frontiers | Research Topics

Cardio-oncology: Mechanisms and therapeutics

Edited by
Feng Cao, Nazish Sayed, Chun Liu and Dong Han

Published in
Frontiers in Cardiovascular Medicine

ISSN 1664-8714
ISBN 978-2-8325-2440-4
DOI 10.3389/978-2-8325-2440-4

About Frontiers

Frontiers is more than just an open access publisher of scholarly articles: it is a pioneering approach to the world of academia, radically improving the way scholarly research is managed. The grand vision of Frontiers is a world where all people have an equal opportunity to seek, share and generate knowledge. Frontiers provides immediate and permanent online open access to all its publications, but this alone is not enough to realize our grand goals.

Frontiers journal series

The Frontiers journal series is a multi-tier and interdisciplinary set of open-access, online journals, promising a paradigm shift from the current review, selection and dissemination processes in academic publishing. All Frontiers journals are driven by researchers for researchers; therefore, they constitute a service to the scholarly community. At the same time, the *Frontiers journal series* operates on a revolutionary invention, the tiered publishing system, initially addressing specific communities of scholars, and gradually climbing up to broader public understanding, thus serving the interests of the lay society, too.

Dedication to quality

Each Frontiers article is a landmark of the highest quality, thanks to genuinely collaborative interactions between authors and review editors, who include some of the world's best academicians. Research must be certified by peers before entering a stream of knowledge that may eventually reach the public - and shape society; therefore, Frontiers only applies the most rigorous and unbiased reviews. Frontiers revolutionizes research publishing by freely delivering the most outstanding research, evaluated with no bias from both the academic and social point of view. By applying the most advanced information technologies, Frontiers is catapulting scholarly publishing into a new generation.

What are Frontiers Research Topics?

Frontiers Research Topics are very popular trademarks of the *Frontiers journals series*: they are collections of at least ten articles, all centered on a particular subject. With their unique mix of varied contributions from Original Research to Review Articles, Frontiers Research Topics unify the most influential researchers, the latest key findings and historical advances in a hot research area.

Find out more on how to host your own Frontiers Research Topic or contribute to one as an author by contacting the Frontiers editorial office: frontiersin.org/about/contact

Cardio-oncology: Mechanisms and therapeutics

Topic editors

Feng Cao — People's Liberation Army General Hospital, China
Nazish Sayed — Stanford University, United States
Chun Liu — Stanford University, United States
Dong Han — People's Liberation Army General Hospital, China

Citation

Cao, F., Sayed, N., Liu, C., Han, D., eds. (2023). *Cardio-oncology: Mechanisms and therapeutics*. Lausanne: Frontiers Media SA. doi: 10.3389/978-2-8325-2440-4

Table of contents

frontiers | Frontiers in Cardiovascular Medicine

TYPE Editorial
PUBLISHED 03 May 2023
DOI 10.3389/fcvm.2023.1198617

OPEN ACCESS

EDITED AND REVIEWED BY
Jun-ichi Abe,
University of Texas MD Anderson Cancer Center, United States

*CORRESPONDENCE
Dong Han
handong123566@163.com

RECEIVED 01 April 2023
ACCEPTED 21 April 2023
PUBLISHED 03 May 2023

CITATION
Ma Y, Cao F and Han D (2023) Editorial: Cardio-oncology: mechanisms and therapeutics.
Front. Cardiovasc. Med. 10:1198617.
doi: 10.3389/fcvm.2023.1198617

Editorial: Cardio-oncology: mechanisms and therapeutics

Yan Ma, Feng Cao and Dong Han*

National Clinical Research Center for Geriatric Diseases, The Second Medical Center, Chinese PLA General Hospital, Beijing, China

KEYWORDS

cardio-oncolody, editoral, mechanisms, cardiotoxcity, prognosis

Editorial on the Research Topic
Cardio-oncology: mechanisms and therapeutics

Cancer and cardiovascular disease share similar risk factors and are both prevalent among aging populations. Individuals with a history of cancer are exposed to a 2–3 times higher chance of getting acute coronary syndrome (ACS), which can persist for up to 10 years after a cancer diagnosis (1). Cancer patients with cardiovascular comorbidity have worse survival rates than cancer patients alone (2, 3). Reciprocally, myocardial infarction also hastens the spread of cancer and worsens the prognosis of cancer patients (4, 5). In this regard, understanding the interaction between cancer and cardiovascular disease may help avoid tackling diseases in a siloed approach and improve the outcome of these patients with comorbidity.

In addition, novel cancer therapies have tremendously improved the survival of cancer patients but also increased treatment-related side effects (6, 7). Cardiovascular toxicities are the most common adverse effects, threatening survival and impairing life quality of the cancer survivors (8). Cancer survivors' early morbidity and death are largely affected by these side effects (9). Understanding the mechanisms underlying anticancer treatment-induced cardiotoxicity can help develop novel therapeutics to avoid or lessen it.

The purpose of this research topic is to bring together a collection of works that provide novel insights into interactions between cancer and cardiovascular disease as well as mechanisms and therapeutics of anticancer treatment-induced cardiotoxicity. All contributions to this research topic concentrate on one or more of the above-mentioned study topics and several studies referenced below are representative.

N^6-Methyladenosine in cyclophosphamide-induced cardiotoxicity

The RNA epitranscriptomics represented by N^6-Methyladenosine (m^6A) are increasingly recognized to play important roles in physiology and disease (10). Cyclophosphamide is frequently prescribed to treat various types of cancers and autoimmune conditions. Accumulated doses of this drug may result in fatal hemorrhagic myocarditis (11). Zhu et al. demonstrated that the pathogenesis of cyclophosphamide-induced cardiotoxicity involves the downregulation of Junctophilin 2 (JPH2) levels. The proper structure and function of junctophilin-2 (JPH2) are recognized to be indispensable for proper excitation-contraction coupling in cardiomyocytes (12). The increased m^6A level of JPH2 mRNA induced by N^6-Methyladenosine writer METTL3 decreased its expression levels, and consequently

dysregulated calcium signaling in cardiomyocytes. These results identified a novel epitranscriptomic mechanism regulating JPH2 expression and offers novel approaches to the management of cyclophosphamide-induced cardiotoxicity.

miR-194-5p contributes to doxorubicin-induced cardiotoxicity

Doxorubicin is a popular anticancer agent but is well-known for its cardiotoxicity in many patients. The mechanisms underlying doxorubicin (DOX)-induced cardiotoxicity remain not fully understood. miRNAs are widely involved in the progression of various cardiovascular diseases (13). Fa et al. revealed the important role of miR-194-5p in the pathogenesis of DOX-induced cardiotoxicity. MiR-194-5p silencing reduced doxorubicin (DOX)-induced cardiotoxicity *in vitro* and *in vivo* by upregulating PAK2 and XBP1s. Overexpression of PAK2 or XBP1s reduced miR-194-5p- exacerbated cardiomyocyte apoptosis. This work was the first to identify a novel pathogenic miR-194-5p/PAK2/XBP1s axis in DOX-induced cardiotoxicity, hence proposing a potential target for the prevention and treatment of DOX-induced cardiotoxicity.

NT-proBNP can predict cardiovascular symptoms caused by Pd-1 inhibitor therapy

In recent years, immunotherapy has achieved great success in cancer treatment. Unfortunately, cardiotoxicity appears to have emerged as an unneglectable issue recently (14). The work by Peng et al. suggested that NT-proBNP could predict cardiovascular symptoms in individuals with myocardial damage following PD-1 inhibitor therapy, while highly sensitive troponin T (hsTnT) is the best cardiac biomarker for mortality prediction in symptomatic patients. This study may help medics to perform risk stratification for patients at an earlier time and to implement effective interventions at the early stage of PD-1 inhibitor-related myocarditis.

A large-scale observation in cancer patients suffering from infective endocarditis

Infective endocarditis (IE) occurs more frequently in cancer patients as compared with the general population (15). IE was predominantly community-acquired (74.8%) in cancer patients, according to Cosyns et al. The most common complications were acute renal failure (25.9%), embolic events (21.7%), and congestive heart failure (18.1%). This is a sizable observational cohort of IE patients with cancer. It sheds light on current IE cancer patient profiles, treatment, and outcomes. Considering the lack of randomized and large-scale observational data on IE cancer patients, this registry provides a unique viewpoint on IE management in cancer patients.

D-Dimer is a predictive factor for cancer therapeutics-related cardiac dysfunction

Improved early detection methods have allowed a larger number of cancer patients with cancer therapeutics-related cardiac dysfunction (CTRCD) to live longer (16). Oikawa et al. consecutively enrolled 169 patients who planned to receive cardiotoxic chemotherapy for 12 months of follow-up and found that the incidence of CTRCD was greater in the high D-dimer group than in the low D-dimer group (16.2 vs. 4.5%, $p = 0.0146$). High D-dimer levels at baseline were an independent predictor of the development of CTRCD, according to multivariable logistic regression analysis [odds ratio 3.93, 95% CI (1.00–15.82), $p = 0.047$]. It is suggested that D-dimer may be a potential predictor of CTRCD and has clinical practical value.

Low LVEF after chemotherapy was associated with blood RNA viruses

It has been hypothesized that immunosuppression after chemotherapy increases opportunistic viral infections (17). Varkoly et al. performed high-throughput sequencing analysis of RNA obtained from blood samples of 28 patients with hematological malignancies who had undergone chemotherapy. The result suggested that patients with low LVEF had influenza orthomyxovirus, avian paramyxovirus, and retrovirus sequences present. This is the first study to use high-throughput, blinded, unbiased sequencing to test for RNA viruses in circulating blood and associate those findings with abnormalities in heart function in patients who have recently finished chemotherapy. This study raises attention to RNA virus infections in individuals with chemotherapy-related cardiomyopathy.

Cardiovascular outcomes in patients with colorectal cancer

Colorectal cancer (CRC) patients are potentially at high cardiovascular risk (18). Hang et al. followed up 197, 699 colorectal cancer patients for 37 months and examined the risks of cardiovascular death (CVD) in patients with CRC. They revealed that CVD ranked first and accounted for 41.69% of the major cause of non-cancer deaths. In addition, the nomogram for CVD prediction in CRC patients was created. This nomogram performed quite well and might assist physicians in providing customized care in clinical settings.

Perspectives

With the generous support from all editors, publishers, reviewers, and authors involved in this research topic, we have successfully finalized this wonderful collection focusing on

mechanisms and therapeutic in Cardio-Oncology. Future studies on the mechanism and management of cardio-oncology are expected to continually improve the survival and life quality of cancer survivors. The enormous issues posed by tumor-cardiovascular comorbidity, however, deserve more attention given its rising incidence and the continuously aging population. There is substantial opportunity for the collaboration between oncologists and cardiologists to work together to improve the outcome of cancer patients with cardiovascular comorbidity.

Author contributions

YM drafted the manuscript. DH and FC revised the paper. All authors listed have made a substantial, direct, and intellectual contribution to the work and approved it for publication.

Conflict of interest

The authors declare that the research was conducted in the absence of any commercial or financial relationships that could be construed as a potential conflict of interest.

Publisher's note

All claims expressed in this article are solely those of the authors and do not necessarily represent those of their affiliated organizations, or those of the publisher, the editors and the reviewers. Any product that may be evaluated in this article, or claim that may be made by its manufacturer, is not guaranteed or endorsed by the publisher.

References

1. Lucà F, Parrini I, Abrignani MG, Rao CM, Piccioni L, Di Fusco SA, et al. Management of acute coronary syndrome in cancer patients: it's high time we dealt with it. *J Clin Med*. (2022) 11(7):1792. doi: 10.3390/jcm11071792

2. Carlson LE, Watt GP, Tonorezos ES, Chow EJ, Yu AF, Woods M, et al. Coronary artery disease in young women after radiation therapy for breast cancer: the WECARE study. *JACC CardioOncol*. (2021) 3:381–92. doi: 10.1016/j.jaccao.2021.07.008

3. Kwok CS, Wong CW, Kontopantelis E, Barac A, Brown S-A, Velagapudi P, et al. Percutaneous coronary intervention in patients with cancer and readmissions within 90 days for acute myocardial infarction and bleeding in the USA. *Eur Heart J*. (2021) 42:1019–34. doi: 10.1093/eurheartj/ehaa1032

4. Romero D. Myocardial infarction promotes breast cancer recurrence. *Nat Rev Clin Oncol*. (2020) 17:520. doi: 10.1038/s41571-020-0418-7

5. Koelwyn GJ, Newman AAC, Afonso MS, van Solingen C, Corr EM, Brown EJ, et al. Myocardial infarction accelerates breast cancer via innate immune reprogramming. *Nat Med*. (2020) 26:1452–8. doi: 10.1038/s41591-020-0964-7

6. Li M, Goldman DP, Chen AJ. Spending on targeted therapies reduced mortality in patients with advanced-stage breast cancer. *Health Aff (Millwood)*. (2021) 40:763–71. doi: 10.1377/hlthaff.2020.01714

7. Seton-Rogers S. Cardiovascular disease and cancer communicate. *Nat Rev Cancer*. (2020) 20:552. doi: 10.1038/s41568-020-0294-6

8. Florido R, Daya NR, Ndumele CE, Koton S, Russell SD, Prizment A, et al. Cardiovascular disease risk among cancer survivors: the atherosclerosis risk in communities (ARIC) study. *J Am Coll Cardiol*. (2022) 80:22–32. doi: 10.1016/j.jacc.2022.04.042

9. Siegel RL, Miller KD, Fuchs HE, Jemal A. Cancer statistics, 2022. *CA Cancer J Clin*. (2022) 72(1):7–33. doi: 10.3322/caac.21708

10. Yang C, Hu Y, Zhou B, Bao Y, Li Z, Gong C, et al. The role of m(6)A modification in physiology and disease. *Cell Death Dis*. (2020) 11:960. doi: 10.1038/s41419-020-03143-z

11. Dhesi S, Chu MP, Blevins G, Paterson I, Larratt L, Oudit GY, et al. Cyclophosphamide-Induced cardiomyopathy: a case report, review, and recommendations for management. *J Investig Med High Impact Case Rep*. (2013) 1:2324709613480346. doi: 10.1177/2324709613480346

12. Garbino A, Wehrens XH. Emerging role of junctophilin-2 as a regulator of calcium handling in the heart. *Acta Pharmacol Sin*. (2010) 31:1019–21. doi: 10.1038/aps.2010.116

13. Barwari T, Joshi A, Mayr M. MicroRNAs in cardiovascular disease. *J Am Coll Cardiol*. (2016) 68:2577–84. doi: 10.1016/j.jacc.2016.09.945

14. Varricchi G, Galdiero MR, Tocchetti CG. Cardiac toxicity of immune checkpoint inhibitors: cardio-oncology meets immunology. *Circulation*. (2017) 136:1989–92. doi: 10.1161/CIRCULATIONAHA.117.029626

15. Grable C, Yusuf SW, Song J, Viola GM, Ulhaq O, Banchs J, et al. Characteristics of infective endocarditis in a cancer population. *Open Heart*. (2021) 8(2):e001664. doi: 10.1136/openhrt-2021-001664

16. Xiao H, Wang X, Li S, Liu Y, Cui Y, Deng X. Advances in biomarkers for detecting early cancer treatment-related cardiac dysfunction. *Front Cardiovasc Med*. (2021) 8:753313. doi: 10.3389/fcvm.2021.753313

17. Badrinath A, Bhatta S, Kloc A. Persistent viral infections and their role in heart disease. *Front Microbiol*. (2022) 13:1030440. doi: 10.3389/fmicb.2022.1030440

18. Koo CY, Tai BC, Chan DKH, Tan LL, Tan KK, Lee CH. Chemotherapy and adverse cardiovascular events in colorectal cancer patients undergoing surgical resection. *World J Surg Oncol*. (2021) 19:21. doi: 10.1186/s12957-021-02125-5

frontiers in Cardiovascular Medicine

ORIGINAL RESEARCH
published: 13 October 2021
doi: 10.3389/fcvm.2021.750186

Luteolin Prevents Cardiac Dysfunction and Improves the Chemotherapeutic Efficacy of Doxorubicin in Breast Cancer

Youyang Shi[1†], Feifei Li[1†], Man Shen[2†], Chenpin Sun[3], Wei Hao[3], Chunyu Wu[3], Ying Xie[1], Shuai Zhang[3], Hongzhi Gao[1], Jianfeng Yang[1], Zhongyan Zhou[4], Dongwen Gao[1], Yuenong Qin[3*], Xianghui Han[1*] and Sheng Liu[1*]*

[1] Longhua Hospital, Shanghai University of Traditional Chinese Medicine, Shanghai, China, [2] School of Pharmacy, Shanghai University of Traditional Chinese Medicine, Shanghai, China, [3] Department of Breast Surgery (Integrated Traditional and Western Medicine), Longhua Hospital, Shanghai University of Traditional Chinese Medicine, Shanghai, China, [4] Department of Cardiovascular Research Laboratory, Longhua Hospital, Shanghai University of Traditional Chinese Medicine, Shanghai, China

Background: Doxorubicin (Dox) is one of the most effective chemotherapy agents used in the treatment of solid tumors and hematological malignancies. However, it causes dose-related cardiotoxicity that may lead to heart failure in patients. Luteolin (Lut) is a common flavonoid that exists in many types of plants. It has been studied for treating various diseases such as hypertension, inflammatory disorders, and cancer. In this study, we evaluated the cardioprotective and anticancer effects of Lut on Dox-induced cardiomyopathy *in vitro* and *in vivo* to explore related mechanisms in alleviating dynamin-related protein (Drp1)-mediated mitochondrial apoptosis.

Methods: MTT and LDH assay were used to determine the viability and toxicity of cardiomyocytes treated with Dox and Lut. Flow cytometry was used to examine ROS levels, and electron and confocal microscopy was employed to assess the mitochondrial morphology. The level of apoptosis was examined by Hoechst 33258 staining. The protein levels of myocardial fission protein and apoptosis-related protein were examined using Western blot. Transcriptome analysis of the protective effect of Lut against Dox-induced cardiac toxicity in myocardial cells was performed using RNA sequencing technology. The protective effects of Lut against cardiotoxicity mediated by Dox in zebrafish were quantified. The effect of Lut increase the antitumor activity of Dox in breast cancer both *in vitro* and *in vivo* were further employed.

Results: Lut ameliorated Dox-induced toxicity in H9c2 and AC16 cells. The level of oxidative stress was downregulated by Lut after Dox treatment of myocardial cells. Lut effectively reduced the increased mitochondrial fission post Dox stimulation in cardiomyocytes. Apoptosis, fission protein Drp1, and Ser616 phosphorylation were also increased post Dox and reduced by Lut. In the zebrafish model, Lut

OPEN ACCESS

Edited by:
Dong Han,
People's Liberation Army General Hospital, China

Reviewed by:
Qiangrong Liang,
New York Institute of Technology, United States
Mingming Zhang,
Tangdu Hospital, China

***Correspondence:**
Sheng Liu
lslhtcm@163.com
Xianghui Han
hanxianghui1106@163.com
Dongwen Gao
dgao3@shutcm.edu.cn
Yuenong Qin
frank_yching@aliyun.com

[†]These authors share first authorship

Specialty section:
This article was submitted to Cardio-Oncology, a section of the journal Frontiers in Cardiovascular Medicine

Received: *30 July 2021*
Accepted: *16 September 2021*
Published: *13 October 2021*

Citation:
Shi Y, Li F, Shen M, Sun C, Hao W, Wu C, Xie Y, Zhang S, Gao H, Yang J, Zhou Z, Gao D, Qin Y, Han X and Liu S (2021) Luteolin Prevents Cardiac Dysfunction and Improves the Chemotherapeutic Efficacy of Doxorubicin in Breast Cancer. Front. Cardiovasc. Med. 8:750186. doi: 10.3389/fcvm.2021.750186

significantly preserved the ventricular function of zebrafish after Dox treatment. Moreover, in the mouse model, Lut prevented Dox-induced cardiotoxicity and enhanced the cytotoxicity in triple-negative breast cancer by inhibiting proliferation and metastasis and inducing apoptosis.

Keywords: luteolin, cardiac dysfunction, doxorubicin, breast cancer, mitochondrial dysfunction

INTRODUCTION

Doxorubicin (Dox), an anthracycline chemotherapeutic agent, has been widely used to treat a variety of tumors including breast cancer, ovarian cancer, and hematological malignancies (1–4). However, the clinical utility of Dox in chemotherapy is limited by its adverse dose-dependent cardiotoxicity, which often results in left ventricular dysfunction, cardiomyopathy, and even heart failure (5, 6). Over the decades, novel insights into Dox-induced oxidative stress in cardiomyocytes emerged since current interventions to lessen the incidence of cardiotoxicity after prolonged Dox treatments are unsatisfactory (7–9). Increasing evidence proved that Dox facilitates cardiomyocyte apoptosis and programmed death by damaging mitochondrial structure and its biologic function, which is ascribed to the disorder of mitochondrial oxidation-reduction homeostasis and mitochondrial dynamics (10). Nevertheless, effective interventions for Dox-induced cardiotoxicity still need to be explored and developed.

Dexrazoxane is the only drug currently approved by the FDA that provides protection against Dox-induced cardiotoxicity. However, dexrazoxane not only causes side effects, such as hematological toxicity and myelosuppression, but also decreases the antitumor efficacy of Dox (11, 12). For instance, the activation of hypoxia-inducible transcription factor, an oncogene, may contribute to the protective effect of dexrazoxane against anthracycline cardiotoxicity in dexrazoxane-treated H9c2 cardiomyocytes (13). Interestingly, numerous studies have demonstrated that different herbal products and bioactive phytochemicals could counterbalance Dox-induced cardiotoxicity as add-on therapies (14, 15). Therefore, developing a drug that confers cardioprotection during Dox treatment and improves the chemotherapeutic efficacy of Dox in cancer cells is important.

Luteolin (Lut), 3′,4′,5′,7′-tetrahydroxyflavone, a naturally occurring flavone, which are widely enriched in plants. Lut has shown beneficial effects in several biological processes including anti-tumorigenesis, anti-inflammation, antiapoptotic activities, and antioxidative stress (**Figure 1A**) (16, 17). Plants rich in Lut have been used as traditional Chinese medicine (TCM) for hypertension, inflammatory diseases, and cancers (14, 18). In China, traditional herbal medicine has been commonly used for the treatment of breast cancer and its complications (19). Among them, *Platycodon grandiflorum* is widely used, alone or in combination with other herbal medicines, to treat patients with early breast cancer receiving anthracycline-based chemotherapy. Our previous clinical study found that *Platycodon grandiflorum* has cardioprotective effects for early breast cancer patients who received Dox-based chemotherapy (20). Basic experiment studies revealed that *Platycodon grandiflorum* prevents Dox-induced cardiotoxicity in a mouse model of breast cancer (21). However, the potential mechanisms behind the cardioprotective effects remain unknown.

Lut is one of the major metabolites upon oral administration of luteolin-7-O-glucoside and is generally absorbed by intestinal mucosa into the systemic circulation after oral administration with an oral bioavailability at ∼26% (22). Importantly, the flavonoid Lut is recognized as an important regulator of myocardial function providing myocardial protection during times of stress and can largely protect the myocardium against IR injury, partly through the downregulation of antioxidant and apoptosis properties (23, 24). Importantly, as the main component of *Platycodon grandiflorum*, Lut exerts multiple cellular effects *in vitro*, including antiproliferative effects in cancer cells and anti-inflammatory and antioxidative effects in various cell types. However, the molecular mechanisms by which Lut exerts these effects remain unclear.

Previous studies shown that Dox may activate apoptotic signaling through multiple mechanisms, including mitochondria-related apoptotic signaling (25). Dox-induced mitochondrial fission is a dynamin-related protein 1 (Drp1) signaling-dependent process, Drp1 might be a potential target against Dox-induced cardiotoxicity (26, 27). Given that hepatotoxicity and heart failure due to different medicines and toxins can be attenuated by Lut, we hypothesized that Lut may have protective effects on cardiotoxicity due to Dox via regulating mitochondrial damage. Therefore, the aim of this work was to investigate the protective effect of Lut against Dox-induced cardiotoxicity. The results showed that this protection was mediated through Drp1-regulated mitochondria-related apoptosis both *in vitro* and *in vivo*. In addition, Lut enhanced the chemotherapeutic efficacy of Dox in breast cancer.

MATERIALS AND METHODS

Cell Cultures

H9c2 (rat cardiomyocytes), AC16 (human cardiomyocytes), 4T1 (mouse breast cancer cell), and MDA-MB-231 (human breast cancer cell) cell lines were purchased from the Cell Bank of the Chinese Academy of Sciences (Shanghai, China). H9c2, AC16, and MDA-MB-231 cells were maintained in DMEM medium supplemented with 10% (v/v) FBS, 100 U/mL penicillin, and 100 mg/L streptomycin. The 4T1 cells were maintained in RPMI 1640 medium supplemented with 10% (v/v) FBS, 100 U/mL penicillin, and 100 mg/L streptomycin. The cells were incubated at 37°C in a 5% CO_2 incubator with saturated humidity.

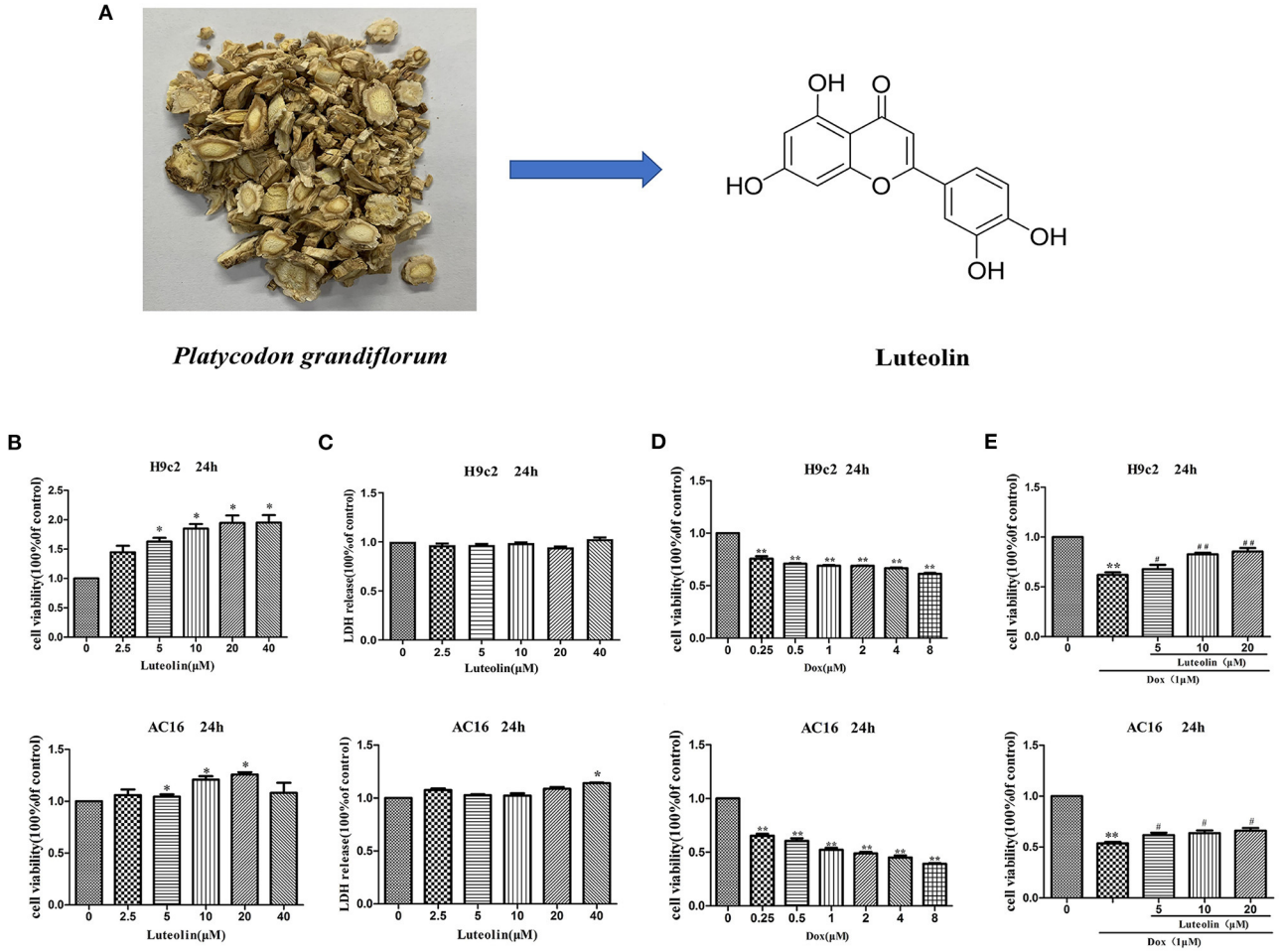

FIGURE 1 | Effect of Lut in attenuating Dox-induced cardiotoxicity in H9c2 and AC16 cells. **(A)** Chemical structure of Lut. **(B,C)** Effects of different concentrations of Lut on cell viability and toxicity in H9c2 and AC16 cells. **(D)** Effects of different concentrations of Dox on cell toxicity in H9c2 and AC16 cells. **(E)** Effects of Lut in attenuating Dox-induced cardiotoxicity in H9c2 and AC16 cells. Mean ± SD, $n = 3$ independent experiment. $^{*}P < 0.05$; $^{**}P < 0.01$ compared with control group. $^{\#}P < 0.05$; $^{\#\#}P < 0.01$ compared with Dox group.

Cell Viability and Cytotoxicity Assays

The cell viability and cytotoxicity of H9c2 and AC16 cells were detected by MTT assay and LDH assays. Briefly, the cells were plated in 96-well plates at a density of 5,000 cells/well, incubated overnight, and then exposed to 1 μM Dox with or without various concentrations of Lut for another 24 h. Cells were supplemented with 20 μL MTT and incubated for 4 h at 37°C. The formazan crystals that formed were subsequently dissolved in 150 μL DMSO, and the OD490 values were measured with a BioTek instrument (Winooski, Vermont, USA). For cytotoxicity assay, the release of LDH into the medium was determined using a Cytotoxicity Detection Kit (Beyotime, Shanghai, China). The absorbance was measured with a microplate reader at 490 nm.

Oxidative Stress Analysis

After 24 h of Dox (1 μM) treatment with or without Lut (20 μM), H9c2 and AC16 cells were loaded with 10 μM DCFH-DA in medium for 30 min at 37°C. After incubation, the ROS levels were measured using a flow cytometer. For SOD analysis, cell supernatants were collected by centrifugation after treatment. The solution was measured by the WST-8 method according to the manufacturer's instructions. The SOD activity was presented as percent inhibition of the reduction of the chromogenic substrate.

Cell Microfilament Cytoskeleton Staining

H9c2 and AC16 cells were seeded into 6-well plates. After 24 h of Dox (1 μM) treatment with or without Lut (20 μM), cells were fixed with 4% paraformaldehyde in PBS for 15 min. Suitable media were washed twice with wash buffer and permeabilized with 0.1% Triton X-100 in PBS for 5 min at room temperature. Following two washes with wash buffer, cells in suitable media were covered with dilute FITC-conjugated phalloidin in PBS immediately prior to use and incubated for 30 min to stain

the actin. Nuclei counterstaining was performed by incubating cells with 0.1 μg/mL DAPI for 15 min. Fluorescence images were captured with a laser scanning confocal microscope.

Cell Apoptosis Analysis

H9c2 and AC16 cells were seeded in 6-well flat-bottom microtiter plates at an initial cell density of 10^5 cells/well and cultured overnight. After 24 h of Dox (1 μM) treatment with or without Lut (20 μM), cells were incubated with fresh medium containing 0.1 mmol/L Hoechst 33258 (Beyotime, Shanghai, China) in the dark for 10 min. The cells were washed three times with PBS, and the apoptotic cells were observed under a fluorescence microscope (Olympus, Tokyo, Japan).

Western Blot

Western blot was used to evaluate the apoptosis-related protein in cells. Primary rabbit antibodies, such as Bax (#2772, 1:1,000), Bcl-2 (#3498, 1:1,000), Bcl-XL (#2764, 1:1,000), Caspase-3 (#9662, 1:1,000), Cleaved Caspase-3 (#9664, 1:1,000), β-actin (#3700, 1:1,000), GAPDH (#5174, 1:1,000), Drp1 (#8570, 1:1,000), phospho-Drp1 (Ser616) (#3455, 1:1,000), and horseradish peroxidase (HRP)-conjugated secondary antibody (#7074s, 1:5,000) were purchased from Cell Signaling Technology, Inc. (Beverly, MA, USA). Cells were washed with PBS for three times and lysed with lysis buffer. After incubation on ice for 30 min, the lysates were centrifuged at 12,000 g for 15 min at 4°C. Protein sample was denatured at 100°C for 10 min, separated by sodium dodecyl sulfate–polyacrylamide gel electrophoresis, and then transferred to PVDF membrane (Millipore). The membrane was incubated with the primary antibodies overnight. Then, the membrane was washed and incubated with secondary HRP-conjugated goat anti-rabbit or anti-mouse antibodies. Finally, the blots were developed with Enhanced ECL System (Beyotime, Shanghai, China), and the signal was quantified by Quantity One software (Bio-Rad).

Confocal Microscopy and Electron Assessment on Mitochondrial Morphology

Mitochondrial morphology was assessed by confocal microscopy. After 24 h of Dox (1 μM) treatment with or without Lut (20 μM), the media were removed from the dish, and staining solution containing MitoTracker probe (Yeasen Biotech, Shanghai, China) was added. The lyophilized MitoTracker was dissolved in anhydrous dimethyl sulfoxide to a final concentration of 100 nmol/L and incubated for 30 min. Images were captured with a laser scanning confocal microscope (Olympus, Tokyo, Japan). Following Dox treatment with or without Lut, the H9c2 and AC16 cells were washed with PBS, collected, and fixed in 2.5% glutaraldehyde for over 2 h at 4°C. The specimens were subsequently rinsed with PBS, fixed in 1% osmium tetroxide for 1–2 h, and then dehydrated sequentially in graded concentrations of 50, 70, 80, 90, and 100% ethanol for 15 min. The specimens were then processed for Epon™ embedding and observed under a transmission electron microscope (CM100, Philips, Netherlands).

Molecular Docking

Molecular docking was used to interpret the binding area of small molecule ligands and macromolecular receptors through computer simulation and then calculate the physical and chemical parameters for predicting the affinity between the two. The mol2 format of the active ingredient was downloaded from the PubChem database. Its energy was minimized through Chem3D and converted into pdb format. Small molecule compounds were imported into AutoDock Tools-1.5.6 software. Water molecules were deleted, atomic charges were added, and atom type was allocated. All flexible keys can be rotated by default and finally saved as a pdbqt file. The PDB format file of the crystal structure of the target was downloaded from the PDB database (Protein Data Bank). Pymol 2.3 software was used to delete irrelevant small molecules in the protein molecule. Then, we imported the protein molecule into the AutoDock Tools-1.5.6 software to delete water molecules and add hydrogen atom, and finally saved it as a pdbqt file. The processed active ingredient is a small molecule ligand, and the protein target is used as a receptor. The center position and length, width, and height of the Grid Box were determined according to the interaction site of the small molecule and the target. Finally, batch docking was carried out through AutoDock vina and python script. In analyzing the molecular docking results, we visualized the binding effect of compounds and proteins using Pymol 2.3 software.

RNA Sequencing

H9c2 and AC16 cells were harvested after drug treatment (three samples per group). The total RNA of each sample was extracted using TRIzol (Thermo Fisher). The quality of the RNA was measured by the Agilent 2100 Bioanalyzer with the RNA 6000 Nano Kit (Agilent, Santa Clara, CA, USA). The RNA concentration, RIN value and fragment length distribution were analyzed. Construction of the sequencing library and RNA sequencing were performed by Sangon (Shanghai, China) using the Illumina NovaSeq Platform.

Identification of Differentially Expressed Genes (DEGs) and Functional Enrichment Analysis

Limma package (version 3.40.2) of R software was used to screen out the DEGs in the Dox–Lut group compared with Lut-treated group and Dox-treated group compared with control group in H9c2 and AC16 cells. "Adjusted $P < 0.05$ and Log (Fold Change| >1)" were defined as the cutoff for the identification of differentially expressed mRNAs. To further confirm the underlying function of potential targets, the data were analyzed by functional enrichment. Gene Ontology (GO) is a widely used tool for annotating genes with functions, especially molecular function (MF), biological pathways (BP), and cellular components (CC). Kyoto Encyclopedia of Genes and Genomes (KEGG) enrichment analysis is a practical database for analytical study of functional annotations and associated high-level genome-wide pathways. The results of functional enrichment are displayed in bubble charts.

Zebrafish Maintenance and Drug Treatment

Tg (cmlc2: GFP) zebrafish with GFP specifically expressed in myocardial cells were used in this study. Zebrafish were maintained as described in the Zebrafish Handbook (28). All animal experiments were approved by the Animal Research Ethics Committee of Shanghai University of Traditional Chinese Medicine. Pair-wise mating (6–12 months old) was used to generate the zebrafish embryos, which were maintained in embryo medium at 28.5°C. All embryos were then raised in the embryo medium containing 1-phenyl-2-thiourea (200 mM) after 48 hpf. Zebrafish (2 dpf) at the same developmental stage were distributed into a 24-well microplate (5 fish per well). After co-treatment with Dox (10 μM) and different concentrations of Lut (5, 10, 20 μM) for 24 h, ventricular functions of zebrafish were examined by assessing various parameters and morphology. The morphology and functions of zebrafish heart were measured by an imaging system comprising a microscope (Olympus). Zebrafish were placed into 1% low-melting-point agarose (Gibco) to restrict their movement, and videos of zebrafish heartbeat were recorded for 10 s at room temperature. The parameters and morphology of ventricular function of zebrafish were measured.

Wound Healing Assay

Cells were seeded in 6-well plates at a density of 1×10^5 cells per well, and when cellular confluence reached about 90%, a 200 μL pipette tip was used to create wounds in confluent cells. After removing the floating cells by washing the scraped surface with PBS, wounded monolayers were photographed with a microscope. Cells were then incubated containing Dox (2 μM) with or without Lut (40 μM) for 24 h. The images of cells migrating into the wound surface and the average distance of migrating cells were determined under a microscope 24 h later.

Colony Formation Assay

To further determine the inhibitory effect of Lut on the tumorigenicity of triple-negative breast cancer (TNBC) cells, colony formation assays were performed. Five hundred 4T1 or MDA-MB-231 cells were seeded into 6-well plates to incubate overnight. The cells were then incubated with Dox (2 μM) with or without Lut (40 μM) for 7–10 days. After fixing with 4% paraformaldehyde and staining with a crystal violet solution, colonies containing more than 30 individual cells were counted under a stereomicroscope.

Cell Invasion Assay

The invasive ability of 4T1 and MDA-MB-231 cells were measured using 24-well Transwell with polycarbonate filters (pore size, 8 μm) coated on the upper side with Matrigel (BD, Bedford, MA, USA). 1×10^3 cells in 100 mL medium were seeded in the top chamber. The bottom chamber contained 10% fetal calf serum medium. After 24 h incubation, non-invasive cells were removed with a cotton swab. Cells that migrated to the bottom surface of the membrane were fixed in formaldehyde, stained with crystal violet solution, and counted under a microscope.

Xenograft Mouse Experiments

Seven-week-old female BALB/c mice (18–20 g) were obtained from the Shanghai SLAC Laboratory Animal Technology Co., Ltd. (Shanghai, China). The animals were housed under standardized conditions in animal facilities at 20 ± 2°C temperature, 40% ± 5% relative humidity, and a 12-h light/dark cycle with dawn/dusk effect. The protocol was approved by the Animal Research Ethics Committee of Shanghai University of Traditional Chinese Medicine (Permit Number: PZSHUTCM18122103). 4T1 cells (2×10^6) were resuspended in 10 mL PBS, and 100 μL of cell suspension was subcutaneously injected into the second pair of breast fat pads on the left side of each mouse. The tumors formed approximately 14 days after the inoculation. Then, all mice were randomly divided into three groups ($n = 5$): control group (ip, saline), Dox group (ip, 2.5 mg/kg Dox), and Dox combined with Lut group (ip 2.5 mg/kg Dox + ip 30 mg/kg Lut). The mice were administered with Dox or Dox combined with Lut solution once per 2 days continuously for 2 weeks. At the experimental endpoint, all animals were euthanized. Then, the size and weight of tumors were measured. Lungs and tumors were excised and then fixed in 4% paraformaldehyde overnight until further analysis. For echocardiographic studies, the mice were anesthetized with 2.5% isoflurane in 95% oxygen and 5% carbon dioxide and then situated in the supine position on a warming platform to maintain the core temperature at 37°C. Cardiac function was evaluated via echocardiography by using a High-Resolution Small Animal Imaging System (Vevo2100, Visual Sonics Inc., Toronto, Canada). Two-dimensional and M-mode echocardiographic images of the long and short axis were recorded. Left ventricular ejection fraction (LVEF) and left ventricular fractional shortening (LVFS) were measured and calculated using the Vevo Strain Software Work Station.

Statistical Analysis

All results are presented as mean ± standard deviation (SD). Two-tailed analysis of variance followed by Dunnett's *post hoc* test and Fisher's test was used to determine the statistical significance. $P < 0.05$ was considered significant for all tests.

RESULTS

Lut Attenuates Dox-Induced Cardiotoxicity in H9c2 and AC16 Cells

The H9c2 (rat) and AC16 (human) cardiomyocytes were treated with elevated concentration (0, 2.5, 5, 10, 20, and 40 μM) of Lut for 24 h. As shown in **Figure 1B**, cell viability was markedly increased with Lut ($P < 0.05$). As detected by LDH assay, the increased Lut concentration was not significantly correlated with LDH release until the Lut concentration was increased to 40 μM ($P < 0.05$; **Figure 1C**). Dox (0, 0.25, 0.5, 1, 2, 4, and 8 μM) treatment for 24 h markedly decreased cell viability ($P < 0.01$; **Figure 1D**). Co-treatment with Lut and Dox significantly increased cell viability compared with Dox alone ($P < 0.05$; **Figure 1E**). Lut could significantly attenuate Dox-induced cardiotoxicity in H9c2 and AC16 cells.

Lut Attenuates Dox-Induced Oxidative Stress and Cytoskeletal Damages in H9c2 and AC16 Cells

We then detected changes of oxidative stress in H9c2 and AC16 cells after 24 h drug treatments using flow cytometry. The results showed that Lut treatment did not significantly change the ROS level, but it could significantly reduce the elevated ROS level induced by Dox ($P < 0.05$; **Figures 2A,B**). Similarly, the decreased SOD activity induced by Dox could be significantly increased by Lut treatment, which could even reach a level higher than that in the Lut-alone group ($P < 0.05$; **Figures 2C,D**). The integrity of the myocardial cytoskeleton plays an important role in the physiological function of the heart. Interestingly, cytoskeleton staining suggested that the cytoskeleton of the Dox treatment group was damaged with disappearance of microfilaments and microtubules in the cell membrane and loss of cell fiber tension. However, this damage could be markedly recovered by Lut in the combined treatment group (white arrows, **Figures 2E,F**). In conclusion, Lut could significantly attenuate Dox-induced oxidative stress and restore cytoskeletal alterations in H9c2 and AC16 cells.

Lut Inhibits Dox-Induced Cardiomyocyte Apoptosis in H9c2 and AC16 Cells

TUNEL assay was performed to assess apoptosis following Lut and Dox treatment in H9c2 and AC16 cells (**Supplementary Figures 1A,B**). Compared with the control group, Dox challenge for 24 h significantly increased cell apoptosis as evidenced by the elevated number of TUNEL-positive cardiomyocytes ($P < 0.05$), while the effect was significantly inhibited by Lut treatment ($P < 0.05$; **Figures 3A,B**). Meanwhile, Western blot indicated that Dox treatment upregulated the levels of Bax and Cleaved Caspase-3 and downregulated Bcl-2 and Bcl-XL levels in H9c2 and AC16 cells. Importantly, the regulation induced by Dox was conversely regulated by Lut treatment ($P < 0.05$; **Figures 3C,D**). Taken together, Lut treatment could significantly inhibit Dox-induced cardiomyocyte apoptosis through the Bax/Bcl-2/Caspase-3 pathway in H9c2 and AC16 cells.

Lut Attenuates Dox-Induced Excessive Mitochondrial Division of H9c2 and AC16 Cells

Next, we explored the effect of Lut on the mitochondrial morphological change of cardiomyocytes induced by Dox. As shown in **Figure 4A**, fluorescence microscopy showed that the mitochondria of normal cardiomyocytes were reticulated. After being stimulated with Dox (1 μM) for 24 h, compared with the normal group, cell mitochondria were divided, and the morphology of cell mitochondria changed significantly, transforming from a reticulate to a punctate phenotype. In addition, compared with the Dox-treated group, Lut (20 μM) markedly inhibited the excessive division of mitochondria and restored the mitochondrial morphology of H9c2 and AC16 cells. Using transmission electron microscopy, we observed the ultrastructure of cells. After 24 h of Dox treatment, vacuoles appeared in cardiomyocytes, and a "hair ball" structure appeared in the mitochondria (red arrow, **Figure 4B**). After Lut treatment, the morphology of cell mitochondria was restored, and the morphology of cell nucleus and chromatin returned to normal.

Lut Attenuates Dox-Induced Drp-1 Phosphorylation in H9c2 and AC16 Cells

We tried to explore the mechanism of Lut to restore Dox-induced mitochondrial morphological alterations and used a molecular docking algorithm to predict the binding mode and affinity between the receptor and the drug molecule in **Figure 5A**. The results suggested a high affinity for docking between Drp-1 and Lut (affinity = −8.31 kcal/mol). Western blot revealed a significantly elevated p-Drp-1/Drp-1 ratio in the Dox-treated group, while the phosphorylation level of Drp-1 significantly decreased with additional Lut treatment in a dose-dependent manner compared with the Dox-treated group ($P < 0.05$; **Figures 5B,C**). Overall, Lut could significantly attenuate Dox-induced mitochondrial morphological changes *via* regulating Drp-1 phosphorylation in H9c2 and AC16 cells.

Lut Reduces Heart Damage Induced by Dox *in vivo*

The protective effects of Lut against cardiotoxicity mediated by Dox in zebrafish were quantified. As shown in **Figure 6A**, we constructed a zebrafish heart injury model using 10 μM Dox. After co-administration of Dox and different concentrations of Lut for 24 h, the zebrafish pericardium of the model group showed obvious edema compared with the negative control group. Moreover, we found a significantly decreased zebrafish heart rate, increased SV–BA distance, and decreased stroke volume in the Dox-induced group ($P < 0.05$; **Figures 6B–D**), indicating severe heart damage. Compared with the doxorubicin-induction group, we found significantly increased heart rate, shortened SV–BA distance, and markedly improved stroke volume of zebrafish after 24 h of intervention with medium and high doses of Lut ($P < 0.05$; **Figures 6B–D**).

Lut Interferes With Dox-Induced Transcriptome Sequencing of Cardiomyocytes in AC16 and H9c2 Cells

Subsequently, to identify DEGs and hallmarks related to the process of Lut in attenuating the toxicity of Dox to cardiomyocytes, we used RNA sequencing and selected upregulated DEGs in the Dox group compared with control group and downregulated DEGs in the Dox–Lut group compared with Dox group. We screened out a total of 137 overlapped hub genes in AC16 cells and 123 overlapped hub genes in H9c2 cells (**Figures 7A,B**). Similarly, we identified downregulated DEGs in the Dox group compared with the control group and upregulated DEGs in the Dox–Lut group compared with the Dox group. Then, we screened out a total of 32 overlapped hub genes in AC16 cells and 814 overlapped hub genes in H9c2 cells (**Figures 7A,B**). Next, we explored the functional annotations of different genes in cardiomyocytes using GO and KEGG algorithm. The DEGs were significantly involved in biological process (GO: BP),

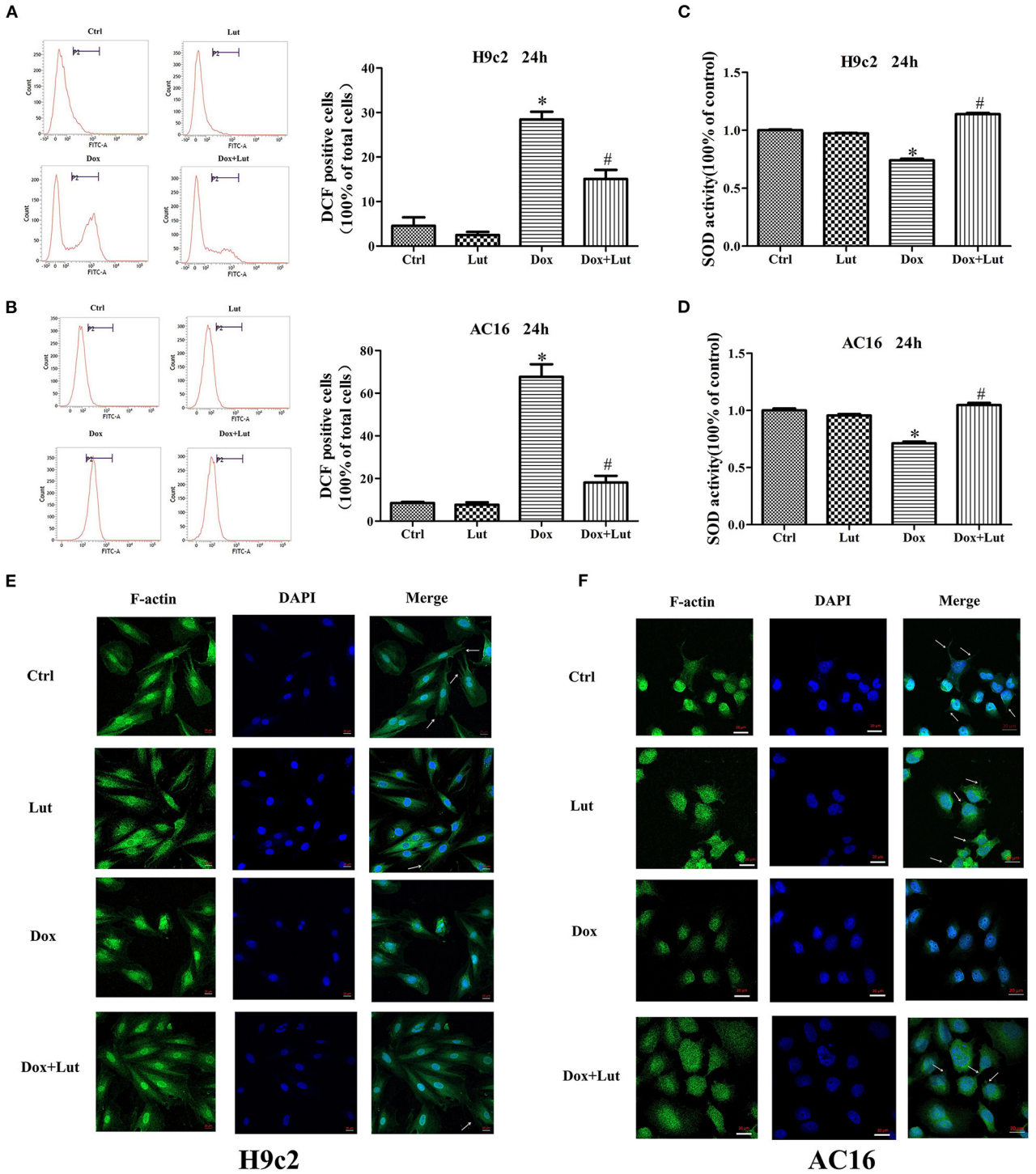

FIGURE 2 | Effect of Lut treatment on Dox-induced oxidative stress and cytoskeletal damages in H9c2 and AC16 cells. **(A,B)** ROS and **(C,D)** SOD levels in H9c2 and AC16 cells after Dox and Lut treatment. **(E,F)** Cytoskeleton staining in H9c2 and AC16 cells after Dox and Lut treatment (630×). White arrows show microfilaments and microtubules. Mean ± SD, $n = 3$ independent experiment. $^{*}P < 0.05$ compared with control group. $^{\#}P < 0.05$ compared with Dox group.

including actin filament bundle organization, Golgi vesicle transport, Ras protein signal transduction, organelle transport along microtubule, microtubule organizing center organization, and microtubule cytoskeleton organization involved in mitosis; cellular function (GO: CC), including chromosomal region, mitotic spindle, P-body, Golgi-associated vesicle membrane, and

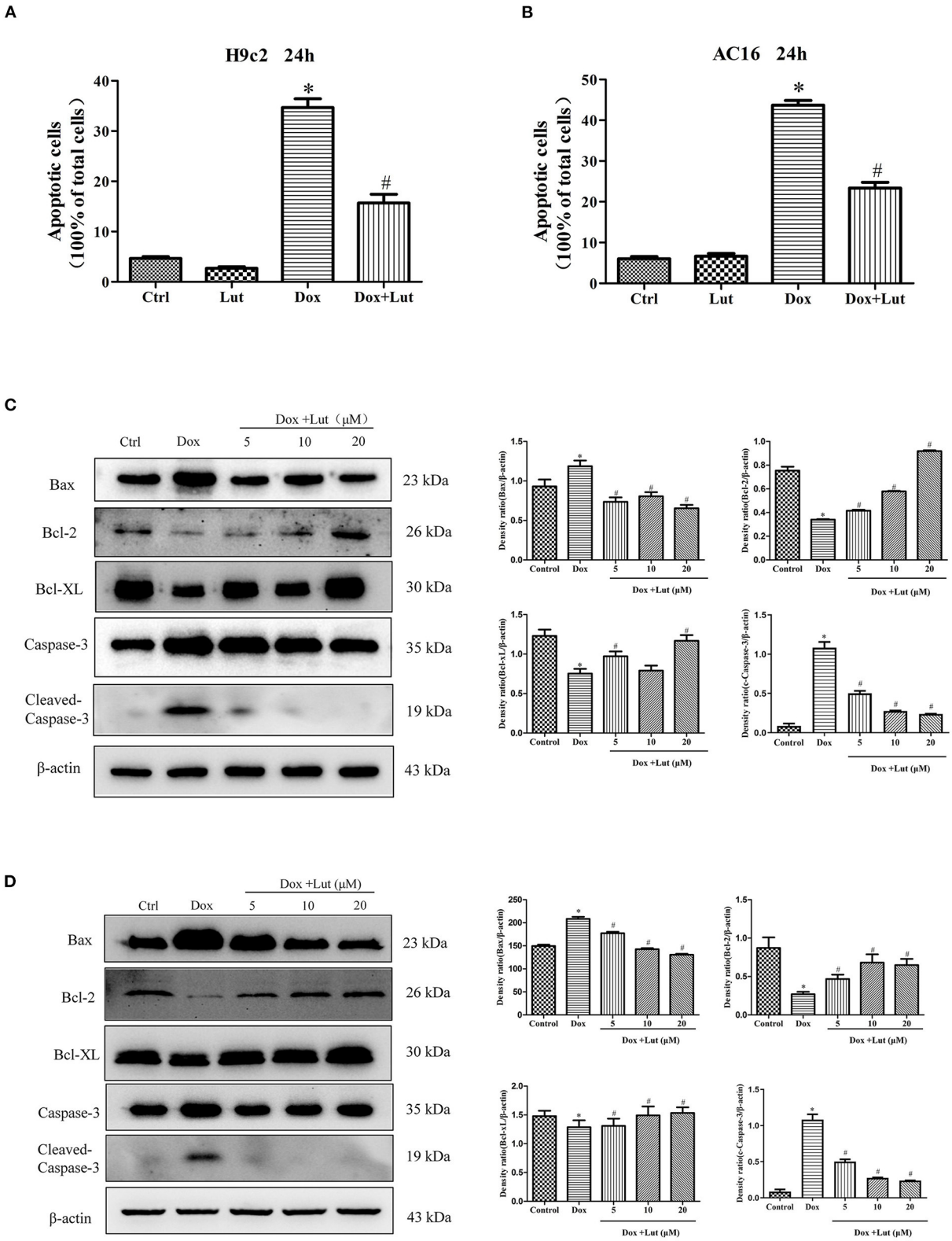

FIGURE 3 | Effect of Lut treatment on Dox-induced cardiomyocyte apoptosis. **(A)** Quantified TUNEL-positive cells from three fields per group in H9c2 and **(B)** AC16 cells. **(C)** Representative Western blot images of H9c2 and **(D)** AC16 apoptosis using Bax, Bcl-2, Bcl-XL, and Cleaved Caspase-3. Mean ± SD, $n = 3$ independent experiment. $^{*}P < 0.05$ compared with control group. $^{\#}P < 0.05$ compared with Dox group.

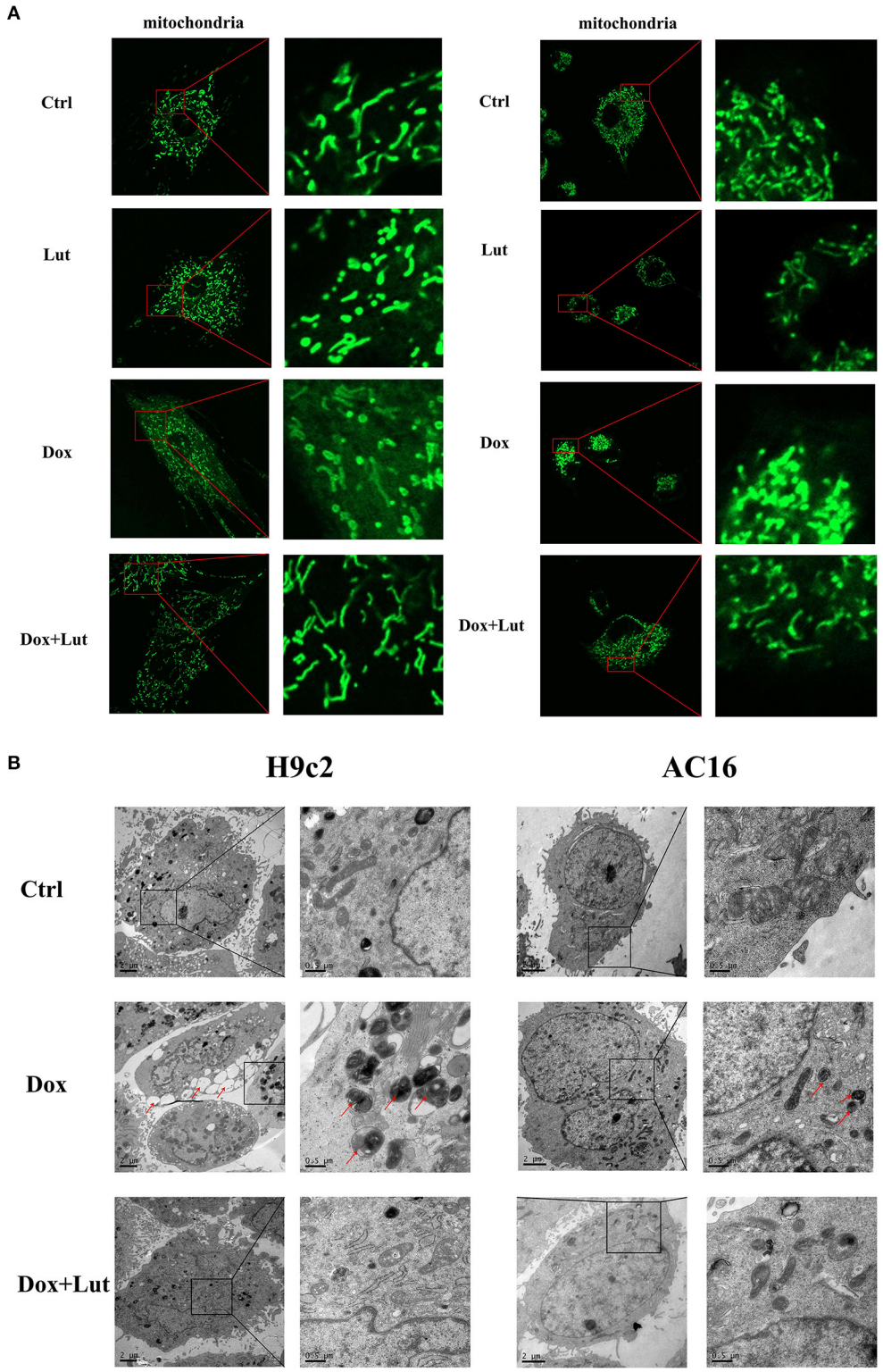

FIGURE 4 | Effect of Lut treatment on Dox-induced changes in cardiomyocyte mitochondrial morphology. **(A)** Representative fluorescence images of the morphology of mitochondria in H9c2 (left) and AC16 (right) cells (630×). **(B)** Transmission electron microscopy images of the morphology of mitochondria in H9c2 (left) and AC16 (right) cells (12,000×). Red arrows show autophagosome.

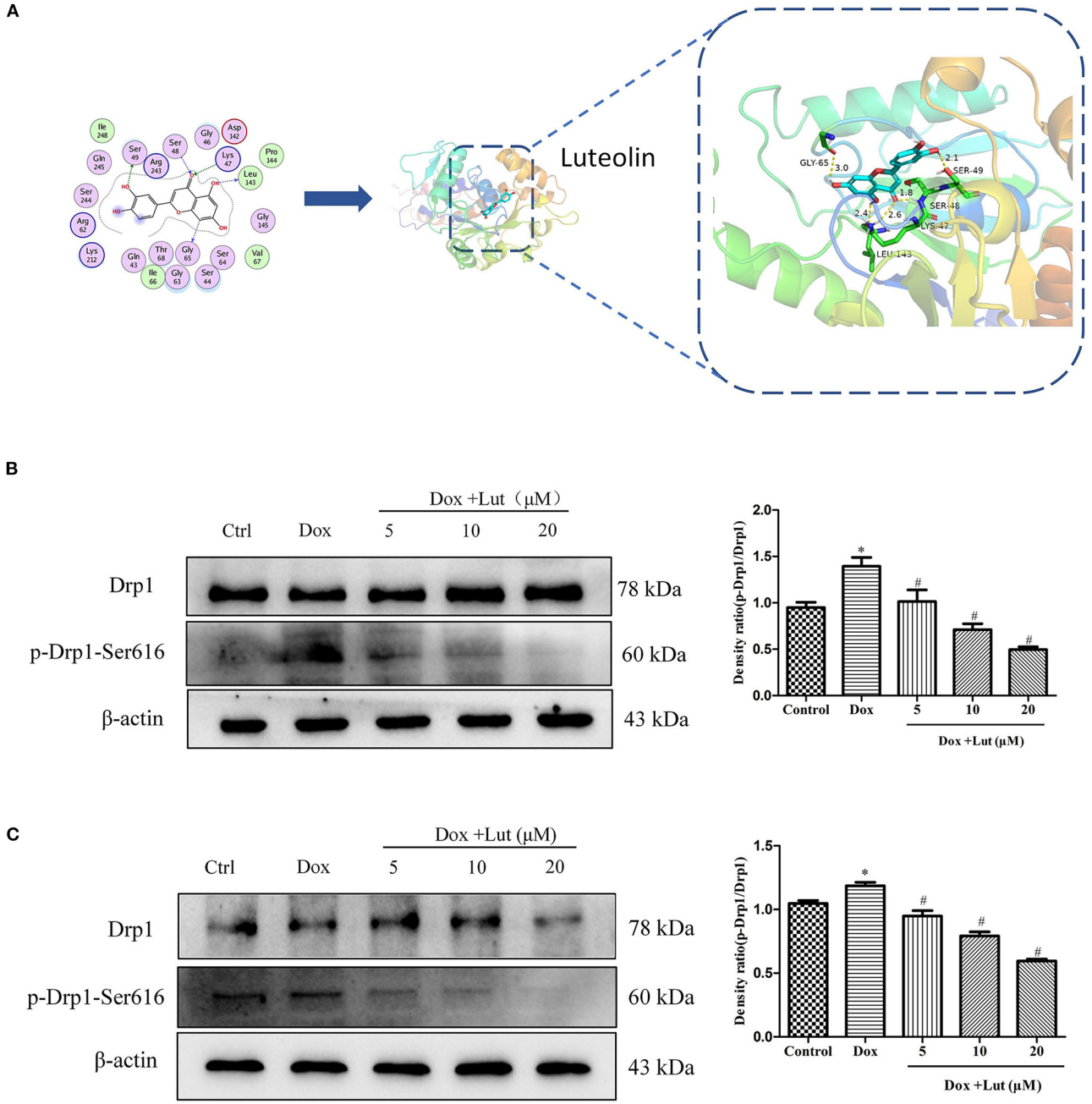

FIGURE 5 | Lut attenuated Dox-induced Drp-1 phosphorylation in H9c2 and AC16 cells. **(A)** Detailed molecular docking simulations. The blue circle on the left represents the binding site of the small-molecule compound, and the bar graph on the right describes the specific form of this interaction. Representative Western blot images of Drp-1 and p-Drp-1 in H9c2 **(B)** and AC16 **(C)** cells. Mean ± SD, $n = 3$ independent experiment. $^{*}P < 0.05$ compared with control group. $^{\#}P < 0.05$ compared with Dox group.

cleavage furrow; and molecular function (GO: MF), including kinase regulator activity, GTPase activator activity, tubulin binding, cytoskeletal protein binding, and microtubule binding (**Figures 7C–E**). Additionally, DEGs of AC16 and H9c2 cells significantly participated in cellular senescence, AMPK signaling pathway, viral carcinogenesis, and human T-cell leukemia virus 1 papillomavirus infection, suggesting that drug-induced cellular senescence may increase the virus susceptibility and carcinogenicity of cardiomyocytes (**Figure 7F**). We found that the DEGs not only markedly participated in Hippo/Wnt, AMPK/MAPK, and TGF-β signaling pathways and animal mitophagy process, but were also involved in transcriptional

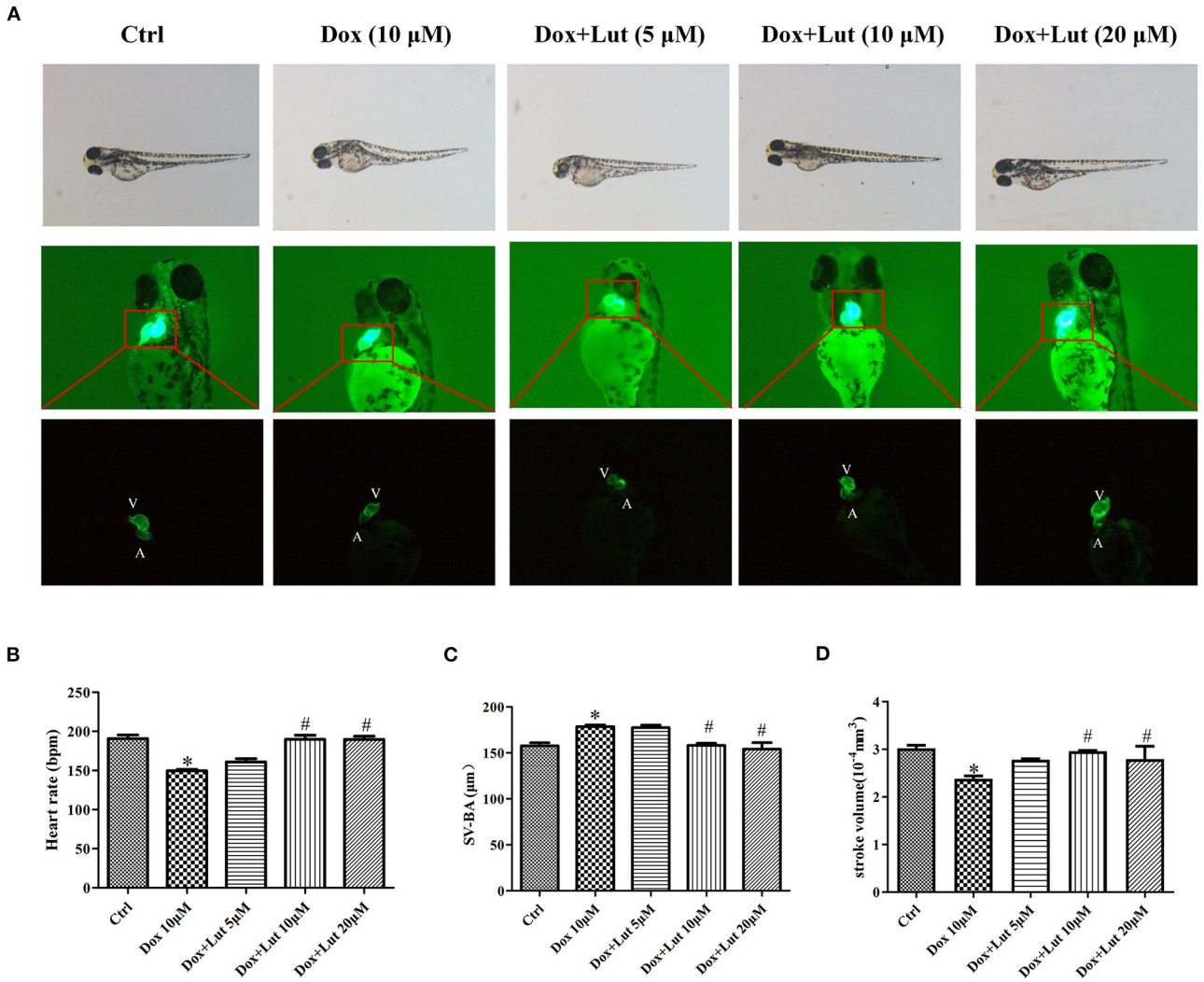

FIGURE 6 | Lut protected the loss of ventricular function in zebrafish. **(A)** Representative images of zebrafish heart after treatment with Dox in the presence or absence of Lut. A: atrium, V: ventricle. Zebrafish were co-treated with Dox and Lut. The changes in **(B)** heart rate and **(C)** SA–BA **(D)** stroke volume were measured. Mean ± SD, $n = 3$ independent experiment. $^{*}P < 0.05$ compared with control group. $^{\#}P < 0.05$ compared with Dox group.

misregulation and pathways in cancers, such as hepatocellular, breast, gastric, and thyroid cancer.

Lut Promotes the Antitumor Effect of Dox in 4T1 and MDA-MB-231 Cells

To further explore the effect of Lut on the antitumor efficacy of Dox, we explored the malignant biological behavior of different treatments in invasive TNBC 4T1 and MDA-MB-231 cell lines. As shown in **Figures 8A,B**, the cell viability was markedly decreased in the Lut-added group compared with the Dox-induced group in 4T1 and MDA-MB-231 cells ($P < 0.05$). Wound healing test showed significantly reduced wound width after 24 h of induction of Lut or Dox compared with the negative control group, while the combination of Lut and Dox remarkably decreased wound healing width compared with the single-drug treatment group ($P < 0.05$; **Figures 8C,D**). In addition, Lut significantly enhanced the antitumor efficacy of Dox by decreasing the colony formation and invasion ability of breast cancer cells ($P < 0.05$; **Figures 8E–H**). In general, Lut could not only significantly inhibit the malignant behavior of tumor cells, but also enhance the antitumor efficacy of Dox in 4T1 and MDA-MB-231 cells.

Lut Promotes Dox-Induced Cell Apoptosis via the Bax/Bcl-2/Caspase-3 Pathway in 4T1 and MDA-MB-231 Cells

Next, we explored the effect of Lut on the apoptosis of triple-negative breast cancer cells induced by Dox. Western blot indicated upregulated levels of Bax and Cleaved Caspase-3 in conjunction with downregulated Bcl-2 levels in Dox-treated

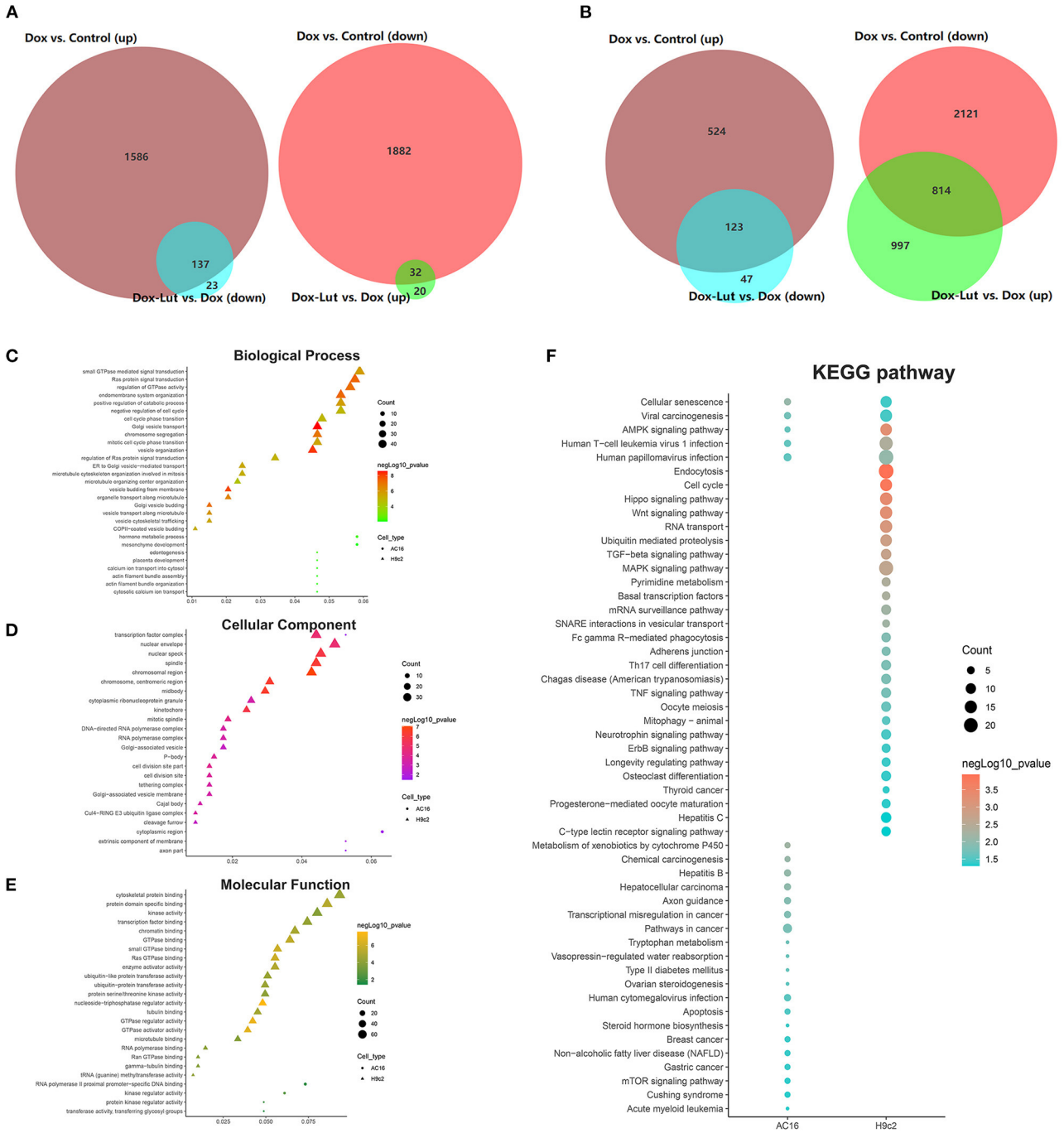

FIGURE 7 | GO and KEGG analysis of DEGs in the Dox–Lut group compared with Dox group. **(A)** Venn diagram. The intersection in the figure is the gene with the opposite differential expression, which is defined as the gene affected by Lut in AC16 and **(B)** H9c2 cells. **(C)** Biological processes, **(D)** cellular component, **(E)** molecular function, and **(F)** KEGG pathways involved in resveratrol-affected genes.

or Lut-treated 4T1 and MDA-MB-231 cells. Importantly, the regulation of cell apoptosis induced by Dox was significantly enhanced by additional Lut treatment ($P < 0.05$; **Figures 9A,B**). Taken together, Lut treatment could significantly enhance Dox-induced tumor cell apoptosis through the Bax/Bcl-2/Caspase-3 pathway in 4T1 and MDA-MB-231 cells.

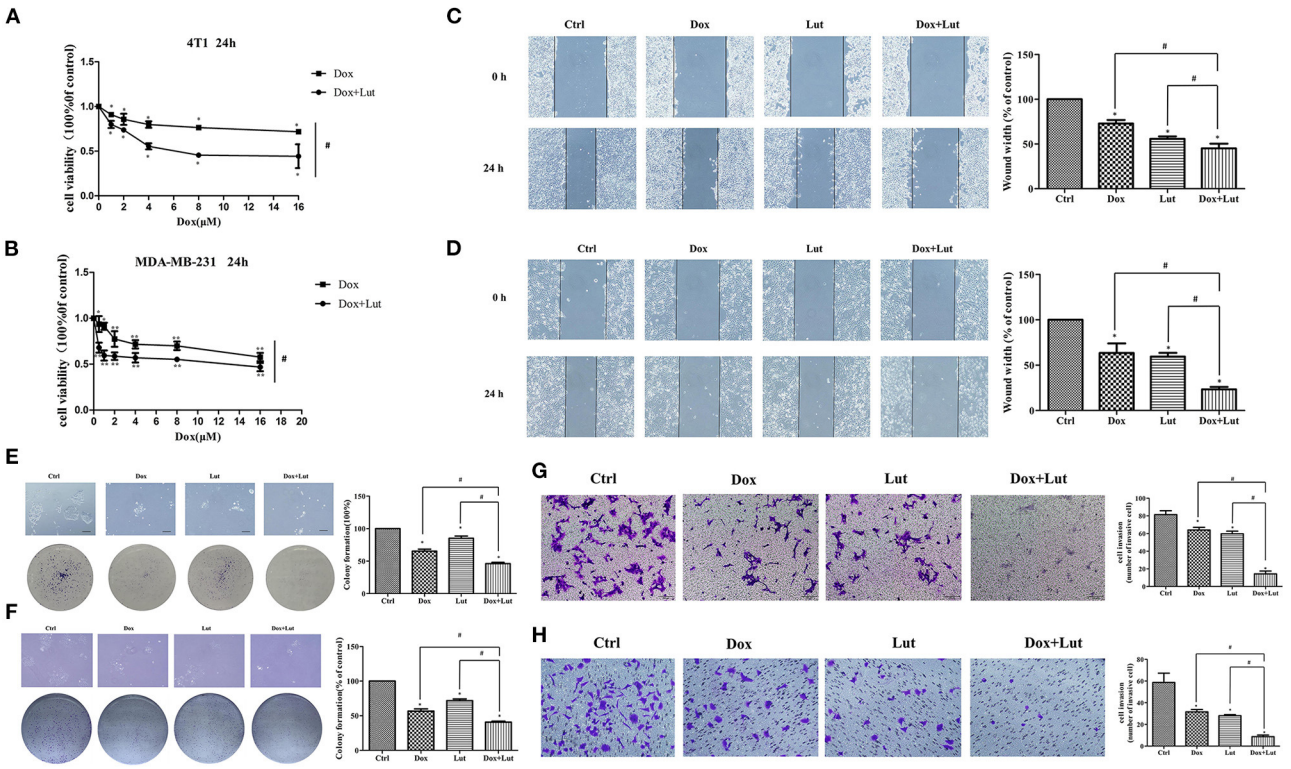

FIGURE 8 | Lut promotes the antitumor effect of Dox in 4T1 and MDA-MB-231 cells. **(A)** 4T1 and **(B)** MDA-MB-231 cells were treated with Dox or Dox added with Lut (40 μM) at concentrations of 0, 1, 2, 4, 8, or 16 μM for 24 h. MTT assays were performed, and cell viability was determined. Photographs and quantification of wounds, colony formation, and cell migration to **(C,E,G)** 4T1 and **(D,F,H)** MDA-MB-231 cells treated with Dox (2 μM) or Dox added with Lut (40 μM). Mean ± SD, n = 3 independent experiment. $^{*}P < 0.05$ compared with control group. $^{\#}P < 0.05$ compared with Dox group.

Lut Prevents the Cardiotoxicity and Promotes the Antitumor Effect Induced by Dox *in vivo*

A xenograft of 4T1 cells in 7-week-old BALB/c mice was established for *in vivo* exploration (**Figure 10A**). Echocardiographic examination showed that the Dox-treated group had an ∼20% decrease in LVEF and LVFS compared with the control group. Lut treatment significantly attenuated cardiac dysfunction in the Dox-treated mice, as indicated by the increased LVEF and LVFS ($P < 0.05$; **Figure 10B**). Additionally, Dox did not alter the cardiac structure, including the diastolic left ventricular internal dimension (LVIDd), diastolic left ventricular posterior wall (LVPWd), and diastolic interventricular septum (IVSd) (**Supplementary Figure 2**). As shown in **Figure 10C**, the tumor volume and weight were significantly decreased in the Dox-induced group compared with the control group and was even further reduced in the Dox–Lut group ($P < 0.05$; **Figure 10C**). Notably, Lut also significantly enhanced the Dox-induced reduction of the number of lung metastatic nodules in xenograft models ($P < 0.05$; **Figure 10D**). Taken together, Lut could significantly promote the antitumor efficiency induced by Dox in a xenograft of highly aggressive 4T1 cells.

DISCUSSION

Breast cancer is one of the most prevalent malignancies and associated with significant morbidity among females worldwide (29). Among the treatments of primary breast cancer, an anthracycline-based regimen is the standard of care (29, 30). According to the latest National Comprehensive Cancer Network guidelines, 5-fluorouracil, epirubicin, and cyclophosphamide adjuvant chemotherapy regimen followed by paclitaxel or paclitaxel combined with anti-human epidermal growth factor-2 trastuzumab is the recommended regimen for breast cancer (31). Anthracyclines represented by Dox are the first-line chemotherapy for breast cancer, and they play an irreplaceable role in current clinical treatment of breast cancer. Unfortunately, the adverse effects of Dox, such as immunosuppression, hepatotoxicity, and especially dose-dependent cardiotoxicity, limit its efficacy and application because treatment-related cardiotoxic adverse events have become one of the common causes of breast cancer mortality (32, 33). Current prevention and treatment cannot effectively solve the problem of Dox-induced cardiotoxicity (34, 35). Therefore, improved approaches to reduce Dox side effects and enhance Dox efficiency need to be developed.

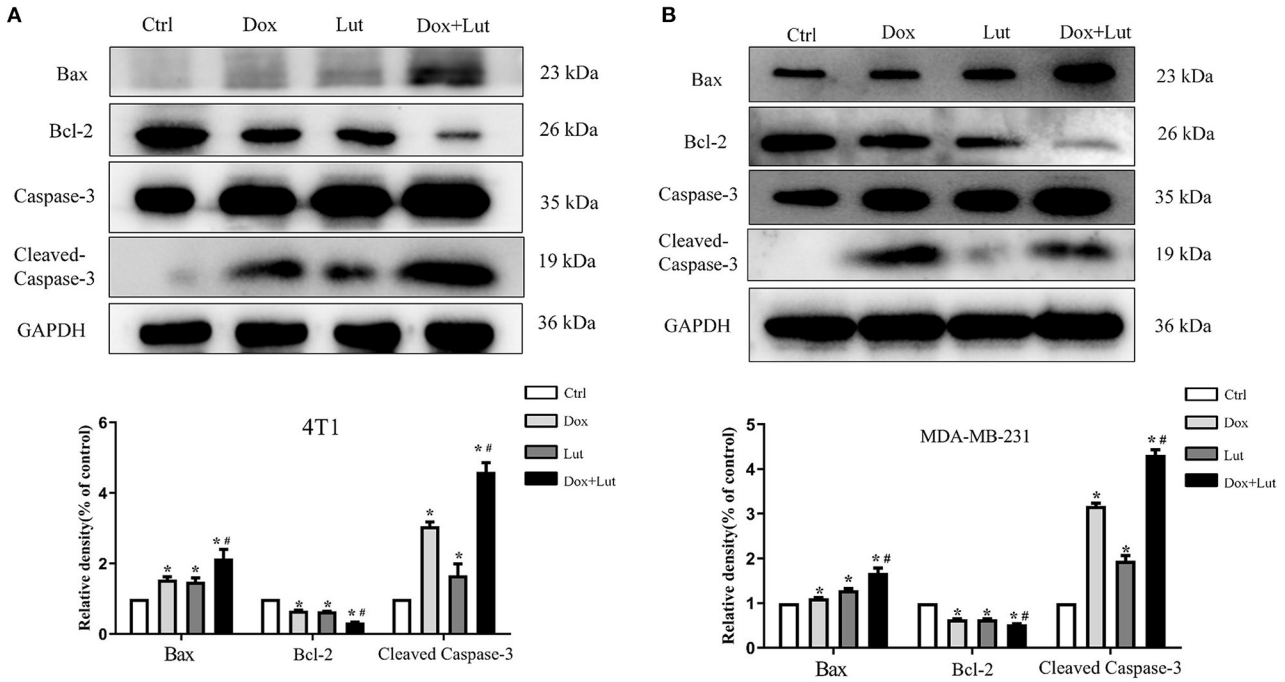

FIGURE 9 | Lut promotes Dox-induced cell apoptosis *via* the Bax/Bcl-2/Caspase-3 pathway in TNBC cancer. Western blot images of Bax, Bcl-2, and Cleaved Caspase-3 expression in 4T1 **(A)** and MDA-MB-231 **(B)** cells after treatment with Dox (2 μM) or Dox added with Lut (40 μM) at the indicated concentrations for 24 h. Quantification of protein expression is shown below the Western blots. $^{*}P < 0.05$ compared with control group. $^{\#}P < 0.05$ compared with Dox group.

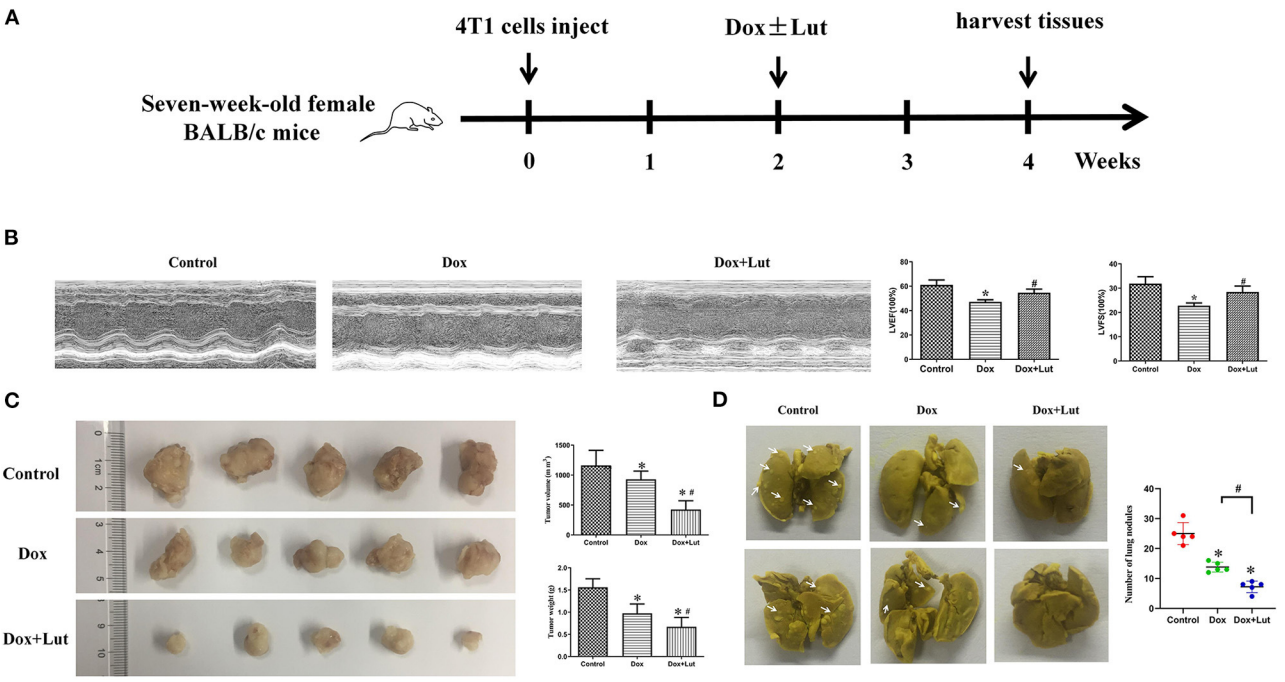

FIGURE 10 | Lut prevents the cardiotoxicity and promotes the antitumor effect induced by Dox *in vivo*. **(A)** Diagram showing the scheme for tumor implantation and Lut treatment. **(B)** Echocardiographic assay was used to determine the attenuated left ventricular dysfunction of Lut on Dox-induced cardiac dysfunction in mice. **(C)** Image of tumors from different groups. The weight and size of the tumor was measured. **(D)** Typical lung nodules in mice from different groups. $^{*}P < 0.05$ compared with control group. $^{\#}P < 0.05$ compared with Dox group.

TCM becoming increasingly important in cancer treatment and modern cardiotoxicity protective pharmacology. The identification of cardiotoxic protective drugs with unique pharmacological effects from TCM has become a new direction (36). For example, Zheng et al. found that the TCM Bu-Shen-Jian-Pi-Fang could inhibit tumor proliferation by enhancing GLUT-1 related glycolysis and may alter the immune-rejection microenvironment in renal cell carcinoma patients (37). Ginsenoside Re functions as an antioxidant, protecting cardiomyocytes from oxidant injury induced by exogenous and endogenous oxidants, and protects against apoptotic cell death (38, 39). Notably, previous attempts to explore the cancer prevention and therapeutic potential of Lut have systematically indicated its potential as an anticancer agent for various cancers (40). Lut can attenuate antitumor activity and drug resistance via reducing Bcl-2 expression in cancer cells (41). Interestingly, a previous study demonstrated the protective features of Lut against Dox-induced cardiotoxicity, possibly related to its ability of improving Drp1-regulated mitochondrial morphology alteration (42). However, it emphasized on TFEB-mediated mitochondrial regulation and the association between Drp-1 and mTOR, thus ignoring the positive effect of Lut in inhibiting Dox-induced cardiotoxicity in cardiomyocytes and tumor cells.

This study showed that Lut, the core component of *Platycodon grandiflorum*, markedly reduced the level of apoptosis and inhibited the activation of the Bax/Bcl-2/Caspase-3 signaling pathway of cardiomyocytes induced by Dox. Moreover, cytoskeleton damage ruptures cardiomyocytes in Dox-induced cardiotoxicity (43). In this work, Lut protected the cardiomyocyte cytoskeleton damage caused by Dox and maintained the integrity of the cardiomyocyte cytoskeleton. Therefore, cardioprotection from the perspective of protecting the cytoskeleton may be an effective target of Lut for the treatment of Dox-induced cardiotoxicity.

Cardiac autophagic processes lead to ROS overproduction and $\Delta\psi m$ dissociation, contributing to mitochondria-mediated apoptosis and death (44, 45). Our present work confirmed that Lut effectively reduced the level of cardiomyocyte oxidative stress and mitochondrial autophagy and inhibited mitochondrial division and the recruitment of Drp-1 phosphorylation. Subsequently, we performed transcriptome analysis to further explore the protective role of Lut in Dox-induced cardiotoxicity. Consistent with previous research (46), our findings indicated the role of Lut in the regulation of mitochondrial morphology, such as Ras protein signal transduction, microtubule cytoskeleton organization, cytoskeletal protein binding, and microtubule binding of molecular function, in GO enrichment analysis. Moreover, we found that the DEGs not only markedly participated in the Hippo/Wnt, AMPK/MAPK, and TGF-β signaling pathways and animal mitophagy process, but were also involved in apoptosis, transcriptional misregulation, and pathways in cancers, such as hepatocellular, breast, gastric, and thyroid cancer. In light of the findings, we carried out follow-up studies on breast cancer cells (4T1 and MDA-MB-231). Notably, Lut exerted a protective effect on Dox-induced cardiotoxicity, improved cardiac function parameters, and enhanced the anticancer therapeutic effects of Dox *in vivo*. Interestingly, combined treatment of Lut and Dox alleviated cardiomyocyte apoptosis but enhanced the apoptosis of breast cancer cells, which were in accordance with previous pharmacokinetics studies highlighting that *Platycodon grandiflorum* combined with Dox can increase the concentration of Dox in the lung and tumor and decrease the concentration of Dox in the heart of breast cancer mice (21). Doubtlessly, the comprehensive findings of Lut and Dox combination in cardiomyocytes and breast cancer cells facilitate its clinical application.

The innovation of this research lies in the mutual verification of *in vivo* and *in vitro* experiments. For the first time, we studied the protective effect of Lut on Dox cardiotoxicity on the basis of a transgenic zebrafish animal model. Second, this study first explored the effect of Lut, the active ingredient of *Platycodon grandiflorum*, on the mitochondrial fusion–division process of cardiomyocytes and the role in the Drp1–Caspase apoptosis signaling pathway. Third, on the basis of transcriptomic sequencing, the mechanism of Lut inhibition of Dox cardiotoxicity was validated in cardiomyocytes and breast cancer cells, which shed light on increasing clinical significance to novel treatment strategies.

Despite the strengths of this study, a number of experimental limitations existed in this study. First and foremost, our study was a cell lines-based study lacking the Dox-induced neonatal rat left ventricle myocyte cardiotoxicity model. Lut retards Dox cardiotoxicity in-depth work is needed in neonatal rat left ventricle myocyte. In addition, the regulation of Lut on Drp-1 phosphorylation and potential binding site remains to be elucidated. Meanwhile, the molecular mechanism of Drp1-dependent mitochondrial autophagy remains unclear. Moreover, the opposite mechanism of Lut-induced apoptosis has not been fully elucidated in cardiomyocytes and tumor cells, more in-depth work is needed for the precise mechanism.

CONCLUSION

The protective effect of Lut against Dox-induced cardiac dysfunction is associated with alleviating Drp1-mediated mitochondrial dysfunction. This study first revealed that Lut could potentiate the anticancer effects of Dox in breast tumor cells via the Bax/Bcl-2/Caspase-3 pathway.

DATA AVAILABILITY STATEMENT

The datasets presented in this study can be found in online repositories. The names of the repository/repositories

and accession number(s) can be found below: NCBI; PRJNA763722, PRJNA763517.

ETHICS STATEMENT

The animal study was reviewed and approved by Shanghai University of Traditional Chinese Medicine.

AUTHOR CONTRIBUTIONS

YS, FL, MS, and CS conducted the experiments. YS analyzed the data and wrote the manuscript. WH, CW, YX, SZ, HG, JY, and ZZ designed the study and revised the manuscript. DG, YQ, and XH supplied technical support. SL provided all of the reagent. All the authors edited and commented on the manuscript.

FUNDING

This study was supported by grants from: National Natural Science Foundation of China (No. 81603629, 81573973, and 81774308).

SUPPLEMENTARY MATERIAL

The Supplementary Material for this article can be found online at: https://www.frontiersin.org/articles/10.3389/fcvm.2021.750186/full#supplementary-material

Supplementary Figure 1 | (A,B) Representative TUNEL staining depicting H9c2 and AC16 cell apoptosis after Dox and Lut treatment (200×). White arrows show positive cells.

Supplementary Figure 2 | Echocardiographic assay was used to determine the attenuated cardiac structure of Lut on Dox-induced cardiac dysfunction in mice.

REFERENCES

1. Li L, Li J, Wang Q, Zhao X, Yang D, Niu L, et al. Shenmai injection protects against doxorubicin-induced cardiotoxicity via maintaining mitochondrial homeostasis. *Front Pharmacol.* (2020) 11:815. doi: 10.3389/fphar.2020.00815
2. De Iuliis F, Salerno G, Corvino R, D'Aniello D, Cefalì K, Taglieri L, et al. Anthracycline-free neoadjuvant chemotherapy ensures higher rates of pathologic complete response in breast cancer. *Clin Breast Cancer.* (2017) 17:34–40. doi: 10.1016/j.clbc.2016.06.010
3. Tung N, Arun B, Hacker MR, Hofstatter E, Toppmeyer DL, Isakoff SJ, et al. TBCRC 031: randomized phase ii study of neoadjuvant cisplatin versus doxorubicin-cyclophosphamide in germline BRCA carriers with HER2-negative breast cancer (the INFORM trial). *J Clin Oncol.* (2020) 38:1539–48. doi: 10.1200/JCO.19.03292
4. Pfisterer J, Shannon CM, Baumann K, Rau J, Harter P, Joly F, et al. Bevacizumab and platinum-based combinations for recurrent ovarian cancer: a randomised, open-label, phase 3 trial. *Lancet Oncol.* (2020) 21:699–709. doi: 10.1016/S1470-2045(20)30142-X
5. Wenningmann N, Knapp M, Ande A, Vaidya TR, Ait-Oudhia S. Insights into doxorubicin-induced cardiotoxicity: molecular mechanisms, preventive strategies, and early monitoring. *Mol Pharmacol.* (2019) 96:219–32. doi: 10.1124/mol.119.115725
6. Osataphan N, Phrommintikul A, Chattipakorn SC, Chattipakorn N. Effects of doxorubicin-induced cardiotoxicity on cardiac mitochondrial dynamics and mitochondrial function: insights for future interventions. *J Cell Mol Med.* (2020) 24:6534–57. doi: 10.1111/jcmm.15305
7. Burridge PW, Li YF, Matsa E, Wu H, Ong SG, Sharma A, et al. Human induced pluripotent stem cell-derived cardiomyocytes recapitulate the predilection of breast cancer patients to doxorubicin-induced cardiotoxicity. *Nat Med.* (2016) 22:547–6. doi: 10.1038/nm.4087
8. Xiao Y, Li J, Qiu L, Jiang C, Huang Y, Liu J, et al. Dexmedetomidine protects human cardiomyocytes against ischemia-reperfusion injury through alpha2-adrenergic receptor/AMPK-dependent autophagy. *Front Pharmacol.* (2021) 12:615424. doi: 10.3389/fphar.2021.615424
9. Wang X, Sun Q, Jiang Q, Jiang Y, Zhang Y, Cao J, et al. Cryptotanshinone ameliorates doxorubicin-induced cardiotoxicity by targeting Akt-GSK-3beta-mPTP pathway *in vitro*. *Molecules.* (2021) 26:1460. doi: 10.3390/molecules26051460
10. Caso S, Maric D, Arambasic M, Cotecchia S, Diviani D. AKAP-Lbc mediates protection against doxorubicin-induced cardiomyocyte toxicity. *Biochim Biophys Acta Mol Cell Res.* (2017) 1864:2336–46. doi: 10.1016/j.bbamcr.2017.09.007
11. Yu X, Ruan Y, Huang X, Dou L, Lan M, Cui J. Dexrazoxane ameliorates doxorubicin-induced cardiotoxicity by inhibiting both apoptosis and necroptosis in cardiomyocytes. *Biochem Biophys Res Commun.* (2020) 523:140–6. doi: 10.1016/j.bbrc.2019.12.027
12. Van Tine BA, Hirbe AC, Oppelt P, Frith AE, Rathore R, Mitchell JD, et al. Interim analysis of the phase II study: noninferiority study of doxorubicin with upfront dexrazoxane plus olaratumab for advanced or metastatic soft-tissue sarcoma. *Clin Cancer Res.* (2021) 27:3854–60. doi: 10.1158/1078-0432.CCR-20-4621
13. Henidi HA, Al-Abbasi FA, El-Moselhy MA, El-Bassossy HM, Al-Abd AM, et al. Despite blocking doxorubicin-induced vascular damage, quercetin ameliorates its antibreast cancer activity. *Oxid Med Cell Longev.* (2020) 20:1–14. doi: 10.1155/2020/8157640
14. Hosseini A, Sahebkar A. Reversal of doxorubicin-induced cardiotoxicity by using phytotherapy: a review. *J Pharmacopuncture.* (2017) 20:243–56. doi: 10.3831/KPI.2017.20.030
15. Ma Y, Yang L, Ma J, Lu L, Wang X, Ren J, et al. Rutin attenuates doxorubicin-induced cardiotoxicity via regulating autophagy and apoptosis. *Biochim Biophys Acta Mol Basis Dis.* (2017) 1863:1904–11. doi: 10.1016/j.bbadis.2016.12.021
16. Lin Y, Shi R, Wang X, Shen HM. Luteolin, a flavonoid with potential for cancer prevention and therapy. *Curr Cancer Drug Targets.* (2008) 8:634–46. doi: 10.2174/156800908786241050
17. Seelinger G, Merfort I, Schempp CM. Anti-oxidant, anti-inflammatory and anti-allergic activities of luteolin. *Planta Med.* (2008) 74:1667–77. doi: 10.1055/s-0028-1088314
18. Harborne JB, Williams CA. Advances in flavonoid research since 1992. *Phytochemistry.* (2000) 55:481–504. doi: 10.1016/S0031-9422(00)00235-1
19. Wang L, Zhang X, Chan JY, Shan L, Cui G, Cui Q, et al. A novel Danshensu derivative prevents cardiac dysfunction and improves the chemotherapeutic efficacy of doxorubicin in breast cancer cells. *J Cell Biochem.* (2016) 117:94–105. doi: 10.1002/jcb.25253
20. Hao W, Shi Y, Qin Y, Sun C, Chen L, Wu C, et al. *Platycodon grandiflorum* protects against anthracycline-induced cardiotoxicity in early breast cancer patients. *Integr Cancer Ther.* (2020) 19:153473542094501. doi: 10.1177/1534735420945017
21. Man S, Youyang S, Sheng L, Guofeng W, Xianghui H, Chenping S, et al. Pharmacokinetics of Platycodonis Radix combined with adriamycin in treating mice with lung metastasis of breast cancer. *Acad J Shanghai Univ Trad Chin Med.* (2019) 33:54–60. doi: 10.16306/j.1008-861x.2019.05.011
22. Lin LC, Pai YF, Tsai TH. Isolation of luteolin and luteolin-7-O-glucoside from Dendranthema morifolium Ramat Tzvel and their pharmacokinetics in rats. *J Agric Food Chem.* (2015) 63:7700–6. doi: 10.1021/jf505848z
23. Yang JT, Qian LB, Zhang FJ, Wang J, Ai H, Tang LH, et al. Cardioprotective effects of luteolin during ischemia-reperfusion injury in rats. *Circ J.* (2011) 75:443–50. doi: 10.1253/circj.cj-10-0381
24. He D, Ma X, Chen Y, Cai Y, Ru X, Bruce IC, et al. Luteolin inhibits pyrogallol-induced apoptosis through the extracellular signal-regulated kinase signaling pathway. *Febs J.* (2012) 279:1834–43. doi: 10.1111/j.1742-4658.2012.08558.x

25. Meng L, Lin H, Zhang J, Lin N, Sun Z, Gao F, et al. Doxorubicin induces cardiomyocyte pyroptosis via the TINCR-mediated posttranscriptional stabilization of NLR family pyrin domain containing 3. *J Mol Cell Cardiol.* (2019) 136:15–26. doi: 10.1016/j.yjmcc.2019.08.009
26. Abdullah CS, Alam S, Aishwarya R, Miriyala S, Bhuiyan MAN, Panchatcharam M, et al. Doxorubicin-induced cardiomyopathy associated with inhibition of autophagic degradation process and defects in mitochondrial respiration. *Sci Rep.* (2019) 9:2002. doi: 10.1038/s41598-018-37862-3
27. Xia Y, Chen Z, Chen A, Fu M, Dong Z, Hu K, et al. LCZ696 improves cardiac function via alleviating Drp1-mediated mitochondrial dysfunction in mice with doxorubicin-induced dilated cardiomyopathy. *J Mol Cell Cardiol.* (2017) 108:138–48. doi: 10.1016/j.yjmcc.2017.06.003
28. Zhou ZY, Zhao WR, Xiao Y, Zhang J, Tang JY, Lee SM. Mechanism study of the protective effects of sodium tanshinone IIA sulfonate against atorvastatin-induced cerebral hemorrhage in zebrafish: transcriptome analysis. *Front Pharmacol.* (2020) 11:551745. doi: 10.3389/fphar.2020.551745
29. Turner N, Biganzoli L, Di Leo A. Continued value of adjuvant anthracyclines as treatment for early breast cancer. *Lancet Oncol.* (2015) 16:e362–9. doi: 10.1016/S1470-2045(15)00079-0
30. Zagar TM, Cardinale DM, Marks LB. Breast cancer therapy-associated cardiovascular disease. *Nat Rev Clin Oncol.* (2016) 13:172–84. doi: 10.1038/nrclinonc.2015.171
31. Gradishar WJ, Anderson BO, Abraham J, Aft R, Agnese D, Allison KH, et al. Breast cancer, version 3.2020, NCCN clinical practice guidelines in oncology. *J Natl Compr Canc Netw.* (2020) 18:452–78. doi: 10.6004/jnccn.2020.0016
32. Shafei A, El-Bakly W, Sobhy A, Wagdy O, Reda A, Aboelenin O, et al. A review on the efficacy and toxicity of different doxorubicin nanoparticles for targeted therapy in metastatic breast cancer. *Biomed Pharmacother.* (2017) 95:1209–18. doi: 10.1016/j.biopha.2017.09.059
33. Yu L, Shi Q, Jin Y, Liu Z, Li J, Sun W. Blockage of AMPK-ULK1 pathway mediated autophagy promotes cell apoptosis to increase doxorubicin sensitivity in breast cancer (BC) cells: an *in vitro* study. *BMC Cancer.* (2021) 21:195. doi: 10.1186/s12885-021-07901-w
34. Denard B, Jiang S, Peng Y, Ye J. CREB3L1 as a potential biomarker predicting response of triple negative breast cancer to doxorubicin-based chemotherapy. *BMC Cancer.* (2018) 18:813. doi: 10.1186/s12885-018-4724-8
35. Wei T, Xiaojun X, Peilong C. Magnoflorine improves sensitivity to doxorubicin (DOX) of breast cancer cells via inducing apoptosis and autophagy through AKT/mTOR and p38 signaling pathways. *Biomed Pharmacother.* (2020) 121:109139. doi: 10.1016/j.biopha.2019.109139
36. Yang X, Liu N, Li X, Yang Y, Wang X, Li L, et al. A review on the effect of traditional chinese medicine against anthracycline-induced cardiac toxicity. *Front Pharmacol.* (2018) 9:444. doi: 10.3389/fphar.2018.00444
37. Zheng J, Xu W, Liu W, Tang H, Lu J, Yu K, et al. Traditional Chinese medicine Bu-Shen-Jian-Pi-Fang attenuates glycolysis and immune escape in clear cell renal cell carcinoma: results based on network pharmacology. *Biosci Rep.* (2021) 41:BSR20204421. doi: 10.1042/BSR20204421
38. Chen J, Li M, Qu D, Sun Y. Neuroprotective effects of red Ginseng saponins in scopolamine-treated rats and activity screening based on pharmacokinetics. *Molecules.* (2019) 24:2136. doi: 10.3390/molecules24112136
39. Zhou TT, Zu G, Wang X, Zhang XG, Li S, Liang ZH, et al. Immunomodulatory and neuroprotective effects of ginsenoside Rg1 in the MPTP(1-methyl-4-phenyl-1,2,3,6-tetrahydropyridine) -induced mouse model of Parkinson's disease. *Int Immunopharmacol.* (2015) 29:334–43. doi: 10.1016/j.intimp.2015.10.032
40. Wang H, Luo Y, Qiao T, Wu Z, Huang Z. Luteolin sensitizes the antitumor effect of cisplatin in drug-resistant ovarian cancer via induction of apoptosis and inhibition of cell migration and invasion. *J Ovarian Res.* (2018) 11:93. doi: 10.1186/s13048-018-0468-y
41. Zheng CH, Zhang M, Chen H, Wang CQ, Zhang MM, Jiang JH, et al. Luteolin from Flos Chrysanthemi and its derivatives: new small molecule Bcl-2 protein inhibitors. *Bioorg Med Chem Lett.* (2014) 24:4672–7. doi: 10.1016/j.bmcl.2014.08.034
42. Xu H, Yu W, Sun S, Li C, Zhang Y, Ren J. Luteolin attenuates doxorubicin-induced cardiotoxicity through promoting mitochondrial autophagy. *Front Physiol.* (2020) 11:113. doi: 10.3389/fphys.2020.00113
43. Bajpai P, Darra A, Agrawal A. Agrawal, microbe-mitochondrion crosstalk and health: an emerging paradigm. *Mitochondrion.* (2018) 39:20–5. doi: 10.1016/j.mito.2017.08.008
44. Bartlett JJ, Trivedi PC, Pulinilkunnil T. Autophagic dysregulation in doxorubicin cardiomyopathy. *J Mol Cell Cardiol.* (2017) 104:1–8. doi: 10.1016/j.yjmcc.2017.01.007
45. Bartlett JJ, Trivedi PC, Yeung P, Kienesberger PC, Pulinilkunnil T. Doxorubicin impairs cardiomyocyte viability by suppressing transcription factor EB expression and disrupting autophagy. *Biochem J.* (2016) 473:3769–89. doi: 10.1042/BCJ20160385
46. Wei B, Lin Q, Ji YG, Zhao YC, Ding LN, Zhou WJ, et al. Luteolin ameliorates rat myocardial ischaemia-reperfusion injury through activation of peroxiredoxin II. *Br J Pharmacol.* (2018) 175:3315–32. doi: 10.1111/bph.14367

Conflict of Interest: The authors declare that the research was conducted in the absence of any commercial or financial relationships that could be construed as a potential conflict of interest.

Publisher's Note: All claims expressed in this article are solely those of the authors and do not necessarily represent those of their affiliated organizations, or those of the publisher, the editors and the reviewers. Any product that may be evaluated in this article, or claim that may be made by its manufacturer, is not guaranteed or endorsed by the publisher.

frontiers in Cardiovascular Medicine

ORIGINAL RESEARCH
published: 08 November 2021
doi: 10.3389/fcvm.2021.763469

The Role of METTL3-Mediated N6-Methyladenosine (m6A) of JPH2 mRNA in Cyclophosphamide-Induced Cardiotoxicity

Min Zhu[1,2†], *Yangong Liu*[1†], *Yuanxiu Song*[1], *Shiqin Zhang*[1], *Chengwen Hang*[1], *Fujian Wu*[3], *Xianjuan Lin*[1], *Zenghui Huang*[4], *Feng Lan*[2,3] *and Ming Xu*[1,5*]

[1] Department of Cardiology and Institute of Vascular Medicine, NHC Key Laboratory of Cardiovascular Molecular Biology and Regulatory Peptides, Key Laboratory of Molecular Cardiovascular Science, Ministry of Education, Beijing Key Laboratory of Cardiovascular Receptors Research, Peking University Third Hospital, Beijing, China, [2] State Key Laboratory of Cardiovascular Disease, National Center for Cardiovascular Diseases, Fuwai Hospital, Key Laboratory of Application of Pluripotent Stem Cells in Heart Regeneration, Chinese Academy of Medical Sciences and Peking Union Medical College, Beijing, China, [3] Beijing Lab for Cardiovascular Precision Medicine, Anzhen Hospital, Capital Medical University, Beijing, China, [4] Key Laboratory of Genetic Network Biology, Institute of Genetics and Developmental Biology, Chinese Academy of Sciences (CAS), Beijing, China, [5] State Key Laboratory of Natural and Biomimetic Drugs, Peking University, Beijing, China

OPEN ACCESS

Edited by:
Feng Cao,
People's Liberation Army General Hospital, China

Reviewed by:
Shijun Hu,
Soochow University, China
Benzhi Cai,
The Second Affiliated Hospital of Harbin Medical University, China

****Correspondence:***
Ming Xu
xuminghi@bjmu.edu.cn

† These authors have contributed equally to this work

Specialty section:
This article was submitted to Cardio-Oncology, a section of the journal Frontiers in Cardiovascular Medicine

Received: *24 August 2021*
Accepted: *07 October 2021*
Published: *08 November 2021*

Citation:
Zhu M, Liu Y, Song Y, Zhang S, Hang C, Wu F, Lin X, Huang Z, Lan F and Xu M (2021) The Role of METTL3-Mediated N6-Methyladenosine (m6A) of JPH2 mRNA in Cyclophosphamide-Induced Cardiotoxicity. Front. Cardiovasc. Med. 8:763469. doi: 10.3389/fcvm.2021.763469

Cyclophosphamide (CYP)-induced cardiotoxicity is a common side effect of cancer treatment. Although it has received significant attention, the related mechanisms of CYP-induced cardiotoxicity remain largely unknown. In this study, we used cell and animal models to investigate the effect of CYP on cardiomyocytes. Our data demonstrated that CYP-induced a prolonged cardiac QT interval and electromechanical coupling time courses accompanied by JPH2 downregulation. Moreover, N6-methyladenosine (m6A) methylation sequencing and RNA sequencing suggested that CYP induced cardiotoxicity by dysregulating calcium signaling. Importantly, our results demonstrated that CYP induced an increase in the m6A level of JPH2 mRNA by upregulating methyltransferases METTL3, leading to the reduction of JPH2 expression levels, as well as increased field potential duration and action potential duration in cardiomyocytes. Our results revealed a novel mechanism for m6A methylation-dependent regulation of JPH2, which provides new strategies for the treatment and prevention of CYP-induced cardiotoxicity.

Keywords: cyclophosphamide, cardiotoxicity, JPH2, m6A methylation, METTL3, cardiomyocyte

INTRODUCTION

Although improved treatments have been effective in increasing the survival of patients with tumors, an increase in the number of side effects of cancer treatment have led to mortality (1, 2). Tumor therapy-induced cardiotoxicity as a common side effect has received increasing attention. Many countries and regions have issued relevant practice guidelines for cardiovascular toxicity induced by cancer treatments (3). Both conventional chemotherapies and targeted drug therapies reportedly induce cardiovascular toxicity events. One traditional antineoplastic agent, cyclophosphamide (CYP), is employed in the treatment of various cancers, including breast, lymphoid, and hematologic malignancies (4). Up to 28% of patients who received a high dose of CYP suffered from cardiac arrhythmias (3) and even heart failure (5). Further, CYP is widely used

in the treatment of other diseases, such as refractory neuromyelitis optica spectrum disorder (200 mg/kg) (6) and rapidly progressive systemic sclerosis (300 mg/kg) (7), all of reportedly cause severe cardiotoxicity. Even in the clinic, oral administration of a low dose (50 or 100 mg/day) for systemic sclerosis or lupus erythematosus for 1 week has caused cardiac electrical alteration (prolonged QT interval) in some patients. However, little is known about the mechanism underlying CYP-related cardiovascular toxicity. In particular, CYP has often been used in combination with other antineoplastic agents, including anthracyclines, docetaxel, and trastuzumab. This has led to difficulty in assessing the contribution of CYP in multidrug schemes (8).

CYP and other alkylating agents are the most common types of DNA damaging agents used in the treatment of various cancers. Alkylating agents exhibit pharmacological toxicity by adding methyl and other hydrocarbon groups to the DNA bases, resulting in base mutations, pair mismatches, and eventually fatal DNA cytotoxicity (9). The pharmacological mechanism is fatal to rapidly proliferating tumor cells. However, the cardiac cytotoxicity induced by alkylating agents is rarely discussed for non-proliferating cardiomyocytes. Because alkylating agents adduct DNA bases (A, T, G, and C) to induce DNA methylation (9), alkylating agents might affect RNA methylation. N6-adenosine methylation (m6A) of RNA transcripts is the most prevalent RNA modification (10). This modification regulates RNA stability (11), gene expression (12), mRNA alternative splicing (13), embryonic and stem cell differentiation (13–15), and various diseases including cancer (16) and cardiac dysfunctions (11, 17). Hence, we hypothesized that CYP induces cardiotoxicity through RNA m6A modification.

We treated rat neonatal cardiomyocytes (NRCMs), human embryonic stem cell-derived cardiomyocytes (hESCs-CMs), and a rat model with CYP to explore solutions for this problem. This was followed by combining action and field potential detections, RNA sequencing, and RNA m6A methylation analysis to explore the toxicity mechanism underlying CYP-induced cardiac electrical and mechanical alterations. Our results may provide drug targets and preventive measures for treating CYP-induced cardiotoxicity.

MATERIALS AND METHODS

Animals

All Sprague-Dawley (SD) rats in this study were purchased from Beijing Vital River Laboratory Animal Technology Company (Beijing, China). Twelve 8-week-old male SD rats with a mean weight of 273.7 ± 3.2 g were randomized into two groups: six rats were subjected to saline (Double Crane Pharmaceutical Co. Ltd, Wuhan, China) peritoneal injection (vehicle group), whereas six rats were intraperitoneally injected with CYP (Jiangsu Hengrui Medicine Co., Ltd. Lianyungang, China) at a dose of 100 mg/kg (CYP treatment group). Echocardiography (echo) and electrocardiography (ECG) were performed at different time points (0, 1, and 3 days).

In vivo ECG Recording

Continuous recordings of heart rate were obtained with a surface ECG. Rats were anesthetized with 3% isoflurane and were subsequently fixed on a wooden board. ECG recording was performed using the limb lead. Three electrodes on an ECG monitor were inserted into the subcutaneous tissues of the rats' left and right shoulders and the right hind leg. The signal was amplified and recorded on a personal computer using an ECG Processor (EP-2B, Softron Beijing Incorporated, China) and stored on a data acquisition program (SP2006, Softron Beijing Incorporated, China).

ECG and Electromechanical Coupling Time Measurement

ECG measurement was performed as described previously (18). ECG was performed using a Vevo 2,100 system (FUJIFILM VisualSonics, Canada), and the cardiac dimensions and functional parameters were measured. The tissue Doppler imaging (TDI) echo combined with ECG was used to measure the electromechanical coupling time at the lateral wall of the left ventricle as described previously (19).

Neonatal Rat Cardiac Myocytes Culture

NRCMs were isolated from newborn SD rats aged 1–2 days as described previously (20). These isolated NRCMs were grown in Dulbecco's modified Eagle's medium supplemented with 10% fetal bovine serum and 100 U/ml penicillin/streptomycin, and maintained at 37°C in 5% CO_2.

Cardiac Differentiation of Human Embryonic Stem Cells (hESC)

H9 human embryonic stem cells were purchased from the Beijing Cellapy Biological Technology Company (Cellapy, China). H9 cells were cultured and differentiated into cardiomyocytes following previously described procedures (21). In brief, H9 cells were cultured on 35-mm dishes (Corning, USA) with PSCeasy hESC culture medium (Cellapy, Beijing, China). Cells were cultured to reach ∼90% confluency and differentiated into ESC-CMs using a chemical method as described previously (22). Immunofluorescent staining with primary antibodies against TNNT2 (Santa Cruz, USA) and α-actinin (Abcam, UK) validated the purity of human cardiomyocytes.

Immunofluorescence

Cells were cultured on glass slides, washed with PBS three times, fixed in 4% paraformaldehyde for 5 min, and then permeabilized with PBS containing 0.5% Triton X-100 (Sigma, USA) for 10 min. After 1 h of blocking with 5% BSA (Amresco, USA), the slides were incubated with primary antibodies followed by incubation with secondary antibodies. After the slides were washed, they were studied with a confocal fluorescence imaging microscope (DMI 4000B, Leica, Germany). The primary and secondary antibodies and their appropriate dilutions are listed in **Supplementary Table 1**.

Microelectrode Array (MEA) Analysis

MEA recording in cardiomyocytes was performed as described previously (23). In brief, 2×10^4 cells were plated on CytoView MEA plates (Axion Biosystems, USA) pre-coated with 5% matrigel, followed by treatment with CYP at different concentrations (0 and 500 μmoL/L). The experimental data were acquired using a Maestro EDGE (Axion Biosystems, USA) according to the MEA operation manual.

RNA Extraction and Quantitative Real-Time PCR

Total RNA was extracted from NRCMs using the TRIzol reagent (Invitrogen) and subjected to reverse transcription (RT) and real-time PCR. The primers used are listed in **Supplementary Table 2**. RT was performed using a 2,720 Thermal Cycler (Applied Biosystems, USA). Real-time PCR was performed using a QuantStudio 3 apparatus (Applied Biosystems, USA).

Western Blot Analysis

Proteins were extracted from cells in RIPA lysis buffer (Solarbio, China) containing 1 mmol/L PMSF (Solarbio, China) and protease inhibitor cocktail (Bimake, China) for western blot analysis. In total, 50 μg of protein were subjected to SDS-PAGE, transferred to a PVDF membrane (Millipore, USA), and incubated with the primary antibodies. These primary antibodies and their appropriate dilutions are listed in **Supplementary Table 1**. The membrane was then incubated with HRP-conjugated goat anti-mouse IgG (1: 2000, ZSGB-BIO) or HRP-conjugated goat anti-rabbit IgG (1: 2000, ZSGB-BIO). GAPDH was used as a control. Protein levels were determined using the Immobilon® Western Chemiluminescent HRP substrate (Millipore, UK).

Cell Treatments

In the CYP treatment assays, 250, 500, and 750 μmol/L of CYP (Selleck, USA) were added to the cell complete culture medium for 2 or 4 days for NRCMs and for 2 or 5 days for hESCs-CMs. To impede the expression of METTL3 in cardiomyocytes, adenoviruses harboring the specific small interference RNA (siRNA) sequences of METTL3 were used individually to infect cardiomyocytes at an optimized MOI for 24 h, followed by treatment with 500 μmol/L CYP for an additional 24 h as the MEA assay. The siRNA and negative control (NC) sequences used are listed in **Supplementary Table 2**.

RNA m6A Dot Blot Assay

An RNA m6A dot blot assay was performed as previously described (24). In brief, 1.5 μg of total RNA was spotted onto a positively charged nylon-based membrane (GE Healthcare), blocked with 5% milk at room temperature for 2 h, and incubated with anti-m6A antibodies (1: 2000, Abcam) at 4 °C overnight and secondary antibodies (1: 3000, Abcam) at room temperature for 2 h. The same RNAs were spotted on the positively charged nylon-based membrane and stained with 0.02% methylene blue in 0.3M sodium acetate (pH 5.2), which ensured loading consistency among different samples.

Methylated RNA Immune Precipitation (MeRIP) Sequencing

High throughput m6A sequencing was performed with the support of Kangchen Biotech (Shanghai, China). Briefly, total RNA was extracted from NRCMs treated with 500 μmol/L CYP or DMSO (solvent control) for 48 h, followed by random fragmentation to 100–150 nucleotides using RNA fragmentation reagents. Fragmented RNA was subjected to m6A antibody immunoprecipitation following the Magna MeRIP m6A kit protocol (17-10499, Merk Millipore, USA) as described previously (25). An RNA library from immunoprecipitated RNA and input RNA was created on an Illumina HiSeq platform. Differential m6A peaks (fold change $\geq$1.5 and $P \leq 0.05$) between CYP and solvent controls were used for gene ontology (GO) enrichment and Kyoto Encyclopedia of Genes and Genomes (KEGG) analysis.

Ca^{2+} Imaging

Ca^{2+} imaging in cardiomyocytes was performed as described previously (21). In brief, hESCs-CMs inoculate with the green fluorescent calcium-modulated protein (GCaMP) calcium sensor (H9-GCaMP-CMs) were seeded onto confocal dishes. Confocal microscope (Leica, TCS5 SP5, Germany) was used for intracellular calcium imaging. Spontaneous Ca^{2+} transients were recorded at 37°C and 5% CO_2 according to the standard line-scan methods (26, 27). A total of 8,192 line scans were acquired for a duration of 8.192 s. The imaging results were analyzed using the Image J and Igor pro software.

Statistical Analysis

All statistical analyses were conducted using the SPSS 20.0 software (IBM Corp., USA) and Graphpad Prism software (version 8.0, GraphPad Software Inc., USA). The data are expressed as the mean ± standard error (SE). A Student's *t*-test detected the differences between groups. *P* values of ≤ 0.05 were considered as statistically significant.

RESULTS

CYP Increased the Field Potential Duration and Decreased the Contractile Amplitudes of Cardiomyocytes

To clarify the cellular significance of CYP in cardiomyocytes, we first performed the CCK-8 assay to examine the effects of CYP on the viability of cardiomyocytes. The result confirmed that CYP had no significant effect on NRCMs viability (**Supplementary Figure 1A**). However, we observed that the levels of atrial natriuretic factor (ANP) and brain natriuretic peptide (BNP) had increased after NRCMs were treated with 500 μmoL/L CYP for 48 h (**Supplementary Figures 1B,C**). These results suggested that CYP induced slight cardiotoxicity, but did not affect cell viability. CYP was closely associated with cardiac arrhythmias related to QT prolongation and the acute and chronic toxicity of chemotherapy (3). A prolonged QT interval is an important monitoring indicator for myocyte toxicity caused by anticancer agents according to the guidelines issued by

the International Conference on Harmonization of Technical Requirements for Registration of Pharmaceuticals for Human Use (28). Therefore, we seeded cardiomyocytes on multielectrode array (MEA) probes to evaluate the effect of CYP on myocardial electrophysiological properties. The time between depolarization and repolarization is the FPD (**Figure 1A**), which corresponds to the QT interval in an ECG. Compared with solvent control (CON), the FPD of NRCMs treated with CYP increased at 12, 24, and 48 h (**Figure 1B**). Meanwhile, the impedance of the CON cells showed no significant changes (**Figure 1C**). We observed that the impedance of NRCMs treated with CYP decreased with time (**Figure 1D**). These observations indicated that CYP negatively regulated the rhythm and contractility of cardiomyocytes.

Furthermore, we used human embryonic stem cell-derived cardiomyocytes (hESCs-CMs) (**Supplementary Figure 1D**) to evaluate the effect of CYP on cellular viability. Consistent with this finding in NRCMs, CYP had no significant effect on the viability of hESCs-CMs (**Supplementary Figure 1E**) but increased the RNA levels of ANP and BNP (**Supplementary Figures 1F,G**). Intriguingly, exposing hESCs-CMs to CYP (500 μmol/L) for 9 days resulted in a significant increase in FPD (**Figure 1E**) and reduction of contractile amplitudes (**Figure 1F**). These results supported QT interval prolongation and cardiac contractile dysfunction in rats.

CYP-Induced Cardiac Electrical and Mechanical Alterations and Decreased Cardiac Contractile Function in Rats

To further investigate the effect of CYP on cardiac functions, we used intraperitoneally injected CYP to treat the rats with CYP at a dose of 100 mg/kg, which was converted from the clinical dose for treatment of cancer. *In vivo* ECG recording data (**Figure 2A**) showed QT interval prolongation in rats after CYP-treatment for 1 day compared with that in rats administered saline (82.17 ± 1.70 vs. 65.17 ± 3.02 ms, $P < 0.001$; **Figure 2B**). Corrected QT interval (QTc) prolongation also showed the same variation as QT prolongation (199.83 ± 4.03 vs. 167.67 ± 6.83 ms, $P < 0.01$; **Figure 2C**). Further, the prolonged QT and QTc would restore to preadministration levels after CYP-treatment for 3 days (**Supplementary Figures 2A,B**). These results were consistent with the clinical side effects of CYP.

Electromechanical coupling disturbances were closely related to the long QT syndrome (29, 30). Hence, we further explored the effect of CYP on cardiac electrical and mechanical alterations. Four electromechanical coupling time courses (Qsb, Qst, Rsb, and Rst) were measured with TDI echo combined with ECG (**Figure 2D**). The measurement results showed that four electromechanical coupling time courses in CYP-treated rats were longer than those in saline controls (**Figures 2E–H**), particularly in terms of Qst and Rst courses ($P < 0.05$, **Figures 2E,G**). Moreover, ultrasound echocardiography (**Figure 2I**) showed that the fractional shortening percentage (FS%; **Figure 2J**) and left ventricular ejection fraction (LVEF; **Figure 2K**) were significantly lower in rats after CYP-treatment for 1 day. These results suggested that CYP induces cardiac electrical and mechanical alterations and decreases the excitation-contraction (E-C) coupling efficiency, leading to cardiac contractile dysfunction. Consistent with the results of QT and QTc, the prolonged electromechanical coupling time courses would restore after CYP treatment for 3 days (**Supplementary Figures 2C–F**) and the decreased FS and LVEF induced by CYP also showed a regression in CYP-treated rats after 3 days (**Supplementary Figures 2G,H**).

CYP-Induced the Decrease of JPH2 Expression in Cardiomyocytes

Previous studies demonstrated that junctophilin-2 (JPH2) that anchor the sarcoplasmic reticulum to T-tubules is the key regulator of Ca^{2+} influx between L-type Ca^{2+} channels (LCCs) and ryanodine receptors (RyRs) and E-C coupling in cardiomyocytes (31, 32), is reportedly associated with atrial fibrillation (33) and arrhythmias (34). Based on the phenomena observed in the above cell and animal experiments, we further investigated the effect of CYP on JPH2 expression in NRCMs and hESCs-CMs at different treatment time points. Notably, a dose-dependent reduction in JPH2 RNA and protein levels occurred in NRCMs treated with CYP for 2 or 4 days (**Figures 3A,B**). Similarly, different concentrations of CYP treatments decreased JPH2 both in RNA and protein levels at day 2 or 5 in hESCs-CMs (**Figures 3C,D**). Similarly, JPH2 downregulation occurred in heart tissues of rats treated with CYP (**Supplementary Figure 3**). These results suggested that CYP induced cardiac electrical and mechanical alterations and cardiac contractile dysfunction by decreasing the expression of JPH2.

To explore the underlying mechanisms involved in the suppression effects of CYP on JPH2 expression in cardiomyocytes, we further investigated the effect of CYP on miR-24 and miR-331 expressions, which were shown to inhibit the expression of JPH2 in our previous studies (31, 35). The real-time PCR analysis revealed that the expression of miR-24 and miR-331 did not significantly change in NRCMs after CYP treatment for 2 days (**Supplementary Figures 4A,B**). Therefore, it suggested that CYP decreased JPH2 expression through other transcriptional regulatory mechanisms.

CYP-Induced Substantial m6A Changes in Cardiomyocytes

N6-methyladenosine (m6A) is the most prevalent modification that widely exists in mRNAs, which is associated with post-transcriptional gene expression regulation (12), and mRNA stabiltity (36). We next investigated whether CYP plays an important role in m6A RNA methylation in NRCMs, considering that CYP can induce nucleic acid methylation. The m6A dot blot testing showed that total m6A levels significantly increased in NRCMs treated with CYP for 2 days (**Figures 4A,B**). Next, methylated RNA immune precipitation sequencing (MeRIP-seq) was performed to compare the global profiling of m6A

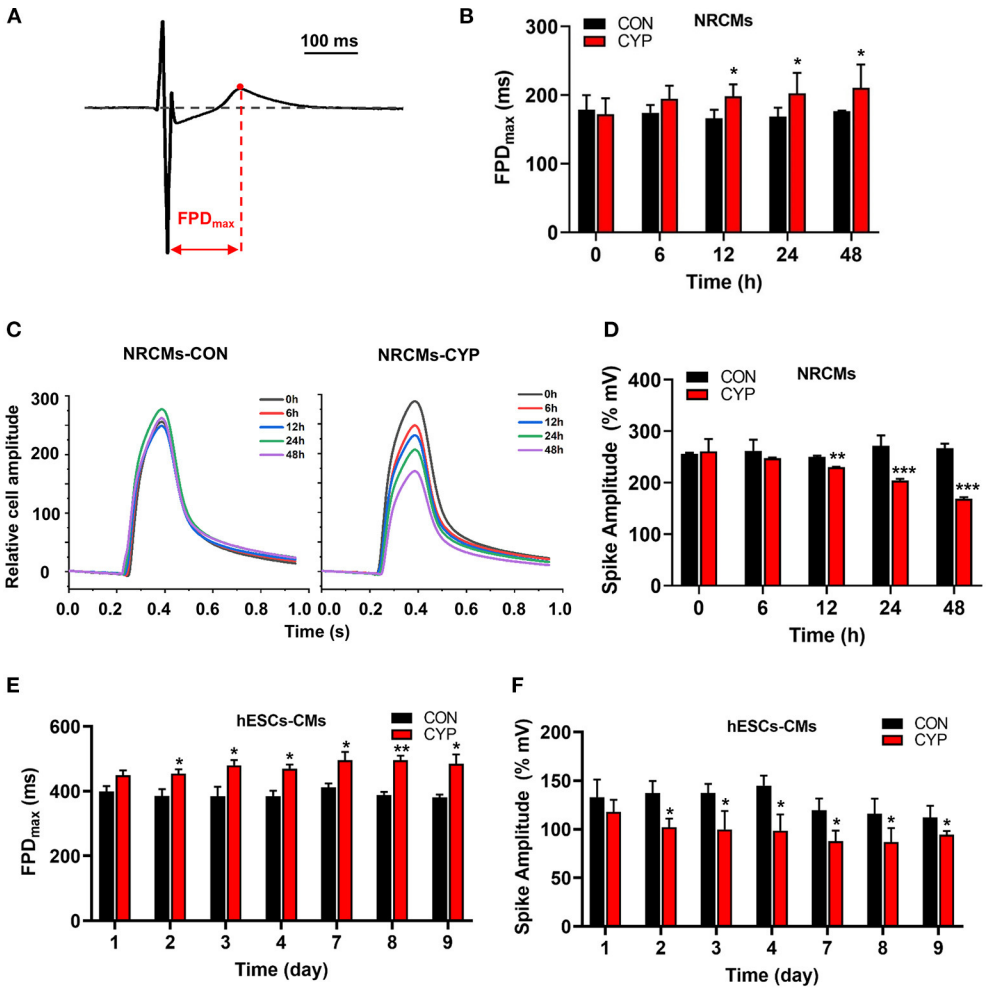

FIGURE 1 | CYP increased the field potential duration (FPD) and decreased contractile amplitudes of cardiomyocytes. **(A)** Schematic of FPD of cardiomyocytes. **(B)** The FPD analysis of NRCMs with 500 μmol/L of CYP at 0, 6, 12, 24, and 48 h. **(C)** Representative images of the relative cell amplitude of NRCMs treated with solvent control (CON) or CYP. The data were shown as the mean of triplicate experimental wells. **(D)** The cell amplitude analysis of NRCMs treated with 500 μmol/L CYP at 0, 6, 12, 24, and 48 h. The FPD **(E)** and cell amplitude **(F)** analysis of hESCs-CMs treated with 500 μmol/L CYP at 1, 2, 3, 4,7,8, and 9 days. The data are shown as the mean±SE, $n = 3$. $^{*}P < 0.05$, $^{**}P < 0.01$, $^{***}P < 0.001$ vs. CON.

target genes between solvent controls and CYP-treated NRCMs. As shown in **Figure 4C**, the sequence motif "GGAC" was highly enriched in m6A immunoprecipitated RNAs, consistent with the findings of previous studies (37, 38). We found 585 significantly increased m6A peaks distributed in 259 genes, whereas 277 genes had 548 statistically decreased m6A peaks in CYP-treated NRCMs relative to controls. Notably, we observed that reduced m6A peaks were mainly localized in the 5′ untranslated region (5′ UTR), whereas increased m6A peaks were distributed in the coding sequence (CDS) and 3′ untranslated region (3′ UTR; **Figure 4D**). The pie charts showed that these statistically differentially distributed m6A peaks were mainly noted in the CDS and 3′ UTR of genes in CYP-treated NRCMs regarding CON cells (**Figure 4E**). To explore the physiological and pathological significance of m6A modification after CYP treatment, we analyzed the KEGG pathway on the significantly altered m6A peaks. Our results showed that upregulated m6A peaks in the CYP-treated NRCMs were significantly related to the cAMP signaling pathway, adrenergic signaling in cardiomyocytes, calcium signaling pathway, GnRH signaling pathway and other dysregulation pathways in cancer (**Figure 4F**).

Furthermore, RNA sequencing was also performed on NRCMs treated with solvent control (CON) or CYP. Compared with CON, 369 genes were significantly downregulated, and 74 genes were upregulated in the CYP-treated group (**Supplementary Figure 5A**). The GO enrichment and KEGG analysis of the total DEGs showed that these DEGs were enriched in the NF-κB, TNF, and calcium signaling pathways (**Supplementary Figures 5B,C**). Remarkably, with the combined MeRIP-seq and RNA-seq results, we found upregulated m6A methylation sites in

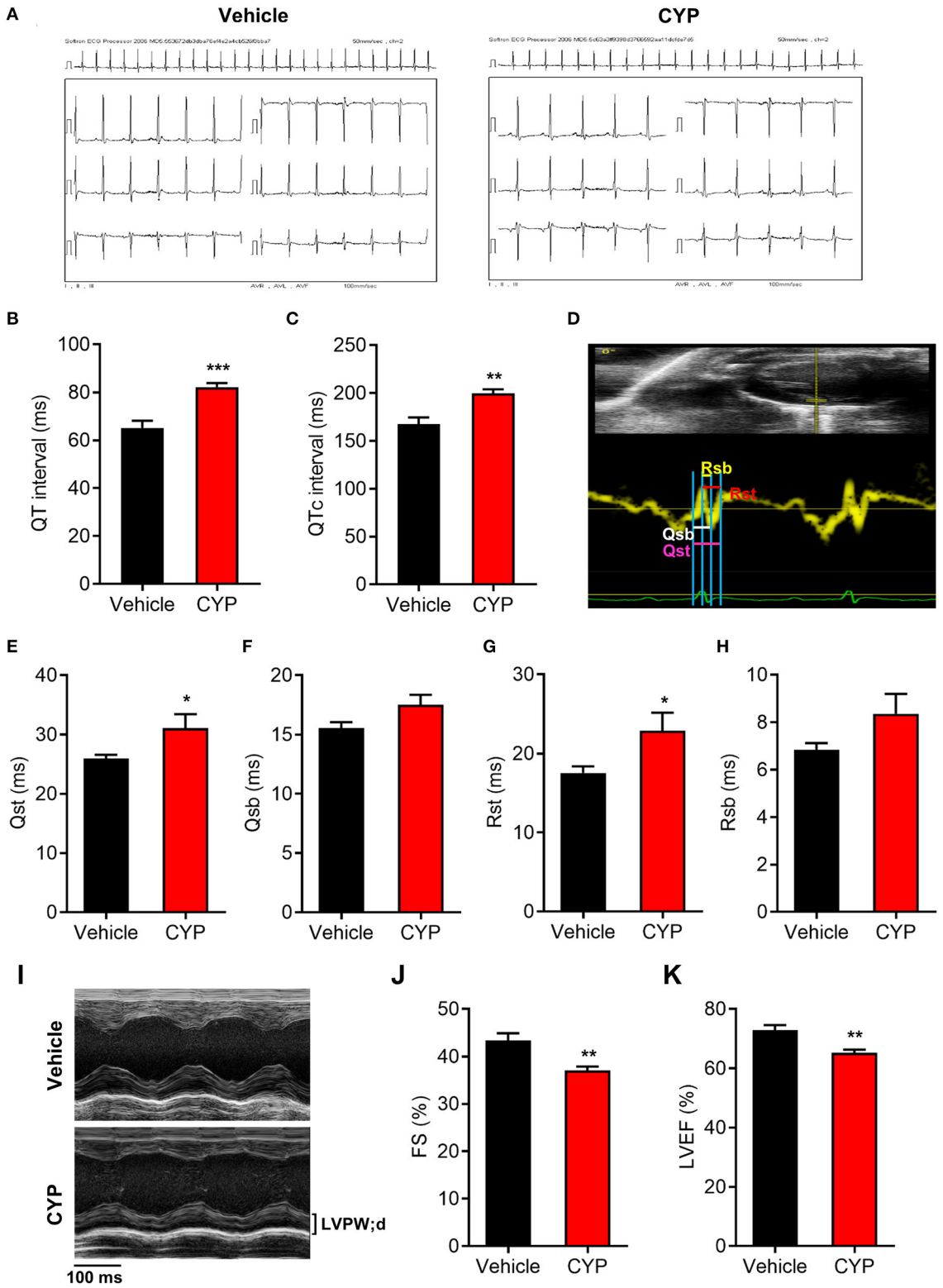

FIGURE 2 | The effect of CYP on QT intervals, cardiac electromechanical coupling and cardiac function. Electrocardiogram recording **(A)** showing QT intervals **(B)** and QTc **(C)** prolongation in rats treated with CYP for 1 day. **(D)** Schematic of four time courses of cardiac electromechanical coupling in the lateral wall of the left ventricle of rats. Qsb time course is the duration from the onset of Q wave on ECG to the beginning of S wave. Qst time course is the duration from the onset of Q wave on ECG to the top of S wave. Rsb time course is the duration from the top of R wave on ECG to the beginning of S wave. Rst time course is the duration from

(Continued)

FIGURE 2 | the top of R wave on ECG to top of S wave. The TDI echo combined with ECG measurement revealed an increase in Qsb **(E)**, Qst **(F)**, Rsb **(G)**, and Rst **(H)** in CYP-treated rats compared with that in vehicle-treated rats. **(I)** Representative M-mode echocardiography in rats treated with vehicle and CYP for 1 day. Echocardiography revealed that fractional shortening (FS) **(J)** and left ventricular ejection fraction (LVEF) **(K)** decreased in CYP-treated rats as compared with that in vehicle-treated rats. The data are represented as mean ± SE, $n = 6$. $^{*}p < 0.05$, $^{**}P < 0.01$, $^{***}P < 0.001$ vs. vehicle.

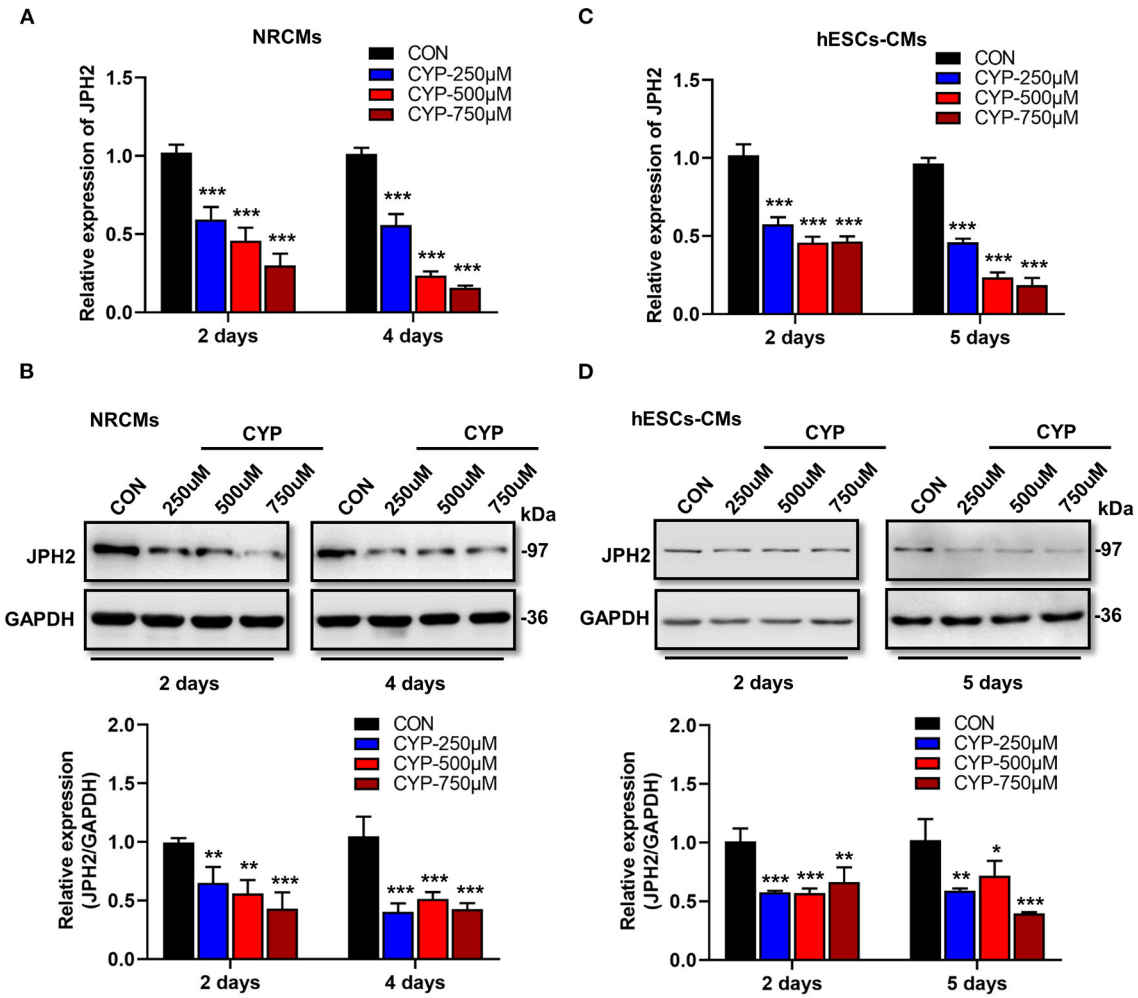

FIGURE 3 | CYP induced the downregulation of JPH2 expression in cardiomyocytes. Real-time PCR **(A)** and western blot **(B)** analysis of JPH2 expression in NRCMs treated with CYP for 2 or 4 days. Real-time PCR **(C)** and western blot **(D)** analysis of JPH2 expression in hESCs-CMs treated with CYP for 2 or 5 days. The data are shown as the mean ± SE of three experiments. $^{*}P < 0.05$, $^{**}P < 0.01$, $^{***}P < 0.001$ vs. CON.

the 5′UTR and CDS of JPH2 mRNA, accompanied with the downregulation of JHP2 expression on the RNA level. These results suggested that CYP induces calcium signaling changes through JPH2 downregulation caused by increasing m6A modification.

CYP-Induced Calcium Handling Abnormalities in hESCs-CMs

Calcium is a fundamental regulator of E-C coupling and electrophysiological signaling in cardiac myocytes (39). The above MeRIP-seq and RNA-seq results showed that the calcium signaling pathway played an important role in CYP-induced cardiotoxicity. We next verified and analyzed the Ca^{2+} handling properties of hESCs-CMs with CYP treatment by using H9-GCaMP derived cardiomyocytes (H9-GCaMP-CMs) (21). Compared with CON, hESCs-CMs treated with different concentrations of CYP (250, 500, and 750 μmoL/L) demonstrated significant Ca^{2+} transient irregularities, which were virtually absent in CON cells. As shown in **Figure 5A**, H9-GCaMP-CMs treated with 250 μmoL/L CYP showed no significant changes in the rhythm of Ca^{2+} transient release and reabsorption regarding CON on day 2. As the treatment time prolonged, the

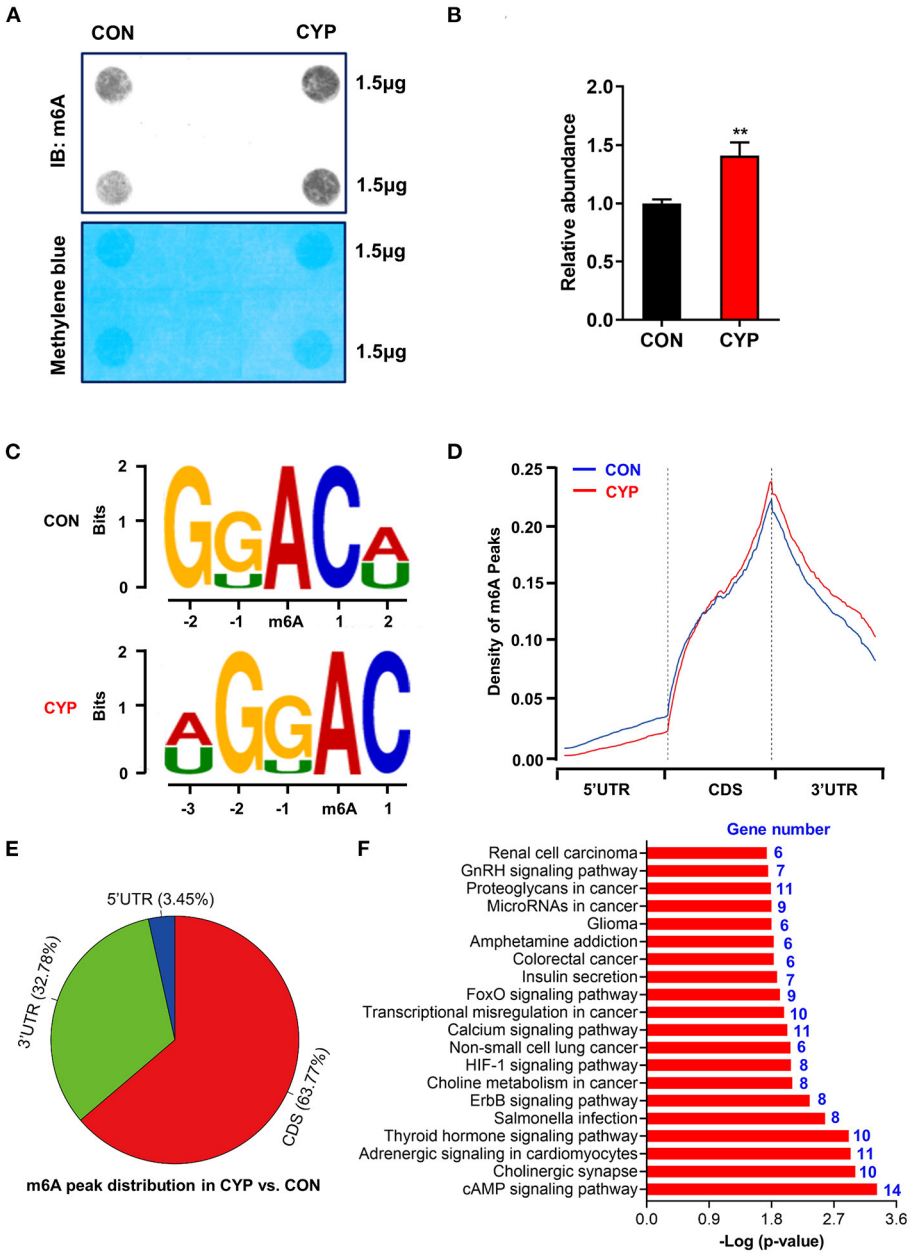

FIGURE 4 | Overview of altered m6A-tagged transcripts landscape in NRCMs with or without CYP. **(A)** The m6A dot blot assay was conducted in NRCMs after treatment with CYP or solvent control (CON) for 2 days. Methylene blue staining was used as the loading control. **(B)** Quantitative analysis of m6A abundance in NRCMs treated with CYP or CON for 2 days. **(C)** Top sequence motif identified from MeRIP-seq peaks in control and CYP-treated NRCMs. **(D)** Metagene plots showing the region of average m6A peaks identified across all transcripts in NRCMs with solvent control or CYP. **(E)** Pie charts showing m6A peak distribution in DEGs between CYP and control (CON) groups. **(F)** The top twenty significantly enriched pathways of upregulation of m6A peaks transcripts. The data are shown as the mean ± SE from three separate experiments. *$P < 0.05$; ** $P < 0.01$; *** $P < 0.001$ vs. CON.

cardiomyocytes exhibited longer Ca^{2+} transient durations on day 4 and slower beating rate, lower Ca^{2+} release amplitude, and longer transient durations on days 6 and 8 (**Figures 5B–D**). We noted a similar pattern of changes in H9-GCaMP-CMs treated with 500 or 750 μmoL/L CYP at different time points. On days 2 and 4, compared with CON, CYP-treated H9-GCaMP-CMs exhibited lower Ca^{2+} release amplitude (**Figure 5B**) and longer transient durations (**Figure 5D**). Interestingly, in addition to lower Ca^{2+} release amplitude, slower Ca^{2+} transient durations

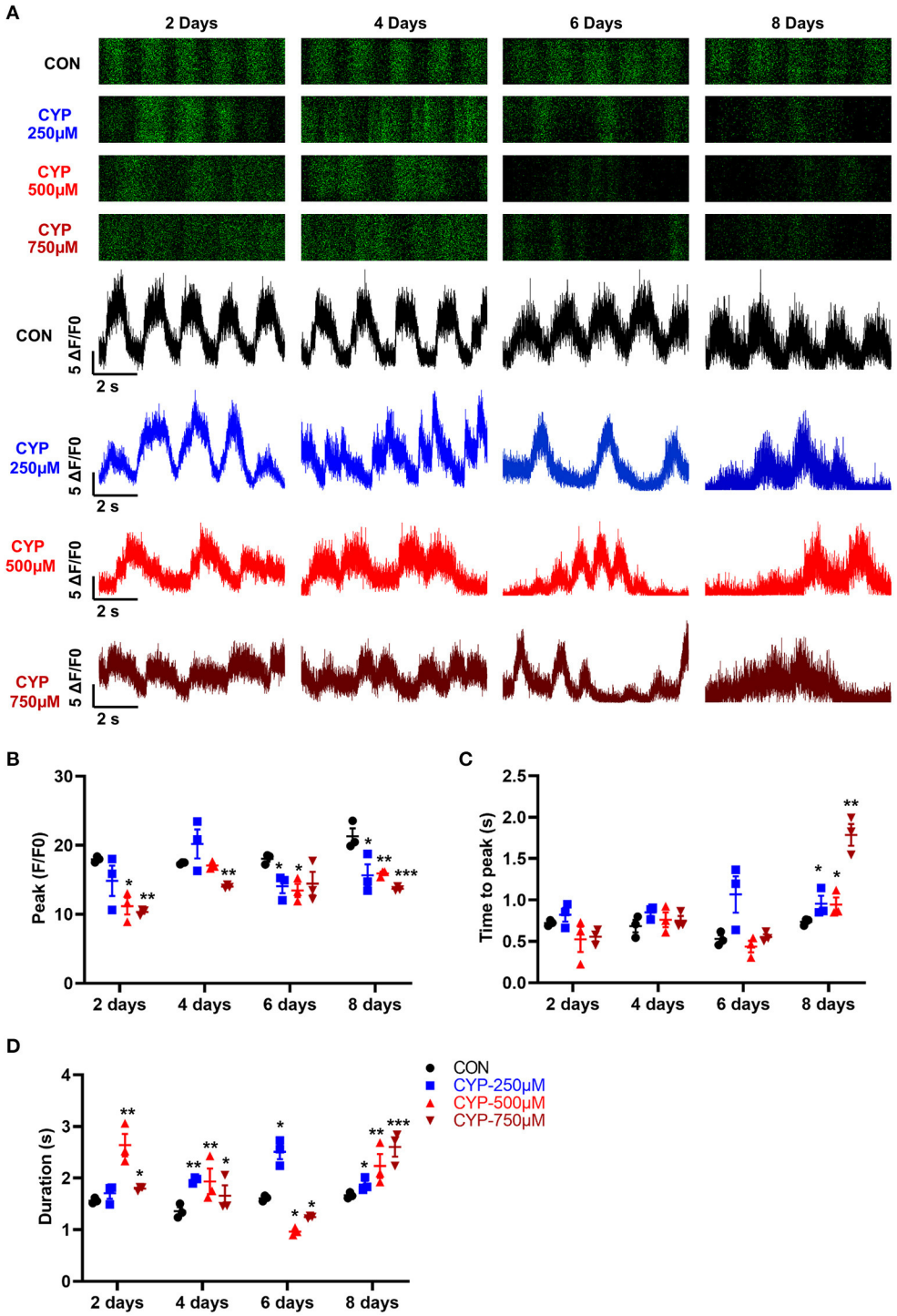

FIGURE 5 | hESCs-CMs treated with CYP exhibited abnormal Ca^{2+} handling properties. **(A)** Representative line-scan images in H9-GCaMP cell-derived cardiomyocytes treated with different concentrations of CYP at 2, 4, 6 and 8 days. Quantification of peak **(B)**, time to peak **(C)**, and calcium transient duration **(D)** in CON and CYP-treated H9-GCaMP-CMs. The data are shown as the mean ± SE, $n = 3$. $^{*}P < 0.05$, $^{**}P < 0.01$, $^{***}P < 0.001$ vs. CON.

were observed to occur in H9-GCaMP-CMs treated with CYP at dose of 500 or 750 μmoL/L(**Figures 5A,D**). On day 8, compared with CON, H9-GCaMP-CMs treated with low, medium and high concentrations of CYP exhibited lower Ca^{2+} release amplitude, and longer time to peak and transient durations (**Figures 5A–D**). These observations

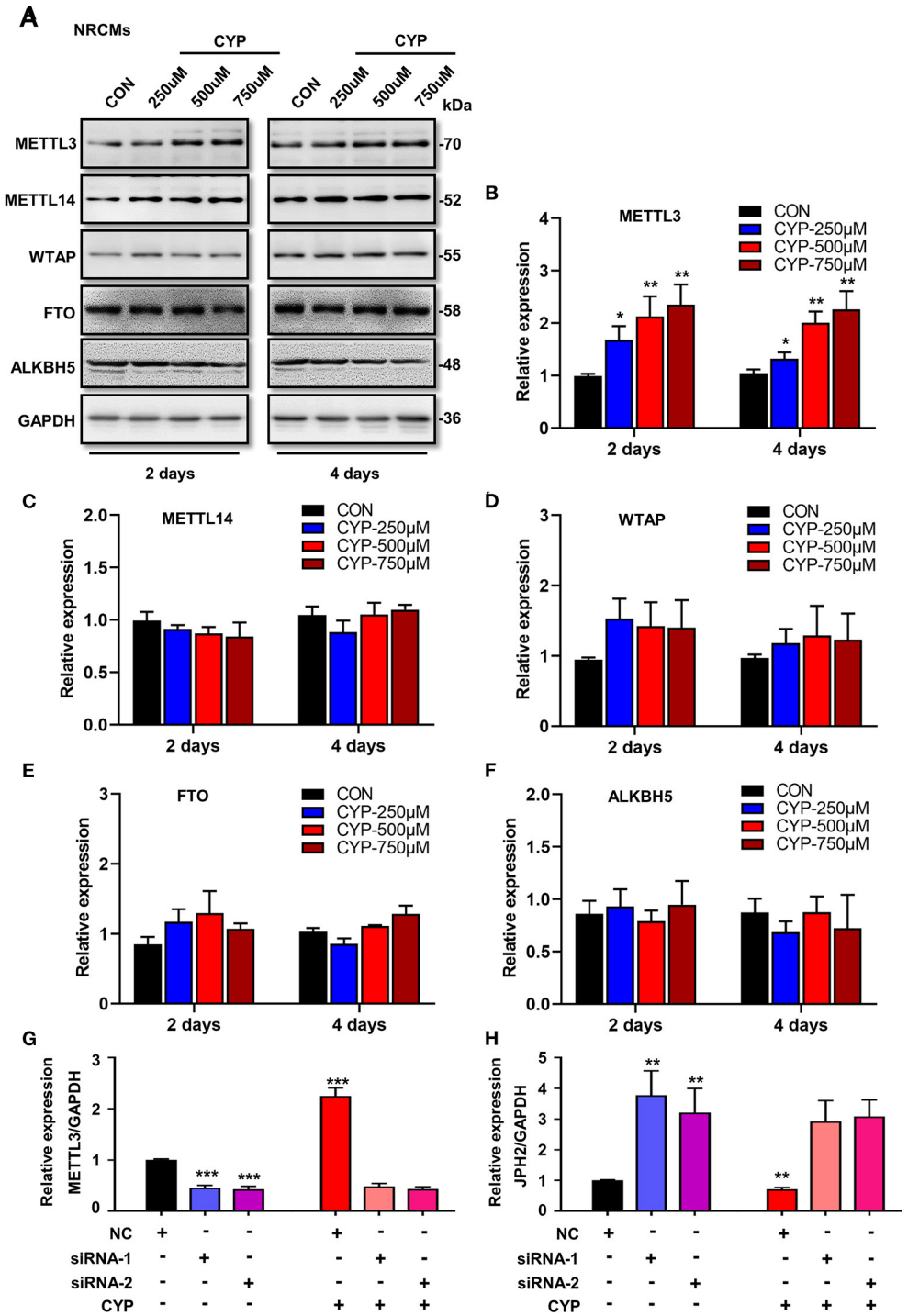

FIGURE 6 | CYP induced the downregulation of JPH2 expression through upregulating METTL3 expression. **(A)** Western blot analyses of METTL3, METTL14, WTAP, FTO and ALKBH5 expression in NRCMs with or without CYP for 2 or 4 days. Quantitative analysis of protein levels of METTL3 **(B)**, METTL14 **(C)**, WTAP **(D)**, FTO **(E)**, and ALKBH5 **(F)** in NRCMs treated with CYP for 2 or 4 days. The data are shown as the mean ± SE of three experiments. $^{*}P < 0.05$, $^{**}P < 0.01$ vs. CON. Real-time PCR analysis of METTL3 **(G)** and JPH2 **(H)** expression in NRCMs transfected with si-METTL3, or NC sequences with/without CYP. CYP did not decrease the expression of JPH2 in METTL3-deficient NRCMs. The data are shown as the mean ± SE of three experiments. $^{**}P < 0.01$; $^{***}P < 0.001$ vs. negative control (NC).

indicated that CYP could induce abnormal electrophysiological and contractile alterations in cardiomyocytes, consistent with the findings of the RNA sequencing and clinical data.

CYP Inhibited JPH2 Expression by Modulating the m6A Writer METTL3

To understand whether m6A RNA methylation plays an important role in the suppression effects of CYP on JPH2 expression in NRCMs, we further investigated the effect of CYP on m6A writers (METTL3, METTL14, and WTAP) and erasers (FTO, and ALKBH5) in CYP-treated cardiomyocytes. Intriguingly, exposing NRCMs to different doses of CYP (250, 500, and 750 umoL/L) for 2 or 4 days resulted in a significant increase in the expression of METTL3 (**Figures 6A,B**), whereas the expression of METTL14, WTAP, FTO, and ALKBH5 was not significantly altered (**Figures 6A,C–F**). Similar results were observed in rats treated with CYP. The RNA level of METTL3 increased in hearts (**Supplementary Figure 6**). These results suggested that CYP induces the m6A methylation of JPH2 mRNA through increasing METTL3 expression, leading to downregulation of JPH2 expression.

To investigate the biological effect of METTL3 on the reduction of JPH2 expression, we designed small interfering RNAs to silence METTL3 in NRCMs. Intriguingly, silencing METTL3 (**Figure 6G**) resulted in an increase in JPH2 expression (**Figure 6H**). Additionally, CYP induced JPH2 downregulation in NRCMs transfected with NC sequences. However, there was no reduction effect of CYP on JPH2 expression in si-METTL3 cardiomyocytes (**Figure 6H**). These data indicated that CYP decreased JPH2 expression by upregulating METTL3.

Disruption of METTL3 Eliminated CYP-Induced Electrical Alterations of Cardiomyocytes

To determine whether the disruption of METTL3 affects cardiac electrical and mechanical alterations in cardiomyocytes, we performed MEA in si-METTL3 and NC cardiomyocytes treated with CYP. Compared with NRCMs treated with NC, the FPD increased in NRCMs treated with CYP for 1 day (**Figure 7A**), whereas knock out of METTL3 significantly eliminated the increased FPD induced by CYP (**Figure 7A**). Similarly, the MEA results showed that the action potential duration (APD) (**Figure 7B**) was prolonged in NRCMs treated with NC after CYP treatment for 1 day (**Figures 7C,D**). However, the prolonged APD did not occur in si-METTL3 cardiomyocytes treated with CYP compared with the NRCMs treated with solvent control (**Figures 7C,D**). The above results demonstrated that the disruption of METTL3 eliminated the electrical alterations of cardiomyocytes induced by CYP.

DISCUSSION

CYP is strongly correlated with cardiac electrical and contractile alterations (3, 40, 41). This study found that CYP was associated with QT prolongation, a decrease in E-C coupling efficiency, and cardiac contractile dysfunction. Specifically, our findings demonstrated that CYP induced RNA m6A modification by upregulating METTL3 expression and suppressing JPH2 expression (**Figure 8**). These results suggested novel therapeutic and preventive targets for CYP-induced cardiotoxicity.

CYP is widely used an antineoplastic and immunosuppressive agent. The cytotoxic effect of CYP is induced by its biologically active metabolites (4, 42). CYP decomposes into acrolein and phoramide mustard (43), which further produces an unstable cation that may attack guanine bases (4), resulting in methylated bases. These DNA methylations lead to mutations and pair mismatches linked with its therapeutic effects on tumor cells. In fact, alkylating agents cause various DNA alkylation lesions including base methylation (9), which also induce RNA methylation. In our study, total m6A levels significantly increased in NRCMs after CYP treatment. Our experimental results showed that the m6A writer METTL3 significantly increased in cardiomyocytes treated with CYP, leading to an increase in m6A methylation of JPH2 mRNA. Promotion of the upregulation of METTL3 expression by CYP needs further exploration, however, the results suggested that RNA methylation played an important role in CYP-induced cardiotoxicity.

Previous study highlighted that CYP induced cardiac apoptosis when administered at a high dose (44), because the metabolite of CYP acrolein could promote the formation of reactive oxygen species (ROS) (45, 46). Hence, some studies have aimed to inhibit reactive oxygen-generators and regenerate other antioxidants that could prevent or treat CYP-induced acute cardiotoxicity (47). In this study, no myocardial death occurred in rats after treatment with CYP. We also observed no significant effect on the viability of cardiomyocytes in NRCMs treated with CYP at high concentrations. However, ANP and BNP both increased in cardiomyocytes treated with CYP, consistent with the findings of a previous study that showed CYP could induce cardiac hypertrophy (44). In this study, there was no obvious ventricular wall thickening in the ultrasound results owing to the short duration of CYP treatment in rats and administration being performed only once. However, increased ANP and BNP levels suggest that the molecular pathological changes may precede structural changes and the prolonged CYP treatment is required for organic changes to occur. Meanwhile, we found cardiac electrical alterations and decreased E-C coupling efficiency in rats after CYP administration. Although FS and LVEF did not decrease to heart failure in rats treated with CYP, these results were a 1-time consequence of CYP treatment with normal doses. Although prolonged QT and QTc interval, as well as E-C coupling time courses would recover after 3 days of administration, our results have implications for some patients with potential risk of ECG abnormalities during therapy for cancer and immune diseases. Interestingly, our data showed that CYP induced cardiac prolonged QT intervals and electromechanical coupling time courses accompanied by the downregulation of JPH2 expression. Calpain hydrolyzes JPH2 at the protein level (48), but CYP-induced decrease in JPH2 expression initiated from the RNA level in this study. To verify whether CYP-induced downregulation of JPH2 expression is mediated by miR-24 (31) and miR-331 (35), we further explored the effect of CYP on the biogenesis of the two miRNAs. There were no increases in the effect of CYP on miR-24 and miR-331, suggesting other regulatory mechanisms for JPH2. Interestingly, our subsequent results showed that m6A RNA methylation was associated with decreased expression of JPH2. These results

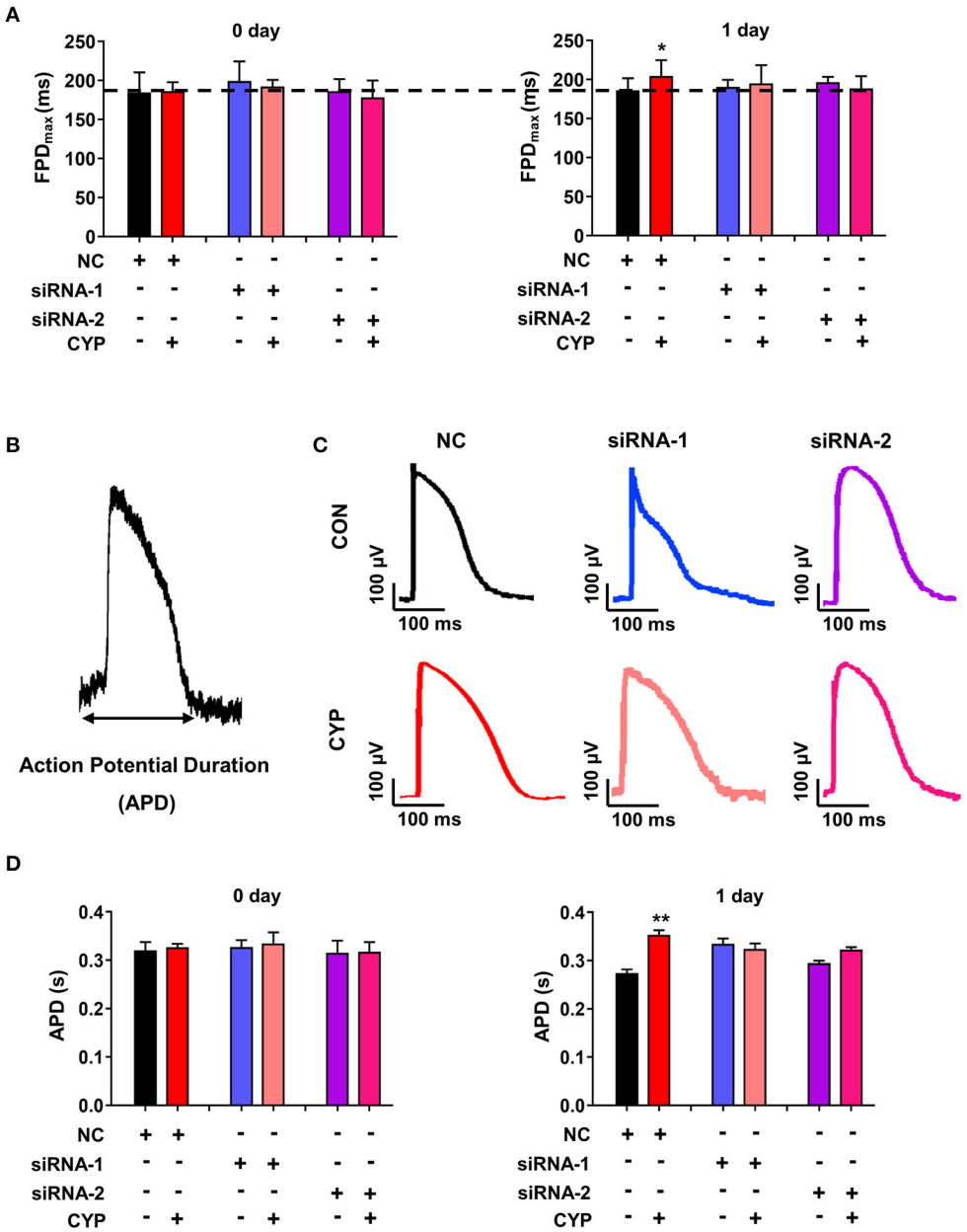

FIGURE 7 | Disruption of METTL3 expression eliminated the increased field potential duration (FPD) and action potential duration (APD) induced by CYP in cardiomyocytes. **(A)** Silencing METTL3 expression eliminated the increase in FPD induced by CYP. **(B)** Schematic of APD by the MEA processing of cardiomyocytes. **(C)** Representative images of APD in NRCMs transfected with si-METTL3, or negative control (NC) sequences with/without CYP. **(D)** Quantification of APD in NRCMs transfected with si-METTL3 or NC sequences with/without CYP. Silencing METTL3 expression eliminated the increased APD induced by CYP. The data are shown as the mean ± SE of three experiments. * $P < 0.05$; ** $P < 0.05$ vs. NC.

suggested that the increase in m6A of JPH2 mRNA is a novel mechanism in CYP-induced cardiotoxicity.

To investigate the mechanisms underlying of CYP-induced cell toxicity, we performed RNA sequencing to explore the potential targets and pathways. Our results showed that these DEGs were enriched in the biological process categories of leukocyte, lymphocyte and T cell-mediated immunity, which corresponded to a recent study that CYP actively recruited macrophages into the bone marrow and eliminated drug-resistant malignant tumor cells (49). However, whether the positive regulation of immunity induces cardiac injury requires further study. These DEGs enriched in molecular function categories of phosphatidylinositol bisphosphate, phosphatidylinositol-4,5-bisphophate binding, ATPase activity,

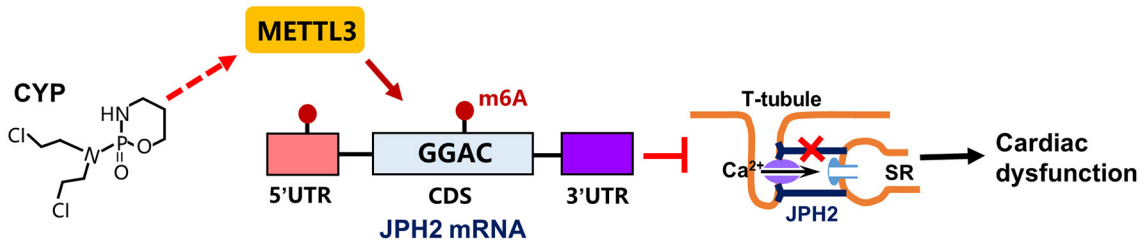

FIGURE 8 | Schematic of CYP-induced cardiac electrical and mechanical alterations. CYP decreased JPH2 expression by upregulating METTL3 expression, leading to Ca^{2+} transient irregularities and cardiac dysfunction.

and metal ion transmembrane transporter activity were associated with reduced ATP production and failure of Ca^{2+} transient in cardiomyocytes. According to this finding, the KEGG analysis showed that these DEGs were involved in the inflammation and calcium signaling pathways. Interestingly, we observed that cAMP signaling and the GnRH pathway were closely associated with the calcium signal and cardiac contraction (50, 51). The calcium signaling pathway was enriched in upregulated DEGs from MeRIP sequencing. In subsequent exploration of the effect of CYP on calcium signal, we found that CYP induces lower calcium release amplitude, and longer time to peak and transient durations. CYP-treated H9-GCaMP-CMs even exhibited lower calcium transient durations. These results are consistent with the adverse cardiac phenotype caused by CYP, suggesting that the calcium signaling pathway plays an important role in CYP-induced cardiotoxicity. Notably, the expression of JPH2, a key regulator for the Ca^{2+} influx and E-C coupling in cardiomyocytes (31, 52), significantly reduced after CYP treatment. Because decreased JPH2 is reportedly associated with atrial fibrillation (33) and arrhythmias (34), consistent with CYP-induced cardiotoxicity events, CYP-induced cardiac electrical and mechanical alterations may be closely related to the downregulation of JPH2 in this study. However, we cannot exclude other potential genes that play roles in regulating the process, such as paralemmin 2 (Palm-2), which upregulated m6A peaks and downregulated gene expression, was associated with cAMP-PKA signaling pathway, which has a strong influence on intracellular cation concentrations in the heart tissue or cardiomyocytes (53).

Previous epidemiological studies have suggested that prolonged QT intervals are closely associated with abnormal sodium, and potassium channels (54). However, the relationships between calcium ion binding protein imbalance and the pathological mechanism of QT prolongation are unknown. Recent studies have shown that Ca^{2+} binding proteins such as calmodulin (55, 56), and triadin (57), are associated with the long QT syndrome. These studies suggested that calcium plays an important role in the pathogenesis of cardiomyocyte repolarization and QT interval prolongation (58). JPH2 is the key regulatory protein that maintains a normal distance between LCCs and RyRs, which are important structures for Ca^{2+} release and recovery in cardiomyocytes. Moreover, a recent study demonstrated that the N-terminal part of JPH2 could bind and interact with caveolin-3 (59), which is a critical mediator for fixing LCCs on caveolar membrane in the plasma membrane and associated with long QT syndrome (60). Caveolin-3 is an important member of muscle-specific structural proteins of caveolae, which are also localized in T-tubules (61). These studies suggested that JPH2 interacts with caveolin-3 to mediate the junctional membrane complexes and Ca^{2+}-induced Ca^{2+} release in the cardiomyocytes (59). Although abnormal JPH2 expression decreases the fixation with caveolin-3, leading to disruption of the normal junctional membrane complexes and efficient Ca^{2+} transient, it may positively affect the QT interval. In this study, CYP induced the downregulation of JPH2 expression, resulting in increased FPD and APD in cardiomyocytes, which would be eliminated by silencing METTL3. Our results suggested that JPH2 aberration is closely related to the long QT syndrome. However, clinical data is warranted to determine whether the absence of JPH2 leads to the prolonged QT interval in future studies.

Despite these encouraging results, it is necessary to point out the limitations of this study. Silencing METTL3 increases the JPH2 expression, and JPH2 is not further downregulated in si-METTL3 NRCMs after CYP treatment. It is significant to use METTL3 knockout transgenic mice to verify whether CYP induced cardiac electrical and mechanical alterations by increasing m6A levels. Additionally, there are m6A methylation sites in both the 5'UTR and CDS of JPH2 mRNA, and the m6A methylation modification sites that regulate the expression of JPH2 need to be further clarified. Furthermore, the m6A levels and JPH2 expression abnormalities in CYP-induced cardiotoxicity should be confirmed in the clinic in future studies.

In summary, our results indicated that CYP-induced cardiac electrical and mechanical alterations and Ca^{2+} dyshomeostasis are associated with m6A methylation modifications and decreased JPH2. Our study found that CYP increased RNA m6A levels by altering METTL3 expression. Furthermore, decreased JPH2 expression plays an important role in CYP-induced cardiac electrical and mechanical alterations by blocking Ca^{2+} influx between transverse tubules and sarcoplasmic reticulum. Our findings demonstrated that RNA m6A methylation is a potential therapeutic intervention for CYP-induced cardiotoxicity.

DATA AVAILABILITY STATEMENT

The datasets presented in this study can be found in online repositories. The names of the repository/repositories and accession number(s) can be found below: https://www.ncbi.nlm.nih.gov/geo/query/acc.cgi?acc=GSE184294.

ETHICS STATEMENT

The animal study was reviewed and approved by the Ethics Committee of Peking University Health Science Centre (LA2021004).

AUTHOR CONTRIBUTIONS

MX and MZ conceived and designed the experiments. MZ and YL performed experiments and acquired data. YS, SZ, CH, XL, and FL provided materials. MZ, YL, and ZH performed data analysis. MZ, YL, and MX wrote the manuscript. All authors contributed to the article and approved the submitted version.

FUNDING

This study was supported by the grants from National Natural Science Foundation of China (81625001 and 81900315) and the National Key Research & Development Program of China (2018YFC1312700 and 2018YFC1312701).

SUPPLEMENTARY MATERIAL

The Supplementary Material for this article can be found online at: https://www.frontiersin.org/articles/10.3389/fcvm.2021.763469/full#supplementary-material

REFERENCES

1. Ferlay J, Steliarova-Foucher E, Lortet-Tieulent J, Rosso S, Coebergh JW, Comber H, et al. Cancer incidence and mortality patterns in Europe: estimates for 40 countries in 2012. *Eur J Cancer.* (2013) 49:1374–403. doi: 10.1016/j.ejca.2012.12.027
2. Siegel R, DeSantis C, Virgo K, Stein K, Mariotto A, Smith T, et al. Cancer treatment and survivorship statistics, 2012. *CA Cancer J Clin.* (2012) 62:220–41. doi: 10.3322/caac.21149
3. Zamorano JL, Lancellotti P, Rodriguez Muñoz D, Aboyans V, Asteggiano R, Galderisi M, et al. 2016 ESC Position Paper on cancer treatments and cardiovascular toxicity developed under the auspices of the ESC Committee for Practice Guidelines: The Task Force for cancer treatments and cardiovascular toxicity of the European Society of Cardiology (ESC). *Eur Heart J.* (2016) 37:2768–801. doi: 10.1093/eurheartj/ehw211
4. Emadi A, Jones RJ, Brodsky RA. Cyclophosphamide and cancer: golden anniversary. *Nat Rev Clin Oncol.* (2009) 6:638–47. doi: 10.1038/nrclinonc.2009.146
5. Wang X, Zhang J, Xu T. Cyclophosphamide-evoked heart failure involves pronounced co-suppression of cytoplasmic thioredoxin reductase activity and non-protein free thiol level. *Eur J Heart Fail.* (2009) 11:154–62. doi: 10.1093/eurjhf/hfn012
6. Dhesi S, Chu MP, Blevins G, Paterson I, Larratt L, Oudit GY, et al. Cyclophosphamide-Induced cardiomyopathy: a case report, review, and recommendations for management. *J Investig Med High Impact Case Rep.* (2013) 1:1–7. doi: 10.1177/2324709613480346
7. van Laar JM, Farge D, Sont JK, Naraghi K, Marjanovic Z, Larghero J, et al. Autologous hematopoietic stem cell transplantation vs intravenous pulse cyclophosphamide in diffuse cutaneous systemic sclerosis: a randomized clinical trial. *JAMA.* (2014) 311:2490–8. doi: 10.1001/jama.2014.6368
8. Mackey JR, Martin M, Pienkowski T, Rolski J, Guastalla JP, Sami A, et al. Adjuvant docetaxel, doxorubicin, and cyclophosphamide in node-positive breast cancer: 10-year follow-up of the phase 3 randomised BCIRG 001 trial. *Lancet Oncol.* (2013) 14:72–80. doi: 10.1016/S1470-2045(12)70525-9
9. Shrivastav N, Li D, Essigmann JM. Chemical biology of mutagenesis and DNA repair: cellular responses to DNA alkylation. *Carcinogenesis.* (2010) 31:59–70. doi: 10.1093/carcin/bgp262
10. Fu Y, Dominissini D, Rechavi G, He C. Gene expression regulation mediated through reversible m6A RNA methylation. *Nat Rev Genet.* (2014) 15:293–306. doi: 10.1038/nrg3724
11. Mathiyalagan P, Adamiak M, Mayourian J, Sassi Y, Liang Y, Agarwal N, et al. FTO-Dependent N(6)-Methyladenosine regulates cardiac function during remodeling and repair. *Circulation.* (2019) 139:518–32. doi: 10.1161/CIRCULATIONAHA.118.033794
12. Yue Y, Liu J, He C. RNA N6-methyladenosine methylation in post-transcriptional gene expression regulation. *Genes Dev.* (2015) 29:1343–55. doi: 10.1101/gad.262766.115
13. Geula S, Moshitch-Moshkovitz S, Dominissini D, Mansour AA, Kol N, Salmon-Divon M, et al. Stem cells. m6A mRNA methylation facilitates resolution of naïve pluripotency toward differentiation. *Science.* (2015) 347:1002–6. doi: 10.1126/science.1261417
14. Chen J, Wang C, Fei W, Fang X, Hu X. Epitranscriptomic m6A modification in the stem cell field and its effects on cell death and survival. *Am J Cancer Res.* (2019) 9:752–64.
15. Zhao BS, He C. Fate by RNA methylation: m6A steers stem cell pluripotency. *Genome Biol.* (2015) 16:43. doi: 10.1186/s13059-015-0609-1
16. Chen M, Wong CM. The emerging roles of N6-methyladenosine (m6A) deregulation in liver carcinogenesis. *Mol Cancer.* (2020) 19:44. doi: 10.1186/s12943-020-01172-y
17. Berulava T, Buchholz E, Elerdashvili V, Pena T, Islam MR, Lbik D, et al. Changes in m6A RNA methylation contribute to heart failure progression by modulating translation. *Eur J Heart Fail.* (2020) 22:54–66. doi: 10.1002/ejhf.1672
18. Keller AM. Positional localization: three-dimensional transthoracic echocardiographic techniques for the measurement of cardiac mass, volume, and function. *Echocardiography.* (2000) 17:745–8. doi: 10.1111/j.1540-8175.2000.tb01232.x
19. Gao J, Zhu M, Yu HY, Wang SQ, Feng XH, Xu M. Excitation-Contraction coupling time is more sensitive in evaluating cardiac systolic function. *Chin Med J.* (2018) 131:1834–9. doi: 10.4103/0366-6999.237395
20. Gao J, Zhu M, Liu RF, Zhang JS, Xu M. Cardiac hypertrophy is positively regulated by MicroRNA-24 in rats. *Chin Med J.* (2018) 131:1333–41. doi: 10.4103/0366-6999.232793
21. Li X, Lu WJ, Li Y, Wu F, Bai R, Ma S, et al. MLP-deficient human pluripotent stem cell derived cardiomyocytes develop hypertrophic cardiomyopathy and heart failure phenotypes due to abnormal calcium handling. *Cell Death Dis.* (2019) 10:610. doi: 10.1038/s41419-019-1826-4
22. Burridge PW, Matsa E, Shukla P, Lin ZC, Churko JM, Ebert AD, et al. Chemically defined generation of human cardiomyocytes. *Nat Methods.* (2014) 11:855–60. doi: 10.1038/nmeth.2999
23. Chang Y, Li YN, Bai R, Wu F, Ma S, Saleem A, et al. hERG-deficient human embryonic stem cell-derived cardiomyocytes for modelling QT prolongation. *Stem Cell Res Ther.* (2021) 12:278. doi: 10.1186/s13287-021-02346-1
24. Zhang Z, Wang M, Xie D, Huang Z, Zhang L, Yang Y, et al. METTL3-mediated N(6)-methyladenosine mRNA modification enhances long-term memory consolidation. *Cell Res.* (2018) 28:1050–61. doi: 10.1038/s41422-018-0092-9
25. Liu X, Liu J, Xiao W, Zeng Q, Bo H, Zhu Y, et al. SIRT1 regulates N(6)-methyladenosine RNA modification in hepatocarcinogenesis by inducing RANBP2-dependent FTO SUMOylation. *Hepatology.* (2020) 72:2029–2050. doi: 10.1002/hep.31222
26. Yazawa M, Hsueh B, Jia X, Pasca AM, Bernstein JA, Hallmayer J, et al. Using induced pluripotent stem cells to investigate cardiac phenotypes in timothy syndrome. *Nature.* (2011) 471:230–4. doi: 10.1038/nature09855

27. Lan F, Lee AS, Liang P, Sanchez-Freire V, Nguyen PK, Wang L, et al. Abnormal calcium handling properties underlie familial hypertrophic cardiomyopathy pathology in patient-specific induced pluripotent stem cells. *Cell Stem Cell.* (2013) 12:101–13. doi: 10.1016/j.stem.2012.10.010
28. Brell JM. Prolonged QTc interval in cancer therapeutic drug development: defining arrhythmic risk in malignancy. *Prog Cardiovasc Dis.* (2010) 53:164–72. doi: 10.1016/j.pcad.2010.05.005
29. Haugaa KH, Edvardsen T, Leren TP, Gran JM, Smiseth OA, Amlie JP. Left ventricular mechanical dispersion by tissue doppler imaging: a novel approach for identifying high-risk individuals with long QT syndrome. *Eur Heart J.* (2009) 30:330–7. doi: 10.1093/eurheartj/ehn466
30. ter Bekke RM, Haugaa KH, van den Wijngaard A, Bos JM, Ackerman MJ, Edvardsen T, et al. Electromechanical window negativity in genotyped long-QT syndrome patients: relation to arrhythmia risk. *Eur Heart J.* (2015) 36:179–86. doi: 10.1093/eurheartj/ehu370
31. Xu M, Wu HD, Li RC, Zhang HB, Wang M, Tao J, et al. Mir-24 regulates junctophilin-2 expression in cardiomyocytes. *Circ Res.* (2012) 111:837–41. doi: 10.1161/CIRCRESAHA.112.277418
32. Zhang HB, Li RC, Xu M, Xu SM, Lai YS, Wu HD, et al. Ultrastructural uncoupling between T-tubules and sarcoplasmic reticulum in human heart failure. *Cardiovasc Res.* (2013) 98:269–76. doi: 10.1093/cvr/cvt030
33. Beavers DL, Wang W, Ather S, Voigt N, Garbino A, Dixit SS, et al. Mutation E169K in junctophilin-2 causes atrial fibrillation due to impaired RyR2 stabilization. *J Am Coll Cardiol.* (2013) 62:2010–9. doi: 10.1016/j.jacc.2013.06.052
34. Beavers DL, Landstrom AP, Chiang DY, Wehrens XH. Emerging roles of junctophilin-2 in the heart and implications for cardiac diseases. *Cardiovasc Res.* (2014) 103:198–205. doi: 10.1093/cvr/cvu151
35. Jin-Jing, Zhang, Li-Peng, Wang, Rong-Chang, Li, et al. Abnormal expression of miR-331 leads to impaired heart function. *Sci Bulletin.* (2019) v.64:63–9. doi: 10.1016/j.scib.2019.05.017
36. Wang X, Lu Z, Gomez A, Hon GC, Yue Y, Han D, et al. N6-methyladenosine-dependent regulation of messenger RNA stability. *Nature.* (2014) 505:117–20. doi: 10.1038/nature12730
37. Lan T, Li H, Zhang D, Xu L, Liu H, Hao X, et al. KIAA1429 contributes to liver cancer progression through N6-methyladenosine-dependent post-transcriptional modification of GATA3. *Mol Cancer.* (2019) 18:186. doi: 10.1186/s12943-019-1106-z
38. Lin S, Choe J, Du P, Triboulet R, Gregory RI. The m(6)A methyltransferase METTL3 promotes translation in human cancer cells. *Mol Cell.* (2016) 62:335–45. doi: 10.1016/j.molcel.2016.03.021
39. Bers DM. Calcium cycling and signaling in cardiac myocytes. *Annu Rev Physiol.* (2008) 70:23–49. doi: 10.1146/annurev.physiol.70.113006.100455
40. Tamargo J, Caballero R, Delpón E. Cancer chemotherapy and cardiac arrhythmias: a review. *Drug Saf.* (2015) 38:129–52. doi: 10.1007/s40264-014-0258-4
41. Gharib MI, Burnett AK. Chemotherapy-induced cardiotoxicity: current practice and prospects of prophylaxis. *Eur J Heart Fail.* (2002) 4:235–42. doi: 10.1016/S1388-9842(01)00201-X
42. Ayash LJ, Wright JE, Tretyakov O, Gonin R, Elias A, Wheeler C, et al. Cyclophosphamide pharmacokinetics: correlation with cardiac toxicity and tumor response. *J Clin Oncol.* (1992) 10:995–1000. doi: 10.1200/JCO.1992.10.6.995
43. Ludeman SM. The chemistry of the metabolites of cyclophosphamide. *Curr Pharm Des.* (1999) 5:627–43.
44. Liu Y, Tan D, Shi L, Liu X, Zhang Y, Tong C, et al. Blueberry anthocyanins-enriched extracts attenuate cyclophosphamide-induced cardiac injury. *PLoS ONE.* (2015) 10:e0127813. doi: 10.1145/2818302
45. Liu W, Zhai X, Wang W, Zheng B, Zhang Z, Fan X, et al. Aldehyde dehydrogenase 2 activation ameliorates cyclophosphamide-induced acute cardiotoxicity via detoxification of toxic aldehydes and suppression of cardiac cell death. *J Mol Cell Cardiol.* (2018) 121:134–44. doi: 10.1016/j.yjmcc.2018.07.006
46. Iqubal A, Iqubal MK, Sharma S, Ansari MA, Najmi AK, Ali SM, et al. Molecular mechanism involved in cyclophosphamide-induced cardiotoxicity: old drug with a new vision. *Life Sci.* (2019) 218:112–31. doi: 10.1016/j.lfs.2018.12.018
47. Mythili Y, Sudharsan PT, Varalakshmi P. dl-alpha-lipoic acid ameliorates cyclophosphamide induced cardiac mitochondrial injury. *Toxicology.* (2005) 215:108–14. doi: 10.1016/j.tox.2005.07.001
48. Wu CY, Chen B, Jiang YP, Jia Z, Martin DW, Liu S, et al. Calpain-dependent cleavage of junctophilin-2 and T-tubule remodeling in a mouse model of reversible heart failure. *J Am Heart Assoc.* (2014) 3:e000527. doi: 10.1161/JAHA.113.000527
49. Lossos C, Liu Y, Kolb KE, Christie AL, Van Scoyk A, Prakadan SM, et al. Mechanisms of lymphoma clearance induced by high-dose alkylating agents. *Cancer Discov.* (2019) 9:944–61. doi: 10.1158/2159-8290.CD-18-1393
50. Patra C, Foster K, Brady MF. *Biochemistry, cAMP, In StatPearls*. Treasure: StatPearls Publishing Copyright © 2020, StatPearls Publishing LLC (2020).
51. Dong F, Skinner DC, Wu TJ, Ren J. The heart: a novel gonadotrophin-releasing hormone target. *J Neuroendocrinol.* (2011) 23:456–63. doi: 10.1111/j.1365-2826.2011.02119.x
52. Takeshima H, Komazaki S, Nishi M, Iino M, Kangawa K. Junctophilins: a novel family of junctional membrane complex proteins. *Mol Cell.* (2000) 6:11–22. doi: 10.1016/S1097-2765(05)00005-5
53. Scholten A, van Veen TA, Vos MA, Heck AJ. Diversity of cAMP-dependent protein kinase isoforms and their anchoring proteins in mouse ventricular tissue. *J Proteome Res.* (2007) 6:1705–17. doi: 10.1021/pr060601a
54. Tester DJ, Will ML, Haglund CM, Ackerman MJ. Compendium of cardiac channel mutations in 541 consecutive unrelated patients referred for long QT syndrome genetic testing. *Heart Rhythm.* (2005) 2:507–17. doi: 10.1016/j.hrthm.2005.01.020
55. Crotti L, Johnson CN, Graf E, De Ferrari GM, Cuneo BF, Ovadia M, et al. Calmodulin mutations associated with recurrent cardiac arrest in infants. *Circulation.* (2013) 127:1009–17. doi: 10.1161/CIRCULATIONAHA.112.001216
56. Reed GJ, Boczek NJ, Etheridge SP, Ackerman MJ. CALM3 mutation associated with long QT syndrome. *Heart Rhythm.* (2015) 12:419–22. doi: 10.1016/j.hrthm.2014.10.035
57. Altmann HM, Tester DJ, Will ML, Middha S, Evans JM, Eckloff BW, et al. Homozygous/compound heterozygous triadin mutations associated with autosomal-recessive long-QT syndrome and pediatric sudden cardiac arrest: elucidation of the triadin knockout syndrome. *Circulation.* (2015) 131:2051–60. doi: 10.1161/CIRCULATIONAHA.115.015397
58. Giudicessi JR, Ackerman MJ. Calcium revisited: new insights into the molecular basis of long-QT syndrome. *Circ Arrhythm Electrophysiol.* (2016) 9. doi: 10.1161/CIRCEP.116.002480
59. Minamisawa S, Oshikawa J, Takeshima H, Hoshijima M, Wang Y, Chien KR, et al. Junctophilin type 2 is associated with caveolin-3 and is down-regulated in the hypertrophic and dilated cardiomyopathies. *Biochem Biophys Res Commun.* (2004) 325:852–6. doi: 10.1016/j.bbrc.2004.10.107
60. Vatta M, Ackerman MJ, Ye B, Makielski JC, Ughanze EE, Taylor EW, et al. Mutant caveolin-3 induces persistent late sodium current and is associated with long-QT syndrome. *Circulation.* (2006) 114:2104–12. doi: 10.1161/CIRCULATIONAHA.106.635268
61. Hagiwara Y, Nishina Y, Yorifuji H, Kikuchi T. Immunolocalization of caveolin-1 and caveolin-3 in monkey skeletal, cardiac and uterine smooth muscles. *Cell Struct Funct.* (2002) 27:375–82. doi: 10.1247/csf.27.375

Conflict of Interest: The authors declare that the research was conducted in the absence of any commercial or financial relationships that could be construed as a potential conflict of interest.

Publisher's Note: All claims expressed in this article are solely those of the authors and do not necessarily represent those of their affiliated organizations, or those of the publisher, the editors and the reviewers. Any product that may be evaluated in this article, or claim that may be made by its manufacturer, is not guaranteed or endorsed by the publisher.

frontiers in Cardiovascular Medicine

ORIGINAL RESEARCH
published: 11 November 2021
doi: 10.3389/fcvm.2021.766996

Cancer and Infective Endocarditis: Characteristics and Prognostic Impact

Bernard Cosyns[1,2†], Bram Roosens[1†], Patrizio Lancellotti[3], Cécile Laroche[4], Raluca Dulgheru[3], Valentina Scheggi[5], Isidre Vilacosta[6], Agnès Pasquet[7,8], Cornelia Piper[9], Graciela Reyes[10], Essam Mahfouz[11], Zhanna Kobalava[12], Lionel Piroth[13], Jarosław D. Kasprzak[14], Antonella Moreo[15], Jean-François Faucher[16], Julien Ternacle[17,18], Marwa Meshaal[19], Aldo P. Maggioni[4,20], Bernard Iung[21] and Gilbert Habib[22,23] on behalf of the EURO-ENDO Investigators Group[‡]*

[1] Centrum Voor Hart- en Vaatziekten (CHVZ), Vrije Universiteit Brussel (VUB), Universitair Ziekenhuis Brussel (UZ Brussel), Brussels, Belgium, [2] In vivo Cellular and Molecular Imaging (ICMI) Center, Vrije Universiteit Brussel (VUB), Brussels, Belgium, [3] Cardiology Department, University Hospital Centre, Centre Hospitalier Universitaire (CHU) Sart Tilman, Liège, Belgium, [4] EURObservational Research Programme, European Society of Cardiology, Antibes, France, [5] Cardiothoracic and Vascular Department, Careggi University Hospital, Florence, Italy, [6] Department of Cardiology, Hospital Clínico San Carlos, Universidad Complutense de Madrid, Madrid, Spain, [7] Pôle de Recherche Cardiovasculaire, Institut de Recherche Expérimentale et Clinique, Université Catholique de Louvain, Brussels, Belgium, [8] Divisions of Cardiology and Cardiothoracic Surgery, Cliniques Universitaires Saint-Luc, Brussels, Belgium, [9] Clinic for General and Interventional Cardiology/Angiology, Herz- und Diabeteszentrum Nordrhein-Westfalen (NRW), Ruhr-Universität Bochum, Bad Oeynhausen, Germany, [10] Echo Lab Department, Hospital de Alta Complejidad en red El Cruce, Florencio Varela, Buenos Aires, Argentina, [11] Mansoura Specialized Medical Hospital, Mansoura University, Mansoura, Egypt, [12] Department of Cardiology, Rossiyskiy Universitet Druzhby Narodov (RUDN) University Moscow, Moscow, Russia, [13] Infectious Diseases Department, University Hospital, INSERM CIC1432, University of Burgundy, Dijon, France, [14] Bieganski Hospital, Medical University of Lodz, Łódź, Poland, [15] A. De Gasperis Cardio Center, ASST Grande Ospedale Metropolitano Niguarda, Milan, Italy, [16] CHU Limoges, Department of Infectious Diseases and Tropical Medicine, Limoges France INSERM, U1094, Limoges, France, [17] Cardiology Department, Henri Mondor Hospital, SOS Endocardites, DHU ATVB, INSERM U955 Team 8, Université Paris-Est Créteil, Créteil, France, [18] Fellow Equipe, Team du Dr Philippe Pibarot, Institut Universitaire de Cardiologie et de Pneumologie de Québec/Quebec Heart and Lung Institute Université Laval, Quebec City, QC, Canada, [19] Cardiology Department, Kasr Al Ainy, Cairo University, Cairo, Egypt, [20] Maria Cecilia Hospital, Gruppo Villa Maria (GVM) Care & Research, Cotignola, Italy, [21] Bichat Hospital, APHP, DHU Fire, Paris Diderot University, Paris, France, [22] AP-HM, La Timone Hospital, Cardiology Department, Marseille, France, [23] Aix Marseille University, IRD, AP-HM, MEPHI, IHU-Mediterranean Infection, Marseille, France

Background: The interplay between cancer and IE has become of increasing interest. This study sought to assess the prevalence, baseline characteristics, management, and outcomes of IE cancer patients in the ESC EORP EURO-ENDO registry.

Methods: Three thousand and eighty-five patients with IE were identified based on the ESC 2015 criteria. Three hundred and fifty-nine (11.6%) IE cancer patients were compared to 2,726 (88.4%) cancer-free IE patients.

Results: In cancer patients, IE was mostly community-acquired (74.8%). The most frequently identified microorganisms were *S. aureus* (25.4%) and Enterococci (23.8%). The most frequent complications were acute renal failure (25.9%), embolic events (21.7%) and congestive heart failure (18.1%). Theoretical indication for cardiac surgery was not significantly different between groups (65.5 vs. 69.8%, $P = 0.091$), but was effectively less performed when indicated in IE patients with cancer (65.5 vs. 75.0%, $P = 0.002$). Compared to cancer-free IE patients, in-hospital and 1-year mortality occurred in 23.4 vs. 16.1%, $P = 0.006$, and 18.0 vs. 10.2%; $P < 0.001$, respectively. In IE cancer patients, predictors of mortality by multivariate analysis were creatinine > 2 mg/dL, congestive heart failure and unperformed cardiac surgery (when indicated).

OPEN ACCESS

Edited by:
Carlo Gabriele Tocchetti, University of Naples Federico II, Italy

Reviewed by:
Zaza Iakobishvili, Clalit Health Services, Israel
Concetta Zito, University of Messina, Italy
Manuel Martínez-Sellés, Gregorio Marañón Hospital, Spain

***Correspondence:**
Bernard Cosyns
bcosyns@gmail.com

[†]*Member of the European Reference Network on Rare or low prevalence Heart diseases (ERN GUARD-HEART)*

[‡]*A complete list of the EURO-ENDO Investigators Group and of the EURO-ENDO National Coordinators is provided in* ***Appendix 1***

Specialty section:
This article was submitted to Cardio-Oncology, a section of the journal Frontiers in Cardiovascular Medicine

Received: *30 August 2021*
Accepted: *21 October 2021*
Published: *11 November 2021*

Citation:
Cosyns B, Roosens B, Lancellotti P, Laroche C, Dulgheru R, Scheggi V, Vilacosta I, Pasquet A, Piper C, Reyes G, Mahfouz E, Kobalava Z, Piroth L, Kasprzak JD, Moreo A, Faucher J-F, Ternacle J, Meshaal M, Maggioni AP, Iung B and Habib G (2021) Cancer and Infective Endocarditis: Characteristics and Prognostic Impact. Front. Cardiovasc. Med. 8:766996. doi: 10.3389/fcvm.2021.766996

Conclusions: Cancer in IE patients is common and associated with a worse outcome. This large, observational cohort provides new insights concerning the contemporary profile, management, and clinical outcomes of IE cancer patients across a wide range of countries.

Keywords: cancer, cardiac surgery, infective endocarditis, registry, valve disease

INTRODUCTION

Infective endocarditis (IE) is a severe disease, associated with important morbidity and mortality (1–4). Some IE patients have active, previously diagnosed cancer. In other patients, IE might be a marker of a new, unsuspected neoplasia (5, 6). The interplay between cancer and IE has become of increasing interest (5, 7). Cancer patients may be at higher risk for IE, because of reduced immunity (e.g., due to antineoplastic therapy), central venous lines or portal catheters (8). Moreover, the clinical presentation of IE patients with cancer could be less specific. Additionally, therapeutic options might be limited, due to frailty and a potentially higher mortality risk in case of surgery.

The ESC EORP European Endocarditis (EURO-ENDO) registry is a multicentre, prospective, observational cohort study of IE patients at hospitals in Europe and ESC-affiliated/non-affiliated countries. The aim of EURO-ENDO is to investigate the care and outcomes of IE (9). This sub-analysis sought to assess the prevalence of cancer in IE patients and to determine baseline characteristics, management, and outcomes compared to IE patients that are free of cancer.

MATERIALS AND METHODS

Study Design and Data Collection

The detailed methodology of the ESC EORP EURO-ENDO registry has been previously reported (9). Briefly, from 1 January 2016 to 31 March 2018, patients older than 18 years who presented with IE were included. Inclusion criteria were a diagnosis of definite IE (or possible IE, but considered and treated as IE) based on the ESC 2015 IE criteria (10). IE patients with previously diagnosed cancer were identified. Cancer was defined as a previous or active, solid tumor, or hematologic malignancy. Data were collected at inclusion and during hospitalization, including demographics, patient history, Charlson index, age, and comorbidities (11). Moreover, data were collected concerning clinical, biological, microbiological, and echocardiographic findings, use of other imaging techniques [computed tomography (CT) scan, 18F-FDG PET/CT, leucocyte scintigraphy], medical therapy, complications, theoretical indications for surgery and in-hospital mortality (9). This study complies with the Declaration of Helsinki. National coordinators, in conjunction with local centers managed the approvals of national or regional ethics committees or Institutional Review Boards, according to local regulations. Informed consent has been obtained from all subjects (or their legally authorized representative).

Abbreviations: CHF, Congestive heart failure; COPD, Chronic obstructive pulmonary disease; CT, Computed tomography; IE, Infective endocarditis; MI, Myocardial infarction; MRI, Magnetic resonance imaging; TIA, Transient ischemic attack; TOE, Transoesophageal echocardiography; TTE, Transthoracic echocardiography.

Data Management and Statistical Analysis

Data were collected by the collecting officers at the participating sites and entered in an online electronic case report form (CRF). Data quality was monitored by the ESC EORP Registry Project and Data management teams. Data quality control followed a data validation plan defined by the Registry Executive Committee team in collaboration with the EORP team. The first author had full access to all the study data and takes responsibility for its integrity and the data analysis. Continuous variables are expressed as mean ± standard deviation or as median and interquartile range. Comparisons among groups have been performed using Kruskall Wallis test for non-parametric data. Categorical variables are expressed as frequency and percentages. Among-group 2 × 2 comparisons were made using Pearson's Chi-squared χ^2-test or Fisher's exact test if any expected cell count was < 5. In other cases, the Monte-Carlo estimate of the exact *P*-value was used. Univariable analysis was applied to both continuous and categorical variables. Pairwise correlations between all candidate variables (variables with $P < 0.10$ in univariable) within the model were tested before proceeding to the multivariable model. In case of correlation, some criteria were not taken into account. Plots of the Kaplan–Meier curves have been used to assess survival and event-free survival. A backward multivariable Cox regression analysis has been performed to evaluate possible predictors of outcomes in cancer patients. A significance level of 0.05 was required to allow a variable to stay within the model. Some measures of model of fit have been considered: concordance and the Goodness of fit test proposed by May and Hosmer. In addition, the proportional hazard ratios assumptions were graphically verified with the Schoenfeld residuals test. All analyses were performed using SAS statistical software version 9.4 (SAS Institute, Inc., Cary, NC, USA).

RESULTS

Three thousand and eighty-five IE patients were included (12). Three hundred and fifty-nine (11.6%) IE patients with cancer were identified and compared to 2,726 (88.4%) IE patients without cancer. IE was definite in 304/359 (84.7%) and possible in 55/359 (15.3%) cancer patients. The age of and most frequent types of cancer can be found in **Supplementary Table 1**.

Patient Demographics and Characteristics

The main demographic and characteristics of IE cancer patients are displayed in **Table 1**. IE was community-acquired in 74.8% and healthcare associated in 25.2% (nosocomial in 18.6%, non-nosocomial in 6.6%), native in 209 (60.4%), prosthetic in 97 (28.0%), device-related in 30 (8.7%), and repaired valve IE in 23 (2.9%) cancer patients. There were no significant differences with the cancer-free group. Valvular IE location was aortic in 52.7%, mitral in 47.0%, tricuspid in 5.7%, pulmonary in 0.9% of IE cancer patients. IE affected two or more valvular locations in 17.9%.

Clinical and Biological Features

Clinical features are displayed in **Supplementary Table 2**. For IE cancer patients, significantly less time passed between first symptoms and first hospitalization (23.7 ± 46.4 vs. 30.1 ± 70.6 days; $P = 0.009$), as well as between first hospitalization and suspected IE (9.1 ± 20.1 vs. 9.2 ± 42.5 days; $P < 0.001$) compared to IE patients without cancer. Platelets were significantly lower in the IE cancer group (194.5 vs. 214 K/mm^3, $P < 0.001$), but otherwise there was no significant difference in biochemistry between groups (data not shown). Blood cultures were positive in 303/359 (84.4%) IE cancer patients (vs. 78.4%, $P = 0.009$). The most frequently identified microorganisms were *S. aureus* in 77/303 (25.4 vs. 31.8%, $P = 0.024$), Enterococci in 72/303 (23.8 vs. 14.8%, $P < 0.001$), and Streptococcus gallolyticus in 33/303 (10.9 vs. 5.9%, $P = 0.001$) IE cancer patients.

Imaging

Transthoracic echocardiography (TTE) was performed in 93.9% and transoesophageal echocardiography (TOE) in 82.2% IE cancer patients. There were significantly more mitral valve vegetations (39.9 vs. 34.8%, $P = 0.020$), but less tricuspid valve vegetations (5.3 vs. 10.5%, $P = 0.008$) in IE cancer patients. No significant difference in vegetation length was found between IE cancer and cancer-free groups (data not shown).

18F-FDG positron emission tomography/computed tomography was performed in 74 (20.6%) and positive in 55 IE cancer patients. There was 69.1% extra-cardiac uptake, vs. 54.3% in cancer-free IE patients ($P = 0.042$). On multislice CT, there was significantly more perivalvular abscess formation in IE cancer compared to cancer-free IE patients (78.6 vs. 50.5%, $P = 0.049$).

In-hospital and One-Year Follow-Up Under Treatment

The main in-hospital complications are shown in **Supplementary Table 3**.

Acute renal failure was the most frequent in hospital complication in IE cancer patients, followed by embolic events and congestive heart failure (CHF).

After 1 year, there was no significant difference in IE recurrence rate ($P = 0.243$) or other complications between groups.

Cancer IE patients were significantly more treated with amoxicillin (35.8 vs. 26.3%; $P < 0.001$), ceftriaxone (36.3 vs. 31.1%; $P = 0.047$) and daptomycin (15.2 vs. 10.6%; $P = 0.010$), but less frequently treated with vancomycin (34.6 vs. 44.9%, $P < 0.001$) compared to cancer-free IE patients.

Following ESC guidelines, theoretical indication for cardiac surgery was not significantly different between both groups (65.5 vs. 69.8%, $P = 0.091$), but was effectively less performed when indicated in IE cancer patients during hospitalization (65.5 vs. 75.0%, $P = 0.002$). The most frequent surgical indication in both groups was infectious (57.4 vs. 64.9%, $P = 0.018$). Reasons for not performing surgery in IE cancer patients were most frequently the surgical risk (80.2 vs. 54.0%, $P < 0.001$), death before surgery (17.3 vs. 22.9%, $P = 0.260$) and patient refusal (16.0 vs. 19.3%, $P = 0.486$), among others.

Death occurred in hospital in 84 (23.4 vs. 16.1%, $P < 0.001$) and at 1-year follow-up in 43 additional IE cancer patients (18.0 vs. 10.2%; $P < 0.001$). Causes of all-cause in-hospital and 1-year mortality are reported in **Tables 2**, **3**, respectively. Predictors of in hospital and 1-year mortality by univariate Cox regression analysis can be found in **Supplementary Tables 4, 5**, respectively. Predictors of in hospital and 1-year mortality by multivariable analysis in IE cancer patients are shown in **Table 4** and **Supplementary Table 6**, respectively.

Kaplan-Meier survival curves for in hospital and 1-year all-cause mortality according to cancer and adjusted for surgery are shown in **Figures 1**, **2**.

DISCUSSION

The following key findings arise from the EURO-ENDO analysis regarding cancer in IE patients: 1. Cancer is common in IE patients with a prevalence of 11.6%. 2. IE cancer patients are significantly older, receive more long-term immune-suppressive treatment and have more IV catheters. 3. The most frequently identified microorganisms are *S. aureus* and Enterococci. The source of infection is mainly community-acquired and preceded by non-dental procedures. 4. In hospital and long-term mortality is significantly increased and often related to the neoplasia. 5. Theoretical indication for cardiac surgery is not significantly different, but surgery is significantly less performed when indicated in IE cancer patients compared to IE patients without cancer.

Demographics, Clinical and Microbiological Characteristics of IE Cancer Patients

Cancer is common in IE patients, with a prevalence of 11.6%. Preceding studies have shown a similar prevalence ranging from 5.6 to 17.6% (6, 8). Prostate- and intestinal neoplasms were found most frequently, which is consistent with previous reports (6, 7). The older age of IE cancer patients has been consistently reported in other series (6, 8, 12). IE cancer patients were more often males, as in the cancer-free group. One study found a slightly significant male predominance in IE cancer patients (6), while another was in agreement with this cohort (8). No gender-based differences were found.

IE cancer patients more often had a history of arterial hypertension, ischemic disease, aortic valve stenosis, atrial

TABLE 1 | Demographics and clinical characteristics of infective endocarditis patients.

	Total	IE + cancer	IE – cancer	*P*-value
Demography				
N	3,085	359	2,726	
Age (years)				
Mean ± SD	59.21 ± 18.06	70.33 ± 11.47	57.74 ± 18.26	<0.001
Median (IQR)	63.0 (46.0–73.0)	72.0 (64.0–79.0)	61.0 (43.0–72.0)	<0.001
< 65 years old	1,655/3,085 (53.6%)	90/359 (25.1%)	1,565/2,726 (57.4%)	<0.001
65–80 years old	1,060/3,085 (34.4%)	191/359 (53.2%)	869/2,726 (31.9%)	
≥80 years old	370/3,085 (12.0%)	78/359 (21.7%)	292/2,726 (10.7%)	
Females (%)	961/3,085 (31.2%)	110/359 (30.6%)	851/2,726 (31.2%)	0.824
History of cardiovascular diseases				
Heart failure	652/2,809 (23.2%)	75/307 (24.4%)	577/2,502 (23.1%)	0.592
Congenital heart disease	362/3,083 (11.7%)	11/359 (3.1%)	351/2,724 (12.9%)	<0.001
Ischemic heart disease	613/2,866 (21.4%)	89/318 (28.0%)	524/2,548 (20.6%)	0.002
Atrial fibrillation	756/2,887 (26.2%)	113/323 (35.0%)	643/2,564 (25.1%)	<0.001
Hypertrophic cardiomyopathy	63/2,809 (2.2%)	4/307 (1.3%)	59/2,502 (2.4%)	0.239
Known valve murmur	955/2,809 (34.0%)	97/307 (31.6%)	858/2,502 (34.3%)	0.347
Previous endocarditis (%)	271/3,085 (8.8%)	33/359 (9.2%)	238/2,726 (8.7%)	0.772
Device therapy	532/3,085 (17.2%)	80/359 (22.3%)	452/2,726 (16.6%)	0.007
History of valve disease				
Aortic valve stenosis	375/2,608 (14.4%)	52/277 (18.8%)	323/2,331 (13.9%)	0.028
Aortic valve surgery	793/3,085 (25.7%)	101/359 (28.1%)	692/2,726 (25.4%)	0.263
Mitral valve surgery	376/3,085 (12.2%)	40/359 (11.1%)	336/2,726 (12.3%)	0.519
Risk factors				
Previous stroke/TIA	337/2,832 (11.9%)	51/312 (16.3%)	286/2,520 (11.3%)	0.010
Previous pulmonary embolism	64/2,802 (2.3%)	14/307 (4.6%)	50/2,495 (2.0%)	0.005
Arterial hypertension	1,483/3,081 (48.1%)	217/358 (60.6%)	1,266/2,723 (46.5%)	<0.001
Previous hemorrhagic events	128/2,802 (4.6%)	23/305 (7.5%)	105/2,497 (4.2%)	0.008
COPD/asthma	315/3,081 (10.2%)	48/358 (13.4%)	267/2,723 (9.8%)	0.034
Chronic renal failure	544/3,083 (17.6%)	79/359 (22.0%)	465/2,724 (17.1%)	0.021
Dialysis	160/544 (29.4%)	15/79 (19.0%)	145/465 (31.2%)	0.028
HIV	31/3,011 (1.0%)	2/349 (0.6%)	29/2,662 (1.1%)	0.572
Hypo/hyperthyroidism	224/2,792 (8.0%)	33/306 (10.8%)	191/2,486 (7.7%)	0.060
Chronic autoimmune disease	106/3,075 (3.4%)	15/357 (4.2%)	91/2,718 (3.3%)	0.406
Current pregnancy	8/3,062 (0.3%)	1/358 (0.3%)	7/2,704 (0.3%)	>0.999
Smoking	750/2,911 (25.8%)	73/330 (22.1%)	677/2,581 (26.2%)	0.108
Intravenous drug dependency	212/3,038 (7.0%)	3/354 (0.8%)	209/2,684 (7.8%)	<0.001
Alcohol abuse	223/2,974 (7.5%)	23/349 (6.6%)	200/2,625 (7.6%)	0.493
Immunosuppressive treatment	104/2,809 (3.7%)	36/307 (11.7%)	68/2,502 (2.7%)	<0.001
Long corticotherapy	126/2,809 (4.5%)	28/307 (9.1%)	98/2,502 (3.9%)	<0.001
Intravenous catheter	248/3,074 (8.1%)	53/358 (14.8%)	195/2,716 (7.2%)	<0.001
Charlson index mean ± SD	3.48 ± 2.92	6.16 ± 3.35	3.13 ± 2.67	<0.001
Antithrombotic treatment on admission	1,686/2,977 (56.6%)	217/340 (63.8%)	1,469/2,637 (55.7%)	0.005
Other non-cardiac intervention				
Colonoscopy	90/2,710 (3.3%)	24/295 (8.1%)	66/2,415 (2.7%)	<0.001
Gastrointestinal intervention	102/3,025 (3.4%)	26/351 (7.4%)	76/2,674 (2.8%)	<0.001
Urogenital intervention	87/3,026 (2.9%)	28/352 (8.0%)	59/2,674 (2.2%)	<0.001
Dental procedure	224/2,849 (7.9%)	16/329 (4.9%)	208/2,520 (8.3%)	0.032

COPD, Chronic obstructive pulmonary disease; HIV, Human Immunodeficiency Virus; IE, Infective endocarditis; TIA, Transient ischemic attack.

TABLE 2 | In-hospital mortality in infective endocarditis patients.

	Total (n = 3,085)	IE + cancer (n = 359)	IE – cancer (n = 2,726)	*P*-value
Death	524/3,085 (17.0%)	84/359 (23.4%)	440/2,726 (16.1%)	<0.001
Cause of death				
Cardiovascular	149/523 (28.5%)	15/84 (17.9%)	134/439 (30.5%)	0.067
Non-cardiovascular	155/523 (29.6%)	25/84 (29.8%)	130/439 (29.6%)	
Cardiovascular + Non-cardiovascular	190/523 (36.3%)	39/84 (46.4%)	151/439 (34.4%)	
Unknown	29/523 (5.5%)	5/84 (6.0%)	24/439 (5.5%)	
If cardiovascular:				
Heart failure	239/339 (70.5%)	40/54 (74.1%)	199/285 (69.8%)	0.530
Arrhythmia	41/339 (12.1%)	3/54 (5.6%)	38/285 (13.3%)	0.108
Cardiac perforation/tamponade	11/339 (3.2%)	4/54 (7.4%)	7/285 (2.5%)	0.080
Acute MI	7/339 (2.1%)	2/54 (3.7%)	5/285 (1.8%)	0.309
Cerebral embolism	41/339 (12.1%)	4/54 (7.4%)	37/285 (13.0%)	0.249
Pulmonary embolism	13/339 (3.8%)	0/54 (0.0%)	13/285 (4.6%)	0.236
Peripheral embolism	3/339 (0.9%)	0/54 (0.0%)	3/285 (1.1%)	>0.999
If non-cardiovascular:				
Neoplasia	12/345 (3.5%)	11/64 (17.2%)	1/281 (0.4%)	<0.001
Sepsis	265/345 (76.8%)	38/64 (59.4%)	227/281 (80.8%)	<0.001

MI, Myocardial infarction.

TABLE 3 | One-year mortality in infective endocarditis patients.

	Total (n = 3,085)	IE + cancer (n = 359)	IE – cancer (n = 2,726)	*P*-value
Death	233/2,108 (11.1%)	43/239 (18.0%)	190/1,869 (10.2%)	<0.001
Cause of death				
Cardiovascular	57/233 (24.5%)	6/43 (14.0%)	51/190 (26.8%)	0.240
Non-cardiovascular	65/233 (27.9%)	16/43 (37.2%)	49/190 (25.8%)	
Cardiovascular + Non-cardiovascular	49/233 (21.0%)	9/43 (20.9%)	40/190 (21.1%)	
Unknown	62/233 (26.6%)	12/43 (27.9%)	50/190 (26.3%)	
If cardiovascular:				
Heart failure	74/106 (69.8%)	9/15 (60.0%)	65/91 (71.4%)	
Arrhythmia	9/106 (8.5%)	3/15 (20.0%)	6/91 (6.6%)	
Cardiac perforation/tamponade	1/106 (0.9%)	0/15 (0.0%)	1/91 (1.1%)	
Acute MI	7/106 (6.6%)	1/15 (6.7%)	6/91 (6.6%)	
Cerebral embolism	7/106 (6.6%)	2/15 (13.3%)	5/91 (5.5%)	
Pulmonary embolism	5/106 (4.7%)	1/15 (6.7%)	4/91 (4.4%)	
Peripheral embolism	1/106 (0.9%)	0/15 (0.0%)	1/91 (1.1%)	
Other cardiovascular	27/106 (25.5%)	1/15 (6.7%)	26/91 (28.6%)	
If non-cardiovascular:				
Neoplasia	22/114 (19.3%)	15/25 (60.0%)	7/89 (7.9%)	
Sepsis	60/114 (52.6%)	7/25 (28.0%)	53/89 (59.6%)	
Other	41/114 (36.0%)	6/25 (24.0%)	35/89 (39.3%)	

MI, Myocardial infarction.

fibrillation and previous stroke, probably due to older age. There exists an overlap between cancer and cardiovascular disease, with shared biological mechanisms, risk factors and genetic predisposition (13). Cancer patients had a less typical clinical presentation with significantly less fever and new heart murmur compared to cancer-free IE patients. Nevertheless, cancer patients were hospitalized and diagnosed significantly faster, probably due to close follow-up care. There was no significant difference in embolic events at admission between groups, despite significant more antithrombotics use in IE cancer

patients. This was probably compensated by the older age and prothrombogenic status in the cancer group.

IE could be a consequence of cancer management, as immunosuppressive therapy, intravenous access and portal catheters were significantly more present in the IE cancer subpopulation, as previously described (6). Nevertheless, the source of infection was mainly community-acquired in this cohort, and comparable to the cancer-free population (74.8 vs. 74.2%, $P = 0.06$). In contrast, previous studies had reported increased nosocomial IE in cancer patients, but the reason for this discrepancy is unclear (6–8, 14). The most frequent preceding non-cardiac interventions performed in IE cancer patients within the last 6 months were non-dental: urogenital and intestinal (including colonoscopy), as previously reported (6, 8). The significantly higher burden of enterococcal IE might be related to the portal of entry, but also to increased age, as seen in the general population (8, 15). As reported in previous studies, *S. aureus* remained the most frequent causative organism (6, 8). These results, combined with low oral Streptococci (8.9 vs. 12.9%, $P = 0.05$) in blood cultures [compared to the general population in the EuroHeart Survey (15%) (16), the 2008 French registry (20.6%) (10), and the International Collaboration on Endocarditis-Prospective Cohort Study (17%)

TABLE 4 | Multivariate Cox regression analysis for in hospital all-cause mortality (1-month period) in IE cancer patients.

	Hazard ratio	95% CI	*P*-value*
Creatinine > 2 mg/dl	2.34	[1.29–4.25]	0.005
Chronic Heart Failure	2.16	[1.18–3.95]	0.013
Surgery: Indication – not performed	2.41	[1.20–4.81]	0.013
Surgery: Indication – performed	0.56	[0.25–1.24]	0.151

Goodness of Fit test: P = 0.50. Concordance = 0.74 – Global Schoenfeld residual test P = 0.21.

**P-value corresponds to the results of the Wald test. For indication – surgery performed, the reference is: no indication.*

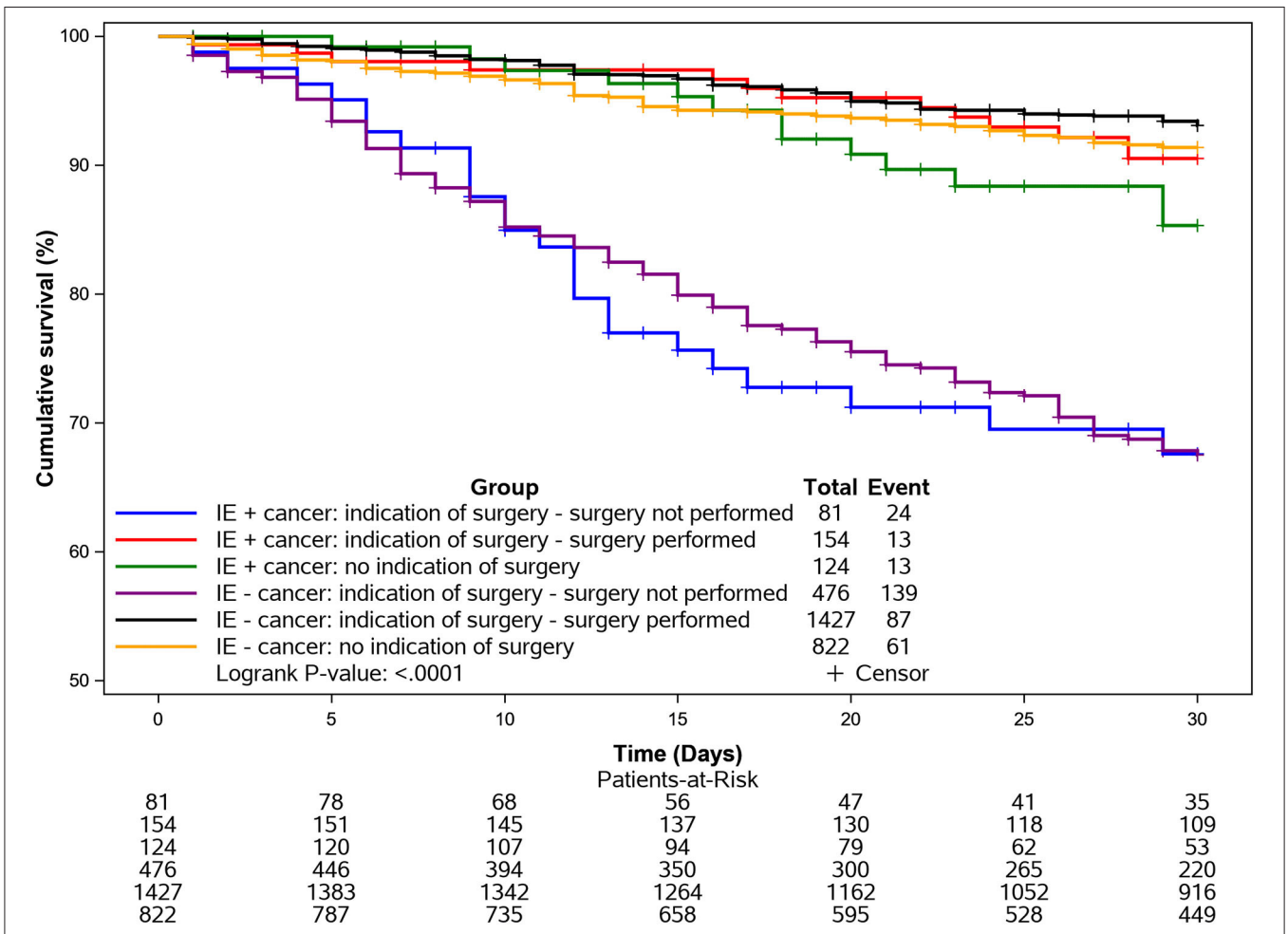

FIGURE 1 | Kaplan-Meier curves for in hospital mortality (1-month) according to cancer and surgery. Mortality was particularly elevated in the IE cancer group when surgery was indicated but not performed.

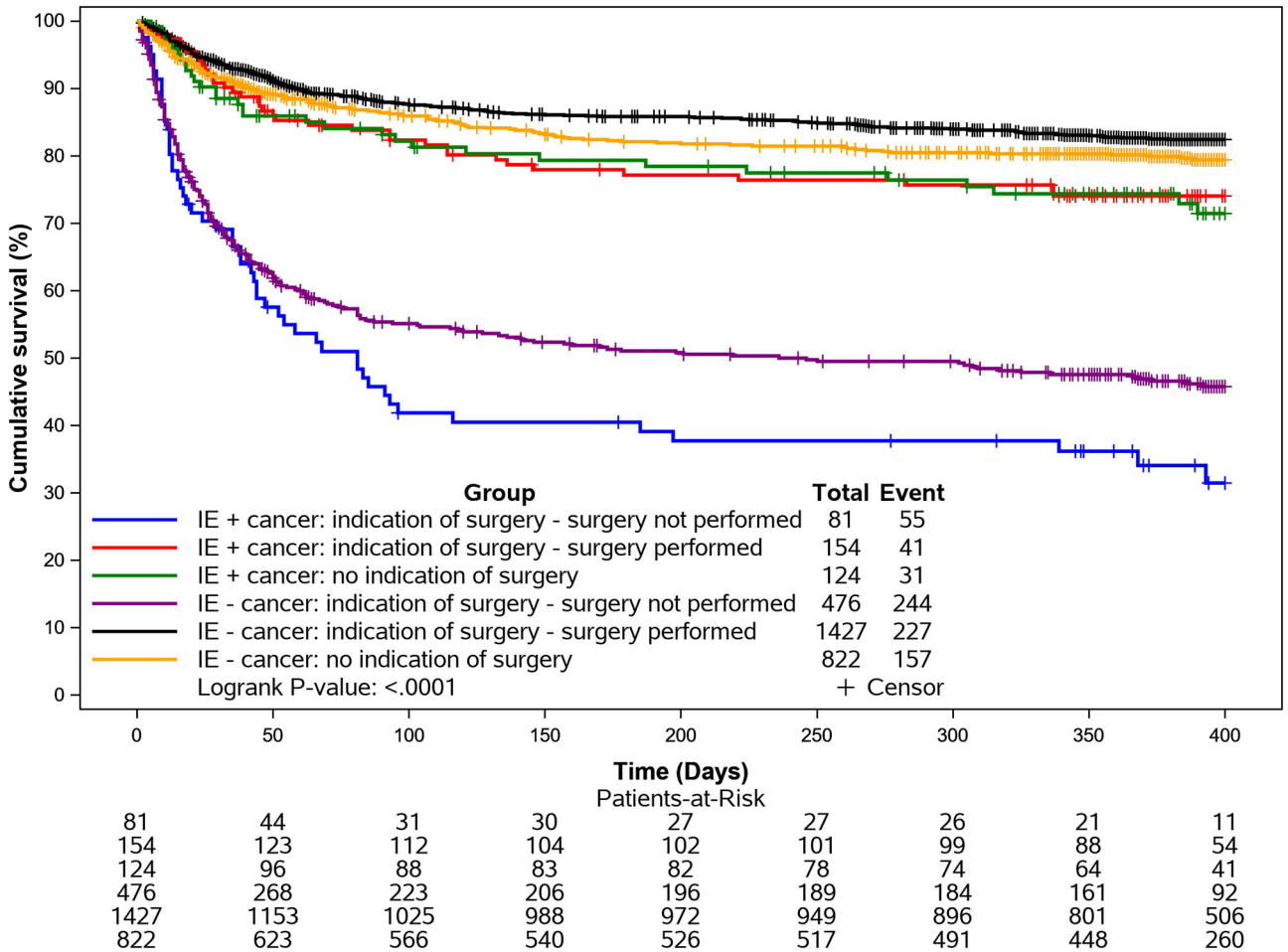

FIGURE 2 | Kaplan-Meier curves for 1-year mortality according to cancer and surgery. Mortality was particularly elevated in the IE cancer group when surgery was indicated but not performed.

(3)], reinforce the recommendations of the 2015 ESC guidelines regarding the restriction of the use of antibiotic prophylaxis to high risk populations undergoing at-risk dental procedures (10). Conversely, there might be opportunities for IE prevention in invasive urogenital and gastrointestinal procedures in cancer patients (8).

About 16% of cancer patients had culture-negative endocarditis, which is lower than previously reported, but not significantly different compared to the non-cancer group (8, 17). In these cases, non-bacterial thrombotic endocarditis could not be ruled out.

Imaging

The transformation in the use of imaging techniques observed in the EURO-ENDO population since the publication of the 2015 ESC guidelines was similarly applicable for IE cancer patients (12). 18F-FDG PET/CT showed more extracardiac liver uptake in IE cancer patients compared to non-cancer patients. Unfortunately, it's difficult to differentiate between metastatic lesions, inflammatory foci and embolic lesions related to IE.

Management and Outcome of IE in Cancer Patients

Surgery

Surgery was performed in ∼50% of patients, similar to previous surveys (3, 16). Bioprosthetic valves were used in most IE cancer patients (aortic bioprosthesis: 76.3 vs. mechanical 14.0%; mitral bioprosthesis: 41.5 vs. mechanical 18.5%): more than in non-cancer patients (aortic bioprosthesis: 56.2%, $P < 0.001$; mitral bioprosthesis: 37.2%, $P = 0.003$) and much higher than observed in the Euro heart survey, in which mechanical prosthesis were more prominent (74%). This change might be related to older age, the possible need for further surgical procedures and to an increased risk of bleeding in some neoplasms (18). Mitral valve repair techniques were also more frequently used in cancer compared to non-cancer IE patients (40 vs. 23.4%; $P = 0.003$). This might be explained by a selection bias in the IE cancer group that was accepted for surgery, with a lower operative risk and less valvular destruction (19). Indication for surgery during hospitalization was comparable in cancer vs. non-cancer IE patients. However, when indicated, cardiac surgery was

effectively less often performed in cancer compared to cancer-free IE patients. Patients of both groups were mainly denied because of high surgical risk or a significant delay leading to death before surgery.

Complications

Acute renal failure was the most frequent complication, followed by embolic events and CHF in IE cancer patients. The older IE cancer group had significantly more underlying chronic renal failure.

There was a significant lower incidence of pulmonary embolism in cancer IE patients. This might be explained by reduced IV drug abuse and less tricuspid valve vegetations in the IE cancer group, as well as a higher proportion of antithrombotic treatment. Nevertheless, this was not reflected by a significant reduction in other embolic events between groups at admission or during hospitalization.

CHF and cardiogenic shock occurred significantly more frequently in IE cancer patients, possibly due to the presence of more cardiovascular disease and frailty in this older population.

In-hospital and 1-Year Mortality

In-hospital and long-term all-cause mortality was significantly increased in IE cancer patients compared to the non-cancer population. However, there was no significant difference in cardiovascular death between groups. A main driver of all-cause mortality in cancer patients was the neoplasia, especially at 1-year follow-up. This might be explained by the necessity to interrupt the cancer treatment due to IE, as noted in previous studies (6, 8). Mortality was particularly elevated in the IE cancer group when surgery was indicated but not performed, emphasizing the need for early discussion with surgeons within the IE team, as recommended by the ESC guidelines (19).

Study Limitations

This sub-analysis has the same inherent limitations as the EURO-ENDO registry, particularly selection bias as the majority of patients (88.2%) were enrolled in high-level centers in western Europe. Moreover, the study is unlikely to be a true population-based sample, as it was based on voluntary participation and thus it is unsure whether all centers included their patients consecutively and prospectively (12). As a consequence, the true prevalence of cancer in IE patients remains uncertain. As this study was selected from IE patients and not cancer patients, we are also unable to provide incidence data on IE in cancer patients. Moreover, all cancer types might not be appropriately represented, details are missing about cancer characteristics (history, stage, active, or previous treatment) and further investigations are warranted in the occurrence of IE in solid vs. non-solid (e.g., hematological) malignancies, as well as the proportion of metastatic cancer which could influence mortality (8). Moreover, the influence of cancer treatment cessation on mortality should also be taken into consideration. The reason for denial of surgery should be more thoroughly investigated in future studies of IE cancer patients. Clinical reasons could range from a high age, frailty, comorbidities, expected poor prognosis from the underlying malignancy to significant immunosuppression which might render surgery either futile or risky. Moreover, the valvular heart disease guidelines are not specifically written for patients with co-existent malignancies.

As cancer plays a major ponderation in the Charlson score, a sub analysis using an adjusted Charlson score excluding cancer is merited. Additionally, data regarding the occurrence of newly discovered cancer in IE patients, e.g., colon cancer diagnosed by colonoscopy, is absent in this registry. It has been suggested that IE could be an early marker or consequence of occult cancer, particularly that of gastrointestinal or urinary origin (6, 7, 20). Finally, it would be of interest to relate preceding invasive procedures for different types of solid cancers to the bacterial etiologies of IE. These limitations were counterbalanced by the high number of enrolled patients, the quality of CRF completion, and representation of a wide range of both university and non-academic hospitals in many countries around the world.

CONCLUSION

This is a large, observational cohort of IE patients with cancer. It provides new insights concerning the contemporary profile, management and clinical outcomes of IE cancer patients. Given the paucity of randomized and large-scale observational data in IE patients with cancer, this registry offers a unique perspective on the current care of IE cancer patients across a wide range of countries.

DATA AVAILABILITY STATEMENT

The original contributions presented in the study are included in the article/**Supplementary Materials**, further inquiries can be directed to the corresponding author.

ETHICS STATEMENT

The studies involving human participants were reviewed and approved by Argentina: Comité de Ética de la Investigación, Hospital Italiano de la Plata; Comité de Ética en Investigación, Hospital El Cruce, Florencio Varela; Comite de Investigaciones Médicas, Instituto de Cardiologia de Corrientes JF Cabral; Belgium: Comité d'Ethique hospitalo-facultaire, Université Catholique de Louvain; Comité Local d'Ethique Hospitalier (O.M. 007), Centre Hospitalier Universitaire Saint Pierre, Bruxelles; Commissie Medische Ethiek (O.G. 016), Universitair Ziekenhuis Brussel; Brazil: Comitê de Ética em Pesquisa da Universidade Federal de São Paulo; Comitê de Ética em Pesquisa do Hospital de Messejana, Fortaleza; Comitê de Ética em Pesquisa do Hospital Israelita Albert Einstein, São Paulo; Comitê de Ética em Pesquisa, Faculdade de Medicina de Marília; Comitê de Ética em Pesquisa, Instituto de Cardiologia, Fundacão Universitaria de Cardiologia, Porto Alegre; Comitê de Ética em Pesquisa, Universidad Federal de Minas Gerais; Canada: Comité d'éthique de la recherche de l'Institut Universitaire de Cardiologie et de Pneumologie de Québec, Université Laval; Comité d'éthique de la recherche du

Centre Intégré Universitaire de Santé et de Services Sociaux du Nord-de-l'Île-de-Montréal; Czech Republic: Etická komise, Fakultní nemocnice Hradec Králové; Etická komise, Všeobecné fakultní nemocnice v Praze; France: Direction générale de la recherche et de l'innovation, Comité Consultatif sur le traitement de l'information en matière de Recherche dans le domaine de la Santé; Germany: Ethik-Kommission an der Medizinishen Fakultät der Universität Leipzig; Ethikkommission der Universität Leipzig, Ethikkommission der Medizinischen Fakultät des Ruhr-Universität Bochum; Ethikkommission der Universität Leipzig, Ethik-Kommission des FB Medizin; Greece: Laiko General Hospital Managing Committee, Athens; Scientific Council of the University Hospital of Ioannina; India: Medanta Instututional Ethics Committee, Medanta the Medicity, Gurgon; Sengupta Hospital & Research Institute Ethics Committee; Iran: University/Regional Research Ethics Committee, Rajaie Cardiovascular Medical and Research Center; Italy: Comitato Etico Campania Sud, Azienda Sanitaria Locale Napoli 3 Sud; Comitato Etico dell'Ospedale San Raffaele, Istituto di Ricovero e Cura a Carattere Scientifico, Milano; Comitato Etico Milano Area 3, Azienda Socio Sanitaria Territoriale Grande Ospedale Metropolitano Niguarda; Comitato Etico Provinciale, Azienda Ospedaliero-Universitaria di Modena; Comitato Etico Regionale per la Sperimentazione Clinica della Provincia di Padova,; Comitato Etico Regionale per la Sperimentazione Clinica della Toscana, Area Vasta Centro, Azienda Ospedaliero-Universitaria Careggi Firenze; Comitato Etico Regionale per la Sperimentazione Clinica della Toscana, Area Vasta Sud Est, Azienda Ospedaliero-Universitaria Senese; Japan: Nagoya City University Internal Review Board for Clinical Studies; Korea: Institutional Review Board, Asan Medical Center; Institutional Review Board, Samsung Medical Center, Seoul; Lithuania: Lietuvos Bioetikos Komitetas, National Ethics Committee, Vilnius; Moldova: Comitetului de Etica a Cercetarii, N.Testemitanu, State University of Medicine and Pharmacy, Chisinau; Netherlands: Medical Ethics Review Committee of VU University Medical Center, Amsterdam; Portugal: Comissão Nacional de Protecção de Dados, Comissão de Ética para Saude de Centro Hospitalar Universitário de Lisboa Central; Romania: Comisia de Etica a Institutului Inimii de Urgenta pentru Boli Cardiovasculare Niculae Stancioiu, Cluj-Napoca; Comisia de Etica in Cercetare-Dezvoltare, Institutului de Boli Cardiovasculare, University of Medicine & Pharmacy, Timisoara; Russia: Local Ethics Committee City Clinical Hospital (named after V. V. Vinogradov), City Clinical Hospital 64 Moscow; Serbia: Etičkog odbora KBC Zemun, Clinical Hopital Center Zemun, Belgrade; Singapore: National Healthcare Group Domain Specific Review Board, National University Heart Centre Singapore; Spain: Comite de Etica de la Investigation Del Hospital Univesitario Ramon Y Cajal; Comité Ético de Investigación Clínica de Cantabria; Comité Ético de Investigación Clínica de Euskadi; Comité Ético de Investigación Clínica del Hospital Clínico de Barcelona; Comité Ético de Investigación Clínica del Hospital Universitari de Tarragona; Comité Ético de Investigación Clínica del Hospital Universitari Vall d'Hebron de Barcelona; Turkey: Baskent University Institutional Review Board and Ethics Committee, Ankara; United Arab Emirates: Dubai Scientific Research Ethics Committee; United Kingdom: London-Chelsea Research Ethics Committee; United States: IRB #1 Washington, MedStar Heart and Vascular Institute, Washington Hospital Center. The patients/participants provided their written informed consent to participate in this study.

AUTHOR CONTRIBUTIONS

All authors listed have made a substantial, direct and intellectual contribution to the work, and approved it for publication.

FUNDING

This work was supported by Abbott Vascular Int. (2011–2021), Amgen Cardiovascular (2009–2018), AstraZeneca (2014–2021), Bayer AG (2009–2018), Boehringer Ingelheim (2009–2019), Boston Scientific (2009–2012), the Bristol Myers Squibb and Pfizer Alliance (2011–2019), Daiichi Sankyo Europe GmbH (2011–2020), the Alliance Daiichi Sankyo Europe GmbH and Eli Lilly and Company (2014–2017), Edwards (2016–2019), Gedeon Richter Plc. (2014–2016), Menarini Int. Op. (2009–2012), MSD-Merck & Co. (2011–2014), Novartis Pharma AG (2014–2020), ResMed (2014–2016), Sanofi (2009–2011), SERVIER (2009–2021), and Vifor (2019–2022).

ACKNOWLEDGMENTS

EORP Oversight Committee, Registry Executive and Steering Committees. The Data collection was conducted by the EORP department of the ESC: Emanuela Fiorucci, as Project Officer; Viviane Missiamenou, Florian Larras, and Rachid Mir Hassaine, as Data Managers. Statistical analyses were performed by Cécile Laroche of the EURObservational Research Programme, European Society of Cardiology, Sophia-Antipolis, France. Overall activities were coordinated and supervised by AM (EORP Scientific Coordinator). Special thanks to the EACVI (European Association of Cardio Vascular Imaging) and to the ESC Working Group on Valvular Heart Disease for their support.

SUPPLEMENTARY MATERIAL

The Supplementary Material for this article can be found online at: https://www.frontiersin.org/articles/10.3389/fcvm.2021.766996/full#supplementary-material

REFERENCES

1. Habib G. Management of infective endocarditis. *Heart*. (2006) 92:124–30. doi: 10.1136/hrt.2005.063719
2. Murdoch DR, Corey RG, Hoen B, Miró M, Fowler VG, Bayer AS, et al. Clinical presentation, etiology, and outcome of infective endocarditis in the 21st century The international collaboration on endocarditis-prospective cohort study. *Arch Intern Med*. (2009) 169:463–73. doi: 10.1001/archinternmed.2008.603
3. San Román JA, López J, Vilacosta I, Luaces M, Sarriá C, Revilla A, et al. Prognostic stratification of patients with left-sided endocarditis determined at admission. *Am J Med*. (2007) 120:369.e1–7. doi: 10.1016/j.amjmed.2006.05.071
4. Chu VH, Cabell CH, Benjamin DK, Kuniholm EF, Fowler VG, Engemann J, et al. Early predictors of in-hospital death in infective endocarditis. *Circulation*. (2004) 109:1745–9. doi: 10.1161/01.CIR.0000124719.61827.7F
5. Thomsen RW, Farkas DK, Friis S, Sværke C, Ording AG, Nørgaard M, et al. Endocarditis and risk of cancer: a danish nationwide cohort study. *Am J Med*. (2013) 126:58–67. doi: 10.1016/j.amjmed.2012.07.026
6. Fernández-Cruz A, Muñoz P, Sandoval C, Fariñas C, Gutiérrez-Cuadra M, Pericás Pulido JM, et al. Infective endocarditis in patients with cancer: a consequence of invasive procedures or a harbinger of neoplasm?: a prospective, multicenter cohort. *Medicine*. (2017) 96:e7913. doi: 10.1097/MD.0000000000007913
7. García-Albéniz X, Hsu J, Lipsitch M, Logan RW, Hernández-Díaz S, Hernán MA. Infective endocarditis and cancer in the elderly. *Eur J Epidemiol*. (2016) 31:41–9. doi: 10.1007/s10654-015-0111-9
8. Kim K, Kim D, Lee SE, Cho IJ, Shim CY, Hong GR, et al. Infective endocarditis in cancer patients - causative organisms, predisposing procedures, and prognosis differ from infective endocarditis in non-cancer patients. *Circ J*. (2019) 83:452–60. doi: 10.1253/circj.CJ-18-0609
9. Habib G, Lancellotti P, Erba PA, Sadeghpour A, Meshaal M, Sambola A, et al. The ESC-EORP EURO-ENDO (European Infective Endocarditis) registry. *Eur Hear J Qual Care Clin Outcomes*. (2019) 5:202–7. doi: 10.1093/ehjqcco/qcz018
10. Habib G, Lancellotti P, Antunes MJ, Grazia Bongiorni M, Casalta JP, Del Zotti F, et al. ESC Guidelines 2015 ESC Guidelines for the management of infective endocarditis The Task Force for the Management of Infective Endocarditis of the European Society of Cardiology (ESC) endorsed by: European Association for Cardio-Thoracic Surgery (EACTS). *Eur Heart J*. 36: 3075–128. doi: 10.1093/eurheartj/ehv319
11. Charlson M, Szatrowski TP, Peterson J, Gold J. Validation of a combined comorbidity index. *J Clin Epidemiol*. (1994) 47:1245–51. doi: 10.1016/0895-4356(94)90129-5
12. Habib G, Erba PA, Iung B, Donal E, Cosyns B, Laroche C, et al. Clinical presentation, aetiology and outcome of infective endocarditis. Results of the ESC-EORP EURO-ENDO (European Infective Endocarditis) registry: a prospective cohort study. *Eur Heart J*. (2019) 40:3222–32B. doi: 10.1093/eurheartj/ehz620
13. Sturgeon KM, Deng L, Bluethmann SM, Zhou S, Trifiletti DM, Jiang C, et al. A population-based study of cardiovascular disease mortality risk in US cancer patients. *Eur Heart J*. (2019) 40:3889–97. doi: 10.1093/eurheartj/ehz766
14. Delahaye F, M'Hammedi A, Guerpillon B, De Gevigney G, Boibieux A, Dauwalder O, et al. Systematic search for present and potential portals of entry for infective endocarditis. *J Am Coll Cardiol*. (2016) 67:151–8. doi: 10.1016/j.jacc.2015.10.065
15. Hubert S, Thuny F, Resseguier N, Giorgi R, Tribouilloy C, Le Dolley Y, et al. Prediction of symptomatic embolism in infective endocarditis: construction and validation of a risk calculator in a multicenter cohort. *J Am Coll Cardiol*. (2013) 62:1384–92. doi: 10.1016/j.jacc.2013.07.029
16. Habib G, Badano L, Tribouilloy C, Vilacosta I, Zamorano JL, Galderisi M, et al. Recommendations for the practice of echocardiography in infective endocarditis. *Eur J Echocardiogr*. (2010) 11:202–19. doi: 10.1093/ejechocard/jeq004
17. Cahill TJ, Prendergast BD. Infective endocarditis. *Lancet*. 387:882–93. doi: 10.1016/S0140-6736(15)00067-7
18. Tornos P, Iung B, Permanyer-Miralda G, Baron G, Delahaye F, Gohlke-Bärwolf C, et al. Infective endocarditis in Europe: lessons from the Euro Heart Survey. *Heart*. (2005) 91:571–5. doi: 10.1136/hrt.2003.032128
19. Bannay A, Hoen B, Duval X, Obadia JF, Selton-Suty C, Le Moing V, et al. The impact of valve surgery on short- and long-term mortality in left-sided infective endocarditis: do differences in methodological approaches explain previous conflicting results? *Eur Heart J*. (2011) 32:2003–15. doi: 10.1093/eurheartj/ehp008
20. Sun LM, Wu JN, Lin CL, Day JD, Liang JA, Liou LR, et al. Infective endocarditis and cancer risk a population-based cohort study. *Medicine*. (2016) 95:e3198. doi: 10.1097/MD.0000000000003198

Conflict of Interest: BI reports personal fees from Edwards Lifesciences, other from Boehringer Ingelheim outside the submitted work. AM reports personal fees from Bayer, personal fees from Fresenius, personal fees from Novartis outside the submitted work.

The remaining authors declare that the research was conducted in the absence of any commercial or financial relationships that could be construed as a potential conflict of interest.

frontiers in Cardiovascular Medicine

REVIEW
published: 19 November 2021
doi: 10.3389/fcvm.2021.758010

Tyrosine Kinase Inhibitors-Induced Arrhythmias: From Molecular Mechanisms, Pharmacokinetics to Therapeutic Strategies

Mengfei Cheng[1†], Fang Yang[2†], Jiahui Liu[1†], Dan Yang[3], Shuo Zhang[1], Yang Yu[1], Shuai Jiang[1] and Mei Dong[1*]*

[1] Department of Pharmacy, Harbin Medical University Cancer Hospital, Harbin, China, [2] The First Department of Respiratory Medical Oncology, Harbin Medical University Cancer Hospital, Harbin, China, [3] Department of Clinical Laboratory, Harbin Medical University Cancer Hospital, Harbin, China

With the development of anti-tumor drugs, tyrosine kinase inhibitors (TKIs) are an indispensable part of targeted therapy. They can be superior to traditional chemotherapeutic drugs in selectivity, safety, and efficacy. However, they have been found to be associated with serious adverse effects in use, such as myocardial infarction, fluid retention, hypertension, and rash. Although TKIs induced arrhythmia with a lower incidence than other cardiovascular diseases, much clinical evidence indicated that adequate attention and management should be provided to patients. This review focuses on QT interval prolongation and atrial fibrillation (AF) which are conveniently monitored in clinical practice. We collected data about TKIs, and analyzed the molecule mechanism, discussed the actual clinical evidence and drug-drug interaction, and provided countermeasures to QT interval prolongation and AF. We also pooled data to show that both QT prolongation and AF are related to their multi-target effects. Furthermore, more than 30 TKIs were approved by the FDA, but most of the novel drugs had a small sample size in the preclinical trial and risk/benefit assessments were not perfect, which led to a suspension after listing, like nilotinib. Similarly, vandetanib exhibits the most significant QT prolongation and ibrutinib exhibits the highest incidence in AF, but does not receive enough attention during treatment.

Keywords: TKIs, QT prolongation, atrial fibrillation, molecule mechanism, therapeutic strategies, pharmacokinetics

OPEN ACCESS

Edited by:
Feng Cao,
People's Liberation Army General Hospital, China

Reviewed by:
Concetta Zito,
University of Messina, Italy
Hari Deshpande,
Yale University, United States

***Correspondence:**
Shuai Jiang
jdyhmu3@163.com
Mei Dong
13804567370@163.com

[†]These authors have contributed equally to this work

Specialty section:
This article was submitted to Cardio-Oncology, a section of the journal Frontiers in Cardiovascular Medicine

Received: *13 August 2021*
Accepted: *25 October 2021*
Published: *19 November 2021*

Citation:
Cheng M, Yang F, Liu J, Yang D, Zhang S, Yu Y, Jiang S and Dong M (2021) Tyrosine Kinase Inhibitors-Induced Arrhythmias: From Molecular Mechanisms, Pharmacokinetics to Therapeutic Strategies. Front. Cardiovasc. Med. 8:758010. doi: 10.3389/fcvm.2021.758010

INTRODUCTION

Protein kinases are enzymes that catalyze adenosine triphosphate (ATP) γ-phosphate transfer to tyrosine residues of the substrate protein and regulate many essential cellular biochemical functions including differentiation, proliferation, and death (1). More than 500 kinases have been discovered, and depending on their substrate specificity, they can be divided into two categories: catalytic tyrosine/tyrosine-like phosphorylation and serine/threonine phosphorylation (2). More than 30% of proteins may be modified by the kinases in the human body (3) and over 50% of proto-oncogene and oncogene products have protein tyrosine kinase activity (4). In this way, tyrosine kinase inhibitors (TKIs) by competitive inhibition of the ATP binding pocket, inhibit tumor proliferation, which has been widely used in cancer target therapy (1, 5).

TKIs can be divided into monoclonal antibody drugs and small molecule TKIs. Monoclonal antibody drugs are mainly bound to unique epitopes on the extracellular matrix to regulate downstream signal transduction, thereby inhibiting the proliferation, invasion, and angiogenesis of tumor cells. Small molecule TKIs act by intracellular inhibition of phosphorylation (6). So, inherently, small molecule TKIs are less selective than monoclonal antibodies and may lead to more adverse effects (AEs).

After the first TKI drug imatinib was approved in the US in 2001, a total of more than 30 TKIs were approved by the FDA up to 2020 (7). Although all the approved TKIs can inhibit BCR-ABL1, they still have different targeted sites and distinctive potency and activity. First-generation TKIs, like imatinib, dramatically improved the 5-year survival from 11 to 90% in Philadelphia chromosome-positive chronic myeloid leukemia (CML) patients (8). Second-generation TKIs, such as nilotinib (9) and dasatinib (10), exhibited the ability to overcome imatinib resistance and a more rapid molecule response. Third-generation TKI ponatinib is the only drug that works against BCR-ABL1^{T315I} mutation (11).

As successful as TKIs are, they still face some challenges, such as AEs caused by drug poor selectivity, drug resistance, and other reasons. According to the FDA's Adverse Effects Reporting System (FARES) database's cardiovascular (CV) toxicity section, TKIs were considered to be the suspected drug in 83.2% of CV events. And torsade de pointes/QT prolongation was considered the only acute event, which had a 6.8% incidence, higher than other anticancer drugs (1.4%) (12). Similarly, correlations were found between QT prolongation with increased risk of polymorphic ventricular tachycardia, which leads to lethal arrhythmia and subsequent sudden cardiac death (SCD) (3, 7, 12). The mechanisms and countermeasures of TKI-induced arrhythmia are still unknown. To this purpose, we wrote this paper to provide a broad overview for the potential of approved TKIs in prolonging QT interval and atrial toxicity and systemic and comprehensive treatment for patients.

As shown in **Figure 1**, the data for this review were identified by searches of PubMed and references from relevant articles using the search terms "TKIs," "QT prolongation," "atrial fibrillation," and "on and off-target." We identified 6,151 records through the PubMed database. We removed 2,759 records as they were review papers ($n = 1{,}267$), meta-analyses ($n = 1{,}181$), or case reports ($n = 311$). A total of 2,931 studies on TKIs combined with other anticancer drugs were also removed. Then, 407 records were excluded by reading the abstract. Finally, 54 records were enrolled. Only articles published in English between 2005 and 2021 were included.

POTENTIAL MOLECULE MECHANISM OF QT PROLONGATION AND ATRIAL TOXICITY

Most TKIs are multi-target drugs, and the target receptors include vascular endothelial growth factor receptor (VEGFR), BCR-ABL, platelet-derived growth factor receptor (PDGFR), epidermal growth factor receptor (EGFR), and c-KIT, etc. (13, 14). Then they regulate the downstream signaling pathways, for example, PI3K, MEK, and AKT, etc. (14, 15). Only a few TKIs have only one or two targets, such as axitinib, bosutinib, and gefitinib (3). Due to the numerous targets of TKIs, the potential mechanisms of TKI-related side effects previously proposed can be divided into: "on-target" and "off-target" (14, 16) effects.

On-Target

On-target means that the targets of TKIs exist in the tumor cell, but also play an important role in other normal organ cells, which may damage the biochemical function of normal cells (17, 18). A typical example of an on-target effect was observed in the Lu et al. trial. They designed an experiment to expose canine ventricular myocytes to drugs that have been demonstrated to prolong QT interval. As the result showed, the inhibition of the PI3K signaling pathway was the actual reason for QT prolongation. After blocking PI3K signaling, with the increase of persistent sodium current (I_{NaP}) and the decrease of L-type calcium current (I_{CaL}) and potassium current (I_{Kr} and I_{Ks}), the total sodium and potassium current change accounted for over 70% of the whole prolongation, not just the potassium channels. And then, PI3K and its second message manager phosphatidylinositol 3,4,5-trisphosphate (PIP3) could affect multiple ion channels, similarly, resulting in action potential duration (APD). They also confirmed this result by breeding mice with reduced PI3K signaling showed QT prolongation (19).

Then, in McMullen's trial, they found that mice with decreased activity of the PI3K-Akt pathway was associated with higher susceptibility to AF and the same observation was relevant in humans. This pathway is an important regulator of cardiac protection under stress conditions. Other experiments also made a hypothesis that AF was related to ROS signaling, which would occur in abnormal Ca^{2+} release and atrial remodeling (20).

Off-Target

Off-target refers to a non-selective TKI acting on normal organ cells. However, the target does not exist in tumor cells (21, 22). Generally, whether a TKI drug has the effect of QT prolongation, we can first observe whether there are fluorophenyl or fluoromethyl-phenyl rings in the molecular structure of the drugs (23). Drugs inhibit the hERG (human ether-a-go-go) subunit with which the channel conducts the main ventricular repolarization potassium current (I_{Kr}) potential during phases 2–3 of the action potential (3, 24, 25). And hERG is regulated by cAMP and cAMP-dependent PKA. Vandetanib has been demonstrated to have values of hERG IC50 of 0.4 μM, and its metabolites are also active. In *in vivo* studies, a dose-dependent increase in QT prolongation has been demonstrated in dogs (3).

For instance, ibrutinib influences tumor cells by inhibiting Bruton tyrosine kinase (BTK); it also has off-target effects on Tec protein tyrosine kinase (TEC) (26). Both BTK and TEC transcripts have been demonstrated to express in cardiac tissue and at a higher expression when AF occurs rather than sinus rhythm. The PI3K-Akt pathway is regulated by BTK and TEC, and plays an important role in cardiac protection under conditions of stress (27).

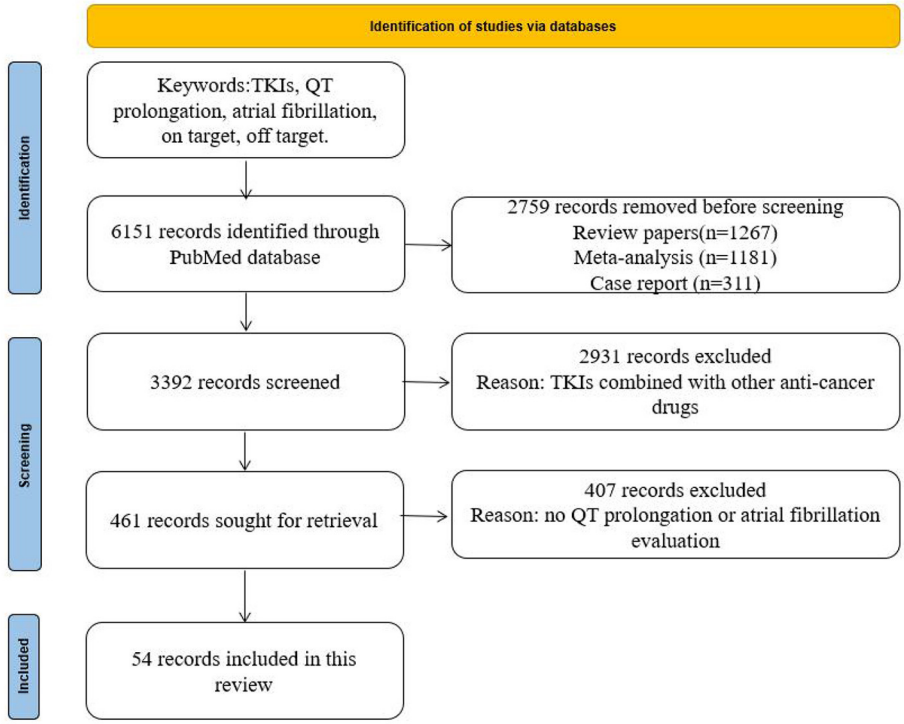

FIGURE 1 | Search strategy and selection criteria.

Even if some drugs act on the same target or class of targets, it cannot be proved that these drugs have the effect of a prolonged QT interval. For example, sorafenib, vandetanib, and axitinib act on VEGFR, but only sorafenib and vandetanib will induce QT prolongation (23).

SELECTED REPRESENTATIVE DRUGS

Vandetanib

Vandetanib has the most significant prolongation of corrected QT interval according to Fridericia's formula (QTcF). It is an oral multitarget TKI drug, which inhibits VEGFR-2, EGFR, and the activity of tyrosine kinase. It was approved for the treatment of metastatic medullary thyroid cancer (MTC) by the FDA in 2011 (28).

In an early report, Ghatalia et al. initiated a meta-analysis about QTcF interval prolongation with VEGFR TKIs (29). They studied 13 clinical trials that included 4,204 patients with multi-tumor types who received 100 or 300 mg of vandetanib daily. The incidence of QT prolongation ranged from 0.3 to 23.9%, AF incidence ranged from 0.43 to 1.79%, and all-grade arrhythmia ranged from 0 to 1.69%. A high dose of vandetanib was associated with a high risk of QT prolongation by the authors. Then, under an approved dosage, phase II trial, multicenter, open-label study, 17 patients with metastatic or recurrent NSCLC with a RET rearrangement and against platinum-based doublet chemotherapy were treated with 300 mg of vandetanib once daily. A total of 6 out of 17 patients had grade 3 AEs, 2 were QT prolongation (11%) (30). In another phase III, double-blind, placebo-controlled clinical trial, 331 patients with advanced or metastatic MTC were randomized 2:1 to receive 300 mg of vandetanib daily orally ($n = 231$) or placebo ($n = 100$). During the treatment, most AEs could be well-managed by dose interruption or reduction, QT prolongation occurred in 14 patients in all grades (31).

Vandetanib is metabolized by cytochrome P450 enzyme (CYP) 3A4, which inhibits or promotes activity by many common drugs (32). In a phase I trial, healthy individuals received 200 mg of itraconazole daily and were given a single dose of 300 mg of vandetanib on day 1 and day 4. A slight increase (9%) was observed in the serum concentration of vandetanib (33). Other substrates of CYP3A4, such as ketoconazole and rifampicin should be considered in the drug combination. In addition, other drugs which may induce QT prolongation need to be considered in the drug combination.

Ibrutinib

Ibrutinib has the highest incidence of AF. It is an oral irreversible small molecule inhibitor of Bruton's tyrosine kinase (BTK), which is inhibited by a covalent bond with the specific cysteine Cys-481 of BTK, thereby inhibiting the proliferation and survival of malignant B cells, as well as reducing their migration and substrate adhesion (34, 35). Through the inhibition of BTK, downstream signaling pathways (MAPK, PI3K, and NF-?B) and phosphorylation functions (PLCγ, ERK, and AKT) are influenced (35–37).

In a preclinical *in vitro* study, it was demonstrated that there were effects on hERG, but no specific risks for human cardiac issues, by the authors. In the *in vivo* safety study of dogs, ibrutinib may increase PR interval, decrease heart rate, and shorten heart rate-corrected QT interval (38). Besides, its use is associated with atrial toxicity. The possible mechanisms are still not entirely clear, but it has been demonstrated that AF is an off-target effect (39). Xiao et al., who used a mouse model and conducted chemo-proteomic analysis of cardiac lysates, found that C-terminal Src kinase (CSK) was the most likely target for ibrutinib-induced AF (40). Jiang et al. created a C57BI/6 mice model where an ibrutinib group received 25 mg/kg/d of ibrutinib and a control group was treated with hydroxypropy1-β-cyclodextrin for 4 weeks. Compared with the control group, the ibrutinib group displayed Ca^{2+} dysregulation in atrial myocytes, it increased spontaneous Ca^{2+} release, CaMKII level, phosphorylated CaMKII, and other related sites, and reduced sarcoplasmic Ca^{2+} capacity (41); both may lead to AF. Ibrutinib is an independent risk factor for the development of atrial arrhythmias, with an incidence of AF of more than 10–15% (42–44). Based on Alexandre's paper, ibrutinib is the most frequent anticancer drug to cause AF (45). In addition to straightforward arrhythmias, other potential effects of ibrutinib on ECG are little known. In early clinical trials, ∼6–16% of participants had an increased risk of AF (46). A review of 16 studies showed that the incidence of ibrutinib-associated AF was 5.77 per 100 person-years (27). Fradley et al. enrolled 137 patients who were treated with ibrutinib, 21 pre- and post-ibrutinib ECG readings were obtained. Compared with the pre ibrutinib ECG, after administration, the ECG showed QT interval shortening from 446 to 437 ms, based on Bazett's formula (47). In another phase II clinical trial, a mean 7.5 ms shortening of the corrected QT interval was found after ibrutinib treatment (34). However, no significant QT effects were found in healthy subjects. Ibrutinib showed concentration-dependent mild shortening of the QT interval and PR prolongation, but seemed to have no significant clinical meaning (38).

Ibrutinib is metabolized by CYP3A4, therefore the coadministration of calcium channel blockers and other enzyme inhibitors should be fully considered. Besides, ibrutinib may increase the P-glycoprotein (P-gp) substrate level, such as digoxin and omeprazole, etc. (27, 48, 49).

Ponatinib

Ponatinib is a third-generation TKI, which was designed by a computational and structure-based approach (50). It was created with a unique carbon-carbon triple bond linkage that overcomes the steric hindrance caused by the T315I mutant in CML or Ph^+ acute lymphoblastic leukemia (ALL) (50, 51). The toxicity is mostly explained as a lack of selectivity, and on and off-target effects. Ponatinib inhibits over 60 kinases, including PDGFR, c-KIT, VEGFR, and EGFR. It also acts on perturbation of pro-survival signaling pathways, the AKT and ERK pathways impact cardiac function (52, 53). And in the Sharma et al. trial, they used human-induced pluripotent stem cell-derived cardiomyocytes (hiPSC-CMs) to evaluate the 21 approved TKIs, and demonstrated that ponatinib is the most toxic (54).

In a pre-clinical trial, ponatinib was not associated with cardiotoxicity. However, it exhibited a high occurrence of cardiac events in follow-up trials (11, 55). One year after being approved by the FDA, ponatinib was suspended because of safety concerns (56). At the dose of 50 mg/kg, the mean tumor volume decreased by 96%, so 45 mg once daily has been suggested, but the label cautions that an optimal dosage has not been identified (52, 57). In Sonnichsen's trial, 39 patients received ponatinib treatment at 30-, 45- and 60-mg dose levels, and the QTcF changes from baseline showed −10.9, −3.9, and −5.0 ms. Seventy-five patients in different dose levels were enrolled to evaluate the PK-PD effect, no significant correlation was found between drug exposure and QT changes (50). For the FDA CV events report for TKIs in 2020, 14.4% were found to be related to ponatinib (12). And in another clinical trial, 78 patients with CML were treated with ponatinib, the most common CAEs were arrhythmia (9%), higher than hypertension (7.7%) and myocardial infarction (3.8%) (58). In a ponatinib vs. imatinib phase III trial, 307 newly diagnosed CML patients were assigned to receive ponatinib ($n = 155$) or imatinib ($n = 152$). The results showed that no significant differences were observed in major molecule response at 12 months, but three serious AFs were observed in the ponatinib group, while no AFs occurred in the imatinib group (59).

Ponatinib is mostly metabolized by CYP3A4/5, but also by the substrates of CYP2C6 and CYP2C8. When co-administered with ketoconazole, the $AUC_{0-\infty}$, AUC_{0-t}, and C_{max} indicated increased exposures to ponatinib of 78, 70, and 47%, respectively. So, a dose decreased to 30 from 45 mg daily could be considered when combined with strong CYP3A4 inhibitors (60, 61).

Nilotinib

Nilotinib also has strong cardiotoxicity. Its ability to prolong QT interval and induce AF is just after that of vandetanib and ibrutinib. It is an orally administered small molecule TKI that was designed with a lipophilic structure which competitively binds to the inactive conformation of the ABL kinase domain and leads to a higher and faster molecule response than imatinib in patients (62, 63). Nilotinib is more selective than imatinib, and does not have an effect on Src, EGFR, and VEGF kinase at a concentration <3,000 nM (64–66). However, it targets PDGFRa, PDGFRb, c-kit, DDR, and colony-stimulating factor receptor 1, which is similar to imatinib (65).

Under the multi-target effect, nilotinib induce cardiotoxicity. In a preclinical safety study, nilotinib inhibited the hERG channel at an IC_{50} value of 0.13 μM (3), and exhibited the signs of QT prolongation in an isolated rabbit heart, but no toxicity in neonatal rat ventricular myocytes (67). There was no evidence that nilotinib had an effect on QTc in dogs at the dose up to 300 mg (3). In a response and safety phase I study, 33 patients with CML-BP were enrolled and received second-line nilotinib treatment. Thirteen patients (39%) achieved a hematologic response. As for arrhythmia, the QTcF increased by 5–15 ms in the study group, and one patient developed AF (grade = 2) (9). Then, in a phase II study, 280 patients with CML were enrolled, 6-month major cytogenetic responses were achieved in 48% of patients, and only 1% (3 of 280) had QTcF > 500 ms (62). In another phase II study, 44 patients with CML-AP

or CML-CP were enrolled, and 6.1% displayed QT prolongation at all grades (68). A positive correlation was found between QT prolongation and nilotinib exposure in many trials (69–71). In patients, as C_{max} increased by 1,000 ng/ml, the QTcF also increased by 4.2 ms; an increase of 1,000 ng/ml in C_{trough} brought on an increase of 6.9 ms in QTcF (70, 71). Contrary to the earlier study, the 2020 FDA CV events report showed that QTc prolongation (any grade) induced by TKI was almost 28.8%, among these events 38.7% was due to nilotinib (12). It was significantly higher than early clinical trials. Alexandre et al. used the World Health Organization (WHO) individual case safety report database, vigibase, to identify the correlation between anticancer drugs and AF. As the results showed, 11,757 of 2,124,646 AF cases were associated with 176 anticancer drugs, and nilotinib accounted for 241 cases (2%) (45).

Nilotinib is also metabolized in the liver and is the competitive inhibitor of CYP3A4/5, CYP2C8, CYP2C9, CYP2D6, and uridine diphosphate glucuronosyltransferase 1A1 (UGT1A1) (72, 73). When co-administered with ketoconazole, the area under the curve (AUC) increased by 3-fold and C_{max} by 1.8-fold (74). Other drugs like rifampicin and esomeprazole reduced the plasma concentration to different degrees (72, 75).

Dasatinib

Dasatinib seems to rarely cause QT interval prolongation events, and pooled safety data suggest that the overall risk for cardiotoxicity is minimal in dasatinib. But it still occurs in clinical use (76). Dasatinib is an effective BCR-ABL inhibitor in the treatment of CML and Philadelphia chromosome-positive acute lymphoblastic leukemia (Ph^+ ALL) after relapse or resistance to imatinib (77, 78). It acts on the targets BCR-ABL, c-Kit, Src family kinases (SFKS), and PDGFR-α/β. By acting on BCR-ABL and the Src family, dasatinib inhibits the downstream PI3K signaling pathway (3, 79), which may induce cardiotoxicity.

The IC_{50} of the effect on hERG is 14.3 μM, which is safer than vandetanib in QT effects. In an *in vivo* study, no QT prolongation was found in monkeys using a body-weight dose strategy (10 or 70 mg/kg). In a clinical trial, 2,182 patients were treated with dasatinib, 21 displayed QT $\geq$ 500 ms, all patients had a mean increase from baseline of 3–5 ms (3). In another retrospective study, 115 cancer patients received dasatinib treatment, 41.7% of patients showed QT prolongation and the mean (SD) of pre- and post- therapeutic QT interval change was 30 ms (12).

Dasatinib influences CYP3A4 and CYP2C8 enzymes and the drug transporter P-gp. In drug-drug interaction, omeprazole, esomeprazole, and pantoprazole will inhibit the P-gp to decrease absorption and lead to higher exposure. Metoclopramide has an additive effect on dasatinib which will increase the incidence of QT interval (80, 81). In a phase I PK and drug interaction study, 17 patients were enrolled to determine whether the coadministration of ketoconazole affected the PK of dasatinib (82). Rhe result showed that ketoconazole led to an increase in dasatinib exposure and may correlate to an ∼6 ms prolongation in QT interval.

The current study showed that QT prolongation occurred in nearly 30% of patients who received TKIs treatment, and 20% were high grade (7). Onco-cardiology is essential for cancer treatment because the incidence of cancer and cardiovascular diseases (CVD) is concentrated in middle-aged and senior patients. During the cancer treatment, it may aggravate CVD, and its side effects may lead to failure of cancer treatment (6). Other unexpected side effects include: Human epidermal growth factor receptor 2 (HER2) and trastuzumab are associated with left ventricular ejection fraction (LVEF) decrease and congestive heart failure (CHF) (83); anti-VEGF drugs were found to significantly increase the incidence of hypertension (84). However, arrhythmia could be induced by lots of targets.

These five TKIs all have obvious characteristics, mechanisms, aim targets, and AEs. Vandetanib and ibrutinib were found to have high incidences of arrhythmia but dasatinib was recommended not to be much concerns about cardiotoxicity. All of them exhibit an effect on QT interval and atria toxicity in clinical application. And, according to the FDA and WHO databases, the impact of some TKIs in QT and AF is much higher than in previous clinical trials (12, 45). Although QT interval prolongation has a lower mortality than hypertension or coronary heart disease, it is convenient as a monitoring strategy of CVD, and evaluation of QT interval changes can maximize the optimization of drug cessation or reduction. The main information of the selected representative drugs is summarized in **Table 1**.

MANAGEMENT

Arrhythmia induced by TKIs is easily monitored and can be an early warning of other serious CVD. For the agents with risk factors, routine monitoring methods such as ECG, blood pressure, electrolytes, and cardiac biomarkers are recommended during the course of treatment. In addition, collecting past medical history and physical function evaluation of patients are recommended to identify those at heightened risk for cardiovascular events. Once the arrhythmia occurs, beta-blockers and type I and III antiarrhythmic drugs are helpful for patients.

Primarily, CVD risk factors should be carefully evaluated before deciding to use TKIs. When patients are diagnosed with underlying diseases, like hypertension, coronary heart disease, diabetes, and other CVDs, they need to be carefully monitored based on their cardiac function. Baseline electrocardiograms (ECGs) should be obtained which will evaluate the risk of arrhythmia. Myoglobin (MYO), B-type natriuretic peptide (BNP), and other biochemical indexes should be obtained and corrected (85–87).

Second, electrolytes should be monitored, especially Na^+, K^+, and Ca^{2+} which have an influence on heart rhythm. Abnormal electrolytes will be a potential risk of arrhythmia and should be corrected immediately (87, 88).

Third, drug-drug interaction should be fully considered. Most TKIs are metabolized by CYP enzymes and transported by P-gp; other drugs influencing CYP enzymes and the competitive bond to P-gp should be fully considered during coadministration. And drugs that have been proved to prolong the QT interval or induce AF should be avoided (89, 90).

TABLE 1 | Target, effect on QT interval/AF, and metabolism of selected representative TKIs.

Name	Vandetanib	Ibrutinib	Ponatinib	Nilotinib	Dasatinib
Target	VEGFR-2; EGFR; RET	BTK; MAPK; PI3K	BCR-ABL; PDGFR; c-KIT; VEGFR; EGFR	BCR-ABL; PDGFR-α/β; c-kit; DDR	BCR-ABL; c-KIT; SFKS; PDGFR-α/β
Effect on QT interval	Prolong QT interval and with a positive drug exposure-dependent risk	Shorten QT interval	Prolong QT interval, no correlation was found between drug exposure and QT prolongation	Prolong QT interval with a positive correlation between exposure and risk	Rarely causes QT interval prolongation
Effect on AF	With a low incidence from 0.43 to 1.79%	Highest incidence of AF, nearly 10–15%	With a low incidence, about 1.29%	With a high incidence followed by ibrutinib	Rarely causes AF
Metabolized by	CYP3A4	CYP3A4	CYP3A4/5, CYP2C6, CYP2C8	CYP3A4	CYP3A4, CYP2C8

Fourth, reducing doses or stopping TKI treatment in time are of vital importance, especially when the QT interval is $\geq$500 ms, or the change of QT is $>$ 60 ms compared with baseline. TKIs could be restarted when the QT is $<$ 450 ms. If ventricular tachycardia, syncope, or other serious cardiovascular adverse reactions occurred again, the drugs should be stopped permanently (76, 91).

Fifth, after taking medicine, if a faint, headache, or irregular heartbeat occurs, healthcare should be provided immediately. The decision of heart rate or rhythm control should be patient-centered and symptom-oriented (87), beta-blockers may be the first choice for heart rate control, and type Ic and type III antiarrhythmic drugs are helpful for heart rhythm (87, 91).

CONCLUSION

To conclude, we focused on the molecule mechanism, clinical outcome, coadministration, and countermeasures of TKI drugs in arrhythmia. There is commonality and variability coexistence in TKI class, studies showed that QT prolongation is the most significant in vandetanib, AF most occurs in ibrutinib, and nilotinib has a high incidence of QT prolongation and AF. Their actual incidence and life-threatening status are higher than preclinical trials, lots of them do not get a black box warning from the FDA. But CVD caused by antitumor drugs needs to be avoided during treatment. Therefore, early diagnosis, convenient monitoring measures, and appropriate treatment methods should be provided to patients. So, ECGs monitoring should be more widely used in cancer patients, existing guidelines should be more specific, more real-world clinical trials need to be done, and on-target and off-target toxicity should be completely understood in the future.

AUTHOR CONTRIBUTIONS

MC and FY collected data and wrote the paper. FY, JL, DY, SZ, and YY collected the literature and information. SJ, MD, and JL reviewed the paper. All authors read and approved the final manuscript.

FUNDING

This work was supported by the Key Program of Harbin Medical University Cancer Hospital Haiyan Fund (no. JJZD2019-03) and the General Program of Harbin Medical University Cancer Hospital Haiyan Fund (no. JJMS2021-25).

REFERENCES

1. Krause DS. Van Etten RA. Tyrosine kinases as targets for cancer therapy. *N Engl J Med*. (2005) 353:172–87. doi: 10.1056/NEJMra044389
2. Grimminger F, Schermuly RT, Ghofrani HA. Targeting non-malignant disorders with tyrosine kinase inhibitors. *Nat Rev*. (2010) 9:956–70. doi: 10.1038/nrd3297
3. Shah RR, Morganroth J, Shah DR. Cardiovascular safety of tyrosine kinase inhibitors: with a special focus on cardiac repolarisation (QT interval). *Drug Saf*. (2013) 36:295–316. doi: 10.1007/s40264-013-0047-5
4. Drake JM, Lee JK, Witte ON. Clinical targeting of mutated and wild-type protein tyrosine kinases in cancer. *Mol Cell Biol*. (2014) 34:1722–32. doi: 10.1128/MCB.01592-13
5. Wu P, Nielsen TE, Clausen MH. Small-molecule kinase inhibitors: an analysis of FDA-approved drugs. *Drug Discovery Today*. (2016) 21:5–10. doi: 10.1016/j.drudis.2015.07.008
6. Chen YC, Chung CC, Lin YK, Chen YJ. Genetic and ethnic modulation of cardiovascular toxicity of vascular endothelial growth factor inhibitors. *Ann Med*. (2018) 50:46–56. doi: 10.1080/07853890.2017.1383629
7. Abu Rmilah AA, Lin G, Begna KH, Friedman PA, Herrmann J. Risk of QTc prolongation among cancer patients treated with tyrosine kinase inhibitors. *Int J Cancer*. (2020) 147:3160–7. doi: 10.1002/ijc.33119
8. Baccarani M, Deininger MW, Rosti G, Hochhaus A, Soverini S, Apperley JF, et al. European LeukemiaNet recommendations for the management of chronic myeloid leukemia: 2013. *Blood*. (2013) 122:872–84. doi: 10.1182/blood-2013-05-501569
9. Kantarjian H, Giles F, Wunderle L, Bhalla K, O'Brien S, Wassmann B, et al. Nilotinib in imatinib-resistant CML and Philadelphia chromosome-positive ALL. *N Engl J Med*. (2006) 354:2542–51. doi: 10.1056/NEJMoa055104
10. Shah NP, Rousselot P, Schiffer C, Rea D, Cortes JE, Milone J, et al. Dasatinib in imatinib-resistant or -intolerant chronic-phase, chronic myeloid leukemia patients: 7-year follow-up of study CA180-034. *Am J Hematol*. (2016) 91:869–74. doi: 10.1002/ajh.24423
11. Cortes JE, Kim DW, Pinilla-Ibarz J. le Coutre PD, Paquette R, Chuah C, et al. Ponatinib efficacy and safety in Philadelphia chromosome-positive leukemia: final 5-year results of the phase 2 PACE trial. *Blood*. (2018) 132:393–404. doi: 10.1182/blood-2016-09-739086
12. Cirmi S, El Abd A, Letinier L, Navarra M, Salvo F. Cardiovascular toxicity of tyrosine kinase inhibitors used in chronic myeloid leukemia: an analysis of

the FDA Adverse Event Reporting System Database (FAERS). *Cancers*. (2020) 12:826. doi: 10.3390/cancers12040826
13. Kim SY, Kim SM, Chang H, Kim BW, Lee YS, Chang HS, Park CS. Safety of tyrosine kinase inhibitors in patients with differentiated thyroid cancer: real-world use of lenvatinib and sorafenib in Korea. *Front Endocrinol*. (2019) 10:384. doi: 10.3389/fendo.2019.00384
14. Hu W, Hirakawa B, Jessen B, Lee M, Aguirre S. A tyrosine kinase inhibitor-induced myocardial degeneration in rats through off-target phosphodiesterase inhibition. *J Appl Toxicol*. (2012) 32:1008–20. doi: 10.1002/jat.2801
15. Wu MD, Moslehi JJ, Lindner JR. Arterial thrombotic complications of tyrosine kinase inhibitors. *Arterioscler Thromb Vasc Biol*. (2021) 41:3–10. doi: 10.1161/ATVBAHA.120.314694
16. Shah RR, Morganroth J. Update on cardiovascular safety of tyrosine kinase inhibitors: with a special focus on QT interval, left ventricular dysfunction and overall risk/benefit. *Drug Saf*. (2015) 38:693–710. doi: 10.1007/s40264-015-0300-1
17. Herman SEM, Montraveta A, Niemann CU, Mora-Jensen H, Gulrajani M, Krantz F, et al. The Bruton Tyrosine Kinase (BTK) inhibitor acalabrutinib demonstrates potent on-target effects and efficacy in two mouse models of chronic lymphocytic leukemia. *Clin Cancer Res*. (2017) 23:2831–41. doi: 10.1158/1078-0432.CCR-16-0463
18. Guo Y, Liu Y, Hu N, Yu D, Zhou C, Shi G, et al. Discovery of zanubrutinib (BGB-3111), a novel, potent, and selective covalent inhibitor of Bruton's tyrosine kinase. *J Med Chem*. (2019) 62:7923–40. doi: 10.1021/acs.jmedchem.9b00687
19. Lu Z, Wu CY, Jiang YP, Ballou LM, Clausen C, Cohen IS, Lin RZ. Suppression of phosphoinositide 3-kinase signaling and alteration of multiple ion currents in drug-induced long QT syndrome. *Sci Trans Med*. (2012) 4:131ra150. doi: 10.1126/scitranslmed.3003623
20. McMullen JR, Boey EJ, Ooi JY, Seymour JF, Keating MJ, Tam CS. Ibrutinib increases the risk of atrial fibrillation, potentially through inhibition of cardiac PI3K-Akt signaling. *Blood*. (2014) 124:3829–30. doi: 10.1182/blood-2014-10-604272
21. Hochhaus A, Baccarani M, Silver RT, Schiffer C, Apperley JF, Cervantes F, et al. European LeukemiaNet 2020 recommendations for treating chronic myeloid leukemia. *Leukemia*. (2020) 34:966–84. doi: 10.1038/s41375-020-0776-2
22. Zhang J, Yang PL, Gray NS. Targeting cancer with small molecule kinase inhibitors. *Nat Rev Cancer*. (2009) 9:28–39. doi: 10.1038/nrc2559
23. Himmel HM, Hoffmann M. QTc shortening with a new investigational cancer drug: a brief case study. *J Pharmacol Toxicol Methods*. (2010) 62:72–81. doi: 10.1016/j.vascn.2010.05.012
24. Vandenberg JI, Perry MD, Perrin MJ, Mann SA, Ke Y, Hill AP. hERG K(+) channels: structure, function, clinical significance. *Physiol Rev*. (2012) 92:1393–478. doi: 10.1152/physrev.00036.2011
25. Cohen IS, Lin RZ, Ballou LM. Acquired long QT syndrome and phosphoinositide 3-kinase. *Trends Cardiovasc Med*. (2017) 27:451–9. doi: 10.1016/j.tcm.2017.05.005
26. Wu J, Liu C, Tsui ST, Liu D. Second-generation inhibitors of Bruton tyrosine kinase. *J Hematol Oncol*. (2016) 9:80. doi: 10.1186/s13045-016-0313-y
27. Ganatra S, Sharma A, Shah S, Chaudhry GM, Martin DT, Neilan TG, et al. Ibrutinib-associated atrial fibrillation. *JACC Clin Electrophysiol*. (2018) 4:1491–500. doi: 10.1016/j.jacep.2018.06.004
28. Commander H, Whiteside G, Perry C. Vandetanib: first global approval. *Drugs*. (2011) 71:1355–65. doi: 10.2165/11595310-000000000-00000
29. Ghatalia P, Je Y, Kaymakcalan MD, Sonpavde G, Choueiri TK. QTc interval prolongation with vascular endothelial growth factor receptor tyrosine kinase inhibitors. *Br J Cancer*. (2015) 112:296–305. doi: 10.1038/bjc.2014.564
30. Lee SH, Lee JK, Ahn MJ, Kim DW, Sun JM, Keam B, et al. Vandetanib in pretreated patients with advanced non-small cell lung cancer-harboring RET rearrangement: a phase II clinical trial. *Ann Oncol*. (2017) 28:292–7. doi: 10.1093/annonc/mdw559
31. Thornton K, Kim G, Maher VE, Chattopadhyay S, Tang S, Moon YJ, et al. Vandetanib for the treatment of symptomatic or progressive medullary thyroid cancer in patients with unresectable locally advanced or metastatic disease: Food US, and Drug Administration drug approval summary. *Clin Cancer Res*. (2012) 18:3722–30. doi: 10.1158/1078-0432.CCR-12-0411
32. Weil A, Martin P, Smith R, Oliver S, Langmuir P, Read J, Molz KH. Pharmacokinetics of vandetanib in subjects with renal or hepatic impairment. *Clin Pharmacokin*. (2010) 49:607–18. doi: 10.2165/11534330-000000000-00000
33. Martin P, Oliver S, Robertson J, Kennedy SJ, Read J, Duvauchelle T. Pharmacokinetic drug interactions with vandetanib during coadministration with rifampicin or itraconazole. *Drugs R&D*. (2011) 11:37–51. doi: 10.2165/11586980-000000000-00000
34. Cameron F, Sanford M. Ibrutinib: first global approval. *Drugs*. (2014) 74:263–71. doi: 10.1007/s40265-014-0178-8
35. Deeks ED. Ibrutinib: a review in chronic lymphocytic leukaemia. *Drugs*. (2017) 77:225–36. doi: 10.1007/s40265-017-0695-3
36. Cheng S, Ma J, Guo A, Lu P, Leonard JP, Coleman M, et al. BTK inhibition targets *in vivo* CLL proliferation through its effects on B-cell receptor signaling activity. *Leukemia*. (2014) 28:649–57. doi: 10.1038/leu.2013.358
37. Herman SE, Mustafa RZ, Gyamfi JA, Pittaluga S, Chang S, Chang B, et al. Ibrutinib inhibits BCR and NF-κB signaling and reduces tumor proliferation in tissue-resident cells of patients with CLL. *Blood*. (2014) 123:3286–95. doi: 10.1182/blood-2014-02-548610
38. de Jong J, Hellemans P, Jiao JJ, Huang Y, Mesens S, Sukbuntherng J, et al. Ibrutinib does not prolong the corrected QT interval in healthy subjects: results from a thorough QT study. *Cancer Chemother Pharmacol*. (2017) 80:1227–37. doi: 10.1007/s00280-017-3471-x
39. Mulder TA, Peña-Pérez L, Berglöf A, Meinke S, Estupiñán HY, Heimersson K, et al. Ibrutinib has time-dependent on- and off-target effects on plasma biomarkers and immune cells in chronic lymphocytic leukemia. *HemaSphere*. (2021) 5:e564. doi: 10.1097/HS9.0000000000000564
40. Xiao L, Salem JE, Clauss S, Hanley A, Bapat A, Hulsmans M, et al. Ibrutinib-mediated atrial fibrillation attributable to inhibition of C-terminal Src kinase. *Circulation*. (2020) 142:2443–55. doi: 10.1161/CIRCULATIONAHA.120.049210
41. Jiang L, Li L, Ruan Y, Zuo S, Wu X, Zhao Q, et al. Ibrutinib promotes atrial fibrillation by inducing structural remodeling and calcium dysregulation in the atrium. *Heart Rhythm*. (2019) 16:1374–82. doi: 10.1016/j.hrthm.2019.04.008
42. Fradley MG, Gliksman M, Emole J, Viganego F, Rhea I, Welter-Frost A, et al. Rates and risk of atrial arrhythmias in patients treated with ibrutinib compared with cytotoxic chemotherapy. *Am J Cardiol*. (2019) 124:539–44. doi: 10.1016/j.amjcard.2019.05.029
43. Leong DP, Caron F, Hillis C, Duan A, Healey JS, Fraser G, et al. The risk of atrial fibrillation with ibrutinib use: a systematic review and meta-analysis. *Blood*. (2016) 128:138–40. doi: 10.1182/blood-2016-05-712828
44. Wiczer TE, Levine LB, Brumbaugh J, Coggins J, Zhao Q, Ruppert AS, et al. Cumulative incidence, risk factors, and management of atrial fibrillation in patients receiving ibrutinib. *Blood Adv*. (2017) 1:1739–48. doi: 10.1182/bloodadvances.2017009720
45. Alexandre J, Salem JE, Moslehi J, Sassier M, Ropert C, Cautela J, et al. Identification of anticancer drugs associated with atrial fibrillation - analysis of the WHO pharmacovigilance database. *Eur Heart J Cardiovasc Pharmacother*. (2020) 7:312–20. doi: 10.1093/ehjcvp/pvaa037
46. Brown JR, Moslehi J, O'Brien S, Ghia P, Hillmen P, Cymbalista F, et al. Characterization of atrial fibrillation adverse events reported in ibrutinib randomized controlled registration trials. *Haematologica*. (2017) 102:1796–805. doi: 10.3324/haematol.2017.171041
47. Fradley MG, Welter-Frost A, Gliksman M, Emole J, Viganego F, Lee DH, et al. Electrocardiographic changes associated with ibrutinib exposure. *Cancer Control*. (2020) 27:1073274820931808. doi: 10.1177/1073274820931808
48. de Zwart L, Snoeys J, De Jong J, Sukbuntherng J, Mannaert E, Monshouwer M. Ibrutinib dosing strategies based on interaction potential of CYP3A4 perpetrators using physiologically based pharmacokinetic modeling. *Clin Pharmacol Therap*. (2016) 100:548–57. doi: 10.1002/cpt.419
49. de Jong J, Hellemans P, De Wilde S, Patricia D, Masterson T, Manikhas G, et al. A drug-drug interaction study of ibrutinib with moderate/strong CYP3A inhibitors in patients with B-cell malignancies. *Leuk Lymphoma*. (2018) 59:2888–95. doi: 10.1080/10428194.2018.1460474
50. Sonnichsen D, Dorer DJ, Cortes J, Talpaz M, Deininger MW, Shah NP, et al. Analysis of the potential effect of ponatinib on the QTc interval in patients with refractory hematological malignancies. *Cancer Chemother Pharmacol*. (2013) 71:1599–607. doi: 10.1007/s00280-013-2160-7

51. Massaro F, Molica M, Breccia M. Ponatinib: a review of efficacy and safety. *Curr Cancer Drug Targets*. (2018) 18:847–56. doi: 10.2174/1568009617666171002142659
52. Singh AP, Umbarkar P, Tousif S, Lal H. Cardiotoxicity of the BCR-ABL1 tyrosine kinase inhibitors: emphasis on ponatinib. *Int J Cardiol*. (2020) 316:214–21. doi: 10.1016/j.ijcard.2020.05.077
53. Gozgit JM, Wong MJ, Moran L, Wardwell S, Mohemmad QK, Narasimhan NI, et al. Ponatinib (AP24534). a multitargeted pan-FGFR inhibitor with activity in multiple FGFR-amplified or mutated cancer models. *Mol Cancer Therap*. (2012) 11:690–9. doi: 10.1158/1535-7163.MCT-11-0450
54. Sharma A, Burridge PW, McKeithan WL, Serrano R, Shukla P, Sayed N, et al. High-throughput screening of tyrosine kinase inhibitor cardiotoxicity with human induced pluripotent stem cells. *Sci Transl Med*. (2017) 9:aaf2584. doi: 10.1126/scitranslmed.aaf2584
55. Breccia M, Pregno P, Spallarossa P, Arboscello E, Ciceri F, Giorgi M, et al. Identification, prevention and management of cardiovascular risk in chronic myeloid leukaemia patients candidate to ponatinib: an expert opinion. *Ann Hematol*. (2017) 96:549–58. doi: 10.1007/s00277-016-2820-x
56. Ariad suspends ponatinib sales. *Cancer Discov*. (2014) 4:6–7. doi: 10.1158/2159-8290.CD-NB2013-163
57. O'Hare T, Shakespeare WC, Zhu X, Eide CA, Rivera VM, Wang F, et al. AP24534. a pan-BCR-ABL inhibitor for chronic myeloid leukemia, potently inhibits the T315I mutant and overcomes mutation-based resistance. *Cancer Cell*. (2009) 16:401–12. doi: 10.1016/j.ccr.2009.09.028
58. Chan O, Talati C, Isenalumhe L, Shams S, Nodzon L, Fradley M, et al. Pinilla-Ibarz J. Side-effects profile and outcomes of ponatinib in the treatment of chronic myeloid leukemia. *Blood Adv*. (2020) 4:530–8. doi: 10.1182/bloodadvances.2019000268
59. Lipton JH, Chuah C, Guerci-Bresler A, Rosti G, Simpson D, Assouline S, et al. Ponatinib versus imatinib for newly diagnosed chronic myeloid leukaemia: an international, randomised, open-label, phase 3 trial. *Lancet Oncol*. (2016) 17:612–21. doi: 10.1016/S1470-2045(16)00080-2
60. Chien JY, Lucksiri A, Ernest CS 2nd, Gorski JC, Wrighton SA, Hall SD. Stochastic prediction of CYP3A-mediated inhibition of midazolam clearance by ketoconazole. *Drug Metab Disposition*. (2006) 34:1208–19. doi: 10.1124/dmd.105.008730
61. Narasimhan NI, Dorer DJ, Niland K, Haluska F, Sonnichsen D. Effects of ketoconazole on the pharmacokinetics of ponatinib in healthy subjects, J Clin Pharmacol. (2013) 53:974–81. doi: 10.1002/jcph.109
62. Kantarjian HM, Giles F, Gattermann N, Bhalla K, Alimena G, Palandri F, et al. Nilotinib (formerly AMN107), a highly selective BCR-ABL tyrosine kinase inhibitor, is effective in patients with Philadelphia chromosome-positive chronic myelogenous leukemia in chronic phase following imatinib resistance and intolerance. *Blood*. (2007) 110:3540–6. doi: 10.1182/blood-2007-03-080689
63. Garnock-Jones KP. Nilotinib: in the first-line treatment of newly diagnosed Philadelphia chromosome-positive chronic myeloid leukaemia in chronic phase. *Drugs*. (2011) 71:1579–90. doi: 10.2165/11207770-000000000-00000
64. Manley PW, Stiefl N, Cowan-Jacob SW, Kaufman S, Mestan J, Wartmann M, et al. Structural resemblances and comparisons of the relative pharmacological properties of imatinib and nilotinib. *Bioorg Med Chem*. (2010) 18:6977–86. doi: 10.1016/j.bmc.2010.08.026
65. Weisberg E, Manley PW, Breitenstein W, Brüggen J, Cowan-Jacob SW, Ray A, et al. Characterization of AMN107, a selective inhibitor of native and mutant Bcr-Abl. *Cancer Cell*. (2005) 7:129–41. doi: 10.1016/j.ccr.2005.01.007
66. Sacha T, Saglio G. Nilotinib in the treatment of chronic myeloid leukemia. *Future Oncol*. (2019) 15:953–65. doi: 10.2217/fon-2018-0468
67. Shopp GM, Helson L, Bouchard A, Salvail D, Majeed M. Liposomes ameliorate Crizotinib- and Nilotinib-induced inhibition of the cardiac IKr channel and QTc prolongation. *Anticancer Res*. (2014) 34:4733–40.
68. Takahashi N, Miura M, Kuroki J, Mitani K, Kitabayashi A, Sasaki O, et al. Multicenter phase II clinical trial of nilotinib for patients with imatinib-resistant or -intolerant chronic myeloid leukemia from the East Japan CML study group evaluation of molecular response and the efficacy and safety of nilotinib. *Biomarker Res*. (2014) 2:6. doi: 10.1186/2050-7771-2-6
69. Kim TD. le Coutre P, Schwarz M, Grille P, Levitin M, Fateh-Moghadam S, et al. Clinical cardiac safety profile of nilotinib. *Haematologica*. (2012) 97:883–9. doi: 10.3324/haematol.2011.058776
70. Larson RA, Yin OQ, Hochhaus A, Saglio G, Clark RE, Nakamae H, et al. Population pharmacokinetic and exposure-response analysis of nilotinib in patients with newly diagnosed Ph+ chronic myeloid leukemia in chronic phase. *Euro J Clin Pharmacol*. (2012) 68:723–33. doi: 10.1007/s00228-011-1200-7
71. Giles FJ, Yin OQ, Sallas WM. le Coutre PD, Woodman RC, Ottmann OG, et al. Nilotinib population pharmacokinetics and exposure-response analysis in patients with imatinib-resistant or -intolerant chronic myeloid leukemia. *Euro J Clin Pharmacol*. (2013) 69:813–23. doi: 10.1007/s00228-012-1385-4
72. Tian X, Zhang H, Heimbach T, He H, Buchbinder A, Aghoghovbia M, et al. Clinical pharmacokinetic and pharmacodynamic overview of Nilotinib, a selective tyrosine kinase inhibitor. *J Clin Pharmacol*. (2018) 58:1533–40. doi: 10.1002/jcph.1312
73. Shibata T, Minami Y, Mitsuma A, Morita S, Inada-Inoue M, Oguri T, et al. Association between severe toxicity of nilotinib and UGT1A1 polymorphisms in Japanese patients with chronic myelogenous leukemia. *Int J Clin Oncol*. (2014) 19:391–6. doi: 10.1007/s10147-013-0562-5
74. Tanaka C, Yin OQ, Smith T, Sethuraman V, Grouss K, Galitz L, et al. Effects of rifampin and ketoconazole on the pharmacokinetics of nilotinib in healthy participants. *J Clin Pharmacol*. (2011) 51:75–83. doi: 10.1177/0091270010367428
75. Zhang H, Sheng J, Ko JH, Zheng C, Zhou W, Priess P, et al. Inhibitory effect of single and repeated doses of nilotinib on the pharmacokinetics of CYP3A substrate midazolam. *J Clin Pharmacol*. (2015) 55:401–8. doi: 10.1002/jcph.434
76. Chaar M, Kamta J, Ait-Oudhia S. Mechanisms, monitoring, and management of tyrosine kinase inhibitors-associated cardiovascular toxicities. *Onco Targets Ther*. (2018) 11:6227–37. doi: 10.2147/OTT.S170138
77. Foa R, Vitale A, Vignetti M, Meloni G, Guarini A, De Propris MS, et al. Dasatinib as first-line treatment for adult patients with Philadelphia chromosome-positive acute lymphoblastic leukemia. *Blood*. (2011) 118:6521–8. doi: 10.1182/blood-2011-05-351403
78. Foà R, Bassan R, Vitale A, Elia L, Piciocchi A, Puzzolo MC, et al. Dasatinib-Blinatumomab for Ph-positive acute lymphoblastic leukemia in adults. *N Engl J Med*. (2020) 383:1613–23. doi: 10.1056/NEJMoa2016272
79. Barbarin A, Abdallah M, Lefevre L, Piccirilli N, Cayssials E, Roy L, et al. Innate T-alphabeta lymphocytes as new immunological components of anti-tumoral "off-target" effects of the tyrosine kinase inhibitor dasatinib. *Sci Rep*. (2020) 10:3245. doi: 10.1038/s41598-020-60195-z
80. Haouala A, Widmer N, Duchosal MA, Montemurro M, Buclin T, Decosterd LA. Drug interactions with the tyrosine kinase inhibitors imatinib, dasatinib, and nilotinib. *Blood*. (2011) 117:e75–87. doi: 10.1182/blood-2010-07-294330
81. Kamath AV, Wang J, Lee FY, Marathe PH. Preclinical pharmacokinetics and in vitro metabolism of dasatinib (BMS-354825): a potent oral multi-targeted kinase inhibitor against SRC and BCR-ABL. *Cancer Chemother Pharmacol*. (2008) 61:365–76. doi: 10.1007/s00280-007-0478-8
82. Johnson FM, Agrawal S, Burris H, Rosen L, Dhillon N, Hong D, et al. Phase 1 pharmacokinetic and drug-interaction study of dasatinib in patients with advanced solid tumors. *Cancer*. (2010) 116:1582–91. doi: 10.1002/cncr.24927
83. Chen T, Xu T, Li Y, Liang C, Chen J, Lu Y, et al. Risk of cardiac dysfunction with trastuzumab in breast cancer patients: a meta-analysis. *Cancer Treatm Rev*. (2011) 37:312–20. doi: 10.1016/j.ctrv.2010.09.001
84. Abdel-Qadir H, Ethier JL, Lee DS, Thavendiranathan P, Amir E. Cardiovascular toxicity of angiogenesis inhibitors in treatment of malignancy: a systematic review and meta-analysis. *Cancer Treatm Rev*. (2017) 53:120–7. doi: 10.1016/j.ctrv.2016.12.002
85. Chang HM, Moudgil R,Scarabelli T, Okwuosa TM, Yeh ETH. Cardiovascular complications of cancer therapy: best practices in diagnosis, prevention, and management: part 1. *J Am Coll Cardiol*. (2017) 70:2536–51. doi: 10.1016/j.jacc.2017.09.1096
86. Zamorano JL, Lancellotti P, Rodriguez Muñoz D, Aboyans V, Asteggiano R, Galderisi M, et al. 2016 ESC Position Paper on cancer treatments and cardiovascular toxicity developed under the auspices of the ESC Committee for Practice Guidelines: The Task Force for cancer treatments and cardiovascular toxicity of the European Society of Cardiology (ESC). *Eur Heart J*. (2016) 37:2768–801. doi: 10.1093/eurheartj/ehw211

87. Wu Q, Bai B, Tian C, Li D, Yu H, Song B, Li B, Chu X. The molecular mechanisms of cardiotoxicity induced by HER2, VEGF, and tyrosine kinase inhibitors: an updated review. *Cardiovasc Drugs Ther*. (2021). doi: 10.1007/s10557-021-07181-3
88. Chang HM, Okwuosa TM, Scarabelli T, Moudgil R, Yeh ETH. Cardiovascular complications of cancer therapy: best practices in diagnosis, prevention, and management: part 2. *J Am Coll Cardiol*. (2017) 70:2552–65. doi: 10.1016/j.jacc.2017.09.1095
89. Suttorp M, Bornhäuser M, Metzler M, Millot F, Schleyer E. Pharmacology and pharmacokinetics of imatinib in pediatric patients. *Expert Rev Clin Pharmacol*. (2018) 11:219–31. doi: 10.1080/17512433.2018.1398644
90. Rimassa L, Danesi R, Pressiani T, Merle P. Management of adverse events associated with tyrosine kinase inhibitors: improving outcomes for patients with hepatocellular carcinoma. *Cancer Treat Rev*. (2019) 77:20–8. doi: 10.1016/j.ctrv.2019.05.004
91. Tsang VHM. Management of treatment-related toxicities in advanced medullary thyroid cancer. *Curr Opin Oncol*. (2019) 31:236–42. doi: 10.1097/CCO.0000000000000534

Conflict of Interest: The authors declare that the research was conducted in the absence of any commercial or financial relationships that could be construed as a potential conflict of interest.

frontiers in Cardiovascular Medicine

SYSTEMATIC REVIEW
published: 19 November 2021
doi: 10.3389/fcvm.2021.752939

N-Acetylcysteine for Cardiac Protection During Coronary Artery Reperfusion: A Systematic Review and Meta-Analysis of Randomized Controlled Trials

Sher Ali Khan[1], *Ashley M. Campbell*[1], *Yingying Lu*[2], *Lingling An*[3,4], *Joseph S. Alpert*[5] *and Qin M. Chen*[1]*

[1] Department of Pharmacy Practice and Science, College of Pharmacy, University of Arizona, Tucson, AZ, United States, [2] Graduate Interdisciplinary Program in Statistics and Data Science, University of Arizona, Tucson, AZ, United States, [3] Department of Biosystems Engineering, College of Agriculture and Life Sciences, University of Arizona, Tucson, AZ, United States, [4] Department of Epidemiology and Biostatistics, Mel & Enid Zuckerman College of Public Health, University of Arizona, Tucson, AZ, United States, [5] Department of Medicine and the Sarver Heart Center, University of Arizona College of Medicine, Tucson, AZ, United States

OPEN ACCESS

Edited by:
Chen Yan,
University of Rochester, United States

Reviewed by:
Si Chen,
University of Rochester, United States
Tingting Wang,
Huazhong University of Science and Technology, China
Jianxin Sun,
Thomas Jefferson University, United States

***Correspondence:**
Qin M. Chen
qchen1@pharmacy.arizona.edu

Specialty section:
This article was submitted to Cardio-Oncology, a section of the journal Frontiers in Cardiovascular Medicine

Received: 03 August 2021
Accepted: 08 October 2021
Published: 19 November 2021

Citation:
Khan SA, Campbell AM, Lu Y, An L, Alpert JS and Chen QM (2021) N-Acetylcysteine for Cardiac Protection During Coronary Artery Reperfusion: A Systematic Review and Meta-Analysis of Randomized Controlled Trials. Front. Cardiovasc. Med. 8:752939. doi: 10.3389/fcvm.2021.752939

Coronary artery reperfusion is essential for the management of symptoms in the patients with myocardial ischemia. However, the benefit of reperfusion often comes at an expense of paradoxical injury, which contributes to the adverse events, and sometimes heart failure. Reperfusion is known to increase the production of reactive oxygen species (ROS). We address whether N-acetylcysteine (NAC) reduces the ROS and alleviates reperfusion injury by improving the clinical outcomes. A literature search for the randomized controlled trials (RCTs) was carried out in the five biomedical databases for testing the effects of NAC in patients undergoing coronary artery reperfusion by percutaneous coronary intervention, thrombolysis, or coronary artery bypass graft. Of 787 publications reviewed, 28 RCTs were identified, with a summary of 2,174 patients. A meta-analysis using the random effects model indicated that NAC administration during or prior to the reperfusion procedures resulted in a trend toward a reduction in the level of serum cardiac troponin (cTn) [95% *CI*, standardized mean difference (SMD) −0.80 (−1.75; 0.15), $p = 0.088$, $n = 262$ for control, 277 for NAC group], and in the incidence of postoperative atrial fibrillation [95% *CI*, relative risk (RR) 0.57 (0.30; 1.06), $p = 0.071$, $n = 484$ for control, 490 for NAC group]. The left ventricular ejection fraction or the measures of length of stay in intensive care unit (ICU) or in hospital displayed a positive trend that was not statistically significant. Among the nine trials that measured ROS, seven showed a correlation between the reduction of lipid peroxidation and improved clinical outcomes. These lines of evidence support the potential benefit of NAC as an adjuvant therapy for cardiac protection against reperfusion injury.

Keywords: N-acetylcysteine, coronary artery bypass, percutaneous coronary intervention, atrial fibrillation, antioxidants, reactive oxygen species, acute coronary syndrome, stable angina

INTRODUCTION

A reperfusion injury has long been an unavoidable complication of the coronary artery revascularization procedures for the patients with acute or chronic myocardial ischemia. Although essential for the survival or for the relief of symptoms, reperfusion can contribute to as much as 40% of the final infarct size (1). The most common reperfusion procedure for the patients with myocardial ischemic is percutaneous coronary intervention (PCI). When reperfusion cannot be achieved successfully by PCI alone or in the setting of multivessel coronary disease, open heart surgery of coronary artery bypass graft (CABG) may be performed. Thrombolytic therapy can be prescribed during PCI, or alone when PCI and CABG are not readily available or impossible to perform due to the condition of a patient. One complication for each of these reperfusion treatments is periprocedural myocardial injury (PMI), which is linked to arrhythmias or reinfarction and in some cases heart failure. The release of massive amounts of reactive oxygen species (ROS) during reperfusion is thought to be an important cause of PMI.

Periprocedural myocardial injury is measurable with a number of clinical parameters, such as elevation of circulating cardiac troponins (cTn) or creatine kinase muscle band (CK-MB). Whereas, the amplitude or duration of cTn elevation can be predictive for the adverse events and heart failure (2–4), the extent of PMI is associated with the incidence of post-operative atrial fibrillation (POAF) (5). As a common complication following an open-heart surgery, the incidence of POAF can reach up to 70% in the patients after an elective CABG (6). POAF can cause stroke and increase the length of stay (LOS) in the intensive care unit (ICU) or in hospital. There is evidence supporting the concept that ROS and cytokine storm play a key role in the pathogenesis of POAF (7).

Despite a well-established association, ROS remains a neglected therapeutic target for the patients undergoing coronary reperfusion procedures. Administration of N-acetylcysteine (NAC) before reperfusion is expected to reduce the ROS generation. While a few randomized controlled trials (RCTs) showed a significant inhibition of cTn or CK-MB release or the incidence of POAF, other RCTs did not report positive outcomes. Given these inconsistences, it is prudent to address whether NAC provides a benefit for the coronary reperfusion procedures through a systematic review and meta-analysis approach.

A few meta-analyses have assessed the cardioprotective effect of NAC during cardiac surgery (8–12). However, each of these reports has a limited number of references. More importantly, none of these reports have included consideration of PCI. About 90% of the patients with ST segment elevation myocardial infarct (STEMI) and 50% of the patients with non-STEMI are treated with PCI (13), supporting the importance of PCI when considering the benefit of NAC during reperfusion. Nevertheless, none of these published meta-analyses have determined the impact of NAC on all the common clinical measures, such as elevation of cTn or CK-MB, change in left ventricular ejection fraction (LVEF), and ICU or hospital length of stay (LOS). In addition, whether the clinical outcomes correlate with the reduction of ROS has not been determined. Here, we address the cardioprotective effect of NAC when administered before PCI, CABG, or thrombolysis by summarizing the data from the publications with relevant clinical measures. In addition, the levels of antioxidants and ROS are captured to support the cause-effect relationship.

METHODS

The Preferred Reporting Items for Systematic Reviews (PRISMA) guideline was adopted for this systematic literature review using an *a-priori* inclusion and exclusion criteria (14).

Inclusion and Exclusion Criteria

A-priori inclusion criteria were: (1) the RCTs assessing the effect of NAC in the patients >18 years old who underwent coronary reperfusion by PCI, CABG, or thrombolysis; (2) NAC was administered within 24 h before or during coronary reperfusion; (3) the RCTs should have measured the effect of NAC in comparison to a control group; (4) the control group should have received either placebo or standard care; (5) the published manuscripts and abstracts for the RCTs; (6) the RCTs published in any language; (7) the RCTs should not have selectively included the participants with any degree of renal insufficiency; and (8) the RCTs published from inception to September 18, 2021.

We excluded those RCTs in which the effect of NAC was not compared with a control group, but instead was compared with another pharmacologic agent. In addition, we excluded those RCTs reporting the trials designed for the selective patients with renal insufficiency, since renal insufficiency itself causes increased levels of cTn and CK-MB (15), potentially underestimating the beneficial effect of NAC on cardiac injury.

We considered both the clinical cardiac endpoints and mechanistic measures in this systematic review. The clinical endpoints included biomarkers of myocardial injury (cTn and CK-MB), cardiac contractility (left ventricular ejection fraction, LVEF), infarct size, incidence of POAF, and postoperative ICU or hospital LOS. The mechanistic measures consisted of markers for total antioxidant capacity (TAC) and ROS. To reduce the complexity of the data, we only extracted the serum and urine levels of the non-clinical markers and excluded the measures from the biopsy samples.

Literature Search and Data Extraction

A comprehensive search strategy was developed with the assistance of a health science librarian (Rachel Walden) using a combination of keywords and controlled vocabulary to identify the studies reporting the use of NAC in the patients undergoing coronary artery reperfusion with PCI, CABG, or thrombolysis. The search strategy was developed for PubMed/Medline (NLM) and was subsequently translated to carry out the searches in four other biomedical bibliographic databases: Embase (Elsevier), Web of Science (Clarivate Analytics), Cumulative Index to Nursing and Allied Health Literature (CINAHL), and Cochrane Library (Wiley). In addition to searching the five bibliographic databases, a search of the gray literature (Clinicaltrials.gov) was

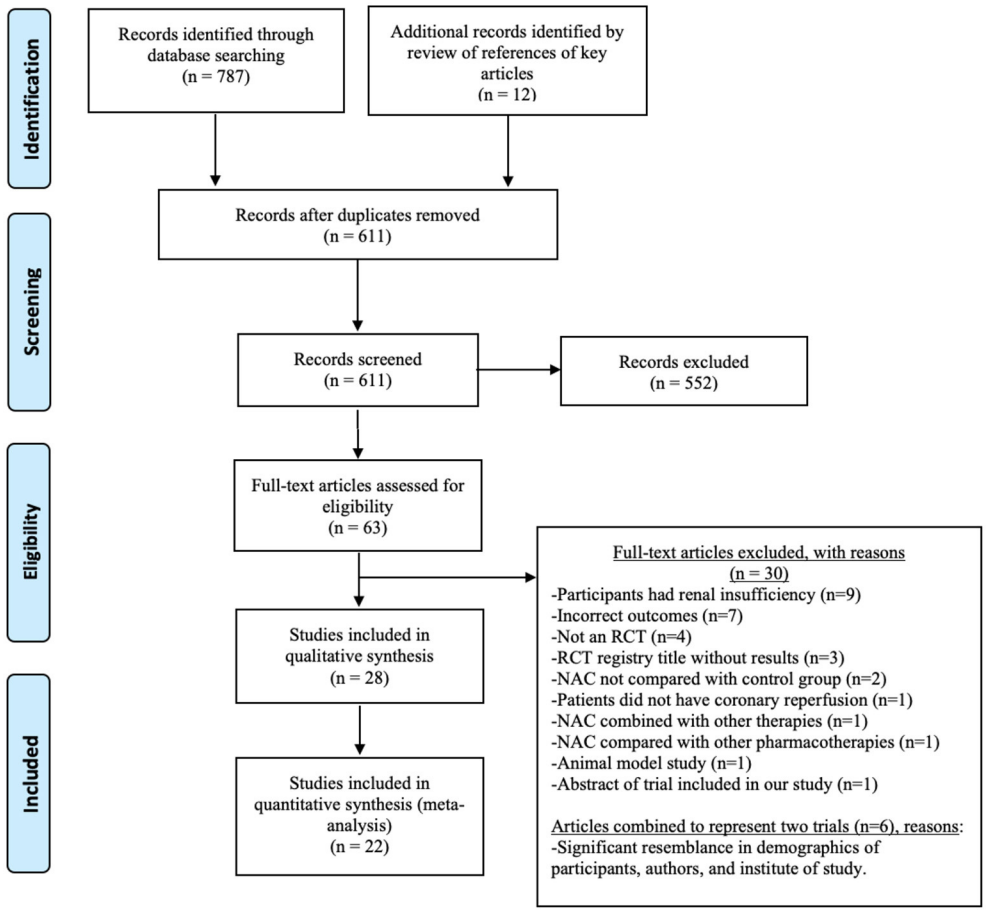

FIGURE 1 | Preferred Reporting Items for Systematic Reviews and Meta-Analyses (PRISMA) flow diagram. The numbers document the literature search results.

performed. We searched for the trials from inception through September 18, 2021.

The following keywords were used to create the search strategy: myocardial reperfusion, T-Plasminogen activator, TPA, activase, alteplase, percutaneous transluminal coronary angioplasty, coronary balloon angioplasty, transluminal coronary balloon dilation, percutaneous coronary revascularization, percutaneous coronary intervention, PCI, coronary artery bypass grafting, CABG, aortocoronary bypass, coronary artery bypass surgery, coronary artery bypass, and acetylcysteine (as shown in **Supplementary Material** for full search strategy).

The primary (SAK) and the secondary reviewer (AMC) independently searched and screened the reports. Rayyan QCRI Systematic Reviews Web Application was used after careful removal of duplicate records (16). No major discrepancies were noted among the two independent reviewers in the shortlisted trials. The primary reviewer extracted the data and assessed the risk of bias for each RCT, while the secondary reviewer validated the data for each publication. Minor discrepancies were noted in the extracted data, which were resolved with discussion reaching a mutual agreement. The PRISMA flowchart summary is shown in **Figure 1**.

Quality Assessment of Included Trials

The revised Cochrane risk of bias tool for randomized trials (RoB2) was applied by the primary and secondary reviewers to assess the risk of bias for each included trial [https://methods.cochrane.org/bias/resources/rob-2-revised-cochrane-risk-bias-tool-randomized-trials (2020, accessed 10 May 2020)]. The following domains were evaluated: random sequence generation, allocation concealment, blinding of patients and personnel, blinding of outcome assessment, and incomplete outcome data. Similar to the data extraction process, minor discrepancies in the risk of bias assessment were resolved through discussion for consensus generation.

Statistical Analysis

The measurements in cTn, CK-MB, LVEF, and LOS were treated as the continuous variables with reported means and SDs, while the incidence of POAF was treated as a dichotomous variable. Instead of applying the fixed effects models, which operate under the assumption that the estimated effects across the studies were pulled from a single population, we employed the random effects models to calculate the pooled effects, as the true effect may derive from a distribution, due to the fact that multiple studies were

pulled from the different populations (17). The Sidik–Jonkman estimator was used for estimating the variance of the distribution of the true effect (18). The false positive rate increases when a small number of studies are enrolled and the outcome measures vary largely between the trials (19, 20).

In this NAC meta-analysis, the number of studies for each of six types of outcome measures varied from 5 to 12. Therefore, the Hartung-Knapp-Sidik-Jonkman method was also utilized to generate more robust estimates of the variance of pooled effects (19). When the outcome measures were continuous variables, the standardized mean difference (SMD) was calculated as a measure of effect size, as this is appropriate when different units were used across the studies (21). The SMD standardizes outcome measures in various units so that they are comparable at the same scale. Within a study, the SMD divides the mean difference of values of a measure by the pooled SD, thus SMD becomes a unitless standardized value. Hence, the SMDs can be compared across the studies for the related measures without the consideration of their respective units. The meta-analysis produces a pooled SMD, which denotes a change in the combined SD for a specific measure.

For dichotomous variables, relative risk (RR), a measure of effect size, was used as the likelihood of an event occurring between the two groups (NAC vs. control). The between-study heterogeneity was reported by I^2. The individual effect size for each study and its weight, as well as confidence interval (CI) for the individual studies and pooled estimates, were included in the results. All the statistical analyses were performed using R version 3.6 (https://www.r-project.org/) (2013, accessed 10 May 2020). Specifically, the meta-analysis was performed by the packages meta (22), metafor (23), and dmetar (24).

RESULTS

Characteristics of the Trials

Figure 1 shows the PRISMA flowchart and the number of publications evaluated, leading to the selection of 28 trials in 32 publications for this systematic review (25–56). The characteristics of the included trials are summarized in **Table 1**. Geographically, the reported trials were carried out in 10 countries: Turkey (10), Iran (5), India (3), Germany (2), Uzbekistan (1), Czech Republic (1), Finland (1), Canada (1), Australia (1), Brazil (1), Korea (1), and China (1). The total sample size, by adding the number of patients in the final statistical analyses for each of the 28 included trials, was 2,174. Among the 26 trials with the gender and age distribution indicated as shown in **Table 1**, the mean age of the patients ranged from 53 to 71.5 years old. The two trials did not disclose the age distribution (30, 56).

N-acetylcysteine was administered *via* intravenous (IV) infusion in the 23 trials and the oral route (PO) in the 3 trials. The two trials administered NAC *via* both IV and PO. One trial did not report the route of NAC administration or dose (30). The dose of NAC ranged from 20 to 150 mg/kg in the 19 trials, and 0.3–4.2 g in nine trials (**Table 1**). NAC was administered during coronary reperfusion in the 16 trials, while 8 trials administered NAC within 30–120 min before the start of reperfusion procedures. Four trials administered NAC the same day but before reperfusion procedure without specifying the timing (25, 28, 30, 34).

Among the 32 publications for the 28 trials included, 30 were journal articles and 2 were published abstracts. Twenty trials assessed the effect of NAC during CABG, five during PCI, two during thrombolysis, and one trail during PCI in combination with thrombolysis. Twenty-one trials had placebo controls, whereas seven practiced standard care in the control group. CABG was mostly elective for coronary artery disease, whereas the PCI and thrombolysis cases were urgent for acute coronary syndrome, except one trial where PCI was elective (39). All the included trials were published in English except one in Chinese (56), which was translated to English.

Risk of Bias Analysis

The results from the risk of bias analysis are indicated in **Figure 2**. Each domain was assigned with a low, unclear, or high risk of bias score. Among the 28 included trials, low risk of bias was noted in the 25 trials, while some concern for risk of bias was noted in 3 trials as indicated in **Figure 2**. None of the trials showed a high risk of bias. Hence all the trials were included for the synthesis of final results.

Effect of NAC Administration on the Clinical Outcomes

Serum cTn Elevation

Eight trials reported the means and SDs for the serum levels of either cardiac troponin I (cTnI) or troponin T (cTnT) following CABG or PCI (25, 33, 34, 40, 42, 46, 47, 49). The units of the measures are indicated in **Figure 3** legend. Two of the reports did not include units for troponin (34, 47). The inquires to the authers of one report were not answered. A meta-analysis using SMD allows us to pool the values of cTnI and cTnT in a scaleless format into one analysis (57). This method does not require units for troponin. The means and SDs were extracted from each trial for the meta-analysis, with the form of troponin measured from each trial indicated in the figure legend (**Figure 3A**). Adding the enrollments from these trials yielded a total number of 271 for NAC and 262 for the control group. With a 95% *CI*, the pooled SMD was −0.80, with a range from −1.75 to 0.15 ($p = 0.088$). The value −0.8 implies that cTn decreased by 0.8 times the pooled SD, which was 1.1, as a result of the NAC treatment when compared with placebo or standard care. This indicates a notable decrease in the cTn levels, even though the *p*-value for such decrease is 0.088, not significant but showing a trend. As expected, a high heterogeneity was observed across the trials ($I^2 = 92\%$, $p < 0.01$).

One trial was not entered into the meta-analysis due to reported median and interquartile ranges (IQR) for cTn, instead of means and SDs (43); hence, ineligible for grouping with the rest of the studies to perform the meta-analysis. This study used low dose NAC, 0.3 g, and did not indicate whether the reduction in the median cTn levels was significant due to NAC treatment [NAC group 4.8 (IQR 2.7, 6.0)] vs. control [5.5 (IQR 2.8, 6.4)]. Overall, our meta-analysis of eight trials suggests that there is a

TABLE 1 | The characteristics of 28 randomized controlled trials (RCTs) meeting the inclusion and exclusion criteria.

References	Origin	Procedure	n (Ctr, NAC)	Age [Yr, Mean ± SD, or *median (IQR)*]		Sex (male) *n* (%)		Route	Ctr Tx	NAC dose
				Ctr	NAC	Ctr	NAC			
Shafiei et al. (25)[a]	Iran	CABG[o]	58 (30, 28)	61.6 ± 7.7	57.7 ± 11.2	14 (46.7)	18 (64.3)	PO	PLB	4.2 g
Soleimani et al. (26)[c]	Iran	CABG[o]	141 (69, 72)	60.7 ± 8.4	62.4 ± 8.9	34 (49.2)	39 (54.1)	IV	PLB	0.05 g/kg
Pasupathy et al. (27)[d]	Australia	PCI[p]	112 (59, 53)	63 ± 14	64 ± 15	31 (52.5)	33 (62.2)	IV	PLB	1.2 g
Aldemir et al. (28)[e]	Turkey	CABG[o]	60 (30, 30)	*70.50 (68–73.2)*	*71.5 (69–73.5)*	22 (73)	18 (60)	IV	PLB	0.15 g/kg
Erdil, et al. (29)	Turkey	CABG[o]	82 (40, 42)	58.8 ± 9.9	58.6 ± 10.1	36 (85)	35 (83.3)	PO, IV	PLB	0.6 g/d × 3 d, 0.3 g
Nizomov et al. (30)[n]	Uzbekistan	PCI[p]	52 (25, 27)	NA	NA	NA	NA	NA	PLB	NA
Jalakandan et al. (31)	India	CABG[o]	50 (25, 25)	56.5 ± 6.7	59.8 ± 8.1	21 (84)	18 (72)	IV	PLB	0.15 g/kg
Talasaz et al. (32)[n] Nozari et al. (33) [b]	Iran	PCI[p]	100 (50, 50)	58.3 ± 11.3	57.6 ± 11.5	36 (72)	42 (84)	IV IC	PLB	IV 0.1 g/kg/30 mins +IC 480 mg/20 mins+IV10 mg/kg/h for 12 h
Talasaz et al. (34)[b]	Iran	PCI[p], TL[p]	88 (38, 50)	*61 (40–86)*	*61 (42–92)*	31 (82)	41 (82)	PO	PLB	1.2 g/d × 3 d
Kazemi et al. (35)	Iran	CABG[o]	240 (120, 120)	58.2 ± 12.7	61.3 ± 9.8	88 (73.3)	91 (75.8)	PO	PLB	1.2 g
Ozaydin et al. (36, 37)[f]	Turkey	CABG[o]	208 (104,104)	62 ± 9	63 ± 9	76 (73.1)	81 (77.9)	IV	PLB	0.05 g/kg
Kim et al. (38)	Korea	CABG[o]	48 (24, 24)	65.3 ± 7.6	60.8 ± 8.4	22 (91.6)	21 (87.5)	IV	PLB	0.1 g/kg
Buyukhatipoglu et al. (39)	Turkey	PCI[o]	60 (30, 30)	61.8 ± 10.0	58.9 ± 11.1	21 (70)	21 (70)	IV	Std	0.6 g
Kurian et al. (40)	India	CABG[o]	50 (25, 25)	60.1 ± 9.4	61.1 ± 10.3	17 (68)	15 (60)	IV	PLB	0.02 g/kg
Thiele et al. (41)[g]	Germany	PCI[p]	251 (125, 126)	*68 (57–75)*	*68 (56–76)*	82 (66)	89 (71)	IV	PLB	1.2 g
Prabhu et al. (42)	India	CABG[o]	53 (25, 28)	53.0 ± 8.1	54.2 ± 9.9	NA	NA	IV	Std	0.05 g/kg
Rodrigues et al. (43)[h]	Brazil	CABG[o]	20 (10, 10)	53 ± 7	54 ± 11	4 (40)	6 (60)	IV	Std	0.3 g
Köksal et al. (44)	Turkey	CABG[o]	30 (15, 15)	62.9 ± 4.9	63.4 ± 5.9	13 (86.6)	11 (73.3)	IV	Std	0.6 g
Ozaydin et al. (45) Peker et al. (46)	Turkey	CABG[o]	115 (57, 58)	59 ± 9	57 ± 11	44 (77.2)	47 (81)	IV	PLB	0.05 g/kg
El-Hamamsy et al. (47)	Canada	CABG[o]	100 (50, 50)	61.3 ± 7.4	59.8 ± 7.8	46 (92)	43 (86)	PO, IV	PLB	0.6 g, 0.05 g/kg
Koramaz et al. (48) Karahan et al. (49)	Turkey	CABG	44 (23, 21)	56.4 ± 3.1	58.6 ± 2.7	13 (56.5)	12 (57.1)	IV	Std	0.05 g/kg
Orhan et al. (50)	Turkey	CABG[o]	20 (10, 10)	61.8 ± 4.32	59.6 ± 5.48	6 (60)	7 (70)	IV	PLB	0.05 g/kg
Fischer et al. (51)[i]	Germany	CABG[o,p]	40 (20, 20)	66.5 ± 6.5	66.2 ± 11.8	19 (95)	12 (60)	IV	PLB	0.1 g/kg,
Sucu et al. (52)	Turkey	CABG[o]	40 (20, 20)	64 ± 6	66 ± 4	14 (70)	15 (75)	IV	PLB	0.050 g/kg/d × 3 d
Eren et al. (53)	Turkey	CABG[o]	20 (10, 10)	60.5 ± 5.7	61.1 ± 4.8	7 (70)	8 (80)	IV	PLB	0.1 g/kg
Vento et al. (54)[j]	Finland	CABG	35 (20, 15)	60.2 ± 1.7	63.1 ± 1.9	20(100)	15(100)	IV	Std	0.098 g/kg
Sochman et al. (55)[k]	Czech	TL[p]	30 (16, 14)	54.2 ± 7.2	52.2 ± 14.3	NA	NA	IV	PLB	0.1 g/kg
Yang et al. (56)	China	TL[p]	27 (7, 20)	NA	NA	NA	NA	IV	Std	1.2 g

Ctr, control group; NAC, N-acetylcysteine group; n, enrollment number; Yr, year/s; IQR, interquartile range; CABG, coronary artery bypass grafting; PCI, percutaneous coronary intervention; TL, thrombolysis; NA, not available; IV, intravenous; IC, intracoronary; PO, per oral; PLB, placebo; Std, standard care; g, gram or grams; Kg, kilogram or kilograms; g/kg, gram of NAC per kg of body weight; d, day or days. The numbers without italic indicate mean +/− standard deviation (SD), whereas the numbers with italic indicate median with interquartile range (IQR) in parentheses.

The trial did not have a funding source unless indicated by "a–m", "a" funding from the Research Deputy of Bushehr University of Medical Science, Iran; "b" funding from the Tehran Heart Center, Tehran University of Medical Sciences; "c" the Research Deputy of Mazandaran University of Medical Sciences; "d" funded by the Australian National Heart Foundation, "e" funding from the University Scientific Research Projects Unit; "f" Daiichi-Sankyo Co provided test-kits for TAC and TOS levels; "g" funding from the University of Leipzig; "h" funded by Fundação de Amparo à Pesquisa do Estado de São Paulo and Fundação de Apoio ao Ensino, Pesquisa e Assistência do Hospital das Clínicas da Faculdade de Medicina de Ribeirão Preto-USP; "i" funding from the German Research Foundation; "j" funded by the Helsinki University Central Hospital; and "k" indicates funding by the Internal Grant Agency of the Ministry of Health of the Czech Republic.

All the trials are journals articles unless indicated by "n", which indicates abstract. Under the procedure for CABG, PCI, or TR, "o" indicates an elective procedure for stable atherosclerotic coronary artery disease, "p" indicates an emergency procedure for unstable atherosclerotic coronary artery disease.

FIGURE 2 | Risk of bias of 28 included trials. The plus sign in green (+) shows "low risk" for bias and the question or exclamation mark in yellow (?/!) shows "some concerns" for bias. None of the trials show high risk for bias per RoB2 analyses.

trend toward the reduced levels of cTn in the NAC group when compared with the control group with 95% *CI*.

Serum CK-MB Elevation

The means and SDs for the serum CK-MB concentrations were reported in 10 trials following CABG, PCI, or only pharmacological therapy (33, 34, 40, 44, 46, 47, 50, 51, 54, 55). With a meta-analysis using a 95% *CI*, we obtained a SMD value of 0.04, ranging from −0.43 to 0.50 ($p = 0.861$) (**Figure 3B**). The heterogeneity was moderate across the trials ($I^2 = 73\%$, $p < 0.01$). One trial was not compatible for the meta-analysis, due to reporting median and IQR instead of the means and SDs. This trial indicated no significant difference between the NAC and control groups [338 (IQR 290, 383) vs. 313 (IQR 260, 356) μmol/L/h, $p = 0.13$] (41). Overall, the NAC treatment had no significant effect on the procedure-associated elevation of CK-MB in the serum.

Infarct Size

Three trials measured the infarct size after a coronary reperfusion procedure at 7 days (27, 41, 55). The infarct size was measured using cardiac magnetic resonance imaging (CMR) (27, 41) or

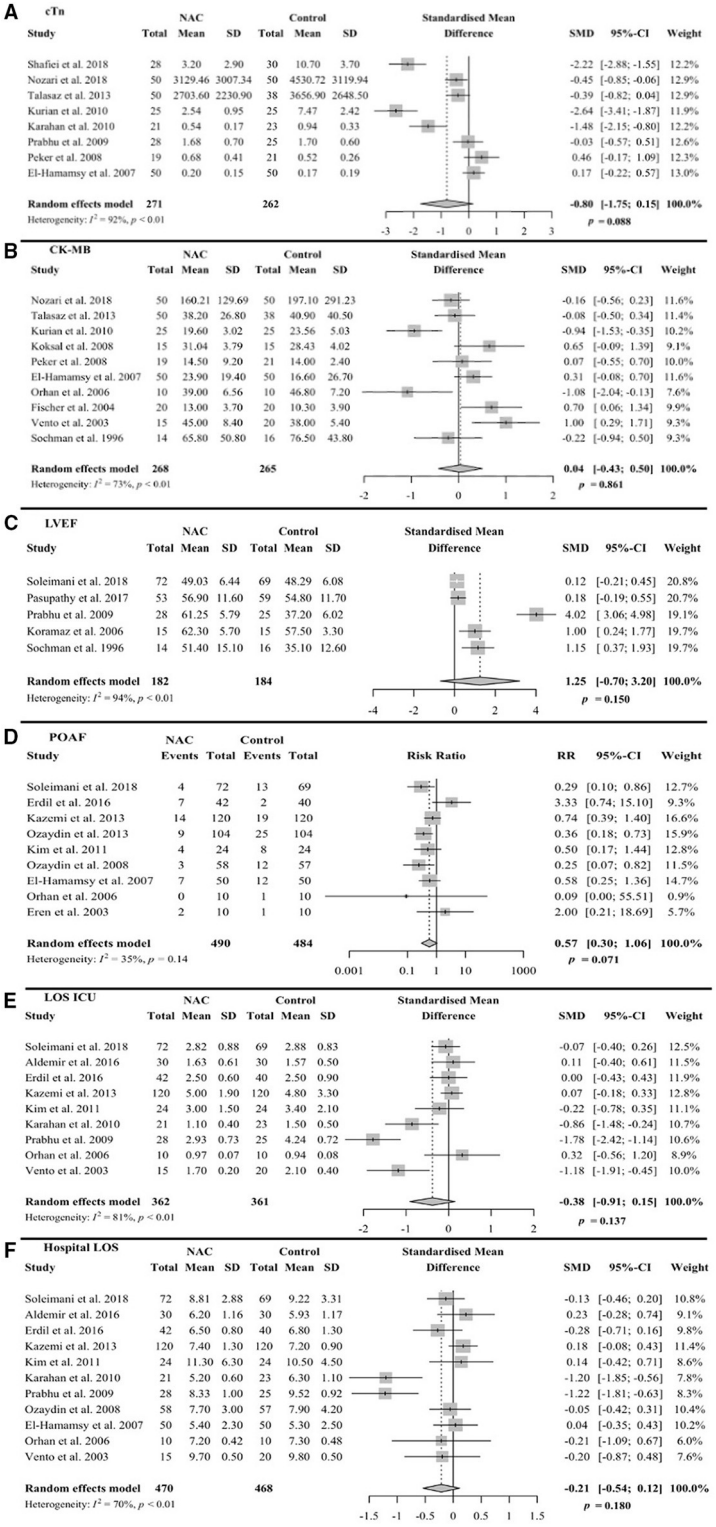

FIGURE 3 | Forest plots of random effects model meta-analysis with 95% confidence interval (CI) comparing NAcetylcysteine (NAC) group vs. control group. The plots are showing standard mean difference (SMD) for continuous variables along with standard deviations (SD) or risk ratio (RR) for binary variables along with events for **(A)** serum troponin levels at 24 h after procedure. Shafiei et al. (25) measured cTnI in ng/ml, Nozari et al. (33) measured high sensitivity TnT (hs-TnT) in ng/dl, Talasaz et al. (32, 34) measured hs-TnT (unit not available, inquires not answered), Kurian et al. (40) measured cTnI in ng/ml, Karahan et al. (49) measured cTnT in ng/ml, Prabhu et al. (42) measured cTnI in ng/ml, Peker et al. (46) measured cTnT in ng/ml, and El-Hamamsy et al. (47) measured cTnT in ng/l (per response to inquires). **(B)** Serum CK-MB levels, **(C)** left ventricular ejection fraction (LVEF), **(D)** post-operative atrial fibrillation (POAF), **(E)** length of stay (LOS) in intensive care unit (ICU), and **(F)** LOS in hospital.

electrocardiography (55). While one trial showed no significant difference [NAC group 17.4% (IQR 9.1, 25.9, $n = 126$) vs. control group 14.3% (IQR 8.0, 26.2, $n = 125$), $p = 0.47$] (41), the two trials reported significantly smaller infarct size in the NAC vs. control groups [11% (IQR 4.1, 16.3, $n = 53$) vs. 16.5% (IQR 10.7, 24.2, $n = 59$), $p = 0.02$; *or* 16.3 ± 10.5, $n = 14$ vs. $24.4\% \pm 9.5$, $n = 16$, $p < 0.05$) (27, 55). Furthermore, Pasupathy et al. (27) measured infarct size at 3 months and reported a significant reduction with the NAC treatment, with the infarct size in the NAC group being 5% on average (IQR 0.7, 12.4, $n = 26$) compared with the control group, which was 10.2% (IQR 6.8, 14.8, $n = 29$ $p = 0.02$). Overall, the two trials showed significant reduction of infarct size, while one trial showed no significant reduction; hence, the results are inconclusive with regard to whether or not NAC can reduce the infarct size.

Left Ventricular Ejection Fraction

Left ventricular ejection fraction was measured within 7 days after coronary reperfusion in the five trials with a sum of 182 enrollments for NAC and 184 for the control group (26, 27, 42, 48, 55). The reported means and SDs were used for the meta-analysis (**Figure 3C**). With a 95% *CI*, the SMD was 1.25 with a range of −0.70 to 3.20 ($p = 0.150$). The heterogeneity was high across the trials ($I^2 = 94\%$, $p < 0.01$). Although the statistical results do not support that NAC had a significant influence on the LVEF, the distribution of means plus SMD value point to a trend of NAC benefit in improving the LVEF.

Not included in the meta-analysis were 4 trials, with a total enrollment of 442, due to reported median instead of means or the differences in time points of the LVEF measurements (27, 30, 41, 56). Nizomov et al. (30) measured LVEF at 1- and 3-month after PCI and indicated a significantly smaller number of participants with LVEF <50% in the NAC vs. control groups [11% vs. 16% at 1 month, $p = 0.046$, and 4% vs. 16% at 3 months, $p = 0.017$], suggesting a benefit of the NAC treatment. Thiele et al. (41) reported that the median values of LVEF measured at 7 days were not significantly different [NAC 52.1% (IQR 43.5, 59.2) vs. control 50.6% (IQR 41.6, 58.6), $p = 0.23$]. Pasupathy et al. (27) did not find a significant difference (NAC $59.6 \pm 11.1\%$ vs. control $56.7 \pm 10.5\%$, $p = 0.33$) in LVEF measured at 3 months. Yang et al. (56) neither revealed the time point of measurement nor reported significant difference in LVEF between the NAC and control groups (57 vs. 53%, no SDs or *p*-values provided). Overall, the results are inconclusive based on the reported median values of LVEF.

Post-operative Atrial Fibrillation

The incidence of POAF was reported in the 9 trials after CABG with a total combined patient number of 490 for NAC and 484 for control (26, 29, 35, 36, 38, 45, 47, 50, 53). It is known that POAF is a rare event following PCI, providing an explanation for the lack of POAF in the PCI trials. The number of patients developing POAF after reperfusion was registered either during the postoperative ICU stay or during the first 3 days of hospital stay. Using the binary outcome of the meta-analysis due to the report of events, we obtained the relative risk (RR) value of 0.57 with 95% *CI*, ranging from 0.30 to 1.06 ($p = 0.071$). The heterogeneity was low across the trials ($I^2 = 35\%$, $P = 0.14$). The meta-analysis points to a reduction, close to 50%, in the incidence of POAF with NAC treatment (**Figure 3D**).

LOS in ICU

The nine trials reported the LOS in ICU with means and SDs for an added-up enrollment of 362 for the NAC group or 361 for the control group (26, 28, 29, 35, 38, 42, 49, 50, 54). The meta-analysis yielded SMD −0.38 with 95% *CI*, ranging −0.91 to 0.15 ($p = 0.137$, **Figure 3E**). The heterogeneity was high across the trials ($I^2 = 81\%$, $p < 0.01$). Although the meta-analysis results did not reveal a significant difference per 95% *CI*, there is a trend toward the reduction of LOS in ICU by the NAC treatment.

LOS in Hospital

Hospital LOS with means and SDs were reported in 11 trials with a total enrollment adding up to 470 (NAC treated) or 468 (control) (26, 28, 29, 35, 38, 42, 45, 47, 49, 50, 54). The meta-analysis produced a SMD of −0.21 with 95% *CI*, ranging −0.54 to 0.12 ($p = 0.180$), and high heterogeneity ($I^2 = 70\%$, $p < 0.01$) (**Figure 3F**). Similar to LOS in ICU, a trend toward the reduction in hospital LOS in the NAC group is shown by the upper boundary of the 95% *CI* close to 0.

Effect of NAC on the Antioxidant Reservoir and ROS

Eighteen publications contained the measures for antioxidants and ROS, among which the nine trials had clinical outcome measures along with the lipid peroxidation product malondialdehyde (MDA). There is a lack of uniformity in the assays or time point of measurements between the studies, and most of the measures at a specific time point have less than five trials, which is not ideal for a meta-analysis. Nevertheless, for most of the measures, there was consistent reduction between the trials.

Total Antioxidant Capacity (TAC)

Seven trials measured the antioxidant levels after the coronary reperfusion procedures (31, 37, 39, 40, 42, 44, 56) (**Table 2**). These studies reported the levels of antioxidants at the baseline and different time points after coronary reperfusion, from 10 min to 48 h. The measurements included reduced glutathione (GSH) or the activities of glutathione peroxidase, glutathione reductase, superoxide dismutase, and catalase in the serum. Two trials reported the outcomes as total antioxidant capacity (TAC) without specifying the scaled measures (37, 39). One trial measured the urine levels of TAC in addition to the serum levels (39).

The measurements of GSH between 1 and 12 h showed significant increases in the three trials (**Table 2**). No significant differences in the activity of glutathione peroxidase were observed, but there was a slight improvement in glutathione reductase in the 2 trials (**Table 2**). The data on superoxide dismutase and catalase are inconsistent among the 3 trials (**Table 2**). Ozaydin et al. (37) reported an improvement of TAC at 24–48 h after NAC, but not by Buyukhatipoglu et al. (39). The latter trial used a much lower dose of NAC (0.6 g, which

TABLE 2 | Total antioxidant capacity (TAC) after coronary artery reperfusion.

References	Measure		Baseline	10 min	30 min	1–12 h	24–48 h
Jalakandan et al. (31)	GSH (nmol/ml)	Ctr	32.79 ± 15.78			24.25 ± 11.56	
		NAC	28.18 ± 10.14			33.82 ± 11.70	
		P	0.225			0.005	
Ozaydin et al. (37)	TAC[a] (mmol Trolox/L)	Ctr	*1.6 (0.7–3.0)*				*1.4 (0.6–3.2)*
		NAC	*1.6 (0.7–2.9)*				*1.9 (0.9–3.9)*
		P	0.89				<0.0001
Buyukhatipoglu et al. (39)	serum TAC (mmol Trolox/L)	Ctr	0.84 ±0.14				0.77 ±0.09
		NAC	0.88 ±0.12				0.81 ±0.07
		P	NS				NS
	urine TAC (mmol Trolox/L)	Ctr	1.52 ± 0.10				1.47 ± 0.16
		NAC	1.56 ± 0.12				1.49 ± 0.10
		P	NS				NS
Kurian et al. (40)	glutathione peroxidase (U/g Hb)	Ctr	6.30 ± 1.2	6.33 ± 1.1	5.89 ± 0.9	5.26 ± 0.9	
		NAC	6.41 ± 1.1	5.41 ± 1.0	4.36 ± 0.8	5.26 ± 0.9	
		P	NS	NS	<0.05	NS	
	glutathione reductase (U/g Hb)	Ctr	1.08 ± 0.16	0.41 ± 0.07	0.42 ± 0.08	0.68 ± 0.08	
		NAC	1.106 ± 0.16	0.426 ± 0.07	0.496 ± 0.08	0.747 ± 0.08	
		P	NS	NS	<0.05	<0.05	
	Superoxide dismutase (U/g Hb)	Ctr	3829.1 ± 323	1218.6 ± 255	1258.9 ± 213	1375.9 ± 221	
		NAC	3938.8 ± 340	1264.7 ± 241	1334.1 ± 254	1461.8 ± 222	
		P	NS	NS	<0.05	<0.05	
	Catalase (pM H_20_2 /min /g Hb)	Ctr	625.72 ± 20.5	985.27 ± 37.6	901.02 ± 36.1	869.93 ± 33.7	
		NAC	620.44 ± 21.73	955.87 ± 39.14	859.47± 35.22	741.38 ± 34.23	
		P	NS	NS	<0.05	<0.05	
Prabhu et al. (42)	GSH [a] (mg/g Hb)	Ctr	0.7 ± 0.08	1.3 ± 0.20		1.25 ± 0.18	1.21 ± 0.15
		NAC	0.75 ± 0.03	1.6 ± 0.10		1.66 ± 0.05	1.31 ± 0.14
		P	NS	<0.001		<0.01	NS
	Glutathione peroxidase[a] (U/g Hb)	Ctr	42.6 ± 2.7	80.4 ± 6.4		59 ± 8	51.6 ± 5.6
		NAC	40.6 ± 3.4	85.7 ± 3.7		62.7 ± 2.7	55 ± 1.4
		P	NS	<0.01		NS	<0.05
	Glutathione reductase[a] (μg/min/g Hb)	Ctr	8.6 ± 0.4	9.9 ± 0.48		10.1 ± 0.5	9.8 ± 0.4
		NAC	8.6 ± 0.4	10.5 ± 0.5		10.4 ± 0.4	9.5 ± 0.1
		P	NS	<0.001		<0.001	NS
	Superoxide dismutase [a] (U/g Hb)	Ctr	367 ± 33	644 ± 31		564 ± 31.8	531 ± 31
		NAC	377 ± 27	708 ± 15		582 ± 18	537 ± 32
		P	NS	<0.001		NS	NS
	Catalase [a] (μmol H_2O_2/ min/g Hb)	Ctr	3.7 ± 1.30	6.0 ± 0.42		5.8 ± 0.60	5.7 ± 0.30
		NAC	4.0 ± 1.0	6.4 ± 0.47		5.8 ± 0.10	5.4 ± 0.40
		P	NS	<0.01		NS	NS
Köksal et al. (44)	Glutathione peroxidase [a] (U/g Hb)	Ctr	24.3 ± 10.7		22.5 ± 8.9		
		NAC	27.7 ± 8.3		28.7 ± 12.9		
		P	NS		NS		
Yang et al. (56)	GSH (mol/L)	Ctr	2.0 ± 2.4			1.4 ± 0.3	1.4 ± 0.4
		NAC	2.2 ± 2.4			2.8 ± 1.3	2.8 ± 1.2
		P	NS			<0.05	<0.05

All numbers represent means ± SDs unless they are italicized, which indicate median (with interquartile ranges, IQR). Ctr: control group, NAC: N-acetylcysteine group. NS: non-significant. "a" indicates that the value was extracted from the figures of the cited publication. TAC: total antioxidant capacity, GSH: reduced glutathione, U/g: units per gram, Hb: Hemoglobin, mmol: millimole(s), nmol: nanomole(s).

translates to 0.01 g/kg per 60 kg body weight) than the average dose of 0.1 g/kg dose. Overall, there is evidence to support the possibility that the administration of NAC before a coronary reperfusion procedure leads to an increase of glutathione redox system activity as expected.

Reactive Oxygen Species

Fourteen publications reported the levels of ROS markers after the coronary reperfusion procedures (25, 27, 31, 37, 39–42, 44, 48, 49, 52, 53, 56) (**Table 3**). The time points of measurements include the baseline and 15 min to 72 h after coronary reperfusion. The ROS was measured as MDA, myeloperoxidase (MPO) activity, oxidized glutathione (GSSG), advanced oxidation protein products (AOPP), or oxidized low density lipoprotein (LDL). The two trials reported the outcomes as the total oxidative stress (TOS) or total oxidant capacity (37, 39). All of these trials measured the serum levels of ROS markers except one trial, which also reported the urinary levels in addition to the serum levels (39).

Malondialdehyde was measured in the 9 trials, all of them showed significant reduction with the NAC treatment at different time points regardless of the reperfusion procedure performed, either PCI, CABG, or thrombolytic therapy (**Table 3**). MPO showed significant reduction in one trial but not the other (**Table 3**). Decreases of oxidized glutathione were observed in one trial (**Table 3**). Overall, there is evidence that the administration of NAC before the coronary reperfusion procedure significantly lowers the levels of ROS markers in the patients receiving NAC at various time points as compared with the control group.

Correlation of ROS Reduction With the Clinical Outcomes

Table 4 compares NAC induced improvements in the TAC or ROS reduction with the clinical outcome measures. It is evident that a significant improvement of TAC or ROS reduction due to NAC correlates with the reduced levels of cTn, increased LVEF, and decreased LOS in ICU or hospital. Such correlation supports the cause-effect relationship of TAC or ROS with the improved clinical outcomes. This suggests that NAC might have mediated the improved clinical outcomes through the reduction of ROS.

Sensitivity Analysis

We performed a sensitivity analysis to assess both the between-study heterogeneity and publication bias to ensure that the pooled effects for meta-analysis were indeed robust (58, 59). Between-study heterogeneity may be caused by a trial with either an extreme enrollment size or a larger impact on the pooled effect. To detect an influential trial, the Cook's distance, a well-established influential point detection method, was used (60). A trial may be considered as an influential case if the Cook's distance is >0.45 (17). **Supplementary Figure 1** shows the Cook's distance for each measure in the meta-analyses, with the potential influential study highlighted in red. For cTn, CK-MB, or POAF, none of the trials have a Cook's distance over 0.45, indicating that there is no influential trial. For LVEF, LOS ICU, or hospital LOS, one potential influential study was detected, which is by Prabhu et al. (42). To verify if the influential trial affects the summary data or the conclusion, we compared the results from the random-effects model with vs. without the influential trial. Removal of Prabhu et al. (42) trial reduced the heterogeneity for LVEF, LOS ICU, or hospital LOS, but did not improve the *p*-value or the direction of SMD (**Supplementary Table 1**), and therefore did not affect our conclusions.

Another potential issue for the meta-analysis is the publication bias due to the trials with a small sample size (17). We checked the small-study effects using the funnel plots, which display the relationship between the SMD of studies against its standard error (61). When there is no publication bias, the distribution of the trials in points (one point represents each trial) is symmetric and fits into the shape of an upside-down funnel. In the case of this NAC meta-analysis, a few trials landed outside the funnel area, but the asymmetry is not across all the different outcome measures (as shown in **Supplementary Figure 2**). Since visual inspection can be subjective, we performed the Egger's regression test (62) to evaluate the asymmetry quantitatively in the funnel plot for the continuous outcome measures, cTn, CK-MB, LVEF, LOS in ICU, and LOS in hospital, and Peters' regression test (63) for the binary outcome measure POAF. The results are shown in **Supplementary Table 2**. None of the statistical tests have a significance at the threshold of 0.05, suggesting that the funnel plots are roughly symmetrical. This indicates that the publication bias is not a major concern in the meta-analysis.

DISCUSSION

The administration of NAC prior to the coronary reperfusion procedures was associated with a trend toward the inhibition of cTn elevation, reduced incidence of POAF, and lowered levels of ROS. The decrease of cTn by NAC treatment is considered notable due to the summary SMD being -0.8 in reference to the SD of 1.1 from the meta-analysis of eight trials (**Figure 3A**). However, the overall *p*-value of 0.088 suggests that the decrease is close to 0.05 but not truly significant in the statistical analysis using 95% *CI*. While improvement in LVEF or reduction in ICU and hospital LOS were not statistically significant at 95% *CI*, the meta-analyses suggested a minor trend toward the improvement for these measures (**Figures 3C,E,F**). The effect of NAC on infarct size remains inconclusive due to the smaller number of trials. CK-MB represents the only outcome that did not show improvement with the administration of NAC. Given the fact that POAF is associated with older age and an increase in all-cause mortality (64), and whereas the level of cTn elevation predicts the incidence of adverse events and the risk of heart failure (2–4), adding NAC as an adjuvant therapy for reperfusion may provide benefit in these parameters. By decreasing these clinical complications, it could be expected that NAC administration might reduce the adverse events and the development of heart failure as well as possibly improving the long-term mortality.

An acute kidney injury (AKI) is often an additional complication of reperfusion procedures. We did not include this measure in our study due to the lack of such information in

TABLE 3 | Total oxidative stress (TOS) after coronary reperfusion.

References	Measure		Baseline	15–30 min	1–3 h	3–8 h	12 h	24 h	48–72 h
Shafiei et al. (25)	MDA (nmol/ml)	ctr	35.96 ± 10.37	42.53 ± 12.37		45.13 ± 12.52			
		NAC	22.92 ± 4.33	14.11 ± 8.02		11.74 ± 6.17			
		p	NS	<0.05		<0.05			
Pasupathy et al. (27)	(log) MDA (μM)	ctr			0.81 ± 0.03				
		NAC			0.82 ± 0.03				
		p			<0.01				
	(log) MPO [a] (ng/ml)	ctr			2.31 ± 0.09				
		NAC			2.37 ± 0.06				
		p			0.64				
Jalakandan et al. (31)	MDA [a] (nmol/ml)	ctr	1.40 ± 0.63		2.26 ± 1.03				
		NAC	1.70 ± 0.87		1.58 ± 1.12				
		p	0.164		0.033				
Ozaydin et al. (37)	TOS [a] (mmol h_2o_2/L)	ctr	*19.2 (4.9–38.8)*						*24.2 (2.2–41.9)*
		NAC	*18.7 (3.0–65.0)*						*19.3 (4.0–41.0)*
		p	0.81						<0.0001
Buyukhatipoglu et al. (39)	Serum TOC (μmol H_2O_2/L)	ctr	13.80 ±3.64					20.38 ±5.58	
		NAC	15.35 ±4.30					18.90 ±5.58	
		p	NS					NS	
	Urine TOC (μmol H_2O_2/L)	ctr	19.46 ±5.96					28.99 ±9.23	
		NAC	21.02 ±7.17					29.27 ±7.99	
		p	NS					NS	
Kurian et al. (40)	MDA (nM/g Hb)	ctr	0.9 ± 0.11	3.379 ± 0.18	3.121 ± 0.18	2.324 ± 0.14			
		NAC	0.955 ± 0.10	2.685 ± 0.19	2.198 ± 0.11	1.501 ± 0.12			
		p	NS	NS	<0.05	<0.05			
Thiele et al. (41)	AOPP [a] (μmol/L) (fold of baseline)	ctr	*40.4 (27.5–54.3)*	1.025 ± 0.32				1.083 ± 1.12	0.9 ± 0.45
		NAC	*40.9 (29.9–58.9)*	0.9 ± 0.67				0.77 (NA)	0.85 (NA)
		p	0.3	NS				<0.05	NS
	oxidized LDL [a] (ng/ml) (fold of baseline)	ctr	*32.3 (12.7–141.8)*	1.07 ± 0.22				1.07 ± 0.34	1.12 ± 0.34
		NAC	*34.8 (16.4–95.1)*	0.91 ± 0.45				0.8 ± 0.45	0.83 ± 0.56
		p	0.94	NS				<0.05	<0.05
Karahan et al. (49)	MDA (nmol/ml)	ctr	1.46 ± 0.23			3.11 ± 0.70	2.81 ± 0.61	2.41 ± 0.56	2.04 ± 0.41
		NAC	1.45 ± 0.24			2.2 ± 0.38	1.85 ± 0.31	1.58 ± 0.27	1.46 ± 0.24
		p	0.909			<0.001	<0.001	<0.001	<0.001
Prabhu et al. (42)	MDA (nM/gHb)	ctr	15 ± 1.3	19 ± 2.5			17.5 ± 1.5	16 ± 1.3	
		NAC	14 ± 2.6	18 ± 2.3			16.5 ± 1.4	14 ± 1.2	
		p	NS	<0.05			<0.05	<0.001	
Köksal et al. (44)	MDA [a] (nmol/ml)	ctr	0.72 ± 0.13		0.89 ± 0.20				
		NAC	0.67 ± 0.13		0.76 ± 0.14				
		p	NS		<0.05				
Koramaz et al. (48)	MDA [a](nmol/ml)	ctr	1.62 ± 0.31			2.6 ± 0.15	2.6 ± 0.77	2.25 ± 0.50	2 ± 0.04
		NAC	1.5 ± 0.31			1.4 ± 0.12	1.4 ± 0.39	1.3 ± 0.31	1.1 ± 0.03
		p	NS			<0.05	<0.05	<0.05	<0.05
Sucu et al. (52)	MPO [a] U (mg protein)$^{-1}$h $^{-1}$	ctr	0.034 ± 0.01		0.062 ± 0.02	0.055 ± 0.02		0.038 ± 0.01	
		NAC	0.032 ± 0.01		0.04 ± 0.06	0.038 ± 0.01		0.031 ± 0.01	
		p	0.592		0.000	0.000		0.000	
	MDA [a] (nmol/ml)	ctr	7.1 ± 5.4		12.6 ± 5.7	14.75 ± 5.9		10.1 ± 4.7	
		NAC	7.5 ± 3.3		8.75 ± 2.9	10.25 ± 2.5		7.8 ± 2.8	
		p	0.675		0.000	0.000		0.000	
Eren et al. (53)	MDA (nmol/ml)	ctr	2.34 ± 0.31	2.84 ± 0.72					
		NAC	2.19 ± 0.42	2.51 ± 0.65					

(Continued)

TABLE 3 | Continued

References	Measure		Baseline	15–30 min	1–3 h	3–8 h	12 h	24 h	48–72 h
		p	NS	0.043					
Yang et al. (56)	GSSH (mol/L)	ctr	0.15 ± 0.23			0.12 ± 0.08		0.11 ± 0.07	
		NAC	0.14 ± 0.11			0.08 ± 0.05		0.05 ± 0.03	
		p	NS			NS		<0.05	

All numbers represent means ± SDs unless they are italicized, which indicate median (with IQRs). Ctr, control group; NAC, N-acetylcysteine group. NS, non-significant. "a" indicates that the values were extracted from figures of the cited reference. MDA, malanodealdehyde; TOC, total oxidant capacity; AOPPs, advanced oxidation protein products; MPO, myeloperoxidase; TOS, total oxidative stress; LDL, low density lipoprotein; GSSH, oxidized glutathione; Hb, Hemoglobin; g, gram(s); L, liter(s); ml, milliliter(s); nmol, nanomole(s).

TABLE 4 | Correlation of reactive oxygen species (ROS) and TAC with the clinical outcomes.

References	*n*	TAC	ROS	cTn	CK-MB	LVEF	POAF	LOS ICU	LOS hospital
Shafiei et al. (25)	58		↓MDA	↑↑↑					
Pasupathy et al. (27)	112		↓MDA			⇑			
Ozaydin et al. (36, 37)	172	↑TAC	↓TOS				↓↓		
Kurian et al. (40)	50	↑SOD, GR	↓MDA		↓				
Karahan et al. (49)	44		↓MDA					↓	↓
Prabhu et al. (42)	53	↑GSH	↓MDA	⟷		↑↑	↓	↓	↓
Köksal et al. (44)	30	⟷GPX	↓MDA		⟷				
Koramaz et al. (48)	30		↓MDA	↓↓		↑		↓	↓↓
Eren et al. (53)	20		↓MDA				⟷		

n, indicates sample size; ROS, reactive oxygen species; TAC, total antioxidant capacity; cTn, cardiac troponin; CK-MB, creatine kinase muscle band; LVEF, left ventricular ejection fraction; POAF, post-operative atrial fibrillation; LOS, length of stay; ICU, intensive care unit; SOD, superoxide dismutase; GR, glutathione reductase; GSH, reduced glutathione; GPX, glutathione peroxidase; MDA, malondialdehyde; TOS, total oxidative stress. ↑indicates increase. ↓indicates decrease. ⇑indicates minor increase. ⟷indicates no change.

majority of the clinical trials on NAC for cardiac protection and the recently published systematic reviews with meta-analysis on the topic. Guo et al. (65) used the random effects model to evaluate the seven clinical trials for the effects of NAC on contrast-induced AKI in the patients with STEMI following PCI. This report showed a significantly reduced rate of AKI and all-cause hospital mortality with NAC compared with the placebo group (65). However, a meta-analysis of eight trials by Mei et al. using the random effects model for perioperative NAC among the patients with cardiac surgery concluded that there was no significant benefit in the prevention of AKI. The American College of Cardiology Foundation (ACCF) and American Heart Association (AHA) Guideline for Coronary Artery Bypass Graft Surgery noted the controversy surrounding the use of NAC for the prevention of CABG-associated AKI (66). However, the benefit of NAC as a potential intervention for POAF was not addressed.

Our data on POAF reduction with NAC are consistent with the published meta-analyses reporting the benefit of NAC for the patients with cardiac surgery. Two meta-analyses used the fixed effects model to determine the impact of NAC on POAF when administered before CABG among the eight trials, and showed a significant reduction of POAF (10, 12). In addition, the reduction of POAF was reported by Liu et al. (9), who summarized 10 publications (without the consideration of redundancy in trials) with meta-analysis using the fixed effects model. Wang et al. (11) registered seven trials for meta-analysis using the random effects model and discovered a trend toward improvement in the incidence of POAF with NAC.

The additional clinical measures are less convincing for the benefit of NAC examining in our data and that of others. Pereira et al. (8), compiled 12 trials for meta-analysis with the random effects model and showed a trend but not statistical significance toward an improvement in the post-operative cardiac insufficiency, ICU LOS, or hospital LOS, and incidence of post-operative acute myocardial infarction or cardiac arrhythmias. Gu et al. (10) did not find that NAC reduced ICU LOS using a fixed effects model for a meta-analysis of four trials. Similarly, Liu et al. (9) did not find significant improvement or a trend toward the improvement of ICU or hospital LOS with five trials. Wang et al. (11) showed neither statistical significance nor a trend toward improvement in the incidence of acute myocardial infarction, the need for ionotropic support, and ICU LOS, or hospital LOS with a random effects model meta-analysis of up to six trials. By consolidating the data from 10 trials, we observed a trend toward but not a significant reduction in LOS in ICU or hospital.

N-acetylcysteine is being used clinically for several decades. The main clinical uses for NAC to date include its mucolytic capacity in bronchi, as an antidote for acetaminophen toxicity, and as a protective agent against contrast-induced nephrotoxicity. NAC as a protective agent against reperfusion injury was first reported in 1992 by Sochman and Peregrin (6, 67, 68), who discovered total recovery of left ventricular

function after acute myocardial infarction when NAC was administered along with the coronary artery thrombolysis during the PCI. Multiple RCTs have been published since to address possible beneficial effects of NAC during the coronary artery reperfusion. Twenty-eight of these RCTs reviewed in this study revealed a trend toward the improvement in several clinical measures, with a correlation to reduction of ROS or lipid peroxidation. The correlation approach provides evidence for the mechanistic basis of the observed benefit of NAC.

Strengths and Limitations

We have included three types of coronary artery revascularization procedures for the clinical practice, PCI, thrombolytics, and CABG. This differs from the other published meta-analyses, which focused on one type of reperfusion procedure. Additionally, we have evaluated the most common clinical measures, cTn or CK-MB, LVEF, POAF, and ICU or hospital LOS, and provided a correlation for the levels of antioxidants or ROS to the clinical measures. This differentiates our study from the other published meta-analyses.

The included RCTs were from multiple countries, with most trials having a placebo control. There were minimal losses to follow-up across the trials. The data were generated from multiple healthcare centers with multi-ethnicities due to a diverse distribution of recruitment among the different countries. Additionally, none of the RCTs presented here were funded by a for-profit organization and the risk of bias was low in most of the trials.

The negative factors affecting our analysis power include limited regions of the trials, sample size, gender distribution, and substantial heterogeneity. While there was no restriction on the country or language for trial inclusion, over 50% of the evaluated studies originated from Turkey (10 trials) or Iran (5 trials), and none of the trials were carried out in the United States. Although many factors may explain the uneven distribution for the trial origins, the genetic background in association with a unique region, and the differences in socioeconomic status for the healthcare provision may prohibit extrapolation of the findings to all case scenarios worldwide. Additionally, most of the included trials had an enrollment below 100 individuals. The participants were mostly middle-aged men, prohibiting the generalization to other age groups or female patients.

We have detected a large between-study heterogeneity in most of the outcome measures, with I^2 varying from 35 to 94% (**Figure 3**). Several variables in the trials contributed to the substantial heterogeneity: (a) non-uniform coronary reperfusion procedures, with either PCI, CABG, or thrombolysis in different trials; (b) the dosage and the route of NAC administration differed among the trials, with three trials using the low doses of NAC, 0.3–0.6 g (39, 43, 44); (c) the patient populations carried distinctive diagnoses, from acute coronary syndrome requiring an emergency reperfusion procedure to stable coronary artery diseases treated with an elective reperfusion protocol; (d) a lack of information on timing from the onset of chest pain to the reperfusion procedures. The large regional differences in such timing may affect the clinical outcome of reperfusion and NAC treatment; and (e) the healthcare facility and supportive infrastructure among the different countries or regions may influence the clinical outcome. If it had been possible to increase the sample sizes or reduce the heterogeneity, the statistical analyses would likely have yielded the *p*-values indicating significant differences supporting the benefit of NAC on multiple clinical outcome measures.

Clinical Implications

Our findings suggest a trend toward the benefit of NAC treatment. The trend in the reduction of cTn suggests a potential reduction of cardiac injury by NAC. It is important to note that NAC, despite its low cost and multiple clinical implications already, is not free of side effects. Nausea and vomiting may be associated with an unpleasant odor during oral intake. For intravenous NAC, an anaphylactoid reaction occurs in 8.2% cases, such as cutaneous (acute flushing, pruritus, and rash) or systemic symptoms (bronchospasm, angioedema, hypotension, and chest pain) (69, 70). Additionally, NAC may have a negative impact on hemostasis in the patients under certain conditions. In a *post-hoc* analysis of an RCT of NAC in the patients undergoing cardiac surgery with an estimated glomerular filtration rate of $\leq$60 ml/min, administration of NAC (100 mg/kg IV bolus, followed by 20 mg/kg/h until 4 h after CABG) was associated with a greater blood loss and an increased need for transfusions (71). Therefore, the benefit of NAC remains to be fully established with larger controlled clinical trials measuring multiple clinical end-points. The risk vs. benefit analysis in such a trial would also be needed.

If well done, the RCTs with large numbers of patients were shown to be positive, then the addition of antioxidant therapy to the patients following reperfusion therapy or cardiopulmonary bypass would be a simple and inexpensive therapy. NAC, vitamin C, and other antioxidant agents are generic, inexpensive, generally safe, and would presumably be administered for a relatively short period of time, possibly hours to days. The long-term clinical implications of such therapy are not yet known and would need to be assessed.

DATA AVAILABILITY STATEMENT

The original contributions presented in the study are included in the article/**Supplementary Material**, further inquiries can be directed to the corresponding author.

AUTHOR CONTRIBUTIONS

SK: study design, building search strategy for six electronic databases, acquisition of data, qualitative analysis, interpretation of data, writing and drafting the manuscript, and coordinating the project. AC: independently reviewed the literature and evaluated all the selected trials, validated the acquisition of data, provided input, and edit to the manuscript. YL: quantitative analysis and conducted meta-analysis. LA: supervising

statistician and manuscript editing. JA: a practicing cardiologist who helped with the clinical interpretation of the data, and manuscript editing. QC: initiated the conception, supervised the study, reviewed the literature, and revised the manuscript. All the authors edited and have approved this version of manuscript to be published.

FUNDING

Research works under QC's direction are supported by NIH R01 GM125212, R01 GM126165, Holsclaw Endowment, and The University of Arizona College of Pharmacy start-up fund.

ACKNOWLEDGMENTS

We appreciate the input from librarian Rachel Walden for the literature search. The authors sincerely thank Ms. Hongting Diao for translating one of our included RCTs from Chinese to English, and Mr. Benjamin Yuchen for English editing of the manuscript.

SUPPLEMENTARY MATERIAL

The Supplementary Material for this article can be found online at: https://www.frontiersin.org/articles/10.3389/fcvm.2021.752939/full#supplementary-material

REFERENCES

1. Yellon DM, Hausenloy DJ. Myocardial reperfusion injury. *N Engl J Med.* (2007) 357:1121–35. doi: 10.1056/NEJMra071667
2. Ottani F, Galvani M, Nicolini FA, Ferrini D, Pozzati A, Di Pasquale G, et al. Elevated cardiac troponin levels predict the risk of adverse outcome in patients with acute coronary syndromes. *Am Heart J.* (2000) 140:917–27. doi: 10.1067/mhj.2000.111107
3. Amin AP, Mukhopadhyay E, Napan S, Mamtani M, Kelly RF, Kulkarni H. Value of early cardiac troponin I to predict long-term adverse events after coronary artery bypass graft surgery in patients presenting with acute coronary syndromes. *Clin Cardiol.* (2009) 32:386–92. doi: 10.1002/clc.20579
4. Stelzle D, Shah ASV, Anand A, Strachan FE, Chapman AR, Denvir MA, et al. High-sensitivity cardiac troponin I and risk of heart failure in patients with suspected acute coronary syndrome: a cohort study. *Eur Heart J Qual Care Clin Outcomes.* (2018) 4:36–42. doi: 10.1093/ehjqcco/qcx022
5. Ben-Yehuda O, Chen S, Redfors B, McAndrew T, Crowley A, Kosmidou I, et al. Impact of large periprocedural myocardial infarction on mortality after percutaneous coronary intervention and coronary artery bypass grafting for left main disease: an analysis from the EXCEL trial. *Eur Heart J.* (2019) 40:1930–41. doi: 10.1093/eurheartj/ehz113
6. Kaireviciute D, Aidietis A, Lip GY. Atrial fibrillation following cardiac surgery: clinical features and preventative strategies. *Eur Heart J.* (2009) 30:410–25. doi: 10.1093/eurheartj/ehn609
7. Engelmann MD, Svendsen JH. Inflammation in the genesis and perpetuation of atrial fibrillation. *Eur Heart J.* (2005) 26:2083–92. doi: 10.1093/eurheartj/ehi350
8. Pereira J, El Dib R, Braz L, Escudero J, Hayes J, Johnston B, et al. N-acetylcysteine use among patients undergoing cardiac surgery: a systematic review and meta-analysis of randomized trials. *PLoS ONE.* (2019) 14:e0213862. doi: 10.1371/journal.pone.0213862
9. Liu XH, Xu CY, Fan GH. Efficacy of N-acetylcysteine in preventing atrial fibrillation after cardiac surgery: a meta-analysis of published randomized controlled trials. *BMC Cardiovasc Disord.* (2014) 14:52. doi: 10.1186/1471-2261-14-52
10. Gu WJ, Wu ZJ, Wang PF, Htet Aung LH, Yin RX. N-acetylcysteine supplementation for the prevention of atrial fibrillation after cardiac surgery: a meta-analysis of eight randomized controlled trials. *BMC Cardiovasc Disord.* (2012) 12:10. doi: 10.1186/1471-2261-12-10
11. Wang G, Bainbridge D, Martin J, Cheng D. N-acetylcysteine in cardiac surgery: do the benefits outweigh the risks? A meta-analytic reappraisal. *J Cardiothorac Vasc Anesth.* (2011) 25:268–75. doi: 10.1053/j.jvca.2010.04.022
12. Baker WL, Anglade MW, Baker EL, White CM, Kluger J, Coleman CI. Use of N-acetylcysteine to reduce post-cardiothoracic surgery complications: a meta-analysis. *Eur J Cardiothorac Surg.* (2009) 35:521–7. doi: 10.1016/j.ejcts.2008.11.027
13. Masoudi FA, Ponirakis A, de Lemos JA, Jollis JG, Kremers M, Messenger JC, et al. Trends in U.S. Cardiovascular Care 2016 Report From 4 ACC National Cardiovascular Data Registries. *J Am Coll Cardiol.* (2017) 69:1427–50. doi: 10.1016/j.jacc.2016.12.005
14. Moher D, Liberati A, Tetzlaff J, Altman DG, Group P. Preferred reporting items for systematic reviews and meta-analyses: the PRISMA statement. *Ann Intern Med.* (2009) 151:264–9. doi: 10.7326/0003-4819-151-4-200908180-00135
15. Chesnaye NC, Szummer K, Bárány P, Heimbürger O, Magin H, Almquist T, et al. Association between renal function and troponin T over time in stable chronic kidney disease patients. *J Am Heart Assoc.* (2019) 8:e013091. doi: 10.1093/ndt/gfz106.FP411
16. Ouzzani M, Hammady H, Fedorowicz Z, Elmagarmid A. Rayyan-a web and mobile app for systematic reviews. *Syst Rev.* (2016) 5:210. doi: 10.1186/s13643-016-0384-4
17. Harrer M, Cuijpers P, Furukawa TA, Ebert DD. *Doing Meta-Analysis with R: A Hands-On Guide*. Boca Raton, FL; London: Chapmann & Hall/CRC Press (2021). doi: 10.1201/9781003107347
18. Sidik K, Jonkman JN. A comparison of heterogeneity variance estimators in combining results of studies. *Stat Med.* (2007) 26:1964–81. doi: 10.1002/sim.2688
19. IntHout J, Ioannidis JP, Borm GF. The Hartung-Knapp-Sidik-Jonkman method for random effects meta-analysis is straightforward and considerably outperforms the standard DerSimonian-Laird method. *BMC Med Res Methodol.* (2014) 14:25. doi: 10.1186/1471-2288-14-25
20. Follmann DA, Proschan MA. Valid inference in random effects meta-analysis. *Biometrics.* (1999) 55:732–7. doi: 10.1111/j.0006-341X.1999.00732.x
21. Higgins JPT, Green S. *Cochrane Handbook for Systematic Reviews of Interventions* (2011).
22. Balduzzi S, Rücker G, G S. How to perform a meta-analysis with R: a practical tutorial. *Evid Based Mental Health.* (2019) 22:153–60. doi: 10.1136/ebmental-2019-300117
23. Viechtbauer W. Conducting meta-analyses in R with the metafor package. *J Statist Software.* (2010) 36:1–48. doi: 10.18637/jss.v036.i03
24. Harrer M, Cuijpers P, Furukawa T, Ebert DD. *dmetar: Companion R Package For The Guide 'Doing Meta-Analysis in R'*. R package version 0.9 (2019).
25. Shafiei E, Bahtoei M, Raj P, Ostovar A, Iranpour D, Akbarzadeh S, et al. Effects of N-acetyl cysteine and melatonin on early reperfusion injury in patients undergoing coronary artery bypass grafting: a randomized, open-labeled, placebo-controlled trial. *Medicine.* (2018) 97:e11383. doi: 10.1097/MD.0000000000011383
26. Soleimani A, Habibi MR, Hasanzadeh Kiabi F, Alipour A, Habibi V, Azizi S, et al. The effect of intravenous N-acetylcysteine on prevention of atrial fibrillation after coronary artery bypass graft surgery: a double-blind, randomised, placebo-controlled trial. *Kardiol Pol.* (2018) 76:99–106. doi: 10.5603/KP.a2017.0183
27. Pasupathy S, Tavella R, Grover S, Raman B, Procter NEK, Du YT, et al. Early use of N-acetylcysteine with nitrate therapy in patients undergoing primary percutaneous coronary intervention for ST-segment-elevation myocardial infarction reduces myocardial infarct size (the

NACIAM Trial [N-acetylcysteine in Acute Myocardial Infarction]). *Circulation.* (2017) 136:894–903. doi: 10.1161/CIRCULATIONAHA.117.027575

28. Aldemir M, Koca H, Baki E, Carsanba G, Kavrut N, Kavakli A, et al. Effects of N-acetyl cysteine on renal functions evaluated by blood neutrophil gelatinase-associated lipocalin levels in geriatric patients undergoing coronary artery bypass grafting. *Anatolian J Cardiol.* (2016) 16:504–11. doi: 10.5152/AnatolJCardiol.2015.6287
29. Erdil N, Eroglu T, Akca B, Disli OM, Yetkin O, Colak MC, et al. The effects of N-acetylcysteine on pulmonary functions in patients undergoing on-pump coronary artery surgery: a double blind placebo controlled study. *Eur Rev Med Pharmacol Sci.* (2016) 20:180–7.
30. Nizomov A, Toshev B, Mukhamedova M, Berdiqulov J, Nizomov A, Toshev B, et al. N-acetylcysteine in a combination therapy reduces myocardial damage in patients with acute coronary syndrome and improves left ventricular function after percutaneous coronary intervention. *Atherosclerosis.* (2016) 252:E184–5. doi: 10.1016/j.atherosclerosis.2016.07.857
31. Jalakandan B, Bhaskaran K, Hiremath V, Jalakandan B, Bhaskaran K, Hiremath VR. Effect of n-acetylcysteine on oxidative stress in patients undergoing off pump coronary artery bypass grafting. *J Evol Medand Dental Sci-jemds.* (2015) 4:13754–63. doi: 10.14260/jemds/2015/1963
32. Talasaz A, Salamzadeh J, Khalili H, Eshraghi A, Bahremand M, Talasaz AH, et al. Evaluating the effect of intracoronary N-acetylcysteine on myocardial reperfusion markers following primary percutaneous coronary intervention in patients with STEMI. *Eur Heart J.* (2013) 34:610. doi: 10.1093/eurheartj/eht309.P3283
33. Nozari Y, Eshraghi A, Talasaz A, Bahremand M, Salamzadeh J, Salarifar M, et al. Protection from reperfusion injury with intracoronary N-acetylcysteine in patients with STEMI undergoing primary percutaneous coronary intervention in a cardiac tertiary center. *Am J Cardiovasc Drugs.* (2018) 18:213–21. doi: 10.1007/s40256-017-0258-8
34. Talasaz AH, Khalili H, Jenab Y, Salarifar M, Broumand MA, Darabi F. N-Acetylcysteine effects on transforming growth factor-beta and tumor necrosis factor-alpha serum levels as pro-fibrotic and inflammatory biomarkers in patients following ST-segment elevation myocardial infarction. *Drugs R D.* (2013) 13:199–205. doi: 10.1007/s40268-013-0025-5
35. Kazemi B, Akbarzadeh F, Safaei N, Yaghoubi A, Shadvar K, Ghasemi K. Prophylactic high-dose oral-N-acetylcysteine does not prevent atrial fibrillation after heart surgery: a prospective double blind placebo-controlled randomized clinical trial. *Pacing Clin Electrophysiol.* (2013) 36:1211–9. doi: 10.1111/pace.12190
36. Ozaydin M, Icli A, Yucel H, Akcay S, Peker O, Erdogan D, et al. Metoprolol vs. carvedilol or carvedilol plus N-acetyl cysteine on post-operative atrial fibrillation: a randomized, double-blind, placebo-controlled study. *Eur Heart J.* (2013) 34:597–604. doi: 10.1093/eurheartj/ehs423
37. Ozaydin M, Peker O, Erdogan D, Akcay S, Yucel H, Icli A, et al. Oxidative status, inflammation, and postoperative atrial fibrillation with metoprolol vs carvedilol or carvedilol plus N-acetyl cysteine treatment. *Clin Cardiol.* (2014) 37:300–6. doi: 10.1002/clc.22249
38. Kim JC, Hong SW, Shim JK, Yoo KJ, Chun DH, Kwak YL. Effect of N-acetylcysteine on pulmonary function in patients undergoing off-pump coronary artery bypass surgery. *Acta Anaesthesiol Scand.* (2011) 55:452–9. doi: 10.1111/j.1399-6576.2011.02407.x
39. Buyukhatipoglu H, Sezen Y, Yildiz A, Bas M, Kirhan I, Ulas T, et al. N-acetylcysteine fails to prevent renal dysfunction and oxidative stress after noniodine contrast media administration during percutaneous coronary interventions. *Pol Arch Med Wewn.* (2010) 120:383-9. doi: 10.20452/pamw.975
40. Kurian GA, Paddikkala J. N-acetylcysteine and magnesium improve biochemical abnormalities associated with myocardial ischaemic reperfusion in South Indian patients undergoing coronary artery bypass grafting: a comparative analysis. *Singapore Med J.* (2010) 51:381–8.
41. Thiele H, Hildebrand L, Schirdewahn C, Eitel I, Adams V, Fuernau G, et al. Impact of high-dose N-acetylcysteine versus placebo on contrast-induced nephropathy and myocardial reperfusion injury in unselected patients with ST-segment elevation myocardial infarction undergoing primary percutaneous coronary intervention. The LIPSIA-N-ACC (Prospective, Single-Blind, Placebo-Controlled, Randomized Leipzig Immediate PercutaneouS Coronary Intervention Acute Myocardial Infarction N-ACC) Trial. *J Am Coll Cardiol.* (2010) 55:2201–9. doi: 10.1016/j.jacc.2009.08.091
42. Prabhu A, Sujatha DI, Kanagarajan N, Vijayalakshmi MA, Ninan B. Effect of N-acetylcysteine in attenuating ischemic reperfusion injury in patients undergoing coronary artery bypass grafting with cardiopulmonary bypass. *Ann Vasc Surg.* (2009) 23:645–51. doi: 10.1016/j.avsg.2008.12.005
43. Rodrigues AJ, Évora PRB, Bassetto S, Alves L Jr, Scorzoni Filho A, Origuela EA, Vicente WVA. Blood cardioplegia with N-acetylcysteine may reduce coronary endothelial activation and myocardial oxidative stress. *Heart Surg Forum.* (2009) 12:E44–E8. doi: 10.1532/HSF98.20081134
44. Köksal H, Rahman A, Burma O, Halifeoglu I, Bayar M. The effects of low dose N-acetylcysteine (NAC) as an adjunct to cardioplegia in coronary artery bypass surgery. *Anatolian J Cardiol.* (2008) 8:437–43.
45. Ozaydin M, Peker O, Erdogan D, Kapan S, Turker Y, Varol E, et al. N-acetylcysteine for the prevention of postoperative atrial fibrillation: a prospective, randomized, placebo-controlled pilot study. *Eur Heart J.* (2008) 29:625–31. doi: 10.1093/eurheartj/ehn011
46. Peker O, Peker T, Erdogan D, Ozaydin M, Kapan S, Sutcu R, et al. Effects of intravenous N-acetylcysteine on periprocedural myocardial injury after on-pump coronary artery by-pass grafting. *J Cardiovasc Surg.* (2008) 49:527–31.
47. El-Hamamsy I, Stevens LM, Carrier M, Pellerin M, Bouchard D, Demers P, et al. Effect of intravenous N-acetylcysteine on outcomes after coronary artery bypass surgery: a randomized, double-blind, placebo-controlled clinical trial. *J Thorac Cardiovasc Surg.* (2007) 133:7–12. doi: 10.1016/j.jtcvs.2006.05.070
48. Koramaz I, Pulathan Z, Usta S, Karahan SC, Alver A, Yaris E, et al. Cardioprotective effect of cold-blood cardioplegia enriched with N-acetylcysteine during coronary artery bypass grafting. *Ann Thorac Surg.* (2006) 81:613–8. doi: 10.1016/j.athoracsur.2005.08.013
49. Karahan SC, Koramaz I, Altun G, Ucar U, Topbas M, Mentese A, et al. Ischemia-modified albumin reduction after coronary bypass surgery is associated with the cardioprotective efficacy of cold-blood cardioplegia enriched with N-acetylcysteine: a preliminary study. *Eur Surg Res.* (2010) 44:30–6. doi: 10.1159/000262324
50. Orhan G, Yapici N, Yuksel M, Sargin M, Senay S, Yalçin AS, et al. Effects of N-acetylcysteine on myocardial ischemia-reperfusion injury in bypass surgery. *Heart Vessels.* (2006) 21:42–7. doi: 10.1007/s00380-005-0873-1
51. Fischer UM, Tossios P, Huebner A, Geissler HJ, Bloch W, Mehlhorn U. Myocardial apoptosis prevention by radical scavenging in patients undergoing cardiac surgery. *J Thorac Cardiovasc Surg.* (2004) 128:103–8. doi: 10.1016/j.jtcvs.2003.11.034
52. Sucu N, Cinel I, Unlu A, Aytacoglu B, Tamer L, Kocak Z, et al. N-Acetylcysteine for preventing pump-induced oxidoinflammatory response during cardiopulmonary bypass. *Surg Today.* (2004) 34:237–42. doi: 10.1007/s00595-003-2699-8
53. Eren N, Cakir O, Oruc A, Kaya Z, Erdinc L. Effects of N-acetylcysteine on pulmonary function in patients undergoing coronary artery bypass surgery with cardiopulmonary bypass. *Perfusion.* (2003) 18:345–50. doi: 10.1191/0267659103pf696oa
54. Vento AE, Nemlander A, Aittomäki J, Salo J, Karhunen J, Rämö OJ. N-acetylcysteine as an additive to crystalloid cardioplegia increased oxidative stress capacity in CABG patients. *Scand Cardiovasc J.* (2003) 37:349–55. doi: 10.1080/14017430310015406
55. Sochman J, Vrbska J, Musilova B, Rocek M. Infarct Size Limitation: acute N-acetylcysteine defense (ISLAND trial): preliminary analysis and report after the first 30 patients. *Clin Cardiol.* (1996) 19:94–100. doi: 10.1002/clc.4960190205
56. Yang J, Stafford I, Arstall MA, Horowitz JD. Effects of N-acetylcysteine on oxidation stress in patients with acute myocardial infarction. *Chinese J Cardiol.* (1996) 24:282–4.
57. Andrade C. Mean Difference, Standardized Mean Difference (SMD), and their use in meta-analysis: as simple as it gets. *J Clin Psychiatry.* (2020) 81:20f13681. doi: 10.4088/JCP.20f13681

58. Patsopoulos NA, Evangelou E, Ioannidis JP. Sensitivity of between-study heterogeneity in meta-analysis: proposed metrics and empirical evaluation. *Int J Epidemiol.* (2008) 37:1148–57. doi: 10.1093/ije/dyn065
59. Copas J, Shi JQ. Meta-analysis, funnel plots and sensitivity analysis. *Biostatistics.* (2000) 1:247–62. doi: 10.1093/biostatistics/1.3.247
60. Cook RD. Detection of influential observation in linear regression. *Technometric.* (1977) 19:15–8. doi: 10.1080/00401706.1977.10489493
61. Pustejovsky JE, Rogers MA. Testing for funnel plot asymmetry of standardized mean differences. *Res Synth Methods.* (2019) 10:57–71. doi: 10.1002/jrsm.1332
62. Egger M, Davey Smith G, Schneider M, Minder C. Bias in meta-analysis detected by a simple, graphical test. *BMJ.* (1997) 315:629–34. doi: 10.1136/bmj.315.7109.629
63. Peters JL, Sutton AJ, Jones DR, Abrams KR, Rushton L. Comparison of two methods to detect publication bias in meta-analysis. *JAMA.* (2006) 295:676–80. doi: 10.1001/jama.295.6.676
64. Almassi GH, Hawkins RB, Bishawi M, Shroyer AL, Hattler B, Quin JA, et al. New-onset postoperative atrial fibrillation impact on 5-year clinical outcomes and costs. *J Thorac Cardiovasc Surg.* (2021) 161:1803–10. doi: 10.1016/j.jtcvs.2019.10.150
65. Guo Z, Liu J, Lei L, Xue Y, Liu L, Huang H, et al. Effect of N-acetylcysteine on prevention of contrast-associated acute kidney injury in patients with STEMI undergoing primary percutaneous coronary intervention: a systematic review and meta-analysis of randomised controlled trials. *BMJ Open.* (2020) 10:e039009. doi: 10.1136/bmjopen-2020-039009
66. Hillis LD, Smith PK, Anderson JL, Bittl JA, Bridges CR, Byrne JG, et al. ACCF/AHA Guideline for Coronary Artery Bypass Graft Surgery. A report of the American College of Cardiology Foundation/American Heart Association Task Force on Practice Guidelines. Developed in collaboration with the American Association for Thoracic Surgery, Society of Cardiovascular Anesthesiologists, and Society of Thoracic Surgeons. *J Am Coll Cardiol.* (2011). 58:e123–210.
67. Sochman J, Peregrin JH. Total recovery of left ventricular function after acute myocardial infarction: comprehensive therapy with streptokinase, N-acetylcysteine and percutaneous transluminal coronary angioplasty. *Int J Cardiol.* (1992) 35:116–8. doi: 10.1016/0167-5273(92)90063-9
68. Sochman J. N-acetylcysteine in acute cardiology: 10 years later: what do we know and what would we like to know? *J Am Coll Cardiol.* (2002) 39:1422–8. doi: 10.1016/S0735-1097(02)01797-7
69. Yarema M, Chopra P, Sivilotti MLA, Johnson D, Nettel-Aguirre A, Bailey B, et al. Anaphylactoid reactions to intravenous N-acetylcysteine during treatment for acetaminophen poisoning. *J Med Toxicol.* (2018) 14:120–7. doi: 10.1007/s13181-018-0653-9
70. Sandilands EA, Bateman DN. Adverse reactions associated with acetylcysteine. *Clin Toxicol.* (2009) 47:81–8. doi: 10.1080/15563650802665587
71. Wijeysundera DN, Karkouti K, Rao V, Granton JT, Chan CT, Raban R, et al. N-acetylcysteine is associated with increased blood loss and blood product utilization during cardiac surgery. *Crit Care Med.* (2009) 37:1929–34. doi: 10.1097/CCM.0b013e31819ffed4

Conflict of Interest: The authors declare that the research was conducted in the absence of any commercial or financial relationships that could be construed as a potential conflict of interest.

Publisher's Note: All claims expressed in this article are solely those of the authors and do not necessarily represent those of their affiliated organizations, or those of the publisher, the editors and the reviewers. Any product that may be evaluated in this article, or claim that may be made by its manufacturer, is not guaranteed or endorsed by the publisher.

frontiers in Cardiovascular Medicine

ORIGINAL RESEARCH
published: 02 December 2021
doi: 10.3389/fcvm.2021.755191

Use of Anti-angiogenic Drugs Potentially Associated With an Increase on Serum AST, LDH, CK, and CK-MB Activities in Patients With Cancer: A Retrospective Study

Qi Zheng[1,2], *Hanzhou Wang*[1], *Wei Hou*[1,2]* *and Ying Zhang*[1,2]*

[1] *Department of Pneumology, Guang'anmen Hospital, China Academy of Chinese Medical Sciences, Beijing, China,*
[2] *Department of Oncology, Guang'anmen Hospital, China Academy of Chinese Medical Sciences, Beijing, China*

Background: There is a large amount of evidence that anti-angiogenic drugs are effective safe. However, few studies have evaluated the specific effects of anti-angiogenic drugs on myocardial enzyme injury biomarkers: aspartate aminotransferase (AST), lactic dehydrogenase (LDH), creatine kinase (CK) and creatine kinase isoenzyme (CK-MB). The purpose of our study was to determine whether anti-angiogenic drugs serum AST, LDH, CK, and CK-MB activities of cancer patients treated with anti-angiogenic drugs.

Methods: This study retrospectively analyzed 81 cancer patients. Patients who had used anti-angiogenic drugs were selected. Serum AST, LDH, CK, and CK-MB activities were measured before and after treatment with anti-angiogenic drugs for 3 weeks.

Results: A total of 16 cancer types were analyzed. The distribution of the cancer types in the patients was mainly concentrated in lung, gastric, and colorectal cancers. The anti-angiogenic treatment markedly increased AST, LDH, CK, and CK-MB activities by 32.51, 7.29, 31.25, and 55.56%, respectively in serum.

Conclusions: Our findings suggest that patients, who had used anti-angiogenic drugs were likely to have elevated AST, LDH, and CK, indicators of myocardial muscle injury. Use of anti-angiogenic drugs should not be assumed to be completely safe and without any cardiovascular risks.

Keywords: anti-angiogenic drugs, cancer, AST, LDH, CK, CK-MB

OPEN ACCESS

Edited by:
Feng Cao,
People's Liberation Army General Hospital, China

Reviewed by:
Mark Mitchell,
Louisiana State University, United States
Fan Yin,
People's Liberation Army General Hospital, China

***Correspondence:**
Ying Zhang
zylzy501@163.com
Wei Hou
houwei1964@163.com

Specialty section:
This article was submitted to Cardio-Oncology, a section of the journal Frontiers in Cardiovascular Medicine

Received: *27 August 2021*
Accepted: *12 November 2021*
Published: *02 December 2021*

Citation:
Zheng Q, Wang H, Hou W and Zhang Y (2021) Use of Anti-angiogenic Drugs Potentially Associated With an Increase on Serum AST, LDH, CK, and CK-MB Activities in Patients With Cancer: A Retrospective Study. Front. Cardiovasc. Med. 8:755191. doi: 10.3389/fcvm.2021.755191

INTRODUCTION

Anti-angiogenic treatment is an effective and targeted therapy strategy that can be used to control and kill tumors (1). Although chemotherapeutics can kill tumor cells, the remaining tumor cells can still survive and continue to grow due to the support of peripheral blood vessels. Meanwhile, abnormal tumor blood vessels reduce the delivery of drugs into tumor tissues, which ultimately leads to limited efficacy of anti-cell proliferation therapy. Therefore, the treatment for cancer should not only be directed against tumor cells, but also against the tumor microenvironment, in particularly tumor angiogenesis (2).

Vascular endothelial growth factor (VEGF) is the master effector of the angiogenic response in cancers (3). Anti-angiogenic drugs can be used to specifically bind to VEGF to prevent it from

interacting with receptors, which play a critical role in tumor blood vessels. Further, this limits exposure to oxygen and other nutrients required for tumor cell growth, thereby weakening the ability of tumor growth and metastasis. Anti-angiogenic agents targeting the VEGF and HIF-α pathways include monoclonal antibodies to VEGF (4), such as bevacizumab and resumumab, small-molecule tyrosine kinase inhibitors (TKIs), such as anlotinib, sorafenib, and sunitinib, and VEGF receptor (VEGFR)2 inhibitors, such as regorafenib and ramucirumab (5). These compounds can lead to a reduction in the tumor blood supply and growth of the tumor blood vessels. Unfortunately, cardiovascular toxicity is a potential limitation associated with the long-term use of anti-angiogenic agents in cancer and requires further study to assess the value of anti-angiogenic treatment.

Aspartate aminotransferase (AST) is a pyridoxal-5′-phosphate-dependent enzyme that is widely distributed in heart, liver, skeletal muscle, kidney and brain. It plays a key role in the metabolism of amino acids, synthesis of purine/pyrimidine bases, urea and protein synthesis, and gluconeogenesis (6). Lactic dehydrogenase (LDH) is a type of enzyme, which plays an important role in making body's energy. It can be found in almost all the body's tissues, including those in the blood, heart, kidneys, brain, and lungs. LDH is released from damaged tissues, and can serve as a biomarker for damaged heart tissue. Creatine kinase (CK) is a guanidino-kinase that catalyzes the reversible phosphorylation of creatine to phosphocreatine, and is primarily distributed in bone and myocardium. The plasma activity of creatine kinase isoenzyme (CK-MB), one of the isoenzymes of CK, is generally used to evaluate acute coronary syndrome. The detection of serum CK isozymes, especially serum CK-MB, is helpful for judging the degree of myocardial injury. Comprehensively, monitoring serum AST, LDH, CK and CK-MB activities for cardiac biomarkers can be valuable for assessing patient status (7, 8).

Unfortunately, few studies have focused on the measuring changes in serum AST, LDH, CK and CK-MB activities before and after anti-angiogenic treatment for cancer. In this study, we conducted a retrospective investigation focused on measuring the changes in serum AST, LDH, CK and CK-MB in serum on cancer patients receiving anti- angiogenic targeted therapy. The results suggested that in serum AST, LDH, CK and CK-MB activities of patients who had used anti-angiogenic drugs were likely to have elevated.

MATERIALS AND METHODS

Patients

This was an observational, retrospective study that obtained informed consent from all subjects, and this research was approved by the Ethics Committee of Guang'anmen hospital, China Academy of Chinese Medical Sciences with code number 2020-073-KT. The study followed the ethical principles of the Declaration of Helsinki 1964.

From Jan 2014 to Dec 2020, cancer 81 patients treated with apatinib, anlotinib, regorafenib, bevacizumab, sorafenib, or sunitinib at the oncology department, Guang'anmen hospital, China Academy of Chinese Medical Sciences were retrospectively recruited for this study. Patients with active infection, systemic corticosteroid treatment within 1 year, or hematological malignancy were excluded since these conditions might affect the hematological laboratory markers. Meanwhile, 81 gender and age matched healthy control were enrolled from physical examination center, Guang'anmen hospital, China Academy of Chinese Medical Sciences.

Data Collection

The following variables were extracted from the medical records of the patients: AST, LDH, CK and CK-MB results, age, gender, histological diagnosis, and the choice of anti-angiogenic drugs (such as apatinib, anlotinib, regorafenib, bevacizumab, sorafenib, or sunitinib), history of prior heart disease, pharmacohistory of cardiovascular drugs, smoking and drinking history, and effect of chemotherapeutic drugs on cardiotoxicity. Additionally, routine complete blood counts and coagulograms (including the AST, LDH, CK and CK-MB activities) were carried out before and after first 1 cycle of therapy The first effective evaluation was proceeded after 21 days of treatment. All the examining were detected in the laboratory department, Guang'anmen hospital, China Academy of Chinese Medical Sciences, by using full-automatic chemistry analyzer (AU5800 series, Beckman Coulter).

Statistical Analysis

Statistical analyses were performed using GraphPad Prism8 (GraphPad Software, San Diego, CA, USA) and SPSS statistical software version 24.0 (SPSS Inc., Chicago, IL, USA). Serum AST, LDH, CK and CK-MB activities after first one cycle of treatment were compared to that with no treatment were analyzed. Considering the predictor variables, such as age, gender, histological diagnosis, and the choice of anti-angiogenic drugs, history of prior heart disease, pharmacohistory of cardiovascular drugs, smoking and drinking history, and effect of chemotherapeutic drugs on cardiotoxicity, the statistics were done by mixed linear modeling. All data were non-normally distributed, that reported by the median, interquartile range, and min-max. The differences between tumor patient group and matched healthy control group were compared with Mann-Whitney U test. A two-sided $P < 0.05$ was deemed as statistically significant.

RESULTS

Patient Characteristics

A total of 81 patients were treated by anti-angiogenic drugs during the study period. **Table 1** presents the detailed patient characteristics. There were 41 (50.6%, 95% CI: 0.397 ∼ 0.615) males and 40 (49.4%, 95% CI: 0.385 ∼ 0.603) females in the total cohort, with a median age of 63 years (Quartiles 25–75%, 56–70). Among the patients, there were 42.0% (34/81, 0.312 ∼ 0.527) have prior heart disease history, 35.8% (29/81, 0.254 ∼ 0.462) have cardiovascular drugs use history. Meanwhile, a total of 34.6% (28/81, 0.242 ∼ 0.449) have smoking history and 23.4% (19/81, 0.142 ∼ 0.327) have drinking history. All the patients have been treated with different chemotherapy, nevertheless,

TABLE 1 | Patients' characteristics.

Variables	N	%	95% CI	
Age				
Median	63			
Quartiles 25–75%	56–70			
Gender				
Male	41	50.6	0.397 ∼ 0.615	
Female	40	49.4	0.385 ∼ 0.603	
Prior heart disease history				
Yes	34	42.0	0.312 ∼ 0.527	
No	47	58.0	0.473 ∼ 0.688	
Cardiovascular drugs use history				
Yes	29	35.8	0.254 ∼ 0.462	
No	52	64.2	0.538 ∼ 0.746	
Smoking history				
Yes	28	34.6	0.242 ∼ 0.449	
No	53	65.4	0.551 ∼ 0.758	
Drinking history				
Yes	19	23.4	0.142 ∼ 0.327	
No	62	76.5	0.673 ∼ 0.858	
Effect of chemotherapeutic drugs on cardiotoxicity				
Yes	3	3.7	−0.004 ∼ 0.078	
No	78	96.3	0.922 ∼ 1.004	
Cancer type				**tumor stage**
Lung cancer	23	28.4	0.186 ∼ 0.382	IV
Gastric cancer	13	16.1	0.081 ∼ 0.240	III∼IV
Colorectal cancer	15	18.5	0.101 ∼ 0.270	IV
Ovarian cancer	5	6.2	0.009 ∼ 0.114	IV
Liver cancer	5	6.2	0.009 ∼ 0.114	IV
Renal cancer	4	4.9	0.002 ∼ 0.097	IV
Metrocarcinoma	3	3.7	−0.004 ∼ 0.078	IV
Esophagus cancer	2	2.5	−0.009 ∼ 0.058	IV
Pancreatic cancer	2	2.5	−0.009 ∼ 0.058	IV
Urethral carcinoma	2	2.5	−0.009 ∼ 0.058	IV
Osteocarcinoma	2	2.5	−0.009 ∼ 0.058	IV
Breast cancer	1	1.2	−0.012 ∼ 0.036	IV
Cholangiocarcinoma	1	1.2	−0.012 ∼ 0.036	IV
Thyroid cancer	1	1.2	−0.012 ∼ 0.036	IV
Duodenal cancer	1	1.2	−0.012 ∼ 0.036	IV
Thymoma	1	1.2	−0.012 ∼ 0.036	IV
Anti-angiogenic therapy				
Apatinib	27	33.3	0.231 ∼ 0.436	
Anlotinib	25	30.9	0.208 ∼ 0.409	
Regorafenib	12	14.8	0.071 ∼ 0.226	
Bevacizumab	10	12.3	0.052 ∼ 0.195	
Sorafenib	6	7.4	0.017 ∼ 0.131	
Sunitinib	1	1.2	−0.012 ∼ 0.036	

there were 3/81 patients were affected by chemotherapeutic drugs on cardiotoxicity.

A total of 28.4% (23/81, 95% CI: 0.186 ∼ 0.382) patients had lung cancer, 16.1% (13/ 81, 95% CI: 0.081 ∼ 0.240) had gastric cancer, 18.5% (15/81, 95% CI: 0.101 ∼ 0.270) had colorectal cancer, 6.2% (5/81, 95% CI: 0.009 ∼ 0.114) had ovarian cancer, and 6.2% (5/81, 95% CI: 0.009 ∼ 0.114) had liver cancer. A small number of renal cancer (4.9%, 4/81), metrocarcinoma (3.7%, 3/81), esophagus cancer (2.5%, 2/81), pancreatic cancer (2.5%, 2/81), urethral carcinoma (2.5%, 2/81), osteocarcinoma (2.5%, 2/81), breast cancer (1.2%, 1/81), cholangiocarcinoma (1.2%, 1/81), thyroid cancer (1.2%, 1/81), duodenal cancer (1.2%, 1/81), and thymoma (1.2%, 1/81) cases were included too. Except one patient is III gastric cancer, all other cancer patients were at staged IV depending on the TNM (Tumor, lymph Node, distant Metastasis). In addition, 27 of 81 patients (33.3%, 95% CI: 0.231 ∼ 0.436) were treated with apatinib, 25 of 81 patients (30.9%, 95% CI: 0.208 ∼ 0.409) were treated with anlotinib, 12 of 81 patients (14.8%, 95% CI: 0.071 ∼ 0.226) were treated with regorafenib, 10 of 81 patients (12.3%, 95% CI: 0.052 ∼ 0.195) were treated with bevacizumab, six patients were treated with sorafenib, and one patient (12.3%) were treated with sunitinib (**Table 1**).

Evaluation of Serum AST and LDH Activities in Patients and Health Control

Table 2 displays the detailed characteristics of serum AST, LDH, CK, and CK-MB activities in patients and health control. Health control was matched in serum AST, LDH. Serum AST and LDH were markedly increased in patients after treatment compared with health control ($p < 0.01$, $p < 0.001$). In addition, it was significantly increased in patients before treatment compared with health control in serum LDH ($p < 0.001$), (**Figure 1**).

The Effects of Predictor Variables on Serum AST, LDH, CK, and CK-MB Activities in Patients

Afterwards, considering the predictor variables, such as age, gender, histological diagnosis, and the choice of anti-angiogenic drugs, history of prior heart disease, pharmacohistory of cardiovascular drugs, smoking and drinking history, and effect of chemotherapeutic drugs on cardiotoxicity, the statistics were done by mixed linear modeling. As **Tables 3**–**6** showed, the influence of age, gender, cancer type, the choice of anti-angiogenic drugs, drinking history, and effect of chemotherapeutic drugs on cardiotoxicity were eliminated in this study.

Exclude the influence of the above factors, the median of AST activities were 18.40 (10.20, 12.10–126.70) before treatment and 26.70 (24.00, 12.00–209.10) after anti-angiogenic treatment, which was markedly decreased ($P = 0.002$). The mean AST activities were 11.26 higher after anti-angiogenic treatment than before, **Tables 2**, **7**. The median of LDH activities were 192.00 (103.00, 100.00–753.00) before treatment and 206 (122.00, 123.00–1,135.00) after anti-angiogenic treatment, which was significantly decreased ($P = 0.022$). The mean LDH activities were 38.58 higher after anti-angiogenic treatment than before, **Tables 2**, **7**.

Interestingly, serum CK and CK-MB activities have been affected by anti-angiogenic treatment, history of prior heart disease, pharmacohistory of cardiovascular drugs, and smoking history. The mean serum CK activities was 14.35, significantly

TABLE 2 | The detailed characteristics of serum AST, LDH, CK and CK-MB activities in patients and health control.

	Group	Number	Median	Interquartile range	Min	Mix
AST	Before treatment	81	18.40	10.20	12.10	126.70
	After treatment	81	26.70	24.00	12.00	209.10
	Health control	81	19.90	6.20	14.30	37.80
LDH	Before treatment	43	192.00	103.00	100.00	753.00
	After treatment	43	206.00	122.00	123.00	1,135.00
	Health control	81	176.00	98.00	119.00	217.00
CK	Before treatment	43	32.00	31.00	12.00	144.00
	After treatment	43	42.00	40.00	10.00	244.00
CK-MB	Before treatment	47	9.00	217.52	0.48	218.00
	After treatment	47	13.00	20.00	0.35	252.00

In our laboratory, 90–50 U/L is adopted as the cut-off value for normal AST; <247 U/L is adopted as the cut-off value for normal LDH; < 171 U/L is adopted as the cut-off value for normal CK; < 25 U/L is used as the cut-off value for normal CK-MB.

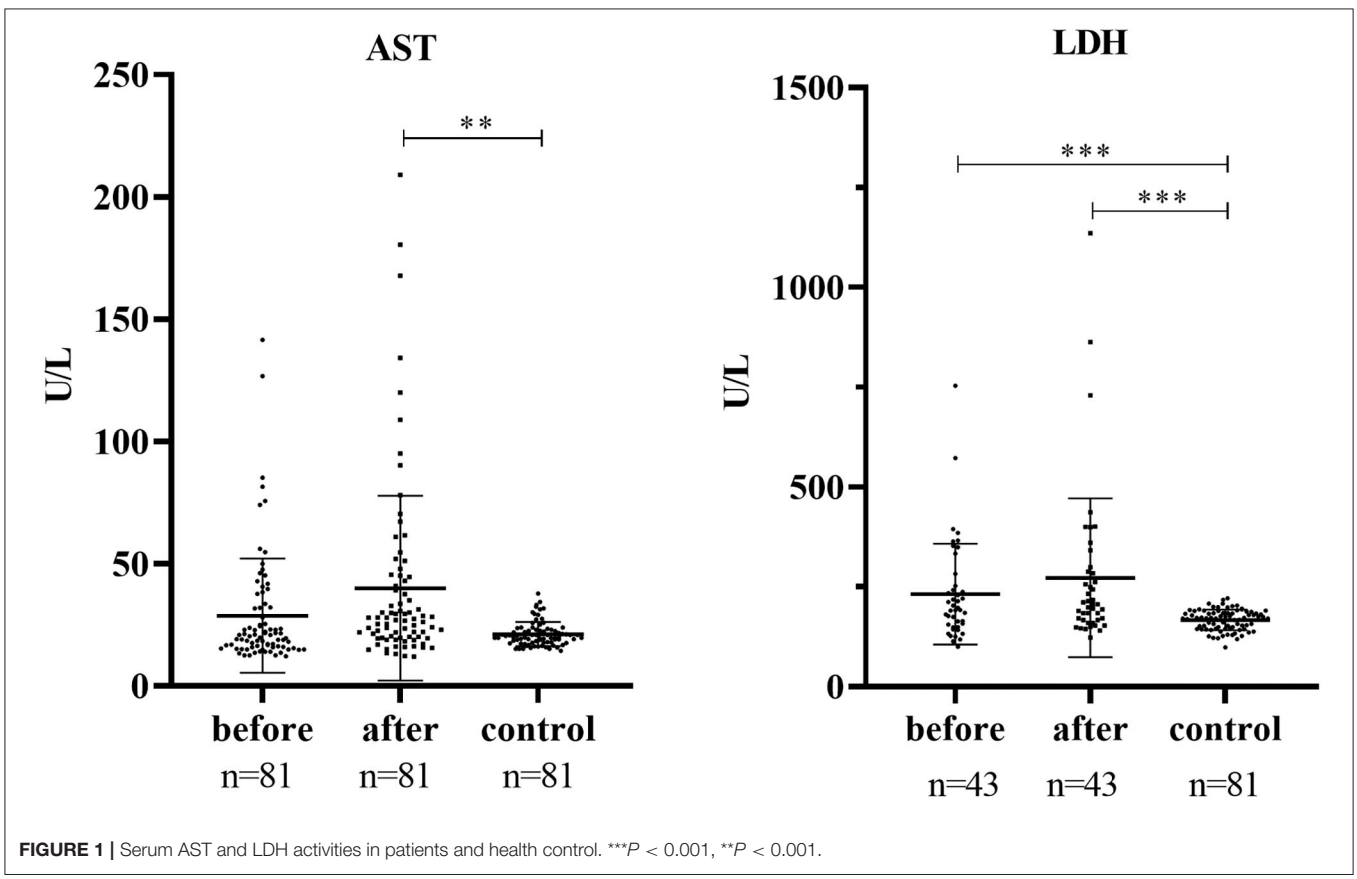

FIGURE 1 | Serum AST and LDH activities in patients and health control. ***$P < 0.001$, **$P < 0.001$.

increased after anti-angiogenic treatment than before ($P = 0.032$). Patients who had cardiovascular drugs history had 84.48 lower serum CK activities ($P = 0.028$) than those without cardiovascular drugs history. Smoking history is another predictor variables, patients who had smoking history was 47.38 higher than those without ($P = 0.042$), **Table 7**. Serum CK-MB activities were mainly history of prior heart disease and cardiovascular drugs. Patients who had prior heart disease history was 129.04 higher serum CK-MB activities ($P = 0.005$) than those without prior heart disease history. Conversely, Patients who had cardiovascular drugs history was 149.10 lower serum CK-MB activities ($P = 0.002$) than those without cardiovascular drugs history.

DISCUSSION

This retrospective study revealed the blood biomarkers, such as AST, LDH and CK were markedly increased with use of anti-angiogenic drugs, indicating that use of anti-angiogenic

TABLE 3 | Type III test of fixed effects of AST.

Source	Numerator df	Denominator df	F	Sig.
Age	1	53.000	0.593	0.445
Gender	1	53	0.672	0.416
Cancer type	15	53	1.679	0.084
Choice of anti-angiogenic drugs	5	53.000	0.550	0.738
Before/after treatment	1	80	10.287	0.002
History of prior heart disease	1	53.000	0.140	0.710
History of cardiovascular drugs	1	53.000	0.984	0.326
Smoking history	1	53	0.000	0.999
Drinking history	1	53.000	0.042	0.838
Effect of chemotherapeutic drugs on cardiotoxicity	1	53.000	0.029	0.866

TABLE 4 | Type III test of fixed effects of LDH.

Source	Numerator df	Denominator df	F	Sig.
Age	1	21.002	0.147	0.705
Gender	1	21.000	0.591	0.451
Cancer type	10	21.006	1.353	0.268
Choice of anti-angiogenic drugs	4	21.006	1.225	0.330
Before/after treatment	1	42.066	5.672	0.022
History of prior heart disease	0	–	–	–
History of cardiovascular drugs	0	–	–	–
Smoking history	1	21.000	3.814	0.064
Drinking history	1	21.004	0.348	0.561
Effect of chemotherapeutic drugs on cardiotoxicity	1	21.000	1.421	0.247

TABLE 5 | Type III test of fixed effects of CK.

Source	Numerator df	Denominator df	F	Sig.
Age	1	21.000	0.461	0.505
Gender	1	21.000	2.961	0.100
Cancer type	9	21.000	1.608	0.177
Choice of anti-angiogenic drugs	4	21.000	0.897	0.483
Before/after treatment	1	42.000	4.946	0.032
History of prior heart disease	1	21.000	4.299	0.051
History of cardiovascular drugs	1	21.000	5.540	0.028
Smoking history	1	21.000	4.708	0.042
Drinking history	1	21.000	0.798	0.382
Effect of chemotherapeutic drugs on cardiotoxicity	1	21.000	0.324	0.575

TABLE 6 | Type III test of fixed effects of CK-MB.

Source	Numerator df	Denominator df	F	Sig.
Age	1	24.000	0.340	0.565
Gender	1	24.000	1.520	0.230
Cancer type	10	24.000	2.034	0.075
Choice of anti-angiogenic drugs	4	24.000	2.042	0.120
Before/after treatment	1	46.000	1.621	0.209
History of prior heart disease	1	24.000	9.675	0.005
History of cardiovascular drugs	1	24.000	12.163	0.002
Smoking history	1	24.000	3.065	0.093
Drinking history	1	24.000	0.016	0.899
Effect of chemotherapeutic drugs on cardiotoxicity	1	24.000	0.299	0.590

drugs may be related to an increased risk of myocardial damage. Moreover, serum CK and CK-MB activities have been affected by history of prior heart disease, cardiovascular drugs, and smoking. The determination of myocardial enzymes mainly includes AST, LDH, CK and CK-MB. When the cardiomyocytes have inflammation (myocarditis) or necrosis (myocardial infarction) due to various reasons, the enzymes contained in the cardiomyocytes can enter the blood, and the activity (content) of these enzymes in the blood increases. Elevation of these serum markers in this study did not exceed the normal upper limit, but it may indicate a tendency for long-term use to accumulate toxicity.

AST is one of the most important aminotransferases in the body. It is mainly found in tissue cells such as myocardium, liver, skeletal muscle, kidney, pancreas, spleen, lung, red blood cells, as well as in normal human plasma, bile, cerebrospinal fluid, and saliva. Medium, but it cannot be detected in urine without kidney damage. The content of AST in the myocardium is the most abundant, so it has certain significance for the diagnosis of myocardial infarction. When acute myocardial infarction (AMI) occurs, the serum AST activity generally rises to 4–5 times the upper limit of the reference value. If it reaches 10–15 times the upper limit of the reference value, it is often fatal infarction occurred. However, the rise of AST is later than CK in AMI, and recovers earlier than LDH, diagnostic value of AST for AMI is becoming less and less. Nevertheless, AST is an indispensable evaluation index in the clinical research of oncology drug evaluation. The study determined the safety and effectiveness of anti-angiogenic therapy with sorafenib and bevacizumab in patients with advanced HCC and results found that dose-limiting toxicities included hypertension, AST increase, creatinine increase, etc. (9). Patients receive intravenous ramucirumab (8 mg/kg) every 2 weeks were observed in a phase 3 clinical trial. Hypertension (34 [12%] of 277 patients treated with ramucirumab), increased AST concentration (15 [5%]), thrombocytopenia (13 [5%]), etc. were occurred with grade 3 or greater adverse events (10). LDH is an extremely important enzyme that regulates the conversion of pyruvate to lactic acid in anaerobic glycolysis and play an important role in cancer metabolism (11). Meanwhile, LDH is a useful marker for predicting the efficacy of bevacizumab-containing chemotherapy in patients with metastatic colorectal cancer (12). It is widely present in the cytoplasm and mitochondria of tissue cells such as liver, heart, skeletal muscle, lung, spleen, brain, red blood

TABLE 7 | Estimates of fixed effect of treatment, cardiovascular drugs history, history of prior heart disease, and smoking history on serum AST, LDH, CK, and CK-MB activities.

Dependent Variable	Parameter	Estimate	SE	df	t	Sig.	95% CI
AST	treatment=before	−11.26	3.51	80	−3.207	0.002	−18.24∼-4.27
	treatment =after	0	0	–	–	–	–
LDH	treatment=before	−38.58	16.20	42	−2.382	0.022	−71.27∼-5.89
	treatment=after	0	0	–	–	–	–
CK	treatment=before	−14.35	6.45	42	−2.224	0.032	−27.37∼-1.33
	treatment=after	0	0				
	cardiovascular drugs history=yes	−84.48	35.89	21	−2.354	0.028	−159.12∼-9.84
	cardiovascular drugs history=no	0	0	–	–	–	–
	smoking history=yes	47.38	21.84	21	2.170	0.042	1.97∼92.80
	smoking history=no	0	0	–	–	–	–
CK-MB	history of prior heart disease=yes	129.04	41.49	24	3.111	0.005	43.42∼214.67
	history of prior heart disease=no	0	0	–	–	–	–
	cardiovascular drugs history=yes	−149.10	42.75	24	−3.488	0.002	−237.34∼-60.86
	cardiovascular drugs history=no	0	0	–	–	–	–

cells, platelets, etc. LDH is a tetramer composed of two different subunits (LDHA and LDHB), forming 5 isoenzymes with M-type and H-type subunits: H4(LD1), MH3(LD2), M2H(LD3), M3H(LD4), M4(LD5). Different tissues have their characteristic isoenzymes. The ratios of LD isoenzymes in the heart, kidney and red blood cells are similar, with LD1 and LD2 dominating. When the myocardium is damaged, the myocardial cell membrane ruptures, and the mitochondria and cytoplasmic substances leak out into the intercellular fluid and periphral blood. In response to the hypoxic characteristic of the tumor microenvironment, cancer cells generate a large amount of lactate *via* the metabolism of glucose and glutamine (13, 14). High levels of LDHA expression serves as a prognostic indicator in patients with different type of cancers (15). LDH increased production of reactive oxygen species and regulate cell apoptosis and autophagy (16). Thus, the role of LDH in tumor biology is more complex and may as a potential target in the treatment of cancer. Although in this study, the elevation of AST and LDH in patients did not exceed the normal upper limit, there was a significant increase in serum AST and LDH activities, compared with the matched healthy control.

But it is regrettable that the serum CK and CK-MB activities of matched healthy control were not found. All healthy control were from a medical examination at our hospital, serum CK and CK-MB activities are not included in the physical examination at present. Interestingly, serum CK and CK-MB activities have been affected by history of prior heart disease, cardiovascular drugs, and smoking.

CK mainly exists in skeletal muscle and cardiac muscle, and brain tissue. CK is an important energy regulating enzyme in the myocardium. Under the energy provided by ATP, it catalyzes the reversible phosphorylation of ATP and creatine to ADP and phosphocreatine in cellular energy metabolism, which can be transported to the cytoplasm and stored. Serum CK can be increased in various types of progressive muscle atrophy. CK begins to increase 2–4 h after AMI and can reach 10–12 times the upper limit of normal. It has higher specificity than AST and LDH for diagnosing myocardial infarction, but the increase of this enzyme lasts for a short time, and it returns to normal after 2–4 days. There are three isoenzyme formations for CK: CK-MB (mostly in the heart), CK-MM (mostly in the muscle), or CK-BB (mostly in the brain) (17). CK-MB activity has been recognized as a specific and sensitive biomarker of clinical and subclinical myocardial injury (8, 18). CK-MB activities are significantly positively correlated with the extent of myocardial injury, so serum CK-MB can be used as a biomarker for AMI (19). The presence of CK-MB in patients with cancers may cause confusion with AMI. Serial determinations of both CK and LDH are of great help in differential diagnosis 3512170. In addition, a previous study demonstrated that an elevated serum CK-MB in cancer patients may be associated with cardiac insufficiency, severe illness status, and have high mortality (20). Even a slight increase in CK-MB indicated the possibility of myocardial infarction (21). There has been no retrospective report focusing on CK, CK-MB and anti-angiogenic therapy. In the present study, both CK and CK-MB levels were significant elevated after use anti-angiogenic drug. Myocardial ischaemia might be the reason for the slight increase in CK and CK-MB. Furthermore, Some studies have demonstrated that CK-MB-to-total-CK ratio could be clinically utilized as a primary screening tool for cancer (22), which is an easily available indicator. In this study, we found that patients who had prior heart disease history had a higher serum CK-MB activities, while in patients who had cardiovascular drugs history had a lower serum CK and CK-MB activities on the contrary. The reason for the result is likely to be that people with previous cardiovascular disease have damage to heart muscle cells, while the drugs reduce the damage, which need to be further studied.

CONCLUSIONS

Our findings suggest that the serum AST, LDH and CK activities of patients who had used anti-angiogenic drugs were likely

to have elevated. History of prior heart disease, cardiovascular drugs, and smoking should be considered in the anti-angiogenic treatment. AST, LDH, CK and CK-MB are indicators of myocardial muscle injury, such as myocarditis or myocardial infarction. Use of anti-angiogenic drugs should not be assumed to be completely safe and without any cardiovascular risks. In addition, attention should also be paid to long-term use to accumulate toxicity. Apparently, the number of cases in patients should be expanded and more detailed research should be done in the future.

DATA AVAILABILITY STATEMENT

The raw data supporting the conclusions of this article will be made available by the authors, without undue reservation.

ETHICS STATEMENT

This was an observational, retrospective study that obtained informed consent from all subjects, and this research was approved by the Ethics Committee of Guang'anmen Hospital, China Academy of Chinese Medical Sciences with code number 2020-073-KT. Written informed consent for participation was not required for this study in accordance with the national legislation and the institutional requirements.

AUTHOR CONTRIBUTIONS

QZ and YZ: conception and design and manuscript writing. YZ and WH: administrative support and manuscript edition. QZ and HW: data extraction and data analysis. All authors contributed to the article and approved the submitted version.

FUNDING

This work was supported by the Fundamental Research Funds for the Central public welfare research institutes (2020YJSZX-3), National Natural Science Foundation of China (No. 82104656) and Beijing Municipal Natural Science Foundation (7214294).

ACKNOWLEDGMENTS

We would like to thank Chen Cheng who worked in marketing and community department of PingCAP helped for programming and cleaning data.

REFERENCES

1. Teleanu RI, Chircov C, Grumezescu AM, Teleanu DM. Tumor angiogenesis and anti-angiogenic strategies for cancer treatment. *J Clin Med.* (2019) 9:84. doi: 10.3390/jcm9010084
2. Wolf-Dennen K, Kleinerman ES. Exosomes: dynamic mediators of extracellular communication in the tumor microenvironment. *Adv Exp Med Biol.* (2020) 1258:189–97. doi: 10.1007/978-3-030-43085-6_13
3. Tanimura K, Yamada T, Omura A, Shiotsu S, Kataoka N, Takeda T, et al. The impact of VEGF inhibition on clinical outcomes in patients with advanced non-small cell lung cancer treated with immunotherapy: a retrospective cohort study. *Front Oncol.* (2021) 11:663612. doi: 10.3389/fonc.2021.663612
4. Fang C, Dai L, Wang C, Fan C, Yu Y, Yang L, et al. Secretogranin II impairs tumor growth and angiogenesis by promoting degradation of hypoxia-inducible factor-1α in colorectal cancer. *Mol Oncol.* (2021). doi: 10.1002/1878-0261.13044
5. Montanino A, Manzo A, Carillio G, Palumbo G, Esposito G, Sforza V, et al. Angiogenesis inhibitors in small cell lung cancer. *Front Oncol.* (2021) 11:655316. doi: 10.3389/fonc.2021.655316
6. Weng SF, Kai J, Guha IN, Qureshi N. The value of aspartate aminotransferase and alanine aminotransferase in cardiovascular disease risk assessment. *Open Heart.* (2015) 2:e000272. doi: 10.1136/openhrt-2015-000272
7. Li JH Li TT, Wu XS, Zeng DL. Effect of gamma globulin combined with creatine phosphate on viral myocarditis. *Am J Transl Res.* (2021) 13:3682–8.
8. Zhu T, Han Q, Zhang X, Hou Q. Effects of Xinnaoning combined with trimetazidine on the levels of CK and its isoenzymes, AST, ALT and LDH in patients with myocardial ischemia. *Am J Transl Res.* (2021) 13:2875–82.
9. Hubbard JM, Mahoney MR, Loui WS, Roberts LR, Smyrk TC, Gatalica Z, et al. Phase I/II randomized trial of sorafenib and bevacizumab as first-line therapy in patients with locally advanced or metastatic hepatocellular carcinoma: north central cancer treatment group trial N0745 (Alliance). *Target Oncol.* (2017) 12:201–9. doi: 10.1007/s11523-016-0467-0
10. Zhu AX, Park JO, Ryoo BY, Yen CJ, Poon R, Pastorelli D, et al. Ramucirumab versus placebo as second-line treatment in patients with advanced hepatocellular carcinoma following first-line therapy with sorafenib (REACH): a randomised, double-blind, multicentre, phase 3 trial. *Lancet Oncol.* (2015) 16:859–70. doi: 10.1016/S1470-2045(15)00050-9
11. Valvona CJ, Fillmore HL, Nunn PB, Pilkington GJ. The regulation and function of lactate dehydrogenase a: therapeutic potential in brain tumor. *Brain Pathol.* (2016) 26:3–17. doi: 10.1111/bpa.12299
12. Shibutani M, Maeda K, Kashiwagi S, Nagahara H, Fukuoka T, Iseki Y, et al. Lactate dehydrogenase is a useful marker for predicting the efficacy of bevacizumab-containing chemotherapy in patients with metastatic colorectal cancer. *Anticancer Res.* (2021) 41:3535–42. doi: 10.21873/anticanres.15141
13. Pérez-Tomás R, Pérez-Guillén I. Lactate in the tumor microenvironment: an essential molecule in cancer progression and treatment. *Cancers (Basel).* (2020) 12:3244. doi: 10.3390/cancers12113244
14. Mishra D, Banerjee D. Lactate dehydrogenases as metabolic links between tumor and stroma in the tumor microenvironment. *Cancers (Basel).* (2019) 11:750. doi: 10.3390/cancers11060750
15. Lv J, Zhou Z, Wang J, Yu H, Lu H, Yuan B, et al. Prognostic value of lactate dehydrogenase expression in different cancers: a meta-analysis. *Am J Med Sci.* (2019) 358:412–21. doi: 10.1016/j.amjms.2019.09.012
16. Urbańska K, Orzechowski A. Unappreciated role of LDHA and LDHB to control apoptosis and autophagy in tumor cells. *Int J Mol Sci.* (2019) 20:2085. doi: 10.3390/ijms20092085
17. Ju-Feng Hsiao, Hsiao-Chen Ning, Po-Wen Gu, Wei-Yee Lin, Pao-Hsien Chu. Clinical role of recurrently elevated macro creatine kinase type 1. *J Clin Lab Anal.* (2008) 22:186–91. doi: 10.1002/jcla.20239
18. Emokpae MA, Nwagbara G. Serum creatine kinase-MB isoenzyme activity among subjects with uncomplicated essential hypertension: any sex differences. *Med Sci (Basel).* (2017) 5:8. doi: 10.3390/medsci5020008
19. Kim S, Um TH, Cho CR, Jeon JS. False-positive elevation of creatine kinase MB mass concentrations caused by macromolecules in a patient who underwent nephrectomy for renal cell carcinoma. *Ann Lab Med.* (2014) 34:405–7. doi: 10.3343/alm.2014.34.5.405
20. Ming Yuan, Li Zang, Aiqing Xu, Mengqi Gong, Qing Liu, Bin Huo, et al. Dynamic Changes of Serum Heart Type-Fatty Acid Binding Protein in Cancer Patients Treated With Immune Checkpoint Inhibitors. *Front Pharmacol.* (2021) 12:748677. doi: 10.3389/fphar.2021.748677
21. Lee JJ, Lee JH, Jeong JW, Chung JY. Fragmented QRS and abnormal creatine kinase-MB are predictors of coronary artery disease in patients with angina and normal electrocardiographys. *Korean J Intern Med.* (2017) 32:469–77. doi: 10.3904/kjim.2015.123

22. Chang CC, Liou CB, Su MJ, Lee YC, Liang CT, Ho JL, et al. Creatine Kinase (CK)-MB-to-Total-CK Ratio: a Laboratory Indicator for Primary Cancer Screening. *Asian Pac J Cancer Prev.* (2015) 16:6599–603. doi: 10.7314/apjcp.2015.16.15.6599

Conflict of Interest: The authors declare that the research was conducted in the absence of any commercial or financial relationships that could be construed as a potential conflict of interest.

Publisher's Note: All claims expressed in this article are solely those of the authors and do not necessarily represent those of their affiliated organizations, or those of the publisher, the editors and the reviewers. Any product that may be evaluated in this article, or claim that may be made by its manufacturer, is not guaranteed or endorsed by the publisher.

frontiers in Cardiovascular Medicine

BRIEF RESEARCH REPORT
published: 03 January 2022
doi: 10.3389/fcvm.2021.792310

Arrhythmia Patterns in Patients on Ibrutinib

Muhammad Fazal[1], Ridhima Kapoor[2], Paul Cheng[1], Albert J. Rogers[1], Sanjiv M. Narayan[1], Paul Wang[1], Ronald M. Witteles[1], Alexander C. Perino[1], Tina Baykaner[1] and June-Wha Rhee[3]**

[1] Department of Medicine, Division of Cardiovascular Medicine, Stanford University, Palo Alto, CA, United States, [2] Department of Medicine, Medical College of Wisconsin, Wauwatosa, WI, United States, [3] Department of Medicine, Division of Cardiology, City of Hope National Cancer Center, Duarte, CA, United States

Introduction: Ibrutinib, a Bruton's tyrosine kinase inhibitor (TKI) used primarily in the treatment of hematologic malignancies, has been associated with increased incidence of atrial fibrillation (AF), with limited data on its association with other tachyarrhythmias. There are limited reports that comprehensively analyze atrial and ventricular arrhythmia (VA) burden in patients on ibrutinib. We hypothesized that long-term event monitors could reveal a high burden of atrial and VAs in patients on ibrutinib.

Methods: A retrospective data analysis at a single center using electronic medical records database search tools and individual chart review was conducted to identify consecutive patients who had event monitors while on ibrutinib therapy.

Results: Seventy-two patients were included in the analysis with a mean age of 76.9 ± 9.9 years and 13 patients (18%) had a diagnosis of AF prior to the ibrutinib therapy. During ibrutinib therapy, most common arrhythmias documented were non-AF supraventricular tachycardia ($n = 32$, 44.4%), AF ($n = 32$, 44%), and non-sustained ventricular tachycardia ($n = 31$, 43%). Thirteen (18%) patients had >1% premature atrial contraction burden; 16 (22.2%) patients had >1% premature ventricular contraction burden. In 25% of the patients, ibrutinib was held because of arrhythmias. Overall 8.3% of patients were started on antiarrhythmic drugs during ibrutinib therapy to manage these arrhythmias.

Conclusions: In this large dataset of ambulatory cardiac monitors on patients treated with ibrutinib, we report a high prevalence of atrial and VAs, with a high incidence of treatment interruption secondary to arrhythmias and related symptoms. Further research is warranted to optimize strategies to diagnose, monitor, and manage ibrutinib-related arrhythmias.

Keywords: cardio-oncology, tyrosine kinase inhibitor, atrial fibrillation, ventricular arrhythmia, ibrutinib, ambulatory event monitor

OPEN ACCESS

Edited by:
Dong Han,
People's Liberation Army General Hospital, China

Reviewed by:
Sri Sundaram,
South Denver Cardiology Associates, United States
Jackson Liang,
University of Michigan, United States

***Correspondence:**
Tina Baykaner
tina4@stanford.edu
June-Wha Rhee
jrhee@coh.org

Specialty section:
This article was submitted to Cardio-Oncology, a section of the journal Frontiers in Cardiovascular Medicine

Received: *10 October 2021*
Accepted: *12 November 2021*
Published: *03 January 2022*

Citation:
Fazal M, Kapoor R, Cheng P, Rogers AJ, Narayan SM, Wang P, Witteles RM, Perino AC, Baykaner T and Rhee J-W (2022) Arrhythmia Patterns in Patients on Ibrutinib. Front. Cardiovasc. Med. 8:792310. doi: 10.3389/fcvm.2021.792310

INTRODUCTION

Atrial fibrillation (AF) is the most common sustained arrhythmia in the world, affecting at least 33 million individuals. The burden of AF has been rapidly increasing worldwide due to growing awareness and the broader application of portable event monitors and wearables and also due to shifts in demographics and an increase in the prevalence of risk factors (1). Moreover, with the

growing use of cancer therapies in clinic, antineoplastic agents such as paclitaxel, mitoxantrone, doxorubicin, and TKIs have been associated with an increased risk of developing AF (2–5).

Ibrutinib is a Bruton's TKI that is used in a growing number of hematologic malignancies. It irreversibly binds Bruton's tyrosine kinase, which plays a critical role in B-cell development and proliferation, and thereby exerts its anticancer activity primarily in B-cell malignancies including chronic lymphocytic leukemia, mantle cell lymphoma, and Waldenström's macroglobulinemia (6). The use of ibrutinib has been associated with increased incidence of AF (5); with limited data on its association with other arrhythmias. These arrhythmias lead to a relatively high treatment interruption rate and cause significant morbidity in this patient population (4). There are limited data to date that comprehensively analyze both atrial and ventricular arrhythmia (VA) burden in patients on ibrutinib, and subsequent referral to subspecialty care, antiarrhythmic drug use, and treatment interruption patterns. Therefore, we hypothesized that long-term event monitors, as defined by continuous ECG monitoring >48 h, could reveal a high burden of atrial and VAs in patients on ibrutinib therapy which may lead to treatment cessation.

METHODS

We performed a single-center, retrospective cohort study to analyze consecutive patients on ibrutinib therapy, who had event monitors of at least 3 days of duration for any indication while on ibrutinib therapy between the years 2014 and 2021.

Data Source and Covariates

Patient data including demographics, past medical history, history of AF, echocardiographic data (including left ventricular ejection fraction (LVEF), left atrial volume index (LAVI), and left atrial diameter), 12-lead ECGs, and event monitors with autotriggers were collected from electronic medical records. Event monitors were manually reviewed to confirm the diagnosis of AF, patterns of other arrhythmias seen, and assess the types of ventricular tachycardia (monomorphic vs. polymorphic). CHA_2DS_2-VASc score was automatically calculated from these data using age, sex, history of heart failure, hypertension, stroke, TIA, vascular disease, and diabetes.

Outcomes

We compared the cohort that had AF seen on the event monitor against the cohort that did not, and the cohort that had ibrutinib held vs. those in whom ibrutinib was continued. We also conducted univariate analyses to identify the correlation between the development of AF and any clinical risk factors including ECG and echocardiographic parameters, and also a correlation between ibrutinib being held and any clinical risk factors.

Statistics

Statistical analyses were done using SPSS version 27 (IBM SPSS Statistics for Mac, IBM Corporation, Armonk, NY). Continuous data are reported as mean ± standard deviation, unless otherwise stated, and are tested for normality using the Shapiro–Wilk test ($p > 0.05$). Independent-samples t-test and Mann–Whitney U test were run to determine whether there were differences in mean values between cohorts and for analysis of continuous data. Categorical variables were compared using the Pearson's chi-squared test or Fisher's exact test where expected frequencies were <5. Statistical significance was assumed at the 5% level. This study was approved by the Institutional Review Board of Stanford University.

RESULTS

Clinical Characteristics

Of 755 patients who were on ibrutinib therapy for hematologic malignancies at Stanford Hospital between 2014 and 2019, 72 patients had event monitors (Zio, iRhythm Technologies, Inc., CA) while on ibrutinib therapy and were included in this analysis (**Table 1**). Thirteen patients (18%) carried a diagnosis of AF prior to ibrutinib therapy but the majority of the patients did not have a screening Holter monitoring, and therefore, the burden of pre-ibrutinib therapy arrhythmia is unknown. The most common indications for event monitoring included atrial arrhythmias (50%), palpitations (23%), abnormal EKG (14%), and syncope (6%). The 72 patients who were included in the analysis had a mean age of 76.9 ± 9.9 years, 25% were women, 68% with a diagnosis of hypertension, 62% with hyperlipidemia, 13% with COPD, 10% with prior history of cardiac surgery, mean BMI of 24.8 ± 4.1, and mean CHA_2DS_2-VASc score of 4 ± 2 (**Figure 1A**). The mean LVEF was 58.1 ± 9.1% and the mean LAVI was 36.4 ± 13.0 (ml/m^2). Thirteen (18%) patients had a history of AF prior to initiation of ibrutinib. The average duration of time on ibrutinib therapy for all patients with event monitors was 31.9 ± 22.3 months. The median number of months on ibrutinib therapy was 28 months (range 1–111 months).

Arrhythmia Patterns on Long-Term Event Monitors

Most common arrhythmias documented were non-AF supraventricular tachycardia (SVT, in $n = 32$, 44.4% of patients), AF ($n = 32$, 44.4%), and non-sustained ventricular tachycardia (NSVT $n = 31$, 43.1%). Fourteen (19.4%) patients had >1% premature atrial contraction (PAC) burden; 16 (22.2%) patients had >1% premature ventricular contraction (PVC) burden (**Figure 1B**). Out of patients that had NSVT, five patients had polymorphic NSVT whereas the rest had monomorphic NSVT. Median QTc in patients with NSVT was 422 ms (range 375–507). Sixteen (22.2%) patients had both NSVT and AF recorded, which is about half of the population which had either NSVT or AF (**Figure 2**). A small proportion of these patients were followed by electrophysiologists ($n = 20$, 27.8%), whereas a higher proportion were followed by cardiologists ($n = 50$, 69.4%).

Factors Associated With Ibrutinib Therapy Interruption

In 18 (25%) patients, ibrutinib therapy was held because of arrhythmias and/or related symptoms (**Table 2**). Six (8.3%) patients were started on antiarrhythmic drugs during ibrutinib

TABLE 1 | Baseline demographics for patients undergoing ibrutinib therapy with cardiac monitor while on ibrutinib, divided by patients in whom therapy was held vs. continued.

Characteristic	All patients ($n = 72$)	Patients in whom ibrutinib was held ($n = 18$)	Patients who continued ibrutinib ($n = 54$)	p
Age (years)	76.9 ± 9.9	78.6 ± 11.2	76.3 ± 9.5	0.391
Sex (*N*, %)				0.753
Male	54 (75.0%)	13 (72.2%)	41 (75.9%)	
Female	18 (25.0%)	5 (27.8%)	13 (24.1%)	
Body mass index (kg/m^2)	24.8 ± 4.1	24.2 ± 3.4	25.1 ± 4.3	0.520
LA volume index (ml/m^2)	36.4 ± 13.0	43.6 ± 16.3	33.6 ± 10.5	**0.008**
EF (%)	58.1 ± 9.1	55.1 ± 11.1	59.2 ± 8.1	0.204
Comorbid medical conditions (*N*, %)	26 (36.1%)	9 (50.0%)	17 (31.5%)	0.157
Congestive heart failure				
Valvular disease	31 (43.1%)	9 (50.0%)	22 (40.7%)	0.492
Hypertension	49 (68.1%)	13 (72.2%)	36 (66.7%)	0.662
Hyperlipidemia	44 (61.8%)	10 (55.6%)	34 (63.0%)	0.557
Diabetes mellitus	13 (18.1%)	2 (11.1%)	11 (20.4%)	0.376
Coronary artery disease	38 (38.9%)	5 (27.8%)	23 (42.6%)	0.264
Obstructive sleep apnea	23 (31.9%)	7 (38.9%)	16 (29.6%)	0.466
Chronic kidney disease	28 (38.9%)	9 (50%)	19 (35.2%)	0.264
History of AF (prior to ibrutinib therapy)	13 (18.1%)	4 (22.2%)	9 (16.7%)	0.725
Duration of Ibrutinib therapy (months)	31.6 ± 22.3	25.6 ± 20.2	33.6 ± 22.8	0.190
Patients on antiarrhythmic drug therapy (*N*, %)	9 (12.5)	5 (27.8%)	4 (7.4%)	**0.038**
Patients on antiarrhythmic drug therapy that was initiated after ibrutinib treatment (*N*, %)	6 (8.3)	4 (22.2%)	2 (3.7%)	**0.031**
Care team involvement (*N*, %)				
General cardiologist	50 (69.4)	16 (88.9%)	34 (63%)	**0.039**
Electrophysiologist	20 (27.8)	8 (44.4%)	12 (22.2%)	0.068

therapy to manage these arrhythmias. Three patients required at least one direct current cardioversion (DCCV) for poorly controlled AF. Interruptions in ibrutinib therapy were associated with >1% PAC burden on event monitor while on ibrutinib therapy ($p = 0.002$) and a prior history of VT ($p = 0.017$); but not with the presence of the PVC burden of >1%, SVT, AF, or NSVT (all, $p > 0.05$) on the event monitor. Neither history of prior AF nor gender correlated with the frequency at which Ibrutinib was held. Patients in whom ibrutinib was held for arrhythmias were more likely to be seen by a cardiac specialist ($p = 0.005$), along with patients on ibrutinib whose Holter monitors showed NSVT ($p < 0.001$). Female patients were referred to a cardiac specialist less frequently than their male counterparts ($p = 0.14$).

When looking at transthoracic echocardiography data, patients in whom ibrutinib was held for arrhythmia had a lower LVEF vs. those in whom ibrutinib was not held, albeit not statistically significant (55.1 ± 10.7 vs. 59.3 ± 8.2%; $p = 0.09$). However, for patients who had an LVEF ≤ 50%, 5 out of 12 (41.7%) had ibrutinib held for arrhythmias, which is considerably higher than the entire cohort (25%). Patients with a larger LA volume index had a higher probability of having ibrutinib held for arrhythmias (LAVI 43.3 ± 15.9 vs. 33.6 ± 10.7 ml/m^2; $p = 0.007$). For those who were detected to have AF on event monitors ($n = 32$, 44%), EF was slightly lower (55.8 ± 8.9% vs. 60.0 ± 8.9%; $p = 0.059$), although it did not reach statistical significance.

There was no statistically significant relationship between AF on event monitor and risk factors such as age, hypertension, EKG, and echocardiographic parameters. No statistically significant difference was found between the cohort that developed AF and the cohort that did not. There was no statistically significant relationship between prior AF history and LA size or EF.

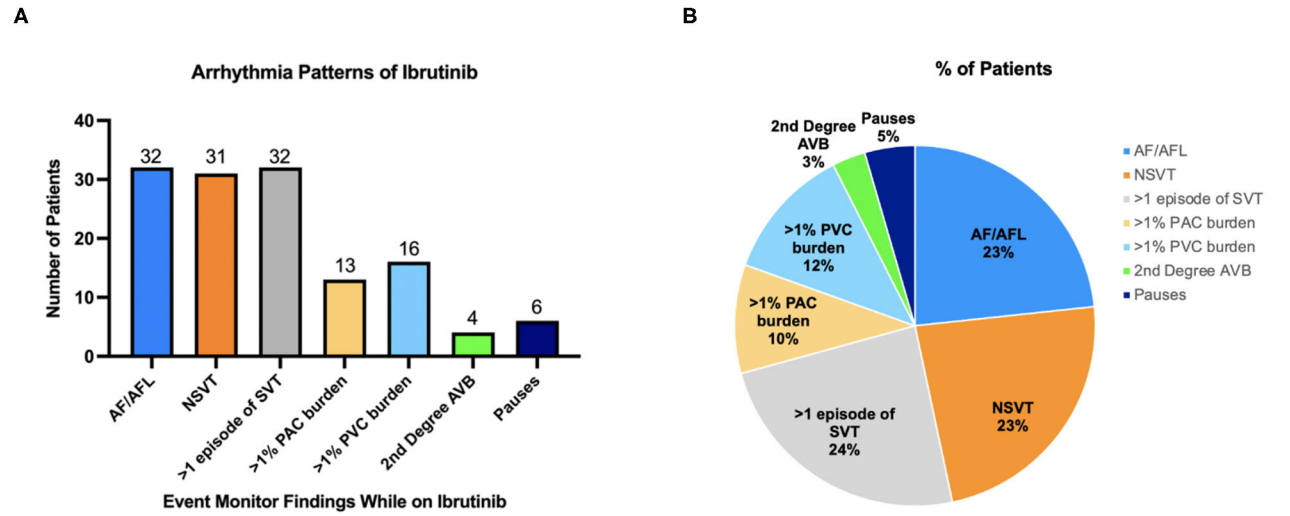

FIGURE 1 | (A) Arrhythmias noted on cardiac monitor while on ibrutinib. **(B)** Distribution of arrhythmias during ibrutinib treatment. The pie chart depicts breakdown of total arrhythmia events detected and showing what the pattern of arrhythmias is on ibrutinib therapy as a percentage of all arrhythmias seen.

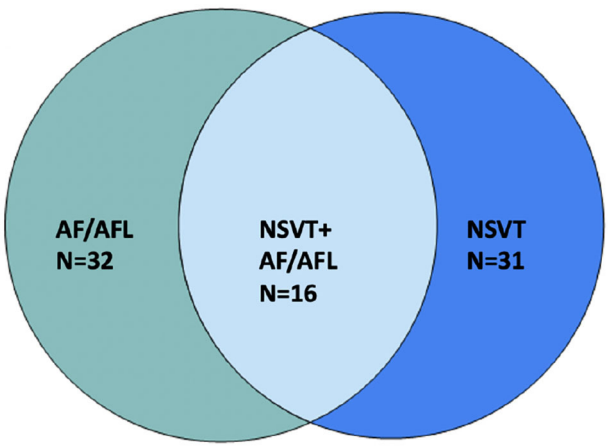

FIGURE 2 | Overlap of atrial and VAs in patients on ibrutinib.

DISCUSSION

In this large dataset of long-term event monitors on patients treated with ibrutinib, we conduct detailed characterization of their arrhythmias which demonstrate a high burden of both atrial and VAs, with a high incidence of treatment interruption secondary to arrhythmias and a low rate of referral to specialists for arrhythmia management.

The incidence of atrial arrhythmias during ibrutinib therapy is well documented, ranging from 8 (7) to 14% (8) in prospective studies, and up to 40% in patients referred to cardio-oncology clinics (9). Compared with other TKIs, ibrutinib therapy has been the most consistent and independent risk factor associated with subsequent AF. These are several-fold higher than the reported incidence of both AF and NSVT on patients with non-cancer who received event monitors (10, 11). Despite the high incidence of AF in this population, it remains unknown which patients are at a higher risk for developing AF. While limited studies suggest advanced age, valvular disease, and prior history of AF to increase this risk (12, 13), these risk factors were not consistently found significant. Moreover, in this study, we did not find significant correlation with any clinical or demographic factors in patients who developed AF, which may be due in part to the limited sample size. We also did not find any significant correlation between the duration of the ibrutinib therapies and the development of AF. To better identify risk factors or predictors of ibrutinib-related AF, a more comprehensive large cohort study would be warranted.

In this study, ibrutinib therapy was held in 18 (25%) patients because of arrhythmias and/or related symptoms. We identified factors such as >1% PAC burden on event monitor while on ibrutinib therapy, a prior history of VT ($p = 0.017$), a high LA volume index, and low LVEF to be significantly associated with increased likelihood of ibrutinib therapy interruption due to arrhythmia or related symptoms. We believe a high LA volume index which correlates with high LA pressure and/or low LVEF may be significant as they can predispose the myocardium to develop subsequent arrhythmia. Otherwise, we were unable to obtain reliable data regarding rates of ibrutinib being held in the cohort that did not have event monitors. According to limited study reports available, rates of ibrutinib discontinuation are as high as 35% and AF seems to be the most common reason for ibrutinib being held in a comparable population of patients with hematologic malignancies (14, 15).

Data regarding VA during ibrutinib or other TKI therapies are rather scant. Some studies have used large registries of patients with cancer and looked at adverse events of VAs while on ibrutinib therapy. They found that even after

TABLE 2 | Detailed personalized information about patients in whom ibrutinib therapy was held.

Patients in whom ibrutinib was held	Reason for ibrutinib interruption	Time on ibrutinib (months)	History of arrhythmia (AF or VT) prior to ibrutinib initiation	EF (%)	NSVT on Zio	QTc (ms)	Re-challenge
Patient 1	New atrial flutter with rapid ventricular response	64	No	41	Yes	419	Yes
Patient 2	Symptomatic persistent AF	17	No	55	N/A	N/A	No
Patient 3	Persistent atrial flutter	23	AF	61	Yes	432	No
Patient 4	Recurrent AF	24	No	68	No	N/A	Yes
Patient 5	New symptomatic AF	5	No	57	No	N/A	No
Patient 6	AF, Tachyarrhythmia mediated LV dysfunction	31	No	42	Yes	445	No
Patient 7	Worsening of existing AF	18	AF	65	Yes	414	No
Patient 8	New AF, bleeding issues with anticoagulation	56	No	60	No	N/A	No
Patient 9	New AF	67	No	51	No	N/A	No
Patient 10	Symptomatic AF	22	No	69	No	N/A	No
Patient 11	Uncontrolled AF	13	AF	42	Yes	445	Yes
Patient 12	New AF	40	No	60	Yes	384	No
Patient 13	New AF	36	No	60	Yes	435	Yes
Patient 14	Symptomatic AF	3	No	70	Yes	410	No
Patient 15	New AF	1	No	57	No	N/A	No
Patient 16	New AF	15	No	56	No	N/A	Yes
Patient 17	New AF	23	No	35	Yes	486	Yes
Patient 18	Recurrent AF	4	AF	41	No	N/A	No

accounting for baseline CV risk factors, ibrutinib was associated with a much higher incidence of VAs compared to similar patients not taking ibrutinib with a risk ratio up to 12.4 (16). When estimating the incidence of VAs in clinical trials involving ibrutinib, it was found that the incidence of VAs was significantly higher in patients receiving ibrutinib therapy compared to non-ibrutinib therapies (17). Yet, the detailed characterization, subtypes, and true incidence of VAs remain unknown as only symptomatic, clinical events were included in the analysis.

This study is unique in that it utilizes Holter event monitors which record all arrhythmic events, inclusive of both symptomatic and asymptomatic, over 2 weeks to comprehensively and unbiasedly characterize VAs among the patients treated with ibrutinib. In this study, the incidence of VAs was substantially higher with NSVTs captured in 43% of patients and a >1% burden of PVCs in up to 22% of symptomatic or arrhythmia-prone patients who were treated with ibrutinib and required Holter monitor screening. The observed rate of NSVT is an order of magnitude higher than the reported incidence of NSVT without known heart disease, which is generally in the range of 0.5–1% (18). Our results support the notion that ibrutinib is associated with a more frequent occurrence of VAs than previously believed. This finding also raises the question of underdiagnosis of VAs in patients treated with ibrutinib and emphasizes the need for further research in and more intensive monitoring of arrhythmias associated with ibrutinib therapy, and also other TKIs.

Multiple mechanisms have been proposed regarding the pathogenesis of TKI-induced arrhythmia. A recent study showed that off-target inhibition of C-terminal Src kinase (CSK), a non-receptor tyrosine kinase that inhibits Src kinase family members, may be responsible for the increased arrhythmogenicity seen with ibrutinib therapy (19). While CSK was reported to be expressed at a lower level in bulk ventricular vs. atrial tissue (19), it was found in both atrial and ventricular myocytes to a similar level (20) at the individual cell level which might explain the high burden of VAs observed in our study. Other proposed mechanisms for VAs due to ibrutinib include QTc prolongation and enhanced automaticity. In our cohort, the QTc of patients who developed NSVT was not found significantly prolonged (median duration of 422 ms).

Limitations of our study include patients enrolled in a single center, relatively small size of patients, and the absence of event monitors in all patients on ibrutinib. Notably, patients included in our study had an event monitor placed due to symptoms, ranging from palpitations to syncope, which can induce a selection bias to overestimate the incidence of arrhythmias in this patient population. Our cohort also consisted of older patients with a mean age of 77 years, more male patients, and patients with a modest burden of cardiovascular risk factors, all of which are known risk factors for developing

atrial or VA. No statistically significant correlation was found between development of AF and clinical risk factors which have been shown to be related in larger studies such as age and hypertension, likely due to the small sample size of our cohort. Given the limited size of the cohort, only descriptive and univariate statistical analyses were performed. Additional clinical data such as alcohol intake data and prescription of other AF-inducing drugs could not be reliably obtained from our retrospective chart review and therefore not included in this analysis. Regarding non-AF SVT, we were unable to further classify the subtypes due to the limited quality of signals. Finally, we were unable to get the rates of ibrutinib discontinuation from the cohort that did not have event monitors placed to compare them to the patients included in this analysis. As such, a prospective and multicenter study would be warranted to better characterize arrhythmia associated with ibrutinib therapy.

CONCLUSION

In this large dataset of Holter monitors on patients treated with ibrutinib, we find a significant burden of both atrial and VAs resulting in treatment interruption due to arrhythmias and related symptoms. Our results highlight the need for intentional monitoring and management of both atrial and VAs when patients are treated with ibrutinib therapy.

DATA AVAILABILITY STATEMENT

The raw data supporting the conclusions of this article will be made available by the authors, without undue reservation.

ETHICS STATEMENT

This study was approved by the Institutional Review Board of Stanford University. Written informed consent for participation was not required for this study in accordance with the national legislation and the institutional requirements.

AUTHOR CONTRIBUTIONS

MF, RK, TB, and J-WR conceived and designed the study. MF and RK collected patient data. PC, AR, MF, RK, and TB analyzed the data. SN, PW, RW, and AP contributed to design the study and provided critical input on the manuscript. MF, RK, TB, and J-WR wrote the manuscript with input from all authors. All authors contributed to the article and approved the submitted version.

FUNDING

This work is supported by National Institutes of Health Grants K08 HL148540 (J-WR), K08 HL153798 (PC), R01 HL83359 (SN), K23 HL145017 (TB), and American Heart Association Career Development Awards (J-WR and PC).

REFERENCES

1. Baptiste F, Cautela J, Ancedy Y, Resseguier N, Aurran T, Farnault L, et al. High incidence of atrial fibrillation in patients treated with ibrutinib. *Open Heart.* (2019) 6:e001049. doi: 10.1136/openhrt-2019-001049
2. Brown JR, Moslehi J, O'Brien S, Ghia P, Hillmen P, Cymbalista F, et al. Characterization of atrial fibrillation adverse events reported in ibrutinib randomized controlled registration trials. *Haematologica.* (2017) 102:1796–805. doi: 10.3324/haematol.2017.171041
3. Chanan-Khan A, Cramer P, Demirkan F, Fraser G, Silva RS, Grosicki S, et al. Ibrutinib combined with bendamustine and rituximab compared with placebo, bendamustine, and rituximab for previously treated chronic lymphocytic leukaemia or small lymphocytic lymphoma (HELIOS): a randomised, double-blind, phase 3 study. *Lancet Oncol.* (2016) 17:200–11. doi: 10.1016/S1470-2045(15)00465-9
4. Chugh SS, Havmoeller R, Narayanan K, Singh D, Rienstra M, Benjamin EJ, et al. Worldwide epidemiology of atrial fibrillation: a Global Burden of Disease 2010 Study. *Circulation.* (2014) 129:837–47. doi: 10.1161/CIRCULATIONAHA.113.005119
5. Fradley MG, Gliksman M, Emole J, Viganego F, Rhea I, Welter-Frost A, et al. Rates and risk of atrial arrhythmias in patients treated with ibrutinib compared with cytotoxic chemotherapy. *Am J Cardiol.* (2019) 124:539–44. doi: 10.1016/j.amjcard.2019.05.029
6. Ganatra S, Sharma A, Shah S, Chaudhry GM, Martin DT, Neilan TG, et al. Ibrutinib-Associated Atrial Fibrillation. *JACC Clin Electrophysiol.* (2018) 4:1491–500. doi: 10.1016/j.jacep.2018.06.004
7. Guha A, Derbala MH, Zhao Q, Wiczer TE, Woyach JA, Byrd JC, et al. Ventricular arrhythmias following ibrutinib initiation for lymphoid malignancies. *J Am Coll Cardiol.* (2018) 72:697–8. doi: 10.1016/j.jacc.2018.06.002
8. Kaakeh Y, Overholser BR, Lopshire JC, Tisdale JE. Drug-induced atrial fibrillation. *Drugs.* (2012) 72:1617–30. doi: 10.2165/11633140-000000000-00000
9. Lampson BL Yu L, Glynn RJ, Barrientos JC, Jacobsen ED, Banerji V, et al. Ventricular arrhythmias and sudden death in patients taking ibrutinib. *Blood.* (2017) 129:2581–4. doi: 10.1182/blood-2016-10-742437
10. Lee C-S, Rattu MA, Kim SS. A review of a novel, Bruton's tyrosine kinase inhibitor, ibrutinib. *J Oncol Pharm Pract.* (2016) 22:92–104. doi: 10.1177/1078155214561281
11. Litvinuková M, Talavera-López C, Maatz H, Reichart D, Worth CL, Lindberg EL, et al. Cells of the adult human heart. *Nature.* (2020) 588:466–72. doi: 10.1038/s41586-020-2797-4
12. Maddocks KJ, Ruppert AS, Lozanski G, Heerema NA, Zhao W, Abruzzo L, et al. Etiology of ibrutinib therapy discontinuation and outcomes in patients with chronic lymphocytic leukemia. *JAMA Oncol.* (2015) 1:80–7. doi: 10.1001/jamaoncol.2014.218
13. Marine JE. Nonsustained ventricular tachycardia in the normal heart: risk stratification and management. *Card Electrophysiol Clin.* (2016) 8:525–43. doi: 10.1016/j.ccep.2016.04.003
14. Mato AR, Nabhan C, Barr PM, Ujjani CS, Hill BT, Lamanna N, et al. Outcomes of CLL patients treated with sequential kinase inhibitor therapy: a real world experience. *Blood.* (2016) 128:2199–205. doi: 10.1182/blood-2016-05-716977
15. Shanafelt TD, Parikh SA, Noseworthy PA, Goede V, Chaffee KG, Bahlo J, et al. Atrial fibrillation in patients with chronic lymphocytic leukemia (CLL). *Leuk Lymphoma.* (2017) 58:1630–9. doi: 10.1080/10428194.2016.1257795
16. Solomon MD, Yang J, Sung SH, Livingston ML, Sarlas G, Lenane JC, et al. Incidence and timing of potentially high-risk arrhythmias detected through long term continuous ambulatory electrocardiographic monitoring. *BMC Cardiovasc Disord.* (2016) 16:35. doi: 10.1186/s12872-016-0210-x
17. van der Hooft CS, Heeringa J, van Herpen G, Kors JA, Kingma JH, Stricker BHC. Drug-induced atrial fibrillation. *J Am Coll Cardiol.* (2004) 44:2117–24. doi: 10.1016/j.jacc.2004.08.053

18. Wiczer TE, Levine LB, Brumbaugh J, Coggins J, Zhao Q, Ruppert AS, et al. Cumulative incidence, risk factors, and management of atrial fibrillation in patients receiving ibrutinib. *Blood Adv*. (2017) 1:1739–48. doi: 10.1182/bloodadvances.2017009720
19. Xiao L, Salem J-E, Clauss S, Hanley A, Bapat A, Hulsmans M, et al. Ibrutinib-Mediated Atrial Fibrillation Attributable to Inhibition of C-Terminal Src Kinase. *Circulation*. (2020) 142:2443–55. doi: 10.1161/CIRCULATIONAHA.120.049210
20. Yenikomshian M, Jarvis J, Patton C, Yee C, Mortimer R, Birnbaum H, et al. Cardiac arrhythmia detection outcomes among patients monitored with the Zio patch system: a systematic literature review. *Curr Med Res Opin*. (2019) 35:1659–70. doi: 10.1080/03007995.2019.1610370

Conflict of Interest: TB has received speaker and consultant fees from Biotronik, Medtronic, and PaceMate unrelated to this work. RW has received consulting fees from Pfizer, Alnylam, Eidos, and Ionis/Akcea unrelated to this work. AP has research support from the American Heart Association, Pfizer Inc. and Bristol Myers Squibb. Consultant for Abbott, Pfizer Inc. and Bristol Myers Squibb.

The remaining authors declare that the research was conducted in the absence of any commercial or financial relationships that could be construed as a potential conflict of interest.

Publisher's Note: All claims expressed in this article are solely those of the authors and do not necessarily represent those of their affiliated organizations, or those of the publisher, the editors and the reviewers. Any product that may be evaluated in this article, or claim that may be made by its manufacturer, is not guaranteed or endorsed by the publisher.

frontiers in Cardiovascular Medicine

REVIEW
published: 12 January 2022
doi: 10.3389/fcvm.2021.821663

The Research Progress of Trastuzumab-Induced Cardiotoxicity in HER-2-Positive Breast Cancer Treatment

Mengmeng Lin[1†], Weiping Xiong[2†], Shiyuan Wang[1], Yingying Li[1], Chunying Hou[1], Chunyu Li[1] and Guohui Li[1*]*

[1] National Cancer Center/National Clinical Research Center for Cancer/Cancer Hospital, Chinese Academy of Medical Sciences and Peking Union Medical College, Beijing, China, [2] Department of Cardiology, Shanghai Putuo District Liqun Hospital, Shanghai, China

OPEN ACCESS

Edited by:
Chun Liu,
Stanford University, United States

Reviewed by:
Nian Liu,
Capital Medical University, China
Zhiqiang Liu,
Beijing Institute of Basic Medical Sciences, China

***Correspondence:**
Chunyu Li
chunyu_li@126.com
Guohui Li
lgh0603@cicams.ac.cn

[†] *These authors have contributed equally to this work*

Specialty section:
This article was submitted to Cardio-Oncology, a section of the journal Frontiers in Cardiovascular Medicine

Received: *24 November 2021*
Accepted: *14 December 2021*
Published: *12 January 2022*

Citation:
Lin M, Xiong W, Wang S, Li Y, Hou C, Li C and Li G (2022) The Research Progress of Trastuzumab-Induced Cardiotoxicity in HER-2-Positive Breast Cancer Treatment. Front. Cardiovasc. Med. 8:821663. doi: 10.3389/fcvm.2021.821663

In recent years, the incidence of breast cancer has been increasing on an annual basis. Human epidermal growth factor receptor-2 (HER-2) is overexpressed in 15-20% human breast cancers, which is associated with poor prognosis and a high recurrence rate. Trastuzumab is the first humanized monoclonal antibody against HER-2. The most significant adverse effect of trastuzumab is cardiotoxicity, which has become an important factor in limiting the safe use of the drug. Unfortunately, the mechanism causing this cardiotoxicity is still not completely understood, and the use of preventive interventions remains controversial. This article focuses on trastuzumab-induced cardiotoxicity, reviewing the clinical application, potential cardiotoxicity, mechanism and discussing the potential interventions through summarizing related researches over the past tens of years.

Keywords: trastuzumab, cardiotoxicity, breast cancer, adverse reaction, rational drug use

INTRODUCTION

Currently, the incidence of breast cancer has been increasing year by year, and now has the greatest incidence of malignant tumors worldwide, with obvious geographical differences. According to GLOBOCAN 2020 estimates of cancer incidence and mortality produced by the International Agency for Research on Cancer, female breast cancer has surpassed lung cancer as the most commonly diagnosed cancer, with an estimated 2.3 million new cases (1). Human epidermal growth factor receptor-2 (HER-2) is an important biomarker for breast cancer as well as a therapeutic target. Of breast cancer patients, 15-20% are HER-2 positive, which is usually considered the most serious subtype due to its poor prognosis and high recurrence rate (2, 3). Trastuzumab is a humanized monoclonal antibody directed against HER-2, initially approved as first-line treatment of HER-2-positive recurrent metastatic breast cancer in 1998. Introduction of trastuzumab to chemotherapeutic regimes has significantly increasing the life expectancy of patients with HER-2 positive, aggressive breast cancer. Meanwhile, there have been increasing reports of trastuzumab-induced cardiotoxicity (TIC) in recent years. To date, the most

relevant clinical solution for TIC is trastuzumab interruption, but this approach may cause cancer recurrence. Therefore, understanding the mechanism of TIC and the related preventive measures is paramount for the safe and effective treatment of HER2-positive breast cancer patients. Here, we have attempted to provide an overview of our current knowledge of this effect, focusing primarily on clinical manifestations, influencing factors and mechanism. We also discussed the prevention and pretreatment, with the goal of providing reference for related research and clinical use.

OVERVIEW OF TRASTUZUMAB FOR HER-2-POSITIVE BREAST CANCER

Trastuzumab is an important HER-2 targeted drug. The gene encoding HER-2 is localized on chromosome 17 (4) and encodes a transmembrane glycoprotein with tyrosine kinase activity that plays an important role in cell survival, proliferation, and differentiation (5, 6). HER-2 is a member of the epidermal growth factor receptor (EGFR) family and has two forms of activation, homodimerization and heterodimerization with other receptors in the family (HER-1, HER-3, HER-4), either of which triggers cellular pathways including MEK/Erk, PI3K/Akt (7, 8). The mechanism of trastuzumab has not been fully elucidated and may be related to inhibiting the formation of the homodimer by binding to the HER2 extracellular structural domain IV, blocking downstream cellular pathways and thus blocking tumor cell proliferation (9, 10). Recently, Tsao et al. (11) found that the dominant therapeutic mechanism of trastuzumab is through its elicitation of tumor associated macrophages, which mediated antibody-dependent cellular phagocytosis. After HER2 overexpression was discovered to be associated to poor clinical outcomes in breast cancer patients, it quickly became the focus of intensive investigations. In 1989, Hudziak et al. (12) found that a mouse monoclonal antibody to HER-2 successfully inhibited the proliferation of breast cancer cells. Researchers humanized mouse-derived 4D5 monoclonal antibodies and the most active of these was named trastuzumab (13). It was approved by the FDA in 1998 for first-line treatment of HER-2-positive recurrent metastatic breast cancer. Trastuzumab in combination with other agents significantly prolonged median survival (25.1 vs. 20.3 months; $p < 0.008$), progression-free survival (7.4 vs. 4.6 months; $p < 0.001$), improved objective remission rates (50 vs. 32%; $p < 0.001$), and reduced one-year mortality (22 vs. 33%; $p < 0.008$) (14). Several large foreign clinical trials have shown that the use of trastuzumab after receiving chemotherapy can significantly reduce the risk of breast cancer recurrence and death (15–17). Furthermore, a joint analysis of two large clinical trials (NCCTG N9831 and NSABP B-31) found that patients with early-stage HER2-positive breast cancer benefited from the addition of trastuzumab to conventional chemotherapy followed by treatment with paclitaxel, resulting in a significant and sustained reduction in cancer recurrence rates and a 37% improvement in overall survival (18). Both *Chinese guidelines for diagnosis and treatment of pancreatic cancer 2019* and *NCCN Clinical Practice Guidelines in Oncology* recommend trastuzumab as the first choice in combination with chemotherapy drugs (19).

CLINICAL MANIFESTATIONS OF TRASTUZUMAB-INDUCED CARDIOTOXICITY

It is generally accepted that, unlike anthracyclines, the cardiotoxicity caused by trastuzumab is not dose-dependent, does not occur in all patients, and is reversible (20). Left ventricular dysfunction (LVD) and heart failure (HF) are relatively common and severe manifestations of cardiotoxicity in cancer therapy (21). The Cardiac Review and Evaluation Committee (CREC) defined the cardiotoxicity as one of the following: (1) cardiomyopathy characterized by a decrease in cardiac left ventricular ejection fraction (LVEF) that was either global or more severe in the septum; (2) symptoms of congestive heart failure (CHF); (3) associated signs of CHF, including but not limited to S3 gallop, tachycardia or both; and (4) decline in LVEF of at least 5 to <55% with accompanying signs or symptoms of CHF or a decline in LVEF of at least 10% to <55% without accompanying signs or symptoms (22). Any of the above can be defined as cardiotoxicity. A frequently used definition of treatment-related cardiotoxicity in clinical trials is an absolute decrease in LVEF of 10% to a value of <55% (23). Of these definitions, there may be differences between individual patients regarding the decrease in LVEF. Researchers analyzed 1,437 echocardiograms from 324 patients over a follow-up period of up to 3.5 years, and revealed three main patterns of LVEF change over time: (1) steady decline over time; (2) mild early and late sustained decline; (3) early significant decline with late partial recovery (24).

In addition to left ventricular dysfunction and heart failure, studies also reported the development of arrhythmias, sick sinus node syndrome, and atrial flutter in patients undergoing treatment with trastuzumab (25). Recently, through a secondary analysis of a clinical trial, investigators found that TIC is characterized by the presence of both left ventricular dysfunction and reversible myocardial inflammation and edema, and that trastuzumab may be associated with deleterious changes in cardiac metabolic phenotype (26).

THE INCIDENCE AND INFLUENCING FACTORS OF TIC

Many clinical studies have demonstrated the cardiotoxicity associated with trastuzumab, and this article focuses on a few large clinical studies of adjuvant therapy with combination or sequential trastuzumab. In the N9831 study (27), in the two trial groups using trastuzumab, the cumulative incidence of CHF or cardiac death over 6 years was 2.8 and 3.4%, respectively, resulting in risks that were 4.7 and 5.7 times higher than not using trastuzumab. The BCIRG006 (17) study found that the addition of trastuzumab after anthracycline treatment significantly increased the odds of CHF, and the risk of decreased LVEF was 1.6 times greater than without trastuzumab.

Furthermore, the incidence of cardiac events reported by NSABP B-31were 1.3% in the control group and 4.0% in the trastuzumab group, with 15.5% of the trastuzumab group discontinuing the drug for cardiac reasons (28). The BIG1-01 (HERA) study (16, 29) conducted a comparative trial of 5102 HER-2 positive early-stage breast cancer patients over 1 and 2 years, respectively. Although the incidence of severe CHF was 0.8% in both groups, the incidence of asymptomatic drop in LVEF was significantly higher in patients on trastuzumab for 2 years (7.2%) than for 1 year (4.1%). The rate of discontinuation of treatment due to TIC was 5.2% during the 1-year period and 9.4% during the 2-year period. Additionally, an 11-year follow-up of the study found that the most of the TIC occurred during the patients' dosing period and no delayed cardiotoxicity was seen (See **Table 1**).

The incidence varies depending on the assay and criteria for cardiotoxicity used by researchers amongst the different clinical trials, as well as on the selection of patients participating in the trials. For example, in the HERA trial, a lower incidence of cardiotoxicity may be due to the exclusion of patients who had a cardiac event prior to treatment from the trial. Because patients with significant disease, including those at high risk for cardiovascular disease, are often excluded from randomized controlled trials, the incidence may differ from the real world. A real-world study based on trastuzumab for cardiotoxicity due to HER2-positive breast cancer that included more than 3,700 study subjects showed a CHF incidence of 2.8%, with a 1.0% incidence of severe CHF (31).

Risk factors for development of TIC include previous anthracycline exposure and conventional cardiovascular risk factors. Several clinical studies have demonstrated that previous anthracycline exposure appears to be the most important factor in worsening cardiotoxicity (32, 33). This may be related to the fact that the inhibition of the HER2 pathway by trastuzumab exacerbates damage caused by oxidative stress induced by anthracyclines, allowing for further accumulation of ROS (34).

In addition to co-administration, conventional cardiovascular risk factors have been associated with TIC. A recently published systematic review and meta-analysis focusing on the relationship between conventional cardiac risk factors and trastuzumab-induced cardiotoxicity in breast cancer treatment showed that age $\geq$ 60 (OR 2.03, 95% CI 1.38-3.00, $P = 0.0004$), hypertension (OR 2.01, 95% CI 1.30-3.09, $P = 0.002$), smoking (OR 1.33, 95% CI 1.07-1.65, $P = 0.01$), diabetes (OR 1.49, 95% CI 1.22-1.81, $P = 0.0001$), family history of coronary artery disease (OR 5.51, 95% CI 1.76-17.25, $P = 0.00001$), known history of coronary artery disease (OR 6.27, 95% CI 2.22-17.69, $P = 0.0005$) were strongly associated with the development of TIC (35). Besides, combination of obesity and being overweight was also a significant influencing factor (36).

MECHANISM OF TRASTUZUMAB-INDUCED CARDIOTOXICITY

The exact mechanism of TIC has not been fully elucidated, and numerous *in vitro* and *in vivo* studies suggest that it may involve multiple cellular and molecular mechanisms (37). The inhibition of NRG-1/HER and downstream signaling pathways has always posed a plausible explanation for TIC, but the underlying molecular mechanisms still remain undefined. In addition, recent research has investigated the inhibition of autophagy and alterations in cellular metabolic pathways in cardiomyocytes as potential causes for the development of cardiotoxicity.

Downregulation of HER2 Signaling and Cardiotoxicity

In addition to being expressed in tumor tissue, HER2 has been shown to be expressed in adult cardiomyocytes along with other members of the family (HER1, HER3 and HER4) (8). HER2, together with its ligand, NRG1, is closely tied to the maintenance of adult cardiac function and the development of cardiomyocytes. When the heart becomes hemodynamically unstable or stimulated, cardiac microvascular endothelial cells can release NRG1 (38, 39). After acting in a paracrine form in cardiomyocytes, NRG1 binds to HER4 and triggers HER4/HER4 homodimerization or HER4/HER2 heterodimerization, which can later trigger a series of pathways including the MAPK pathway and PI3K-Akt (40).

The activation of the Akt family can trigger many proteins through phosphorylation, thereby initiating tumor cell survival and inhibiting apoptosis (41). Ravingerova et al. (42) used a chronic cardiac ischemia rat model to discover that Akt also increases glucose and lipid metabolism in cardiomyocytes through nutrient uptake and ensures energy in cardiomyocytes during hypoxia. Furthermore, the activation of the PI3K-Akt pathway promotes nitric oxide (NO) production in adult ventricular myocytes, thereby protecting them from oxidative stress. Moreover, Akt can initiate alterations in mitochondrial respiration, thereby reducing reactive oxygen species (ROS) production and improving cell survival. If HER2 signaling is blocked, PI3K-Akt pathway blockade will cause the accumulation of ROS in cardiomyocytes, thereby triggering the apoptosis of cardiomyocytes (43).

The MAPK pathway is another pathway associated with TIC. The MAPK pathway consists mainly of three protein kinases, Raf/MEK/ERK, that cascade to amplify external signals and thus cause cell proliferation and differentiation (44). Meanwhile, the phosphorylation of ERK1/2, inhibits the opening of the mitochondrial osmotic transition pore and suppresses the decrease in membrane potential, thus stabilizing mitochondrial function (45).

In summary, the activation of NRG1/HER and downstream signaling pathways plays an important role in protecting the stability of cardiac function. Trastuzumab inhibits the dimerization of HER4/HER2 by binding to HER2 and thereby inhibiting the above pathways (see **Figure 1**), which may be one of the potential mechanisms for TIC. In fact, NRG1/HER signaling in the heart is part of a stress-activated compensatory system that plays a minor role under physiological conditions, but can play a protective role when the heart is exposed to cardiotoxic drugs or ischemia, which is consistent with the reality

TABLE 1 | Cardiac toxicity induced by trastuzumab.

TRIAL (Ref.)	Median follow-up time	Enrolled patients	Design	Asymptomatic drop in LVEF (≥10-55%)	Severe CHF/CE
NCCTG(Alliance)N9831 (27)	9.2	1,944	AC-paclitaxel AC-paclitaxel-H AC-paclitaxel plus H-H	20.5% 19.6% 22.5%	0.6% 2.8% 3.4%
BCIRG006 (17)	5	3,222	AC-docetaxel plus H AC-docetaxel Docetaxel-carboplatin-H	18.6% 11.2% 9.4%	2.0% 0.7% 0.4%
NSABP B-31 (28)	7	1,830	AC-paclitaxel AC-paclitaxel plus H-H	NO MENTIONED	1.3% 4.0%
HERA(BIG1-01) (29)	8	3,387	Observation 1 Year of H 2 Year of H	0.9% 4.1% 7.2%	0 0.8% 0.8%
PHARE (30)	3.5	3,384	1 year of AC-H 6 months of AC-H	6%(CHF, or LVEF ≥ 10-55%) 2%(CHF, or LVEF ≥ 10-55%)	

A, anthracyclines; C, cyclophosphamide; H, trastuzumab; CE, cardiac event.
CHF, congestive heart failure.

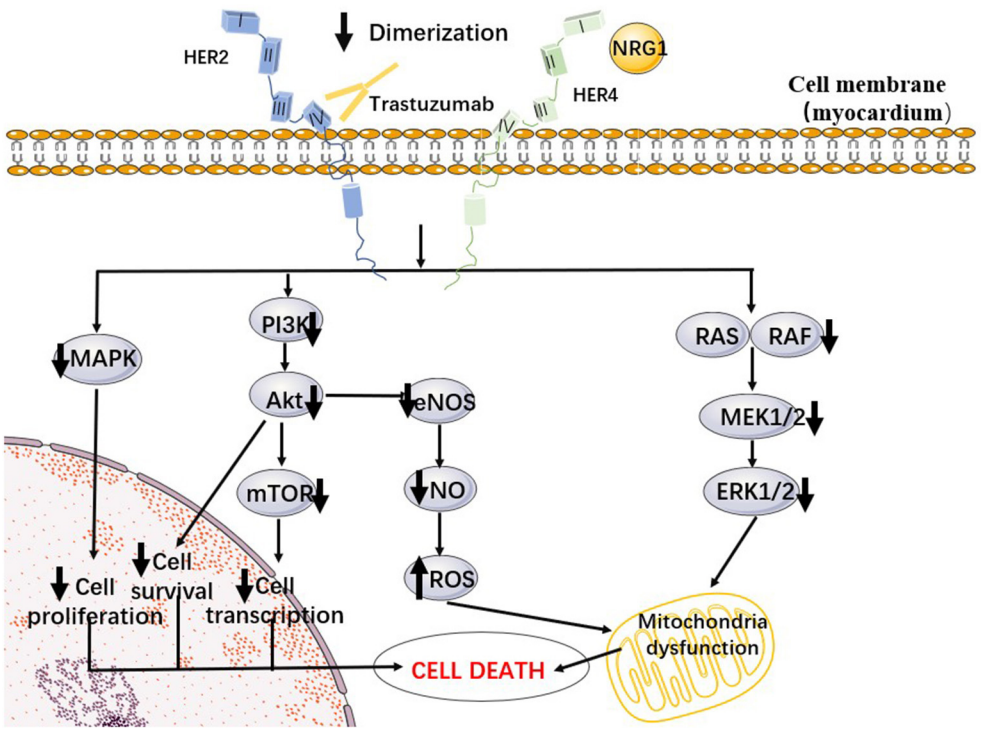

FIGURE 1 | A proposed cellular mechanism of the cardiotoxicity of trastuzumab. Trastuzumab inhibited Her2/4 dimerization, preventing autophosphorylation and subsequent downstream pathways such as PI3K/Akt and MAPK.

that trastuzumab increases cardiotoxicity when combined with anthracyclines (46, 47).

Inhibition of Autophagy

Autophagy is a catabolic process that aims to recycle cellular components and damaged organelles in response to different stress conditions (48). Thomas et al. found that deletion of the anti-apoptotic protein MCL-1 in mouse cardiomyocytes leads to the inhibition of autophagy, eventually resulting in heart failure, and further indicated that MCL-1 deficiency is associated with mitochondrial dysfunction (49). Mohan et al. found that trastuzumab treatment decreased the protein expression of autophagy-related signaling molecules such as ATG5-12, ATG7, ATG14, and Beclin 1, and also demonstrated that trastuzumab-mediated inhibition of autophagy resulted in increased ROS production in cardiomyocytes (50). In earlier years, some

researchers found that anthracycline increases autophagy and that this is closely related to its cardiotoxicity, which also suggests that anthracyclines and trastuzumab differ in their mechanisms of inducing cardiotoxicity (51, 52).

Alterations of Cardiomyocyte Metabolism

The inhibition of the NRG1/HER signaling pathway still does not fully answer the question of why trastuzumab causes cardiotoxicity. For example, TIC is often reversible in clinical settings, which contradicts the above explanation that blocking the HER2 pathway leads to cardiomyocyte apoptosis. Alterations in cardiac energy metabolism are a key feature of heart failure and are thought to exacerbate its progression (53). Necela et al. (54) found that after trastuzumab treatment, there was a reduction in glucose uptake in human induced pluripotent stem cell-derived cardiomyocytes (IPSC-CMs) as well as a significant downregulation of SLC6A6. SLC6A6 is a metabolism-related gene, and SLC6A6 knockout mice exhibit a cardiomyopathy with myocardial atrophy phenotype, which also provides a potential mechanism for TIC (55). Recently, investigators have found that clinically relevant doses of trastuzumab impaired the contractile and calcium regulatory functions of IPSC-CMs but did not lead to cardiomyocyte death, and that further RNA-SEQ with subsequent functional analysis revealed that mitochondrial dysfunction and altered cardiac energy metabolic pathways were the main causes of the TIC phenotypes, thus suggesting that metabolic modulators are important for the treatment of TIC (56).

PREVENTION AND TREATMENT OF TIC

Monitoring of TIC

Strict monitoring of cardiotoxicity during the treatment of trastuzumab facilitates timely adjustment of dosing and optimization of treatment regimens by clinicians. LVEF, measured by cardiovascular magnetic resonance (CMR) or 2-dimensional echocardiography (2DE), is currently the most commonly used index for monitoring left ventricular function, but LVEF has limitations and often underestimates cardiac compromise in patients. In a retrospective study, investigators found that baseline left ventricular end-diastolic volume (LEVD) was an independent predictor of cardiotoxicity and more reliably identified patients at high risk of cardiotoxicity (57). Besides, echocardiographic measurement of longitudinal shortening of the heart during contraction, or global longitudinal strain (GLS), can identify early changes in left ventricular contractility before ejection fraction (EF) declines. Researchers found that ΔGLS at 6 months were predictors of decrease in EF at 12 months (58). And GLS-guided cardioprotective therapy (CPT) prevents reduction in LVEF and development of cardiac dysfunction in high-risk patients undergoing potentially cardiotoxic chemotherapy, compared with usual care (59). Improvements in testing technology have allowed for the emergence of serum biomarkers that play an increasing role in the monitoring of cardiotoxicity. The 2016 ESC Position Paper on cancer treatments and cardiovascular toxicity published by the European Society of Cardiology (ESC) proposed that the use of serum biomarkers is an important tool for baseline risk assessment and diagnosis of cardiovascular disease. The statement recommends cardiac troponin (CTn) baseline measurement for all cancer patients, as the strongest independent predictor of cardiotoxicity, and in patients with early invasive HER2+ breast cancer undergoing neoadjuvant or adjuvant therapy. B-type natriuretic peptide (BNP)/amino-terminal pro-B-type natriuretic peptide (NT-proBNP) with CTn testing were recommended after receiving trastuzumab (60). In recent years, soluble growth-stimulating expression gene 2 protein (sST2) has received wide attention as a novel heart failure marker. Some studies have shown that sST2 levels correlate with the severity of heart failure, LVEF and NT-proBNP in patients (61). In addition, Zhang et al. (62) analyzed 65 HER2-positive breast cancer patients treated with trastuzumab and applied ordered logistic regression to analyze the relationship between serum miR-222-3p and adverse events and found that serum miR-222-3p was a potential predictor of TIC.

Choosing an Anthracycline-Free Regimen

In the BCIRG006 clinical trial, the regimen combining anthracyclines with trastuzumab had similar long-term survival rates as the paclitaxel and cyclophosphamide combined with trastuzumab regimen, while the incidence of cardiotoxicity in the latter group was much lower than former (17). A randomized multicenter phase III trial of 438 patients with stage II and III HER2-positive breast cancer showed an estimated 3-year event-free survival rate of 93% in patients treated with anthracyclines and 94% in patients not using, while decrease in LVEF was more common in the anthracycline group (63). This suggests that avoiding anthracyclines when using trastuzumab in favor of other classes of drugs may reduce the likelihood of cardiac events without compromising efficacy.

In addition to its use in combination with chemotherapeutic agents, trastuzumab has shown a good prognosis in combination with other antitumor drugs. Unlike trastuzumab, pertuzumab is a humanized monoclonal antibody against the extracellular structural domain II region of HER2, which inhibits the heterodimerization of HER2 with HER3, thereby blocking pathways including phosphatidylinositol 3-kinase (PI3K/AKT/mTOR) and mitogen-activated protein kinase (RAS/RAF/MEK/ERK) (64, 65). It acts at a different site from trastuzumab in the extracellular structural domain of HER2 and there may be a synergistic effect when they are combined (see **Figure 2**). The NeoSphere phase II study evaluated the efficacy and safety of trastuzumab with pertuzumab in combination with docetaxel in HER2-positive breast cancer patients treated with neoadjuvant therapy, and showed that the dual-target combination chemotherapy significantly increased the pathologic complete remission rate (pCR) as compared to the single-target, while the adverse effects were broadly consistent with the trastuzumab monotherapy arm (66). Furthermore, the TRYPHAENA trial demonstrated that the combination of trastuzumab and pertuzumab, whether co-administered with anthracyclines or with carboplatin, was usually well-tolerated and also showed a higher rate of pCR and a lower incidence of cardiotoxicity in the anthracycline-free trial group (67).

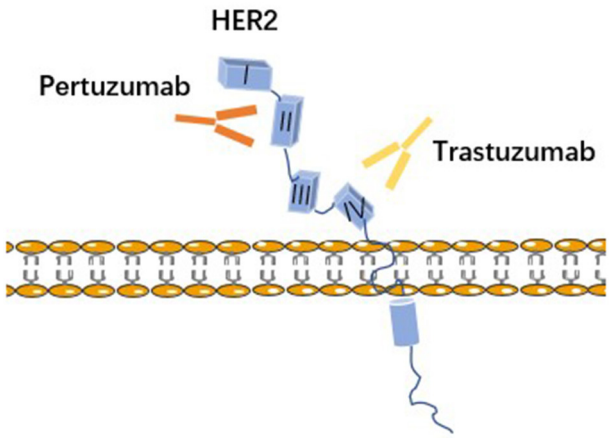

FIGURE 2 | Trastuzumab and pertuzumab bind to different regions on HER2. Trastuzumab is a humanized monoclonal antibody to IV subdomain of HER2. Pertuzumab is a humanized monoclonal antibody to subdomain II of the dimerization arm of HER2.

Similarly, the PEONY study demonstrated that dual-targeted combination therapy significantly improved the pCR rate (68). The 2019 NCCN guidelines recommend the TCHP regimen [trastuzumab (H) + pertuzumab (P) in combination with docetaxel (T) + carboplatin (C)] as a first-line treatment option for HER-2-positive breast cancer. This regimen is anthracycline-free and therefore has a higher safety profile for patients with potentially dangerous cardiac function.

Pharmacological Prevention

Unlike anthracyclines, LVD caused by trastuzumab is usually reversible, thus the ESMO guidelines mainly recommend strategies such as observation and discontinuation of the drug (69). However, a large retrospective cohort study found that discontinuation of trastuzumab led to adverse clinical outcomes (70). Therefore, it is necessary to use appropriate cardioprotective agents in the clinical setting.

Angiotensin-Converting Enzyme Inhibitor or β-Receptor Inhibitors

Early research found that NRG-1/HER signaling regulates myocardial contractility and is influenced by circulating catecholamines and angiotensin-II in animal models (39). This may provide some theoretical basis for the use of ACEI or β-receptor inhibitors in the prevention of TIC. Several small randomized trials and single-center studies have also reported that ACEI and β-blockers ameliorate chemotherapy-induced cardiotoxicity, but these studies all emphasized high-dose anthracycline-induced cardiotoxicity and have limited clinical applicability in TIC (71, 72). In 2016, the MANTICORE 101-Breast randomized clinical trial specifically investigated the pharmacological prevention of TIC and found that Perindopril and Bisoprolol were well-tolerated in the prevention of TIC and attenuated the decrease in LVEF, but trastuzumab-induced left ventricular remodeling was not reversed (73). In another randomized clinical trial, however, concomitant use of the angiotensin II receptor inhibitor Candesartan did not prevent a reduction in LVEF (74). In 2019, researchers evaluated the preventive effect of Lisinopril and Carvedilol on cardiotoxicity with or without anthracyclines prior to trastuzumab administration and found that both drugs were more protective in patients who had exposure to anthracyclines. Patients receiving pharmacological interventions were more likely to benefit compared to the placebo group [(75); **Table 2**].

Statins

A retrospective case control study found that in women with HER2+ breast cancer receiving trastuzumab-based therapy with or without anthracyclines, concomitant statin use was associated with a lower risk of cardiotoxicity (76). And a recent meta-analysis also showed that patients receiving statins during cancer treatment had a lower incidence of cardiotoxicity and were more likely to maintain LVEF during the follow-up period, suggesting that statins have the potential to mitigate the cardiotoxic effects of anthracyclines and trastuzumab (77). Rosuvastatin is a statin with anti-lipid peroxidation effects (78). Kabel et al. (79) found that rosuvastatin had a protective effect against TIC in mice due to the antioxidant and anti-inflammatory properties combined with its ability to induce STAT-3 expression and preserve the morphology of the cardiomyocytes. This study also demonstrated better results in combination with ubiquinone, the oxidized form of coenzyme Q10.

AMPK Agonist

AMPK (Adenosine 5'-monophosphate (AMP)-activated protein kinase) is considered to be a key regulatory kinase of myocardial energy metabolism (80). Recently, researchers identified mitochondrial dysfunction and altered cardiac energy metabolic pathways as important potential mechanisms of trastuzumab-induced cardiotoxicity (56). Susheel et al. (81) found that low-dose metformin improved mitochondrial function and provided significant myocardial protection against ischemic heart failure by activating AMPK and downstream signaling pathways involving eNOS and PGC-1. Wang et al. (82) observed a heterodimeric shift of AMPKα2 to AMPKα1 in the hearts of heart failure patients and mice with transverse artery constriction. They further found that overexpression of AMPKα2 prevented drug-induced chronic heart failure by increasing mitochondrial phagocytosis and improving mitochondrial function in isolated adult mouse cardiomyocytes. This is consistent with the finding that AMPK agonists (AICAR, metformin) improve trastuzumab-induced symptoms of cardiac insufficiency in IPSC-CMS (56). Although there are no relevant clinical studies to prove whether an AMPK agonist has the function of preventing trastuzumab cardiotoxicity, targeting cellular energy metabolism is a potential research direction. Additionally, it has been shown that activation of AMPK can inhibit the growth of breast cancer cells and increase the sensitivity of breast cancer as well as various other cancers, to chemotherapy and radiotherapy (83). Therefore, it is of great clinical interest to investigate whether AMPK agonists can be used to combat TIC.

TABLE 2 | Primary cardiac prevention studies in patients with breast cancer receiving trastuzumab.

References	Enrolled patients	Treatment	Cardiac prevention strategy	Results
Heck et al. (72)	130	Epirubicin ($n = 28$ with trastuzumab)	candesartan 32 mg, metoprolol 100 mg, placebo (2 x 2 design)	Absolute LVEF change: 2.6% in placebo, 0.8% in candesartan;
Pituskin et al. (73)	99	Trastuzumab ($n = 22$ with doxorubicin)	perindopril 8 mg, bisoprolol 10 mg, placebo (1:1:1)	LVEDVI not different among arms
Boekhout et al. (74)	206	Epirubicin with trastuzumab	candesartan 32 mg, placebo	LVEF decline: 19% in candesartan, 16% in placebo
Guglin et al. (75)	468	Trastuzumab ($n = 189$ with doxorubicin)	carvedilol 10 mg, lisinopril 10 mg, placebo	LVEF decline: 32% in placebo, 29% in carvedilol, 30% in lisinopril.

LVEDVI, left ventricular end-diastolic volume index.

TABLE 3 | Active ingredients of Chinese medicine against cytotoxic drug–induced cardiotoxicity through regulation of the PI3K/Akt signaling pathway.

Active ingredients of Chinese medicine (Ref.)	Experimental model	dose/route/time	Treatment	Findings
Ferulic acid Apigenin (85)	Wistar rats	100 mg/kg; p.o. for 7 days	Doxorubicin	↓NF-κB/PKC-δ ↓p53/p38/JNK ↑PI3K/ Akt/mTOR
	Cardiomyocytes	50 μM for 24 h		
Salvianolic acid B (86)	BALB/c mice	2 mg/kg; i.v., for 7 days	Doxorubicin arsenic trioxide	↑PI3K/Akt ↓ GSK3β/ER
	Cardiomyocytes	10 μM for 12 h		
Paeonol (87)	BALB/C Mice	50 mg/kg, for 6 days	Epirubicin	↓PI3K/Akt/mTOR ↓NF-κB
	H9c2 cells	50 mg/kg, for 6 days		
Rutin (88)	C57BL/6 mice	30 and 50 mg/kg; i.v. for 7 days	Pirarubicin	↑PI3K/Akt/mTOR ↓NF-κB
	H9c2 cells	10, 30, 50, and 70 μM for 1 h		
Astragalus polysaccharide (89)	C57BL/6 mice	1.5 g/kg; p.o. for 3 days	Doxorubicin	↑PI3K/Akt ↓p38 MAPK
	Rat Cardiac Myocytes	50 μg/ml for 1 h		
Calycosin (90)	Kunming mice	50 and 100 mg/kg; i.p. for 7 days	Doxorubicin	↑PI3K-Akt ↑Sirt1/NLRP3
	H9c2 cells	200 μM for 24h		
Total flavonoids from Clinopodium Chinense (91)	Male Sprague-Dawley (SD) rats	80 mg/kg, i.p. for 15 days	Doxorubicin	↑PI3K/Akt ↑Nrf2/HO-1
	H9c2 cells	6.25, 12.5, 25, and 50 μg/ml for 24 h		
Ginkgolide B (92)	C57BL/10 mice	100 mg/kg, i.p. for 5days	Doxorubicin	↑PI3K/Akt ↓p38 MAPK
	H9c2 cells	1, 5 and 50 μM for 30 min		
Saponins from leaves of Panax Quinquefolius (93)	ICR mice	125 and 250 mg/kg; p.o. for 15 days	Cisplatin	↓NF-κB ↑PI3K/Akt/GSK-3β
Neferine (94)	H9c2 cells	10 μM for 24 h	Doxorubicin	↑IGF-IR/PI3K/Akt

Potential Role of Traditional Chinese Medicine on TIC

There are many studies on the prevention and treatment of anthracycline-induced cardiotoxicity in Traditional Chinese Medicine (TCM), but reports regarding TIC are rare. The inhibition of the NRG1/HER pathway is one of the possible mechanisms of TIC. It has been suggested that activation of Akt may protect cardiac function by inhibiting apoptosis (84). Many active ingredients in Chinese medicine have been reported

to show protective effects against cardiac injury by interfering with the PI3K/Akt signaling pathway, as shown in **Table 3** (85–94). In addition, Zhang et al. (95) used network pharmacology analysis to find that Shenmai injection has multi-target and multi-pathway synergistic effects, which may exert myocardial protective effects through the PI3K-Akt signaling pathway and tumor microRNAs. The Shenmai injection treatment group improved cardiac structure and function, reduced myocardial pathological damage as well as the number of autophagic vesicles in mice compared with the control group. Targeting the inhibition of autophagy by trastuzumab, Liu et al. (96) investigated the protective mechanism of ginsenoside Rg2 against TIC in human cardiac myocytes (HCMs), and found that it could induce autophagy in HCMs by upregulating the expression levels of p-Akt, p-mTOR, Beclin 1, LC3, and ATG5, thus providing protection against TIC. At present, TCM is playing an increasing adjuvant role in the process of cancer treatment, while its role in the prevention and treatment of TIC has yet to be fully explored. Further in-depth studies are of great significance to ensure the safe use of trastuzumab as well as to promote the development of TCM in China.

SUMMARY AND PROSPECTS

Trastuzumab is a landmark agent in the treatment of HER2-positive breast cancer. It has changed the treatment paradigm for HER2-positive breast cancer patients and has no alternative to its status as a first-line drug for breast cancer. At the same time, its cardiotoxicity remains a major constraint to its use. The mechanism of trastuzumab cardiotoxicity has not been fully elucidated, and there is no specific drug to prevent it in clinical practice. Fewer studies have been conducted specifically on the cardiotoxicity of trastuzumab than on anthracyclines. Researchers should further clarify the mechanism of TIC, establish a reasonable model of myocardial injury, determine appropriate detection indicators, and conduct research on relevant cardioprotective agents in response to the mechanism in order to provide the possibility of safer use of trastuzumab. In addition, TCM has shown great potential in the prevention of antineoplastic drug-induced cardiotoxicity, and while few studies have been conducted specifically for trastuzumab, this provides a research direction for the prevention and treatment of TIC. There are several hurdles at the clinical study level given that studies evaluating patients treated with trastuzumab alone are lacking, strategies to prevent anthracycline-induced cardiotoxicity are not always applicable to trastuzumab, and the definition and evaluation metrics of cardiotoxicity have yet to be standardized. In clinical application, physicians as well as pharmacists should fully understand the risk factors and fully evaluate basic information such as age, previous cardiovascular history, medication history, and the physical condition of patients before drug administration. In addition, high-risk patients need to be monitored closely throughout the oncology treatment process. These efforts will maximize efficacy while minimizing adverse effects.

AUTHOR CONTRIBUTIONS

ML and WX assorted information and drafted the manuscript. SW polished the language. YL and CH offered advice about the structure. CL and GL governed the whole process and offered advice. All authors contributed to the article and approved the submitted version.

FUNDING

This work was supported by Beijing Hope Run Special Find of Cancer Foundation of China (LC2020L03) and Beijing Municipal Science and Technology Commission (Z181100001618003).

REFERENCES

1. Sung H, Ferlay J, Siegel RL, Laversanne M, Soerjomataram I, Jemal A, et al. Global cancer statistics 2020: GLOBOCAN estimates of incidence and mortality worldwide for 36 cancers in 185 countries. *CA Cancer J Clin.* (2021) 71:209-49. doi: 10.3322/caac.21660
2. Zhang L, Yu J. Role of apoptosis in colon cancer biology, therapy, and prevention. *Curr Colorectal Cancer Rep.* (2013) 9:331–40. doi: 10.1007/s11888-013-0188-z
3. Gonzalez-Angulo AM, Litton JK, Broglio KR, Meric-Bernstam F, Rakkhit R, Cardoso F, et al. High risk of recurrence for patients with breast cancer who have human epidermal growth factor receptor 2-positive, node-negative tumors 1 cm or smaller. *J Clin Oncol.* (2009) 27:5700-6. doi: 10.1200/JCO.2009.23.2025
4. Beser AR, Tuzlali S, Guzey D, Dolek Guler S, Hacihanefioglu S, Dalay N. HER-2, TOP2A and chromosome 17 alterations in breast cancer. *Pathol Oncol Res.* (2007) 13:180-5. doi: 10.1007/BF02893497
5. Witton CJ, Reeves JR, Going JJ, Cooke TG, Bartlett JM. Expression of the HER1-4 family of receptor tyrosine kinases in breast cancer. *J Pathol.* (2003) 200:290-7. doi: 10.1002/path.1370
6. Morrison G, Fu X, Shea M, Nanda S, Giuliano M, Wang T, et al. Therapeutic potential of the dual EGFR/HER2 inhibitor AZD8931 in circumventing endocrine resistance. *Breast Cancer Res Treat.* (2014) 144:263-72. doi: 10.1007/s10549-014-2878-x
7. Jiang Z, Zhou M. Neuregulin signaling and heart failure. *Curr Heart Fail Rep.* (2010) 7:42-7. doi: 10.1007/s11897-010-0003-y
8. Vermeulen Z, Segers VF, De Keulenaer GW. ErbB2 signaling at the crossing between heart failure and cancer. *Basic Res Cardiol.* (2016) 111:60. doi: 10.1007/s00395-016-0576-z
9. Spector NL, Blackwell KL. Understanding the mechanisms behind trastuzumab therapy for human epidermal growth factor receptor 2-positive breast cancer. *J Clin Oncol.* (2009) 27:5838-47. doi: 10.1200/JCO.2009.22.1507
10. Molina MA, Codony-Servat J, Albanell J, Rojo F, Arribas J, Baselga J. Trastuzumab (herceptin), a humanized anti-Her2 receptor monoclonal antibody, inhibits basal and activated Her2 ectodomain cleavage in breast cancer cells. *Cancer Res.* (2001) 61:4744-9.
11. Tsao LC, Crosby EJ, Trotter TN, Agarwal P, Hwang BJ, Acharya C, et al. CD47 blockade augmentation of trastuzumab antitumor efficacy dependent on antibody-dependent cellular phagocytosis. *JCI Insight.* (2019) 4:e131882. doi: 10.1172/jci.insight.131882
12. Hudziak RM, Lewis GD, Winget M, Fendly BM, Shepard HM, Ullrich A. p185HER2 monoclonal antibody has antiproliferative effects in vitro and sensitizes human breast tumor cells to tumor necrosis factor. *Mol Cell Biol.* (1989) 9:1165-72. doi: 10.1128/mcb.9.3.1165-1172.1989

13. Carter P, Presta L, Gorman CM, Ridgway JB, Henner D, Wong WL, et al. Humanization of an anti-p185HER2 antibody for human cancer therapy. *Proc Natl Acad Sci USA*. (1992) 89:4285-9. doi: 10.1073/pnas.89.10.4285
14. Slamon DJ, Leyland-Jones B, Shak S, Fuchs H, Paton V, Bajamonde A, et al. Use of chemotherapy plus a monoclonal antibody against HER2 for metastatic breast cancer that overexpresses HER2. *N Engl J Med.* (2001) 344:783-92. doi: 10.1056/NEJM200103153441101
15. Halyard MY, Pisansky TM, Dueck AC, Suman V, Pierce L, Solin L, et al. Radiotherapy and adjuvant trastuzumab in operable breast cancer: tolerability and adverse event data from the NCCTG Phase III Trial N9831. *J Clin Oncol.* (2009) 27:2638-44. doi: 10.1200/JCO.2008.17.9549
16. Cameron D, Piccart-Gebhart MJ, Gelber RD, Procter M, Goldhirsch A, de Azambuja E, et al. 11 years' follow-up of trastuzumab after adjuvant chemotherapy in HER2-positive early breast cancer: final analysis of the HERceptin Adjuvant (HERA) trial. *Lancet.* (2017) 389:1195-205. doi: 10.1016/S0140-6736(16)32616-2
17. Slamon D, Eiermann W, Robert N, Pienkowski T, Martin M, Press M, et al. Adjuvant trastuzumab in HER2-positive breast cancer. *N Engl J Med.* (2011) 365:1273-83. doi: 10.1056/NEJMoa0910383
18. Perez EA, Romond EH, Suman VJ, Jeong JH, Sledge G, Geyer CE, Jr., et al. Trastuzumab plus adjuvant chemotherapy for human epidermal growth factor receptor 2-positive breast cancer: planned joint analysis of overall survival from NSABP B-31 and NCCTG N9831. *J Clin Oncol.* (2014) 32:3744-52. doi: 10.1200/JCO.2014.55.5730
19. Gradishar WJ, Anderson BO, Abraham J, Aft R, Agnese D, Allison KH, et al. Breast cancer, Version 3.2020, NCCN Clinical Practice Guidelines in Oncology. *J Natl Compr Canc Netw.* (2020) 18:452-78. doi: 10.6004/jnccn.2020.0016
20. Chen J, Long JB, Hurria A, Owusu C, Steingart RM, Gross CP. Incidence of heart failure or cardiomyopathy after adjuvant trastuzumab therapy for breast cancer. *J Am Coll Cardiol.* (2012) 60:2504-12. doi: 10.1016/j.jacc.2012.07.068
21. Zamorano JL, Lancellotti P, Munoz DR, Aboyans V, Asteggiano R, Galderisi M, et al. [2016 ESC position paper on cancer treatments and cardiovascular toxicity developed under the auspices of the ESC Committee for Practice Guidelines]. *Kardiol Pol.* (2016) 74:1193-233. doi: 10.5603/KP.2016.0156
22. Seidman A, Hudis C, Pierri MK, Shak S, Paton V, Ashby M, et al. Cardiac dysfunction in the trastuzumab clinical trials experience. *J Clin Oncol.* (2002) 20:1215-21. doi: 10.1200/JCO.2002.20.5.1215
23. Jordan JH, Todd RM, Vasu S, Hundley WG. Cardiovascular magnetic resonance in the oncology patient. *JACC Cardiovasc Imaging.* (2018) 11:1150-72. doi: 10.1016/j.jcmg.2018.06.004
24. Demissei BG, Finkelman BS, Hubbard RA, Smith AM, Narayan HK, Narayan V, et al. Cardiovascular function phenotypes in response to cardiotoxic breast cancer therapy. *J Am Coll Cardiol.* (2019) 73:248-9. doi: 10.1016/j.jacc.2018.10.057
25. Karaca M, Kocoglu H, Bilgetekin I, Ozet A, Sahinli H, Demir H, et al. Ventricular bigeminal rhythm associated with trastuzumab: a potential cardiac side effect. *J Cancer Res Ther.* (2018) 14:S536-7. doi: 10.4103/0973-1482.183557
26. Kirkham AA, Pituskin E, Thompson RB, Mackey JR, Koshman SL, Jassal D, et al. Cardiac and cardiometabolic phenotyping of trastuzumab-mediated cardiotoxicity: a secondary analysis of the MANTICORE trial. *Eur Heart J Cardiovasc Pharmacother.* (2021). doi: 10.1093/ehjcvp/pvab016. [Epub ahead of print].
27. Advani PP, Ballman KV, Dockter TJ, Colon-Otero G, Perez EA. Long-term cardiac safety analysis of NCCTG N9831 (Alliance) Adjuvant Trastuzumab Trial. *J Clin Oncol.* (2016) 34:581-7. doi: 10.1200/JCO.2015.61.8413
28. Romond EH, Jeong JH, Rastogi P, Swain SM, Geyer CE, Jr., Ewer MS, et al. Seven-year follow-up assessment of cardiac function in NSABP B-31, a randomized trial comparing doxorubicin and cyclophosphamide followed by paclitaxel (ACP) with ACP plus trastuzumab as adjuvant therapy for patients with node-positive, human epidermal growth factor receptor 2-positive breast cancer. *J Clin Oncol.* (2012) 30:3792-9. doi: 10.1200/JCO.2011.40.0010
29. de Azambuja E, Procter MJ, van Veldhuisen DJ, Agbor-Tarh D, Metzger-Filho O, Steinseifer J, et al. Trastuzumab-associated cardiac events at 8 years of median follow-up in the Herceptin Adjuvant trial (BIG 1-01). *J Clin Oncol.* (2014) 32:2159-65. doi: 10.1200/JCO.2013.53.9288
30. Pivot X, Romieu G, Debled M, Pierga JY, Kerbrat P, Bachelot T, et al. 6 months versus 12 months of adjuvant trastuzumab for patients with HER2-positive early breast cancer (PHARE): a randomised phase 3 trial. *Lancet Oncol.* (2013) 14:741-8. doi: 10.1016/S1470-2045(13)70225-0
31. Lidbrink E, Chmielowska E, Otremba B, Bouhlel A, Lauer S, Liste Hermoso M, et al. A real-world study of cardiac events in > 3700 patients with HER2-positive early breast cancer treated with trastuzumab: final analysis of the OHERA study. *Breast Cancer Res Treat.* (2019) 174:187-96. doi: 10.1007/s10549-018-5058-6
32. Naumann D, Rusius V, Margiotta C, Nevill A, Carmichael A, Rea D, et al. Factors predicting trastuzumab-related cardiotoxicity in a real-world population of women with HER2+ breast cancer. *Anticancer Res.* (2013) 33:1717-20.
33. Leung HW, Chan AL. Trastuzumab-induced cardiotoxicity in elderly women with HER-2-positive breast cancer: a meta-analysis of real-world data. *Expert Opin Drug Saf.* (2015) 14:1661-71. doi: 10.1517/14740338.2015.1089231
34. Anjos M, Fontes-Oliveira M, Costa VM, Santos M, Ferreira R. An update of the molecular mechanisms underlying doxorubicin plus trastuzumab induced cardiotoxicity. *Life Sci.* (2021) 280:119760. doi: 10.1016/j.lfs.2021.119760
35. Koulaouzidis G, Yung AE, Yung DE, Skonieczna-Zydecka K, Marlicz W, Koulaouzidis A, et al. Conventional cardiac risk factors associated with trastuzumab-induced cardiotoxicity in breast cancer: systematic review and meta-analysis. *Curr Probl Cancer.* (2021) 2021:100723. doi: 10.1016/j.currproblcancer.2021.100723
36. Guenancia C, Lefebvre A, Cardinale D, Yu AF, La Ladoire S, Ghiringhelli F, et al. Obesity as a risk factor for anthracyclines and trastuzumab cardiotoxicity in breast cancer: a systematic review and meta-analysis. *J Clin Oncol.* (2016) 34:3157-65. doi: 10.1200/JCO.2016.67.4846
37. Wu Q, Bai B, Tian C, Li D, Yu H, Song B, et al. The molecular mechanisms of cardiotoxicity induced by HER2, VEGF, and tyrosine kinase inhibitors: an updated review. *Cardiovasc Drugs Ther.* (2021). doi: 10.1007/s10557-021-07181-3. [Epub ahead of print].
38. Rupert CE, Coulombe KL. The roles of neuregulin-1 in cardiac development, homeostasis, and disease. *Biomark Insights.* (2015) 10(Suppl 1):1-9. doi: 10.4137/BMI.S20061
39. Lemmens K, Doggen K, De Keulenaer GW. Role of neuregulin-1/ErbB signaling in cardiovascular physiology and disease: implications for therapy of heart failure. *Circulation.* (2007) 116:954-60. doi: 10.1161/CIRCULATIONAHA.107.690487
40. Geissler A, Ryzhov S, Sawyer DB. Neuregulins: protective and reparative growth factors in multiple forms of cardiovascular disease. *Clin Sci.* (2020) 134:2623-43. doi: 10.1042/CS20200230
41. Gordon LI, Burke MA, Singh AT, Prachand S, Lieberman ED, Sun L, et al. Blockade of the erbB2 receptor induces cardiomyocyte death through mitochondrial and reactive oxygen species-dependent pathways. *J Biol Chem.* (2009) 284:2080-7. doi: 10.1074/jbc.M804570200
42. Ravingerova T, Matejikova J, Neckar J, Andelova E, Kolar F. Differential role of PI3K/Akt pathway in the infarct size limitation and antiarrhythmic protection in the rat heart. *Mol Cell Biochem.* (2007) 297:111-20. doi: 10.1007/s11010-006-9335-z
43. Rochette L, Guenancia C, Gudjoncik A, Hachet O, Zeller M, Cottin Y, et al. Anthracyclines/trastuzumab: new aspects of cardiotoxicity and molecular mechanisms. *Trends Pharmacol Sci.* (2015) 36:326-48. doi: 10.1016/j.tips.2015.03.005
44. Yang S, Liu G. Targeting the Ras/Raf/MEK/ERK pathway in hepatocellular carcinoma. *Oncol Lett.* (2017) 13:1041-7. doi: 10.3892/ol.2017.5557
45. Liu F, Yang X, Geng M, Huang M. Targeting ERK, an Achilles' Heel of the MAPK pathway, in cancer therapy. *Acta Pharm Sin B.* (2018) 8:552-62. doi: 10.1016/j.apsb.2018.01.008
46. Hedhli N, Huang Q, Kalinowski A, Palmeri M, Hu X, Russell RR, et al. Endothelium-derived neuregulin protects the heart against ischemic injury. *Circulation.* (2011) 123:2254-62. doi: 10.1161/CIRCULATIONAHA.110.991125
47. Liu FF, Stone JR, Schuldt AJ, Okoshi K, Okoshi MP, Nakayama M, et al. Heterozygous knockout of neuregulin-1 gene in mice exacerbates doxorubicin-induced heart failure. *Am J Physiol Heart Circ Physiol.* (2005) 289:H660-6. doi: 10.1152/ajpheart.00268.2005

48. Filomeni G, De Zio D, Cecconi F. Oxidative stress and autophagy: the clash between damage and metabolic needs. *Cell Death Differ.* (2015) 22:377-88. doi: 10.1038/cdd.2014.150
49. Thomas RL, Roberts DJ, Kubli DA, Lee Y, Quinsay MN, Owens JB, et al. Loss of MCL-1 leads to impaired autophagy and rapid development of heart failure. *Genes Dev.* (2013) 27:1365-77. doi: 10.1101/gad.215871.113
50. Mohan N, Shen Y, Endo Y, ElZarrad MK, Wu WJ. Trastuzumab, but Not pertuzumab, dysregulates HER2 signaling to mediate inhibition of autophagy and increase in reactive oxygen species production in human cardiomyocytes. *Mol Cancer Ther.* (2016) 15:1321-31. doi: 10.1158/1535-7163.MCT-15-0741
51. Lu L, Wu W, Yan J, Li X, Yu H, Yu X. Adriamycin-induced autophagic cardiomyocyte death plays a pathogenic role in a rat model of heart failure. *Int J Cardiol.* (2009) 134:82-90. doi: 10.1016/j.ijcard.2008.01.043
52. Dirks-Naylor AJ. The role of autophagy in doxorubicin-induced cardiotoxicity. *Life Sci.* (2013) 93:913-6. doi: 10.1016/j.lfs.2013.10.013
53. Doenst T, Nguyen TD, Abel ED. Cardiac metabolism in heart failure: implications beyond ATP production. *Circ Res.* (2013) 113:709-24. doi: 10.1161/CIRCRESAHA.113.300376
54. Necela BM, Axenfeld BC, Serie DJ, Kachergus JM, Perez EA, Thompson EA, et al. The antineoplastic drug, trastuzumab, dysregulates metabolism in iPSC-derived cardiomyocytes. *Clin Transl Med.* (2017) 6:5. doi: 10.1186/s40169-016-0133-2
55. Ito T, Kimura Y, Uozumi Y, Takai M, Muraoka S, Matsuda T, et al. Taurine depletion caused by knocking out the taurine transporter gene leads to cardiomyopathy with cardiac atrophy. *J Mol Cell Cardiol.* (2008) 44:927-37. doi: 10.1016/j.yjmcc.2008.03.001
56. Kitani T, Ong SG, Lam CK, Rhee JW, Zhang JZ, Oikonomopoulos A, et al. Human-induced pluripotent stem cell model of trastuzumab-induced cardiac dysfunction in patients with breast cancer. *Circulation.* (2019) 139:2451-65. doi: 10.1161/CIRCULATIONAHA.118.037357
57. Bergamini C, Torelli F, Ghiselli L, Rossi A, Trevisani L, Vinco G, et al. Left ventricular end-diastolic volume as early indicator of trastuzumab-related cardiotoxicity in HER2+ breast cancer patients: results from a single-center retrospective study. *Minerva Cardioangiol.* (2017) 65:278-87. doi: 10.23736/S0026-4725.16.04278-X
58. Negishi K, Negishi T, Hare JL, Haluska BA, Plana JC, Marwick TH. Independent and incremental value of deformation indices for prediction of trastuzumab-induced cardiotoxicity. *J Am Soc Echocardiogr.* (2013) 26:493-8. doi: 10.1016/j.echo.2013.02.008
59. Thavendiranathan P, Negishi T, Somerset E, Negishi K, Penicka M, Lemieux J, et al. Strain-guided management of potentially cardiotoxic cancer therapy. *J Am Coll Cardiol.* (2021) 77:392-401. doi: 10.1016/j.jacc.2020.11.020
60. Zamorano JL, Lancellotti P, Rodriguez Munoz D, Aboyans V, Asteggiano R, Galderisi M, et al. 2016 ESC Position Paper on cancer treatments and cardiovascular toxicity developed under the auspices of the ESC Committee for Practice Guidelines: the Task Force for cancer treatments and cardiovascular toxicity of the European Society of Cardiology (ESC). *Eur J Heart Fail.* (2017) 19:9-42. doi: 10.1093/eurheartj/ehw211
61. Aimo A, Januzzi JL, Jr., Bayes-Genis A, Vergaro G, Sciarrone P, Passino C, et al. Clinical and prognostic significance of sST2 in heart failure: JACC review topic of the week. *J Am Coll Cardiol.* (2019) 74:2193-203. doi: 10.1016/j.jacc.2019.08.1039
62. Zhang S, Wang Y, Wang Y, Peng J, Yuan C, Zhou L, et al. Serum miR-222-3p as a double-edged sword in predicting efficacy and trastuzumab-induced cardiotoxicity for HER2-positive breast cancer patients receiving neoadjuvant target therapy. *Front Oncol.* (2020) 10:631. doi: 10.3389/fonc.2020.00631
63. van der Voort A, van Ramshorst MS, van Werkhoven ED, Mandjes IA, Kemper I, Vulink AJ, et al. Three-year follow-up of neoadjuvant chemotherapy with or without anthracyclines in the presence of dual ERBB2 blockade in patients with ERBB2-positive breast cancer: a secondary analysis of the TRAIN-2 randomized, phase 3 trial. *JAMA Oncol.* (2021) 7:978-84. doi: 10.1001/jamaoncol.2021.1371
64. Agus DB, Gordon MS, Taylor C, Natale RB, Karlan B, Mendelson DS, et al. Phase I clinical study of pertuzumab, a novel HER dimerization inhibitor, in patients with advanced cancer. *J Clin Oncol.* (2005) 23:2534-43. doi: 10.1200/JCO.2005.03.184
65. Capelan M, Pugliano L, De Azambuja E, Bozovic I, Saini KS, Sotiriou C, et al. Pertuzumab: new hope for patients with HER2-positive breast cancer. *Ann Oncol.* (2013) 24:273-82. doi: 10.1093/annonc/mds328
66. Gianni L, Pienkowski T, Im YH, Roman L, Tseng LM, Liu MC, et al. Efficacy and safety of neoadjuvant pertuzumab and trastuzumab in women with locally advanced, inflammatory, or early HER2-positive breast cancer (NeoSphere): a randomised multicentre, open-label, phase 2 trial. *Lancet Oncol.* (2012) 13:25-32. doi: 10.1016/S1470-2045(11)70336-9
67. Schneeweiss A, Chia S, Hickish T, Harvey V, Eniu A, Hegg R, et al. Pertuzumab plus trastuzumab in combination with standard neoadjuvant anthracycline-containing and anthracycline-free chemotherapy regimens in patients with HER2-positive early breast cancer: a randomized phase II cardiac safety study (TRYPHAENA). *Ann Oncol.* (2013) 24:2278-84. doi: 10.1093/annonc/mdt182
68. Shao Z, Pang D, Yang H, Li W, Wang S, Cui S, et al. Efficacy, safety, and tolerability of pertuzumab, trastuzumab, and docetaxel for patients with early or locally advanced ERBB2-positive breast cancer in Asia: the PEONY phase 3 randomized clinical trial. *JAMA Oncol.* (2020) 6:e193692. doi: 10.1001/jamaoncol.2019.3692
69. Curigliano G, Lenihan D, Fradley M, Ganatra S, Barac A, Blaes A, et al. Management of cardiac disease in cancer patients throughout oncological treatment: ESMO consensus recommendations. *Ann Oncol.* (2020) 31:171-90. doi: 10.1016/j.annonc.2019.10.023
70. Dang CT, Yu AF, Jones LW, Liu J, Steingart RM, Argolo DF, et al. Cardiac surveillance guidelines for trastuzumab-containing therapy in early-stage breast cancer: getting to the heart of the matter. *J Clin Oncol.* (2016) 34:1030-3. doi: 10.1200/JCO.2015.64.5515
71. Bosch X, Rovira M, Sitges M, Domenech A, Ortiz-Perez JT, de Caralt TM, et al. Enalapril and carvedilol for preventing chemotherapy-induced left ventricular systolic dysfunction in patients with malignant hemopathies: the OVERCOME trial (preventiOn of left Ventricular dysfunction with Enalapril and caRvedilol in patients submitted to intensive ChemOtherapy for the treatment of Malignant hEmopathies). *J Am Coll Cardiol.* (2013) 61:2355-62. doi: 10.1016/j.jacc.2013.02.072
72. Heck SL, Mecinaj A, Ree AH, Hoffmann P, Schulz-Menger J, Fagerland MW, et al. Prevention of cardiac dysfunction during adjuvant breast cancer therapy (PRADA): extended follow-up of a 2x2 factorial, randomized, placebo-controlled, double-blind clinical trial of candesartan and metoprolol. *Circulation.* (2021) 143:2431-40. doi: 10.1161/CIRCULATIONAHA.121.054698
73. Pituskin E, Mackey JR, Koshman S, Jassal D, Pitz M, Haykowsky MJ, et al. Multidisciplinary approach to novel therapies in cardio-oncology Research (MANTICORE 101-Breast): a randomized trial for the prevention of trastuzumab-associated cardiotoxicity. *J Clin Oncol.* (2017) 35:870-7. doi: 10.1200/JCO.2016.68.7830
74. Boekhout AH, Gietema JA, Milojkovic Kerklaan B, van Werkhoven ED, Altena R, Honkoop A, et al. Angiotensin II-receptor inhibition with candesartan to prevent trastuzumab-related cardiotoxic effects in patients with early breast cancer: a randomized clinical trial. *JAMA Oncol.* (2016) 2:1030-7. doi: 10.1001/jamaoncol.2016.1726
75. Guglin M, Krischer J, Tamura R, Fink A, Bello-Matricaria L, McCaskill-Stevens W, et al. Randomized trial of lisinopril versus carvedilol to prevent trastuzumab cardiotoxicity in patients with breast cancer. *J Am Coll Cardiol.* (2019) 73:2859-68. doi: 10.1016/j.jacc.2019.03.495
76. Calvillo-Arguelles O, Abdel-Qadir H, Michalowska M, Billia F, Suntheralingam S, Amir E, et al. Cardioprotective effect of statins in patients with HER2-positive breast cancer receiving trastuzumab therapy. *Can J Cardiol.* (2019) 35:153-9. doi: 10.1016/j.cjca.2018.11.028
77. Obasi M, Abovich A, Vo JB, Gao Y, Papatheodorou SI, Nohria A, et al. Correction to: statins to mitigate cardiotoxicity in cancer patients treated with anthracyclines and/or trastuzumab: a systematic review and metaanalysis. *Cancer Causes Control.* (2021) 32:1407-9. doi: 10.1007/s10552-021-01495-1
78. Moon GJ, Kim SJ, Cho YH, Ryoo S, Bang OY. Antioxidant effects of statins in patients with atherosclerotic cerebrovascular disease. *J Clin Neurol.* (2014) 10:140-7. doi: 10.3988/jcn.2014.10.2.140
79. Kabel AM, Elkhoely AA. Targeting proinflammatory cytokines, oxidative stress, TGF-beta1 and STAT-3 by rosuvastatin and ubiquinone to ameliorate trastuzumab cardiotoxicity. *Biomed Pharmacother.* (2017) 93:17-26. doi: 10.1016/j.biopha.2017.06.033

80. Kim TT, Dyck JR. Is AMPK the savior of the failing heart? *Trends Endocrinol Metab.* (2015) 26:40-8. doi: 10.1016/j.tem.2014.11.001
81. Gundewar S, Calvert JW, Jha S, Toedt-Pingel I, Ji SY, Nunez D, et al. Activation of AMP-activated protein kinase by metformin improves left ventricular function and survival in heart failure. *Circ Res.* (2009) 104:403-11. doi: 10.1161/CIRCRESAHA.108.190918
82. Wang B, Nie J, Wu L, Hu Y, Wen Z, Dong L, et al. AMPKalpha2 protects against the development of heart failure by enhancing mitophagy *via* PINK1 phosphorylation. *Circ Res.* (2018) 122:712-29. doi: 10.1161/CIRCRESAHA.117.312317
83. Carling D. AMPK signalling in health and disease. *Curr Opin Cell Biol.* (2017) 45:31-7. doi: 10.1016/j.ceb.2017.01.005
84. Chaanine AH, Hajjar RJ. AKT signalling in the failing heart. *Eur J Heart Fail.* (2011) 13:825-9. doi: 10.1093/eurjhf/hfr080
85. Sahu R, Dua TK, Das S, De Feo V, Dewanjee S. Wheat phenolics suppress doxorubicin-induced cardiotoxicity *via* inhibition of oxidative stress, MAP kinase activation, NF-kappaB pathway, PI3K/Akt/mTOR impairment, and cardiac apoptosis. *Food Chem Toxicol.* (2019) 125:503-19. doi: 10.1016/j.fct.2019.01.034
86. Chen R, Sun G, Yang L, Wang J, Sun X. Salvianolic acid B protects against doxorubicin induced cardiac dysfunction via inhibition of ER stress mediated cardiomyocyte apoptosis. *Toxicol Res.* (2016) 5:1335-45. doi: 10.1039/C6TX00111D
87. Wu J, Sun C, Wang R, Li J, Zhou M, Yan M, et al. Cardioprotective effect of paeonol against epirubicin-induced heart injury via regulating miR-1 and PI3K/AKT pathway. *Chem Biol Interact.* (2018) 286:17-25. doi: 10.1016/j.cbi.2018.02.035
88. Fei J, Sun Y, Duan Y, Xia J, Yu S, Ouyang P, et al. Low concentration of rutin treatment might alleviate the cardiotoxicity effect of pirarubicin on cardiomyocytes *via* activation of PI3K/AKT/mTOR signaling pathway. *Biosci Rep.* (2019) 39:BSR20190546. doi: 10.1042/BSR20190546
89. Cao Y, Ruan Y, Shen T, Huang X, Li M, Yu W, et al. Astragalus polysaccharide suppresses doxorubicin-induced cardiotoxicity by regulating the PI3k/Akt and p38MAPK pathways. *Oxid Med Cell Longev.* (2014) 2014:674219. doi: 10.1155/2014/674219
90. Zhai J, Tao L, Zhang S, Gao H, Zhang Y, Sun J, et al. Calycosin ameliorates doxorubicin-induced cardiotoxicity by suppressing oxidative stress and inflammation via the sirtuin 1-NOD-like receptor protein 3 pathway. *Phytother Res.* (2020) 34:649-59. doi: 10.1002/ptr.6557
91. Zhang HJ, Chen RC, Sun GB, Yang LP, Zhu YD, Xu XD, et al. Protective effects of total flavonoids from Clinopodium chinense (Benth.) O. Ktze on myocardial injury *in vivo* and *in vitro via* regulation of Akt/Nrf2/HO-1 pathway. *Phytomedicine.* (2018) 40:88-97. doi: 10.1016/j.phymed.2018.01.004
92. Gao J, Chen T, Zhao D, Zheng J, Liu Z. Ginkgolide B Exerts cardioprotective properties against doxorubicin-induced cardiotoxicity by regulating reactive oxygen species, Akt and calcium signaling pathways *in vitro* and *in vivo*. *PLoS ONE.* (2016) 11:e0168219. doi: 10.1371/journal.pone.0168219
93. Xing JJ, Hou JG, Liu Y, Zhang RB, Jiang S, Ren S, et al. Supplementation of Saponins from Leaves of Panax quinquefolius mitigates Cisplatin-evoked cardiotoxicity *via* inhibiting oxidative stress-associated inflammation and apoptosis in mice. *Antioxidants.* (2019) 8:347. doi: 10.3390/antiox8090347
94. Bharathi Priya L, Baskaran R, Huang CY, Vijaya Padma V. Neferine modulates IGF-1R/Nrf2 signaling in doxorubicin treated H9c2 cardiomyoblasts. *J Cell Biochem.* (2018) 119:1441-52. doi: 10.1002/jcb.26305
95. Zhang X, Lv S, Zhang W, Jia Q, Wang L, Ding Y, et al. Shenmai injection improves doxorubicin cardiotoxicity *via* miR-30a/Beclin 1. *Biomed Pharmacother.* (2021) 139:111582. doi: 10.1016/j.biopha.2021.111582
96. Liu G, Qi X, Li X, Sun F. Ginsenoside Rg2 protects cardiomyocytes against trastuzumab-induced toxicity by inducing autophagy. *Exp Ther Med.* (2021) 21:473. doi: 10.3892/etm.2021.9904

Conflict of Interest: The authors declare that the research was conducted in the absence of any commercial or financial relationships that could be construed as a potential conflict of interest.

Publisher's Note: All claims expressed in this article are solely those of the authors and do not necessarily represent those of their affiliated organizations, or those of the publisher, the editors and the reviewers. Any product that may be evaluated in this article, or claim that may be made by its manufacturer, is not guaranteed or endorsed by the publisher.

frontiers in Cardiovascular Medicine

ORIGINAL RESEARCH
published: 21 January 2022
doi: 10.3389/fcvm.2021.807754

D-Dimer Is a Predictive Factor of Cancer Therapeutics-Related Cardiac Dysfunction in Patients Treated With Cardiotoxic Chemotherapy

Masayoshi Oikawa, Daiki Yaegashi, Tetsuro Yokokawa, Tomofumi Misaka, Takamasa Sato, Takashi Kaneshiro, Atsushi Kobayashi, Akiomi Yoshihisa, Kazuhiko Nakazato, Takafumi Ishida and Yasuchika Takeishi*

Department of Cardiovascular Medicine, Fukushima Medical University, Fukushima, Japan

OPEN ACCESS

Edited by:
Dong Han,
People's Liberation Army General Hospital, China

Reviewed by:
Nicola Maurea,
G. Pascale National Cancer Institute Foundation (IRCCS), Italy
Steven Philip Grover,
University of North Carolina at Chapel Hill, United States

***Correspondence:**
Masayoshi Oikawa
moikawa@fmu.ac.jp

Specialty section:
This article was submitted to Cardio-Oncology, a section of the journal Frontiers in Cardiovascular Medicine

Received: *02 November 2021*
Accepted: *16 December 2021*
Published: *21 January 2022*

Citation:
Oikawa M, Yaegashi D, Yokokawa T, Misaka T, Sato T, Kaneshiro T, Kobayashi A, Yoshihisa A, Nakazato K, Ishida T and Takeishi Y (2022) D-Dimer Is a Predictive Factor of Cancer Therapeutics-Related Cardiac Dysfunction in Patients Treated With Cardiotoxic Chemotherapy. Front. Cardiovasc. Med. 8:807754. doi: 10.3389/fcvm.2021.807754

Background: D-dimer is a sensitive biomarker for cancer-associated thrombosis, but little is known about its significance on cancer therapeutics-related cardiac dysfunction (CTRCD).

Methods: Consecutive 169 patients planned for cardiotoxic chemotherapy were enrolled and followed up for 12 months. All patients underwent echocardiography and blood test at baseline and at 3-, 6-, and 12 months.

Results: The patients were divided into two groups based on the level of D-dimer (>1.65 μg/ml or ≦ 1.65 μg/ml) at baseline before chemotherapy: high D-dimer group (n = 37) and low D-dimer group (n = 132). Left ventricular ejection fraction (LVEF) decreased at 3- and 6 months after chemotherapy in high D-dimer group [baseline, 65.2% (62.8–71.4%); 3 months, 62.9% (59.0–67.7%); 6 months, 63.1% (60.0–67.1%); 12 months, 63.3% (58.8–66.0%), $p = 0.03$], but no change was observed in low D-dimer group. The occurrence of CTRCD within the 12-month follow-up period was higher in the high D-dimer group than in the low D-dimer group (16.2 vs. 4.5%, $p = 0.0146$). Multivariable logistic regression analysis revealed that high D-dimer level at baseline was an independent predictor of the development of CTRCD [odds ratio 3.93, 95% CI (1.00–15.82), $p = 0.047$].

Conclusion: We should pay more attention to elevated D-dimer levels not only as a sign of cancer-associated thrombosis but also the future occurrence of CTRCD.

Keywords: cardio-oncology, D-dimer, cancer therapeutics-related cardiac dysfunction, heart failure, troponin I

INTRODUCTION

Recent advances in the diagnosis and treatment of cancers improve its prognosis. However, anticancer drugs, namely, anthracyclines, monoclonal antibodies, tyrosine kinase inhibitors, etc., induce cardiac dysfunction, resulting in poor prognosis in cancer survivors (1). Several cardiac biomarkers and echocardiographic parameters, such as troponins, myeloperoxidase,

interleukin-1β (IL-1β), Nucleotide-binding domain-like receptor family pyrin domain containing 3, and reduced global longitudinal strain, are proposed to detect the early phase of cancer therapeutics-related cardiac dysfunction (CTRCD) and prompt cardioprotective treatment can improve cardiac function (2–7). Although those parameters are useful, careful monitoring is required for all patients to detect early signs of CTRCD. Thus, a novel biomarker that identifies high-risk patients before chemotherapy is desirable to perform effective clinical monitoring.

D-dimer is a sensitive biomarker for cancer-associated thrombosis, but accumulating evidence suggests that pretreatment D-dimer can be used as a prognostic biomarker for patients with solid tumors (8). In cardiovascular fields, elevated D-dimer is associated with not only thromboembolic events but also heart failure mortality in heart failure patients with reduced and preserved ejection fraction (EF) (9, 10).

Although D-dimer is a promising biomarker in the cardio-oncology field, little is known about the relationship between D-dimer and CTRCD. The present study aimed to evaluate the predictive impact of D-dimer before chemotherapy on the development of CTRCD.

METHODS

Study Subjects and Protocol

We enrolled 202 consecutive cancer patients, planned for cardiotoxic chemotherapy, such as anthracyclines, human epidermal growth factor receptor 2 (HER2) inhibitors, tyrosine kinase inhibitors, and proteasome inhibitors, at Fukushima Medical University hospital from November 2016 to March 2019 (**Figure 1**). Patients were excluded if they died or were transferred to other hospitals within 12 months follow-up period ($n = 33$). The remaining 169 patients were divided into two groups based on the cut-off value of D-dimer, which was defined by the receiver operator characteristic curve analysis to detect the occurrence of CTRCD (**Figure 2**).

Hypertension was defined as a history of use of an antihypertensive drug or systolic blood pressure of ≥140 mmHg and/or diastolic blood pressure ≥90 mmHg. Diabetes was defined as recent use of insulin treatment or hypoglycemic drug or hemoglobin A1c ≥6.5%. Dyslipidemia was defined as a history of use of cholesterol-lowering drugs, or triglyceride was ≥150 mg/dl, low-density lipoprotein cholesterol was ≥140 mg/dl, and/or high-density lipoprotein cholesterol was ≤40 mg/dl. A cumulative dose of anthracycline was expressed as a doxorubicin equivalent (1). HER2 inhibitors included trastuzumab and pertuzumab. Tyrosine kinase inhibitors included dabrafenib, trametinib, lenvatinib, sorafenib, dasatinib, bevacizumab, and pazopanib. Proteasome inhibitors included carfilzomib and bortezomib. Radiation therapy was defined as irradiation to the mediastinum and/or the heart field within the follow-up period. Transthoracic echocardiography and blood sampling test were performed at baseline as well as at 3, 6, and 12 months after the administration of cardiotoxic chemotherapy. All procedures used in this research were approved by the Ethical Committee of Fukushima Medical University.

Echocardiography

Transthoracic echocardiography was performed by a trained sonographer, and images were checked by another trained sonographer and an echo-cardiologist. We measured cardiac function using EPIQ 7G (Philips Healthtech, Best, The Netherlands). Left ventricular (LV) EF was calculated using the modified Simpson's method according to the guideline from the American Society of Echocardiography and the European Association of Cardiovascular Imaging (11). The LV mass was calculated using the following formula:

$$\textit{Left ventricular (LV) mass} = 0.8 \times \left[1.04 \times \left\{ \left(\begin{array}{l} \textit{LV diastolic diameter} + \\ \textit{interventricular septum wall} \\ \textit{thicness} + \textit{LV posterior wall thicness} \end{array} \right)^3 - (\textit{LV diastolic diameter})^3 \right\} \right] + 0.6\,\text{g (11)}.$$

Cancer therapeutics-related cardiac dysfunction was defined as a decrease in EF by more than 10% points, to a value <53% (12). The LV end-diastolic volume index, LV end-systolic volume index, LV mass index, and left atrial volume index were measured using the B-mode ultrasound.

Blood Sampling

High sensitivity cardiac troponin I (TnI) was measured using an assay based on Luminescent Oxygen Channeling Immunoassay technology and run on a Dimension EXL Integrated Chemistry System (Siemens Healthcare Diagnostics, Deerfield, IL, USA). B-type natriuretic peptide (BNP) levels were measured using a specific immunoradiometric assay (Shionoria BNP kit, Shionogi, Osaka, Japan). D-dimer was measured using a latex agglutination method (Lias Auto D-dimer Neo, Sysmex, Kobe, Japan).

Statistical Analysis

All statistical analyses were performed using Prism 9 (GraphPad Software, San Diego, CA, USA) or R software packages version 3.6.3 (R core team 2020, Vienna, Austria). We used the Shapiro-Wilk test to discriminate which variables were normally or not normally distributed. Normally distributed variables were shown as mean ± SD. Non-normally distributed variables were indicated by a median with interquartile range. Category variables were shown in numbers and percentages. Student's *t*-test was used for variables following a normal distribution, the Mann-Whitney U-test was used for variables of the non-normal distribution, and the chi-square test was used for categorical variables. The time course of EF (baseline, 3-, 6-, and 12 months after the administration of anthracyclines) was evaluated using the Friedman test.

Logistic regression analysis was performed to identify the variables to predict the occurrence of CTRCD. We selected variables relating to the general condition and cardiac function, i.e., age, echocardiographic parameters, use of anthracyclines, BNP, hemoglobin, estimated glomerular filtration ratio, and the elevation of D-dimer. The variables presenting $p < 0.05$ in the

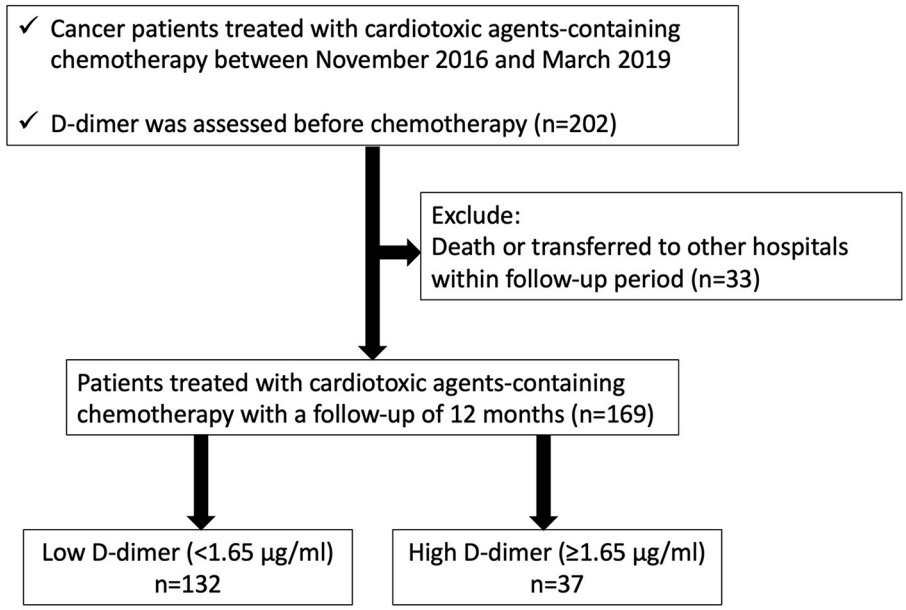

FIGURE 1 | Patient cohort selection.

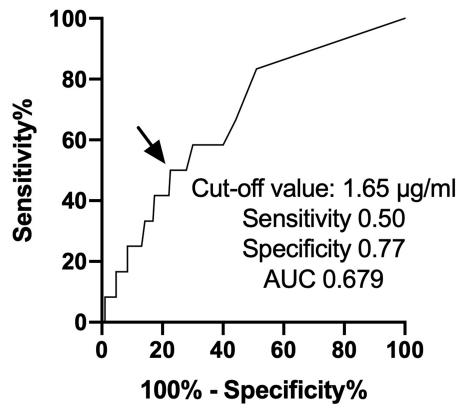

FIGURE 2 | ROC curve analysis of D-dimer predicting the occurrence of cancer therapeutics-related cardiac dysfunction. ROC, receiver operator characteristic curve.

univariable analysis were entered into the multivariable analysis. A receiver operating characteristic curve analysis was performed to determine the optimal cut-off value of the D-dimer for predicting the occurrence of CTRCD. The p of 0.05 or less was defined as significant.

RESULTS

First, we performed a receiver operating characteristic curve analysis to identify the threshold level of D-dimer to predict the occurrence of CTRCD (**Figure 2**). A total of 12 patients suffered from CTRCD within 12 months follow-up period. When we set the cut-off value of D-dimer at 1.65 μg/ml, sensitivity, specificity, and area under the curve to predict CTRCD were 50.0%, 80.3%, and 0.661, respectively. Then, we divided the patients into two groups based on the cut-off value. **Table 1** shows patient characteristics at the baseline before chemotherapy. There were no statistical differences in age, sex, and the usage of angiotensin-converting enzyme inhibitors/angiotensin II receptor blockers and β-blockers. The high D-dimer group included a lower rate of breast cancer (35 vs. 67%, $p = 0.0005$), a higher rate of ovarian/uterine cancer (19 vs. 6%, $p = 0.0151$), and a higher rate of leukemia (16 vs. 4%, $p = 0.0068$) than low D-dimer group. Echocardiographic data demonstrated that EF was slightly higher in the high D-dimer group (67 ± 5 vs. $64 \pm 5\%$, $p = 0.0019$). In laboratory data, the high D-dimer group showed lower hemoglobin values and higher BNP values.

Time-dependent changes in EF are displayed in **Figure 3**. Low D-dimer group showed no changes in EF within the follow-up period, but EF was decreased at 3- and 6 months after chemotherapy in high D-dimer group [baseline, 65.2% (62.8–71.4%); 3 months, 62.9% (59.0–67.7%); 6 months, 63.1% (60.0–67.1%); 12 months, 63.3% (58.8–66.0%), $p = 0.03$, **Figures 3A,B**]. The reduction of EF from baseline was larger in high D-dimer group than in low D-dimer group (3 months: -4.0 ± 7.1 vs. -0.5 ± 5.3, $p = 0.0015$; 6 months: -4.8 ± 8.0 vs. -0.2 ± 6.2, $p = 0.0004$; 12 months: -4.5 ± 7.3 vs. $-0.4 \pm 6.6\%$, $p = 0.0024$).

The occurrence of CTRCD during the 12-month follow-up period was higher in the high D-dimer group than in the low D-dimer group (16.2 vs. 4.5%, $p = 0.0146$). Multivariable logistic regression analysis revealed that LV end-diastolic volume index [odds ratio 0.95, 95% CI (0.91–0.99), $p = 0.0122$] and high D-dimer levels [odds ratio 3.93, 95% CI (1.00–15.82), $p = 0.0469$] before chemotherapy were independent predictors of the development of CTRCD (**Table 2**).

TABLE 1 | Baseline clinical characteristics of patients with elevated or non-elevated D-dimer.

Variable	Entire cohort (n = 169)	Low D-dimer (n = 132)	High D-dimer (n = 37)	P-value
Age, years	57 ± 12	56 ± 12	58 ± 14	0.6265
Female, *n* (%)	146 (86%)	117 (89%)	29 (78%)	0.1078
Medications				
Use of ACEi or ARB	23	18	5	0.9846
Use of β-blockers	4	3	1	0.8791
Cancer types				
Breast cancer, *n* (%)	101 (60%)	88 (67%)	13 (35%)	0.0005
Lymphoma, *n* (%)	28 (17%)	20 (15%)	8 (22%)	0.3495
Ovarian or uterine cancer, *n* (%)	15 (9%)	8 (6%)	7 (19%)	0.0151
Leukemia, *n* (%)	11 (7%)	5 (4%)	6 (16%)	0.0068
Bone cancer, *n* (%)	2 (2%)	2 (2%)	0 (0%)	0.4513
Other cancers, *n* (%)	12 (7%)	9 (7%)	3 (8%)	0.7872
Cancer therapy				
Anthracyclines	138 (82%)	104 (79%)	34 (92%)	0.0687
HER2 inhibitors	36 (21%)	31 (23%)	5 (14%)	0.1905
Tyrosine kinase inhibitors	8 (5%)	6 (5%)	2 (5%)	0.8277
Proteasome inhibitors	5 (3%)	5 (4%)	0 (0%)	0.2295
Dose of anthracyclines(doxorubicin equivalent), mg/m^2	200 [161–240]	200 [180–240]	180 [112–300]	0.3874
Radiation therapy, *n* (%)	20 (12%)	15 (11%)	5 (14%)	0.7205
Cardiovascular risk factors				
Hypertension, *n* (%)	40 (24%)	31 (24%)	9 (24%)	0.9154
Smoking history, *n* (%)	47 (28%)	37 (28%)	10 (27%)	0.9042
Diabetes mellitus, *n* (%)	16 (10%)	13 (10%)	3 (8%)	0.7493
Dyslipidemia, *n* (%)	44 (26%)	38 (29%)	6 (16%)	0.1235
Echocardiographic parameter				
LV end-diastolic volume index, mm/m^2	45 [36–55]	45 [36–55]	46 [36–55]	0.6517
LV end-systolic volume index, mm/m^2	15 [13–20]	15 [13–19]	16 [12–20]	0.6431
LV mass index, g/m^2	70 [59–85]	70 [59–85]	75 [60–87]	0.4644
LA volume index, ml/m^2	23 [17–30]	23 [17–28]	23 [19–32]	0.3159
LV ejection fraction, %	65 ± 5	64 ± 5	67 ± 5	0.0019
E/A	1.0 [0.8–1.2]	1.0 [0.8–1.2]	0.9 [0.8–1.1]	0.5788
Laboratory data				
Aspartate aminotransferase, IU/L	19 [15–23]	19 [16–23]	19 [15–26]	0.7973
Alanine aminotransferase, IU/L	15 [12–22]	15 [12–21]	15 [12–23]	0.7960
eGFR, ml/min/1.73 m^2	72 [64–85]	73 [65–82]	69 [57–88]	0.3472
Hemoglobin, g/dl	13 [11–14]	13 [12–14]	11 [9–13]	0.0001
Uretic acid, mg/dl	4.7 ± 1.4	4.6 ± 1.3	4.7 ± 1.7	0.8197
B-type natriuretic peptide, pg/ml	12 [7–22]	11 [7–20]	17 [9–38]	0.0440
Troponin I, ng/ml	0.017 [0.017–0.017]	0.017 [0.017–0.017]	0.017 [0.017–0.017]	0.5440
D-dimer, μg/ml	0.6 [0.5–1.4]	0.5 [0.5–0.7]	3.1 [2.2–8.1]	<0.0001

ACEi, angiotensin converting enzyme inhibitor; ARB, angiotensin II receptor blocker; HER2, human epidermal growth factor receptor 2; LV, left ventricular; E/A, early to late diastolic transmitral flow velocity; eGFR, estimated glomerular filtration ratio.

DISCUSSION

In the present study, we revealed the predictive features of D-dimer in patients treated with cardiotoxic agents. First, the threshold level of D-dimer was 1.65 μg/ml to predict the development of CTRCD. Second, EF was decreased time-dependently in high D-dimer patients. Third, the occurrence of CTRCD was significantly higher in high D-dimer patients.

D-dimer is a pivotal biomarker of hypercoagulability and thrombosis. Fibrin-bound plasmin degrades the fibrin network into soluble fragments D-dimers and E fragments, thus increased levels of D-dimer represent a global activation of coagulation and fibrinolysis (13). Cancers produce hypercoagulable and prothrombotic situations by secreting several pro-thromboembolic factors, such as mucins, cysteine protease, and tissue factors (14). Therefore, thrombi are easily generated in patients with cancer, and thromboembolism is the second

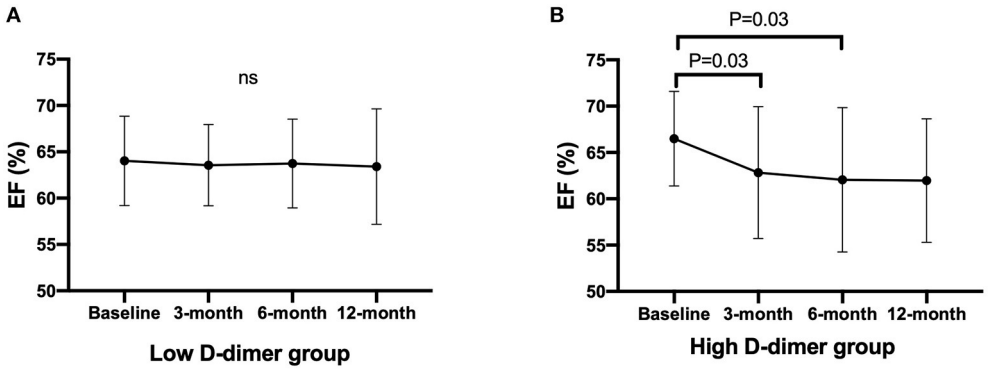

FIGURE 3 | Time-dependent changes in EF after chemotherapy. Data are expressed in mean with SD. Statistics is performed using Friedman's test with Dunn's multiple comparisons test. EF, ejection fraction. **(A)** Changes in EF in the low D-dimer group. **(B)** Changes in EF in the high D-dimer group. EF, ejection fraction.

TABLE 2 | Parameters associated with the occurrence of CTRCD.

	Univariate		Multivariate	
	OR (95% CI)	***P*-value**	**OR (95% CI)**	***P*-value**
Age, per 1 year increase	1.01 (0.96–1.05)	0.8470		
Male	1.79 (0.32–33.57)	0.5852		
Use of anthracyclines	1.18 (0.29–7.94)	0.8353		
BNP, per 1 pg/ml increase	0.99 (0.98–1.02)	0.4239		
LV ejectioin fraction, per 1% increase	1.07 (0.95–1.22)	0.2591		
LV end-diastolic volume index, per 1 ml/m^2 increase	0.95 (0.91–0.99)	0.0099	0.95 (0.91–0.99)	0.0122
E/A, per 1 increase	0.24 (0.05–1.39)	0.0934		
Left atrial volume index, per 1 ml/m^2 increase	0.99 (0.94–1.05)	0.7157		
Hemoglobin, per 1 g/dl increase	1.13 (0.85–1.45)	0.3539		
Estimated GFR, per 1 ml/min/1.73 m^2	0.98 (0.95–1.02)	0.2989		
Elevated D-dimer (1.65 mg/dl)	4.07 (1.20–13.84)	0.0218	3.93 (1.00–15.82)	0.0469

CTRCD, cancer therapeutics-related cardiac dysfunction; BNP, B-type natriuretic peptide; E/A, early to late diastolic transmitral flow velocity; LV, left ventricular; GFR, glomerular filtration ratio.

leading cause of cancer-related morbidity and mortality (15, 16). Although D-dimer is an established and widely used biomarker for the screening of thrombus formation in patients with cancer, prognostic features of D-dimer have become clinically overt recently. The link between D-dimer and cancer progression is reported in several papers (17, 18), and higher levels of D-dimer are associated with poor prognosis in cancer patients (18). Although the precise mechanisms are still complex and uncovered, the pro-coagulable state may produce a suitable milieu for cancer progression by recruitment of pro-metastatic leukocytes, adhesion to the endothelium, transendothelial migration, and restriction in natural killer cell-mediated clearance of micrometastasis (19, 20). Accumulating evidence showed that abnormal inflammation and oxidative stress are key factors to the development of heart failure, and these also play important roles in cancer progression and thrombus formation (21–25). For example, IL-1β, a representative inflammatory cytokine, induces cardiac dysfunction and thrombus formation (26). IL-1β activates myddosome complex, such as nuclear factor κB, myeloid differentiation factor 88, cryopyrin, and p38-MAPK, in cardiomyocytes, leading to dysregulates metabolism in the sarcoplasmic reticulum, calcium homeostasis, and myocardial apoptosis and necrosis (7). In addition, IL-1β increased pro-coagulant state through activating tissue factor-dependent mechanisms in endothelial cells (27). Gomes et al. reported that blockade of IL-1 receptor abolished the neutrophil extracellular traps-dependent pro-thrombotic state and attenuated cancer-associated thrombosis in murine breast cancer model (25). Considering the fact that inflammation is a major contributor to cardiac dysfunction and thrombus formation, cancer patients with high D-dimer may be predisposed to cardiac dysfunction due to a chronic inflammatory state. Cardiotoxic chemotherapeutic agents are crucial and indispensable to performing cancer treatment. Anthracyclines induce pro-inflammatory responses by increasing tumor necrosis factor α (TNF-α), IL-1β, and IL-6, leading to tumor cell death (28). Not only anthracyclines but also targeted chemotherapy, such as trastuzumab and bevacizumab, increased inflammatory cytokines after the treatment (29, 30). In the present study, the patients with a high D-dimer group may already have been exposed to an inflammatory state before chemotherapy and were vulnerable to additional inflammatory

stress by cardiotoxic agents, resulting in the development of CTRCD. To elucidate the precise mechanisms was beyond this study, but the importance of D-dimer should be noted in the cardio-oncology field. Intervention with Pravastatin in Ischemic Disease (LIPID) study revealed that elevated D-dimer levels predict long-term risk of arterial and venous events, cardiovascular disease mortality, in addition to that, increased cancer incidence and mortality rate (31). To the best of our knowledge, this is the first report assessing the relationship between D-dimer levels and the development of CTRCD. The importance of D-dimer should be taken into account when managing patients with cancer who are treated with cardiotoxic chemotherapy.

LIMITATION

This study has several limitations. First, this study was performed using a relatively small number of patients and a short follow-up period by a single center. Slight differences in EF at baseline may be due to the small sample size of the high D-dimer group. Second, although not statistically significant, a higher proportion of patients in the high D-dimer group received anthracycline-containing chemotherapies. This might affect the results in the reduction in EF in the high D-dimer group. Longer follow-up and larger population data were needed to confirm the importance of D-dimer to the development of CTRCD and cardiovascular prognosis. Third, D-dimer has modest sensitivity and specificity to predict CTRCD in the present study. The mechanisms by which CTRCD development must be complicated, thereby predicting CTRCD by a single biomarker is still challenging. D-dimer is frequently analyzed in daily clinical practice to detect cancer-associated thrombosis. Therefore, we think D-dimer is easy and useful for predicting both CTRCD and thrombus formation.

CONCLUSION

Elevated D-dimer is a pivotal biomarker to predict CTRCD. D-dimer should be taken into account when managing cancer patients treated with cardiotoxic chemotherapy.

DATA AVAILABILITY STATEMENT

The raw data supporting the conclusions of this article will be made available by the authors, without undue reservation.

ETHICS STATEMENT

The studies involving human participants were reviewed and approved by Ethical Committee of Fukushima Medical University Hospital. The patients/participants provided their written informed consent to participate in this study.

AUTHOR CONTRIBUTIONS

MO created the study design, analyzed the data, and drafted the manuscript. DY created the study design and analyzed the data. TM, TS, TK, and AK acquired the data. AY, KN, TI, and YT interpreted the data and revised the manuscript. All authors contributed to the conception, design, critical revision, and final approval of this manuscript.

FUNDING

JSPS KAKENHI (Grant Number JP20K08493).

ACKNOWLEDGMENTS

The authors thank Ms. H. Kobayashi for data management.

REFERENCES

1. Zamorano JL, Lancellotti P, Munoz DR, Aboyans V, Asteggiano R, Galderisi M, et al. 2016 ESC position paper on cancer treatments and cardiovascular toxicity developed under the auspices of the ESC committee for practice guidelines: the task force for cancer treatments and cardiovascular toxicity of the European society of cardiology (ESC). *Eur Heart J.* (2016) 37:2768–801. doi: 10.1093/eurheartj/ehw211
2. Oikawa M, Yoshihisa A, Yokokawa T, Misaka T, Yaegashi D, Miyata M, et al. Cardiac troponin I predicts elevated B-type natriuretic peptide in patients treated with anthracycline-containing chemotherapy. *Oncology.* (2020) 98:653–60. doi: 10.1159/000507585
3. Ky B, Putt M, Sawaya H, French B, Januzzi JL Jr, Sebag IA, et al. Early increases in multiple biomarkers predict subsequent cardiotoxicity in patients with breast cancer treated with doxorubicin, taxanes, and trastuzumab. *J Am Coll Cardiol.* (2014) 63:809–16. doi: 10.1016/j.jacc.2013.10.061
4. Thavendiranathan P, Negishi T, Somerset E, Negishi K, Penicka M, Lemieux J, et al. Strain-guided management of potentially cardiotoxic cancer therapy. *J Am Coll Cardiol.* (2021) 77:392–401. doi: 10.1016/j.jacc.2020.11.020
5. Cardinale D, Colombo A, Bacchiani G, Tedeschi I, Meroni CA, Veglia F, et al. Early detection of anthracycline cardiotoxicity and improvement with heart failure therapy. *Circulation.* (2015) 131:1981–8. doi: 10.1161/CIRCULATIONAHA.114.013777
6. Quagliariello V, De Laurentiis M, Cocco S, Rea G, Bonelli A, Caronna A, et al. NLRP3 as putative marker of ipilimumab-induced cardiotoxicity in the presence of hyperglycemia in estrogen-responsive and triple-negative breast cancer cells. *Int J Mol Sci.* (2020) 21:7802. doi: 10.3390/ijms21207802
7. Quagliariello V, Paccone A, Iovine M, Cavalcanti E, Berretta M, Maurea C, et al. Interleukin-1 blocking agents as promising strategy for prevention of anticancer drug-induced cardiotoxicities: possible implications in cancer patients with COVID-19. *Eur Rev Med Pharmacol Sci.* (2021) 25:6797–812. doi: 10.26355/eurrev_202111_27124
8. Li W, Tang Y, Song Y, Chen SH, Sisliyan N, Ni M, et al. Prognostic role of pretreatment plasma D-dimer in patients with solid tumors: a systematic review and meta-analysis. *Cell Physiol Biochem.* (2018) 45:1663–76. doi: 10.1159/000487734
9. Zhang X, Wang S, Sun L, Fang S, Yu B. Prognostic value of D-dimer in acute myocardial infarction complicated by heart failure with preserved ejection fraction. *ESC Heart Fail.* (2020) 7:4118–25. doi: 10.1002/ehf2.13027
10. de Boer RA, Nayor M. deFilippi CR, Enserro D, Bhambhani V, Kizer JR, et al. Association of cardiovascular biomarkers with incident heart failure with preserved and reduced ejection fraction. *JAMA Cardiol.* (2018) 3:215–24. doi: 10.1001/jamacardio.2017.4987
11. Lang RM, Badano LP, Mor-Avi V, Afilalo J, Armstrong A, Ernande L, et al. Recommendations for cardiac chamber quantification by echocardiography in adults: an update from the American Society of Echocardiography and

the European Association of Cardiovascular Imaging. *J Am Soc Echocardiogr.* (2015) 28:1–39. doi: 10.1016/j.echo.2014.10.003
12. Plana JC, Galderisi M, Barac A, Ewer MS, Ky B, Scherrer-Crosbie M, et al. Expert consensus for multimodality imaging evaluation of adult patients during and after cancer therapy: a report from the American Society of Echocardiography and the European Association of Cardiovascular Imaging. *J Am Soc Echocardiogr.* (2014) 27:911–39. doi: 10.1016/j.echo.2014.07.012
13. Kyrle PA, Eichinger S. D-dimer for long-term risk prediction in patients after acute coronary syndrome. Jack of all trades, or master of none? *Circulation.* (2018) 138:724–6. doi: 10.1161/CIRCULATIONAHA.118.033670
14. Varki A. Trousseau's syndrome: multiple definitions and multiple mechanisms. *Blood.* (2007) 110:1723–9. doi: 10.1182/blood-2006-10-053736
15. Prandoni P, Falanga A, Piccioli A. Cancer and venous thromboembolism. *Lancet Oncol.* (2005) 6:401–10. doi: 10.1016/S1470-2045(05)70207-2
16. Tuzovic M, Herrmann J, Iliescu C, Marmagkiolis K, Ziaeian B, Yang EH. Arterial thrombosis in patients with cancer. *Curr Treat Options Cardiovasc Med.* (2018) 20:40. doi: 10.1007/s11936-018-0635-x
17. Han D. ó Hartaigh B, Lee JH, Cho IJ, Shim CY, Chang HJ, et al. Impact of D-dimer for prediction of incident occult cancer in patients with unprovoked venous thromboembolism. *PLoS ONE.* (2016) 11:e0153514. doi: 10.1371/journal.pone.0153514
18. Ay C, Dunkler D, Pirker R, Thaler J, Quehenberger P, Wagner O, et al. High D-dimer levels are associated with poor prognosis in cancer patients. *Haematologica.* (2012) 97:1158–64. doi: 10.3324/haematol.2011.054718
19. Lucotti S, Muschel RJ. Platelets and Metastasis: New implications of an old interplay. *Front Oncol.* (2020) 10:1350. doi: 10.3389/fonc.2020.01350
20. Palumbo JS, Talmage KE, Massari JV, La Jeunesse CM, Flick MJ, Kombrinck KW, et al. Tumor cell-associated tissue factor and circulating hemostatic factors cooperate to increase metastatic potential through natural killer cell-dependent and-independent mechanisms. *Blood.* (2007) 110:133–41. doi: 10.1182/blood-2007-01-065995
21. Bertero E, Canepa M, Maack C, Ameri P. Linking heart failure to cancer: Background evidence and research perspectives. *Circulation.* (2018) 138:735–42. doi: 10.1161/CIRCULATIONAHA.118.033603
22. Koene RJ, Prizment AE, Blaes A, Konety SH. Shared risk factors in cardiovascular disease and cancer. *Circulation.* (2016) 133:1104–14. doi: 10.1161/CIRCULATIONAHA.115.020406
23. Barrera G. Oxidative stress and lipid peroxidation products in cancer progression and therapy. *ISRN Oncol.* (2012) 2012:137289. doi: 10.5402/2012/137289
24. Jang JH, Kim DH, Surh YJ. Dynamic roles of inflammasomes in inflammatory tumor microenvironment. *NPJ Precis Oncol.* (2021) 5:18. doi: 10.1038/s41698-021-00154-7
25. Gomes T, Várady CBS, Lourenço AL, Mizurini DM, Rondon AMR, Leal AC, et al. IL-1β blockade attenuates thrombosis in a neutrophil extracellular trap-dependent breast cancer model. *Front Immunol.* (2019) 10:2088. doi: 10.3389/fimmu.2019.02088
26. Bevilacqua MP, Pober JS, Majeau GR, Cotran RS, Gimbrone MA Jr. Interleukin 1 (IL-1) induces biosynthesis and cell surface expression of procoagulant activity in human vascular endothelial cells. *J Exp Med.* (1984) 160:618–23. doi: 10.1084/jem.160.2.618
27. Puhlmann M, Weinreich DM, Farma JM, Carroll NM, Turner EM, Alexander HR. Jr. Interleukin-1beta induced vascular permeability is dependent on induction of endothelial tissue factor (TF) activity. *J Transl Med.* (2005) 3:37. doi: 10.1186/1479-5876-3-37
28. Tocchetti CG, Ameri P, de Boer RA, D'Alessandra Y, Russo M, Sorriento D, et al. Cardiac dysfunction in cancer patients: beyond direct cardiomyocyte damage of anticancer drugs: novel cardio-oncology insights from the joint 2019 meeting of the ESC Working Groups of Myocardial Function and Cellular Biology of the Heart. *Cardiovasc Res.* (2020) 116:1820–34. doi: 10.1093/cvr/cvaa222
29. Dhesy-Thind S, Kumar V, Snider-McNair A, Shortt C, Mukherjee SD, Ellis P, et al. Cardiac and inflammation biomarker profile after initiation of adjuvant trastuzumab therapy. *Clin Chem.* (2013) 59:327–9. doi: 10.1373/clinchem.2012.192419
30. El-Hajjar L, Jalaleddine N, Shaito A, Zibara K, Kazan JM, El-Saghir J, et al. Bevacizumab induces inflammation in MDA-MB-231 breast cancer cell line and in a mouse model. *Cell Signal.* (2019) 53:400–12. doi: 10.1016/j.cellsig.2018.11.007
31. Simes J, Robledo KP, White HD, Espinoza D, Stewart RA, Sullivan DR, et al. D-dimer predicts long-term cause-specific mortality, cardiovascular events, and cancer in patients with stable coronary heart disease: LIPID study. *Circulation.* (2018) 138:712–23. doi: 10.1161/CIRCULATIONAHA.117.029901

Conflict of Interest: The authors declare that the research was conducted in the absence of any commercial or financial relationships that could be construed as a potential conflict of interest.

Publisher's Note: All claims expressed in this article are solely those of the authors and do not necessarily represent those of their affiliated organizations, or those of the publisher, the editors and the reviewers. Any product that may be evaluated in this article, or claim that may be made by its manufacturer, is not guaranteed or endorsed by the publisher.

frontiers in Cardiovascular Medicine

MINI REVIEW
published: 24 January 2022
doi: 10.3389/fcvm.2022.839644

Demystifying the Relationship Between Metformin, AMPK, and Doxorubicin Cardiotoxicity

*Manrose Singh[1], Akito T. Nicol[1], Jaclyn DelPozzo[1], Jia Wei[2], Mandeep Singh[1], Tony Nguyen[1], Satoru Kobayashi[1] and Qiangrong Liang[1]**

[1] Department of Biomedical Sciences, College of Osteopathic Medicine, New York Institute of Technology, Old Westbury, NY, United States, [2] Department of Cardiology, The Second Affiliated Hospital of Xi'an Jiaotong University, Xian, China

Doxorubicin (DOX) is an extremely effective and wide-spectrum anticancer drug, but its long-term use can lead to heart failure, which presents a serious problem to millions of cancer survivors who have been treated with DOX. Thus, identifying agents that can reduce DOX cardiotoxicity and concurrently enhance its antitumor efficacy would be of great clinical value. In this respect, the classical antidiabetic drug metformin (MET) has stood out, appearing to have both antitumor and cardioprotective properties. MET is proposed to achieve these beneficial effects through the activation of AMP-activated protein kinase (AMPK), an essential regulator of mitochondrial homeostasis and energy metabolism. AMPK itself has been shown to protect the heart and modulate tumor growth under certain conditions. However, the role and mechanism of the hypothesized MET-AMPK axis in DOX cardiotoxicity and antitumor efficacy remain to be firmly established by *in vivo* studies using tumor-bearing animal models and large-scale prospective clinical trials. This review summarizes currently available literature for or against a role of AMPK in MET-mediated protection against DOX cardiotoxicity. It also highlights the emerging evidence suggesting distinct roles of the AMPK subunit isoforms in mediating the functions of unique AMPK holoenzymes composed of different combinations of isoforms. Moreover, the review provides a perspective regarding future studies that may help fully elucidate the relationship between MET, AMPK and DOX cardiotoxicity.

Keywords: doxorubicin, metformin, AMPK, doxorubicin cardiotoxicity, cardio-oncology

OPEN ACCESS

Edited by:
Dong Han,
People's Liberation Army General Hospital, China

Reviewed by:
Xing Fu,
Louisiana State University Agricultural Center, United States

****Correspondence:***
Qiangrong Liang
qliang03@nyit.edu

Specialty section:
This article was submitted to Cardio-Oncology, a section of the journal Frontiers in Cardiovascular Medicine

Received: *20 December 2021*
Accepted: *04 January 2022*
Published: *24 January 2022*

Citation:
Singh M, Nicol AT, DelPozzo J, Wei J, Singh M, Nguyen T, Kobayashi S and Liang Q (2022) Demystifying the Relationship Between Metformin, AMPK, and Doxorubicin Cardiotoxicity. Front. Cardiovasc. Med. 9:839644. doi: 10.3389/fcvm.2022.839644

INTRODUCTION

The anthracycline doxorubicin (DOX) has been widely used for over 5 decades and is a highly effective chemotherapeutic agent for the treatment of a broad spectrum of cancers including various solid tumors and leukemia. Unfortunately, DOX chemotherapy can cause severe cardiotoxic effects (1–3). Acute toxicity occurs immediately after treatment and is generally transient. Chronic cardiotoxicity is more serious and culminates in irreversible congestive heart failure. Currently, only the iron chelator dexrazoxane has been approved for limited clinical use for reducing DOX cardiotoxicity in certain pediatric or breast cancer patients (4–7). Given the continuing widespread use of DOX in cancer chemotherapies, it is imperative to identify

new strategies that can protect against DOX cardiotoxicity without compromising the anti-tumor activity of DOX. Metformin (MET), a drug used for the first-line treatment of type 2 diabetes, has been suggested as such a dual-function agent that can simultaneously decrease DOX cardiotoxicity (8–11) and increase its anticancer activity (12, 13). The differential effects of MET on cardiomyocytes and cancer cells may be related to the differences in cellular energy metabolism. Cardiomyocytes are highly dependent on mitochondria for energy supply, while cancer cells primarily use glycolysis-generated ATP. Therefore, drugs such as MET that modulate mitochondrial function may have substantially different effects on the heart as compared to tumors. AMP-activated protein kinase (AMPK), a cellular energy sensor, is activated by MET and implicated in both cardioprotection and tumor growth. Most cell-based studies have suggested AMPK as a downstream effector of MET that functions to reduce DOX cardiotoxicity (9, 11, 14–17). However, the role of AMPK in cancer has been controversial (18). It remains uncertain whether and how AMPK affects the ability of MET to modulate DOX cardiotoxicity or tumor growth *in vivo*. This mini-review will extract evidence from currently available literature for or against a role of AMPK in MET-mediated protection against DOX cardiotoxicity. For the effects of MET and AMPK in antitumor therapies, the readers are referred to other review articles published elsewhere (18–24).

DOX CARDIOTOXICITY IS A SERIOUS CLINICAL PROBLEM

Dox is an extremely effective and wide-spectrum antineoplastic drug that can lead to dose-dependent cardiotoxicity, culminating in heart failure (1–3). This presents a serious problem to millions of cancer survivors who have been treated with DOX. Indeed, the cardiovascular mortality in cancer survivors exceeds that caused by cancer *per se* (25). DOX cardiotoxicity is even more significant in childhood cancer since about half of all pediatric patients are treated with anthracyclines and many childhood cancer survivors go on to develop cardiac dysfunction (26–28). Due to the dose-dependent risk, the lifetime cumulative dose of DOX has been recommended not to exceed 450 mg/m^2 per patient (1). Thus, DOX cardiotoxicity is a significant life-long health concern for cancer survivors.

DOX INDUCES CARDIOTOXICITY VIA MULTIPLE MECHANISMS

Several mechanisms have been proposed to account for the ability of DOX to produce cardiotoxicity. DOX is concentrated in the mitochondria and its quinone moiety is reduced by the oxidoreductases to a semiquinone form which in turn donates its excess electron to O_2, leading to the formation of reactive oxygen species (ROS) including superoxide anions (29, 30). Although the long-held ROS and oxidative stress theory of DOX cardiotoxicity is strongly supported by numerous animal studies (31–33), clinical trials have failed to demonstrate the efficacy of antioxidant supplements in reducing DOX-triggered cardiac injury (34, 35), suggesting that oxidative stress is not the only mechanism that mediates DOX cardiotoxicity. Interestingly, DOX has been shown to either bind with free iron (36) or cause mitochondrial iron accumulation in the heart (37), which may directly cause mitochondria-dependent ferroptosis or produce additional ROS intensifying the oxidative stress (38). The contribution of iron to DOX cardiotoxicity is demonstrated by the ability of the iron chelator dexrazoxane to attenuate DOX-induced cardiomyopathy (4, 5, 37). Another recognized culprit of DOX cardiotoxicity is mitochondrial dysfunction (39). Being the major site of DOX-induced ROS production, mitochondria themselves are vulnerable to oxidative injury. DOX interacts with the acidic lipoprotein cardiolipin in the inner mitochondrial membrane, resulting in its peroxidation and the opening of mitochondrial permeability transition pores which in turn triggers cytochrome c release and apoptosis (40, 41). The third mechanism proposed for DOX cardiotoxicity is through its effect on topoisomerase IIβ (TOPIIβ). While the antitumor effect of DOX is through DNA intercalation and TOPIIα inhibition (42–44), DOX also binds to TOPIIβ which is expressed mainly in quiescent cells such as cardiomyocytes. Mice null for TOPIIβ do not exhibit cardiotoxic effects with DOX treatment (45), suggesting that TOPIIβ is a major mediator of DOX cardiotoxicity. DOX is proposed to complex with TOPIIβ, leading to the activation of p53 mediated DNA damage pathways and the inhibition of genes implicated in mitochondrial biogenesis. Interestingly, dexrazoxane is shown to protect the heart by transiently depleting TOPIIβ levels in cardiomyocytes, suggesting that dexrazoxane may reduce DOX cardiotoxicity via both TOPIIβ depletion and iron chelation (46). The last potential mechanism of DOX cardiotoxicity relates to autophagy, a catabolic process for the cell to degrade long-lived proteins and organelles in the lysosome. The exact function of autophagy in DOX cardiotoxicity remains hotly debated, which is not surprising given the dynamic nature of the multi-step autophagic process and the numerous pathways implicated in its regulation. Indeed, DOX has been shown to either activate autophagy (17, 47–50) or inhibit autophagy (51–53), paradoxically, both of which contribute to cardiotoxicity. Adding to the confusion, DOX-triggered suppression of autophagy is seemingly cardioprotective (54). These conflicting results may be attributable to the differences in the experimental models used, the developmental stages of cardiomyopathy, and the dose and duration of DOX treatment, as well as the methods applied to manipulate different steps of the autophagic process and the techniques used to measure autophagic activities (49, 55). An early sign of DOX-induced mitochondrial damage is the loss of mitochondrial membrane potential (56–58). The latter is a major mechanism that triggers mitochondrial degradation by autophagy, a process known as mitophagy. However, as with autophagy, it remains controversial whether DOX activates or inhibits mitophagy and whether mitophagy contributes to or protects against DOX cardiotoxicity (59–62).

Abbreviations: DOX, doxorubicin; MET, metformin; ROS, reactive oxygen species; AMPK, AMP-activated protein kinase; TOPIIα/β, topoisomerase IIα/β; ACE, angiotensin-converting enzyme; IGF1, Insulin-like growth factor 1; P-gp, P-glycoprotein; LKB1, Liver Kinase B1; MEFs, mouse embryonic fibroblasts.

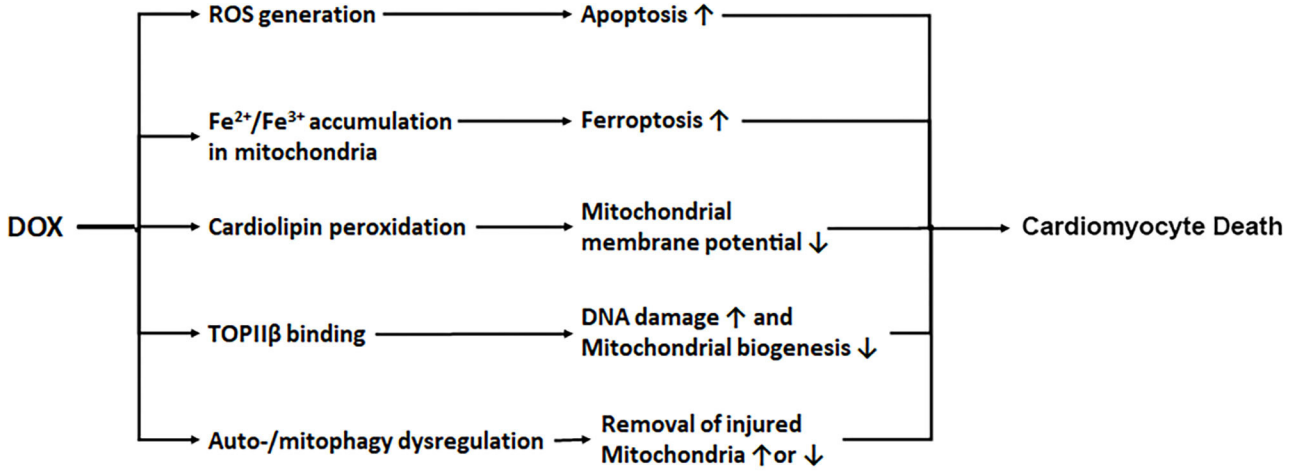

FIGURE 1 | DOX induces cardiotoxicity via multiple mechanisms. DOX enters mitochondria triggering increased production of ROS, iron accumulation, cardiolipin peroxidation, and mitochondrial injury. DOX also binds to topoisomerase IIβ (TOPIIβ), resulting in DNA damage and reduced mitochondrial biogenesis. In addition, DOX causes autophagy/mitophagy dysfunction, leading to either reduced or excessive elimination of injured mitochondria, worsening cardiac injury.

Further investigation is needed to measure mitophagy flux and elucidate the role of mitophagy in DOX cardiotoxicity by using more reliable approaches and more clinically relevant animal models. In summary, it is likely that DOX induces cardiotoxicity via multiple mechanisms, including ROS generation, iron accumulation, cardiolipin peroxidation/mitochondrial injury, topoisomerase binding, and autophagy/mitophagy dysfunction (**Figure 1**).

NEW STRATEGIES TO DIMINISH DOX CARDIOTOXICITY IN CANCER PATIENTS ARE DESPERATELY NEEDED

The current approach for reducing DOX cardiotoxicity is to limit the overall cumulative dose of the drug. However, this also narrows the therapeutic window for cancer treatment. Other strategies for limiting its cardiotoxicity have been pursued. Attempts to develop chemical analogs that retain anti-tumor properties but have reduced cardiotoxicity have had minimal success (63). Liposomal DOX has improved pharmacokinetics and reduced accumulation in the heart (64) but has failed to replace conventional DOX for treatment of most solid tumors (65). An additional approach is to combine DOX with a cardioprotective agent during treatment. Common neurohormonal antagonists, such as β-adrenergic receptor blockers and angiotensin-converting enzyme inhibitors, are routinely used for treating non-cancer-related heart failure, but they are not recommended for preventing and managing DOX cardiotoxicity due to the marginal benefits and related adverse events (66). Currently, only the iron chelator dexrazoxane has been approved for clinical use for reducing DOX cardiotoxicity (4, 5). Unfortunately, dexrazoxane is not a ubiquitous treatment for anthracycline cardiotoxicity, and its use has been limited to pediatric patients with high risk acute lymphoblastic leukemia and breast cancer patients on high doses of DOX, given the possibility of dexrazoxane to cause myelosuppression and secondary malignancies (6, 67, 68). Therefore, it is imperative to develop new strategies to protecting against DOX-induced heart damage without compromising the anti-tumor activity of DOX. In this regard, the antidiabetic drug metformin (MET) has appeared to be such a promising dual-function agent that can improve the clinical use of DOX.

METFORMIN PROTECTS THE HEART AGAINST VARIOUS PATHOLOGICAL CONDITIONS INCLUDING DOX CARDIOTOXICITY

Metformin (MET) is an oral biguanide agent that was first utilized to treat diabetes in France in 1957 (69) and approved by the US FDA in 1994 and has since been widely used as the first-line treatment for Type II diabetes due to its safety, efficacy and tolerability (70, 71). MET has been shown to protect the heart in people with or without diabetes mellitus (72). Indeed, MET is associated with decreased risk of heart failure (73) and reduced cardiovascular mortality independent of its glucose lowering effects (74). The cardioprotective effects of MET have been repeatedly confirmed by numerous pre-clinical studies under various cardiac conditions (75–79). Not surprisingly, MET can also reduce DOX cardiotoxicity in many animal studies (8–11). This may hold true in humans as well, given the ability of MET to attenuate radiation cardiotoxicity in breast cancer patients (80). Unfortunately, a phase II clinical trial "Use of Metformin to Reduce Cardiac Toxicity in Breast Cancer" was prematurely terminated due to its failure to meet target accrual (https://clinicaltrials.gov/ct2/show/NCT02472353). Apparently, further clinical trials are needed to confirm the cardioprotective effects of MET in cancer patients

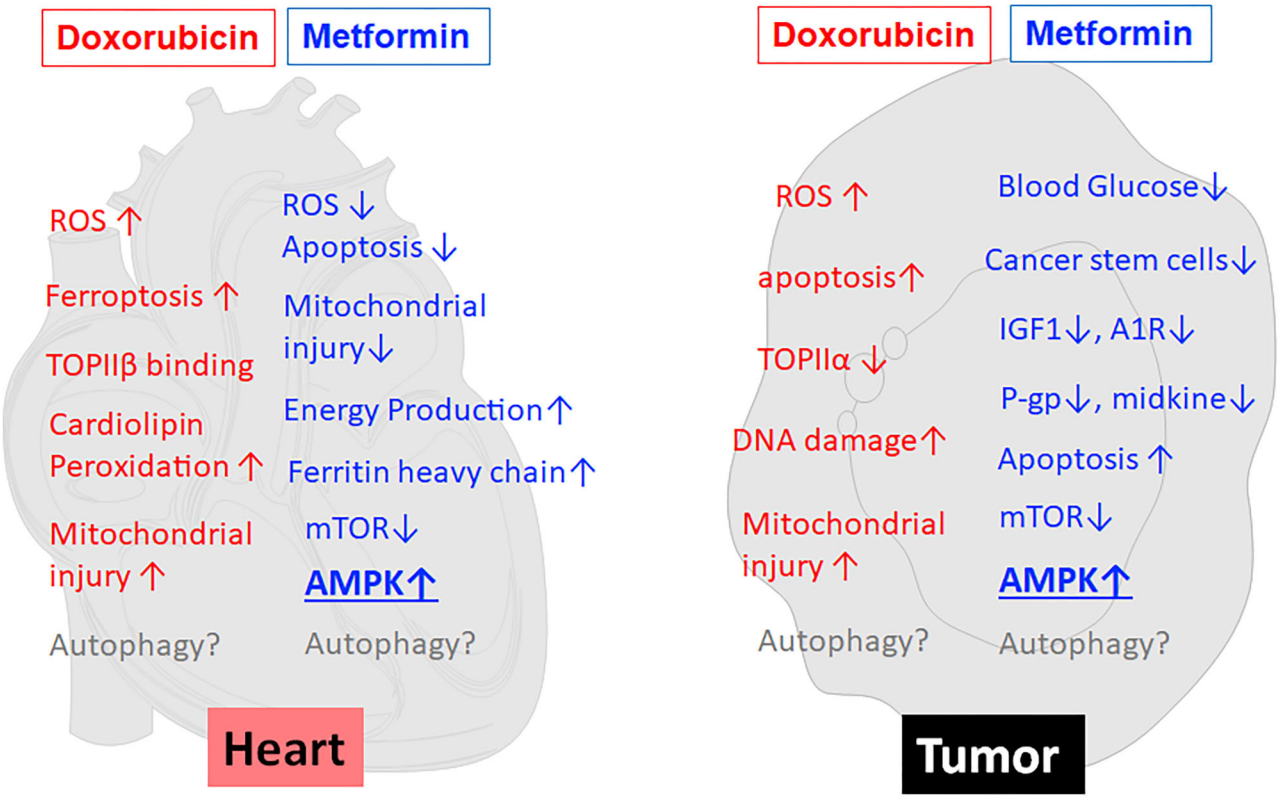

FIGURE 2 | MET reduces the toxic effects of DOX on cardiomyocytes but concurrently enhances the anticancer effects of DOX on tumor cells. As shown in the left panel (heart), MET antagonizes DOX cardiotoxicity through several mechanisms, including attenuation of ROS generation and oxidative stress, inhibition of mitochondrial damage and maintenance of energy production, increased expression of ferritin heavy chain, and activation of AMPK. At the same time, MET enhances DOX antitumor effects (tumor, the right panel) through reduction of blood glucose, inhibition of cancer stem cells, reduction of IGF-1, modulation of adenosine A1 receptor (A1R), down-regulation of drug-resistant gene P-glycoprotein (P-gp), induction of apoptosis, inhibition of midkine, inhibition of mTOR, and activation of AMPK. Of note, AMPK activation has been suggested to be the major mechanism that mediates both the anti-tumor and cardioprotective effects of MET. On the other hand, the effects of MET on autophagy/mitophagy are not very clear. ↑, increase or upregulation; ↓, inhibition or downregulation; ROS, Reactive oxygen species; TOPII, Topoisomerase II; A1R, Adenosine A1 receptor; IGF1, Insulin-like growth factor 1; P-gp, P-glycoprotein.

treated with DOX. MET has been suggested to antagonize DOX cardiotoxicity through several mechanisms (left panel in **Figure 2**), including attenuation of ROS generation and oxidative stress, inhibition of mitochondrial damage and maintenance of energy production (82), normalization of autophagy markers (8), increased expression of ferritin heavy chain in cardiomyocytes, and activation of AMP-activated protein kinase (AMPK) (11). The role of AMPK in MET-induced protection against DOX cardiotoxicity has been supported by numerous studies either in cultured cells or in animals (8–11).

METFORMIN HAS ANTITUMOR PROPERTIES THAT MAY SYNERGIZE WITH THE ANTITUMOR ACTIVITY OF DOX

Several epidemiological studies, meta-analyses and animal studies have revealed that MET has anti-neoplastic and chemopreventive activities (20, 81) despite mixed results observed in other studies (82, 83). Indeed, diabetic patients taking MET have significantly reduced risk of cancer and lower cancer-related mortality (84–89). Several small-scale clinical trials have shown the ability of MET to induce favorable cellular and molecular changes in cancer patients (90–93). For example, clinical trials in pre-surgical endometrial cancer patients exhibited a significant decrease in Ki67 with MET monotherapy (19). Another study showed the ability of MET to inhibit the increase of Insulin-like growth factor 1 (IGF-1) and maintain the levels of IGF binding protein-1 although the progression-free survival was not affected (91). In addition, numerous animal studies have shown that MET can enhance the anticancer activity of DOX (11–13, 94, 95). Thus, it is highly desirable that large scale randomized clinical trials be conducted to confirm the usefulness of MET in cancer chemotherapy. Nevertheless, given the demonstrated anti-tumor and cardioprotective properties of MET, it is reasonable to believe that MET can be used in DOX-containing chemotherapy to enhance the antitumor activity of DOX and at the same time to reduce its cardiotoxic effect (96). Metformin is believed to exert its antitumor effects via multiple mechanisms (right panel in

Figure 2), including activation of AMPK and inhibition of mTOR (13, 97, 98), reduction of blood glucose (21), reduction of insulin and IGF-1(98), inhibition of cancer stem cells (99), modulation of adenosine A1 receptor (100), down-regulating drug-resistant gene P-glycoprotein (P-gp) (94), inhibition of midkine (101), and induction of apoptosis (102, 103). Among them, AMPK activation has been suggested to be the major mechanism that mediates both the anti-tumor and cardioprotective effects of metformin (11, 13, 21, 97). If this is true, modulation of AMPK *per se* should improve the application of DOX in antitumor therapy.

AMPK SIGNALING MAY PROTECT AGAINST DOX CARDIOTOXICITY

AMP-activated protein kinase (AMPK) is a heterotrimeric protein kinase composed of a catalytic α subunit and two regulatory subunits (β and γ). Each subunit has multiple isoforms encoded by distinct genes (α1, α2, β1, β2, γ1, γ2, and γ3), and they combine to form 12 different AMPK holoenzymes (104). All isoforms except for γ3 are expressed in mouse and human heart, which can form 8 AMPK holoenzymes (105). As an energy sensor, AMPK detects and reacts to fluctuations in intracellular ATP levels under normal and stress conditions. The activated AMPK affects multiple metabolic pathways to maintain an energy homeostasis conducive to stress resistance and cell survival (106). There has been continuous intense research targeting AMPK for the treatment of multiple prevalent diseases, such as obesity, diabetes, cancer and cardiovascular diseases (107–109). Using AMPK deficient mice and chemical activators of AMPK such as AICAR and MET, numerous studies have shown that AMPK exerts a cardioprotective effect against myocardial ischemic injury (110, 111), diabetic cardiomyopathy (112), pathological cardiac remodeling (113), and heart failure (109). However, the use of MK-8722, a pan-AMPK activator, induces cardiac hypertrophy despite its ability to improve glucose homeostasis in rodents and rhesus monkeys (114), casting some doubt on the notion that AMPK activation always benefits the heart. Indeed, the gain-of-function mutations of the AMPK γ2 subunit result in severe cardiomyopathy in humans (115, 116), suggesting that the activation of some AMPK isoforms or holoenzymes can be detrimental to the heart under certain conditions. Interestingly, AMPK holoenzymes containing the α2 rather than the α1 subunit are the primary mediators of the cardiac phenotype of γ2 mutations (117), suggesting that α1-AMPK may play a different role than α2-AMPK, which underscores the complexity of isoform-specific functions of AMPK. This isoform-specific phenomenon was also observed in skeletal muscle where α2 but not α1 AMPK is responsible for AICAR-induced glucose uptake (118). When it comes to DOX cardiotoxicity, most cell-based studies have suggested AMPK as cardioprotective (9, 11, 14–17) despite the fact that DOX has been reported to either increase or decrease cardiac AMPK activity depending on the dose and duration of DOX treatment as well as the experimental models used (59, 119, 120). Pharmacological agents including MET, statins and many others can simultaneously activate AMPK and protect against DOX cardiotoxicity, but this remains an association and the causality between these two effects has not been established (119, 120). For example, the proposed role of AMPK in MET-mediated protection against DOX cardiotoxicity remains to be determined by using genetic animal models lacking AMPK function. Also, it remains essentially unknown which of the 8 isoform-specific AMPK holoenzymes mediates the putative protective effects on DOX cardiotoxicity *in vivo*.

AMPK PLAYS TEMPORAL AND ISOFORM-DEPENDENT DICHOTOMOUS ROLES IN CANCER

AMPK is considered to be both a tumor suppressor and an oncogene depending on the context (22). Studies have suggested AMPK as a tumor suppressor before disease arises, which is further enhanced by the biguanide phenformin. However, once cancer has occurred, AMPK becomes a tumor promoter to enhance cancer cell survival by protecting against metabolic, oxidative and genotoxic stresses (23). Indeed, the Liver Kinase B1 (LKB1)/AMPK pathway contributes to tumor cell survival by promoting cellular sensing of and adaptation to bioenergetic stress. Repression of LKB1 by miR-17∼92 sensitizes MYC-dependent lymphoma to biguanide treatment (121). In addition, a loss of both AMPK α1 and α2 subunit isoforms in H-Ras-transformed mouse embryonic fibroblasts (MEFs) caused a complete failure of their growth *in vivo* in immunodeficient mice (122). However, a loss of AMPK α2 alone caused the tumors to grow more rapidly (123), suggesting isoform-dependent differential effects of AMPK on tumor growth. In summary, whether AMPK behaves as a tumor suppressor or a promoter depends on the developmental stage of the tumor and the specific isoform of the AMPK subunits.

MET ACTIVATES AMPK, BUT IT IS UNKNOWN IF AMPK IS RESPONSIBLE FOR CARDIOPROTECTION BY MET

Met has been shown to activate the AMPK pathway, and this has been proposed as the major mechanism that mediates the cardioprotective (9, 11, 109, 119, 120) and antitumor (13, 96, 97, 124) effects of MET. Thus, pharmacologically activating the AMPK pathway seems to be a two-birds-with-one-stone strategy to simultaneously reduce DOX cardiotoxicity and enhance its antitumor activity. However, it remains to be determined whether AMPK is indeed responsible for the potential double benefits of MET in humans or in clinically relevant animal models. Indeed, MET is shown to reduce pathological cardiac remodeling in the absence of AMPKα2 (76), suggesting the possibility that MET may reduce DOX cardiotoxicity independently of AMPK. Given the dual role of AMPK in tumor growth, it is equally unclear if the antitumor effects of MET are mediated by AMPK or its subunit isoforms.

SUMMARY AND FUTURE PERSPECTIVES

MET has been safely used to treat diabetes for several decades, making it a good candidate for repurposing (19). Indeed, many animal and preclinical studies suggest that MET has both cardioprotective and antitumor properties, which lends itself as a promising adjuvant drug for DOX anticancer therapies to reduce cardiotoxicity. MET is proposed to achieve these beneficial effects through the activation of AMPK that itself has been shown to protect the heart and modulate tumor growth under certain conditions. However, the role and mechanism of the hypothesized MET-AMPK axis in DOX cardiotoxicity and antitumor efficacy have not been firmly established. Convincing *in vivo* studies using tumor-bearing animal models and large-scale prospective clinical trials are needed to fully establish MET as an effective antitumor agent either alone or together with DOX. Also, the proposed role of AMPK in MET-mediated protection against DOX cardiotoxicity should be validated in genetic animal models lacking AMPK in the heart. Given the emerging evidence suggesting distinct functional roles of the AMPK isoforms, it is important to investigate how different AMPK holoenzymes containing unique combinations of isoforms will modulate the ability of DOX to affect either heart function or tumor growth. Future studies should also explore the cellular and molecular mechanisms that account for the differential responses of cardiomyocytes vs. cancer cells to DOX and MET, either individually or in combination. Without any doubt, answers to the above questions are expected to have a positive impact on the treatment of many types of cancers with DOX. For example, if it is firmly established that MET can reduce DOX cardiotoxicity and concurrently maintain its antitumor activity, the results could be rapidly translated into use for cancer patients because MET has been used in diabetic patients for decades. Specifically, including MET in a therapeutic protocol could reduce the amount of DOX needed to achieve the same antitumor effect. Alternatively, MET could make it possible to use larger doses of DOX to eradicate cancer more effectively without increasing cardiac damage. In short, MET could improve the therapeutic window for DOX, allowing greater flexibility in designing regimens for treating cancer. Finally, a comprehensive understanding of the relationship between DOX cardiotoxicity, antitumor efficacy, and individual isoforms of AMPK will guide novel mechanism-based therapeutic strategies that target AMPK.

AUTHOR CONTRIBUTIONS

ManrS, AN, JD, JW, MandS, and TN contributed to sections of the first draft. SK made the figures and edited the manuscript. QL wrote the outline, edited the draft, and finalized the manuscript. All authors contributed to the article and approved the submitted version.

FUNDING

This line of research in the laboratory was supported by an in-house grant from New York Institute of Technology College of Osteopathic Medicine (NYITCOM) to QL and a research grant from the American Osteopathic Association (AOA, #2007816) to TN.

REFERENCES

1. Swain SM, Whaley FS, Ewer MS. Congestive heart failure in patients treated with doxorubicin: a retrospective analysis of three trials. *Cancer.* (2003) 97:2869–79. doi: 10.1002/cncr.11407
2. Singal PK, Iliskovic N. Doxorubicin-induced cardiomyopathy. *N Engl J Med.* (1998) 339:900–5. doi: 10.1056/NEJM199809243391307
3. Minotti G, Menna P, Salvatorelli E, Cairo G, Gianni L. Anthracyclines: molecular advances and pharmacologic developments in antitumor activity and cardiotoxicity. *Pharmacol Rev.* (2004) 56:185–229. doi: 10.1124/pr.56.2.6
4. Injac R, Strukelj B. Recent advances in protection against doxorubicin-induced toxicity. *Technol Cancer Res Treat.* (2008) 7:497–516. doi: 10.1177/153303460800700611
5. Hasinoff BB, Herman EH. Dexrazoxane: how it works in cardiac and tumor cells. Is it a prodrug or is it a drug? *Cardiovasc Toxicol.* (2007) 7:140–4. doi: 10.1007/s12012-007-0023-3
6. Tebbi CK, London WB, Friedman D, Villaluna D, De Alarcon PA, Constine LS, et al. Dexrazoxane-associated risk for acute myeloid leukemia/myelodysplastic syndrome and other secondary malignancies in pediatric Hodgkin's disease. *J Clin Oncol.* (2007) 25:493–500. doi: 10.1200/JCO.2005.02.3879
7. Swain SM, Whaley FS, Gerber MC, Ewer MS, Bianchine JR, Gams RA. Delayed administration of dexrazoxane provides cardioprotection for patients with advanced breast cancer treated with doxorubicin-containing therapy. *J Clin Oncol.* (1997) 15:1333–40. doi: 10.1200/JCO.1997.15.4.1333
8. Zilinyi R, Czompa A, Czegledi A, Gajtko A, Pituk D, Lekli I, et al. The cardioprotective effect of metformin in doxorubicin-induced cardiotoxicity: the role of autophagy. *Molecules.* (2018) 23:1184. doi: 10.3390/molecules23051184
9. Kobashigawa LC, Xu YC, Padbury JF, Tseng YT, Yano N. Metformin protects cardiomyocyte from doxorubicin induced cytotoxicity through an AMP-activated protein kinase dependent signaling pathway: an *in vitro* study. *PLoS ONE.* (2014) 9:e104888. doi: 10.1371/journal.pone.0104888
10. Asensio-Lopez MC, Lax A, Pascual-Figal DA, Valdes M, Sanchez-Mas J. Metformin protects against doxorubicin-induced cardiotoxicity: involvement of the adiponectin cardiac system. *Free Radic Biol Med.* (2011) 51:1861–871. doi: 10.1016/j.freeradbiomed.2011.08.015
11. Ajzashokouhi AH, Bostan HB, Jomezadeh V, Hayes AW, Karimi G. A review on the cardioprotective mechanisms of metformin against doxorubicin. *Hum Exp Toxicol.* (2019) 39:237–48. doi: 10.1177/0960327119888277
12. Li Y, Luo J, Lin MT, Zhi P, Guo WW, Han M, et al. Co-delivery of metformin enhances the antimultidrug resistant tumor effect of doxorubicin by improving hypoxic tumor microenvironment. *Mol Pharm.* (2019) 16:2966–79. doi: 10.1021/acs.molpharmaceut.9b00199
13. El-Ashmawy NE, Khedr NF, El-Bahrawy HA, Abo Mansour. HE. Metformin augments doxorubicin cytotoxicity in mammary carcinoma through activation of adenosine monophosphate protein kinase pathway. *Tumour Biol.* (2017) 39:1010428317692235. doi: 10.1177/1010428317692235
14. Liu D, Ma Z, Di S, Yang Y, Yang J, Xu L, et al. AMPK/PGC1alpha activation by melatonin attenuates acute doxorubicin cardiotoxicity via alleviating mitochondrial oxidative damage and apoptosis. *Free Radic Biol Med.* (2018) 129:59–72. doi: 10.1016/j.freeradbiomed.2018.08.032
15. Liu MH, Lin XL, Guo DM, Zhang Y, Yuan C, Tan TP, et al. Resveratrol protects cardiomyocytes from doxorubicin-induced apoptosis

through the AMPK/P53 pathway. *Mol Med Rep.* (2016) 13:1281–86. doi: 10.3892/mmr.2015.4665
16. Liu D, Ma Z, Xu L, Zhang X, Qiao S, Yuan J. PGC1alpha activation by pterostilbene ameliorates acute doxorubicin cardiotoxicity by reducing oxidative stress via enhancing AMPK and SIRT1 cascades. *Aging.* (2019) 11:10061–73. doi: 10.18632/aging.102418
17. Chen K, Xu X, Kobayashi S, Timm D, Jepperson T, Liang Q. Caloric restriction mimetic 2-deoxyglucose antagonizes doxorubicin-induced cardiomyocyte death by multiple mechanisms. *J Biol Chem.* (2011) 286:21993–2006. doi: 10.1074/jbc.M111.225805
18. Russell FM, Hardie DG. AMP-activated protein kinase: do we need activators or inhibitors to treat or prevent cancer? *Int J Mol Sci.* (2020) 22:186. doi: 10.3390/ijms22010186
19. Chae YK, Arya A, Malecek MK, Shin DS, Carneiro B, Chandra S, et al. Repurposing metformin for cancer treatment: current clinical studies. *Oncotarget.* (2016) 7:40767–80. doi: 10.18632/oncotarget.8194
20. Kheirandish M, Mahboobi H, Yazdanparast M, Kamal W, Kamal MA. Anti-cancer effects of metformin: recent evidences for its role in prevention and treatment of cancer. *Curr Drug Metab.* (2018) 19:793–7. doi: 10.2174/1389200219666180416161846
21. Aljofan M, Riethmacher D. Anticancer activity of metformin: a systematic review of the literature. *Future Sci OA.* (2019) 5:FSO410. doi: 10.2144/fsoa-2019-0053
22. Liang J, Mills GB. AMPK: a contextual oncogene or tumor suppressor? *Cancer Res.* (2013) 73:2929–35. doi: 10.1158/0008-5472.CAN-12-3876
23. Vara-Ciruelos D, Russell FM, Hardie DG. The strange case of AMPK and cancer: Dr Jekyll or Mr Hyde? (dagger). *Open Biol.* (2019) 9:190099. doi: 10.1098/rsob.190099
24. Samuel SM, Varghese E, Kubatka P, Triggle CR, Busselberg D. Metformin: the answer to cancer in a flower? Current knowledge and future prospects of metformin as an anti-cancer agent in breast cancer. *Biomolecules.* (2019) 9:846. doi: 10.3390/biom9120846
25. Hoffman RK, Kim BJ, Shah PD, Carver J, Ky B, Ryeom S. Damage to cardiac vasculature may be associated with breast cancer treatment-induced cardiotoxicity. *Cardiooncology.* (2021) 7:15. doi: 10.1186/s40959-021-00100-3
26. van der Pal HJ, van Dalen EC, Hauptmann M, Kok WE, Caron HN, van den Bos C, et al. Cardiac function in 5-year survivors of childhood cancer: a long-term follow-up study. *Arch Intern Med.* (2010) 170:1247–255. doi: 10.1001/archinternmed.2010.233
27. Maeda M. Late effects of childhood cancer: life-threatening issues. *J Nippon Med Sch.* (2008) 75:320–4. doi: 10.1272/jnms.75.320
28. Mancilla TR, Iskra B, Aune GJ. Doxorubicin-induced cardiomyopathy in children. *Comprehens Physiol.* (2019) 9:905–31. doi: 10.1002/cphy.c180017
29. Link G, Tirosh R, Pinson A, Hershko C. Role of iron in the potentiation of anthracycline cardiotoxicity: identification of heart cell mitochondria as a major site of iron-anthracycline interaction. *J Lab Clin Med.* (1996) 127:272–8. doi: 10.1016/S0022-2143(96)90095-5
30. Songbo M, Lang H, Xinyong C, Bin X, Ping Z, Liang S. Oxidative stress injury in doxorubicin-induced cardiotoxicity. *Toxicol Lett.* (2019) 307:41–8. doi: 10.1016/j.toxlet.2019.02.013
31. Yen HC, Oberley TD, Vichitbandha S, Ho YS, St Clair. D. K. The protective role of manganese superoxide dismutase against adriamycin-induced acute cardiac toxicity in transgenic mice. *J Clin Investig.* (1996) 98:1253–60. doi: 10.1172/JCI118909
32. Siveski-Iliskovic N, Hill M, Chow DA, Singal PK. Probucol protects against adriamycin cardiomyopathy without interfering with its antitumor effect. *Circulation.* (1995) 91:10–15. doi: 10.1161/01.CIR.91.1.10
33. Sun X, Zhou Z, Kang YJ. Attenuation of doxorubicin chronic toxicity in metallothionein-overexpressing transgenic mouse heart. *Cancer Res.* (2001) 61:3382–7.
34. Gianni L, Herman EH, Lipshultz SE, Minotti G, Sarvazyan N, Sawyer DB. Anthracycline cardiotoxicity: from bench to bedside. *J Clin Oncol.* (2008) 26:3777–84. doi: 10.1200/JCO.2007.14.9401
35. Ladas EJ, Jacobson JS, Kennedy DD, Teel K, Fleischauer A, Kelly KM. Antioxidants and cancer therapy: a systematic review. *J Clin Oncol.* (2004) 22:517–28. doi: 10.1200/JCO.2004.03.086
36. Kalyanaraman B. Teaching the basics of the mechanism of doxorubicin-induced cardiotoxicity: have we been barking up the wrong tree? *Redox Biol.* (2020) 29:101394. doi: 10.1016/j.redox.2019.101394
37. Ichikawa Y, Ghanefar M, Bayeva M, Wu R, Khechaduri A, Naga Prasad SV, et al. Cardiotoxicity of doxorubicin is mediated through mitochondrial iron accumulation. *J Clin Investig.* (2014) 124:617–30. doi: 10.1172/JCI72931
38. Tadokoro T, Ikeda M, Ide T, Deguchi H, Ikeda S, Okabe K, et al. Mitochondria-dependent ferroptosis plays a pivotal role in doxorubicin cardiotoxicity. *JCI Insight.* (2020) 5:e132747. doi: 10.1172/jci.insight.132747
39. Wallace KB, Sardao VA, Oliveira PJ. Mitochondrial determinants of doxorubicin-induced cardiomyopathy. *Circ Res.* (2020) 126:926–41. doi: 10.1161/CIRCRESAHA.119.314681
40. Lebrecht D, Kokkori A, Ketelsen UP, Setzer B, Walker UA. Tissue-specific mtDNA lesions and radical-associated mitochondrial dysfunction in human hearts exposed to doxorubicin. *J Pathol.* (2005) 207:436–44. doi: 10.1002/path.1863
41. Varga ZV, Ferdinandy P, Liaudet L, Pacher P. Drug-induced mitochondrial dysfunction and cardiotoxicity. *Am J Physiol Heart Circ Physiol.* (2015) 309:H1453–67. doi: 10.1152/ajpheart.00554.2015
42. Pommier Y, Leo E, Zhang H, Marchand C. DNA topoisomerases and their poisoning by anticancer and antibacterial drugs. *Chem Biol.* (2010) 17:421–33. doi: 10.1016/j.chembiol.2010.04.012
43. Thorn CF, Oshiro C, Marsh S, Hernandez-Boussard T, McLeod H, Klein TE, et al. Doxorubicin pathways: pharmacodynamics and adverse effects. *Pharmacogenet Genomics.* (2011) 21:440–6. doi: 10.1097/FPC.0b013e32833ffb56
44. Marinello J, Delcuratolo M, Capranico G. Anthracyclines as topoisomerase ii poisons: from early studies to new perspectives. *Int J Mol Sci.* (2018) 19:3480. doi: 10.3390/ijms19113480
45. Zhang S, Liu X, Bawa-Khalfe T, Lu LS, Lyu YL, Liu LF, et al. Identification of the molecular basis of doxorubicin-induced cardiotoxicity. *Nat Med.* (2012) 18:1639–42. doi: 10.1038/nm.2919
46. Deng S, Yan T, Jendrny C, Nemecek A, Vincetic M, Godtel-Armbrust U, et al. Dexrazoxane may prevent doxorubicin-induced DNA damage via depleting both topoisomerase II isoforms. *BMC Cancer.* (2014) 14:842. doi: 10.1186/1471-2407-14-842
47. Kobayashi S, Volden P, Timm D, Mao K, Xu X, Liang Q. Transcription factor GATA4 inhibits doxorubicin-induced autophagy and cardiomyocyte death. *J Biol Chem.* (2010) 285:793–804. doi: 10.1074/jbc.M109.070037
48. Xu X, Chen K, Kobayashi S, Timm D, Liang Q. Resveratrol attenuates doxorubicin-induced cardiomyocyte death via inhibition of p70 S6 kinase 1-mediated autophagy. *J Pharmacol Exp Ther.* (2012) 341:183–95. doi: 10.1124/jpet.111.189589
49. Ding Y, Sun X, Xu X. TOR-autophagy signaling in adult zebrafish models of cardiomyopathy. *Autophagy.* (2012) 8:142–3. doi: 10.4161/auto.8.1.18536
50. Zhu W, Soonpaa MH, Chen H, Shen W, Payne RM, Liechty EA, et al. Acute doxorubicin cardiotoxicity is associated with p53-induced inhibition of the mammalian target of rapamycin pathway. *Circulation.* (2009) 119:99–106. doi: 10.1161/CIRCULATIONAHA.108.799700
51. Sishi BJ, Loos B, van Rooyen J, Engelbrecht AM. Autophagy upregulation promotes survival and attenuates doxorubicin-induced cardiotoxicity. *Biochem Pharmacol.* (2013) 85:124–34. doi: 10.1016/j.bcp.2012.10.005
52. Kawaguchi T, Takemura G, Kanamori H, Takeyama T, Watanabe T, Morishita K, et al. Prior starvation mitigates acute doxorubicin cardiotoxicity through restoration of autophagy in affected cardiomyocytes. *Cardiovasc Res.* (2012) 96:456–65. doi: 10.1093/cvr/cvs282
53. Li DL, Wang ZV, Ding G, Tan W, Luo X, Criollo A, et al. Doxorubicin blocks cardiomyocyte autophagic flux by inhibiting lysosome acidification. *Circulation.* (2016) 133:1668–87. doi: 10.1161/CIRCULATIONAHA.115.017443
54. Xiao B, Hong L, Cai X, Mei S, Zhang P, Shao L. The true colors of autophagy in doxorubicin-induced cardiotoxicity. *Oncol Lett.* (2019) 18:2165–72. doi: 10.3892/ol.2019.10576
55. Montalvo RN, Doerr V, Kwon OS, Talbert EE, Yoo JK, Hwang MH, et al. Protection against doxorubicin-induced cardiac dysfunction is not maintained following prolonged autophagy inhibition. *Int J Mol Sci.* (2020) 21:8105. doi: 10.3390/ijms21218105

56. Solem LE, Henry TR, Wallace KB. Disruption of mitochondrial calcium homeostasis following chronic doxorubicin administration. *Toxicol Appl Pharmacol.* (1994) 129:214–22. doi: 10.1006/taap.1994.1246
57. Hasinoff BB, Schnabl KL, Marusak RA, Patel D, Huebner E. Dexrazoxane (ICRF-187) protects cardiac myocytes against doxorubicin by preventing damage to mitochondria. *Cardiovasc Toxicol.* (2003) 3:89–99. doi: 10.1385/CT:3:2:89
58. Carvalho RA, Sousa RP, Cadete VJ, Lopaschuk GD, Palmeira CM, Bjork JA, et al. Metabolic remodeling associated with subchronic doxorubicin cardiomyopathy. *Toxicology.* (2010) 270:92–8. doi: 10.1016/j.tox.2010.01.019
59. Koleini N, Kardami E. Autophagy and mitophagy in the context of doxorubicin-induced cardiotoxicity. *Oncotarget.* (2017) 8:46663–80. doi: 10.18632/oncotarget.16944
60. Hoshino A, Mita Y, Okawa Y, Ariyoshi M, Iwai-Kanai E, Ueyama T, et al. Cytosolic p53 inhibits Parkin-mediated mitophagy and promotes mitochondrial dysfunction in the mouse heart. *Nat Commun.* (2013) 4:2308. doi: 10.1038/ncomms3308
61. Yin J, Guo J, Zhang Q, Cui L, Zhang L, Zhang T, et al. Doxorubicin-induced mitophagy and mitochondrial damage is associated with dysregulation of the PINK1/parkin pathway. *Toxicol In Vitro.* (2018) 51:1–10. doi: 10.1016/j.tiv.2018.05.001
62. Catanzaro MP, Weiner A, Kaminaris A, Li C, Cai F, Zhao F, et al. Doxorubicin-induced cardiomyocyte death is mediated by unchecked mitochondrial fission and mitophagy. *FASEB J.* (2019) 33:11096–108. doi: 10.1096/fj.201802663R
63. Ludke AR, Al-Shudiefat AA, Dhingra S, Jassal DS, Singal PK. A concise description of cardioprotective strategies in doxorubicin-induced cardiotoxicity. *Can J Physiol Pharmacol.* (2009) 87:756–63. doi: 10.1139/Y09-059
64. Smith LA, Cornelius VR, Plummer CJ, Levitt G, Verrill M, Canney P, et al. Cardiotoxicity of anthracycline agents for the treatment of cancer: systematic review and meta-analysis of randomised controlled trials. *BMC Cancer.* (2010) 10:337. doi: 10.1186/1471-2407-10-337
65. Fukuda A, Tahara K, Hane Y, Matsui T, Sasaoka S, Hatahira H, et al. Comparison of the adverse event profiles of conventional and liposomal formulations of doxorubicin using the FDA adverse event reporting system. *PLoS ONE.* (2017) 12:e0185654. doi: 10.1371/journal.pone.0185654
66. Bansal N, Adams MJ, Ganatra S, Colan SD, Aggarwal S, Steiner R, et al. Strategies to prevent anthracycline-induced cardiotoxicity in cancer survivors. *Cardiooncology.* (2019) 5:18. doi: 10.1186/s40959-019-0054-5
67. Swain SM, Whaley FS, Gerber MC, Weisberg S, York M, Spicer D, et al. Cardioprotection with dexrazoxane for doxorubicin-containing therapy in advanced breast cancer. *J Clin Oncol.* (1997) 15:1318–32. doi: 10.1200/JCO.1997.15.4.1318
68. Seif AE, Walker DM, Li Y, Huang YS, Kavcic M, Torp K, et al. Dexrazoxane exposure and risk of secondary acute myeloid leukemia in pediatric oncology patients. *Pediatr Blood Cancer.* (2015) 62:704–9. doi: 10.1002/pbc.25043
69. Bailey CJ. Metformin: historical overview. *Diabetologia.* (2017) 60:1566–76. doi: 10.1007/s00125-017-4318-z
70. Rena G, Hardie DG, Pearson ER. The mechanisms of action of metformin. *Diabetologia.* (2017) 60:1577–85. doi: 10.1007/s00125-017-4342-z
71. Fujita Y, Inagaki N. Metformin: clinical topics and new mechanisms of action. *Diabetol Int.* (2017) 8:4–6. doi: 10.1007/s13340-016-0300-0
72. Varjabedian L, Bourji M, Pourafkari L, Nader ND. Cardioprotection by metformin: beneficial effects beyond glucose reduction. *Am J Cardiovasc Drugs.* (2018) 18:181–93. doi: 10.1007/s40256-018-0266-3
73. Eurich DT, McAlister FA, Blackburn DF, Majumdar SR, Tsuyuki RT, Varney J, et al. Benefits and harms of antidiabetic agents in patients with diabetes and heart failure: systematic review. *BMJ.* (2007) 335:497. doi: 10.1136/bmj.39314.620174.80
74. Johnson JA, Majumdar SR, Simpson SH, Toth EL. Decreased mortality associated with the use of metformin compared with sulfonylurea monotherapy in type 2 diabetes. *Diabetes Care.* (2002) 25:2244–8. doi: 10.2337/diacare.25.12.2244
75. Nesti L, Natali A. Metformin effects on the heart and the cardiovascular system: a review of experimental and clinical data. *Nutr Metab Cardiovasc Dis.* (2017) 27:657–69. doi: 10.1016/j.numecd.2017.04.009
76. Xu X, Lu Z, Fassett J, Zhang P, Hu X, Liu X, et al. Metformin protects against systolic overload-induced heart failure independent of AMP-activated protein kinase alpha2. *Hypertension.* (2014) 63:723–8. doi: 10.1161/HYPERTENSIONAHA.113.02619
77. Tzanavari T, Varela A, Theocharis S, Ninou E, Kapelouzou A, Cokkinos DV, et al. Metformin protects against infection-induced myocardial dysfunction. *Metabolism.* (2016) 65:1447–58. doi: 10.1016/j.metabol.2016.06.012
78. Soraya H, Clanachan AS, Rameshrad M, Maleki-Dizaji N, Ghazi-Khansari M, Garjani A. Chronic treatment with metformin suppresses toll-like receptor 4 signaling and attenuates left ventricular dysfunction following myocardial infarction. *Eur J Pharmacol.* (2014) 737:77–84. doi: 10.1016/j.ejphar.2014.05.003
79. Loi H, Boal F, Tronchere H, Cinato M, Kramar S, Oleshchuk O, et al. Metformin protects the heart against hypertrophic and apoptotic remodeling after myocardial infarction. *Front Pharmacol.* (2019) 10:154. doi: 10.3389/fphar.2019.00154
80. Yu JM, Hsieh MC, Qin L, Zhang J, Wu SY. Metformin reduces radiation-induced cardiac toxicity risk in patients having breast cancer. *Am J Cancer Res.* (2019) 9:1017–026.
81. Zi F, Zi H, Li Y, He J, Shi Q, Cai Z. Metformin and cancer: an existing drug for cancer prevention and therapy. *Oncol Lett.* (2018) 15:683–90. doi: 10.3892/ol.2017.7412
82. Mallik R, Chowdhury TA. Metformin in cancer. *Diabetes Res Clin Pract.* (2018) 143:409–19. doi: 10.1016/j.diabres.2018.05.023
83. Pacal L, Kankova K. Metformin in oncology - how far is its repurposing as an anticancer drug? *Klin Onkol.* (2020) 33:107–13. doi: 10.14735/amko2020107
84. Berstein LM, Boyarkina MP, Teslenko SY. Familial diabetes is associated with reduced risk of cancer in diabetic patients: a possible role for metformin. *Med Oncol.* (2012) 29:1308–13. doi: 10.1007/s12032-011-9840-0
85. Evans JM, Donnelly LA, Emslie-Smith AM, Alessi DR, Morris AD. Metformin and reduced risk of cancer in diabetic patients. *BMJ.* (2005) 330:1304–5. doi: 10.1136/bmj.38415.708634.F7
86. Currie CJ, Poole CD, Jenkins-Jones S, Gale EA, Johnson JA, Morgan CL. Mortality after incident cancer in people with and without type 2 diabetes: impact of metformin on survival. *Diabetes Care.* (2012) 35:299–304. doi: 10.2337/dc11-1313
87. Libby G, Donnelly LA, Donnan PT, Alessi DR, Morris AD, Evans JM. New users of metformin are at low risk of incident cancer: a cohort study among people with type 2 diabetes. *Diabetes Care.* (2009) 32:1620–5. doi: 10.2337/dc08-2175
88. Tseng CH. Metformin is associated with a lower incidence of benign brain tumors: a retrospective cohort study in patients with type 2 diabetes mellitus. *Biomolecules.* (2021) 11:1405. doi: 10.3390/biom11101405
89. Tseng CH. Metformin and risk of malignant brain tumors in patients with type 2 diabetes mellitus. *Biomolecules.* (2021) 11:578831. doi: 10.3389/fphar.2020.578831
90. Reni M, Dugnani E, Cereda S, Belli C, Balzano G, Nicoletti R, et al. (Ir)relevance of metformin treatment in patients with metastatic pancreatic cancer: an open-label, randomized phase ii trial. *Clin Cancer Res.* (2016) 22:1076–85. doi: 10.1158/1078-0432.CCR-15-1722
91. Zheng Y, Zhu J, Zhang H, Liu Y, Sun H. Metformin plus first-line chemotherapy versus chemotherapy alone in the treatment of epithelial ovarian cancer: a prospective open-label pilot trial. *Cancer Chemother Pharmacol.* (2019) 84:1349–57. doi: 10.1007/s00280-019-03963-7
92. Nanni O, Amadori D, De Censi A, Rocca A, Freschi A, Bologna A, et al. Metformin plus chemotherapy versus chemotherapy alone in the first-line treatment of HER2-negative metastatic breast cancer. The MYME randomized, phase 2 clinical trial. *Breast Cancer Res Treat.* (2019) 174:433–42. doi: 10.1007/s10549-018-05070-2
93. Trucco M, Barredo JC, Goldberg J, Leclerc GM, Hale GA, Gill J, et al. A phase I window, dose escalating and safety trial of metformin in combination with induction chemotherapy in relapsed refractory acute lymphoblastic leukemia: metformin with induction chemotherapy of vincristine, dexamethasone, PEG-asparaginase, and doxorubicin. *Pediatr Blood Cancer.* (2018) 65:e27224. doi: 10.1002/pbc.27224
94. Li Y, Wang M, Zhi P, You J, Gao JQ. Metformin synergistically suppress tumor growth with doxorubicin and reverse drug resistance by inhibiting the

expression and function of P-glycoprotein in MCF7/ADR cells and xenograft models. *Oncotarget.* (2018) 9:2158–174. doi: 10.18632/oncotarget.23187
95. Pateliya B, Burade V, Goswami S. Enhanced antitumor activity of doxorubicin by naringenin and metformin in breast carcinoma: an experimental study. *Naunyn Schmiedebergs Arch Pharmacol.* (2021) 394:1949–61. doi: 10.1007/s00210-021-02104-3
96. Viollet B, Guigas B, Sanz Garcia N, Leclerc J, Foretz M, Andreelli F. Cellular and molecular mechanisms of metformin: an overview. *Clin Sci.* (2012) 122:253–70. doi: 10.1042/CS20110386
97. Cho SY, Lee HJ, Lee HJ, Jung DB, Kim H, Sohn EJ, et al. Activation of AMP-activated protein kinase alpha and extracelluar signal-regulated kinase mediates CB-PIC-induced apoptosis in hypoxic SW620 colorectal cancer cells. *Evid Based Complement Altern Med.* (2013) 2013:974313. doi: 10.1155/2013/974313
98. Sosnicki S, Kapral M, Weglarz L. Molecular targets of metformin antitumor action. *Pharmacol Rep.* (2016) 68:918–25. doi: 10.1016/j.pharep.2016.04.021
99. Malinowski B, Musiala N, Wicinski M. Metformin's modulatory effects on miRNAs function in cancer stem cells-a systematic review. *Cells.* (2020) 9:1401. doi: 10.3390/cells9061401
100. Lan B, Zhang J, Zhang P, Zhang W, Yang S, Lu D, et al. Metformin suppresses CRC growth by inducing apoptosis via ADORA1. *Front Biosci.* (2017) 22:248–57. doi: 10.2741/4484
101. Karadeniz Z, Aynacioglu AS, Bilir A, Tuna MY. Inhibition of midkine by metformin can contribute to its anticancer effects in malignancies: a proposal mechanism of action of metformin in context of endometrial cancer prevention and therapy. *Med Hypotheses.* (2020) 134:109420. doi: 10.1016/j.mehy.2019.109420
102. Sharma P, Kumar S. Metformin inhibits human breast cancer cell growth by promoting apoptosis via a ROS-independent pathway involving mitochondrial dysfunction: pivotal role of superoxide dismutase (SOD). *Cell Oncol.* (2018) 41:637–650. doi: 10.1007/s13402-018-0398-0
103. Tsai CC, Chuang TW, Chen LJ, Niu HS, Chung KM, Cheng JT, et al. Increase in apoptosis by combination of metformin with silibinin in human colorectal cancer cells. *World J Gastroenterol.* (2015) 21:4169–77. doi: 10.3748/wjg.v21.i14.4169
104. Ross FA, MacKintosh C, Hardie DG. AMP-activated protein kinase: a cellular energy sensor that comes in 12 flavours. *FEBS J.* (2016) 283:2987–3001. doi: 10.1111/febs.13698
105. Kim M, Shen M, Ngoy S, Karamanlidis G, Liao R, Tian R. AMPK isoform expression in the normal and failing hearts. *J Mol Cell Cardiol.* (2012) 52:1066–73. doi: 10.1016/j.yjmcc.2012.01.016
106. Viollet B, Athea Y, Mounier R, Guigas B, Zarrinpashneh E, Horman S, et al. AMPK: lessons from transgenic and knockout animals. *Front Biosci.* (2009) 14:19–44. doi: 10.2741/3229
107. Day EA, Ford RJ, Steinberg GR. AMPK as a therapeutic target for treating metabolic diseases. *Trends Endocrinol Metab.* (2017) 28:545–60. doi: 10.1016/j.tem.2017.05.004
108. Jeon SM. Regulation and function of AMPK in physiology and diseases. *Exp Mol Med.* (2016) 48:e245. doi: 10.1038/emm.2016.81
109. Li X, Liu J, Lu Q, Ren D, Sun X, Rousselle T, et al. AMPK: a therapeutic target of heart failure-not only metabolism regulation. *Biosci Rep.* (2019) 39:BSR20181767. doi: 10.1042/BSR20181767
110. Gundewar S, Calvert JW, Jha S, Toedt-Pingel I, Ji SY, Nunez D, et al. Activation of AMP-activated protein kinase by metformin improves left ventricular function and survival in heart failure. *Circ Res.* (2009) 104:403–411. doi: 10.1161/CIRCRESAHA.108.190918
111. Zarrinpashneh E, Carjaval K, Beauloye C, Ginion A, Mateo P, Pouleur AC, et al. Role of the alpha2-isoform of AMP-activated protein kinase in the metabolic response of the heart to no-flow ischemia. *Am J Physiol Heart Circ Physiol.* (2006) 291:H2875–83. doi: 10.1152/ajpheart.01032.2005
112. Xie Z, Lau K, Eby B, Lozano P, He C, Pennington B, et al. Improvement of cardiac functions by chronic metformin treatment is associated with enhanced cardiac autophagy in diabetic OVE26 mice. *Diabetes.* (2011) 60:1770–8. doi: 10.2337/db10-0351
113. Zhang P, Hu X, Xu X, Fassett J, Zhu G, Viollet B, et al. AMP activated protein kinase-alpha2 deficiency exacerbates pressure-overload-induced left ventricular hypertrophy and dysfunction in mice. *Hypertension.* (2008) 52:918–24. doi: 10.1161/HYPERTENSIONAHA.108.114702
114. Myers RW, Guan HP, Ehrhart J, Petrov A, Prahalada S, Tozzo E, et al. Systemic pan-AMPK activator MK-8722 improves glucose homeostasis but induces cardiac hypertrophy. *Science.* (2017) 357:507–11. doi: 10.1126/science.aah5582
115. Arad M, Benson DW, Perez-Atayde AR, McKenna WJ, Sparks EA, Kanter RJ, et al. Constitutively active AMP kinase mutations cause glycogen storage disease mimicking hypertrophic cardiomyopathy. *J Clin Investig.* (2002) 109:357–62. doi: 10.1172/JCI0214571
116. Blair E, Redwood C, Ashrafian H, Oliveira M, Broxholme J, Kerr B, et al. Mutations in the gamma(2) subunit of AMP-activated protein kinase cause familial hypertrophic cardiomyopathy: evidence for the central role of energy compromise in disease pathogenesis. *Hum Mol Genet.* (2001) 10:1215–20. doi: 10.1093/hmg/10.11.1215
117. Ahmad F, Arad M, Musi N, He H, Wolf C, Branco D, et al. Increased alpha2 subunit-associated AMPK activity and PRKAG2 cardiomyopathy. *Circulation.* (2005) 112:3140–8. doi: 10.1161/CIRCULATIONAHA.105.550806
118. Jorgensen SB, Viollet B, Andreelli F, Frosig C, Birk JB, Schjerling P, et al. Knockout of the alpha2 but not alpha1 5'-AMP-activated protein kinase isoform abolishes 5-aminoimidazole-4-carboxamide-1-beta-4-ribofuranosidebut not contraction-induced glucose uptake in skeletal muscle. *J Biol Chem.* (2004) 279:1070–9. doi: 10.1074/jbc.M306205200
119. Timm KN, Tyler DJ. The role of AMPK activation for cardioprotection in doxorubicin-induced cardiotoxicity. *Cardiovasc Drugs Ther.* (2020) 34:255–69. doi: 10.1007/s10557-020-06941-x
120. Chen J, Zhang S, Pan G, Lin L, Liu D, Liu Z, et al. Modulatory effect of metformin on cardiotoxicity induced by doxorubicin via the MAPK and AMPK pathways. *Life Sci.* (2020) 249:117498. doi: 10.1016/j.lfs.2020.117498
121. Izreig S, Gariepy A, Kaymak I, Bridges HR, Donayo AO, Bridon G, et al. Repression of LKB1 by miR-17 approximately 92 sensitizes MYC-dependent lymphoma to biguanide treatment. *Cell Rep Med.* (2020) 1:100014. doi: 10.1016/j.xcrm.2020.100014
122. Laderoute KR, Amin K, Calaoagan JM, Knapp M, Le T, Orduna J, et al. 5'-AMP-activated protein kinase (AMPK) is induced by low-oxygen and glucose deprivation conditions found in solid-tumor microenvironments. *Mol Cell Biol.* (2006) 26:5336–47. doi: 10.1128/MCB.00166-06
123. Phoenix KN, Devarakonda CV, Fox MM, Stevens LE, Claffey KP. AMPKalpha2 suppresses murine embryonic fibroblast transformation and tumorigenesis. *Genes Cancer.* (2012) 3:51–62. doi: 10.1177/1947601912452883
124. Peng M, Darko KO, Tao T, Huang Y, Su Q, He C, et al. Combination of metformin with chemotherapeutic drugs via different molecular mechanisms. *Cancer Treat Rev.* (2017) 54:24–33. doi: 10.1016/j.ctrv.2017.01.005

Conflict of Interest: The authors declare that the research was conducted in the absence of any commercial or financial relationships that could be construed as a potential conflict of interest.

frontiers in Cardiovascular Medicine

REVIEW
published: 07 February 2022
doi: 10.3389/fcvm.2022.813883

New Insights in Early Detection of Anticancer Drug-Related Cardiotoxicity Using Perfusion and Metabolic Imaging

Farah Cadour[1,2], *Franck Thuny*[3] *and Joevin Sourdon*[1,2]*

[1] Aix-Marseille Université, CNRS, CRMBM, Marseille, France, [2] APHM, Hôpital Universitaire Timone, CEMEREM, Marseille, France, [3] Aix-Marseille University, University Mediterranean Center of Cardio-Oncology, Unit of Heart Failure and Valvular Heart Diseases, Department of Cardiology, North Hospital, Assistance Publique - Hôpitaux de Marseille, Centre for CardioVascular and Nutrition Research (C2VN), Inserm 1263, Inrae 1260, Marseille, France

Cardio-oncology requires a good knowledge of the cardiotoxicity of anticancer drugs, their mechanisms, and their diagnosis for better management. Anthracyclines, anti-vascular endothelial growth factor (VEGF), alkylating agents, antimetabolites, anti-human epidermal growth factor receptor (HER), and receptor tyrosine kinase inhibitors (RTKi) are therapeutics whose cardiotoxicity involves several mechanisms at the cellular and subcellular levels. Current guidelines for anticancer drugs cardiotoxicity are essentially based on monitoring left ventricle ejection fraction (LVEF). However, knowledge of microvascular and metabolic dysfunction allows for better imaging assessment before overt LVEF impairment. Early detection of anticancer drug-related cardiotoxicity would therefore advance the prevention and patient care. In this review, we provide a comprehensive overview of the cardiotoxic effects of anticancer drugs and describe myocardial perfusion, metabolic, and mitochondrial function imaging approaches to detect them before over LVEF impairment.

Keywords: cardio-oncology, cardiotoxicity, perfusion, metabolism, mitochondria, magnetic resonance spectroscopy or MRS, magnetic resonance imaging, nuclear imaging

OPEN ACCESS

Edited by:
Feng Cao,
People's Liberation Army General Hospital, China

Reviewed by:
Michele Russo,
University of Turin, Italy
Rohit Moudgil,
Cleveland Clinic, United States

***Correspondence:**
Joevin Sourdon
joevin.sourdon@univ-amu.fr

Specialty section:
This article was submitted to Cardio-Oncology, a section of the journal Frontiers in Cardiovascular Medicine

Received: *12 November 2021*
Accepted: *06 January 2022*
Published: *07 February 2022*

Citation:
Cadour F, Thuny F and Sourdon J (2022) New Insights in Early Detection of Anticancer Drug-Related Cardiotoxicity Using Perfusion and Metabolic Imaging. Front. Cardiovasc. Med. 9:813883. doi: 10.3389/fcvm.2022.813883

INTRODUCTION

Cancer therapy significantly improves patient survival but is sometimes accompanied by cardiotoxic effects. Cardiotoxic complications can range from myocardial abnormalities, valvular abnormalities, pericardial diseases, coronary artery disease (CAD), and alteration in left ventricle ejection fraction (LVEF).

Anthracyclines, one of the most used and oldest chemotherapies, are the archetypal cardiotoxic anticancer drug, ultimately leading to the heart failure (1). In addition, the emerging field of cardio-oncology has seen the development of new anticancer drugs such as antiangiogenics also leading to cardiotoxicity with endothelial dysfunction, forcing a reconsideration of the stages, timing, and levels of cardiotoxicity.

Initial evaluation of LVEF and subsequent evaluation under anticancer therapy is paramount as the most guidelines for cardiotoxicity are based on LVEF impairment (2). To date, echocardiography remains the most frequently used method to detect LVEF alteration, but also

by assessment of left ventricle (LV) longitudinal strain evaluation that might identify early LVEF dysfunction (3). Although not considered the first-line method, cardiac magnetic resonance imaging (CMR) can assess cardiac anatomy, structure, and tissue properties in addition to LVEF.

These modalities have been able to detect impaired cardiac function in the later stages of cardiac side effects (4). Myocardial perfusion imaging and metabolic imaging are powerful approaches providing novel biomarkers that can improve early detection of cardiotoxicity before irreversible cardiac damage occurs. This review summarizes the alterations in cardiac perfusion and metabolism that occur in anticancer drug-related cardiotoxicity and the advantage of assessing perfusion and metabolism non-invasively in the beating heart with cardiac imaging.

MYOCARDIAL VASCULAR AND METABOLIC EFFECTS OF ANTICANCER DRUGS

Overview of the Link Between Myocardial Circulation and Metabolism

There is a close relationship between myocardial blood circulation, which delivers oxygen and nutrients, tissue metabolism, and oxidative stress. The heart has a very high energy demand to sustain contractile function and synthesizes adenosine triphosphate (ATP) through oxidative metabolism of free fatty acids (FFA), glucose, ketones, and lactate (5).

The adult heart normally obtains 50–70% of its ATP from fatty acid β-oxidation in the presence of oxygen. However, it must adapt, switching from one substrate to another, to sustain demand depending upon the metabolic state and physical conditions at the time (5). Under well-perfused aerobic conditions, glucose and FFA are catabolized into pyruvate or acyl-CoA, respectively, both of which are catabolized to acetyl-CoA to enter the tricarboxylic acid (TCA, Krebs) cycle. Most of the energy supply is then derived from the mitochondrial oxidative phosphorylation system. The main cardiac energy reserve is phosphocreatine (PCr), which is maintained by the following creatine kinase (CK) reaction:

$$PCr + ADP + H^{+} \leftrightarrow ATP + Creatine$$

This system facilitates intracellular delivery of energy from mitochondria to cytoplasmic sites of ATP utilization and maintains a high level of ATP during changes in energy demand (6).

Direct damage to the mitochondria, blood supply, and myocardial metabolism will be responsible for abnormal production of reactive oxygen species (ROSs). ROS are reactive intermediates of the molecular oxygen that are essentially generated during mitochondrial oxidative phosphorylation (7). Cellular sources of ROSs are cardiomyocytes, endothelial cells, stromal cells, and inflammatory cells in the heart (8). One of the major ROSs is the proximal mitochondrial ROSs (superoxide anion), which can be generated by a loss of ATP production or when there is a high NADH/NAD^{+} ratio in the mitochondrial matrix (9). An imbalance between ROS production and antioxidant cell response leads to endothelial dysfunction, the release of proinflammatory cytokines, and vasoconstriction of epicardial and microvascular coronary arteries (10). The heart is particularly sensitive to oxidative stress because of its low-antioxidant resources (11–13). One of the main mechanisms of ROS leading to endothelial dysfunction is the uncoupling of endothelial nitric oxide (NO) synthase, which usually facilitates NO production (14), ultimately leading to reduce NO bioavailability. Indeed, the endothelium synthetizes the NO (15), which acts as a vasodilator, an antithrombotic, and an anti-atherosclerotic molecule (14). Endothelial nitric oxide synthase (eNOS) is the type III of NO synthases (NOS) that will lead to NO radicals synthesis from L-arginine and is expressed in endothelial cells. But in the inflammatory situation, the other NO synthases are neuronal NOS (type I) and inducible NOS (iNOS, type II). The latter will be expressed in blood vessels under pathological conditions such as inflammation or oxidative stress (16). Major cell structure and function damages will result reaction of NO with superoxide anion leading to peroxynitrite (17).

Interestingly, initial vascular injury also results in the production of ROSs species derived from NAD(P)H (18). Oxidative inflammation will ultimately cause adventitial fibrosis and smooth muscle hypertrophy (18). The latter phenomenon can also be observed in the media and intima through paracrine effects of adventitial inflammation. As a result, medial layers of vessels do not respond to NO to adapt blood flow and assure normal myocardial perfusion (19), resulting in impaired endothelium-dependent relaxation.

It is important to bear in mind that impaired myocardial perfusion and/or subsequent alteration of metabolic pathways, substrate preferences, and bioenergetics (i.e., reduced PCr/ATP ratio) might contribute to the development of several common cardiovascular diseases (20). For these reasons, perfusion and metabolic imaging are preferred methods to study early vascular and metabolic cardiotoxic effects.

Anticancer Drugs

The vascular and metabolic cardiotoxic effects of the various anticancer drugs are given in **Table 1**.

Anthracyclines

Anthracyclines are a group of chemotherapy broadly used in cancer treatment, with doxorubicin (DOX) being one of the most widely used. Its cardiotoxicity is well-known with cumulative toxicity ultimately leading to permanent cardiac alteration (21). The initial alteration of this end state is thought to be at a microvascular level through ROS production (22–24), with mitochondrial superoxide production increasing with DOX dose (25).

Excessive production of ROS by DOX leads to apoptosis, cardiac function impairment, inflammation, and vascular injury (25, 26). Both the cardiomyocytes and arterial endothelial cells can experience mitochondrial dysfunction under anthracyclines (27, 28). These properties suggest that, in addition to its known direct effect on deoxyribonucleic acid through topoisomerase II beta inhibition (29), endothelial cells injury could be one

TABLE 1 | Myocardial vascular and metabolic effects of common anticancer drugs.

Anticancer drugs	Mechanisms of cardiotoxicity
Anthracyclines	Microcirculation alteration
	Endothelial dysfunction (NO)
	Microcirculation increased thickening
	Altered oxidative metabolism
	Impaired energetics
	ROS
	Mitochondrial dysfunction
Antimetabolites	Vasospasm
	Vasoconstriction
	Endothelial dysfunction (NO)
	Smooth cell dysfunction
	Altered oxidative metabolism
	Impaired energetics
	Mitochondrial dysfunction
	ROS
RTKi	Inhibits angiogenesis
	Endothelial dysfunction (NO)
	Vasoconstriction
	Altered oxidative metabolism
	Myocardial insulin resistance pattern
	Impaired energetics
	ROS
	Mitochondrial dysfunction
Anti-VEGF Ab	Inhibits angiogenesis
	Capillary rarefaction
	Impaired energetics
	ROS
	Mitochondrial dysfunction
Anti-HER2 Ab	Microcirculation alteration (neuregulin 1)
	Disruption of cardioprotective *Neuregulin-1* pathway
	ROS
	Mitochondrial dysfunction
ICI	Microcirculation alteration → vascular sequelae
	Dysregulated myocardial metabolism
Taxanes	Impaired energetics
	Endothelial damage
	Capillary rarefaction
Alkylating agents	Endothelial dysfunction (NO)
	ROS
	Free fatty acids accumulation
	Vasoconstriction
	Mitochondrial dysfunction

Ab, antibody; NO, nitric oxide; ROS, reactive oxygen species.

cause of anthracycline cardiotoxicity. Although anthracyclines cardiotoxicity is usually detected at a stage of altered ejection (21), studies suggest that anthracyclines cardiotoxicity occurs in a continuum, challenging the hypothesis of irreversible cardiac injury (30, 31).

Current guidelines suggest monitoring of patients with cancer undergoing chemotherapy by echocardiography since most definitions of cardiotoxicity are based on LVEF decline (2), but the literature reports microcirculation changes long before any LVEF or contraction alterations occur (31, 32). This myocardial perfusion alteration could be the result of increased arterial walls thickening, which can occur early and even after a single DOX injection (31, 33), but is more overt with repeated injections (33). The increase in intima-media thickness under anthracyclines (34) is in part secondary to oxidative inflammation. Thus, anthracyclines cardiotoxicity appears at the histological level and these microcirculation alterations appear to be an early form of the well-known anthracyclines cardiotoxicity, suggesting modalities to assess the initial endothelial cell damage and better prevent its progression. Moreover, the combination of radiotherapy with anthracyclines potentiates heart damage. Radiotherapy has been reported as responsible for cardiac perfusion defect development, however, myocardial perfusion imaging of the combination of radiotherapy with anthracyclines remains poorly described (32).

Antimetabolites

5-Fluorouracil (5-FU) is a part of antimetabolite agents and is commonly used in the treatment of malignancies. One of the major cardiotoxicities of 5-FU is coronary vasospasm that can lead to ischemia. Its mechanism remains uncertain, with some suggesting an endothelial-dependent mechanism through endothelial dysfunction, but others an endothelium-independent with vasoconstriction of dysfunctional smooth muscle cells (35). Studies in animal models demonstrated that altered erythrocyte metabolism decreases erythrocyte ability to bring oxygen to the myocardium (36, 37). 5-FU reduces oxidative metabolism (38), impairs energetics (38), and induces mitochondrial uncoupling reducing aerobic efficiency (39). At a subcellular level, the toxicity of 5-FU and another antimetabolite drug, the capecitabine, have been shown to be mediated through oxidative stress with ROS generation leading to altered mitochondrial membrane potential in isolated rat cardiomyocytes (40).

Alkylating Agents

One of the main alkylating agents, mostly used in hematologic cancers, is cyclophosphamide, for which dose-mediated cardiotoxicity is one of the notable toxic effects. The metabolites of cyclophosphamide reported to be involved in cardiotoxicity are acrolein and 4-hydroxy-cyclophosphamide. These metabolites are involved in ROS generation (41, 42) that damage mitochondrial membrane by decreasing its detoxifying capacity, but also by disrupting normal vasotone response pathway through NO reduction or an increase in the vasoconstrictor endothelin-1 (23). In addition, cyclophosphamide is responsible for FFA accumulation and reduction of ATP production resulting in the release of proinflammatory cytokines (41). Cardiac microscopic findings of alkylating agents consist of interstitial damages, myocardial necrosis, vacuolar changes, and intramural changes in small coronary vessels (43). Similar

disturbances have also been reported with cisplatin-based chemotherapy, another alkylating agent (44).

Taxanes

Taxanes are antimicrotubules whose main cardiotoxicity is disruption of cardiac rhythm and conduction. Heart failure (possibly in combination with DOX), ischemia, and microvascular rarefaction because of the endothelial damage might also occur (45).

Receptor Tyrosine Kinase Inhibitors

Receptor tyrosine kinase inhibitors (RTKi) include sorafenib, pazopanib, and sunitinib. As a part of antiangiogenic therapy, RTKi inhibits the tyrosine kinase activity of the vascular endothelial growth factor (VEGF) receptor, thereby blocking the VEGF pathway, but also platelet-derived growth factor receptors and c-kit (46). Oxidative stress and dysregulation of NO signaling have been proposed to mediate RTKi-induced hypertension, as they are known to be involved in the VEGF pathway (47, 48). However, sunitinib-induced hypertension has been associated with upregulation of the endothelin peptide (49–51), a potent vasconstrictor known to induce cardiac endothelial dysfunction (52). Experimental studies investigating the effects of VEGFR blockade on cardiac microvasculature did not reveal any changes in the number of capillaries (50, 53). Nevertheless, sunitinib induces a loss of coronary microvascular pericytes in mice (53), which might explain the impaired coronary flow reserve (CFR) of sunitnib-induced cardiotoxicity (49, 53).

Carbohydrate metabolism is altered in the myocardium of sunitinib-treated mice, which exhibits higher glucose uptake, higher gene expression of pyruvate dehydrogenase kinase, and of the pyruvate kinase isoform 2 (54), a signature of fetal myocardium in which the metabolism is mostly anaerobic. The sensor of cardiac energetic metabolism, AMP-activated protein kinase, is inhibited by sunitinib (55). Energy impairment because of the loss of mitochondrial membrane potential resulting in reduced ATP has been reported in the early stages of sunitinib-treated cardiomyocytes (56).

In a comparative study, only sorafenib among others RTKi directly impaired mitochondrial function and oxidative metabolism at clinically concentrations (57), but ROS generation was documented in several RTKi-treated myocardium (58, 59).

Anti-vascular Endothelial Growth Factor (VEGF) Monoclonal Antibody

Another antiangiogenic approach consists of blocking VEGF with a humanized monoclonal antibody, which traps endogenous VEGF and inhibits its binding with the receptor. Bevacizumab was the first anti-VEGF antibody with a rate of sytemic hypertension as high as 70%, probably because of the vascular resistance, endothelial dysfunction, and capillary rarefection (39). Bevacizumab induces mitochondrial dysfunction plus ROS formation in isolated rat heart (60, 61) and in isolated cardiomyocytes (62).

Anti-human Epidermal Growth Factor Receptor (HER 2)

Human epidermal growth factor receptor 2 is a receptor that promotes cell growth, proliferation, and repair in the body. Tumors can hijack these functions to proliferate. Therefore, one treatment option is to specifically target this receptor, with anti-HER2 therapy, led by Trastuzumab, which has revolutionized the treatment and prognostic of patients with HER2 positive breast cancer (63). Trastuzumab will result in ROS production, mitochondrial dysfunction, and proapoptotic signals release in cardiomyocytes (64). Unlike anthracyclines, cardiotoxicity of anti-HER2 is dose-independent and often reversible. However, it results in greater cardiotoxicity in the presence of or after anthracyclines (65).

Anti-HER2 might cause cardiomyocyte damage by disrupting the neuregulin-1 axis that normally activates protective pathways in response to stress (66), which could lead to LVEF decrease. Neuregulin-1 is a cardioactive growth factor that normally participates in the dimerization of HER receptors on cardiomyocytes to provide cell protection. However, the fact that neuregulin-1 is released from the endothelial cells in the heart leads to the question of whether the impaired LVEF is due to a direct impact of anti-HER2 on cardiomyocytes or an indirect impact *via* endothelial cells of the altered coronary microvasculature (67). Interestingly, a decrease in neuregulin-1 levels has been associated with CAD (68). The same neuregulin-1/HER pathway may also explain the increased susceptibility to anthracyclines cardiotoxicity when the two treatments are combined.

Immune Checkpoint Inhibitors (ICIs)

Immune checkpoint inhibitors are monoclonal antibodies that restore antitumor immunity by targeting inhibitory receptors on the lymphocytes surface, such as cytotoxic T-lymphocyte-associated protein 4, programmed cell death receptor 1 (PD1), and its ligand. By reactivating the immune response against the tumor, ICIs can lead to immune-related cardiovascular adverse events that, although rare, present a case-fatality rate as high as 50% (69). The most-reported cardiac complications of ICIs are ICI-induced myocarditis but also pericardial diseases, cardiomyopathy, myocardial fibrosis, and acute heart failure (70). Microvascular damage leading to vascular sequelae has also been reported with ICI (10). Furthermore, studies are needed to explore all the different pathways involved in the cardiotoxicity of ICIs with possible yet unknown microcirculation damage. A recent *in vivo* study in mice showed that anti-PD1 drugs cause myocardial dysfunction and altered myocardial metabolism, suggesting damage at a subcellular level (71).

IMAGING

Imaging modalities in cardio-oncology and their assessment of anticancer-drug-related cardiotoxicity are given in **Figure 1**.

Perfusion Imaging

Perfusion imaging involves assessing the delivery of oxygen and nutrients to tissues through blood flow. It aims to describe

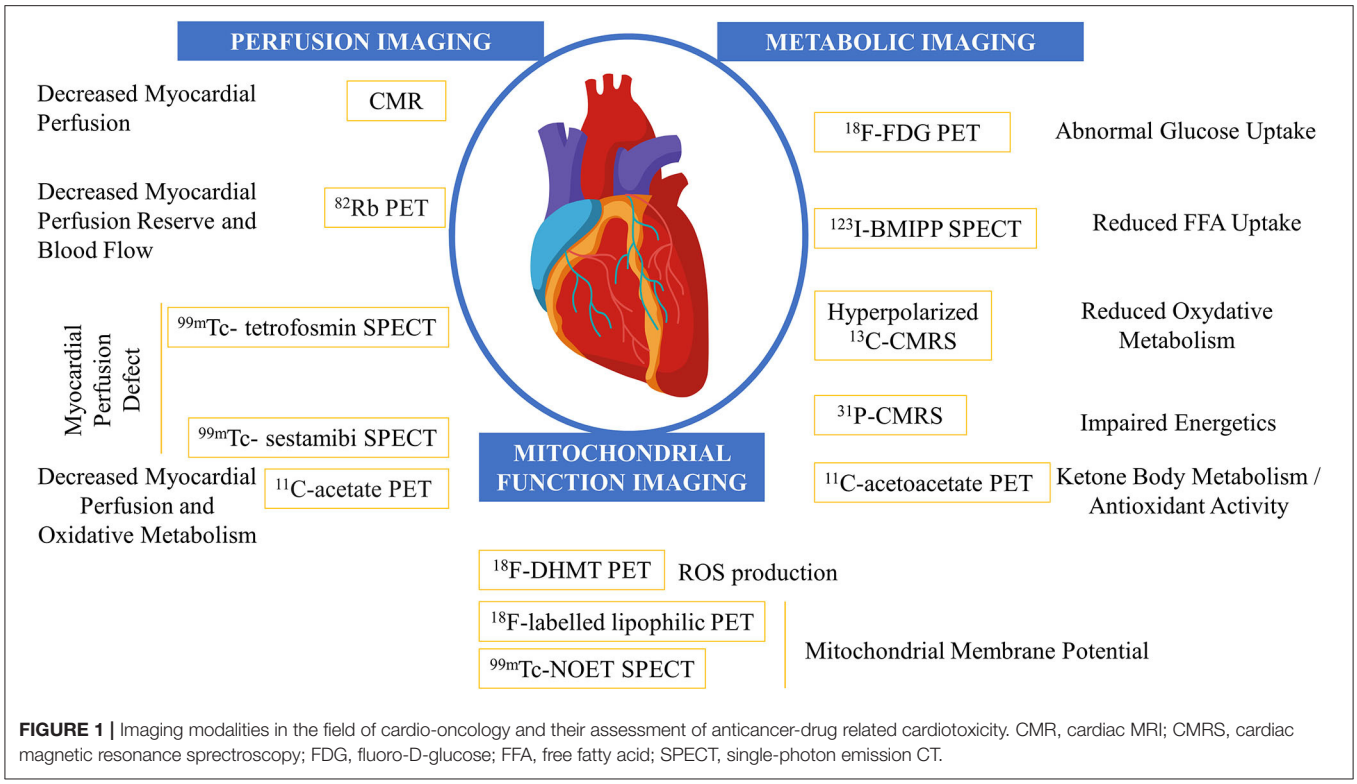

FIGURE 1 | Imaging modalities in the field of cardio-oncology and their assessment of anticancer-drug related cardiotoxicity. CMR, cardiac MRI; CMRS, cardiac magnetic resonance sprectroscopy; FDG, fluoro-D-glucose; FFA, free fatty acid; SPECT, single-photon emission CT.

microvasculature that can be altered under the effect of anticancer drugs. Since 1997, Hasdai et al. reported that coronary endothelial dysfunction may be associated with myocardial perfusion defects (72). Both radiotherapy and chemotherapy have shown to be associated with microvascular dysfunction (2), although the effect of non-radiation therapies on the latter is less well-described (31). Knowing the effects of anticancer drugs on myocardial microcirculation, myocardial perfusion imaging appears to be an attractive modality to detect anticancer drug-related myocardial toxicity. Moreover, by the time cardiotoxicity-associated LV dysfunction is detectable by echocardiography, it is often too late, emphasizing the need to assess the initial microvasculature dysfunction to better prevent it.

Symptomatic oxygen supply-demand mismatch can be evaluated invasively by invasive coronary angiography (ICA), but myocardial microcirculation disturbance can occur before any visible epicardial coronary on ICA (73), requiring blood flow measurements to assess myocardial function. Myocardial malperfusion can be unmasked through fractional flow reserve (FFR), which is an invasive measurement under hyperemia to determine the significance of an epicardial coronary artery stenosis, with an FFR $\leq$ 0.80 considered to be ischemia prone (74), and defined as the ratio of maximal blood flow distal to proximal to the stenosis. The invasive measurement of CFR is intended to study the vascular bed and describe the myocardial reserve capacity for vasodilatation, and is defined as the ratio of maximal hyperemic to the resting coronary blood flow (75).

Another interesting measure to evaluate coronary microvascular dysfunction is the index of microcirculatory resistance (IMR) (76) which is an index of coronary microvasculature and considered as abnormal if $\geq$25 independently of epicardial stenosis (77). However, these different parameters remain invasive, which could explain their low use in clinical practice for monitoring patients undergoing anticancer therapy, and should be discussed with respect to non-invasive techniques for the assessment of myocardial perfusion, which we review here.

Nuclear Imaging

Nuclear imaging techniques include single-photon emission computerized tomography (SPECT) and PET. These techniques are based on the detection of radioactive gamma rays and photons (after positrons annihilation) from an injected radioactive compound, respectively.

Single-Photon Emission CT (SPECT)

Impairment of epicardial arteries vasodilatation, by evaluation of change in coronary diameters under pharmacological stress, has been reported after DOX infusions on CT angiography suggesting dysfunction of smooth cells and the microvascular bed (78). However, the resolution of cardiac CT is insufficient to visually assess microvessels, underlining the need for cardiac perfusion CT to assess myocardial microcirculation by detecting hypoperfused territories. Coupling of metabolic information by traditional radiotracers ^{201}Tl-chloride, ^{99m}Tc- sestamibi, and ^{99m}Tc- tetrofosmin, is obtained by myocardial perfusion SPECT. SPECT is performed at rest and under stress, which can be achieved by exercise or pharmacologically with vasodilators (79).

The added value of SPECT is that the radiotracers will be delivered to the myocardium in proportion to flow and therefore be able to unmask a myocardial perfusion defect secondary to CAD. Territories with myocardial perfusion abnormalities may not only be secondary to CAD but reflect the myocardial cardiotoxicity at a microvascular level.

Studies have reported increased perfusion defects in DOX-treated patients with a history of radiotherapy (32, 80). Galluci et al., have suggested myocardial perfusion abnormalities, assessed by SPECT, without LVEF dysfunction in patients who had undergone chemotherapy and radiotherapy (32). However, this observational study could not strictly conclude that the findings were only due to the chemotherapy because of the lack of a control group before cancer treatment, and because of the inclusion of patients with a history of radiotherapy.

Some studies described LVEF dysfunction after the introduction of DOX in patients with cancer (81), but there are very little data on the incidence of SPECT perfusion defect in patients under DOX alone. One study on 36 patients with breast carcinoma evaluated before and after anthracyclines found no significant perfusion defect after anthracyclines (34), leaving the question of myocardial perfusion monitoring with ^{99m}Tc-sestamibi SPECT subject open to debate.

Positron Emission Tomography

Compared with SPECT, PET allows assessment of myocardial blood flow with better spatial resolution and sensitivity. CFR can be quantified as the ratio of myocardial blood flow between stress and rest on PET (82). The most commonly used and validated radionuclide for cardiac perfusion evaluation is rubidium-82 (^{82}Rb) (82). Although ^{82}Rb PET is often used for semiquantitative myocardial perfusion, it may assess coronary microvascular function by absolute quantification of myocardial perfusion and myocardial perfusion (or flow) reserve (MPR) (83). MPR is the ratio of stress flow to resting flow and describes the capacity of the coronary bed to maximize flow (84).

Myocardial perfusion reserve has been reported to be decreased after DOX exposure, representing a possible early marker of DOX myocardial cardiotoxicity (85). Detection of changes in mitochondrial function, estimation of myocardial blood flow and myocardial oxygen consumption, and thus, the ability of coronary arteries to respond to stress, can also be assessed by ^{11}C-acetate rest stress PET. Using the latter, a decrease in myocardial perfusion and oxygen consumption reserve in DOX-treated rats compared with the control animals has been reported (86). ^{11}C-acetate PET is not only used to investigate DOX cardiotoxicity but has also been evaluated in sunitinib-induced cardiotoxicity. Similarly, an *in vivo* study in rats described a decrease in myocardial perfusion, evaluated by ^{11}C-acetate PET, as early as 5 days after treatment initiation (87).

Cardiac MR

Common practices remain the assessment of cardiotoxicity by echocardiography because of its ability and availability to detect LVEF alteration, which is the current standard for oncologic treatment cardiotoxicity (88). However, the gold standard in LVEF evaluation remains CMR imaging (89). But in addition to LVEF assessment, it is currently admitted that CMR with vasodilator stress perfusion should be performed to non-invasively investigate microvascular dysfunction (90). Yet, we know that anthracyclines may be responsible for myocardial damage at a histologic level long before any overt LVEF decrease (91). Although most studies of anthracyclines have focused on their effect on myocyte damages (92), more recent studies suggest that DOX cardiotoxicity may present as direct vascular injury and arterial damage with coronary arteriolar wall abnormalities (31, 33, 93, 94). Some mechanisms of microcirculation damage arise from increased thickening of microcirculatory arterioles and loss of smooth muscle cells, which may contribute to myocardial perfusion defects.

Thus, the literature reports that DOX cardiotoxicity results in microvascular dysfunction, and we know that microvascular can technically be assessed by myocardial perfusion on CMR. We had to wait until 2021 to finally find a study that proved *in vivo* that there was a reduction in myocardial perfusion well before any overt LVEF alteration. Indeed, to the best of our knowledge, Galán-Arriola et al. (31) were the first to describe in large animals the impact of DOX on coronary microcirculation, assessed by CMR but also by invasive measurement and histology, under different DOX protocols. In this study, the alteration of myocardial perfusion by CMR followed a similar pattern to that observed in the assessment of microcirculatory function by CFR. Indeed, they showed that in the early stages of DOX treatment, there was a decline in CMR perfusion. This decline in perfusion was present although LVEF, cardiac motion, cardiac contractility were not impaired; and was persistent as long-term changes with cumulative doses of DOX.

Myocardial perfusion assessment by CMR is a validated non-invasive assessment of microvascular CAD (95) and has been shown to outperform SPECT in detecting obstructive CAD (96–99). Newer CMR techniques that could quantitatively detect epicardial and microvascular CAD have correlated well with IMR and FFR measurements (77), and coronary sinus flow evaluation could be a good surrogate for CFR measurements (100). Although to the best of our knowledge, no study has yet reported myocardial perfusion CMR findings of anthracyclines-treated patients, it is legitimate to speculate that vasoconstriction and increased wall thickness of the heart microvasculature may reveal a myocardial perfusion defect and decreased myocardial blood flow reserve. Myocardial perfusion is acquired during the first pass of gadolinium-based contrast agents, based on an ECG-triggered fast T1-sensitive pulse sequences that can be acquired both at rest and with stress. The additional benefit of stress in CMR perfusion compared with resting perfusion alone is still debated but is theoretically used to unmask myocardial perfusion defect that could be compensated at rest (101). Indeed, stress could reveal insufficient coronary reserve resulting in decreased perfusion and ischemia in territories with thickened vessels walls and impaired ability to respond to stress-induced vasodilation. Although the mechanisms leading to 5-FU-related cardiotoxicity are numerous and detailed elsewhere (102), ischemia, especially secondary to vasospasm, can be imaged by perfusion defect in the coronary territory of the vasospasm (103, 104).

Regarding the evaluation of anti-VEGF myocardial cardiotoxicity with perfusion CMR, there are very sparse data in the literature. A small study on 9 patients evaluated both resting and stress perfusion with CMR before treatment and at 4 and 6 weeks of treatment (105). They were able to show a decrease in myocardial blood flow on resting perfusion after treatment introduction but no difference under stress, and an increase in vascular permeability. These preliminary findings suggest that anti-VEGF cardiotoxicity leads to microvascular constriction, which may, fortunately, be reversible, and that microvascular endothelial dysfunction may be responsible in part for impaired LVEF.

Metabolic Imaging

Metabolic imaging focuses and targets changes in metabolic pathways and energetics. It includes CMRS and nuclear imaging techniques such as SPECT and PET.

Cardiac Magnetic Resonance Spectroscopy

Cardiac magnetic resonance spectroscopy has several advantages for metabolic imaging since it is able of measuring several metabolic biomarkers without using ionizing radiation (106). Metabolites containing proton (^{1}H) such as creatine or lipids; containing carbon (^{13}C) such as glucose, and containing phosphorus (^{31}P) such as PCr or ATP can be assessed by CMRS. In addition, the development of ^{31}P saturation magnetic resonance spectroscopy allows the measurement of the metabolic rate of ATP production *via* the enzyme creatine kinase (= CK flux) (106, 107).

Early studies performed on isolated animal hearts have demonstrated several alterations in the cardiac metabolic. The injection of [1-^{13}C]glucose into isolated perfused hearts treated for 10 weeks with anthracyclines highlighted altered glycolytic metabolism (108). Similarly, abnormal cardiac bioenergetics, as revealed by a reduced PCr/ATP ratio, was measured with ^{31}P-CMRS in an isolated animal hearts of acute (109) and chronic (110–112) anthracycline-related cardiotoxicity. In addition, Bittner et al. showed that hearts chronically exposed to DOX failed to adapt metabolically, as evidenced by the delayed recovery of PCr after hemodynamic stress (113). Recently, Henderson et al. showed that acute and clinically relevant exposure to DOX in isolated, perfused rat hearts induced a reduction in energy reserve, as measured by a decrease in PCr, in response to the cardiac-stimulant isoproterenol (114). These studies demonstrated abnormal cardiac energetics production and utilization, even in the setting of acute anthracycline exposure. Interestingly, the myocardial PCr/ATP ratio was reduced after 6 weeks of anthracycline treatment without evidence of cardiac damage in an *in vivo* study (110). In addition, the authors showed a strong correlation between cardiac energetics and LV systolic and diastolic dysfunction after 8 and 10 weeks of treatment. The same group then demonstrated that the absolute concentration of PCr was decreased in DOX-treated mice and that ^{31}P-CMRS also detected a reduced rate of ATP synthesis through CK reaction (115). Importantly, overexpression of cardiac-specific myofibrillar isoform of CK restored impaired PCr and CK flux, which was associated with improved LVEF and survival in DOX-treated mice (115), opening up a new possibility for preventive therapy.

Recent research has focused on improving the signal-to-noise ratio of conventional CMRS, with the development of hyperpolarization CMRS: the injection of hyperpolarized [1-^{13}C]pyruvate and [2-^{13}C]pyruvate enables measurement of the flux through the pyruvate dehydrogenase (PDH) complex and TCA flux, respectively (116). A decrease in PDH flux, representative of reduced oxidative mitochondrial carbohydrate metabolism, was observed in the myocardium of DOX-treated rats for 3 weeks without impairment of cardiac function (117). After 6 weeks of treatment, the authors showed, in addition to reduced PDH activity, a decrease of TCA cycle flux and impaired cardiac function. This altered carbohydrate metabolism reflected the loss of mitochondrial integrity, which was not because of the oxidative stress in this study, and preceded cardiac function impairment.

The exploration of cardiac energetics in the clinic has been recently proposed. The authors found no difference in cardiac PCr/ATP ratio of anthracycline-treated women despite a 5% reduction in LVEF between the start and end treatment (118). This could be explained, at least in part, by the small number of patients in whom CMRS was possible (11 patients).

Nuclear Imaging

Several radiopharmaceuticals can be used as biomarkers of myocardial metabolism using nuclear imaging, the two best known being iodine-123 betamethyl-iodophenyl-pentadecanoic acid (BMIPP) for the assessment of myocardial FFA uptake and 2'-deoxy-2'-[^{18}F]fluoro-D-glucose (FDG) for the assessment of cardiac glucose uptake. Because myocardial metabolism is tightly regulated, the heart switches from FFA metabolism to glycolysis in high-insulin/glucose levels and low oxygen by increasing its glucose transporter protein translocation to the plasma membrane (119). Hence, PET with FDG under fasting condition is preferred for oncology study (minimize myocardial uptake) but is performed under fasted condition or with glucose load after an overnight fasting for cardiac study (maximize myocardial uptake).

Early studies conducted two decades ago showed a significantly lower myocardial BMIPP uptake in patients treated with DOX (120) and taxanes (121), but other studies showed that only one in four (122), and one in six (123) patients displayed hypomyocardial BMIPP accumulation. Importantly, modeling of kinetics, which was measured by the acquisition of dynamic time sequences in the latter study, revealed a significant decrease in BMIPP flux in DOX-treated patients (123). This analysis more accurately reflects the features of fatty acid metabolism disorders by measuring the metabolic flux of the tracer rather than its accumulation in the myocardium. The lower cardiac uptake of BMIPP, which is a biomarker of impaired fatty acid beta-oxidation, was predictive of LV dysfunction (120).

An exciting exploration in cardio-oncology is ketone body imaging. This has been proposed with cardiac ^{11}C-acetoacetate PET. As a ketone body, acetoacetate can be used as a substrate by the heart and be involved in cardioprotection through its antioxidant activity plus mitochondrial membrane repair

(124, 125). Greater uptake and retention of ^{11}C-acetoacetate in the myocardium was found in non-fasted rats treated for 6 weeks with DOX, which may be associated with mitochondrial membrane alteration (126). Although it has been studied only once in this field, ketone body imaging may hold promise as a theranostic approach.

In 2012, Borde et al. first described enhanced ^{18}F-FDG uptake in the myocardium of DOX-treated patients, highlighting the ability of PET to early detect cardiotoxicity (127). Similar observations have been reproduced by others attempting to better understand the increased myocardial ^{18}F-FDG uptake in animals and patients treated with chemotherapy. First, DOX dose-dependently increased myocardial metabolic flux of ^{18}F-FDG measured by dynamic PET in the fasted mice (128). The same group demonstrated that a low pretreatment ^{18}F-FDG standardized uptake value (SUV) in Hodgkin's disease patients may predict the development of chemotherapy-induced cardiotoxicity, which was subsequently detected by a higher myocardial ^{18}F-FDG SUV (128). Another study showed that 12% of 121 patients with breast cancer treated with anthracycline or trastuzumab had increased ^{18}F-FDG uptake in the right ventricle, which was significantly associated with cardiotoxicity (129). Second, increased LV ^{18}F-FDG uptake correlated with LVEF decline after two cycles and at the end of DOX therapy in a retrospective study including a cohort of 43 patients (130). Another interesting study explored ^{18}F-FDG myocardial uptake and myocardial perfusion (through ^{99m}Tc-tetrofosmin SPECT) in a retrospective cohort of 332 patients followed for malignant disorders (131). As part of an oncologic PET protocol, patients were fasted to avoid myocardial ^{18}F-FDG uptake: 36% of patients had no ^{18}F-FDG uptake, 22.5% had diffuse ^{18}F-FDG uptake, 8% had focal ^{18}F-FDG uptake, and 30.5% had a focal uptake overlying the diffuse pattern ^{18}F-FDG uptake. Among all the patients, multivariate logistic regression identified focal myocardial ^{18}F-FDG uptake as a predictor of impaired LVEF and myocardial perfusion (131). It is important to bear in mind two interesting points. First, no direct mechanisms that could explain the increased cardiac ^{18}F-FDG uptake have been explored in these reports. This could be because of the recruitment of inflammatory cells, switch to anaerobic glycolysis, or being associated with other pathological mechanisms. Second, the correlation between ^{18}F-FDG uptake and LV function was made at the same time, which cannot directly prove the ability of early detection of cardiotoxicity before the decline of LV function. In terms of mechanisms and correlations, the increase in cardiac uptake of ^{18}F-FDG seven days after DOX treatment in mice was directly correlated with oxidative stress and antioxidant mechanisms assessed by biochemical measurements (132). This is particularly interesting knowing the close relationship between metabolic imbalance (i.e., mismatch of oxidative metabolism plus reduced ATP production) and ROS generation in mitochondria (133, 134).

Chemotherapy-induced cardiotoxicity is not limited to an increase in ^{18}F-FDG uptake. The SUV of ^{18}F-FDG was significantly reduced in the fasted rats treated for 6 weeks (135) and in non-fasted rats treated for 4 weeks (136) with DOX. ^{18}F-FDG PET could have detected a loss of cell viability and necrosis in these experimental models, which was associated with decreased LVEF (136). This supports the fact that dietary status is important in the cardiac ^{18}F-FDG PET investigation.

With respect to antiangiogenic therapies, few reports have described the role of ^{18}F-FDG PET. In 2011, a case report described decreased myocardial ^{18}F-FDG uptake in patients treated with imatinib plus sorafenib who later developed a cardiac event (137). Later, O'Farrell et al. also showed an increase in ^{18}F-FDG uptake 2–3 days after the introduction of sunitinib in mice and 5 days in rats (87). In another study, sunitnib induced higher ^{18}F-FDG uptake after 1 week of treatment in fasted mice but not in non-fasted mice (138), highlighting once again a role of the dietary status on myocardial ^{18}F-FDG uptake for further investigations. In both studies, this early side effect was associated with a switch from oxidative metabolism to glycolytic metabolism (138) and correlated with late myocardial hypertrophy measured after 6 weeks of treatment (139). Moreover, the metabolic flux of ^{18}F-FDG from the blood to the cytoplasmatic glycolysis, measured by dynamic time sequence acquisition and kinetic modeling, was reduced after 3 weeks of treatment (87, 138) with sunitinib and was associated with an insulin resistance pattern (138).

Mitochondrial Function Imaging

In-vivo assessment of cardiotoxicity-induced ROS production is tempting as there is a close relationship between altered circulation, metabolism, and oxidative stress. ^{18}F-labeled analog of dihydroethidium (^{18}F-DHMT) is a radioactive compound that can assess free radicals because it is trapped in the cell when oxidized by ROS (140, 141). In an initial *in-vivo* study in mice, the authors reported a 2-fold increase in cardiac retention of ^{18}F-DHMT after a single injection of DOX, which revealed ROS production compared with controls (141). This observation was later confirmed with an increased cardiac uptake of ^{18}F-DHMT in DOX-treated rats following 4 and 6 weeks of treatment (142). Interestingly, no impairment of cardiac function was found after 4 weeks of treatment, but 6 weeks of DOX treatment induced a decrease in LVEF (142). In another study, dynamic time sequence ^{18}F-DHMT PET and kinetic modeling confirmed higher absolute quantification of myocardial ROS production in beagle dogs following 2 weeks of DOX treatment (143).

Similarly, new radiopharmaceuticals have been developed to assess early DOX myocardial cardiotoxicity detection, such as ^{18}F-labeled lipophilic cation PET tracers (144). Its principle is to image mitochondrial damage by ^{18}F-labeled lipophilic tracers, which diffuse across mitochondrial membranes depending upon the mitochondrial membrane potential (144). The tracers will therefore accumulate in cardiac tissue in case of mitochondrial damage, which is one of the possible mechanisms of myocardial cardiotoxicity of DOX, allowing early detection of its cardiotoxicity.

In SPECT imaging, in the same perspective, the usual ^{99m}Tc-sestamibi, which is used to assess myocardial perfusion, is also a lipophilic cation and so its myocardial distribution depends on the mitochondrial membrane potential additionally to regional myocardial perfusion. Safee et al. recently demonstrated in a rat model a correction tool to free the ^{99m}Tc-sestamibi from its

TABLE 2 | This table summarizes early perfusion, metabolic and mitochondrial function imaging findings suggestive of DOX myocardial toxicity that subsequently revealed impaired left ventricle ejection fraction.

Reference	Early myocardial toxicity with no overt cardiac dysfunction	Late cardiac dysfunction	Species
Saito et al. (120)	Reduced ^{123}I-BMIPP [2 to 3 weeks]	Decreased LVEF [variable]	Human
Maslov et al. (110)	Decreased PCr/ATP ratio [6 weeks]	Systolic and diastolic dysfunction [8 and 10 weeks]	Mouse
Bauckneht et al. (128)	Lower pre-treatment ^{18}F-FDG Increased ^{18}F-FDG [4-6 weeks and 6 months follow up]	Decreased LVEF [median = 27 months, range 8-96]	Human
Boutagy et al. (142)	Increased ^{18}F-DHMT [4 weeks]	Decreased LVEF [6 weeks]	Rat
Timm et al. (117)	Decreased PDH flux [3 weeks]	Decreased LVEF [6 weeks]	Rat
Galán-Arriola et al. (31)	Decreased CMR-determined myocardial perfusion Decreased CFR [weeks 6]	Decreased LVEF [weeks 16]	Pig

[time] = from the beginning of treatment to the assessment of alteration on imaging.
CFR, coronary flow reserve; CMR, cardiac MRI; ^{18}F-DHMT, ^{18}F-labeled analog of dihydroethidium; DOX, doxorubicin; ^{18}F-FDG, ^{18}F-Fluoro-D-glucose; ^{123}I-BMIPP, ^{123}I-Betamethyl-iodophenyl-pentadecanoic acid; LVEF, left ventricle ejection fraction; PCr, phosphocreatine; PDH, pyruvate dehydrogenase.

perfusion imaging, to assess only the mitochondrial potential, and thus, its possible perturbation by anthracyclines (145). They proposed to correct the ^{99m}Tc-sestamibi with a lipophilic uncharged radiotracer that would thus be a perfusion tracer independent of the mitochondrial membrane potential [the bis (N-ethoxy-N-ethyldithiocarbamato)nitrido ^{99m}Tc(V)]. The latter ^{99m}Tc-NOET would, therefore, be able to detect DOX cardiotoxicity through its mitochondrial damage.

PERSPECTIVES

We are convinced that the assessment of the mechanisms of anticancer drug cardiotoxicity by imaging is a cornerstone in the new era of cardio-oncology. **Table 2** supports our assertion by summarizing studies that demonstrate DOX-induced cardiotoxicity early before overt LVEF impairment (**Table 2**).

Imaging Opportunities

We have seen throughout this review that most studies have been conducted in animal models. We are confident that this research has been and will be of great importance for the development of a standardized protocol to predict drug-related cardiotoxicity and to test preventive interventions.

Early detection of metabolism and vascular alteration is paramount to prevent DOX-induced permanent cardiac dysfunction (**Table 2**) and could be extended to other anticancer drugs since several vascular and metabolic cardiotoxic effects have been described in this review (**Table 1**). The assessment of myocardial cardiotoxicity by CMR seems to be of interest, to seek other complications of oncologic therapies such as ICI-induced cardiotoxicity. The major cardiotoxicity reported in this therapeutic class is myocarditis, with CMR being of great importance when suspected (146). Although not a commonly used modality for myocardial inflammation (147), increased ^{18}F-FDG uptake on PET could be found in myocarditis, including in ICI myocarditis (148). Interestingly, ^{18}F-FDG uptake has also been reported as a marker of anthracyclines cardiotoxicity, either *via* inflammatory response or altered myocardial metabolism (149). Fusion between ^{18}F-FDG and CMR have also been reported (148) for simultaneous vascular, metabolic, and functional imaging and may benefit from creatine measurement with proton CMRS (150) since creatine is decreased in both ischemic (151) and non-ischemic (152) cardiovascular disease.

Clinical Feasibilities

Because most studies of perfusion and metabolic imaging have been performed in animal models, their clinical relevance in routine practice is questionable. Anyhow, further clinical studies are required to ensure the utility of early detection of anticancer drugs.

Cardiac magnetic resonance imaging appears to be a non-invasive, radiation-free tool for monitoring patients with cancer, capable of imaging microcirculation, metabolism, and myocardial inflammation, which could be offered routinely before and after the introduction of an anticancer drug. We believe that CMR could be a justifiable perfusion approach as a part of standard patient care. Indeed, we have seen that altered myocardial perfusion in large animal models has been

reported by resting myocardial perfusion on CMR (31). Multiple other CMR parameters have been reported to be related to cardiotoxicity of anticancer drugs (153–156), so the addition of a rapid perfusion sequence to the CMR protocol would be sufficient to obtain an argument for cardiotoxic effect. As the gold standard, CMR would also provide an accurate evaluation of LVEF. Unfortunately, LVEF assessment is so far performed in daily practice by echocardiography because of the lack of access to CMR. This would be the only limitation we see for its routine integration into the health care of patients with cancer.

We believe that the use of nuclear perfusion imaging in daily practice is difficult to justify. One of the main possible obstacles is the use of radiation and the cost of the technique that would allow assessment of myocardial perfusion without assessing oncologic follow-up. Nevertheless, it may be interesting to consider the integration of ^{18}F-FDG PET in the follow-up of patients with cancer in order to assess tumor progression and, at the same time, to look for possible cardiotoxic effects. Indeed, the most PET scans for oncology monitoring use ^{18}F-FDG, which is also, as mentioned earlier, sensitive to myocardial metabolic imbalance and also to myocardial inflammation. This capability of PET for whole-body imaging would be attractive in patients with cancer to concomitantly allow imaging of tumor progression in addition to an assessment of myocardial toxicity, thus providing a unique modality. We believe that further studies regarding the place of PET imaging in the future of cardio-oncology are required.

CONCLUSION

Early detection of cardiotoxicity is crucial and offers the opportunity for early therapeutic intervention. In this review, we have shown that perfusion imaging, metabolic imaging, and mitochondrial function imaging are capable of assessing myocardial cardiotoxic effects of cancer therapeutics before irreversible cardiac damage occurs (**Figure 1**, **Table 2**). Knowledge of these possible early imaging findings in anticancer drug-related myocardial toxicity could change the paradigm of "late-onset cardiotoxicity." Earlier detection would allow for better prevention, with specific therapeutics attempting in part to reduce oxidative stress. Current guidelines on cardiotoxicity do not include myocardial and metabolic perfusion imaging, but in light of this review, it may be worthwhile to add these parameters to better detect and prevent dramatic progression.

AUTHOR CONTRIBUTIONS

FC and JS contributed equally to this study and wrote the manuscript. FT did proofreading and provided useful advice. All authors contributed to the article and approved the submitted version.

FUNDING

This study was performed by a laboratory member of the France Life Imaging Network (grant ANR-11-INBS-0006).

REFERENCES

1. Schwartz RG, McKenzie WB, Alexander J, Sager P, D'Souza A, Manatunga A, et al. Congestive heart failure and left ventricular dysfunction complicating doxorubicin therapy. Seven-year experience using serial radionuclide angiocardiography. *Am J Med.* (1987) 82:1109–18. doi: 10.1016/0002-9343(87)90212-9
2. Burrage MK, Ferreira VM. The use of cardiovascular magnetic resonance as an early non-invasive biomarker for cardiotoxicity in cardio-oncology. *Cardiovasc Diagn Ther.* (2020) 10:610–24. doi: 10.21037/cdt-20-165
3. Jordan JH, Todd RM, Vasu S, Hundley WG. Cardiovascular magnetic resonance in the oncology patient. *JACC Cardiovasc Imaging.* (2018) 11:1150–72. doi: 10.1016/j.jcmg.2018.06.004
4. Pizzino F, Vizzari G, Qamar R, Bomzer C, Carerj S, Zito C, et al. Multimodality imaging in cardiooncology. *J Oncol.* (2015) 2015:263950. doi: 10.1155/2015/263950
5. Taegtmeyer H, Golfman L, Sharma S, Razeghi P, van Arsdall M. Linking gene expression to function: metabolic flexibility in the normal and diseased heart. *Ann N Y Acad Sci.* (2004) 1015:202–13. doi: 10.1196/annals.1302.017
6. Saks V, Dzeja P, Schlattner U, Vendelin M, Terzic A, Wallimann T. Cardiac system bioenergetics: metabolic basis of the Frank-Starling law. *J Physiol.* (2006) 571:253–73. doi: 10.1113/jphysiol.2005.101444
7. Ray PD, Huang B-W, Tsuji Y. Reactive oxygen species (ROS) homeostasis and redox regulation in cellular signaling. *Cell Signal.* (2012) 24:981–90. doi: 10.1016/j.cellsig.2012.01.008
8. Varricchi G, Ameri P, Cadeddu C, Ghigo A, Madonna R, Marone G, et al. Antineoplastic drug-induced cardiotoxicity: a redox perspective. *Front Physiol.* (2018) 9:167. doi: 10.3389/fphys.2018.00167
9. Murphy MP. How mitochondria produce reactive oxygen species. *Biochem J.* (2009) 417:1–13. doi: 10.1042/BJ20081386
10. Soufer A, Baldassarre LA. The role of cardiac magnetic resonance imaging to detect cardiac toxicity from cancer therapeutics. *Curr Treat Options Cardiovasc Med.* (2019) 21:28. doi: 10.1007/s11936-019-0732-5
11. Minotti G, Menna P, Salvatorelli E, Cairo G, Gianni L. Anthracyclines: molecular advances and pharmacologic developments in antitumor activity and cardiotoxicity. *Pharmacol Rev.* (2004) 56:185–229. doi: 10.1124/pr.56.2.6
12. Minotti G, Salvatorelli E, Menna P. Pharmacological foundations of cardio-oncology. *J Pharmacol Exp Ther.* (2010) 334:2–8. doi: 10.1124/jpet.110.165860
13. Sourdon J, Keceli G, Lindsey ML, Paolocci N. Death of an antioxidant brings heart failure with preserved ejection fraction to life: 5-oxoproline and post-ischaemic cardio-renal dysfunction. *Cardiovasc Res.* (2018) 114:1819–21. doi: 10.1093/cvr/cvy239
14. Tang X, Luo Y-X, Chen H-Z, Liu D-P. Mitochondria, endothelial cell function, and vascular diseases. *Front Physiol.* (2014) 5:175. doi: 10.3389/fphys.2014.00175
15. Chow AY, Chin C, Dahl G, Rosenthal DN. Anthracyclines cause endothelial injury in pediatric cancer patients: a pilot study. *J Clin Oncol.* (2006) 24:925–8. doi: 10.1200/JCO.2005.03.5956
16. Pautz A, Art J, Hahn S, Nowag S, Voss C, Kleinert H. Regulation of the expression of inducible nitric oxide synthase. *Nitric Oxide.* (2010) 23:75–93. doi: 10.1016/j.niox.2010.04.007
17. Heeringa P, van Goor H, Moshage H, Klok PA, Huitema MG, de Jager A, et al. Expression of iNOS, eNOS, and peroxynitrite-modified proteins in experimental anti-myeloperoxidase associated crescentic glomerulonephritis. *Kidney Int.* (1998) 53:382–93. doi: 10.1046/j.1523-1755.1998.00780.x

18. Csányi G, Taylor WR, Pagano PJ. NOX and inflammation in the vascular adventitia. *Free Radic Biol Med.* (2009) 47:1254–66. doi: 10.1016/j.freeradbiomed.2009.07.022
19. Ueno H, Kanellakis P, Agrotis A, Bobik A. Blood flow regulates the development of vascular hypertrophy, smooth muscle cell proliferation, and endothelial cell nitric oxide synthase in hypertension. *Hypertension.* (2000) 36:89–96. doi: 10.1161/01.HYP.36.1.89
20. Neubauer S. The failing heart–an engine out of fuel. *N Engl J Med.* (2007) 356:1140–51. doi: 10.1056/NEJMra063052
21. Hader SN, Zinkevich N, Norwood Toro LE, Kriegel AJ, Kong A, Freed JK, et al. Detrimental effects of chemotherapy on human coronary microvascular function. *Am J Physiol Heart Circ Physiol.* (2019) 317:H705–10. doi: 10.1152/ajpheart.00370.2019
22. Wolf MB, Baynes JW. The anti-cancer drug, doxorubicin, causes oxidant stress-induced endothelial dysfunction. *Biochim Biophys Acta.* (2006) 1760:267–71. doi: 10.1016/j.bbagen.2005.10.012
23. Soultati A, Mountzios G, Avgerinou C, Papaxoinis G, Pectasides D, Dimopoulos M-A, et al. Endothelial vascular toxicity from chemotherapeutic agents: preclinical evidence and clinical implications. *Cancer Treat Rev.* (2012) 38:473–83. doi: 10.1016/j.ctrv.2011.09.002
24. Wojcik T, Buczek E, Majzner K, Kolodziejczyk A, Miszczyk J, Kaczara P, et al. Comparative endothelial profiling of doxorubicin and daunorubicin in cultured endothelial cells. *Toxicol In Vitro.* (2015) 29:512–21. doi: 10.1016/j.tiv.2014.12.009
25. Mukhopadhyay P, Rajesh M, Bátkai S, Kashiwaya Y, Haskó G, Liaudet L, et al. Role of superoxide, nitric oxide, and peroxynitrite in doxorubicin-induced cell death *in vivo* and *in vitro*. *Am J Physiol Heart Circ Physiol.* (2009) 296:H1466–83. doi: 10.1152/ajpheart.00795.2008
26. Wang S, Kotamraju S, Konorev E, Kalivendi S, Joseph J, Kalyanaraman B. Activation of nuclear factor-kappaB during doxorubicin-induced apoptosis in endothelial cells and myocytes is pro-apoptotic: the role of hydrogen peroxide. *Biochem J.* (2002) 367:729–40. doi: 10.1042/bj20020752
27. Chaosuwannakit N, D'Agostino R, Hamilton CA, Lane KS, Ntim WO, Lawrence J, et al. Aortic stiffness increases upon receipt of anthracycline chemotherapy. *J Clin Oncol.* (2010) 28:166–72. doi: 10.1200/JCO.2009.23.8527
28. Pennell DJ, Sechtem UP, Higgins CB, Manning WJ, Pohost GM, Rademakers FE, et al. Clinical indications for cardiovascular magnetic resonance (CMR): consensus Panel report. *J Cardiovasc Magn Reson.* (2004) 6:727–65. doi: 10.1081/JCMR-200038581
29. Zhang S, Liu X, Bawa-Khalfe T, Lu L-S, Lyu YL, Liu LF, et al. Identification of the molecular basis of doxorubicin-induced cardiotoxicity. *Nat Med.* (2012) 18:1639–42. doi: 10.1038/nm.2919
30. Medeiros-Lima DJM, Carvalho JJ, Tibirica E, Borges JP, Matsuura C. Time course of cardiomyopathy induced by doxorubicin in rats. *Pharmacol Rep.* (2019) 71:583–90. doi: 10.1016/j.pharep.2019.02.013
31. Galán-Arriola C, Vílchez-Tschischke JP, Lobo M, López GJ, de Molina-Iracheta A, Pérez-Martínez C, et al. Coronary microcirculation damage in anthracycline cardiotoxicity. *Cardiovasc Res.* (2021) doi: 10.1093/cvr/cvab053. [Epub ahead of print].
32. Gallucci G, Coccaro M, Storto G, Lapadula L, Tartarone A, Nappi A, et al. The clinical impact of a cardiologic follow-up in breast cancer survivors: an observational study. *Int J Immunopathol Pharmacol.* (2010) 23:1221–7. doi: 10.1177/039463201002300426
33. Eckman DM, Stacey RB, Rowe R, D'Agostino R, Kock ND, Sane DC, et al. Weekly doxorubicin increases coronary arteriolar wall and adventitial thickness. *PLoS ONE.* (2013) 8:e57554. doi: 10.1371/journal.pone.0057554
34. Kalábová H, Melichar B, Ungermann L, DoleŽal J, Krčmová L, Kašparová M, et al. Intima-media thickness, myocardial perfusion and laboratory risk factors of atherosclerosis in patients with breast cancer treated with anthracycline-based chemotherapy. *Med Oncol.* (2011) 28:1281–7. doi: 10.1007/s12032-010-9593-1
35. Kinhult S, Albertsson M, Eskilsson J, Cwikiel M. Antithrombotic treatment in protection against thrombogenic effects of 5-fluorouracil on vascular endothelium: a scanning microscopy evaluation. *Scanning.* (2001) 23:1–8. doi: 10.1002/sca.4950230101
36. Tsibiribi P, Bui-Xuan C, Bui-Xuan B, Lombard-Bohas C, Duperret S, Belkhiria M, et al. Cardiac lesions induced by 5-fluorouracil in the rabbit. *Hum Exp Toxicol.* (2006) 25:305–9. doi: 10.1191/0960327106ht628oa
37. Kinhult S, Albertsson M, Eskilsson J, Cwikiel M. Effects of probucol on endothelial damage by 5-fluorouracil. *Acta Oncol.* (2003) 42:304–8. doi: 10.1080/02841860310004409
38. Matsubara I, Kamiya J, Imai S. Cardiotoxic effects of 5-fluorouracil in the guinea pig. *Jpn J Pharmacol.* (1980) 30:871–9. doi: 10.1016/S0021-5198(19)52945-6
39. Tamatsu H, Nakazawa M, Imai S, Watari H. 31P-topical nuclear magnetic resonance (31P-TMR) studies of cardiotoxic effects of 5-fluorouracil (5-FU) and 5'-deoxy-5-fluorouridine (5'-DFUR). *Jpn J Pharmacol.* (1984) 34:375–9. doi: 10.1016/S0021-5198(19)52291-0
40. Eskandari MR, Moghaddam F, Shahraki J, Pourahmad J. A comparison of cardiomyocyte cytotoxic mechanisms for 5-fluorouracil and its pro-drug capecitabine. *Xenobiotica.* (2015) 45:79–87. doi: 10.3109/00498254.2014.942809
41. Kurauchi K, Nishikawa T, Miyahara E, Okamoto Y, Kawano Y. Role of metabolites of cyclophosphamide in cardiotoxicity. *BMC Res Notes.* (2017) 10:406. doi: 10.1186/s13104-017-2726-2
42. Clarke L, Waxman DJ. Oxidative metabolism of cyclophosphamide: identification of the hepatic monooxygenase catalysts of drug activation. *Cancer Res.* (1989) 49:2344–50.
43. Colvin M. *Alkylating Agents. Holland-Frei Cancer Medicine.* 6th ed. (2003). Available online at: https://www.ncbi.nlm.nih.gov/books/NBK12772/ (accessed October 31, 2021).
44. Herradón E, González C, Uranga JA, Abalo R, Martín MI, López-Miranda V. Characterization of cardiovascular alterations induced by different chronic cisplatin treatments. *Front Pharmacol.* (2017) 8:196. doi: 10.3389/fphar.2017.00196
45. Hsu P-Y, Mammadova A, Benkirane-Jessel N, Désaubry L, Nebigil CG. Updates on anticancer therapy-mediated vascular toxicity and new horizons in therapeutic strategies. *Front Cardiovasc Med.* (2021) 8:694711. doi: 10.3389/fcvm.2021.694711
46. Hartmann JT, Kanz L. Sunitinib and periodic hair depigmentation due to temporary c-KIT inhibition. *Arch Dermatol.* (2008) 144:1525–6. doi: 10.1001/archderm.144.11.1525
47. Lévy BI. Blood pressure as a potential biomarker of the efficacy angiogenesis inhibitor. *Ann Oncol.* (2009) 20:200–3. doi: 10.1093/annonc/mdp018
48. Facemire CS, Nixon AB, Griffiths R, Hurwitz H, Coffman TM. Vascular endothelial growth factor receptor 2 controls blood pressure by regulating nitric oxide synthase expression. *Hypertension.* (2009) 54:652–8. doi: 10.1161/HYPERTENSIONAHA.109.129973
49. Kappers MHW, van Esch JHM, Sluiter W, Sleijfer S, Danser AHJ, van den Meiracker AH. Hypertension induced by the tyrosine kinase inhibitor sunitinib is associated with increased circulating endothelin-1 levels. *Hypertension.* (2010) 56:675–81. doi: 10.1161/HYPERTENSIONAHA.109.149690
50. Lankhorst S, Kappers MHW, van Esch JHM, Smedts FMM, Sleijfer S, Mathijssen RHJ, et al. Treatment of hypertension and renal injury induced by the angiogenesis inhibitor sunitinib: preclinical study. *Hypertension.* (2014) 64:1282–9. doi: 10.1161/HYPERTENSIONAHA.114.04187
51. Dhaun N, Webb DJ. Receptor tyrosine kinase inhibition, hypertension, and proteinuria: is endothelin the smoking gun? *Hypertension.* (2010) 56:575–7. doi: 10.1161/HYPERTENSIONAHA.110.155762
52. Lerman A, Holmes DR, Bell MR, Garratt KN, Nishimura RA, Burnett JC. Endothelin in coronary endothelial dysfunction and early atherosclerosis in humans. *Circulation.* (1995) 92:2426–31. doi: 10.1161/01.CIR.92.9.2426
53. Chintalgattu V, Rees ML, Culver JC, Goel A, Jiffar T, Zhang J, et al. Coronary microvascular pericytes are the cellular target of sunitinib malate induced cardiotoxicity. *Sci Transl Med.* (2013) 5:187ra69. doi: 10.1126/scitranslmed.3005066

54. Rees ML, Subramaniam J, Li Y, Hamilton DJ, Frazier OH, Taegtmeyer H. A PKM2 signature in the failing heart. *Biochem Biophys Res Commun.* (2015) 459:430–6. doi: 10.1016/j.bbrc.2015.02.122
55. Hasinoff BB, Patel D, O'Hara KA. Mechanisms of myocyte cytotoxicity induced by the multiple receptor tyrosine kinase inhibitor sunitinib. *Mol Pharmacol.* (2008) 74:1722–8. doi: 10.1124/mol.108.050104
56. Kerkela R, Woulfe KC, Durand J-B, Vagnozzi R, Kramer D, Chu TF, et al. Sunitinib-induced cardiotoxicity is mediated by off-target inhibition of AMP-activated protein kinase. *Clin Transl Sci.* (2009) 2:15–25. doi: 10.1111/j.1752-8062.2008.00090.x
57. Will Y, Dykens JA, Nadanaciva S, Hirakawa B, Jamieson J, Marroquin LD, et al. Effect of the multitargeted tyrosine kinase inhibitors imatinib, dasatinib, sunitinib, and sorafenib on mitochondrial function in isolated rat heart mitochondria and H9c2 cells. *Toxicol Sci.* (2008) 106:153–61. doi: 10.1093/toxsci/kfn157
58. Rainer PP, Doleschal B, Kirk JA, Sivakumaran V, Saad Z, Groschner K, et al. Sunitinib causes dose-dependent negative functional effects on myocardium and cardiomyocytes. *BJU Int.* (2012) 110:1455–62. doi: 10.1111/j.1464-410X.2012.11134.x
59. Ma W, Liu M, Liang F, Zhao L, Gao C, Jiang X, et al. Cardiotoxicity of sorafenib is mediated through elevation of ROS level and CaMKII activity and dysregulation of calcium homoeostasis. *Basic Clin Pharmacol Toxicol.* (2020) 126:166–80. doi: 10.1111/bcpt.13318
60. Sabet NS, Atashbar S, Khanlou EM, Kahrizi F, Salimi A. Curcumin attenuates bevacizumab-induced toxicity via suppressing oxidative stress and preventing mitochondrial dysfunction in heart mitochondria. *Naunyn Schmiedebergs Arch Pharmacol.* (2020) 393:1447–57. doi: 10.1007/s00210-020-01853-x
61. Mohammad Khanlou E, Atashbar S, Kahrizi F, Shokouhi Sabet N, Salimi A. Bevacizumab as a monoclonal antibody inhibits mitochondrial complex II in isolated rat heart mitochondria: ameliorative effect of ellagic acid. *Drug Chem Toxicol.* (2020) 1–8. doi: 10.1080/01480545.2020.1715423. [Epub ahead of print].
62. Li Y, Tian W, Yue D, Chen C, Li C, Zhang Z, et al. Bevacizumab-induced mitochondrial dysfunction, endoplasmic reticulum stress, and erk inactivation contribute to cardiotoxicity. *Oxid Med Cell Longev.* (2021) 2021:5548130. doi: 10.1155/2021/5548130
63. Bartsch R, Wenzel C, Steger GG. Trastuzumab in the management of early and advanced stage breast cancer. *Biologics.* (2007) 1:19–31.
64. ElZarrad MK, Mukhopadhyay P, Mohan N, Hao E, Dokmanovic M, Hirsch DS, et al. Trastuzumab alters the expression of genes essential for cardiac function and induces ultrastructural changes of cardiomyocytes in mice. *PLoS ONE.* (2013) 8:e79543. doi: 10.1371/journal.pone.0079543
65. Farolfi A, Melegari E, Aquilina M, Scarpi E, Ibrahim T, Maltoni R, et al. Trastuzumab-induced cardiotoxicity in early breast cancer patients: a retrospective study of possible risk and protective factors. *Heart.* (2013) 99:634–9. doi: 10.1136/heartjnl-2012-303151
66. Timolati F, Ott D, Pentassuglia L, Giraud M-N, Perriard J-C, Suter TM, et al. Neuregulin-1 beta attenuates doxorubicin-induced alterations of excitation-contraction coupling and reduces oxidative stress in adult rat cardiomyocytes. *J Mol Cell Cardiol.* (2006) 41:845–54. doi: 10.1016/j.yjmcc.2006.break08.002
67. Giordano FJ, Gerber H-P, Williams S-P, VanBruggen N, Bunting S, Ruiz-Lozano P, et al. A cardiac myocyte vascular endothelial growth factor paracrine pathway is required to maintain cardiac function. *Proc Natl Acad Sci USA.* (2001) 98:5780–5. doi: 10.1073/pnas.091415198
68. Geisberg CA, Wang G, Safa RN, Smith HM, Anderson B, Peng X-Y, et al. Circulating neuregulin-1β levels vary according to the angiographic severity of coronary artery disease and ischemia. *Coron Artery Dis.* (2011) 22:577–82. doi: 10.1097/MCA.0b013e32834d3346
69. Salem J-E, Manouchehri A, Moey M, Lebrun-Vignes B, Bastarache L, Pariente A, et al. Cardiovascular toxicities associated with immune checkpoint inhibitors: an observational, retrospective, pharmacovigilance study. *Lancet Oncol.* (2018) 19:1579–89. doi: 10.1016/S1470-2045(18)30608-9
70. Heinzerling L, Ott PA, Hodi FS, Husain AN, Tajmir-Riahi A, Tawbi H, et al. Cardiotoxicity associated with CTLA4 and PD1 blocking immunotherapy. *J Immunother Cancer.* (2016) 4:50. doi: 10.1186/s40425-016-0152-y
71. Michel L, Helfrich I, Hendgen-Cotta UB, Mincu R-I, Korste S, Mrotzek SM, et al. Targeting early stages of cardiotoxicity from anti-PD1 immune checkpoint inhibitor therapy. *Eur Heart J.* (2021) ehab430. doi: 10.1093/eurheartj/ehab430. [Epub ahead of print].
72. Hasdai D, Gibbons RJ, Holmes DR, Higano ST, Lerman A. Coronary endothelial dysfunction in humans is associated with myocardial perfusion defects. *Circulation.* (1997) 96:3390–5. doi: 10.1161/01.CIR.96.10.3390
73. Behrenbeck TR, McCollough CH, Miller WL, Williamson EE, Leng S, Kline TL, et al. Early changes in myocardial microcirculation in asymptomatic hypercholesterolemic subjects: as detected by perfusion CT. *Ann Biomed Eng.* (2014) 42:515–25. doi: 10.1007/s10439-013-0934-z
74. Garcia D, Harbaoui B, van de Hoef TP, Meuwissen M, Nijjer SS, Echavarria-Pinto M, et al. Relationship between FFR, CFR and coronary microvascular resistance - Practical implications for FFR-guided percutaneous coronary intervention. *PLoS ONE.* (2019) 14:e0208612. doi: 10.1371/journal.pone.0208612
75. Gould KL, Kirkeeide RL, Buchi M. Coronary flow reserve as a physiologic measure of stenosis severity. *J Am Coll Cardiol.* (1990) 15:459–74. doi: 10.1016/S0735-1097(10)80078-6
76. Lee B-K, Lim H-S, Fearon WF, Yong AS, Yamada R, Tanaka S, et al. Invasive evaluation of patients with angina in the absence of obstructive coronary artery disease. *Circulation.* (2015) 131:1054–60. doi: 10.1161/CIRCULATIONAHA.114.012636
77. Kotecha T, Martinez-Naharro A, Boldrini M, Knight D, Hawkins P, Kalra S, et al. automated pixel-wise quantitative myocardial perfusion mapping by CMR to detect obstructive coronary artery disease and coronary microvascular dysfunction: validation against invasive coronary physiology. *JACC Cardiovasc Imaging.* (2019) 12:1958–69. doi: 10.1016/j.jcmg.2018.12.022
78. Feher A, Boutagy NE, Stendahl JC, Hawley C, Guerrera N, Booth CJ, et al. Computed tomographic angiography assessment of epicardial coronary vasoreactivity for early detection of doxorubicin-induced cardiotoxicity. *JACC CardioOncol.* (2020) 2:207–19. doi: 10.1016/j.jaccao.2020.05.007
79. Fathala A. Myocardial perfusion scintigraphy: techniques, interpretation, indications and reporting. *Ann Saudi Med.* (2011) 31:625–34. doi: 10.4103/0256-4947.87101
80. Hardenbergh PH, Munley MT, Bentel GC, Kedem R, Borges-Neto S, Hollis D, et al. Cardiac perfusion changes in patients treated for breast cancer with radiation therapy and doxorubicin: preliminary results. *Int J Radiat Oncol Biol Phys.* (2001) 49:1023–8. doi: 10.1016/S0360-3016(00)01531-5
81. Chernov VI, Kravchuk TL, Zelchan RV, Goldberg VE. [Radionuclide methods in the assessment of anthracycline-induced cardiotoxicity]. *Kardiologiia.* (2015) 55:57–62. doi: 10.18565/cardio.2015.7.57-62
82. Ghotbi AA, Kjaer A, Hasbak P. Review: comparison of PET rubidium-82 with conventional SPECT myocardial perfusion imaging. *Clin Physiol Funct Imaging.* (2014) 34:163–70. doi: 10.1111/cpf.12083
83. Hagemann CE, Ghotbi AA, Kjær A, Hasbak P. Quantitative myocardial blood flow with Rubidium-82 PET: a clinical perspective. *Am J Nucl Med Mol Imaging.* (2015) 5:457–68.
84. Ziadi MC, de Kemp R, Beanlands RSB, Small GR. Looking for trouble: reduced myocardial flow reserve following anthracyclines. *J Nucl Cardiol.* (2020) 27:1708–13. doi: 10.1007/s12350-018-01564-0
85. Laursen AH, Elming MB, Ripa RS, Hasbak P, Kjær A, Køber L, et al. Rubidium-82 positron emission tomography for detection of acute doxorubicin-induced cardiac effects in lymphoma patients. *J Nucl Cardiol.* (2020) 27:1698–07. doi: 10.1007/s12350-018-1458-6
86. Croteau E, Gascon S, Bentourkia M, Langlois R, Rousseau JA, Lecomte R, Bénard F. [11C]Acetate rest-stress protocol to assess myocardial perfusion and oxygen consumption reserve in a model of congestive heart failure in rats. *Nucl Med Biol.* (2012) 39:287–94. doi: 10.1016/j.nucmedbio.2011.07.010

87. O'Farrell AC, Evans R, Silvola JMU, Miller IS, Conroy E, Hector S, et al. A novel Positron Emission Tomography (PET) approach to monitor cardiac metabolic pathway remodeling in response to sunitinib malate. *PLoS ONE.* (2017) 12:e0169964. doi: 10.1371/journal.pone.0169964
88. Plana JC, Galderisi M, Barac A, Ewer MS, Ky B, Scherrer-Crosbie M, et al. Expert consensus for multimodality imaging evaluation of adult patients during and after cancer therapy: a report from the American Society of Echocardiography and the European Association of Cardiovascular Imaging. *J Am Soc Echocardiogr.* (2014) 27:911–39. doi: 10.1016/j.echo.2014.07.012
89. Bellenger NG, Burgess MI, Ray SG, Lahiri A, Coats AJ, Cleland JG, et al. Comparison of left ventricular ejection fraction and volumes in heart failure by echocardiography, radionuclide ventriculography and cardiovascular magnetic resonance; are they interchangeable? *Eur Heart J.* (2000) 21:1387–96. doi: 10.1053/euhj.2000.2011
90. Hubert A, Seitz A, Pereyra VM, Bekeredjian R, Sechtem U, Ong P. Coronary artery spasm: the interplay between endothelial dysfunction and vascular smooth muscle cell hyperreactivity. *Eur Cardiol.* (2020) 15:e12. doi: 10.15420/ecr.2019.20
91. Ewer MS, Ali MK, Mackay B, Wallace S, Valdivieso M, Legha SS, et al. A comparison of cardiac biopsy grades and ejection fraction estimations in patients receiving Adriamycin. *J Clin Oncol.* (1984) 2:112–7. doi: 10.1200/JCO.1984.2.2.112
92. Gianni L, Herman EH, Lipshultz SE, Minotti G, Sarvazyan N, Sawyer DB. Anthracycline cardiotoxicity: from bench to bedside. *J Clin Oncol.* (2008) 26:3777–84. doi: 10.1200/JCO.2007.14.9401
93. Bar-Joseph H, Ben-Aharon I, Tzabari M, Tsarfaty G, Stemmer SM, Shalgi R. *In vivo* bioimaging as a novel strategy to detect doxorubicin-induced damage to gonadal blood vessels. *PLoS ONE.* (2011) 6:e23492. doi: 10.1371/journal.pone.0023492
94. Murata T, Yamawaki H, Yoshimoto R, Hori M, Sato K, Ozaki H, et al. Chronic effect of doxorubicin on vascular endothelium assessed by organ culture study. *Life Sci.* (2001) 69:2685–95. doi: 10.1016/S0024-3205(01)01352-2
95. Hamirani YS, Kramer CM. Cardiac MRI assessment of myocardial perfusion. *Future Cardiol.* (2014) 10:349–58. doi: 10.2217/fca.14.18
96. Kwong RY, Ge Y, Steel K, Bingham S, Abdullah S, Fujikura K, et al. Cardiac magnetic resonance stress perfusion imaging for evaluation of patients with chest pain. *J Am Coll Cardiol.* (2019) 74:1741–55. doi: 10.1016/j.jacc.2019.07.074
97. Nagel E, Greenwood JP, McCann GP, Bettencourt N, Shah AM, Hussain ST, et al. Magnetic resonance perfusion or fractional flow reserve in coronary disease. *N Engl J Med.* (2019) 380:2418–28. doi: 10.1056/NEJMoa1716734
98. Schwitter J, Wacker CM, Wilke N, Al-Saadi N, Sauer E, Huettle K, et al. MR-IMPACT II: magnetic resonance imaging for myocardial perfusion assessment in coronary artery disease trial: perfusion-cardiac magnetic resonance vs. single-photon emission computed tomography for the detection of coronary artery disease: a comparative multicentre, multivendor trial. *Eur Heart J.* (2013) 34:775–81. doi: 10.1093/eurheartj/ehs022
99. Greenwood JP, Maredia N, Younger JF, Brown JM, Nixon J, Everett CC, et al. Cardiovascular magnetic resonance and single-photon emission computed tomography for diagnosis of coronary heart disease (CE-MARC): a prospective trial. *Lancet.* (2012) 379:453–60. doi: 10.1016/S0140-6736(11)61335-4
100. Indorkar R, Kwong RY, Romano S, White BE, Chia RC, Trybula M, et al. Global coronary flow reserve measured during stress cardiac magnetic resonance imaging is an independent predictor of adverse cardiovascular events. *JACC Cardiovasc Imaging.* (2019) 12:1686–95. doi: 10.1016/j.jcmg.2018.08.018
101. Kirkham AA, Virani SA, Campbell KL. The utility of cardiac stress testing for detection of cardiovascular disease in breast cancer survivors: a systematic review. *Int J Womens Health.* (2015) 7:127–40. doi: 10.2147/IJWH.S68745
102. Sara JD, Kaur J, Khodadadi R, Rehman M, Lobo R, Chakrabarti S, et al. 5-fluorouracil and cardiotoxicity: a review. *Ther Adv Med Oncol.* (2018) 10:1758835918780140. doi: 10.1177/1758835918780140
103. Pirozzolo G, Martínez Pereyra V, Hubert A, Guenther F, Sechtem U, Bekeredjian R, et al. Coronary artery spasm and impaired myocardial perfusion in patients with ANOCA: predictors from a multimodality study using stress CMR and acetylcholine testing. *Int J Cardiol.* (2021) 343:5–11. doi: 10.1016/j.ijcard.2021.09.003
104. Yilmaz A, Mahrholdt H, Athanasiadis A, Sechtem U. Non-invasive evaluation of coronary vasospasm using a combined hyperventilation and cold-pressure-test perfusion CMR protocol. *J Cardiovasc Magn Reson.* (2007) 9:759–64. doi: 10.1080/10976640701544662
105. Dobbin SJH, Mangion K, Berry C, Roditi G, Basak S, Sourbron S, et al. Cardiotoxicity and myocardial hypoperfusion associated with anti-vascular endothelial growth factor therapies: prospective cardiac magnetic resonance imaging in patients with cancer. *Eur J Heart Fail.* (2020) 22:1276–7. doi: 10.1002/ejhf.1847
106. Sourdon J, Lewsey SC, Schär M, Weiss RG. Measuring myocardial energetics with cardiovascular magnetic resonance spectroscopy. *Heart Fail Clin.* (2021) 17:149–56. doi: 10.1016/j.hfc.2020.08.011
107. Weiss RG, Gerstenblith G, Bottomley PA. ATP flux through creatine kinase in the normal, stressed, and failing human heart. *Proc Natl Acad Sci USA.* (2005) 102:808–13. doi: 10.1073/pnas.0408962102
108. Chatham JC, Hutchins GM, Glickson JD. Altered glucose metabolism in adriamycin-induced heart failure. *Biochim Biophys Acta.* (1992) 1138:1–5. doi: 10.1016/0925-4439(92)90143-B
109. Chatham JC, Cousins JP, Glickson JD. The relationship between cardiac function and metabolism in acute adriamycin-treated perfused rat hearts studied by 31P and 13C NMR spectroscopy. *J Mol Cell Cardiol.* (1990) 22:1187–97. doi: 10.1016/0022-2828(90)90082-D
110. Maslov MY, Chacko VP, Hirsch GA, Akki A, Leppo MK, Steenbergen C, et al. Reduced *in vivo* high-energy phosphates precede adriamycin-induced cardiac dysfunction. *Am J Physiol Heart Circ Physio.* (2010) 299:H332–7. doi: 10.1152/ajpheart.00727.2009
111. Dekker T, van Echteld CJ, Kirkels JH, Ruigrok TJ, van Hoesel QG, de Jong WH, et al. Chronic cardiotoxicity of adriamycin studied in a rat model by 31P NMR. *NMR Biomed.* (1991) 4:16–24. doi: 10.1002/nbm.1940040104
112. Nicolay K, Aue WP, Seelig J, van Echteld CJ, Ruigrok TJ, de Kruijff B. Effects of the anti-cancer drug adriamycin on the energy metabolism of rat heart as measured by *in vivo* 31P-NMR and implications for adriamycin-induced cardiotoxicity. *Biochim Biophys Acta.* (1987) 929:5–13. doi: 10.1016/0167-4889(87)90234-5
113. Bittner V, Reeves RC, Digerness SB, Caulfield JB, Pohost GM. 31P NMR spectroscopy in chronic adriamycin cardiotoxicity. *Magn Reson Med.* (1991) 17:69–81. doi: 10.1002/mrm.1910170112
114. Henderson KA, Borders RB, Ross JB, Abdulalil A, Gibbs S, Skowronek AJ, et al. Integration of cardiac energetics, function and histology from isolated rat hearts perfused with doxorubicin and doxorubicin-ol; a model for use in drug safety evaluations. *J Pharmacol Toxicol Methods.* (2018) 94:54–63. doi: 10.1016/j.vascn.2018.08.004
115. Gupta A, Rohlfsen C, Leppo MK, Chacko VP, Wang Y, Steenbergen C, et al. Creatine kinase-overexpression improves myocardial energetics, contractile dysfunction and survival in murine doxorubicin cardiotoxicity. *PLoS ONE.* (2013) 8:e74675. doi: 10.1371/journal.pone.0074675
116. Schroeder MA, Clarke K, Neubauer S, Tyler DJ. Hyperpolarized magnetic resonance: a novel technique for the *in vivo* assessment of cardiovascular disease. *Circulation.* (2011) 124:1580–94. doi: 10.1161/CIRCULATIONAHA.111.024919
117. Timm KN, Perera C, Ball V, Henry JA, Miller JJ, Kerr M, et al. Early detection of doxorubicin-induced cardiotoxicity in rats by its cardiac metabolic signature assessed with hyperpolarized MRI. *Commun Biol.* (2020) 3:692. doi: 10.1038/s42003-020-01440-z
118. Macnaught G, Oikonomidou O, Rodgers CT, Clarke W, Cooper A, McVicars H, et al. Cardiac energetics before, during, and after anthracycline-based chemotherapy in breast cancer patients using 31P magnetic resonance spectroscopy: a pilot study. *Front Cardiovasc Med.* (2021) 8:653648. doi: 10.3389/fcvm.2021.653648
119. Hue L, Beauloye C, Marsin A-S, Bertrand L, Horman S, Rider MH. Insulin and ischemia stimulate glycolysis by acting on the same targets through different and opposing signaling pathways. *J Mol Cell Cardiol.* (2002) 34:1091–7. doi: 10.1006/jmcc.2002.2063
120. Saito K, Takeda K, Okamoto S, Okamoto R, Makino K, Tameda Y, et al. Detection of doxorubicin cardiotoxicity by using iodine-123 BMIPP

early dynamic SPECT: quantitative evaluation of early abnormality of fatty acid metabolism with the Rutland method. *J Nucl Cardiol.* (2000) 7:553–61. doi: 10.1067/mnc.2000.108351

121. Saito K, Takeda K, Imanaka-Yoshida K, Imai H, Sekine T, et al. Assessment of fatty acid metabolism in taxan-induced myocardial damage with iodine-123 BMIPP SPECT: comparative study with myocardial perfusion, left ventricular function, and histopathological findings. *Ann Nucl Med.* (2003) 17:481–8. doi: 10.1007/BF03006439
122. Nousiainen T, Vanninen E, Jantunen E, Remes J, Kuikka J, Hartikainen J. Anthracycline-induced cardiomyopathy: long-term effects on myocardial cell integrity, cardiac adrenergic innervation and fatty acid uptake. *Clin Physiol.* (2001) 21:123–8. doi: 10.1046/j.1365-2281.2001.00292.x
123. Kitagawa K, Takeda K, Saito K, Okamoto S, Makino K, Maeda H, et al. Differences in fatty acid metabolic disorder between ischemic myocardium and doxorubicin-induced myocardial damage: assessment using BMIPP dynamic SPECT with analysis by the Rutland method. *J Nucl Med.* (2002) 43:1286–94.
124. Maalouf M, Sullivan PG, Davis L, Kim DY, Rho JM. Ketones inhibit mitochondrial production of reactive oxygen species production following glutamate excitotoxicity by increasing NADH oxidation. *Neuroscience.* (2007) 145:256–64. doi: 10.1016/j.neuroscience.2006.11.065
125. Fukao T, Lopaschuk GD, Mitchell GA. Pathways and control of ketone body metabolism: on the fringe of lipid biochemistry. *Prostaglandins Leukot Essent Fatty Acids.* (2004) 70:243–51. doi: 10.1016/j.plefa.2003.11.001
126. Croteau E, Tremblay S, Gascon S, Dumulon-Perreault V, Labbé SM, Rousseau JA, et al. [(11)C]-Acetoacetate PET imaging: a potential early marker for cardiac heart failure. *Nuclear Med Biol.* (2014) 41:863–70. doi: 10.1016/j.nucmedbio.2014.08.006
127. Borde C, Kand P, Basu S. Enhanced myocardial fluorodeoxyglucose uptake following Adriamycin-based therapy: evidence of early chemotherapeutic cardiotoxicity? *World J Radiol.* (2012) 4:220–3. doi: 10.4329/wjr.v4.i5.220
128. Baucknehtt M, Ferrarazzo G, Fiz F, Morbelli S, Sarocchi M, Pastorino F, et al. Doxorubicin effect on myocardial metabolism as a prerequisite for subsequent development of cardiac toxicity: a translational 18F-FDG PET/CT observation. *J Nucl Med.* (2017) 58:1638–45. doi: 10.2967/jnumed.117.191122
129. Kim J, Cho S-G, Kang S-R, Yoo SW, Kwon SY, Min J-J, et al. Association between FDG uptake in the right ventricular myocardium and cancer therapy-induced cardiotoxicity. *J Nucl Cardiol.* (2020) 27:2154–63. doi: 10.1007/s12350-019-01617-y
130. Sarocchi M, Baucknehtt M, Arboscello E, Capitanio S, Marini C, Morbelli S, et al. An increase in myocardial 18-fluorodeoxyglucose uptake is associated with left ventricular ejection fraction decline in Hodgkin lymphoma patients treated with anthracycline. *J Transl Med.* (2018) 16:295. doi: 10.1186/s12967-018-1670-9
131. Haider A, Bengs S, Schade K, Wijnen WJ, Portmann A, Etter D, Fröhlich S, et al. Myocardial 18F-FDG uptake pattern for cardiovascular risk stratification in patients undergoing oncologic PET/CT. *J Clin Med.* (2020) 9:E2279. doi: 10.3390/jcm9072279
132. Baucknehtt M, Pastorino F, Castellani P, Cossu V, Orengo AM, Piccioli P, et al. Increased myocardial 18F-FDG uptake as a marker of Doxorubicin-induced oxidative stress. *J Nucl Cardiol.* (2020) 27:2183–94. doi: 10.1007/s12350-019-0break1618-x
133. Peoples JN, Saraf A, Ghazal N, Pham TT, Kwong JQ. Mitochondrial dysfunction and oxidative stress in heart disease. *Exp Mol Med.* (2019) 51:1–13. doi: 10.1038/s12276-019-0355-7
134. Zhou B, Tian R. Mitochondrial dysfunction in pathophysiology of heart failure. *J Clin Invest.* (2018) 128:3716–26. doi: 10.1172/JCI120849
135. Shen L-J, Lu S, Zhou Y-H, Li L, Xing Q-M, Xu Y-L. Developing a rat model of dilated cardiomyopathy with improved survival. *J Zhejiang Univ Sci B.* (2016) 17:975–83. doi: 10.1631/jzus.B1600257
136. Oudot A, Courteau A, Guillemin M, Vrigneaud J-M, Walker PM, Brunotte F, et al. [123I]MIBG is a better early marker of anthracycline cardiotoxicity than [18F]FDG: a preclinical SPECT/CT and simultaneous PET/MR study. *EJNMMI Res.* (2021) 11:92. doi: 10.1186/s13550-021-00835-1
137. Toubert M-E, Vercellino L, Faugeron I, Lussato D, Hindie E, Bousquet G. Fatal heart failure after a 26-month combination of tyrosine kinase inhibitors in a papillary thyroid cancer. *Thyroid.* (2011) 21:451–4. doi: 10.1089/thy.2010.0270
138. Sourdon J, Lager F, Viel T, Balvay D, Moorhouse R, Bennana E, et al. Cardiac metabolic deregulation induced by the tyrosine kinase receptor inhibitor sunitinib is rescued by endothelin receptor antagonism. *Theranostics.* (2017) 7:2757–74. doi: 10.7150/thno.19551
139. Sourdon J, Facchin C, Certain A, Viel T, Robin B, Lager F, et al. Sunitinib-induced cardiac hypertrophy and the endothelin axis. *Theranostics.* (2021) 11:3830–8. doi: 10.7150/thno.49837
140. Zhang W, Cai Z, Li L, Ropchan J, Lim K, Boutagy NE, et al. Optimized and automated radiosynthesis of [18F]DHMT for translational imaging of reactive oxygen species with positron emission tomography. *Molecules.* (2016) 21:E1696. doi: 10.3390/molecules21121696
141. Chu W, Chepetan A, Zhou D, Shoghi KI, Xu J, Dugan LL, et al. Development of a PET radiotracer for non-invasive imaging of the reactive oxygen species, superoxide, *in vivo*. *Org Biomol Chem.* (2014) 12:4421–31. doi: 10.1039/C3OB42379D
142. Boutagy NE, Wu J, Cai Z, Zhang W, Booth CJ, Kyriakides TC, et al. *In vivo* reactive oxygen species detection with a novel positron emission tomography tracer, 18F-DHMT, allows for early detection of anthracycline-induced cardiotoxicity in rodents. *JACC Basic Transl Sci.* (2018) 3:378–90. doi: 10.1016/j.jacbts.2018.02.003
143. Wu J, Boutagy NE, Cai Z, Lin S-F, Zheng M-Q, Feher A, et al. Feasibility study of PET dynamic imaging of [18F]DHMT for quantification of reactive oxygen species in the myocardium of large animals. *J Nucl Cardiol.* (2020). doi: 10.1007/s12350-020-02184-3. [Epub ahead of print].
144. McCluskey SP, Haslop A, Coello C, Gunn RN, Tate EW, Southworth R, et al. Imaging of chemotherapy-induced acute cardiotoxicity with 18F-labeled lipophilic cations. *J Nucl Med.* (2019) 60:1750–6. doi: 10.2967/jnumed.119.226787
145. Safee ZM, Baark F, Waters ECT, Veronese M, Pell VR, Clark JE, et al. Detection of anthracycline-induced cardiotoxicity using perfusion-corrected 99mTc sestamibi SPECT. *Sci Rep.* (2019) 9:216. doi: 10.1038/s41598-018-36721-5
146. Michel L, Rassaf T, Totzeck M. Cardiotoxicity from immune checkpoint inhibitors. *Int J Cardiol Heart Vasc.* (2019) 25:100420. doi: 10.1016/j.ijcha.2019.100420
147. Nensa F, Kloth J, Tezgah E, Poeppel TD, Heusch P, Goebel J, et al. Feasibility of FDG-PET in myocarditis: comparison to CMR using integrated PET/MRI. *J Nucl Cardiol.* (2018) 25:785–94. doi: 10.1007/s12350-016-0616-y
148. Chen Y, Jia Y, Liu Q, Shen Y, Zhu H, Dong X, et al. Myocarditis related to immune checkpoint inhibitors treatment: two case reports and literature review. *Ann Palliat Med.* (2021) 10:8512–7. doi: 10.21037/apm-20-2620
149. Baucknehtt M, Morbelli S, Fiz F, Ferrarazzo G, Piva R, Nieri A, et al. A score-based approach to 18F-FDG PET images as a tool to describe metabolic predictors of myocardial doxorubicin susceptibility. *Diagnostics.* (2017) 7:E57. doi: 10.3390/diagnostics7040057
150. Sourdon J, Roussel T, Costes C, Viout P, Guye M, Ranjeva J-P, et al. Comparison of single-voxel 1H-cardiovascular magnetic resonance spectroscopy techniques for *in vivo* measurement of myocardial creatine and triglycerides at 3T. *J Cardiovasc Magn Reson.* (2021) 23:53. doi: 10.1186/s12968-021-00748-x
151. Bottomley PA, Weiss RG. Non-invasive magnetic-resonance detection of creatine depletion in non-viable infarcted myocardium. *Lancet.* (1998) 351:714–8. doi: 10.1016/S0140-6736(97)06402-7
152. Nakae I, Mitsunami K, Matsuo S, Inubushi T, Morikawa S, Tsutamoto T, et al. Myocardial creatine concentration in various nonischemic heart diseases assessed by 1H magnetic resonance spectroscopy. *Circ J.* (2005) 69:711–6. doi: 10.1253/circj.69.711
153. Drafts BC, Twomley KM, D'Agostino R, Lawrence J, Avis N, Ellis LR, et al. Low to moderate dose anthracycline-based chemotherapy is associated with early noninvasive imaging evidence of subclinical cardiovascular disease. *JACC Cardiovasc Imaging.* (2013) 6:877–85. doi: 10.1016/j.jcmg.2012.11.017
154. Neilan TG, Coelho-Filho OR, Shah RV, Feng JH, Pena-Herrera D, Mandry D, et al. Myocardial extracellular volume by cardiac magnetic resonance imaging in patients treated with anthracycline-based chemotherapy. *Am J Cardiol.* (2013) 111:717–22. doi: 10.1016/j.amjcard.2012.11.022

155. Fallah-Rad N, Lytwyn M, Fang T, Kirkpatrick I, Jassal DS. Delayed contrast enhancement cardiac magnetic resonance imaging in trastuzumab induced cardiomyopathy. *J Cardiovasc Magn Reson.* (2008) 10:5. doi: 10.1186/1532-429X-10-5
156. Jordan JH, Vasu S, Morgan TM, D'Agostino RB, Meléndez GC, Hamilton CA, et al. Anthracycline-associated T1 mapping characteristics are elevated independent of the presence of cardiovascular comorbidities in cancer survivors. *Circ Cardiovasc Imaging.* (2016) 9:e004325. doi: 10.1161/CIRCIMAGING.115.004325

Conflict of Interest: The authors declare that the research was conducted in the absence of any commercial or financial relationships that could be construed as a potential conflict of interest.

Publisher's Note: All claims expressed in this article are solely those of the authors and do not necessarily represent those of their affiliated organizations, or those of the publisher, the editors and the reviewers. Any product that may be evaluated in this article, or claim that may be made by its manufacturer, is not guaranteed or endorsed by the publisher.

frontiers in Cardiovascular Medicine

ORIGINAL RESEARCH
published: 17 February 2022
doi: 10.3389/fcvm.2022.758324

A Concomitant Cancer Diagnosis Is Associated With Poor Cardiovascular Outcomes Among Acute Myocardial Infarction Patients

Xiang Peng [1,2†], Zhuozhong Wang [1,2†], Muhua Cao [1,2†], Yuqi Zheng [1,2], Ya'nan Tian [1,2], Li Yu [1,2], Wenjun Ni [1,2], Shanjie Wang [1,2], Zhifeng Qin [1,2], Suhong Zhao [1,2], Jinwei Tian [1,2] and Bo Yu [1,2*]*

[1] Department of Cardiology, The Second Affiliated Hospital of Harbin Medical University, Harbin, China, [2] The Key Laboratory of Myocardial Ischemia, Harbin Medical University, Ministry of Education, Harbin, China

OPEN ACCESS

Edited by:
Feng Cao,
People's Liberation Army General Hospital, China

Reviewed by:
Paolo Spallarossa,
San Martino Hospital (IRCCS), Italy
Frank Ernst,
CTI Clinical Trial and Consulting, United States

***Correspondence:**
Bo Yu
dryu_hmu@163.com
Jinwei Tian
tianjinweidr2009@163.com

[†]These authors have contributed equally to this work and share first authorship

Specialty section:
This article was submitted to Cardio-Oncology, a section of the journal Frontiers in Cardiovascular Medicine

Received: 13 August 2021
Accepted: 27 January 2022
Published: 17 February 2022

Citation:
Peng X, Wang Z, Cao M, Zheng Y, Tian Y, Yu L, Ni W, Wang S, Qin Z, Zhao S, Tian J and Yu B (2022) A Concomitant Cancer Diagnosis Is Associated With Poor Cardiovascular Outcomes Among Acute Myocardial Infarction Patients. Front. Cardiovasc. Med. 9:758324. doi: 10.3389/fcvm.2022.758324

Background and Aims: With the increasing coexistence of cardiovascular disease and cancer in contemporary clinical practice, studies on the outcomes in acute myocardial infarction (AMI) patients with cancer has not been systematically investigated. This study sought to investigated the effect of coexisting cancer on the treatment and clinical outcomes among AMI patients.

Methods: We retrospectively integrated and analyzed cardiovascular data of 6,607 AMI patients between June 2016 and December 2019. Patients with cancer were compared with pair-matched cancer-naive patients. Cox proportional hazards models were constructed to compare the differences in outcomes.

Results: Of 6,607 patients, 2.3% ($n = 150$) had been diagnosed with cancer. Patients with cancer were older (70.3 ± 10.0 vs. 63.9 ± 11.5 years, $P < 0.001$) and had a higher burden of comorbidities. Moreover, patients with cancer tended to receive clopidogrel (52.0 vs. 40.0%, $P = 0.004$) rather than ticagrelor (45.6 vs. 58.2%, $P = 0.003$) than those without cancer. After pairwise matching, patients with cancer were less likely to undergo in-hospital percutaneous coronary intervention (61.3 vs. 70.0%, $P = 0.055$). And after 3-year follow-up, the cumulative incidence of cardiovascular death (14.0 vs. 8.3%; adjusted HR, 1.93; 95% CI, 1.11–3.39; $P = 0.021$) among patients with cancer was significantly higher than that among the matched controls, a similar pattern was observed for the composite outcome of cardiovascular death, non-fatal myocardial infarction, and non-fatal stroke (16.0 vs. 10.3%; adjusted HR, 1.98; 95% CI, 1.21–3.26; $P = 0.007$). Moreover, patients with a historical cancer diagnosis within 5 years had a higher risk of cardiovascular ischemic events.

Conclusions: AMI patients with a concomitant diagnosis of cancer tended to be treated with conservative therapies and were at substantially higher risk for adverse cardiovascular outcomes.

Keywords: cancer, acute myocardial infarction, cardiovascular outcomes, percutaneous coronary intervention, conservative therapies

INTRODUCTION

Cancer and cardiovascular disease are the leading causes of disease-related death worldwide, together accounting for nearly 70% (1). Due to earlier detection and modern treatment regimens, cancer-related mortality has decreased significantly (2), and two-thirds of patients with cancer can survive at least 5 years with the disease (3). Likewise, there has been a global decline in deaths from acute myocardial infarction (AMI) (4). Although cancer and cardiovascular disease are regarded as two distinct disease processes, there is a considerable overlap of risk factors for these diseases, such as advanced age, diabetes (5), smoking (6), and obesity (7). As life expectancy increases, non-cancer-related mortality from cardiovascular disease has become more important during cancer survivorship (8, 9), and cardiovascular disease has been shown to be the leading cause of death in cancer patients (10, 11).

When cancer patients present with AMI, their management poses unique challenges for clinicians. Many old and new emerging anti-cancer agents are associated with cardiovascular toxicities (12, 13). The lasting cardiovascular side effects of cancer treatments means that the compensatory reserve for acute clinical events such as AMI may also be reduced (14). At a cumulative (i.e., lifetime) dose of 400–450 mg/m^2 doxorubicin, a 10% rate of heart failure can be expected among patients aged over 65 years (15). In addition, cancer is commonly associated with hematologic and coagulation abnormalities (16), which poses a major obstacle to percutaneous coronary intervention (PCI) and the use of antithrombotic agents. Unfortunately, patients with cancer are commonly excluded from randomized controlled trials exploring best practices for the treatment of AMI, leading to a scarcity of reliable data on clinical outcomes in this cohort to guide clinical decision-making, which compounds the dilemma faced by clinicians.

Therefore, in this retrospective cohort study, we analyzed the clinical characteristics, treatment patterns, and outcomes in AMI patients with cancer and sought to define the influence of cancer duration and treatment pattern on the cardiovascular outcomes.

MATERIALS AND METHODS

Study Design and Patient Population

A retrospective, single-center study was performed at the Second Affiliated Hospital of Harbin Medical University, which was approved by the ethics committee of Harbin Medical University. The study procedures were conducted in compliance with the principles of the Declaration of Helsinki, and patient information was collected anonymously. All AMI patients from June 2016 to December 2019 were included in the study. Myocardial infarction (MI) was defined according to the fourth universal definition of MI (17). The population included in the final analysis consisted of 6,607 AMI patients. All detailed clinical data of those patients were collected from electronic medical records, including age, sex, type of malignancy, cardiovascular risk factors [smoking status, hypertension, hyperlipidemia, diabetes mellitus, and previous coronary heart disease (CHD)], treatment, and outcomes. During a 3-year follow-up period, patients were surveyed semi-annually *via* telephone about major adverse events using a standardized questionnaire.

Outcomes

Our primary outcome was defined as cardiovascular mortality during follow-up. Secondary outcomes included all-cause mortality, major adverse cardiovascular and cerebrovascular events (MACCE), non-fatal MI, non-fatal stroke, and revascularization. MACCE is composed of cardiovascular death, non-fatal myocardial infarction, or non-fatal stroke.

Statistical Analysis

For all statistical tests, a two-tailed P-value < 0.05 indicated statistical significance, and data analyses were performed using R version 3.6.2 software (R Institute Inc.). Continuous variables are presented as the means ± standard deviations (SDs) if normally distributed or presented as medians with interquartile ranges (IQRs) if non-normally distributed. discrete variables are presented as frequencies (percentages), and missing data were excluded from the summary statistic calculations. To evaluate the differences in baseline characteristics between unmatched groups, Student's t-test was used for nearly normally distributed continuous variables, the Wilcoxon rank-sum test was used for non-normally distributed continuous and ordinal discrete variables, and Categorical data have been compared using the χ^2 or Fisher's exact test. Furthermore, to make the two groups comparable with regard to the vast majority of baseline characteristics, pairwise matching was performed *via* a greedy matching algorithm to match each pair of reference patients and patients with cancer according to the following restrictions: (1) age within 1 year, (2) sex, (3) hyperlipidemia status, (4) smoking status, and (5) diabetes status. The control group allowed a variable number of reference matches and a maximum of 4 matches per patient with cancer. Except for unpaired patients, each patient pair was used once in the further analyses. Comparisons between reference patients and patients with cancer were tested *via* the same test for baseline characteristics and outcomes. To evaluate the incremental relative risk increase among subgroups in the heterogeneity analysis, models were fit with an indicator for any history of cancer and with another indicator for the subgroup. Forest plots were drawn to analyze the heterogeneity of the effect of coexisting cancer on the event risk between subgroups.

RESULTS

Patient Characteristics

A total of 6,607 AMI patients were included between June 2016 and December 2019. Among those patients, 150 (2.3%) had been diagnosed with cancer. According to the order of frequencies, the most prevalent malignancies were lung (31, 20.7%), colorectum (21, 14.0%), stomach (19, 12.7%), and breast (15, 10.0%) cancers (**Supplementary Table S1**).

The characteristics of the overall cohort and matched cohort are summarized in **Table 1**. Before matching, the group of patients with cancer was older (70.3 ± 10.0 vs. 63.9 ± 11.5 years, $P < 0.001$) and had higher proportions of patients with

TABLE 1 | Clinical characteristics.

	Unmatched			Matched		
	No cancer	**Cancer**	***P*-value**	**No cancer**	**Cancer**	***P*-value**
N	6,457	150		542	150	
Age	63.9 ± 11.5	70.3 ± 10.0	<0.001	70.3 ± 9.4	70.3 ± 10.0	>0.999
Male	4,447 (68.9)	93 (62.0)	0.088	340 (62.7)	93 (62.0)	0.946
STEMI	4,156 (65.5)	85 (64.4)	0.861	331 (62.0)	85 (64.4)	0.681
BMI[a]	24.9 ± 3.7	24.5 ± 3.8	0.179	24.9 ± 3.6	24.5 ± 3.8	0.295
Risk factors						
Hypertension[a]	3,428 (53.2)	89 (60.1)	0.110	312 (57.7)	89 (60.1)	0.657
Hyperlipidemia[a]	1,462 (22.7)	46 (31.3)	0.018	160 (29.5)	46 (31.3)	0.753
Diabetes[a]	1,559 (24.2)	57 (38.3)	<0.001	194 (35.8)	57 (38.3)	0.648
Current smoker[a]	3,140 (48.7)	46 (31.1)	<0.001	170 (31.4)	46 (31.1)	>0.999
Comorbidities						
Coronary heart disease[a]	1,656 (25.7)	66 (44.9)	<0.001	145 (26.8)	66 (44.9)	<0.001
History of MI[a]	711 (11.0)	32 (21.8)	<0.001	60 (11.1)	32 (21.8)	0.001
History of stroke[a]	1,320 (20.5)	30 (20.4)	>0.999	142 (26.2)	30 (20.4)	0.183
History of PCI[a]	470 (7.3)	24 (16.3)	<0.001	32 (5.9)	24 (16.3)	<0.001
History of CABG[a]	18 (0.3)	1 (0.7)	0.349[b]	0 (0.0)	1 (0.7)	0.213[b]
Peripheral vascular disease[a]	158 (2.5)	10 (6.8)	0.002	19 (3.5)	10 (6.8)	0.127
Liver disease[a]	130 (2.0)	6 (4.1)	0.147	13 (2.4)	6 (4.1)	0.412
Chronic kidney disease[a]	239 (3.7)	14 (9.5)	<0.001	26 (4.8)	14 (9.5)	0.048
Clinical presentation						
LDL-C, umol/mL[a]	2.0 ± 5.6	1.8 ± 0.6	0.646	1.9 ± 0.8	1.8 ± 0.6	0.701
Troponin I, ng/mL[a]	2.1 (0.3–10.9)	1.7 (0.4–8.6)	0.687	2.1 (0.4–11.9)	1.7 (0.4–8.6)	0.456
Pro-BNP, pg/mL[a]	294.0 (82.0–1,156.0)	428.5 (102.8–428.5)	0.353	473.0 (119.0–2,018.0)	428.5 (102.8–428.5)	0.085
LVEF ≤ 40%	409 (6.3)	4 (2.7)	0.096	39 (7.3)	4 (2.7)	0.062
Diastolic cardiac dysfunction[a]	3,808 (63.2)	88 (62.9)	>0.999	356 (70.2)	88 (62.9)	0.119
Angiographic presentation						
Lesion location						
LM	313 (4.9)	8 (5.3)	0.935	41 (7.6)	8 (5.3)	0.430
LAD	3,979 (61.6)	89 (59.3)	0.628	341 (63.5)	89 (59.3)	0.403
LCX	1,729 (26.8)	31 (20.7)	0.114	142 (26.4)	31 (20.7)	0.182
RCA	3,266 (50.6)	70 (46.7)	0.387	286 (53.3)	70 (46.7)	0.182
TIMI flow 0 or 1 in any lesion	2,396 (37.1)	53 (35.3)	0.720	205 (38.2)	53 (35.3)	0.589
In-hospital procedures						
PCI	4,261 (66.0)	92 (61.3)	0.270	376 (70.0)	92 (61.3)	0.055
PTCA	849 (13.2)	17 (11.3)	0.597	47 (8.75)	17 (11.3)	0.422
Thrombus suction pipe	1,456 (22.6)	32 (21.3)	0.800	102 (19.0)	32 (21.3)	0.601
Thrombolysis[a]	268 (4.2)	6 (4.1)	>0.999	14 (2.6)	6 (4.1)	0.495
Aspirin[a]	6,285 (97.4)	143 (96.0)	0.439	523 (97.4)	143 (96.0)	0.525
Clopidogrel[a]	2,582 (40.0)	77 (52.0)	0.004	246 (45.8)	77 (52.0)	0.212
Ticagrelor[a]	3,760 (58.2)	68 (45.6)	0.003	285 (53.1)	68 (45.6)	0.130
Statin[a]	6,263 (97.0)	143 (96.0)	0.616	520 (96.8)	143 (96.0)	0.795
ACEI[a]	3,026 (46.9)	67 (45.3)	0.761	251 (46.7)	67 (45.3)	0.822
ARB[a]	174 (2.7)	6 (4.1)	0.455	19 (3.5)	6 (4.1)	0.961
Beta-blocker[a]	3,947 (61.1)	88 (59.5)	0.743	332 (61.8)	88 (59.5)	0.669
In-hospital complications						
Reinfarction[a]	5 (0.1)	0 (0.0)	>0.999	0 (0.0)	0 (0.0)	1
Malignant arrhythmia	204 (3.2)	2 (1.3)	0.301	25 (4.7)	2 (1.3)	0.107
Cardiogenic shock[a]	142 (2.2)	2 (1.3)	0.663	13 (2.4)	2 (1.3)	0.624
Cardiopulmonary arrest[a]	93 (1.4)	1 (0.7)	0.658	9 (1.7)	1 (0.7)	0.598
Death	154 (2.4)	2 (1.3)	0.571	15 (2.8)	2 (1.3)	0.471

Values are mean ± SD, median (interquartile range) or n (%).

[a]Include some missing values since some patients did not accept these examinations.

[b]Result of fisher's exact test.

ACEI, angiotensin-converting enzyme inhibitor; ARB, angiotensin receptor blocker; BMI, body mass index; CABG, coronary artery bypass grafting; LAD, left anterior descending artery; LDL-C, low-density lipoprotein cholesterol; LM, left main coronary artery; LVEF, left ventricular ejection fraction; MI, myocardial infarction; NT-proBNP, N-terminal pro–brain natriuretic peptide; PCI, percutaneous coronary intervention; PTCA, percutaneous transluminal coronary angioplasty; SD, standard deviation; STEMI, ST segment elevation myocardial infarction; TIMI, Thrombolysis In Myocardial Infarction.

hyperlipidemia (31.3 vs. 22.7%, $P = 0.018$) and diabetes (38.3 vs. 24.2%, $P < 0.001$). The group of patients with cancer had a lower proportion of current smokers (31.1 vs. 48.7%, $P < 0.001$) but higher proportions of patients with comorbidities. Furthermore, the group of patients with cancer had higher proportions of patients with previous CHD (44.9 vs. 25.7%, $P < 0.001$), previous MI (21.8 vs. 11.0%, $P < 0.001$) and previous PCI (16.3 vs. 7.3%, $P < 0.001$) than the group without cancer. During hospitalization, patients with cancer tended to receive clopidogrel (52.0 vs. 40.0%, $P = 0.004$) rather than ticagrelor (45.6 vs. 58.2%, $P = 0.003$) given an aspirin background. In addition, matching was possible for 542 pairs of reference patients and patients with cancer, and those patients constituted our matched study groups. After controlling for these heterogeneous covariates, such as age, sex, diabetes, smoking habits, and hyperlipidemia, the baseline characteristics were similar between the groups after

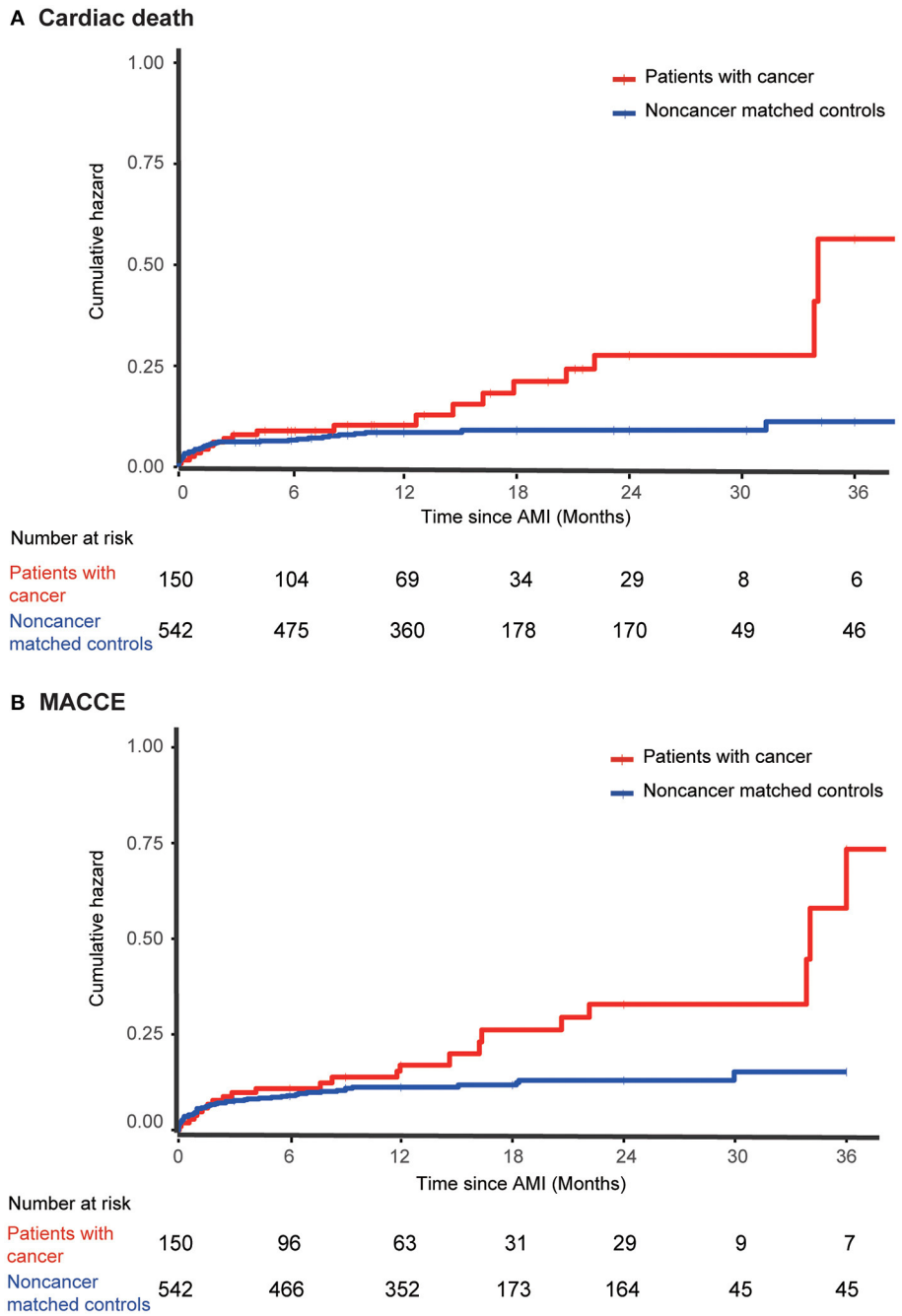

FIGURE 1 | Clinical outcomes among AMI patients with and without cancer. Displayed are the cumulative incidence curves for **(A)** cardiac mortality and **(B)** MACCE for cancer patients vs. controls. AMI, acute myocardial infarction; MACCE, major adverse cardiovascular and cerebrovascular events.

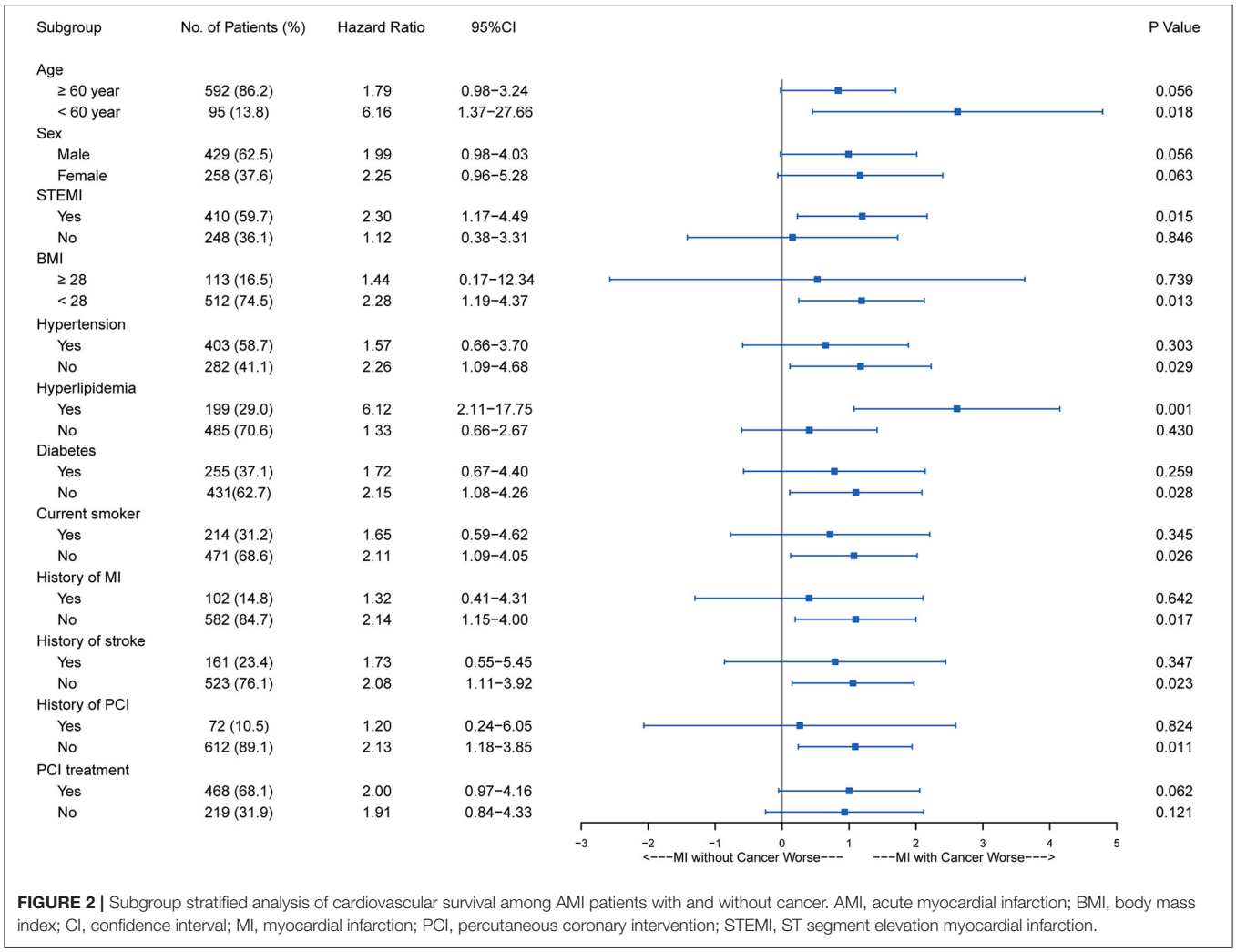

FIGURE 2 | Subgroup stratified analysis of cardiovascular survival among AMI patients with and without cancer. AMI, acute myocardial infarction; BMI, body mass index; CI, confidence interval; MI, myocardial infarction; PCI, percutaneous coronary intervention; STEMI, ST segment elevation myocardial infarction.

matching with the exception of higher proportions of patients with previous CHD (44.9 vs. 26.8%, $P < 0.001$), previous MI (21.8 vs. 11.1%, $P = 0.001$) and previous PCI (16.3 vs. 5.9%, $P < 0.001$) in the group of patients with cancer than in the matched controls. Moreover, patients with cancer were less likely to undergo in-hospital PCI (61.3 vs. 70.0%, $P = 0.055$).

Outcomes in the Cancer and Matched Non-cancer Groups

With regard to the long-term outcomes, patients with cancer had a significantly higher cumulative incidence of all-cause mortality (22.7 vs. 9.8%; adjusted HR, 2.40; 95% CI, 1.52–3.79; $P < 0.001$) (**Supplementary Figure S1**) and cardiovascular mortality (14.0 vs. 8.3%; adjusted HR, 1.934; 95% CI, 1.11–3.39; $P = 0.021$) (**Figure 1**; **Supplementary Table S2**). MACCE were also significantly higher in the patients with cancer than in the matched non-cancer group (16.0 vs. 10.3%; adjusted HR, 1.98; 95% CI, 1.21–3.26; $P = 0.007$). Moreover, there was no significant difference in MI (2.7 vs. 1.7%; adjusted HR, 1.64; 95% CI, 0.50–5.41; $P = 0.419$), stroke (0.7 vs. 0.9%; adjusted HR, 0.84; 95% CI, 0.10–7.34; $P = 0.876$), and revascularization (1.3 vs. 4.6%; adjusted HR, 0.259; 95% CI, 0.061–1.097; $P = 0.067$) between patients with or without cancer. Cardiovascular mortality tended to be similar across all pre-specified subgroups (**Figure 2**), as was all-cause mortality and MACCE (**Supplementary Figures S2**, **S3**).

Among 150 patients with cancer, 52 had a historical cancer diagnosis beyond 5 years before AMI, 59 had a historical cancer diagnosis within 5 years before AMI, and the other 39 had a current cancer diagnosis after AMI. The incidences of all-cause mortality, cardiovascular mortality and MACCE were significantly higher among patients with a historical cancer diagnosis within 5 years than among those without cancer (adjusted HR, 3.38; 95% CI, 1.88–6.04; $P < 0.001$; adjusted HR, 2.59; 95% CI, 1.25–5.35; $P = 0.010$; and adjusted HR, 2.66; 95% CI, 1.39–5.11; $P = 0.003$, respectively) (**Table 2**). A similar pattern was observed for all-cause mortality among patients with a current cancer diagnosis (adjusted HR, 2.71; 95% CI, 1.25–5.88; $P = 0.012$).

TABLE 2 | Outcomes according to the timing of the cancer diagnosis.

Outcome	Events (N/All)	HR (95%CI) (Cancer vs. no cancer)	*P*-value	Adjusted HR[a] (95%CI) (Cancer vs. no cancer)	Adjusted *P*-value[a]
All-cause death					
All cancer	34/87	2.465 (1.581–3.843)	<0.001	2.402 (1.523–3.789)	<0.001
History > 5 years	8	1.460 (0.692–3.081)	0.320	1.453 (0.685–3.082)	0.331
History ≤ 5 years	16	3.271 (1.833–5.836)	<0.001	3.375 (1.884–6.044)	<0.001
Current	10	3.099 (1.523–6.304)	0.002	2.708 (1.248–5.875)	0.012
Cardiac death					
All cancer	21/66	2.075 (1.206–3.569)	0.008	1.934 (1.105–3.386)	0.021
History > 5 years	6	1.717 (0.730–4.040)	0.216	1.649 (0.697–3.904)	0.255
History ≤ 5 years	10	2.550 (1.239–5.246)	0.011	2.589 (1.253–5.348)	0.010
Current	5	1.879 (0.674–5.241)	0.228	1.348 (0.406–4.473)	0.626
MACCE					
All cancer	24/80	2.302 (1.251–3.303)	0.004	1.982 (1.205–3.261)	0.007
History > 5 years	7	1.530 (0.697–3.358)	0.289	1.542 (0.700–3.397)	0.282
History ≤ 5 years	11	2.571 (1.346–4.910)	0.004	2.661 (1.385–5.111)	0.003
Current	6	2.031 (0.814–5.071)	0.129	1.647 (0.578–4.692)	0.350

CI, confidence interval; HR, hazard ratio; MACCE, major adverse cardiovascular and cerebrovascular events.

[a]*HRs were calculated using adjustments for history of coronary heart disease, history of myocardial infarction, history of percutaneous coronary intervention and history of chronic kidney disease.*

DISCUSSION

The main findings of this study are as follows: (a) among AMI patients, those with cancer were generally older and more often presented with comorbidities than those without cancer; (b) patients with cancer tended to be treated with conservative medical strategies with a weaker P2Y12 inhibitor in dual antiplatelet therapy (DAPT) and less PCI; (c) patients with cancer had a significantly higher incidence of cardiovascular mortality and MACCE; (d) patients with a historical cancer diagnosis within 5 years had a higher risk of cardiovascular ischemic events.

Patients With Cancer Tended to Be Treated With Less PCI

We found that patients with cancer are less likely to undergo PCI treatment during hospitalization than those without cancer, and they were also less likely to undergo revascularization during follow-up. According to previous data, patients with active cancer have ∼2- and 3-fold higher risks of 90 days for readmission with AMI or major bleeding after PCI, respectively, than patients without cancer (18). Thus, clinicians are often wary of performing invasive therapies in patients with cancer. However, data from large retrospective studies showed that PCI results in significantly lower risks of in-hospital all-cause mortality and MACCE than conservative treatment, irrespective of whether the patient had a cancer diagnosis, and PCI did not increase the risk of in-hospital complications, including massive bleeding and stroke (19). To date, there has been no large randomized trial to assess the benefits and risks of invasive and conservative approaches to treating AMI in patients with cancer, and such patients are often excluded from clinical trials. The current guidelines recommend that percutaneous revascularization should be considered even in cancer patients with an expected survival duration of <1 year (20). Balloon angioplasty without stents are recommended to limit the duration of antiplatelet therapy. If stents need to be used, those with fast reendothelialization rates may be a better choice.

Clinicians Prefer Conservative Clopidogrel Rather Than Ticagrelor for Aspirin-Based DAPT

The coexistence of high risks of ischemia and major bleeding presents a challenge for clinicians when treating AMI patients with cancer with regard to antiplatelet therapy. When faced with this dilemma, clinicians prefer conservative approaches with regard to aspirin-based DAPT. A less potent P2Y12 inhibitor, namely, clopidogrel rather than ticagrelor, was administered to AMI patients with cancer, but there is a lack of reliable evidence to confirm the greater benefits of clopidogrel among such high-risk patients.

Patients With Cancer Had a Significantly Higher Incidence of Adverse Cardiovascular Outcomes Than Those Without Cancer

A previous study that included 6,563,255 AMI patients revealed that patients with cancer, irrespective of the cancer type, had higher risks of in-hospital mortality, MACCE, and stroke than those without cancer (21). Inflammation plays a vital role in the progression of both cancer and atherosclerotic lesions (including CHD) (22). Although the mechanism underlying this association is unclear, we propose that local malignancies might increase vascular wall inflammation by releasing inflammatory cytokines

and that this circulatory inflammation might subsequently lead to progressive coronary atherosclerosis. In addition, cardiotoxicity can be a major complication of cancer treatment, radiotherapy is recognized as a cardiovascular risk factor among patients with cancer, and many anticancer drugs (anthracyclines, vinca alkaloid anti-metabolites, and biologics) are known to be closely associated with acute early and late cardiovascular adverse events. Perhaps because of the overlap of common risk factors for cancer and CHD and the susceptibility to atherosclerosis caused by oncology treatments (such as radiation therapy or tyrosine kinase inhibitors), patients with cancer tend to exhibit a relatively higher cardiovascular risk. In particular, there was no significant difference in cardiovascular mortality and MACCE for 1 year, but we found that there was no significant difference in cardiovascular mortality and MACCE for 1 year (**Supplementary Table S3**), and the 3-year incidences of all-cause mortality, cardiovascular mortality and MACCE were significantly higher among patients with cancer than among those without cancer (**Supplementary Table S2**). These problems highlight the fact that cardiovascular diseases become more important during the long-term survival of patients with cancer. Advances in screening, big data, targeted and immune therapies, and significant new knowledge of cancer biology are changing the prevention, detection, diagnosis, treatment and survival of cancer. However, the current treatments are still mostly based on extrapolation from non-cancer patient data, and there remain some gaps in achieving the goal of personalized treatment for AMI patients with cancer.

Patients With a Historical Cancer Diagnosis Within 5 Years Had a Higher Risk of Adverse Cardiovascular Outcomes Among All Subgroups

Furthermore, subgroup analysis was performed according to the time between the diagnosis of cancer and the occurrence of AMI. The results showed that the incidences of all-cause death, cardiovascular death and MACCE in the group with a historical cancer diagnosis within 5 years were significantly higher than in those without cancer, and the risks in that subgroup were the highest among all subgroups. This connection is not accidental, and a large-scale study from Sweden also found that patients with cancer had the highest risk of CHD in the first 6 months after diagnosis (23). Another previous study reported similar results: the risks of in-hospital mortality and MACCEs were higher by at least 50% among AMI patients with a current cancer diagnosis than among those without cancer, whereas they were not higher among patients with a historical cancer diagnosis (21). Our findings also underscore the importance of vigilance in cardiovascular risk monitoring after cancer treatment. It is critical to continue assessing the risk of potential cardiovascular events among patients with cancer, and future randomized trials are needed to evaluate the effectiveness of such surveillance.

Limitations

(a) We acknowledge all limitations inherent to a retrospective, single-center study, which restrict the generalization of our findings and the inference of causality. (b) The overall cancer population was relatively small, and the subgroups related to cardiovascular safety concerns were potentially underpowered. In addition, the patients with cancer were a heterogeneous population with different cancer types and stages, and the sample size was too small to evaluate each cancer type separately. (c) Although the data for AMI patients were abundant, the lack of complete cancer history and cancer types may be considered a limitation of this study. The missing data on cancer metastasis, stages, and cancer treatment limits the further understanding of the differences in outcomes between AMI patients with cancer and those without cancer.

CONCLUSIONS

AMI patients with cancer tended to have a significantly higher risk of cardiovascular adverse outcomes than those without cancer. Given the limited evidence-based guidance, clinicians are more likely to empirically initiate conservative treatment when faced with the dilemma of ischemia and the risk of major bleeding. Thus, it is vital to raise awareness of cardiovascular risk management and continuously optimize cardiovascular treatment among patients with cancer.

DATA AVAILABILITY STATEMENT

The raw data supporting the conclusions of this article will be made available by the authors, without undue reservation.

ETHICS STATEMENT

The studies involving human participants were reviewed and approved by the Ethics Committee of Harbin Medical University. The patients/participants provided their written informed consent to participate in this study.

AUTHOR CONTRIBUTIONS

XP, ZW, BY, and JT: study concept and design. XP, ZW, MC, YZ, YT, LY, and WN: acquisition of data. XP and ZW: analysis and interpretation of data and drafting of the manuscript. MC, SW, ZQ, and SZ: critical revision of the manuscript for intellectual content. XP and ZW: statistical analysis. BY and JT: obtaining funding. All authors gave final approval and agreed to be accountable for all aspects of the work, ensuring integrity and accuracy.

FUNDING

This work was supported by grants from the National Natural Science Foundation of China (Grant Nos. 91739113, 81971715 to JT and 81827806 to BY), the Applied Technology Research and Development Program of Heilongjiang Province (Grant No. GA20C007 to JT), the National Key R&D Program of China (Grant No. 2016YFC1301100 to BY), the Fok Ying-Tong Education Foundation for Young Teachers (171032 to JT) and

the Foundation of Guangxi Key Laboratory of Diabetic Systems Medicine (GKLCDSM-20200101-01 to JT).

SUPPLEMENTARY MATERIAL

The Supplementary Material for this article can be found online at: https://www.frontiersin.org/articles/10.3389/fcvm.2022.758324/full#supplementary-material

Supplementary Figure S1 | Clinical outcomes among AMI patients with and without cancer. Displayed are the cumulative incidence curves for **(A)** all-cause mortality, **(B)** MI, **(C)** stroke, and **(D)** revascularization for cancer patients vs. controls. AMI, acute myocardial infarction; MI, myocardial infarction.

Supplementary Figure S2 | Subgroup stratified analysis of all-cause mortality among AMI patients with and without cancer. AMI, acute myocardial infarction; BMI, body mass index; CI, confidence interval; MI, myocardial infarction; PCI, percutaneous coronary intervention; STEMI, ST segment elevation myocardial infarction.

Supplementary Figure S3 | Subgroup stratified analysis of MACCE among AMI patients with and without cancer. AMI, acute myocardial infarction; BMI, body mass index; CI, confidence interval; MACCE, major adverse cardiovascular and cerebrovascular events; MI, myocardial infarction; PCI, percutaneous coronary intervention; STEMI, ST segment elevation myocardial infarction.

Supplementary Table S1 | Pathological types in the 150 patients with cancer.

Supplementary Table S2 | Cumulative incidence of outcomes among AMI patients with and without cancer.

Supplementary Table S3 | Cumulative incidence of 1-year outcomes among AMI patients with and without cancer.

REFERENCES

1. World Health Organization. *Noncommunicable Diseases Country Profiles*. (2018). Available online at: https://www.who.int/nmh/publications/ncd-profiles-2018/en/ (accessed February 25, 2021).
2. Ryerson AB, Eheman CR, Altekruse SF, Ward JW, Jemal A, Sherman RL et al. Annual report to the nation on the status of cancer, 1975-2012, featuring the increasing incidence of liver cancer. *Cancer.* (2016) 122:1312–37. doi: 10.1002/cncr.29936
3. CDC Centers for Disease Control and Prevention. *Two Out of 3 People with Invasive Cancer are Surviving 5 Years or More*. Available online at: https://www.cdc.gov/media/releases/2015/p0312-cancer-survivors.html (accessed February 25, 2021).
4. Hall M, Dondo TB, Yan AT, Goodman SG, Bueno H, Chew DP, et al. Association of clinical factors and therapeutic strategies with improvements in survival following non-ST-elevation myocardial infarction, 2003-2013. *JAMA*. (2016) 316:1073–82. doi: 10.1001/jama.2016.10766
5. Giovannucci E, Harlan DM, Archer MC, Bergenstal RM, Gapstur SM, Habel LA, et al. Diabetes and cancer: a consensus report. *Diabetes Care.* (2010) 33:1674–85. doi: 10.2337/dc10-0666
6. Lortet-Tieulent J, Goding Sauer A, Siegel RL, Miller KD, Islami F, Fedewa SA, et al. State-level cancer mortality attributable to cigarette smoking in the United States. *JAMA Intern Med.* (2016) 176:1792–8. doi: 10.1001/jamainternmed.2016.6530
7. Basen-Engquist K, Chang M. Obesity and cancer risk: recent review and evidence. *Curr Oncol Rep.* (2011) 13:71–6. doi: 10.1007/s11912-010-0139-7
8. DeSantis CE, Lin CC, Mariotto AB, Siegel RL, Stein KD, Kramer JL, et al. Cancer treatment and survivorship statistics, 2014. *CA Cancer J Clin.* (2014) 64:252–71. doi: 10.3322/caac.21235
9. Colzani E, Liljegren A, Johansson AL, Adolfsson J, Hellborg H, Hall PF, et al. Prognosis of patients with breast cancer: causes of death and effects of time since diagnosis, age, and tumor characteristics. *J Clin Oncol.* (2011) 29:4014–21. doi: 10.1200/JCO.2010.32.6462
10. Ye Y, Otahal P, Marwick TH, Wills KE, Neil AL, Venn AJ. Cardiovascular and other competing causes of death among patients with cancer from 2006 to 2015: an Australian population-based study. *Cancer.* (2019) 125:442–52. doi: 10.1002/cncr.31806
11. Yeh ET, Bickford CL. Cardiovascular complications of cancer therapy: incidence, pathogenesis, diagnosis, and management. *J Am Coll Cardiol.* (2009) 53:2231–47. doi: 10.1016/j.jacc.2009.02.050
12. Moslehi JJ. Cardiovascular toxic effects of targeted cancer therapies. *N Engl J Med.* (2016) 375:1457–67. doi: 10.1056/NEJMra1100265
13. Yeh ET, Chang HM. Oncocardiology-past, present, and future: a review. *JAMA Cardiol.* (2016) 1:1066–72. doi: 10.1001/jamacardio.2016.2132
14. Duran JM, Makarewich CA, Trappanese D, Gross P, Husain S, Dunn J, et al. Sorafenib cardiotoxicity increases mortality after myocardial infarction. *Circ Res.* (2014) 114:1700–12. doi: 10.1161/CIRCRESAHA.114.303200
15. Eschenhagen T, Force T, Ewer MS, de Keulenaer GW, Suter TM, Anker SD, et al. Cardiovascular side effects of cancer therapies: a position statement from the Heart Failure Association of the European Society of Cardiology. *Eur J Heart Fail.* (2011) 13:1–10. doi: 10.1093/eurjhf/hfq213
16. De Cicco M. The prothrombotic state in cancer: pathogenic mechanisms. *Crit Rev Oncol Hematol.* (2004) 50:187–96. doi: 10.1016/j.critrevonc.2003.10.003
17. Thygesen K, Alpert JS, Jaffe AS, Chaitman BR, Bax JJ, Morrow DA, et al. Fourth universal definition of myocardial infarction 2018. *J Am Coll Cardiol.* (2018) 72:2231–64. doi: 10.1016/j.jacc.2018.08.1038
18. Kwok CS, Wong CW, Kontopantelis E, Barac A, Brown SA, Velagapudi P, et al. Percutaneous coronary intervention in patients with cancer and readmissions within 90 days for acute myocardial infarction and bleeding in the USA. *Eur Heart J.* (2021) 42:1019–34. doi: 10.1093/eurheartj/ehaa1032
19. Mohamed MO, Van Spall HGC, Kontopantelis E, Alkhouli M, Barac A, Elgendy IY, et al. Effect of primary percutaneous coronary intervention on in-hospital outcomes among active cancer patients presenting with ST-elevation myocardial infarction: a propensity score matching analysis. *Eur Heart J Acute Cardiovasc Care.* (2021) 10:829–39. doi: 10.1093/ehjacc/zuaa032
20. Iliescu CA, Grines CL, Herrmann J, Yang EH, Cilingiroglu M, Charitakis K, et al. SCAI Expert consensus statement: evaluation, management, and special considerations of cardio-oncology patients in the cardiac catheterization laboratory (endorsed by the cardiological society of india, and sociedad Latino Americana de Cardiologia intervencionista). *Catheter Cardiovasc Interv.* (2016) 87:E202–23. doi: 10.1002/ccd.26375
21. Bharadwaj A, Potts J, Mohamed MO, Parwani P, Swamy P, Lopez-Mattei JC, et al. Acute myocardial infarction treatments and outcomes in 65 million patients with a current or historical diagnosis of cancer in the USA. *Eur Heart J.* (2020) 41:2183–93. doi: 10.1093/eurheartj/ehz851
22. Libby P, Ridker PM. Inflammation and atherosclerosis: role of C-reactive protein in risk assessment. *Am J Med.* (2004) 116(Suppl. 6A):9S−16S. doi: 10.1016/j.amjmed.2004.02.006
23. Zoller B, Ji J, Sundquist J, Sundquist K. Risk of coronary heart disease in patients with cancer: a nationwide follow-up study from

Sweden. *Eur J Cancer*. (2012) 48:121–8. doi: 10.1016/j.ejca.2011.09.015

Conflict of Interest: The authors declare that the research was conducted in the absence of any commercial or financial relationships that could be construed as a potential conflict of interest.

Publisher's Note: All claims expressed in this article are solely those of the authors and do not necessarily represent those of their affiliated organizations, or those of the publisher, the editors and the reviewers. Any product that may be evaluated in this article, or claim that may be made by its manufacturer, is not guaranteed or endorsed by the publisher.

frontiers in Cardiovascular Medicine

REVIEW
published: 17 February 2022
doi: 10.3389/fcvm.2022.810262

Risk Factors for the Comorbidity of Hypertension and Renal Cell Carcinoma in the Cardio-Oncologic Era and Treatment for Tumor-Induced Hypertension

*Zhengqing Ba[1], Ying Xiao[1,2], Ming He[3], Dong Liu[1], Hao Wang[1], Hanyang Liang[1] and Jiansong Yuan[1,4]**

[1] Department of Cardiology, Fuwai Hospital, National Center for Cardiovascular Diseases, Chinese Academy of Medical Sciences and Peking Union Medical College, Beijing, China, [2] Xiangya School of Medicine, Central South University, Changsha, China, [3] Department of Infectious Diseases, Peking University First Hospital, Beijing, China, [4] Key Laboratory of Pulmonary Vascular Medicine, Fuwai Hospital, National Center for Cardiovascular Diseases, Chinese Academy of Medical Sciences and Peking Union Medical College, Beijing, China

OPEN ACCESS

Edited by:
Dong Han,
People's Liberation Army General Hospital, China

Reviewed by:
Keyue Ding,
Queen's University, Canada
Aditi Jain,
Institute for Stem Cell Science and Regenerative Medicine (inStem), India

***Correspondence:**
Jiansong Yuan
jsyuantg@163.com

Specialty section:
This article was submitted to Cardio-Oncology, a section of the journal Frontiers in Cardiovascular Medicine

Received: 06 November 2021
Accepted: 17 January 2022
Published: 17 February 2022

Citation:
Ba Z, Xiao Y, He M, Liu D, Wang H, Liang H and Yuan J (2022) Risk Factors for the Comorbidity of Hypertension and Renal Cell Carcinoma in the Cardio-Oncologic Era and Treatment for Tumor-Induced Hypertension. Front. Cardiovasc. Med. 9:810262. doi: 10.3389/fcvm.2022.810262

Advances in tumor diagnosis and treatment, especially the use of targeted therapies, have remarkably improved the survival rate of patients with renal cell carcinoma (RCC), accompanied by higher hypertension (HTN) incidence among patients with RCC, reflecting the coming of a cardio-oncologic era. Therefore, for patients with RCC and HTN simultaneously, finding risk factors for the comorbidity and giving better clinical treatment have been urgent problems. In this review, we thoroughly investigated risk factors for the comorbidity of HTN and RCC based on preclinical and clinical studies. Firstly, RCC and HTN may have common risk factors, such as obesity, smoking, and other modifiable lifestyles. Secondly, RCC and HTN may lead to each other directly or indirectly by their therapies. We then discussed measures of reducing the comorbidity and treatment of HTN in patients with RCC. We also discussed the deficiency of current studies and pointed out future directions. In conclusion, this review aims to deepen the understanding of cardio-oncology and bring benefit to the population who are at high risk of getting or have already got RCC and HTN simultaneously.

Keywords: hypertension, kidney cancer, comorbidity, targeted therapy, antihypertensive drug, cardio-oncology

INTRODUCTION

The prevalence of hypertension (HTN) and renal cell carcinoma (RCC) keeps increasing. In 2019, one-third of people between 30 and 70 years old were estimated to have HTN globally and the number has doubled from 648 to 1.2 billion in the past 3 decades (1). HTN was the most frequent comorbidity with malignant tumors, seen in 38% of patients with cancer (2). RCC accounted for about 90% of renal malignancies (3). According to GLOBOCAN in 2020, the patients with kidney cancer were more than 1.2 million and new cases were estimated to be 431,288 globally (4). RCC prevalence in the United States was increasing owing to a higher incidence which had doubled compared with the incidence in 1975 (15.6 vs. 7.1 per 100,000 persons) and longer 5-year relative survival (75.6 vs. 52.3%), reported by the SEER program (5).

Since the prevalence of HTN and RCC is increasing, patients with RCC and HTN simultaneously are estimated to increase for the following reasons: HTN is a potential risk factor for RCC (6) and RCC can cause HTN due to paraneoplastic syndrome (7), nephrectomy (8), and targeted therapies (9). Besides, prolonged survival rates and modern lifestyles may increase the comorbidity of HTN and RCC (10). The above-mentioned situation raised our questions: (1) What are the risk factors for the comorbidity of HTN and RCC in cardio-oncologic era? (2) How to decrease the comorbidity of HTN and RCC? (3) How to give better antihypertensive treatment for the patients with RCC with HTN? To answer these questions, we did a thorough search and reviewed the relationship between HTN and RCC based on clinical evidence and basic researches (**Figure 1**).

METHODS

A literature review of publications about RCC and HTN has been performed. A manuscript outline was formed before searching for relevant publications. PubMed (1946–2021) and Cochrane Library (1996–2021) were employed as the source of initial searches. Hand searching was also used to find relevant studies in PubMed and other websites (e.g., FDA and SEER). Besides, valuable publications recommended by experts were included as well. Key search words include HTN, antihypertensive agents, and kidney neoplasms. Detailed search queries and search results are available (**Supplementary Material**). In total, 7,279 studies were found. These studies were screened for eligibility using title and abstract. The remaining studies were then retrieved as full texts and checked with inclusion and exclusion criteria. We considered studies that were related to: (1) epidemiology about RCC or HTN; (2) risk factors causing RCC or HTN; (3) mechanisms for the formation of RCC or HTN; (4) treatment of HTN in patients with RCC. We excluded studies that were: (1) not in English; (2) duplicate; (3) clinical studies with similar results but lower evidence level or out of date; and (4) could not find full text. The review process is conducted independently by 3 authors. Discrepancies were solved by consensus.

COMMON MODIFIABLE RISK FACTORS

Obesity, inadequate physical activity and alcohol are well-known dose-dependent risk factors for HTN (11). The relationship between smoking and HTN is complex, but it is certain that cessation of smoking can dramatically reduce the cardiovascular disease burden (12). It is noteworthy that obesity, smoking, and inadequate physical activity are also risk factors for RCC (13) while alcohol exerts a protective effect on RCC development (14). Besides, diets play important roles in HTN and RCC. For example, excess salt intake increases blood pressure (BP) (11), whereas heavy meat and fatty food are risk factors for RCC, and lack of vegetables or fruits may also increase RCC incidence (15), but the common unhealthy diets for both RCC and HTN still need further study. In summary, obesity, smoking, and inadequate physical activity are common modifiable risk factors for RCC and HTN, we will discuss the clinical evidence and potential mechanisms below.

Obesity as a Risk Factor for RCC

A meta-analysis of 24 cohort studies showed that the relative risk (RR) of kidney cancer was 35% higher ($RR = 1.35$, 95% CI = 1.27–1.43) in overweight [body mass index (BMI): 25–30] and 76% higher (1.76, 1.61–1.91) in patients of obesity (BMI > 30) compared with the normal weight population (16). Several indicators of obesity were used in clinical studies, such as BMI, waist and hip circumference, and body fat percentage, but the results were consistent (15). A large cohort study demonstrated that per unit increase in BMI will increase 5% risk of RCC (17). Both pre-existing obesity in adulthood and obesity near diagnosis of RCC could increase the risk of renal cancer [odds ratio (OR) = 1.6, same] (18). Of note, a cohort study in Japan demonstrated that low BMI (<21) may also increase the risk of kidney cancer [hazard ratio (HR) = 1.86; 95% CI: 1.01–3.45] compared with BMI of 23.0–24.9 (19). Interestingly, obesity was found to increase the risk of clear-cell RCC while decreasing the risk of papillary RCC (14). Such heterogeneity may be associated with demographic difference considering the fact that papillary RCC is more common in women, the older and the black (20).

Obesity-induced chronic renal hypoxia may play an oncogenic role mainly through upregulating the vascular endothelial growth factor (VEGF) pathway (21). Obesity could cause lipid peroxidation and then facilitate the formation of RCC (22). Obesity-induced renal hyperfiltration may increase the exposure to oncogenic nephrotoxins (23). Increased estrogen in adiposity patients also facilitates RCC by upregulating the insulin-like growth factor-1 (IGF-1) receptor, enhancing the oncogenic influence of IGF-1 (24). Metabolism disorders caused by obesity are also oncogenic. Overexpressed insulin and IGF-1 could promote the formation of RCC. Adiponectin, secreted by fatty tissue, is an anti-angiogenic factor by suppressing the VEGF pathway. However, the serum adiponectin is expressed lower in obesity (15). Besides, increased leptin in obesity, which is a kind of adipokine, promotes RCC by regulating VEGF, the Janus kinase/signal transducer and activator of transcription 3 and extracellular signal-regulated kinase 1/2 pathways (25). Obesity-induced inflammatory response increases levels of interleukin-6, which is also an oncogenic adipokine because it can protect RCC cells from immune attacks (26).

Insulin resistance and increased circulating insulin observed in obesity could induce HTN by increasing renal sodium reabsorption and activating the sympathetic nervous system (27). Elevated leptin can also promote HTN mediated by increasing

Abbreviations: ACEI, angiotensin-converting enzyme inhibitor; a-MSH, a-melanocyte-stimulating hormone; ARB, angiotensin receptor blockade; BMI, body mass index; BP, blood pressure; CCB, calcium channel blocker; DBP, diastolic blood pressure; HR, hazard ratio; HTN, hypertension; IGF-1, insulin-like growth factor-1; mRCC, metastatic RCC; mTOR, mammalian target of rapamycin; OR, odds ratio; OS, overall survival; PFS, progression-free survival; PN, partial nephrectomy; RCC, renal cell carcinoma; RR, relative risk; RN, radical nephrectomy; SBP, systolic blood pressure; tHTN, targeted therapy-related HTN; TKI, tyrosine kinase inhibitor; VEGF, vascular endothelial growth factor; VSP, vascular endothelial growth factor signaling pathway.

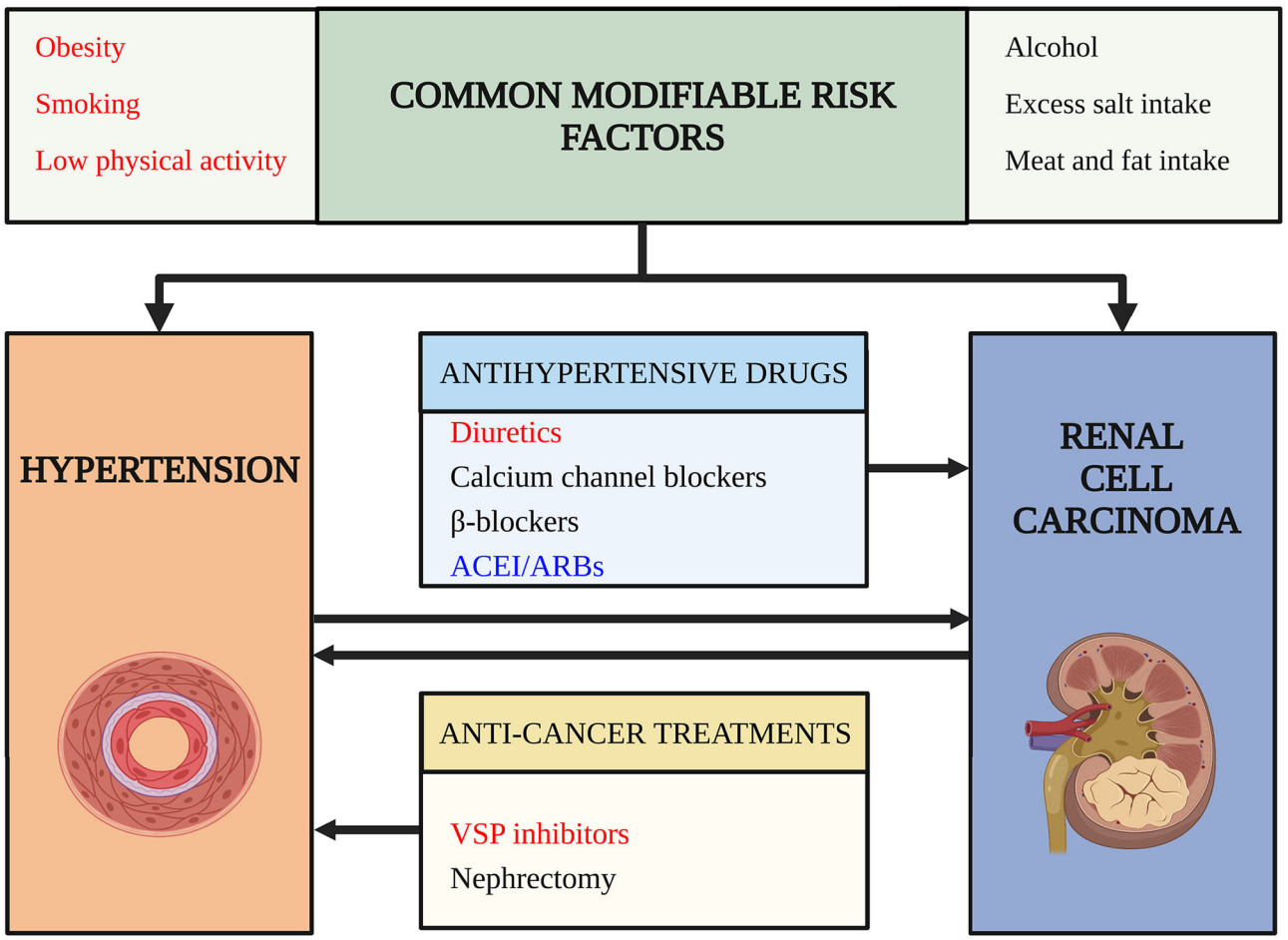

FIGURE 1 | Risk factors for comorbidity of hypertension (HTN) and renal cell carcinoma (RCC). This figure outlines risk factors for the comorbidity of hypertension and renal cell carcinoma. Arrows indicate a potential causality relationship. Words in red color highlight risk factors confirmed by high-level evidence and have achieved consensus. Words in black color indicate risk factors lack strong evidence or the evidence are still conflictive. Words in blue indicate risk factors that may decrease the risk of comorbidity and have protective roles. ACEI/ARB, angiotensin-converting enzyme inhibitors/angiotensin receptor blockades; VSP, vascular endothelial growth factor signaling pathway.

sympathetic nervous system activity (28). Furthermore, a-melanocyte-stimulating hormone (a-MSH) that is a hormone secreted by melanocytes could regulate BP by suppressing adrenocorticotropic hormone. Interestingly, a-MSH could also inhibit obesity progress by targeting melanocortin 4 receptor. Therefore, it is hypothesized that sunshine may increase levels of a-MSH and then protect obese patients from inflammation-induced HTN (29).

Smoking as a Risk Factor for RCC

A meta-analysis of 24 studies reported that smokers have a higher risk for RCC (*RR* = 1.38, 95% *CI*: 1.27–1.50) and a dose-dependent relationship was seen both in men and women (30). Remarkably, passive smoking increases the risk of RCC either (31). Cessation of smoking for more than 30 years reduced 50% risk of RCC (*CI*: 0.3–0.8), while quitting smoking shorter than 30 years showed no significant difference in RCC incidence (32). A retrospective study revealed that smoking is positively related to increased risk of clear-cell RCC rather than papillary RCC. However, this heterogeneity may be attributable to the skewed distribution of smoking patterns (14).

Some ingredients contained in cigarettes are carcinogenic. Nicotine could induce angiogenesis of RCC, while N-nitrosamines and Benzo[α]pyrene diol epoxide correlate with renal oxidative stress which could lead to DNA damage or gene aberration, thus facilitating the formation of RCC (15). Smoking-related chronic respiratory diseases and carbon monoxide could cause hypoxia of renal tissue (10) and lipid peroxidation is another possible mechanism (22).

Grassi et al. (33) found that smoking-induced acute increase of BP attributes to higher dose of catecholamines at the neuroeffector junctions. In addition, smoking was demonstrated to cause increased arterial wave reflection and stiffness of large arteries, thus enhancing BP (34). Smokers with atherosclerotic renal artery stenosis were more common than non-smokers, and renal vascular stenosis could cause refractory HTN (35).

Low Physical Activity as a Risk Factor for RCC

Low physical activity is regarded as a risk factor for RCC (36–38). An American cohort study of 482,386 participants with a median follow-up of 8.2 years showed that the multivariate RR for those with current exercise more than 4 times per week was 0.77 (95% *CI*: 0.64–0.92) compared with the never exercise population. Besides, regular exercise and activity in youth is also protective (36). Similarly, a meta-analysis including 19 studies, which was conducted in 2013, showed that adequate physical activity was a protective factor for RCC ($RR = 0.88$, 95% *CI*: 0.79–0.97) (37). Physical activity like running or walking had a dose–response relationship with a decreased risk (1.9% risk decline per metabolic equivalents hour/week) of kidney cancer after adjustment for age and sex (38).

Physical activity may decrease the risk of RCC in a directly or indirectly manner. Physical activity could directly inhibit RCC formation by decreasing insulin resistance, circulating IGF-1, and lipid peroxidation (37). Some researchers thought the lack of exercise was an indirect risk factor because a low level of energy consumption could cause obesity and subsequently promotes RCC formation (13). Furthermore, more activity could prevent HTN and diabetes, which are also confounding factors (38).

The mechanisms for inactivity-induced HTN have not been clearly demonstrated. Murine studies showed that insulin resistance and imbalance of sympathetic and vagus nerves are potential reasons (39). Another animal study demonstrated that resistance training could contribute to the regulation of vessel constriction and keep luminal diameter (40). Other factors that explain inactivity-induced HTN include vascular resistance, arterial stiffness, oxidative stress, inflammation, BMI, and endothelial function (41).

HTN AS A DIRECT RISK FACTOR FOR RCC

A meta-analysis of 18 prospective studies and 14 case–control studies showed that each 10 mmHg increase of systolic BP (SBP) led to 5% higher risk (95% *CI*: 1.03–1.06) of RCC and 10 mmHg increase of diastolic BP (DBP) with 7% higher risk (95% *CI*: 1.04–1.10) (42). However, extremely high pressure (SBP $>$ 150 mmHg or DBP $>$ 100 mmHg) will cause a rapid increase of RCC incidence rather than linear growth (6, 43). It is noteworthy that even high-normal BP (SBP: 130–140 mmHg, DBP: 80–90 mmHg) could increase the risk of RCC (44).

Women with HTN may be more susceptible to RCC. A recent meta-analysis showed that women with HTN have a 54% higher risk than men ($RR = 63$ vs. 29%), but the difference was substantially reduced (1.40, 1.12–1.74 for men and 1.54, 1.17–2.04 for women) after adjustment for age, cigarette, family history of RCC, obesity, alcohol, and physical activity (42).

Age may influence the incidence of RCC in the patients of HTN while this hypothesis is still controversial. A study suggested that HTN was not an independent risk factor for RCC in adolescence (45), while another study got the opposite conclusion that younger patients with HTN were more likely to develop RCC (44).

It is worth mentioning that HTN may have a synergistic effect with obesity on RCC formation. A prospective study showed that the risk of obesity-caused RCC will increase significantly when BP was very high (SBP $>$ 160 mmHg or DBP $>$ 100 mmHg) (6).

A cohort study conducted in Sweden with a mean follow-up of 16 years among 3,63,992 men using repeated measurements of BP showed that RCC incidence decreased with the reduction of BP and especially, in those with a reduction of more than 14 mmHg in DBP, the RR for RCC decreased 40% (46). Thus, HTN is a modifiable risk factor for RCC and effective control of BP is of great value.

However, some factors may influence the reliability of these researches. HTN shares several common risk factors with RCC (43), which highlights the necessity of sufficient adjustment for these confounding factors during the investigation of the causality between HTN and RCC. Besides, the way of defining and measuring HTN varies (47). Of note, if RCC were diagnosed in patients with HTN in the first several years after enrollment in a cohort, it is difficult to determine the occurrence sequence of RCC and HTN. But such bias could be avoided by excluding data of the first several years of follow-up (46). In conclusion, well-designed prospective studies are warranted to clarify their causality.

As to the mechanisms of HTN-induced RCC, HTN could result in chronic inflammation, making the kidney in a state of hypoxia and then upregulating the expression of hypoxia-inducible factors, causing overexpressed VEGF and platelet-derived growth factors which could facilitate the tumor genesis (2). Overexpressed angiotensin receptors and angiotensin-converting enzyme in the patients with HTN could upregulate the angiotensin II, and cause the overexpression of oncogenic VEGF (42, 48). In addition, HTN is related to dysfunction and remodeling of blood vessels, which could increase the number of reactive oxygen species and eventually promote the formation and progress of tumor (44). Similar to obesity, an increased level of lipid peroxidation in the patients of HTN is supposed to participate in RCC carcinogenesis (22).

ANTIHYPERTENSIVE DRUGS AS A POTENTIAL RISK FACTOR FOR RCC

In general, antihypertensive drugs are not risk factors for cancers (49). However, a recent cohort study in Korea showed that the use of antihypertensive drugs in patients of HTN was related to increased risk of RCC ($HR = 1.74$, 95% *CI*: 1.64–1.84) and those with two or more classes of antihypertensive drugs have an even higher risk ($HR = 1.80$, 95% *CI*: 1.69–1.91) without adjusting for HTN (44). Another cohort study supported this result after adjusting for HTN, sex, age, BMI, and smoking (6). There seemed to be a linear relationship between the RCC incidence and the duration of antihypertensive drugs, and the risk will increase 2% per year (95% *CI*: 1.01–1.02) (50). However, different kinds of antihypertensive drugs play different roles in RCC development. Diuretics have been convincingly shown to be tumorigenic for kidney, while angiotensin-converting enzyme inhibitor/angiotensin receptor blockades (ACEI/ARBs)

are possible anti-cancer drugs. The role of calcium channel blockers (CCB) and β-blockers is still in dispute. The tumorigenic role of these antihypertensive drugs will be elaborated below.

Diuretics

Many researchers argued that diuretics are risk factors for RCC (47, 48, 50–53). A systematic review of observational studies in 2020 found that diuretics could increase 34% RCC risk (95% *CI*: 1.19–1.51) (50). Another meta-analysis showed that the risk effect of diuretics was still significant after adjustment for smoking, obesity, and HTN (47). Several cohort studies and case–control studies drew similar conclusions (48, 51). Women with diuretics ($OR = 1.92$, 95% *CI*: 1.59–2.33) seemed to have a higher risk of RCC than men ($OR = 1.18$, 95% *CI*: 0.93–1.49) (47). The sexual difference may be explained by the hypothesis that estrogens could intensify the effect of thiazide in the distal tubule, and women consume more diuretics than men (52). Some possible underlying mechanisms may explain the carcinogenic role of diuretics. First, hydrochlorothiazide could be converted in the stomach to nitroso derivatives and cause genetic mutations (53). Second, diuretics may exert a little carcinogenic function on their target, the renal tubular cells (51). More detailed preclinical studies are necessary to clarify the possible tumorigenic mechanisms of diuretics.

Calcium Channel Blockers

The role of CCB on RCC carcinogenesis has not been determined yet (54). In patients without HTN, the use of CCB increased the risk of papillary RCC rather than clear-cell RCC, demonstrated by a retrospective study (55). CCB may predispose the patients with HTN to RCC by impeding DNA fragmentation and cell apoptosis (44). However, other clinical studies showed insignificant results which denied its carcinogenic role (54).

β-Blockers

The role of β-blockers for RCC incidence is less well-studied. A recent cohort study showed that β-blockers have higher HR for RCC than other antihypertensive drugs (44). However, another large cohort study showed that β-blockers may not increase the risk of total cancer incidence (56). Thus, the exact role of β-blockers as a possible cancer-promotor is far from clear.

Angiotensin-Converting Enzyme Inhibitors/Angiotensin Receptor Blockades

The role of ACEI/ARBs is still in dispute (57). A meta-analysis showed that ACEI increased the risk of RCC ($RR = 1.50$, 95% *CI*: 1.01–2.23) (58). ACEI may increase the amount of bradykinin which may facilitate RCC formation (57). Interestingly, ACEI/ARBs are also considered as possible anti-cancer drugs since overexpressed angiotensin receptors and angiotensin II is associated with upregulated VEGF (59).

Even though many clinical studies have managed to clarify the causality between antihypertensive drugs and RCC, there are still no conclusive results because of some limitations. Firstly, it is quite difficult to exclude the effect of HTN *per se* (10). For example, a large prospective study in 2008 showed that in those with SBP < 160 mmHg or DBP < 100 mmHg, the use of antihypertensive drugs did not show a significant difference compared with non-users while in those with poorly controlled BP, antihypertensive medication increased the risk of RCC, which highlighted the confounding role of HTN (6). Secondly, other confounding factors like age, sex, obesity, smoking, and physical activity are sometimes not adjusted because of the small sample size or poor statistical design. Thus, a well-designed large prospective clinical study is needed to clarify the relationship between antihypertensive drugs and RCC.

RCC DIRECTLY CAUSE HTN

The HTN directly caused by RCC is considered as a manifestation of paraneoplastic syndrome and in the population with malignant HTN, the prevalence of RCC was 1.2%, much higher than those without malignant HTN (0.01%) (7), indicating malignant HTN could be a clue for the diagnosis of RCC. The severity of paraneoplastic HTN varies and can sometimes cause refractory HTN. Most of the paraneoplastic HTN will recover after nephrectomy (60–62).

Tumor compression, renal arteriovenous fistula, and ureteral obstruction could cause renal ischemia, thus activating the rein-angiotensin-aldosterone system, leading to HTN (63, 64). Besides, ectopic hormones secretion, such as catecholamines, erythropoietin correlated with paraneoplastic HTN (7, 60). Hypercalcemia, which increased vascular resistance or indirectly increased catecholamines, could also cause HTN (61, 62). In addition, paraneoplastic nodular polyarteritis correlated with renal vascular HTN (59). It is rarely reported that brain metastasis from RCC could cause intracranial HTN by compressing dural venous sinuses (65).

TREATMENT OF RCC CAUSE HTN

The treatment of RCC mainly includes surgery for localized RCC, targeted therapy, and immunotherapy for metastatic RCC (mRCC) (3). The excision of kidney jeopardizes kidney function and then increases the risk of cardiovascular disorders, such as coronary heart disease, HTN, cardiomyopathy, heart failure (HF), and dysrhythmias (66). Considering that partial nephrectomy (PN) can better preserve kidney function than radical nephrectomy (RN), PN is recommended to treat patients with early stage tumors (3). Nephrectomy-related HTN (NR-HT) has been reported by several studies, but robust high-level evidence is still needed (8, 67–69). The use of targeted therapies, especially vascular endothelial growth factor signaling pathway (VSP) inhibitors, has remarkably increase the life expectancy of patients with mRCC while the increased risk of cardiovascular events turns out to be its obvious side effect (5, 70). Apart from HTN, VSP inhibitors could also cause venous thromboembolism (VTE), HF, arterial thromboembolism (ATE), myocardial infarction (MI), long Q-T syndrome (LQTS) and Torsade de Pointes (TdP). Detailed information is listed in **Table 1**. Immnunotherapy is also a first-line therapy for mRCC but significant cardiovascular side effects have not been found yet (3, 70).

TABLE 1 | Incidence of targeted therapy associated hypertension (HTN) in patients with metastatic renal cell carcinoma (mRCC).

Drugs	FDA approved year	Any grade HTN (%)	Grade 3/4 HTN (%)	Other associated cardiovascular complications
Temsirolimus	2007	7	-	VTE, thrombophlebitis
Everolimus	2009	1–10	3	Non-infectious pneumonitis with pulmonary HTN, VTE, tachycardia, HF
Bevacizumab	2004	4–34	1–11	ATE, VTE, HF
Sorafenib	2005	12–34	4–11	MI, LQTS
Sunitinib	2006	24–41	8–15	MI, HF, cardiomyopathy, LQTS, TdP
Pazopanib	2009	13–57	4	LQTS, TdP, HF, ATE, VTE, thrombotic microangiopathy
Axitinib	2012	40–42	8–16	ATE, VTE, HF, MI
Lenvatinib	2015	42	13	cardiomyopathy, HF, ATE, LQTS
Cabozantinib	2016	37–81	15–28	MI, ATE, VTE
Tivozanib	2021	44–45	12–22	HF, MI, ATE, VTE

This table shows data about incidence of tHTN collected from FDA, Phase III clinical trials and meta-analysis or other high-grade evidences. The Grade 3/4 HTN data about Temsirolimus has not been found. HTN, hypertension; VTE, venous thromboembolism; HF, heart failure; ATE, arterial thromboembolism; MI, myocardial infarction; LQTS, long Q-T syndrome; TdP, Torsade de Pointes.

Nephrectomy-Related HTN

As for PN, a cross-sectional survey showed that PN was independently associated with NR-HT ($OR = 2.93$, $p = 0.022$) (8). There are several hypotheses for NR-HT after PN. The compressed renal parenchyma due to renal hematoma, bolsters, or sclerotic tissue could cause insufficient renal perfusion and renin-angiotensin system activation, which refers to the "page kidney" hypothesis (71). In addition, vascular clamping in PN process could cause vasculitis and intimal hyperplasia, which would aggravate renal artery stenosis, resulting in the decline of glomerular capillary pressure and activated rennin-angiotensin system, leading to NR-HT (72). However, some studies drew opposite conclusions (67, 73). A retrospective study involving 264 patients with PN showed that BP had no significant change after surgery (67). A plausible explanation is that PN may treat paraneoplastic HTN, which can mask NR-HT, thus resulting in a statistically insignificant difference. Another study showed the BP decreased 1.9 mmHg ($p = 0.01$) in 5 years after PN and the decrease of BP is thought to be associated with more BP measurements during follow-up and increased antihypertensive medications (73). Considering the conflicting results, well-designed prospective researches are warranted for NR-HT.

As for RN, it is still uncertain for its facilitating HTN role owing to insufficient evidence. After more than 10 years of follow-up, a small cohort study showed that 40% of patients with RN developed NR-HT and the mechanisms of RN leading to NR-HT are most likely due to functional renal parenchyma deficits and secondary end-stage renal disease (68). However, another cross-sectional cohort study showed that there was no significant difference in BP among RCC patients who underwent RN (69). Besides, the circadian rhythm of BP may also be affected after bilateral RN (74).

Targeted Treatment-Related HTN

Targeted therapies for mRCC have prolonged the overall survival (OS) and progression-free survival (PFS) significantly and now have been listed as the standard treatment for mRCC (3). However, the number of patients with mRCC complicated with targeted therapy-related HTN (tHTN) as the on-target effect has dramatically increased (75).

These targeted drugs for mRCC mainly include VSP inhibitors and phosphatidylinositol-3-kinase–protein kinase B/mammalian target of rapamycin (mTOR) inhibitors. Bevacizumab is a monoclonal antibody to VEGF, often accompanied by the use of IFN-α (3). Multitargeted tyrosine kinase inhibitors (TKIs), which can bind to VEGF receptors and suppress the VEGF pathway, include sunitinib, sorafenib, pazopanib, axitinib, tivozanib, and cabozantinib (76). The mTOR inhibitor includes everolimus and temsirolimus (3). According to a report of real-world treatment patterns, the most common first-line used of targeted drugs in 2015 in the United States are sunitinib and pazopanib accounting for about 70% (77).

Strong evidence showed that targeted therapy, especially VSP inhibitors, could induce HTN. We collect data about tHTN from FDA (70), Phase III clinical trials, meta-analysis, or other high-grade evidence RCC (78–84) (**Table 1**). The Common Terminology Criteria for Adverse Events classified the tHTN into 5 grades. A meta-analysis of randomized controlled trials in 2015 showed that patients with TKIs have a significantly higher grade 3 or 4 HTN incidence compared with IFN-α or placebo ($RR = 6.00$, 95% CI: 3.36–10.69) (9). A large retrospective real-world study from 2006 to 2015 showed the total tHTN incidence rate was 69.1 per 100 patient-years and VSP inhibitors were higher than mTOR inhibitors (71.7 vs. 47.8 per patient-years) (77). The newer generation of VSP inhibitors which are more powerful to inhibit the VEGF pathway, tended to have higher HTN incidence (85). In addition, higher doses and longer duration of VSP inhibitors will increase the incidence and degree of HTN, which showed a dose-dependent relationship (2, 85, 86). Germline polymorphisms (86), high SBP at baseline (87), aging and other cardiovascular risk factors (88) may also affect the onset of tHTN. The tHTN could occur within hours or days after receiving VSP inhibitors (9) and drop quickly after drug withdrawal (89). The average onset time of tHTN was 131 days for bevacizumab (78), 116.5 days for mTOR inhibitors, and 70.0 days for VSP inhibitors (77). The newly proved lenvatinib has a median onset time of 35 days, reported by the FDA (70).

The use of antihypertensive drugs may affect the onset time of severe HTN (9).

The mechanisms for tHTN are still elusive. VSP inhibitors could cause depletion of nitric oxide and prostacyclin which are vasodilators as well as increased vasoconstrictive endothelin-1 (89). In addition, increased reactive oxygen species, functional decreased microvascular density, increased vascular stiffness, and salt sensitivity are other possible reasons (90).

The tHTN could be seen as a biomarker for the on-target effect of VSP inhibitors and indicated a better prognosis (75). A multicenter retrospective study in 2020 demonstrated that patients with tHTN had higher PFS (12 months, 95% *CI* = 9–21 months) than those without tHTN (9 months, 95% *CI*: 7–12 months) (86). Similar results were shown among other TKIs and Bevacizumab (2, 75).

However, HTN that is not induced by targeted therapy could increase the risk of RCC mortality (*OR* = 1.75, 95% *CI*: 1.61–1.90) demonstrated by a review such as 6,964 patients of RCC in 2002 (91). Severe HTN in patients of RCC could cause HF, leukoencephalopathy, suspend, or cessation of targeted drugs (75, 90), which will do harm to the prognosis and well-control of BP during targeted therapy could improve prognosis (92).

Selection of Antihypertensive Drugs for tHTN

There is no conclusion about the best antihypertensive drugs for tHTN (81). The current opinion is the selection of antihypertensive drugs should be individualized, but there are indeed some preferences (93).

Angiotensin-converting enzyme inhibitors/ angiotensin receptor blockades are potential better antihypertensive drugs for VSP inhibitors users. Several retrospective studies showed that patients of mRCC treated with sunitinib or other VSP inhibitors had better OS and PFS if received ACEI/ARBs (92, 94). ACEI/ARBs may be more recommended in patients with mRCC undergoing nephrectomy, considering its renal protective function (95). ACEI/ARBs could also treat proteinuria and left ventricular systolic dysfunction induced by targeted treatment (81, 90). ACEI/ARBs may prevent sarcopenia in patients with RCC and then reduce overexposure and toxicity of TKIs which could decrease the treatment interruption rate (95). However, a case report claimed that ACEI may decrease the effect of bevacizumab in ovarian cancer (96) and another case reported that combinatorial therapy of ACEI and everolimus may increase the risk of angioedema (97). A pooled-analysis reported that baseline use of ACEI/ARB is not significantly associated with OS or PFS (81). Thus, even with much supporting evidence, the priority of ACEI/ARB in mRCC needs further studies.

Dihydropyridine CCB can control tHTN as well as other antihypertensive drugs, considering the function of inhibiting arterial wall contractility (98). In addition, CCB was thought to inhibit chemoresistance of RCC and thus enhance drug efficacy (88). Besides, animal studies showed that CCB could increase the density of micro-vessels (89). But non-dihydropyridine CCB should not be used in patients receiving VSP inhibitors because they would competitively inhibit the activity of P450 3A4, thus increasing the circulating VSP inhibitors concentrations (2).

A retrospective study showed that the patients with mRCC treated with sunitinib or pazopanib with β-blockers have better PFS and OS than other antihypertensive drugs (99). Animal studies have shown that β-blockers could inhibit the proliferation of cancer, but the anti-cancer role of β-blockers in human is still in controversy (100).

The use of diuretics should consider the probability of dehydration and electrolyte disorders, since patients treated with VSP inhibitors like sunitinib have the higher risk of diarrhea and electrolyte imbalances (95). Fluid retention due to sodium excretion depletion may explain tHTN occurred weeks later and diuretics are a potential preference in this condition (101).

DISCUSSION

What Are the Risk Factors for Comorbidity of HTN and RCC?

The relationship between HTN and RCC is complex (**Figure 1**). HTN and RCC share several common modifiable risk factors, such as obesity, smoking, and low physical activity. These risk factors may induce RCC and HTN through several common mechanisms, for example, chronic inflammation, oxidative stress like lipid peroxidation, interleukin-6, insulin, IGF-1, leptin, and VEGF pathway (48). There are also some potential common risk factors, like unhealthy diet, alcohol, but need further study to confirm their roles.

Hypertension is a direct risk factor for RCC with a dose-dependent relationship. HTN may also play a synergistic role with other risk factors like obesity to facilitate RCC. Meanwhile, the risk of RCC caused by antihypertensive drugs has not been excluded and diuretics are with great suspicion to cause RCC. Notably, ACEI/ARBs are potential anti-cancer drugs considering their mechanisms of function.

Renal cell carcinoma can directly cause HTN by the formation of arteriovenous fistula, tumor compression-induced renin secretion, ectopic hormone syndromes, paraneoplastic vasculitis, and brain metastasis. Treatment of RCC can also induce HTN. Nephrectomy may affect BP. The use of targeted therapy is strongly associated with HTN. This kind of increased BP is short-term, reversible, and dose-dependent and indicates the effect of targeted therapy. As to medicine for tHTN, there is no strong evidence proving a preference for a certain kind of antihypertensive drugs.

There are some guiltless factors responsible for the increasing comorbidity. For example, population growth and aging, advances in cancer treatment and prolonged survival, widespread use of advanced imaging techniques, improved public awareness for annual medical examination (44, 48, 102).

How to Decrease the Comorbidity of HTN and RCC?

There are some factors that we can handle to decrease the comorbidity and the suggestions are discussed below (**Figure 2**).

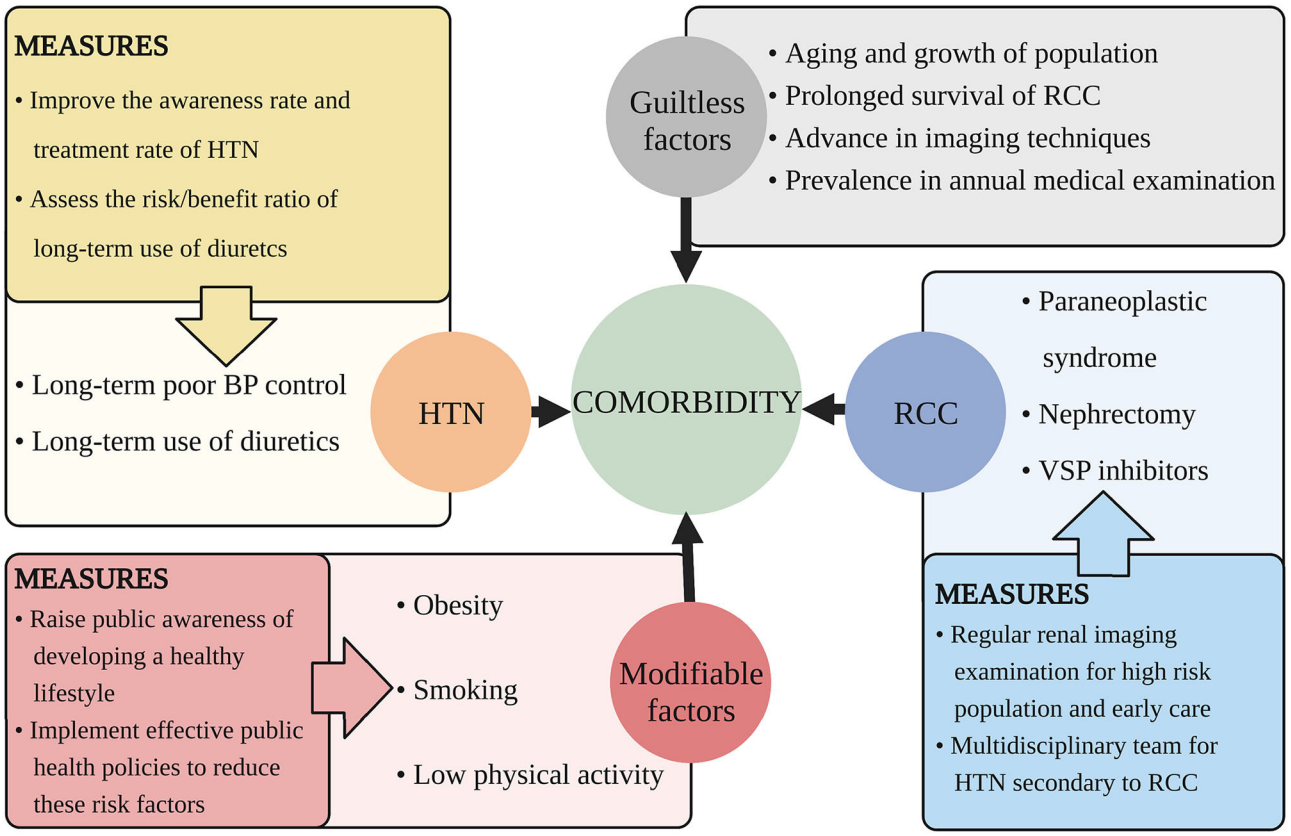

FIGURE 2 | Suggested measures for decreasing the comorbidity of HTN and RCC. This figure illustrates aspects that cause the increasing comorbidity of HTN and RCC and proposes related measures. HTN, hypertension; RCC, renal cell carcinoma; BP, blood pressure; VSP, vascular endothelial growth factor signaling pathway.

Obesity, smoking, and lack of physical activity all show a dose-dependent relationship with RCC and HTN. Obesity was supposed to be associated with 78% patients of HTN, and increased 60% risk of RCC (90). The risk of RCC doubled in people smoking more than 20 cigarettes a day while cessation of smoking more than 30 years reduced the 50% risk of RCC (32). Adequate physical activity can reduce 12% risk of RCC (37). It is known that prevention is more favorable than treatment, both for patients and for society. Thus, public awareness of developing a healthy lifestyle should be raised and effective public health policies should be implemented to reduce the modifiable risk factors.

Poor control of essential HTN facilitates the rising prevalence of RCC. Globally, it is estimated that only half patients of HTN are diagnosed and one-fifth patients of HTN have well-controlled BP (1). Thus, improvement of the awareness and treatment rate of HTN is quite urgent.

Diuretics exert a potential carcinogenic effect, thus it should be prescribed after comprehensive thought of the risk/benefit ratio (103). For those with severe HF, refractory HTN, or edema, the benefit is higher than the risk. Considering the carcinogenic risk of diuretics is low and needs long-term accumulation to be significant, younger women who need decades of use of diuretics are at high risk than the elderly and if not necessary, better change to other antihypertensive drugs.

For those with obesity, smoking exposure, low activity, and unhealthy diets, the risk of RCC or HTN is high. For those with long-term HTN and diuretics history, RCC will occur in higher possibility. People with malignant HTN also have a higher incidence of RCC (7). These groups with a high risk of RCC are recommended for regular renal imaging examination. And for those already diagnosed with RCC and HTN, cardio-oncologic teams are needed to give better clinical care.

How to Give Better Antihypertensive Treatment for the Patients With RCC With HTN?

Regular and accurate BP measurement is fundamental. If the patients with RCC are treated with nephrectomy and targeted therapy, clinicians need to predict the possible changes of blood pressure and monitor BP regularly. As to tHTN, guideline recommend well-controlled BP before targeted treatment and weekly monitor during the first treatment cycle and monitor every 2–3 weeks in the remaining treatment cycle (76). For

those with a history of HTN or coronary heart disease, the risk of cardiovascular event is significantly higher when receiving VSP inhibitors and should be monitored with caution (104). Hypotension may also occur as a manifestation of hypersensitivity/infusion reactions when receiving targeted therapy (70). Thus, BP should be monitored throughout the infusion process and necessary supportive care should be prepared. Notably, white-coat HTN, masked HTN may conceal the exact BP, so out-of-office measurements are also necessary (105).

Well-control of BP can improve the prognosis of RCC by preventing severe cardiovascular diseases or discontinuation of targeted drugs (104). The HTN caused by VSP inhibitors is usually mild and reversible (106). According to ACC/AHA guidelines, for people taking VSP inhibitors, the recommended BP is below 140/90 and below 130/80 if with cardiovascular risk factors (105). However, there is limited evidence to support this antihypertensive target. The patients with RCC with VSP inhibitors developed stage I HTN or DBP increased >20 mmHg should use antihypertensive drugs (107). The pros and cons of each kind of antihypertensive drugs have been discussed above. If the HTN could not be controlled well with a single agent, consider combined therapy methods. If the HTN is uncontrolled with end organ damage, the cessation of VSP inhibitors is recommended (108). Paraneoplastic HTN is usually reversible after renal tumor removal and there is a lack of evidence for antihypertensive therapies for NR-HT. Besides, better pain control and psychotherapy are necessary in the control of BP in the patients with RCC (2).

However, in view of the lack of high-level evidence for the management of HTN in the patients with RCC and different comorbidity conditions of patients, the strategy of blood pressure control is often best guided by a team of oncologist, cardiologist, and clinical pharmacist (108). It is necessary to improve the understanding of "cardio-oncology" among health professionals. The term "cardio-oncology" highlights the complex relationship between cardiovascular diseases and cancer, and encourages the corporation of cardiovascular specialists and oncologists to give better clinical care for cancer survivors.

CONCLUSIONS

In modern society, owing to the change of lifestyle and use of VSPs, the number of patients with HTN and RCC simultaneously is increasing, which turns out to be a heavy disease burden. This review thoroughly investigated the relationship between RCC and HTN from basic, epidemiological, and clinical aspects, aiming to deepen the understanding of the comorbidity and benefit of these patients. However, many problems remain to be resolved. Apart from obesity, smoking, and low physical activity, there are still other possible common modifiable risk factors without robust evidence. Besides, the exact roles of antihypertensive drugs on tumor formation are uncertain and high quality evidence regarding the management of HTN secondary to RCC is far from enough to generate guidance for clinicians. Thus, we appealed to the corporation of basic scientists, public health officers, oncologists, cardiologists, and other health experts to solve these cardio-oncologic problems.

AUTHOR CONTRIBUTIONS

ZB and JY: conception and thoroughly searching related papers. ZB, YX, MH, DL, HW, HL, and JY: drafting of the manuscript or revising it critically for important intellectual content. YX and ZB: drawing illustrations. JY: final approval of the manuscript submitted. All authors contributed to the article and approved the submitted version.

ACKNOWLEDGMENTS

The authors thank Jiawei Huang, Wei Zhu, and Fanzhou Zeng, for their kind advice on medical writing support. The authors thank BioRender.com because the pictures were drawn by their software.

SUPPLEMENTARY MATERIAL

The Supplementary Material for this article can be found online at: https://www.frontiersin.org/articles/10.3389/fcvm.2022.810262/full#supplementary-material

REFERENCES

1. NCD Risk Factor Collaboration. Worldwide trends in hypertension prevalence and progress in treatment and control from 1990 to 2019: a pooled analysis of 1201 population-representative studies with 104 million participants. *Lancet.* (2021) 398:957–80. doi: 10.1016/s0140-6736(21)01330-1
2. Kidoguchi S, Sugano N, Tokudome G, Yokoo T, Yano Y, Hatake K, et al. New concept of onco-hypertension and future perspectives. *Hypertension.* (2021) 77:16–27. doi: 10.1161/hypertensionaha.120.16044
3. Ljungberg B, Albiges L, Abu-Ghanem Y, Bensalah K, Dabestani S, Fernández-Pello S, et al. European Association of Urology Guidelines on renal cell carcinoma: the 2019 update. *Eur Urol.* (2019) 75:799–810. doi: 10.1016/j.eururo.2019.02.011
4. Sung H, Ferlay J, Siegel RL, Laversanne M, Soerjomataram I, Jemal A, et al. Global cancer statistics 2020: GLOBOCAN estimates of incidence and mortality worldwide for 36 cancers in 185 countries. *CA Cancer J Clin.* (2021) 71:209–49. doi: 10.3322/caac.21660
5. SEER Program. *Cancer Stat Facts: Kidney and Renal Pelvis Cancer*. Available online at: https://seer.cancer.gov/statfacts/html/kidrp.html (accessed October 13, 2021).
6. Weikert S, Boeing H, Pischon T, Weikert C, Olsen A, Tjonneland A, et al. Blood pressure and risk of renal cell carcinoma in the European prospective investigation into cancer and nutrition. *Am J Epidemiol.* (2008) 167:438–46. doi: 10.1093/aje/kwm321
7. Handler J. Renal cell carcinoma and hypertension. *J Clin Hypertens.* (2005) 7:249–51. doi: 10.1111/j.1524-6175.2005.04108.x
8. Fukushima H, Inoue M, Kijima T, Yoshida S, Yokoyama M, Ishioka J, et al. Incidence and risk factors of hypertension following partial nephrectomy in patients with renal tumors: a cross-sectional study of postoperative home blood pressure and antihypertensive medications. *Clin Genitourin Cancer.* (2020) 18:e619–28. doi: 10.1016/j.clgc.2020.02.004

9. Tan Q, Wang W, Long Y, Chen G. Therapeutic effects and associated adverse events of multikinase inhibitors in metastatic renal cell carcinoma: a meta-analysis. *Exp Ther Med.* (2015) 9:2275–80. doi: 10.3892/etm.2015.2427
10. Chow WH, Dong LM, Devesa SS. Epidemiology and risk factors for kidney cancer. *Nat Rev Urol.* (2010) 7:245–57. doi: 10.1038/nrurol.2010.46
11. Carey RM, Muntner P, Bosworth HB, Whelton PK. Prevention and control of hypertension: JACC health promotion series. *J Am Coll Cardiol.* (2018) 72:1278–93. doi: 10.1016/j.jacc.2018.07.008
12. Njølstad I, Arnesen E, Lund-Larsen PG. Smoking, serum lipids, blood pressure, and sex differences in myocardial infarction. A 12-year follow-up of the Finnmark Study. *Circulation.* (1996) 93:450–6. doi: 10.1161/01.CIR.93.3.450
13. Washio M, Mori M, Mikami K, Miki T, Watanabe Y, Nakao M, et al. Cigarette smoking and other risk factors for kidney cancer death in a Japanese population: Japan Collaborative Cohort Study for evaluation of cancer risk (JACC study). *Asian Pac J Cancer Prev.* (2014) 14:6523–8. doi: 10.7314/apjcp.2013.14.11.6523
14. van de Pol JA, George L, van den Brandt PA, Baldewijns M, Schouten LJ. Etiologic heterogeneity of clear-cell and papillary renal cell carcinoma in the Netherlands Cohort Study. *Int J Cancer.* (2021) 148:67–76. doi: 10.1002/ijc.33193
15. Kabaria R, Klaassen Z, Terris MK. Renal cell carcinoma: links and risks. *Int J Nephrol Renovasc Dis.* (2016) 9:45–52. doi: 10.2147/ijnrd.S75916
16. Liu X, Sun Q, Hou H, Zhu K, Wang Q, Liu H, et al. The association between BMI and kidney cancer risk: an updated dose-response meta-analysis in accordance with PRISMA guideline. *Medicine.* (2018) 97:e12860. doi: 10.1097/MD.0000000000012860
17. Bjørge T, Tretli S, Engeland A. Relation of height and body mass index to renal cell carcinoma in two million Norwegian men and women. *Am J Epidemiol.* (2004) 160:1168–76. doi: 10.1093/aje
18. Beebe-Dimmer JL, Colt JS, Ruterbusch JJ, Keele GR, Purdue MP, Wacholder S, et al. Body mass index and renal cell cancer: the influence of race and sex. *Epidemiology.* (2012) 23:821–8. doi: 10.1097/EDE.0b013e31826b7fe9
19. Sawada N, Inoue M, Sasazuki S, Iwasaki M, Yamaji T, Shimazu T, et al. Body mass index and subsequent risk of kidney cancer: a prospective cohort study in Japan. *Ann Epidemiol.* (2010) 20:466–72. doi: 10.1016/j.annepidem.2010.03.008
20. Purdue MP, Moore LE, Merino MJ, Boffetta P, Colt JS, Schwartz KL, et al. An investigation of risk factors for renal cell carcinoma by histologic subtype in two case-control studies. *Int J Cancer.* (2013) 132:2640–7. doi: 10.1002/ijc.27934
21. Rini BI, Small EJ. Biology and clinical development of vascular endothelial growth factor-targeted therapy in renal cell carcinoma. *J Clin Oncol.* (2005) 23:1028–43. doi: 10.1200/JCO.2005.01.186
22. Gago-Dominguez M, Castelao JE. Lipid peroxidation and renal cell carcinoma: further supportive evidence and new mechanistic insights. *Free Radic Biol Med.* (2006) 40:721–33. doi: 10.1016/j.freeradbiomed.2005.09.026
23. Griffin KA, Kramer H, Bidani AK. Adverse renal consequences of obesity. *Am J Physiol Renal Physiol.* (2008) 294:F685–96. doi: 10.1152/ajprenal.00324.2007
24. Sun L, Chao F, Luo B, Ye D, Zhao J, Zhang Q, et al. Impact of estrogen on the relationship between obesity and renal cell carcinoma risk in women. *EBioMedicine.* (2018) 34:108–12. doi: 10.1016/j.ebiom.2018.07.010
25. Klinghoffer Z, Yang B, Kapoor A, Pinthus JH. Obesity and renal cell carcinoma: epidemiology, underlying mechanisms and management considerations. *Expert Rev Anticancer Ther.* (2009) 9:975–87. doi: 10.1586/era.09.51
26. Yao X, Huang J, Zhong H, Shen N, Faggioni R, Fung M, et al. Targeting interleukin-6 in inflammatory autoimmune diseases and cancers. *Pharmacol Ther.* (2014) 141:125–39. doi: 10.1016/j.pharmthera.2013.09.004
27. Salvetti A, Brogi G, Di Legge V, Bernini GP. The inter-relationship between insulin resistance and hypertension. *Drugs.* (1993) 46(Suppl 2):149–59. doi: 10.2165/00003495-199300462-00024
28. Shek EW, Brands MW, Hall JE. Chronic leptin infusion increases arterial pressure. *Hypertension.* (1998) 31:409–14. doi: 10.1161/01.hyp.31.1.409
29. Kotsis V, Nilsson P, Grassi G, Mancia G, Redon J, Luft F, et al. New developments in the pathogenesis of obesity-induced hypertension. *J Hypertens.* (2015) 33:1499–508. doi: 10.1097/hjh.0000000000000645
30. Hunt JD, van der Hel OL, McMillan GP, Boffetta P, Brennan P. Renal cell carcinoma in relation to cigarette smoking: meta-analysis of 24 studies. *Int J Cancer.* (2005) 114:101–8. doi: 10.1002/ijc.20618
31. Hu J, Ugnat A-M. Active and passive smoking and risk of renal cell carcinoma in Canada. *Eur J Cancer.* (2005) 41:770–8. doi: 10.1016/j.ejca.2005.01.003
32. Parker AS, Cerhan JR, Janney CA, Lynch CF, Cantor KP. Smoking cessation and renal cell carcinoma. *Ann Epidemiol.* (2003) 13:245–51. doi: 10.1016/s1047-2797(02)00271-5
33. Grassi G, Seravalle G, Calhoun DA, Bolla GB, Giannattasio C, Marabini M, et al. Mechanisms responsible for sympathetic activation by cigarette smoking in humans. *Circulation.* (1994) 90:248–53. doi: 10.1161/01.cir.90.1.248
34. Virdis A, Giannarelli C, Neves MF, Taddei S, Ghiadoni L. Cigarette smoking and hypertension. *Curr Pharm Des.* (2010) 16:2518–25. doi: 10.2174/138161210792062920
35. Mackay A, Brown JJ, Cumming AM, Isles C, Lever AF, Robertson JI. Smoking and renal artery stenosis. *Br Med J.* (1979) 2:770. doi: 10.1136/bmj.2.6193.770
36. Moore SC, Chow WH, Schatzkin A, Adams KF, Park Y, Ballard-Barbash R, et al. Physical activity during adulthood and adolescence in relation to renal cell cancer. *Am J Epidemiol.* (2008) 168:149–57. doi: 10.1093/aje/kwn102
37. Behrens G, Leitzmann MF. The association between physical activity and renal cancer: systematic review and meta-analysis. *Br J Cancer.* (2013) 108:798–811. doi: 10.1038/bjc.2013.37
38. Williams PT. Reduced risk of incident kidney cancer from walking and running. *Med Sci Sports Exerc.* (2014) 46:312–7. doi: 10.1249/MSS.0b013e3182a4e89c
39. Moraes-Silva IC, Mostarda C, Moreira ED, Silva KA, dos Santos F, Angelis K de, et al. Preventive role of exercise training in autonomic, hemodynamic, and metabolic parameters in rats under high risk of metabolic syndrome development. *J Appl Physiol.* (2013) 114:786–91. doi: 10.1152/japplphysiol.00586.2012
40. Araujo AJ de, Santos AC, Souza KD, Aires MB, Santana-Filho VJ, Fioretto ET, et al. Resistance training controls arterial blood pressure in rats with L-NAME- induced hypertension. *Arq Bras Cardiol.* (2013) 100:339–46. doi: 10.5935/abc.20130051
41. Diaz KM, Shimbo D. Physical activity and the prevention of hypertension. *Curr Hypertens Rep.* (2013) 15:659–68. doi: 10.1007/s11906-013-0386-8
42. Seretis A, Cividini S, Markozannes G, Tseretopoulou X, Lopez DS, Ntzani EE, et al. Association between blood pressure and risk of cancer development: a systematic review and meta-analysis of observational studies. *Sci Rep.* (2019) 9:8565. doi: 10.1038/s41598-019-45014-4
43. Hidayat K, Du X, Zou SY, Shi BM. Blood pressure and kidney cancer risk: meta-analysis of prospective studies. *J Hypertens.* (2017) 35:1333–44. doi: 10.1097/hjh.0000000000001286
44. Kim CS, Han KD, Choi HS, Bae EH, Ma SK, Kim SW. Association of hypertension and blood pressure with kidney cancer risk: a nationwide population-based cohort study. *Hypertension.* (2020) 75:1439–46. doi: 10.1161/hypertensionaha.120.14820
45. Leiba A, Kark JD, Afek A, Derazne E, Keinan-Boker L, Shamiss A, et al. Hypertension in adolescence is not an independent risk factor for renal cancer: a cohort study of 918,965 males. *J Am Soc Hypertens.* (2013) 7:283–8. doi: 10.1016/j.jash.2013.04.003
46. Chow WH, Gridley G, Fraumeni JF Jr., Järvholm B. Obesity, hypertension, and the risk of kidney cancer in men. *N Engl J Med.* (2000) 343:1305–11. doi: 10.1056/nejm200011023431804
47. Corrao G, Scotti L, Bagnardi V, Sega R. Hypertension, antihypertensive therapy and renal-cell cancer: a meta-analysis. *Curr Drug Saf.* (2007) 2:125–33. doi: 10.2174/157488607780598296
48. Koene RJ, Prizment AE, Blaes A, Konety SH. Shared risk factors in cardiovascular disease and cancer. *Circulation.* (2016) 133:1104–14. doi: 10.1161/circulationaha.115.020406
49. Copland E, Canoy D, Nazarzadeh M, Bidel Z, Ramakrishnan R, Woodward M, et al. Antihypertensive treatment and risk of cancer: an individual participant data meta-analysis. *Lancet Oncol.* (2021) 22:558–70. doi: 10.1016/s1470-2045(21)00033-4
50. Xie Y, Xu P, Wang M, Zheng Y, Tian T, Yang S, et al. Antihypertensive medications are associated with the risk of kidney and bladder cancer:

a systematic review and meta-analysis. *Aging.* (2020) 12:1545–62. doi: 10.18632/aging.102699
51. Schouten LJ, van Dijk BA, Oosterwijk E, Hulsbergen-van de Kaa CA, Kiemeney LA, Goldbohm RA, et al. Hypertension, antihypertensives and mutations in the Von Hippel-Lindau gene in renal cell carcinoma: results from the Netherlands Cohort Study. *J Hypertens.* (2005) 23:1997–2004. doi: 10.1097/01.hjh.0000186023.74245.48
52. Messerli FH. Diuretic therapy and renal cell carcinoma—another controversy? *Eur Heart J.* (1999) 20:1441–2. doi: 10.1053/euhj.1999.1534
53. Messerli FH. Risk factors for renal cell carcinoma: hypertension or diuretics? *Kidney Int.* (2005) 67:774–5. doi: 10.1111/j.1523-1755.2005.67190.x
54. Grossman E, Messerli FH, Goldbourt U. Antihypertensive therapy and the risk of malignancies. *Eur Heart J.* (2001) 22:1343–52. doi: 10.1053/euhj.2001.2729
55. Colt JS, Hofmann JN, Schwartz K, Chow WH, Graubard BI, Davis F, et al. Antihypertensive medication use and risk of renal cell carcinoma. *Cancer Causes Control.* (2017) 28:289–97. doi: 10.1007/s10552-017-0857-3
56. Hole DJ, Hawthorne VM, Isles CG, McGhee SM, Robertson JW, Gillis CR, et al. Incidence of and mortality from cancer in hypertensive patients. *BMJ.* (1993) 306:609. doi: 10.1136/bmj.306.6878.609
57. Sobczuk P, Szczylik C, Porta C, Czarnecka AM. Renin angiotensin system deregulation as renal cancer risk factor. *Oncol Lett.* (2017) 14:5059–68. doi: 10.3892/ol.2017.6826
58. Yoon C, Yang H-S, Jeon I, Chang Y, Park SM. Use of angiotensin-converting-enzyme inhibitors or angiotensin-receptor blockers and cancer risk: a meta-analysis of observational studies. *CMAJ.* (2011) 183:E1073–84. doi: 10.1503/cmaj.101497
59. Miyajima A, Kikuchi E, Kosaka T, Oya M. Angiotensin II type 1 receptor antagonist as an angiogenic inhibitor in urogenital cancer. *Rev Recent Clin Trials.* (2009) 4:75–8. doi: 10.2174/157488709788185996
60. Rosenbach LM, Xefteris ED. Erythrocytosis associated with carcinoma of the kidney. *JAMA.* (1961) 176:136–7. doi: 10.1001/jama.1961.63040150001012
61. Eiam-Ong S, Eiam-Ong S, Punsin P, Sitprija V, Chaiyabutr N. Acute hypercalcemia-induced hypertension: the roles of calcium channel and alpha-1 adrenergic receptor. *J Med Assoc Thai.* (2004) 87:410–8.
62. Ahmed U, Chatterjee T, Kandula M. Polyarteritis Nodosa: an unusual case of paraneoplastic process in renal cell carcinoma. *J Community Hosp Intern Med Perspect.* (2020) 10:73–5. doi: 10.1080/20009666.2019.1703374
63. Dahl T, Eide I, Fryjordet A. Hypernephroma and hypertension. Two case reports. *Acta Med Scand.* (1981) 209:121–4.
64. Ogunmola OJ, Onyema C, Babatunde Bakare TI, Olabinri EO, Bamigboye-Taiwo OT, Adaje AO, et al. A 10-year old girl with resistant hypertension without significant indication of an underlying renal cell carcinoma, misdiagnosed as malaria. *Am J Case Rep.* (2019) 20:1434–9. doi: 10.12659/AJCR.916588
65. Marvin E, Synkowski J, Benko M. Tumor cerebri: Metastatic renal cell carcinoma with dural venous sinus compression leading to intracranial hypertension; a case report. *Surg Neurol Int.* (2017) 8:175. doi: 10.4103/sni.sni_69_17
66. Capitanio U, Terrone C, Antonelli A, Minervini A, Volpe A, Furlan M, et al. Nephron-sparing techniques independently decrease the risk of cardiovascular events relative to radical nephrectomy in patients with a T1a-T1b renal mass and normal preoperative renal function. *Eur Urol.* (2015) 67:683–9. doi: 10.1016/j.eururo.2014.09.027
67. Lawrentschuk N, Trottier G, Mayo K, Rendon RA. Effects of partial nephrectomy on postoperative blood pressure. *Korean J Urol.* (2012) 53:154–8. doi: 10.4111/kju.2012.53.3.154
68. Nestler S, Levien P, Neisius A, Thomas C, Kamal MM, Hampel C, et al. Incidence of cardiovascular events after nephrectomy - a single centre, matched pair analysis between donor and tumour nephrectomy in a long term follow-up. *Urol Int.* (2016) 97:142–7. doi: 10.1159/000446248
69. Inoue M, Fujii Y, Yokoyama M, Saito K, Numao N, Kihara K. Progression of hypertension after partial nephrectomy in patients with renal tumors: a preliminary report. *Int J Urol.* (2015) 22:797–8. doi: 10.1111/iju.12794
70. U.S. Food and Drug administration. *Drugs@FDA: FDA-Approved Drugs.* Available online at: https://www.accessdata.fda.gov/scripts/cder/daf (accessed October 15, 2021).
71. Smyth A, Collins CS, Thorsteinsdottir B, Madsen BE, Oliveira GH, Kane G, et al. Page kidney: etiology, renal function outcomes and risk for future hypertension. *J Clin Hypertens.* (2012) 14:216–21. doi: 10.1111/j.1751-7176.2012.00601.x
72. Ploth DW, Fitzgibbon W. Pathophysiology of altered renal function in renal vascular hypertension. *Am J Kidney Dis.* (1994) 24:652–9. doi: 10.1016/S0272-6386(12)80227-7
73. Gupta N, Ganesan V, Gao TM, Zabell J, Campbell SC, Haber GP. The effect of partial nephrectomy on blood pressure in patients with solitary kidney. *World J Urol.* (2021) 39:1577–82. doi: 10.1007/s00345-020-03354-1
74. Uzu T, Takeji M, Kanasaki M, Isshiki K, Araki S, Sugiomoto T, et al. Change in circadian rhythm of blood pressure by bilateral radical nephrectomy and haemodialysis: a case report. *J Hum Hypertens.* (2006) 20:549–50. doi: 10.1038/sj.jhh.1002027
75. Liu Y, Zhou L, Chen Y, Liao B, Ye D, Wang K, et al. Hypertension as a prognostic factor in metastatic renal cell carcinoma treated with tyrosine kinase inhibitors: a systematic review and meta-analysis. *BMC Urol.* (2019) 19:49. doi: 10.1186/s12894-019-0481-5
76. Jesus-Gonzalez N de, Robinson E, Moslehi J, Humphreys BD. Management of antiangiogenic therapy-induced hypertension. *Hypertension.* (2012) 60:607–15. doi: 10.1161/hypertensionaha.112.196774
77. Pal S, Gong J, Mhatre SK, Lin SW, Surinach A, Ogale S, et al. Real-world treatment patterns and adverse events in metastatic renal cell carcinoma from a large US claims database. *BMC Cancer.* (2019) 19:548. doi: 10.1186/s12885-019-5716-z
78. Shepard DR, Garcia JA. Toxicity associated with the long-term use of targeted therapies in patients with advanced renal cell carcinoma. *Expert Rev Anticancer Ther.* (2009) 9:795–805. doi: 10.1586/era.09.29
79. Di Lorenzo G, Porta C, Bellmunt J, Sternberg C, Kirkali Z, Staehler M, et al. Toxicities of targeted therapy and their management in kidney cancer. *Eur Urol.* (2011) 59:526–40. doi: 10.1016/j.eururo.2011.01.002
80. Kirkali Z. Adverse events from targeted therapies in advanced renal cell carcinoma: the impact on long-term use. *BJU Int.* (2011) 107:1722–32. doi: 10.1111/j.1464-410X.2010.09985.x
81. Derosa L, Izzedine H, Albiges L, Escudier B. Hypertension and angiotensin system inhibitors in patients with metastatic renal cell carcinoma. *Oncol Rev.* (2016) 10:298. doi: 10.4081/oncol.2016.298
82. Schmidinger M, Danesi R. Management of adverse events associated with cabozantinib therapy in renal cell carcinoma. *Oncologist.* (2018) 23:306–15. doi: 10.1634/theoncologist.2017-0335
83. Bæk Møller N, Budolfsen C, Grimm D, Krüger M, Infanger M, Wehland M, et al. Drug-induced hypertension caused by multikinase inhibitors (sorafenib, sunitinib, lenvatinib and axitinib) in renal cell carcinoma treatment. *Int J Mol Sci.* (2019) 20:4712. doi: 10.3390/ijms20194712
84. Campia U, Moslehi JJ, Amiri-Kordestani L, Barac A, Beckman JA, Chism DD, et al. Cardio-oncology: vascular and metabolic perspectives: a scientific statement from the American Heart Association. *Circulation.* (2019) 139:e579–602. doi: 10.1161/cir.0000000000000641
85. Versmissen J, Mirabito Colafella KM, Koolen SL, Danser AH. Vascular cardio-oncology: vascular endothelial growth factor inhibitors and hypertension. *Cardiovasc Res.* (2019) 115:904–14. doi: 10.1093/cvr/cvz022
86. Dienstmann R, Braña I, Rodon J, Tabernero J. Toxicity as a biomarker of efficacy of molecular targeted therapies: focus on EGFR and VEGF inhibiting anticancer drugs. *Oncologist.* (2011) 16:1729–40. doi: 10.1634/theoncologist.2011-0163
87. Izumi K, Itai S, Takahashi Y, Maolake A, Namiki M. Predictive factor and antihypertensive usage of tyrosine kinase inhibitor-induced hypertension in kidney cancer patients. *Oncol Lett.* (2014) 8:305–8. doi: 10.3892/ol.2014.2060
88. Milan A, Puglisi E, Ferrari L, Bruno G, Losano I, Veglio F. Arterial hypertension and cancer. *Int J Cancer.* (2014) 134:2269–77. doi: 10.1002/ijc.28334
89. Ptinopoulou AG, Sprangers B. Tyrosine kinase inhibitor-induced hypertension-marker of anti-tumour treatment efficacy or cardiovascular risk factor? *Clin Kidney J.* (2021) 14:14–7. doi: 10.1093/ckj/sfaa174
90. van Dorst DC, Dobbin SJ, Neves KB, Herrmann J, Herrmann SM, Versmissen J, et al. Hypertension and prohypertensive antineoplastic therapies in cancer patients. *Circ Res.* (2021) 128:1040–61. doi: 10.1161/circresaha.121.318051

91. Grossman E, Messerli FH, Boyko V, Goldbourt U. Is there an association between hypertension and cancer mortality? *Am J Med.* (2002) 112:479–86. doi: 10.1016/s0002-9343(02)01049-5
92. Penttilä P, Rautiola J, Poussa T, Peltola K, Bono P. Angiotensin inhibitors as treatment of sunitinib/pazopanib-induced hypertension in metastatic renal cell carcinoma. *Clin Genitourin Cancer.* (2017) 15:384–90.e3. doi: 10.1016/j.clgc.2016.12.016
93. Cohen JB, Geara AS, Hogan JJ, Townsend RR. Hypertension in cancer patients and survivors: epidemiology, diagnosis, and management. *JACC CardioOncol.* (2019) 1:238–51. doi: 10.1016/j.jaccao.2019.11.009
94. Yang J, Yang X, Gao L, Zhang J, Yi C, Huang Y. The role of the renin-angiotensin system inhibitors in malignancy: a review. *Am J Cancer Res.* (2021) 11:884–97.
95. Porta C, Szczylik C. Tolerability of first-line therapy for metastatic renal cell carcinoma. *Cancer Treat Rev.* (2009) 35:297–307. doi: 10.1016/j.ctrv.2008.12.003
96. Emile G, Pujade-Lauraine E, Alexandre J. Should we use the angiotensin-converting enzyme inhibitors for the treatment of anti-VEGF-induced hypertension? *Ann Oncol.* (2014) 25:1669–70. doi: 10.1093/annonc/mdu197
97. Rothermundt C, Gillessen S. Angioedema in a patient with renal cell cancer treated with everolimus in combination with an angiotensin-converting enzyme inhibitor. *J Clin Oncol.* (2013) 31:e57–8. doi: 10.1200/jco.2012.44.5106
98. Ivanyi P, Beutel G, Drewes N, Pirr J, Kielstein JT, Morgan M, et al. Therapy of treatment-related hypertension in metastatic renal-cell cancer patients receiving sunitinib. *Clin Genitourin Cancer.* (2017) 15:280–90.e3. doi: 10.1016/j.clgc.2016.10.004
99. Fiala O, Ostašov P, Rozsypalová A, Hora M, Šorejs O, Šustr J, et al. Impact of concomitant cardiovascular medication on survival of metastatic renal cell carcinoma patients treated with sunitinib or pazopanib in the first line. *Target Oncol.* (2021) 16:643–52. doi: 10.1007/s11523-021-00829-y
100. Masur K, Niggemann B, Zanker KS, Entschladen F. Norepinephrine-induced migration of SW 480 colon carcinoma cells is inhibited by beta-blockers. *Cancer Res.* (2001) 61:2866–9.
101. Saito K, Fujii H, Kono K, Hirabayashi K, Yamatani S, Watanabe K, et al. Changes in blood pressure during treatment with the tyrosine kinase inhibitor lenvatinib. *Clin Kidney J.* (2021) 14:325–31. doi: 10.1093/ckj/sfaa137
102. Miller KD, Nogueira L, Mariotto AB, Rowland JH, Yabroff KR, Alfano CM, et al. Cancer treatment and survivorship statistics, 2019. *CA Cancer J Clin.* (2019) 69:363–85. doi: 10.3322/caac.21565
103. Grossman E, Messerli FH. Diuretics and renal cell carcinoma—what is the risk/benefit ration? *Kidney Int.* (1999) 56:1603–4. doi: 10.1046/j.1523-1755.1999.00713-3.x
104. Di Lorenzo G, Autorino R, Bruni G, Cartenì G, Ricevuto E, Tudini M, et al. Cardiovascular toxicity following sunitinib therapy in metastatic renal cell carcinoma: a multicenter analysis. *Ann Oncol.* (2009) 20:1535–42. doi: 10.1093/annonc/mdp025
105. Marvel FA, Whelton SP, Blumenthal RS. A cardio-oncology cardiovascular prevention framework. *JACC CardioOncol.* (2019) 1:252–5. doi: 10.1016/j.jaccao.2019.11.012
106. Schmidinger M, Zielinski CC, Vogl UM, Bojic A, Bojic M, Schukro C, et al. Cardiac toxicity of sunitinib and sorafenib in patients with metastatic renal cell carcinoma. *J Clin Oncol.* (2008) 26:5204–12. doi: 10.1200/jco.2007.15.6331
107. Maitland ML, Bakris GL, Black HR, Chen HX, Durand JB, Elliott WJ, et al. Initial assessment, surveillance, and management of blood pressure in patients receiving vascular endothelial growth factor signaling pathway inhibitors. *J Natl Cancer Inst.* (2010) 102:596–604. doi: 10.1093/jnci/djq091
108. Essa H, Dobson R, Wright D, Lip GY. Hypertension management in cardio-oncology. *J Hum Hypertens.* (2020) 34:673–81. doi: 10.1038/s41371-020-0391-8

Conflict of Interest: The authors declare that the research was conducted in the absence of any commercial or financial relationships that could be construed as a potential conflict of interest.

Publisher's Note: All claims expressed in this article are solely those of the authors and do not necessarily represent those of their affiliated organizations, or those of the publisher, the editors and the reviewers. Any product that may be evaluated in this article, or claim that may be made by its manufacturer, is not guaranteed or endorsed by the publisher.

frontiers in Cardiovascular Medicine

REVIEW
published: 25 February 2022
doi: 10.3389/fcvm.2022.812578

Cardiomyocyte Atrophy, an Underestimated Contributor in Doxorubicin-Induced Cardiotoxicity

De-Shu Chen[1,2,3], *Jing Yan*[1,2,3]* *and Ping-Zhen Yang*[1,2,3]*

[1] Department of Cardiology, Laboratory of Heart Center, Zhujiang Hospital, Southern Medical University, Guangzhou, China, [2] Heart Center of Zhujiang Hospital, Guangdong Provincial Biomedical Engineering Technology Research Center for Cardiovascular Disease, Guangzhou, China, [3] Heart Center of Zhujiang Hospital, Sino-Japanese Cooperation Platform for Translational Research in Heart Failure, Guangzhou, China

Left ventricular (LV) mass loss is prevalent in doxorubicin (DOX)-induced cardiotoxicity and is responsible for the progressive decline of cardiac function. Comparing with the well-studied role of cell death, the part of cardiomyocyte atrophy (CMA) playing in the LV mass loss is underestimated and the knowledge of the underlying mechanism is still limited. In this review, we summarized the recent advances in the DOX-induced CMA. We found that the CMA caused by DOX is associated with the upregulation of FOXOs and "atrogenes," the activation of transient receptor potential canonical 3-NADPH oxidase 2 (TRPC3-Nox2) axis, and the suppression of IGF-1-PI3K signaling pathway. The imbalance of anabolic and catabolic process may be the common final pathway of these mechanisms. At last, we provided some strategies that have been demonstrated to alleviate the DOX-induced CMA in animal models.

Keywords: doxorubicin, cardiotoxicity, cardiomyocyte atrophy, left ventricular mass loss, cell death

OPEN ACCESS

Edited by:
Nazish Sayed,
Stanford University, United States

Reviewed by:
Beshay Zordoky,
University of Minnesota Twin Cities, United States
Anindita Das,
Virginia Commonwealth University, United States

***Correspondence:**
Ping-Zhen Yang
y_pingzhen@126.com
Jing Yan
yanve1008@126.com

Specialty section:
This article was submitted to Cardio-Oncology, a section of the journal Frontiers in Cardiovascular Medicine

Received: *10 November 2021*
Accepted: *11 January 2022*
Published: *25 February 2022*

Citation:
Chen D-S, Yan J and Yang P-Z (2022) Cardiomyocyte Atrophy, an Underestimated Contributor in Doxorubicin-Induced Cardiotoxicity. Front. Cardiovasc. Med. 9:812578. doi: 10.3389/fcvm.2022.812578

INTRODUCTION

Doxorubicin (DOX), the most prescribed anthracycline chemotherapy agent, remains one of the most commonly used anti-cancer drugs among the world while its clinical application is limited by its cumulative dose-dependent cardiotoxicity (1, 2). The congestive heart failure (CHF) is the end stage of DOX-induced cardiotoxicity (DIC) and predicts poor prognosis. The incidence of DOX-related CHF reaches to 26% in patients received DOX at a cumulative dose of 550 mg/m^2 (3). The health of patients with cancer and cancer survivors is threatened by the DIC, unfortunately, the number of both is large. For cancer survivors only, it was reported that there are more than 16.9 million cancer survivors until January 1, 2019 in the United States; this number is estimated to reach more than 22.1 million in the next decade based on the growth and aging of the population alone (4). Nowadays, several strategies are recommended for patients planning to receive high-dose anthracyclines to prevent DIC, such as the use of dexrazoxane or liposomal formulation of doxorubicin, continuous doxorubicin infusion (evidence based; strength of recommendation: moderate) (5). However, there is still lack of evidence to confirm whether these strategies are safe and effective for all patients with cancer receiving chemotherapy (5–7). Although small clinical

trials have revealed that conventional drug of heart failure therapy may be beneficial against DIC (8, 9). Cardinale et al. reported that with conventional heart failure therapy, only 11% patients showed complete recovery from DIC in a heterogeneous cohort study of 2,625 patients (10). Therefore, it is vital to uncover the key mechanism of DIC and find a new approach to prevent it.

Several studies have revealed that anthracycline-based chemotherapy (ANbC) accounts for the left ventricular (LV) mass loss in patients with cancer and cancer survivors. In patients receiving ANbC, the LV mass decrease was detected as early as 1 month after the initiation of the therapy (11) and a 5% reduction in LV mass in 6 month was found based on the cardiovascular magnetic resonance detection (12). In the studies focusing on the pediatric and adult cancer survivors, the LV mass reduction still exists more than 20 years after the ANbC therapy (13–17). The severity of LV mass loss is correlative with the cumulative dose of DOX (14, 18). Further, there may not be a safe dose of DOX to avoid cardiotoxicity for that the cardiac abnormalities, such as significantly reduced LV mass and dimension was found in patients who received as low as 45 mg/m^2 cumulative dose (18).

Although there are multi-factors that can be resulted into the LV mass loss, for example, cancer-associated cachexia like food intake reduction and excess catabolism (19), heart load alteration (20), denervation (21), and bed rest (22). Jordan et al. found that the reduction of LV mass is not necessarily accompanied with the decline of body weight and the heart failure (HF) symptom is not associated with the body weight decrease in patients who received ANbC, indicating a process other than cancer-associated cachexia leads to LV mass loss (12). Consistent finding was reported in animal models, DOX itself caused the heart weight loss in healthy mice and the heart weight (HW)/body weight (BW) index decreases in a dose-dependent fashion of DOX treatment, implicating the possibility that the HW loss is out of portion of BW loss and is caused by the chemotherapy (11). Intriguingly, Pietzsch et al. reported that the cardiac dysfunction induced by cancer alone would nearly recover to the base line, while tumor-bearing mice with DOX treatment showed lower survival rate in the acute phase and long-lasting damage in the gene expression system (23).

The LV mass loss is correlative to the decline of life quality (12) and the increase of major adverse cardiovascular events, such as cardiovascular death, implantable cardioverter-defibrillator therapy, and decompensated heart failure (14). Generally, the LV afterload decreases, the LV mass reduces (20). However, a high afterload was paradoxically found in ANbC-treated patient (12). The same phenomenon was found in animal models. Matsumura et al. found that DOX caused the cardiac atrophy and induced higher blood pressure after angiotensin II treatment (24). In addition, DOX-treated juvenile mice failed to develop cardiac hypertrophic response to late-onset hypertension induced by angiotensin II, which resulted into higher blood pressure, cardiac output decline, and overt mortality (24). Maayah et al. also reported that DOX treatment led to the impairment of the adaptive hypertrophic response to hypertrophic stimuli (25). Insufficient ventricular mass plus high chronic afterload contributes to the progressive contractile deficit, decreased cardiac output, and the establishment of cardiomyopathy (18). These may explain why hypertension markedly increased the risk for coronary artery disease, HF, valvular disease, and arrhythmia in aging adult survivors of childhood cancer (26).

The LV mass loss derives from both cell death (27, 28) and cardiomyocyte atrophy (CMA) (11), leads to cardiac atrophy. It should be noted that cardiac atrophy is different from CMA. The term of cardiac atrophy generally defined as an acquired reduction in the size and mass of the heart (29), is usually evaluated by HW, HW/BW ratio, or HW/tibia length (TL) ratio in animal DIC model. A great number of studies have revealed that DOX caused cardiac atrophy, as indicated by the decrease of HW, HW/TL ratio or HW/BW ratio (30–35). However, several studies reported that DOX caused a reduction of HW and BW, did not affect or increase the HW/BW ratio (36–38). It was reported that the delivery of DOX through intraperitoneal route resulted into peritoneal damage, which interfered the food intake and absorption and caused BW loss (39). Therefore, the preserved or increased HW/BW ratio may originate from the greater BW reduction. Therefore, it may be more appropriate to evaluate the cardiac atrophy by HW/TL ratio or HW alone, which is more evident mostly.

Despite numerous studies focusing on the cell death, less attention was paid on the CMA in DIC studies. However, the weight of cardiomyocyte apoptosis in DIC might be overstated (40). Several studies demonstrated that the contribution of cardiomyocyte apoptosis is low in acute DIC model. Willis et al. reported that CMA rather than cell death determines the cardiac atrophy in acute DIC mice model. They sacrificed mice 7 days after injected with DOX (20 mg/kg) and found that there were barely no increase of serum Troponin-I level and TUNEL-stained cell number in DOX treated mice, however, a 44% reduction of cell cross-section area and an obvious cardiac atrophy were detected (11). Little doxorubicin-induced apoptotic effect in acute DIC model was reported by other groups (41–44). However, it was also reported that DOX caused a great amount of apoptotic cardiomyocyte in an acute DIC model (45–47). Maybe apoptosis plays less important role in cardiac atrophy of acute DIC than we thought. While in a chronic DIC model, cardiomyocyte may undergo a hypertrophy response in a compensated manner (48), CMA was also found in a chronic DIC model (49–51). The controversial results will require further research to clarify, and the role of CMA in the DIC model should be evaluated. In a study including 27 women with breast cancer, patients received the cardiac magnetic resonance image exam at 351–700 days after anthracycline therapy (240 mg/m^2). Ferreira et al. found that the LV mass index in these patients is correlated with intracellular water lifetime (τic; a cardiomyocyte size maker) other than with extracellular volume (ECV), indicating that the cardiac atrophy originates from CMA (52). Cell size shrinkage alone accounted for an ∼44% reduction in LV mass, while the increased ECV may attenuate the LV mass loss (52). Except for apoptosis, other forms of cell death had been found and demonstrated to participate in DIC (27), the relative contribution of cell death and CMA in DOX-induced cardiac atrophy needs further studies to illustrate.

Here, we aim to emphasize the importance of CMA in cardiac atrophy, summarize the current knowledge of the effect of DOX on CMA, and provide insight into the underlying molecular mechanism of it, finally discuss some approaches that have been identified to protect it.

MOLECULAR MECHANISM

Forkhead Box O1 (FOXO1)

Forkhead box O (FOXO) proteins are transcription factors regulating multi physiological and pathological processes included in cardiovascular system. The family contains four members in human, FOXO1, FOXO3, FOXO4, and FOXO6 (53). FOXOs are key regulators in maintaining the muscle mass (54). Depletion of FOXOs has been reported to prevent the muscle loss and weakness through suppressing autophagy–lysosome systems (ALS) and ubiquitin–proteasome systems (UPS) *via* inhibiting the AKT activity (55). Sengupta et al. reported that FOXOs activation may reduce the cardiomyocyte size by promoting autophagy (56). Additionally, Skurk et al. (57) reported that AKT-FOXO3a signaling regulates cardiomyocyte cell size against hypertrophy *via* mediating the expression of atrophy-related genes "atrogenes". Actually, FOXOs regulates half of the atrogenes by binding their promoters, such as muscle RING finger 1 (MuRF1), muscle atrophy gene-1 (atrogin-1/MAFbx), and Bcl-2 19-kDa interacting protein 3 (Bnip3) (55). Atrogin-1 and MuRF-1 are two members of E3 ubiquitin ligases mastering the ubiquitin-mediated protein degradation (58). Bnip3, an autophagy-related gene, has been reported to regulate CMA in a model of mechanical unloading (59).

It has been reported that high dose (20 mg/kg) of DOX treatment activated FOXO1 phosphorylation at Ser-249 and upregulated nuclear FOXO1 levels, accompanied with the increased expression of its target gene, MuRF1 within 24 h. Pharmacological inhibition of FOXO1 with AS1842856 decreased MuRF1 and prevented DOX-induced CMA and LV mass loss (60). Consistently, Willis et al. reported that DOX treatment resulted into a significant upregulation of MuRF1 and Bnip3, while MuRF1 depletion reversed DOX-induced cardiac atrophy in mice (11). Yamamoto et al. reported that DOX-induced CMA was abrogated by MG-132, a proteasome inhibitor, indicating that the atrophy response is involved in the UPS (61). Wang et al. reported that 3-MA, an autophagy inhibitor, alleviated the DOX-induced CMA *in vitro* and Ghrelin, a multi-functional peptide hormone, attenuated DOX-induced CMA by inhibiting the excessive autophagy (62) (**Figure 1**).

The expression of FOXO1 and its target genes might be induced by DOX in a time- and dose-dependent manner. Low dose (5 mg/kg) of DOX failed to induce MuRF1 expression at 24 h (60). In addition, the mRNA levels of FOXO1and Atrogin-1 were not upregulated in mice 7 days after injected with 20 mg/kg DOX (11).

In conclusion, DOX triggers catabolic process involving the induction of ALS and UPS *via* activating FOXO1 and its target genes, which contributes to the CMA. However, FOXOs are classified as tumor suppressor genes (63), inhibition of FOXOs may compromise the anti-tumor effect of DOX. Therefore, more precise and comprehensive studies need to be conducted to figure out if FOXOs inhibition is benefit in DIC therapy in patients with cancer (**Figure 1**).

Transient Receptor Potential Canonical 3 (TRPC3)-NADPH Oxidase 2 (Nox2) Axis

Transient receptor potential canonical (TRPC) proteins, regulating intracellular Ca^{2+}, K^{+}, and Na^{+}, are involved in a variety of physiological and pathological processes in cardiovascular system (64). It has been reported that TRPC3 is a risk factor deteriorating the pathological cardiac remodeling (65, 66). TRPC3 was upregulated underlying the DOX-induced hypoxia stress, silence of TRPC3 ameliorated DOX-induced CMA (29). NADPH oxidase 2 (Nox2) is a key regulator accounting for the major reactive oxygen species (ROS) generation in response to cardiac injury. Nox2 knock-out mice exhibited ameliorated CMA and improved the cardiac function against accumulative DOX toxicity, which may be associated with the decrease of NADPH oxidase activity and oxidation (67).

Transient receptor potential canonical 3 (TRPC3) protects Nox2 from proteasome-dependent degradation *via* interacting with it at the specific C-terminal sites and promotes its activation by regulating Ca^{2+} entry (65). The functional interaction of TRPC3 and Nox2 is required for DOX-induced CMA, as the supplement of the TRPC3-C terminal fragment peptide, which disrupted the TRPC3-Nox2 complex without affecting the TRPC3 channel activity, attenuated DOX-induced CMA (29). Further, pharmacological inhibition of TRPC3-Nox2 complex by pyrazole-3 (Pyr3) abrogated DOX-induced CMA and ameliorated cardiotoxicity (29).

However, the downstream mechanism of TRPC3-Nox2 in DOX-induced CMA remains poorly known. It was reported that the mitochondrial dysfunction promoted muscle disuse atrophy by increasing oxidation stress, impairing Ca^{2+} handling, and activating associated cellular degradation processes (68, 69). TRPC3 was found to translocate to the mitochondria to mediate mitochondrial Ca^{2+} homeostasis and regulate the mitochondrial function (70). The number of evidence has revealed that the TRPC3-induced ROS emission and mitochondrial dysfunction participate in cardiac remodeling (65, 66, 71). Ca^{2+} overload is one of the major causes of DIC, Chen et al. reported that the upregulation of TRPC3 and TRPC6 contributed to the Ca^{2+} overload in DIC (72). Calmodulin is a ubiquitously expressed calcium binding protein which plays a key role in transducing intracellular calcium signal (73). Trifluoperazine, a strong calmodulin antagonist, was found to alleviate myofibril degeneration and cardiac atrophy induced by DOX (74). Calpains are Ca^{2+}-activated neutral cysteine proteases and comprise two major molecules, calpain-1 and calpain-2 (75). Min et al. reported that DOX-induced skeleton and cardiac atrophy requiring the increased mitochondrial emission of ROS and calpain activation (76). Therefore, it can be speculated that DOX might induce CMA through TPRC3-Nox2 axis by disrupting the mitochondrial function, increasing Ca^{2+} entry, and activating the Ca^{2+}-associated calpain protein degradation system (**Figure 1**).

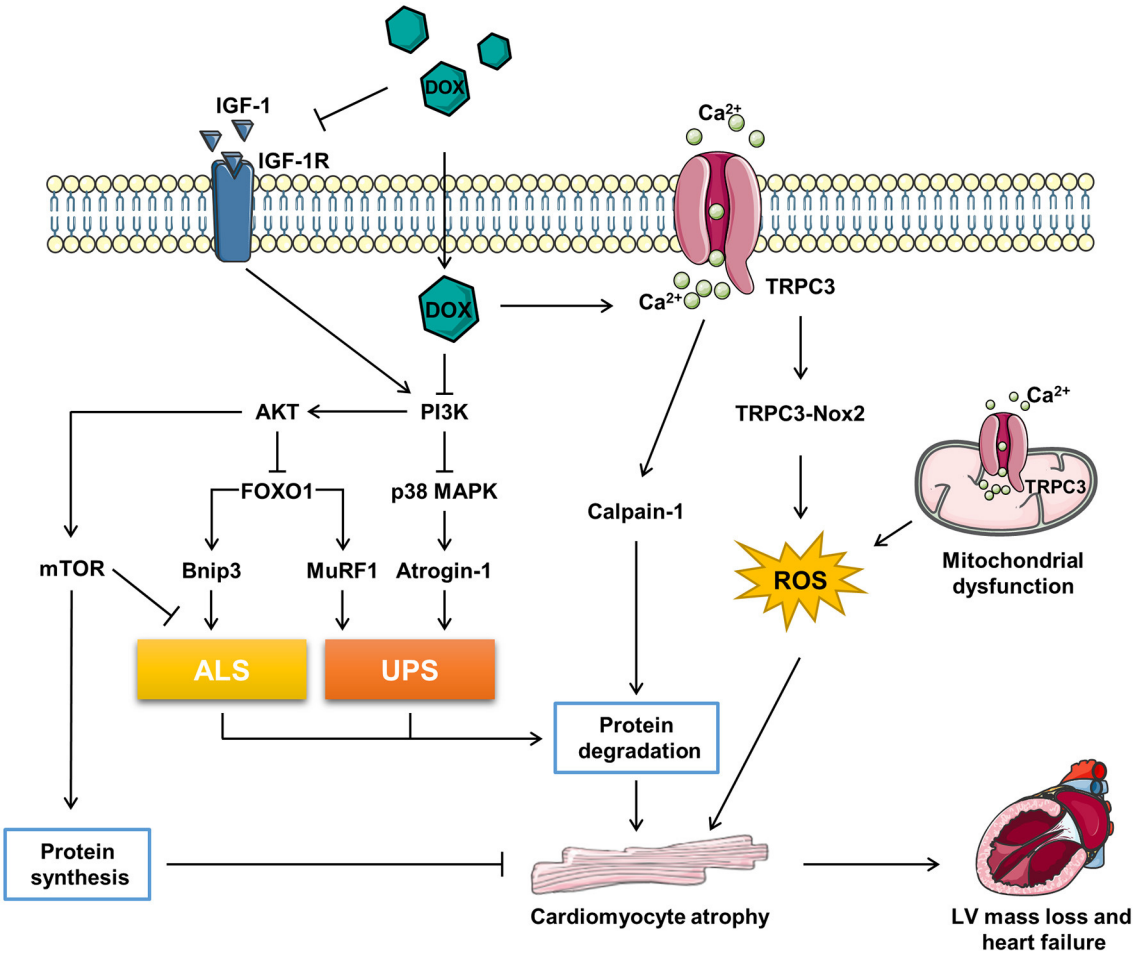

FIGURE 1 | The related molecular mechanism of doxorubicin (DOX)-induced cardiomyocyte atrophy (CMA). ALS, autophagy–lysosome systems; atrogin-1/MAFbx, muscle atrophy gene-1; Bnip3, Bcl-2 19-kDa interacting protein 3; DOX, doxorubicin; FOXO1, forkhead box O1; IGF-1, insulin-like growth factor; IGF-1R, IGF-1 receptor; MuRF1, muscle RING finger 1; mTOR, mammalian target of rapamycin; Nox2, NADPH oxidase 2; PI3K, phosphoinositide 3-kinase; p38 MAPK, p38 mitogen-activated protein kinase; TRPC3, transient receptor potential canonical 3; UPS, ubiquitin–proteasome systems.

Phosphoinositide 3-Kinase (PI3K)

Insulin-Like Growth Factor 1 (IGF-1) and PI3K

Insulin-like growth factor 1 (IGF-1), a key growth factor controlling both anabolic and catabolic pathways, plays a critical role in modulating the muscle size and function (76). IGF-1 binding to IGF-1 receptor (IGF-1R) leads to increased phosphorylation of insulin receptor substrate-1 (ISR-1), which recruits phosphoinositide 3-kinase (PI3K) and activates downstream the AKT signaling pathway (77). Besides, IGF binding protein (IGFBP) regulated IGF-1 activity by keeping it away from IGF-1R (78). DOX was reported to impair IGF-1R and upregulate IGFBP *via* p53 activation in H9C2 cells (79, 80). Restoration of IGF-1R-PI3K-AKT signaling pathway increased the cell survival ability against DIC (79, 80). Apart from that, exogenous IGF-1 (81) or insulin (82) were reported to alleviated DOX-induced cardiomyocyte apoptosis *via* stimulating PI3K-AKT. Interestingly, Mousa et al. discovered that the co-treatment of human umbilical cord blood mesenchymal stem cells (hUCB-MSCs) and carvedilol alleviated DOX-induced decrease of cardiac muscle fiber diameter, which is accompanied with the elevation of IGF-1, GATA-binding protein 4 (GATA-4), and vascular endothelial growth factor (VEGF) (83). Studies have uncovered that IGF-1 is a pro-hypertrophic inducer in cardiomyocyte (84, 85). Further, exogenous IGF-1 reversed cisplatin-induced skeleton muscle atrophy through inhibiting PI3K-AKT-FOXO mediated UPS (86). Overexpression of IGF-1 was also found to ameliorate cardiac atrophy in spinal muscular atrophy mice (87). However, whether IGF-1/IGF-1R have the potent to rescue CMA induced by DOX remains unknown (**Figure 1**).

PI3K and AKT

The PI3K-AKT signaling pathway plays a vital role in regulating the muscle hypertrophy and atrophy response (77). Studies have revealed that DOX inhibited PI3K-AKT activity both *in vivo* and *in vitro* (79, 88–90). PI3K, a lipid kinase family transducing

receptor tyrosine kinase signaling, is aberrantly upregulated in human cancers frequently (91). Though targeting PI3K is effective in cancer therapy, inadvertently increases its side effect on the heart (92). PI3K is a key note in growth factor signaling as well as a modulator in heart muscle mass and contractility (93). Brent et al. found that specific inhibition of PI3Kα by BYL719 decreased the cross-sectional area of cardiomyocyte and induced cardiac atrophy (94). The use of PI3K inhibitor enhanced the anti-tumor effect of chemotherapy drugs, such as DOX (95, 96), while cotreatment of DOX and BYL719 aggravated CMA and cardiotoxicity compared with DOX alone (94). In addition, several studies shed the relationship of PI3K-AKT and cardiac atrophy as well. For example, Chen et al. found that total flavonoids stimulated PI3K-AKT and attenuated DOX-induced HW loss, while inhibition of PI3K-AKT abrogated the protection of total flavonoids against DIC (97). Meeran et al. revealed that nerolidol, a sesquiterpene from the essential oils of aromatic plants, alleviated DOX-induced cardiac atrophy possibly *via* the PI3K-AKT pathway (88). Intriguingly, both upregulation and downregulation of PI3K-AKT triggered by DOX has been reported (98, 99). The discrepancy may be explained by different DIC models and detected time. Interestingly, Cao et al. found that AKT activity was induced by DOX in the beginning, while this was suppressed in the long term (100). In addition, it was reported that PI3Kγ inhibition ameliorated DOX-induced CMA and cardiotoxicity as well as reduced tumor growth (101). Therefore, the role of PI3K-AKT in DIC requires deeper research to clarify and subunit specific inhibition of PI3K might be a promising idea.

Phosphoinositide 3-kinase-AKT activation promotes FOXOs to transport from nucleus to cytoplasm, where FOXOs are sequestered by 14-3-3 proteins and stay inactive (102). Several studies have revealed that the inhibition of PI3K-AKT signaling pathway promoted muscle atrophy *via* FOXOs-mediated activation of UPS (103–105). Moreover, Spurthi et al. reported that toll-like receptor 2 deficiency suppressed PI3K-AKT and activated FOXO1-atrogin-1/MuRF1, which resulted into cardiac atrophy in aging mice (106). Ni et al. found that angiotensin II induced cardiac hypertrophy *via* PI3K-AKT-FOXO pathway (107). Therefore, DOX-induced CMA may be associated with PI3K-AKT-FOXO pathway, which need further exploration. Worth to mention, Yamamoto et al. reported that DOX treatment induced a rapid increase of atrogin-1 mRNA expression *via* activation of p38 mitogen-activated protein kinase (MAPK) pathway without modulating the AKT-FOXO pathway (61).

Mammalian target of rapamycin (mTOR), acts as a serine/threonine kinase, plays an important role in regulating the protein synthesis and modulating autophagy by phosphorylating p70S6K and 4E-BP and Ulk-1, respectively (108, 109). The activity of mTOR regulates the cell growth and organ size (110). The AKT-mTOR axis has been reported to be involved in cardiac hypertrophy during volume overload (111). Further, the PI3K-AKT-mTOR signaling pathway has been found to participate in the DOX-induced skeleton muscle atrophy and cancer cachexia-related cardiac atrophy (112, 113). DOX was reported to impair AKT-mTOR axis by several research (82, 114–117). As reported, β2-agonist formoterol was reported to decrease protein degradation partially through inhibiting PI3K-AKT-mTOR mediated ALS, which prevented the muscle mass loss in fasted mice (118). Apart from that, the activation of PI3K-AKT signaling pathway prevented muscle atrophy *via* mTOR-mediated inhibition of ALS (119, 120). Wang et al. found that ghrelin ameliorated DOX-induced CMA by inhibiting excess autophagy *via* stimulating mTOR (62). Additionally, Hullin et al. revealed that enalapril protected against cardiotoxicity and CMA caused by DOX possibly through activating the PI3K-AKT-mTOR pathway (50). To sum up, DOX might cause CMA *via* inhibiting protein synthesis and activating ALS by suppressing the PI3K-AKT-mTOR pathway (**Figure 1**).

PI3K and p38 MAPK

The p38 MAPK family, which responses to the stress stimuli, plays an important role in cardiac development and function (121). The *in vivo* and *in vitro* evidence has shown that DOX activated the p38 MAPK pathway, which contributed to the DIC (89, 100, 122, 123). McLean et al. reported that suppression of PI3Kα with BYL719 or DOX activated p38 MAPK (94). The stimulation of p38 MAPK is correlative with the muscle wasting. Puigserver et al. found that p38 MAPK activation led to mitochondrial uncoupling and energy expenditure in muscle wasting (124). In addition, Fukawa et al. reported that cancer-secreted inflammatory factors resulted into the excessive fatty acid oxidation and the activation of p38 MAPK, which led to muscle atrophy (125). Several studies have revealed that the activation of p38 MAPK was responsible for DOX-induced CMA. Szeto-Schiller 31 (SS31), an antioxidant peptide, inhibited p38 MAPK phosphorylation and CMA induced by DOX (122). Diosgenin, a steroidal saponin of Dioscorea opposite, alleviated DOX-induced HW and HW/BW ratio reduction possibly *via* suppressing p38 MAPK (123). Further, therapeutic inhibition of p38 MAPK signaling mitigated DOX-induced CMA (94). However, the mechanism that downstream the p38 MAPK in DOX-induced CMA is beyond well established. It was reported that p38 MAPK activation resulted into the upregulation of atrogin-1 and the activation of catabolic process in cancer-induced muscle wasting (126). Pharmacological inhibition of p38 MAPK blunted DOX-induced atrogin-1 upregulation in cardiomyocytes and overexpression of atrogin-1 resulted into CMA (61). Besides, Odeh et al. reported that compromised p38 MAPK activity prevented the denervation-induced muscle atrophy through inhibiting UPS, decreasing oxidation stress, and increased clearance of damaged mitochondria (127). Ding et al. found that Activin A induced skeleton muscle atrophy *via* p38 mediated activation of UPS and autophagy, shown by the upregulation of atrogin-1 and LC3II (128). Therefore, DOX may induce CMA by activating catabolic process though PI3K-p38-atrogin-1 signaling pathway (**Figure 1**).

THERAPY STRATEGIES

Exercise

Appropriate exercise has been demonstrated to be beneficial for alleviating the muscle atrophy and improving the muscle strength (129). Wang et al. reported that moderate aerobic

exercise decreased DOX exposure in cardiac tissue without altering the microvascular density (130). They found that moderate aerobic exercise during DOX treatment counteracted heart mass loss and cardiac function decline in juvenile tumor-bearing nude mice, while failed to preserve the cardiac function when exercise started after the closure of chemotherapy (130). Gomes-Santos et al. (131) found that aerobic exercise training prevented CMA, ameliorated cardiac atrophy, and attenuated exercise intolerance in mice developed with chronic DIC. While the LVEF reduction and fibrosis were not mitigated by it. Several studies have revealed the molecular mechanism underlying the effect of exercise in ameliorating DOX-induced CMA. Activation of TRPC3-Nox2 pathway contributes to the DOX-induced CMA, it was reported that voluntary exercise downregulated TRPC3 and Nox2 in a posttranslational manner (29). Further, it was reported that exercise upregulated IGF-1 mRNA expression (132) and activated PI3K-AKT impaired by DOX (133). Additionally, Kavazis et al. reported that the short-term endurance exercise training attenuated mRNA expression of some negative regulators of cardiac mass, such as FOXO1, MuRF1, myostatin but not atrogin-1, and Bnip3, which was probably associated with the activation of AMPK/PGC-1α pathway (134).

Non-Coding RNA (NcRNA)

Non-coding RNA (ncRNA), such as microRNA, small interference RNA (siRNA), long non-coding RNA (lncRNA), and circular RNA (cirRNA), plays an important role in regulating the cardiovascular system (135). Hu et al. reported that DOX treatment resulted into miR-200a downregulation both *in vivo* and *in vitro*, overexpression of miR-200a alleviated DOX-induced cardiac atrophy and cardiac dysfunction *via* nuclear factor (erythroid-derived 2)-like 2 (Nrf2) activation (136). Li et al. (137) also found that DOX caused elevation of miR-451 expression and miR-451 inhibition prevented the whole body wasting and cardiac atrophy and alleviated cardiotoxicity through AMPK signaling pathway in DIC mice. Moreover, Gupta et al. found that miR-212/132, a pro-hypertrophic cluster, ameliorated DOX-induced CMA and improved cardiac function by inhibiting downstream fat storage-inducing transmembrane protein 2 (Fitm2) (138). In addition, they found that Quaking, an RNA-binding protein, exerted cardiac protective effect against DOX-induced CMA and cardiotoxicity *via* mediating cardiac cirRNAs derived from Titin (Ttn), Formin homology 2 domain containing 3 (Fhod3), and Striatin calmodulin-binding protein 3 (Strn3) (139). It seems that interfering with ncRNAs may provide a new strategy in reversing the DOX-induced CMA, however, the related studies remain limited.

Hormones and Growth Factors

Growing evidence has demonstrated that part of endogenous hormones and growth factors have protective effect in cardiovascular diseases (140–143). Vascular endothelial growth factor-B (VEGF-B), one of the five known members of VEGF that regulate endothelial function (144), has been demonstrated to show potent in promoting coronary arteriogenesis and physiological cardiac hypertrophy (145). Räsänen et al. reported that overexpression of VEGF-B reversed CMA and cardiac mass loss through protecting endothelial in DOX-treated mice without compromising the anti-tumor effect of DOX (146). Li et al. (44) reported that exogenous supplementation of erythropoietin ameliorated DOX-induced CMA and cardiac dysfunction. The same team found that the atrophic response was attenuated by giving granulocyte colony-stimulating factor (G-CSF) in acute DIC mice in their following study (43). Interestingly, Esaki et al. reported that artificial upregulation of hepatocyte growth factor (HGF) at 2 weeks after the establishment of acute DIC model mitigated DOX-induced CMA and cardiac dysfunction (42). The related mechanism underlies the anti-atrophic effect of erythropoietin, G-CSF, and HGF might be similar, which was related to the activation of extracellular signal-regulated kinase (ERK) as well as the restoration of the expression of GATA-4 and its downstream 3 sarcomeric proteins, myosin heavy chain, troponin I, and desmin (42–44). GATA-4, a member of the GATA family of zinc finger transcription factors, is a major transcription factor regulating sarcomeric genes (147). DOX treatment caused a decrease in the level of GATA-4 DNA-binding activity as a result of downregulation of GATA-4 (148), which downregulated the sarcomeric proteins, and resulted into the degeneration of myofibrils in response to DOX.

Polyphenolic Compounds

The plant-derived polyphenolic compounds exert powerful antioxidant activity and have showed their beneficial effects in cardiovascular disease, such as DIC (149). The polyphenolic compounds can be classified as flavonoids, stilbenes, phenolic acids, and lignans based on the molecular structure (150). Rutin, a polyphenolic flavonoid, prevented DOX-induced cardiac atrophy and dysfunction *via* inhibiting excessive autophagy, reducing apoptosis, and restoring AKT activity (151). Isorhapontigenin, a new derivative of stilbene, alleviated CMA and cardiac atrophy caused by DOX, which is associated with the upregulation of yes-associated protein 1 expression (31). Resveratrol (3,5,4′-trihydroxy-trans-stilbene, RES), a natural polyphenol which can be found mainly in grapes, red wine, soy, and peanuts, has been well studied in DIC protection (152). Earlier, Zhang et al. found that RES prevented DOX-induced HW, BW, HW/BW ratio reduction, and cardiotoxicity *via* sirtuin 1(SIRT1)-p53 pathway (153). Furthermore, Arafa et al. revealed that RES was capable of alleviating cardiac atrophy caused by DOX (154). Several studies have implicated the possible molecular mechanism of the protection of RES on DOX-induced cardiac atrophy. It was reported that RES inhibited DOX-induced catabolic process as indicated by the downregulation of MuRF1 and ubiquitin-specific protease 7 (USP7) *via* increasing the deacetylase activity of SIRT1 in young mice (155). RES was reported to suppress DOX-induced p38 MAPK activation (24, 156) and restore VEGF-B and AKT impaired by DOX (157). Recently, Maayah et al. reported that RES ameliorated DOX-induced cardiac atrophy and cardiotoxicity through inhibiting nucleotide-binding domain-like receptor protein-3 (NLRP3) and systemic inflammation in juvenile mice (25). Interestingly, they found that RES restored DOX-induced deficiency of compensated

hypertrophic response to the late-onset hypertension, as indicated by the alleviated CMA and increased heart wall thickness (25). Of note, some polyphenolic compounds have shown the effectiveness against cancer cells both *in vivo* and *in vitro* (158).

Clinical Drugs

The advantage of clinical drugs is the proved relative safety and the convenience for application. Here, we presented several studies about the protective effect of clinical drugs in DOX-induced CMA. Although the results of clinical study showed that only 11% patients showed complete recovery from DIC receiving conventional HF drugs (10), which may be associated with the underlying mechanism of DIC is cardiac atrophy rather than pathological hypertrophy. Losartan, a clinical used AT1 receptor antagonist, exerted cardioprotective effect against DOX-induced CMA possibly by inhibiting the Nox2 activity (67). Controversial studies about the effect of eplerenone on DIC were reported (50, 159). Enalapril, an angiotensin converting enzyme inhibitor (ACEI), attenuated DOX-induced CMA possibly *via* stimulating the PI3K-AKT-mTOR pathway and maintaining the normal levels of connective tissue growth factor (50). So, it reminds us that is it possible for some specific group population to benefit from the conventional HF drugs in DIC therapy? Oral supplementation of folic acid prevented myofibrils disruption, ameliorated DOX-induced CMA, and improved cardiac function (160). Of note, Durham et al. reported that upregulation of high-density lipoprotein (HDL) by overexpressing apolipoprotein A1 abrogated DOX-induce CMA in mice, which was required for the high-affinity HDL receptor, scavenger receptor class B type 1 (49). This study implicates that a lipid-lowering therapy may be beneficial for DOX-induced CMA.

The phosphodiesterase 5 (PDE5) inhibitors, such as tadalafil, sildenafil, and vardenafil, have been demonstrated to show protection in cardiovascular system (161). Koka et al. revealed that tadalafil, a long-acting selective inhibitor of cGMP-specific PDE5, improved cardiac function, reduced oxidation stress, attenuated apoptosis, and prevented cardiac atrophy in DIC mice (162). Prysyazhna et al. found that tadalafil protected against DOX-induced LV mass loss *via* attenuating protein kinase G Iαoxidation (163). Moreover, Jin et al. reported that tadalafil ameliorated the downregulation of 3 sarcomeric proteins, myosin heavy chain, troponin I, desmin, and alleviated CMA caused by DOX in mice (41). Another PDE5 inhibitor, sildenafil, has been verified to attenuate cardiac dysfunction, apoptosis, mitochondrial damage, and myofibrillar disarray induced by DOX (164). Multiple studies have reported that the administration of PDE5 inhibitors did not affect the anticancer effect but enhanced chemotherapeutic efficacy of DOX in animal tumor models (165–168). However, Poklepovic et al. found that sildenafil was safe, but did not show cardiac protection following DOX treatment in a small randomized clinical trial (169). The effect of sildenafil in DIC will require deeper research to verify. Worth to mention, several studies have shed light into the cardiac protective effect of other PDE inhibitors against DIC. Nishiyama et al. found that ibudilast, a PDE4 inhibitor already used in clinic, exerted cardioprotective effect against DOX-induced CMA by interfering the TRPC3-Nox2 complex without affecting the TRPC3 activity (170). Recently, Chen et al. reported that PDE10A deficiency ameliorated DOX-induced CMA and cardiotoxicity *via* cGMP and cAMP, and PDE10A inhibition antagonized tumor growth (171). Inspiringly, the safety of several PDE10A inhibitors have been demonstrated in phase I clinical trial (171). Zhang et al. revealed that PDE1C deficiency or suppression of ameliorated DOX-induced cardiac atrophy and improved cardiac function *via* adenosine A2 receptor stimulation (172). Cilostazol, a potent PDE3 inhibitor, also alleviated HW loss in DIC (173).

DISCUSSION

In this review, we pointed out the importance of CMA in DIC and then, summarized recent advances in the molecular mechanism and the promising therapy strategies of DOX-induced CMA. Here, we paid more attention to the studies involving DOX-induced CMA, but not merely cardiac atrophy. Cardiac atrophy is a common finding and a major cause in the DIC. The weight of CMA in cardiac atrophy might be greater than we thought before. In addition, the reversibility of DIC also supports it (174). We are not going to say that we should downgrade the role of cell death yet. Although several studies have reported that little apoptotic effect was found in acute DIC models, the part of cardiomyocyte necrosis was not evaluated (11, 42–44). The apoptotic rate may be underestimated due to the secondary necrosis (175, 176). So, the relative contribution of CMA and cell death in DOX-induced cardiac atrophy is worth to elucidate in the future study. Inhibiting cellular degradation processes and promoting synthesis processes might be the key idea in preventing the DOX-induced CMA. The DOX-induced CMA is a degenerated process, which explains the protective effect of pro-growth therapy, such as exercise and supplementation of growth factors. Pathological hypertrophy is found in multi cardiovascular diseases; however, appropriate hypertrophy can be helpful for alleviating the DOX-induced CMA as proved by Gupta et al. (138). Considering that the cardiac regeneration technology is still far from application in clinic nowadays (177), reversing CMA serves an alternative and promising strategy in DIC therapy.

AUTHOR CONTRIBUTIONS

D-SC collected the literature and wrote the manuscript. JY and P-ZY conceived the idea and supervised the manuscript. All authors agree to be accountable for the content of the work. All authors contributed to the article and approved the submitted version.

FUNDING

This work was supported by the National Natural Science Foundation of China (Grant Nos. 82070247 and 82000249) and the Guangdong Basic and Applied Basic Research Foundation (Grant No. 2020A1515111028).

REFERENCES

1. Chang HM, Moudgil R, Scarabelli T, Okwuosa TM, Yeh E. Cardiovascular complications of cancer therapy: best practices in diagnosis, prevention, and management: part 1. *J Am Coll Cardiol.* (2017) 70:2536–51. doi: 10.1016/j.jacc.2017.09.1096
2. Chang HM, Okwuosa TM, Scarabelli T, Moudgil R, Yeh E. Cardiovascular complications of cancer therapy: best practices in diagnosis, prevention, and management: part 2. *J Am Coll Cardiol.* (2017) 70:2552–65. doi: 10.1016/j.jacc.2017.09.1095
3. Swain SM, Whaley FS, Ewer MS. Congestive heart failure in patients treated with doxorubicin: a retrospective analysis of three trials. *Cancer-Am Cancer Soc.* (2003) 97:2869–79. doi: 10.1002/cncr.11407
4. Miller KD, Nogueira L, Mariotto AB, Rowland JH, Yabroff KR, Alfano CM, et al. Cancer treatment and survivorship statistics, 2019. *CA Cancer J Clin.* (2019) 69:363–85. doi: 10.3322/caac.21565
5. Armenian SH, Lacchetti C, Barac A, Carver J, Constine LS, Denduluri N, et al. Prevention and monitoring of cardiac dysfunction in survivors of adult cancers: american society of clinical oncology clinical practice guideline. *J Clin Oncol.* (2017) 35:893–911. doi: 10.1200/JCO.2016.70.5400
6. Upshaw JN. Cardioprotective strategies to prevent cancer treatment-related cardiovascular toxicity: a review. *Curr Oncol Rep.* (2020) 22:72. doi: 10.1007/s11912-020-00923-w
7. Vejpongsa P, Yeh ET. Prevention of anthracycline-induced cardiotoxicity: challenges and opportunities. *J Am Coll Cardiol.* (2014) 64:938–45. doi: 10.1016/j.jacc.2014.06.1167
8. Lee M, Chung WB, Lee JE, Park CS, Park WC, Song BJ, et al. Candesartan and carvedilol for primary prevention of subclinical cardiotoxicity in breast cancer patients without a cardiovascular risk treated with doxorubicin. *Cancer Med.* (2021) 10:3964–73. doi: 10.1002/cam4.3956
9. Gupta V, Kumar SS, Agrawal V, Bali ST. Role of ace inhibitors in anthracycline-induced cardiotoxicity: a randomized, double-blind, placebo-controlled trial. *Pediatr Blood Cancer.* (2018) 65:e27308. doi: 10.1002/pbc.27308
10. Cardinale D, Colombo A, Bacchiani G, Tedeschi I, Meroni CA, Veglia F, et al. Early detection of anthracycline cardiotoxicity and improvement with heart failure therapy. *Circulation.* (2015) 131:1981–8. doi: 10.1161/CIRCULATIONAHA.114.013777
11. Willis MS, Parry TL, Brown DI, Mota RI, Huang W, Beak JY, et al. Doxorubicin exposure causes subacute cardiac atrophy dependent on the striated muscle-specific ubiquitin ligase murf1. *Circ Heart Fail.* (2019) 12:e5234. doi: 10.1161/CIRCHEARTFAILURE.118.005234
12. Jordan JH, Castellino SM, Meléndez GC, Klepin HD, Ellis LR, Lamar Z, et al. Left ventricular mass change after anthracycline chemotherapy. *Circ Heart Fail.* (2018) 11:e4560. doi: 10.1161/CIRCHEARTFAILURE.117.004560
13. Tham EB, Haykowsky MJ, Chow K, Spavor M, Kaneko S, Khoo NS, et al. Diffuse myocardial fibrosis by t1-mapping in children with subclinical anthracycline cardiotoxicity: relationship to exercise capacity, cumulative dose and remodeling. *J Cardiovasc Magn Reson.* (2013) 15:48. doi: 10.1186/1532-429X-15-48
14. Neilan TG, Coelho-Filho OR, Pena-Herrera D, Shah RV, Jerosch-Herold M, Francis SA, et al. Left ventricular mass in patients with a cardiomyopathy after treatment with anthracyclines. *Am J Cardiol.* (2012) 110:1679–86. doi: 10.1016/j.amjcard.2012.07.040
15. Armstrong GT, Plana JC, Zhang N, Srivastava D, Green DM, Ness KK, et al. Screening adult survivors of childhood cancer for cardiomyopathy: comparison of echocardiography and cardiac magnetic resonance imaging. *J Clin Oncol.* (2012) 30:2876–84. doi: 10.1200/JCO.2011.40.3584
16. Iarussi D, Galderisi M, Ratti G, Tedesco MA, Indolfi P, Casale F, et al. Left ventricular systolic and diastolic function after anthracycline chemotherapy in childhood. *Clin Cardiol.* (2001) 24:663–9. doi: 10.1002/clc.4960241006
17. De Wolf D, Suys B, Maurus R, Benoit Y, Verhaaren H, Matthijs D, et al. Dobutamine stress echocardiography in the evaluation of late anthracycline cardiotoxicity in childhood cancer survivors. *Pediatr Res.* (1996) 39:504–12. doi: 10.1203/00006450-199603000-00020
18. Lipshultz SE, Lipsitz SR, Sallan SE, Dalton VM, Mone SM, Gelber RD, et al. Chronic progressive cardiac dysfunction years after doxorubicin therapy for childhood acute lymphoblastic leukemia. *J Clin Oncol.* (2005) 23:2629–36. doi: 10.1200/JCO.2005.12.121
19. Baracos VE, Martin L, Korc M, Guttridge DC, Fearon K. Cancer-associated cachexia. *Nat Rev Dis Primers.* (2018) 4:17105. doi: 10.1038/nrdp.2017.105
20. Cooper GT, Kent RL, Mann DL. Load induction of cardiac hypertrophy. *J Mol Cell Cardiol.* (1989) 21:11–30. doi: 10.1016/0022-2828(89)90768-2
21. Takano H, Ozawa H, Kobayashi I, Hamaoka S, Nakajima A, Nakamura T, et al. Atrophic nerve fibers in regions of reduced mibg uptake in doxorubicin cardiomyopathy. *J Nucl Med.* (1995) 36:2060–1.
22. Dorfman TA, Levine BD, Tillery T, Peshock RM, Hastings JL, Schneider SM, et al. Cardiac atrophy in women following bed rest. *J Appl Physiol.* (1985) (2007) 103: 8-16. doi: 10.1152/japplphysiol.01162.2006
23. Pietzsch S, Wohlan K, Thackeray JT, Heimerl M, Schuchardt S, Scherr M, et al. Anthracycline-free tumor elimination in mice leads to functional and molecular cardiac recovery from cancer-induced alterations in contrast to long-lasting doxorubicin treatment effects. *Basic Res Cardiol.* (2021) 116:61. doi: 10.1007/s00395-021-00902-7
24. Matsumura N, Zordoky BN, Robertson IM, Hamza SM, Parajuli N, Soltys CM, et al. Co-administration of resveratrol with doxorubicin in young mice attenuates detrimental late-occurring cardiovascular changes. *Cardiovasc Res.* (2018) 114:1350–9. doi: 10.1093/cvr/cvy064
25. Maayah ZH, Alam AS, Takahara S, Soni S, Ferdaoussi M, Matsumura N, et al. Resveratrol reduces cardiac nlrp3-inflammasome activation and systemic inflammation to lessen doxorubicin-induced cardiotoxicity in juvenile mice. *Febs Lett.* (2021) 595:1681–95. doi: 10.1002/1873-3468.14091
26. Armstrong GT, Oeffinger KC, Chen Y, Kawashima T, Yasui Y, Leisenring W, et al. Modifiable risk factors and major cardiac events among adult survivors of childhood cancer. *J Clin Oncol.* (2013) 31:3673–80. doi: 10.1200/JCO.2013.49.3205
27. Christidi E, Brunham LR. Regulated cell death pathways in doxorubicin-induced cardiotoxicity. *Cell Death Dis.* (2021) 12:339. doi: 10.1038/s41419-021-03614-x
28. Zhang YW, Shi J, Li YJ, Wei L. Cardiomyocyte death in doxorubicin-induced cardiotoxicity. *Arch Immunol Ther Exp (Warsz).* (2009) 57:435–45. doi: 10.1007/s00005-009-0051-8
29. Shimauchi T, Numaga-Tomita T, Ito T, Nishimura A, Matsukane R, Oda S, et al. Trpc3-nox2 complex mediates doxorubicin-induced myocardial atrophy. *JCI Insight.* (2017) 2. doi: 10.1172/jci.insight.93358
30. Hou K, Shen J, Yan J, Zhai C, Zhang J, Pan JA, et al. Loss of trim21 alleviates cardiotoxicity by suppressing ferroptosis induced by the chemotherapeutic agent doxorubicin. *Ebiomedicine.* (2021) 69:103456. doi: 10.1016/j.ebiom.2021.103456
31. Wang P, Wang M, Hu Y, Chen J, Cao Y, Liu C, et al. Isorhapontigenin protects against doxorubicin-induced cardiotoxicity via increasing yap1 expression. *Acta Pharm Sin B.* (2021) 11:680–93. doi: 10.1016/j.apsb.2020.10.017
32. Tadokoro T, Ikeda M, Ide T, Deguchi H, Ikeda S, Okabe K, et al. Mitochondria-dependent ferroptosis plays a pivotal role in doxorubicin cardiotoxicity. *JCI Insight.* (2020) 5. doi: 10.1172/jci.insight.132747
33. Hu C, Zhang X, Wei W, Zhang N, Wu H, Ma Z, et al. Matrine attenuates oxidative stress and cardiomyocyte apoptosis in doxorubicin-induced cardiotoxicity via maintaining ampkα/ucp2 pathway. *Acta Pharm Sin B.* (2019) 9:690–701. doi: 10.1016/j.apsb.2019.03.003
34. Fang X, Wang H, Han D, Xie E, Yang X, Wei J, et al. Ferroptosis as a target for protection against cardiomyopathy. *Proc Natl Acad Sci U S A.* (2019) 116:2672–80. doi: 10.1073/pnas.1821022116
35. Lu J, Li J, Hu Y, Guo Z, Sun D, Wang P, et al. Chrysophanol protects against doxorubicin-induced cardiotoxicity by suppressing cellular parylation. *Acta Pharm Sin B.* (2019) 9:782–93. doi: 10.1016/j.apsb.2018.10.008
36. Singla DK, Johnson TA, Tavakoli DZ. Exosome treatment enhances anti-inflammatory m2 macrophages and reduces inflammation-induced pyroptosis in doxorubicin-induced cardiomyopathy. *Cells-Basel.* (2019) 8. doi: 10.3390/cells8101224
37. Sharifiaghdam Z, Dalouchi F, Sharifiaghdam M, Shaabani E, Ramezani F, Nikbakht F, et al. Curcumin-coated gold nanoparticles attenuate doxorubicin-induced cardiotoxicity via regulating apoptosis in a mouse model. *Clin Exp Pharmacol Physiol.* (2022) 49:70–83. doi: 10.1111/1440-1681.13579

38. Abu-Khudir R, Ibrahim WM, Shams ME, Salama AF. Trehalose alleviates doxorubicin-induced cardiotoxicity in female swiss albino mice by suppression of oxidative stress and autophagy. *J Biochem Mol Toxicol.* (2021) 35:e22859. doi: 10.1002/jbt.22859
39. Li DL, Wang ZV, Ding G, Tan W, Luo X, Criollo A, et al. Doxorubicin blocks cardiomyocyte autophagic flux by inhibiting lysosome acidification. *Circulation.* (2016) 133:1668–87. doi: 10.1161/CIRCULATIONAHA.115.017443
40. Kankeu C, Clarke K, Passante E, Huber HJ. Doxorubicin-induced chronic dilated cardiomyopathy-the apoptosis hypothesis revisited. *J Mol Med (Berl).* (2017) 95:239–48. doi: 10.1007/s00109-016-1494-0
41. Jin Z, Zhang J, Zhi H, Hong B, Zhang S, Guo H, et al. Beneficial effects of tadalafil on left ventricular dysfunction in doxorubicin-induced cardiomyopathy. *J Cardiol.* (2013) 62:110–6. doi: 10.1016/j.jjcc.2013.03.018
42. Esaki M, Takemura G, Kosai K, Takahashi T, Miyata S, Li L, et al. Treatment with an adenoviral vector encoding hepatocyte growth factor mitigates established cardiac dysfunction in doxorubicin-induced cardiomyopathy. *Am J Physiol Heart Circ Physiol.* (2008) 294:H1048–57. doi: 10.1152/ajpheart.01102.2007
43. Li L, Takemura G, Li Y, Miyata S, Esaki M, Okada H, et al. Granulocyte colony-stimulating factor improves left ventricular function of doxorubicin-induced cardiomyopathy. *Lab Invest.* (2007) 87:440–55. doi: 10.1038/labinvest.3700530
44. Li L, Takemura G, Li Y, Miyata S, Esaki M, Okada H, et al. Preventive effect of erythropoietin on cardiac dysfunction in doxorubicin-induced cardiomyopathy. *Circulation.* (2006) 113:535–43. doi: 10.1161/CIRCULATIONAHA.105.568402
45. Arunachalam S, Nagoor MM, Azimullah S, Sharma C, Goyal SN, Ojha S. Nerolidol attenuates oxidative stress, inflammation, and apoptosis by modulating nrf2/mapk signaling pathways in doxorubicin-induced acute cardiotoxicity in rats. *Antioxidants (Basel).* (2021) 10. doi: 10.3390/antiox10060984
46. Zhang WB, Zheng YF, Wu YG. Inhibition of mir-128-3p attenuated doxorubicin-triggered acute cardiac injury in mice by the regulation of ppar-γ. *Ppar Res.* (2021) 2021:7595374. doi: 10.1155/2021/7595374
47. Ma ZG, Kong CY, Wu HM, Song P, Zhang X, Yuan YP, et al. Toll-like receptor 5 deficiency diminishes doxorubicin-induced acute cardiotoxicity in mice. *Theranostics.* (2020) 10:11013–25. doi: 10.7150/thno.47516
48. Jafarinezhad Z, Rafati A, Ketabchi F, Noorafshan A, Karbalay-Doust S. Cardioprotective effects of curcumin and carvacrol in doxorubicin-treated rats: stereological study. *Food Sci Nutr.* (2019) 7:3581–8. doi: 10.1002/fsn3.1210
49. Durham KK, Chathely KM, Mak KC, Momen A, Thomas CT, Zhao YY, et al. Hdl protects against doxorubicin-induced cardiotoxicity in a scavenger receptor class b type 1-, pi3k-, and akt-dependent manner. *Am J Physiol Heart Circ Physiol.* (2018) 314:H31–44. doi: 10.1152/ajpheart.00521.2016
50. Hullin R, Métrich M, Sarre A, Basquin D, Maillard M, Regamey J, et al. Diverging effects of enalapril or eplerenone in primary prevention against doxorubicin-induced cardiotoxicity. *Cardiovasc Res.* (2018) 114:272–81. doi: 10.1093/cvr/cvx162
51. Zhu W, Shou W, Payne RM, Caldwell R, Field LJ. A mouse model for juvenile doxorubicin-induced cardiac dysfunction. *Pediatr Res.* (2008) 64:488–94. doi: 10.1203/PDR.0b013e318184d732
52. Ferreira DST, Quinaglia ACST, Osorio CF, Shah R, Neilan TG, Velloso L, et al. Anthracycline therapy is associated with cardiomyocyte atrophy and preclinical manifestations of heart disease. *JACC Cardiovasc Imaging.* (2018) 11:1045–55. doi: 10.1016/j.jcmg.2018.05.012
53. Calissi G, Lam EW, Link W. Therapeutic strategies targeting foxo transcription factors. *Nat Rev Drug Discov.* (2021) 20:21–38. doi: 10.1038/s41573-020-0088-2
54. Sanchez AM, Candau RB, Bernardi H. Foxo transcription factors: their roles in the maintenance of skeletal muscle homeostasis. *Cell Mol Life Sci.* (2014) 71:1657–71. doi: 10.1007/s00018-013-1513-z
55. Milan G, Romanello V, Pescatore F, Armani A, Paik JH, Frasson L, et al. Regulation of autophagy and the ubiquitin-proteasome system by the foxo transcriptional network during muscle atrophy. *Nat Commun.* (2015) 6:6670. doi: 10.1038/ncomms7670
56. Sengupta A, Molkentin JD, Yutzey KE. Foxo transcription factors promote autophagy in cardiomyocytes. *J Biol Chem.* (2009) 284:28319–31. doi: 10.1074/jbc.M109.024406
57. Skurk C, Izumiya Y, Maatz H, Razeghi P, Shiojima I, Sandri M, et al. The foxo3a transcription factor regulates cardiac myocyte size downstream of akt signaling. *J Biol Chem.* (2005) 280:20814–23. doi: 10.1074/jbc.M500528200
58. Gumucio JP, Mendias CL. Atrogin-1, murf-1, and sarcopenia. *Endocrine.* (2013) 43:12–21. doi: 10.1007/s12020-012-9751-7
59. Cao DJ, Jiang N, Blagg A, Johnstone JL, Gondalia R, Oh M, et al. Mechanical unloading activates foxo3 to trigger bnip3-dependent cardiomyocyte atrophy. *J Am Heart Assoc.* (2013) 2:e16. doi: 10.1161/JAHA.113.000016
60. Xia P, Chen J, Liu Y, Fletcher M, Jensen BC, Cheng Z. Doxorubicin induces cardiomyocyte apoptosis and atrophy through cyclin-dependent kinase 2-mediated activation of forkhead box o1. *J Biol Chem.* (2020) 295:4265–76. doi: 10.1074/jbc.RA119.011571
61. Yamamoto Y, Hoshino Y, Ito T, Nariai T, Mohri T, Obana M, et al. Atrogin-1 ubiquitin ligase is upregulated by doxorubicin via p38-map kinase in cardiac myocytes. *Cardiovasc Res.* (2008) 79:89–96. doi: 10.1093/cvr/cvn076
62. Wang X, Wang XL, Chen HL, Wu D, Chen JX, Wang XX, et al. Ghrelin inhibits doxorubicin cardiotoxicity by inhibiting excessive autophagy through ampk and p38-mapk. *Biochem Pharmacol.* (2014) 88:334–50. doi: 10.1016/j.bcp.2014.01.040
63. Farhan M, Wang H, Gaur U, Little PJ, Xu J, Zheng W. Foxo signaling pathways as therapeutic targets in cancer. *Int J Biol Sci.* (2017) 13:815–27. doi: 10.7150/ijbs.20052
64. Bon RS, Wright DJ, Beech DJ, Sukumar P. Pharmacology of trpc channels and its potential in cardiovascular and metabolic medicine. *Annu Rev Pharmacol Toxicol.* (2021) doi: 10.1146/annurev-pharmtox-030121-122314
65. Kitajima N, Numaga-Tomita T, Watanabe M, Kuroda T, Nishimura A, Miyano K, et al. Trpc3 positively regulates reactive oxygen species driving maladaptive cardiac remodeling. *Sci Rep.* (2016) 6:37001. doi: 10.1038/srep37001
66. Numaga-Tomita T, Kitajima N, Kuroda T, Nishimura A, Miyano K, Yasuda S, et al. Trpc3-gef-h1 axis mediates pressure overload-induced cardiac fibrosis. *Sci Rep.* (2016) 6:39383. doi: 10.1038/srep39383
67. Zhao Y, McLaughlin D, Robinson E, Harvey AP, Hookham MB, Shah AM, et al. Nox2 nadph oxidase promotes pathologic cardiac remodeling associated with doxorubicin chemotherapy. *Cancer Res.* (2010) 70:9287–97. doi: 10.1158/0008-5472.CAN-10-2664
68. Ji LL, Yeo D. Mitochondrial dysregulation and muscle disuse atrophy. *F1000Res.* (2019) 8. doi: 10.12688/f1000research.19139.1
69. Hyatt H, Deminice R, Yoshihara T, Powers SK. Mitochondrial dysfunction induces muscle atrophy during prolonged inactivity: a review of the causes and effects. *Arch Biochem Biophys.* (2019) 662:49–60. doi: 10.1016/j.abb.2018.11.005
70. Feng S, Li H, Tai Y, Huang J, Su Y, Abramowitz J, et al. Canonical transient receptor potential 3 channels regulate mitochondrial calcium uptake. *Proc Natl Acad Sci U S A.* (2013) 110:11011–6. doi: 10.1073/pnas.1309531110
71. Ma T, Lin S, Wang B, Wang Q, Xia W, Zhang H, et al. Trpc3 deficiency attenuates high salt-induced cardiac hypertrophy by alleviating cardiac mitochondrial dysfunction. *Biochem Biophys Res Commun.* (2019) 519:674–81. doi: 10.1016/j.bbrc.2019.09.018
72. Chen RC, Sun GB, Ye JX, Wang J, Zhang MD, Sun XB. Salvianolic acid b attenuates doxorubicin-induced er stress by inhibiting trpc3 and trpc6 mediated ca(2+) overload in rat cardiomyocytes. *Toxicol Lett.* (2017) 276:21–30. doi: 10.1016/j.toxlet.2017.04.010
73. Sorensen AB, Søndergaard MT, Overgaard MT. Calmodulin in a heartbeat. *Febs J.* (2013) 280:5511–32. doi: 10.1111/febs.12337
74. Goda AE, Elenany AM, Elsisi AE. Novel in vivo potential of trifluoperazine to ameliorate doxorubicin-induced cardiotoxicity involves suppression of nf-κb and apoptosis. *Life Sci.* (2021) 283:119849. doi: 10.1016/j.lfs.2021.119849
75. Goll DE, Thompson VF, Li H, Wei W, Cong J. The calpain system. *Physiol Rev.* (2003) 83:731–801. doi: 10.1152/physrev.00029.2002
76. Min K, Kwon OS, Smuder AJ, Wiggs MP, Sollanek KJ, Christou DD, et al. Increased mitochondrial emission of reactive oxygen species and calpain activation are required for doxorubicin-induced cardiac and skeletal muscle myopathy. *J Physiol.* (2015) 593:2017–36. doi: 10.1113/jphysiol.2014.286518

77. Yoshida T, Delafontaine P. Mechanisms of igf-1-mediated regulation of skeletal muscle hypertrophy and atrophy. *Cells-Basel.* (2020) 9. doi: 10.3390/cells9091970
78. Ren J, Samson WK, Sowers JR. Insulin-like growth factor i as a cardiac hormone: physiological and pathophysiological implications in heart disease. *J Mol Cell Cardiol.* (1999) 31:2049–61. doi: 10.1006/jmcc.1999.1036
79. Alzahrani AM, Rajendran P, Veeraraghavan VP, Hanieh H. Cardiac protective effect of kirenol against doxorubicin-induced cardiac hypertrophy in h9c2 cells through nrf2 signaling via pi3k/akt pathways. *Int J Mol Sci.* (2021) 22. doi: 10.3390/ijms22063269
80. Fabbi P, Spallarossa P, Garibaldi S, Barisione C, Mura M, Altieri P, et al. Doxorubicin impairs the insulin-like growth factor-1 system and causes insulin-like growth factor-1 resistance in cardiomyocytes. *Plos ONE.* (2015) 10:e124643. doi: 10.1371/journal.pone.0124643
81. Chae HJ, Kim HR, Bae J, Chae SU, Ha KC, Chae SW. Signal transduction of the protective effect of insulin like growth factor-1 on adriamycin-induced apoptosis in cardiac muscle cells. *Arch Pharm Res.* (2004) 27:324–33. doi: 10.1007/BF02980068
82. Lee BS, Oh J, Kang SK, Park S, Lee SH, Choi D, et al. Insulin protects cardiac myocytes from doxorubicin toxicity by sp1-mediated transactivation of survivin. *Plos One.* (2015) 10:e135438. doi: 10.1371/journal.pone.0135438
83. Mousa H, Abdel AS, Abbas N. Umbilical cord blood-mesenchymal stem cells and carvedilol reduce doxorubicin- induced cardiotoxicity: possible role of insulin-like growth factor-1. *Biomed Pharmacother.* (2018) 105:1192–204. doi: 10.1016/j.biopha.2018.06.051
84. Fernández C, Torrealba N, Altamirano F, Garrido-Moreno V, Vásquez-Trincado C, Flores-Vergara R, et al. Polycystin-1 is required for insulin-like growth factor 1-induced cardiomyocyte hypertrophy. *Plos One.* (2021) 16:e255452. doi: 10.1371/journal.pone.0255452
85. Ito H, Hiroe M, Hirata Y, Tsujino M, Adachi S, Shichiri M, et al. Insulin-like growth factor-i induces hypertrophy with enhanced expression of muscle specific genes in cultured rat cardiomyocytes. *Circulation.* (1993) 87:1715–21. doi: 10.1161/01.CIR.87.5.1715
86. Sakai H, Asami M, Naito H, Kitora S, Suzuki Y, Miyauchi Y, et al. Exogenous insulin-like growth factor 1 attenuates cisplatin-induced muscle atrophy in mice. *J Cachexia Sarcopenia Muscle.* (2021) doi: 10.1002/jcsm.12760
87. Tsai LK, Chen CL, Ting CH, Lin-Chao S, Hwu WL, Dodge JC, et al. Systemic administration of a recombinant aav1 vector encoding igf-1 improves disease manifestations in sma mice. *Mol Ther.* (2014) 22:1450–9. doi: 10.1038/mt.2014.84
88. Meeran M, Azimullah S, Mamoudh HH, Sharma C, Kumar S, Goyal SN, et al. Nerolidol, a sesquiterpene from the essential oils of aromatic plants, attenuates doxorubicin-induced chronic cardiotoxicity in rats. *J Agric Food Chem.* (2021) 69:7334–43. doi: 10.1021/acs.jafc.0c05667
89. Venkatesan B, Prabhu SD, Venkatachalam K, Mummidi S, Valente AJ, Clark RA, et al. Wnt1-inducible signaling pathway protein-1 activates diverse cell survival pathways and blocks doxorubicin-induced cardiomyocyte death. *Cell Signal.* (2010) 22:809–20. doi: 10.1016/j.cellsig.2010.01.005
90. Sahu R, Dua TK, Das S, De Feo V, Dewanjee S. Wheat phenolics suppress doxorubicin-induced cardiotoxicity via inhibition of oxidative stress, map kinase activation, nf-κb pathway, pi3k/akt/mtor impairment, and cardiac apoptosis. *Food Chem Toxicol.* (2019) 125:503–19. doi: 10.1016/j.fct.2019.01.034
91. Yang Q, Jiang W, Hou P. Emerging role of pi3k/akt in tumor-related epigenetic regulation. *Semin Cancer Biol.* (2019) 59:112–24. doi: 10.1016/j.semcancer.2019.04.001
92. McMullen JR, Jay PY. Pi3k(p110alpha) inhibitors as anti-cancer agents: minding the heart. *Cell Cycle.* (2007) 6:910–3. doi: 10.4161/cc.6.8.4124
93. Crackower MA, Oudit GY, Kozieradzki I, Sarao R, Sun H, Sasaki T, et al. Regulation of myocardial contractility and cell size by distinct pi3k-pten signaling pathways. *Cell.* (2002) 110:737–49. doi: 10.1016/S0092-8674(02)00969-8
94. McLean BA, Patel VB, Zhabyeyev P, Chen X, Basu R, Wang F, et al. Pi3kα pathway inhibition with doxorubicin treatment results in distinct biventricular atrophy and remodeling with right ventricular dysfunction. *J Am Heart Assoc.* (2019) 8:e10961. doi: 10.1161/JAHA.118.010961
95. Mohlin S, Hansson K, Radke K, Martinez S, Blanco-Apiricio C, Garcia-Ruiz C, et al. Anti-tumor effects of pim/pi3k/mtor triple kinase inhibitor ibl-302 in neuroblastoma. *Embo Mol Med.* (2019) 11:e10058. doi: 10.15252/emmm.201810058
96. Kim SJ, Jung KH, Son MK, Park JH, Yan HH, Fang Z, et al. Tumor vessel normalization by the pi3k inhibitor hs-173 enhances drug delivery. *Cancer Lett.* (2017) 403:339–53. doi: 10.1016/j.canlet.2017.06.035
97. Chen RC, Xu XD, Zhi LX, Sun GB, Zhu YD, Dong X, et al. Total flavonoids from clinopodium chinense (benth.) O. Ktze protect against doxorubicin-induced cardiotoxicity *in vitro* and *in vivo*. *Evid Based Complement Alternat Med.* (2015) 2015:472565. doi: 10.1155/2015/472565
98. Li L, Li J, Wang Q, Zhao X, Yang D, Niu L, et al. Shenmai injection protects against doxorubicin-induced cardiotoxicity via maintaining mitochondrial homeostasis. *Front Pharmacol.* (2020) 11:815. doi: 10.3389/fphar.2020.00815
99. Kalantary-Charvadeh A, Sanajou D, Hemmati-Dinarvand M, Marandi Y, Khojastehfard M, Hajipour H, et al. Micheliolide protects against doxorubicin-induced cardiotoxicity in mice by regulating pi3k/akt/nf-kb signaling pathway. *Cardiovasc Toxicol.* (2019) 19:297–305. doi: 10.1007/s12012-019-09511-2
100. Cao Y, Ruan Y, Shen T, Huang X, Li M, Yu W, et al. Astragalus polysaccharide suppresses doxorubicin-induced cardiotoxicity by regulating the pi3k/akt and p38mapk pathways. *Oxid Med Cell Longev.* (2014) 2014:674219. doi: 10.1155/2014/674219
101. Li M, Sala V, De Santis MC, Cimino J, Cappello P, Pianca N, et al. Phosphoinositide 3-kinase gamma inhibition protects from anthracycline cardiotoxicity and reduces tumor growth. *Circulation.* (2018) 138:696–711. doi: 10.1161/CIRCULATIONAHA.117.030352
102. Ronnebaum SM, Patterson C. The foxo family in cardiac function and dysfunction. *Annu Rev Physiol.* (2010) 72:81–94. doi: 10.1146/annurev-physiol-021909-135931
103. Stitt TN, Drujan D, Clarke BA, Panaro F, Timofeyva Y, Kline WO, et al. The igf-1/pi3k/akt pathway prevents expression of muscle atrophy-induced ubiquitin ligases by inhibiting foxo transcription factors. *Mol Cell.* (2004) 14:395–403. doi: 10.1016/S1097-2765(04)00211-4
104. Sandri M, Sandri C, Gilbert A, Skurk C, Calabria E, Picard A, et al. Foxo transcription factors induce the atrophy-related ubiquitin ligase atrogin-1 and cause skeletal muscle atrophy. *Cell.* (2004) 117:399–412. doi: 10.1016/S0092-8674(04)00400-3
105. Liu L, Hu R, You H, Li J, Liu Y, Li Q, et al. Formononetin ameliorates muscle atrophy by regulating myostatin-mediated pi3k/akt/foxo3a pathway and satellite cell function in chronic kidney disease. *J Cell Mol Med.* (2021) 25:1493–506. doi: 10.1111/jcmm.16238
106. Spurthi KM, Sarikhani M, Mishra S, Desingu PA, Yadav S, Rao S, et al. Toll-like receptor 2 deficiency hyperactivates the foxo1 transcription factor and induces aging-associated cardiac dysfunction in mice. *J Biol Chem.* (2018) 293:13073–89. doi: 10.1074/jbc.RA118.001880
107. Ni YG, Berenji K, Wang N, Oh M, Sachan N, Dey A, et al. Foxo transcription factors blunt cardiac hypertrophy by inhibiting calcineurin signaling. *Circulation.* (2006) 114:1159–68. doi: 10.1161/CIRCULATIONAHA.106.637124
108. Mizushima N. The role of the atg1/ulk1 complex in autophagy regulation. *Curr Opin Cell Biol.* (2010) 22:132–9. doi: 10.1016/j.ceb.2009.12.004
109. Wang X, Proud CG. The mtor pathway in the control of protein synthesis. *Physiology (Bethesda).* (2006) 21:362–9. doi: 10.1152/physiol.00024.2006
110. Csibi A, Blenis J. Hippo-yap and mtor pathways collaborate to regulate organ size. *Nat Cell Biol.* (2012) 14:1244–5. doi: 10.1038/ncb2634
111. Ikeda M, Ide T, Fujino T, Matsuo Y, Arai S, Saku K, et al. The akt-mtor axis is a pivotal regulator of eccentric hypertrophy during volume overload. *Sci Rep.* (2015) 5:15881. doi: 10.1038/srep15881
112. Hiensch AE, Bolam KA, Mijwel S, Jeneson J, Huitema A, Kranenburg O, et al. Doxorubicin-induced skeletal muscle atrophy: elucidating the underlying molecular pathways. *Acta Physiol (Oxf).* (2020) 229:e13400. doi: 10.1111/apha.13400
113. Murphy KT. The pathogenesis and treatment of cardiac atrophy in cancer cachexia. *Am J Physiol Heart Circ Physiol.* (2016) 310:H466–77. doi: 10.1152/ajpheart.00720.2015
114. Nie L, Liu M, Chen J, Wu Q, Li Y, Yi J, et al. Hydrogen sulfide ameliorates doxorubicin-induced myocardial fibrosis in rats via the pi3k/akt/mtor pathway. *Mol Med Rep.* (2021) 23. doi: 10.3892/mmr.2021.11938

115. Zhang J, Wang M, Ding W, Zhao M, Ye J, Xu Y, et al. Resolvin e1 protects against doxorubicin-induced cardiotoxicity by inhibiting oxidative stress, autophagy and apoptosis by targeting akt/mtor signaling. *Biochem Pharmacol.* (2020) 180:114188. doi: 10.1016/j.bcp.2020.114188
116. Zhang X, Hu C, Kong CY, Song P, Wu HM, Xu SC, et al. Fndc5 alleviates oxidative stress and cardiomyocyte apoptosis in doxorubicin-induced cardiotoxicity via activating akt. *Cell Death Differ.* (2020) 27:540–55. doi: 10.1038/s41418-019-0372-z
117. Bharathi PL, Baskaran R, Huang CY, Vijaya PV. Neferine modulates igf-1r/nrf2 signaling in doxorubicin treated h9c2 cardiomyoblasts. *J Cell Biochem.* (2018) 119:1441–52. doi: 10.1002/jcb.26305
118. Gonçalves DA, Silveira WA, Manfredi LH, Graça FA, Armani A, Bertaggia E, et al. Insulin/igf1 signalling mediates the effects of β(2) -adrenergic agonist on muscle proteostasis and growth. *J Cachexia Sarcopenia Muscle.* (2019) 10:455–75. doi: 10.1002/jcsm.12395
119. Tang G, Du Y, Guan H, Jia J, Zhu N, Shi Y, et al. Butyrate ameliorate skeletal muscle atrophy in diabetic nephropathy via enhancing gut barrier function and ffa2-mediated pi3k/akt/mtor signals. *Br J Pharmacol.* (2021) doi: 10.22541/au.160688559.90642598/v1
120. Yin D, Lin D, Xie Y, Gong A, Jiang P, Wu J. Neuregulin-1β alleviates sepsis-induced skeletal muscle atrophy by inhibiting autophagy via akt/mtor signaling pathway in rats. *Shock.* (2021) doi: 10.1097/SHK.0000000000001860
121. Romero-Becerra R, Santamans AM, Folgueira C, Sabio G. P38 mapk pathway in the heart: new insights in health and disease. *Int J Mol Sci.* (2020) 21. doi: 10.3390/ijms21197412
122. Zhang L, Feng M, Wang X, Zhang H, Ding J, Cheng Z, et al. Peptide szeto-schiller 31 ameliorates doxorubicin-induced cardiotoxicity by inhibiting the activation of the p38 mapk signaling pathway. *Int J Mol Med.* (2021) 47. doi: 10.3892/ijmm.2021.4896
123. Chen CT, Wang ZH, Hsu CC, Lin HH, Chen JH. In vivo protective effects of diosgenin against doxorubicin-induced cardiotoxicity. *Nutrients.* (2015) 7:4938–54. doi: 10.3390/nu7064938
124. Puigserver P, Rhee J, Lin J, Wu Z, Yoon JC, Zhang CY, et al. Cytokine stimulation of energy expenditure through p38 map kinase activation of ppargamma coactivator-1. *Mol Cell.* (2001) 8:971–82. doi: 10.1016/S1097-2765(01)00390-2
125. Fukawa T, Yan-Jiang BC, Min-Wen JC, Jun-Hao ET, Huang D, Qian CN, et al. Excessive fatty acid oxidation induces muscle atrophy in cancer cachexia. *Nat Med.* (2016) 22:666–71. doi: 10.1038/nm.4093
126. Zhang G, Jin B, Li YP. C/ebpβ mediates tumour-induced ubiquitin ligase atrogin1/mafbx upregulation and muscle wasting. *Embo J.* (2011) 30:4323–35. doi: 10.1038/emboj.2011.292
127. Odeh M, Tamir-Livne Y, Haas T, Bengal E. P38α mapk coordinates the activities of several metabolic pathways that together induce atrophy of denervated muscles. *Febs J.* (2020) 287:73–93. doi: 10.1111/febs.15070
128. Ding H, Zhang G, Sin KW, Liu Z, Lin RK, Li M, et al. Activin a induces skeletal muscle catabolism via p38β mitogen-activated protein kinase. *J Cachexia Sarcopenia Muscle.* (2017) 8:202–12. doi: 10.1002/jcsm.12145
129. He N, Ye H. Exercise and muscle atrophy. *Adv Exp Med Biol.* (2020) 1228:255–67. doi: 10.1007/978-981-15-1792-1_17
130. Wang F, Iskra B, Kleinerman E, Alvarez-Florez C, Andrews T, Shaw A, et al. Aerobic exercise during early murine doxorubicin exposure mitigates cardiac toxicity. *J Pediatr Hematol Oncol.* (2018) 40:208–15. doi: 10.1097/MPH.0000000000001112
131. Gomes-Santos IL, Jordão CP, Passos CS, Brum PC, Oliveira EM, Chammas R, et al. Exercise training preserves myocardial strain and improves exercise tolerance in doxorubicin-induced cardiotoxicity. *Front Cardiovasc Med.* (2021) 8:605993. doi: 10.3389/fcvm.2021.605993
132. Werner C, Hanhoun M, Widmann T, Kazakov A, Semenov A, Pöss J, et al. Effects of physical exercise on myocardial telomere-regulating proteins, survival pathways, and apoptosis. *J Am Coll Cardiol.* (2008) 52:470–82. doi: 10.1016/j.jacc.2008.04.034
133. Sequeira CM, Martins MA, Alves R, Nascimento A, Botti G, Rocha VN, et al. Aerobic exercise training attenuates doxorubicin-induced ultrastructural changes in rat ventricular myocytes. *Life Sci.* (2021) 264:118698. doi: 10.1016/j.lfs.2020.118698
134. Kavazis AN, Smuder AJ, Powers SK. Effects of short-term endurance exercise training on acute doxorubicin-induced foxo transcription in cardiac and skeletal muscle. *J Appl Physiol.* (1985) 117:223–30. doi: 10.1152/japplphysiol.00210.2014
135. Poller W, Dimmeler S, Heymans S, Zeller T, Haas J, Karakas M, et al. Non-coding rnas in cardiovascular diseases: diagnostic and therapeutic perspectives. *Eur Heart J.* (2018) 39:2704–16. doi: 10.1093/eurheartj/ehx165
136. Hu X, Liu H, Wang Z, Hu Z, Li L. Mir-200a attenuated doxorubicin-induced cardiotoxicity through upregulation of nrf2 in mice. *Oxid Med Cell Longev.* (2019) 2019:1512326. doi: 10.1155/2019/1512326
137. Li J, Wan W, Chen T, Tong S, Jiang X, Liu W. Mir-451 silencing inhibited doxorubicin exposure-induced cardiotoxicity in mice. *Biomed Res Int.* (2019) 2019:1528278. doi: 10.1155/2019/1528278
138. Gupta SK, Garg A, Avramopoulos P, Engelhardt S, Streckfuss-Bömeke K, Batkai S, et al. Mir-212/132 cluster modulation prevents doxorubicin-mediated atrophy and cardiotoxicity. *Mol Ther.* (2019) 27:17–28. doi: 10.1016/j.ymthe.2018.11.004
139. Gupta SK, Garg A, Bär C, Chatterjee S, Foinquinos A, Milting H, et al. Quaking inhibits doxorubicin-mediated cardiotoxicity through regulation of cardiac circular RNA expression. *Circ Res.* (2018) 122:246–54. doi: 10.1161/CIRCRESAHA.117.311335
140. Räsänen M, Sultan I, Paech J, Hemanthakumar KA, Yu W, He L, et al. Vegf-b promotes endocardium-derived coronary vessel development and cardiac regeneration. *Circulation.* (2021) 143:65–77. doi: 10.1161/CIRCULATIONAHA.120.050635
141. Gallo S, Sala V, Gatti S, Crepaldi T. Cellular and molecular mechanisms of hgf/met in the cardiovascular system. *Clin Sci (Lond).* (2015) 129:1173–93. doi: 10.1042/CS20150502
142. Lipsic E, Schoemaker RG, van der Meer P, Voors AA, van Veldhuisen DJ, van Gilst WH. Protective effects of erythropoietin in cardiac ischemia: from bench to bedside. *J Am Coll Cardiol.* (2006) 48:2161–7. doi: 10.1016/j.jacc.2006.08.031
143. Harada M, Qin Y, Takano H, Minamino T, Zou Y, Toko H, et al. G-csf prevents cardiac remodeling after myocardial infarction by activating the jak-stat pathway in cardiomyocytes. *Nat Med.* (2005) 11:305–11. doi: 10.1038/nm1199
144. Bry M, Kivelä R, Leppänen VM, Alitalo K. Vascular endothelial growth factor-b in physiology and disease. *Physiol Rev.* (2014) 94:779–94. doi: 10.1152/physrev.00028.2013
145. Bry M, Kivelä R, Holopainen T, Anisimov A, Tammela T, Soronen J, et al. Vascular endothelial growth factor-b acts as a coronary growth factor in transgenic rats without inducing angiogenesis, vascular leak, or inflammation. *Circulation.* (2010) 122:1725–33. doi: 10.1161/CIRCULATIONAHA.110.957332
146. Räsänen M, Degerman J, Nissinen TA, Miinalainen I, Kerkelä R, Siltanen A, et al. Vegf-b gene therapy inhibits doxorubicin-induced cardiotoxicity by endothelial protection. *Proc Natl Acad Sci U S A.* (2016) 113:13144–9. doi: 10.1073/pnas.1616168113
147. Suzuki YJ, Evans T. Regulation of cardiac myocyte apoptosis by the gata-4 transcription factor. *Life Sci.* (2004) 74:1829–38. doi: 10.1016/j.lfs.2003.10.002
148. Kim Y, Ma AG, Kitta K, Fitch SN, Ikeda T, Ihara Y, et al. Anthracycline-induced suppression of gata-4 transcription factor: implication in the regulation of cardiac myocyte apoptosis. *Mol Pharmacol.* (2003) 63:368–77. doi: 10.1124/mol.63.2.368
149. Alotaibi BS, Ijaz M, Buabeid M, Kharaba ZJ, Yaseen HS, Murtaza G. Therapeutic effects and safe uses of plant-derived polyphenolic compounds in cardiovascular diseases: a review. *Drug Des Devel Ther.* (2021) 15:4713–32. doi: 10.2147/DDDT.S327238
150. Michalska M, Gluba A, Mikhailidis DP, Nowak P, Bielecka-Dabrowa A, Rysz J, et al. The role of polyphenols in cardiovascular disease. *Med Sci Monit.* (2010) 16:A110–9.
151. Ma Y, Yang L, Ma J, Lu L, Wang X, Ren J, et al. Rutin attenuates doxorubicin-induced cardiotoxicity via regulating autophagy and apoptosis. *Biochim Biophys Acta Mol Basis Dis.* (2017) 1863:1904–11. doi: 10.1016/j.bbadis.2016.12.021

152. Hu LF, Lan HR, Li XM, Jin KT. A systematic review of the potential chemoprotective effects of resveratrol on doxorubicin-induced cardiotoxicity: focus on the antioxidant, antiapoptotic, and anti-inflammatory activities. *Oxid Med Cell Longev.* (2021) 2021:2951697. doi: 10.1155/2021/2951697
153. Zhang C, Feng Y, Qu S, Wei X, Zhu H, Luo Q, et al. Resveratrol attenuates doxorubicin-induced cardiomyocyte apoptosis in mice through sirt1-mediated deacetylation of p53. *Cardiovasc Res.* (2011) 90:538–45. doi: 10.1093/cvr/cvr022
154. Arafa MH, Mohammad NS, Atteia HH, Abd-Elaziz HR. Protective effect of resveratrol against doxorubicin-induced cardiac toxicity and fibrosis in male experimental rats. *J Physiol Biochem.* (2014) 70:701–11. doi: 10.1007/s13105-014-0339-y
155. Sin TK, Tam BT, Yung BY, Yip SP, Chan LW, Wong CS, et al. Resveratrol protects against doxorubicin-induced cardiotoxicity in aged hearts through the sirt1-usp7 axis. *J Physiol.* (2015) 593:1887–99. doi: 10.1113/jphysiol.2014.270101
156. Ruan Y, Dong C, Patel J, Duan C, Wang X, Wu X, et al. Sirt1 suppresses doxorubicin-induced cardiotoxicity by regulating the oxidative stress and p38mapk pathways. *Cell Physiol Biochem.* (2015) 35:1116–24. doi: 10.1159/000373937
157. Tian W, Yang L, Liu Y, He J, Yang L, Zhang Q, et al. Resveratrol attenuates doxorubicin-induced cardiotoxicity in rats by up-regulation of vascular endothelial growth factor b. *J Nutr Biochem.* (2020) 79:108132. doi: 10.1016/j.jnutbio.2019.01.018
158. Kubczak M, Szustka A, Rogalińska M. Molecular targets of natural compounds with anti-cancer properties. *Int J Mol Sci.* (2021) 22. doi: 10.3390/ijms222413659
159. Lother A, Bergemann S, Kowalski J, Huck M, Gilsbach R, Bode C, et al. Inhibition of the cardiac myocyte mineralocorticoid receptor ameliorates doxorubicin-induced cardiotoxicity. *Cardiovasc Res.* (2018) 114:282–90. doi: 10.1093/cvr/cvx078
160. Octavia Y, Kararigas G, de Boer M, Chrifi I, Kietadisorn R, Swinnen M, et al. Folic acid reduces doxorubicin-induced cardiomyopathy by modulating endothelial nitric oxide synthase. *J Cell Mol Med.* (2017) 21:3277–87. doi: 10.1111/jcmm.13231
161. Das A, Durrant D, Salloum FN, Xi L, Kukreja RC. Pde5 inhibitors as therapeutics for heart disease, diabetes and cancer. *Pharmacol Ther.* (2015) 147:12–21. doi: 10.1016/j.pharmthera.2014.10.003
162. Koka S, Das A, Zhu SG, Durrant D, Xi L, Kukreja RC. Long-acting phosphodiesterase-5 inhibitor tadalafil attenuates doxorubicin-induced cardiomyopathy without interfering with chemotherapeutic effect. *J Pharmacol Exp Ther.* (2010) 334:1023–30. doi: 10.1124/jpet.110.170191
163. Prysyazhna O, Burgoyne JR, Scotcher J, Grover S, Kass D, Eaton P. Phosphodiesterase 5 inhibition limits doxorubicin-induced heart failure by attenuating protein kinase g iα oxidation. *J Biol Chem.* (2016) 291:17427–36. doi: 10.1074/jbc.M116.724070
164. Fisher PW, Salloum F, Das A, Hyder H, Kukreja RC. Phosphodiesterase-5 inhibition with sildenafil attenuates cardiomyocyte apoptosis and left ventricular dysfunction in a chronic model of doxorubicin cardiotoxicity. *Circulation.* (2005) 111:1601–10. doi: 10.1161/01.CIR.0000160359.49478.C2
165. Booth L, Roberts JL, Cruickshanks N, Conley A, Durrant DE, Das A, et al. Phosphodiesterase 5 inhibitors enhance chemotherapy killing in gastrointestinal/genitourinary cancer cells. *Mol Pharmacol.* (2014) 85:408–19. doi: 10.1124/mol.113.090043
166. Li Q, Shu Y. Pharmacological modulation of cytotoxicity and cellular uptake of anti-cancer drugs by pde5 inhibitors in lung cancer cells. *Pharm Res.* (2014) 31:86–96. doi: 10.1007/s11095-013-1134-0
167. Das A, Durrant D, Mitchell C, Mayton E, Hoke NN, Salloum FN, et al. Sildenafil increases chemotherapeutic efficacy of doxorubicin in prostate cancer and ameliorates cardiac dysfunction. *Proc Natl Acad Sci U S A.* (2010) 107:18202–7. doi: 10.1073/pnas.1006965107
168. Chang JF, Hsu JL, Sheng YH, Leu WJ, Yu CC, Chan SH, et al. Phosphodiesterase type 5 (pde5) inhibitors sensitize topoisomerase ii inhibitors in killing prostate cancer through pde5-independent impairment of HR and NHEJ DNA repair systems. *Front Oncol.* (2018) 8:681. doi: 10.3389/fonc.2018.00681
169. Poklepovic A, Qu Y, Dickinson M, Kontos MC, Kmieciak M, Schultz E, et al. Randomized study of doxorubicin-based chemotherapy regimens, with and without sildenafil, with analysis of intermediate cardiac markers. *Cardiooncology.* (2018) 4. doi: 10.1186/s40959-018-0033-2
170. Nishiyama K, Numaga-Tomita T, Fujimoto Y, Tanaka T, Toyama C, Nishimura A, et al. Ibudilast attenuates doxorubicin-induced cytotoxicity by suppressing formation of trpc3 channel and nadph oxidase 2 protein complexes. *Br J Pharmacol.* (2019) 176:3723–38. doi: 10.1111/bph.14777
171. Chen S, Chen J, Shi H, Mickelsen D, Yan C. Abstract mp265: the role of phosphodiesterase 10a in tumor growth and doxorubicin-induced cardiotoxicity. *Circ Res.* (2021) 129:P265. doi: 10.1161/res.129.suppl_1.MP265
172. Zhang Y, Knight W, Chen S, Mohan A, Yan C. Multiprotein complex with trpc (transient receptor potential-canonical) channel, pde1c (phosphodiesterase 1c), and a2r (adenosine a2 receptor) plays a critical role in regulating cardiomyocyte camp and survival. *Circulation.* (2018) 138:1988–2002. doi: 10.1161/CIRCULATIONAHA.118.034189
173. Koh JS, Yi CO, Heo RW, Ahn JW, Park JR, Lee JE, et al. Protective effect of cilostazol against doxorubicin-induced cardiomyopathy in mice. *Free Radic Biol Med.* (2015) 89:54–61. doi: 10.1016/j.freeradbiomed.2015.07.016
174. Narezkina A, Nasim K. Anthracycline cardiotoxicity. *Circ Heart Fail.* (2019) 12:e5910. doi: 10.1161/CIRCHEARTFAILURE.119.005910
175. Silva MT. Secondary necrosis: the natural outcome of the complete apoptotic program. *Febs Lett.* (2010) 584:4491–9. doi: 10.1016/j.febslet.2010.10.046
176. Leist M, Single B, Castoldi AF, Kühnle S, Nicotera P. Intracellular adenosine triphosphate (atp) concentration: a switch in the decision between apoptosis and necrosis. *J Exp Med.* (1997) 185:1481–6. doi: 10.1084/jem.185.8.1481
177. Kasai-Brunswick TH, Carvalho AB, Campos DCA. Stem cell therapies in cardiac diseases: current status and future possibilities. *World J Stem Cells.* (2021) 13:1231–47. doi: 10.4252/wjsc.v13.i9.1231

Conflict of Interest: The authors declare that the research was conducted in the absence of any commercial or financial relationships that could be construed as a potential conflict of interest.

frontiers in Cardiovascular Medicine

ORIGINAL RESEARCH
published: 07 March 2022
doi: 10.3389/fcvm.2022.815916

MicroRNA-194-5p Attenuates Doxorubicin-Induced Cardiomyocyte Apoptosis and Endoplasmic Reticulum Stress by Targeting P21-Activated Kinase 2

*Hongge Fa[1,2], Dandan Xiao[1], Wenguang Chang[3], Lin Ding[1], Lanting Yang[1], Yu Wang[1], Mengyu Wang[1] and Jianxun Wang[1]**

[1] School of Basic Medicine, Qingdao University, Qingdao, China, [2] Qingdao Women and Children's Hospital, Qingdao University, Qingdao, China, [3] Institute for Translational Medicine, Qingdao University, Qingdao, China

OPEN ACCESS

Edited by:
Feng Cao,
People's Liberation Army General Hospital, China

Reviewed by:
Benzhi Cai,
The Second Affiliated Hospital of Harbin Medical University, China
Shanjie Wang,
Harbin Medical University, China
Qiangrong Liang,
New York Institute of Technology, United States
Mei Han,
Hebei Medical University, China

***Correspondence:**
Jianxun Wang
wangjx@qdu.edu.cn

Specialty section:
This article was submitted to Cardio-Oncology, a section of the journal Frontiers in Cardiovascular Medicine

Received: 16 November 2021
Accepted: 10 February 2022
Published: 07 March 2022

Citation:
Fa H, Xiao D, Chang W, Ding L, Yang L, Wang Y, Wang M and Wang J (2022) MicroRNA-194-5p Attenuates Doxorubicin-Induced Cardiomyocyte Apoptosis and Endoplasmic Reticulum Stress by Targeting P21-Activated Kinase 2. Front. Cardiovasc. Med. 9:815916. doi: 10.3389/fcvm.2022.815916

Objective: Many studies have reported that microRNAs (miRs) are involved in the regulation of doxorubicin (DOX)-induced cardiotoxicity. MiR-194-5p has been reported significantly upregulated in patients with myocardial infarction; however, its role in myocardial diseases is still unclear. Various stimuluses can trigger the endoplasmic reticulum (ER) stress and it may activate the apoptosis signals eventually. This study aims to explore the regulatory role of miR-194-5p in DOX-induced ER stress and cardiomyocyte apoptosis.

Methods: H9c2 was treated with 2 μM DOX to induce apoptosis, which is to stimulate the DOX-induced cardiotoxicity model. The expression of miR-194-5p was detected by quantitative real-time PCR (qRT-PCR); the interaction between miR-194-5p and P21-activated kinase 2 (PAK2) was tested by dual luciferase reporter assay; terminal deoxynucleotidyl transferase dUTP nick-end labeling (TUNEL) assay and caspase-3/7 activity were used to assess apoptosis; trypan blue staining was applied to measure cell death; Western blotting was performed to detect protein expressions; and ER-related factors splicing X-box binding protein 1 (XBP1s) was detected by polyacrylamide gel electrophoresis and immunofluorescence to verify the activation of ER stress.

Results: MiR-194-5p was upregulated in cardiomyocytes and mouse heart tissue with DOX treatment, while the protein level of PAK2 was downregulated. PAK2 was predicted as the target of miR-194-5p; hence, dual luciferase reporter assay indicated that miR-194-5p directly interacted with PAK2 and inhibited its expression. TUNEL assay, caspase-3/7 activity test, and trypan blue stain results showed that either inhibition of miR-194-5p or overexpression of PAK2 reduced DOX-induced cardiomyocyte apoptosis. Silencing of miR-194-5p also improved DOX-induced cardiac dysfunction. In addition, DOX could induce ER stress in H9c2, which led to XBP1 and caspase-12 activation. The expression level of XBP1s with DOX treatment increased first then decreased. Overexpression of XBP1s suppressed DOX-induced caspase-3/7 activity elevation as well as the expression of cleaved caspase-12, which protected cardiomyocyte from apoptosis. Additionally, the activation of XBP1s was regulated by miR-194-5p and PAK2.

Conclusion: Our findings revealed that silencing miR-194-5p could alleviate DOX-induced cardiotoxicity *via* PAK2 and XBP1s *in vitro* and *in vivo*. Thus, the novel miR-194-5p/PAK2/XBP1s axis might be the potential prevention/treatment targets for cancer patients receiving DOX treatment.

Keywords: doxorubicin, cardiotoxicity, miR-194-5p, ER stress, apoptosis

INTRODUCTION

Doxorubicin (DOX) is a broad-spectrum antitumor drug that can be used to treat a variety of cancers. However, the clinical utility of DOX is confined due to its cumulative cardiotoxicity (1, 2). In the past decades, the mechanisms of DOX-induced cardiotoxicity have been extensively studied, mainly including accumulation of reactive oxygen species (ROS), mitochondrial dysfunction, endoplasmic reticulum (ER) stress, and disturbance of calcium homeostasis (3–8). However, the exact mechanism underlying DOX cardiotoxicity has not been fully discovered. In addition, the aberrant apoptosis caused cardiomyocytes number decrease is the predominant cellular event in DOX-induced cardiomyopathy, which was confirmed by morphological changes and terminal deoxinucleotidyl transferase dUTP nick-end labeling (TUNEL) assay (9–11). Therefore, to further explore the mechanisms of DOX-induced cardiomyocytes apoptosis will help minimize its adverse effects and benefit the clinical application.

MicroRNA (miR, miRNA) is a type of non-coding RNA with a length of approximately 22 nucleotides, and they exert their functions by degrading target mRNAs and inhibiting protein expressions, therefore, participate in various biological processes, such as proliferation, migration, differentiation, and cell death (12, 13). Many studies have reported that miRNAs play important roles in the DOX-induced cardiotoxicity (14–17). Recently, it has been reported that miR-194 is upregulated in the serum of patients with myocardial infarction and is closely correlated with impaired cardiac function (18). In addition, the expression level of circulating exosomal miR-194 was also upregulated in patients with obese cardiomyopathy, which was closely related to the mitochondrial activity and cardiac function (19). However, the role of miR-194 in DOX-induced cardiotoxicity is unclear.

P21-activated kinase 2 (PAK2), a Rac1/Cdc42 activated signaling effector, belongs to the PAK family of serine/threonine kinases (20). The antiapoptotic effect of PAK2 has been demonstrated in multiple cancer studies (21–23). Recently, PAK2 has been reported to exert cardioprotective role by improving ER function through the inositol-requiring enzyme 1 (IRE1)/X-box binding protein 1 (XBP1)-dependent pathway (24). In cardiomyocytes hypoxia and reoxygenation model, the decrease of PAK2 is associated with ER stress, oxidative stress, calcium overload, caspase-12 (cas-12) activation, and apoptosis (25). Activation of 5′ AMP-activated protein kinase (AMPK)-p21-activated kinase 2 (PAK2) signaling attenuated ER stress and myocardial apoptosis induced by ischemia/reperfusion injury (26). Nonetheless, the role of PAK2 in DOX-induced cardiotoxicity has not been elucidated.

It has been reported that ER stress is involved in DOX-induced cardiotoxicity (27, 28). When the ER is under stress that cannot afford the excessive unfolded proteins to be processed, the unfolded protein response (UPR) is triggered to restore the ER homeostasis (29, 30). Severe or prolonged ER stress will switch the cells from adaptive phase to apoptosis. XBP1 is the key transcription factor in the IRE pathway in response to UPR. During UPR, XBP1 is activated and its mRNA is cleaved to form the splicing XBP1 (XBP1s) (31). XBP1s can bind to ER stress response elements in promoters of many UPR target genes, therefore help to fold and degrade proteins, promoting ER adaption and cytoprotection (32, 33). Studies reported that XBP1s also plays a key role in cardiovascular disease. A recent study showed that XBP1s modulates vascular endothelial growth factor-mediated cardiac angiogenesis and contributes to the development of adaptive hypertrophy (34). Similarly, in the transgenic mouse model, overexpression of XBP1s showed protective effect on reperfusion injury (35). However, the role of XBP1 in DOX-induced cardiotoxicity needs further study.

In this study, we reported that the expression of miR-194-5p increased in DOX-induced cardiomyocytes and mouse heart tissue and was involved in the regulation of DOX-induced cardiotoxicity by targeting PAK2. Inhibition of miR-194-5p attenuated DOX-induced apoptosis, and PAK2 showed important role in maintaining endoplasmic reticulum homeostasis to exert cardioprotective effects *via* the key transcription factor-XBP1. The present results revealed the regulatory role of miR-194-5p/PAK2/XBP1s axis in DOX-induced cardiotoxicity and provided a theoretical basis for the development of therapeutic targets.

MATERIALS AND METHODS

Animal Experiments

A 8-week old male C57BL/6J mice were randomly divided into the 4 groups: the control group, the DOX treatment group, the DOX and antagomir negative control group, and the DOX and miR-194-5p antagomir group. All the mice were housed on a 12-h light/12-h dark cycle in a pathogen-free environment and allowed *ad libitum* access to food and water. Adenovirus-harbored miR-194-5p antagomir (5×10^{10} vector genomes) was synthesized by Hanbio Corporation Ltd. (Shanghai, China). The animals in the antagomir group and its negative control (NC) group were injected *via* tail vein with miR-194-5p antagomir 50 μl or same dosage of antagomir NC. On day 7, the experimental groups (DOX group, DOX + antagomir NC group, and DOX + miR-194-5p antagomir group) were intraperitoneally injected with DOX hydrochloride

15 mg/kg once. Same dose of normal saline was injected to the control group. Cardiac function was tested 1 week after DOX administration and mice were euthanized after *in vivo* evaluations of cardiac function. Then, hearts were rapidly excised and immediately cut into two parts. One part was snap-frozen in liquid nitrogen and the remaining part was fixed in 4% polyformaldehyde solution and embedded in paraffin. All the procedures involving animals were reviewed and approved by the Institutional Animal Care and Use Committee of Qingdao University Medical College.

Cell Culture and Treatment

H9c2 cells (rat cardiomyocytes) were purchased from the Shanghai Institutes for Biological Sciences (Shanghai, China), which were cultured in Dulbecco's Modified Eagle's Medium (DMEM) (Gibco; Thermo Fisher Scientific, Waltham, MA, United States) supplemented with 10% fetal bovine serum (FBS), 100 U/ml penicillin, 100 μg/ml streptomycin, and 110 mg/l sodium pyruvate at 37°C in a humidified atmosphere containing 5% CO_2. The cells were treated with 2 μM or 0.2 μM DOX (Aladdin., Shanghai, China) at the indicated times.

Cell Transfection

H9c2 cells were transfected with the Lipofectamine 3000 Transfection Reagent when they reached approximately 70% confluence for 24 h according to the manufacturer's instructions. PAK2 and XBP1s were cloned into the pcDNA3.1 expression and synthesized by Tsingke (Beijing, China). The empty vector of pcDNA3.1 and scramble control were used as negative controls for overexpression and small interfering RNA (siRNA), respectively. MiR-mimic, miR-inhibitor, and si_PAK2 were purchased from Shanghai GenePharma (Shanghai, China). Their sequences are shown in **Table 1**.

Quantitative Real-Time PCR

Total RNA obtained from the H9c2 cells or left ventricle tissue was extracted using Trizol reagent. RNA was reverse transcribed with HiScript III RT SuperMix for qPCR (+ gDNA WIper) reverse transcription kit (Vazyme, Nanjing, China) for mRNA levels testing. Stem-loop quantitative real-time PCR (qRT-PCR) for mature miRNAs was performed as previously described (36) with miRNA 1st Strand cDNA Synthesis Kit (by stem-loop) (Vazyme, Nanjing, China) for miRNA levels testing. The miR-194-5p stem-loop primer sequence: 5′-GT CGTATCCAGTGCAGGGTCCGAGGTATTCGCACTGGATAC GACTCCACA-3′. According to the manufacturer's instructions, the cDNA was mixed with the corresponding fluorescent dye SYBR, and the test was carried out in the CFX96 real-time PCR system (Bio-Rad, Hercules, CA, United States). The results were put into the $2-^{\Delta\Delta}$CT formula for calculation. MiR-194-5p expression was normalized to that of U6, while XBP1s mRNA level was normalized to that of glyceraldehyde 3-phosphate dehydrogenase (GAPDH). The primers are shown in **Table 2**.

TABLE 1 | The sequences of synthesized mimic, inhibitor, small-interfering RNA (siRNA).

Gene	Sequence
miR-194-5p mimic	F: UGUAACAGCAACUCCAUGUGGA
	R: CACAUGGAGUUGCUGUUACAUU
mimic-NC	F: UUCUCCGAACGUGUCACGUTT
	R: ACGUGACACGUUCGGAGAATT
miR-194-5p inhibitor	5′-UCCACAUGGAGUUGCUGUUACA-3′
Negative control	5′-CAGUACUUUUGUGUAGUACAA-3′
Si_PAK2	5′-GGGAAUGGAAGGCUCAGUUTT-3′
Scramble control	5′-UUCUCCGAACGUGUCACGUTT-3′

TABLE 2 | Real-time quantitative PCR (qRT-PCR) primers used in this study.

Gene	Sequence
U6	F: ATTGGAACGATACAGAGAAGATT
	R: GGAACGCTTCACGAATTTG
miR-194-5p	F: CGCGTGTAACAGCAACTCCA
	R: AGTGCAGGGTCCGAGGTATT
GAPDH	F: GCCCATCACCATCTTCCAGGAG
	R: GAAGGGGCGGAGATGATGAC
XBP1s	F: TGAGAACCAGGAGTTAAG
	R: CCTGCACCTGCTGCGGAC

Cell Apoptosis Assay

The sterile slides were placed in the 24-well plate and then the H9c2 cells were planted on top of the slides. After transfection and treatment, 4% paraformaldehyde added to fix the cells for at least 1 h in room temperature. Cell apoptosis was characterized *via* a TUNEL assay using the TUNEL Apoptosis Detection Kit (YEASEN, Shanghai, China) according to the manufacturer's instructions. The samples were mounted with mounting medium containing 4′,6′-diamidino-2-phenylindole (DAPI) (Vector Laboratories, Burlingame, CA, United States) to stain nuclei. The stained-glass slides were observed and photographed under a fluorescence microscope. The percentage of the apoptotic nuclei was calculated by the number of apoptotic cells/the number of total nuclei. We randomly measured 150 cells from each experiment to calculate the apoptotic rate. Caspase-3/7 activity assay was performed using the Caspase 3/7 Activity Assay Kit (Meilunbio, Dalian, China) according to the manufacturer's instructions. Masson's trichrome staining was performed using the staining kit (Solarbio, Beijing, China) following the manufacturer's instructions.

Trypan Blue Stain

Cell death rate was measured by trypan blue stain (Solarbio, Beijing, China). The supernatant and adherent cells were collected. The cell was prepared and stained by trypan blue according to the manufacturer's instructions. The percentage of the cell death was calculated by the number of trypan blue positive cells/the number of total cells, which were counted under the microscope.

Western Blot Analysis

Total protein was extracted from H9c2 cells or mouse left ventricle tissue by the radio immunoprecipitation assay

(RIPA) Lysis Buffer (Solarbio, Beijing, China) according to the manufacturer's instructions. Proteins were separated by electrophoresis on the sodium dodecyl sulfate-polyacrylamide gel electrophoresis (SDS-PAGE) (10–12% polyacrylamide gels) and then transferred to polyvinylidene fluoride (PVDF) membranes. Subsequently, the PVDF membranes were blocked in 5% non-fat milk for 2 h and then incubated overnight at 4°C with anti-PAK2 (1:1,000, Cell Signaling Technology, Danvers, MA, United States), or anti-XBP1s (1:1,000, Cell Signaling Technology, Danvers, MA, United States), or anti-β-actin (1:2,000, Santa Cruz Biotechnology, Dallas, TX, United States), or anti-GAPDH (1:100,000, ABclonal, Wuhan, China), or anti-cas-12 (1:2,000, Abcam, United States) primary antibodies after washing with TBS-Tween 20 (TBST) three times, 10 min each time. Horseradish peroxidase (HRP)-conjugated secondary antibodies were incubated at room temperature for 1 h, then washed with TBST three times, 10 min each time. Membranes were visualized using enhanced chemiluminescence. Protein expression was quantified using ImageJ, and β-actin or GAPDH was used as the internal control.

Dual-Luciferase Reporter Gene Assay

The wild-type (WT) and mutated-type (MT) PAK2 fragments of the miR-194-5p binding region were, respectively, inserted into the pGL3 vector immediately downstream of the stop codon of the luciferase gene, to synthesize the reporter gene plasmid (Tsingke, Beijing, China). A luciferase activity assay was performed as described previously (37). Briefly, phRL-TK reporter plasmid and miR-194-5p mimic (or mimic-NC) were cotransfected into HEK-293 cells, which were seeded in 48-well plates. The cells were collected and lysed after 24 h, then the firefly and Renilla luciferase activities were detected by the Dual–Luciferase Reporter Assay System (Promega, Madison, WI, United States). Firefly luciferase activities were normalized to Renilla luciferase activity.

Polymerase Chain Reaction Product Polyacrylamide Gel Electrophoresis

The extracted RNA was first reverse transcribed into cDNA with HiScript III RT SuperMix for qPCR (+ gDNA wiper) (Vazyme, Nanjing, China). The cDNA was amplified by PCR with Gold Mix rapid PCR enzyme (Tsingke, Beijing, China). About 10% of polyacrylamide gel (per 10 ml: 30% acrylamide 3.33 ml, 10X TBE 1 ml, ddH_2O 5.614 ml, N,N,N′,N′-Tetramethylethylenediamine (TEMED) 5 μl, 10% ammonium persulfate (APS) 50 μl) were prepared. Electrophoresis was performed in 1 × TBE solution and the PCR products were separated. Then gel was stained in Gelred non-toxic nucleic acid dye in the dark (dye: water = 1:10,000 ratio) for 30 min and visualized using chemiluminescence.

Immunofluorescence

Cells were planted and fixed in the same manner as TUNEL assay. About 0.5% Triton X-100 was used for cell permeability treatment for 30 min. After discarded Triton X-100, cells were rinsed with phosphate-buffered saline (PBS) for three times, 5 min each time. Blocked with goat serum for 1 h, then washed with PBS for three times, 5 min each time. Added primary antibody and incubated overnight at 4°C, then washed with PBS. Fluorescent secondary antibody was added and incubated in dark for 1 h. After washing with PBS, slides were mounted with DAPI to stain nuclei. The slides were observed and photographed using an inverted two-photon laser confocal microscope.

Echocardiographic Assessment

Generally, mice were mildly anesthetized with intraperitoneal injection of 4% chloral hydrate 0.1 ml/10 g, and the hair over the chest region was removed. The mice were then placed in a supine position and transthoracic echocardiography was performed using a VINNO 6 Lab system (VINNO, Suzhou, China). Two-dimensional guided M-mode tracings were recorded in parasternal long and short axis views at the level of the papillary muscles. Left ventricular ejection fraction (EF) and fractional shortening (FS) were recorded by the system. All the measurements were obtained for greater than three beats and averaged.

Statistical Analysis

The experimental data were analyzed using GraphPad Prism version 5 software and the data were presented as mean ± SD. *T*-test was used to compare the data between the two groups. One-way ANOVA was used to compare the mean values of multiple groups. Tukey's *post hoc* test was used for pairwise comparison between the multiple groups. All the experiments were repeated three times and $p < 0.05$ was indicated as statistically significant.

RESULTS

MicroRNA-194-5p Participated in Doxorubicin-Induced Cardiomyocyte Apoptosis

We first investigated the sequences of miR-194-5p, and found that they are homologous in human, rat, and mouse according to miRBASE (miRBASE Sequence database-release 22.1). In order to explore the role of miR-194-5p in DOX-induced cardiotoxicity, rat myocardial cell line H9c2 was treated with 2 μM DOX to simulate the cell model of DOX-induced cardiotoxicity. With 2 μM DOX treatment, the expression of miR-194-5p increased in a time-dependent manner (**Figure 1A**). Transfection with miR-194-5p inhibitor could effectively suppress the expression of miR-194-5p (**Figure 1B**), while transfection with miR-194-5p mimic enhanced its expression (**Figure 1C**). Next, we further studied the potential role of miR-194-5p in DOX-induced cardiomyocytes apoptosis. When miR-194-5p expression was inhibited, DOX-induced apoptosis was significantly reduced on TUNEL assay (**Figures 1D,E**). In addition, inhibition of miR-194-5p attenuated DOX-induced caspase-3/7 activity elevation (**Figure 1F**). On the other hand, in order to demonstrate whether miR-194-5p participate in regulating the sensitivity of cardiomyocytes

to DOX, low dose of DOX (0.2 μM) was used to treat cardiomyocytes. Under low DOX concentration stimulation, overexpression of miR-194-5p sensitized cardiomyocytes to cas-3/7 activity elevation (**Figure 1G**). Since apoptosis is the predominant cell death mode in DOX-induced cardiotoxicity, the detection of cell death rate can also reflect the degree of DOX-induced cardiotoxicity. Finally, increased cell death induced by low dose DOX was further aggravated by miR-194-5p mimic (**Figure 1H**). Taken together, miR-194-5p was upregulated in cardiomyocytes with DOX treatment, and inhibition of miR-194-5p could alleviate DOX-induced apoptosis.

MicroRNA-194-5p Directly Targeted P21-Activated Kinase 2

It was predicted that miR-194-5p directly binds to PAK2 3′ untranslated region (UTR) region on the bioinformatics program TargetScan. Moreover, PAK2 has conserved binding sites for miR-194-5p (**Figure 2A**). Hence, we tested PAK2 expression level in DOX-treated H9c2, and the result showed that its expression level was significantly decreased 12 h after treatment (**Figure 2B**). Then, we speculated the regulatory effect of miR-194-5p on DOX-induced cardiomyocyte apoptosis achieved by targeting PAK2. To verify whether miR-194-5p directly binds to PAK2, we first constructed the luciferase plasmid containing the wild type of the predicted PAK2 3′UTR binding site (WT) or mutant binding site (MT) (**Figure 2C**). Dual luciferase reporter assay demonstrated that the fluorescence activity was inhibited when the WT plasmid was cotransfected with miR-194-5p mimic. The fluorescence activity remained unchanged when the MT plasmid was cotransfected with a miR-194-5p mimic, which indicated that miR-194-5p directly bound to PAK2 3′UTR region (**Figure 2D**). Next, we transfected miR-194-5p inhibitor and mimic into H9c2 cells to investigate their effects on PAK2 protein expression. MiR-194-5p inhibitor enhanced PAK2 expression (**Figure 2E**), while miR-194-5p mimic suppressed PAK2 expression (**Figure 2F**). These results indicated that miR-194-5p directly targeted PAK2 and negatively regulated its expression.

P21-Activated Kinase 2 Attenuated Doxorubicin-Induced Cardiomyocyte Apoptosis

We further investigated the role of PAK2 in DOX-induced cardiomyocytes apoptosis. The PAK2 plasmid was able to enhance its expression and si_PAK2 inhibited the expression (**Figures 3A,B**). Functionally, overexpression of PAK2 significantly decreased DOX-induced apoptosis (**Figures 3C,D**) and caspase-3/7 activity (**Figure 3E**). In addition, PAK2 overexpression abolished the effects of miR-194-5p on DOX-induced cell death (**Figure 3F**), indicating that PAK2 was the downstream target of miR-194-5p. Contrarily, cell death induced by 0.2 μM DOX was further increased with si_PAK2 (**Figure 3G**). The above findings indicated that the PAK2 could alleviate apoptosis in H9c2 cells exposed to DOX treatment.

X-Box Binding Protein 1 Participated in Doxorubicin-Induced Cardiotoxicity

It has been reported that DOX-induced cardiotoxicity may activate multiple UPR pathways (28). The key transcription factor XBP1s is regulated by PAK2 in the heart (24). Therefore, we first explored the XBP1s expression in DOX-induced cardiotoxicity. Similarly, H9c2 was treated with 2 μM DOX for the indicated time, and the XBP1s expression reached peak at 3 h and decreased thereafter, which indicated the activation of the IRE/XBP1 pathway of UPR (**Figures 4A,B**).

Cas-12 as an indicator of ER-mediated apoptosis was investigated as well. The expression of its activated form—cleaved cas-12 (cl cas-12) was significantly increased 12 h onward under 2 μM DOX treatment (**Figures 4A,C**). Next, we detected the mRNA level of XBP1s, and the result showed the same trend with its protein expression levels (**Figure 4D**). When XBP1 was activated, XBP1 mRNA was spliced and 26 bases were cut off to form the splicing XBP1, also known as its activated form (XBP1s). Thus, we measured the cDNA level after reverse transcription from total RNA. The results also showed that significant XBP1s band appeared at 3 h after DOX treatment (**Figure 4E**). It has been reported that the XBP1s can be translocated from cytoplasm to nucleus once activated (38), and this can be confirmed by immunofluorescence experiments (**Figure 4F**). Next, Thapsigargin, an ER stress inducer, was used as the positive control to verify that DOX could trigger the UPR and activate the XBP1s (**Figures 4G,H**). The inhibition of the ER stress by 4-PBA inhibited the DOX-triggered XBP1s at 3 h (**Figure 4I**). Taken together, the UPR was involved in DOX-induced cardiotoxicity, in which XBP1 was activated. In addition, the XBP1s expression reached its peak at 3 h in DOX-treated H9c2, and then decreased.

X-Box Binding Proteins 1 Attenuated Doxorubicin-Induced Cardiomyocyte Apoptosis

Several studies have reported that XBP1s plays protective roles in the heart. In our study, we also confirmed the role of XBP1s in DOX-induced cardiotoxicity. The overexpression of XBP1s was verified by WB after transfection of XBP1s plasmid (**Figure 5A**). Cleaved caspase-12 expression increased in DOX-induced cardiomyocytes, indicating that the DOX-induced ER-related apoptosis, which decreased when XBP1s was overexpressed (**Figure 5B**). In addition, the overexpression of XBP1s significantly inhibited the DOX-induced increase in cas-3/7 activity (**Figure 5C**). Trypan blue stain assay showed the same result that the overexpression of XBP1s inhibited increased cell death rate induced by the DOX (**Figure 5D**). These results indicated that XBP1s could alleviate the ER-related apoptosis induced by the DOX and play the cardioprotective role.

Activation of XBP1 has been shown to require the presence of PAK2 in cardiomyocytes. Next, we verified the relationship between miR-194-5p, PAK2 and XBP1s on the regulation of cardiomyocyte apoptosis. Firstly, inhibition of

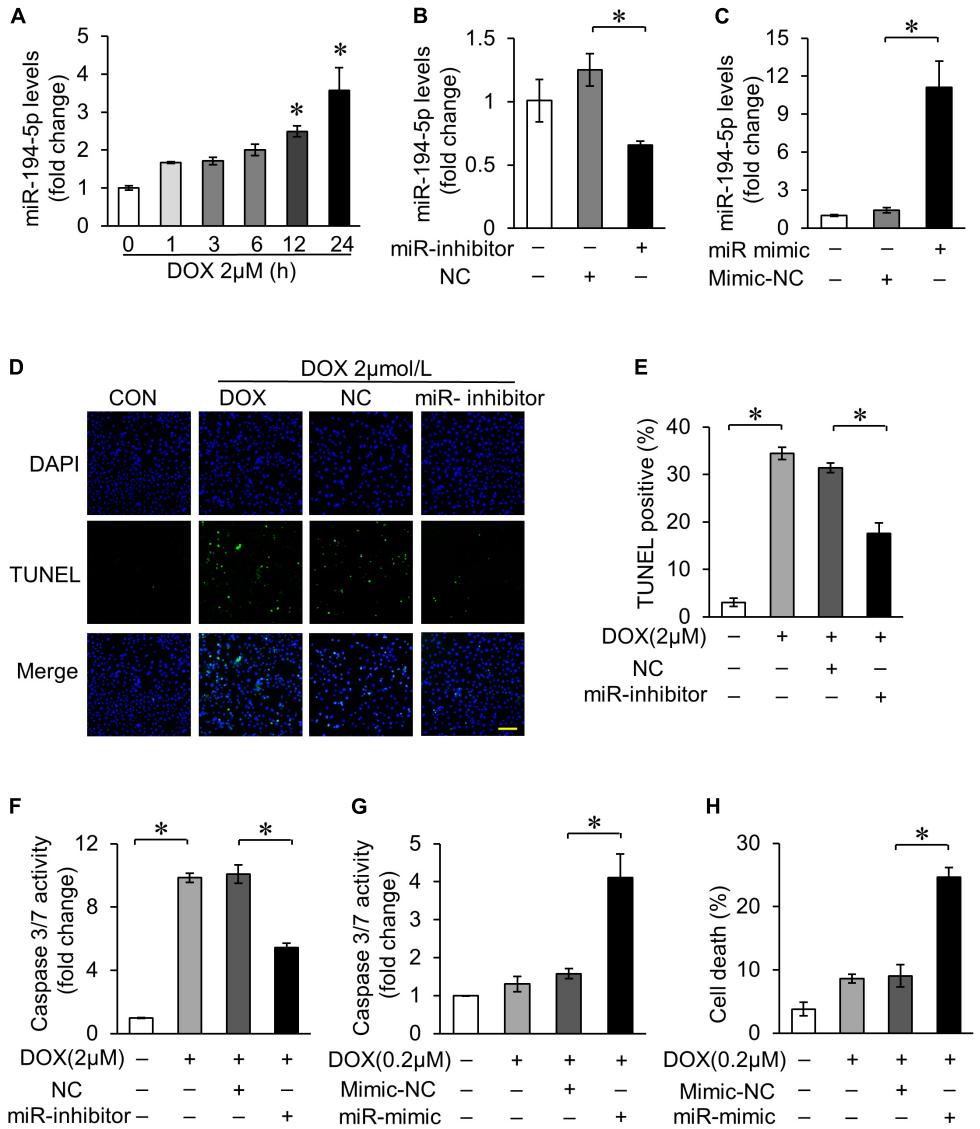

FIGURE 1 | MiR-194-5p participated in doxorubicin (DOX)-induced cardiomyocyte apoptosis. **(A)** H9c2 cells were treated with 2 μM DOX for the indicated times. The expression levels of miR-194-5p were measured by qRT-PCR. *$p < 0.01$ vs. control. **(B)** MiR-194-5p expression after transfection with miR-194-5p inhibitor for 24 h was measured by real-time quantitative PCR (qRT-PCR). **(C)** MiR-194-5p expression after transfection with miR-194-5p mimic for 24 h was measured by qRT-PCR. **(D–F)** Suppressed miR-194-5p expression with miR-194-5p inhibitor for 24 h and exposed cells to 2 μM DOX for 24 h. Apoptosis was detected by terminal deoxinucleotidyl transferase dUTP nick-end labeling (TUNEL) assay **(D)**. Green, TUNEL-positive nuclei; blue, 4,6-diamidino-2-phenylindole (DAPI)-stained nuclei; scale bar, 200 μm. Statistical analysis of TUNEL-positive cells **(E)** and caspase 3/7 activity **(F)** are shown. **(G,H)** Enhanced miR-194-5p expression with miR-194-5p mimic for 24 h and exposed cells to 0.2 μM DOX for 24 h. Caspase-3/7 activity **(G)** and cell death rate **(H)** are shown. All the experiments have been performed independently in triplicate, and the data were expressed as mean ± SD. *$p < 0.01$ as indicated.

miR-194-5p could alleviate the downregulation of XBP1s expression and the upregulation of cl cas-12 expression levels under the DOX treatment (**Figure 6A**). Next, PAK2 restoration by transfection with its overexpression plasmid also reduced the downregulation of XBP1s expression and the upregulation of cl cas-12 expression levels (**Figure 6B**). When cotransfected, XBP1s partially eliminated miR-194-5p mimic caused elevation of cleaved cas-12 and cell death (**Figures 6C,D**). Similarly, XBP1s also partially eliminated si_PAK2 caused elevation of cleaved cas-12 level and cell death (**Figures 6E,F**). Thus, those data suggested that miR-194-5p and PAK2 regulated DOX-induced cardiomyocyte apoptosis *via* XBP1s.

MicroRNA-194-5p Was Involved in Doxorubicin-Induced Cardiotoxicity *in vivo*

We further explored the role of miR-194-5p in the DOX-induced cardiotoxicity in the mouse model. We found

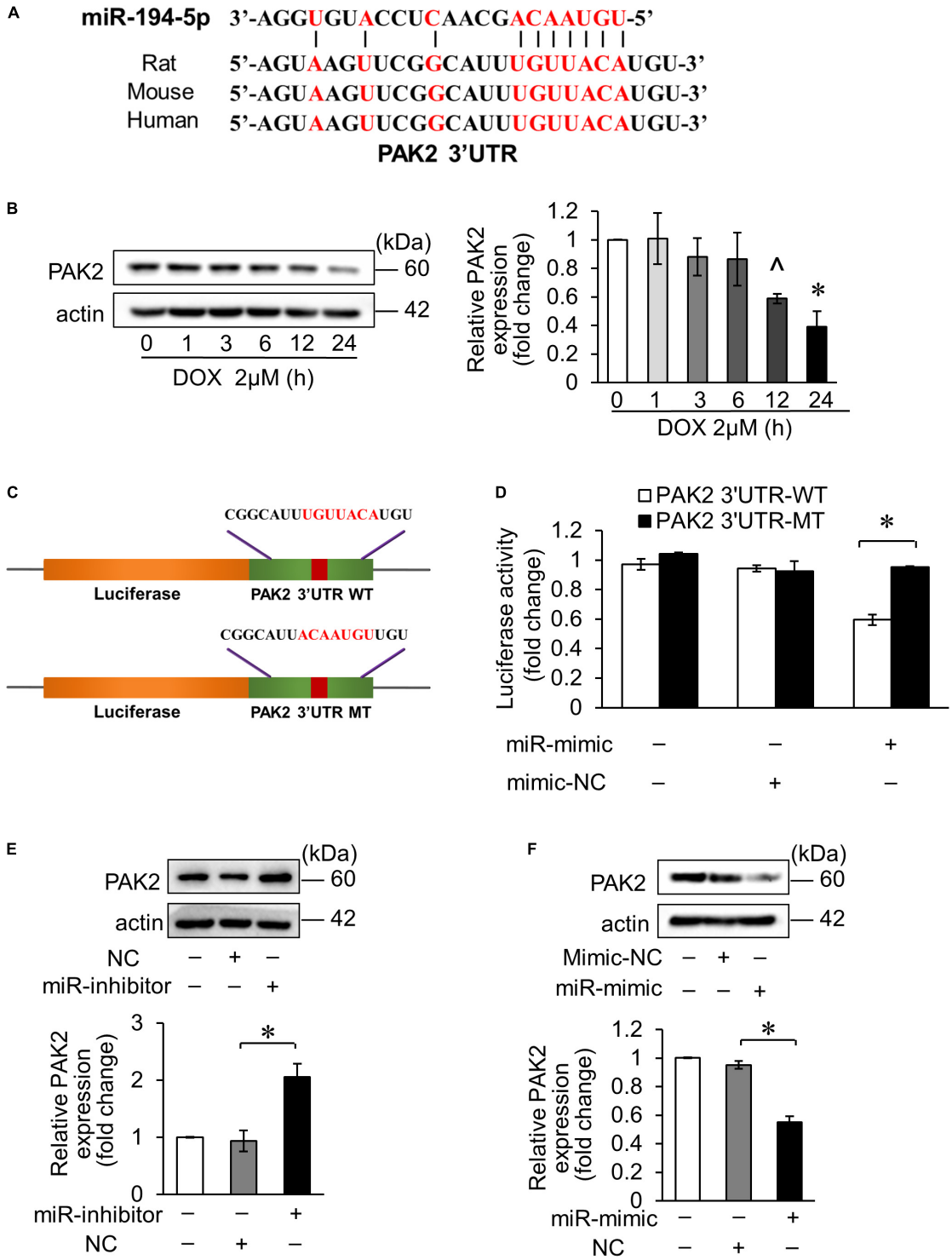

FIGURE 2 | MiR-194-5p directly targeted PAK2. **(A)** Prediction of the PAK2 3′UTR potential binding site of miR-194-5p *via* bioinformatics program TargetScan. Potential complementary bases are shown in red. **(B)** H9c2 were treated with 2 μM DOX for the indicated times. The expression levels of PAK2 were detected by Western blots and the quantitative histogram was shown. $\wedge p < 0.05$ vs. control. $^{*}p < 0.01$ vs. control. **(C)** Schematic diagram of the reporter containing the putative miR-194-5p binding site in the PAK2 3′UTR region. WT, wild-type; MT, mutant. **(D)** Luciferase activity detected in HEK-293 cells transfected with miR-194-5p mimic or negative control along with luciferase reporter constructs, as indicated. **(E)** H9c2 was transfected with miR-194-5p inhibitor for 24 h. The expression levels of PAK2 were detected by Western blot and the quantitative histogram was shown. **(F)** H9c2 was transfected with miR-194-5p mimic for 24 h. The expression levels of PAK2 were detected by Western blot and the quantitative histogram was shown. All the experiments have been performed independently in triplicate, and the data were expressed as mean ± SD. $^{*}p < 0.01$ as indicated.

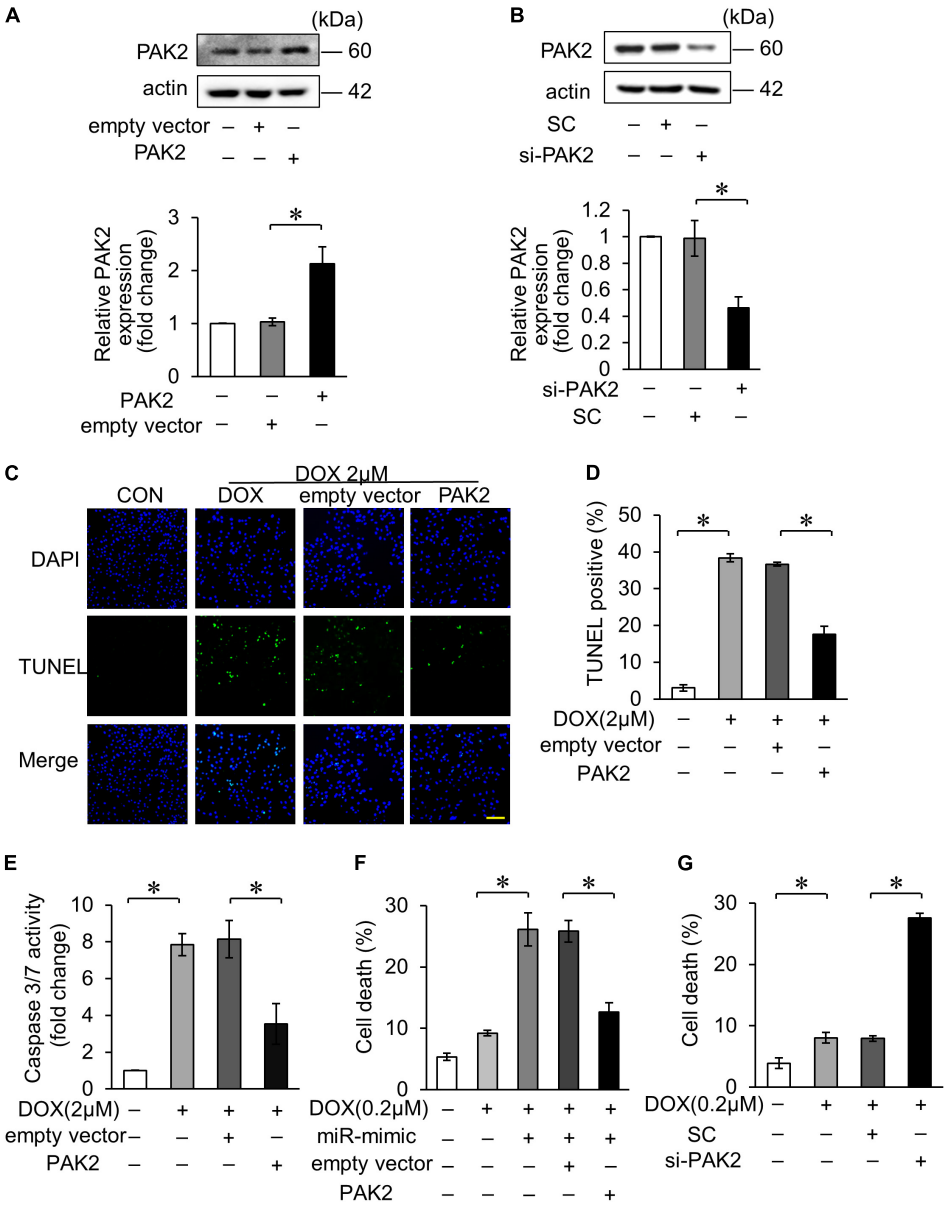

FIGURE 3 | PAK2 attenuated DOX-induced cardiomyocyte apoptosis. **(A)** H9c2 was transfected with PAK2-overexpressing plasmid for 24 h. The expression levels of PAK2 were detected by Western blot and the quantitative histogram was shown. **(B)** H9c2 was transfected with PAK2 small-interfering RNA (siRNA) for 24 h. The expression levels of PAK2 were detected by Western blot and the quantitative histogram was shown. **(C–E)** Enhanced PAK2 expression with PAK2-overexpressing plasmid for 24 h and exposed to 2 μM DOX for 24 h. Apoptosis was detected by TUNEL assay **(C)**. Green, TUNEL-positive nuclei; blue, DAPI-stained nuclei; scale bar, 200 μm. Statistical analysis of TUNEL-positive cells **(D)** and caspase-3/7 activity **(E)** are shown. **(F)** H9c2 was cotransfected with miR-194-5p mimic and PAK2-overexpressing plasmid for 24 h and then exposed to 0.2 μM DOX for 24 h. Cell death rate was analyzed. **(G)** H9c2 was transfected with PAK2 siRNA for 24 h and exposed to 0.2 μM DOX for 24 h. Cell death rate was analyzed. All the experiments have been performed independently in triplicate, and the data were expressed as mean ± SD. *$p < 0.01$ as indicated.

that DOX treatment induced an increase in miR-194-5p expression levels in the heart (**Figure 7A**). Moreover, the protein expression levels of PAK2, XBP1s decreased, and cl cas-12 level increased (**Figure 7B**). Next, we validated the role of miR-194-5p *in vivo*. Injection with adenovirus-harbored miR-194-5p antagomir could reverse the expression of PAK2, XBP1s, and cl cas-12 induced by the DOX (**Figure 7B**). Furthermore, suppression of the miR-194-5p significantly improved cardiac function (**Figures 7C,D**), attenuated DOX-induced cardiomyocyte apoptosis (**Figures 7E,F**), and ameliorated myocardial fibrosis (**Figure 7G**). Taken together, our *in vivo* results showed a significant protective role of miR-194-5p antagomir in the DOX-induced cardiotoxicity.

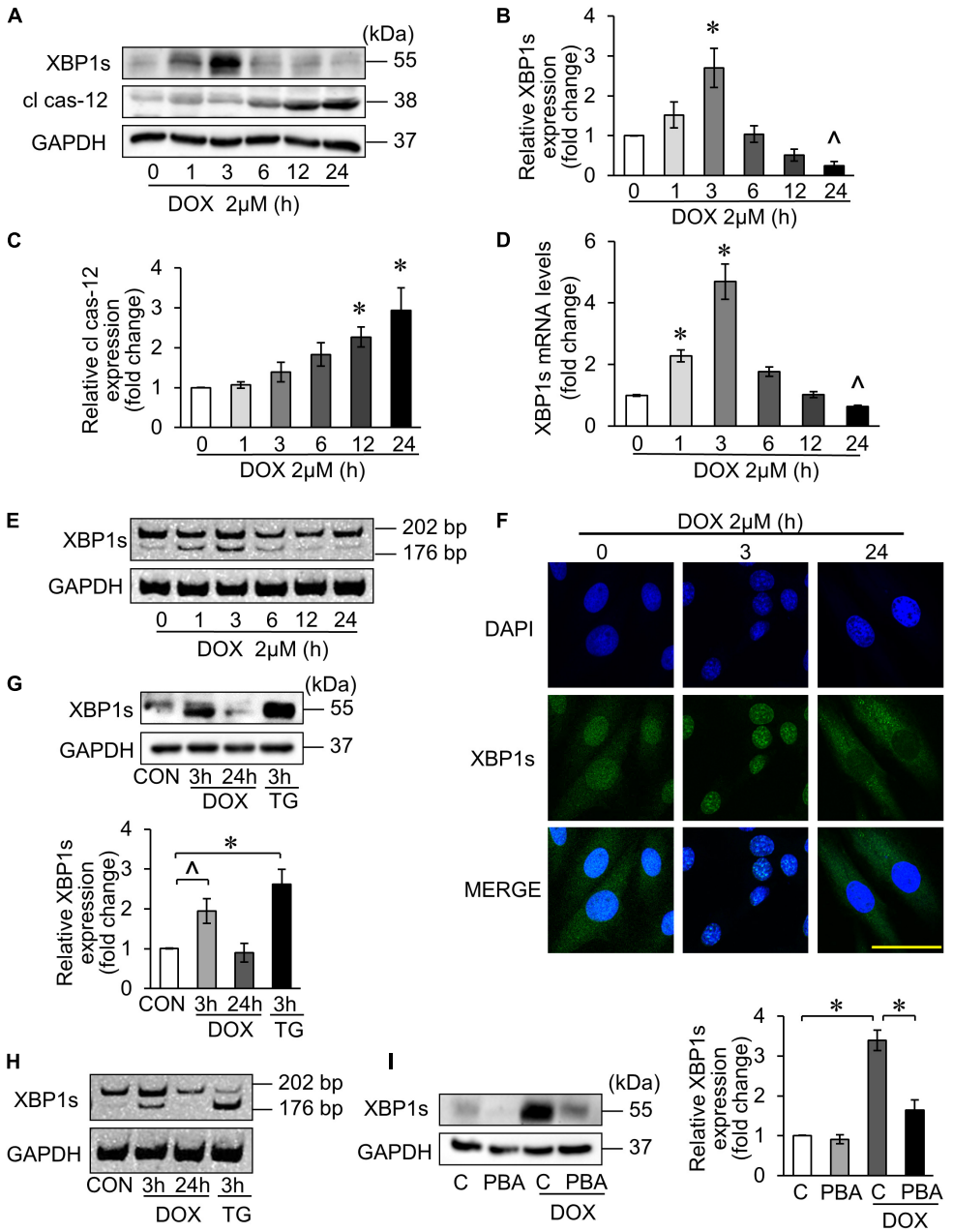

FIGURE 4 | X-box binding protein 1 (XBP1) participated in DOX-induced cardiotoxicity. **(A–E)** H9c2 was treated with 2 μM DOX for the indicated times. The XBP1s levels were detected using Western blots **(A)** and the quantitative histogram was shown **(B,C)**, and also detected using qRT-PCR **(D)**. $\wedge p < 0.05$ vs. control. $^*p < 0.01$ vs. control. Spliced bands of XBP1 were detected by polyacrylamide gel electrophoresis **(E)**. **(F)** H9c2 was treated with 2 μM DOX for 3 and 24 h. The localization of XBP1s in cells was detected by immunofluorescence experiment. Green, XBP1s; blue, DAPI-stained nuclei; scale bar, 50 μm. **(G,H)** H9c2 was treated with 2 μM DOX or 50 nM TG for the indicated times. The XBP1s levels were detected by Western blots and the quantitative histogram was shown **(G)**, and the spliced bands were detected by polyacrylamide gel electrophoresis **(H)**. TG, thapsigargin. **(I)** H9c2 was treated with 2 μM DOX for 3 h, which was pre-treated with 5 mM 4-PBA for 3 h. The XBP1s levels were detected by Western blots and the quantitative histogram was shown. All the experiments have been performed independently in triplicate, and the data were expressed as mean ± SD. $\wedge p < 0.05$ vs. control. $^*p < 0.01$ vs. control.

DISCUSSION

Doxorubicin is the representative of anthracycline family, one of the most widely used effective antitumor drugs. However, DOX-induced cardiotoxicity is the major limiting factor for its application, and the cardiomyopathy may not be detected until years after the DOX completion. It has been reported that 10% of patients receiving DOX developed symptomatic cardiomyopathy within 15 years after the end of treatment (39). Studies over the years have revealed that oxidative stress and mitochondrial

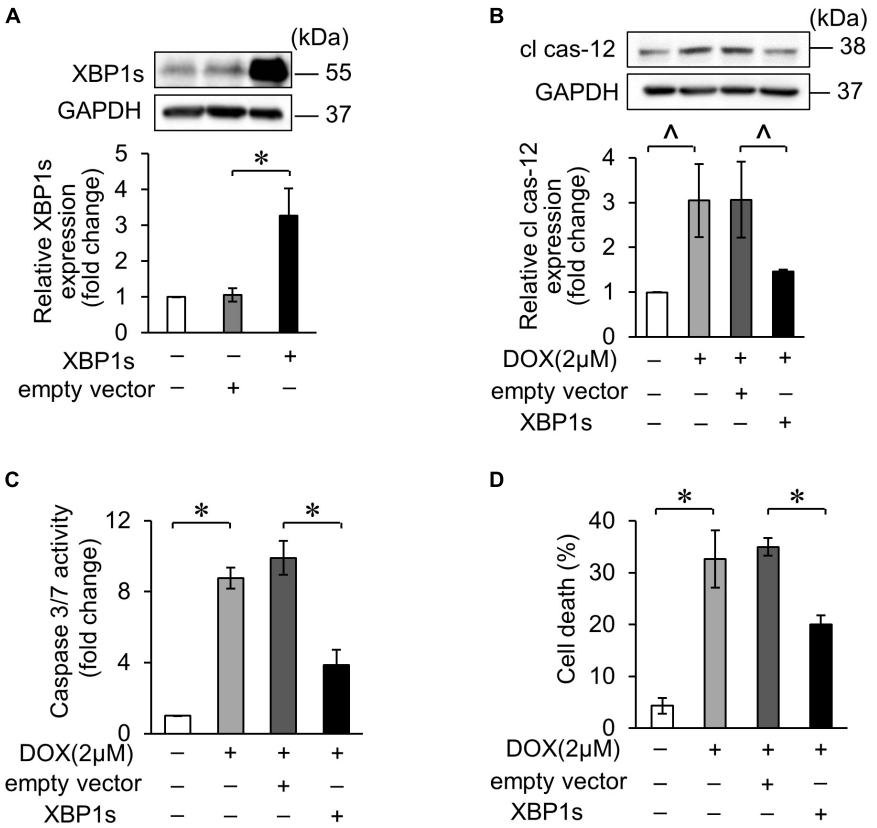

FIGURE 5 | XBP1s attenuated DOX-induced cardiomyocyte endoplasmic reticulum (ER) stress and apoptosis. **(A)** H9c2 was transfected with XBP1s-overexpressing plasmid for 24 h. The expression levels of XBP1s were determined using Western blot and the quantitative histogram was shown. **(B–D)** Enhanced XBP1s expression in H9c2 cells with XBP1s-overexpressing plasmid for 24 h and exposed to 2 μM DOX for 24 h. The expression levels of cleaved caspase-12 were determined using Western blot and the quantitative histogram was shown **(B)**. Caspase-3/7 activity **(C)** and cell death rate **(D)** were analyzed. All the experiments have been performed independently in triplicate, and the data were expressed as mean ± SD. $\wedge p < 0.05$ vs. control. $^{*}p < 0.01$ vs. control.

damage are the predominant mechanisms of DOX-induced cardiotoxicity. However, the simply use of antioxidants does not provide much protection against heart damage caused by DOX (40). This suggests that the DOX-induced cardiotoxicity may be the result of multiple mechanisms. In this study, we explored the molecular mechanisms involved in ER stress-related DOX cardiotoxicity, which provides a new strategy for the prevention and control of DOX-induced cardiotoxicity.

A growing number of studies have proposed miRNAs as potential targets for the DOX-induced cardiotoxicity. For example, in the DOX-induced cardiotoxicity, miR-15b-5p, miR-23a, miR-29b, and miR-146a have been proved to be related to mitochondrial damage; miR-30 family, miR-140-5p, and miR-451 are related to oxidative stress; miR-378 is associated with the ER stress and miR-320 is related to the microvascular density (17). We reported here that miR-194-5p participated in the DOX-induced cardiotoxicity and suppression of miR-194-5p alleviated the DOX-induced cardiomyocyte apoptosis.

In recent years, the role of ER stress in the DOX-induced cardiomyopathy gained attentions. Studies have shown that the DOX caused significant ER dilatation in human hearts (27). The effectors of ER stress were activated in the DOX-treated heart tissue, indicating that UPR was involved in regulating cardiomyocyte survival or death. Recent study has shown that PAK2 regulation of the protective ER function was through the IRE1/XBP1-dependent UPR pathway and this regulation was conferred by PAK2 inactivation of PP2A. Mice with PAK2 deletion showed defective response to ER stress, increasing cardiomyocyte damage (24). In our study, we demonstrated that PAK2 as the target gene of miR-194-5p exerted antiapoptotic effect in the DOX-induced cardiotoxicity.

In addition, the activation of the transcription factor XBP1 upregulates the expression of ER chaperone and ER associated degradation (ERAD) components to relieve ER stress and promotes cell survival (38). For example, $XBP1^{-/-}$ livers showed increased apoptosis, and $XBP1^{-/-}$ mouse embryos could not survive, while XBP1 transgenic reversed this embryonic lethality (41). In cardiovascular disease, cardiomyocyte-specific deletion of XBP1 aggravated cardiac dysfunction in ischemia-reperfusion injury, suggesting that XBP1s has a protective effect (35). The expression of XBP1s was decreased in the heart tissue of both human and rodents with heart failure, heart-specific XBP1 overexpression prevented the development of cardiac dysfunction, and XBP1s

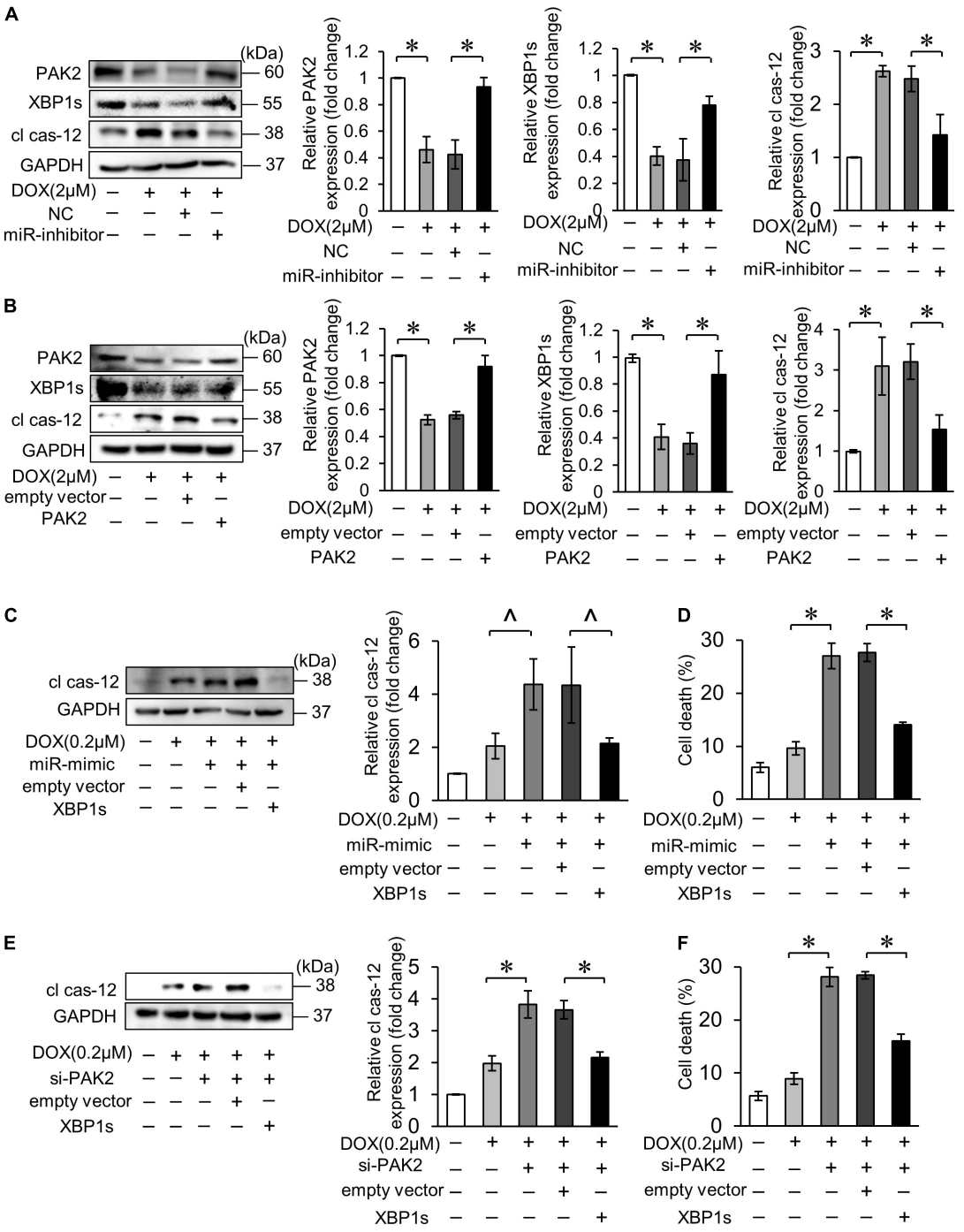

FIGURE 6 | MiR-194-5p participated in DOX-induced ER stress and cardiomyocyte apoptosis through PAK2 and XBP1s. **(A)** Suppressed miR-194-5p expression with miR-194-5p inhibitor for 24 h and exposed to 2 μM DOX for 24 h. The expression levels of PAK2, XBP1s, and cleaved caspase-12 were detected by Western blot and the quantitative histogram was shown. **(B)** Enhanced PAK2 expression with PAK2-overexpressing plasmid for 24 h and exposed to 2 μM DOX for 24 h. The expression levels of PAK2, XBP1s, and cleaved caspase-12 were detected by Western blot and the quantitative histogram was shown. **(C,D)** H9c2 was cotransfected with miR-194-5p mimic and XBP1s-overexpressing plasmid for 24 h, then exposed to 0.2 μM DOX for 24 h. The expression levels of cleaved caspase-12 were detected by Western blot and the quantitative histogram was shown **(C)** and cell death rate was analyzed **(D)**. **(E,F)** H9c2 was co-transfected with PAK2 siRNA and XBP1s-overexpressing plasmid for 24 h, then exposed to 0.2 μM DOX for 24 h. The expression levels of cleaved caspase-12 were detected by Western blot and the quantitative histogram was shown **(E)** and cell death rate was analyzed **(F)**. All the experiments have been performed independently in triplicate, and the data were expressed as mean ± SD. $\wedge p < 0.05$ vs. control. $^{*}p < 0.01$ vs. control.

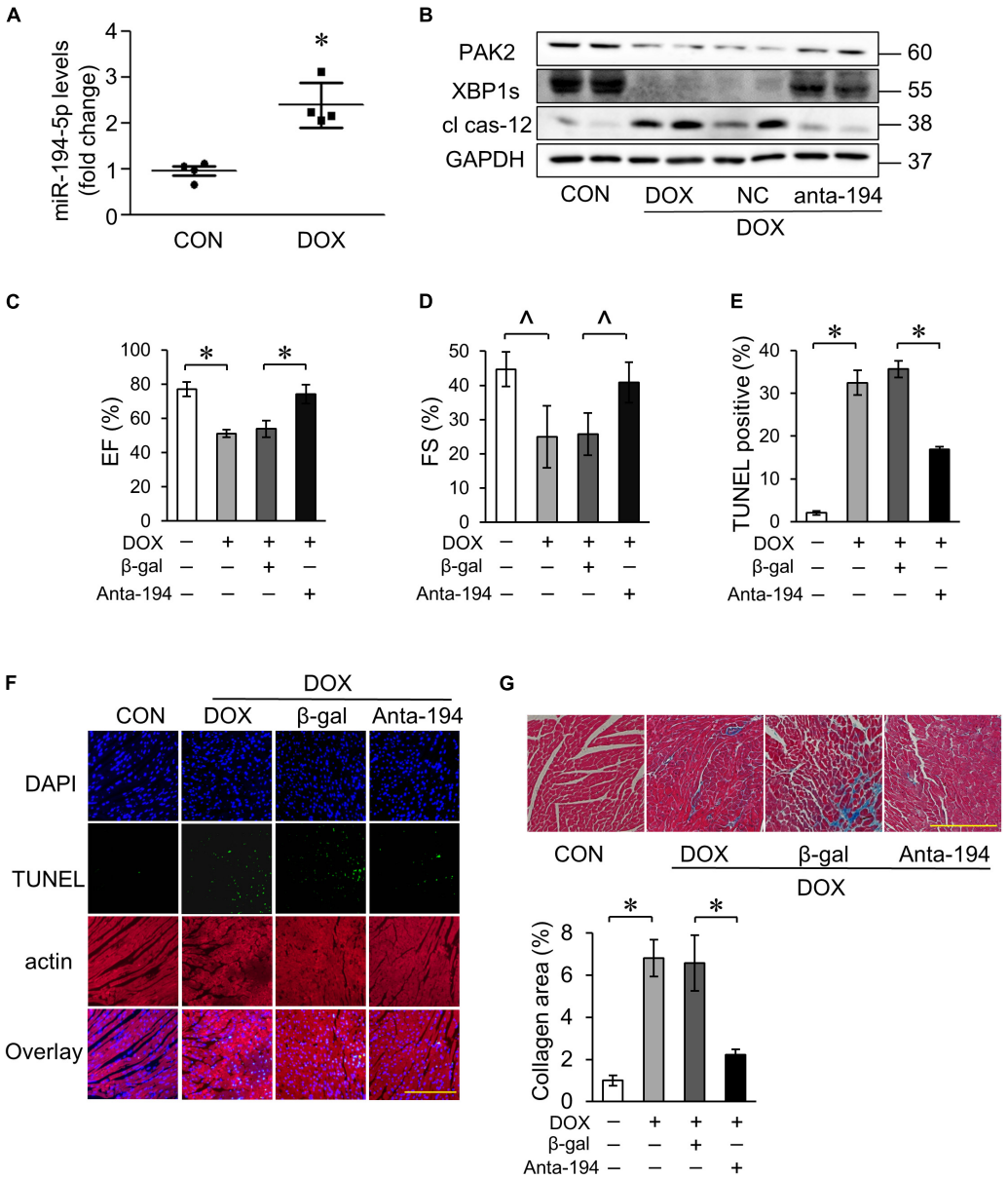

FIGURE 7 | MiR-194-5p was involved in DOX-induced cardiotoxicity *in vivo*. **(A)** The expression levels of miR-194-5p in mice heart tissue were detected after DOX treatment by qRT-PCR. **(B)** Adenovirus-harbored anta-miR-194-5p was injected into the mice 1 week before DOX treatment. The expression levels of PAK2, XBP1s and cleaved caspase-12 were detected by Western blot. Echocardiographic analysis of left ventricular cardiac function in mice, EF **(C)** and FS **(D)** results are shown. EF, ejection fraction; FS, fractional shortening. Apoptosis was measured by TUNEL assay **(F)** and apoptotic rates were analyzed **(E)**. Green, TUNEL-positive nuclei; blue, DAPI (4,6-diamidino-2-phenylindole)-stained nuclei; scale bar, 500 μm. **(G)** Masson trichrome staining for collagen performed. scale bar, 200 μm. Anta-194, adenovirus-harbored miR-194-5p antagomir. $N = 4$, and the data were expressed as mean ± SD. $\wedge p < 0.05$ vs. control. $^{*}p < 0.01$ vs. control.

stimulated adaptive heart growth by activating mammalian target of rapamycin (mTOR) signal (42). In vascular smooth muscle cells, XBP1s promoted the repair of vascular injury or the formation of neointimal (43). These results indicated that XBP1s is involved in the regulation of cardiovascular disease and plays a protective role. Besides, other ER stress sensor, such as, binding immunoglobulin protein (BiP) was reported to bind to the IRE1 and protein kinase R-like endoplasmic reticulum kinase (PERK) *via* its nuclei binding domain (44); ER stress with prolonged activation of the UPR-initiated apoptotic cell death *via* the upregulation of C/EBP-homologus protein (CHOP). Previous studies showed that the DOX treatment increased CHOP, BiP, and cas-12 activation to initiated apoptosis (45, 46). In the case of DOX-induced cardiotoxicity, a study also revealed that XBP1s significantly inhibited the cleaved cas-12 expression (an ER-specific apoptotic factor) and alleviated cell apoptosis (27). This present study, we measured levels of cl cas-12 by

the DOX treatment to indicate the apoptosis induced by ER stress, and further to investigate the changes of XBP1s during the ER stress. The expression of XBP1s was increased and nuclear translocated when applied DOX to H9c2 within 3 h, indicating that the DOX-induced UPR and alleviated ER stress by increasing XBP1s expression in a short time. With the extension of induction time, the level of XBP1s decreased, which was consistent with the decrease of PAK2 expression level and indicated that lack of PAK2 affected the activation of IRE/XBP1 pathway. Functionally, XBP1s as the downstream factor of miR-194-5p and PAK2, protected from DOX-induced cardiotoxicity.

Our result was consistent with other studies, showing that the XBP1s exerts cardioprotective effect. However, the expression levels of XBP1s under DOX treatment remain controversial. In a similar study of DOX-induced cardiotoxicity, the expression of XBP1s was downregulated in both 15 mg/kg (i.p.) DOX injected Institute of Cancer Research (ICR) mouse heart tissue and DOX-treated cardiomyocytes (27). In a study using SD rats, there was no significant change of XBP1s expression level in rat heart tissue after a single injection of DOX at 20 mg/kg (i.p.) (47). In another study on the role of ER stress in regulating the DOX-induced cardiotoxicity, XBP1 expression was upregulated in the heart tissues of C57BL/6J mice with a single injection of 20 mg/kg DOX (i.p.) (48). Unfortunately, neither of the latter two studies was conducted *in vitro* experiments nor was the function of XBP1 explored. These contrary results may be partially due to species heterogeneity, the difference in the dosage of DOX, and the selected myocardial tissue sites. These results indicated that ER stress is involved in the complexity of pathological mechanism regulation, and different induction conditions and external factors may cause different degrees of damage.

Currently, studies on miR-194 in cardiovascular diseases have involved in its serum expressions and the association with cardiac function impairment, suggesting the potential of miR-194 as a circulating marker. MiRNAs attracted extensive attention as potential biomarkers because they have many advantages: high conserved between species (12), partial tissue specificity (49), and stability of expression in circulation (50). In addition, miRNAs can be detected using sensitive techniques such as quantitative real-time PCR and next-generation sequencing. Therefore, whether miR-194-5p expression is also upregulated in circulation during the DOX-induced cardiotoxicity, and whether this abnormal expression can be used as a biomarker of the DOX-induced myocardial injury, remains to be further explored.

CONCLUSION

In the DOX-induced cardiotoxicity, the miR-194-5p expression level was upregulated, and inhibition of miR-194-5p expression significantly alleviated the DOX-induced cardiotoxicity *in vitro* and *in vivo*, suggesting that the upregulation of miR-194-5p may be the cause of DOX-induced cardiotoxicity. Mechanically, miR-194-5p directly targeted PAK2 inhibited its expression, and participated in the regulation of DOX-induced cardiomyocyte apoptosis by affecting ER stress. Overexpression of PAK2 or XBP1s partially eliminated miR-194-5p induced cardiomyocytes apoptosis. Our study first identified the regulatory role of miR-194-5p/PAK2/XBP1s axis in DOX-induced cardiotoxicity, which provides a potential target for the prevention or treatment of the DOX-induced cardiotoxicity in its clinical applications.

DATA AVAILABILITY STATEMENT

The raw data supporting the conclusions of this article will be made available by the authors, without undue reservation.

ETHICS STATEMENT

The animal study was reviewed and approved by Ethics Committee Medical College of Qingdao University.

AUTHOR CONTRIBUTIONS

HF and JW conceived and designed the study, and drafted the manuscript. HF, DX, and LD conducted most of the *in vitro* experiments and data analysis. WC, LY, and YW conducted the *in vivo* study. MW participated in collecting data. All authors reviewed and approved the manuscript.

FUNDING

This study was supported by the National Natural Science Foundation of China (Grant Nos. 81770232 and 81970253) and Natural Science Foundation of Shandong Province (ZR2019ZD28).

REFERENCES

1. Carvalho FS, Burgeiro A, Garcia R, Moreno AJ, Carvalho RA, Oliveira PJ. Doxorubicin-induced cardiotoxicity: from bioenergetic failure and cell death to cardiomyopathy. *Med Res Rev.* (2014) 34:106–35. doi: 10.1002/med.21280
2. Cardinale D, Sandri MT, Martinoni A, Tricca A, Civelli M, Lamantia G, et al. Left ventricular dysfunction predicted by early troponin I release after high-dose chemotherapy. *J Am Coll Cardiol.* (2000) 36:517–22. doi: 10.1016/s0735-1097(00)00748-8
3. Songbo M, Lang H, Xinyong C, Bin X, Ping Z, Liang S. Oxidative stress injury in doxorubicin-induced cardiotoxicity. *Toxicol Lett.* (2019) 307:41–8. doi: 10.1016/j.toxlet.2019.02.013
4. Davies KJ, Doroshow JH. Redox cycling of anthracyclines by cardiac mitochondria. I. Anthracycline radical formation by NADH dehydrogenase. *J Biol Chem.* (1986) 261:3060–7.
5. Green PS, Leeuwenburgh C. Mitochondrial dysfunction is an early indicator of doxorubicin-induced apoptosis. *Biochim Biophys Acta.* (2002) 1588:94–101. doi: 10.1016/s0925-4439(02)00144-8
6. Arai M, Tomaru K, Takizawa T, Sekiguchi K, Yokoyama T, Suzuki T, et al. Sarcoplasmic reticulum genes are selectively down-regulated in cardiomyopathy produced by doxorubicin in rabbits. *J Mol Cell Cardiol.* (1998) 30:243–54. doi: 10.1006/jmcc.1997.0588
7. Arai M, Yoguchi A, Takizawa T, Yokoyama T, Kanda T, Kurabayashi M, et al. Mechanism of doxorubicin-induced inhibition of sarcoplasmic reticulum

Ca(2+)-ATPase gene transcription. *Circ Res.* (2000) 86:8–14. doi: 10.1161/01.res.86.1.8
8. Childs AC, Phaneuf SL, Dirks AJ, Phillips T, Leeuwenburgh C. Doxorubicin treatment in vivo causes cytochrome C release and cardiomyocyte apoptosis, as well as increased mitochondrial efficiency, superoxide dismutase activity, and Bcl-2:Bax ratio. *Cancer Res.* (2002) 62:4592–8.
9. Lee Y, Gustafsson AB. Role of apoptosis in cardiovascular disease. *Apoptosis.* (2009) 14:536–48. doi: 10.1007/s10495-008-0302-x
10. Arola OJ, Saraste A, Pulkki K, Kallajoki M, Parvinen M, Voipio-Pulkki LM. Acute doxorubicin cardiotoxicity involves cardiomyocyte apoptosis. *Cancer Res.* (2000) 60:1789–92.
11. Delpy E, Hatem SN, Andrieu N, de Vaumas C, Henaff M, Rucker-Martin C, et al. Doxorubicin induces slow ceramide accumulation and late apoptosis in cultured adult rat ventricular myocytes. *Cardiovasc Res.* (1999) 43:398–407. doi: 10.1016/s0008-6363(99)00142-x
12. Ambros V. microRNAs: tiny regulators with great potential. *Cell.* (2001) 107:823–6. doi: 10.1016/s0092-8674(01)00616-x
13. Bartel DP. MicroRNAs: genomics, biogenesis, mechanism, and function. *Cell.* (2004) 116:281–97. doi: 10.1016/s0092-8674(04)00045-5
14. Wan Q, Xu T, Ding W, Zhang X, Ji X, Yu T, et al. miR-499-5p attenuates mitochondrial fission and cell apoptosis via p21 in doxorubicin cardiotoxicity. *Front Genet.* (2018) 9:734. doi: 10.3389/fgene.2018.00734
15. Wang JX, Zhang XJ, Feng C, Sun T, Wang K, Wang Y, et al. MicroRNA-532-3p regulates mitochondrial fission through targeting apoptosis repressor with caspase recruitment domain in doxorubicin cardiotoxicity. *Cell Death Dis.* (2015) 6:e1677. doi: 10.1038/cddis.2015.41
16. Ji X, Ding W, Xu T, Zheng X, Zhang J, Liu M, et al. MicroRNA-31-5p attenuates doxorubicin-induced cardiotoxicity via quaking and circular RNA Pan3. *J Mol Cell Cardiol.* (2020) 140:56–67. doi: 10.1016/j.yjmcc.2020.02.009
17. Fa HG, Chang WG, Zhang XJ, Xiao DD, Wang JX. Noncoding RNAs in doxorubicin-induced cardiotoxicity and their potential as biomarkers and therapeutic targets. *Acta Pharmacol Sin.* (2021) 42:499–507. doi: 10.1038/s41401-020-0471-x
18. Matsumoto S, Sakata Y, Suna S, Nakatani D, Usami M, Hara M, et al. Circulating p53-responsive microRNAs are predictive indicators of heart failure after acute myocardial infarction. *Circ Res.* (2013) 113:322–6. doi: 10.1161/CIRCRESAHA.113.301209
19. Nie H, Pan Y, Zhou Y. Exosomal microRNA-194 causes cardiac injury and mitochondrial dysfunction in obese mice. *Biochem Biophys Res Commun.* (2018) 503:3174–9. doi: 10.1016/j.bbrc.2018.08.113
20. Bagrodia S, Taylor SJ, Creasy CL, Chernoff J, Cerione RA. Identification of a mouse p21Cdc42/Rac activated kinase. *J Biol Chem.* (1995) 270:22731–7. doi: 10.1074/jbc.270.39.22731
21. Xing J, Wang Z, Xu H, Liu C, Wei Z, Zhao L, et al. Pak2 inhibition promotes resveratrol-mediated glioblastoma A172 cell apoptosis via modulating the AMPK-YAP signaling pathway. *J Cell Physiol.* (2020) 235:6563–73. doi: 10.1002/jcp.29515
22. Wang Y, Tong J, Lin H, Ma L, Xu Y. CCHE1 accelerated the initiation of oral squamous cell carcinoma through enhancing PAK2 expression by sponging miR-922. *J Oral Pathol Med.* (2020) 49:636–44. doi: 10.1111/jop.12995
23. Tian L, Han F, Yang J, Ming X, Chen L. Long noncoding RNA LINC01006 exhibits oncogenic properties in cervical cancer by functioning as a molecular sponge for microRNA285p and increasing PAK2 expression. *Int J Mol Med.* (2021) 47:1. doi: 10.3892/ijmm.2021.4879
24. Binder P, Wang S, Radu M, Zin M, Collins L, Khan S, et al. Pak2 as a novel therapeutic target for cardioprotective endoplasmic reticulum stress response. *Circ Res.* (2019) 124:696–711. doi: 10.1161/CIRCRESAHA.118.312829
25. Wang S, Bian W, Zhen J, Zhao L, Chen W. Melatonin-mediated Pak2 activation reduces cardiomyocyte death through suppressing hypoxia reoxygenation injury-induced endoplasmic reticulum stress. *J Cardiovasc Pharmacol.* (2019) 74:20–9. doi: 10.1097/FJC.0000000000000678
26. Xu L, Cai Y, Wang Y, Xu C. Meteorin-like (METRNL) attenuates myocardial ischemia/reperfusion injury-induced cardiomyocytes apoptosis by alleviating endoplasmic reticulum stress via activation of AMPK-PAK2 signaling in H9C2 cells. *Med Sci Monit.* (2020) 26:e924564. doi: 10.12659/MSM.924564
27. Fu HY, Sanada S, Matsuzaki T, Liao Y, Okuda K, Yamato M, et al. Chemical endoplasmic reticulum chaperone alleviates doxorubicin-induced cardiac dysfunction. *Circ Res.* (2016) 118:798–809. doi: 10.1161/CIRCRESAHA.115.307604
28. Yarmohammadi F, Rezaee R, Haye AW, Karimi G. Endoplasmic reticulum stress in doxorubicin-induced cardiotoxicity may be therapeutically targeted by natural and chemical compounds: a review. *Pharmacol Res.* (2021) 164:105383. doi: 10.1016/j.phrs.2020.105383
29. Hebert DN, Molinari M. In and out of the ER: protein folding, quality control, degradation, and related human diseases. *Physiol Rev.* (2007) 87:1377–408. doi: 10.1152/physrev.00050.2006
30. Minamino T, Kitakaze M. ER stress in cardiovascular disease. *J Mol Cell Cardiol.* (2010) 48:1105–10. doi: 10.1016/j.yjmcc.2009.10.026
31. Korennykh AV, Egea PF, Korostelev AA, Finer-Moore J, Zhang C, Shokat KM, et al. The unfolded protein response signals through high-order assembly of Ire1. *Nature.* (2009) 457:687–93. doi: 10.1038/nature07661
32. Yoshida H, Matsui T, Yamamoto A, Okada T, Mori K. XBP1 mRNA is induced by ATF6 and spliced by IRE1 in response to ER stress to produce a highly active transcription factor. *Cell.* (2001) 107:881–91. doi: 10.1016/s0092-8674(01)00611-0
33. Calfon M, Zeng H, Urano F, Till JH, Hubbard SR, Harding HP, et al. IRE1 couples endoplasmic reticulum load to secretory capacity by processing the XBP-1 mRNA. *Nature.* (2002) 415:92–6. doi: 10.1038/415092a
34. Duan Q, Ni L, Wang P, Chen C, Yang L, Ma B, et al. Deregulation of XBP1 expression contributes to myocardial vascular endothelial growth factor-A expression and angiogenesis during cardiac hypertrophy in vivo. *Aging Cell.* (2016) 15:625–33. doi: 10.1111/acel.12460
35. Wang ZV, Deng Y, Gao N, Pedrozo Z, Li DL, Morales CR, et al. Spliced X-box binding protein 1 couples the unfolded protein response to hexosamine biosynthetic pathway. *Cell.* (2014) 156:1179–92. doi: 10.1016/j.cell.2014.01.014
36. Lee Y, Ahn C, Han J, Choi H, Kim J, Yim J, et al. The nuclear RNase III Drosha initiates microRNA processing. *Nature.* (2003) 425:415–9. doi: 10.1038/nature01957
37. Wang JX, Zhang XJ, Li Q, Wang K, Wang Y, Jiao JQ, et al. MicroRNA-103/107 regulate programmed necrosis and myocardial ischemia/reperfusion injury through targeting FADD. *Circ Res.* (2015) 117:352–63. doi: 10.1161/CIRCRESAHA.117.305781
38. Bashir S, Banday M, Qadri O, Bashir A, Hilal N, Nida IF, et al. The molecular mechanism and functional diversity of UPR signaling sensor IRE1. *Life Sci.* (2021) 265:118740. doi: 10.1016/j.lfs.2020.118740
39. Zhang YW, Shi J, Li YJ, Wei L. Cardiomyocyte death in doxorubicin-induced cardiotoxicity. *Arch Immunol Ther Exp (Warsz).* (2009) 57:435–45. doi: 10.1007/s00005-009-0051-8
40. Bjelogrlic SK, Radic J, Jovic V, Radulovic S. Activity of d,l-alpha-tocopherol (vitamin E) against cardiotoxicity induced by doxorubicin and doxorubicin with cyclophosphamide in mice. *Basic Clin Pharmacol Toxicol.* (2005) 97:311–9. doi: 10.1111/j.1742-7843.2005.pto_166.x
41. Lee AH, Chu GC, Iwakoshi NN, Glimcher LH. XBP-1 is required for biogenesis of cellular secretory machinery of exocrine glands. *EMBO J.* (2005) 24:4368–80. doi: 10.1038/sj.emboj.7600903
42. Wang X, Deng Y, Zhang G, Li C, Ding G, May HI, et al. Spliced X-box binding protein 1 stimulates adaptive growth through activation of mTOR. *Circulation.* (2019) 140:566–79. doi: 10.1161/CIRCULATIONAHA.118.038924
43. Angbohang A, Huang L, Li Y, Zhao Y, Gong Y, Fu Y, et al. X-box binding protein 1-mediated COL4A1s secretion regulates communication between vascular smooth muscle and stem/progenitor cells. *J Biol Chem.* (2021) 296:100541. doi: 10.1016/j.jbc.2021.100541
44. Kopp MC, Larburu N, Durairaj V, Adams CJ, Ali MMU. UPR proteins IRE1 and PERK switch BiP from chaperone to ER stress sensor. *Nat Struct Mol Biol.* (2019) 26:1053–62. doi: 10.1038/s41594-019-0324-9
45. Oyadomari S, Mori M. Roles of CHOP/GADD153 in endoplasmic reticulum stress. *Cell Death Differ.* (2004) 11:381–9. doi: 10.1038/sj.cdd.4401373
46. Bagchi AK, Malik A, Akolkar G, Jassal DS, Singal PK. Endoplasmic reticulum stress promotes iNOS/NO and influences inflammation in the development of

doxorubicin-induced cardiomyopathy. *Antioxidants (Basel).* (2021) 10:1897. doi: 10.3390/antiox10121897

47. Montalvo RN, Doerr V, Min K, Szeto HH, Smuder AJ. Doxorubicin-induced oxidative stress differentially regulates proteolytic signaling in cardiac and skeletal muscle. *Am J Physiol Regul Integr Comp Physiol.* (2020) 318:R227–33. doi: 10.1152/ajpregu.00299.2019
48. Wang Z, Wang M, Liu J, Ye J, Jiang H, Xu Y, et al. Inhibition of TRPA1 attenuates doxorubicin-induced acute cardiotoxicity by suppressing oxidative stress, the inflammatory response, and endoplasmic reticulum stress. *Oxid Med Cell Longev.* (2018) 2018:5179468. doi: 10.1155/2018/5179468
49. Liang Y, Ridzon D, Wong L, Chen C. Characterization of microRNA expression profiles in normal human tissues. *BMC Genomics.* (2007) 8:166. doi: 10.1186/1471-2164-8-166
50. Turchinovich A, Weiz L, Langheinz A, Burwinkel B. Characterization of extracellular circulating microRNA. *Nucleic Acids Res.* (2011) 39:7223–33. doi: 10.1093/nar/gkr254

Conflict of Interest: The authors declare that the research was conducted in the absence of any commercial or financial relationships that could be construed as a potential conflict of interest.

frontiers in Cardiovascular Medicine

ORIGINAL RESEARCH
published: 11 March 2022
doi: 10.3389/fcvm.2022.821162

RNA Virus Gene Signatures Detected in Patients With Cardiomyopathy After Chemotherapy; A Pilot Study

Kyle Varkoly[1,2†], Shaoyuan Tan[3†], Roxana Beladi[2,4], David Fonseca[2], Isabela Rivabem Zanetti[2], Simona Kraberger[5], Chintan Shah[6], Jordan R. Yaron[2,7], Liqiang Zhang[2], Michael Juby[2], Ayman Fath[8], Sriram Ambadapadi[2], Melanie House[9], Paul Maranian[2], Carl J. Pepine[9], Arvind Varsani[5,7], Jan Moreb[10], Stacey Schultz-Cherry[3] and Alexandra R. Lucas[2,9,11]*

[1] Department of Internal Medicine, McLaren Macomb Hospital- Michigan State University College of Human Medicine, Mt Clemens, MI, United States, [2] Center for Personalized Diagnostics, The Biodesign Institute, Arizona State University, Tempe, AZ, United States, [3] Department of Infectious Diseases, St. Jude Children's Research Hospital, Memphis, TN, United States, [4] Department of Neurological Surgery, Ascension Providence Hospital- Michigan State University College of Human Medicine, Southfield, MI, United States, [5] The Biodesign Center of Fundamental and Applied Microbiomics, Center for Evolution and Medicine, School of Life Sciences, Arizona State University, Tempe, AZ, United States, [6] Division of Hematology/Oncology, Department of Medicine, University of Florida, Gainesville, FL, United States, [7] School for Engineering of Matter, Transport and Energy, Ira A. Fulton Schools of Engineering, Arizona State University, Tempe, AZ, United States, [8] Department of Internal Medicine, Dignity Health, Creighton University, Phoenix, AZ, United States, [9] Division of Cardiology, Department of Medicine, University of Florida, Gainesville, FL, United States, [10] Hematologic Malignancies, Transplantation and Cellular Therapy Program, Forsyth Medical Center, Derrick L Davis Cancer Center, Winston-Salem, NC, United States, [11] Center for Immunotherapy, Vaccines and Virotherapy, The Biodesign Institute, Arizona State University, Tempe, AZ, United States

OPEN ACCESS

Edited by:
Chun Liu,
Stanford University, United States

Reviewed by:
Abdelrahman Ibrahim Abushouk,
Cleveland Clinic, United States
Shuang Li,
Medical University of South Carolina, United States

***Correspondence:**
Alexandra R. Lucas
arlucas5@asu.edu

[†] These authors have contributed equally to this work and share first authorship

Specialty section:
This article was submitted to Cardio-Oncology, a section of the journal Frontiers in Cardiovascular Medicine

Received: *23 November 2021*
Accepted: *20 January 2022*
Published: *11 March 2022*

Citation:
Varkoly K, Tan S, Beladi R, Fonseca D, Zanetti IR, Kraberger S, Shah C, Yaron JR, Zhang L, Juby M, Fath A, Ambadapadi S, House M, Maranian P, Pepine CJ, Varsani A, Moreb J, Schultz-Cherry S and Lucas AR (2022) RNA Virus Gene Signatures Detected in Patients With Cardiomyopathy After Chemotherapy; A Pilot Study. Front. Cardiovasc. Med. 9:821162. doi: 10.3389/fcvm.2022.821162

Background: Viral infections are pervasive and leading causes of myocarditis. Immune-suppression after chemotherapy increases opportunistic infections, but the incidence of virus-induced myocarditis is unknown.

Objective: An unbiased, blinded screening for RNA viruses was performed after chemotherapy with correlation to cardiac function.

Methods: High-throughput sequencing of RNA isolated from blood samples was analyzed following chemotherapy for hematological malignancies ($N = 28$) and compared with left ventricular ejection fraction (LVEF).

Results: On initial rigorous analysis, low levels of influenza orthomyxovirus and avian paramyxovirus sequences were detectable, but without significant correlation to LVEF ($r = 0.208$). A secondary broad data mining analysis for virus sequences, without filtering human sequences, detected significant correlations for paramyxovirus with LVEF after chemotherapy ($r = 0.592$, $P < 0.0096$). Correlations were similar for LVEF pre- and post- chemotherapy for orthomyxovirus ($R = 0.483$, $P < 0.0421$). Retrovirus detection also correlated with LVEF post ($r = 0.453$, $p < 0.0591$), but not pre-chemotherapy, but is suspect due to potential host contamination. Detectable phage and anellovirus had no correlation. Combined sequence reads (all viruses) demonstrated significant correlation ($r = 0.621$, $P < 0.0078$). Reduced LVEF was not associated with chemotherapy ($P =$ NS).

Conclusions: This is the first report of RNA virus screening in circulating blood and association with changes in cardiac function among patients post chemotherapy,

using unbiased, blinded, high-throughput sequencing. Influenza orthomyxovirus, avian paramyxovirus and retrovirus sequences were detectable in patients with reduced LVEF. Further analysis for RNA virus infections in patients with cardiomyopathy after chemotherapy is warranted.

Keywords: virus, infection, RNA, immune suppression, chemotherapy, LVEF, cardiomyopathy, cancer

INTRODUCTION

The use of chemotherapy in treatment for neoplastic disease is associated with frequent side effects and non-therapeutic toxicities (1–3). Chemotherapy associated cardiac toxicity is well-described for some chemotherapeutic agents, however, for many agents the cause of cardiac toxicity is not defined (1–3). Chemotherapy-associated heart failure has considerable associated mortality and morbidity. Amongst 3,234,256 cancer patients in the United States, 38% have died from cancer and about 1 in 3 have died from cardiovascular disease (CVD). Among the deaths from CVD, 76% were in patients younger than 35 years. The incidence of all chemotherapy-associated cardiotoxicities is reported to be ∼10% in all treated patients, and this is projected to increase as more patients receive chemotherapy (1–3).

Chemotherapy induces leukocyte cytotoxicity and immune suppression with increased risk of opportunistic infections, including bacteria, fungi and viruses (4–6). Viruses are the most common cause for myocarditis in patients without cancer or chemotherapy (7–9) and myocarditis is linked to a wide array of viruses, in some cases with severe heart failure (10–17). While opportunistic bacterial and fungal infections are frequently reported after chemotherapy and immunosuppression, opportunistic viral infections are less often reported. Herpesvirus, hepatitis B/C, influenza and parainfluenza viruses, respiratory syncytial virus (RSV), and retrovirus infections have been reported after chemotherapy (7–9), but the role of viruses in myocarditis in immunosuppressed patients after chemotherapy has not been studied. Opportunistic viral infection after chemotherapy is thus predicted to contribute to heart damage and heart failure.

Among the RNA viruses, Coxsackie virus B3 (CVB3), human parvovirus B19 (B19V), measles, retroviruses and influenza viruses have been implicated in myocarditis among other viruses, and these viruses have been detected after chemotherapy (7–16). B19V and the enterovirus, coxsackievirus, are considered leading causes of viral myocarditis (7–15). DNA viruses are also linked to myocarditis, specifically cytomegalovirus (CMV), Epstein bar virus (EBV), human herpes simplex virus-6 (HHV6) also cause myocarditis (17–19). In the past year, the RNA virus, Severe Acute Respiratory Syndrome Coronavirus 2 (SARS-CoV-2) infection has also been implicated in acute myocarditis (14–16). Viral infections thus present a risk for myocarditis after immune suppression with chemotherapy.

In patients with chronic unexplained heart failure positive for B19V and treated with intravenous immunoglobulins (IVIG), a significant decrease in B19V load has been observed with improved cardiac function, symptoms, and decreased end diastolic volume (8). Other treatments that selectively target specific viruses, such as acyclovir that inactivates herpes simplex virus (HSV) DNA polymerase for herpes myocarditis or antiretroviral therapy for human immunodeficiency virus (HIV) infections have proven beneficial (8–19). Development of new vaccines to target viral infections are highly effective as for SARS-CoV-2 and COVID-19, but viruses with the potential to cause chemotherapy induced myocarditis must be identified in order to develop effective vaccines and treatments.

Accordingly, we postulated that immune suppression caused by chemotherapy, or by the cancer itself, will increase susceptibility to viral infections, and therefore myocarditis. This study presents an unbiased, blinded screen for RNA viruses in blood samples obtained from patients after chemotherapy for hematological malignancies. In this pilot study, reductions in measured left ventricular ejection fraction (LVEF) on 2D echocardiogram were correlated with measured levels of detected RNA virus gene signatures. To the best of our knowledge, this is the first screen for detectable RNA virus sequences in blood samples from cancer patients with evidence for myocarditis and reduced LVEF after chemotherapy. Information on opportunistic viral infections seen after immune suppression and chemotherapy will foster a defined preventative approach, such as development of vaccines or treatment with specific anti-viral agents designed to reduce the risk of cardiac damage.

MATERIALS AND METHODS

Patient Population

Twenty-eight patients were enrolled in the Cardio-Oncology (AL) and the Hematologic Malignancies / Stem Cell Transplantation clinics (SC, JM) at the University of Florida after written informed consent. All patients and samples were assigned a randomized number after informed consent. The study was approved by the Institutional Review Boards (IRB) at all institutions involved in the study.

Patient ages ranged from 18 to 85 years; all had a diagnosis of cancer and a range of chemotherapeutic agents including dexamethasone, lanolidomide, rituximab, bortezomib, and cyclophosphamide, as well as combinations as noted (**Table 1**; **Figure 1**). The majority of patients had a history of hematological malignancy (25/26 hematological malignancy and 1/26 breast cancer) (**Table 1**). Six patients had a history of prior diagnosed ischemic heart disease, one with documented coronary artery disease and stent implant. Of the enrolled patients, 26 had complete viral sequencing (ST, SS-C) (**Table 1**). Eighteen patients had LVEF measured post chemotherapy, 22 patients had

TABLE 1 | Study patient demographics.

Patient ID	Diagnosis	Age	Chemotherapy	Repeat chemotherapy	Stage	Diagnosis of prior heart disease	Ejection fraction (EF) prior to chemotherapy	Ejection fraction (EF) post chemotherapy
PJ0266_R2	Multiple myeloma (MM)	70–85	Velcade and dexamethasone (2010–2012) –> 12/7/2012 (ASCT)–>revlimid maintainance (2013 till 1/2015)	None	IIIA	No	60	30
PJ0267_R2	Follicular lymphoma	80–85	Bendamustine and rituximab(1/19/2016–4/12/2016) f/b rituximab 8/2016–1/2018)	Rituximab	IIA	IHD	60	40
PJ0268_R2	Multiple myeloma (MM)	60–65	Revlimid, velcade, dexa (1st)–> CVD	CVD,	IIIB	No	60	50
PJ0269_R2	Chronic lymphocytic leukemia (CLL)	75–80	Ibrutinib	NA	NA	IHD	60	NA
PJ0270_R2	Multiple myeloma (MM)	70–75	Revlimid, velcade	NA	IIIA	IHD	60	NA
PJ0271_R2	Multiple myeloma (MM)	70–75	Velcade, dexamethasone–> pomalidomide, dex	NA	IA	No	60	NA
PJ0272_R2	Mantle cell lymphoma	50–55	Rituximab, fludarabine, cyclophosphamide-> busulfan, cyclophosphamide, vincristine (conditioning)_-> rituximab maintenance	NA	IVA	No	60	60
PJ0273_R2	Multiple myeloma (MM)	50–55	Velcade, revlimid, dexa (2014)–> revlimid (2015, 2016)–> melphalan and transplant	Revlimid, transplant	NA	No	NA	60
PJ0274_R2	Multiple myeloma (MM)-kappa LC	45–50	RVD	RVD, ASCT, velcade	IIIA (II)	No	60	65
PJ0275_R2	Multiple myeloma (MM)-IgG kappa	70–75	CTX/velcade	Dexa, CTX, VCR, Mel,	IIA (I)	IHD	30	40
PJ0276_R2	Multiple myeloma (MM)-IgG lambda	70–72	RT, CVD	Dara/Velcade/Dexa	IIIA	No	60	NA
PJ0277_R2	Multiple myeloma (MM)-IgG kappa	50–55	RVD-CVD, revlimid maitenance, relapse #1, Kyprolis, pomalyst, VBCP	VBCP, Dara	IA (I)	No	55	55

(Continued)

TABLE 1 | Continued

Patient ID	Diagnosis	Age	Chemotherapy	Repeat chemotherapy	Stage	Diagnosis of prior heart disease	Ejection fraction (EF) prior to chemotherapy	Ejection fraction (EF) post chemotherapy
PJ0278_R2	Multiple myeloma (MM)-KLC	50–55	CVD	Revlimid, velcade, melflufen, Dexa	IIIB (III)	No	35	45
PJ0279_R2	Multiple myeloma (MM)-PCL-LLC	65–70	CVDX 4	Revlimid, prednisone	NA	No	60	40
PJ0280_R2	Multiple myeloma (MM)-KLC	65–70	CVD X 4	Revlimid	IIIA (I)	No	60	ND
PJ0281_R2	Multiple myeloma (MM)-KLC	65–70	VD X 6	None	IB (II)	No	NA	70
PJ0282_R2	Multiple myeloma (MM)-IgG kappa	75–80	VTD, RVD	CVD, PD, PD+Elo, Dara, Dara+Velcade	IIIA (?)	No	60	60
PJ0283_R2	Multiple myeloma (MM)-IgA Lambda	65–70	CVD	Revlimid maintenance	IIIA (II)	No	60	ND
PJ0284_R2	Multiple myeloma (MM)-IgG lambda, Acute lymphocytic leukemia (ALL)	60–65	VD	Revlimid maintenance	IIIA (II)	No	60	55
PJ0285_R2	Multiple myeloma (MM)-IgG kappa	70–75	CVD	Revlimid, RVD, Kyprolis, pomalidomide	IIIA (?)	No	55	20
PJ0286_R2	Multiple myeloma (MM)-IgG lambda	70–75	Thal/Dexa	Revlimid, CTX, RCD, high dose kyprolis	IIIA (II)	No	60	55
PJ0287_R2	Multiple myeloma (MM)-IgG kappa	70–75	VAD	Revlimid maintenance, velcade/pomalidomide/dexa Dara, CTX, CVD,PD, VBCP,Kyprolis, VTD-PACE		No	55	25%
PJ0288_R2	Cirrhosis, DCIS, CAD	50–55	TAM	NA		IHD	65	60
PJ0289_R2	Multiple myeloma	70–75	Velcade and dexa (2010–2012) –> 12/7/2012 (ASCT)–>revlimid maintainance (2013 till 1/2015)	NA		No	NA	NA
PJ0290_R2	Follicular lymphoma	80–85	Bendamustine and rituximab(1/19/2016 - 4/12/2016) f/b rituximab 8/2016- 1/2018)	Rituximab	IIA	IHD	60%	40–45%
PJ0291_R2	Multiple myeloma	60–65	Revlimid, velcade, dexa (1st)–> CVD	NA		NA	NA	NA

dexa, dexamethasone; RVD, revlimid, velcade, dexa; ASCT, autologous stem cell transplant; CTX, cyclophosphamide; DCIS, ductal carcinoma in situ; VCR, vincristine; CVD, velcade, cyclophosphamide, dexa; Mel, melphalan; Dara, daratumumab; VD, velcade and dexamethasone; RT, radiation therapy; VBCP, vincristine, BCNU, cyclophosphamide, and prednisone; Thal/Dex, thalidomide and dexamethasone; PD, pomalidomide and dexamethasone; PD+ Elo, PD and Elotuzumab; VTD, velcade, thalidomide and dexa; VAD, vincristine, Adriamycin and dexamethasone; RCD, revlimid, cyclophosphamide and dexa; VTD-PACE, Velcade, thalidomide, dexamethasone, platinum, Adriamycin, cyclophosphamide, and etoposide; TAM, tamoxifen.

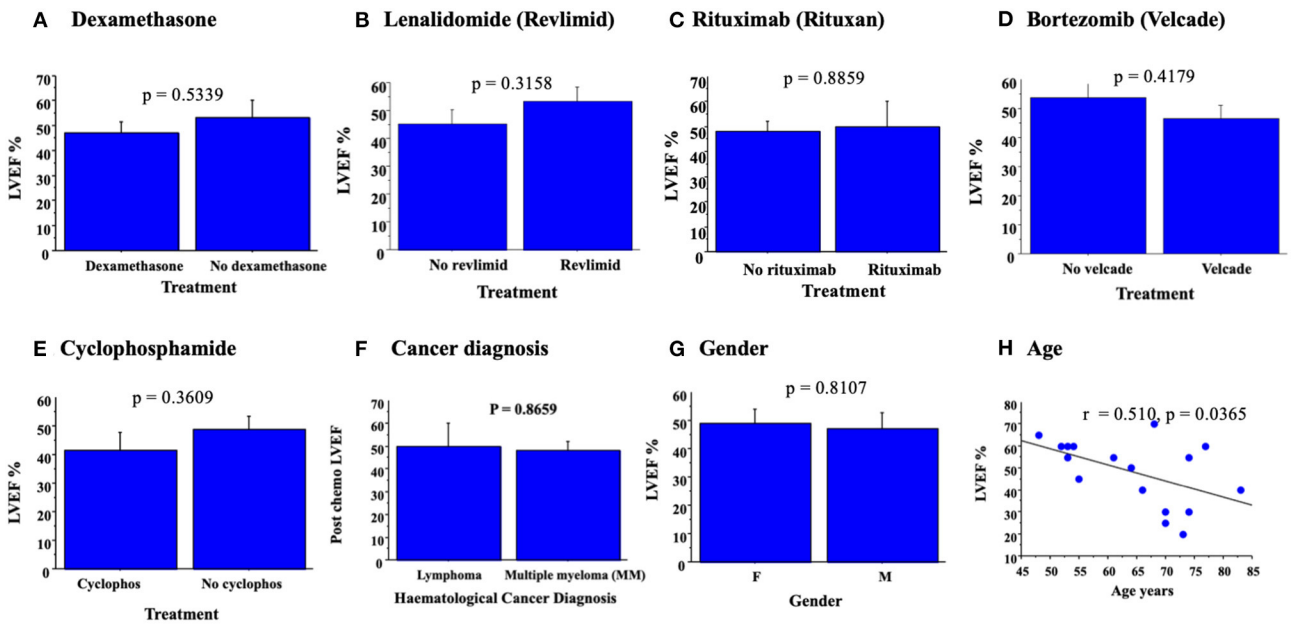

FIGURE 1 | Bar graphs demonstrating mean LVEF ± SE with chemotherapy. No significant change in LVEF, as assessed by ANOVA, was detected for treatments with dexamethasone **(A)**, revlimid **(B)**, lenolidomide **(C)**, bortezomib **(D)**, cyclophosphamide **(E)**, cancer diagnosed **(F)**, or gender **(G)**. Simple regression analysis demonstrates a significant correlation between LVEF post chemotherapy and increased age **(H)**.

LVEF measured before chemotherapy, and 16 had both. One patient had confirmation of LVEF by cardiac catheterization. Chemotherapy given was recorded for each patient. Echocardiograms were ordered by the attending physician based upon perceived clinical risk, but were not mandated. Cardiac dysfunction was defined as a decrease in ejection fraction (EF) <45% as demonstrated on echocardiography. LVEF data was available but more comprehensive data such as fractional shortening was not provided.

Virome Sequencing of Blood Samples

Blood samples were obtained 2–4 weeks after chemotherapy, once informed consent was obtained. Venous blood was collected in clinic at 2–4 weeks after the last chemotherapy in tubes containing 3 mL of Ethylenediaminetetraacetic acid (EDTA). RNALater (Life Technologies, Bleiswijk, The Netherlands) was added at a ratio of 2:1 RNALater to whole blood and samples stored at −80°C until analysis. Blood samples were anonymized blood samples and were sent to St Jude's Hospital (SCC, ST); where investigators were masked to cancer type, chemotherapy, and LVEF findings.

Samples were fragmented prior to RNA extraction as previously described (20). RNA was isolated using the QIAamp cador Pathogen Mini kit (Qiagen, Hilden, Germany) according to manufacturer's instructions. First strand synthesis was completed using the random-primer technique described by Wang et al. (21). Briefly, Super Script III (Invitrogen, Carlsbad, CA, USA) first strand synthesis was carried out using primer A (5'-GTTTCCCAGTCACGATANNNNNNNNN), followed by Sequenase (Affymetrix, Santa Clara, CA, USA) for second strand synthesis. Finally, PCR amplification utilized Primer B (5'-GTTTCCCAGTCACGATA) for 40 cycles. Samples were electrophoresed in an agarose gel to confirm product.

Samples were run on a 1% agarose gel and imaged to confirm the presence of DNA (between 500 bp and 1 kb). To prepare for sequencing, samples were purified using AMPure XP beads (Beckman Coulter, Brea, CA, USA) followed by analysis on a Qubit fluorometer (Thermo Fisher Scientific, Waltham, MA, USA). A Nextera DNA library preparation kit (Illumina, San Diego, CA, USA) was used for sample genome sequencing using the Illumina MiSeq Amplicon application for virome reference genomes. Quality control of input nucleic acid and final libraries were checked using Agilent TapeStation 4200.

Bioinformatics Analysis

In an initial analysis, Illumina sequencing data sets were examined for viral pathogen detection. The quality of raw reads was assessed using FastQC (version 0.11.9) (https://www.bioinformatics.babraham.ac.uk/projects/fastqc/). Trimmomatic was used to trim the adapters from the paired-end reads (22). Taxonomic classification was performed for blood samples using Kraken2 (version 2.0.7b). Illumina sequencing data sets were initially analyzed for detection of RNA viruses (23–25). The RNA viral reads that were viral-like were also checked using BLASTn against a viral RefSeq database. Sequencing data is available, Bioproject accession number NCBI, PRJNA794842, temporary submission ID SUB10902989, release date: 2022-01-06.

For the broader viral RNA sequence analysis (SS-C, ST), a custom viral database, containing complete viral genomes cross referenced to RefSeq (ftp://ftp.ncbi.nlm.nih.gov/refseq/release/)

with taxonomic classifications, was built using Kraken2 (26). Following that, Kraken reports were analyzed, visualized and summarized using Pavian [(27), **Supplementary Figure 1**]. The database used for taxonomic classification included all viral genomes in RefSeq. Contigs sequences were used to identify the viral genetic sequences. To verify that human endogenous retrovirus K (HERV K) is detected correctly, we extracted the raw reads that classify as HERV K. The extracted raw retrovirus K reads were then mapped to human endogenous retrovirus reference genome (NC_022518.1) and human reference genome (GRCh38) separately. The quality of mapping to both reference genomes was assessed.

Statistical Analysis—Correlation of Viral Genetic Sequences With Cardiac Function and Chemotherapy

Levels of viral gene sequences detected in blood samples were correlated with heart function (LVEF) before and after chemotherapy using simple regression analysis with confirmation by our statisticians (PM,AV,SK at ASU; ST, SS-C at St Judes). All statistics were performed using Statview, version 5.01 (SAS, Inc., Cary, NC) or Graphpad Prism (GraphPad). Multiple-group comparisons were performed using analysis of variance (ANOVA) with Fishers protected least significant difference (PLSD) and unpaired two-tailed Student's *t*-test for subgroup analysis. A $P < 0.05$ is considered significant.

RESULTS

Analysis of Associations Between Cardiac Function and Chemotherapy

No significant correlation was detected for the specific chemotherapy given to each patient and LVEF post chemotherapy, measured as LVEF (**Table 1**); $p = 0.5339$ for dexamethasone (**Figure 1A**), $p = 0.3158$; lenolidamide (**Figure 1B**), $p = 0.3158$; rituximab (**Figure 1C**), $p = 0.8859$; bortezomib (**Figure 1D**), $p = 0.4179$; and cyclophosphamide (**Figure 1E**), $p = 0.3609$. When a chemotherapeutic agent was used in only one of the patients, this was considered an inadequate number to allow analysis for correlation with LVEF. Analysis of changes in LVEF with specific cancer diagnosis demonstrated no significant correlation between diagnosed cancer type and LVEF (**Figure 1F**, $p = 0.8659$). No significant association was made between patient sex and measured LVEF ($p = 0.8107$, **Figure 1G**). Simple regression analysis did demonstrate a significant correlation between an increased age of patients and reduced LVEF, both pre and post chemotherapy (for post chemotherapy—$r = 0.510$, $p < 0.0365$) (**Figure 1H**). The minority of patients were receiving cardiovascular medications at enrollment, 6/ 26 patients had diagnosis of IHD listed (**Table 1**; ANOVA $P = 0.056$) and diagnosed IHD and CVD medications were not associated with changes in LVEF ($p = 0.8659$).

High Throughput Sequencing of RNA Virus in Blood Samples From Patients

Low levels of RNA virus sequences were detected in blood samples isolated from patients post chemotherapy. Detection of virus sequences using a strict, blinded analysis with either Blastn or Kraken 2 programs, and removing all potential contaminating human sequences, detected low levels of paramyxovirus and orthomyxovirus, as representative of potential opportunistic infections. The avian Avulavirus, a paramyxovirus, and Influenza A, an orthomyxovirus, were consistently identified on sequence analysis using both methods for RNA Seq analysis (Blastn and Kraken 2), indicating low levels of these RNA viruses after chemotherapy. The paramyxovirus avian Avulavirus and the orthomyxovirus Influenza A were the most frequently identified sequences.

Effects of Chemotherapy on Strict RNA Virus Sequence Read Detection

Potential correlations were assessed for detected RNA virus sequences and treatments with individual chemotherapeutic agents. Levels of virus sequences detected were increased with bortezomib and dexamethasone (**Figure 2**), however, there was only a trend toward increased detection of virus sequences in blood samples; $p = 0.0623$ for orthomyxovirus detection (**Figure 2A**), $p = 0.1726$ for paramyxovirus detection (**Figure 2B**) and $p = 0.0767$ for retrovirus sequences (**Figure 2C**) after bortezomib and $p = 0.1061$ for paramyxovirus (**Figure 2D**) after dexamethasone, none reaching significance. Analysis of a combined count of all detected RNA virus sequences in patients with bortezomib chemotherapy again detected a borderline increase ($p = 0.053$) (**Figure 2E**). Lenolidomide and cyclophosphamide treatment had no clear trend nor significant change in RNA virus gene sequence detection. In contrast, rituximab treatment was associated with a non-significant trend toward decreased virus sequence detection (not shown). Detection of RNA virus sequences in blood samples from cancer patients was not linked to gender ($p = 0.1028$, **Figure 2F**) nor age ($p = 0.245$, **Figure 2G**).

Initial Strict Analysis of RNA Virus Sequence Detection and Cardiac Function After Chemotherapy

On an initial rigorous, or strict, analysis, removing all potential contaminating human, bacterial or phage sequences, RNA virus sequences in the paramyxovirus (28) and orthomyxovirus (29) families were detected. Virus sequence detection was read blinded by four investigators (ST, SS-C, AV, AL). No significant correlations were detected for measured LVEF post chemotherapy; $r = 0.177$ for paramyxovirus ($p = 0.4961$, **Figure 3A**), and $r = 0.208$ for orthomyxovirus ($p = 0.4229$, **Figure 3B**). Screening for LVEF and a combined analysis of paramyxovirus and orthomyxovirus virus sequences detected a minimal, but again non-significant, increase in the correlation with reductions in LVEF reported on 2D echo post chemotherapy ($r = 0.233$, $p = 0.3732$, **Figure 3C**). This would suggest that RNA virus gene signatures are detectable at low levels in blood samples

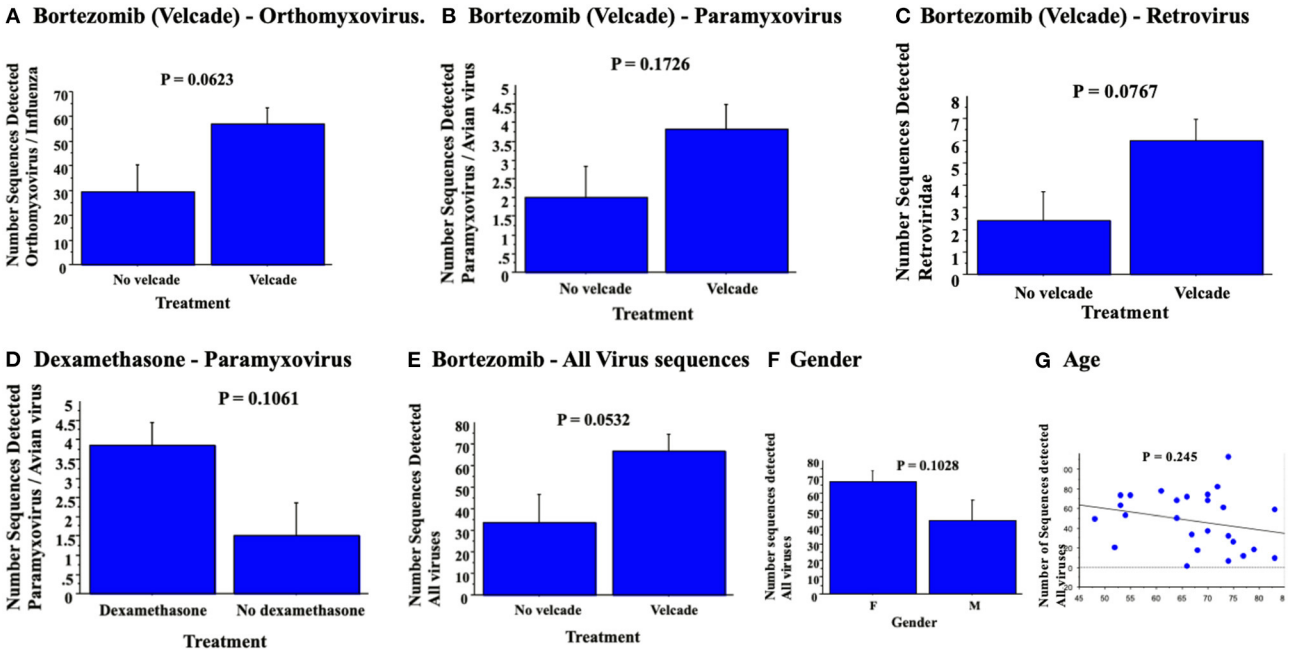

FIGURE 2 | RNA virus sequence reads detected in blood samples demonstrated no significant association for orthomyxovirus **(A)**, paramyxovius **(B)** nor retrovirus **(C)** with bortezomib or with dexamethasone for detected paramyxovirus reads **(D)**. Bortezomib chemotherapy was associated with a trend toward detection of all paramyxo-, orthomyxo- and retro-virus sequences detected **(E)**. Analysis for virus detection with gender (**F**, ANOVA) and age (**G**, simple regression analysis) detected no significant changes.

from patients with reduced LVEF post chemotherapy, but do not have a significant correlation for reduced LVEF for individual detectable viruses in this small patient cohort.

Secondary Custom Database Analysis of RNA Virus Sequence Detection and Cardiac Function After Chemotherapy

A secondary, broad, customized Kraken2 database was next designed to detect a wider spectrum of RNA virus sequences as a metagenome analysis platform. This secondary analysis was performed without rigorous filtering of potential human genome sequences, and accepting both unidirectional as well as bidirectional reads. With this broad analysis an increased correlation was detectable for RNA virus sequences (Illustrated via Pavian software, **Supplementary Figure 1**). Bidirectional reads were used for analysis of correlations between detected virus gene signatures with measured LVEF post chemotherapy. Correlations of virus sequence detection with LVEF recorded prior to chemotherapy was used as a control to assess changes in LVEF prior to treatment with chemotherapy.

Paramyxovirus sequence detection and retrovirus sequence detection, using bidirectional reads from this more permissive analysis, had increased correlation when comparing LVEF post chemotherapy and LVEF measured pre chemotherapy; For paramyxovirus the correlation increased from r = 0.484 pre chemotherapy LVEF ($P < 0.0452$) to r = 0.592 for LVEF measured post chemotherapy ($P < 0.0096$, **Figure 4A**), with a clear increase in significance. Albeit both achieve significance.

Conversely, orthomyxovirus sequence detection, specifically for influenza A, had similar correlations when comparing paramyxovirus sequence reads to LVEF measured prior to or after chemotherapy (r = 0.513 pre, $P < 0.0248$ and r = 0.483 post, $P < 0.0421$). Although both analyses for influenza A reached significance prior to or after chemotherapy, the fact that there was a significant and greater correlation prior to chemotherapy would suggest no specific association between orthomyxovirus detection and developing cardiac dysfunction after chemotherapy. Overall, orthomyxovirus and paramyxovirus sequences were again detected in this broad, less strict analysis, but with increased numbers of detectable reads using this custom platform.

Other RNA virus sequence reads were also detected using this broad analysis (**Figure 5**). One of the most prominent was the retrovirus HERV K (30). For retrovirus sequences, the correlation increased from r = 0.034 for LVEF measured pre chemotherapy ($P = 0.8904$, non-significant) to r = 0.453 post chemotherapy with a borderline trend toward significance ($P = 0.0591$, **Figure 5C**). Retrovirus sequences detected were predominantly human endogenous retrovirus K (HERV K), a retrovirus commonly detected in the human genome. Retrovirus sequences may represent activation from the native human cell genome, during the stress of cancer, chemotherapy or extrinsic infections.

Among other sequences detected there were Molivirus, Pandoravirus and Pandoravirus dulcis, Lambdina fiscellaria

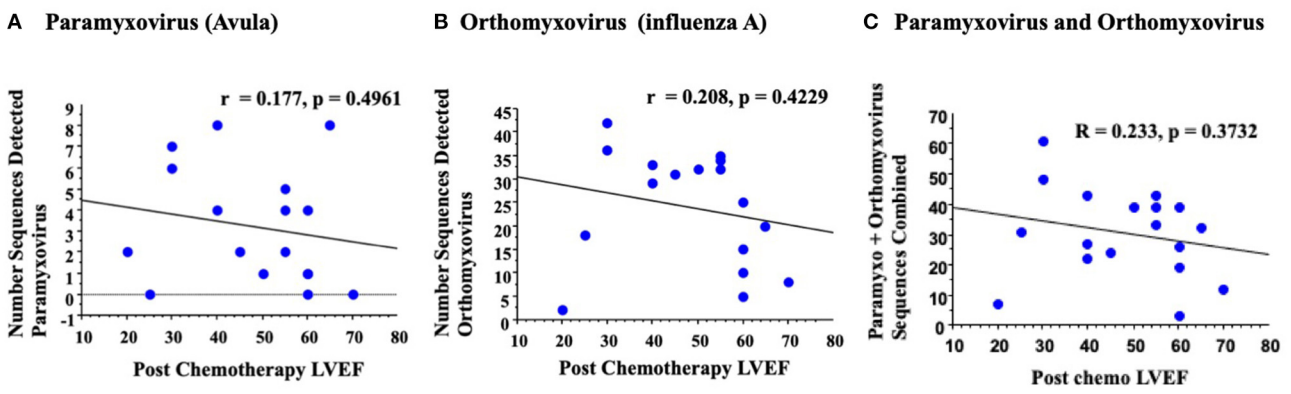

FIGURE 3 | An initial rigorous analysis for detected virus sequences in blood samples with reduced LVEF detected no significant correlation. Analysis of paramyxovirus **(A)** orthomyxovirus **(B)** or total combined paramyxovirus and orthomyxovirus **(C)** sequences detected no significant correlation on simple regression analysis.

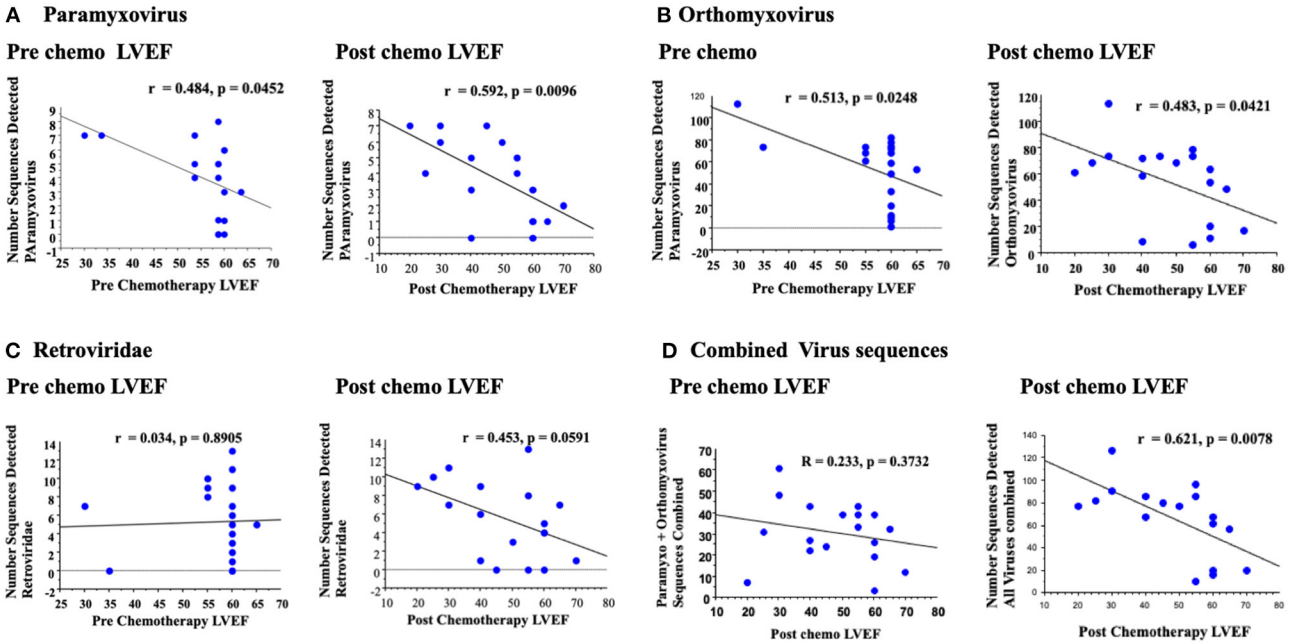

FIGURE 4 | A secondary broad analysis demonstrated a correlation between paramyxovirus bidirectional sequence reads with LVEF pre and post chemotherapy, but with greater correlation and significance post chemotherapy LVEF **(A)**. Similar correlations were detected for orthomyxovirus both pre and post chemotherapy **(B)**. Retrovirus reads had no detectable correlation with LVEF pre chemotherapy, but a trend to increased correlation post chemotherapy **(C)**. Analysis of all RNA virus reads for paramyxovirus, orthomyxovirus and retrovirus reads detected a significant correlation for changes in LVEF post chemotherapy **(D)**.

nucleopolyhedrovirus, Leukania separata nucleopolyhedrovirus, and several phage including Proteus virus mirabilis Isfaham, Aeromonas virus 25AhydR2PP and Aes 12, Caulobacter virus CcrBL10, Vibrio phage Eugene 12A 10, Streptomyces virus Izzy, and Pseudomonas phage OBP and PAJU2. None of these additional virus sequence reads demonstrated significant correlations for changes in LVEF post or even pre chemotherapy for hematological cancers (**Figure 5** illustrates some of these analyses). For these virus sequences compared to LVEF post chemotherapy, the following r values were obtained: Molivirus r = 0.251, $P = 0.3306$; Pandoravirus and Pandoravirus dulcis r = 0.015, $P = 0.9538$; Lambdina fiscellaria nucleopolyhedrovirus r = 0.435, $P = 0.3289$; Leukania separata nucleopolyhedrovirus r = 0.114–0.201, $P = 0.4372$–0.6725; and several phage including Lactococcus phage BK5-T r = 0.228, $P = 0.3625$; Streptomyces virus Izzy r = 0.221, $P = 0.4104$; Proteus mirabilis virus Isfaham r = 0.433, $P = 0.0826$; Aeromonas virus 25AhydR2PP r = 0.447, $P = 0.1088$; Aes 12 r= 0.124, $P = -0.6483$; Caulobacter virus CcrBL10 r = 0225, $P = 0.3849$; Vibrio phage Eugene 12A 10 r = 0.376, $P = 0.5429$, Pseudomonas phage OBP and PAJU2, r = 0.240–0.356, $P = 0.1927$–0.3536. A circular DNA Anellovirus, signature was detected in one patient with multiple myeloma and demonstrated no correlation.

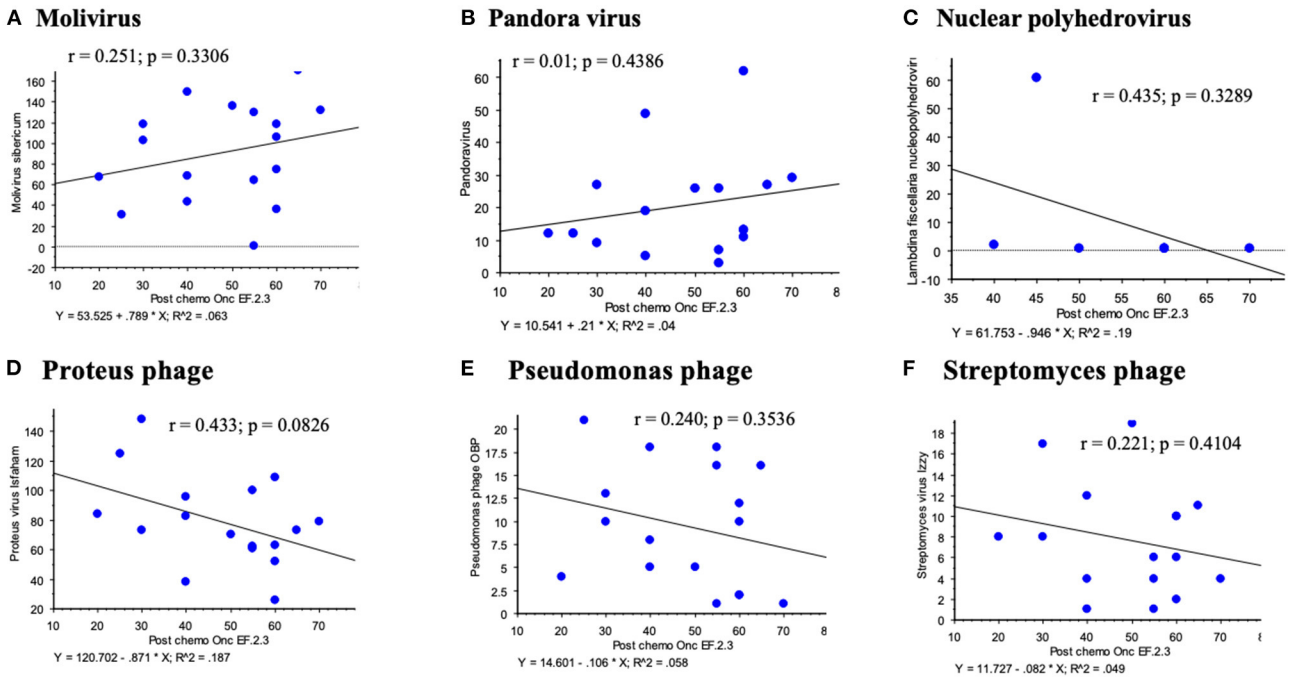

FIGURE 5 | Other virus sequences detected on the broader platform for RNA viruses demonstrated no significant correlations between viral sequence reads and LVEF post chemotherapy; Molivirus **(A)**, Pandora virus **(B)**, Panderina fiscellaria nucleopolyhedrovirus **(C)**, Proteus **(D)**, Pseudomonas phage **(E)** and Streptomyces **(F)** phage.

A potential correlation between changes in LVEF pre and post chemotherapy with an analysis of a combined RNA virus sequence reads for virus sequence detection where trends toward increased RNA viral sequence correlations with reduced LVEF were demonstrated was then examined. A combined read for detcted paramyxo- orthomyxo- and retro-virus sequnces was assessed using this broad screen (**Figure 4D**). On this final analysis of combined RNA virus sequences for each sample, the correlation increased from r = 0.233 ($p = 0.3732$) for pre chemo LVEF to r = 0.621 ($P < 0.0078$) for post chemo LVEF, a markedly significant increase. Thus, increased detection of three detectable RNA virus sequence reads, paramyxo, orthomyxo- and retro-viruses after chemotherapy did demonstrate an apparent significant association with measured reductions in LVEF after chemotherapy (**Figure 4D**).

DISCUSSION

Dilated cardiomyopathy in cancer patients is a critically important complication after chemotherapy produced by cardiotoxicity with associated increased mortality (1–3). Immunosuppression with secondary opportunistic viral infection increases the risk for virus-induced myocarditis and heart damage after chemotherapy (4–9). Individual chemotherapeutic regimes have proven cardiotoxicity, but there are multiple molecular mechanisms for cardiac damage that differ for individual chemotherapeutic agents and some have no known etiology for cardiotoxicity (31–35). Viral infections are a leading cause for myocarditis in patients without cancer or chemotherapy (7–16, 36) and immunosuppression after chemotherapy increases the risk for opportunistic viral infections. We have performed a pilot study to screen for potential correlations between RNA virus sequences detected in blood samples and reduced LVEF post chemotherapy in patients with hematological tumors.

Chemotherapy is used for both hematological cancers and solid tumors with proven cytotoxicity, with a variety of non-therapeutic and potentially adverse side effects. Myocardial toxicity leads to left ventricular dysfunction (LVD), heart failure (HF), endothelial dysfunction, thrombogenesis, ischemia, vasospasm, pericardial disease, hypertension, and rhythm disturbances (1–3, 31–35). Incidence and cardiotoxic effects vary with individual chemotherapy agents. The incidence of LVD is 3–26% for Doxyrubicin (anthracycline), 7–28% for Cyclophosphamide, 17% for Ifosfamide, 1–3% for Bevacuzimab 2–28% for Trastuzumab therapy and 0.5–1.7% for Imatinib mesylate therapy (1, 2). Causes for cardiac toxicity varies from direct cardiomyocyte toxicity to vascular injury. Several mechanisms have been proposed for each class of agent, but individual chemotherapeutic reagents have differing molecular targets and reported causes for heart damage; there is, as might be expected, no unifying mechanism. The mechanism underlying anthracycline-induced cardiotoxicity has been reported as interference with topoisomerase II beta and secondary free-radical formation; apoptosis; transcriptional changes in intracellular adenosine triphosphate (ATP); reduced sarcoplasmic reticulum calcium-ATPase expression; prolonged depression in cardiac glutathione peroxidase

activity; and respiratory defects associated with mitochondrial deoxyribonucleic acid damage (12, 31–35). Cyclophosphamide-induced cardiotoxicity is postulated to be caused by endothelial injury through toxic metabolites that damage cardiomyocytes and secondary intracapillary microemboli and coronary vasospasm (1, 2). The mechanism of HF associated with bevacizumab is believed to be associated with uncontrolled HTN and inhibition of vascular endothelial growth factor (VEGF)/VEGF receptor signaling (1–3). Damage to the myocardium after treatment with chemotherapy thus has differing etiologies dependent upon the underlying cancer, treatment used, and the cause is incompletely defined for many newer chemotherapies. The potential for viral infection and secondary myocarditis after immunosuppression with chemotherapy for cancer has not been systematically examined as a potential cause for cardiomyopathy after chemotherapy.

In this study we measured RNA virus sequences in blood samples obtained from patients after chemotherapy using RNA Seq screening, RNA isolates were assessed both by an initial rigorous analysis that removed any potential human sequence contamination as well as with a subsequent broader, customized virome analysis. This was an unbiased screen for the detection of RNA virus sequences in venous blood samples in cancer patients receiving chemotherapy. On the initial more rigorous analysis, both paramyxovirus and orthomyxovirus sequences were detectable, but had no clear correlation with changes in LVEF (**Figure 3**). The orthomyxovius Influenza A has a well-known association with viral myocarditis, but demonstrated similar correlations with LVEF measured prior to, or after, chemotherapy (6–9). Both paramyxovirus and orthomyxovirus families have been reported as causes for myocarditis in patients without known prior cancer or chemotherapy. The detectable sequences for orthomyxovirus matched to influenza A (29) and those for paramyxovirus with avulavirus (28). On a secondary broad analysis using a customized screen, we were able to detect larger numbers of RNA virus sequences for orthomyxovirus influenza A and paramyxovirus Avulavirus, as well as a larger array of RNA viruses including retroviruses, insect viruses and phage. In this second analysis we identified correlations between the detected paramyxovirus and retrovirus with changes in LVEF.

The increase in the paramyxovirus Avulavirus, sequences does demonstrate an increase in sequence detection and reduced LVEF after chemotherapy, with a greater correlation for post chemotherapy LVEF than for pre-chemotherapy LVEF. Orthomyxovirus influenza A was also detected, but with similar detected sequence counts and correlations for LVEF measured pre- or post-chemotherapy (**Figure 4B**); this correlation was stronger for pre-chemotherapy. Influenza is a common upper respiratory infection and the detection of this orthomyxovirus may be attributed to the prevalence of influenza A virus in the general population, with a generalized increase in an immunocompromised cohort. This suggests a general association of influenza A, the orthomyxovirus, with a reduction in LVEF that is unrelated to chemotherapy. The paramyxovirus Avulavirus sequence detection was also detectable, but the correlation was greater for LVEF measured after chemotherapy, albeit a small increase (**Figure 4A**). On the secondary, broader analysis, the greatest increase in correlation was seen with the HERV K retrovirus sequence on the post chemotherapy sample. Simple regression analysis for pre-chemotherapy LVEF analysis exhibited a flat, unresponsive regression with no evidence for correlation with LVEF pre chemotherapy, but with a clear inverted, negative correlation for detected HERV K sequences with post-chemotherapy LVEF (**Figure 4C**).

Retroviruses are reported to represent up to 8% of the human genome (37–41). Retrovirus sequence detection may represent activation of latent human retroviruses rather than opportunistic infection, as has been reported. Retrovirus K reads may represent reactivation from the human genome induced by the stress from chemotherapy and/ or cancer. Blast confirmation indicated that all reads belonged to the human genome suggesting reactivation rather than *de novo* infections. HERV-K is the most transcriptionally active retrovirus in man, representing up to 8% of the human genome, and thus may also represent a contamination. HERV-K has been associated with neurodegenerative disorders, cancer, and an overall higher tumor burden (38–41). HERV K genes, like nuclear protein-1, has important roles in the generation of reactive oxygen species and other tumorigenic characteristics that may act in synergy with chemotherapeutics to decrease LVEF. HERV-K has also been reported to be upregulated after chemotherapy and could suggest that the stress of chemotherapy or the immunosuppression may have induced increased HERV-K expression.

Phage infect bacteria and alter bacterial responses after chemotherapy. We detected some phage sequences and these might be considered contaminants, as are the pandoraviruses. However, recent reports have demonstrated high levels of phage in many organs outside the gut (42, 43). Increased levels of phage are reported in the circulating blood in patients with increased gut permeability in leukemic patients where "leaky gut" is suspected to allow phages to translocate from the gut to the plasma (43). In this study, no correlation was uncovered between the detected phage sequences and insect virus reads with LVEF post chemotherapy (**Figure 5**). No correlation was found between anellovirus and reduced LVEF. These identified virus reads likely represent incidental detection of DNA viruses during analysis of RNA virus cDNA.

Bortezomib was associated with a borderline increase in detection of viral sequences ($P = 0.0532$). Other than age, none of the other parameters, chemotherapeutic agent, gender, cancer diagnosis and none of the other chemotherapeutic drugs demonstrated clear correlations with reduced LVEF pre- or post-chemotherapy.

This study was realized as an unbiased survey, a pilot study, to detect RNA virus sequences in blood samples in post chemotherapy patients with hematological cancers. In this study we were able to detect paramyxovirus, orthomyxovirus, and retroviruses in venous blood samples taken post chemotherapy for hematological malignancy. With a broad analysis, correlations were detected with LVEF measured post chemotherapy. This is, however, limited to a correlation without a definitive cause-and effect. A comprehensive analysis of correlations between detected virus sequences and reduced LVEF with scheduled blood samples, LVEF analysis, and heart damage markers prior to and after chemotherapy should be considered and has the potential to demonstrate chemotherapy induced

immune suppression and the risk of heart damage due to viral infection and/or reactivation.

LIMITATIONS OF STUDY

This study is limited by the small numbers of patients studied, variability in temporality of blood sample collection, as well as an incomplete data set for echocardiogram measured LVEF and longer term follow up for cardiac function. A control group of patients not receiving chemotherapy is not available, however the pre-treatment LVEF analysis by 2D echo provide an internal control. Echocardiograms were ordered at the discretion of the attending clinic physician and not all patients had LVEF measured.

CONCLUSIONS

In summary, low levels of RNA virus sequences are detectable in venous blood samples taken from patients with hematological cancers after chemotherapy. Analysis of these detected RNA virus sequences suggest that there is increased detection of RNA virus sequences in blood samples from patients after chemotherapy. Chemotherapeutic immune suppression increases the risk for chemotherapy induced myocarditis and cardiomyopathy with reduced LVEF. A comprehensive, structured study of cancer patients for sequential detection for RNA virus sequences after chemotherapy and correlation with LVEF analysis at predetermined follow up times, as well as an analysis for other markers for cardiac damage and immunosuppression is needed. A structured sequential analysis, as well as a comparison to patients without chemotherapy, will allow identification of opportunistic viral infections and identify potential approaches to prevent or treat viruses identified as risk factors for myocarditis and cardiomyopathy after chemotherapy.

CLINICAL PERSPECTIVES—TRANSLATIONAL OUTLOOK

Further investigation into the role of RNA viruses as a significant underlying etiology for myocarditis and cardiomyopathy after chemotherapy with associated immunosuppression is needed.

Understanding the role of virus induced myocarditis and cardiomyopathy after chemotherapy will allow for further treatment, both preventative through vaccines and for selective anti-viral treatment.

DATA AVAILABILITY STATEMENT

The original contributions presented in the study are publicly available. This data can be found here: NCBI, BioProject, PRJNA79842.

ETHICS STATEMENT

The studies involving human participants were reviewed and approved by Biodesign Institute, ASU IRB and Department of Medicine, Shands Hospital, University of Florida. The patients/participants provided their written informed consent to participate in this study.

AUTHOR CONTRIBUTIONS

KV, ST, RB, MJ, SS-C, CP, and AL designed the experiment and wrote the manuscript. ST, SA, CS, MH, SS-C, and AL managed participant recruitment and were responsible for sample acquisition and preservation. AL, ST, KV, RB, SK, JY, LZ, MJ, PM, and AV analyzed and interpreted the data. All authors contributed to manuscript revision, provided important intellectual contributions, and approved the submitted version.

FUNDING

This work was supported by Biodesign, ASU startup funding (AL), American Heart Association (AL), National Institutes of Health (AL), and St Jude Children's Research Hospital (SS-C).

SUPPLEMENTARY MATERIAL

The Supplementary Material for this article can be found online at: https://www.frontiersin.org/articles/10.3389/fcvm.2022.821162/full#supplementary-material

Supplementary Figure 1 | Pavian software illustrations of detected RNA virus reads detected based on Kraken 2 analyses for all individual patient samples.

REFERENCES

1. Chang H-M, Moudgil R, Scarabelli T, Okwuosa TM, Yeh ETH. Cardiovascular complications of cancer therapy: best practices in diagnosis, prevention, and management-Part 1. *J Am Coll Cardiol.* (2017) 70:2536–51. doi: 10.1016/j.jacc.2017.09.1096
2. Stoltzfus KC, Zhang Y, Sturgeon K, Sinoway LI, Trifiletti DM, Chinchilli VN, et al. Fatal heart disease among cancer patients. *Nat Comm.* (2020) 11:1–8. doi: 10.1038/s41467-020-15639-5
3. Yeh ETH, Ewer MS, Moslehi J, Dlugosz-Danecka M, Banchs J, Chang HM, et al. Mechanisms clinical course of cardiovascular toxicity of cancer treatment I. *Oncol Semin Oncol.* (2019) 46:397–402. doi: 10.1053/j.seminoncol.2019.10.006
4. Morrison VA. Immunosuppression associated with novel chemotherapy agents and monoclonal antibodies. *Clin Inf Dis.* (2014) 59:S360–4. doi: 10.1093/cid/ciu592
5. Nesher L, Rolston KV. The current spectrum of infection in cancer patients with chemotherapy related neutropenia. *Infection.* (2014) 42:5–13. doi: 10.1007/s15010-013-0525-9
6. Hijano DR, Maron G, Hayden RT. Respiratory viral infections in patients with cancer or undergoing hematopoietic cell transplant. *Front Microbiol.* (2018) 9:3097. doi: 10.3389/fmicb.2018.03097
7. Abelmann WH. Virus and the heart. *Circulation.* (1971) 44:950–6. doi: 10.1161/01.CIR.44.5.950
8. Hazebroek M, Dennert R, Heymans S. Virus infection of the heart - unmet therapeutic needs. *Antivir Chem Chemother.* (2012) 22:249–53. doi: 10.3851/IMP2047
9. Van Linthout S, Tschöpe C. Viral myocarditis: a prime example for endomyocardial biopsy guided diagnosis and therapy. *Curr Opin Cardiol.* (2018) 33:325–33. doi: 10.1097/HCO.0000000000000515
10. Dennert R, Velthuis S, Schalla S, Eurlings L, van Suylen RJ, van Paassen P, et al. Intravenous immunoglobulin therapy for patients with idiopathic

cardiomyopathy and endomyocardial biopsy-proven high PVB19 viral load. *Antivir Ther*. (2010) 15:193–201. doi: 10.3851/IMP1516
11. Zhou L, He X, Gao B, Xiong S. Inhibition of histone deacetylase activity aggravates Coxsackievirus B3-induced myocarditis by promoting viral replication and myocardial apoptosis. *J Virol*. (2015) 89:10512–23. doi: 10.1128/JVI.01028-15
12. Wang D, Chen Y, Jiang J, Zhou A, Pan L, Chen Q, et al. Carvedilol has stronger anti-inflammation and anti-virus effects than metoprolol in murine model with coxsackievirus B3-induced viral myocarditis. *Gene*. (2014) 547:195–201. doi: 10.1016/j.gene.2014.06.003
13. Chang S, Zhi C, Li H, Huang D, Fan Q, Cui J, et al. Umifenovir effectively inhibits IL-10 dependent persistent Coxsackie B4 virus infection. *Antiviral Res*. (2017) 141:165–73. doi: 10.1016/j.antiviral.2017.02.018
14. Guzik TJ, Mohiddin SA, Dimarco A, Patel V, Savvatis K, Federica M, et al. COVID-19 and the cardiovascular system: implications for risk assessment, diagnosis, and treatment options. *Cardiovasc Res*. (2020) 116:1666–87. doi: 10.1093/cvr/cvaa106
15. Hendren NS, Drazner MH, Bozkurt B, Cooper LT Jr. Description and proposed management of the acute COVID-19 cardiovascular syndrome. *Circulation*. (2020) 141:1903–14. doi: 10.1161/CIRCULATIONAHA.120.047349
16. Quagliariello V, Bonelli A, Caronna A, Conforti G, Iovine M, Carbone A, et al. SARS-CoV-2 Infection and cardiooncology: from cardiometabolic risk factors to outcomes in cancer patients. *Cancers*. (2020) 12:3316–41. doi: 10.3390/cancers12113316
17. El Chaer F, Shah DP, Chemaly RF. How I treat resistant cytomegalovirus infection in hematopoietic cell transplantation recipients. *Blood*. (2016) 128:2624–36. doi: 10.1182/blood-2016-06-688432
18. Handous I, Achour B, Marzouk M, Rouis S, OHazgui O, Ines Brini I, et al. Co-infections of human herpesviruses (CMV, HHV6, HHV-7 and EBV) in non-transplant acute leukemia patients undergoing chemotherapy. *Virol J*. (2020) 17:37. doi: 10.1186/s12985-020-01302-4
19. Wu Y-T, Li X, Liu Z-l, Xu Z, Dai W, Zhang K, et al. Hepatitis B virus reactivation and antiviral prophylaxis during lung cancer chemotherapy: systematic review and meta- analysis. *PLoS ONE*. (2017) 12:e0179680. doi: 10.1371/journal.pone.0179680
20. Legoff J, Resche-Rigon M, Bouquet J, Robin M, Naccache SN, Séverine Mercier-Delarue S, et al. (2017). The eukaryotic gut virome in hematopoietic cell transplantation: new clues in enteric graft-versus-host disease. *Nat Med*. 23:1080–5. doi: 10.1038/nm.4380
21. Wang D, Urisman A, Liu YT, Springer M, Ksiazek TG, Erdman DD, et al. (2003). Viral discovery and sequence recovery using DNA microarrays. *PLoS Biol*. 1:E2. doi: 10.1371/journal.pbio.0000002
22. Bolger AM, Lohse M, Usadel B. Trimmomatic: a flexible trimmer for Illumina sequence data. *Bioinformatics*. (2014) 30:2114–20. doi: 10.1093/bioinformatics/btu170
23. Boonham N, Kreuze J, Winter S, van der Vlugt R, Bergervoet J, Tomlinson J, et al. Methods in virus diagnostics: From ELISA to next generation sequencing. *Virus Res*. (2014) 186:20–31. doi: 10.1016/j.virusres.2013.12.007
24. Huang B, Jennison A, Whiley D, McMahon J, Hewitson G, Graham R, et al. Illumina sequencing of clinical samples for virus detection in a public health laboratory. *Sci Reports*. (2019) 9:5409. doi: 10.1038/s41598-019-41830-w
25. Takeuchi S, Kawada J-I, Okuno Y, Horiba K, Suzuki T, Torii Y, et al. Identification of potential pathogenic viruses in patients with acute myocarditis using next generation sequencing. *J Mol Virol*. (2018) 90:1814–21. doi: 10.1002/jmv.25263
26. Derrick E, Wood DE, Lu J, Langmead B. Improved metagenomic analysis with Kraken 2. *Genome Biol*. (2019) 20:257. doi: 10.1186/s13059-019-1891-0
27. Breitwieser FP, Salzberg SL. Pavian: interactive analysis of metagenomics data for microbiome studies and pathogen identification. *Bioinformatics*. (2020) 36:1303–4. doi: 10.1093/bioinformatics/btz715
28. Ashraf A, Mahboob S, Andleeb R, Ijaz MU, Shah MS. Status updates of Newcastle disease and amelioration effects of medicinal plants against Newcastle disease virus: A review. *Acta Virol*. (2018) 62:3–15. doi: 10.4149/av_2018_101
29. Rezkalla SH, Kloner RA. Influenza-related viral myocarditis. *WMJ*. (2010) 109:209–13.
30. Garcia-Montojo M, Doucet-O'Hare T, Henderson L, Nath A. Human endogenous retrovirus K (HML-2): a comprehensive review. *Crit Rev Microbiol*. (2018) 44:715–38. doi: 10.1080/1040841X.2018.1501345
31. Songbo M, Lang H, Xinyong C, Bin X, Ping Z, Liang S. Oxidative stress injury in doxorubicin-induced cardiotoxicity. *Toxicol Lett*. (2019) 307:41–8. doi: 10.1016/j.toxlet.2019.02.013
32. Wouters KA, Kremer LCM, Miller TL, Herman EH, Lipshultz SE. Protecting against anthracycline-induced myocardial damage: a review of the most promising strategies. *Br J Haem*. (2005) 131:561–78. doi: 10.1111/j.1365-2141.2005.05759.x
33. Lyu YL, Kerrigan JE, Lin CP, Azarova AM, Tsai Y-C, Ban Y, et al. Topoisomerase IIbeta mediated DNA double-strand breaks: implications in doxorubicin cardiotoxicity and prevention by dexrazoxane. *Cancer Res*. (2007) 67:8839–46. doi: 10.1158/0008-5472.CAN-07-1649
34. Ni C, Ma P, Wang R, Lou X, Liu X, Qin Y, et al. Doxorubicin-induced cardiotoxicity involves IFNγ-mediated metabolic reprogramming in cardiomyocytes. *J Pathol*. (2019) 247:320–32. doi: 10.1002/path.5192
35. Nicolazzi MA, Carnicelli A, Fuorlo M, Scaldaferri A, Masetti R, Landolfi R, et al. Anthracycline and trastuzumab-induced cardiotoxicity in breast cancer. *Eur Rev Med Pharmacol Sci*. (2018) 22:2175–85. doi: 10.26355/eurrev_201804_14752
36. Olejniczak M, Schwartz M, Webber E, Shaffer A, Perry TE. Viral myocarditis - incidence, diagnosis and management. *J Cardiothorac Vasc Anesth*. (2020) 34:1591–601. doi: 10.1053/j.jvca.2019.12.052
37. Barmak K, Harhaj E, Grant C, Alefantis T, Wigdahl B. Human T cell leukemia virus type Iinduced disease: pathways to cancer and neurodegeneration. *Virology*. (2003) 30:1–12. doi: 10.1016/S0042-6822(02)00091-0
38. Stengel S, Fiebig U, Kurth R, Denner J. Regulation of human endogenous retrovirus-K expression in melanomas by CpG methylation. *Genes Chromosomes Cancer*. (2010) 49:401411. doi: 10.1002/gcc.20751
39. Dolei A, Ibba G, Piu C, Serra C. Expression of HERV Genes as possible biomarker and target in neurodegenerative diseases. *Int J Mol Sci 20*. (2019) 20:3706. doi: 10.3390/ijms20153706
40. Ko EJ, Ock MS, Choi YH, Iovanna JL, Mun S, Han S, et al. Human Endogenous Retrovirus (HERV)-K env gene knockout affects tumorigenic characteristics of nupr1 gene in DLD-1 colorectal cancer cells. *Int J Mol Sci*. (2021) 22:3941. doi: 10.3390/ijms22083941
41. Argaw-Denboba A, Balestrieri E, Serafino A, Cipriani C, Bucci I, Sorrentino R, et al. HERV-K activation is strictly required to sustain CD133+ melanoma cells with stemness features. *J Exp Clin Cancer Res*. (2017) 36:20. doi: 10.1186/s13046-016-0485-x
42. Chan BK, Sistrom M, Wertz JE, Kortright KE, Narayan D, Turner PE. Phage selection restores antibiotic sensitivity in MDR *Pseudomonas aeruginosa*. *Sci Rep*. (2016) 6:26717. doi: 10.1038/srep26717
43. Yin XR, Liu P, Xu X, Xia Y, Huang K-Z, Wang Q-D, et al. Elevated plasma phage load as a marker for intestinal permeability in leukemic patients. *Med Microbiol Immunol*. (2020) 209:693–703. doi: 10.1007/s00430-020-00694-y

Conflict of Interest: The authors declare that the research was conducted in the absence of any commercial or financial relationships that could be construed as a potential conflict of interest.

Publisher's Note: All claims expressed in this article are solely those of the authors and do not necessarily represent those of their affiliated organizations, or those of the publisher, the editors and the reviewers. Any product that may be evaluated in this article, or claim that may be made by its manufacturer, is not guaranteed or endorsed by the publisher.

frontiers in Cardiovascular Medicine

REVIEW
published: 15 March 2022
doi: 10.3389/fcvm.2022.829553

Multimodality Advanced Cardiovascular and Molecular Imaging for Early Detection and Monitoring of Cancer Therapy-Associated Cardiotoxicity and the Role of Artificial Intelligence and Big Data

Jennifer M. Kwan[1], *Evangelos K. Oikonomou*[1], *Mariana L. Henry*[2] *and Albert J. Sinusas*[1,3,4]*

[1] Section of Cardiovascular Medicine, Yale University School of Medicine, New Haven, CT, United States, [2] Geisel School of Medicine at Dartmouth, Hanover, NH, United States, [3] Department of Radiology and Biomedical Imaging, Yale University School of Medicine, New Haven, CT, United States, [4] Department of Biomedical Engineering, Yale University, New Haven, CT, United States

OPEN ACCESS

Edited by:
Chun Liu,
Stanford University, United States

Reviewed by:
Ian Chen,
VA Palo Alto Health Care System, United States
Concetta Zito,
University of Messina, Italy

***Correspondence:**
Albert J. Sinusas
albert.sinusas@yale.edu

Specialty section:
This article was submitted to Cardio-Oncology, a section of the journal Frontiers in Cardiovascular Medicine

Received: 06 December 2021
Accepted: 12 January 2022
Published: 15 March 2022

Citation:
Kwan JM, Oikonomou EK, Henry ML and Sinusas AJ (2022) Multimodality Advanced Cardiovascular and Molecular Imaging for Early Detection and Monitoring of Cancer Therapy-Associated Cardiotoxicity and the Role of Artificial Intelligence and Big Data. Front. Cardiovasc. Med. 9:829553. doi: 10.3389/fcvm.2022.829553

Cancer mortality has improved due to earlier detection *via* screening, as well as due to novel cancer therapies such as tyrosine kinase inhibitors and immune checkpoint inhibitions. However, similarly to older cancer therapies such as anthracyclines, these therapies have also been documented to cause cardiotoxic events including cardiomyopathy, myocardial infarction, myocarditis, arrhythmia, hypertension, and thrombosis. Imaging modalities such as echocardiography and magnetic resonance imaging (MRI) are critical in monitoring and evaluating for cardiotoxicity from these treatments, as well as in providing information for the assessment of function and wall motion abnormalities. MRI also allows for additional tissue characterization using T1, T2, extracellular volume (ECV), and delayed gadolinium enhancement (DGE) assessment. Furthermore, emerging technologies may be able to assist with these efforts. Nuclear imaging using targeted radiotracers, some of which are already clinically used, may have more specificity and help provide information on the mechanisms of cardiotoxicity, including in anthracycline mediated cardiomyopathy and checkpoint inhibitor myocarditis. Hyperpolarized MRI may be used to evaluate the effects of oncologic therapy on cardiac metabolism. Lastly, artificial intelligence and big data of imaging modalities may help predict and detect early signs of cardiotoxicity and response to cardioprotective medications as well as provide insights on the added value of molecular imaging and correlations with cardiovascular outcomes. In this review, the current imaging modalities used to assess for cardiotoxicity from cancer

treatments are discussed, in addition to ongoing research on targeted molecular radiotracers, hyperpolarized MRI, as well as the role of artificial intelligence (AI) and big data in imaging that would help improve the detection and prognostication of cancer-treatment cardiotoxicity.

Keywords: cardiotoxicity, cardiovascular imaging, big data, cancer therapy-associated cardiotoxicity, molecular imaging

INTRODUCTION

Cancer incidence is expected to increase by 50% by 2050, but over the past two decades, cancer mortality has improved in part due to earlier detection *via* screening and the advent of novel therapies such as tyrosine kinase inhibitors (TKI) for cancers like chronic myelogenous leukemia (CML), liver, gastrointestinal and lung cancers, as well as immunotherapy, such as checkpoint inhibitors, for metastatic disease and an expanding list of indications including triple negative breast cancer, lung cancer, melanoma, bladder cancer, and renal cell cancer (1–6).

However, with the rise of newer oncologic therapies, there have been a spectrum of adverse cardiovascular toxicities including cardiomyopathy (CM), myocardial infarction, myocarditis, arrhythmia, hypertension (HTN) and thrombosis that have been associated with these agents. More traditional cardiotoxic agents like anthracyclines (i.e., doxorubicin), one of the most widely used class of chemotherapeutics due to improved overall cancer and survival outcomes has been shown to alter myocardial energetics, promote mitochondrial dysfunction, increase reactive oxygen species levels leading to activation of matrix metalloproteases, inhibit topoisomerase IIb and cause DNA strand breaks, thereby promoting cardiomyopathy (7–9).

HER2 inhibitors like trastuzumab has also been shown to increase risk of CM *via* antagonizing important pro survival as well as other important signal transduction pathways for metabolism in the heart (10). Platinum agents like cisplatin have been shown to increase oxidative stress and increased apoptosis and has been associated with cardiomyopathy in rare instances (11). Alkylating agents like cyclophosphamide, which can cause oxidative damage and direct endothelial cell damage have been linked to myocarditis and cardiomyopathy (12). Antimetabolites like 5 fluorouracil (5FU), which is commonly used in head and neck cancers as well as gastrointestinal cancers has been shown to increase risk of coronary vasospasm and myocardial infarction (13, 14). Multiple myeloma therapies (bortezomib, lenalidomide) and vascular endothelial growth factor (VEGF) inhibitors like bevacizumab have been associated with thrombosis and hypertension by promoting endothelial cell dysfunction (15–18). TKIs like ibrutinib has been associated with atrial fibrillation, while other TKIs such as ponatinib, sorafenib, sunitinib have been associated with CM and myocardial infarction (MI) (19–21).

Of the close to 2 million patients diagnosed with cancer in 2019, it is estimated that 38.5% are eligible for ICI therapy (22, 23). In addition to increased risk of myocarditis, pericarditis and vasculitis, immune checkpoint inhibitors (ICI) have been associated with increased risk of plaque rupture/acceleration of atherosclerosis and thrombosis (24). ICI myocarditis is characterized by lymphocytic infiltration with CD4 and CD8 cells and mortality is high if not identified and if left untreated (25).

Newer immunotherapies may also increase risk of myocarditis, such as cellular therapies like CART and molecular inhibitors such as CCR4 antagonist, mogamulizumab, which is used to treat T cell lymphomas (26–28). However, evaluation of the earliest signs of immune cell infiltration in the myocarditis process is limited (**Table 1**; **Figure 1**). Imaging modalities like echocardiography (echo) and magnetic resonance imaging (MRI) are routinely used to monitor and evaluate for the aforementioned oncologic therapy related cardiotoxicity, with both allowing for assessment of function and wall motion abnormalities and MRI allowing for additional tissue characterization using T1, T2, extracellular volume (ECV) and delayed gadolinium enhancement (DGE) assessment. While nuclear studies like multi-gated acquisition (MUGA) scans have fallen out of favor for the evaluation of cardiomyopathy mediated by oncologic therapy due to the higher sensitivity, and availability of echo and MRI, emerging nuclear imaging using molecularly targeted radiotracers may confer more specificity and help elucidate the mechanisms of cardiotoxicity, many of which are already in clinical use for oncology purposes and thus can be adapted to evaluate their signal/role in cardiotoxicity (**Table 1**). In addition to molecular targets, hyperpolarized MRI has emerged as a potential imaging modality to evaluate effects of oncologic therapy on cardiac metabolism and has reached human studies. Finally, artificial intelligence and big data of imaging modalities including electrocardiograms may be able to help predict and detect early signs of cardiotoxicity and response to cardioprotective medications once cardiomyopathy develops but also help provide insights on diagnostic and prognostic value of molecular based imaging. We review current imaging modalities used to assess for cardiovascular toxicities associated with oncologic therapies and highlight ongoing research in the areas of molecular imaging, targeted molecular radiotracers and hyperpolarized MRI as well as the role of artificial intelligence (AI) and big data in imaging that would help improve detection, prognostication of oncologic therapy related cardiotoxicity.

Abbreviations: AI, artificial intelligence; CM, cardiomyopathy; CML, chronic myelogenous leukemia; DGE, delayed gadolinium enhancement; DNA, Deoxyribonucleic acid; ECV, extracellular volume; GLS, global longitudinal strain; ICI, checkpoint inhibitors; HER2, human epidermal growth factor receptor 2; HF, heart failure; HTN, hypertension; MI, myocardial infarction; MUGA, multigated acquisition; ROS, reactive oxygen species; TdP, torsades de pointe; TKI, tyrosine kinase inhibitor; VTE, venous thromboembolism.

TABLE 1 | Cancer therapy, associated CV toxicity and imaging assessment.

Cancer therapy	Associated CV toxicity	Imaging modality/method for evaluating cardiotoxicity	Novel molecular imaging approaches	Stage preclinical vs. clinical
Anthracyclines: Doxorubicin, daunorubicin	Cardiomyopathy (29) Early stages of toxicity	MRI, echo, nuclear	Molecular nuclear imaging for cardiotoxicity:	
			SPECT radiotracers:	
			^{123}I-meta-iodobenzylguanidine (MIBG) (30)	Clinical
			^{99m}Tc-RP805 (31)	Preclinical
			^{111}In-antimyosin (30)	Clinical (32)
			^{99m}Tc-annexin (33)	Clinical (34)
			PET radiotracers:	
			^{18}F-DHMT (35)	Preclinical
			^{68}Ga-Galmydar (36)	Preclinical
			Changes in metabolism:	
			Hyperpolarized magnetic resonance (37)	Clinical
			^{13}C pyruvate (38, 39)	
Other: Topoisomerase I/II inhibitors, taxols, cyclophosphamide, paclitaxel			Hyperpolarized magnetic resonance (37)	Clinical
Platinum agents: cisplatin, oxaliplatin, carboplatin				
Checkpoint inhibitors				
Pembrolizumab	Myocarditis (40), vasculitis, pericarditis (41, 42), atherosclerosis (43)	Echo for function/strain, MRI for function, tissue characterization i.e.,	Molecular imaging for myocarditis:	
Ipilimumab		MRI:	^{89}Zr-DFO-CD4 and ^{89}Zr-DFO-CD8a (44)	Clinical
Nivolumab		Edema/scar imaging	^{68}Ga-FAPI (45)	Clinical
Atezolizumab		PET:		
Avelumab		^{18}FDG to evaluate for vasculitis.	Fibrosis imaging:	
Cemiplimab		^{82}Rb to evaluate for ischemic disease	^{68}Ga-collagelin (46)	Preclinical
		SPECT:		
		^{99m}Tc-tetrofosmin or ^{99m}Tc-sestamibi to evaluate for ischemic disease		
TKIs				
Imatinib	HF (47)	MRI, echo, nuclear SPECT		
Bosutinib	Thrombosis (48)		Thrombosis imaging	
			Evaluation of fibrin	
			^{64}CU-FBP8 (49)	Clinical trials (50)
			Evaluation of glycoprotein IIb/IIIa receptor	
Dasatinib	Thrombosis (51), HTN, QT prolongation (52)		^{18}F-GP1 (53)	Clinical trial (53)
Ponatinib	Thrombosis (54), HF (55), HTN, ischemia	MRI, echo		
Nilotinib	Thrombosis, QTC prolongation (52)			
Ibrutinib	A Fib (19)			
Sunitinib	HF (56), HTN, QTC prolongation (57)	MRI, echo		

(Continued)

TABLE 1 | Continued

Cancer therapy	Associated CV toxicity	Imaging modality/method for evaluating cardiotoxicity	Novel molecular imaging approaches	Stage preclinical vs. clinical
Sorafenib	MI, HF, HTN, QTC prolongation	CT coronary, PET/SPECT for ischemic evaluation	Hyperpolarized magnetic resonance ^{68}Ga-DOTATATE (58)	Clinical Clinical (59)
Vendetanib	HF, HTN (60), QTC prolongation, TdP (61)			
Afatinib	None so far (62)			
Erlotinib	MI (rare) (63)			
Lapatinib	HF, QT prolongation (64)	MRI, echo		
Gefitinib	HF (65)	MRI, echo		
axitinib	HF, HTN (66)	MRI, echo		
bevacizumab	HTN, thrombosis		Hyperpolarized magnetic resonance to evaluate hypertensive stress (67)	Clinical
Trastuzumab	Heart failure (68–70)	MRI, ECHO, nuclear (MUGA)		
Pertuzumab				
Neratinib				
Tucatinib				
Anti metabolite				
5 FU	Coronary vasospasm (14, 71)	CT coronary, PET or SPECT to rule out obstructive disease	Hyperpolarized magnetic resonance	Clinical

CURRENT IMAGING MODALITIES USED TO INTERROGATE ONCOLOGIC THERAPY CARDIOTOXICITY

Echo and MRI in Evaluation of Cardiotoxicity

Cardiotoxicity due to anthracycline use (often dose dependent, but can occur at any dose) are common, up to 5% with cumulative doses <400 mg/kg, but up to 20% for those treated with 700 mg/kg or more (72). HER2 inhibitor mediated cardiomyopathy can occur in 5–10% of patients and is increased when given in conjunction with anthracyclines up to 27% (73, 74). Oncologic therapy mediated cardiomyopathy can be evaluated by traditional imaging modalities such as echo and MRI, which are able to evaluate wall motion, left and right ventricular function and even early signs of toxicity *via* changes in strain, namely global longitudinal strain (75, 76). The European Society for Medical Oncology (ESMO) and the American Society of Echo (ASE) recommend 2D/3D echo or MRI for assessing left ventricular function including strain for monitoring of known cardiotoxic therapies such as anthracyclines or anti-Her2 therapies and the American Society of Clinical Oncology (ASCO) recommends echo or MRI as first line imaging modalities with MUGA as a second line if echo/MRI are not available or if not technically feasible for MRI (77–81). Due to reduced variability compared to 2D echo, 3D echo or MRI are recommended for sequential follow up (82).

In addition to being the gold standard for volumetrics and ejection fraction, MRI has additional evaluation capabilities including tissue characterization for injured cells such as changes in ECV and increased native T1 times, shown with anthracycline use and increased T2 relaxation times with anthracycline toxicity (83–86). The presence of DGE post trastuzumab, a HER2 inhibitor, was associated with cardiomyopathy (87).

Strain as a Predictor of Cardiomyopathy

Feature tracking global longitudinal strain (GLS) was first used in echo to show that it could be predictive of future cardiomyopathy in multiple studies of cancer patients undergoing cardiotoxic chemotherapy with anthracycline or trastuzumab. For example, an increase in GLS >12 or 15% was associated with a significant drop in LVEF >10% 6 months after in several studies (88, 89). MRI has subsequently shown that use of tagging, feature tracking strain or fast strain encoded (SENC) assessment are sensitive and highly accurate in detecting subclinical cardiotoxicity as evidenced by an increase in GLS for patients on cardiotoxic chemotherapy such as anthracyclines, with SENC having a higher accuracy that was less dependent on loading conditions (90–94). However, strain assessment in MRI is largely used in a research setting and is not routinely used in the clinical practice yet.

MRI Evaluation of Adverse Immune Related Cardiac Events

ICI myocarditis can occur in 1–2% of patients and has a high mortality of up to 50% if untreated (25, 95). MRI has become a work horse for evaluation of immunotherapy related cardiotoxicities. In addition to T1, and ECV changes, T2 abnormalities allow for assessment of myocardial edema in patients on checkpoint inhibitors with concern for myocarditis or pericarditis and DGE, a marker of myocardial injury

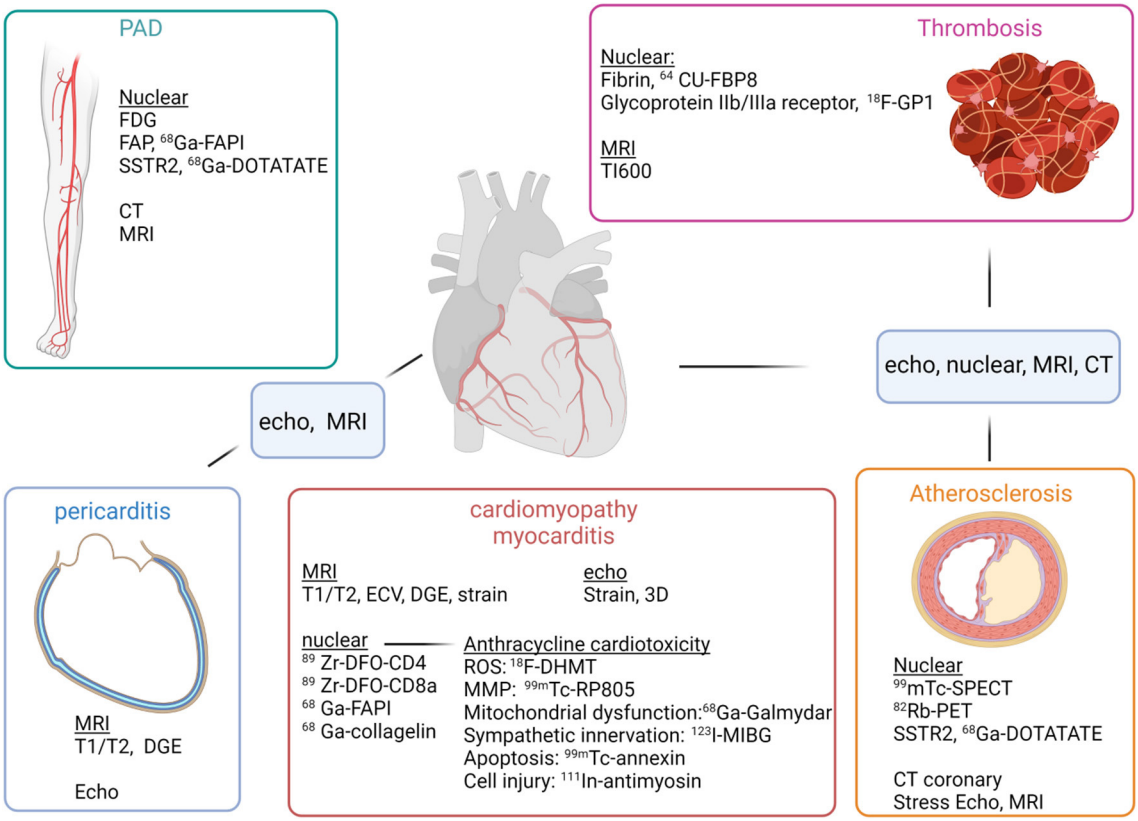

FIGURE 1 | Imaging modalities and evaluation of cardiotoxicities of oncologic therapies. For evaluation of peripheral artery disease (PAD) (top left), FDG, FAP and SSTR2 imaging may be able to identify vulnerable plaque, while CT and MRI can help evaluate degree of stenosis. For evaluation of thrombosis (top right), nuclear imaging may be able to identify early clot formation with radiotracers directed at fibrin or glycoprotine IIb/IIIa, and MRI can use a long inversion time to identify thrombus, as with TI600. For evaluation of cardiomyopathy/myocarditis (middle), echo and MRI can evaluate ejection fraction as well as myocardial strain. For myocarditis, MRI can evaluate tissue characteristics such as T1, T2 and DGE, which are now components of the Lake Louise criteria for myocarditis. Nuclear can evaluate for T cell infiltration using tracers targeting CD4, CD8 cells. Tracers directed against FAP, such as ^{68}Ga-FAPI has been shown to be increased in an animal model of checkpoint inhibitor myocarditis. Evaluation of pericarditis (bottom left), a complication of checkpoint inhibitors can be assessed by echo for detection of pericardial effusion, but with greater specificity MRI can identify edema and DGE. Atherosclerosis (bottom right) can be evaluated by traditional SPECT and PET techniques to evaluate for perfusion with stress and rest. CT coronary is now first line for evaluation of those with intermediate risk chest pain to rule out obstructive disease. Stress MRI or DGE can also be performed to evaluate for prior myocardial infarction as well as myocardial viability.

or scarring is another tissue characterization parameter that can evaluate for immunotherapy toxicities. MRI is recommended by specialty society guidelines as part of the evaluation and monitoring of ICI myocarditis using the Lake Louise criteria, updated in 2018 to require both increased myocardial signal intensity ratio >2 or increased myocardial relaxation times or visible myocardial edema in T2-weighted images and increased myocardial relaxation times or extracellular volume fraction or DGE in T1-weighted images for the imaging diagnosis of myocarditis (80, 96–100). However, DGE is non-specific and cannot distinguish from cell damage vs. end stage fibrosis and current standard clinical imaging modalities are lacking in assessment of potential molecular correlates, such as collagen deposition and scar. Thus, molecularly targeted imaging tracers may shed light on both mechanism and help increase the specificity of cardiac imaging findings.

MOLECULAR TARGETED NUCLEAR IMAGING MODALITIES TO EVALUATE ONCOLOGIC THERAPY RELATED ADVERSE CARDIOVASCULAR PATHOLOGIES

Molecular Nuclear Imaging for Evaluation of Anthracycline Cardiotoxicity

Anthracycline mediated cardiotoxicity has been associated with an increase in reactive oxygen species (ROS) levels in the heart. ROS levels have been shown to confer cardiotoxicity by increased apoptosis, inflammation, mitochondrial dysfunction and activation of matrix metalloproteases (31). Molecular nuclear imaging studies have helped shed light on mechanisms of anthracycline mediated cardiotoxicity. Increased ROS levels in an animal model of doxorubicin cardiotoxicity showed that a novel

PET tracer, ^{18}F-labeled radioanalog of dihydroethidium, [^{18}F]-6-(4-((1-(2-fluoroethyl)-1H-1,2,3-triazol-4-yl)methoxy)phenyl)-5-methyl-5,6 dihydrophenanthridine-3, 8-diamine ([^{18}F]·DHMT), which targets superoxide, was able to reveal an elevation in superoxide levels in the heart at least 2 weeks prior to a drop in the left ventricular ejection fraction (35). ROS activation of MMPs downstream can then promote adverse cardiac remodeling (101). Renin-angiotensin-aldosterone system (RAAS) activation has been shown to augment the progression of anthracycline induced cardiotoxicity and inhibition *via* RAAS inhibitors like angiotensin receptor blockers or angiotensin converting enzyme inhibitors have been able to prevent and treat anthracycline mediated cardiomyopathy (102, 103). Use of a novel angiotensin receptor-neprilysin Inhibitor, sacubitril/valsartan in a rodent model of anthracycline cardiotoxicity was able to attenuate cardiotoxicity. MMP imaging of activated MMPs using SPECT radiotracer ^{99m}Tc-RP805 showed that sacubitril/valsartan in conjunction with doxorubicin was able to significantly attenuate MMP activation as well as prevent a decline in LVEF compared to doxorubicin alone vs. doxorubicin and valsartan groups. Myocardial MMP activity as assessed by ^{99m}Tc-RP805 uptake was inversely related to left ventricular ejection fraction (31). In addition to MMP activation and adverse remodeling, ROS can also injure endothelial cells. Anthracycline use has been associated with capillary loss in the heart in some rodent models and protection of endothelial cells with vascular endothelial growth factor-B (VEGF-B) treatment led to preservation of capillary mass (104).

ROS has also been shown to confer mitochondrial dysfunction. Disruption of mitochondrial membrane potential in mitochondrial dysfunction mediated by anthracycline can be evaluated by ^{68}Ga-Galmydar. In a rodent model, uptake of ^{68}Ga-Galmydar was reduced by 2-fold with anthracycline treatment compared to control and in H9c2 rat cardiomyoblasts, this was associated with activation of the apoptosis cascade (36).

Early markers of anthracycline cardiotoxicity include an increased uptake of indium-111-labeled antimyosin in the heart, which occurs due to myocyte damage and subsequent association of antimyosin with myosin, which is normally intracellular. Increased uptake of ^{111}In-antimyosin in patients on anthracycline was associated with LV dysfunction (30). Detection of the earliest stages of apoptosis can also signal early toxicity. Annexin V has a high affinity for phosphatidylserine, which gets exposed on the cell surface during apoptosis. Use of annexin V imaging has allowed for detection of cells undergoing apoptosis. In a rodent model of doxorubicin cardiotoxicity, radiolabeled annexin V, ^{99m}Tc-annexin was used to visualize apoptosis that corresponded to histological evidence of apoptosis on TUNEL staining (33). Finally, sympathetic nervous innervation of the myocardium has also been shown to be disrupted with anthracycline toxicity. An assessment of myocardial sympathetic innervation impairment was done by evaluating a radiotracer that is an analog of norepinephrine, iodine-123-labeled meta-iodobenzylguanidine (^{123}I-MIBG). A decrease in ^{123}I-MIBG uptake with increasing cumulative doses of anthracyclines in human patients was associated with LV dysfunction. However, it takes higher cumulative doses of anthracycline to see a drop in ^{123}I-MIBG uptake, thus this agent would be less useful if earlier detection of toxicity is desired. However, ^{123}I-MIBG is clinically available and routinely used to evaluate for adrenaline secreting tumors (30) (**Figure 2**).

CD4, CD8 Imaging in ICI Myocarditis

Molecularly targeted radiotracers in nuclear medicine are emerging to evaluate processes such as fibrosis, inflammation and thrombosis, extending beyond nuclear cardiology's traditional use to evaluate perfusion deficits in ischemic heart disease *via* single photon emission computed tomography (SPECT) and positron emission tomography (PET), tissue viability or inflammation with PET fluorodeoxyglucose (FDG), which evaluates for glucose uptake predominantly by inflammatory cells, such as myeloid and T cells (106). These processes are common adverse effects of oncologic and immunotherapies.

Detection of the earliest signs of myocardial inflammation in ICI myocarditis, which occurs in 1-2% of patients on these agents remains a clinical challenge (95, 107). The ability to detect the initial infiltration of inflammatory cells such as CD4 or CD8 cells before injury has occurred could help reduce morbidity and high mortality associated with this condition (25). Emerging molecularly targeted probes against CD4, ^{89}Zr-DFO-CD4 and CD8 cells, ^{89}Zr-DFO-CD8a may be a potential avenue to detect inflammation at these earliest of stages, which can prompt more frequent follow ups, biomarker checking and earlier therapy (44). Determining specificity of these findings will also be important as to avoid withholding cancer fighting immunotherapy or treatment with steroids, which may potentially lower the efficacy of the immunotherapy agent (108–110). Checkpoint inhibitors have been shown to accelerate atherosclerosis and increase risk of plaque rupture in addition to the risk for myocarditis and pericarditis by driving increased inflammatory cells, including CD8 T cell infiltration into plaques in animal models and patients on checkpoint inhibitors (43, 111, 112). Thus, evaluation of atherosclerotic lesions with CD8 radiotracers, may be able to identify those at risk for myocardial infarction in patients on checkpoint inhibitor therapy.

Detection of Vulnerable Plaque

Both checkpoint inhibitor use and certain TKIs like ponatinib and sorafenib have been associated with increased risk of myocardial infarction (43, 113). ICIs have also been associated with increased risk of stroke (114). Use of ICIs have been associated with increased infiltration of CD3, CD8 and CD68 cells, markers for T cells and macrophages respectively into atherosclerotic lesions (115). Increased somatostatin receptor 2 (SSTR2) on the cell surface of inflammatory macrophages is a marker of macrophage activation. In a study of symptomatic stroke patients, increased uptake of SSTR2 in culprit vessels assessed by PET tracer ^{68}Ga-DOTATATE was shown to predict plaque rupture (58). Thus, evaluation of SSRT2 levels in patients on ICI therapy may help identify vulnerable plaques and warrants further investigation. The mechanisms for TKI mediated MI on the other hand are attributed to endothelial cell dysfunction and activation of apoptosis pathways, although direct evidence for MI mechanisms are still lacking, thus further research would be

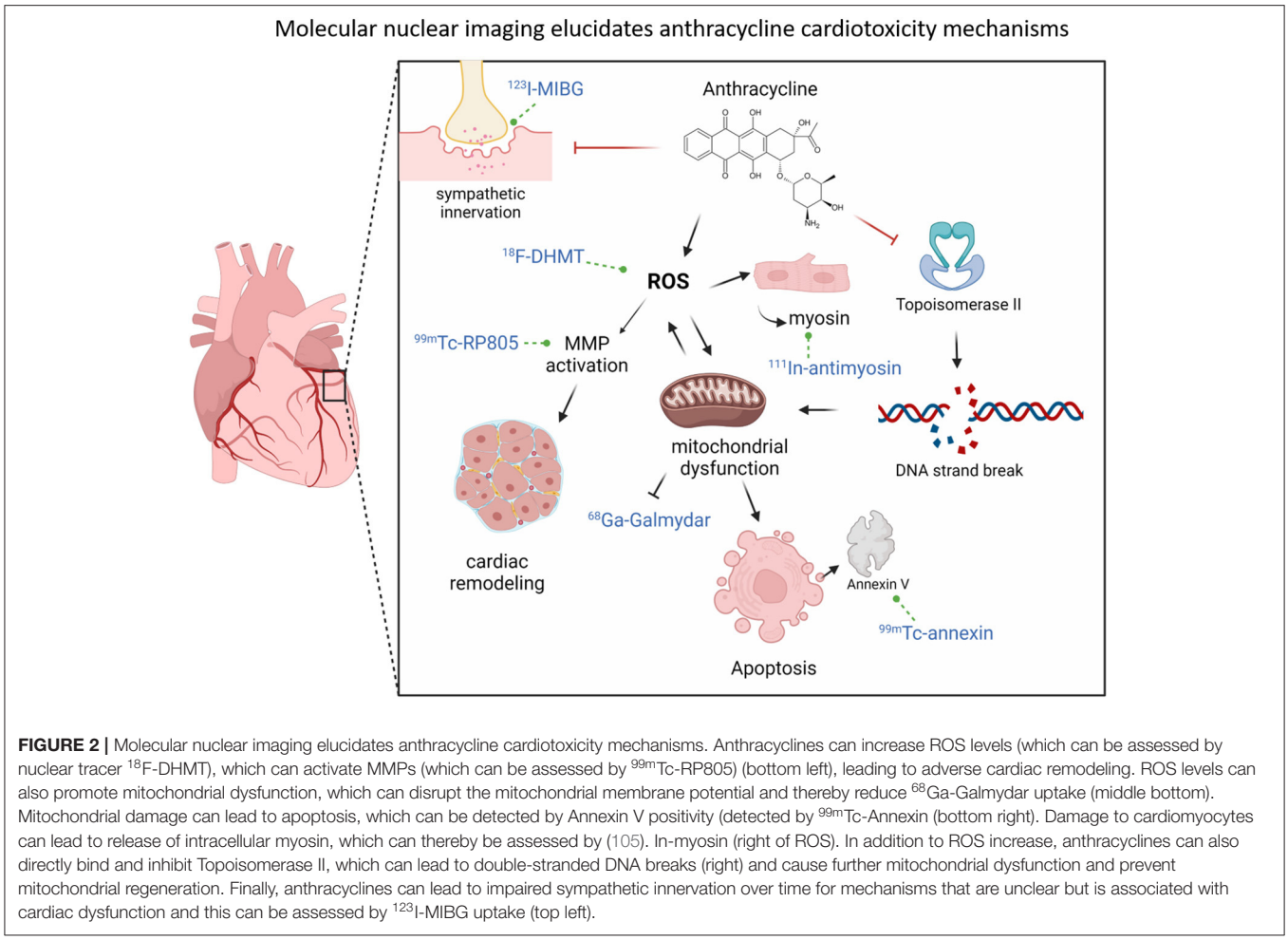

FIGURE 2 | Molecular nuclear imaging elucidates anthracycline cardiotoxicity mechanisms. Anthracyclines can increase ROS levels (which can be assessed by nuclear tracer ^{18}F-DHMT), which can activate MMPs (which can be assessed by ^{99m}Tc-RP805) (bottom left), leading to adverse cardiac remodeling. ROS levels can also promote mitochondrial dysfunction, which can disrupt the mitochondrial membrane potential and thereby reduce ^{68}Ga-Galmydar uptake (middle bottom). Mitochondrial damage can lead to apoptosis, which can be detected by Annexin V positivity (detected by ^{99m}Tc-Annexin (bottom right). Damage to cardiomyocytes can lead to release of intracellular myosin, which can thereby be assessed by (105). In-myosin (right of ROS). In addition to ROS increase, anthracyclines can also directly bind and inhibit Topoisomerase II, which can lead to double-stranded DNA breaks (right) and cause further mitochondrial dysfunction and prevent mitochondrial regeneration. Finally, anthracyclines can lead to impaired sympathetic innervation over time for mechanisms that are unclear but is associated with cardiac dysfunction and this can be assessed by ^{123}I-MIBG uptake (top left).

needed to see if macrophage activation is involved and whether activated macrophage imaging would help risk stratify patients on these TKIs (113).

FAP Imaging in ICI Myocarditis

Another potential marker of early stages of ICI myocarditis is fibroblast activating protein (FAP), which is a protein that gets significantly upregulated in cancer tissue, atherosclerosis, arthritis and fibrosis. It is emerging as an imaging marker for fibroblast activation and fibrosis (116, 117). A PET radiotracer tracer targeting FAP is ^{68}Ga-FAPI. In a recent study, ^{68}Ga-FAPI was shown to be a potential early marker of ICI myocarditis with median standardized uptake values (SUV) 1.79 (IQR 1.62, 1.85) in myocarditis patients vs. 1.15 (IQR 0.955, 1.52) in non-myocarditis patients (45). FAP has also been used to evaluate post myocardial infarction fibrosis, but its level in the blood vessels and myocardium of patients on checkpoint inhibitors is unclear (118, 119).

PD1 Imaging as a Potential Risk Factor for ICI Myocarditis

Another challenge with checkpoint inhibitor myocarditis is trying to figure out who is at increased risk. Programmed cell death protein 1 (PD1), a target of checkpoint inhibitors like pembrolizumab and its expression on cardiomyocytes warrants additional research as a potential risk factor. PET radiotracer, ^{64}Cu-DOTA-pembrolizumab can detect PD1 in rodent hearts as well as on the surface of human blood cells and may be used in such an investigation (120).

MRI DGE Limitations in Fibrosis Assessment and Collagen Imaging

A higher burden of DGE and presumed scarring in hypertrophic cardiomyopathy is associated with worse cardiovascular and death outcomes (121, 122). In a retrospective study of ICI myocarditis patients who underwent cMRI, DGE evaluation did not correlate with cardiovascular outcomes, nor fibrosis, with only 35% of pathology proven fibrosis cases showing DGE on MRI (96, 121, 123, 124). Further, of the 56 patients with histopathology available either through biopsy or autopsy, 98% had lymphocytic infiltration but only 38% had DGE and 26% with T2 positivity (96). Thus in addition to evaluation of lymphocytic infiltration with targeted radiotracers for CD4 and CD8 cells to identify early stages of myocarditis and increase sensitivity of diagnosis, late stages of myocardial injury that can result in scar and thus collagen deposition can be evaluated

by radiotracers targeting collagen. The PET radiotracer ^{68}Ga-collagelin targets collagen, which can help quantify the burden of scarring or end stage fibrosis, which was shown to be able to detect pulmonary fibrosis in a mouse model of bleomycin induced pulmonary fibrosis and correlated with fibrosis on pathology (46) (**Figure 3**). MRI with DGE is able to evaluate for possible scarring, but it is not able to distinguish between early vs. late stage fibrosis, with the former having potential reversibility and may partially explain the differential outcomes we see between HCM and ICI myocarditis patients when it comes to the differences in the fibrosis processes between the two conditions and correlation of scar burden as quantified by DGE and outcomes (125). There is also a MRI collagen type I targeted probe EP-3533 that is conjugated to gadolinium, which was shown to be able to visualize pulmonary, liver and bowel fibrosis in rodent models, but these have not yet advanced to use in humans (126–128).

Thrombosis Imaging

Pathologic thromboses like pulmonary embolism (PE), deep vein thrombosis (DVT) carries high morbidity and mortality (129). Cancer patients are at increased risk of thrombosis and some of their oncologic therapies can increase that risk further (130, 131). ICI, VEGF inhibitors and lenalidomide have been associated with increased thrombosis risk. Increasing the sensitivity of diagnosing blood clots so treatment can be timely instigated may help avoid complications and help improve outcomes (132–134). Radiotracers that can target fibrin, a molecular precursor of blood clotting can be useful in detection of blood clots. PET radiotracer ^{64}CU-FBP8 can target fibrin and has been used to identify thrombi in animal models, particularly earlier stages of clots (49). Another PET radiotracer, ^{18}F-GP1 that targets the glycoprotein IIb/IIIa receptors on activated platelets and has been demonstrated to detect venous thrombosis and arterial thromboses (53, 135). A phase 1, first-in-human study of ^{18}F-GP1 positron emission tomography for imaging acute arterial thrombosis is underway (53). These PET thrombosis imaging agents may be of utility for detection of DVTs and PEs in cancer patients, especially for those who may have contraindications to contrast, such as those with chronic kidney disease or those who have an allergy to contrast.

MOLECULAR MRI AND MR SPECTROSCOPY

Hyperpolarized MRI for Evaluation of Cardiac Metabolism *in vivo*

As the human heart failures, it has been shown to shift its metabolism from predominantly fatty acid oxidation to more glucose utilization (136). Changes in oxidative phosphorylation or substrate utilization may reflect early signs of cardiotoxicity, yet *in vivo* real time detection of cardiac metabolism has been limited to small studies with radioactive tracers using PET. More recently, substrate utilization and metabolism have been evaluated using magnetic resonance (MR) imaging and spectroscopy. Hyperpolarized carbon-13 (^{13}C) labeled pyruvate imaging is different from standard clinical MRI using gadolinium contrast, in that it provides information on how tissue uses carbon-based nutrients (37). In rodent models of anthracycline cardiotoxicity, carbon-13 MR spectroscopy (MRS) was used to assess changes to oxidative phosphorylation and tricarboxylic acid (TCA) cycle flux *in vivo*. These studies showed that doxorubicin lead to reduced cardiac oxidative phosphorylation in a rat model as evidenced by increased ^{13}C lactate production (38). First in human MRS was used to evaluate tumor metabolism in prostate cancer and ongoing clinical trials are evaluating hyperpolarized MR in tumor metabolism and correlations with outcomes in prostate and pancreatic cancer (137–139). First use of hyperpolarized ^{13}C metabolic MRI in human heart involved evaluation of pyruvate metabolism in healthy individuals (39). Hyperpolarized MR imaging may allow for visualization of changes in cardiac energetics, particularly from fatty acid metabolism to more glucose utilization in an evolving cardiomyopathy in response to cardiotoxic chemotherapy and to evaluate response to cardioprotective medications such as beta blockers and angiotensin converting enzyme inhibitors in real time (140).

Apoptosis Evaluation by MRI

Various chemotherapy agents, most notably anthracyclines are known to increase cardiomyocyte apoptosis. Molecular MRI probes conjugated to superparamagnetic iron oxide (SPIO) and human annexin was shown to be able to visualize apoptosis in real time in a rodent model following ischemia and post doxorubicin exposure, but these MRI molecular probes have not gone beyond animal studies thus far but have the potential to detect early signs of cell death in the myocardium (105, 141).

Inflammation Imaging by MRI

In addition to T1, ECV and T2 signal changes, use of ultrasmall superparamagnetic particles of iron oxide (USPIOs) in MRI may confer insights on inflammation *via* increased macrophage activity. USPIOs have been shown to be taken up by macrophages and correlates with plaque inflammation in animal studies (142). In a study of patients with severe carotid stenosis, uptake of USPIOs corresponded to inflamed plaques on histology. Uptake of USPIOs induced areas of signal loss on T_2^*-weighted magnetic resonance imaging within the vessel wall. Whether this can help predict plaque vulnerability in those on checkpoint inhibitors or help identify ICI myocarditis is untested and warrants further investigation (143). However, this has been used clinically and may have potential to distinguish vulnerable plaque from less vulnerable plaque.

Barriers to Advancing Molecular Imaging

For the molecular imaging tracers that are already clinically used, barriers to use include radiation exposure, so deciding who should get the test, when to get it and how often will have to be established. For example, if FAP is associated with ICI myocarditis as a potential early marker, then perhaps it should be obtained when there is suspicion for myocarditis or when troponin becomes positive. Timed with evaluation of this marker for residual disease, it can also help with monitoring of resolution

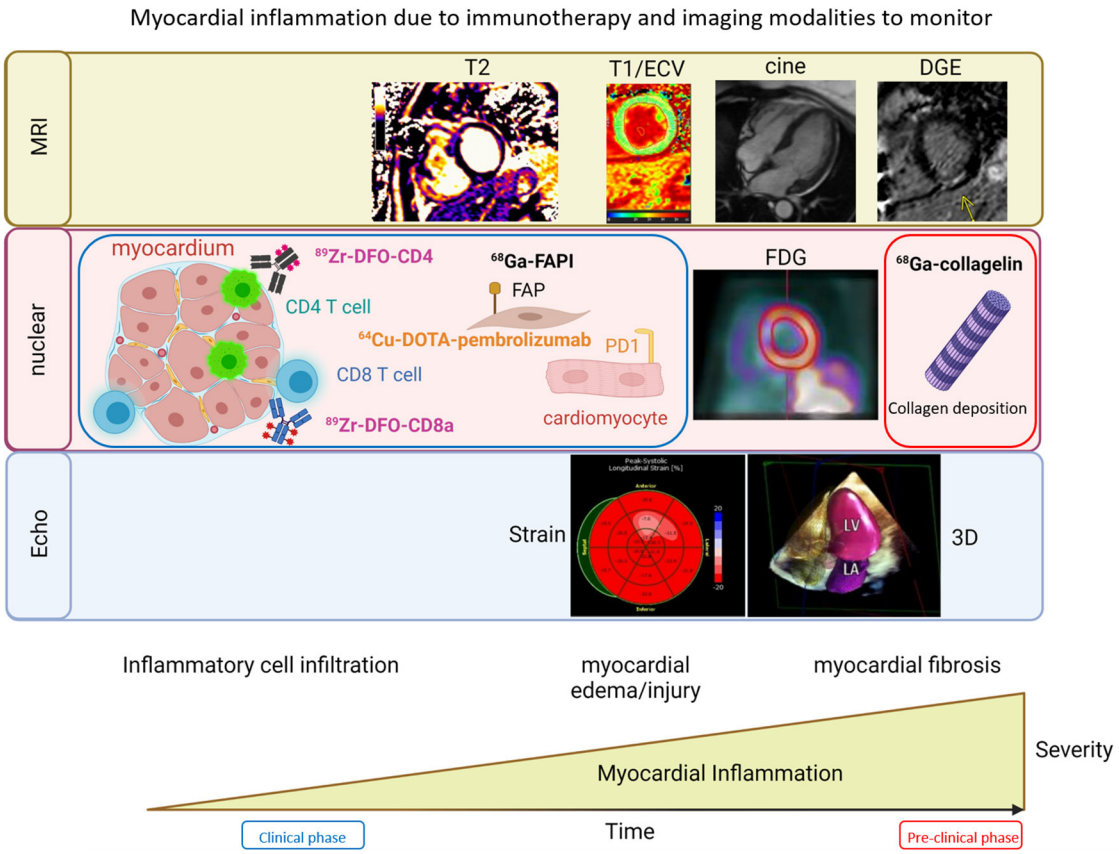

FIGURE 3 | Imaging modalities in the evaluation of immunotherapy related cardiotoxicities. Imaging modalities that can be used to monitor myocardial inflammation due to immunotherapy include: **MRI** (top) using tissue characterization assessments such as T2, T1/ECV, delayed gadolinium enhancement (DGE) and cine to evaluate wall motion and function; **Nuclear Imaging** (middle) approaches involving molecularly targeted probes conjugated to radiotracers facilitating evaluation of CD4 cells with ^{89}Zr-DFO-CD4, CD8 cells with ^{89}Zr-DFO-CD8, early signs of fibrosis with fibroblast activation protein (FAP), expression of PD1 on cardiomyocytes, which can be seen with ^{64}Cu-DOTA-pembrolizumab and may reflect increased risk of checkpoint inhibitor myocarditis, FDG that allows for monitoring of inflammation, and the final stages of inflammation with tissue damage and fibrosis and scar deposition assessed with collagen imaging with ^{68}Ga collagelin; **Echocardiography** (bottom) is able to evaluate regional and global strain to detect signs of chemotherapy related toxicity and myocarditis.

of myocarditis, potentially complementing cardiac MRI or taking place of MRI for those who cannot tolerate MRI, which is usually used for monitoring. Access is another challenge. Access to molecular nuclear studies are often available through large hospital systems and for agents with shorter radioisotope half-lives like Gallium-68 (^{68}Ga) with average half-life of 68 min, an onsite germanium-68/gallium-68 generator is needed along with accompanying nuclear accreditation, thus, more rural hospitals or private practices may have to refer out to larger centers in order to obtain these tests at high volume imaging centers (144). Finally, nuclear studies tend to be more expensive than echo and either on par or more expensive than MRI studies due to the costs associated with radiolabeled probes, thus being able to get these studies approved can also be a challenge for providers even if it is clinically used and indicated. For the molecular tracers that are in the preclinical stage, the usual barriers exist for clinical translation, including establishing safety, a favorable target to noise ratio in humans and correlation with outcomes to achieve FDA approval and ultimately clinical use. For those radiotracers that are already in clinical use for oncology indications, such as FAP, CD4, CD8 and PD1, incidental detection in the heart and correlation with outcomes is possible and can be further explored for future dedicated cardiac imaging and may provide unique clinical value. The power of machine learning, artificial intelligence and big data in evaluation of imaging signals can help unlock patterns that humans may not readily be able to see, such as in a recent evaluation of cardiac fibrosis by T1 imaging by MRI and be able to correlate these imaging findings with outcomes (145).

ROLE OF ARTIFICIAL INTELLIGENCE (AI) AND BIG DATA IN CARDIO-ONCOLOGY AND IMAGING

Overview of Current AI Applications in Cardio-Oncology

Artificial intelligence (AI), through the training of machine and deep learning models, has shown remarkable potential in the prevention and diagnosis of cancer therapeutics-related

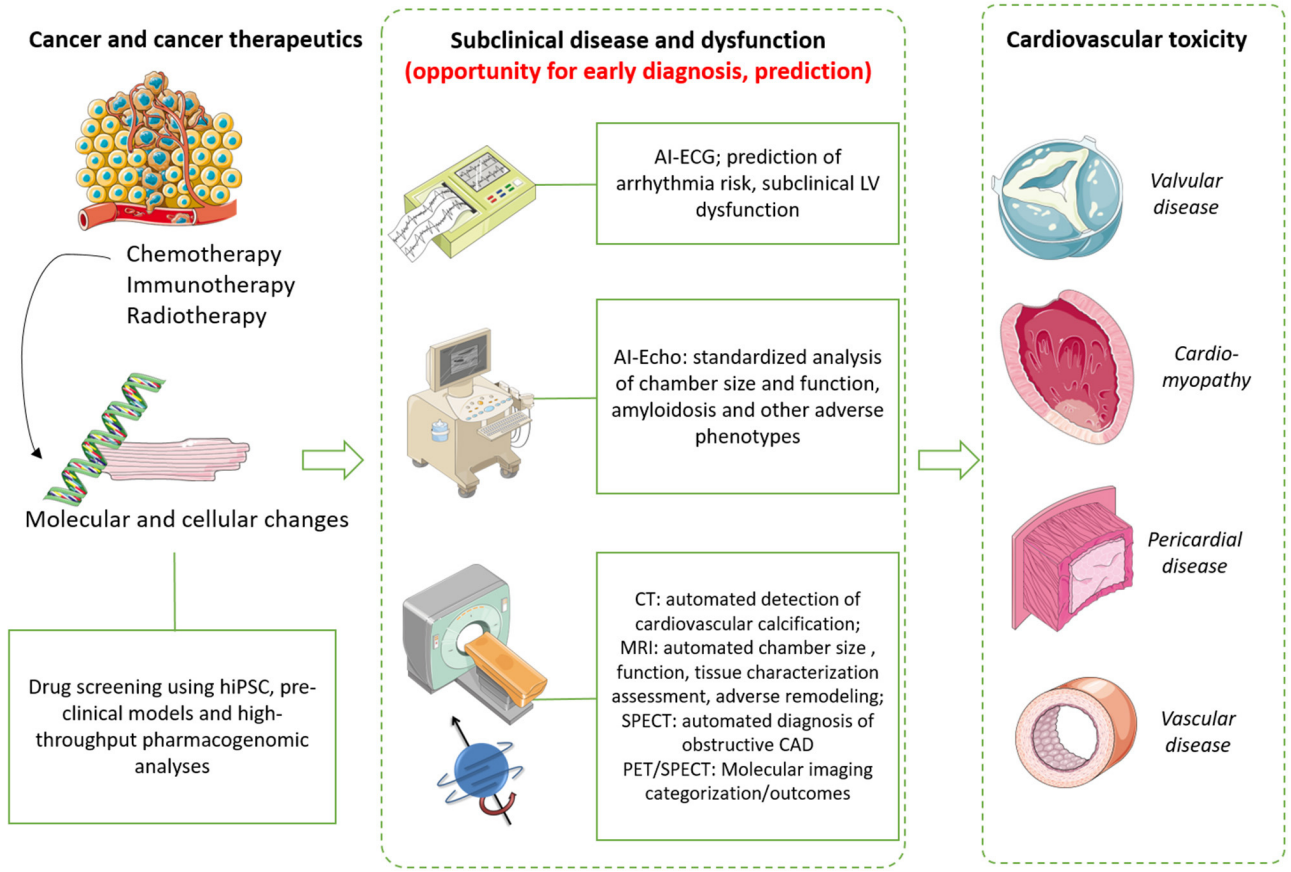

FIGURE 4 | Applications of artificial intelligence, big data in cardio-oncology. Artificial intelligence (AI) can improve our understanding of the early molecular and phenotypic changes that occur prior to the development of clinical cancer therapeutics-related cardiac dysfunction. Machine learning approaches enable high-throughput screening of novel therapeutics using preclinical models, such as induced pluripotent stem cells as well as *in silico* simulations using libraries of drugs and molecular targets. In the clinical setting, AI can improve risk prediction of left ventricular dysfunction, arrhythmias as well as facilitate accurate and standardized assessment of chamber size, function and coronary calcification, all hallmarks of cardiovascular disease that can be caused or exacerbated by cancer therapeutics. Therefore, AI offers an opportunity for early diagnosis and deployment of strategies to prevent the progression to overt cardiovascular disease. Images have been reproduced under a Creative Commons Attribution 3.0 Unported License from smart.servier.com. CAD, coronary artery disease; CT, computed tomography; ECG, electrocardiography; hiPSC, human induced pluripotent stem cell; LV, left ventricular; MRI, magnetic resonance imaging; SPECT, single photon emission computed tomography.

cardiac dysfunction (CTRCD). With applications across all stages of the natural history of CTRCD, AI can assist scientists and physicians in screening for molecular interactions between novel therapeutic agents and the cardiovascular system, as well as detecting subclinical cardiovascular effects prior to the development of overt clinical disease (**Figure 4**).

At the pre-clinical stage, AI techniques have been used for high-throughput screening of cancer agents using a variety of disease models. These range from human induced pluripotent stem cell-derived cardiomyocytes (hiPSC-CMs) exposed to antineoplastic agents, screening of drug libraries to detect agents that interact with channel proteins resulting in QT prolongation, all the way to exome sequencing to identify variants in cardiac injury pathway genes that protect against anthracycline-induced cardiotoxicity and dual transcriptomic and molecular machine learning to predict different types of cardiotoxic response (146–150). Such approaches can de-risk early-stage drug discovery but also contribute to post-marketing surveillance to maximize patient safety. On the same note, pharmacovigilance in cardio-oncology can be assisted by machine learning-guided monitoring of electronic health records that includes patient demographics, echocardiography, laboratory values to detect signals suggestive of increased cardiac risk with specific therapies or practices (151, 152).

For therapies that form the mainstay of cancer therapy, ranging from chemotherapy to immunotherapy and radiation therapy, active surveillance protocols have been proposed and implemented, particularly for therapies with known cardiotoxic effects, such as anthracyclines and HER-2/neu inhibitors. Here, non-invasive cardiac imaging (by means of transthoracic echocardiography and/or magnetic resonance

imaging (MRI)) and electrocardiography (ECG) represent the modalities of choice in the screening of conditions, such as anthracycline-induced cardiotoxicity and immune checkpoint-induced myocarditis (78, 153). Whereas AI applications in cardiovascular imaging have traditionally been developed in the general population, shared phenotypes seen in both CTRCD and non-cancer-related cardiac dysfunction, may extend the use of these technologies to cardio-oncology.

An expanding body of research has in fact demonstrated the ability of deep learning-enhanced interpretation of ECG in screening for and improving the diagnosis of left ventricular dysfunction, essentially functioning as a gatekeeper to the use of more advanced imaging modalities (154). It is notable that this tool was tested in a randomized controlled trial and demonstrated effectiveness in increasing the early diagnosis of decreased left ventricular ejection fraction (LVEF) without an increase in the use of echocardiography (155). Similarly, AI-guided ECG assessment can also predict the future incidence of atrial fibrillation (156). In childhood cancer survivors, machine learning algorithms of baseline and follow up ECGs were able to predict future cardiomyopathy (157). However, whether these results generalize to cardio-oncology, such as in the monitoring of anthracycline or Herceptin mediated cardiotoxicity, or ibrutinib-associated atrial fibrillation remains unknown and should be explored in future studies (158, 159).

AI has contributed to a more efficient and standardized interpretation of several non-invasive cardiovascular imaging modalities. For instance, in the field of transthoracic echocardiography, deep learning video-based models now enables fast and automated calculation of LVEF, with variance that is comparable to that or even lower of a human observer (160, 161). Similarly, combined assessment of ECG- and echocardiography-derived AI models has shown good discrimination in detecting cardiac amyloidosis, a rare disorder that is however more prevalent among patients with cancer compared to the general population (162). Similar approaches can be found in the field of computed tomography (CT) imaging, where automated tools enable an accurate assessment of coronary artery calcium burden, which can be generalized to both gated and non-gated CT scans of the chest, with the latter often used in the staging or monitoring of patients (163, 164). Therefore, such tools may refine a patient's baseline cardiovascular risk and inform risk-benefit discussions about the deployment of potentially cardiotoxic therapies. Finally, automated chamber size quantification, tissue characterization parameters such as T1, T2, extracellular volume and functional indices that can be extracted from cardiac MRI images can have the ability to confer insights into cardiotoxicity including the potential to identify early to late cardiotoxicity mediated by chemotherapy or immunotherapy agents *via* detection of changes in chamber size, abnormal T1, T2 relaxation times and delayed gadolinium enhancement patterns (86, 95, 96, 99, 145, 165–167). Deep learning models have also shown promise in the standardized interpretation of functional nuclear modalities, such as SPECT (single photon emissions computed tomography) myocardial perfusion imaging with good discrimination for the presence of obstructive coronary artery disease (168). However, as these tools become clinically available, prospective validation and possibly recalibration specifically in patients with cancer will be required to ensure their validity and generalizability.

Strengths and Weaknesses of Current Methods and Barriers for Clinical Translation

To better understand the strengths and weaknesses of AI applications in cardio-oncology, one first needs to review key definitions. AI refers to the ability of an automated system to perform tasks that are typically characteristic of human intelligence, such as image and pattern recognition, as well as prediction and classification. *Machine learning* describes the process by which a system gains the ability to perform such tasks. This learning process can be further divided into *supervised* and *unsupervised learning*. The former describes the analysis of labeled datasets with the goal of predicting the label of a given datapoint based on a set of independent predictors. The latter refers to the analysis of unlabeled and unclassified datasets where the algorithm attempts to discover patterns within the data on its own. Algorithms may range from traditional regression models to deep neural networks, consisting of multiple layers of neurons and nodes which operate in a manner similar to the human brain (169, 170). However, independent of the algorithm used, machine learning systems rely on high-quality input to deliver high-quality output. This is where "big data" become relevant, describing the need for datasets that are large enough to ensure adequate variance, remain representative of their original and target populations, enable time-efficient analyses and have been carefully rather opportunistically curated to address a specific question (171).

With those key concepts in mind, some of the limitations of machine learning applications in cardio-oncology become apparent. First, cardiovascular disease is often listed as an exclusion criterion in major cancer trials, thus resulting in under-representation of patients with cardiovascular disease in pivotal cancer trials (172). However, the inclusion of cardiovascular outcomes in cancer trials will be able to help fill this data gap if sufficient baseline and follow up data are acquired (molecular biomarkers, baseline imaging prior to oncologic therapy and follow up that can be used as input). Second, while AI systems can learn patterns in the data, explaining what drives those predictions or establishing causal inference is not a straightforward task (173). Moreover, cancer is a highly heterogeneous condition with multiple molecular, histological, and clinical subtypes that often respond differently to the same therapies (174). Therefore, ensuring generalizability of models across different cancer subtypes, treatments and patient populations may be an insurmountable task without access to vast amounts of accurately labeled data. Third, there is often significant delay in the timing between data collection, model training and the final model deployment. As a result, AI models are often outdated when deployed for clinical use, thus highlighting the need for more efficient pathways that would enable real-time updates. Finally, AI models are bias-prone often reproducing biases that are inherently present in the datasets

used for training. Ensuring representation of diverse patient populations is of paramount importance to promote an equitable impact of AI in healthcare delivery and outcomes (175).

Future Applications of AI in Cardio-Oncology and Molecular Imaging

With careful consideration of these limitations, AI has the potential to advance cardio-oncology in many different directions. Radiomic applications, which extract several metrics based on the shape, dimensions, signal density and spatial interrelationship of voxel signals in a given tissue, have been found to be superior to conventional readouts in reflecting tissue composition, as well as metabolic or inflammatory activity (176–178). In fact, some of the most exciting applications of AI lie beyond structural imaging in molecular imaging. In the recent past, deep learning and generative adversarial networks have successfully reconstructed PET images directly from raw sinogram data effectively maximizing image quality (179, 180). In other applications, AI tools have generated full-dose PET images from low-dose images, thus maximizing signal-to-noise ratio at lower radiation levels (181, 182). In another example, convolutional neural networks have enabled the development of cMRI virtual native imaging technologies which generate late gadolinium enhancement-like images in an accurate and reproducible manner without the need for contrast administration (183). Though originally developed in patients with hypertrophic cardiomyopathy, this technology may be of value in cardio-oncology and the monitoring of ICI-myocarditis. Further, for molecular imaging targeting biomarkers like FAP and PD1, these are already used clinically in oncology to monitor for residual disease and assess response to immunotherapy respectively, thus if the heart is captured in existing data sets, AI/ML can help to predict whether the presence of these markers are associated with adverse cardiovascular outcomes. Coupled with improvements in the speed and accuracy of segmentation algorithms, AI can accelerate the clinical deployment of molecular imaging approaches in the timely detection of cardiovascular toxicity (184).

CONCLUSIONS

Imaging advances, particularly molecularly targeted imaging modalities may help detect cardiotoxicities at the earliest stages with greater specificity, shed light on mechanism as well as response to cardioprotective medications such as beta blockers, angiotensin converting enzyme inhibitors, etc. Newer MRI metabolic evaluation techniques such as hyperpolarized MRI may allow for a non-invasive approach to evaluate cardiac metabolism in real time. To complement imaging studies, use of AI and big data on imaging parameters and forthcoming molecular imaging datasets, in addition to patient demographics may help predict or detect cardiovascular toxicities at their earliest stages. Inclusion of diverse patient cohorts as well as cardiovascular parameters/biomarkers and imaging in cancer trials can enable AI/Ml to increase accurate categorization as well prediction models in cardio-oncology patients. Additional research in these areas and advancing animal studies toward human studies may further help improve cardiovascular outcomes in cancer patients.

AUTHOR CONTRIBUTIONS

JK led the development of the manuscript, writing, and generation of figures. EO contributed to writing and generation of figures. MH contributed to writing, assisting with editing and organizing of the manuscript. AJS oversaw the writing, editing, and review of the manuscript. All authors contributed to the article and approved the submitted version.

FUNDING

This work was funded by NIH R01 HL113352, R01 HL121226, R01 HL123949, and R01 HL154345 associated with AJS.

ACKNOWLEDGMENTS

Biorender was used to create **Figures 1–3**.

REFERENCES

1. Weir HK, Thompson TD, Stewart SL, White MC. Cancer incidence projections in the United States between 2015 and 2050. *Prevent Chronic Dis.* (2021) 18:E59. doi: 10.5888/pcd18.210006
2. Eckstein N, Röper L, Haas B, Potthast H, Hermes U, Unkrig C, et al. Clinical pharmacology of tyrosine kinase inhibitors becoming generic drugs: the regulatory perspective. *J Exp Clin Cancer Res.* (2014) 33:1. doi: 10.1186/1756-9966-33-15
3. Vito A, Salem O, El-Sayes N, MacFawn IP, Portillo AL, Milne K, et al. Immune checkpoint blockade in triple negative breast cancer influenced by B cells through myeloid-derived suppressor cells. *Commun Biol.* (2021) 4:1–19. doi: 10.1038/s42003-021-02375-9
4. Schmid P, Adams S, Rugo HS, Schneeweiss A, Barrios CH, Iwata H, et al. Atezolizumab and nab-paclitaxel in advanced triple-negative breast cancer. *New Engl J Med.* (2018) 379:2109–21. doi: 10.1056/NEJMoa1809615
5. Siegel RL, Miller KD, Fuchs HE, Jemal A. Cancer statistics, 2021. *CA Cancer J Clin.* (2021) 71:9–29. doi: 10.3322/caac.21654
6. Vaddepally RK, Kharel P, Pandey R, Garje R, Chandra AB. Review of indications of FDA-approved immune checkpoint inhibitors per NCCN guidelines with the level of evidence. *Cancers.* (2020) 12:738. doi: 10.3390/cancers12030738
7. Guha A, Caraballo C, Jain P, Miller PE, Owusu-Guha J, Clark KAA, et al. Outcomes in patients with anthracycline-induced cardiomyopathy undergoing left ventricular assist devices implantation. *ESC Heart Failure.* (2021) 8:2866–75. doi: 10.1002/ehf2.13362
8. Russo M, della Sala A, Tocchetti CG, Porporato PE, Ghigo A. Metabolic aspects of anthracycline cardiotoxicity. *Curr Treat Options Oncol.* (2021) 22:1–21. doi: 10.1007/s11864-020-00812-1
9. Zhang S, Liu X, Bawa-Khalfe T, Lu LS Lyu YL, Liu LF, et al. Identification of the molecular basis of doxorubicin-induced cardiotoxicity. *Nat Med.* (2012) 18:1639–42. doi: 10.1038/nm.2919
10. Rosen SD. Trastuzumab induced cardiomyopathy: Wider implications for cardio-oncology. *Heart.* (2013) 99:599–600. doi: 10.1136/heartjnl-2012-303495

11. Hu Y, Sun B, Zhao B, Mei D, Gu Q, Tian Z. Cisplatin-induced cardiotoxicity with midrange ejection fraction: a case report and review of the literature. *Medicine.* (2018) 97:e13807. doi: 10.1097/MD.0000000000013807
12. Dhesi S, Chu MP, Blevins G, Paterson I, Larratt L, Oudit GY, et al. Cyclophosphamide-induced cardiomyopathy. *J Investig Med High Impact Case Rep.* (2013) 1:2324709613480346. doi: 10.1177/2324709613480346
13. Chong JH, Ghosh AK. Coronary artery vasospasm induced by 5-fluorouracil: proposed mechanisms, existing management options and future directions. *Interv Cardiol Rev.* (2019) 14:89. doi: 10.15420/icr.2019.12
14. Lestuzzi C, Vaccher E, Talamini R, Lleshi A, Meneguzzo N, Viel E, et al. Effort myocardial ischemia during chemotherapy with 5-fluorouracil: an underestimated risk. *Ann Oncol.* (2014) 25:1059–64. doi: 10.1093/annonc/mdu055
15. Hirsh J. Risk of thrombosis with lenalidomide and its prevention with aspirin. *Chest.* (2007) 131:275–7. doi: 10.1378/chest.06-2360
16. Li A, Wu Q, Warnick G, Li S, Libby EN, Garcia DA, et al. The incidence of thromboembolism for lenalidomide versus thalidomide in older patients with newly diagnosed multiple myeloma. *Ann Hematol.* (2020) 99:121–6. doi: 10.1007/s00277-019-03860-2
17. Alahmari AK, Almalki ZS, Alahmari AK, Guo JJ. Thromboembolic events associated with bevacizumab plus chemotherapy for patients with colorectal cancer: a meta-analysis of randomized controlled trials. *Am Health Drug Benefits.* (2016) 9:221.
18. Syrigos KN, Karapanagiotou E, Boura P, Manegold C, Harrington K. Bevacizumab-induced hypertension: pathogenesis and management. *BioDrugs.* (2011) 25:159–69. doi: 10.2165/11590180-000000000-00000
19. Khalid S, Yasar S, Khalid A, Spiro T, Haddad A, Daw H. Management of atrial fibrillation in patients on ibrutinib: a cleveland clinic experience. *Cureus.* (2018) 10:e2701. doi: 10.7759/cureus.2701
20. Uraizee I, Cheng S, Moslehi J. Reversible cardiomyopathy associated with sunitinib and sorafenib. *New Engl J Med.* (2011) 365:1649–50. doi: 10.1056/NEJMc1108849
21. Chen MH, Kerkelä R, Force T. Mechanisms of cardiac dysfunction associated with tyrosine kinase inhibitor cancer therapeutics. *Circulation.* (2008) 118:84–95. doi: 10.1161/CIRCULATIONAHA.108.776831
22. Siegel RL, Miller KD, Jemal A. Cancer statistics, 2019. *CA Cancer J Clin.* (2019) 69:7–34. doi: 10.3322/caac.21551
23. Haslam A, Gill J, Prasad V. Estimation of the percentage of US patients with cancer who are eligible for immune checkpoint inhibitor drugs. *JAMA Netw Open.* (2020) 3:e200423. doi: 10.1001/jamanetworkopen.2020.0423
24. Bar J, Markel G, Gottfried T, Percik R, Leibowitz-Amit R, Berger R, et al. Acute vascular events as a possibly related adverse event of immunotherapy: a single-institute retrospective study. *Eur J Cancer.* (2019) 120:122–31. doi: 10.1016/j.ejca.2019.06.021
25. Mahmood SS, Fradley MG, Cohen JV, Nohria A, Reynolds KL, Heinzerling LM, et al. Myocarditis in patients treated with immune checkpoint inhibitors. *J Am Coll Cardiol.* (2018) 71:1755–64. doi: 10.1016/j.jacc.2018.02.037
26. Alvi RM, Frigault MJ, Fradley MG, Jain MD, Mahmood SS, Awadalla M, et al. Cardiovascular events among adults treated with chimeric antigen receptor T-cells (CAR-T). *J Am Coll Cardiol.* (2019) 74:3099–108. doi: 10.1016/j.jacc.2019.10.038
27. Kwan JM, Henry ML, Cook K, Higgins A, Cuomo J, Foss F, et al. Adverse cardiovascular events in patients treated with mogamulizumab. *Am Heart J Plus Cardiol Res Pract.* (2021) 9:100049. doi: 10.1016/j.ahjo.2021.100049
28. Kwan JM, Odanovic N, Arbune A, Higgins A, Henry M, Greif D, et al. Mogamulizumab-associated acute myocarditis in a patient with T-Cell lymphoma. *JACC: Case Rep.* (2021) 3:1018–23. doi: 10.1016/j.jaccas.2021.04.001
29. Chatterjee K, Zhang J, Honbo N, Karliner JS. Doxorubicin cardiomyopathy. *Cardiology.* (2010) 115:155–62. doi: 10.1159/000265166
30. Carrio I, Estorch M, Berna L, Lopez-Pousa J, Tabernero J, Torres G. Indium-111-antimyosin and iodine-123-MIBG studies in early assessment of doxorubicin cardiotoxicity. *J Nuclear Med.* (1995) 36:2044–9.
31. Boutagy NE, Feher A, Pfau D, Liu Z, Guerrera NM, Freeburg LA, et al. Dual angiotensin receptor-neprilysin inhibition with sacubitril/valsartan attenuates systolic dysfunction in experimental doxorubicin-induced cardiotoxicity. *JACC: CardioOncol.* (2020) 2:774–87. doi: 10.1016/j.jaccao.2020.09.007
32. Bhattacharya S, Liu X. jie, Senior R, Jain D, Leppo JA, Lahiri A. 111In antimyosin antibody uptake is related to the age of myocardial infarction. *Am Heart J.* (1991) 122:1583–7. doi: 10.1016/0002-8703(91)90274-L
33. Bennink RJ, van den Hoff MJ, van Hemert FJ, de Bruin KM, Spijkerboer AL, Vanderheyden JL, et al. Annexin V imaging of acute doxorubicin cardiotoxicity (apoptosis) in rats. *J Nuclear Medicine.* (2004) 45:842–8. Available online at: https://jnm.snmjournals.org/content/45/5/842/tab-article-info
34. Blankenberg FG, Kalinyak J, Liu L, Koike M, Cheng D, Goris ML, et al. 99mTc-HYNIC-annexin V SPECT imaging of acute stroke and its response to neuroprotective therapy with anti-Fas ligand antibody. *Eur J Nucl Med Mol Imag.* (2006) 33:566–74. doi: 10.1007/s00259-005-0046-6
35. Boutagy NE, Wu J, Cai Z, Zhang W, Booth CJ, Kyriakides TC, et al. In vivo reactive oxygen species detection with a novel positron emission tomography tracer, 18F-DHMT, allows for early detection of anthracycline-induced cardiotoxicity in rodents. *JACC Basic Transl Sci.* (2018) 3:378–90. doi: 10.1016/j.jacbts.2018.02.003
36. Sivapackiam J, Kabra S, Speidel S, et al. 68Ga-Galmydar: a PET imaging tracer for noninvasive detection of Doxorubicin-induced cardiotoxicity. *PLoS ONE.* (2019) 14:e0215579. doi: 10.1371/journal.pone.0215579
37. Rider OJ, Tyler DJ. Clinical implications of cardiac hyperpolarized magnetic resonance imaging. *J Cardiovasc Magn Reson.* (2013) 15:1–9. doi: 10.1186/1532-429X-15-93
38. Timm KN, Perera C, Ball V, Henry JA, Miller JJ, Kerr M, et al. Early detection of doxorubicin-induced cardiotoxicity in rats by its cardiac metabolic signature assessed with hyperpolarized MRI. *Commun Biol.* (2020) 3:1–10. doi: 10.1038/s42003-020-01440-z
39. Cunningham CH, Lau JYC, Chen AP, Geraghty BJ, Perks WJ, Roifman I, et al. Hyperpolarized 13C metabolic MRI of the human heart: initial experience. *Circ Res.* (2016) 119:1177–82. doi: 10.1161/CIRCRESAHA.116.309769
40. Inayat F, Masab M, Gupta S, Ullah W. New drugs and new toxicities: pembrolizumab-induced myocarditis. *BMJ Case Reports.* (2018) 2018:bcr-2017. doi: 10.1136/bcr-2017-223252
41. Yun S, Vincelette ND, Mansour I, Hariri D, Motamed S. Late onset ipilimumab-induced pericarditis and pericardial effusion: a rare but life threatening complication. *Case Rep Oncol Med.* (2015) 2015:1–5. doi: 10.1155/2015/794842
42. Chen DY, Huang WK, Wu VC, Chang WC, Chen JS, Chuang CK, et al. Cardiovascular toxicity of immune checkpoint inhibitors in cancer patients: A review when cardiology meets immuno-oncology. *J Formosan Med Assoc.* (2020) 119:1461–75. doi: 10.1016/j.jfma.2019.07.025
43. Drobni ZD, Alvi RM, Taron J, Zafar A, Murphy SP, Rambarat PK, et al. Association between immune checkpoint inhibitors with cardiovascular events and atherosclerotic plaque. *Circulation.* (2020) 6:877–85. doi: 10.1161/CIRCULATIONAHA.120.049981
44. Kristensen LK, Fröhlich C, Christensen C, Melander MC, Poulsen TT, Galler GR, et al. CD4+ and CD8a+ PET imaging predicts response to novel PD-1 checkpoint inhibitor: studies of Sym021 in syngeneic mouse cancer models. *Theranostics.* (2019) 9:8221. doi: 10.7150/thno.37513
45. Finke D, Heckmann MB, Herpel E, Katus HA, Haberkorn U, Leuschner F, et al. Early detection of checkpoint inhibitor-associated myocarditis using 68Ga-FAPI PET/CT. *Frontiers in Cardiovasc Med.* (2021) 8:54. doi: 10.3389/fcvm.2021.614997
46. Désogère P, Tapias LF, Hariri LP, Rotile NJ, Rietz TA, Probst CK, et al. Type I collagen-Targeted PET probe for pulmonary fibrosis detection and staging in preclinical models. *Sci Transl Med.* (2017) 9:eaaf4696. doi: 10.1126/scitranslmed.aaf4696
47. The cancer drug imatinib can cause cardiotoxicity. *Nat Clin Pract Cardiovasc Med.* (2007) 4:8. doi: 10.1038/ncpcardio0699
48. Cortes JE, Jean Khoury H, Kantarjian H, Brümmendorf TH, Mauro MJ, Matczak E, et al. Long-term evaluation of cardiac and vascular toxicity in patients with Philadelphia chromosome-positive leukemias treated with bosutinib. *Am J Hematol.* (2016) 91:606–16. doi: 10.1002/ajh.24360
49. Blasi F, Oliveira BL, Rietz TA, Rotile NJ, Naha PC, Cormode DP, et al. Multisite thrombus imaging and fibrin content estimation with a single whole-body PET scan in rats. *Arterioscler Thromb Vasc Biol.* (2015) 35:2114–21. doi: 10.1161/ATVBAHA.115.306055

50. Case Medical Research. PET. Fibrin Imaging of DVT and PE. Available online at: https://wwwclinicaltrialsgov/. (2019).
51. Haguet H, Bouvy C, Delvigne AS, Modaffari E, Wannez A, Sonveaux P, et al. The risk of arterial thrombosis in patients with chronic myeloid leukemia treated with second and third generation BCR-ABL tyrosine kinase inhibitors may be explained by their impact on endothelial cells: an in-vitro study. *Front Pharmacol.* (2020) 11:1007. doi: 10.3389/fphar.2020.01007
52. Abu Rmilah AA, Lin G, Herrmann J. Risk of QTc interval prolongation among cancer patients treated with tyrosine kinase inhibitors. *J Clin Oncol.* (2019) 37(15_suppl):3160–7. doi: 10.1200/JCO.2019.37.15_suppl.3033
53. Chae SY, Kwon TW, Jin S, Kwon SU, Sung C, Oh SJ, et al. A phase 1, first-in-human study of 18 F-GP1 positron emission tomography for imaging acute arterial thrombosis. *EJNMMI Res.* (2019) 9:1–10. doi: 10.1186/s13550-018-0471-8
54. Merkulova A, Mitchell SC, Stavrou EX, Forbes GL, Schmaier AH. Ponatinib treatment promotes arterial thrombosis and hyperactive platelets. *Blood Adv.* (2019) 3:2312. doi: 10.1182/bloodadvances.2019000034
55. Singh AP, Glennon MS, Umbarkar P, Gupte M, Galindo CL, Zhang Q, et al. Ponatinib-induced cardiotoxicity: delineating the signalling mechanisms and potential rescue strategies. *Cardiovasc Res.* (2019) 115:966–77. doi: 10.1093/cvr/cvz006
56. Chu TF, Rupnick MA, Kerkela R, Dallabrida SM, Zurakowski D, Nguyen L, et al. Cardiotoxicity associated with tyrosine kinase inhibitor sunitinib. *Lancet.* (2007) 370:2011–9. doi: 10.1016/S0140-6736(07)61865-0
57. Kloth JS, Pagani A, Verboom MC, Malovini A, Napolitano C, Kruit WH, et al. Incidence and relevance of QTc-interval prolongation caused by tyrosine kinase inhibitors. *Br J Cancer.* (2015) 112:1011–6. doi: 10.1038/bjc.2015.82
58. Tarkin JM, Joshi FR, Evans NR, Chowdhury MM, Figg NL, Shah AV, et al. Detection of atherosclerotic inflammation by 68Ga-DOTATATE PET compared to [18F]FDG PET imaging. *J Am Coll Cardiol.* (2017) 69:1774–91. doi: 10.1016/j.jacc.2017.01.060
59. Sanli Y, Garg I, Kandathil A, Kendi T, Zanetti MJ, Kuyumcu S, et al. Neuroendocrine tumor diagnosis and management: 68 Ga-DOTATATE PET/CT. *Am J Roentgenol.* (2018) 211:267–77. doi: 10.2214/AJR.18.19881
60. Qi WX, Shen Z, Lin F, Sun YJ, Min DL, Tang LN, et al. Incidence and risk of hypertension with vandetanib in cancer patients: A systematic review and meta-analysis of clinical trials. *Br J Clin Pharmacol.* (2013) 75:919–30. doi: 10.1111/j.1365-2125.2012.04417.x
61. Zang J, Wu S, Tang L, Xu X, Bai J, Ding C, et al. Incidence and risk of QTc interval prolongation among cancer patients treated with vandetanib: a systematic review and meta-analysis. *PLoS ONE.* (2012) 7:e30353. doi: 10.1371/journal.pone.0030353
62. Ewer MS, Patel K, O'Brien D, Lorence RM. Cardiac safety of afatinib: a review of data from clinical trials. *Cardio-Oncology.* (2015) 1:1–8. doi: 10.1186/s40959-015-0006-7
63. Ding S, Long F, Jiang S. Acute myocardial infarction following erlotinib treatment for NSCLC: a case report. *Oncol Lett.* (2016) 11:4240–4. doi: 10.3892/ol.2016.4508
64. Coppola C, Rienzo A, Piscopo G, Barbieri A, Arra C, Maurea N. Management of QT prolongation induced by anti-cancer drugs: target therapy and old agents. Different algorithms for different drugs. *Cancer Treatment Rev.* (2018) 63:135–43. doi: 10.1016/j.ctrv.2017.11.009
65. Omori S, Oyakawa T, Naito T, Takahashi T. Gefitinib-induced cardiomyopathy in epidermal growth receptor-mutated NSCLC. *J Thoracic Oncol.* (2018) 13:e207–8. doi: 10.1016/j.jtho.2018.05.020
66. Kadowaki H, Ishida J, Akazawa H, Yagi H, Saga-Kamo A, Umei M, et al. Axitinib induces and aggravates hypertension regardless of prior treatment with tyrosine kinase inhibitors. *Circul Rep.* (2021) 3:CR21. doi: 10.1253/circrep.CR-21-0008
67. Tougaard RS, Hansen ES, Laustsen C, Lindhardt J, Schroeder M, Bøtker HE, et al. Acute hypertensive stress imaged by cardiac hyperpolarized [1-13C]pyruvate magnetic resonance. *Magn Reson Med.* (2018) 80:2053–61. doi: 10.1002/mrm.27164
68. Guan J, Zhang M. Cardiotoxicity of anthracycline-free targeted oncological therapies in HER2-positive breast cancer (Review). *Oncol Lett.* (2021) 21:1. doi: 10.3892/ol.2020.12361
69. Sengupta PP, Northfelt DW, Gentile F, Zamorano JL, Khandheria BK. Trastuzumab-induced cardiotoxicity: heart failure at the crossroads. *Mayo Clinic Proc.* (2008) 83:197–203. doi: 10.1016/S0025-6196(11)60840-9
70. Lenihan D, Suter T, Brammer M, Neate C, Ross G, Baselga J. Pooled analysis of cardiac safety in patients with cancer treated with pertuzumab. *Ann Oncol.* (2012) 23:791–800. doi: 10.1093/annonc/mdr294
71. Yildirim M, Parlak C, Sezer C, Eryilmaz R, Kaya C, Yildiz M. Coronary vasospasm secondary to 5-fluorouracil and its management: case report. *Eurasian J Med.* (2011) 43:54. doi: 10.5152/eajm.2011.11
72. Curigliano G, Cardinale D, Dent S, Criscitiello C, Aseyev O, Lenihan D, et al. Cardiotoxicity of anticancer treatments: epidemiology, detection, and management. *CA Cancer J Clin.* (2016) 66:309–25. doi: 10.3322/caac.21341
73. Tu CM, Chu KM, Yang SP, Cheng SM, Wang W. Trastuzumab (Herceptin)-associated cardiomyopathy presented as new onset of complete left bundle-branch block mimicking acute coronary syndrome: a case report and literature review. *Am J Emerg Med.* (2009) 27:903. doi: 10.1016/j.ajem.2008.11.012
74. Mohan N, Jiang J, Dokmanovic M, Wu WJ. Trastuzumab-mediated cardiotoxicity: current understanding, challenges, and frontiers. *Antibody Therap.* (2018) 1:13–7. doi: 10.1093/abt/tby003
75. Celutkiene J, Pudil R, López-Fernández T, Grapsa J, Nihoyannopoulos P, Bergler-Klein J, et al. Role of cardiovascular imaging in cancer patients receiving cardiotoxic therapies: a position statement on behalf of the Heart Failure Association (HFA), the European Association of Cardiovascular Imaging (EACVI) and the Cardio-Oncology Council of the European Society of Cardiology (ESC). *Eur J Heart Fail.* (2020) 22:1504–24. doi: 10.1002/ejhf.1957
76. Gripp E de A, de Oliveira GE, Feijó LA, Garcia MI, Xavier SS, de Sousa AS. Global longitudinal strain accuracy for cardiotoxicity prediction in a cohort of breast cancer patients during anthracycline and/or trastuzumab treatment. *Arq Bras Cardiol.* (2018) 110:140–50. doi: 10.5935/abc.20180021
77. Curigliano G, Cardinale D, Suter T, Plataniotis G, De Azambuja E, Sandri MT, et al. Cardiovascular toxicity induced by chemotherapy, targeted agents and radiotherapy: ESMO clinical practice guidelines. *Ann Oncol.* (2012) 23(SUPPL. 7):vii155–66. doi: 10.1093/annonc/mds293
78. Plana JC, Galderisi M, Barac A, Ewer MS, Ky B, Scherrer-Crosbie M, et al. Expert consensus for multimodality imaging evaluation of adult patients during and after cancer therapy: a report from the American Society of Echocardiography and the European Association of Cardiovascular Imaging. *Eur Heart J Cardiovasc Imaging.* (2014) 15:1603–93. doi: 10.1093/ehjci/jeu192
79. Schneider BJ, Naidoo J, Santomasso BD, Lacchetti C, Adkins S, Anadkat M, et al. Management of immune-related adverse events in patients treated with immune checkpoint inhibitor therapy: ASCO guideline update. *J Clin Oncol.* (2021) 39:4073–126. doi: 10.1200/JCO.21.01440
80. Ferreira VM, Schulz-Menger J, Holmvang G, Kramer CM, Carbone I, Sechtem U, et al. Cardiovascular magnetic resonance in nonischemic myocardial inflammation: expert recommendations. *J Am Coll Cardiol.* (2018) 72:3158–76. doi: 10.1016/j.jacc.2018.09.072
81. Biersmith MA, Tong MS, Guha A, Simonetti OP, Addison D. Multimodality cardiac imaging in the era of emerging cancer therapies. *J Am Heart Assoc.* (2020) 9:e013755. doi: 10.1161/JAHA.119.013755
82. Lambert J, Lamacie M, Thampinathan B, Altaha MA, Esmaeilzadeh M, Nolan M, et al. Variability in echocardiography and MRI for detection of cancer therapy cardiotoxicity. *Heart.* (2020) 106:817–23. doi: 10.1136/heartjnl-2019-316297
83. Salerno M, Sharif B, Arheden H, Kumar A, Axel L, Li D, et al. Recent advances in cardiovascular magnetic resonance techniques and applications. *Circ Cardiovasc Imaging.* (2017) 47:e003951. doi: 10.1161/CIRCIMAGING.116.003951
84. Neilan TG, Coelho-Filho OR, Shah RV, Feng JH, Pena-Herrera D, Mandry D, et al. Myocardial extracellular volume by cardiac magnetic resonance imaging in patients treated with anthracycline-based chemotherapy. *Am J Cardiol.* (2013) 111:717–22. doi: 10.1016/j.amjcard.2012.11.022
85. Jordan JH, Vasu S, Morgan TM, D'Agostino RB Jr, Meléndez GC, Hamilton CA, et al. Anthracycline-associated T1 mapping characteristics are elevated independent of the presence of cardiovascular comorbidities

in cancer survivors. *Circul Cardiovasc Imag.* (2016) 9:e004325. doi: 10.1161/CIRCIMAGING.115.004325
86. Lustberg MB, Reinbolt R, Addison D, Ruppert AS, Moore S, Carothers S, et al. Early detection of anthracycline-induced cardiotoxicity in breast cancer survivors with T2 cardiac magnetic resonance. *Circul Cardiovasc Imag.* (2019) 12:e008777. doi: 10.1161/CIRCIMAGING.118.008777
87. Fallah-Rad N, Lytwyn M, Fang T, Kirkpatrick I, Jassal DS. Delayed contrast enhancement cardiac magnetic resonance imaging in trastuzumab induced cardiomyopathy. *J Cardiovasc Magn Reson.* (2008) 10:1–4. doi: 10.1186/1532-429X-10-5
88. Thavendiranathan P, Poulin F, Lim KD, Plana JC, Woo A, Marwick TH. Use of myocardial strain imaging by echocardiography for the early detection of cardiotoxicity in patients during and after cancer chemotherapy: a systematic review. *J Am College Cardiol.* (2014) 63(25 PART A):2751–68. doi: 10.1016/j.jacc.2014.01.073
89. Oikonomou EK, Kokkinidis DG, Kampaktsis PN, Amir EA, Marwick TH, Gupta D, et al. Assessment of prognostic value of left ventricular global longitudinal strain for early prediction of chemotherapy-induced cardiotoxicity: a systematic review and meta-analysis. *JAMA Cardiol.* (2019) 4:1007–18. doi: 10.1001/jamacardio.2019.2952
90. Löffler AI, Salerno M. Cardiac MRI for the evaluation of oncologic cardiotoxicity. *J Nuclear Cardiol.* (2018) 25:2148–58. doi: 10.1007/s12350-018-1293-9
91. Drafts BC, Twomley KM, D'Agostino R, Lawrence J, Avis N, Ellis LR, et al. Low to moderate dose anthracycline-based chemotherapy is associated with early noninvasive imaging evidence of subclinical cardiovascular disease. *JACC: Cardiovasc Imag.* (2013) 6:877–85. doi: 10.1016/j.jcmg.2012.11.017
92. Jordan JH, Sukpraphrute B, Meléndez GC, Jolly MP, D'Agostino RB, Hundley WG. Early myocardial strain changes during potentially cardiotoxic chemotherapy may occur as a result of reductions in left ventricular end-diastolic volume: the need to interpret left ventricular strain with volumes. *Circulation.* (2017) 135:2575–7. doi: 10.1161/CIRCULATIONAHA.117.027930
93. Giusca S, Korosoglou G, Montenbruck M, Geršak B, Schwarz AK, Esch S, et al. Multiparametric early detection and prediction of cardiotoxicity using myocardial strain, T1 and T2 mapping, and biochemical markers: a longitudinal cardiac resonance imaging study during 2 years of follow-up. *Circul Cardiovasc Imag.* (2021) 14:e012459. doi: 10.1161/CIRCIMAGING.121.012459
94. Steen H, Montenbruck M, Gersak B, Schwarz AK, Esch S, Kelle S, et al. Intramyocardial fast-SENC is less impacted by compensatory mechanisms while monitoring cardiotoxic effects of chemotherapy than echocardiography and conventional CMR: the PREFECT study. *Eur Heart J.* (2020) 41(Supplement_2): ehaa946–1222. doi: 10.1093/ehjci/ehaa946.1222
95. D'Souza M, Nielsen D, Svane IM, Iversen K, Rasmussen PV, Madelaire C, et al. The risk of cardiac events in patients receiving immune checkpoint inhibitors: a nationwide Danish study. *Eur Heart J.* (2021) 42:1621–31. doi: 10.1093/eurheartj/ehaa884
96. Zhang L, Awadalla M, Mahmood SS, Nohria A, Hassan MZ, Thuny F, et al. Cardiovascular magnetic resonance in immune checkpoint inhibitor-associated myocarditis. *Eur Heart J.* (2020) 41:1733–43. doi: 10.1093/eurheartj/ehaa051
97. Faron A, Isaak A, Mesropyan N, Reinert M, Schwab K, Sirokay J, et al. Cardiac MRI depicts immune checkpoint inhibitor–induced myocarditis: a prospective study. *Radiology.* (2021) 301:602–9. doi: 10.1148/radiol.2021210814
98. Arbune A, Soufer A, Baldassarre LA. Clinical and advanced MRI techniques for detection of checkpoint inhibitor associated myocarditis. *Curr Cardiovasc Imag Rep.* (2020) 13:1–10. doi: 10.1007/s12410-019-9521-5
99. Higgins AY, Arbune A, Soufer A, Ragheb E, Kwan JM, Lamy J, et al. Left ventricular myocardial strain and tissue characterization by cardiac magnetic resonance imaging in immune checkpoint inhibitor associated cardiotoxicity. *PLoS ONE.* (2021) 16:e0246764. doi: 10.1371/journal.pone.0246764
100. Palaskas N, Lopez-Mattei J, Durand JB, Iliescu C, Deswal A. Immune checkpoint inhibitor myocarditis: pathophysiological characteristics, diagnosis, and treatment. *J Am Heart Assoc.* (2020) 9:e013757. doi: 10.1161/JAHA.119.013757
101. Mukhopadhyay P, Rajesh M, Bátkai S, Kashiwaya Y, Hasko G, Liaudet L, et al. Role of superoxide, nitric oxide, and peroxynitrite in doxorubicin-induced cell death in vivo and in vitro. *Am J Physiol Heart Circul Physiol.* (2009) 296:H1466–83. doi: 10.1152/ajpheart.00795.2008
102. Guglin M, Krischer J, Tamura R, Fink A, Bello-Matricaria L, McCaskill-Stevens W, et al. Randomized trial of lisinopril versus carvedilol to prevent trastuzumab cardiotoxicity in patients with breast cancer. *J Am Coll Cardiol.* (2019) 73:2859–68. doi: 10.1016/j.jacc.2019.03.495
103. Sawicki KT, Sala V, Prever L, Hirsch E, Ardehali H, Ghigo A. Preventing and treating anthracycline cardiotoxicity: new insights. *Annu Rev Pharmacol Toxicol.* (2021) 61:3–8. doi: 10.1146/annurev-pharmtox-030620-104842
104. Räsänen M, Degerman J, Nissinen TA, Miinalainen I, Kerkelä R, Siltanen A, et al. VEGF-B gene therapy inhibits doxorubicin-induced cardiotoxicity by endothelial protection. *Proc Natl Acad Sci USA.* (2016) 113:13144–9. doi: 10.1073/pnas.1616168113
105. Dash R, Chung J, Chan T, Yamada M, Barral J, Nishimura D, et al. A molecular MRI probe to detect treatment of cardiac apoptosis in vivo. *Magn Reson Med.* (2011) 66:1152–62. doi: 10.1002/mrm.22876
106. Reinfeld BI, Madden MZ, Wolf MM, Chytil A, Bader JE, Patterson AR, et al. Cell-programmed nutrient partitioning in the tumour microenvironment. *Nature.* (2021) 593:282–8. doi: 10.1038/s41586-021-03442-1
107. Makunts T, Saunders IM, Cohen I. v., Li M, Moumedjian T, Issa MA, et al. Myocarditis occurrence with cancer immunotherapy across indications in clinical trial and post-marketing data. *Sci Rep.* (2021) 11:1–15. doi: 10.1038/s41598-021-96467-5
108. Pan EY, Merl MY, Lin K. The impact of corticosteroid use during anti-PD1 treatment. *J Oncol Pharm Pract.* (2020) 26:814–22. doi: 10.1177/1078155219872786
109. Maslov D, Tawagi K, Kc M, Simenson V, Yuan H, Parent C, et al. Timing of steroid initiation and response rates to immune checkpoint inhibitors in metastatic cancer. *J ImmunoTherapy Cancer.* (2021) 9:2312–6. doi: 10.1136/jitc-2020-002261
110. Ricciuti B, Dahlberg SE Adeni A, Sholl LM, Nishino M, Awad MM. Immune checkpoint inhibitor outcomes for patients with non-small-cell lung cancer receiving baseline corticosteroids for palliative versus nonpalliative indications. *J Clin Oncol.* (2019) 37:1927–34. doi: 10.1200/JCO.19.00189
111. Poels K, van Leent MMT, Boutros C, Tissot H, Roy S, Meerwaldt AE, et al. Immune checkpoint inhibitor therapy aggravates T cell–driven plaque inflammation in atherosclerosis. *JACC: CardioOncology.* (2020) 2:599–610. doi: 10.1016/j.jaccao.2020.08.007
112. Newman JL, Stone JR. Immune checkpoint inhibition alters the inflammatory cell composition of human coronary artery atherosclerosis. *Cardiovasc Pathol.* (2019) 43:107148. doi: 10.1016/j.carpath.2019.107148
113. Chaar M, Kamta J, Ait-Oudhia S. Mechanisms, monitoring, and management of tyrosine kinase inhibitors–associated cardiovascular toxicities. *OncoTargets Therapy.* (2018). 11: 6227–37. doi: 10.2147/OTT.S170138
114. Jain P, Gutierrez J, Guha A, Jain C, Patil N, Shen T, et al. 641 incidence and risk factors for stroke associated with immune checkpoint inhibitor therapy in cancer patients using real-world clinical data. *J ImmunoTherapy Cancer.* (2020) 8(Suppl 3):A677–8. doi: 10.1136/jitc-2020-SITC2020.0641
115. Champion SN, Stone JR. Immune checkpoint inhibitor associated myocarditis occurs in both high-grade and low-grade forms. *Modern Pathol.* (2020) 33:99–108. doi: 10.1038/s41379-019-0363-0
116. Fitzgerald AA, Weiner LM. The role of fibroblast activation protein in health and malignancy. *Cancer Metastasis Rev.* (2020) 39:783–803. doi: 10.1007/s10555-020-09909-3
117. Kratochwil C, Flechsig P, Lindner T, Abderrahim L, Altmann A, Mier W, et al. 68Ga-FAPI PET/CT: tracer uptake in 28 different kinds of cancer. *J Nuclear Med.* (2019) 60:801–5. doi: 10.2967/jnumed.119.227967
118. Varasteh Z, Mohanta S, Robu S, Braeuer M, Li Y, Omidvari N, et al. Molecular imaging of fibroblast activity after myocardial infarction using a 68Ga-labeled fibroblast activation protein inhibitor, FAPI-04. *J Nuclear Med.* (2019) 60:1743–9. doi: 10.2967/jnumed.119.226993
119. Kessler L, Kupusovic J, Ferdinandus J, Hirmas N, Umutlu L, Zarrad F, et al. Visualization of fibroblast activation after myocardial infarction using 68Ga-FAPI PET. *Clin Nucl Med.* (2021) 46:810–3. doi: 10.1097/RLU.0000000000003745

120. Natarajan A, Patel CB, Habte F, Gambhir SS. Dosimetry prediction for clinical translation of 64Cu-pembrolizumab ImmunoPET targeting human PD-1 expression. *Sci Rep.* (2018) 8:1–11. doi: 10.1038/s41598-017-19123-x
121. Dohy Z, Szabo L, Toth A, Czimbalmos C, Horvath R, Horvath V, et al. Prognostic significance of cardiac magnetic resonance-based markers in patients with hypertrophic cardiomyopathy. *Int J Cardiovasc Imag.* (2021) 37:2027–36. doi: 10.1007/s10554-021-02165-8
122. Kamp NJ, Chery G, Kosinski AS, Desai MY, Wazni O, Schmidler GS, et al. Risk stratification using late gadolinium enhancement on cardiac magnetic resonance imaging in patients with hypertrophic cardiomyopathy: a systematic review and meta-analysis. *Prog Cardiovasc Dis.* (2021) 66:10–6. doi: 10.1016/j.pcad.2020.11.001
123. Papavassiliu T, Germans T, Flüchter S, Doesch C, Suriyakamar A, Haghi D, et al. CMR findings in patients with hypertrophic cardiomyopathy and atrial fibrillation. *J Cardiovasc Magn Reson.* (2009) 11:1–9. doi: 10.1186/1532-429X-11-34
124. Jordà P, García-Álvarez A. Hypertrophic cardiomyopathy: sudden cardiac death risk stratification in adults. *Glob Cardiol Sci Pract.* (2018) 2018:25. doi: 10.21542/gcsp.2018.25
125. Franco A, Javidi S, Ruehm SG. Delayed myocardial enhancement in cardiac magnetic resonance imaging. *J Radiol Case Rep.* (2015) 9:6. doi: 10.3941/jrcr.v9i6.2328
126. Caravan P, Yang Y, Zachariah R, Schmitt A, Mino-Kenudson M, Chen HH, et al. Molecular magnetic resonance imaging of pulmonary fibrosis in mice. *Am J Respir Cell Mol Biol.* (2013) 49:1120–6. doi: 10.1165/rcmb.2013-0039OC
127. Farrar CT, Gale EM, Kennan R, Ramsay I, Masia R, Arora G, et al. CM-101: type I collagen-targeted MR imaging probe for detection of liver fibrosis. *Radiology.* (2018) 287:581–9. doi: 10.1148/radiol.2017170595
128. Li Z, Lu B, Lin J, He S, Huang L, Wang Y, et al. A Type I collagen-targeted mr imaging probe for staging fibrosis in Crohn's disease. *Front Mol Biosci.* (2021) 8:1–11. doi: 10.3389/fmolb.2021.762355
129. Gupta A, Day JR, Streiff MB, Takemoto C, Jung K, Abro C, et al. Mortality and associated comorbidities among patients hospitalized for deep vein thrombosis and pulmonary embolism in the United States: results from a nationally representative database. *Blood.* (2020) 136(Supplement 1):39–40. doi: 10.1182/blood-2020-136867
130. Razak NBA, Jones G, Bhandari M, Berndt MC, Metharom P. Cancer-associated thrombosis: An overview of mechanisms, risk factors, and treatment. *Cancers.* (2018) 10:380. doi: 10.3390/cancers10100380
131. Debbie Jiang MD, Alfred Ian Lee MD. Thrombotic risk from chemotherapy and other cancer therapies. *Cancer Treat Res.* (2019) 179:87-101. doi: 10.1007/978-3-030-20315-3_6
132. Moik F, Chan WSE, Wiedemann S, Hoeller C, Tuchmann F, Aretin MB, et al. Incidence, risk factors, and outcomes of venous and arterial thromboembolism in immune checkpoint inhibitor therapy. *Blood.* (2021) 137:1669–78. doi: 10.1182/blood.2020007878
133. Meyer G. Effective diagnosis and treatment of pulmonary embolism: Improving patient outcomes. *Arch Cardiovasc Dis.* (2014) 107:406–14. doi: 10.1016/j.acvd.2014.05.006
134. Klok FA, Zondag W, van Kralingen KW, van Dijk APJ, Tamsma JT, Heyning FH, et al. Patient outcomes after acute pulmonary embolism: a pooled survival analysis of different adverse events. *Am J Respir Crit Care Med.* (2010) 181:501–6. doi: 10.1164/rccm.200907-1141OC
135. Kim C, Lee JS, Han Y, Chae SY, Jin S, Sung C, et al. Glycoprotein IIb/IIIa receptor imaging with 18 F-GP1 PET for acute venous thromboembolism: An open-label, nonrandomized, phase 1 study. *J Nucl Med.* (2019) 60:244–9. doi: 10.2967/jnumed.118.212084
136. Dávila-Román VG, Vedala G, Herrero P, De Las Fuentes L, Rogers JG, Kelly DP, et al. Altered myocardial fatty acid and glucose metabolism in idiopathic dilated cardiomyopathy. *J Am College Cardiol.* (2002) 40:271–7. 01967-8 doi: 10.1016/S0735-1097(02)01967-8
137. Nelson SJ, Kurhanewicz J, Vigneron DB, Larson PEZ, Harzstark AL, Ferrone M, et al. Metabolic imaging of patients with prostate cancer using hyperpolarized [1-13C]pyruvate. *Sci Transl Med*. (2013) 5:198ra108. doi: 10.1126/scitranslmed.3006070
138. ClinicalTrials.gov. *Magnetic Resonance Imaging (MRI) With Hyperpolarized Pyruvate (13C) as Diagnostic Tool in Advanced Prostate Cancer*. San Francisco, CA (2020). Available online at: ClinicalTrials.gov
139. ClinicalTrials.gov. *Hyperpolarized 13C Pyruvate MRI for Treatment Response Assessment in Patients With Locally Advanced or Metastatic Pancreatic Cancer*. ClinicalTrials.gov.
140. van Bilsen M, van Nieuwenhoven FA, van der Vusse GJ. Metabolic remodelling of the failing heart: Beneficial or detrimental? *Cardiovasc Res*. (2009). 81:420–8. doi: 10.1093/cvr/cvn282
141. Dash R, Chan T, Yamada M, Paningbatan M, Myagmar B-E, Swigart P, et al. Cardiac magnetic resonance of targeted annexin-iron oxide labeling detects cardiac cell death in vivo after doxorubicin and myocardial infarction. *J Cardiovasc Magn Reson.* (2009) 11:1–316. doi: 10.1186/1532-429X-11-S1-O8
142. Ruehm SG, Corot C, Vogt P, Kolb S, Debatin JF. Magnetic resonance imaging of atherosclerotic plaque with ultrasmall superparamagnetic particles of iron oxide in hyperlipidemic rabbits. *Circulation.* (2001) 103:415–22. doi: 10.1161/01.CIR.103.3.415
143. Trivedi RA, Mallawarachi C. U-King-Im JM, Graves MJ, Horsley J, Goddard MJ, et al. Identifying inflamed carotid plaques using in vivo USPIO-enhanced MR imaging to label plaque macrophages. *Arterioscl Thromb Vascul Biol.* (2006) 26:1601–6. doi: 10.1161/01.ATV.0000222920.59760.df
144. Banerjee SR, Pomper MG. Clinical applications of Gallium-68. *Appl Radiat Isotop.* (2013) 76:2–13. doi: 10.1016/j.apradiso.2013.01.039
145. Nauffal V, Achille P di, Klarqvist MDR, Cunningham JW, Pirruccello JP, Weng L-C, et al. Genetics of myocardial interstitial fibrosis in the human heart and association with disease running title: genetic and phenotypic associations of myocardial interstitial fibrosis. *medRxiv*. doi: 10.1101/2021.11.05.21265953
146. Sharma A, Burridge PW, McKeithan WL, Serrano R, Shukla P, Sayed N, et al. High-throughput screening of tyrosine kinase inhibitor cardiotoxicity with human induced pluripotent stem cells. *Sci Transl Med*. (2017) 9: eaaf2584. doi: 10.1126/scitranslmed.aaf2584
147. Grafton F, Ho J, Ranjbarvaziri S, Farshidfar F, Budan A, Steltzer S, et al. Deep learning detects cardiotoxicity in a high-content screen with induced pluripotent stem cell-derived cardiomyocytes. *Elife.* (2021) 10:e68714. doi: 10.7554/eLife.68714.sa2
148. Cai C, Guo P, Zhou Y, Zhou J, Wang Q, Zhang F, et al. Deep learning-based prediction of drug-induced cardiotoxicity. *J Chem Inf Model.* (2019) 59:1073–84. doi: 10.1021/acs.jcim.8b00769
149. Chaix MA, Parmar N, Kinnear C, Lafreniere-Roula M, Akinrinade O, Yao R, et al. Machine learning identifies clinical and genetic factors associated with anthracycline cardiotoxicity in pediatric cancer survivors. *JACC: CardioOncology.* (2020) 2:690–706. doi: 10.1016/j.jaccao.2020.11.004
150. Mamoshina P, Bueno-Orovio A, Rodriguez B. Dual transcriptomic and molecular machine learning predicts all major clinical forms of drug cardiotoxicity. *Front Pharmacol.* (2020) 11:639. doi: 10.3389/fphar.2020.00639
151. Zhou Y, Hou Y, Hussain M, Brown SA, Budd T, Tang WW, et al. Machine learning–based risk assessment for cancer therapy–related cardiac dysfunction in 4300 longitudinal oncology patients. *J Am Heart Assoc.* (2020) 9:e019628. doi: 10.1161/JAHA.120.019628
152. Heilbroner SP, Few R, Neilan TG, Mueller J, Chalwa J, Charest F, et al. Predicting cardiac adverse events in patients receiving immune checkpoint inhibitors: a machine learning approach. *J ImmunoTherapy Cancer.* (2021) 9:2545. doi: 10.1136/jitc-2021-002545
153. Curigliano G, Lenihan D, Fradley M, Ganatra S, Barac A, Blaes A, et al. Management of cardiac disease in cancer patients throughout oncological treatment: ESMO consensus recommendations. *Ann Oncol.* (2020) 31:171–90. doi: 10.1016/j.annonc.2019.10.023
154. Attia ZI, Kapa S, Lopez-Jimenez F, McKie PM, Ladewig DJ, Satam G, et al. Screening for cardiac contractile dysfunction using an artificial intelligence–enabled electrocardiogram. *Nat Med.* (2019) 25:70–4. doi: 10.1038/s41591-018-0240-2
155. Yao X, Rushlow DR, Inselman JW, McCoy RG, Thacher TD, Behnken EM, et al. Artificial intelligence–enabled electrocardiograms for identification of patients with low ejection fraction: a pragmatic, randomized clinical trial. *Nat Med*. (2021) 2021:27815-9. doi: 10.1038/s41591-021-01335-4
156. Attia ZI, Noseworthy PA, Lopez-Jimenez F, Asirvatham SJ, Deshmukh AJ, Gersh BJ, et al. An artificial intelligence-enabled ECG algorithm for the identification of patients with atrial fibrillation during sinus rhythm:

a retrospective analysis of outcome prediction. *Lancet.* (2019) 394:861–7. doi: 10.1016/S0140-6736(19)31721-0
157. Güntürkün F, Akbilgic O, Davis RL, Armstrong GT, Howell RM, Jefferies JL, et al. Artificial intelligence–assisted prediction of late-onset cardiomyopathy among childhood cancer survivors. *JCO Clin Cancer Inform.* (2021) 5:459–68. doi: 10.1200/CCI.20.00176
158. Cardinale D, Iacopo F, Cipolla CM. Cardiotoxicity of anthracyclines. *Front Cardiovasc Med.* (2020) 7:26. doi: 10.3389/fcvm.2020.00026
159. Ganatra S, Sharma A, Shah S, Chaudhry GM, Martin DT, Neilan TG, et al. Ibrutinib-associated atrial fibrillation. *JACC: Clin Electrophysiol.* (2018) 4:1491–500. doi: 10.1016/j.jacep.2018.06.004
160. Ouyang D, He B, Ghorbani A, Yuan N, Ebinger J, Langlotz CP, et al. Video-based AI for beat-to-beat assessment of cardiac function. *Nature.* (2020) 580:252–6. doi: 10.1038/s41586-020-2145-8
161. Ghorbani A, Ouyang D, Abid A, He B, Chen JH, Harrington RA, et al. Deep learning interpretation of echocardiograms. *NPJ Digital Med.* (2020) 3:1–10. doi: 10.1038/s41746-019-0216-8
162. Goto S, Mahara K, Beussink-Nelson L, Ikura H, Katsumata Y, Endo J, et al. Artificial intelligence-enabled fully automated detection of cardiac amyloidosis using electrocardiograms and echocardiograms. *Nat Commun.* (2021) 12:1–12. doi: 10.1038/s41467-021-22877-8
163. Eng D, Chute C, Khandwala N, Rajpurkar P, Long J, Shleifer S, et al. Automated coronary calcium scoring using deep learning with multicenter external validation. *NPJ Digital Medicine.* (2021) 4:1–13. doi: 10.1038/s41746-021-00460-1
164. Zeleznik R, Foldyna B, Eslami P, Weiss J, Alexander I, Taron J, et al. Deep convolutional neural networks to predict cardiovascular risk from computed tomography. *Nat Commun.* (2021) 12:1–9. doi: 10.1038/s41467-021-20966-2
165. Bai W, Sinclair M, Tarroni G, Oktay O, Rajchl M, Vaillant G, et al. Automated cardiovascular magnetic resonance image analysis with fully convolutional networks. *J Cardiovasc Magn Reson.* (2018) 20:1–12. doi: 10.1186/s12968-018-0471-x
166. de Souza TF, Silva TQ, Antunes-Correa L, Drobni ZD, Costa FO, Dertkigil SS, et al. Cardiac magnetic resonance assessment of right ventricular remodeling after anthracycline therapy. *Sci Rep.* (2021) 11:1. doi: 10.1038/s41598-021-96630-y
167. Muehlberg F, Funk S, Zange L, von Knobelsdorff-Brenkenhoff F, Blaszczyk E, Schulz A, et al. Native myocardial T1 time can predict development of subsequent anthracycline-induced cardiomyopathy. *ESC Heart Failure.* (2018) 5:620–9. doi: 10.1002/ehf2.12277
168. Betancur J, Commandeur F, Motlagh M, Sharir T, Einstein AJ, Bokhari S, et al. Deep learning for prediction of obstructive disease from fast myocardial perfusion SPECT: a multicenter study. *JACC: Cardiovasc Imag.* (2018) 11:1654–63. doi: 10.1016/j.jcmg.2018.01.020
169. Kagiyama N, Shrestha S, Farjo PD, Sengupta PP. Artificial intelligence: practical primer for clinical research in cardiovascular disease. *J Am Heart Assoc.* (2019) 8:e012788. doi: 10.1161/JAHA.119.012788
170. Dey D, Slomka PJ, Leeson P, Comaniciu D, Shrestha S, Sengupta PP, et al. Artificial intelligence in cardiovascular imaging: JACC state-of-the-art review. *J Am Coll Cardiol.* (2019) 73:1317–35. doi: 10.1016/j.jacc.2018.12.054
171. Antoniades C, Oikonomou EK. Artificial intelligence in cardiovascular imaging—principles, expectations, and limitations. *Eur Heart J.* (2021). doi: 10.1093/eurheartj/ehab678. [Epub ahead of print].
172. Bonsu J, Charles L, Guha A, Awan F, Woyach J, Yildiz V, et al. Representation of patients with cardiovascular disease in pivotal cancer clinical trials. *Circulation.* (2019) 139:2594–6. doi: 10.1161/CIRCULATIONAHA.118.039180
173. Petch J, Di S, Nelson W. Opening the black box: the promise and limitations of explainable machine learning in cardiology. *Can J Cardiol.* (2021) 38:204–13. doi: 10.1016/j.cjca.2021.09.004
174. Dagogo-Jack I, Shaw AT. Tumour heterogeneity and resistance to cancer therapies. *Nat Rev Clin Oncol.* (2018) 15:81–94. doi: 10.1038/nrclinonc.2017.166
175. Noseworthy PA, Attia ZI, Brewer LC, Hayes SN, Yao X, Kapa S, et al. Assessing and mitigating bias in medical artificial intelligence: the effects of race and ethnicity on a deep learning model for ECG analysis. *Circul Arrhyth Electrophysiol.* (2020) 13:e007988. doi: 10.1161/CIRCEP.119.007988
176. Di Noto T, von Spiczak J, Mannil M, Gantert E, Soda P, Manka R, et al. Radiomics for distinguishing myocardial infarction from myocarditis at late gadolinium enhancement at MRI: Comparison with subjective visual analysis. *Radiol Cardiothor Imag.* (2019) 1:e180026. doi: 10.1148/ryct.2019180026
177. Kolossváry M, Maurovich-Horvat P. Radiomics: the link between radiology and histology? *Circul Cardiovasc Imag.* (2019) 12:e009990. doi: 10.1161/CIRCIMAGING.119.009990
178. Oikonomou EK, Williams MC, Kotanidis CP, Desai MY, Marwan M, Antonopoulos AS, et al. A novel machine learning-derived radiotranscriptomic signature of perivascular fat improves cardiac risk prediction using coronary CT angiography. *Eur Heart J.* (2019) 40:3529–43. doi: 10.1093/eurheartj/ehz592
179. Häggström I, Schmidtlein CR, Campanella G, Fuchs TJ. DeepPET: A deep encoder–decoder network for directly solving the PET image reconstruction inverse problem. *Med Image Anal.* (2019) 54:253–62. doi: 10.1016/j.media.2019.03.013
180. Cui J, Liu X, Wang Y, Liu H. Deep reconstruction model for dynamic PET images. *PLoS ONE.* (2017) 12:e0184667. doi: 10.1371/journal.pone.0184667
181. Kaplan S, Zhu YM. Full-dose PET image estimation from low-dose PET image using deep learning: a pilot study. *J Digit Imaging.* (2019) 32:773–8. doi: 10.1007/s10278-018-0150-3
182. Ouyang J, Chen KT, Gong E, Pauly J, Zaharchuk G. Ultra-low-dose PET reconstruction using generative adversarial network with feature matching and task-specific perceptual loss. *Med Phys.* (2019) 46:3555–64. doi: 10.1117/12.2512946
183. Zhang Q, Burrage MK, Lukaschuk E, Shanmuganathan M, Popescu IA, Nikolaidou C, et al. Toward replacing late gadolinium enhancement with artificial intelligence virtual native enhancement for gadolinium-free cardiovascular magnetic resonance tissue characterization in hypertrophic cardiomyopathy. *Circulation.* (2021) 144:589–9. doi: 10.1161/CIRCULATIONAHA.121.054432
184. Seo H, Badiei Khuzani M, Vasudevan V, Huang C, Ren H, Xiao R, et al. Machine learning techniques for biomedical image segmentation: an overview of technical aspects and introduction to state-of-art applications. *Med Phys.* (2020) 47:e148–67. doi: 10.1002/mp.13649

Conflict of Interest: AJS is a limited partner and consultant of MicroVide, LLC, which holds the license for the use of 99mTc-RP805 in myocardial applications.

The authors declare that the research was conducted in the absence of any commercial or financial relationships that could be construed as a potential conflict of interest.

Publisher's Note: All claims expressed in this article are solely those of the authors and do not necessarily represent those of their affiliated organizations, or those of the publisher, the editors and the reviewers. Any product that may be evaluated in this article, or claim that may be made by its manufacturer, is not guaranteed or endorsed by the publisher.

frontiers in Cardiovascular Medicine

ORIGINAL RESEARCH
published: 23 March 2022
doi: 10.3389/fcvm.2022.849175

Alteration of N^6-Methyladenosine mRNA Methylation in a Human Stem Cell-Derived Cardiomyocyte Model of Tyrosine Kinase Inhibitor-Induced Cardiotoxicity

Yan Ma[1†], *Xian Liu*[2†], *Yiming Bi*[1], *Tianhu Wang*[1], *Cheng Chen*[1], *Yabin Wang*[1], *Dong Han*[1*] *and Feng Cao*[1*]

[1] National Clinical Research Center for Geriatric Diseases, The Second Medical Center, Chinese People's Liberation Army (PLA) General Hospital, Beijing, China, [2] Department of Pharmaceutical Sciences, Beijing Institute of Radiation Medicine, Beijing, China

OPEN ACCESS

Edited by:
Praveen K. Dubey,
University of Alabama at Birmingham,
United States

Reviewed by:
Tousif Sultan,
University of Alabama at Birmingham,
United States
Fnu Shiridhar,
University of Central Florida,
United States

***Correspondence:**
Dong Han
handong123566@163.com
Feng Cao
fengcao8828@163.com

[†]These authors have contributed equally to this work and share first authorship

Specialty section:
This article was submitted to Cardio-Oncology, a section of the journal Frontiers in Cardiovascular Medicine

Received: 05 January 2022
Accepted: 23 February 2022
Published: 23 March 2022

Citation:
Ma Y, Liu X, Bi Y, Wang T, Chen C, Wang Y, Han D and Cao F (2022) Alteration of N^6-Methyladenosine mRNA Methylation in a Human Stem Cell-Derived Cardiomyocyte Model of Tyrosine Kinase Inhibitor-Induced Cardiotoxicity. Front. Cardiovasc. Med. 9:849175. doi: 10.3389/fcvm.2022.849175

Background: N^6-methyladenosine (m^{6}A) plays important roles in various cardiovascular diseases (CVDs), including cardiac hypertrophy and heart failure. Sunitinib (SUN) is a tyrosine kinase inhibitor (TKI) that is widely used in the treatment of different types of solid and blood tumors, but its efficacy is restricted by a concomitant rise in cardiotoxicities. However, the methylation modification of m^{6}A messenger RNA (mRNA) in cardiomyocytes treated with TKI has not been investigated.

Methods: The global m^{6}A methylation level of SUN-induced cardiotoxicity was detected by m^{6}A dot blot and colorimetric methylation assay. MeRIP-Seq (methylated RNA immunoprecipitation sequencing) and RNA-seq (RNA sequencing, input) were employed to depict the landscapes of transcriptome and epitranscriptome in TKI. Changes in major m^{6}A-related enzymes were detected by qRT-PCR and Western blot. In addition, the effects of FTO on SUN-induced cardiotoxicity were evaluated by gain and loss of function studies.

Results: In this study, we observed that the m^{6}A methylation level was significantly elevated in SUN-treated human-induced pluripotent stem cell-derived cardiomyocytes (hiPSC-CMs) and paralleled a positively correlated cellular damage level. Through a genome-wide analysis of m^{6}A mRNA methylation by methylated RNA immunoprecipitation sequencing (MeRIP-seq) and input RNA sequencing (RNA-seq), we identified a total of 2,614 peaks with significant changes, of which 1,695 peaks were significantly upregulated and 919 peaks were significantly downregulated. Quantitative reverse transcription PCR (RT-qPCR), immunofluorescence, and Western blotting revealed that the RNA demethylase fat mass and obesity-associated protein (FTO) was downregulated, whereas the RNA methylases methyltransferase-like 14 (METTL14) and wilms' tumor 1-associating protein (WTAP) were upregulated. Furthermore, gain- and loss-of-function studies substantiated that FTO is cardioprotective in TKI.

Conclusion: This study deciphered the methylation modification of m^{6}A mRNA in hiPSC-CMs post-TKI treatment and determined that FTO may be a promising therapeutic target for TKI-induced cardiotoxicity.

Keywords: tyrosine kinase inhibitor (TKI), hiPSC-CMs, N^6-methyladenosine, FTO, cardiotoxicity

INTRODUCTION

Tyrosine kinase inhibitors (TKIs) have been widely used in the treatment of various types of cancer, some of which are in different stages of clinical development, which shows the importance of tyrosine kinase as the main target of new antitumor drugs (1). However, the widespread use of TKIs was restricted due to their cardiovascular toxicity, which threatened patients' medication compliance and quality of life (2). Therefore, the study of the cardiovascular toxicity mechanism of TKIs is of great significance for circumventing these cardiovascular complications. Sunitinib (SUN), a small-molecule, multitarget receptor tyrosine kinase (RTK) inhibitor, was approved by the US Food and Drug Administration (FDA) in 2006 to treat kidney cancer, gastrointestinal stromal tumors, and endocrine tumors (3). Its targets include vascular endothelial growth factor receptors (VEGFRs), platelet-derived growth factor (PDGFR), and mast/stem cell growth factor receptor (SCFR) (4). In the cardiovascular system, SUN impairs cell signal transduction, cell cycle regulation, and cell metabolism, increasing the incidence of cardiac events in patients with cancer (5). However, cardioprotective strategies based on these mechanisms are controversial and have not been proven in humans, suggesting that SUN-mediated cardiotoxicity may also be mediated by other mechanisms (6).

Ribonucleic acid methylation constitutes more than 60% of all the RNA modifications and N^6-methyladenosine (m^{6}A) is the most prevalent RNA modification in mammalian mRNA and long non-coding RNAs (lncRNAs) (7, 8). The m^{6}A modification mainly occurs on adenine in the "RRACH" motif and its state is tightly controlled by "writer" methyltransferases (methyltransferase-like 3 (METTL3), methyltransferase-like 14 (METTL14), and wilms' tumor 1-associating protein (WTAP)), "eraser" demethylases [fat mass and obesity-associated protein (FTO) and Alk B homologue 5 (ALKBH5)], and "reader" m^{6}A binding proteins (YT homology domain containing1 (YTHDC1), YTHDC2, YT homology domain family (YTHDF1), YTHDF2, YTHDF3, heterogeneous nuclear ribonucleo protein C (HNRNPC), heterogeneous nuclear ribonucleoprotein A2B1 (HNRNPA2B1), eukaryotic initiation factor 3A (EIF3A), and EIF3C) (9, 10). Ample evidence suggests that m^{6}A modification regulates a variety of RNA metabolic processes, such as mRNA stability, splicing, nuclear transport, and translation capabilities (11–13). Given the importance of m^{6}A modification in RNA metabolism, we were, thus, curious to discover whether m^{6}A modification had potential effects on TKI-induced cardiotoxicity.

Abbreviations: METTL14, methyltransferase-like 14; WTAP, Wilms' tumor 1-associating protein; ALKBH5, Alk B homologue 5; YTHDF, CYT homology domain family, HNRNPC, heterogeneous nuclear ribonucleo protein C; HNRNPA2B1, heterogeneous nuclear ribonucleoprotein A2B1; EIF3A, eukaryotic initiation factor 3A; RPMI, Roswell Park Memorial Institute; IWR-1, Wnt/β-catenin inhibitor; FB23-2, FTO Demethylase inhibitor; RIPA, Radio-Immunoprecipitation Assay; PVDF, poly vinyli dene fluoride; TBST, Tris-Buffered Saline and Tween; ECL, enhanced chemiluminescence; GAPDH, glyceraldehyde-3- phosphate dehydrogenase; DTT, DL-Dithiothreitol; MIT, Massachusetts Institute of Technology; AAV9, adeno-associated virus 9.

Furthermore, previous studies have proposed a cardioprotective role of m^{6}A demethylase FTO-mediated demethylating effects in various cardiovascular pathologies. First, reduced FTO expression was observed in failing human hearts and hypoxic cardiomyocytes, thereby increasing m^{6}A in RNA and deteriorating cardiomyocyte contractile dysfunction via regulating the methylation of cardiac contractile transcripts (7). Moreover, elevated m^{6}A-RNA methylation and FTO repression were causatively involved in myocardial inflammation and dysfunction during endotoxemia in mice (14). Another study showed that FTO overexpression mitigated apoptosis of hypoxia-/reoxygenation-treated myocardial cells by demethylating Mhrt (15). However, the role of FTO in TKI-induced myocardial injury remains to be further revealed.

In this study, we used methylated RNA immunoprecipitation sequencing (MeRIP-seq) and input RNA sequencing (RNA-seq) to study the transcriptome and m^{6}A modification epitranscriptome in human-induced pluripotent stem cell-derived cardiomyocytes (hiPSC-CMs) treated with SUN. To gain further insights into the pathological significance of m^{6}A modification in TKI-induced cardiotoxicity, the Gene Ontology (GO) and the Kyoto Encyclopedia of Genes and Genomes (KEGG) pathway enrichment analyses were performed on the key genes identified by MeRIP-seq and input RNA-seq. Furthermore, we revealed a cardioprotective role of FTO in SUN-treated hiPSC-CMs. This study is the first study to show that m^{6}A methylation may play an indispensable role in TKI-induced cardiotoxicity.

MATERIALS AND METHODS

Cell Culture

Urinary epithelial cell-derived hiPSCs were cultured in Matrigel (Invitrogen, Carlsbad, California, USA)-coated 6-well plates in E8 medium (Invitrogen, Carlsbad, California, USA) containing 0.5% penicillin/streptomycin. HiPSCs were induced to differentiate into cardiomyocytes when cultured at 80% confluence, as previously reported (16, 17). In short, cells were treated with 6 μM of selective inhibition CHIR99021, a selective inhibitor of glycogen synthase kinase 3ß, in roswell park memorial institute (RPMI) medium supplemented with B27 (Invitrogen, Carlsbad, California, USA) for 48 h, followed by 5 μM of Wnt/β-catenin inhibitor (IWR-1), a Wnt antagonist (Sigma-Aldrich), for another 48 h, and the medium was changed every 3 days. On the 10th day, the beating cardiomyocytes were purified by the glucose starvation method for 5 days for further tests.

Isolation and Culture of Cardiac Microvascular Endothelial Cells (CMECs) and Cardiac Fibroblasts (CFs)

Primary CMECs and CFs were isolated, cultured, characterized, and subjected to subsequent experiments, as previously reported (18, 19).

Silence and Overexpression of FTO

We employed commercially available ready-to-use lentiviral constructs pLenti-GIII-CMV (Applied Biological Materials

Incorporation, CAT. NO 210500610196) and FTO small hairpin RNA (shRNA) lentiviral particles (Santa Cruz Biotechnology Incorporation, CAT. NO sc-75002-V) to overexpress or knockdown FTO in hiPSC-CMs. The transfection process was done as per the manufacturer's instructions. Lentivirus particles were transfected at a multiplicity of infection (MOI) of 20.

Cell Viability Assay

Cell viability was detected with a Cell Counting Kit-8 (CCK-8) (C0037, Beyotime, Shanghai, China). The culture medium was aspirated and the precoated Matrigel hiPSC-CMs were washed with phosphate-buffered saline (PBS) once. Then, 100 μl of working buffer was added to hiPSC-CMs in 96-well plates and the cells were incubated at 37°C for 30 min in the dark. A microplate reader (Tecan, Switzerland) was used to automatically measure the absorbance at a wavelength of 450 nm.

Drug Treatment

Our preliminary results showed that the half-maximal inhibitory concentration (IC50) of SUN treatment for 24 h (cell viability serving as the readout) is around 6 μM (**Supplementary Figure S1A**); thus, the subsequent experiments were carried out with 6 μM SUN (SU11248, Sellect, Shanghai, China) treatment for 24 h and equal volume of dimethyl sulfoxide (DMSO) treatment for 24 h served as the control group. For FTO Demethylase inhibitor (FB23-2) (S8837, Sellect, Shanghai, China) treatment, 20 μM FB23-2 was added simultaneously with SUN for 24 h. The concentration of FB23-2 was chosen based on a previous report (20).

Western Blot Analysis

Cell protein was extracted with Radio-Immunoprecipitation Assay (RIPA) Lysis Solution (P0013C, Beyotime, Shanghai, China) from hiPSC-CMs for Western blot detection. Protein extractions and molecular weight standards were separated by 10% sodium dodecyl sulfate-polyacrylamide gel electrophoresis (SDS-PAGE) gels and transferred to poly vinyli dene fluoride (PVDF) membranes (Bio-Rad, USA). After blocking, the membrane was incubated with primary antibodies [methyltransferase-like 3, (METTL3) ab195352, Abcam; METTL14, ab220030, Abcam; FTO, ab126605, Abcam; ALKBH5 aa302-330, LifeSpan Biosciences; WTAP, 56501, Cell Signaling Technology; and glyceraldehyde-3-phosphate dehydrogenase (GAPDH) ab8245, Abcam] at 4°C overnight in a 5% bovine serum albumin (BSA) blocking solution. After being washed with Tris-Buffered Saline and Tween (TBST) buffer, the membrane was incubated in 5% blocking buffer for 1 h at room temperature with the secondary antibody (1:800 dilution, 7074, Cell Signaling Technology, USA) at the recommended dilution. Protein bands were detected with the enhanced chemiluminescence (ECL) chemiluminescent kit (P0018S, Beyotime, Shanghai, China) in a dark room and assessed with Image Lab software (Bio-Rad, USA).

N^6-Methyladenosine Dot Blot

The mRNA was isolated with the Dynabeads® mRNA Purification Kit (61006, Invitrogen, Carlsbad, California, USA) and the purity of mRNA was detected by the NanoDrop method for further tests. The serially diluted mRNA was denatured at a high temperature of 95°C and cooled immediately after denaturation. The 2 μl sample was transferred directly onto a nucleic acid-optimized nylon membrane (1620153, Bio-Rad, USA). After a regimen UV cross-linking and methylene blue (M4591, Sigma-Aldrich, USA) staining, the membrane was blocked by soaking in 5% BSA buffer and incubated with the anti-m^{6}A antibody (ab284130, Abcam, Shanghai, China) in 5% BSA for 30 min at room temperature. Then, the membrane was incubated with horseradish peroxidase (HRP)-conjugated secondary antibody (ab97051, Abcam, Shanghai, China) for 30 min, followed by incubation with the ECL reagent (P0018S, Beyotime, Shanghai, China) for 1 min, covered with plastic wrap, and exposed to different lengths of exposure in a dark room. The test sample was compared with the signal of the standard sample to detect its concentration.

m^{6}A RNA Methylation Assay (Colorimetric)

The m^{6}A RNA Methylation Assay Kit (ab185912, Abcam, Shanghai, China) was used to measure the m^{6}A level of mRNA. According to the instructions, 80 μl of binding solution was added to each well and negative control, diluted positive control, and 200 ng of mRNA were added to each well and incubated at 37°C for 90 min. Fifty microliter of diluted capture antibody was added for incubation at room temperature for 60 min and then 50 μl of diluted detection antibody was added to each well for 30 min. Finally, 100 μl of developing solution was used for the reaction and after incubation in the dark at room temperature for 10 min, stop solution was added and the absorbance was measured at 450 nm.

Lactate Dehydrogenase (LDH) Release

The LDH Release Detection Kit (C0016, Beyotime, Shanghai, China) was used to detect cell cytotoxicity according to the instructions. Sixty microliter of LDH detection working solution was added to each well. The sample was incubated at room temperature (∼25°C) in the dark for 30 min. Then, the absorbance was measured at 490 nm.

Quantitative Reverse Transcription PCR (RT-qPCR)

Total RNA was extracted from hiPSC-CMs using the RNAsimple Total RNA Kit (DP419, Tiangen, Beijing, China). One microgram of total RNA was used for complementary DNA (cDNA) synthesis reaction, as previously described (21). The isolated mRNA was reverse transcribed into cDNA with the High Capacity cDNA Reverse Transcription Kit (4368814, Invitrogen, Carlsbad, California, USA) and cDNA was amplified with the Takara's Perfect Real-Time PCR Kit (RR037A, Takara Bio, Otsu, Japan). The primers and probes were ordered from TaqMan (Invitrogen, Carlsbad, California, USA). The relative level of each mRNA was quantified by GAPDH and expressed as a relative ratio.

Methylated RNA Immunoprecipitation Sequencing

Guangzhou Epibiotek Corporation Ltd. (Guangzhou, China) provided the MeRIP-seq service. Briefly, m^{6}A RNA immunoprecipitation was performed with the GenSeq^{TM} m^{6}A RNA IP Kit (GE-ET-001, GenSeq Incorporation, China) according to the manufacturer's instructions. Both the input samples were obtained by ribosomal RNA (rRNA) removal and smart principles and first-strand cDNA PCR-enriched library fragments were synthesized. The magnetic bead library fragments were purified by DNA and the ultrafine RNA methylated m^{6}A detection library was obtained. The library quality was evaluated using the Bioptic Qsep100 Analyzer (Agilent Technologies Incorporation, USA). Library sequencing was performed on an Illumina HiSeq instrument in PE150 sequencing mode.

Methylated RNA Immunoprecipitation Sequencing Data Processing

Cutadapt (version 2.5) was used to trim adapters and filter for sequences. The remaining reads were then aligned to the human Ensemble genome GRCh38 (mouse Ensemble genome GRCm38) using Hisat2 aligner (version 2.1.0) under the following parameters: "–rna-strandness RF." m^{6}A peaks were identified using the exome Peak R package (version 2.13.2) under the parameter: "peak_cutoff_*p*-value = 0.05, peak_cutoff_false discovery rate (FDR) = NA, and fragment_length = 200."

Differential m^{6}A peaks were identified using the exome Peak R package under the following parameters: "peak_cutoff_*p*-value = 0.05, peak_cutoff_FDR = NA, and fragment_length = 200." The GO and the KEGG analyses were performed using the cluster profile R package (version 3.6.0). m^{6}A RNA-related genomic features were visualized using the Guitar R package (version 1.16.0). Identified m^{6}A peaks with p-values < 0.05 were chosen for the *de-novo* motif analysis using homer (version 4.10.4) under the parameter "-len 6-rna."

Long RNA-seq

The Epi^{TM} Mini LongRNA-SEQ Kit (E1802, Epibiotek, Guangzhou, China) and the Epi^{TM} DNA Clean Beads Kit (R1809, Epibiotek, Guangzhou, China) was used for long RNA sequencing. DNase I was added to the RNA samples and digested at 37°C for 30 min to remove the residual DNA in the samples and the RNA was purified and recovered by magnetic beads. rRNA removal and RNA fragmentation: 5XRT buffer was added to sample RNA, a rRNA probe, and a temperature gradient reaction was used to fragment RNA samples and remove rRNA. Synthesis of first-strand cDNA: EpiScript^{TM} IV, RNase inhibitor, DL-Dithiothreitol (DTT), Template-Switching oligonucleotide (TSO), and random primers were added to the RNA samples in Step 2. After mixing with the wall of the tube, rapid centrifugation was carried out in the PCR machine according to the following procedures: 37°C, 90 min; 70°C, 15 min. 2XpfuMax HiFi PCR ProMix and sequencing primers were added to the first-strand cDNA samples and then amplified in a PCR apparatus after mixing. The Epi^{TM} DNA Clean Beads were used to purify PCR products in a 1X ratio. DNA fragments (300–400 bp) were recovered from the purified products with magnetic beads in a 0.65/0.2X ratio for a second round of PCR amplification to enrich 300–400 bp DNA fragments. The Bioptic Qsep100 Analyzer was used to conduct quality inspection of the library to detect whether the size distribution of the library conformed to the theoretical size.

Ribonucleic Acid Sequencing Data Processing

Cutadapt (version 2.5) was used to trim adapters and filter for sequences and the remaining reads were then aligned to the human Ensemble genome GRCh38 (mouse Ensemble genome GRCm38) using Hisat2 aligner (version 2.1.0) under the parameter "–rna-strandness RF." The reads mapping the genome were calculated using feature counts (version 1.6.3). Differential gene expression analysis was performed using the DESeq2 R package. Enrichment analysis was performed using the clusterProfiler R package for the GO terms and the KEGG database pathways.

Immunostaining and Immunofluorescence Analysis

Human-induced pluripotent stem cell-derived cardiomyocytes were separated and placed in 6-well plates (Corning, New York, USA). The combined staining of α-actinin (ab137346, Abcam), immunoglobulin G (IgG) H&L (Alexa Fluor® 488) (ab150077, Abcam), and propidium iodide (PI) 1 μg/ml (ST511, Beyotime, Shanghai, China) was used to detect cardiomyocyte death. The nucleus was stained with 4′,6-diamidino-2-phenylindole (DAPI) (C1002, Beyotime, Shanghai China) and the dead cells were labeled with PI to pass through the damaged cell membrane. A Nikon A1R HD25 confocal microscope was used to capture images. The total number of cells in the PI-positive and five randomly selected fields was counted using ImageJ software by a researcher blinded to the treatment assignments. A manual pipeline (CellProfiler, Broad Institute of Massachusetts Institute of Technology (MIT) and Harvard in Cambridge) was used to determine the cell surface area (22). Briefly, 5 to 6 random pictures were taken with 20X magnification and 150–200 cells/per condition were analyzed in order to determine cell size following the instructions of the software.

Statistical Analyses

Continuous data are expressed as the mean ± SD unless otherwise specified. Comparisons between the two or more groups were performed using the Student's *t*-test and ANOVA for normal variables or the Mann–Whitney *U* test and the Kruskal–Wallis test for non-normal variables. R software (version 3.4.2) and GraphPad Prism software (version 8.00) were used for statistical analysis. Biological replicates (individual mice) are shown as individual data points superimposed on bar charts. Significance was conventionally accepted at $p < 0.05$.

RESULTS

Global m^{6}A Level Was Upregulated in SUN-Injured hiPSC-CMs

The treatment dose and duration of SUN were determined based on preliminary experiments. Our preliminary results showed that the IC50 of SUN treatment for 24 h

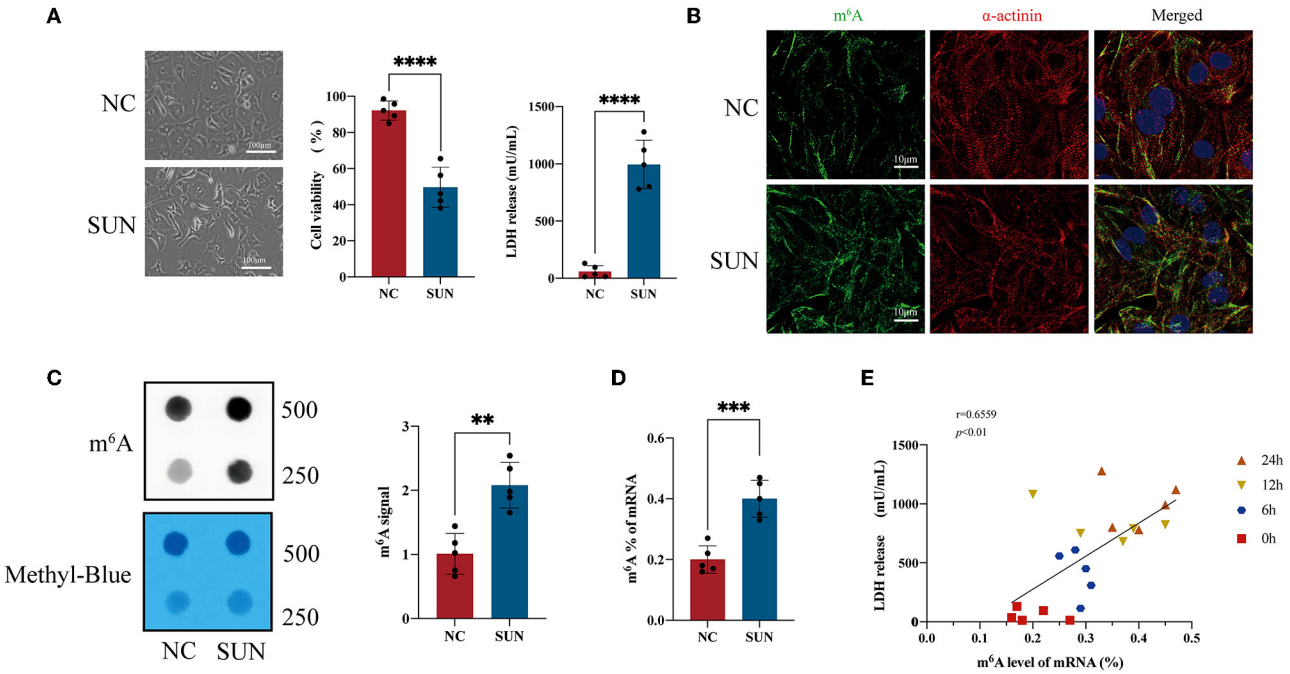

FIGURE 1 | The global N^6-methyladenosine (m^{6}A) methylation level of sunitinib (SUN)-treated human-induced pluripotent stem cell-derived cardiomyocytes (hiPSC-CMs). **(A)** Representative images after SUN treatment for 24 h and measurement of lactate dehydrogenase (LDH) release level and cell viability are shown (n = 5). **(B)** The levels of m^{6}A methylation in the normal control (NC) and SUN groups detected by m^{6}A antibody-based immunofluorescence. Red denotes α-actinin, green denotes m^{6}A, and blue denotes 4′,6-diamidino-2-phenylindole (DAPI). **(C)** The m^{6}A level of total RNA of hiPSC-CMs is indicated by an m^{6}A dot blot. Corresponding RNAs were loaded equally by a 2-fold serial dilution with 500 ng and 250 ng of methylene blue staining served as a loading control. **(D)** The RNA m^{6}A level detected by the colorimetric method. **(E)** The m^{6}A level of messenger RNA (mRNA) and the level of LDH release exhibit a time-dependent gradual increase after SUN treatment and the two indicators are positively correlated. "**" indicates $p < 0.01$, "***" indicates $p < 0.001$, and "****" indicates $p < 0.0001$.

(cell viability serving as the readout) is around 6 μM (**Supplementary Figure S1A**); thus, the subsequent experiments were carried out with 6 μM SUN treatment for 24 h and equal volume of DMSO treatment for 24 h served as the control group. Furthermore, we also explored the time kinetics of 6 μM SUN in hiPSC-CMs; these results were given in **Supplementary Figure S1B**.

Figure 1A shows the optical microscope morphology of hiPSC-CMs treated with 6 μM of SUN for 24 h. The cell surface area decreased, accompanied by a significant elevation in LDH release and a significant reduction in cell viability in SUN-treated hiPSC-CMs. Furthermore, the immunofluorescence results suggested that the global m^{6}A levels in the SUN group increased and that the structure of myocardial sarcomeres became disorganized (**Figure 1B**). The m^{6}A dot blot validated that the global m^{6}A level was indeed elevated in the SUN group (**Figure 1C**). In addition, the colorimetric kit method also verified the upregulation of the global m^{6}A level (**Figure 1D**). Linear regression was used to analyze the relationship between the mRNA m^{6}A level and LDH release of hiPSC-CMs after SUN treatment and it was found that a positive correlation was identified between the global m^{6}A level and LDH release (r = 0.6096, $p < 0.01$) and the global m^{6}A level and LDH release gradually increased as the treatment time was prolonged (**Figure 1E**). Overall, these results indicated that the dysregulated m^{6}A modification in SUN-injured hiPSC-CMs may play important roles in TKI-induced cardiotoxicity.

Overview of the m^{6}A Methylation Map in SUN-Injured hiPSC-CMs

Next, to further decipher the role of elevated m^{6}A in SUN-injured hiPSC-CMs, three biological copies of hiPSC-CMs from either the normal control (NC) group or the SUN group were sent for MeRIP-seq and m^{6}A MeRIP enrichment regions (peaks) were analyzed after sample normalization (**Figure 2A**). The m^{6}A modification mostly occurred in mRNAs (**Figure 2B**). A total of 16,399 m^{6}A peaks from 4,499 coding gene transcripts (mRNAs) were identified in the NC group. In the SUN group, there were 16,732 m^{6}A peaks within 4,427 mRNAs (**Figure 2C**). To reveal the preferential distribution of m^{6}A in transcripts, the metagene profiles of all the identified m^{6}A peaks in the entire transcriptome were probed. The results show that the m^{6}A peak is preferentially enriched in two sets of coding DNA sequences (CDSs) and the 3′-untranslated region (UTR) (**Figures 2D,E**). To learn whether a consensus motif existed in the identified m^{6}A peaks, we used HOMER software to map the m^{6}A methylation. The results showed that m^{6}A mainly exists in the consensus sequence of 5-RRAH-3′ and 5-RRAH-3′ (R = A or G; H = A, C, or U) (14). Among the identified m^{6}A peaks, the top five conserved

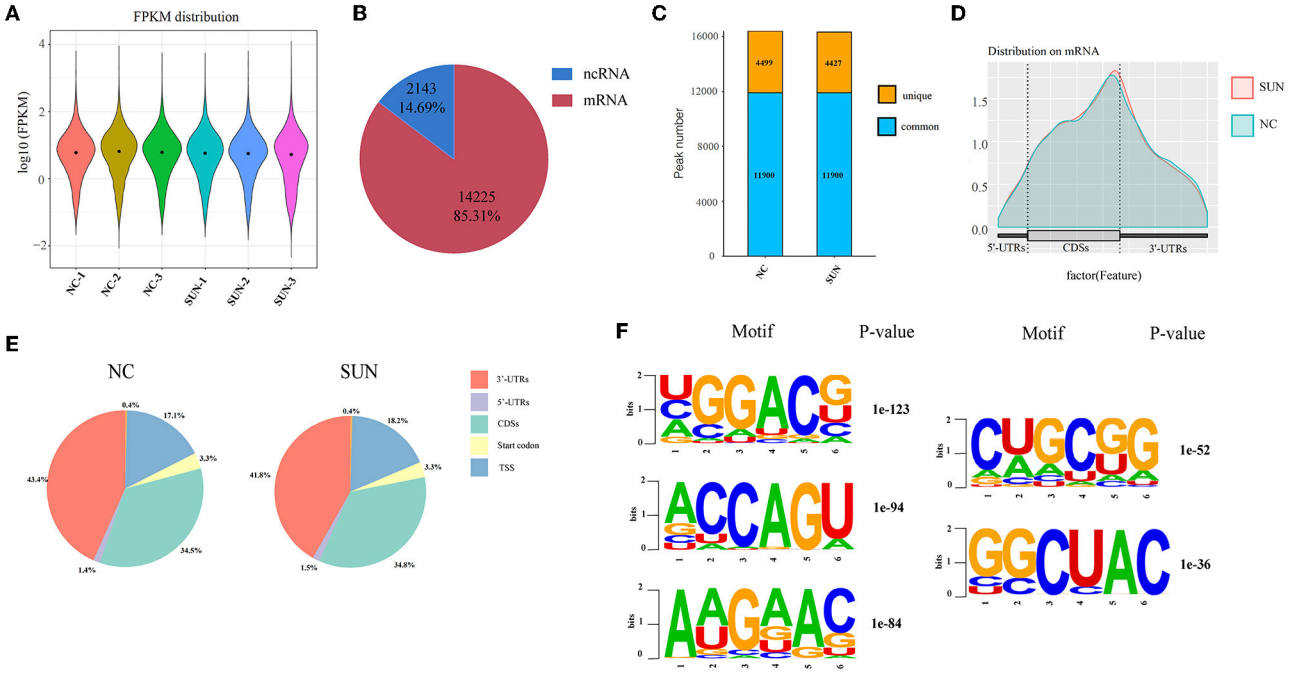

FIGURE 2 | Overview of the m^{6}A methylation map in SUN-treated hiPSC-CMs. **(A)** Sequencing sequences were compared to the genome and the distribution intensity and abundance of normalized expression quantities are described. **(B)** Pie chart showing the distribution of m^{6}A peaks in mRNAs and non-coding RNAs (ncRNAs). **(C)** The histogram displays the unique and common m^{6}A peaks in the two sets of mRNAs. **(D)** The density curve shows the distribution of the m^{6}A peak on the transcript, which is divided into three parts: 5′-UTR, CDSs, and 3′-UTRs. **(E)** Pie charts showing the proportion of the m^{6}A peak distribution in the NC and SUN groups. **(F)** The top five motifs enriched across the m^{6}A peaks. SUN, sunitinib; CDS, coding DNA sequence; UTR, untranslated region.

motifs are shown in **Figure 2F**, which was consistent with the well-known "RRACH" consensus motif of m^{6}A modification.

Conjoint Analysis of the MeRIP-seq and RNA-seq Data in SUN-Injured hiPSC-CMs

To further clarify the changes in m^{6}A methylation associated with TKI-induced cardiotoxicity, we performed a conjoint analysis of the MeRIP-seq and RNA-seq data. As shown in **Figure 3A**, 20,072 m^{6}A peaks (representing 9,892 genes) were identified and there were 2,614 differentially methylated peaks (representing 2,066 genes), among which 919 differentially methylated peaks had hypermethylation and 1,695 differentially methylated peaks had hypomethylation at the log fold change cutoff of (±1) and FDR cutoff of <0.05. The top 10 hypermethylated genes and the top 10 hypomethylated genes are shown in **Table 1**. The analysis of the differentially methylated peak (DMPeaks) distribution at different chromosome loci revealed that the chromosomes with the most m^{6}A methylation were chromosome 1 with 308 m^{6}A methylation peaks, chromosome 2 with 170 m^{6}A methylation peaks, and chromosome 17 with 164 m^{6}A methylation peaks (**Figure 3B**). In parallel, RNA-seq was used to determine the transcriptome profile of altered genes. We identified 1,906 differentially expressed genes (DEGs) between the NC and SUN groups, including 990 upregulated DEGs and 916 downregulated DEGs (fold changes 2, $p < 0.05$; **Figures 3C,D**). The top 10 upregulated mRNAs and the top 10 downregulated mRNAs are shown in **Table 2**. Furthermore, among the 20,072 m^{6}A peaks (representing 9,892 genes) identified, there were 2,614 differentially methylated peaks (representing 2,066 genes), 919 hypermethylated peaks, and 1,695 hypomethylated peaks. Accordingly, we identified 244 mRNAs with significant changes in their m^{6}A peaks and levels and they could be divided into four quadrants: both the mRNA expression and m^{6}A peaks were upregulated (55), mRNA and m^{6}A peaks were both downregulated (74), m^{6}A peaks were upregulated and mRNA peaks were downregulated (37), and m^{6}A peaks were downregulated and mRNA peaks were upregulated (78) (**Figure 3E**). We have validated the transcriptomic study by examining the gene expression level of top 5 upregulated and top 5 downregulated protein coding genes among the 244 intersection genes by RT-qPCR assay. The RT-qPCR results were mostly consistent with RNA-seq (**Supplementary Figure S2**), which might be helpful to solidify our sequencing result. The list of 244 DEGs with significant differential m^{6}A peaks is given in **Supplementary Table S2**. Their GO term for enrichment analysis is given in **Supplementary Figure S3**. The GO analysis showed that the biological functions of the 244 mRNAs were mainly enriched in mitogen-activated protein kinase (MAPK) and p53 signaling pathway, while the KEGG analysis repetitiously pointed to apoptotic signaling pathways.

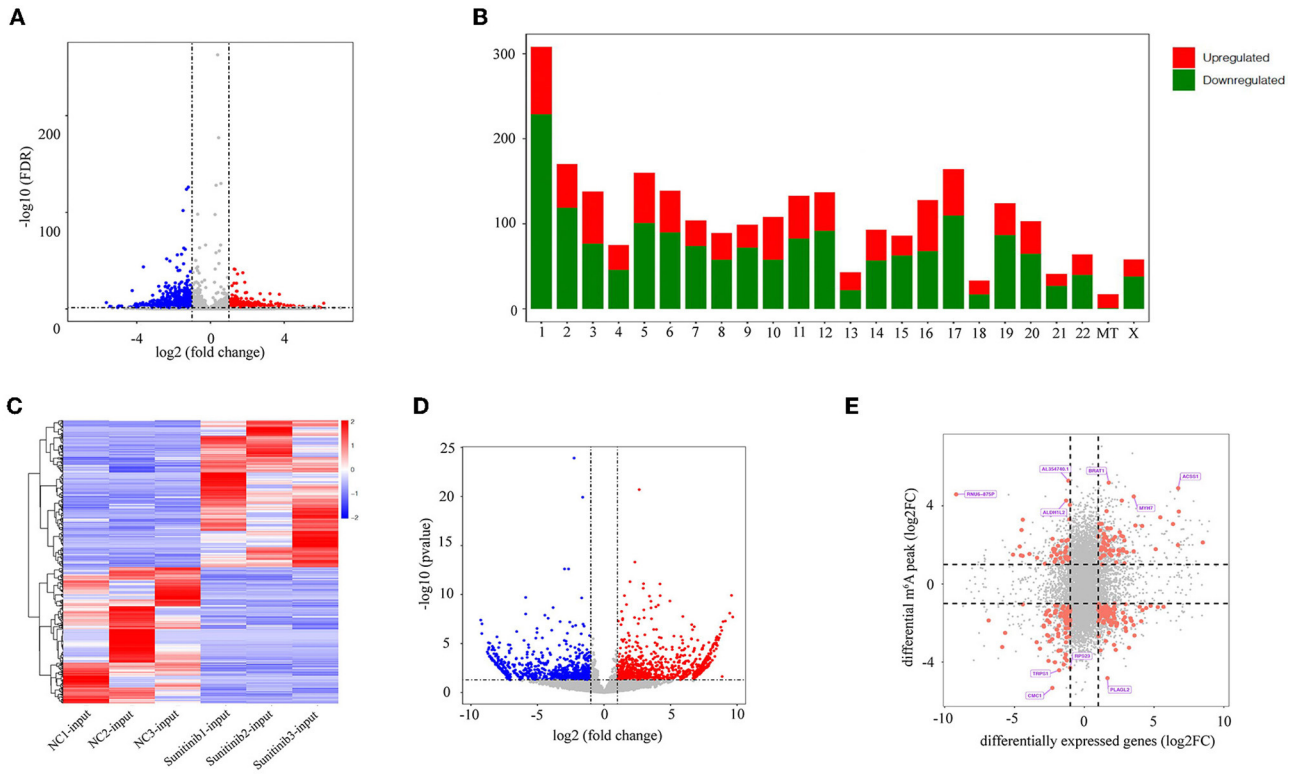

FIGURE 3 | Joint analysis of methylated RNA immunoprecipitation sequencing (MeRIP-seq) and RNA sequencing (RNA-seq) data. **(A)** The volcano plot shows the difference in m^{6}A methylation peaks, fold changes ≥2, and *p*-values < 0.05. The red image represents the high methylation peak of m^{6}A and the blue image represents the low methylation peak of m^{6}A. **(B)** The histogram shows the distribution of the m^{6}A peak on chromosomes. **(C)** Heatmap showing upregulated and downregulated mRNAs. **(D)** The volcano map shows differentially expressed genes, *p*-value < 0.05, and double change ≥2. The red area represents upregulated genes and the blue area represents downregulated genes. **(E)** Four-quadrant diagram showing the relationship between mRNA m^{6}A methylation and mRNA expression.

The GO and the KEGG Enrichment Analyses Revealed the Biological Information Underlying DEGs and Differentially Methylated Genes (DMGs)

To explore the physiological and pathological significance of the DEGs and DMGs, the GO and the KEGG pathway analyses were performed on the key genes identified. The GO analysis showed that the biological functions of upregulated DEGs were mainly enriched in the regulation of angiogenesis and apoptosis signaling pathways (**Figure 4A**). The downregulated DEGs were mainly involved in microtubule cytoskeleton organization, endomembrane system organization, protein tetramerization, and protein heterodimerization (**Figure 4B**). Through the KEGG analysis, the upregulated DEGs were mainly enriched in pathways in cell adhesion molecules (CAMs), extracellular matrix (ECM)-receptor interaction, and ribosome biogenesis in eukaryotes (**Figure 4C**). The downregulated DEGs were mainly involved in cancer pathways, the MAPK signaling pathway, cytokine–cytokine receptor interactions, and the p53 signaling pathway (**Figure 4D**). In addition, we also performed enrichment analyses on DMGs. These genes were mainly enriched in pathways such as nuclear transport, nucleocytoplasmic transport, regulation of cell cycle phase transition, and histone modification (**Figure 4E**). The KEGG analyses showed that these DMGs were related to pathways in cancer, focal adhesion, regulation of actin cytoskeleton, and protein processing in the endoplasmic reticulum (**Figure 4F**).

Expression of FTO Was Downregulated, While the Expressions of MELLT14 and ALKBH5 Were Upregulated in SUN-Treated hiPSC-CMs

To further explore whether the m^{6}A modification enzyme was involved in SUN-induced hiPSC-CM injury, we examined the expression levels of major methyltransferases and demethylases. Compared with the NC group, the mRNA expression levels of the methylases WTAP and METTL14 in the SUN group were significantly upregulated ($p < 0.05$), whereas the mRNA expression level of FTO (demethylase) was significantly downregulated in the SUN group ($p < 0.01$) (**Figure 5A**). The downregulation of FTO was again verified in the SUN group by immunofluorescence (IF) staining (**Figure 5B**). However, the expression of the other two enzymes, METTL3 and ALKBH5, was not altered in SUN-treated hiPSC-CMs. Consistent with the

TABLE 1 | List of the top 10 hypomethylated genes and the top 10 hypermethylated genes.

Genes	Description	Chromosome	Peak start	Peak end	log_2 Fold change	*P*-value	Up/down
FAM69B	Family with sequence similarity 69 member B	9	136,723,693	136,724,020	−5.65	1.023e-8	Down
ATXN1	Ataxin 1	6	16,300,520	16,300,791	−5.46	1.58e-4	Down
SLC30A6	Solute carrier family 30 member 6	2	32,224,109	32,224,289	−5.39	4.07e-4	Down
JAM2	Junctional adhesion molecule 2	21	25,716,872	25,717,262	−5.04	0.0036	Down
NRDE2	Nuclear RNAi defective 2	14	90,270,343	90,270,584	−5.02	3.31e-4	Down
MANEL	Mannosidase like protein	1	37,799,732	37,800,181	−4.98	5.89e-5	Down
PLAGL2	Pleiomorphicad-enomagene like 2	20	32,195,399	32,195,639	−4.82	7.41e-5	Down
TRPS1	Trichorhinophalangeal syndrome type 1	8	115,412,594	115,412,805	−4.42	0.0024	Down
TSPAN5	Tetraspanin 5	4	98,472,253	98,472,524	−4.33	0.0013	Down
RPS23	Ribosomal protein S23	5	82,275,563	82,275,772	−4.29	0.0043	Down
RGMB	Repulsive guidance molecules B	5	98,795,779	98,796,079	6.15	4.47e-8	Up
TTN	Titin	2	178,693,982	178,702,575	5.98	0.0035	Up
NEBL	Nebulette	10	20,831,577	20,845,420	5.89	0.0010	Up
FABP3	Fat acid binding protein 3	1	31,369,427	31,372,984	5.64	1.70e-4	Up
STOX2	Stork head box 2	4	184,009,557	184,009,768	4.98	0.0051	Up
DYRK3	Dual-specificity tyrosine-(Y)-phosphorylation regulated kinase 3	1	206,647,569	206,647,839	4.94	0.0054	Up
BRAT1	Breast cancer type 1 associated ring domain 1	7	2,542,069	2,542,339	4.83	1.15e-4	Up
ZNF697	Zinc finger protein 697	1	119,624,014	119,625,981	4.52	1.82e-5	Up
LSM14A	RNA-associated protein 55A,	19	34,228,887	34,229,157	4.49	1.70e-5	Up
CCDC184	Coiled-coil domain containing 184	12	48,184,769	48,185,096	4.44	4.57e-4	Up

TABLE 2 | List of the top 10 upregulated messenger RNAs (mRNAs) and the top 10 downregulated mRNAs.

	Description	log2 Fold change	*P*-value	Up/down
CATSPER2	The cation channel of sperm receptor 2	−9.1720856	1.01E-07	Down
ITGB7	Integrin Beta 7	−8.6837258	3.99E-05	Down
CLDN20	Claudin 20	−8.6824254	8.49E-06	Down
GMPR	Guanosine monophosphate reductase	−8.6137908	0.00021296	Down
USP50	Ubiquitin-specific peptidase 50	−8.5858481	9.24E-06	Down
PCDHA7	Protocadherin alpha 7	−8.402541	0.00040126	Down
ZP1	Zona pellucida glycoprotein 1	−8.3886407	0.00054659	Down
SLC37A4	Glucose-6-phosphate transporter member 4	−8.3131318	2.82E-05	Down
KCNC1	Potassium voltage-gated channel 1	−8.2366521	0.00065662	Down
LPAR4	Lysophosphatidic acid receptor 4	−8.1447607	0.00105897	Down
PGF	Vascular endothelial growth factor	9.66737242	2.05E-08	Up
AVPI1	Arginine vasopressin-induced 1	9.44284665	8.06E-09	Up
ANKRD45	Ankyrin repeat domain 45	9.11522806	5.18E-08	Up
TNFRSF10A	Tumor necrosis factor receptor superfamily member 10A	8.94685039	5.80E-08	Up
MYOCD	Myocardin	8.87253755	0.02317118	Up
NPTX1	Neuronal pentraxin 1	8.84367054	4.82E-07	Up
SLCO4A1	Solute carrier organic anion transporter family, member 4A1	8.77762835	2.14E-07	Up
MEDAG	Mesenteric estrogen-dependent adipogenesis protein	8.60841757	2.70E-06	Up
IGSF9	Immunoglobulin superfamily, member 9	8.51141356	1.63E-05	Up
SULT1C2	Sulfotransferase family, cytosolic 2C	8.49784929	2.13E-06	Up

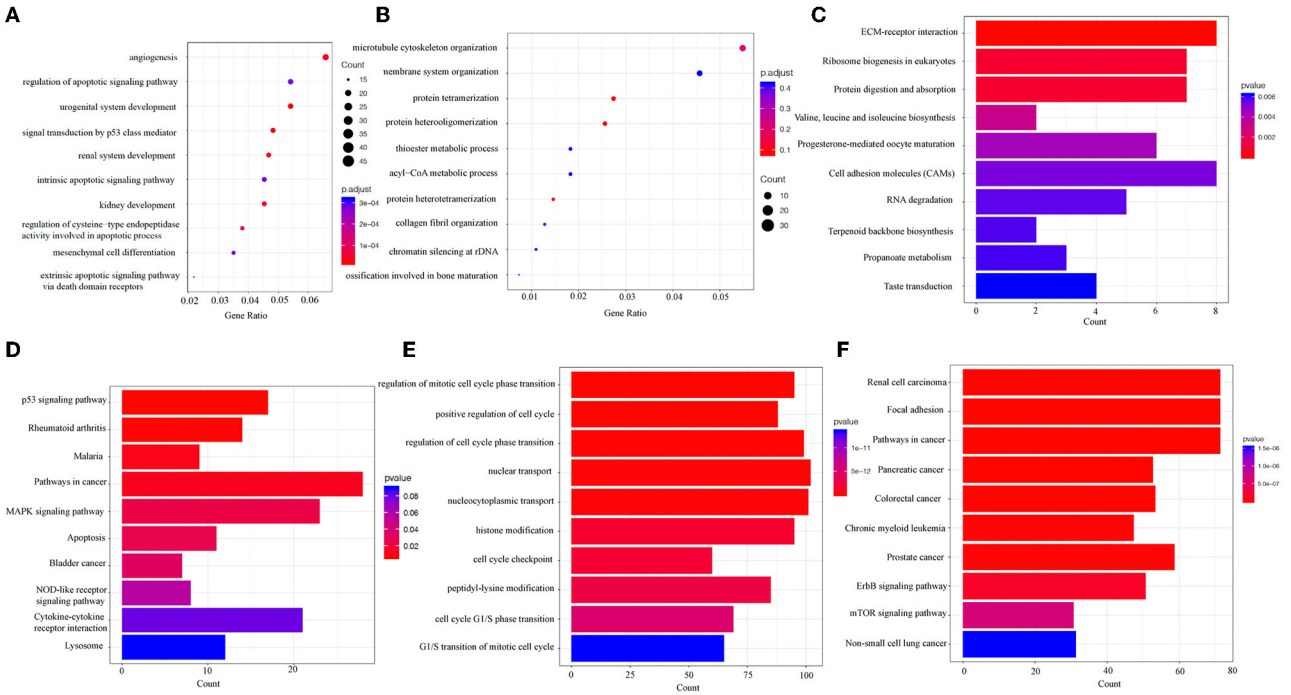

FIGURE 4 | The Gene Ontology (GO) and the Kyoto Encyclopedia of Genes and Genomes (KEGG) analyses reveal the biological information behind the differences in mRNA expression levels and m^{6}A methylation modification. **(A,B)** The top 10 enriched GO terms of upregulated and downregulated DEGs. **(C,D)** The top 10 enriched KEGG pathways of upregulated and downregulated DEGs. **(E,F)** The top 10 enriched GO terms and KEGG pathways of DMGs. DEGs, differentially expressed genes. DMGs, differentially methylated genes. "Gene ratio," number of genes annotated to the specific GO term/number of all the genes with the GO database annotations. "Count," number of genes annotated to the specific GO term.

mRNA expression data, the protein levels of WTAP, METTL14, and FTO exhibited similar trends in SUN-treated hiPSC-CMs (**Figure 5C**). Collectively, these results indicated that the downregulated FTO as well as the upregulated METTL14 and WTAP might account for the increased global m^{6}A level in SUN-injured hiPSC-CMs.

FTO Downregulation Aggravated SUN-Induced hiPSC-CM Injury

Next, we employed FB23-2, a potent and selective FTO inhibitor that directly binds to FTO and selectively inhibits FTOs m^{6}A demethylase activity to examine the role of FTO in SUN-induced hiPSC-CM injury. For FB23-2 treatment, 20 μM FB23-2 was added simultaneously with SUN for 24 h. The concentration of FB23-2 was chosen based on a previous report (20). We examined the effect of FB23-2 on global m^{6}A level by m^{6}A dot blot. The results verified a ∼1.7-fold upregulation of global m^{6}A level. Cell death was evaluated by PI staining after 24 h of treatment. Interestingly, SUN-induced hiPSC-CM death was exacerbated in the FB23-2 + SUN group (**Figures 6A,B**). This effect was not observed in normal hiPSC-CMs, indicating that FB23-2 alone would not affect the cell viability of hiPSC-CMs. Furthermore, SUN-induced hiPSC-CM atrophy was also aggravated in the FB23-2 + SUN group, as evidenced by a smaller cell surface area (**Figures 6A,C**). The colorimetric test kit for LDH release again validated the findings obtained from the PI staining (**Figure 6D**). In addition, we knocked down FTO using a FTO shRNA lentiviral particles. The silencing efficiency and inhibited FTO activity as revealed by elevated global m^{6}A level were confirmed (**Supplementary Figures S6A,B**). We observed that FTO shRNA phenocopied the effects of FTO inhibitor in terms of elevating PI-positive cell death, LDH release, and reducing cell surface area (**Figures 6A–D**). Taken together, these results indicate that FTO plays a protective role in SUN-induced hiPSC-CM injury.

To further explore the role of FTO in SUN-induced cardiotoxicity, we employed a lentivirus construct to overexpress FTO. After verifying the FTO mRNA and global m^{6}A level, we transfected hiPSC-CMs with the FTO lentivirus construct or empty vector. The results showed that FTO overexpression by lentivirus construct successfully induced a ∼2-fold upregulation of FTO expression and a ∼40% downregulation of global m^{6}A level (**Supplementary Figures S5A,B**). Furthermore, FTO overexpression significantly reduced LDH release and improved cell viability in SUN-challenged hiPSC-CMs (**Supplementary Figures S5C,D**).

To justify that SUN-altered m^{6}A effects are cardiomyocytes specific or not, we treated CMECs and CFs with 60 nM or 10 μM SUN for 18 h, respectively, referring to the concentration and duration reported in previous studies (23, 24). We then measured the global m^{6}A level of mRNA and the transcripts levels of FTO mRNA. Interestingly enough, both the CMECs and

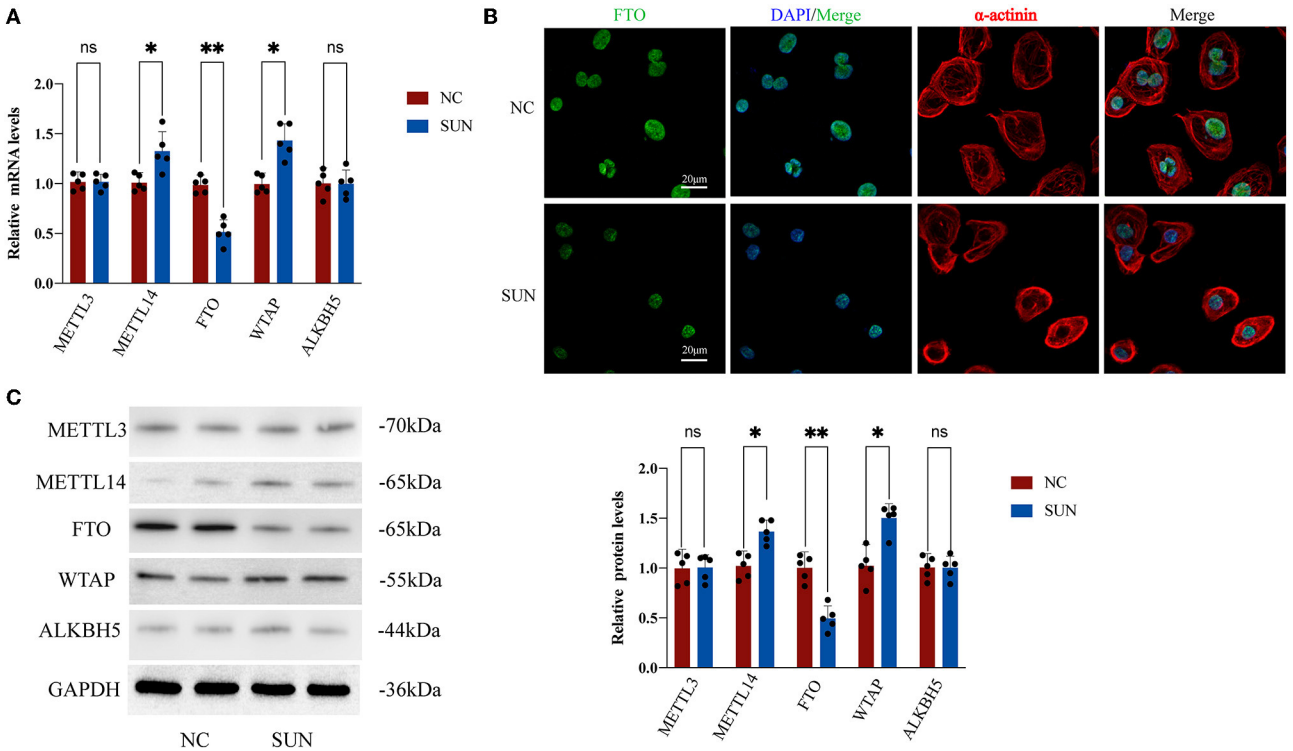

FIGURE 5 | Changes in m^{6}A methyltransferase and demethylase expression levels in hiPSC-CMs treated with SUN. **(A)** Reverse transcription PCR (RT-PCR) of METTL3, ALKBH5, fat mass and obesity-associated protein (FTO), METTL14, and WTAP; the NC group ($n = 5$) and the SUN group ($n = 5$). **(B)** The levels of FTO expression in the NC and SUN groups as detected by immunofluorescence. Red denotes α-actinin, green denotes FTO, and blue denotes DAPI. **(C)** The protein expression levels of methyltransferase and demethylase as detected by Western blot ($n = 5$). NS, non-significant, "*" indicates $p < 0.05$ and "**" indicates $p < 0.01$.

CFs failed to show significant changes in these two parameters in response to SUN (**Supplementary Figures S7A,B,D,E**). Furthermore, cotreatment of FTO inhibitor FB23-2 did not alter the reduced cell viability in response to SUN as revealed by CCK-8 assay (**Supplementary Figures S7C,F**). These results might indicate that the reported effects are cardiomyocytes specific.

DISCUSSION

In this study, we performed a genome-wide analysis of m^{6}A mRNA methylation by MeRIP-seq and RNA-seq in a human stem cell-derived cardiomyocyte model of TKI-induced cardiotoxicity. Our major findings include the following: (a) the global m^{6}A level was upregulated in SUN-injured hiPSC-CMs; (b) downregulated FTO as well as upregulated METTL14 and WTAP might account for the increased global m^{6}A level in SUN-injured hiPSC-CMs; (c) m^{6}A modification was associated with the occurrence and course of TKI-induced cardiotoxicity to some extent; and (d) protected against SUN-induced hiPSC-CM injury. Nevertheless, the specific mechanism of m^{6}A methylation in TKI-induced cardiotoxicity remains to be further studied in the future.

Recent studies have shown that m^{6}A is involved in the occurrence and development of cancers and cardiac dysfunction. RNA methyltransferases, demethylases, and m^{6}A-binding proteins are frequently altered in human cancer tissues from various organ sources, influencing cancer transcription and oncoprotein expression, cancer cell proliferation, survival, tumor initiation, progression, and metastasis (25, 26). However, there is no consensus on whether altered m^{6}A is oncogenic or tumor suppressive. In comparison, studies have reported that m^{6}A methylation and FTO have decreased expressions in various pathologic conditions including heart failure and endotoxemia- and hypoxia-/reoxygenation-induced cardiac cell injuries (7, 14, 15). In accordance with our present finding, most studies suggest that elevated m^{6}A level that result from elevated methylases or reduced demethylases is a deleterious factor for the onset and progression of various cardiovascular diseases (27).

Recently, m^{6}A methylation was revealed to play important roles in various cardiovascular diseases, but its role in TKI-induced cardiotoxicity has rarely been studied. In this study, we found that the cell viability of hiPCS-CMs treated with SUN decreased, whereas the release of LDH increased, which suggested that SUN had a damaging effect on hiPSC-CMs. IF staining showed that the m^{6}A levels of the SUN group were elevated and the m^{6}A dot blot also verified this elevation. Moreover, we also found that the global m^{6}A methylation level in SUN-treated hiPSC-CMs was positively correlated with LDH release. Therefore, we employed MeRIP-seq and RNA-seq to

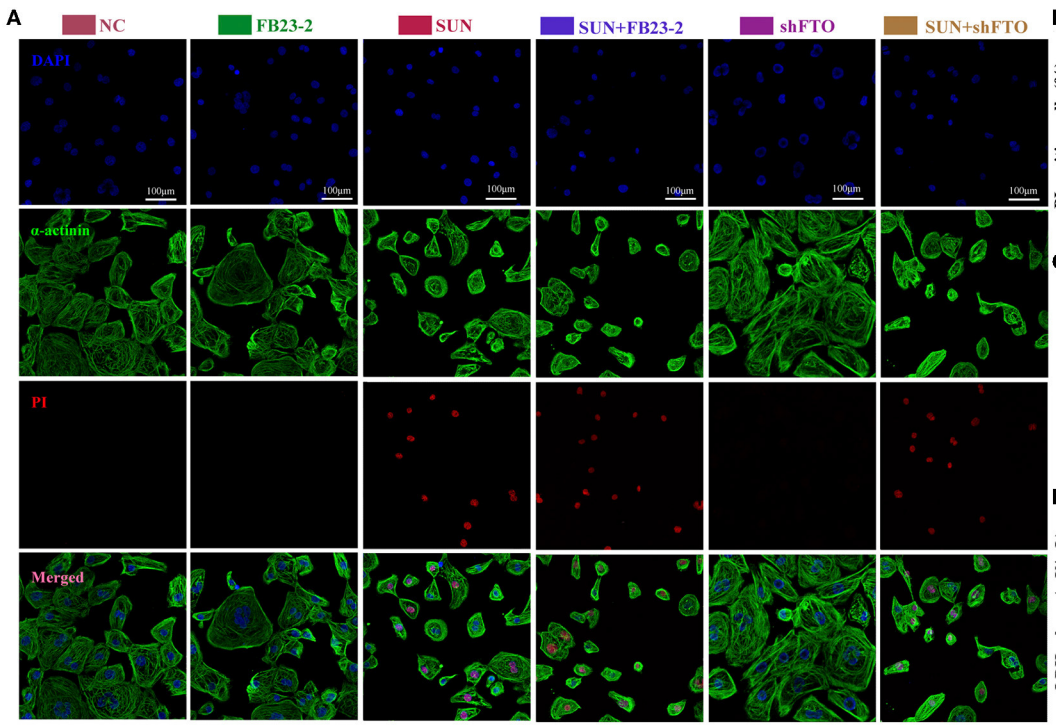

FIGURE 6 | The FTO inhibitor FB23-2 and knocking down of FTO aggravated SUN-induced hiPSC-CM injury. **(A)** Multiple immunofluorescences staining of DAPI (blue), propidium iodide (PI) (red), and α-actinin (green) to detect hiPSC-CM death. **(B)** The proportions of PI-positive cardiomyocytes ($n = 5$). **(C)** The cell surface area was detected and analyzed by CellProfiler pipeline ($n = 5$). **(D)** Measurement of LDH release levels ($n = 5$). NS, non-significant, "*" indicates $p < 0.05$, "**" indicates $p < 0.01$, and "****" indicates $p < 0.0001$.

study the transcriptome and methylome in SUN-treated hiPSC-CMs. Through further joint analysis of MeRIP-seq and RNA-seq data, we found significant differences between the m^{6}A methylation and mRNA expression levels of 244 genes. We surmised that these potential genes, through m^{6}A methylation, are potentially involved in the occurrence and development of TKI-induced cardiotoxicity.

We further conducted the GO and the KEGG analyses of differentially expressed m^{6}A methylated genes. Biological processes and pathways indicated apoptotic signaling pathways that were repetitiously enriched by upregulated DEGs. This enrichment pattern coincides with previous SUN cardiotoxicity studies. For instance, a previous study in isolated cardiomyocytes and mice scrutinized the potential mechanisms of SUN-associated cardiac effects. This study concluded that mitochondrial injury and cardiomyocyte apoptosis accounted for SUN-associated cardiotoxicity (28). In a more recent report, apoptotic cell death resulting from mitochondrial damage with reactive oxygen species (ROS) accumulation was shown to be the important contributing mechanism of cardiotoxicity associated with SUN (29). Conversely, thioester and acetyl-CoA metabolic pathways were significantly enriched by downregulated DEGs. Thioesters play a prominent role in metabolism. The central metabolite acetyl-CoA is a thioester that is produced mainly by oxidative decarboxylation of pyruvate or by fatty acid degradation. It is, thus, possible that SUN-induced cardiotoxicity can be ascribed to interrupted mitochondrial energy production. Interestingly, SUN was previously reported to induce loss of mitochondrial membrane potential and energy rundown in cardiomyocytes (30). Thus, this study further supports the notion that apoptosis induction and energy reduction are the crucial mechanisms of SUN-associated cardiotoxicity.

Fat mass and obesity-associated protein is the first demethylase discovered to be involved in m^{6}A modification. Recent high-quality studies have confirmed that FTO plays fundamental roles in many cardiac physiological and pathological processes. Increased m^{6}A in RNA was associated with decreased FTO mRNA and protein expression in human and mouse failing hearts. Moreover, adeno-associated virus 9 (AAV9)-mediated myocardial FTO overexpression restores cardiac function in mouse models of myocardial infarction, whereas cardiomyocyte-restricted knockout of FTO mice deteriorates cardiac function (27). Further mechanistic studies revealed that FTO overexpression selectively demethylates cardiac contractile transcripts, thus blocking their degradation and improving their stability and expression under ischemia, which eventually contributed to reduced fibrosis and enhanced angiogenesis (7). Another study found that FTO alleviated cardiac dysfunction by regulating glucose uptake and glycolysis in mice with pressure overload-induced heart failure, the effects of which were associated with demethylation of the glycolysis-related gene *Pgam2* (31). In addition, a similar study reported that FTO cardiomyocyte-specific knockout worsened cardiac dysfunction through transcription-independent mechanisms

of translation regulation (32). All these reports support a cardioprotective role of FTO in different cardiac pathologies. In this study, we detected the major methylases and demethylases in SUN-treated hiPSC-CMs and found that FTO was significantly downregulated. To verify the role of FTO in SUN-induced cardiotoxicity, we treated hiPSC-CMs with FB23-2, a potent and selective FTO inhibitor and demonstrated that FB23-2 can aggravate the cell injury elicited by SUN, cause damage to the sarcomeres of cardiomyocytes, and deteriorate cell atrophy. Together with previous findings, this study might add a conceptual framework for targeting FTO as a therapeutic for various cardiovascular diseases. Notably, this study also found that the expression levels of METTL14 and WTAP increased in SUN-treated hiPSC-CMs and their functional roles remain to be further clarified.

This study failed to reveal the downstream regulatory mechanisms by which SUN-stimulated m^{6}A upregulation regulates the mRNA expression of related genes, which warrants further investigations. Nonetheless, we have depicted the m^{6}A modification landscape of SUN-treated hiPSC-CMs with transcriptome-wide unbiased epitranscriptomics and revealed a potential role of m^{6}A and m^{6}A eraser FTO in SUN-induced cardiotoxicity, which would lay a solid foundation for further detailed mechanistic studies.

CONCLUSION

This study provides the first overview of the m^{6}A methylation map in SUN-injured hiPSC-CMs to decipher the RNA post-transcriptional epigenetic mechanisms of TKI-induced cardiotoxicity. Through MeRIP-seq, we found that the m^{6}A methylation level in 2,614 mRNAs changed significantly. Combined analysis of the m^{6}A peak and mRNA expression showed that 244 mRNAs were significantly changed after SUN treatment. These genes with varying levels of m^{6}A modification may play an important role in the process of TKI-induced cardiotoxicity. In addition, we found that inhibiting FTO can aggravate the myocardial toxicity caused by SUN, which suggests a novel therapeutic target for TKI-induced cardiotoxicity.

DATA AVAILABILITY STATEMENT

The data presented in the study are deposited in the NCBI Gene Expression Omnibus (GEO) database repository, accession number GSE192913.

AUTHOR CONTRIBUTIONS

FC and DH conceived and designed the experiments, provided financial support, co-wrote the article, and edited the manuscript. YM and XL performed the experiments. YM, XL, YB, TW, CC, and YW analyzed the data. All authors contributed to the article and approved the submitted version.

FUNDING

This study was supported by the National Natural Science Foundation of China (82100372, 81820108019, and 91939303), the Innovative Project of Chinese PLA General Hospital (CX19028), the Key Health Care Projects of National Health Commission (2020ZD05), National Postdoctoral Program for Innovative Talents (BX20200154), Beijing Nova Program (Z211100002121048), and the Basic Research Reinforcement Project (2021-JCJQ-JJ-1079).

ACKNOWLEDGMENTS

We acknowledge Jie Zhou for valuable comments on data analysis, Yanfei Zhang for assistance on the generation and amplification of cDNA templates.

SUPPLEMENTARY MATERIAL

The Supplementary Material for this article can be found online at: https://www.frontiersin.org/articles/10.3389/fcvm.2022.849175/full#supplementary-material

REFERENCES

1. Thomas A, Rajan A, Giaccone G. Tyrosine kinase inhibitors in lung cancer. *Hematol Oncol Clin North Am*. (2012) 26:589–605. doi: 10.1016/j.hoc.2012.02.001
2. Moslehi JJ, Deininger M. Tyrosine kinase inhibitor-associated cardiovascular toxicity in chronic myeloid leukemia. *J Clin Oncol*. (2015) 33:4210–8. doi: 10.1200/JCO.2015.62.4718
3. Bex A, Mulders P, Jewett M, Wagstaff J, van Thienen JV, Blank CU, et al. Comparison of immediate vs deferred cytoreductive nephrectomy in patients with synchronous metastatic renal cell carcinoma receiving sunitinib: the SURTIME randomized clinical trial. *JAMA Oncol*. (2019) 5:164270. doi: 10.1001/jamaoncol.2018.5543
4. Ferrari SM, Centanni M, Virili C, Miccoli M, Ferrari P, Ruffilli I, et al. Sunitinib in the treatment of thyroid cancer. *Curr Med Chem*. (2019) 26:963272. doi: 10.2174/0929867324666171006165942
5. Chintalgattu V, Rees ML, Culver JC, Goel A, Jiffar T, Zhang J, et al. Coronary microvascular pericytes are the cellular target of sunitinib malate-induced cardiotoxicity. *Sci Transl Med*. (2013) 5:187ra69. doi: 10.1126/scitranslmed.3005066
6. Yang Y, Bu P. Progress on the cardiotoxicity of sunitinib: prognostic significance, mechanism and protective therapies. *Chem Biol Interact*. (2016) 257:125:31. doi: 10.1016/j.cbi.2016.08.006
7. Mathiyalagan P, Adamiak M, Mayourian J, Sassi Y, Liang Y, Agarwal N, et al. FTO-dependent N-methyladenosine regulates cardiac function during remodeling and repair. *Circulation*. (2019) 139:518:32. doi: 10.1161/CIRCULATIONAHA.118.033794
8. Liu Z-X, Li L-M, Sun H-L, Liu S-M. Link between m6A modification and cancers. *Front Bioeng Biotechnol*. (2018) 6:89. doi: 10.3389/fbioe.2018.00089
9. Meyer KD, Patil DP, Zhou J, Zinoviev A, Skabkin MA, Elemento O, et al. 5' UTR m(6)A promotes cap-independent translation. *Cell*. (2015) 163:999–1010. doi: 10.1016/j.cell.2015.10.012
10. Gao R, Ye M, Liu B, Wei M, Ma D, Dong K. m6A modification: a double-edged sword in tumor development. *Front Oncol*. (2021) 11:679367. doi: 10.3389/fonc.2021.679367

11. Tang Y, Chen K, Song B, Ma J, Wu X, Xu Q, et al. m6A-Atlas: a comprehensive knowledgebase for unraveling the N6-methyladenosine (m6A) epitranscriptome. *Nucleic Acids Res*. (2021) 49:D134–43. doi: 10.1093/nar/gkaa692
12. Li Y, Gu J, Xu F, Zhu Q, Chen Y, Ge D, Lu C. Molecular characterization, biological function, tumor microenvironment association and clinical significance of m6A regulators in lung adenocarcinoma. *Brief Bioinform*. (2021) 22:bbaa225. doi: 10.1093/bib/bbaa225
13. Chen X-Y, Zhang J, Zhu J-S. The role of mA RNA methylation in human cancer. *Mol Cancer*. (2019) 18:103. doi: 10.1186/s12943-019-1033-z
14. Dubey PK, Patil M, Singh S, Dubey S, Ahuja P, Verma SK, Krishnamurthy P. Increased m6A-RNA methylation and FTO suppression is associated with myocardial inflammation and dysfunction during endotoxemia in mice. *Mol Cell Biochem*. (2021) 477:129–41. doi: 10.1007/s11010-021-04267-2
15. Shen W, Li H, Su H, Chen K, Yan J. FTO overexpression inhibits apoptosis of hypoxia/reoxygenation-treated myocardial cells by regulating m6A modification of Mhrt. *Mol Cell Biochem*. (2021) 476:2171–9. doi: 10.1007/s11010-021-04069-6
16. Han D, Wang Y, Wang Y, Dai X, Zhou T, Chen J, et al. The tumor-suppressive human circular RNA CircITCH sponges miR-330-5p to ameliorate doxorubicin-induced cardiotoxicity through upregulating SIRT6, survivin, and SERCA2a. *Circ Res*. (2020) 127:e108–25. doi: 10.1161/CIRCRESAHA.119.316061
17. Qiu Y, Ma Y, Jiang M, Li S, Zhang J, Chen H, et al. Melatonin alleviates LPS-induced pyroptotic cell death in human stem cell-derived cardiomyocytes by activating autophagy. *Stem Cells Int*. (2021) 2021:8120403. doi: 10.1155/2021/8120403
18. Wang D, Luo P, Wang Y, Li W, Wang C, Sun D, et al. Glucagon-like peptide-1 protects against cardiac microvascular injury in diabetes via a cAMP/PKA/Rho-dependent mechanism. *Diabetes*. (2013) 62:1697–708. doi: 10.2337/db12-1025
19. Li X, Han D, Tian Z, Gao B, Fan M, Li C, et al. Activation of cannabinoid receptor type II by AM1241 ameliorates myocardial fibrosis via Nrf2-mediated inhibition of TGF-d inhid3 pathway in myocardial infarction mice. *Cell Physiol Biochem*. (2016) 39:1521–36. doi: 10.1159/000447855
20. Zhao T, Wang J, Wu Y, Han L, Chen J, Wei Y, et al. Increased m6A modification of RNA methylation related to the inhibition of demethylase FTO contributes to MEHP-induced Leydig cell injury. *Environ Pollut*. (2021) 268:115627. doi: 10.1016/j.envpol.2020.115627
21. Han D, Wang Y, Chen J, Zhang J, Yu P, Zhang R, et al. Activation of melatonin receptor 2 but not melatonin receptor 1 mediates melatonin-conferred cardioprotection against myocardial ischemia/reperfusion injury. *J Pineal Res*. (2019) 67:e12571. doi: 10.1111/jpi.12571
22. Carpenter AE, Jones TR, Lamprecht MR, Clarke C, Kang IH, Friman O, et al. CellProfiler: image analysis software for identifying and quantifying cell phenotypes. *Genome Biol*. (2006) 7:R100. doi: 10.1186/gb-2006-7-10-r100
23. Chiusa M, Hool S-L, Truetsch P, Djafarzadeh S, Jakob SM, Seifriz F, et al. Cancer therapy modulates VEGF signaling and viability in adult rat cardiac microvascular endothelial cells and cardiomyocytes. *J Mol Cell Cardiol*. (2012) 52:1164–75. doi: 10.1016/j.yjmcc.2012.01.022
24. McMullen CJ, Chalmers S, Wood R, Cunningham MR, Currie S. Sunitinib and imatinib display differential cardiotoxicity in adult rat cardiac fibroblasts that involves a role for calcium/calmodulin dependent protein kinase II. *Front Cardiovasc Med*. (2020) 7:630480. doi: 10.3389/fcvm.2020.630480
25. Lan Q, Liu PY, Haase J, Bell JL, Hüttelmaier S, Liu T. The critical role of RNA mA methylation in cancer. *Cancer Res*. (2019) 79:1285–92. doi: 10.1158/0008-5472.CAN-18-2965
26. Ma S, Chen C, Ji X, Liu J, Zhou Q, Wang G, et al. The interplay between m6A RNA methylation and noncoding RNA in cancer. *J Hematol Oncol*. (2019) 12:121. doi: 10.1186/s13045-019-0805-7
27. Wu S, Zhang S, Wu X, Zhou X. mA RNA methylation in cardiovascular diseases. *Mol Ther*. (2020) 28:2111–9. doi: 10.1016/j.ymthe.2020.08.010
28. Chu TF, Rupnick MA, Kerkela R, Dallabrida SM, Zurakowski D, Nguyen L, et al. Cardiotoxicity associated with tyrosine kinase inhibitor sunitinib. *Lancet*. (2007) 370:2011–19. doi: 10.1016/S0140-6736(07)61865-0
29. Bouitbir J, Alshaikhali A, Panajatovic MV, Abegg VF, Paech F, Krähenbühl S. Mitochondrial oxidative stress plays a critical role in the cardiotoxicity of sunitinib: running title: sunitinib and oxidative stress in hearts. *Toxicology*. (2019) 426:152281. doi: 10.1016/j.tox.2019.152281
30. Kerkela R, Woulfe KC, Durand J-B, Vagnozzi R, Kramer D, Chu TF, et al. Sunitinib-induced cardiotoxicity is mediated by off-target inhibition of AMP-activated protein kinase. *Clin Transl Sci*. (2009) 2:15(20. doi: 10.1111/j.1752-8062.2008.00090.x
31. Zhang B, Jiang H, Wu J, Cai Y, Dong Z, Zhao Y, et al. m6A demethylase FTO attenuates cardiac dysfunction by regulating glucose uptake and glycolysis in mice with pressure overload-induced heart failure. *Signal Transduct Target Ther*. (2021) 6:377. doi: 10.1038/s41392-021-00699-w
32. Berulava T, Buchholz E, Elerdashvili V, Pena T, Islam MR, Lbik D, et al. Changes in m6A RNA methylation contribute to heart failure progression by modulating translation. *Eur J Heart Fail*. (2020) 22:54:20. doi: 10.1002/ejhf.1672

Conflict of Interest: The authors declare that the research was conducted in the absence of any commercial or financial relationships that could be construed as a potential conflict of interest.

Publisher's Note: All claims expressed in this article are solely those of the authors and do not necessarily represent those of their affiliated organizations, or those of the publisher, the editors and the reviewers. Any product that may be evaluated in this article, or claim that may be made by its manufacturer, is not guaranteed or endorsed by the publisher.

frontiers in Cardiovascular Medicine

ORIGINAL RESEARCH
published: 25 March 2022
doi: 10.3389/fcvm.2022.742193

Divergent Cardiac Effects of Angiotensin II and Isoproterenol Following Juvenile Exposure to Doxorubicin

Kevin Agostinucci[1†], Marianne K. O. Grant[1†], Davis Seelig[2], Doğacan Yücel[3,4], Jop van Berlo[3,4], Alessandro Bartolomucci[3], Jason R. B. Dyck[5] and Beshay N. Zordoky[1]*

[1] Department of Experimental and Clinical Pharmacology, University of Minnesota College of Pharmacy, Minneapolis, MN, United States, [2] Department of Veterinary Clinical Sciences, University of Minnesota College of Veterinary Medicine, St. Paul, MN, United States, [3] Department of Integrative Biology and Physiology, University of Minnesota Medical School, Minneapolis, MN, United States, [4] Department of Medicine, Lillehei Heart Institute, University of Minnesota Medical School, Minneapolis, MN, United States, [5] Department of Pediatrics, Faculty of Medicine and Dentistry, Cardiovascular Research Centre, University of Alberta, Edmonton, AB, Canada

OPEN ACCESS

Edited by:
Nazish Sayed,
Stanford University, United States

Reviewed by:
Yuri D'Alessandra,
Monzino Cardiology Center (IRCCS), Italy
Carmine Savoia,
Sapienza University of Rome, Italy
Martino Deidda,
University of Cagliari, Italy

***Correspondence:**
Beshay N. Zordoky
zordo001@umn.edu

[†] These authors have contributed equally to this work

Specialty section:
This article was submitted to Cardio-Oncology, a section of the journal Frontiers in Cardiovascular Medicine

Received: 15 July 2021
Accepted: 18 February 2022
Published: 25 March 2022

Citation:
Agostinucci K, Grant MKO, Seelig D, Yücel D, van Berlo J, Bartolomucci A, Dyck JRB and Zordoky BN (2022) Divergent Cardiac Effects of Angiotensin II and Isoproterenol Following Juvenile Exposure to Doxorubicin. Front. Cardiovasc. Med. 9:742193. doi: 10.3389/fcvm.2022.742193

Hypertension is the most significant risk factor for heart failure in doxorubicin (DOX)-treated childhood cancer survivors. We previously developed a two-hit mouse model of juvenile DOX-induced latent cardiotoxicity that is exacerbated by adult-onset angiotensin II (ANGII)-induced hypertension. It is still not known how juvenile DOX-induced latent cardiotoxicity would predispose the heart to pathologic stimuli that do not cause hypertension. Our main objective is to determine the cardiac effects of ANGII (a hypertensive pathologic stimulus) and isoproterenol (ISO, a non-hypertensive pathologic stimulus) in adult mice pre-exposed to DOX as juveniles. Five-week-old male C57BL/6N mice were administered DOX (4 mg/kg/week) or saline for 3 weeks and then allowed to recover for 5 weeks. Thereafter, mice were administered either ANGII (1.4 mg/kg/day) or ISO (10 mg/kg/day) for 14 days. Juvenile exposure to DOX abrogated the hypertrophic response to both ANGII and ISO, while it failed to correct ANGII- and ISO-induced upregulation in the hypertrophic markers, ANP and BNP. ANGII, but not ISO, worsened cardiac function and exacerbated cardiac fibrosis in DOX-exposed mice as measured by echocardiography and histopathology, respectively. The adverse cardiac remodeling in the DOX/ANGII group was associated with a marked upregulation in several inflammatory and fibrotic markers and altered expression of *Ace*, a critical enzyme in the RAAS. In conclusion, juvenile exposure to DOX causes latent cardiotoxicity that predisposes the heart to a hypertensive pathologic stimulus (ANGII) more than a non-hypertensive stimulus (ISO), mirroring the clinical scenario of worse cardiovascular outcome in hypertensive childhood cancer survivors.

Keywords: anthracycline-induced cardiotoxicity, doxorubicin, angiotensin II, hypertension, isoproterenol

INTRODUCTION

The survival rate of childhood cancer has increased from 60% to more than 85%, thanks to advanced diagnosis, treatment, and care models (1). Indeed, there are more than 500,000 childhood cancer survivors in the United States and this number is expected to increase. Although the increased survivorship is a cause for celebration, up to 73% of childhood cancer survivors suffer from long-term health complications (2). Cardiovascular disease is one of the most common long-term complications in survivors and the second leading cause of death in childhood cancer survivors after secondary malignancy (2). The high burden of cardiovascular diseases in childhood cancer survivors is mainly attributed to cardiotoxic cancer treatments such as anthracyclines and radiation therapy (3). Doxorubicin (DOX) is an anthracycline chemotherapeutic agent widely used in the treatment of lymphoma, leukemia, and other pediatric cancers, despite its known cardiotoxic effects (4). Since the severe cardiotoxic effects of DOX are dependent on the cumulative dose, the current treatment protocols usually do not exceed this threshold. Therefore, the rates of severe cardiovascular complications have declined in recent years. However, it has also been shown that low cumulative doses of DOX cause subclinical cardiotoxicity in childhood cancer survivors (5–7).

DOX-induced subclinical cardiotoxicity predisposes the survivors to adult-onset cardiovascular risk factors in a two-hit manner (8, 9). Given the expected long survivorship life in childhood cancer survivors, many of them would develop multiple cardiovascular risk factors later in their adult life, which can be considered as "second hits." Since hypertension is the most significant cardiovascular risk factor for all adverse cardiac events, including heart failure and cardiac death, in anthracycline-treated childhood cancer survivors (10), we have recently developed a two-hit mouse model of juvenile DOX-induced latent cardiotoxicity that is exacerbated by adult-onset angiotensin II (ANGII)-induced hypertension (11). Nevertheless, it is still not known how juvenile DOX-induced latent cardiotoxicity would predispose the heart to other cardiovascular pathologic stimuli that do not cause hypertension. In the current study, we characterize the detrimental synergy in the DOX/ANGII model in parallel to a new model wherein juvenile DOX exposure is followed by adult-onset catecholamine stress by daily injections of isoproterenol (ISO). ISO is a non-specific beta-adrenoceptor agonist that is commonly used to induce a dose-dependent cardiac pathology without elevating blood pressure (12–15). Characterizing both DOX/ANGII and DOX/ISO models is critical to understanding why hypertension is the most significant risk factor for cardiovascular morbidity and mortality in anthracycline-treated childhood cancer survivors and thereby devising effective therapeutic strategies against this significant clinical problem.

Abbreviations: ANGII, Angiotensin II; DOX, Doxorubicin; ISO, Isoproterenol.

MATERIALS AND METHODS

Animals

Animal procedures were approved by the Institutional Animal Care and Use Committee (IACUC) at the University of Minnesota (Protocol ID: 1807-36187A). Animal housing and all animal procedures were performed at the University of Minnesota according to the approved protocol. Male 4-week old C57BL/6N mice were purchased from Charles River Laboratories. All mice were housed in groups of 3-4 mice per cage, maintained under standard specific pathogen free (SPF) conditions, and given food and water *ad libitum* in a 14 h light/10 h dark cycle and at 21 ± 2°C. After a 1-week acclimation period, 5-week old mice were administered either DOX (4 mg/kg/week for 3 weeks, DOX group) or equivalent volume of sterile normal saline (control group). The mice were monitored twice per week and were weighed once weekly. Five-weeks following the last DOX injection at the age of 12 weeks (the age of young adult mice), control and DOX-treated mice were assigned to either the ANGII or ISO experiments. In the ANGII experiment (**Figure 1A**), control and DOX-exposed mice were infused with ANGII (1.4 mg/kg/day) or sterile normal saline for 14 days through subcutaneously implanted ALZET osmotic mini-pumps (Durect Corp, Cupertino, CA) to induce hypertension as previously reported (11, 16, 17). Animals were anesthetized with isoflurane (2-3%) and surgical site was clipped then cleaned with betadine and alcohol. Anesthetic level was assessed by toe pinch and respiratory rate. A skin incision was made with surgical scissors in the mid-scapular area, a filled pump was inserted into the pocket, and the wound was closed with skin staples. For analgesia, animals were administered carprofen (5 mg/kg) just prior to the surgery and daily for 3 days following surgery and monitored for any signs of infection or suture opening. In the ISO experiment (**Figure 1E**), 10 mg/kg ISO or an equivalent volume of sterile normal saline was administered by subcutaneous daily injection for 14 days as previously reported (12). At the end of the experiment, mice were humanely euthanized by decapitation under isoflurane anesthesia and hearts were harvested.

Echocardiography

All heart function and wall thickness data was measured using echocardiography. Baseline cardiac function was assessed 5 weeks after the last DOX treatment on the day prior to the start of the 14 day ANGII or ISO challenge. To determine the response to prolonged ANGII administration, cardiac function was assessed by echocardiography on the 15th day after implanting the mini-osmotic pumps containing either saline or ANGII in control and DOX-treated mice (n = 6-9 per group). To determine the response to ISO administration, cardiac function was assessed by echocardiography 24 h following the last dose of ISO or sterile saline injections in control and DOX-treated mice (n = 6 per group). Echocardiography was performed using the Vevo 2100 system (VisualSonics, Inc., Toronto, Ontario, Canada) equipped with an MS400 transducer. Anesthesia was induced with 3% isoflurane in oxygen and maintained at 1-2% during the procedure. Mice were secured in a supine position on a heated

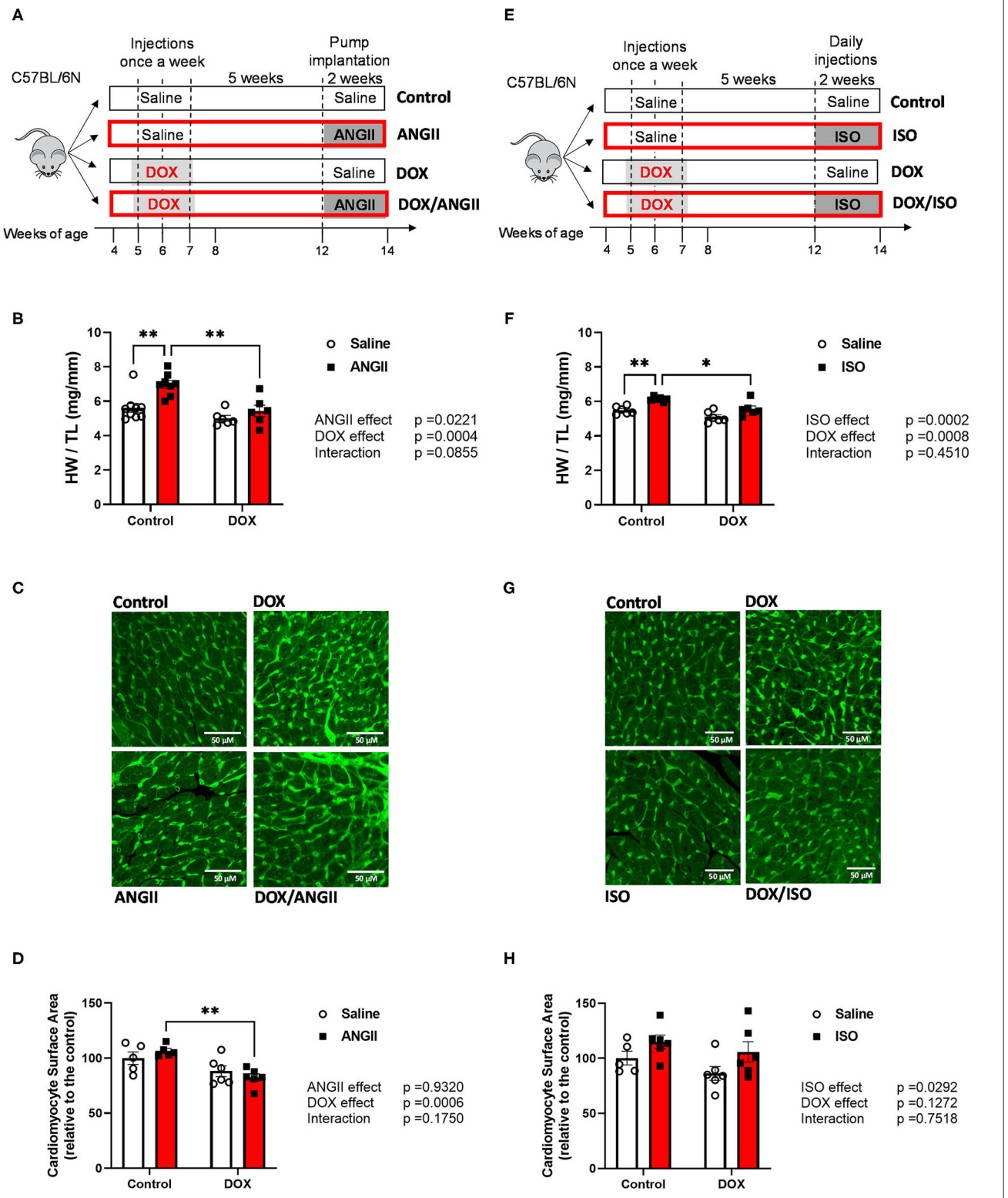

FIGURE 1 | Experimental design of the two-hit models of latent DOX cardiotoxicity using ANGII **(A)** or ISO **(E)** as second hits. Male 5-week old mice were administered DOX (4 mg/kg/week) or saline for 3 weeks and allowed to recover for 5 weeks prior to exposure to ANGII infusion (1.4 mg/kg/day for 14 days) or ISO injections (10 mg/kg/day for 14 days). Hypertrophic response to ANGII and ISO is abrogated by juvenile exposure to DOX. **(B,F)** Heart weight to tibial length ratio (HW/TL) (n = 6-9 per group). **(C,G)** Representative heart sections. **(D,H)** Quantification of cardiomyocyte surface area; bar scale = 50µM. Values are represented as means ± SEM. Statistical significance of pairwise comparisons was determined by two-way ANOVA with Tukey's *post-hoc* analysis (*$p < 0.05$, **$p < 0.01$). ANGII, Angiotensin II; DOX, doxorubicin; ISO, isoproterenol.

physiologic monitoring stage. Parasternal short axis images of the left ventricle were obtained in M-Mode at the level of the papillary muscles. Endocardial and epicardial borders were manually traced over three cardiac cycles and measures of cardiac function and morphometry were calculated using VisualSonics cardiac measurement package of the Vevo 2100.

Histopathology

Left ventricular (LV) heart sections were collected, fixed in 10% neutral buffered formalin and embedded in paraffin. Four-micron sections were stained with hematoxylin and eosin (H&E) or Masson's trichrome stain. Histopathologic evaluation was performed by a board-certified veterinary pathologist who was blinded to the experimental group. Inflammation and fibrosis were assessed as follows: 0, absent; 1, minimal inflammation or fibrosis; 2, mild inflammation or fibrosis; 3, moderate inflammation or fibrosis; and 4, marked inflammation or fibrosis. Sections from each heart were also immunohistochemically stained for expression of MAC-2 (galectin-3). In brief, four-micron sections were dewaxed and rehydrated prior to antigen retrieval. Thereafter, sections were incubated with anti-galectin-3 antibody (clone M3/38, Cedarlane Labs, Burlington, NC) according to manufacturer's instruction. The number of MAC-2 positive cells was manually quantified on the five most cellular 200X images. To measure cardiomyocyte cross-sectional surface area from histological sections, we stained dewaxed and rehydrated sections with Fluorescein isothiocyanate-conjugated wheat germ agglutinin (5 μg/ml, Vector Laboratories FL-1021) and 4′,6-diamidino-2-phenylindole (DAPI, Invitrogen D3571). Stained slides were mounted with Vectashield (Vector Laboratories H-1000). Images were acquired using a Nikon TiE or a Zeiss Axio Images M1 microscope, both equipped with a digital black/white camera. Wheat germ agglutinin binds to glycosylated proteins, which are enriched in the membranes of cells. Based on the difference in size between cardiomyocytes and non-cardiomyocytes, we traced the area of cardiomyocytes using Image J. We selected areas where cardiomyocytes had a round shape, indicative of a cross-sectioned cardiomyocytes. We traced at least 100 cardiomyocytes per heart in different areas of a cross-sectioned heart. Images were quantified by a researcher blinded to the treatment.

RNA Extraction and Real-Time PCR

Total RNA was extracted from 20 mg frozen heart tissue using 300 μl Trizol reagent (Life Technologies, Carlsbad, CA) according to manufacturer's instructions. RNA concentrations were measured at 260 nm using a NanoDrop 8000 spectrophotometer (Thermo Fisher Scientific, Wilmington, DE) and first-strand cDNA was synthesized from 1.5 μg total RNA using the high-capacity cDNA reverse transcription kit (Applied Biosystems, Foster City, CA) according to manufacturer's instructions. Specific mRNA expression was quantified by real-time PCR using SYBR Green (Applied Biosystems) and performed on an ABI 7900HT instrument (Applied Biosystems). Thermocycler conditions were as follows: 95°C for 10 min, followed by 40 PCR cycles of denaturation at 95°C for 15 s, and annealing/extension at 60°C for 1 min. Gene expression was determined using previously published primers for atrial natriuretic peptide (*ANP*), b-type natriuretic peptide *(BNP),* Cyclooxygenase-2 *(Cox2),* Collagen 1a1 *(Col1a1),* Collagen 3a1 *(Col3a1),* Galectin-3 *(Lgals3),* Angiotensin converting enzyme *(Ace),* ANGII type 1 receptor-*a (Agtr1a),* and ANGII type 1 receptor-b *(Agtr1b)*. Primer sequences are listed in **Supplementary Table 1**. The mRNA expression levels were normalized to beta-actin and are expressed relative to the control group. Relative gene expression was determined by the ΔΔCT method. Primer specificity and purity of the final PCR product were confirmed by melting curve analysis.

Statistical Analysis

Data were analyzed using GraphPad Prism software (version 9.0, La Jolla, CA) and are presented as individual data points and their means ± standard errors of the mean (SEM). Comparisons among different treatment groups were performed by ordinary two-way analysis of variance (ANOVA), followed by Tukey's multiple comparison *post-hoc* analysis. Comparisons between two groups were performed by unpaired student's two-tailed *t*-test. Statistical analyses for histopathologic grading were performed using the non-parametric Kruskal-Wallis test. A *p*-value of <0.05 was taken to indicate statistical significance.

RESULTS

Juvenile Exposure to DOX Abrogated the Hypertrophic Response to Both ANGII and ISO

Juvenile exposure to DOX (4 mg/kg/week for 3 weeks) did not cause significant morbidity or mortality in mice, similar to our earlier study (11). In addition, treatments with either ANGII or ISO were not associated with significant morbidity or mortality, when administered to control or DOX-treated mice (**Supplementary Figure 1**).

Corroborating previous studies (16, 18), 2 weeks of ANGII infusion or ISO injections caused cardiac hypertrophy in control mice as demonstrated by an increase in the heart weight to tibia length (HW/TL) (**Figures 1B,F**). Remarkably, juvenile exposure to DOX prevented both ANGII- and ISO-induced cardiac hypertrophy as evident by a reduction in HW/TL (**Figures 1B,F**). To follow on this result, we measured cardiomyocyte surface area to determine if the reduction of heart weight is due to cardiomyocyte atrophy (**Figures 1C,D,G,H**). Mice exposed to DOX/ANGII had the smallest surface area among the groups and this group was significantly different from mice treated with ANGII only (**Figures 1C,D**). No statistically significant differences in cardiomyocyte surface area were observed in mice treated with ISO (**Figures 1G,H**). Images shown are representative images for each group, where wheat germ agglutinin staining is pseudo-colored green (**Figures 1C,G**).

Measurements of ANP and BNP mRNA expressions were assessed to determine the cardiotoxicity that was induced on the heart by the pharmacological interventions. There were no differences observed in ANP and BNP mRNA expression between control and ANGII treated mice. The combination

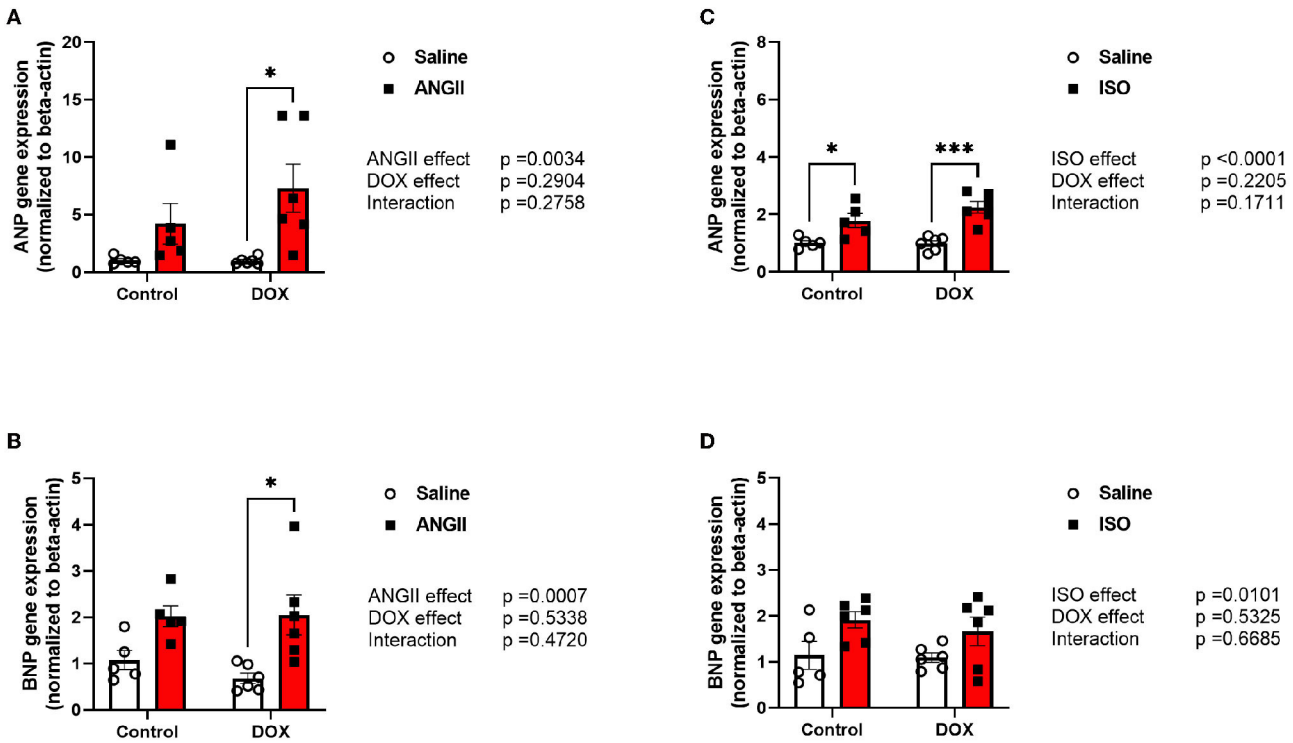

FIGURE 2 | Juvenile exposure to DOX fails to correct ANGII- and ISO-induced upregulation of hypertrophic markers. Male 5-week old mice were administered DOX (4 mg/kg/week) or saline for 3 weeks and allowed to recover for 5 weeks prior to exposure to **(A,B)** ANGII (1.4 mg/kg/day for 14 days) or **(C,D)** ISO (10 mg/kg/day for 14 days). The mRNA expression of *ANP* **(A,C)** and *BNP* **(B,D)** was determined by real-time PCR (n = 5-6 per group); results were normalized to beta-actin and are expressed relative to the control group. Values are represented as means ± SEM. Statistical significance of pairwise comparisons was determined by two-way ANOVA with Tukey's *post-hoc* analysis (*$p < 0.05$, ***$p < 0.001$). ANGII, Angiotensin II; ANP, atrial natriuretic peptide; BNP, B-type natriuretic peptide; DOX, doxorubicin; ISO, Isoproterenol.

of DOX/ANGII significantly increased the expression of these markers compared to DOX alone (**Figures 2A,B**). On the other hand, it appears that DOX did not exacerbate the ISO mediated increases in ANP and BNP since no statistically significant differences were observed between DOX/ISO and ISO alone (**Figures 2C,D**).

ANGII but Not ISO Worsens Cardiac Function in DOX-Exposed Mice

There were no significant changes in systolic cardiac function 5 weeks after the last DOX treatment, as evidenced by no significant difference in ejection fraction or fractional shortening (**Table 1**). Cardiac output and stroke volume were significantly lower in DOX-exposed mice than that in saline-treated mice, which was associated with a reduction in LV mass and wall thickness (**Table 1**). Neither DOX nor ANGII alone was sufficient to significantly reduce the cardiac function in mice (**Figures 3A–D**); however, juvenile exposure to DOX followed by adult-onset ANGII-induced hypertension caused a significant deterioration in cardiac function parameters as shown by a decrease in cardiac output (**Figure 3B**), stroke volume (**Figure 3C**), and ejection fraction (**Figure 3D**). Intriguingly, when DOX-exposed mice were subjected to ISO as a second cardiovascular hit, the cardiac function of DOX/ISO-treated mice did not significantly differ from the other groups (**Figures 3E–H**). **Tables 2**, **3** show detailed echocardiography measurements after 14 days of ANGII, ISO, or saline treatment in control and DOX-treated mice.

ANGII but Not ISO Worsens Cardiac Fibrosis in DOX-Exposed Mice

Histopathology analysis using H&E and Masson's trichrome stains revealed marked inflammatory cell infiltration and cardiac fibrosis in the DOX/ANGII group as compared to the control (**Figures 4A–C**). Although a few mice in the DOX and ANGII groups showed signs of cardiac fibrosis at varying degrees, neither DOX nor ANGII alone was sufficient to cause a statistically significant effect on cardiac fibrosis (**Figure 4C**). The combination of DOX and ANGII significantly increased fibrosis suggesting that DOX potentiates the fibrosis inducing action of ANGII. On the other hand, ISO treatment caused modest, but statistically significant, cardiac fibrosis which was not exacerbated by DOX treatment (**Figures 4D–F**). To ascertain the molecular determinants of the observed fibrotic changes, we measured gene expression of several inflammatory and fibrotic markers. ANGII caused a significant induction of the inflammatory marker *Cox-2* (**Figure 5A**) and the fibrotic markers, *Col1a1* and *Col3a1* (**Figures 5B,C**). Juvenile exposure

TABLE 1 | Cardiac function and morphometry measured by trans-thoracic echocardiography in control and DOX-treated mice 5 weeks following the last DOX administration.

Parameter	Control mean (SEM)	DOX mean (SEM)
CO (ml/min)	18.19 (0.6730)	15.59** (0.4575)
SV (μl)	42.73 (1.608)	37.51** (0.6720)
EF (%)	54.72 (1.792)	55.18 (1.879)
FS (%)	28.33 (1.121)	28.53 (1.162)
LV Mass (mg)	128.0 (4.310)	101.4**** (2.111)
LVESV (μl)	37.95 (2.564)	32.90 (2.742)
LVEDV (μl)	84.02 (3.644)	75.60 (2.650)
LVAW;s (mm)	1.373 (0.02731)	1.280 (0.04129)
LVAW;d (mm)	1.017 (0.02067)	0.9286* (0.02676)
LVPW;s (mm)	1.124 (0.03176)	0.9752*** (0.02614)
LVPW;d (mm)	0.7967 (0.02410)	0.6684**** (0.01267)
HR (bpm)	427 (5)	416 (11)

*Values are presented as mean ± standard error of the mean (SEM) (N = 22-23). Statistical significance was determined using an unpaired t-test. *p < 0.05, **p < 0.01, ***p < 0.001, ****p < 0.0001 vs. control. DOX, doxorubicin; CO, cardiac output; SV, stroke volume; EF, ejection fraction; FS, fractional shortening; LV, left ventricle; LVESV, LV end systolic volume; LVEDV, LV end diastolic volume; LVAW;s, LV anterior wall systole; LVAW;d, LV anterior wall diastole; LVPW;s, LV posterior wall systole; LVPW;d, LV posterior wall diastole; HR, heart rate.*

to DOX mildly but not significantly exacerbated ANGII-induced upregulation of inflammatory and fibrotic markers (**Figures 5A–C**). Marked increases in inflammatory and fibrotic markers were observed in DOX/ANGII treated mice compared to mice only treated with DOX. On the other hand, DOX/ISO had no exacerbating effect on *Cox-2* or *Col3a1* expression (**Figures 5D,F**), while there was a significant reduction in *Col1a1* expression in the DOX/ISO treated mice compared to ISO alone (**Figure 5E**).

Since macrophage infiltration plays an important role in cardiac fibrosis, we measured the expression the fibrotic marker galectin-3 by measuring MAC-2 positive cells by immunohistochemistry as well as the gene expression of galectin-3 *(Lgals-3)*. As expected, ANGII caused a significant increase in the number of MAC-2 positive cells (**Figures 6A,B**) but not a significant induction of *Lgals-3* gene expression (**Figure 6C**). In agreement with the exacerbation of cardiac fibrosis in the DOX/ANGII group, DOX/ANGII-treated mice had the highest number of MAC-2 positive cells (**Figures 6A,B**). Juvenile exposure to DOX significantly aggravated ANGII-induced upregulation of *Lgals-3* gene expression (**Figure 6C**). ISO caused a modest but significant increase in the number of MAC-2 positive cells (**Figures 6D,E**) and caused a significant upregulation of *Lgal-3* gene expression (**Figure 6F**). However, juvenile exposure to DOX did not change the effects of ISO on these parameters (**Figures 6D–F**).

Perturbed RAAS Gene Expression in the DOX/ANGII Model

Since DOX has been shown to alter the renin-angiotensin-aldosterone-system (RAAS) in different ways (19), we sought to determine whether DOX-induced alteration in the RAAS may have played a role in the detrimental synergy between DOX and ANGII. To this end, we determined the effects of DOX, ANGII, and DOX/ANGII on expression of the RAAS genes in the heart. Interestingly, the gene expression of angiotensin converting enzyme (*Ace*) was significantly upregulated in the DOX/ANGII group compared to DOX alone (**Figure 7A**). Next, measurements of the *Atgr1a* and *Atgr1b*, the gene encoding for the ANGII type 1 receptor (AT1) were measured and no statistically significant differences were observed among the groups (**Figures 7B,C**).

DISCUSSION

Childhood cancer survivors have a considerably increased risk for premature cardiovascular diseases (20), with an estimated 15 times higher risk of heart failure than their siblings who did not have cancer (2). Nearly 50% of pediatric cancer patients receive anthracyclines such as doxorubicin (DOX), which are known to cause cardiotoxicity (21). Although the risk of anthracycline-induced cardiotoxicity increases with a higher anthracycline cumulative dose (22), latent (subclinical) cardiotoxicity occurs in children who receive low doses of anthracyclines (5–7). Anthracycline-induced subclinical cardiotoxicity is characterized by reduction in the left ventricular mass, mild cardiac fibrosis, and modest decline in ejection fraction (5–7). This latent cardiotoxicity can be unmasked and overt cardiomyopathy precipitated by other cardiovascular risk factors in adulthood, in a two-hit manner (10). We designed the current experimental protocol to mimic the scenario in cancer survivors that undergo DOX treatment at young age. With this protocol, we are able to show that latent cardiotoxicity caused by juvenile exposure to DOX is exacerbated when adult mice undergo a hypertensive "second-hit" on the heart. We used ANGII and ISO as two pharmacological agents that both increase the stress on the heart through distinct mechanisms. In this report, we show that the combination of DOX and ANGII causes the most changes to heart size, cardiac function and fibrosis. While the combination of DOX and ISO shows modest changes in heart size, cardiac function and fibrosis are not affected (**Figure 8**).

Most preclinical models of juvenile DOX-induced cardiotoxicity used high cumulative doses of DOX that were enough to cause immediate or delayed cardiac dysfunction (23–26). Although clinically relevant, animal models for juvenile DOX cardiotoxicity have rarely adopted the two-hit models. Huang *et al.* demonstrated that low doses of DOX administered to very young mice, at postnatal day 5, did not cause immediate cardiac dysfunction. DOX-exposed mice developed normally and had no obvious cardiac dysfunction as adults. However, juvenile exposure to DOX exacerbated cardiac pathology in response to an adult-onset pathologic stimulus (myocardial infarction) and even a physiologic stimulus (swimming exercise) (27). Since hypertension is the most significant cardiovascular risk factor for all adverse cardiac events, including heart failure and cardiac death, in anthracycline-treated childhood cancer survivors (10), we have recently developed another two-hit mouse model of juvenile DOX-induced latent cardiotoxicity

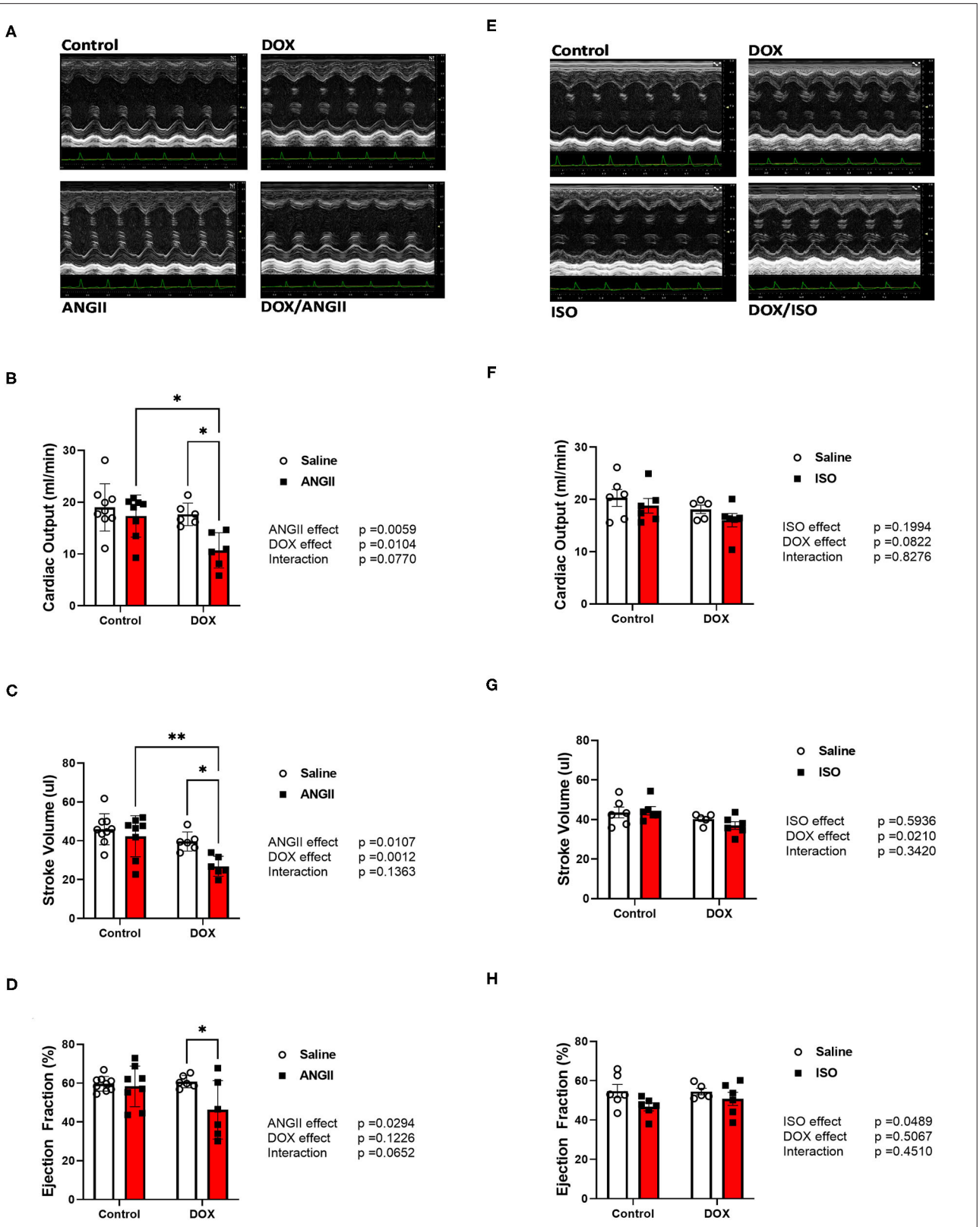

FIGURE 3 | ANGII, but not ISO, worsens cardiac function in DOX-exposed mice. Male 5-week old mice were administered DOX (4 mg/kg/week) or saline for 3 weeks and allowed to recover for 5 weeks prior to exposure to **(A–D)** ANGII (1.4 mg/kg/day for 14 days) or **(E–H)** ISO (10 mg/kg/day for 14 days). Cardiac function was determined by trans-thoracic echocardiography (n = 5-9 per group). **(A,E)** Representative M-Mode images from parasternal short axis view of the heart. **(B,F)** Cardiac output. **(C,G)** Stroke volume. **(D,H)** Ejection fraction. Values are represented as means ± SEM. Statistical significance of pairwise comparisons was determined by two-way ANOVA with Tukey's *post-hoc* analysis (*$p < 0.05$, **$p < 0.01$). ANGII, Angiotensin II; DOX, doxorubicin; ISO, isoproterenol.

TABLE 2 | Cardiac function and morphometry measured by trans-thoracic echocardiography in control, ANGII, DOX, DOX/ANGII-treated mice.

Parameter	Control mean (SEM)	ANGII mean (SEM)	DOX mean (SEM)	DOX/ANGII mean (SEM)	ANGII effect		DOX effect		Interaction effect	
					Effect size (%)	*P*-value	Effect size (%)	*P*-value	Effect size (%)	*P*-value
CO (ml/min)	18.998 (1.518)	17.328 (1.434)	17.667 (0.885)	10.695[b,c] (1.393)	20.67	0.0059	17.55	0.0104	7.776	0.0770
SV (μl)	45.953 (2.659)	42.330 (3.744)	39.634 (2.012)	26.866[b,c] (2.117)	16.02	0.0107	28.29	0.0012	4.986	0.1363
EF (%)	59.651 (1.258)	58.340 (3.707)	60.786 (1.299)	46.235[c] (6.151)	15.10	0.0294	7.222	0.1226	10.52	0.0652
FS (%)	31.432 (0.844)	32.044 (0.843)	30.825 (2.498)	23.195 (3.701)	7.473	0.1198	13.57	0.0397	10.31	0.0701
LV mass (mg)	129.918 (6.306)	147.820 (6.334)	110.631 (7.536)	119.872 (9.024)	8.849	0.0733	26.80	0.0033	0.9011	0.5562
LVESV (μl)	31.627 (2.931)	31.681 (5.289)	26.048 (2.645)	34.595 (6.427)	3.360	0.3536	0.3225	0.7720	3.276	0.3595
LVEDV (μl)	77.578 (5.390)	74.009 (7.285)	65.682 (4.635)	61.460 (6.247)	1.323	0.5393	13.03	0.0621	0.009296	0.9588
LVAW;s (mm)	1.475 (0.055)	1.614 (0.083)	1.412 (0.067)	1.340[b] (0.029)	0.7565	0.6144	18.94	0.0172	7.446	0.1220
LVAW;d (mm)	1.087 (0.030)	1.166 (0.038)	1.094 (0.053)	1.128 (0.020)	7.913	0.1558	0.5889	0.6929	1.237	0.5677
LVPW;s (mm)	1.125 (0.041)	1.310[a] (0.060)	1.035 (0.014)	1.097[b] (0.055)	14.74	0.0183*	22.06	0.0049	3.690	0.2184
LVPW;d (mm)	0.792 (0.025)	0.936[a] (0.046)	0.701 (0.019)	0.898[c] (0.052)	42.00	0.0002	5.985	0.1046	1.026	0.4920
HR (bpm)	411 (16)	413 (13)	446 (8)	390 (26)	8.487	0.1244	0.5206	0.6971	9.698	0.1016

Values are presented as mean ± standard error of the mean (SEM) (N = 6-9). Statistical significance was determined using Two-way ANOVA with Tukey post-hoc test. [a]significant difference ($p < 0.05$) vs. control, [b]significant difference ($p < 0.05$) vs. ANGII, [c]significant difference ($p < 0.05$) vs. DOX. DOX, doxorubicin; ANGII, angiotensin II; CO, cardiac output; SV, stroke volume; EF, ejection fraction; FS, fractional shortening; LV, left ventricle; LVESV, LV end systolic volume; LVEDV, LV end diastolic volume; LVAW;s, LV anterior wall systole; LVAW;d, LV anterior wall diastole; LVPW;s, LV posterior wall systole; LVPW;d, LV posterior wall diastole; HR, heart rate.

that is exacerbated by adult-onset ANGII-induced hypertension (11). Similar to Huang et al., we demonstrated that low doses of DOX (4 mg/kg/week for 3 weeks) did not cause immediate cardiac dysfunction in juvenile mice, but predisposed to late-occurring detrimental cardiovascular changes when the mice were challenged by ANGII-induced hypertension (11). However, unlike Huang et al., our DOX administration regimen starts at 5 weeks of age, equivalent to 10 years in human life. Therefore, these dosage regimens model latent cardiotoxicity in anthracycline-treated pediatric cancer patients who do not immediately develop overt cardiac dysfunction but are left with "weaker" hearts that predispose them to other cardiovascular insults, corroborating the findings of several clinical studies (5, 28–31).

Nevertheless, it is still not known how this low-dose DOX regimen would predispose the heart to other cardiovascular pathologic stimuli that do not cause hypertension. To answer this question, we subjected control and DOX-treated mice to a regimen of ISO injections (10 mg/kg/day for 14 days). ISO is a non-specific beta-adrenoceptor agonist that is commonly used to induce a dose-dependent cardiac pathology without elevating blood pressure (12–15). We have previously demonstrated that this dosage regimen causes cardiac hypertrophy, mild cardiac dysfunction, and modest cardiac fibrosis in C57BL/6N male mice (12). In the current study, we characterize the DOX/ANGII model in parallel to the DOX/ISO model to better understand why hypertension is the most significant risk factor for cardiovascular morbidity and mortality in anthracycline-treated childhood cancer survivors.

Cardiac atrophy and thinning of the LV ventricular walls are common late effects of anthracycline therapy in childhood cancer survivors (32–35). Intriguingly, a study has shown that reduction in the LV mass is associated with worsening of heart failure symptomatology independent of LV ejection fraction in adult cancer survivors (36), demonstrating the predictive value of LV mass. However, the association between LV mass and heart failure symptomatology has not been determined in childhood cancer survivors. We previously demonstrated that juvenile exposure to DOX prevented the adaptive cardiac hypertrophy in response to ANGII-induced hypertension (11). However, it is not known whether juvenile exposure to DOX would also prevent adaptive cardiac hypertrophy in response to other hypertrophic stimuli. In the current study, juvenile exposure to DOX prevented the adaptive cardiac hypertrophy in response to both ANGII and ISO. Indeed, ANGII and ISO cause cardiac hypertrophy *via* different pathways. ANGII induces cardiac hypertrophy directly

TABLE 3 | Cardiac function and morphometry measured by trans-thoracic echocardiography in control, ISO, DOX, and DOX/ISO-treated mice.

Parameter	Control mean (SEM)	ISO mean (SEM)	DOX mean (SEM)	DOX/ISO mean (SEM)	ISO effect		DOX effect		Interaction effect	
					Effect size (%)	*P*-value	Effect size (%)	*P*-value	Effect size (%)	*P*-value
CO (ml/min)	20.277 (1.611)	18.780 (1.382)	18.099 (0.816)	16.006 (1.281)	7.235	0.1994	13.78	0.0822	0.1995	0.8276
SV (μl)	43.548 (2.741)	44.475 (2.125)	40.238 (1.203)	36.981 (1.920)	1.095	0.5936	23.52	0.0210*	3.530	0.3420
EF (%)	54.733 (3.368)	46.709 (1.998)	54.491 (1.682)	50.739 (3.336)	18.03	0.0489	1.865	0.5067	2.372	0.4547
FS (%)	28.337 (2.205)	23.328 (1.151)	27.932 (1.088)	25.679 (2.004)	17.80	0.0510	1.277	0.5834	2.563	0.4390
LV Mass (mg)	123.532 (4.444)	142.947[a] (4.850)	111.599 (5.807)	115.680[b] (4.893)	13.08	0.0291	36.40	0.0009	5.570	0.1400
LVESV (μl)	38.702 (4.164)	52.299 (4.359)	34.158 (2.724)	38.550 (4.384)	16.04	0.0404	16.59	0.0375	4.200	0.2744
LVEDV (μl)	80.931 (4.542)	100.300[a] (5.185)	81.370 (2.362)	79.407[b] (4.553)	11.08	0.0659	15.30	0.0334	16.64	0.0273
LVAW;s (mm)	1.330 (0.087)	1.307 (0.062)	1.313 (0.074)	1.242 (0.062)	2.127	0.5230	1.685	0.5693	0.5551	0.7432
LVAW;d (mm)	1.025 (0.046)	1.076 (0.025)	0.983 (0.047)	1.010 (0.054)	3.619	0.3911	6.931	0.2395	0.3312	0.7935
LVPW;s (mm)	1.114 (0.054)	0.989 (0.026)	0.959 (0.070)	1.047 (0.058)	0.4790	0.7384	3.546	0.3681	16.95	0.0582
LVPW;d (mm)	0.794 (0.042)	0.780 (0.015)	0.690 (0.033)	0.734 (0.028)	0.9204	0.6328	22.68	0.0262	3.506	0.3552
HR (bpm)	463 (10)	421 (14)	449 (11)	430 (18)	19.78	0.0390	0.1030	0.8746	2.785	0.4158

Values are presented as mean ± standard error of the mean (SEM) (N = 5-6). Statistical significance was determined using Two-way ANOVA with Tukey post-hoc test. [a]Significant difference ($p < 0.05$) vs. control, [b]significant difference ($p < 0.05$) vs. ISO. DOX, doxorubicin; ISO, isoproterenol; CO, cardiac output; SV, stroke volume; EF, ejection fraction; FS, fractional shortening; LV, left ventricle; LVESV, LV end systolic volume; LVEDV, LV end diastolic volume; LVAW;s, LV anterior wall systole; LVAW;d, LV anterior wall diastole; LVPW;s, LV posterior wall systole; LVPW;d, LV posterior wall diastole; HR, heart rate.

through activating the AT1 receptors on cardiomyocytes and indirectly through elevating the afterload (37). In contrast, ISO activates the beta-adrenoceptors on cardiomyocytes to elicit a direct hypertrophic effect (37). ISO-induced tachycardia may also contribute to its hypertrophic effect indirectly. The ability of DOX to prevent cardiac hypertrophy in response to both pathologic stimuli suggest that DOX interferes with common downstream pathways fundamental to the development of cardiac hypertrophy.

Although high-dose DOX causes cardiac atrophy due to apoptotic and necrotic cell death and loss of cardiomyocytes (38), experimental studies using low/divided-dose DOX have suggested that DOX-induced cardiomyocyte atrophy is the main culprit leading to cardiac atrophy and reduction of LV mass with minimal apoptotic cell death (39, 40). We demonstrate that mice with juvenile exposure to DOX had the smallest cardiomyocyte surface area after ANGII exposure. These experimental observations have recently been supported by a clinical study reporting that the reduction in LV mass after anthracycline therapy is due to cardiomyocyte atrophy in breast cancer patients (41). Another recent preclinical study has shown that acute DOX administration causes dose-dependent cardiac atrophy that parallels the decrease in contractile function (39). In our current study, we demonstrate that chronic administration of low-dose DOX caused cardiac atrophy without reducing the contractile function of the heart. The contractile function of the heart was only affected when the juvenile exposure of DOX was followed by ANGII-induced hypertension. ANGII cause pathologic cardiac hypertrophy characterized by the induction of fetal gene expression such as *ANP* and *BNP*, adverse cardiac remodeling, and reduction in cardiac function parameters. Therefore, in the current work, we determined the effect of juvenile DOX exposure on these parameters. Although we previously showed that juvenile exposure to DOX induced *ANP* gene expression 1 week after the last DOX injection (11), there is no significant change in *ANP* or *BNP* in DOX-exposed mice 7 weeks after the last DOX injection. Only the combination of DOX/ANGII was able to significantly elevate the markers of pathological hypertrophy. Although juvenile exposure to DOX prevented the hypertrophic growth of the heart in response to ANGII, it did not abrogate the molecular determinants of pathological cardiac hypertrophy induced by these stimuli.

We also determined the effect of juvenile exposure to DOX on cardiac remodeling in response to both ANGII and ISO. In our previous study describing the DOX/ANGII model (11), the effect on cardiac fibrosis had not been determined.

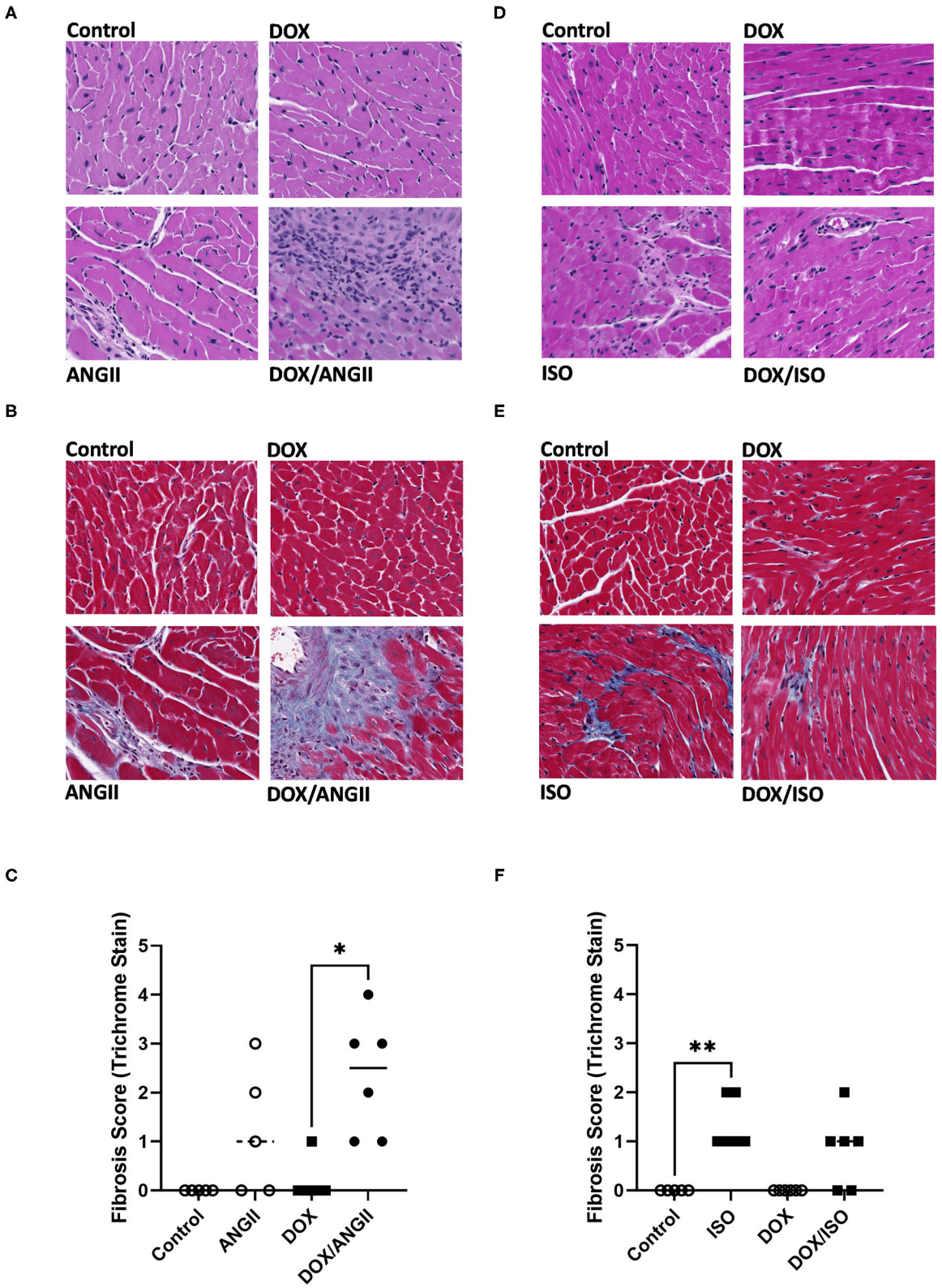

FIGURE 4 | ANGII, but not ISO, worsens cardiac fibrosis in DOX-exposed mice. Male 5-week old mice were administered DOX (4 mg/kg/week) or saline for 3 weeks and allowed to recover for 5 weeks prior to exposure to **(A–C)** ANGII (1.4 mg/kg/day for 14 days) or **(D–F)** ISO (10 mg/kg/day for 14 days). Representative images from H&E **(A,D)** and Masson's trichrome stained heart sections **(B,E)**. **(C,F)** Semi-quantification of fibrosis score derived from Masson's trichrome stain (n = 5-6 per group). Statistical significance was determined by non-parametric Kruskal-Wallis test (*$p < 0.05$, **$p < 0.01$). ANGII, Angiotensin II; DOX, doxorubicin; H&E, hematoxylin and eosin; ISO, isoproterenol.

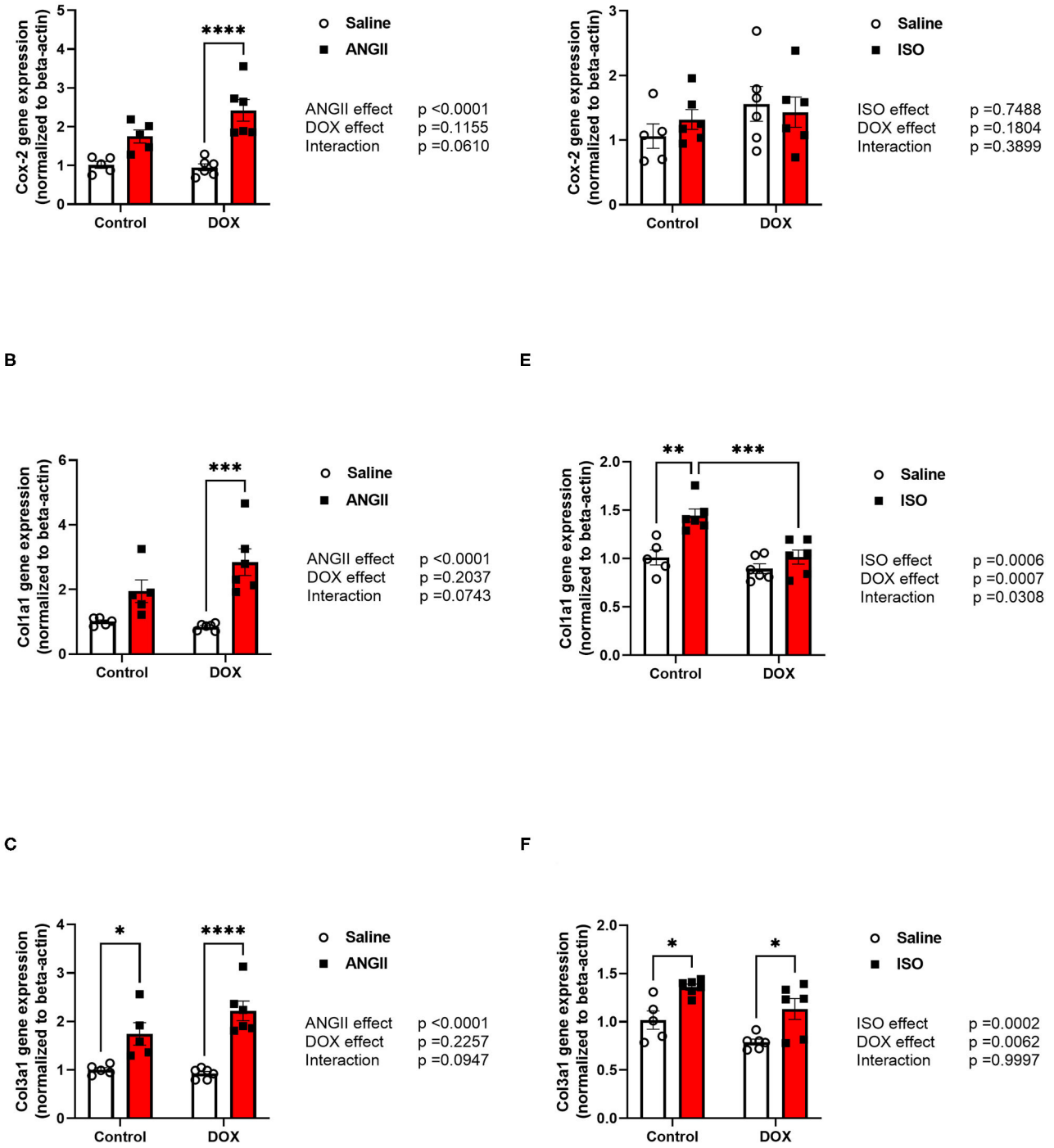

FIGURE 5 | ANGII, but not ISO, exacerbates the upregulation of inflammatory and fibrotic markers in DOX-exposed mice. Male 5-week old mice were administered DOX (4 mg/kg/week) or saline for 3 weeks and allowed to recover for 5 weeks prior to exposure to **(A–C)** ANGII (1.4 mg/kg/day for 14 days) or **(D–F)** ISO (10 mg/kg/day for 14 days). The mRNA expression of **(A,D)** the inflammatory marker *Cox-2*, and the fibrotic markers **(B,E)** *Col1a1* and **(C,F)** *Col3a1* was determined by real-time PCR ($n = 5$-6 per group). Results were normalized to beta-actin and are expressed relative to the control group. Statistical significance of pairwise comparisons was determined by two-way ANOVA with Tukey's *post-hoc* analysis ($^{*}p < 0.05$, $^{**}p < 0.01$, $^{***}p < 0.001$, $^{****}p < 0.0001$). ANGII, Angiotensin II; DOX, doxorubicin; ISO, isoproterenol.

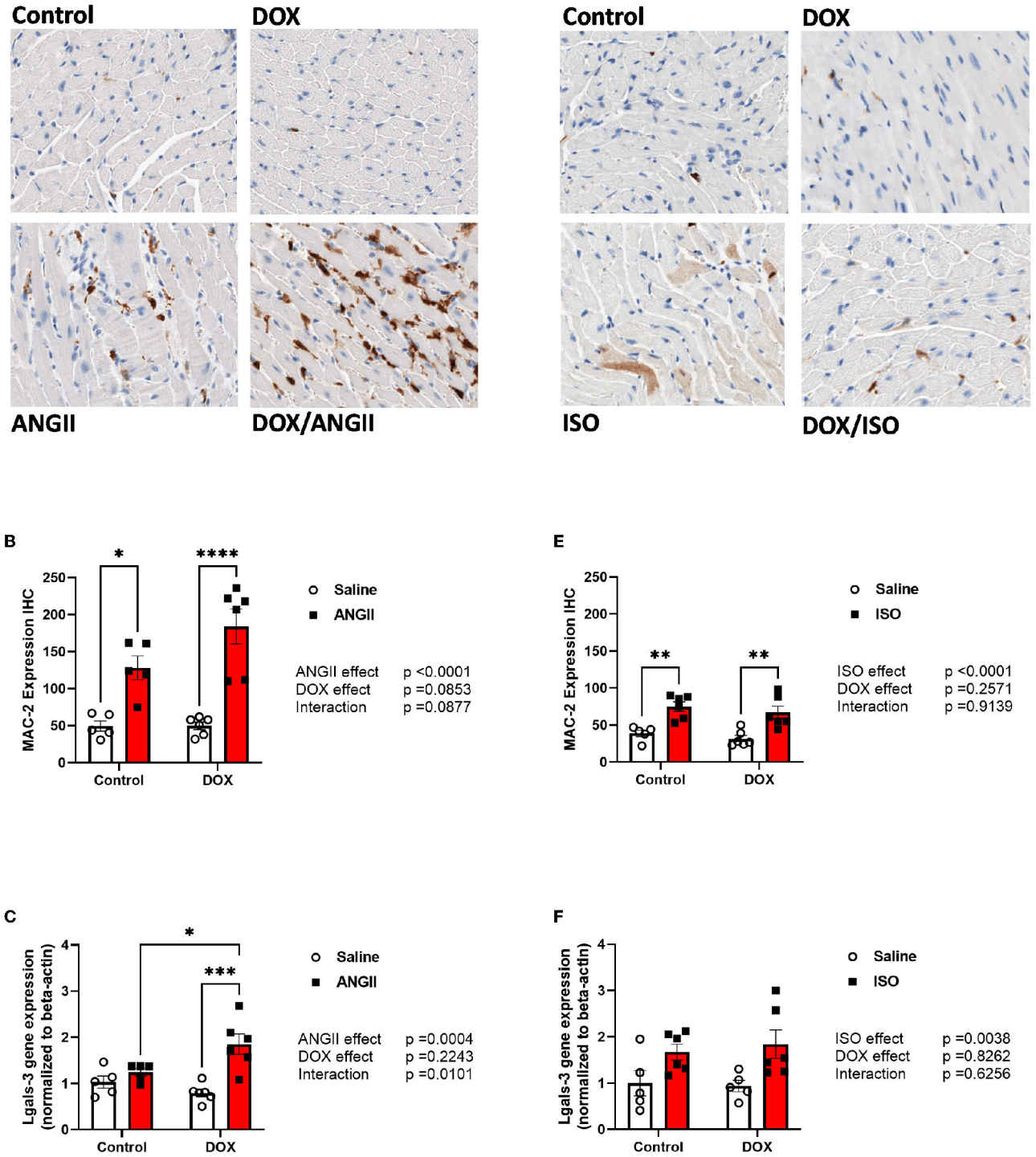

FIGURE 6 | ANGII, but not ISO, exacerbates the upregulation of MAC-2 in DOX-exposed mice. Male 5-week old mice were administered DOX (4 mg/kg/week) or saline for 3 weeks and allowed to recover for 5 weeks prior to exposure to **(A–C)** ANGII (1.4 mg/kg/day for 14 days) or **(D–F)** ISO (10 mg/kg/day for 14 days). Representative images from **(A,D)** MAC-2 stained heart sections. **(B,E)** Semi-quantification of MAC-2 positive cells (n = 5-6 per group). The mRNA expression of **(C,F)** *Lgals-3* was determined by real-time PCR (n = 5-6 per group). Results were normalized to beta-actin and are expressed relative to the control group. Statistical significance of pairwise comparisons was determined by two-way ANOVA with Tukey's *post-hoc* analysis (*$p < 0.05$, **$p < 0.01$, ***$p < 0.001$, ****$p < 0.0001$). ANGII, Angiotensin II; DOX, doxorubicin; ISO, isoproterenol; Lgals-3, lectin, galactoside-binding, soluble-3.

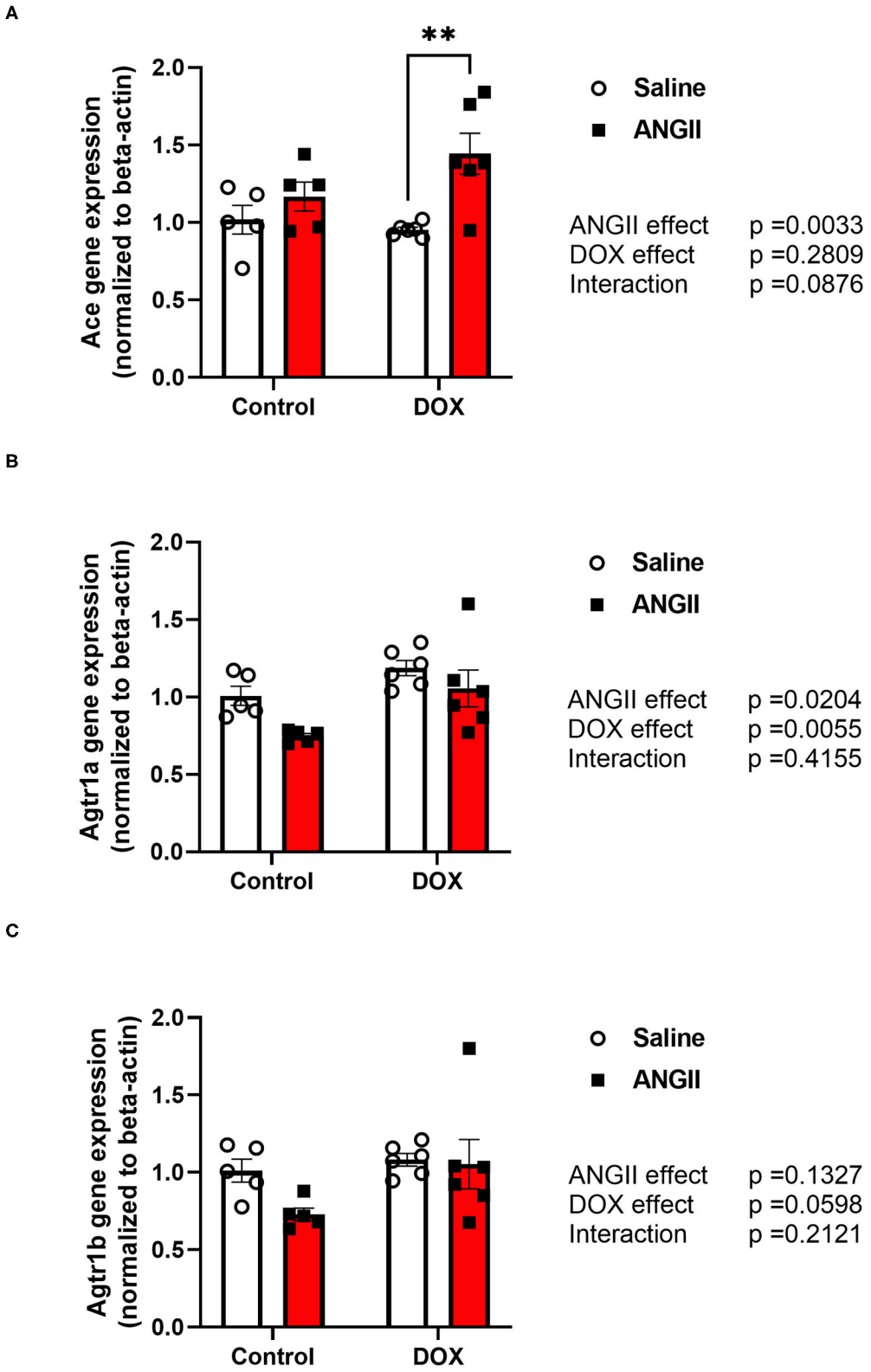

FIGURE 7 | Perturbation of the RAAS pathway in the DOX/ANGII model. Male 5-week old mice were administered DOX (4 mg/kg/week) or saline for 3 weeks and allowed to recover for 5 weeks prior to exposure to ANGII (1.4 mg/kg/day for 14 days). The mRNA expression of **(A)** *Ace*, **(B)** *Agtr1a*, and **(C)** *Agtr1b* was determined by real-time PCR (n = 5-6 per group). Results were normalized to beta-actin and are expressed relative to the control group. Statistical significance of pairwise comparisons was determined by two-way ANOVA with Tukey's *post-hoc* analysis (**$p < 0.01$). Ace, Angiotensin converting enzyme; Agtr1a, Angiotensin II type1 receptor-a; Agtr1b, Angiotensin II type1 receptor-b; ANGII, Angiotensin II; DOX, doxorubicin.

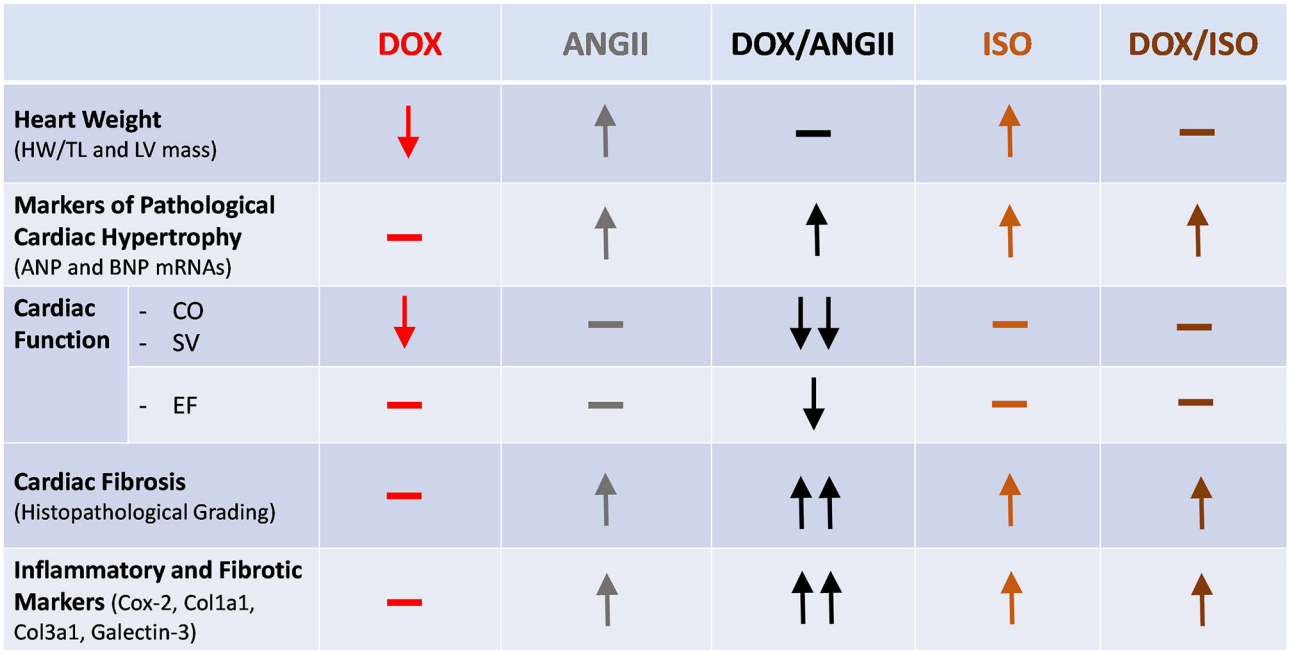

FIGURE 8 | Divergent cardiac effects of ANGII and ISO in adult mice pre-exposed to DOX as juveniles. Male 5-week old mice were administered DOX (4 mg/kg/week) or saline for 3 weeks and allowed to recover for 5 weeks prior to exposure to ANGII (1.4 mg/kg/day for 14 days) or ISO (10 mg/kg/day for 14 days). Juvenile exposure to DOX prevented both ANGII- and ISO-induced cardiac hypertrophy, but failed to correct the upregulation in hypertrophic markers. ANGII, but not ISO, worsened cardiac function, exacerbated cardiac fibrosis, and upregulated inflammatory and fibrotic markers in DOX-exposed mice. ANGII, Angiotensin II; DOX, doxorubicin; ISO, isoproterenol.

In the current study, we demonstrate that juvenile exposure to DOX did not cause significant cardiac fibrosis in naïve mice, but it exacerbated ANGII-induced cardiac fibrosis. The exacerbated cardiac fibrosis was associated with a marked upregulation in several inflammatory and fibrotic markers in the DOX/ANGII-treated mice. Importantly, MAC-2 positive cells and the expression of *Lgals-3* gene encoding galectin-3 were much higher in hearts of DOX/ANGII-treated mice than in hearts of mice receiving either DOX or ANGII alone. In contrast to cardiac atrophy, which is a consistent feature of anthracycline-induced cardiotoxicity, the prevalence and extent of cardiac fibrosis in anthracycline-treated childhood cancer survivors is controversial. In a cohort of childhood cancer survivors, the prevalence of left ventricular and right ventricular fibrosis was 9 and 38%, respectively; however, these values were not compared to a healthy control group (42). Some studies report anthracycline-treated childhood cancer survivors to show modest myocardial fibrosis as evident by an increased extracellular volume fraction (35). On the other hand, other studies demonstrate the absence of a statistically significant increase in myocardial fibrosis in survivors compared to healthy control subjects (43, 44). Since there is no clinical data reporting the association between myocardial fibrosis and cardiovascular risk factors in anthracycline-treated survivors, it may be possible that the discrepancy in these clinical studies arise from the confounding effect of other cardiovascular diseases, particularly hypertension.

In contrast to the DOX/ANGII model, juvenile exposure to DOX did not exacerbate ISO-induced cardiac fibrosis. Surprisingly, the gene expression of the fibrotic marker collagen 1a1 was lower in DOX/ISO-treated mice as compared to mice treated with ISO alone. DOX-induced cardiotoxicity has been shown to attenuate the acute effects of ISO on the heart including its positive inotropic effect (45), acute decrease of myocardial stiffness (46), and stimulation of adenylyl cyclase (47). Nevertheless, the impact of DOX exposure on the chronic effects of ISO has not been previously reported. ANGII-induced increase in afterload coupled with DOX-induced thinning of the left ventricular walls is expected to markedly increase ventricular wall stress according to the Law of LaPlace. Since ISO does not increase the afterload, its effects on the heart of DOX-exposed mice would be expected to be much milder.

DOX-induced cardiotoxicity has been shown to be more severe in hypertensive experimental animals than in normotensive ones (48–50). An important distinction between these studies and our model is the fact that these studies administered DOX to already hypertensive animals, while in our model DOX is administered to young normotensive mice then challenged by ANGII-induced hypertension in their adult life, 5 weeks after the last DOX injection. In an attempt to determine the mechanism of the detrimental synergy between juvenile exposure to DOX and adult-onset ANGII-induced hypertension, we determined the effect of these experimental conditions on

the renin-angiotensin-aldosterone-system (RAAS) genes. In the current study, juvenile exposure to DOX had no significant effect on the expression of *Ace*, *Agtr1a*, and *Agtr1b* genes. Nevertheless, there was a significant upregulation in *Ace* gene expression in the DOX/ANGII group. Similarly, juvenile exposure to DOX prevented ANGII-induced downregulation of *Agtr1a*, which encodes the AT1 receptor. ANGII mediates its detrimental effects *via* the AT1 receptors, while AT2 receptors mediate cardioprotective effects. DOX has been previously shown to alter the RAAS in different ways (19). DOX has been shown to significantly increase the expression of AT1 receptors and reduce that of AT2 receptors in a rat model of DOX-induced heart failure (51). Although there was no significant change in the mRNA expression of RAAS genes in the hearts of rabbits treated with a single dose of DOX (52), the plasma and myocardial levels of ANGII were increased three-fold in a rat model of DOX-induced heart failure (53). DOX treatment has also been shown to increase myocardial ACE activity in the cardiac tissues of hamsters (54). Intriguingly, angiotensin receptor blockers (ARBs) have been shown to ameliorate anthracycline-induced cardiotoxicity in animal models (55–57). Importantly, a recent meta-analysis shows that RAAS antagonists were the most efficient drugs to prevent anthracycline-induced cardiotoxicity with 84% risk reduction (58).

The current study has some limitations that warrant discussion. First, we have not measured the blood pressure in our experimental groups. We previously reported that juvenile exposure to DOX caused an increase in blood pressure, which was further exacerbated by ANGII infusion (11). ISO is a beta-adrenergic agonist that does not increase blood pressure, as previously reported by several other investigators (14). We also did not measure the plasma levels of natriuretic peptides, ANP and BNP. Although the induction of fetal gene expression as a hallmark of pathologic hypertrophy is usually assessed by measuring the gene expression of ANP and BNP (59, 60), measuring plasma levels of these peptides would have strengthened our conclusions.

In conclusion, this study shows that juvenile exposure to DOX differentially exacerbates ANGII—but not ISO-induced adverse cardiac remodeling. There was a marked detrimental synergy between juvenile exposure to DOX followed by ANGII-induced hypertension, which resulted in cardiac dysfunction and adverse cardiac remodeling. This preclinical mouse model highlights the clinical finding that hypertension is the most significant risk factor for heart failure in anthracycline-treated childhood cancer survivors. Since ANGII may cause cardiac damage through direct mechanism beyond elevating blood pressure, future studies are planned to delineate the mechanisms of these deleterious effects by targeting elements of RAAS system.

DATA AVAILABILITY STATEMENT

The raw data supporting the conclusions of this article will be made available by the authors, without undue reservation.

ETHICS STATEMENT

The animal study was reviewed and approved by Institutional Animal Care and Use Committee (IACUC) at the University of Minnesota (Protocol ID: 1807-36187A).

AUTHOR CONTRIBUTIONS

MG, KA, and DY: performed experiments. MG, KA, DS, JB, and BZ: analyzed data. KA, MG, and BZ: wrote the manuscript. AB, JD, and BZ: contributed to conception and design of the study.

FUNDING

This work was supported by the National Heart, Lung, and Blood Institute (NHLBI) grant R01HL151740 (BZ and AB), the St. Baldrick's Foundation for Childhood Cancer (Award ID 638335, BZ and AB); and the National Institutes of Health's National Center for Advancing Translational Sciences, grant UL1TR002494 (BZ). AB was funded by a Minnesota Partnership for Biotechnology and Medical Genomics #18.04. JD is a Canada Research Chair in Molecular Medicine and is funded by a Foundation Grant awarded by the Canadian Institutes for Health Research (CIHR) and by a Women and Children's Health Research Institute (WCHRI) grant, University of Alberta.

ACKNOWLEDGMENTS

The authors are grateful for the scientific discussions with Dr. Chetan Shenoy (Division of Cardiology, Department of Medicine, University of Minnesota Medical School). Experiments using the NanoDrop 8000 and ABI 7900 HT were done with staff support at the University of Minnesota Genomics Center. Experiments using the Vevo 2100 echocardiography system were done with staff support at the University of Minnesota Imaging Center. Processing of heart tissues for histopathological analysis was performed with staff support at the Comparative Pathology Shared Resource, University of Minnesota Masonic Cancer Center. Statistical analysis of the results was performed in consultation with staff from the Biostatistics and Bioinformatics Core shared resource of the Masonic Cancer Center, University of Minnesota supported by NIH grant P30CA077598 and by the National Center for Advancing Translational Sciences of the National Institutes of Health Award Number UL1-TR002494.

SUPPLEMENTARY MATERIAL

The Supplementary Material for this article can be found online at: https://www.frontiersin.org/articles/10.3389/fcvm.2022.742193/full#supplementary-material

REFERENCES

1. Dixon SB, Chow EJ, Hjorth L, Hudson MM, Kremer LCM, Morton LM, et al. The future of childhood cancer survivorship: challenges and opportunities for continued progress. *Pediatr Clin North Am.* (2020) 67:1237-51. doi: 10.1016/j.pcl.2020.07.013
2. Oeffinger KC, Mertens AC, Sklar CA, Kawashima T, Hudson MM, Meadows AT, et al. Childhood cancer survivor, chronic health conditions in adult survivors of childhood cancer. *N Engl J Med.* (2006) 355:1572-82. doi: 10.1056/NEJMsa060185
3. van der Pal HJ, van Dalen EC, van Delden E, van Dijk IW, Kok WE, Geskus RB, et al. High risk of symptomatic cardiac events in childhood cancer survivors. *J Clin Oncol.* (2012) 30:1429-37. doi: 10.1200/JCO.2010.33.4730
4. van Dalen EC, Raphael MF, Caron HN, Kremer LC. Treatment including anthracyclines versus treatment not including anthracyclines for childhood cancer. *Cochrane Database Syst Rev.* (2011) CD006647. doi: 10.1002/14651858.CD006647.pub3
5. Leger K, Slone T, Lemler M, Leonard D, Cochran C, Bowman WP, et al. Subclinical cardiotoxicity in childhood cancer survivors exposed to very low dose anthracycline therapy. *Pediatr Blood Cancer.* (2015) 62:123-7. doi: 10.1002/pbc.25206
6. Vandecruys E, Mondelaers V, De Wolf D, Benoit Y, Suys B. Late cardiotoxicity after low dose of anthracycline therapy for acute lymphoblastic leukemia in childhood. *J Cancer Surviv.* (2012) 6:95-101. doi: 10.1007/s11764-011-0186-6
7. Yeh ET, Vejpongsa P. Subclinical cardiotoxicity associated with cancer therapy: early detection and future directions. *J Am Coll Cardiol.* (2015) 65:2523-5. doi: 10.1016/j.jacc.2015.04.012
8. Jones LW, Haykowsky MJ, Swartz JJ, Douglas PS, Mackey JR. Early breast cancer therapy and cardiovascular injury. *J Am Coll Cardiol.* (2007) 50:1435-41. doi: 10.1016/j.jacc.2007.06.037
9. Shenoy C, Klem I, Crowley AL, Patel MR, Winchester MA, Owusu C, et al. Cardiovascular complications of breast cancer therapy in older adults. *Oncologist.* (2011) 16:1138-43. doi: 10.1634/theoncologist.2010-0348
10. Armstrong GT, Oeffinger KC, Chen Y, Kawashima T, Yasui Y, Leisenring W, et al. Modifiable risk factors and major cardiac events among adult survivors of childhood cancer. *J Clin Oncol.* (2013) 31:3673-80. doi: 10.1200/JCO.2013.49.3205
11. Matsumura N, Zordoky BN, Robertson IM, Hamza SM, Parajuli N, Soltys CM, et al. Co-administration of resveratrol with doxorubicin in young mice attenuates detrimental late-occurring cardiovascular changes. *Cardiovasc Res.* (2018) 114:1350-9. doi: 10.1093/cvr/cvy064
12. Grant MKO, Abdelgawad IY, Lewis CA, Seelig D, Zordoky BN. Lack of sexual dimorphism in a mouse model of isoproterenol-induced cardiac dysfunction. *PLoS ONE.* (2020) 15:e0232507. doi: 10.1371/journal.pone.0232507
13. Zordoky BN, Aboutabl ME, El-Kadi AO. Modulation of cytochrome P450 gene expression and arachidonic acid metabolism during isoproterenol-induced cardiac hypertrophy in rats. *Drug Metab Dispos.* (2008) 36:2277-86. doi: 10.1124/dmd.108.023077
14. Berthonneche C, Peter B, Schupfer F, Hayoz P, Kutalik Z, Abriel H, et al. Cardiovascular response to beta-adrenergic blockade or activation in 23 inbred mouse strains. *PLoS ONE.* (2009) 4:e6610. doi: 10.1371/journal.pone.0006610
15. Faulx MD, Ernsberger P, Vatner D, Hoffman RD, Lewis W, Strachan R, et al. Strain-dependent beta-adrenergic receptor function influences myocardial responses to isoproterenol stimulation in mice. *Am J Physiol Heart Circ Physiol.* (2005) 289:H30-6. doi: 10.1152/ajpheart.00636.2004
16. Dolinsky VW, Chakrabarti S, Pereira TJ, Oka T, Levasseur J, Beker D, et al. Resveratrol prevents hypertension and cardiac hypertrophy in hypertensive rats and mice. *Biochim Biophys Acta.* (2013) 1832:1723-33. doi: 10.1016/j.bbadis.2013.05.018
17. Matsumura N, Robertson IM, Hamza SM, Soltys CM, Sung MM, Masson G, et al. A novel complex I inhibitor protects against hypertension-induced left ventricular hypertrophy. *Am J Physiol Heart Circ Physiol.* (2017) 312:H561-70. doi: 10.1152/ajpheart.00604.2016
18. Fan D, Takawale A, Basu R, Patel V, Lee J, Kandalam V, et al. Differential role of TIMP2 and TIMP3 in cardiac hypertrophy, fibrosis, diastolic dysfunction. *Cardiovasc Res.* (2014) 103:268-80. doi: 10.1093/cvr/cvu072
19. Sobczuk P, Czerwinska M, Kleibert M, Cudnoch-Jedrzejewska A. Anthracycline-induced cardiotoxicity and renin-angiotensin-aldosterone system-from molecular mechanisms to therapeutic applications. *Heart Fail Rev.* (2022) 27:295–319. doi: 10.1007/s10741-020-09977-1
20. Faber J, Wingerter A, Neu MA, Henninger N, Eckerle S, Munzel T, et al. Burden of cardiovascular risk factors and cardiovascular disease in childhood cancer survivors: data from the German CVSS-study. *Eur Heart J.* (2018) 39:1555-62. doi: 10.1093/eurheartj/ehy026
21. van Dalen EC, Raphael MF, Caron HN, Kremer LC. Treatment including anthracyclines versus treatment not including anthracyclines for childhood cancer. *Cochrane Database Syst Rev.* (2009) CD006647. doi: 10.1002/14651858.CD006647.pub2
22. Nysom K, Holm K, Lipsitz SR, Mone SM, Colan SD, Orav EJ, et al. Relationship between cumulative anthracycline dose and late cardiotoxicity in childhood acute lymphoblastic leukemia. *J Clin Oncol.* (1998) 16:545-50. doi: 10.1200/JCO.1998.16.2.545
23. Chakouri N, Farah C, Matecki S, Amedro P, Vincenti M, Saumet L, et al. Screening for *in-vivo* regional contractile defaults to predict the delayed Doxorubicin Cardiotoxicity in Juvenile Rat. *Theranostics.* (2020) 10:8130-42. doi: 10.7150/thno.47407
24. Zhu W, Reuter S, Field LJ. Targeted expression of cyclin D2 ameliorates late stage anthracycline cardiotoxicity. *Cardiovasc Res.* (2019) 115:960-5. doi: 10.1093/cvr/cvy273
25. Nagiub M, Filippone S, Durrant D, Das A, Kukreja RC. Long-acting PDE5 inhibitor tadalafil prevents early doxorubicin-induced left ventricle diastolic dysfunction in juvenile mice: potential role of cytoskeletal proteins. *Can J Physiol Pharmacol.* (2017) 95:295-304. doi: 10.1139/cjpp-2016-0551
26. Zhu W, Zhang W, Shou W, Field LJ. P53 inhibition exacerbates late-stage anthracycline cardiotoxicity. *Cardiovasc Res.* (2014) 103:81-9. doi: 10.1093/cvr/cvu118
27. Huang C, Zhang X, Ramil JM, Rikka S, Kim L, Lee Y, et al. Juvenile exposure to anthracyclines impairs cardiac progenitor cell function and vascularization resulting in greater susceptibility to stress-induced myocardial injury in adult mice. *Circulation.* (2010) 121:675-83. doi: 10.1161/CIRCULATIONAHA.109.902221
28. Tham EB, Haykowsky MJ, Chow K, Spavor M, Kaneko S, Khoo NS, et al. Diffuse myocardial fibrosis by T1-mapping in children with subclinical anthracycline cardiotoxicity: relationship to exercise capacity, cumulative dose and remodeling. *J Cardiovasc Magn Reson.* (2013) 15:48. doi: 10.1186/1532-429X-15-48
29. Cetin S, Babaoglu K, Basar EZ, Deveci M, Corapcioglu F. Subclinical anthracycline-induced cardiotoxicity in long-term follow-up of asymptomatic childhood cancer survivors: assessment by speckle tracking echocardiography. *Echocardiography.* (2018) 35:234-40. doi: 10.1111/echo.13743
30. Germanakis I, Kalmanti M, Parthenakis F, Nikitovic D, Stiakaki E, Patrianakos A, et al. Correlation of plasma N-terminal pro-brain natriuretic peptide levels with left ventricle mass in children treated with anthracyclines. *Int J Cardiol.* (2006) 108:212-5. doi: 10.1016/j.ijcard.2005.05.006
31. Yazaki K, Takahashi K, Shigemitsu S, Yamada M, Iso T, Kobayashi M, et al. In-depth insight into the mechanisms of cardiac dysfunction in patients with childhood cancer after anthracycline treatment using layer-specific strain analysis. *Circ J.* (2018) 82:715-23. doi: 10.1253/circj.CJ-17-0874
32. Lipshultz SE, Lipsitz SR, Sallan SE, Simbre VC, 2nd, Shaikh SL, et al. Long-term enalapril therapy for left ventricular dysfunction in doxorubicin-treated survivors of childhood cancer. *J Clin Oncol.* (2002) 20:4517-22. doi: 10.1200/JCO.2002.12.102
33. Lipshultz SE, Miller TL, Lipsitz SR, Neuberg DS, Dahlberg SE, Colan SD, et al. Continuous versus bolus infusion of doxorubicin in children with all: long-term cardiac outcomes. *Pediatrics.* (2012) 130:1003-11. doi: 10.1542/peds.2012-0727
34. Lipshultz SE, Lipsitz SR, Kutok JL, Miller TL, Colan SD, Neuberg DS, et al. Impact of hemochromatosis gene mutations on cardiac status in doxorubicin-treated survivors of childhood high-risk leukemia. *Cancer.* (2013) 119:3555-62. doi: 10.1002/cncr.28256
35. Mawad W, Mertens L, Pagano JJ, Riesenkampff E, Reichert MJE, Mital S, et al. Effect of anthracycline therapy on myocardial function and markers of fibrotic

remodelling in childhood cancer survivors. *Eur Heart J Cardiovasc Imaging.* (2020) 22:435-42. doi: 10.1093/ehjci/jeaa093
36. Jordan JH, Castellino SM, Melendez GC, Klepin HD, Ellis LR, Lamar Z, et al. Left ventricular mass change after anthracycline chemotherapy. *Circ Heart Fail.* (2018) 11:e004560. doi: 10.1161/CIRCHEARTFAILURE.117.004560
37. Takano APC, Senger N, Barreto-Chaves MLM. The endocrinological component and signaling pathways associated to cardiac hypertrophy. *Mol Cell Endocrinol.* (2020) 518:110972. doi: 10.1016/j.mce.2020.110972
38. Dhingra R, Margulets V, Chowdhury SR, Thliveris J, Jassal D, Fernyhough P, et al. Bnip3 mediates doxorubicin-induced cardiac myocyte necrosis and mortality through changes in mitochondrial signaling. *Proc Natl Acad Sci USA.* (2014) 111:E5537-44. doi: 10.1073/pnas.1414665111
39. Willis MS, Parry TL, Brown DI, Mota RI, Huang W, Beak JY, et al. Doxorubicin exposure causes subacute cardiac atrophy dependent on the striated muscle-specific ubiquitin ligase MuRF1. *Circ Heart Fail.* (2019) 12:e005234. doi: 10.1161/CIRCHEARTFAILURE.118.005234
40. Li J, Wang PY, Long NA, Zhuang J, Springer DA, Zou J, et al. p53 prevents doxorubicin cardiotoxicity independently of its prototypical tumor suppressor activities. *Proc Natl Acad Sci USA.* (2019) 116:19626-34. doi: 10.1073/pnas.1904979116
41. Ferreira de Souza TA, Quinaglia CST, Osorio Costa F, Shah R, Neilan TG, Velloso L, et al. Anthracycline therapy is associated with cardiomyocyte atrophy and preclinical manifestations of heart disease. *JACC Cardiovasc Imaging.* (2018) 11:1045-55. doi: 10.1016/j.jcmg.2018.05.012
42. Cheung YF, Lam WW, Ip JJ, Cheuk DK, Cheng FW, Yang JY, et al. Myocardial iron load and fibrosis in long term survivors of childhood leukemia. *Pediatr Blood Cancer.* (2015) 62:698-703. doi: 10.1002/pbc.25369
43. Tong X, Li VW, Liu AP, So EK, Chan Q, Ho KK, et al. Cardiac magnetic resonance T1 mapping in adolescent and young adult survivors of childhood cancers. *Circ Cardiovasc Imaging.* (2019) 12:e008453. doi: 10.1161/CIRCIMAGING.118.008453
44. Ylanen K, Poutanen T, Savikurki-Heikkila P, Rinta-Kiikka I, Eerola A, Vettenranta K. Cardiac magnetic resonance imaging in the evaluation of the late effects of anthracyclines among long-term survivors of childhood cancer. *J Am Coll Cardiol.* (2013) 61:1539-47. doi: 10.1016/j.jacc.2013.01.019
45. Kizaki K, Akatsuka K, Momozaki M, Fujimori Y, Uchide T, Temma K, et al. Changes in myocardial beta1-adrenergic receptor and stimulatory G-protein gene expression after chronic treatment with doxorubicin in rat. *J Vet Med Sci.* (2004) 66:989-92. doi: 10.1292/jvms.66.989
46. Falcao-Pires I, Fontes-Sousa AP, Lopes-Conceicao L, Bras-Silva C, Leite-Moreira AF. Modulation of myocardial stiffness by beta-adrenergic stimulation–its role in normal and failing heart. *Physiol Res.* (2011) 60:599-609. doi: 10.33549/physiolres.932088
47. Nagami K, Yoshikawa T, Suzuki M, Wainai Y, Anzai T, Handa S. Abnormal beta-adrenergic transmembrane signaling in rabbits with adriamycin-induced cardiomyopathy. *Jpn Circ J.* (1997) 61:249-55. doi: 10.1253/jcj.61.249
48. Kala P, Bartuskova H, Pitha J, Vanourkova Z, Kikerlova S, Jichova S, et al. Deleterious effects of hyperactivity of the renin-angiotensin system and hypertension on the course of chemotherapy-induced heart failure after doxorubicin administration: a study in Ren-2 transgenic rat. *Int J Mol Sci.* (2020) 21:9337. doi: 10.3390/ijms21249337
49. Zordoky BN, Radin MJ, Heller L, Tobias A, Matise I, Apple FS, et al. The interplay between genetic background and sexual dimorphism of doxorubicin-induced cardiotoxicity. *Cardiooncology.* (2016) 2:4. doi: 10.1186/s40959-016-0013-3
50. Sharkey LC, Radin MJ, Heller L, Rogers LK, Tobias A, Matise I, et al. Differential cardiotoxicity in response to chronic doxorubicin treatment in male spontaneous hypertension-heart failure (SHHF), spontaneously hypertensive. (SHR), and Wistar Kyoto. (WKY) rats. *Toxicol Appl Pharmacol.* (2013) 273:47-57. doi: 10.1016/j.taap.2013.08.012
51. Zong WN, Yang XH, Chen XM, Huang HJ, Zheng HJ, Qin XY, et al. Regulation of angiotensin-(1-7) and angiotensin II type 1 receptor by telmisartan and losartan in adriamycin-induced rat heart failure. *Acta Pharmacol Sin.* (2011) 32:1345-50. doi: 10.1038/aps.2011.96
52. Boucek RJ, Jr, Miracle A, Anderson M, Engelman R, Atkinson J, Dodd DA. Persistent effects of doxorubicin on cardiac gene expression. *J Mol Cell Cardiol.* (1999) 31:1435-46. doi: 10.1006/jmcc.1999.0972
53. Zheng M, Kang YM, Liu W, Zang WJ, Bao CY, Qin DN. Inhibition of cyclooxygenase-2 reduces hypothalamic excitation in rats with adriamycin-induced heart failure. *PLoS ONE.* (2012) 7:e48771. doi: 10.1371/journal.pone.0048771
54. Okumura K, Jin D, Takai S, Miyazaki M. Beneficial effects of angiotensin-converting enzyme inhibition in adriamycin-induced cardiomyopathy in hamsters. *Jpn J Pharmacol.* (2002) 88:183-8. doi: 10.1254/jjp.88.183
55. Matouk AI, Taye A, Heeba GH, El-Moselhy MA. Quercetin augments the protective effect of losartan against chronic doxorubicin cardiotoxicity in rats. *Environ Toxicol Pharmacol.* (2013) 36:443-50. doi: 10.1016/j.etap.2013.05.006
56. Soga M, Kamal FA, Watanabe K, Ma M, Palaniyandi S, Prakash P, et al. Effects of angiotensin II receptor blocker. (candesartan) in daunorubicin-induced cardiomyopathic rats. *Int J Cardiol.* (2006) 110:378-85. doi: 10.1016/j.ijcard.2005.08.061
57. Ibrahim MA, Ashour OM, Ibrahim YF, El-Bitar HI, Gomaa W, Abdel-Rahim SR. Angiotensin-converting enzyme inhibition and angiotensin AT(1)-receptor antagonism equally improve doxorubicin-induced cardiotoxicity and nephrotoxicity. *Pharmacol Res.* (2009) 60:373-81. doi: 10.1016/j.phrs.2009.05.007
58. Abdel-Qadir H, Ong G, Fazelzad R, Amir E, Lee DS, Thavendiranathan P, et al. Interventions for preventing cardiomyopathy due to anthracyclines: a Bayesian network meta-analysis. *Ann Oncol.* (2017) 28:628-33. doi: 10.1093/annonc/mdw671
59. Ellmers LJ, Knowles JW, Kim HS, Smithies O, Maeda N, Cameron VA. Ventricular expression of natriuretic peptides in Npr1(-/-) mice with cardiac hypertrophy and fibrosis. *Am J Physiol Heart Circ Physiol.* (2002) 283:H707-14. doi: 10.1152/ajpheart.00677.2001
60. Gutte H, Oxbol J, Kristoffersen US, Mortensen J, Kjaer A. Gene expression of ANP, BNP and ET-1 in the heart of rats during pulmonary embolism. *PLoS ONE.* (2010) 5:e11111. doi: 10.1371/journal.pone.0011111

Author Disclaimer: The content is solely the responsibility of the authors and does not necessarily represent the official views of the National Institutes of Health.

Conflict of Interest: The authors declare that the research was conducted in the absence of any commercial or financial relationships that could be construed as a potential conflict of interest.

Publisher's Note: All claims expressed in this article are solely those of the authors and do not necessarily represent those of their affiliated organizations, or those of the publisher, the editors and the reviewers. Any product that may be evaluated in this article, or claim that may be made by its manufacturer, is not guaranteed or endorsed by the publisher.

frontiers | Frontiers in Cardiovascular Medicine

ORIGINAL RESEARCH
published: 14 April 2022
doi: 10.3389/fcvm.2022.867867

An Olive Oil Mill Wastewater Extract Improves Chemotherapeutic Activity Against Breast Cancer Cells While Protecting From Cardiotoxicity

Nadia Benedetto[1†], *Luana Calabrone*[1†], *Karolina Gutmańska*[1], *Nicoletta Macrì*[1], *Maria Grazia Cerrito*[2], *Riccardo Ricotta*[3], *Giuseppe Pelosi*[1,4], *Antonino Bruno*[1,5*], *Douglas M. Noonan*[1,5‡] *and Adriana Albini*[6*‡]

[1] IRCCS MultiMedica, Milan, Italy, [2] School of Medicine and Surgery, University of Milano-Bicocca, Monza, Italy, [3] IRCCS MultiMedica, Sesto San Giovanni, Italy, [4] Department of Oncology and Hemato-Oncology, University of Milan, Milan, Italy, [5] Immunology and General Pathology Laboratory, Department of Biotechnology and Life Sciences, University of Insubria, Varese, Italy, [6] European Institute of Oncology (IEO) IRCCS, Milan, Italy

OPEN ACCESS

Edited by:
Nazish Sayed,
Stanford University, United States

Reviewed by:
Nicola Maurea,
G. Pascale National Cancer Institute Foundation (IRCCS), Italy
Alessandra Cuomo,
Federico II University Hospital, Italy

***Correspondence:**
Adriana Albini
adriana.albini@ieo.it
Antonino Bruno
antonino.bruno@uninsubria.it

[†]These authors have contributed equally to this work
[‡]These authors share senior authorship

Specialty section:
This article was submitted to Cardio-Oncology, a section of the journal Frontiers in Cardiovascular Medicine

Received: 01 February 2022
Accepted: 14 March 2022
Published: 14 April 2022

Citation:
Benedetto N, Calabrone L, Gutmańska K, Macrì N, Cerrito MG, Ricotta R, Pelosi G, Bruno A, Noonan DM and Albini A (2022) An Olive Oil Mill Wastewater Extract Improves Chemotherapeutic Activity Against Breast Cancer Cells While Protecting From Cardiotoxicity. Front. Cardiovasc. Med. 9:867867. doi: 10.3389/fcvm.2022.867867

Cardiovascular toxicity in cancer patients receiving chemotherapy remains one of the most undesirable side effects, limiting the choice of the most efficient therapeutic regimen, including combinations of different anticancer agents. Anthracyclines (doxorubicin) and antimetabolites (5-fluorouracil (5-FU), capecitabine) are among the most known agents used in breast cancer and other neoplasms and are associated with cardiotoxic effects. Extra-virgin olive oil (EVOO) is rich in polyphenols endowed with antioxidant cardioprotective activities. Olive mill wastewater (OMWW), a waste product generated by EVOO processing, has been reported to be enriched in polyphenols. In this study, we investigated the activities of polyphenol-rich extract from OMWW, A009, in cooperation with chemotherapy on two breast cancer cell lines, namely, BT459 and MDA-MB-231, in a cardio-oncology perspective. The effects of A009 on cardiac cells were also investigated with and without chemotherapeutic agents. Cell viability was determined on BT459 and MDA-MB-231 (i.e., breast cancer cells) and H9C2 (i.e., rat cardiomyocytes) cells, using 3-(4,5-dimethylthiazol-2-yl)-2,5-diphenyltetrazolium bromide (MTT) assay. A spheroids assay was used as a 3D *in vitro* model on BT459 and MDA-MB-231 cells. For *in vivo* studies, the murine sponge assay of angiogenesis was used as a model of breast cancer-associated vascularization. The embryo of *Danio rerio* (zebrafish) was used to detect the cardioprotective activities of the OMWW. We found that the A009 extract exhibited antiangiogenic activities induced by breast cancer cell supernatants and increased T-cell recruitment *in vivo*. The combination of the OMWW extracts with doxorubicin or 5-FU limited BT459 and MDA-MB-231 cell viability and the diameter of 3D spheroids, while mitigating their toxic effects on the rat H9C2 cardiomyocytes. Cardioprotective effects were observed by the combination of OMWW extracts with doxorubicin in zebrafish embryos. Finally, in human cardio myocytes, we observed 5-FU-induced upregulation of the inflammatory, senescence-associated cytokine IL6 and

p16 genes, which expression was reduced by OMWW treatment. Our study demonstrates that the polyphenol-rich purified OMWW extract A009 combined with cancer chemotherapy could represent a potential candidate for cardiovascular protection in breast cancer patients, while increasing the effects of breast cancer chemotherapy.

Keywords: chemotherapy, breast cancer, polyphenol, olive, cardiomyocyte

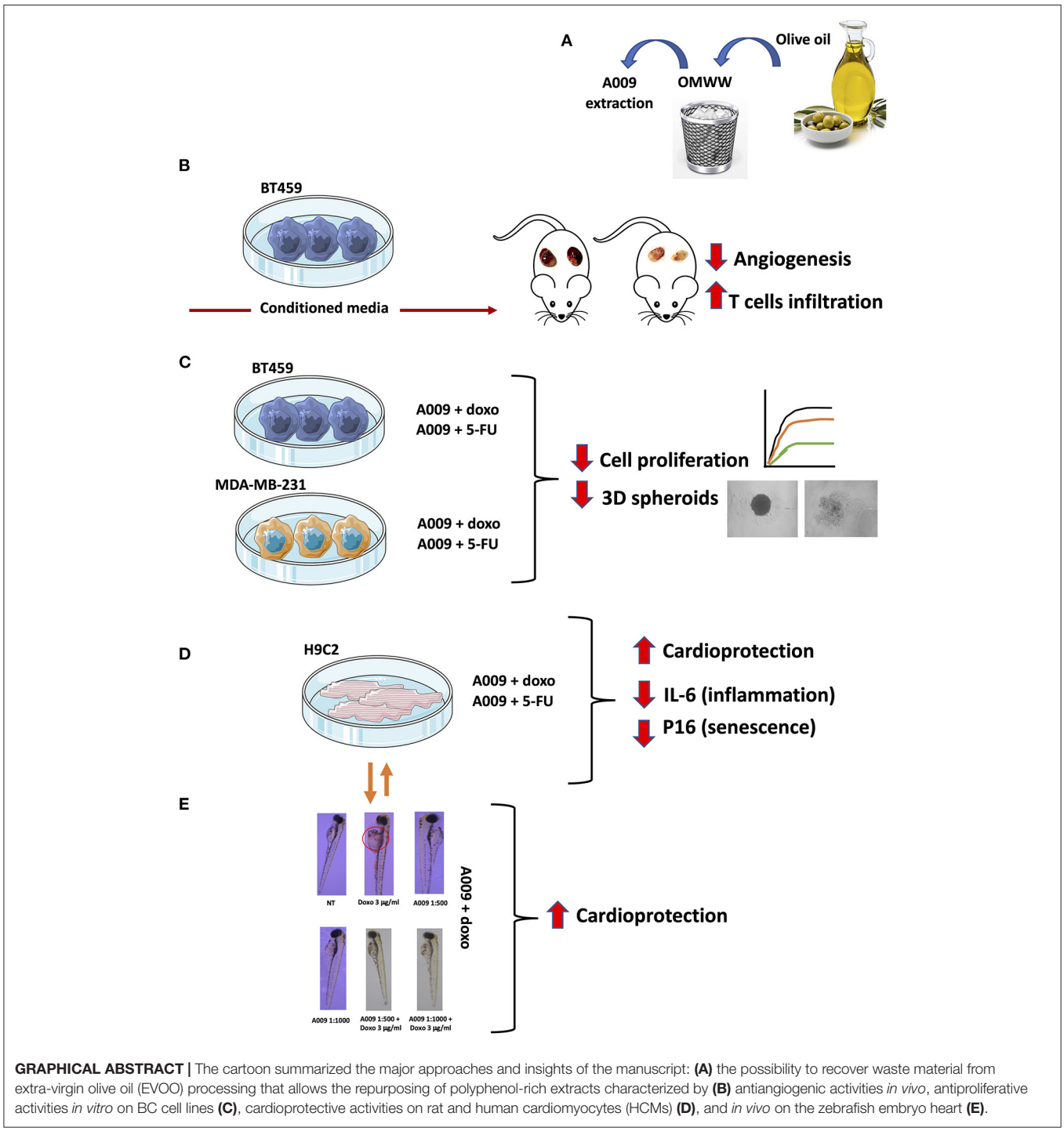

GRAPHICAL ABSTRACT | The cartoon summarized the major approaches and insights of the manuscript: **(A)** the possibility to recover waste material from extra-virgin olive oil (EVOO) processing that allows the repurposing of polyphenol-rich extracts characterized by **(B)** antiangiogenic activities *in vivo*, antiproliferative activities *in vitro* on BC cell lines **(C)**, cardioprotective activities on rat and human cardiomyocytes (HCMs) **(D)**, and *in vivo* on the zebrafish embryo heart **(E)**.

INTRODUCTION

Together with cardiovascular diseases, cancer still accounts as a major cause of death in the world (1, 2). Breast cancer (BC) is the fifth most prevalent cause of cancer death worldwide and is the most common malignancy among women (3). BC is characterized by the presence of several different subtypes, which are generally classified as hormone receptor (HR)-positive and human epidermal growth factor receptor 2 (HER2)-overexpressing BCs or triple negative BC. The presence of the markers has allowed the development of targeted therapies. Tumors without the expression of HR or HER2 are classified as triple-negative BC (TNBC). TNBC has a higher mortality rate than HR-positive or HER-2-overexpressing BC because of its high recurrence rate and metastatic potential (4).

Among the current strategies for the treatment of TNBC, chemotherapy represents the major option (5, 6). Taxanes (e.g., paclitaxel and docetaxel) and anthracyclines (e.g., doxorubicin and epirubicin) are usually the main choice (7), in combination with platinum (e.g., carboplatin), antimetabolites [e.g., capecitabine, similar to 5-fluorouracil (5-FU)] and/or alkylating agent (e.g., cyclophosphamide); however, their possible toxicity, low aqueous solubility, and rapid *in vivo* clearance can represent a limit (7, 8). All these agents are often used in combination with targeted therapy.

Despite the great medical and pharmaceutical advances, these limitations remain a big challenge. According to the Food and Drug Administration (FDA), about 1 million of severe adverse drug events (ADEs) were reported in only 1 year in the United States, including death (9). Chemotherapy-induced cardiotoxicity is one of the most common ADEs and can cause more or less serious manifestations, such as changes in ECG, arrhythmia, bradycardia, tachycardia, and heart failure, which lead to an increase in morbidity and mortality (7, 9). In this complex contest, prevention still remains the most promising approach for all types of cancer. Natural products or agents derived from foods and beverages (or their synthetic analogs) have been found to exert antitumor and tumor-preventive activities in diverse preclinical settings, and some are currently employed in the clinic. Among them, phenolic compounds have gained the attention of the scientific community, thanks to their plethora of beneficial effects on health, that include antibacterial, anti-inflammatory, and anticancer activities. Also, several preclinical studies, including those published by our research group, showed that diverse phytocompounds, while synergizing with chemotherapeutic drugs, have cardioprotective activity (10, 11).

Southern European countries have lower incidence of cancer and cardiovascular disease than northern European countries or the United States. The Mediterranean diet has been proposed as the main protective factor for this benefit (12). In this context, angioprevention is an important concept to consider, since angiogenesis prevention through bioactive compounds present in the Mediterranean diet components could explain in part the chemopreventive effect of this diet model in cancer (13–17). Extra-virgin olive oil (EVOO) is a major component of the Mediterranean diet, with numerous beneficial effects, which concern the ability to prevent diseases that can be linked to oxidative damage, such as neurodegenerative diseases, cancer, and cardiovascular diseases (18). EVOO protective role is due to its enriched content in phytochemicals: the main fraction (95–97%) is the lipophilic one, which is represented by both monounsaturated and polyunsaturated fatty acids (i.e., omega-3 and omega-6) (19). The polar fraction is mainly represented by polyphenolic compounds like oleuropein, tyrosol, and hydroxytyrosol, which possess strong anti-inflammatory and antioxidant properties (20). A major issue within the industrial processing of EVOO is the generation of large amount of liquid waste product, including, olive mill wastewater (OMWW) (21, 22). The high content of pollutants within the waste requires special disposal and cost-effective procedures that significantly impact both the health environment and the industrial management. In contrast, it has been found that OMWW is rich in polyphenolic compounds, endowed with antibacterial and antioxidant activities, thus representing a valid product to be considered in scientific research (23).

We previously reported that the A009 polyphenol-rich extracts, purified form OMWW, exhibit chemopreventive and angiopreventive properties, *in vitro* and *in vivo*, in different cancer types (e.g., lung, colon, and prostate cancer cells) and endothelial cells (11, 24–27).

In this study, we investigated the A009 effect on tumor growth of BC cells, alone or in combination with a chemotherapeutic agent. In addition, we examined the potential A009 cardioprotective activity, against chemotherapy-induced cardiovascular damages, using both *in vitro* and *in vivo* models (i.e., *Danio rerio* and *Mus musculus*). In this study, we focused on doxorubicin and 5-FU, which are very prominent, highly active anticancer drugs, however, endowed with cardiotoxic effects. Work flow is described in the **Graphical Abstract**.

MATERIALS AND METHODS

Chemicals

5-Fluorouracil was purchased from Sigma-Aldrich and was dissolved in dimethyl sulfoxide (DMSO) and used for *in vitro* experiments as detailed below. Doxorubicin hydrochloride (Doxo) was purchased from Abcam and was dissolved in Milli-Q water. 3-(4,5-dimethylthiazol-2-yl)-2,5-diphenyltetrazolium bromide (MTT) was purchased from Sigma-Aldrich. The synthetic hydroxytyrosol (Hyt), ≥98% in purity, was purchased from Cayman Chemicals (Ann Arbor, MI, USA). Hyt was dissolved in ethanol (EtOH). DMSO and EtOH vehicles were used as controls.

Preparation of A009 Extracts

Olive oil mill wastewaters were kindly provided by Agriturismo Fattoria La Vialla (Castiglion Fibocchi, Arezzo, Italy) and used to obtain the phenol-rich purified extract A009 (Patent No. 1420804; No. 1420805). The experiments were performed using the extract A009. The extraction procedures of A009 obtained from OMWW and its polyphenol content have been previously

described (24). The polyphenol content of the A009 extract is shown in **Supplementary Table 1**.

Cell Line Culture and Maintenances

The human metastatic BC cells, e.g., MDA-MB-231 (purchased from ATCC), were maintained in the Dulbecco's Modified Eagle's Medium (Gibco-BRL) supplemented with 10% fetal bovine serum (FBS) (Euroclone), 2 mM L-glutamine (Euroclone), 100 U/ml penicillin, and 100 μg/ml streptomycin (Euroclone), at 37°C, 5% CO_2. The human BC cell line BT549 (purchased from ATCC) was grown in Roswell Park Memorial Institute (RPMI) 1640 supplemented with 10% FBS, 2 mM L-glutamine, 100 U/ml penicillin and 100 μg/ml streptomycin, and 0.023 U/ml insulin at 37°C, 5% CO_2. The human cardiomyocytes (HCMs, purchased by PromoCell) cells were maintained in the Myocyte Growth Medium (PromoCell) plus Myocyte supplements mix (PromoCell), in addition to 10% FBS, 2 mM L-glutamine, 100 U/ml penicillin, and 100 μg/ml streptomycin, at 37°C, 5% CO_2. The rat cardiomyocytes cell line H9C2 (purchased by PromoCell) was maintained in DMEM-F12, supplemented with 10% FBS, 2 mM L-glutamine, 100 U/ml penicillin, and 100 μg/ml streptomycin. All the cell lines used in the study were routinely checked for eventual mycoplasma contamination, before being used.

Generation of Conditioned Media

Conditioned media (CM), for subsequent *in vivo* studies, was obtained from the BT459 BC cell line. Briefly, 3×10^6 BT459 were seeded into t100 Petri dishes (Corning) in RPMI 1640 supplemented with 10% FBS, 2 mM L-glutamine, 100 U/ml penicillin and 100 μg/ml streptomycin, and 0.023 U/ml insulin at 37°C, 5% CO_2. When cells reached 80% of confluency, cells were starved for 48 h in 10 ml serum-free RMPI medium. Finally, CM were collected, residual cells and debris were discarded, by centrifugation, and concentrated with Concentricon devices (Millipore, Temecula, CA) with a 5 kDa membrane pore cutoff.

In vivo Angiogenesis Sponge Assay as a Model of Breast Cancer-Associated Angiogenesis

To use a rapid model of breast cancer-associated angiogenesis *in vivo* (28–30), the ability of A009 (1:250) to inhibit vascularization, induced by CM of BC cell lines, was investigated using the UltiMatrix (Biotechne) Matrigel sponge assay in mice. Briefly, liquid UltiMatrix (10 mg/ml) was mixed with 50 μg of total protein BT459-concentrated CM, alone or in combination with the A009 extract (1:250 dilution) and inoculated in cold liquid form, which polymerizes *in vivo*. UltiMatrix alone or UltiMatrix supplemented with a cocktail of proangiogenic factors VEGF, TNFα and Heparin (VTH) (100 ng/ml vascular endothelial growth factor (VEGF)-A, 2 ng/ml tumor necrosis factor (TNF)-α, and 25 U/ml heparin) were used as negative and positive controls, respectively. Each mixture was brought to a final volume of 0.6 ml and injected subcutaneously into the right and left flanks of 6–8-week-old C57/BL6 female mice (Charles River Laboratories, Calco (Lecco), Italy) with a cold syringe. All animals were housed in a conventional animal facility with 12 h light/dark cycles and fed *ad libitum*. Manipulation of animals was performed in accordance with the Italian and European Community guidelines (D.L. 2711/92 No.116; 86/609/EEC Directive), the 3 R's declaration, and approved by the institutional ethics committee. All the procedures applied were approved by the local animal experimentation ethics committee (ID# #06_16 Noonan) of the University of Insubria and by the Health Ministry (ID#225/2017-PR).

Groups of 3–7 mice were used for each treatment. At body temperature, the UltiMatrix polymerizes to a solid gel and becomes vascularized in response to angiogenic substances. Four days following injection, the gel plugs were recovered and divided into two parts. One half was formalin-fixed, paraffin-embedded to generate paraffin blocks processed for histological analysis; the other half from gel plugs was minced and diluted in water to measure the hemoglobin content with a Drabkin's Reagent Kit (Sigma-Aldrich), and part was mechanically processed for the subsequent flow cytometry analysis.

Immunohistochemistry Analysis of Utimatrix Sponges

All the processing for the immunohistochemistry analysis on the Utimatrix sponges were performed by the Unit of Pathological Anatomy, IRCCS MultiMedica, Milan, Italy, by a routine system on an automated immunostainer (BenchMark ULTRA IHC/*in situ* hybridization System, Ventana-Roche Group, Basel, Switzerland). Hematoxylin and Eosin-stained sections were used to acquire micrographs, at 40× magnification.

Flow Cytometry Analysis for Cell Infiltrate in the UltiMatrix Plugs

Part of the recovered UltiMatrix plugs were mechanically processed by scissors, then placed into 70 mm cell strainers (BD Biosciences), and pressured with a syringe swab. The cell suspension obtained was used for the flow cytometry analysis to detect the immune cell infiltrate. Cells were stained for 30 min at 4°C, at dark, with the following fluorophore-conjugated antimouse antibodies, all purchased from BD Biosciences: CD45-BUV395, F4/80-PECF594, CD3e-BB700, and NK1.1-BV650. For fluorescence-activated cell sorting (FACS) analysis, viable cells were gated according to physical parameters (FSC/SSC). Following the gating of $CD45^+$ cells, immune cells were identified as follows: $CD45^+$:$F4/80^+$ cells (macrophages), $CD3^+$ cells (total T cells), and $CD3^-NK1.1^+$ cells (total NK cells).

Assessment of Combination Effect of Chemotherapy and A009 on Breast Cancer Cell Lines and Rat Cardiomyocytes by MTT Assay

To investigate whether the A009 extract could synergize with chemotherapy, cell viability of the BC cell lines MDA-MB-231 and BT549 was evaluated by the MTT assay (**Supplementary Table 2**). The 2×10^3 cells of BT549 and MDA-MB-231 BC cell lines were seeded in 96-well plates and, after adhesion, treated with A009 extract (dilution 1:800) and Hyt (dilution 1:800) for 24 h. The medium was then substituted

with the chemotherapy drug 5-FU 100 μM or Doxorubicin 1 μM, alone or in combination with A009 or Hyt for 48 and 72 h. At each time point, media were replaced with fresh complete medium, supplemented with 0.5 mg/ml MTT reagent, and then incubated for 3 h at 37°C with 5% CO_2. This colorimetric assay is based on the reduction of a yellow tetrazolium salt (3-(4,5-dimethylthiazol2-yl)-2,5-diphenyltetrazolium bromide or MTT) to purple formazan crystals by metabolically active cells. The viable cells contain NAD(P)H-dependent oxidoreductase enzymes that reduce the MTT to formazan. MTT was removed, and formazan crystals were dissolved using 100% DMSO. The darker the solution, the greater the number of viable, metabolically active cells. The absorbance was recorded at 570 nm wavelength with the microplate spectrophotometer SpectraMax M2 (Molecular Devices, Sunnyvale, CA). To evaluate the effects of the A009 extracts on chemotherapy-induced cardiotoxicity, the same experiment was repeated on rat cardiomyocytes H9C2 cells (**Supplementary Table 2**).

Generation of Tumor Spheroids

We investigated the capability of the A009 extract to synergize with chemotherapy, in reducing the generation of BC tumor spheroids. BT459 or MDA-MB-231 cells were cultured in 20 μl hanging drops at a density of 4×10^3 cells/drop, in complete RPMI medium, with or without treatment. After spheroids formation, which typically occurs within 24 h, the spheroids were transferred to 96-well plates, containing 100 μl/well of fresh culture medium with or without treatment (one spheroid/well), previously coated with 2% agar and growth on the bottom of 60 mm tissue culture dish, at 37 °C and 5% CO_2. BT459 and MDA-MB-231 spheroids were treated with the A009 extract + 5-FU 100 μM combination, or the A009 extract + Doxo 1 μM combination, or A009 extract or 5-FU alone. Growth of the spheroidal colonies was monitored for the following days, replacing culture medium and treatments, with fresh ones, each 48 h. Images were acquired at 3, 6, and 12 days, following spheroid generation and treatments. Untreated and treated spheroids' area was measured, for each time point, using the ImageJ software and normalized for the respective area at day 3. The diameter was calculated based on the spheroid area, using the $d = \sqrt{(4A/\pi)}$ formula. Finally, the average area, between treatment groups, was compared.

In vivo Studies on Zebrafish Embryos

To evaluate the cardioprotective effect of the A009 extract, we used the embryos of *Danio rerio* (zebrafish), a robust animal model for cardiovascular diseases (31–33). Zebrafish eggs were incubated at a temperature of 26 ± 1°C, in a 12:12 h light:dark regime. Developmental stages were identified according to Kimmel et al. (34). Eggs were collected and washed two times with ISO-water (80 mM $CaCl_2$, 20 mM $MgSO_4$, 30.8 mM $NaHCO_3$, and 3.09 mM KCl) according to DIN ISO 150888 (International Organization for Standardization (ISO), 2009). All experiments were performed on zebrafish embryos exposed to the indicated agents for 24, 48, and 72 h post fertilization (hpf). Ten fertilized eggs were maintained in 24-well plates, with a proportion of 1 embryo/2 ml of solution. Embryos received A009 (dilutions 1:1,000 or 1:500), alone or in combination with the cardiotoxic agent doxorubicin (3 μg/ml) or left untreated. Embryo development was monitored at 48 and 72 hpf using an inverted stereomicroscope (Leica), by tracing the development of eyes, heartbeat, blood circulation, pigmentation, body shape malformations, edemas, detachment of the tail, and delay in development. The effect on embryo viability was determined by counting the number of dead embryos per experimental condition. Several parameters to trace the treatment induced congenital embryo abnormalities were monitored as listed in **Supplementary Tables 3, 4**. Congenital embryo abnormalities monitored included ischemia in the yolk sack (IS-YS), malformation of the heart (M.HT), ischemia in the tail (IS-TA), malformation of the tail (MT), yolk sack malformation (YS-DE), swim bladder malformation (SWB-DE), pericardial edema (PE), and ischemia in the brain (IS-BR).

Quantitative Real-Time PCR

Total RNA was extracted from HCM exposed to A009 (dilution 1:800) alone or in combination with 5-FU 100 μM for 24 h. The TRIzol method was used, following separation with chloroform precipitation of RNA with isopropanol (Sigma-Aldrich). The RNA pellet was washed twice with 75% ethanol (Sigma-Aldrich) and resuspended in nuclease-free water. RNA concentration was determined using the Nanodrop Spectrophotometer ND-1000 (Thermo Fisher Scientific). Reverse transcription was performed using the SuperScript VILO cDNA synthesis kit (Thermo Fisher Scientific), starting from 1,000 ng of total RNA. Quantitative real-time PCR was performed using SYBR GreenMasterMix (Applied Biosystems) on the QuantStudio 6 Flex RealTime PCR System Software (Applied Biosystems). All reactions were performed in duplicate. The relative gene expression was indicated as relative to nontreated cells, normalized to the housekeeping gene 18S. IL-6 (Fw-*AGACAGCCACTCACCT CTTCAG*, Rv-*TTCTGCCAGTGCCTCTTTGCTG*), p16 (Fw-*CTCGTGCTGATGCTACTGAGGA*, Rv-*GGTCGGCGCAGTTGG GCTCC*), and the housekeeping 18S (Fw-*CGCAGCTAGGAATA ATGGAATAGG*, Rv *CATGGCCTCAGTTCCGAAA*) primers, for qPCR, were designed using the NCBI Primer BLAST tool and purchased from Integrated DNA Technologies (IDT, Coralville, IA, USA).

Statistical Analysis

The statistical significance between multiple datasets was determined using the GraphPad Prism software v9. Flow cytometry data were analyzed using the FlowJo software, v10. Data are expressed as means ± SEM, one-way ANOVA, followed by the Tukey's *post-hoc* test. The $p \leq 0.05$ were considered statistically significant.

RESULTS

A009 Inhibits Angiogenesis *in vivo*

To evaluate the effect of the extract A009 (dilution 1:250) on angiogenesis, a hallmark of cancer, induced by CM of BC cells *in vivo*, a Matrigel sponge assay was performed in C57/BL6 female mice. We found that the A009 extract (1:250) was able to reduce the angiogenic activities exerted by the BT549 BC CM, as revealed by the colorimetric analysis of

the excised UltiMatrix plugs (**Figure 1A**). The A009 extract (1:250) was able to reduce the total hemoglobin content in the treated plugs, as compared with those containing the BT549 BC CM alone, in a statistically significant dependent manner (**Figure 1A**). Proangiogenic recruitment of endothelial cells was also decreased as demonstrated by histological staining (**Figure 1C**). Given the immune-modulatory properties of the A009 extract, we tested its ability to enhance immune cell number in the exposed sponge, following excision. We found that the A009 extract (1:250) was able to increase the infiltration of T cells in treated plugs, as compared with those containing the BT549 BC CM alone; in a statistically significant manner (**Figure 1B**), macrophages and NK cells are non-significantly modified (**Supplementary Figure 1**).

Effect of A009 on Cell Viability of BC Cell Lines in 2D and 3D Models *in vitro*

The effect of the A009 extract on tumor cell viability was investigated using the MTT assay. BT549 and MDA-MB-231 BC cell lines were pretreated with A009 extract (dilution 1:800) or Hyt (dilution of the major polyphenol present in the A009 extract, 1:800) for 24 h. The medium was then replaced with the chemotherapeutic drug Doxo 1 μM or 5-FU 100 μM, alone or in combination with the A009 extract or Hyt. Cells were treated for 48 and 72 h. The schedule of treatments and pretreatments is depicted in **Supplementary Figure 2**. Cell metabolic activity assessed by MTT of BT549 and MDA-MB-231 cells, receiving pretreatment with the extract A009 or Hyt, followed by the co-administration of these compounds with the chemotherapy drug 5-FU, was reduced compared with that of the cells receiving the 5-FU alone (**Figures 2A,B**). The same effect occurs on BT549 and MDA-MB-231 (**Figure 3B**), when treated with the A009 extract in combination with doxorubicin (**Figures 3A,B**). These results showed that the addition of chemotherapy to the A009 extract acts in an additive way reducing BC cell viability *in vitro*. We translated our results from a 2D to a 3D *in vitro* model of BC, by generating tumor spheroids, further treated following the same schedule applied for the 2D models. We observed that the combination of the A009 extract (1:800) with the chemotherapeutic agents 5-FU or Doxo synergized in blocking the generation of BC spheroids that morphologically appear less stable and with reduced diameter, within the time frame of treatments (**Figures 4A–D**).

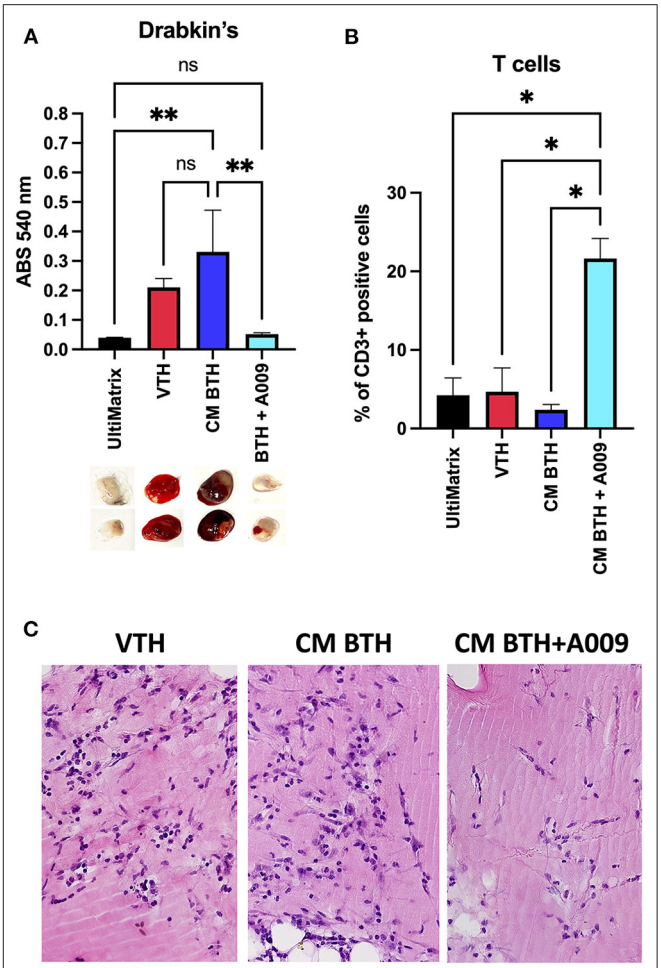

FIGURE 1 | Effects of the A009 extract on angiogenesis and immune cell infiltration *in vivo*. The effects of the A009 on angiogenesis, induced by CM of BC cell lines, and immune cell infiltration *in vivo*, was evaluated by the UltiMatrix Matrigel sponge assay. **(A)** Determination of the hemoglobin content in the excised pugs, using the Drabkin's assay and visual inspection of excised pellets; **(B)** determination of T-cell infiltration, detected as $CD3^+$ cells, in the plugs by flow cytometry. Data are shown as mean ± SEM, one-way ANOVA, $^*p < 0.05$ and $^{**}p < 0.01$. VTH (vascular endothelial growth factor (VEGF), tumor necrosis factor (TNF)-α, heparin), CM BTH (CM BT549 + heparin), A009 extract. Hemoglobin is decreased by A009 and T-cell infiltrates are increased. **(C)** Histological examination of pellets. Sections of paraffin embedded plugs were stained with hematoxylin eosin. VTH: VEGF-TNF-α-heparin containing UltiMatrix show angiogenesis. Pellets with BTH conditioned media show angiogenesis with many vessels. Pellets with A009 in addition to BTH CM show reduced angiogenesis with few vessels.

Cardioprotective Effect of A009 on Rat Cardiomyocytes

Based on our previous published article on the cardioprotective properties of the A009 extracts against chemotherapy-induced damages in models of prostate cancers (11), we also tested whether a similar scenario could be observed with chemotherapeutic agents used in BC treatment, such as 5-FU and Doxo. We observed that the rat cardiomyocyte cell line H9C2 exhibited less reduced cell proliferation, when co-treated with the A009 + 5-FU (**Figure 5**) or A009 + Doxo (**Figure 6**), both at 48 and 72 h, as compared to 5-FU or Doxo alone. 5-FU and Doxo were toxic, while A009 or Hyt alone did not show cardiotoxicity. In addition, the co-administration of A009 or Hyt with the chemotherapy drugs does not increase damage induced by the drugs, Hyt + 5-FU after 48 and 72 h, and both Hyt + Doxo and A009 + Doxo after 48 and 72 h.

Cardioprotective Effects of A009 Extract in Zebrafish Embryos

We extended our *in vitro* results to the zebrafish (*Danio rerio*) animal model. Zebrafish embryos were exposed to

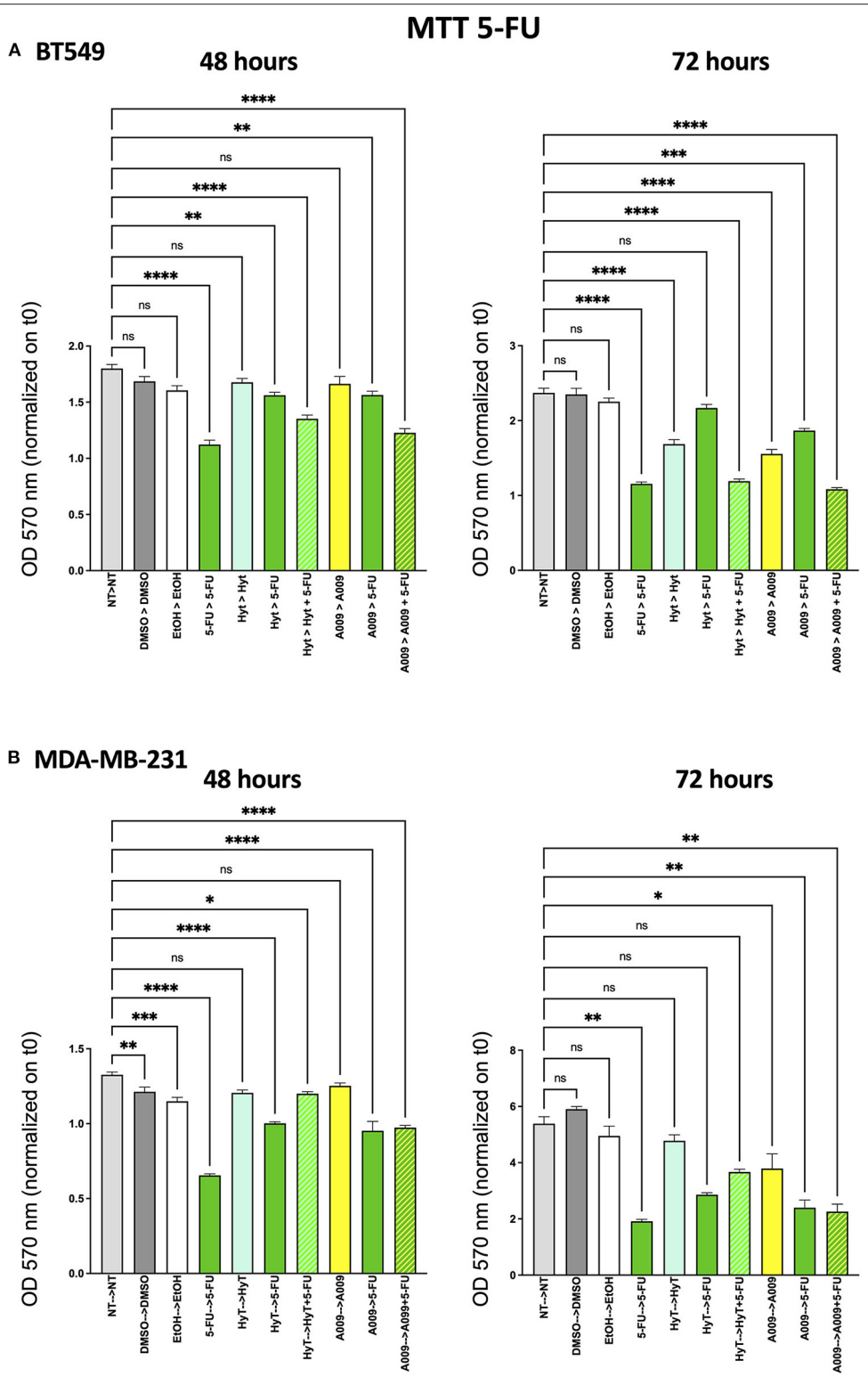

FIGURE 2 | Effects of the A009 extract in combination with 5-fluorouracil (5-FU) on breast cancer cell lines. BT549 **(A)** and MDA-MB-231 **(B)** cells were pretreated with extract A009 (dilution 1:800) or hydroxytyrosol (Hyt) (same concentration as that present in the 1:800 diluted A009 extract), for 24 h. Later, the medium was replaced with 5-FU 100 μM alone or in combination with A009 or Hyt for 48 and 72 h. Proliferation was detected by the MMT assay at the indicated time points. The experiments were performed in quadruplicate and repeated two times. Results are expressed as the mean of the absorbance normalized on the T0 ± SEM, one-way ANOVA, $*p < 0.05$, $**p < 0.01$, $***p < 0.001$, and $****p < 0.0001$. A009 activity was enhanced by addition of chemotherapy towards breast cancer cells.

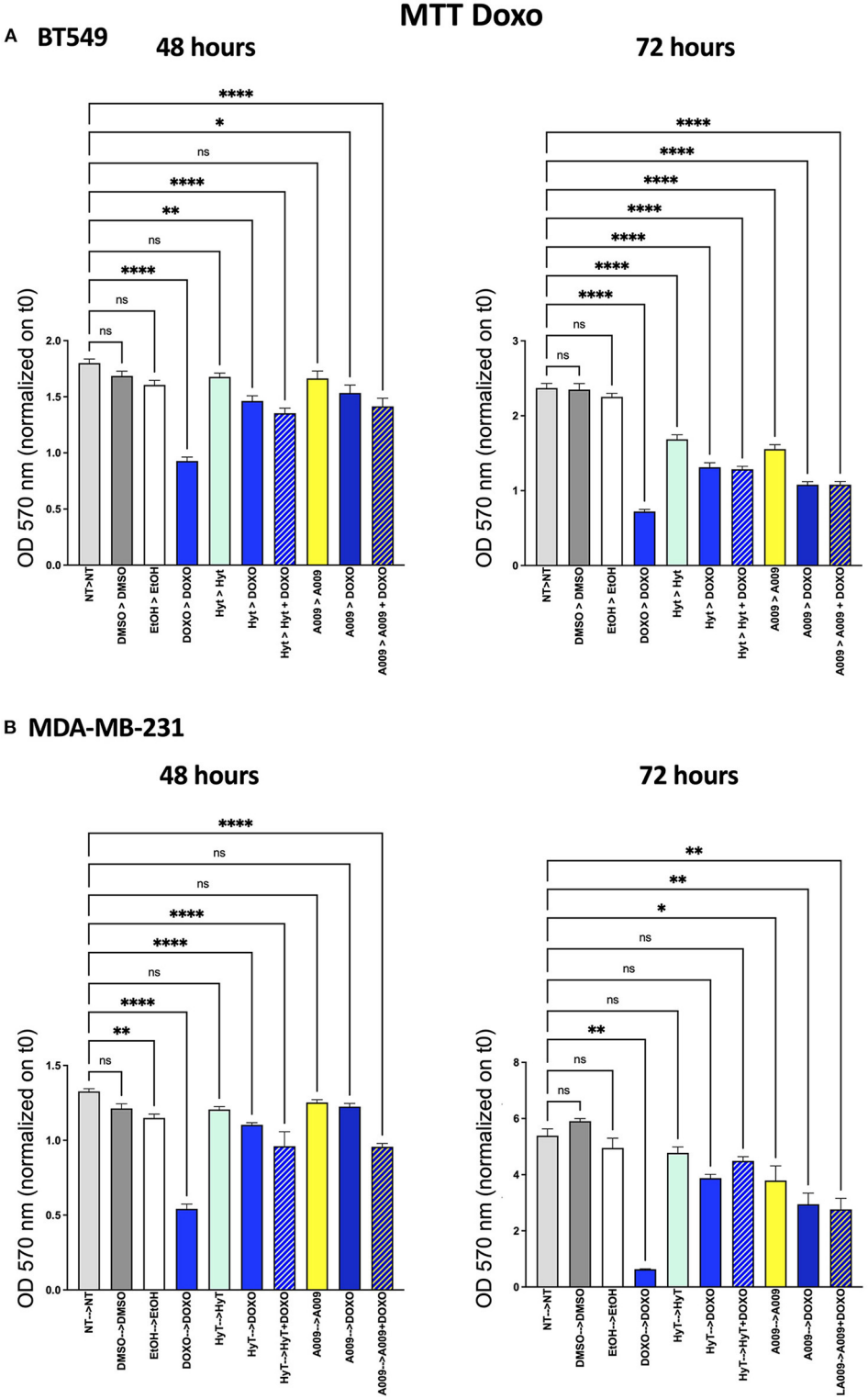

FIGURE 3 | Effects of the A009 extract in combination with doxorubicin on breast cancer cell lines. BT549 **(A)** and MDA-MB-231 **(B)** cells were pretreated with extract A009 (dilution 1:800) or Hyt (same concentration as that present in the 1:800 diluted A009 extract), for 24 h. Later, the medium was replaced with doxorubicin 1 μM alone or in combination with A009 or Hyt for 48 and 72 h. Proliferation was detected by the MMT assay at the indicated time points. The experiments were performed in quadruplicate and repeated two times. Results are expressed as the mean of the absorbance normalized on the T0 ± SEM, one-way ANOVA, $*p < 0.05$, $**p < 0.01$, and $****p < 0.0001$. A009 activity was enhanced by addition of chemotherapy toward breast cancer cells.

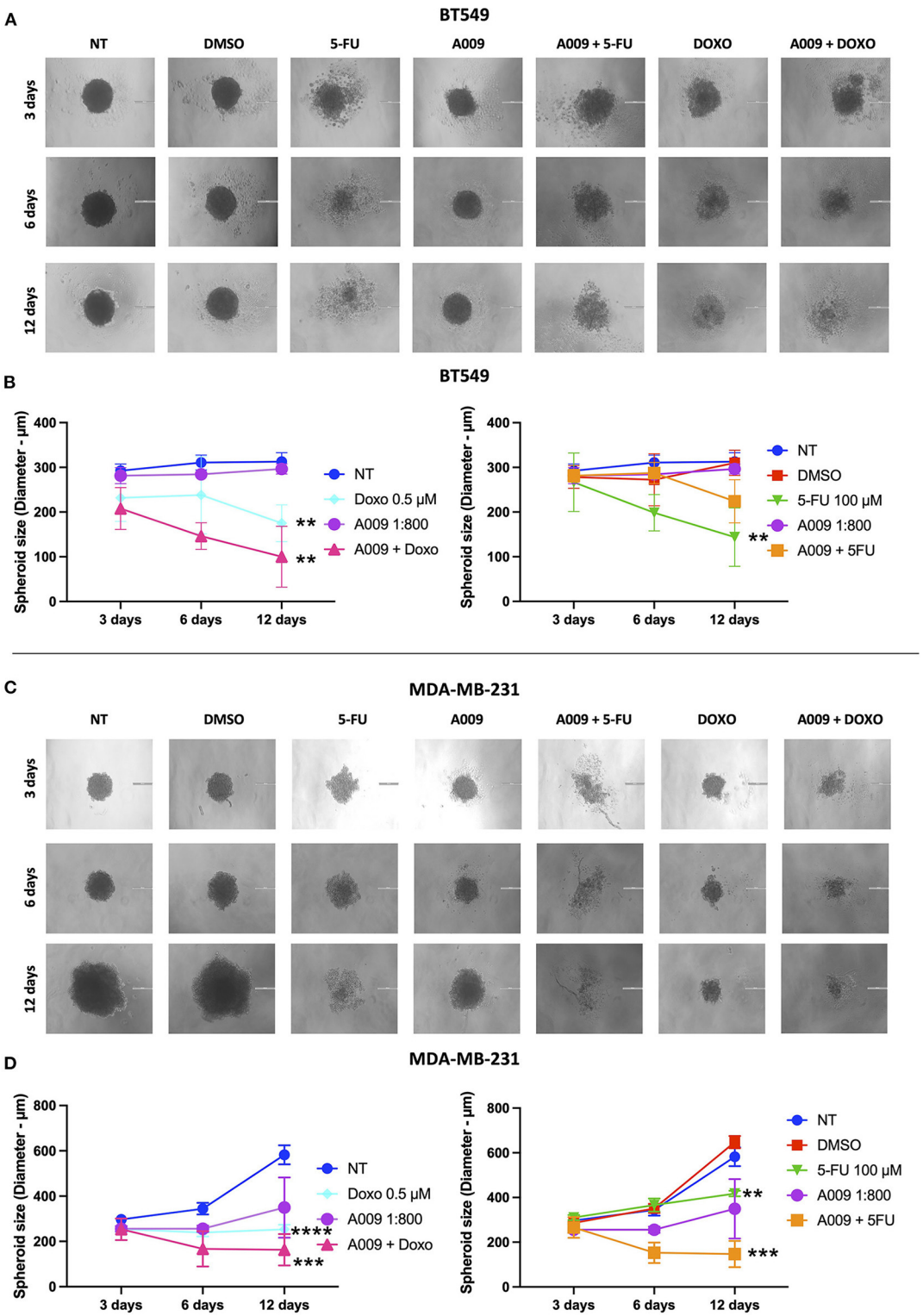

FIGURE 4 | Effects of the combination A009+chemotherapy on breast cancer spheroids. Single spheroids were generated by culturing 4 x 10^3 BT549 or MDDA-MB-231 cells in nonadherent conditions. BT459 **(A,B)** and MDA-MB-231 **(C,D)** spheroids were treated with the combination of A009 extract + 5-FU or Doxo, A009 or drugs alone, for 3, 6, and 12 days. During the treatment kinetic, spheroid diameters were detected, and spheroid macrophotographs were captured. The experiments were performed in quadruplicate and repeated two times. Scale bar = 200 µm. Data are shown as mean ± SEM, two-way ANOVA, $^{**}p < 0.01$, $^{***}p < 0.001$, and $^{****}p < 0.0001$. A009 combinations with chemotherapy reduced size of breast cancer cell spheroids.

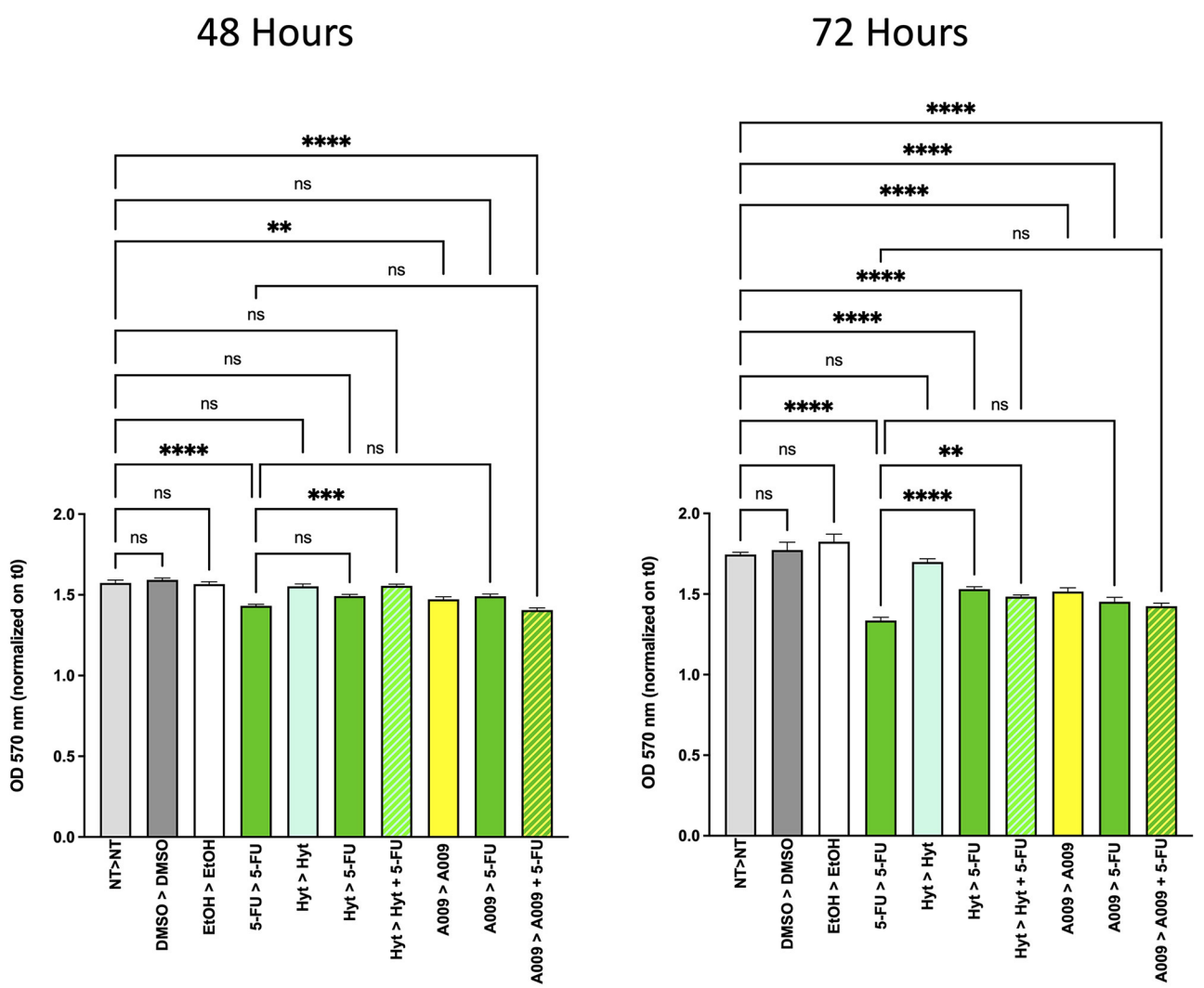

FIGURE 5 | Effects of the A009 extract in combination with 5-FU on rat cardiomyocytes. H9C2 cells were pretreated with extract A009 (dilution 1:800) or Hyt (same concentration as that present in the 1:800 diluted A009 extract), for 24 h. Later, the medium was replaced with 5-FU 100 μM alone or in combination with A009 or Hyt for 48 and 72 h. Proliferation was detected by the MMT assay at the indicated time points. The experiments were performed in quadruplicate and repeated two times. Results are expressed as the mean of the absorbance normalized on the T0 ± SEM, one-way ANOVA, $^{**}p < 0.01$, $^{***}p < 0.001$, and $^{****}p < 0.0001$. A009 combinations with chemotherapy were less toxic toward cardiomyocytes than toward breast cancer cells.

Doxo, alone or in combination with the A009 extract (dilution 1:1,000 or 1:500). We observed that the treatment of zebrafish embryos with doxorubicin (3 g/ml) significantly reduced their cardiac area at 48 and 72 h of treatment (**Figures 7A,B**). The co-treatment with A009 was able to reverse the doxorubicin-induced cardiotoxic effect, in terms of cardiac area, following 48 and 72 h of treatment (**Figures 7A,B**). The polyphenolic concentrate alone does not change the viability of the embryos.

Furthermore, we observed that co-treatment of embryos with the A009 extract and doxorubicin resulted in decreased numbers of embryos displaying congenital abnormalities, when compared with embryos treated with doxorubicin alone (**Supplementary Tables 3, 4**).

Effect of A009 on Inflammation and Induction of Senescence Associated With Chemotherapy in Human Cardiomyocytes

Chemotherapy is often associated with damages to the heart that result in exacerbated cardiac inflammation and generation of senescent phenotype in cardiomyocytes. Il6 is among

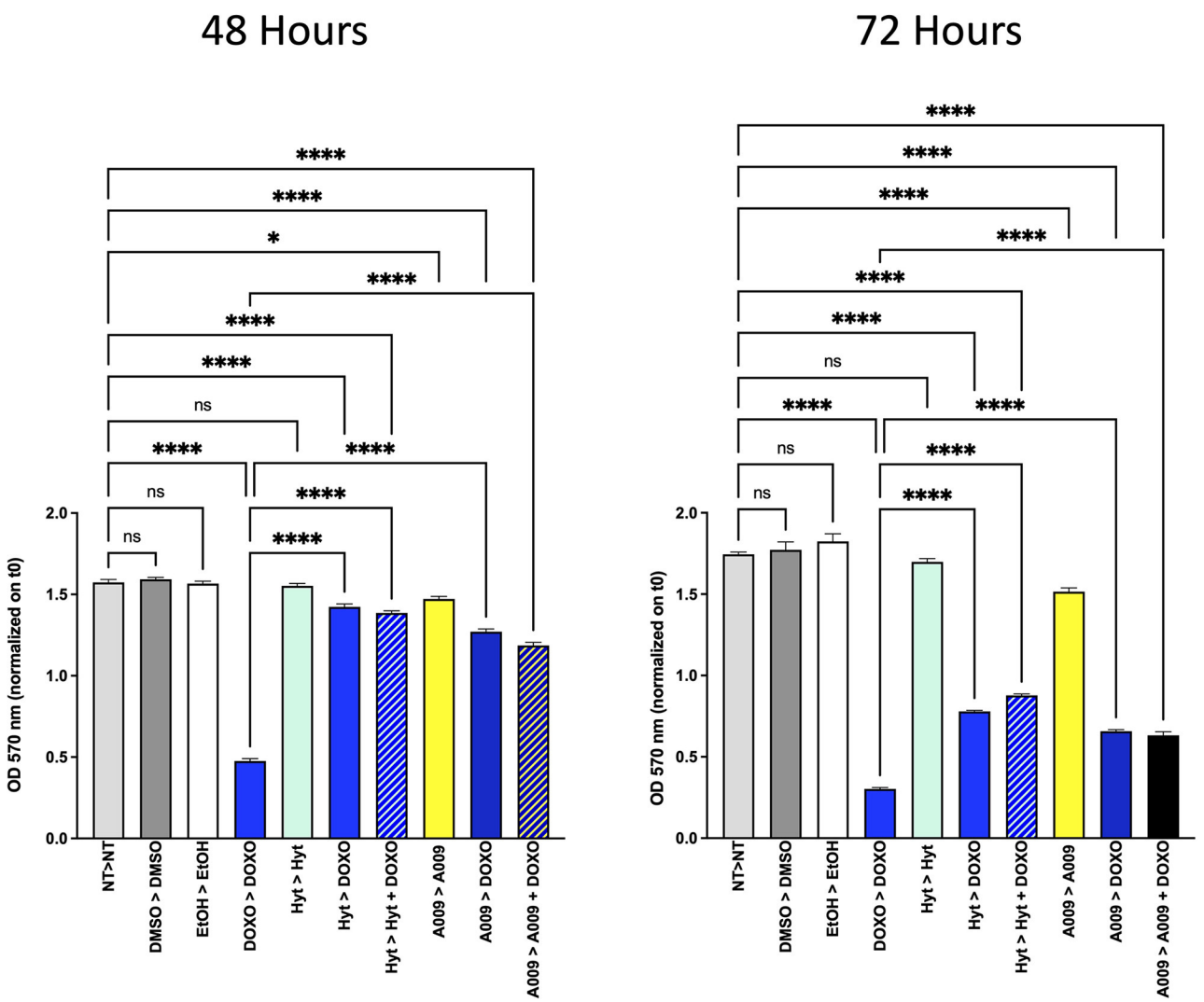

FIGURE 6 | Effects of the A009 extract in combination with doxorubicin on rat cardiomyocytes. H9C2 cells were pretreated with extract A009 (dilution 1:800) or Hyt (same concentration as that present in the 1:800 diluted A009 extract), for 24 h. Later, the medium was replaced with and without Doxo 1 μM alone or in combination with A009 or Hyt for 48 and 72 h. Proliferation was detected by the MMT assay at the indicated time points. The experiments were performed in quadruplicate and repeated two times. Results are expressed as the mean of the absorbance normalized on the T0 ± SEM, one-way ANOVA, $^{*}p < 0.05$ and $^{****}p < 0.0001$. A009 combinations with chemotherapy were less toxic toward cardiomyocytes than toward breast cancer cells.

the cytokines involved in the cardiac inflammation and participating to the induction of the senescent-associated secretory phenotype (SASP), while p16 is a senescence marker. We investigated the effect of A009 on IL-6 and p16 gene expression, both molecules linking inflammation and senescence, following chemotherapy-induced (i.e., 5-FU) cardiac damages, on HCM cells. We found that HCM cells, exposed to the combination of A009 extract (1:800) and 5-FU 100 μM, exhibit decreased transcript levels of IL-6 (**Figure 8A**) and p16 (**Figure 8B**), as compared to HCM treated with 5-FU alone, in a statistically significant dependent manner.

DISCUSSION

Chemotherapy, alone or in combination with other therapies (i.e., targeted, antiangiogenic therapies), along with surgery and radiotherapy is still a major option in BC treatment. However, cancer chemotherapy-induced cardiotoxicity remains a relevant obstacle, thus limiting the therapeutic options (alone or in combination) for cancer patients (10, 35–37). This largely impacts on the management of oncologic patients, requiring more efforts to overcome the generation of side effects, following cancer chemotherapy that remains the treatment of election (10, 35–37). With the knowledge of such a relevant unmet clinical

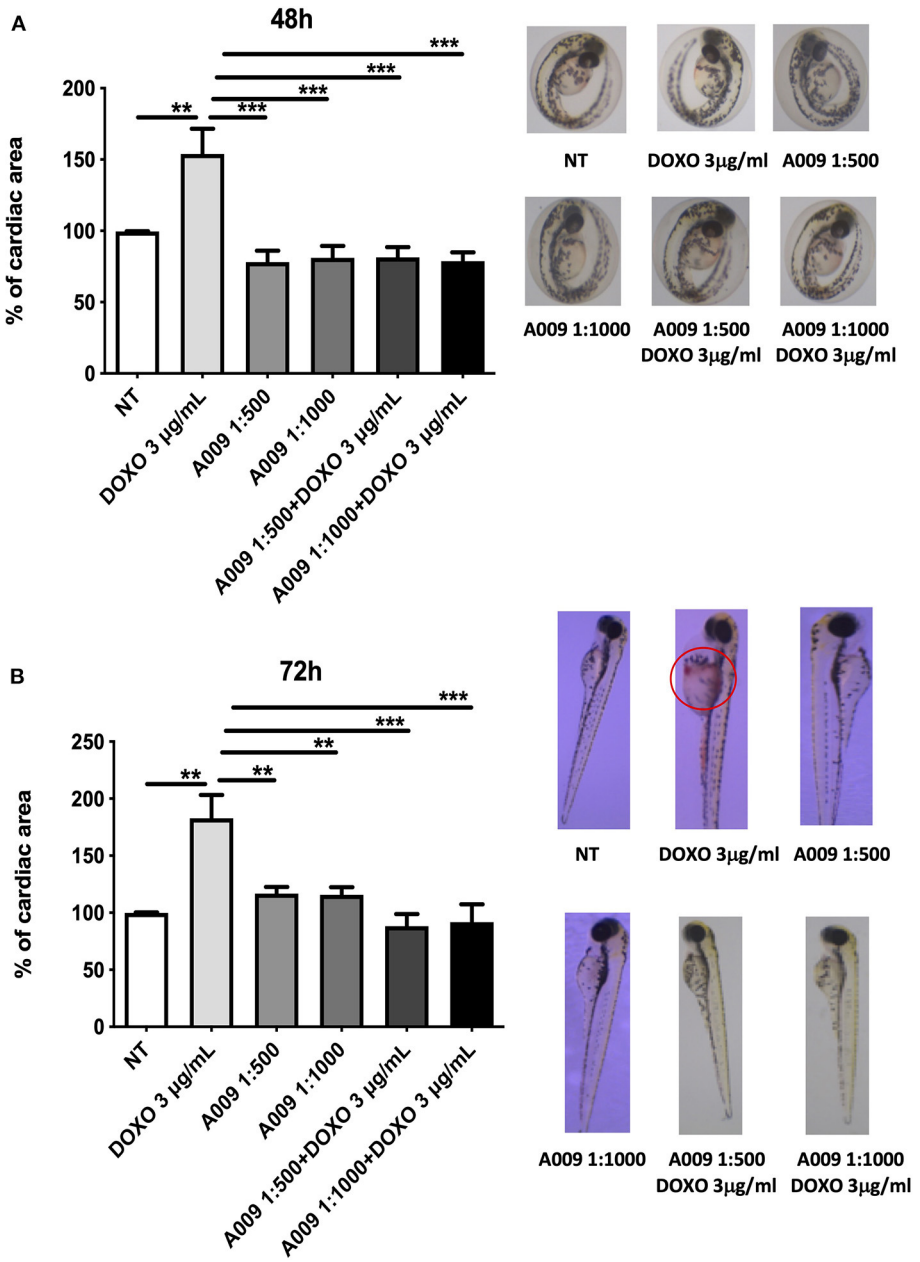

FIGURE 7 | Cardioprotective effects of A009 extract in zebrafish embryos. The cardioprotective effects of the A009 extract on chemotherapy-induced cardiotoxicity was investigated in zebrafish embryos. All experiments were performed on zebrafish embryos exposed to doxorubicin (3 µg/ml) alone, A009 (dilution 1:1,000, 1:500), or the combination of doxorubicin (µg/ml) and A009 (dilution 1:1,000, 1:500) for 48 h **(A)** and 72 h **(B)** post fertilization (hpf). Embryo micrographs for all the experimental conditions are shown. Data for cardiac area are shown as fold% increased over control. Data are shown as mean ± SEM, one-way ANOVA, $^{**}p < 0.01$ and $^{***}p < 0.001$. DOX, doxorubicin; A009 batch extract; NT, not treated. A009 combinations with chemotherapy were protective toward the heart.

need, together with the identification of robust biomarkers able to predict chemotherapy-induced cardiovascular effects, prevention remains the most accessible option to manage such an issue (10, 35, 36), and cardio-oncology is a flourishing field of investigation (38, 39).

Polyphenols account as the major dietary-derived molecules endowed with beneficial effects on human health, based on their ability to target tumor cells, while sparing or recovering damaged normal/healthy cells. In this context, EVOO accounts as one of the most abundant dietary sources of polyphenols, within the Mediterranean diet. Interestingly, also the waste products derived by EVOO processing have been reported to be rich in polyphenols with beneficial health effects, such as hydroxytyrosol. We have previously demonstrated that the

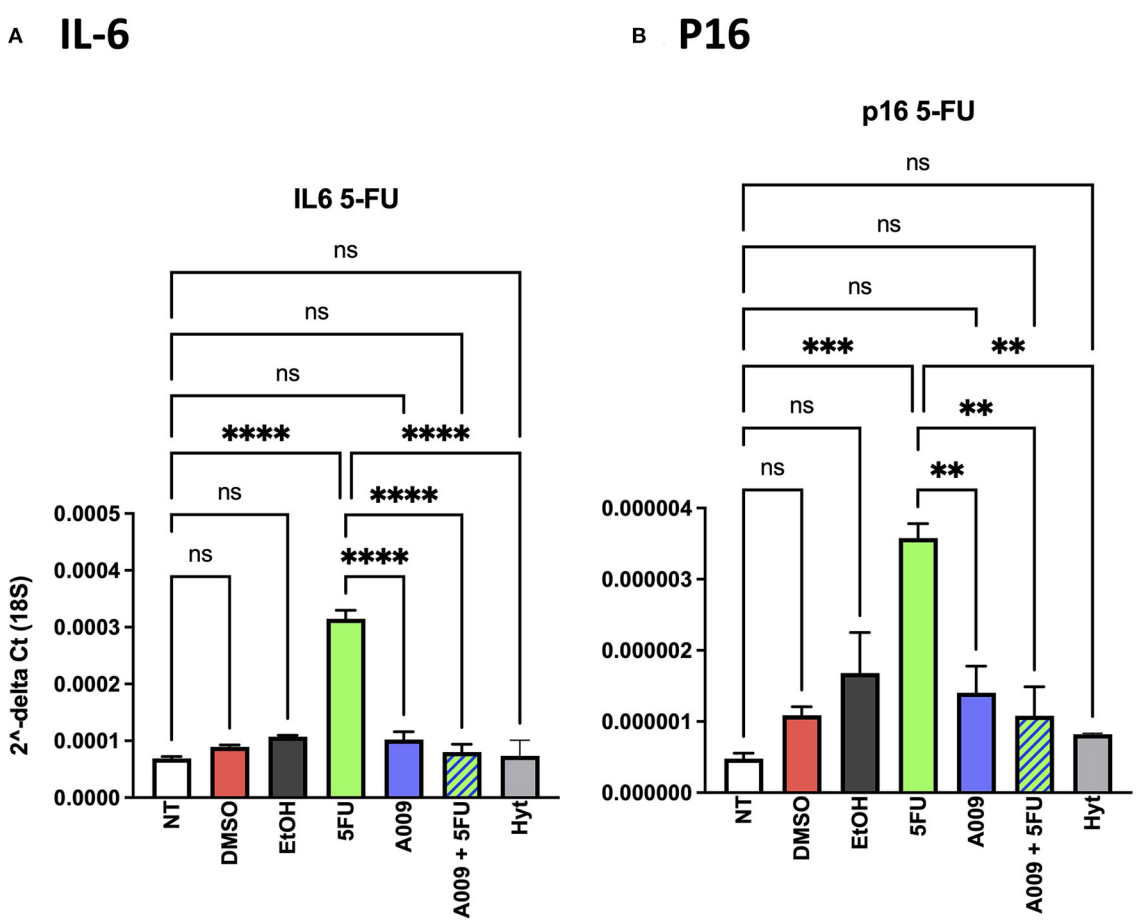

FIGURE 8 | Effects of the A009 extract on interleukin (IL)-6 and p16 expression in human cardiac myocytes by qPCR. The ability of A009 (dilution 1:800) to inhibit **(A)** IL-6 and **(B)** p16 expression in HCM was determined, following 24 h of stimulation, by qPCR. Data are shown as mRNA relative expression, normalized to 18S and control, mean ± SEM, one-way ANOVA, $^{**}p < 0.01$, $^{***}p < 0.001$, and **** $p < 0.0001$. A009 combinations with chemotherapy reduced IL6 and p16 expression.

polyphenol-rich OMWW extract, A009, from EVOO is endowed with antiangiogenic properties and chemopreventive activities in the context of colon and prostate cancers, both *in vitro* and *in vivo*. Recently, we also showed, in *in vitro* and *in vivo* models of prostate cancer, that the combination of the A009 extract with chemotherapy resulted in increasing chemopreventive and antitumor activities, while mitigating the chemotherapy-induced damages to cardiomyocytes and mice hearts.

Starting from our previous results of antiangiogenic effects of the A009 extracts, in this study, we tested the ability of A009 to limit angiogenesis, a hallmark of cancer, *in vivo*, induced by CM from the BT549 BC cell line in a Matrigel sponge model that we contributed to develop (27–29). We found that the A009 extract limits angiogenesis *in vivo*, induced by factors present in the BT549 cell CM. We also observed that the BT459 CM sponges from mice treated with the A009 extract show increased infiltration of $CD3^{+}$T cells, suggesting a potential contribution of the OMWW extract in the recruitment of immune cells.

We then tested the capability of the combination of the A009 extract with chemotherapeutic agents clinically employed in BC, to act on BC cell proliferation. We found that both the BT549 and MDA-MB-231 cells, following exposure to the A009 + 5-FU or A009 + Doxo combination, exhibited reduced cell proliferation, as compared with those treated with A009 alone. We observed additive effects by treating BT459 and MDA-MB-231 cell spheroids, with the A009 + drug combination. These results show that the combination of chemotherapy with the A009 extract further reduces BC cell viability *in vitro*.

A peculiar capability of polyphenols resides in their ability to target transformed malignant cells (40) also cooperating with chemotherapeutic agents (11, 40, 41), while sparing healthy cells or recovering healthy cells undergoing stress conditions and cellular damages (42–44). Based on this evidence and on our previous published article on the cardioprotective properties of the A009 extract against chemotherapy-induced damages, in models of prostate cancers, we tested whether

a cardio-oncological prevention scenario could be observed, using chemotherapeutic agents used for BC treatment, such as doxorubicin and fluoropyrimidines. The combination of A009 extract to chemotherapy mitigate the effects of reduced cell proliferation, mediates by 5-FU alone on rat cardiomyocytes. We found that this cardioprotective effect of the A009 extract occurs also *in vivo*: zebrafish embryos exposed to A009 extract + Doxo combination show rescue of cardiac area, as compared with those treated with Doxo alone.

OMWW extracts are not toxic to the animals, and in a cohort of healthy, individuals were highly tolerated with no toxicity (11).

Inflammation represents a peculiar hallmark of chronic diseases, such as cancer, metabolic, and cardiovascular disorders (45–48). Chemotherapy-induced cardiovascular side effects also include exacerbated inflammation, together with induction of cell senescence and of an SASP. We previously demonstrated that cardiovascular toxicities associated with the anticancer agent 5-FU include the induction of a senescent phenotype in HCMs and endothelial cells (49).

IL-6 accounts as a relevant cytokine in the inflammatory process (50) and is highly represented in the cytokine milieu characterizing the SASP phenotype (51, 52). In line with this evidence, we found that HCMs treated with 5-FU, have increased transcript levels of IL-6 and the senescence marker p16. We observed that the combination of the A009 extract with 5-FU can reduce the expression level of IL-6 and p16, induced by the 5-FU. This suggests the potential capability of the A009 extracts to exert cardioprotective activities also acting on the inflammation/senescence pathways in cardiomyocytes exposed to chemotherapeutic agents.

CONCLUSION

Our study suggests that in a cardio-oncological prevention perspective, a polyphenol-rich purified OMWW extract A009 combined with cancer chemotherapy, could represent a potential candidate for cardiovascular protection in patients with BC, while increasing effects of BC chemotherapy.

DATA AVAILABILITY STATEMENT

The raw data supporting the conclusions of this article will be made available by the authors, without undue reservation.

ETHICS STATEMENT

All the procedures applied were approved by the Local Animal Experimentation Ethics Committee (ID# #06_16 Noonan) of the University of Insubria and by the Health Ministry (ID#225/2017-PR).

AUTHOR CONTRIBUTIONS

DN, AB, RR, and AA: conceptualization, writing revision, and data curation. AB, DN, and AA: formal analysis and supervision. DN and AA: funding acquisition and project administration. NB, LC, KG, MGC, GP and AB: methodology. NB and LC: writing—original draft. GP and MGC: writing revision. All authors contributed to the article and approved the submitted version.

FUNDING

This work has been supported by Italian Ministry of Health Ricerca Corrente—IRCCS MultiMedica.

ACKNOWLEDGMENTS

We are grateful to Paola Corradino for bibliography. LC has a fellowship from the Stazione Zoologica Anton Dohrn, Naples, Italy. NB is a PhD fellow of Basilicata University. KG is an Erasmus fellow from Poland.

SUPPLEMENTARY MATERIAL

The Supplementary Material for this article can be found online at: https://www.frontiersin.org/articles/10.3389/fcvm.2022.867867/full#supplementary-material

Supplementary Figure 1 | Macrophages and natural killer (NK) cells in the UltiMatrix sponge assay. Changes in macrophages and NK cells upon treatment are nonsignificant.

Supplementary Table 1 | Phenolic composition of A009 obtained by high-performance liquid chromatography coupled with mass spectrometry (HPLC-DADMS-MS). Samples were analyzed by HPLC with UV-vis and MS detection. The identification of phenolic compounds from samples was carried out as previously reported by interpreting their mass spectra determined *via* LC-MS-MS and comparing with the data reported in the literature.

Supplementary Table 2 | Treatment's scheme of 3-(4,5-dimethylthiazol-2-yl)-2,5-diphenyltetrazolium bromide (MTT) assay on BT549, MDA-MB-231, and H9C2 cell lines. Cells were treated with A009 extract (dilutions 1:800) and Hyt (dilution 1:800) for 24 h. The medium was then substituted with the chemotherapy drug 5-FU 100 μM or Doxo 1 μM, alone or in combination with A009 or Hyt for 48 and 72 h.

Supplementary Tables 3, 4 | Presence of congenital alterations in zebrafish embryos, during single agent (A009, dilution 1:1,000, 1:500) alone, doxorubicin (3 μg/ml) alone, or the combination of doxorubicin and the A009 extract treatments, was monitored. Data are presented as the frequency (%) of events per experimental condition, at 24 **(A)** and 48 **(B)** h of treatment. Ischemia in Yolk Sack (IS-YS); malformation of heart (M.HT); ischemia in the tail (IS-TA); malformation of the tail (MT); yolk sack malformation (YS-DE); swim bladder malformation (SWB-DE); pericardial edema (PE); ischemia in the brain (IS-BR). Congenital alterations are mitigated by A009.

REFERENCES

1. Sturgeon KM, Deng L, Bluethmann SM, Zhou S, Trifiletti DM, Jiang C, et al. A population-based study of cardiovascular disease mortality risk in US cancer patients. *Eur Heart J.* (2019) 40:3889–97. doi: 10.1093/eurheartj/ehz766
2. Kitsis RN, Riquelme JA, Lavandero S. Heart disease and cancer: are the two killers colluding? *Circulation.* (2018) 138:692–5. doi: 10.1161/CIRCULATIONAHA.118.033907
3. Sung H, Ferlay J, Siegel RL, Laversanne M, Soerjomataram I, Jemal A, et al. Global Cancer Statistics 2020: GLOBOCAN estimates of incidence and mortality worldwide for 36 cancers in 185 countries. *CA Cancer J Clin.* (2021) 71:209–49. doi: 10.3322/caac.21660
4. Lin NU, Vanderplas A, Hughes ME, Theriault RL, Edge SB, Wong YN, et al. Clinicopathologic features, patterns of recurrence, and survival among women with triple-negative breast cancer in the National Comprehensive Cancer Network. *Cancer.* (2012) 118:5463–72. 10.1002/cncr.27581
5. Tsang JYS, Tse GM. Molecular classification of breast cancer. *Adv Anat Pathol.* (2020) 27:27–35. 10.1097/PAP.0000000000000232
6. Collignon J, Lousberg L, Schroeder H, Jerusalem G. Triple-negative breast cancer: treatment challenges and solutions. *Breast Cancer.* (2016) 8:93–107. 10.2147/BCTT.S69488
7. Cardinale D, Iacopo F, Cipolla CM. Cardiotoxicity of anthracyclines. *Front Cardiovasc Med.* (2020) 7:26. doi: 10.3389/fcvm.2020.00026
8. Martin-Sabroso C, Fraguas-Sanchez AI, Raposo-Gonzalez R, Torres-Suarez AI. Perspectives in breast and ovarian cancer chemotherapy by nanomedicine approach: nanoformulations in clinical research. *Curr Med Chem.* (2021) 28:3271–86. doi: 10.2174/0929867327666200819115403
9. Sonawane KB, Cheng N, Hansen RA. Serious adverse drug events reported to the FDA: analysis of the FDA adverse event reporting system 2006-2014 database. *J Manag Care Spec Pharm.* (2018) 24:682–90. doi: 10.18553/jmcp.2018.24.7.682
10. Albini A, Pennesi G, Donatelli F, Cammarota R, De Flora S, Noonan DM. Cardiotoxicity of anticancer drugs: the need for cardio-oncology and cardio-oncological prevention. *J Natl Cancer Inst.* (2010) 102:14–25. doi: 10.1093/jnci/djp440
11. Albini A, Festa MMG, Ring N, Baci D, Rehman M, Finzi G, et al. A polyphenol-rich extract of olive mill wastewater enhances cancer chemotherapy effects, while mitigating cardiac toxicity. *Front Pharmacol.* (2021) 12:694762. doi: 10.3389/fphar.2021.694762
12. Sofi F, Abbate R, Gensini GF, Casini A. Accruing evidence on benefits of adherence to the Mediterranean diet on health: an updated systematic review and meta-analysis. *Am J Clin Nutr.* (2010) 92:1189–96. doi: 10.3945/ajcn.2010.29673
13. Albini A, Tosetti F, Li VW, Noonan DM Li WW. Cancer prevention by targeting angiogenesis. *Nat Rev Clin Oncol.* (2012) 9:498–509. doi: 10.1038/nrclinonc.2012.120
14. Tosetti F, Noonan DM, Albini A. Metabolic regulation and redox activity as mechanisms for angioprevention by dietary phytochemicals. *Int J Cancer.* (2009) 125:1997–2003. doi: 10.1002/ijc.24677
15. Araldi EM. Dell'aica I, Sogno I, Lorusso G, Garbisa S, Albini A. Natural and synthetic agents targeting inflammation and angiogenesis for chemoprevention of prostate cancer. *Curr Cancer Drug Targets.* (2008) 8:146–55. doi: 10.2174/156800908783769382
16. Albini A, Noonan DM, Ferrari N. Molecular pathways for cancer angioprevention. *Clin Cancer Res.* (2007) 13:4320–5. doi: 10.1158/1078-0432.CCR-07-0069
17. Noonan DM, Benelli R, Albini A. Angiogenesis and cancer prevention: a vision. *Recent Results Cancer Res.* (2007) 174:219–24. doi: 10.1007/978-3-540-37696-5_19
18. Maruca A, Catalano R, Bagetta D, Mesiti F, Ambrosio FA, Romeo I, et al. The Mediterranean diet as source of bioactive compounds with multi-targeting anti-cancer profile. *Eur J Med Chem.* (2019) 181:111579. doi: 10.1016/j.ejmech.2019.111579
19. Nocella C, Cammisotto V, Fianchini L, D'Amico A, Novo M, Castellani V, et al. Extra virgin olive oil and cardiovascular diseases: benefits for human health. *Endocr Metab Immune Disord Drug Targets.* (2018) 18:4–13. doi: 10.2174/1871530317666171114121533
20. Foscolou A, Critselis E, Panagiotakos D. Olive oil consumption and human health: a narrative review. *Maturitas.* (2018) 118:60–6. doi: 10.1016/j.maturitas.2018.10.013
21. Vougogiannopoulou K, Angelopoulou MT, Pratsinis H, Grougnet R, Halabalaki M, Kletsas D, et al. Chemical and biological investigation of olive mill waste water - OMWW secoiridoid lactones. *Planta Med.* (2015) 81:1205–12. doi: 10.1055/s-0035-1546243
22. El-Abbassi A, Kiai H, Hafidi A. Phenolic profile and antioxidant activities of olive mill wastewater. *Food Chem.* (2012) 132:406–12. doi: 10.1016/j.foodchem.2011.11.013
23. Azaizeh H, Halahlih F, Najami N, Brunner D, Faulstich M, Tafesh A. Antioxidant activity of phenolic fractions in olive mill wastewater. *Food Chem.* (2012) 134:2226–34. doi: 10.1016/j.foodchem.2012.04.035
24. Baci D, Gallazzi M, Cascini C, Tramacere M, De Stefano D, Bruno A, et al. Downregulation of pro-inflammatory and pro-angiogenic pathways in prostate cancer cells by a polyphenol-rich extract from olive mill wastewater. *Int J Mol Sci.* (2019) 20:307. doi: 10.3390/ijms20020307
25. Gallazzi M, Festa M, Corradino P, Sansone C, Albini A, Noonan DM. An extract of olive mill wastewater downregulates growth, adhesion and invasion pathways in lung cancer cells: involvement of CXCR4. *Nutrients.* (2020) 12:903. doi: 10.3390/nu12040903
26. Bassani B, Rossi T, De Stefano D, Pizzichini D, Corradino P, Macrì N, et al. Potential chemopreventive activities of a polyphenol rich purified extract from olive mill wastewater on colon cancer cells. *J Funct Foods.* (2016) 27:236–48.
27. Rossi T, Bassani B, Gallo C, Maramotti S, Noonan DM, Albini A, et al. Effect of a purified extract of olive mill waste water on endothelial cell proliferation, apoptosis, migration and capillary-like structure *in vitro* and *in vivo*. *J Bioanal Biomed*. (2015) S12:006.
28. Albini A, Fontanini G, Masiello L, Tacchetti C, Bigini D, Luzzi P, et al. Angiogenic potential *in vivo* by Kaposi's sarcoma cell-free supernatants and HIV-1 tat product: inhibition of KS-like lesions by tissue inhibitor of metalloproteinase-2. *AIDS.* (1994) 8:1237–44. doi: 10.1097/00002030-199409000-00004
29. Benton G, Arnaoutova I, George J, Kleinman HK, Koblinski J. Matrigel: from discovery and ECM mimicry to assays and models for cancer research. Adv Drug Deliv Rev. 2014;79-80:3-18. doi: 10.1016/j.addr.2014.06.005
30. Passaniti A, Taylor RM, Pili R, Guo Y, Long PV, Haney JA, et al. Simple, quantitative method for assessing angiogenesis and antiangiogenic agents using reconstituted basement membrane, heparin, and fibroblast growth factor. *Lab Invest.* (1992) 67:519–28.
31. Nguyen CT, Lu Q, Wang Y, Chen JN. Zebrafish as a model for cardiovascular development and disease. *Drug Discov Today Dis Models.* (2008) 5:135–40. doi: 10.1016/j.ddmod.2009.02.003
32. Ding Y, Bu H, Xu X. Modeling inherited cardiomyopathies in adult zebrafish for precision medicine. *Front Physiol.* (2020) 11:599244. doi: 10.3389/fphys.2020.599244
33. Choi TY, Choi TI, Lee YR, Choe SK, Kim CH. Zebrafish as an animal model for biomedical research. *Exp Mol Med.* (2021) 53:310–7. doi: 10.1038/s12276-021-00571-5
34. Kimmel CB, Ballard WW, Kimmel SR, Ullmann B, Schilling TF. Stages of embryonic development of the zebrafish. *Dev Dyn.* (1995) 203:253–310. doi: 10.1002/aja.1002030302
35. Han X, Zhou Y, Liu W. Precision cardio-oncology: understanding the cardiotoxicity of cancer therapy. *NPJ Precis Oncol.* (2017) 1:31. doi: 10.1038/s41698-017-0034-x
36. Fernandez-Ruiz I. Cardioprotection: cardiotoxicity of anticancer therapy. *Nat Rev Cardiol.* (2016) 13:183. doi: 10.1038/nrcardio.2016.39
37. Molteni LP, Rampinelli I, Cergnul M, Scaglietti U, Paino AM, Noonan DM, et al. Capecitabine in breast cancer: the issue of cardiotoxicity during fluoropyrimidine treatment. *Breast J.* (2010) 16 Suppl 1:S45–8. doi: 10.1111/j.1524-4741.2010.01004.x
38. Lyon AR, Dent S, Stanway S, Earl H, Brezden-Masley C, Cohen-Solal A, et al. Baseline cardiovascular risk assessment in cancer patients scheduled to receive cardiotoxic cancer therapies: a position statement and new risk assessment tools from the Cardio-Oncology Study Group of the Heart Failure Association of the European Society of Cardiology in collaboration with the International Cardio-Oncology Society. *Eur J Heart Fail.* (2020) 22:1945–60. doi: 10.1002/ejhf.1920

39. Alvarez-Cardona JA, Ray J, Carver J, Zaha V, Cheng R, Yang E, et al. Cardio-oncology education and training: JACC council perspectives. *J Am Coll Cardiol.* (2020) 76:2267–81. doi: 10.1016/j.jacc.2020.08.079
40. Chairez-Ramirez MH. de la Cruz-Lopez KG, Garcia-Carranca A. Polyphenols as antitumor agents targeting key players in cancer-driving signaling pathways. *Front Pharmacol.* (2021) 12:710304. doi: 10.3389/fphar.2021.710304
41. Mahbub AA, Le Maitre CL, Haywood-Small SL, Cross NA, Jordan-Mahy N. Polyphenols act synergistically with doxorubicin and etoposide in leukaemia cell lines. *Cell Death Discov.* (2015) 1:15043. doi: 10.1038/cddiscovery.2015.43
42. Forman HJ, Zhang H. Targeting oxidative stress in disease: promise and limitations of antioxidant therapy. *Nat Rev Drug Discov.* (2021) 20:689–709. doi: 10.1038/s41573-021-00233-1
43. Sharifi-Rad M, Anil Kumar NV, Zucca P, Varoni EM, Dini L, Panzarini E, et al. Lifestyle, oxidative stress, and antioxidants: back and forth in the pathophysiology of chronic diseases. *Front Physiol.* (2020) 11:694. doi: 10.3389/fphys.2020.00694
44. Shi Y, Li F, Shen M, Sun C, Hao W, Wu C, et al. Luteolin prevents cardiac dysfunction and improves the chemotherapeutic efficacy of doxorubicin in breast cancer. *Front Cardiovasc Med.* (2021) 8:750186. doi: 10.3389/fcvm.2021.750186
45. Steven S, Frenis K, Oelze M, Kalinovic S, Kuntic M, Bayo Jimenez MT, et al. Vascular inflammation and oxidative stress: major triggers for cardiovascular disease. *Oxid Med Cell Longev.* (2019) 2019:7092151.
46. Multhoff G, Molls M, Radons J. Chronic inflammation in cancer development. *Front Immunol.* (2011) 2:98. doi: 10.3389/fimmu.2011.00098
47. Mantovani A, Allavena P, Sica A, Balkwill F. Cancer-related inflammation. *Nature.* (2008) 454:436–44. doi: 10.1038/nature07205
48. Hotamisligil GS. Inflammation and metabolic disorders. *Nature.* (2006) 444:860–7.
49. Focaccetti C, Bruno A, Magnani E, Bartolini D, Principi E, Dallaglio K, et al. Effects of 5-fluorouracil on morphology, cell cycle, proliferation, apoptosis, autophagy and ROS production in endothelial cells and cardiomyocytes. *PLoS One.* (2015) 10:e0115686. doi: 10.1371/journal.pone.0115686
50. Unver N, McAllister F. IL-6 family cytokines: Key inflammatory mediators as biomarkers and potential therapeutic targets. *Cytokine Growth Factor Rev.* (2018) 41:10–7. doi: 10.1016/j.cytogfr.2018.04.004
51. Kumari R, Jat P. Mechanisms of cellular senescence: cell cycle arrest and senescence associated secretory phenotype. *Front Cell Dev Biol.* (2021) 9:645593. doi: 10.3389/fcell.2021.645593
52. Li Y, Kracun D, Dustin CM, El Massry M, Yuan S, Goossen CJ, et al. Forestalling age-impaired angiogenesis and blood flow by targeting NOX: Interplay of NOX1, IL-6, and SASP in propagating cell senescence. *Proc Natl Acad Sci USA*. (2021) 118:e2015666118. doi: 10.1073/pnas.2015666118

Conflict of Interest: The authors declare that the research was conducted in the absence of any commercial or financial relationships that could be construed as a potential conflict of interest.

Publisher's Note: All claims expressed in this article are solely those of the authors and do not necessarily represent those of their affiliated organizations, or those of the publisher, the editors and the reviewers. Any product that may be evaluated in this article, or claim that may be made by its manufacturer, is not guaranteed or endorsed by the publisher.

frontiers | Frontiers in Cardiovascular Medicine

REVIEW
published: 15 April 2022
doi: 10.3389/fcvm.2022.847012

Cardiotoxicity of Anticancer Drugs: Molecular Mechanisms and Strategies for Cardioprotection

Marco Bruno Morelli[1†], Chiara Bongiovanni[2,3†], Silvia Da Pra[2,3†], Carmen Miano[2†], Francesca Sacchi[2,3†], Mattia Lauriola[3] and Gabriele D'Uva[2,3]*

[1] Scientific and Technological Pole, IRCCS MultiMedica, Milan, Italy, [2] National Laboratory of Molecular Biology and Stem Cell Engineering, National Institute of Biostructures and Biosystems (INBB), Bologna, Italy, [3] Department of Experimental, Diagnostic and Specialty Medicine (DIMES), University of Bologna, Bologna, Italy

Chemotherapy and targeted therapies have significantly improved the prognosis of oncology patients. However, these antineoplastic treatments may also induce adverse cardiovascular effects, which may lead to acute or delayed onset of cardiac dysfunction. These common cardiovascular complications, commonly referred to as cardiotoxicity, not only may require the modification, suspension, or withdrawal of life-saving antineoplastic therapies, with the risk of reducing their efficacy, but can also strongly impact the quality of life and overall survival, regardless of the oncological prognosis. The onset of cardiotoxicity may depend on the class, dose, route, and duration of administration of anticancer drugs, as well as on individual risk factors. Importantly, the cardiotoxic side effects may be reversible, if cardiac function is restored upon discontinuation of the therapy, or irreversible, characterized by injury and loss of cardiac muscle cells. Subclinical myocardial dysfunction induced by anticancer therapies may also subsequently evolve in symptomatic congestive heart failure. Hence, there is an urgent need for cardioprotective therapies to reduce the clinical and subclinical cardiotoxicity onset and progression and to limit the acute or chronic manifestation of cardiac damages. In this review, we summarize the knowledge regarding the cellular and molecular mechanisms contributing to the onset of cardiotoxicity associated with common classes of chemotherapy and targeted therapy drugs. Furthermore, we describe and discuss current and potential strategies to cope with the cardiotoxic side effects as well as cardioprotective preventive approaches that may be useful to flank anticancer therapies.

Keywords: cardiotoxicity, cardioncology, cardiomyocyte death, cardiomyocyte dysfunction, cardiomyocyte survival, chemotherapy, targeted therapy, cardioprotection

OPEN ACCESS

Edited by:
Chun Liu,
Stanford University, United States

Reviewed by:
Lichao Liu,
Stanford University, United States
Shane Rui Zhao,
Stanford University, United States

***Correspondence:**
Gabriele D'Uva
gabrielematteo.duva2@unibo.it

† These authors have contributed equally to this work

Specialty section:
This article was submitted to Cardio-Oncology, a section of the journal Frontiers in Cardiovascular Medicine

Received: *31 December 2021*
Accepted: *03 March 2022*
Published: *15 April 2022*

Citation:
Morelli MB, Bongiovanni C, Da Pra S, Miano C, Sacchi F, Lauriola M and D'Uva G (2022) Cardiotoxicity of Anticancer Drugs: Molecular Mechanisms and Strategies for Cardioprotection. Front. Cardiovasc. Med. 9:847012. doi: 10.3389/fcvm.2022.847012

INTRODUCTION

The introduction of antineoplastic drugs has been a turning point for prognosis improvement in oncology patients. However, a large number of chemotherapeutic agents have adverse cardiovascular effects, leading to acute or delayed onset of cardiac dysfunction, commonly referred to as cardiotoxicity. Although the definition of cardiotoxicity is not universally accepted, in clinical practice, cardiotoxicity commonly indicates a decline in patients' cardiac function measured as

left ventricle ejection fraction (LVEF). Various organizations and clinical committees defined cardiotoxicity using different threshold changes in LVEF [reviewed in (1)]. Treatment with anthracyclines, namely the chemotherapy class of drugs that generated the most concerns about cardiotoxicity, is associated with an incidence of cardiac dysfunction ranging between 2% and 48% [reviewed in (2–7)]. The Cardiac Review and Evaluation Committee (CREC), a retrospective study aiming at the evaluation of the cardiotoxicity of the anti-HER2 agent trastuzumab with or without concomitant anthracycline treatment, defined cardiotoxicity as a reduction in LVEF of at least 5% to below 55% with concomitant signs or symptoms of congestive heart failure (CHF), or a decrease in LVEF of at least 10% to below 55% without associated signs or symptoms (8). Although the assessment of LVEF is a well-established clinical procedure for the early recognition of cardiotoxic side effects to prevent irreversible cardiac damage and heart failure (HF), a reduction in LVEF may not be an effective parameter to detect a subclinical myocardial dysfunction that subsequently evolves in a symptomatic CHF (9) [reviewed in (1, 10)].

During the last decades, the cardiotoxic effects of several classes of chemotherapy drugs (anthracyclines, fluoropyrimidines, taxanes, and alkylating agents) and targeted therapies (targeting monoclonal antibodies and kinase inhibitors) were documented, and the underlying molecular mechanisms were investigated to suggest and develop potential strategies to avoid or reduce these effects (**Table 1**). Based on retrospective pathophysiological analysis of cancer patients with HF after chemotherapy, cardiotoxic side effects can be defined as irreversible (type I) or reversible (type II) [reviewed in (11, 12)]. Irreversible cardiotoxicity (type I) is usually observed in anticancer regimes causing injury and loss of cardiac myocytes. These effects are mainly observed after administration of anthracyclines and alkylating drugs, and to a lesser degree with fluoropyrimidines. According to the class of anticancer agents, the underlying mechanisms may involve cardiomyocyte-intrinsic and/or indirect mechanisms. For example, anthracyclines are associated with a high incidence of HF as consequence of irreversible cardiac damages through impairment of cardiomyocyte-intrinsic mechanisms leading to cell death [reviewed in (5, 7, 13–15)]. Despite administration of alkylating drugs and fluoropyrimidines may also cause cardiomyocyte death and thus irreversible cardiac damage, the main mechanism appears to be mediated by a vasculature dysfunction and/or thromboembolic ischemia. However, anticancer agents may also impair cardiomyocyte function without inducing cell death. This type of cardiac dysfunction is typically reversible and is associated with a lower incidence of HF (type II cardiotoxicity). Mechanistically, it has been suggested that reversible cardiotoxicity may be consequent to the deregulation of cardiomyocyte-intrinsic mechanisms and/or alteration of other cardiac populations and extracellular factors, in particular paracrine factors, in turn influencing cardiomyocyte function [reviewed in (4)]. Targeting monoclonal antibodies or tyrosine kinase inhibitors (TKIs) are typically associated with reversible cardiac damages, and their adverse effects derive by the signaling impairment of cardioprotective factors for cardiomyocytes, such as Neuregulin-1 (NRG1), or for other cardiac cell populations, such as vascular endothelial growth factor (VEGF), and platelet-derived growth factor (PDGF) [reviewed in (13, 16)].

Importantly, the comprehension of different cellular and molecular mechanisms by which common classes of chemotherapy and targeted therapy drugs induce cardiotoxic effects is critical for developing efficient strategies for prevention, early detection, and treatment. Several therapeutical approaches have already been proposed to cope with the cardiotoxic side effects of anticancer therapies, including iron-chelating drugs, β-blockers, renin-angiotensin-aldosterone system inhibitors, sodium-glucose cotransporter-2 (SGLT2) inhibitors, late inward sodium current (INaL) selective inhibitors, phosphodiesterase-5 inhibitors, metabolic agents, statins, and growth factors. As future therapeutic goal, moving toward a protective chemoprevention approach, we need well-tolerated drugs that may flank chemotherapy to reduce clinical and subclinical cardiotoxic side effects, without interfering with the action of the antineoplastic treatments (17).

CARDIOTOXICITY MECHANISMS ASSOCIATED WITH COMMON CLASSES OF CHEMOTHERAPY DRUGS AND TARGETED THERAPY

Chemotherapy Drugs

Anthracyclines

The anthracyclines, such as doxorubicin, daunorubicin, and epirubicin, are a class of broad-spectrum anticancer drugs extracted from *Streptomyces* bacterium. These compounds are used to treat different adult and pediatric hematologic cancers, such as leukemia and lymphomas, as well as many solid tumors, including breast, stomach, uterine, ovarian, bladder and lung cancers. However, anthracyclines are associated with a dose-dependent risk of cardiomyopathy and HF [reviewed in (2–7)]. Specifically, in the absence of risk factors, **doxorubicin** is tolerated up to a cumulative dose of 300 mg/m^2, with a rate of HF of less than 2% (18). Retrospective studies have shown that an estimated 3–5% of patients, without other risk factors, would experience doxorubicin-related HF at a cumulative dose of 400 mg/m^2, increasing at 7–26% and 18–48% for a dose of 550 and 700 mg/m^2, respectively (18, 19). Based on these evident cardiotoxic effects, high-dose treatments with anthracycline are no longer administrated, but sub-acute and chronic cardiac effects are still a clinical problem. The use of second-generation analogs of doxorubicin, namely **epirubicin or idarubicin**, exhibits improvements in their therapeutic index, but the risks of inducing cardiomyopathy are not abated [reviewed in (6)]. Mitoxantrone, which is an anthracenedione, an anthracycline analog, can also damage the cardiac muscle cells, thus resulting in cardiac dysfunction (20) [reviewed in (21, 22)].

Importantly, a large body of evidence indicates that cardiomyopathy develops at lower doses of anthracyclines in the presence of risk factors, including hypertension, arrhythmias,

TABLE 1 | Main features and mechanisms of cardiotoxic side effect of chemotherapies and targeted therapies along with mitigating strategies.

Anti-cancer agent	Epidemiology of the cardiotoxicity	Cardiotoxic effect	Cellular and molecular mechanisms of cardiotoxicity	Mitigating strategies
Anthracyclines (e.g., doxorubicin, daunorubicin, epirubicin, idarubicin) **and anthracycline analogs** (e.g., mitoxantrone)	Patients without risk factors: <2% of doxorubicin-related heart failure for a cumulative dose of 300 mg/m^2; 3–5% for a cumulative dose of 400 mg/m^2; 7–26% for a dose of 550 mg/m^2; 18–48% for a dose of 700 mg/m^2 (18, 19). In patients with risk factors cardiomyopathy may occur at low doses of anthracyclines [reviewed in (23, 24)].	Permanent damage due to cardiomyocyte death [reviewed in (34)].	Mitochondrial dysfunction in cardiomyocytes induced by formation of reactive oxygen species (ROS), iron-catalyzed formation of free radicals, lipid peroxidation, and cardiolipin sequestration (44, 45) [reviewed in (6, 14, 34, 38)]. Alteration of mitochondria structural integrity in cardiomyocytes (55). DNA double-strand breaks (DSBs) in cardiomyocytes induced by topoisomerase 2 (Top2) (45, 56) [reviewed in (4, 6)].	**Iron-chelating drug**: dexrazoxane (56, 202, 203, 206) [reviewed in (14, 204, 207)]. **β-Blockers** [reviewed in (16, 37)]: metoprolol (216, 217) carvedilol (220–226) nebivolol (228, 230, 231). **RAAS inhibitors:** ACE-Is such as enalapril, captopril, lisinopril, and ramipril (235–237, 239–241), ARBs such as candesartan and telmisartan (216, 242–245), aldosterone antagonists (251). **Combination of RAAS inhibitors and β-blockers** (33, 247). **SGLT2 selective inhibitors**: empagliflozin (256–259). **INaL inhibitor:** ranolazine (261, 262, 264). **Phosphodiesterase-5 inhibitors**: sildenafil, tadalafil (267–269). **Metabolic agents:** butyric acid (273), β-hydroxybutyrate (276). **Statins** (279–282). **Growth factors:** neuregulins (134, 284, 285, 287), G-CSF (289), erythropoietin (290). **PPARα activators**: fenofibrate (292). **Remote ischemic preconditioning** (293).
		Maladaptive effects on fibroblasts, endothelial cells, vascular smooth muscle cells and immune cells, leading to pathological left ventricular remodeling [reviewed in (67)].	Increased transforming growth factor beta (TGF-β) signaling and myofibroblasts activation [reviewed in (67)]. Increased endothelial cell permeability [reviewed in (67)]. Activation of immune cells [reviewed in (67)].	
Fluoropyrimidines (e.g., 5-fluorouracil, capecitabine)	1–19% cardiotoxic events [reviewed in (69, 73, 75)].	Generally reversible coronary artery spasm, although cardiomyocyte death and loss may occur as consequence of coronary artery thrombosis and myocardial infarction [reviewed in (69, 75, 76)], as well as directly through cardiomyocyte-intrinsic mechanisms (77).	Protein kinase C-mediated vasoconstriction in vascular smooth muscle cells (78) [reviewed in (69)]. Reduced oxygen transport capacity of erythrocytes, inducing relative ischemia of the myocardium (79). Increased ROS production in endothelial cells, leading to cell senescence and death, in turn triggering a procoagulant state (77) [reviewed in (69)]. ROS production and induction of cardiomyocyte apoptosis and autophagy (77).	**β-Blockers**, together with **calcium channel blockers, nitrates, and aspirin** [reviewed in (68, 71, 213)].

(Continued)

TABLE 1 | (Continued)

Anti-cancer agent	Epidemiology of the cardiotoxicity	Cardiotoxic effect	Cellular and molecular mechanisms of cardiotoxicity	Mitigating strategies
Taxanes (e.g., paclitaxel)	3–20% cardiotoxic events (81, 82) [reviewed in (84)].	Mild, primarily QT interval prolongation, followed by bradycardia and atrial fibrillation (82).	Hypersensitivity reaction with massive histamine release with consequent disturbance of the conduction system and arrhythmia (82). Increased ROS production by cardiomyocyte mitochondria, collapse of mitochondrial membrane potential and opening of mitochondrial permeability transition pore (91).	**Anti-inflammatory**: glucocorticoids [reviewed in (37, 88, 90)]. **Anti-histamine drugs**: histamine receptor blockers [reviewed in (37, 88, 90)].
	Exacerbate anthracycline-induced toxicity (93).	Increment of anthracycline-induced congestive heart failure (92).	Pharmacokinetic interference of doxorubicin elimination by paclitaxel [reviewed in (94)].	
Alkylating drugs (e.g., cisplatin, cyclophosphamide, ifosfamide, mitomycin)	7–32% of patients (96) [reviewed in (97)].	Permanent damage due to thromboembolic events and vascular damage, in turn inducing cardiomyocyte degeneration and necrosis (99) [reviewed in (87)].	Increased platelet reactivity by activation of arachidonic pathway [reviewed in (87)]. Oxidative stress and direct endothelial capillary damage with resultant extravasation of proteins, erythrocytes, and toxic metabolites, in turn causing a damage to the myocardium [reviewed in (99)].	**Amino acids:** taurine (102). **NADPH oxidase inhibitors:** apocynin (101).
		Pro-inflammatory effects leading to pathological left ventricular remodeling (101).	Expression of proinflammatory chemokines and cytokines driven by increased NFkB activation (101, 102).	
ERBB targeting monoclonal antibodies (e.g., trastuzumab, pertuzumab) **and tyrosine kinase inhibitors** (e.g., lapatinib, tucatinib)	Cardiotoxicity in 2–5% of **trastuzumab**-treated patients, leading to heart failure in 1–4% of the cases (151–153) [reviewed in (155, 156)]. Limited data regarding the sole **pertuzumab** cardiotoxicity [reviewed in (37, 297)]. The risk of heart failure is increased by the addition of pertuzumab to trastuzumab plus chemotherapy regimes (171). 2–5% LVEF reduction in patients treated with **lapatinib**, and in 1% of patients treated with tucatinib [reviewed in (173)]. Combination of lapatinib with trastuzumab does not increase cardiotoxicity (175).	Generally reversible alteration of cardiomyocyte contractile function {trastuzumab [reviewed in (8, 158)] and pertuzumab [reviewed in (174)].	Inhibition of the signaling activated by Neuregulin-1 (NRG1), a paracrine growth factor released by cardiac endothelial cells [reviewed in (110–112)].	**β-Blockers**: bisoprolol (215). **RAAS inhibitors:** ACE-Is such as perindopril (215). **Combination of RAAS inhibitors (ACE-Is) and β-blockers** (248, 249). **INaL inhibitor:** ranolazine (265, 266). **Statins** (283).

(Continued)

TABLE 1 | (Continued)

Anti-cancer agent	Epidemiology of the cardiotoxicity	Cardiotoxic effect	Cellular and molecular mechanisms of cardiotoxicity	Mitigating strategies
	May exacerbate anthracycline-induced toxicity, reaching 28% of heart failure incidence when **trastuzumab** is **combined with anthracyclines** (165).	Exacerbation of anthracycline-induced permanent damage through increased cardiomyocyte death (140).	Increase in anthracycline-induced ROS accumulation and consequent cardiomyocyte death (167).	**β-Blockers** (214): bisoprolol (216), carvedilol (226). **RAAS inhibitors:** ACE-Is such as lisinopril (226). **Statins** (283).
VEGFR/PDGFR tyrosine kinase inhibitors (e.g., sunitinib, sorafenib)	Up to 47% of patients receiving sunitinib treatment experienced hypertension, up to 28% showed LV dysfunction, and 8% developed congestive heart failure [reviewed in (15)].	Generally reversible [reviewed in (37, 76, 193)].	Sunitinib- or sorafenib-induced VEGFR inhibition reduces the production of the vasorelaxant nitric oxide (NO) by endothelial cells, in turn resulting in hypertension. In turn, hypertension may lead to capillary rarefaction, which may cause LV dysfunction [reviewed in (15, 194)]. Sunitinib- or sorafenib-induced VEGFR inhibition reduces angiogenesis resulting in LV dysfunction [reviewed in (15, 194)]. Sunitinib- or sorafenib-induced PDGFR inhibition induces the loss of pericytes, leading to coronary microvascular dysfunction and LV dysfunction [reviewed in (15, 194)].	**SGLT2 selective inhibitors**: empagliflozin (260).
BCL-ABL tyrosine kinase inhibitors (e.g., imatinib, ponatinib)	Despite initial fears (196), the rate of cardiotoxicity upon imatinib treatment was shown to be extremely low, with less than 1% of the patients developing heart failure [reviewed in (37, 197)]. More than 20% of patients receiving ponatinib treatment experienced adverse cardiovascular event, 5% developed congestive heart failure [reviewed in (181, 197)].	Generally reversible (181).	Ponatinib-induced cardiotoxic effects were suggested to be consequent to thrombotic microangiopathy and consequent ischemia (199).	**Growth factors:** neuregulins [proof-of-principle study in (200), reviewed in (197)].

coronary disease, combination with other anticancer agents as well as genetic predisposition to cardiotoxicity [reviewed in (17, 23, 24)]. In this regard, among the genetic factors increasing the susceptibility to anthracycline-induced cardiotoxic effects, the role of specific single-nucleotide polymorphisms (SNPs) is emerging [reviewed in (24, 25)]. Indeed, heritability analysis on multiple cell lines unveiled SNPs from 30 genes giving a greater predisposition to daunorubicin-induced cardiotoxicity (26). Specifically, several SNPs associated with anthracycline cardiotoxicity affect genes involved in anthracycline metabolism, transport, or downstream cytotoxic effects. For example, studies on pediatric cohorts enlightened polymorphisms in CBR1 and CBR3 genes (encoding for carbonyl reductases) associated with enhanced cardiotoxicity susceptibility in children with cancer (27), polymorphisms in ABCC1 and ABCC5 genes (encoding for ATP-binding cassette transporters) associated with increased anthracycline-induced cardiac dysfunction in acute lymphoblastic leukemia patients (28, 29), polymorphisms in SLC22A gene (encoding for a solute carrier) (30), as well as polymorphisms in genes playing a role in iron homeostasis (31), and others [reviewed in (25, 32)]. Oppositely, SNPs in endothelial nitric oxide synthase (NOS3) gene have been reported to be cardioprotective in patients upon a high dose of doxorubicin (29).

Cardiac injury after anthracycline administration occurs with every dose, as documented by the analysis of cardiac-biopsy specimens a few hours after a single dose of anthracycline [reviewed in (7)]. Although the vast majority (98%) of cases of anthracycline cardiotoxicity being detected within the first year after completing the treatment (33), anthracycline-induced cardiotoxicity can also manifest months to years after completing chemotherapy (33). From a pathophysiological point of view, anthracyclines were suggested to induce cardiotoxicity through cardiomyocyte-intrinsic mechanisms as well as other mechanisms involving other cardiac cell types (**Figure 1**). Importantly, anthracycline-induced cardiac damage may be permanent due to cardiomyocyte death through several biological processes, including apoptosis, autophagy, necrosis, necroptosis, pyroptosis, and ferroptosis [reviewed in (34)]. In this regard, the alteration of mitochondrial function and integrity emerged as a distinctive feature of anthracycline-induced cardiomyopathy [reviewed in (7, 34–39)]. Mitochondria network is well developed in the cardiac muscle, occupying 36–40% of the cardiomyocyte volume and producing around 90% of the cellular energy [reviewed in (40–43)]. Among the complex underlying molecular mechanisms involved in anthracycline-induced mitochondrial dysfunction is worth to mention the formation of reactive oxygen species (ROS), iron-catalyzed formation of free radicals, lipid peroxidation, and cardiolipin sequestering (44, 45) [reviewed in (6, 14, 34, 38)]. In this regard, in cardiac mitochondria, anthracyclines can be reduced by NAD(P)H-oxidoreductases and converted to unstable metabolites, such as doxorubicin-semiquinone radicals, which can react with molecular oxygen (O_2), producing superoxide anion-free radicals and hydrogen peroxide (O_2^- and H_2O_2) (46) [reviewed in (37)]. ROS generated by anthracyclines affect the activity of many mitochondrial enzyme complexes, such as NOSs, NAD(P)H oxidases, catalase, and glutathione peroxidase (GPx), leading to DNA, protein, and lipid damage, and consequently to cardiomyocyte death [reviewed in (39, 47, 48)]. Moreover, anthracyclines, such as doxorubicin, have been reported to impair cardiac iron homeostasis, resulting in its overload in the cardiac tissue [reviewed in (14, 49, 50)]. Accordingly, patients with anthracycline-induced cardiac dysfunction exhibit higher iron levels in cardiac mitochondria, compared to healthy individuals or patients suffering from anthracycline-independent cardiac dysfunction (44). Doxorubicin can, in fact, chelate the free intracellular iron and form iron-doxorubicin complexes, which, in turn, are able to react with O_2, further increasing the generation of ROS [reviewed in (4, 14, 49, 50)]. In addition, anthracyclines can directly interfere with the main iron-transporting/-binding proteins. For example, doxorubicin can impair cellular iron mobilization, resulting in its accumulation within ferritin (51), and can reduce the expression of the mitochondrial iron exporter ABCB8 (44). Recent studies have also focused on the detrimental role of mitochondrial iron-doxorubicin complexes triggering cardiomyocyte ferroptosis, a kind of programmed cell death dependent on iron and induced by lethal lipid peroxidation (52) [reviewed in (50)]. In this regard, doxorubicin-induced cardiotoxicity in mouse models was shown to be consequent to a decrease in the expression levels of glutathione peroxidase 4 (GPx4), which is a scavenger for lipid peroxides, in turn inducing peroxidation of unsaturated fatty acids and lipids (52). Anthracyclines are also linked to mitochondria damage because of their high affinity to cardiolipin, a mitochondrial membrane phospholipid that is involved in apoptotic pathways [reviewed in (35, 53)]. Mechanistically, doxorubicin sequesters cardiolipin avoiding its anchorage to cytochrome C or lipid-protein interfaces, thus contributing to mitochondrial dysfunction and ROS formation (54) [reviewed in (35, 53)]. Along with the impaired cardiac mitochondrial function, anthracyclines have been demonstrated to alter the structural integrity of mitochondria. Indeed, it has been reported that doxorubicin stimulates the receptor-interacting protein 3 (RIPK3)-induced activation of Ca^{2+}-calmodulin-dependent protein kinase (CaMKII), thus triggering the opening of mitochondrial permeability transition pore (MTPT), and ultimately inducing necroptotic cardiomyocyte death (55).

Several lines of evidence have suggested that nuclear damage induced by topoisomerase 2 (Top2) is another pivotal event in anthracyclines' cardiotoxic effects (45, 56) [reviewed in (4, 6)]. Specifically, doxorubicin intercalates into DNA and interacts with both Top2-alpha (Top2α) and Top2-beta (Top2β), which are enzymes responsible for managing DNA tangles and super-coils. Top2α is highly expressed in proliferating cancerous cells but not in quiescent tissues; therefore, it is considered one of the key molecular targets of anthracycline anti-tumoral effect (56). Cardiomyocyte toxicity stems from the fact that doxorubicin interacts with cardiac Top2-β, the only isoform expressed by adult mammalian cardiomyocytes. Consequently, the Top2β-doxorubicin-DNA complex induces DNA double-strand breaks (DSBs), ultimately promoting cardiomyocyte death (45, 56).

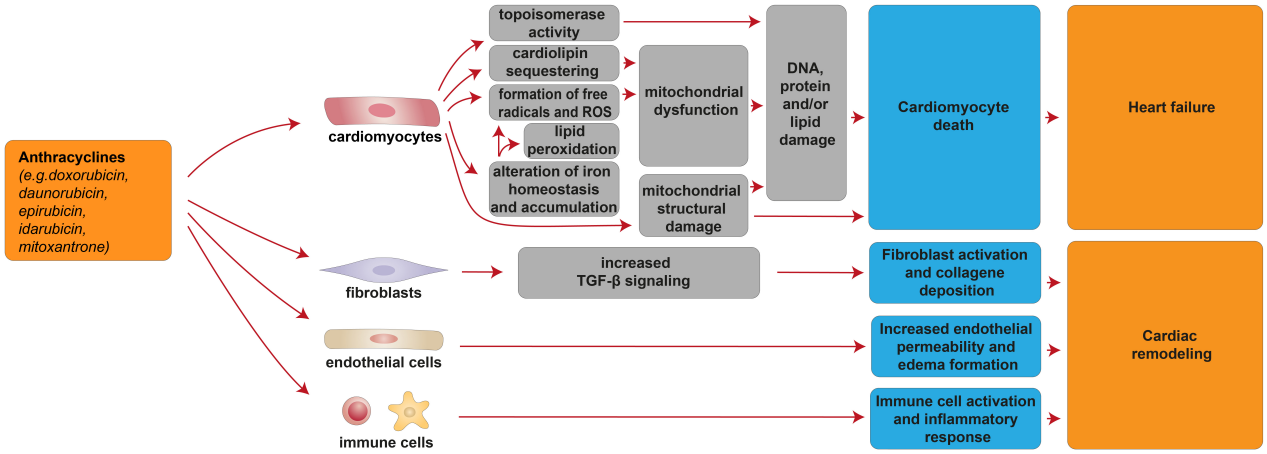

FIGURE 1 | Cellular and molecular mechanisms of the cardiotoxic effects exerted by anthracyclines. Schematic diagram showing the impact of anthracyclines on a multitude of cardiomyocyte-intrinsic mechanisms leading to mitochondrial dysfunction and structural damage and/or DNA damage by topoisomerase activity, in turn leading to cardiomyocyte death and heart failure. Additional mechanisms of anthracycline-induced cardiotoxicity include deregulation of fibroblasts, endothelial, and immune cells, in turn concurring to cardiac remodeling.

Tumor protein P53 (p53) has also been implicated in anthracyclines' cardiotoxic response, although its involvement is currently controversial. Indeed, it has been reported that DNA breaks, induced by acute doxorubicin administration, lead to activation of the DNA damage response (DDR) network, in turn activating p53, which ultimately promotes the apoptotic cascade (57) [reviewed in (58)]. Moreover, in response to cell stress, p53 was shown to accumulate in the cytosol and to localize in mitochondria, triggering a series of death-events related to mitochondrial dysfunction, such as the permeabilization of the mitochondrial outer membrane (MOMP), the release of cytochrome C, the opening of the mitochondrial permeability transition pore (PTP), the impairment of mitochondria, and the production of ROS (59–63). Mice depleted for p53 exhibit a less impaired mitochondrial integrity and reduced cardiac dysfunction following doxorubicin treatment [reviewed in (5)]. In addition, doxorubicin-activated p53 has been shown to contribute to metabolic derangement by inhibiting mitophagy events (45) [reviewed in (4)]. As a result of cytosolic accumulation, p53 binds Parkin and abrogates its translocation to damaged mitochondria and their subsequent clearance by mitophagy (64) [reviewed in (5)]. These results support p53 as a key player in anthracycline-related cardiomyopathies (61, 62) [reviewed in (4)]. Nevertheless, other studies unveiled opposite effects depending on the dosage and timing of doxorubicin-induced cellular stress. Indeed, upon low doses of doxorubicin, which more closely recapitulate the clinical settings, it has been reported a protective role of p53, counteracting the late-onset cardiomyopathy and without activation of p53-dependent cell death cascades (65, 66).

In addition to cardiomyocyte-intrinsic mechanisms, anthracyclines exhibit a wide range of maladaptive effects on other cardiac populations, including fibroblasts, endothelial cells, vascular smooth muscle cells, and immune cells [reviewed in (67)]. In particular, doxorubicin administration was shown to increase endothelial cellular permeability, in turn causing edema formation [reviewed in (67)], to induce ROS-dependent activation of transforming growth factor beta (TGFβ) signaling, in turn triggering myofibroblast activation and collagen deposition [reviewed in (67)], and to induce the activation of the innate immune system and inflammatory response [reviewed in (67)]. Overall, these events were suggested to lead to pathological left ventricular remodeling [reviewed in (67)].

Fluoropyrimidines

Fluoropyrimidines exert the second most common cause of chemotherapy-induced cardiotoxicity [reviewed in (68–74)]. This antimetabolite drug class, which includes **5-fluorouracil (5-FU)** and its prodrug **capecitabine**, is incorporated into DNA or RNA, thus acting as cytostatic agent for the clinical treatment of colorectal, breast, gastric, pancreatic, prostate, and bladder cancers [reviewed in (74)]. Fluoropyrimidines are generally well tolerated; nevertheless, 1–18% of the patients receiving fluoropyrimidines experiences cardiovascular toxicity [reviewed in (69–71, 73–75)]. Cardiovascular side effects associated with fluoropyrimidines include a generally reversible coronary artery spasm and myocardial ischemia, although cardiomyocyte death and loss may occur as consequence of coronary artery thrombosis and myocardial infarction [reviewed in (69, 75, 76)], as well as directly through cardiomyocyte-intrinsic mechanisms (77). These adverse effects were suggested to be mediated by vascular smooth muscle cells, erythrocytes, endothelial cells as well as directly by cardiomyocytes (**Figure 2**). From a molecular point of view, 5-FU was reported to induce protein kinase C-mediated vasoconstriction in vascular smooth muscle cells (78) [reviewed in (69)]. 5-FU was also shown to reduce the oxygen transport capacity of erythrocytes, inducing relative ischemia of the myocardium (79). 5-FU administration was also suggested to induce increased ROS production in endothelial cells, leading to cell senescence and death (77), in turn

triggering a procoagulant state and acute thrombotic events [reviewed in (69)]. Finally, direct cardiomyocyte toxicity after fluoropyrimidine administration has also been suggested. Indeed, 5-FU has also been demonstrated to favor ROS production and to induce cardiomyocyte apoptosis and autophagy (77).

Taxanes

Taxanes, such as **paclitaxel**, are antimitotic agents that stabilize microtubules in the mitotic spindle, thus blocking cell cycle progression. These chemotherapy drugs are widely employed in cancer treatment, including breast, lung, and ovarian cancers. However, significant toxicities limit the effectiveness of taxane-based treatment regimens (80). Taxane administration is reported to induce cardiotoxic events in 3–20% of the patients (81, 82) [reviewed in (83–85)]. Taxane-induced cardiotoxic effects include QT interval prolongation, followed by bradycardia and atrial fibrillation (82). Because taxane-induced cardiotoxicity appears to be mild in most cases and reversible upon discontinuation of the therapy, no specific agents are recommended for their management [reviewed in (86, 87)].

The underlying cellular and molecular mechanisms of taxane-induced cardiotoxicity are unclear; however, a few hypotheses have been proposed (**Figure 3**). Among them, hypersensitivity reaction with a massive histamine release and consequent disturbance of the conduction system and arrhythmia has been proposed (82). Hence, the administration of anti-inflammatory (glucocorticoids) and anti-histamine drugs (histamine receptor blockers), is suggested as prophylactic therapy for the management of cardiac anaphylaxis induced by taxanes [reviewed in (37, 88–90)]. Another hypothesis is cardiomyocyte damage through the drug's actions on subcellular organelles (82). In this regard, taxanes were suggested to increase ROS production by cardiomyocyte mitochondria, the opening of mitochondrial permeability transition pore and the collapse of mitochondrial membrane potential (91).

Among taxanes, paclitaxel has been shown to exacerbate anthracycline-induced toxicity. Indeed, combined treatment with paclitaxel and doxorubicin augmented HF events (92) and increased histopathological alterations of cardiac tissue, with extensive necrosis (93). This effect was suggested to derive from a pharmacokinetic interference of doxorubicin elimination by paclitaxel [reviewed in (94)]. No interaction between doxorubicin and other taxanes (such as docetaxel) has been reported; in line, **docetaxel** showed no increase in cardiac toxicity when combined with doxorubicin [reviewed in (94)].

Alkylating Drugs

Alkylating drugs, such as cisplatin, cyclophosphamide, ifosfamide, mitomycin, are crosslinking agents inducing ROS production, DNA damage and apoptosis in cancer cells [reviewed in (95)]. **Cisplatin** is mostly used in combination with other chemotherapy drugs to overcome drug-resistance and reduce toxicity [reviewed in (95)]. Cisplatin-based chemotherapy has been reported to cause cardiovascular diseases, particularly myocardial infarction and angina, in a range of 7–32% of patients (96) [reviewed in (97)]. In patients treated with cisplatin, a long-term unfavorable cardiovascular risk profile was observed, with hypercholesterolemia, hypertriglyceridemia, hypertension and insulin-resistance evaluated after more than 10 years from remission (98). The cardiotoxic effects of alkylating agents may be permanent and a few cellular and molecular mechanisms were suggested to contribute to these processes (**Figure 4**). Indeed, cisplatin administration has been linked with thromboembolic events associated with platelet aggregation and vascular damage (99) [reviewed in (87)], in turn resulting in cardiomyocyte degeneration and necrosis. The increased platelet aggregation was suggested as a direct consequence of cisplatin on the activation of the arachidonic pathway in platelets [reviewed in (87)]. The endothelial capillary damage was suggested to derive from a cisplatin-dependent increase in oxidative stress (99). Indeed, cisplatin has also been shown to induce oxidative stress in myocardial tissue, with decreased activity of glutathione and antioxidant enzymes (100, 101). The consequence of cisplatin-induced endothelial injury was suggested to be the extravasation of proteins, erythrocytes, and toxic metabolites, in turn causing damage to the myocardium (99). Finally, cisplatin has also been suggested to activate NF-κB in the cardiac tissue (101), in turn increasing the expression of proinflammatory chemokines and cytokines (102). This mechanism was proposed to result in cardiac remodeling (101), and extensive degeneration and fragmentation of cardiac muscle fibers (102).

The alkylating agent **cyclophosphamide** at high doses can cause hemorrhagic cell necrosis and may lead to HF; however, with the lower doses currently used, these side effects are infrequent (103).

Targeted Therapy

ERBB Targeted Therapies

Growth factor receptors of the ERBB family (EGFR/ERBB1, ERBB2, ERBB3, and ERBB4) play a key role in the development and progression of a variety of solid cancers [reviewed in (104–106)]. After the binding of soluble ligands, ERBB kinase receptors arrange in homo- or heterodimer complexes, which activate the tyrosine kinase activity and the consequent signaling events leading to the modulation of cell survival, proliferation, migration, and differentiation [reviewed in (104–107)]. ERBB2 (also known as HER2) receptor is a proto-oncogene frequently amplified and overexpressed in many human cancers. Unlike the other ERBB receptors, ERBB2 is unable to bind ligands but heterodimerizes with other ERBB receptors, stabilizing the ligand interaction with the coupled receptors, enhancing and diversifying the ligand-induced receptor signaling (108) [reviewed in (107)]. Several strategies have been developed to target the key role of ERBB2 signaling in tumor development and progression. Successful approaches are represented by treatment with humanized ERBB2-targeting antibodies (e.g., trastuzumab and pertuzumab) and tyrosine kinase multi-HER inhibitors (e.g., lapatinib, tucatinib, afatinib, neratinib, and dacomitinib), which effectively showed ERBB2 inhibition and tumor regression, particularly in the treatment of mammary carcinomas [reviewed in (109)].

The cardiotoxicity of ERBB2-directed therapeutics is consequent to the inhibition of the signaling activated by

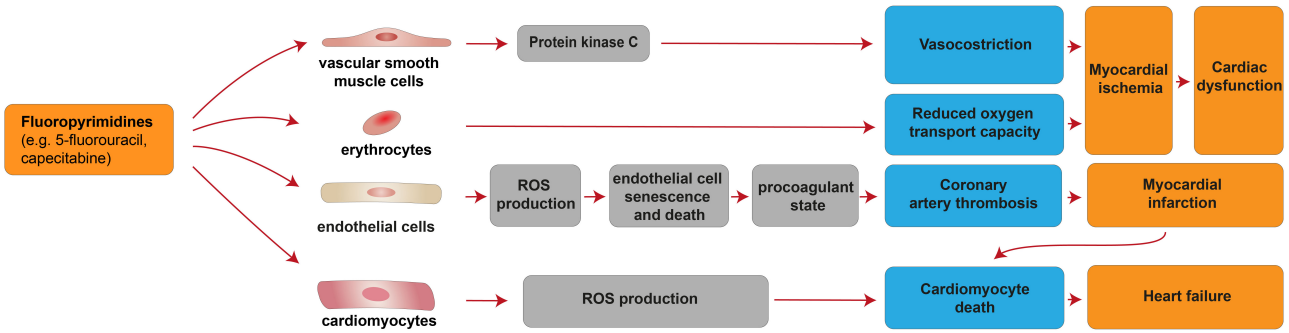

FIGURE 2 | Cellular and molecular mechanisms of the cardiotoxic effects exerted by fluoropyrimidines. Schematic diagram showing the impact of fluoropyrimidines on cardiac dysfunction due to myocardial ischemia induced by deregulation of vascular smooth muscle cells and erythrocytes. Additional mechanisms of taxane-induced cardiotoxicity include heart failure, consequent to cardiomyocyte death induced by cardiomyocyte-intrinsic mechanisms (increased ROS production) or myocardial infarction consequent to coronary artery thrombosis caused by endothelial cell senescence and death.

Neuregulin-1 (NRG1), a paracrine growth factor released by cardiac endothelial cells featuring pivotal functions in the heart (**Figure 5**) [reviewed in (110–112)]. NRG1, together with its tyrosine kinase receptors ERBB4, ERBB3, and ERBB2, is essential for heart development (113–115) [reviewed in (110, 116, 117)] and tunes heart regenerative, inflammatory, fibrotic, and metabolic processes (118, 119) [reviewed in (110, 117, 120–122)]. In cardiomyocytes, the most prominently expressed NRG1 receptors are ERBB4 and ERBB2 (123) and NRG1 stimulates fetal/neonatal cardiomyocyte proliferation, hypertrophy, sarcomerogenesis, and survival (114, 115, 124–127) [reviewed in (110, 116, 117, 120, 121)]. ERBB2 forms heterodimers with ERBB4 and is necessary for NRG1-elicited cardiomyocyte proliferation during embryonic and neonatal stages (122, 124). However, cardiac ERBB2 expression levels decline soon after birth in mice, as part of the mechanism leading to cardiomyocyte terminal differentiation, cell cycle withdrawal and loss of cardiac regenerative ability (124) [reviewed in (122)].

Despite low levels described in adulthood, ERBB2 appears to play a role in the prevention of dilated cardiomyopathy. Indeed, mice with ventricular-restricted deletion of ERBB2 exhibited multiple independent parameters of dilated cardiomyopathy, such as chamber dilatation, wall thinning, and decreased contractility (128). Decreased NRG1 signaling in postnatal life is associated with adverse cardiac function and susceptibility to stress [reviewed in (110, 116)]. The expression and activation of ERBB4 and ERBB2 receptors were found lower in myocardium from HF patients (129). In mice subjected to pressure overload, ERBB4 and ERBB2 undergo relevant reduction at mRNA and protein levels with the progression to HF (130).

Conversely, enhanced activity of NRG1 counteracts cardiac remodeling and HF progression [reviewed in (110, 116)]. Systemic administration of NRG1 improves cardiac function following various types of cardiac injuries in adult mice (115, 127, 131, 132) [reviewed in (110, 133)] and HF patients (117, 134–136) [reviewed in (137)].

Cardiac upregulation of ERBB2 was documented upon adverse hemodynamic or other stressful or toxic stimuli, including anthracycline therapies (138, 139). This increase is required to sustain cardiomyocyte survival and cardiac function under stress conditions. Indeed, cardiomyocytes isolated from mice with ventricular-restricted deletion of ERBB2 were more susceptible to anthracycline toxicity, revealing a role for ERBB2 in cardiomyocyte survival upon chemotherapy administration (128). Conversely, cardiac-specific overexpression of ERBB2 in mice has been shown to decrease cardiomyocyte death upon doxorubicin administration (140).

EGFR (also known as ERBB1) is associated with cancer progression and its inhibition *via* monoclonal antibodies (such as cetuximab and panitumumab) or TKIs (such as erlotinib and gefitinib) has been the first strategy evaluated among growth factor receptors targeting therapies (141, 142). Nowadays, EGFR inhibitors are clinically used for the treatment of several solid cancers, including lung, head and neck, colorectal, and pancreatic cancers (142). Although cetuximab-associated cardiotoxicity has been reported in the clinical literature, the incidence of cardiac events in patients remains very low (143, 144).

ERBB Targeting Monoclonal Antibodies

Trastuzumab, the first ERBB2-targeting humanized monoclonal antibody, binds the extracellular domain IV of ERBB2 receptor leading to the inhibition of ligand-independent heterodimerization between ERBB2 and other ERBB family members (145, 146) [reviewed in (105, 147)]. From a clinical perspective, the cardiotoxicity of monoclonal antibodies targeting ERBB2, such as trastuzumab, is moderate and reversible [reviewed in (148–150)]. Trastuzumab monotherapy is associated with cardiotoxicity in 2–5% of patients, leading to HF in 1–4% of the cases (151–153) [reviewed in (154–157)]. The mechanism of trastuzumab-induced cardiotoxicity appears to be the alteration of cardiomyocyte contractile function without cardiomyocyte death [reviewed in (8, 158)]. Interestingly, Erbb2 gene polymorphisms that alter the ERBB2 protein sequence have been identified, and two of them (Ile 655 Val and Pro 1170 Ala) were associated with an increased risk of cardiotoxicity from trastuzumab therapy (32, 159–164). Importantly, with the concomitant association of trastuzumab and anthracyclines, HF incidence increased to 28% (165, 166).

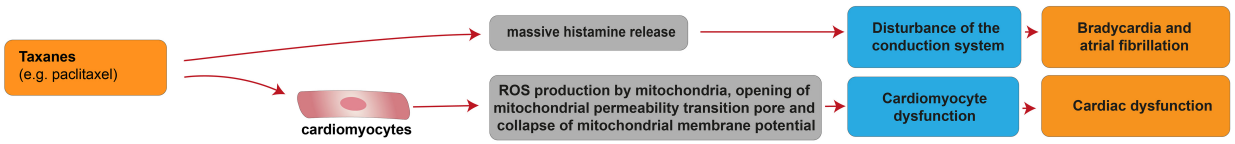

FIGURE 3 | Cellular and molecular mechanisms of the cardiotoxic effects exerted by taxanes. Schematic diagram showing the main cardiotoxic effects of taxanes, namely atrial fibrillation and cardiac dysfunction, as a result of the disturbance of the conduction system or cardiomyocyte dysfunction, respectively.

Thus, trastuzumab-mediated blockade of ERBB2 signaling increases anthracycline-induced toxicity. The molecular mechanism underlying this combinatorial phenomenon may be due to the key role of ERBB2 in the management of oxidative stress in the heart: interrupting the neuregulin/ERBB2 axis, which is responsible for the activation of the glutathione reductase system, facilitates the anthracycline-induced accumulation of ROS and subsequent calcium influx, finally leading to caspase activation and cardiomyocyte death (167). Once anti-ERBB2 agents inhibit the ERBB2 protective mechanisms in cardiomyocytes, the doxorubicin oxidative damage was reported to increase (158) [reviewed in (37)].

Pertuzumab, a new generation of ERBB2-targeting therapies, is an antibody against domain II specifically designed to inhibit ligand-induced ERBB2 heterodimerization (168, 169). The data regarding the sole pertuzumab cardiotoxicity effects are still limited. Currently, combining trastuzumab/pertuzumab and trastuzumab/lapatinib, in order to induce a dual blockade of HER2, is part of the standard of care (170). In this regard, a recent study reporting a systematic review of eight randomized controlled trials showed that the risk of HF is increased by the addition of pertuzumab to trastuzumab plus chemotherapy therapeutic regimens (171).

ERBB Kinase Inhibitors

Tyrosine kinase inhibitors selectively target and inhibit several oncogenic relevant receptor-tyrosine kinases (RTKs), inducing survival benefits in therapies for various hematological and solid cancers [reviewed in (172)]. TKIs include single-targeted and multi-targeted TKIs. A small group of small TKIs, including lapatinib (ERBB2 and EGFR inhibitor), tucatinib (ERBB2 inhibitor), erlotinib (EGFR inhibitor), gefitinib (EGFR inhibitor), afatinib (EGFR, ERBB2, and ERBB4 inhibitor), neratinib (EGFR, ERBB2, and ERBB4 inhibitor), and dacomitinib (EGFR, ERBB2, and ERBB4 inhibitor), has been developed to target ERBB receptors. However, these ERBB blockers can also exert cardiac toxicity in treated patients. In particular, about 2–5% of patients treated with lapatinib displayed a reduced LVEF, and similar effects were reported in 1% of patients treated with tucatinib [reviewed in (173)]. The decline in cardiac function is generally reversible [reviewed in (174)]. Regarding combinatorial anti-ERBB strategies, little is known about the cardiotoxic potential of ERBB2 double blockade with trastuzumab plus lapatinib. Although stronger inhibition of the HER2 pathway using two anti-HER2 drugs was initially expected to result in greater impairment of cardiomyocytes, preclinical tests suggested a possible cardioprotective mechanism exerted by lapatinib. Adjuvant Lapatinib and/or Trastuzumab Treatment Optimisation (ALTTO), a randomized, multi-center, open-label, phase III study of adjuvant lapatinib plus trastuzumab treatment in patients with HER2/ERBB2 positive primary breast cancers (ClinicalTrials.gov, identifier NCT00490139), as well as other clinical trials with double ERBB2 blockade, support the safety of lapatinib plus trastuzumab treatment, since a lower, although not statistically significant, incidence of cardiac events was detected in patients in the trastuzumab plus lapatinib arm. This evidence does not imply that lapatinib has a cardioprotective effect, nor that it should be a preferred option for patients with an increased risk of cardiotoxicity (175).

Afatinib, an ERBB family blocker, approved for the first-line treatment of advanced non-small cell lung cancer (NSCLC) with EGFR mutations, is one of the few TKIs with a low risk of cardiotoxicity [reviewed in (176)]. Finally, cardiac side effects of the irreversible pan-ERBB inhibitor neratinib [reviewed in (177)] were reported neither in phase I clinical studies in solid tumors (178, 179) nor in a phase II trial in advanced HER2-positive breast cancer (179).

Multi-Targeted Tyrosine Kinase Inhibitors

In addition to single- or multi-targeted ERBB family inhibitors (see the previous paragraph), other multi-targeted TKIs were developed to effectively block multiple pathways of intracellular signal transduction. The broad kinase-signaling inhibition of several TKIs, such as sunitinib, sorafenib, imatinib, and nilotinib, includes the vascular endothelial growth factor receptors (VEGFRs), platelet-derived growth factor receptors (PDGFRs), BCR-ABL, and c-KIT. This wide action results in a strong anti-malignancy effect of this class of drugs, although correlated with reversible myocardial dysfunctions with a wide range of severity (180) [reviewed in (37, 181–183)]. Clinical analysis of TKI anti-tumoral therapies shows that compounds with broader off-target effects as kinases inhibitors (lower selectivity in targeting a specific kinase) correlated to higher degree of cardiotoxicity, particularly in case the inhibited kinase plays a role in the maintenance of the cardiovascular system (184–186) [reviewed in (37)]. In this regard, sunitinib, which targets VEGFR/PDGFR and interferes with more than 30 tyrosine kinases; sorafenib, which targets VEGFR/PDGFR and inhibits at least 15 tyrosine kinases, including RAF/MEK/ERK pathway, and ponatinib, which targets BCR-ABL and several other RTKs, are responsible for major clinical concerns related to cardiotoxicity (172) [reviewed in (37, 187, 188)]. Of note, these three compounds (sunitinib, sorafenib, and sonatinib) target VEGF, PDGFR, and c-Kit, namely three tyrosine kinase receptors

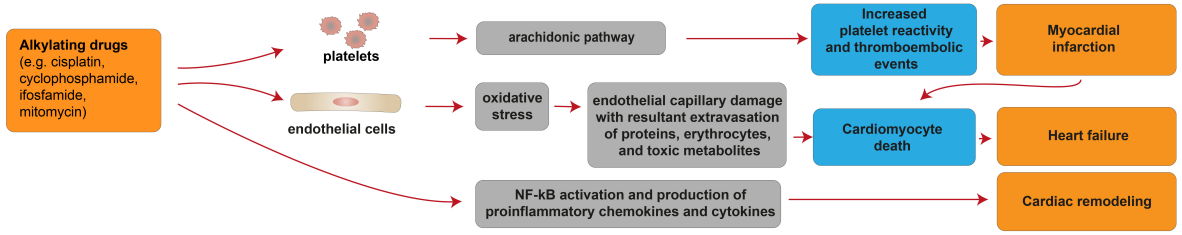

FIGURE 4 | Cellular and molecular mechanisms of the cardiotoxic effects exerted by alkylating drugs. Schematic diagram showing the impact of alkylating agents in promoting heart failure due to cardiomyocyte death consequent to myocardial infarction. Additional mechanisms of alkylating drug-induced cardiotoxicity include heart failure consequent to cardiomyocyte death induced by oxidative stress and cardiac remodeling following activation of pro-inflammatory pathways.

involved in multiple key functions in the cardiovascular system, whose inhibition is likely the cause of the observed cardiotoxic effects (**Figure 6**). Particularly, **sunitinib**, which presents an effective multi-targeted inhibition of growth-factor receptors able to reduce the angiogenesis and tumor cell survival/proliferation (182, 189), is considered more cardiotoxic than other anti-angiogenic and TKI drugs (182). Based on clinical studies, 47% of patients receiving sunitinib treatment exhibited hypertension, up to 28% showed LV dysfunction, and 8% developed CHF [reviewed in (15)]. Patients with pre-existing cardiovascular diseases or previous cardio-toxicant exposure show even higher risks [reviewed in (190–192)]. However, cardiac dysfunctions induced by sunitinib and other inhibitors of tyrosine kinases have shown high reversibility; after treatment withdrawal, hypertension and cardiac dysfunction were alleviated or wholly restored (193) [reviewed in (37)]. Indeed, the majority of sunitinib-treated patients were able to carry on with sunitinib therapy following the resolution of cardiovascular events (193). Similarly, reversible cardiotoxicity has been reported upon sorafenib treatment [reviewed in (76)].

The cellular and molecular details of the observed elevated blood pressure and cardiac dysfunction in patients treated with anti-VEGF/PDGFR drugs, such as sunitinib and sorafenib, are not fully understood. Nevertheless, sunitinib- and sorafenib-induced VEGFR inhibition was suggested to reduce the production of the vasodilator nitric oxide (NO) by endothelial cells, in turn resulting in hypertension [reviewed in (15, 194)]. Hypertension is known to lead to capillary rarefaction, which may be responsible for the cardiac dysfunction observed in sunitinib and sorafenib-treated patients [reviewed in (15)]. Indeed, given the high energy dependency, the heart is usually highly vulnerable to any altered blood supply. However, the capillary rarefaction potentially responsible for cardiac dysfunction may also be a direct consequence of reduced angiogenesis following sunitinib- or sorafenib-induced VEGFR inhibition [reviewed in (15, 194)]. Further, sunitinib- or sorafenib-induced PDGFR inhibition was suggested to induce the loss of pericytes, in turn leading to coronary microvascular dysfunction (195) [reviewed in (15, 194)]. Sunitinib, as an off-target effect, has also been suggested to inhibit AMPK activity, in turn inducing energy depletion in cardiomyocytes (184). However, another study found that sunitinib treatment in cardiomyocytes does not affect cellular ATP levels and that myocytes are not protected from sunitinib by pre-treatment with AMPK-activating drug metformin (189).

Imatinib, a TKI that inhibits BCR-ABL fusion protein, c-KIT, and PDGFR, is used to treat chronic myeloid leukemia and gastrointestinal stromal cancers. Despite initial fears (196), the rate of cardiotoxicity upon imatinib treatment was shown to be very low, with less than 1% of the patients developing HF [reviewed in (37, 197)]. Nevertheless, the inhibition of CaMKII in adult rat cardiac fibroblasts was shown to reduce the production of mitochondrial superoxide triggered by sunitinib and imatinib treatments (198).

Interestingly, **ponatinib**, a BCR-ABL kinase inhibitor developed to treat patients with imatinib resistance driven by T315I "gatekeeper" mutation, has been associated with a high rate of cardiovascular adverse events. Indeed, more than 20% of patients receiving ponatinib treatment experienced adverse cardiovascular events, and 5% developed CHF [reviewed in (181, 197)]. Of note, these cardiotoxic effects are often reversible with interruption of the therapy (181). The mechanisms of ponatinib-induced cardiotoxic effects are unclear; however, they were suggested to be consequent to thrombotic microangiopathy and consequent ischemia (**Figure 6**) (199), although cardiomyocyte death was also reported to occur in the zebrafish model (200).

STRATEGIES TO REDUCE ANTICANCER DRUG-ASSOCIATED CARDIOVASCULAR TOXICITY

Several therapeutical approaches already known in clinical usage have been proposed to reduce cardiotoxicities, such as iron-chelating drugs, β-blockers, renin-angiotensin-aldosterone system (RAAS) inhibitors, SGLT2 inhibitors, late inward sodium current (INaL) selective inhibitors, phosphodiesterase-5 inhibitors, metabolic agents, statins as well as growth factors and hormones [previously reviewed in (201)]. Here we will discuss these classes of drugs, focusing on their mechanisms of action and the therapeutic validity and effectiveness.

Iron-Chelating Drugs

The iron-chelating drug dexrazoxane has been identified as one of the most promising cardioprotective therapies in these last years and represents the only FDA-approved drug

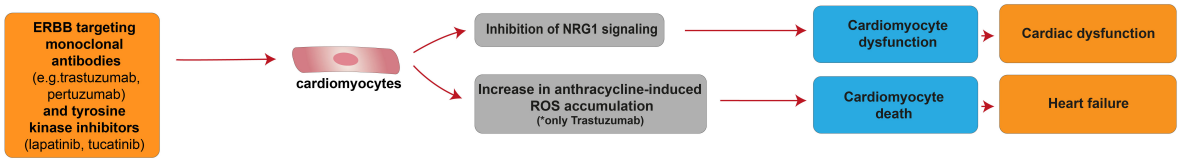

FIGURE 5 | Cellular and molecular mechanisms of the cardiotoxic effect exerted by ERBB targeting monoclonal antibodies and tyrosine kinase inhibitors. Schematic diagram showing the impact of ERBB targeting therapies on cardiomyocyte dysfunction caused by the impairment of Neuregulin-1 signaling. However, in combination with anthracyclines, anti-HER2 monoclonal antibody trastuzumab may also induce heart failure as a consequence of cardiomyocyte death induced by ROS accumulation.

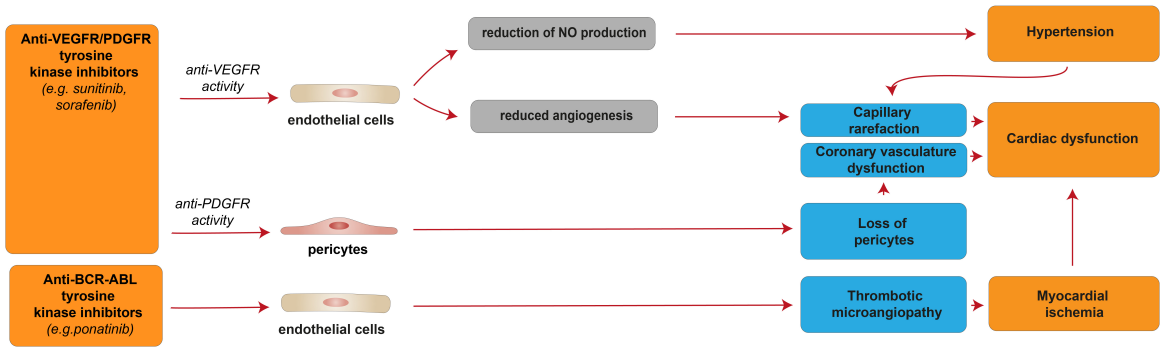

FIGURE 6 | Cellular and molecular mechanisms of the cardiotoxic effects exerted by VEGFR/PDGFR and BCR-ABL and tyrosine kinase inhibitors. Schematic diagram showing the impact of VEGFR/PDGFR and BCR-ABL inhibition, resulting in a reversible cardiac disfunction. Anti-VEFGR activity impairs cardiac function by inducing capillary rarefaction consequent to reduced angiogenesis or hypertension derived from reduced NO production. Anti-PDGFR activity induces cardiac dysfunction by promoting the loss of pericytes, which in turn impairs the coronary vasculature. Anti-BCR-ABL inhibition may results in myocardial ischemia and cardiac dysfunction consequent to thrombotic microangiopathy.

specific for anthracycline-induced cardiotoxicity (202, 203). Dexrazoxane is a pro-drug that rapidly turns into its active form after entering in cardiomyocytes, in turn counteracting the formation of anthracyclines-iron complexes and the subsequent adverse cardiac effects [reviewed in (204)]. Importantly, the development of iron-chelating drugs to prevent anthracycline-induced cardiotoxicity has emerged as an approach of relevant clinical importance in the context of the genetic predisposition of patients suffering from iron-related genetic disorders, such as hereditary hemochromatosis (31, 205). Initially, the cardioprotective functions of this iron chelator were ascribed majorly to its ability to affect iron regulatory proteins and reduce iron accumulation (206) [reviewed in (14, 207)]. However, additional mechanisms have been suggested to drive the cardioprotective activity exerted by dexrazoxane following anthracycline administration. Specifically, dexrazoxane has been shown to modify the topoisomerase 2 (Top2β) configuration preventing its interface with anthracyclines, thereby avoiding the Top2-DNA cleavage complexes (56, 208). Close derivatives of dexrazoxane lacking the interaction with Top2β were found not to be protective in relevant chronic anthracycline cardiotoxicity models (206, 209). Thus, cardioprotective effects of dexrazoxane in chronic anthracycline cardiotoxicity were suggested to derive from the inhibition of the interaction between anthracyclines and Top2β, rather than to its metal-chelating action (209) [reviewed in (210)].

Recently, a study on the cardioprotective effects of dexrazoxane, based on seven randomized trials and two retrospective trials for a total of 2177 patients with breast cancer receiving anthracyclines with or without trastuzumab reported that dexrazoxane reduces the risk of clinical HF and cardiac events in these patients without significantly impacting cancer outcomes (203). Thus, dexrazoxane represents a therapeutical strategy to limit anthracycline cardiotoxicity.

β-Blockers

β-blockers, also known as beta-adrenergic blocking agents, are a class of drugs that blocks the effects of the hormone epinephrine (adrenaline), causing the heart to beat more slowly and with less force, thus lowering blood pressure. These drugs are predominantly used to manage the reduction in left ventricular ejection fraction (LVEF), preventing symptomatic HF and protecting the heart from a second heart attack event after the first one (secondary prevention) [reviewed in (211, 212)]. The choice of β-blockers as a therapy for cardiac dysfunctions associated with anticancer drugs is mostly based on the dual cardioprotective role exerted by antihypertensive or antiarrhythmic drugs, which preserve cardiovascular function while inhibiting tumor angiogenesis [reviewed in (212)]. β-blockers, together with calcium channel blockers, nitrates, and aspirin are recommended for the management of fluoropyrimidines-induced cardiotoxicity as

therapies for angina chest pain, albeit the absence of randomized controlled trials to support their efficacy [reviewed in (68, 71, 213)]. Furthermore, a large number of observations indicate β-adrenergic receptor signaling alterations as a feature of anthracycline-induced cardiomyopathy and in other forms of dilated cardiomyopathies [reviewed in (16, 37)]. A retrospective survey between 2005 and 2010 on 920 breast cancer patients who received anthracyclines and trastuzumab showed an association of continuous β-blocker treatment with a significantly lower incidence of HF events (214). **Bisoprolol**, another second-generation β-blocker, showed stronger efficacy compared to angiotensin-converting-enzyme inhibitor (ACE-I) **perindopril** in attenuating the LVEF decline in patients who received trastuzumab, even though it was unable to avoid left ventricular remodeling (215). However, administration of **metoprolol**, a second-generation β-blocker, did not affect LVEF decline determined by adjuvant, anthracycline-containing regimens with or without trastuzumab and radiation (216) and showed a non-statistically significant reduction in the incidence of anthracycline-induced HF events (217).

In *in vitro* and *ex vivo* set-up, **carvedilol**, a non-selective β- and α1-AR antagonist with strong antioxidant properties, reduced doxorubicin-induced ROS release and cardiomyocyte apoptosis (218) as well as mitochondrial respiration dysfunctions and calcium overloading (219). In rat models of doxorubicin-induced cardiomyopathy, carvedilol showed a significant cardioprotective effect, while **atenolol**, a β-blocker selective for β1-AR and without antioxidant properties, did not, thus suggesting that carvedilol cardioprotective efficacy relies more on its antioxidant properties than on the β-AR blocking action (220). In clinical trials of patients undergoing anthracycline chemotherapy, the prophylactic use of carvedilol decreased the ventricular dysfunction (221–223). In children receiving anthracyclines for acute lymphocytic leukemia, pre-treatment with carvedilol reduced troponin, diastolic dysfunction, and lactate dehydrogenase levels (224, 225). Furthermore, a randomized trial on 468 breast cancer patients treated with anthracyclines with/without trastuzumab showed reduced cardiotoxicity upon carvedilol administration, hence recommending carvedilol as a strategy to reduce trastuzumab interruptions (226).

Nebivolol is a cardio-selective β-blocker with mild vasodilating effects due to its interaction with the arginine/NO pathway [reviewed in (227)]. In isolated perfused rat hearts model of anthracycline-induced cardiotoxicity, treatment with nebivolol increased NO levels and significantly reduced oxidative stress, and improved cardiac function (228). Mechanistically, experiments in the rat model suggested that nebivolol administration reduces alterations in cardiomyocyte histomorphometry induced by doxorubicin through modulation of caspase-3, NO synthase (NOS), and TNF-α (229). In randomized placebo-controlled studies, the prophylactic use of nebivolol preserved the cardiac diastolic and systolic function from anthracycline-induced toxicity (230, 231).

To date, the cardioprotective efficacy of β-blockers needs to be further validated in large clinical trials. In addition, in clinical practice, the usage of β-blockers is hampered by their adverse effects in fragile patients, indicating their possible application only in patients with a high cardiotoxicity risk.

Renin-Angiotensin-Aldosterone System Inhibitors

Several studies showed that alteration of the RAAS has a crucial role in modulating anthracycline-induced cardiotoxicity [reviewed in (232)]. Therefore, the development of RAAS inhibitors, including ACE-Is, angiotensin receptor type 1 blockers (ARBs), as well as aldosterone antagonists, may be effective in the prevention and treatment of anthracycline-induced cardiotoxicity [reviewed in (232, 233)].

Angiotensin-converting-enzyme inhibitors, such as enalapril, captopril, lisinopril, and ramipril, impair the conversion of angiotensin I to angiotensin II, with a consequent decrease of angiotensin II receptor type 1 (AT1R) stimulation and its downstream signaling. These compounds have been demonstrated effective in the treatment of hypertension, as well as in reducing mortality in left ventricular dysfunction after myocardial infarction and CHF (234). Preclinical studies in animal models have demonstrated that ACE-Is, such as enalapril, captopril, and lisinopril, can effectively counteract the cardiotoxic effects after single high-dose, multiple low-doses or chronic exposure of anthracyclines (235–238). Mechanistically, ACE-Is' therapy has been shown to result in the neutralization of ROS damage, reduction of interstitial fibrosis, limitation of intracellular calcium overload, along with improvement of mitochondrial respiration and cardiomyocyte metabolism (235, 236) [reviewed in (232)]. In retrospective clinical analysis, **enalapril** administration to doxorubicin-induced HF children increased cardiac hemodynamic parameters; however, these parameters declined after a few years (239). ACE-I therapy with **ramipril or enalapril** was also shown to induce the recovery of cardiac parameters in patients with doxorubicin-induced cardiac function decline (240). However, no significant improvement in exercise ability or contractile state of pediatric cancer patients receiving anthracyclines was also reported upon enalapril administration, albeit with reduction of left ventricular end-systolic wall stress (241). Clinical trials on HER2-positive breast cancer patients under anthracycline-trastuzumab therapy enlightened cardioprotective effects upon the administration of the ACE-I **lisinopril** (226).

Angiotensin receptor type 1 blockers, such as candesartan and telmisartan, inhibit angiotensin II binding to AT1R. In preclinical rat models, **candesartan** significantly reversed the daunorubicin-induced myocardial pathological changes and cardiac dysfunction (242). Candesartan administration was shown to significantly alleviate the decline in LVEF occurring during adjuvant, anthracycline-containing regimens with or without trastuzumab and radiation (216). Furthermore, in a small prospective study of 49 patients free from cardiovascular diseases and affected by solid cancers, **telmisartan** treatment starting before chemotherapy was able to reduce epirubicin-induced ROS damage by antagonizing the pro-inflammatory signals and reversing the early myocardial impairment (243). Telmisartan administration was also associated with long-lasting

(up to 18 months) protection from early and acute myocardial dysfunction in patients treated with epirubicin (244, 245). In contrast, the administration of candesartan was unable to protect against the decrease in left ventricular ejection fraction during or shortly after trastuzumab treatment (246).

Importantly, clinical trials have also shown that a combination of ACE-Is or ARBs and β-blockers has beneficial effects in treating cardiotoxicity induced by anthracyclines and/or anti-HER2 agents. Indeed, the combination of ACE-Is (enalapril) and β-blockers significantly reduced the incidence of cardiac dysfunction along with prevention of the onset of late cardiotoxicity in patients receiving anthracyclines (33, 247). A small phase I trial conducted on 20 women suffering from breast cancer assessed the safety of continuing trastuzumab treatment despite cardiotoxicity onset if patients received ACE-Is and β-blockers following a staggered protocol (248). Another study unveiled the combination of ACE-Is, β-blockers and close cardiac monitoring as an effective strategy for cardioprotection in patients receiving HER2-targeted therapies (249).

Further studies focused on the cardioprotective role of **aldosterone antagonists**, which inhibit the last step of the RAAS and are already known for their beneficial effects on injury-induced cardiac remodeling and fibrosis [reviewed in (250)]. In a small clinical trial, spironolactone has been reported to prevent anthracycline-related cardiac dysfunction in breast cancer patients (251).

Sodium-Glucose Cotransporter-2 Inhibitors

Sodium-glucose cotransporter-2 selective inhibitors (empagliflozin, canagliflozin, and dapagliflozin) are a group of compounds that have been shown to have protective effects on the progression of HF [reviewed in (252)]. Indeed, EMPA-REG OUTCOME trial demonstrated that empagliflozin reduces major adverse cardiovascular events, cardiovascular death, and hospitalization rates for HF (253). Similarly, EMPEROR-Preserved trials found a reduced risk of HF hospitalization for 9718 patients with HF treated with empagliflozin (254). In a new systematic review meta-analysis of seven studies, for a total of 5,150 HF patients, empagliflozin was effective in reducing cardiovascular death or hospitalization for worsening HF condition (255). Therefore, SGLT2 inhibitors represent a promising treatment for chronic HF patients.

Recently, the potentially protective effects of SGLT2 inhibitors on the cardiac dysfunction induced by chemotherapies and targeted therapies were also investigated in preclinical studies in animal models. In this regard, protective effect by empagliflozin against anthracycline-induced cardiac impairment, diastolic dysfunction, and maladaptive cardiac remodeling has been documented (256–259). Mechanistically, empagliflozin was suggested to reduce ferroptosis, inflammatory response (NF-κB signaling), apoptosis, and fibrosis induced by doxorubicin through the involvement of NLRP3 and MyD88-related pathway (257, 258). A recent pre-clinical study reported that empagliflozin can also improve the cardiac dysfunction induced by anti-VEGFR/PDGFR multi-TKI sunitinib, *via* regulation of cardiomyocyte autophagy, in turn mediated by the AMPK-mTOR signaling pathway (260).

Late Inward Sodium Current Inhibitors

Selective inhibitors of late inward sodium current (INaL), such as ranolazine, have proven effective in treating experimental HF in several experimental models of cardiac dysfunction given its antiarrhythmic, anti-ischemic, and ATP-sparing features. Experimental evidence suggests that anthracyclines indirectly induce INaL hyperactivation, resulting in cytosolic calcium overload (261–263). INaL hyperactivation contributes to mitochondrial calcium depletion and dysregulation that, in turn, triggers mitochondrial ROS generation (oxidative stress), as well as NAD(P)H and ATP depletion (energetic stress); as a result, these events lead to cardiomyocyte impairment, diastolic dysfunction, and HF progression (261, 262, 264). Importantly, in animal models of doxorubicin-induced cardiotoxicity, ranolazine administration attenuated diastolic cardiac dysfunction and prevented worsening of systolic function by reducing oxidative stress and cardiomyocyte functional derangements (261, 262, 264). Moreover, ranolazine limited trastuzumab-induced cardiac dysfunction in mice by acting as a regulator of cardiac redox balance (265). In a very small randomized clinical study on 24 low-risk patients with diastolic dysfunction induced by anthracycline-based or fluoropyrimidine-/platinum-based therapies, patients were treated for 5 weeks with ranolazine or standard therapy, observing a complete recovery from diastolic dysfunction in all subjects in ranolazine group (12 patients) (266). Thus, the therapeutic use of this drug is promising, although needs validation in large clinical trials specific for each type of chemotherapy.

Phosphodiesterase-5 Inhibitors

Phosphodiesterase-5 inhibitors, such as sildenafil and tadalafil, were demonstrated to induce cardioprotective effects in animal models affected by doxorubicin cardiac toxicity (267–269). **Sildenafil** demonstrated cardioprotective activity against anthracycline-induced cardiac dysfunction by inducing the opening of mitochondrial K_{ATP} channels, leading to preserving mitochondrial potential and functions, myofibrillar integrity, and preventing cardiomyocyte apoptosis (267). The cardiac effects of sildenafil were also suggested to be dependent on the NO-signaling pathway since its protective activity was abolished by both L-NAME (inhibitor of NOS) and 5-hydroxydecanoate (inhibitor of ATP-sensitive K+ channels) (270). **Tadalafil's** effects on cardiotoxicity reduction, instead, were suggested to be mainly due to NO-mediated increases of protein kinase G (PKG) activity and cGMP signaling, which is significantly reduced by doxorubicin administration (268, 269).

Metabolic Agents

Butyric acid, a short-chain fatty acid produced daily by the gut microbiota, has proven beneficial in models of cardiovascular diseases (271) [reviewed in (272)]. A novel butyric acid derivative, phenylalanine-butyramide (FBA), has

been shown to protect animal models from doxorubicin-induced cardiotoxicity by decreasing oxidative stress and improving mitochondrial function (273). Of note, FBA prevented doxorubicin-induced cardiomyocyte apoptosis, left ventricular dilatation, and fibrosis (273).

Another metabolic agent, **β-hydroxybutyrate (BHB)**, produced by fatty-acid oxidation in the liver under the fasting state, was shown to play a cardioprotective role in diabetic and HF with preserved ejection fraction (HFpEF) mouse models, when administrated as a dietary supplement or directly injected (274, 275). Interestingly, BHB was also reported to induce protection against anthracycline-induced cardiac function decline and partially reverted the maladaptive remodeling, characterized by increased cardiomyocyte size and decreased fibrosis (276). *In vitro*, BHB administration reduces oxidative stress and ameliorates mitochondrial functions, decreasing cardiomyocyte cell injury and apoptosis (276).

Statins

Statins reduce cholesterol synthesis by inhibiting the enzyme HMG CoA reductase. However, statins have emerged as pleiotropic factors playing a positive role on the cardiovascular system, including ROS production and oxidative stress, and the consequent cardiac mitochondrial dysfunction [reviewed in (277, 278)]. Importantly, the treatment of breast cancer patients undergoing anthracycline-based therapy with statins has been reported to be associated with a lower risk for HF and to prevent the decrease of the left ventricular ejection fraction (279–282). A similar cardioprotective activity of statins was reported for trastuzumab-based therapies (283).

Growth Factors

Administration of the growth factor **Neuregulin-1 (NRG1β)** has been shown to improve cardiac function following injury in adult mice (127, 134) [reviewed in (110, 133)] and in HF patients (135, 136) [reviewed in (137)]. Importantly, administration of NRG1β has also been shown to protect cardiac myocytes from anthracycline-induced apoptosis (134, 167, 284, 285) [reviewed in (286)]. Further, NRG1 administration in the zebrafish model was reported to reduce cardiomyocyte apoptosis induced by the multi-TKI ponatinib (200) [reviewed in (197)]. However, NRG1β is not clinically relevant as a therapy for cardiomyopathy induced by anticancer drugs because of its well-established cancer-promoting role. To solve this issue, an engineered bivalent NRG1 (NN), which preferentially induces ERBB4 homodimer formation in cardiomyocytes, has been developed and shown to protect against doxorubicin-induced cardiotoxicity, maintaining the same cardioprotective properties of NRG1 but with reduced pro-neoplastic potential (287). Nevertheless, although up to now there is no evidence in the literature about detrimental side effects in response to bivalent NRG1, NN has not been recruited into a clinical trial yet. Further studies are therefore recommended to assess if this combinatorial treatment is sufficient to mitigate the cardiotoxic side effects of chemotherapeutic agents.

Granulocyte colony-stimulating factor (G-CSF) is a hematopoietic growth factor that affects proliferation and differentiation, especially of progenitors of the neutrophil and granulocyte lineages, therefore it is currently used clinically in combination with doxorubicin to counteract doxorubicin-induced myelosuppression (288). Interestingly, a role for G-CSF has also been suggested in doxorubicin-induced cardiomyopathy. Indeed, an attenuation of cardiomyocyte atrophic degeneration and a decrease of myocardial fibrosis have been reported after G-CSF administration in doxorubicin-treated mice (289). Intriguingly, G-CSF was suggested to exert an anti-atrophic and anti-inflammatory activity directly on cardiomyocytes (289).

Among stromal cells, the beneficial role of endothelial progenitor cells (EPCs) has emerged to counteract the cardiotoxicity of cancer therapies. For example, **erythropoietin (EPO)** has been shown to promote angiogenesis by increasing the number of EPCs, thereby improving cardiac function after doxorubicin treatment (290).

Other Strategies

A few other strategies were suggested to reduce the adverse cardiovascular side effects of common chemotherapies and targeted therapies. In this regard, the sulfur-containing amino acid **taurine** (2-aminoethanesulfonic acid) has been shown to exert beneficial effects in CHF, ischemic heart disease, hypertension, atherosclerosis, and diabetic cardiomyopathy (291). Intriguingly, taurine was also shown to reduce cisplatin-induced cardiotoxicity by suppressing the generation of ROS, ER stress, and inflammation (102). **Apocynin**, a specific NADPH oxidase inhibitor, has been shown to reduce cisplatin-induced oxidative stress, inflammation and apoptosis (101).

Preclinical studies demonstrated that **fenofibrate**, a PPARα activator, counteracted doxorubicin-induced cardiotoxicity in mice by increasing circulating EPCs, stimulating cardiac NO activation and inducing the production of pro-angiogenic factors such as SDF-1 and VEGF (292).

Besides molecular strategies, **remote ischemic preconditioning (RIPC)**, which consists of reversible repetitive interruptions in blood flow, ischemia, and reperfusion, seems a good approach to reduce anthracycline-induced cardiotoxicity (293). Indeed, large animals, subjected to RIPC before each doxorubicin injection, have shown a preserved cardiac contractility and mitochondrial integrity, concomitantly with a higher cardiac performance and reduced fibrosis (293).

CONCLUSION AND FUTURE PERSPECTIVES

Although anticancer therapies greatly improve survival and quality of life of oncological patients, their negative impact on cardiac well-being is a very critical issue. In addition to common risk factors, such as age, hypertension, arrhythmias, and coronary disease, it has emerged the identification of genetic variants related to an increased predisposition to cardiotoxicity of chemotherapies and targeted therapies, in particular for anthracyclines and anti-HER2 therapies. Thus, the development of individualized treatments, based on the forecast of the cardiotoxic side effects, may acquire a considerable clinical

relevance for the future perspective. Importantly, the cellular and molecular mechanisms mediating the cardiotoxicity of common classes of chemotherapy and targeted therapy drugs are emerging, providing a rationale for the development of novel strategies for cardioprotection. Recent clinical trials have tested multiple cardioprotective drugs, highlighting the ability of some of them in counteracting or limiting the cardiotoxic effects of anticancer treatments. However, many of these therapeutic strategies still have certain limits and need some precautions. Among them, the lack of validation in large clinical trials, the underlying molecular mechanisms still not fully understood, as well as the risk-benefit controversies. In this regard, it is extremely important to take into account the tolerability of the adverse effects that these therapies may entail, including fatigue and dizziness, in patients already fatigued by antitumoral therapy.

Despite multiple cellular and molecular mechanisms being suggested to mediate the cardiotoxic effect of anti-cancer drugs, cardiomyocyte death has emerged as the major cause of long-term irreversible cardiac disfunction. These important side effects have been documented for anthracyclines, fluoropyrimidines, and alkylating drugs. This is because lost cardiomyocytes cannot be efficiently regenerated due to the very low ability of the adult mammalian heart to produce new cardiomyocytes (294, 295) [reviewed in (296)]. Although the cytotoxic effect of anticancer treatments resides on a wide range of biological mechanisms, the development of strategies aiming at increasing cardiomyocyte survival is thus encouraged to reduce anticancer drug-induced cardiomyocyte death and the consequent permanent damage. In the future, the administration of cardiomyocyte survival factors flanking chemotherapy and targeted therapies should be further explored. In this regard, a plethora of factors and signaling pathways has been shown to trigger endogenous cardiomyocyte proliferation for cardiac regenerative strategies [reviewed in (296)], thus their modulation may be also explored for cancer patients with permanent damage by anticancer drugs. Some of these factors also regulate cardiomyocyte survival, thus their modulation may be tested as a preventive strategy to reduce permanent cardiotoxic effect of anticancer drugs. Obviously, the potential interfering with the action of the antineoplastic treatments should be carefully evaluated.

In conclusion, cardiovascular adverse effects resulting from antineoplastic therapies are important concerns for the health of cancer patients and could question the choice of undertaking or interrupting treatments. Nowadays, some drugs have been clinically tested to counteract the cardiotoxicity related to anticancer care, and we here propose a further evaluation of factors that up to now are mainly known for their role in cardiomyocyte proliferation and survival, as promising strategies for protection and/or regeneration of the cardiac tissue. Moreover, an increasing synergistic effort would be required for the oncologic and cardiologic research fields to assure cancer patients a long-term relapse-free survival and high-quality cardiovascular health.

AUTHOR CONTRIBUTIONS

All authors significantly contributed to the writing of the manuscript.

FUNDING

This project was supported by the Fondazione Cariplo to GD'U and ML (Grant Number: GR 2017-0800) and by Ministry of Health – Ricerca Corrente – IRCCS MultiMedica.

REFERENCES

1. Lambert J, Thavendiranathan P. Controversies in the definition of cardiotoxicity: do we care? – American college of cardiology. *Am Coll Cardiol.* (2016). Available online at: https://www.acc.org/latest-in-cardiology/articles/2016/07/07/14/59/controversies-in-the-definition-of-cardiotoxicity (accessed February 13, 2022).
2. Cardinale D, Iacopo F, Cipolla CM. Cardiotoxicity of anthracyclines. *Front Cardiovasc Med.* (2020) 7:26. doi: 10.3389/fcvm.2020.00026
3. Menna P, Salvatorelli E. Primary prevention strategies for anthracycline cardiotoxicity: a brief overview. *Chemotherapy.* (2017) 62:159–68. doi: 10.1159/000455823
4. Mercurio V, Pirozzi F, Lazzarini E, Marone G, Rizzo P, Agnetti G, et al. Models of heart failure based on the cardiotoxicity of anticancer drugs. *J Card Fail.* (2016) 22:449–58. doi: 10.1016/j.cardfail.2016.04.008
5. Menna P, Paz OG, Chello M, Covino E, Salvatorelli E, Minotti G. Anthracycline cardiotoxicity. *Expert Opin Drug Saf.* (2012) 11(Suppl. 1):S21–36. doi: 10.1517/14740338.2011.589834
6. Minotti G, Menna P, Salvatorelli E, Cairo G, Gianni L. Anthracyclines: molecular advances and pharmacologic developments in antitumor activity and cardiotoxicity. *Pharmacol Rev.* (2004) 56:185–229. doi: 10.1124/pr.56.2.6
7. Sawyer DB. Anthracyclines and heart failure. *N Engl J Med.* (2013) 368:1154–6. doi: 10.1056/NEJMCIBR1214975
8. Seidman A, Hudis C, Pierri MK, Shak S, Paton V, Ashby M, et al. Cardiac dysfunction in the trastuzumab clinical trials experience. *J Clin Oncol.* (2002) 20:1215–21. doi: 10.1200/JCO.2002.20.5.1215
9. Plana JC, Galderisi M, Barac A, Ewer MS, Ky B, Scherrer-Crosbie M, et al. Expert consensus for multimodality imaging evaluation of adult patients during and after cancer therapy: a report from the American society of echocardiography and the European association of cardiovascular imaging. *Eur Hear J Cardiovasc Imaging.* (2014) 15:1063–93. doi: 10.1093/ehjci/jeu192
10. Vaduganathan M, Prasad V. Cardiovascular risk assessment in oncological clinical trials: is there a role for centralized events adjudication? *Eur J Heart Fail.* (2016) 18:128–32. doi: 10.1002/ejhf.457
11. Ewer MS, Lippman SM. Type II chemotherapy-related cardiac dysfunction: time to recognize a new entity. *J Clin Oncol.* (2005) 23:2900–2. doi: 10.1200/JCO.2005.05.827
12. Suter TM, Ewer MS. Cancer drugs and the heart: importance and management. *Eur Heart J.* (2013) 34:1102–11. doi: 10.1093/eurheartj/ehs181
13. Ky B, Vejpongsa P, Yeh ETH, Force T, Moslehi JJ. Emerging paradigms in cardiomyopathies associated with cancer therapies. *Circ Res.* (2013) 113:754–64. doi: 10.1161/CIRCRESAHA.113.300218
14. Gammella E, Maccarinelli F, Buratti P, Recalcati S, Cairo G. The role of iron in anthracycline cardiotoxicity. *Front Pharmacol.* (2014) 5:25. doi: 10.3389/fphar.2014.00025
15. Hahn VS, Lenihan DJ, Ky B. Cancer therapy-induced cardiotoxicity: basic mechanisms and potential cardioprotective therapies. *J Am Heart Assoc.* (2014) 3:e000665. doi: 10.1161/JAHA.113.000665
16. Molinaro M, Ameri P, Marone G, Petretta M, Abete P, Di Lisa F, et al. Recent advances on pathophysiology, diagnostic and therapeutic insights in cardiac dysfunction induced by antineoplastic drugs. *Biomed Res Int.* (2015) 2015:138148. doi: 10.1155/2015/138148

17. Albini A, Pennesi G, Donatelli F, Cammarota R, De Flora S, Noonan DM. Cardiotoxicity of anticancer drugs: the need for cardio-oncology and cardio-oncological prevention. *J Natl Cancer Inst.* (2010) 102:14–25. doi: 10.1093/jnci/djp440
18. Swain SM, Whaley FS, Ewer MS. Congestive heart failure in patients treated with doxorubicin: a retrospective analysis of three trials. *Cancer.* (2003) 97:2869–79. doi: 10.1002/cncr.11407
19. Von Hoff DD, Layard MW, Basa P, Davis HL, Von Hoff AL, Rozencweig M, et al. Risk factors for doxorubicin-induced congestive heart failure. *Ann Intern Med.* (1979) 91:710–7. doi: 10.7326/0003-4819-91-5-710
20. Shaikh AY, Suryadevara S, Tripathi A, Ahmed M, Kane JL, Escobar J, et al. Mitoxantrone-induced cardiotoxicity in acute myeloid leukemia-a velocity vector imaging analysis. *Echocardiography.* (2016) 33:1166–77. doi: 10.1111/echo.13245
21. Damiani RM, Moura DJ, Viau CM, Caceres RA, Henriques JAP, Saffi J. Pathways of cardiac toxicity: comparison between chemotherapeutic drugs doxorubicin and mitoxantrone. *Arch Toxicol.* (2016) 90:2063–76. doi: 10.1007/s00204-016-1759-y
22. Saletan S. Mitoxantrone: an active, new antitumor agent with an improved therapeutic index. *Cancer Treat Rev.* (1987) 14:297–303. doi: 10.1016/0305-7372(87)90021-1
23. Qiu S, Zhou T, Qiu B, Zhang Y, Zhou Y, Yu H, et al. Risk factors for anthracycline-induced cardiotoxicity. *Front Cardiovasc Med.* (2021) 8:736854. doi: 10.3389/fcvm.2021.736854
24. Tromp J, Steggink LC, Van Veldhuisen DJ, Gietema JA, van der Meer P. Cardio-oncology: progress in diagnosis and treatment of cardiac dysfunction. *Clin Pharmacol Ther.* (2017) 101:481–90. doi: 10.1002/cpt.614
25. Chang VY, Wang JJ. Pharmacogenetics of chemotherapy-induced cardiotoxicity. *Curr Oncol Rep.* (2018) 20:52. doi: 10.1007/s11912-018-0696-8
26. Duan S, Bleibel WK, Huang RS, Shukla SJ, Wu X, Badner JA, et al. Mapping genes that contribute to daunorubicin-induced cytotoxicity. *Cancer Res.* (2007) 67:5425–33. doi: 10.1158/0008-5472.CAN-06-4431
27. Blanco JG, Sun C-L, Landier W, Chen L, Esparza-Duran D, Leisenring W, et al. Anthracycline-related cardiomyopathy after childhood cancer: role of polymorphisms in carbonyl reductase genes–a report from the children's oncology group. *J Clin Oncol.* (2012) 30:1415–21. doi: 10.1200/JCO.2011.34.8987
28. Semsei AF, Erdelyi DJ, Ungvari I, Csagoly E, Hegyi MZ, Kiszel PS, et al. ABCC1 polymorphisms in anthracycline-induced cardiotoxicity in childhood acute lymphoblastic leukaemia. *Cell Biol Int.* (2012) 36:79–86. doi: 10.1042/CBI20110264
29. Krajinovic M, Elbared J, Drouin S, Bertout L, Rezgui A, Ansari M, et al. Polymorphisms of ABCC5 and NOS3 genes influence doxorubicin cardiotoxicity in survivors of childhood acute lymphoblastic leukemia. *Pharmacogenomics J.* (2016) 16:530–5. doi: 10.1038/tpj.2015.63
30. Visscher H, Rassekh SR, Sandor GS, Caron HN, van Dalen EC, Kremer LC, et al. Genetic variants in SLC22A17 and SLC22A7 are associated with anthracycline-induced cardiotoxicity in children. *Pharmacogenomics.* (2015) 16:1065–76. doi: 10.2217/pgs.15.61
31. Miranda CJ, Makui H, Soares RJ, Bilodeau M, Mui J, Vali H, et al. Hfe deficiency increases susceptibility to cardiotoxicity and exacerbates changes in iron metabolism induced by doxorubicin. *Blood.* (2003) 102:2574–80. doi: 10.1182/blood-2003-03-0869
32. Yang X, Li G, Guan M, Bapat A, Dai Q, Zhong C, et al. Potential gene association studies of chemotherapy-induced cardiotoxicity: a systematic review and meta-analysis. *Front Cardiovasc Med.* (2021) 8:651269. doi: 10.3389/fcvm.2021.651269
33. Cardinale D, Colombo A, Bacchiani G, Tedeschi I, Meroni CA, Veglia F, et al. Early detection of anthracycline cardiotoxicity and improvement with heart failure therapy. *Circulation.* (2015) 131:1981–8. doi: 10.1161/CIRCULATIONAHA.114.013777
34. Renu K, V G A, P B TP, Arunachalam S. Molecular mechanism of doxorubicin-induced cardiomyopathy – an update. *Eur J Pharmacol.* (2018) 818:241–53. doi: 10.1016/j.ejphar.2017.10.043
35. Wallace KB, Sardão VA, Oliveira PJ. Mitochondrial determinants of doxorubicin-induced cardiomyopathy. *Circ Res.* (2020) 126:926–41. doi: 10.1161/CIRCRESAHA.119.314681
36. Murabito A, Hirsch E, Ghigo A. Mechanisms of anthracycline-induced cardiotoxicity: is mitochondrial dysfunction the answer? *Front Cardiovasc Med.* (2020) 7:35. doi: 10.3389/fcvm.2020.00035
37. Tocchetti CG, Cadeddu C, Di Lisi D, Femminò S, Madonna R, Mele D, et al. From molecular mechanisms to clinical management of antineoplastic drug-induced cardiovascular toxicity: a translational overview. *Antioxid Redox Signal.* (2019) 30:2110–53. doi: 10.1089/ars.2016.6930
38. Ghigo A, Li M, Hirsch E. New signal transduction paradigms in anthracycline-induced cardiotoxicity. *Biochim Biophys Acta.* (2016) 1863:1916–25. doi: 10.1016/j.bbamcr.2016.01.021
39. Pagliaro P, Penna C. Redox signalling and cardioprotection: translatability and mechanism. *Br J Pharmacol.* (2015) 172:1974–95. doi: 10.1111/bph.12975
40. Bonora M, Wieckowski MR, Sinclair DA, Kroemer G, Pinton P, Galluzzi L. Targeting mitochondria for cardiovascular disorders: therapeutic potential and obstacles. *Nat Rev Cardiol.* (2019) 16:33–55. doi: 10.1038/s41569-018-0074-0
41. Brown DA, Perry JB, Allen ME, Sabbah HN, Stauffer BL, Shaikh SR, et al. Expert consensus document: mitochondrial function as a therapeutic target in heart failure. *Nat Rev Cardiol.* (2017) 14:238–50. doi: 10.1038/nrcardio.2016.203
42. Murphy E, Ardehali H, Balaban RS, DiLisa F, Dorn GW, Kitsis RN, et al. Mitochondrial function, biology, and role in disease: a scientific statement from the american heart association. *Circ Res.* (2016) 118:1960–91. doi: 10.1161/RES.0000000000000104
43. Aon MA, Cortassa S. Mitochondrial network energetics in the heart. *Wiley Interdiscip Rev Syst Biol Med.* (2012) 4:599–613. doi: 10.1002/wsbm.1188
44. Ichikawa Y, Ghanefar M, Bayeva M, Wu R, Khechaduri A, Naga Prasad SV, et al. Cardiotoxicity of doxorubicin is mediated through mitochondrial iron accumulation. *J Clin Invest.* (2014) 124:617–30. doi: 10.1172/JCI72931
45. Zhang S, Liu X, Bawa-Khalfe T, Lu L-S, Lyu YL, Liu LF, et al. Identification of the molecular basis of doxorubicin-induced cardiotoxicity. *Nat Med.* (2012) 18:1639–42. doi: 10.1038/nm.2919
46. Davies KJA, Doroshow JH. Redox cycling of anthracyclines by cardiac mitochondria. I. Anthracycline radical formation by NADH dehydrogenase. *J Biol Chem.* (1986) 261:3060–7. doi: 10.1016/s0021-9258(17)35746-0
47. Tullio F, Angotti C, Perrelli M-G, Penna C, Pagliaro P. Redox balance and cardioprotection. *Basic Res Cardiol.* (2013) 108:392. doi: 10.1007/s00395-013-0392-7
48. Penna C, Mancardi D, Rastaldo R, Pagliaro P. Cardioprotection: a radical view free radicals in pre and postconditioning. *Biochim Biophys Acta.* (2009) 1787:781–93. doi: 10.1016/j.bbabio.2009.02.008
49. Christidi E, Brunham LR. Regulated cell death pathways in doxorubicin-induced cardiotoxicity. *Cell Death Dis.* (2021) 12:339. doi: 10.1038/s41419-021-03614-x
50. Qin Y, Guo T, Wang Z, Zhao Y. The role of iron in doxorubicin-induced cardiotoxicity: recent advances and implication for drug delivery. *J Mater Chem B.* (2021) 9:4793–803. doi: 10.1039/d1tb00551k
51. Kwok JC, Richardson DR. Anthracyclines induce accumulation of iron in ferritin in myocardial and neoplastic cells: inhibition of the ferritin iron mobilization pathway. *Mol Pharmacol.* (2003) 63:849–61. doi: 10.1124/mol.63.4.849
52. Tadokoro T, Ikeda M, Ide T, Deguchi H, Ikeda S, Okabe K, et al. Mitochondria-dependent ferroptosis plays a pivotal role in doxorubicin cardiotoxicity. *JCI insight.* (2020) 5:e132747. doi: 10.1172/jci.insight.132747
53. Kagan VE, Bayir HA, Belikova NA, Kapralov O, Tyurina YY, Tyurin VA, et al. Cytochrome c/cardiolipin relations in mitochondria: a kiss of death. *Free Radic Biol Med.* (2009) 46:1439–53. doi: 10.1016/j.freeradbiomed.2009.03.004
54. Parker MA, King V, Howard KP. Nuclear magnetic resonance study of doxorubicin binding to cardiolipin containing magnetically oriented phospholipid bilayers. *Biochim Biophys Acta.* (2001) 1514:206–16. doi: 10.1016/s0005-2736(01)00371-6
55. Zhang T, Zhang Y, Cui M, Jin L, Wang Y, Lv F, et al. CaMKII is a RIP3 substrate mediating ischemia- and oxidative stress-induced myocardial necroptosis. *Nat Med.* (2016) 22:175–82. doi: 10.1038/nm.4017
56. Lyu YL, Kerrigan JE, Lin C-P, Azarova AM, Tsai Y-C, Ban Y, et al. Topoisomerase IIbeta mediated DNA double-strand breaks: implications

in doxorubicin cardiotoxicity and prevention by dexrazoxane. *Cancer Res.* (2007) 67:8839–46. doi: 10.1158/0008-5472.CAN-07-1649
57. McSweeney KM, Bozza WP, Alterovitz W-L, Zhang B. Transcriptomic profiling reveals p53 as a key regulator of doxorubicin-induced cardiotoxicity. *Cell Death Discov.* (2019) 5:102. doi: 10.1038/s41420-019-0182-6
58. Pilié PG, Tang C, Mills GB, Yap TA. State-of-the-art strategies for targeting the DNA damage response in cancer. *Nat Rev Clin Oncol.* (2019) 16:81–104. doi: 10.1038/s41571-018-0114-z
59. Marchenko ND, Zaika A, Moll UM. Death signal-induced localization of p53 protein to mitochondria. A potential role in apoptotic signaling. *J Biol Chem.* (2000) 275:16202–12. doi: 10.1074/jbc.275.21.16202
60. Nakagawa T, Shimizu S, Watanabe T, Yamaguchi O, Otsu K, Yamagata H, et al. Cyclophilin D-dependent mitochondrial permeability transition regulates some necrotic but not apoptotic cell death. *Nature.* (2005) 434:652–8. doi: 10.1038/nature03317
61. Baumann K. Cell death: multitasking p53 promotes necrosis. *Nat Rev Mol Cell Biol.* (2012) 13:480–1. doi: 10.1038/nrm3401
62. Vaseva AV, Marchenko ND, Ji K, Tsirka SE, Holzmann S, Moll UM. p53 opens the mitochondrial permeability transition pore to trigger necrosis. *Cell.* (2012) 149:1536–48. doi: 10.1016/j.cell.2012.05.014
63. Blandino G, Valenti F, Sacconi A, Di Agostino S. Wild type- and mutant p53 proteins in mitochondrial dysfunction: emerging insights in cancer disease. *Semin Cell Dev Biol.* (2020) 98:105–17. doi: 10.1016/j.semcdb.2019.05.011
64. Maj MA, Ma J, Krukowski KN, Kavelaars A, Heijnen CJ. Inhibition of mitochondrial p53 accumulation by PFT-μ prevents cisplatin-induced peripheral neuropathy. *Front Mol Neurosci.* (2017) 10:108. doi: 10.3389/fnmol.2017.00108
65. Li J, Wang P-Y, Long NA, Zhuang J, Springer DA, Zou J, et al. p53 prevents doxorubicin cardiotoxicity independently of its prototypical tumor suppressor activities. *Proc Natl Acad Sci USA.* (2019) 116:19626–34. doi: 10.1073/pnas.1904979116
66. Nishi M, Wang P-Y, Hwang PM. Protective role of p53 in doxorubicin-induced cardiomyopathy as a mitochondrial disease. *Mol Cell Oncol.* (2020) 7:1724598. doi: 10.1080/23723556.2020.1724598
67. Gambardella J, Trimarco B, Iaccarino G, Sorriento D. Cardiac nonmyocyte cell functions and crosstalks in response to cardiotoxic drugs. *Oxid Med Cell Longev.* (2017) 2017:1089359. doi: 10.1155/2017/1089359
68. Jurczyk M, Król M, Midro A, Kurnik-Łucka M, Poniatowski A, Gil K. Cardiotoxicity of fluoropyrimidines: epidemiology, mechanisms, diagnosis, and management. *J Clin Med.* (2021) 10:4426. doi: 10.3390/jcm10194426
69. Shiga T, Hiraide M. Cardiotoxicities of 5-fluorouracil and other fluoropyrimidines. *Curr Treat Options Oncol.* (2020) 21:27. doi: 10.1007/s11864-020-0719-1
70. Deac AL, Burz CC, Bocsan IC, Buzoianu AD. Fluoropyrimidine-induced cardiotoxicity. *World J Clin Oncol.* (2020) 11:1008–17. doi: 10.5306/wjco.v11.i12.1008
71. Depetris I, Marino D, Bonzano A, Cagnazzo C, Filippi R, Aglietta M, et al. Fluoropyrimidine-induced cardiotoxicity. *Crit Rev Oncol Hematol.* (2018) 124:1–10. doi: 10.1016/j.critrevonc.2018.02.002
72. Sorrentino MF, Kim J, Foderaro AE, Truesdell AG. 5-fluorouracil induced cardiotoxicity: review of the literature. *Cardiol J.* (2012) 19:453–8. doi: 10.5603/cj.2012.0084
73. Saif MW, Shah MM, Shah AR. Fluoropyrimidine-associated cardiotoxicity: revisited. *Expert Opin Drug Saf.* (2009) 8:191–202. doi: 10.1517/14740330902733961
74. Alter P, Herzum M, Soufi M, Schaefer JR, Maisch B. Cardiotoxicity of 5-fluorouracil. *Cardiovasc Hematol Agents Med Chem.* (2006) 4:1–5. doi: 10.2174/187152506775268785
75. Madeddu C, Deidda M, Piras A, Cadeddu C, Demurtas L, Puzzoni M, et al. Pathophysiology of cardiotoxicity induced by nonanthracycline chemotherapy. *J Cardiovasc Med (Hagerstown).* (2016) 17(Suppl. 1):S12–8. doi: 10.2459/JCM.0000000000000376
76. Ewer MS, Ewer SM. Cardiotoxicity of anticancer treatments. *Nat Rev Cardiol.* (2015) 12:547–58. doi: 10.1038/nrcardio.2015.65
77. Focaccetti C, Bruno A, Magnani E, Bartolini D, Principi E, Dallaglio K, et al. Effects of 5-fluorouracil on morphology, cell cycle, proliferation, apoptosis, autophagy and ROS production in endothelial cells and cardiomyocytes. *PLoS One.* (2015) 10:e0115686. doi: 10.1371/journal.pone.0115686
78. Mosseri M, Fingert HJ, Varticovski L, Chokshi S, Isner JM. *In vitro* evidence that myocardial ischemia resulting from 5-fluorouracil chemotherapy is due to protein kinase C-mediated vasoconstriction of vascular smooth muscle. *Cancer Res.* (1993) 53:3028–33.
79. Spasojević I, Jelić S, Zakrzewska J, Bacić G. Decreased oxygen transfer capacity of erythrocytes as a cause of 5-fluorouracil related ischemia. *Molecules.* (2008) 14:53–67. doi: 10.3390/molecules14010053
80. Marupudi NI, Han JE, Li KW, Renard VM, Tyler BM, Brem H. Paclitaxel: a review of adverse toxicities and novel delivery strategies. *Expert Opin Drug Saf.* (2007) 6:609–21. doi: 10.1517/14740338.6.5.609
81. Osman M, Elkady MA. Prospective study to evaluate the effect of paclitaxel on cardiac ejection fraction. *Breast Care (Basel).* (2017) 12:255–9. doi: 10.1159/000471759
82. Rowinsky EK, McGuire WP, Guarnieri T, Fisherman JS, Christian MC, Donehower RC. Cardiac disturbances during the administration of taxol. *J Clin Oncol.* (1991) 9:1704–12. doi: 10.1200/JCO.1991.9.9.1704
83. Batra A, Patel B, Addison D, Baldassarre LA, Desai N, Weintraub N, et al. Cardiovascular safety profile of taxanes and vinca alkaloids: 30 years FDA registry experience. *Open Hear.* (2021) 8:e001849. doi: 10.1136/openhrt-2021-001849
84. Schlitt A, Jordan K, Vordermark D, Schwamborn J, Langer T, Thomssen C. Cardiotoxicity and oncological treatments. *Dtsch Arztebl Int.* (2014) 111:161–8. doi: 10.3238/arztebl.2014.0161
85. Arbuck SG, Strauss H, Rowinsky E, Christian M, Suffness M, Adams J, et al. A reassessment of cardiac toxicity associated with taxol. *J Natl Cancer Inst Monogr.* (1993) 117–30. Available online at: https://pubmed.ncbi.nlm.nih.gov/7912518/ (accessed February 24, 2022).
86. Rosa GM, Gigli L, Tagliasacchi MI, Di Iorio C, Carbone F, Nencioni A, et al. Update on cardiotoxicity of anti-cancer treatments. *Eur J Clin Invest.* (2016) 46:264–84. doi: 10.1111/eci.12589
87. Schimmel KJM, Richel DJ, van den Brink RBA, Guchelaar H-J. Cardiotoxicity of cytotoxic drugs. *Cancer Treat Rev.* (2004) 30:181–91. doi: 10.1016/j.ctrv.2003.07.003
88. Geiger S, Lange V, Suhl P, Heinemann V, Stemmler H-J. Anticancer therapy induced cardiotoxicity: review of the literature. *Anticancer Drugs.* (2010) 21:578–90. doi: 10.1097/CAD.0b013e3283394624
89. Finley RS, Rowinsky EK. Patient care issues: the management of paclitaxel-related toxicities. *Ann Pharmacother.* (1994) 28:S27–30. doi: 10.1177/10600280940280S507
90. Rowinsky EK, Eisenhauer EA, Chaudhry V, Arbuck SG, Donehower RC. Clinical toxicities encountered with paclitaxel (taxol). *Semin Oncol.* (1993) 20:1–15.
91. Varbiro G, Veres B, Gallyas F, Sumegi B. Direct effect of taxol on free radical formation and mitochondrial permeability transition. *Free Radic Biol Med.* (2001) 31:548–58. doi: 10.1016/s0891-5849(01)00616-5
92. Gianni L, Viganò L, Locatelli A, Capri G, Giani A, Tarenzi E, et al. Human pharmacokinetic characterization and *in vitro* study of the interaction between doxorubicin and paclitaxel in patients with breast cancer. *J Clin Oncol.* (1997) 15:1906–15. doi: 10.1200/JCO.1997.15.5.1906
93. Saad SY, Najjar TAO, Alashari M. Cardiotoxicity of doxorubicin/paclitaxel combination in rats: effect of sequence and timing of administration. *J Biochem Mol Toxicol.* (2004) 18:78–86. doi: 10.1002/jbt.20012
94. Sparano JA. Doxorubicin/taxane combinations: cardiac toxicity and pharmacokinetics. *Semin Oncol.* (1999) 26:14–9.
95. Dasari S, Tchounwou PB. Cisplatin in cancer therapy: molecular mechanisms of action. *Eur J Pharmacol.* (2014) 740:364–78. doi: 10.1016/j.ejphar.2014.07.025
96. Haugnes HS, Wethal T, Aass N, Dahl O, Klepp O, Langberg CW, et al. Cardiovascular risk factors and morbidity in long-term survivors of testicular cancer: a 20-year follow-up study. *J Clin Oncol.* (2010) 28:4649–57. doi: 10.1200/JCO.2010.29.9362
97. Alexandre J, Moslehi JJ, Bersell KR, Funck-Brentano C, Roden DM, Salem J-E. Anticancer drug-induced cardiac rhythm disorders: current knowledge and basic underlying mechanisms. *Pharmacol Ther.* (2018) 189:89–103. doi: 10.1016/j.pharmthera.2018.04.009

98. Meinardi MT, Gietema JA, van der Graaf WTA, van Veldhuisen DJ, Runne MA, Sluiter WJ, et al. Cardiovascular morbidity in long-term survivors of metastatic testicular cancer. *J Clin Oncol.* (2000) 18:1725–32. doi: 10.1200/JCO.2000.18.8.1725
99. Al-Majed AA, Sayed-Ahmed MM, Al-Yahya AA, Aleisa AM, Al-Rejaie SS, Al-Shabanah OA. Propionyl-L-carnitine prevents the progression of cisplatin-induced cardiomyopathy in a carnitine-depleted rat model. *Pharmacol Res.* (2006) 53:278–86. doi: 10.1016/j.phrs.2005.12.005
100. El-Awady E-SE, Moustafa YM, Abo-Elmatty DM, Radwan A. Cisplatin-induced cardiotoxicity: mechanisms and cardioprotective strategies. *Eur J Pharmacol.* (2011) 650:335–41. doi: 10.1016/j.ejphar.2010.09.085
101. El-Sawalhi MM, Ahmed LA. Exploring the protective role of apocynin, a specific NADPH oxidase inhibitor, in cisplatin-induced cardiotoxicity in rats. *Chem Biol Interact.* (2014) 207:58–66. doi: 10.1016/j.cbi.2013.11.008
102. Chowdhury S, Sinha K, Banerjee S, Sil PC. Taurine protects cisplatin induced cardiotoxicity by modulating inflammatory and endoplasmic reticulum stress responses. *Biofactors.* (2016) 42:647–64. doi: 10.1002/biof.1301
103. Braverman AC, Antin JH, Plappert MT, Cook EF, Lee RT. Cyclophosphamide cardiotoxicity in bone marrow transplantation: a prospective evaluation of new dosing regimens. *J Clin Oncol.* (1991) 9:1215–23. doi: 10.1200/JCO.1991.9.7.1215
104. Arteaga CL, Engelman JA. ERBB receptors: from oncogene discovery to basic science to mechanism-based cancer therapeutics. *Cancer Cell.* (2014) 25:282–303. doi: 10.1016/j.ccr.2014.02.025
105. Yarden Y, Pines G. The ERBB network: at last, cancer therapy meets systems biology. *Nat Rev Cancer.* (2012) 12:553–63. doi: 10.1038/nrc3309
106. Lemmon MA, Schlessinger J. Cell signaling by receptor tyrosine kinases. *Cell.* (2010) 141:1117–34. doi: 10.1016/j.cell.2010.06.011
107. Citri A, Yarden Y. EGF-ERBB signalling: towards the systems level. *Nat Rev Mol Cell Biol.* (2006) 7:505–16. doi: 10.1038/nrm1962
108. Tzahar E, Waterman H, Chen X, Levkowitz G, Karunagaran D, Lavi S, et al. A hierarchical network of interreceptor interactions determines signal transduction by Neu differentiation factor/neuregulin and epidermal growth factor. *Mol Cell Biol.* (1996) 16:5276–87. doi: 10.1128/MCB.16.10.5276
109. Wang J, Xu B. Targeted therapeutic options and future perspectives for HER2-positive breast cancer. *Signal Transduct Target Ther.* (2019) 4:34. doi: 10.1038/s41392-019-0069-2
110. Odiete O, Hill MF, Sawyer DB. Neuregulin in cardiovascular development and disease. *Circ Res.* (2012) 111:1376–85. doi: 10.1161/CIRCRESAHA.112.267286
111. De Keulenaer GW, Doggen K, Lemmens K. The vulnerability of the heart as a pluricellular paracrine organ: lessons from unexpected triggers of heart failure in targeted ErbB2 anticancer therapy. *Circ Res.* (2010) 106:35–46. doi: 10.1161/CIRCRESAHA.109.205906
112. Fuller SJ, Sivarajah K, Sugden PH. ErbB receptors, their ligands, and the consequences of their activation and inhibition in the myocardium. *J Mol Cell Cardiol.* (2008) 44:831–54. doi: 10.1016/j.yjmcc.2008.02.278
113. Del Monte-Nieto G, Ramialison M, Adam AAS, Wu B, Aharonov A, D'Uva G, et al. Control of cardiac jelly dynamics by NOTCH1 and NRG1 defines the building plan for trabeculation. *Nature.* (2018) 557:439–71. doi: 10.1038/s41586-018-0110-6
114. Lai D, Liu X, Forrai A, Wolstein O, Michalicek J, Ahmed I, et al. Neuregulin 1 sustains the gene regulatory network in both trabecular and nontrabecular myocardium. *Circ Res.* (2010) 107:715–27. doi: 10.1161/CIRCRESAHA.110.218693
115. Liu J, Bressan M, Hassel D, Huisken J, Staudt D, Kikuchi K, et al. A dual role for ErbB2 signaling in cardiac trabeculation. *Development.* (2010) 137:3867–75. doi: 10.1242/dev.053736
116. Wadugu B, Kuhn B. The role of neuregulin/ErbB2/ErbB4 signaling in the heart with special focus on effects on cardiomyocyte proliferation. *Am J Physiol Hear Circ Physiol.* (2012) 302:H2139–47. doi: 10.1152/ajpheart.00063.2012ajpheart.00063.2012
117. Pentassuglia L, Sawyer DB. The role of neuregulin-1beta/ErbB signaling in the heart. *Exp Cell Res.* (2009) 315:627–37. doi: 10.1016/j.yexcr.2008.08.015
118. Hedhli N, Huang Q, Kalinowski A, Palmeri M, Hu X, Russell RR, et al. Endothelium-derived neuregulin protects the heart against ischemic injury. *Circulation.* (2011) 123:2254–62. doi: 10.1161/CIRCULATIONAHA.110.991125
119. Hedhli N, Dobrucki LW, Kalinowski A, Zhuang ZW, Wu X, Russell RR, et al. Endothelial-derived neuregulin is an important mediator of ischaemia-induced angiogenesis and arteriogenesis. *Cardiovasc Res.* (2012) 93:516–24. doi: 10.1093/cvr/cvr352
120. De Keulenaer GW, Feyen E, Dugaucquier L, Shakeri H, Shchendrygina A, Belenkov YN, et al. Mechanisms of the multitasking endothelial protein NRG-1 as a compensatory factor during chronic heart failure. *Circ Heart Fail.* (2019) 12:e006288. doi: 10.1161/CIRCHEARTFAILURE.119.006288
121. Harvey RP, Wystub-Lis K, del Monte-Nieto G, Graham RM, Tzahor E. Cardiac regeneration therapies – targeting neuregulin 1 signalling. *Hear Lung Circ.* (2016) 25:4–7. doi: 10.1016/j.hlc.2015.08.014
122. D'Uva G, Tzahor E. The key roles of ERBB2 in cardiac regeneration. *Cell Cycle.* (2015) 14:2383–4. doi: 10.1080/15384101.2015.1063292
123. Zhao YY, Sawyer DR, Baliga RR, Opel DJ, Han X, Marchionni MA, et al. Neuregulins promote survival and growth of cardiac myocytes. Persistence of ErbB2 and ErbB4 expression in neonatal and adult ventricular myocytes. *J Biol Chem.* (1998) 273:10261–9. doi: 10.1074/jbc.273.17.10261
124. D'Uva G, Aharonov A, Lauriola M, Kain D, Yahalom-Ronen Y, Carvalho S, et al. ERBB2 triggers mammalian heart regeneration by promoting cardiomyocyte dedifferentiation and proliferation. *Nat Cell Biol.* (2015) 17:627–38. doi: 10.1038/ncb3149
125. Polizzotti BD, Ganapathy B, Walsh S, Choudhury S, Ammanamanchi N, Bennett DG, et al. Neuregulin stimulation of cardiomyocyte regeneration in mice and human myocardium reveals a therapeutic window. *Sci Transl Med.* (2015) 7:281ra45. doi: 10.1126/scitranslmed.aaa5171
126. Gemberling M, Karra R, Dickson AL, Poss KD. Nrg1 is an injury-induced cardiomyocyte mitogen for the endogenous heart regeneration program in zebrafish. *Elife.* (2015) 4:e05871. doi: 10.7554/eLife.05871
127. Bersell K, Arab S, Haring B, Kuhn B. Neuregulin1/ErbB4 signaling induces cardiomyocyte proliferation and repair of heart injury. *Cell.* (2009) 138:257–70. doi: 10.1016/j.cell.2009.04.060S0092-8674(09)00522-4
128. Crone SA, Zhao Y-YY, Fan L, Gu Y, Minamisawa S, Liu Y, et al. ErbB2 is essential in the prevention of dilated cardiomyopathy. *Nat Med.* (2002) 8:459–65. doi: 10.1038/nm0502-459nm0502-459
129. Rohrbach S, Niemann B, Silber RE, Holtz J. Neuregulin receptors erbB2 and erbB4 in failing human myocardium – depressed expression and attenuated activation. *Basic Res Cardiol.* (2005) 100:240–9. doi: 10.1007/s00395-005-0514-4
130. Rohrbach S, Yan X, Weinberg EO, Hasan F, Bartunek J, Marchionni MA, et al. Neuregulin in cardiac hypertrophy in rats with aortic stenosis. Differential expression of erbB2 and erbB4 receptors. *Circulation.* (1999) 100:407–12. doi: 10.1161/01.cir.100.4.407
131. Mendes-Ferreira P, Maia-Rocha C, Adão R, Mendes MJ, Santos-Ribeiro D, Alves BS, et al. Neuregulin-1 improves right ventricular function and attenuates experimental pulmonary arterial hypertension. *Cardiovasc Res.* (2016) 109:44–54. doi: 10.1093/cvr/cvv244
132. Gu A, Jie Y, Sun L, Zhao S, Mingyan E, You Q. RhNRG-1β protects the myocardium against irradiation-induced damage *via* the ErbB2-ERK-SIRT1 signaling pathway. *PLoS One.* (2015) 10:e0137337. doi: 10.1371/journal.pone.0137337
133. Xu Y, Li X, Liu X, Zhou M. Neuregulin-1/ErbB signaling and chronic heart failure. *Adv Pharmacol.* (2010) 59:31–51. doi: 10.1016/S1054-3589(10)59002-1
134. Liu X, Gu X, Li Z, Li X, Li H, Chang J, et al. Neuregulin-1/erbB-activation improves cardiac function and survival in models of ischemic, dilated, and viral cardiomyopathy. *J Am Coll Cardiol.* (2006) 48:1438–47. doi: 10.1016/j.jacc.2006.05.057
135. Gao R, Zhang J, Cheng L, Wu X, Dong W, Yang X, et al. A Phase II, randomized, double-blind, multicenter, based on standard therapy, placebo-controlled study of the efficacy and safety of recombinant human neuregulin-1 in patients with chronic heart failure. *J Am Coll Cardiol.* (2010) 55:1907–14. doi: 10.1016/j.jacc.2009.12.044
136. Lenihan DJ, Anderson SA, Lenneman CG, Brittain E, Muldowney JAS, Mendes L, et al. A phase I, single ascending dose study of cimaglermin alfa (neuregulin 1β3) in patients with systolic dysfunction and heart failure. *JACC Basic to Transl Sci.* (2016) 1:576–86. doi: 10.1016/j.jacbts.2016.09.005
137. Sawyer DB, Caggiano A. Neuregulin-1beta for the treatment of systolic heart failure. *J Mol Cell Cardiol.* (2011) 51:501–5. doi: 10.1016/j.yjmcc.2011.06.016

138. de Korte MA, de Vries EG, Lub-de Hooge MN, Jager PL, Gietema JA, van der Graaf WT, et al. 111Indium-trastuzumab visualises myocardial human epidermal growth factor receptor 2 expression shortly after anthracycline treatment but not during heart failure: a clue to uncover the mechanisms of trastuzumab-related cardiotoxicity. *Eur J Cancer.* (2007) 43:2046–51. doi: 10.1016/j.ejca.2007.06.024
139. Gabrielson K, Bedja D, Pin S, Tsao A, Gama L, Yuan B, et al. Heat shock protein 90 and ErbB2 in the cardiac response to doxorubicin injury. *Cancer Res.* (2007) 67:1436–41. doi: 10.1158/0008-5472.CAN-06-3721
140. Belmonte F, Das S, Sysa-Shah P, Sivakumaran V, Stanley B, Guo X, et al. ErbB2 overexpression upregulates antioxidant enzymes, reduces basal levels of reactive oxygen species, and protects against doxorubicin cardiotoxicity. *Am J Physiol Heart Circ Physiol.* (2015) 309:H1271–80. doi: 10.1152/ajpheart.00517.2014
141. Harding J, Burtness B. Cetuximab: an epidermal growth factor receptor chimeric human-murine monoclonal antibody. *Drugs Today.* (2005) 41:107–27. doi: 10.1358/dot.2005.41.2.882662
142. Ciardiello F, Tortora G. EGFR antagonists in cancer treatment. *N Engl J Med.* (2008) 358:1160–74. doi: 10.1056/NEJMra0707704
143. Ishiguro M, Watanabe T, Yamaguchi K, Satoh T, Ito H, Seriu T, et al. Japanese post-marketing surveillance of cetuximab (Erbitux®) in patients with metastatic colorectal cancer. *Jpn J Clin Oncol.* (2012) 42:287–94. doi: 10.1093/jjco/hys005
144. Huang W-T, Chen H-H, Yeh C-H, Lu Y-C, Hwang W-S, Huang J-S, et al. A postmarketing surveillance study on erbitux (cetuximab) in patients with metastatic colorectal cancer refractory to irinotecan-containing treatment. *J Investig Med.* (2013) 61:1108–14. doi: 10.2310/JIM.0b013e3182a6799d
145. Cho H-S, Mason K, Ramyar KX, Stanley AM, Gabelli SB, Denney DW, et al. Structure of the extracellular region of HER2 alone and in complex with the Herceptin fab. *Nature.* (2003) 421:756–60. doi: 10.1038/nature01392
146. Junttila TT, Akita RW, Parsons K, Fields C, Lewis Phillips GD, Friedman LS, et al. Ligand-independent HER2/HER3/PI3K complex is disrupted by trastuzumab and is effectively inhibited by the PI3K inhibitor GDC-0941. *Cancer Cell.* (2009) 15:429–40. doi: 10.1016/j.ccr.2009.03.020
147. Hynes NE, Lane HA. ERBB receptors and cancer: the complexity of targeted inhibitors. *Nat Rev Cancer.* (2005) 5:341–54. doi: 10.1038/nrc1609
148. Perez EA. Cardiac issues related to trastuzumab. *Breast.* (2004) 13:171–2. doi: 10.1016/j.breast.2004.02.008
149. Perez EA, Rodeheffer R. Clinical cardiac tolerability of trastuzumab. *J Clin Oncol.* (2004) 22:322–9. doi: 10.1200/JCO.2004.01.120
150. Keefe DL. Trastuzumab-associated cardiotoxicity. *Cancer.* (2002) 95:1592–600. doi: 10.1002/cncr.10854
151. Yavas O, Yazici M, Eren O, Oyan B. The acute effect of trastuzumab infusion on ECG parameters in metastatic breast cancer patients. *Swiss Med Wkly.* (2007) 137:556–8. doi: 10.4414/smw.2007.11899
152. Vogel CL, Cobleigh MA, Tripathy D, Gutheil JC, Harris LN, Fehrenbacher L, et al. Efficacy and safety of trastuzumab as a single agent in first-line treatment of HER2-overexpressing metastatic breast cancer. *J Clin Oncol.* (2002) 20:719–26. doi: 10.1200/JCO.2002.20.3.719
153. Cobleigh MA, Vogel CL, Tripathy D, Robert NJ, Scholl S, Fehrenbacher L, et al. Multinational study of the efficacy and safety of humanized anti-HER2 monoclonal antibody in women who have HER2-overexpressing metastatic breast cancer that has progressed after chemotherapy for metastatic disease. *J Clin Oncol.* (1999) 17:2639–48. doi: 10.1200/JCO.1999.17.9.2639
154. Lin M, Xiong W, Wang S, Li Y, Hou C, Li C, et al. The research progress of trastuzumab-induced cardiotoxicity in HER-2-positive breast cancer treatment. *Front Cardiovasc Med.* (2021) 8:821663. doi: 10.3389/fcvm.2021.821663
155. Healey Bird BRJ, Swain SM. Cardiac toxicity in breast cancer survivors: review of potential cardiac problems. *Clin Cancer Res.* (2008) 14:14–24. doi: 10.1158/1078-0432.CCR-07-1033
156. Hudis CA, Clifford H. Trastuzumab – mechanism of action and use in clinical practice. *N Engl J Med.* (2007) 357:39–51. doi: 10.1056/nejmra043186
157. Morris PG, Hudis CA. Trastuzumab-related cardiotoxicity following anthracycline-based adjuvant chemotherapy: how worried should we be? *J Clin Oncol.* (2010) 28:3407–10. doi: 10.1200/JCO.2009.26.0125
158. Ewer MS, Ewer SM. Troponin I provides insight into cardiotoxicity and the anthracycline-trastuzumab interaction. *J Clin Oncol.* (2010) 28:3901–4. doi: 10.1200/JCO.2010.30.6274
159. Beauclair S, Formento P, Fischel JL, Lescaut W, Largillier R, Chamorey E, et al. Role of the HER2 [Ile655Val] genetic polymorphism in tumorogenesis and in the risk of trastuzumab-related cardiotoxicity. *Ann Oncol Off J Eur Soc Med Oncol.* (2007) 18:1335–41. doi: 10.1093/annonc/mdm181
160. Roca L, Diéras V, Roché H, Lappartient E, Kerbrat P, Cany L, et al. Correlation of HER2, FCGR2A, and FCGR3A gene polymorphisms with trastuzumab related cardiac toxicity and efficacy in a subgroup of patients from UNICANCER-PACS 04 trial. *Breast Cancer Res Treat.* (2013) 139:789–800. doi: 10.1007/s10549-013-2587-x
161. Han X, Diao L, Xu Y, Xue W, Ouyang T, Li J, et al. Association between the HER2 Ile655Val polymorphism and response to trastuzumab in women with operable primary breast cancer. *Ann Oncol Off J Eur Soc Med Oncol.* (2014) 25:1158–64. doi: 10.1093/annonc/mdu111
162. Gómez Peña C, Dávila-Fajardo CL, Martínez-González LJ, Carmona-Sáez P, Soto Pino MJ, Sánchez Ramos J, et al. Influence of the HER2 Ile655Val polymorphism on trastuzumab-induced cardiotoxicity in HER2-positive breast cancer patients: a meta-analysis. *Pharmacogenet Genomics.* (2015) 25:388–93. doi: 10.1097/FPC.0000000000000149
163. Stanton SE, Ward MM, Christos P, Sanford R, Lam C, Cobham MV, et al. Pro1170 Ala polymorphism in HER2-neu is associated with risk of trastuzumab cardiotoxicity. *BMC Cancer.* (2015) 15:267. doi: 10.1186/s12885-015-1298-6
164. Vazdar L, Gabrić ID, Kruljac I, Pintarić H, Šeparović R, Kirigin Biloš LS, et al. Influence of Ile655Val polymorphism on trastuzumab-induced cardiotoxicity in early-stage HER2 positive breast cancer. *Sci Rep.* (2021) 11:14395. doi: 10.1038/s41598-021-93634-6
165. Slamon DJ, Leyland-Jones B, Shak S, Fuchs H, Paton V, Bajamonde A, et al. Use of chemotherapy plus a monoclonal antibody against HER2 for metastatic breast cancer that overexpresses HER2. *N Engl J Med.* (2001) 344:783–92. doi: 10.1056/nejm200103153441101
166. Cardinale D, Colombo A, Torrisi R, Sandri MT, Civelli M, Salvatici M, et al. Trastuzumab-induced cardiotoxicity: clinical and prognostic implications of troponin I evaluation. *J Clin Oncol.* (2010) 28:3910–6. doi: 10.1200/JCO.2009.27.3615
167. Timolati F, Ott D, Pentassuglia L, Giraud MN, Perriard JC, Suter TM, et al. Neuregulin-1 beta attenuates doxorubicin-induced alterations of excitation-contraction coupling and reduces oxidative stress in adult rat cardiomyocytes. *J Mol Cell Cardiol.* (2006) 41:845–54. doi: 10.1016/j.yjmcc.2006.08.002
168. Capelan M, Pugliano L, De Azambuja E, Bozovic I, Saini KS, Sotiriou C, et al. Pertuzumab: new hope for patients with HER2-positive breast cancer. *Ann Oncol.* (2013) 24:273–82. doi: 10.1093/annonc/mds328
169. Franklin MC, Carey KD, Vajdos FF, Leahy DJ, De Vos AM, Sliwkowski MX. Insights into ErbB signaling from the structure of the ErbB2-pertuzumab complex. *Cancer Cell.* (2004) 5:317–28. doi: 10.1016/S1535-6108(04)00083-2
170. von Minckwitz G, Procter M, de Azambuja E, Zardavas D, Benyunes M, Viale G, et al. Adjuvant pertuzumab and trastuzumab in early HER2-positive breast cancer. *N Engl J Med.* (2017) 377:122–31. doi: 10.1056/NEJMoa1703643
171. Alhussein MM, Mokbel A, Cosman T, Aghel N, Yang EH, Mukherjee SD, et al. Pertuzumab cardiotoxicity in patients with HER2-positive cancer: a systematic review and meta-analysis. *CJC Open.* (2021) 3:1372–82. doi: 10.1016/j.cjco.2021.06.019
172. Force T, Krause DS, Van Etten RA. Molecular mechanisms of cardiotoxicity of tyrosine kinase inhibition. *Nat Rev Cancer.* (2007) 7:332–44. doi: 10.1038/nrc2106
173. Schlam I, Swain SM. HER2-positive breast cancer and tyrosine kinase inhibitors: the time is now. *NPJ Breast Cancer.* (2021) 7:56. doi: 10.1038/s41523-021-00265-1
174. Perez EA, Koehler M, Byrne J, Preston AJ, Rappold E, Ewer MS. Cardiac safety of lapatinib: pooled analysis of 3689 patients enrolled in clinical trials. *Mayo Clin Proc.* (2008) 83:679–86. doi: 10.4065/83.6.679
175. Eiger D, Pondé NF, Agbor-Tarh D, Moreno-Aspitia A, Piccart M, Hilbers FS, et al. Long-term cardiac outcomes of patients with HER2-positive breast cancer treated in the adjuvant lapatinib and/or trastuzumab treatment

optimization trial. *Br J Cancer.* (2020) 122:1453–60. doi: 10.1038/s41416-020-0786-x
176. Ewer MS, Patel K, O'Brien D, Lorence RM. Cardiac safety of afatinib: a review of data from clinical trials. *Cardio Oncol.* (2015) 1:3. doi: 10.1186/s40959-015-0006-7
177. Sendur MAN, Aksoy S, Altundag K. Cardiotoxicity of novel HER2-targeted therapies. *Curr Med Res Opin.* (2013) 29:1015–24. doi: 10.1185/03007995.2013.807232
178. Wong K-K, Fracasso PM, Bukowski RM, Lynch TJ, Munster PN, Shapiro GI, et al. A phase I study with neratinib (HKI-272), an irreversible pan ErbB receptor tyrosine kinase inhibitor, in patients with solid tumors. *Clin Cancer Res.* (2009) 15:2552–8. doi: 10.1158/1078-0432.CCR-08-1978
179. Ito Y, Suenaga M, Hatake K, Takahashi S, Yokoyama M, Onozawa Y, et al. Safety, efficacy and pharmacokinetics of neratinib (HKI-272) in Japanese patients with advanced solid tumors: a phase 1 dose-escalation study. *Jpn J Clin Oncol.* (2012) 42:278–86. doi: 10.1093/jjco/hys012
180. Novo G, Di Lisi D, Bronte E, Macaione F, Accurso V, Badalamenti G, et al. Cardiovascular toxicity in cancer patients treated with tyrosine kinase inhibitors: a real-world single-center experience. *Oncology.* (2020) 98:445–51. doi: 10.1159/000505486
181. Singh AP, Umbarkar P, Tousif S, Lal H. Cardiotoxicity of the BCR-ABL1 tyrosine kinase inhibitors: emphasis on ponatinib. *Int J Cardiol.* (2020) 316:214–21. doi: 10.1016/j.ijcard.2020.05.077
182. Yang Y, Bu P. Progress on the cardiotoxicity of sunitinib: prognostic significance, mechanism and protective therapies. *Chem Biol Interact.* (2016) 257:125–31. doi: 10.1016/j.cbi.2016.08.006
183. Yang B, Papoian T. Preclinical approaches to assess potential kinase inhibitor-induced cardiac toxicity: past, present and future. *J Appl Toxicol.* (2018) 38:790–800. doi: 10.1002/jat.3584
184. Hasinoff BB, Patel D, O'Hara KA. Mechanisms of myocyte cytotoxicity induced by the multiple receptor tyrosine kinase inhibitor sunitinib. *Mol Pharmacol.* (2008) 74:1722–8. doi: 10.1124/mol.108.050104
185. Hasinoff BB, Patel D. Mechanisms of myocyte cytotoxicity induced by the multikinase inhibitor sorafenib. *Cardiovasc Toxicol.* (2010) 10:1–8. doi: 10.1007/s12012-009-9056-0
186. Hasinoff BB, Patel D. The lack of target specificity of small molecule anticancer kinase inhibitors is correlated with their ability to damage myocytes *in vitro*. *Toxicol Appl Pharmacol.* (2010) 249:132–9. doi: 10.1016/j.taap.2010.08.026
187. Cheng H, Force T. Molecular mechanisms of cardiovascular toxicity of targeted cancer therapeutics. *Circ Res.* (2010) 106:21–34. doi: 10.1161/CIRCRESAHA.109.206920
188. Green MR, Newton MD, Fancher KM. Off-target effects of BCR-ABL and JAK2 inhibitors. *Am J Clin Oncol.* (2016) 39:76–84. doi: 10.1097/COC.0000000000000023
189. Kerkela R, Woulfe KC, Durand J-B, Vagnozzi R, Kramer D, Chu TF, et al. Sunitinib-induced cardiotoxicity is mediated by off-target inhibition of AMP-activated protein kinase. *Clin Transl Sci.* (2009) 2:15–25. doi: 10.1111/j.1752-8062.2008.00090.x
190. Zhu X, Stergiopoulos K, Wu S. Risk of hypertension and renal dysfunction with an angiogenesis inhibitor sunitinib: systematic review and meta-analysis. *Acta Oncol.* (2009) 48:9–17. doi: 10.1080/02841860802314720
191. Wu S, Chen JJ, Kudelka A, Lu J, Zhu X. Incidence and risk of hypertension with sorafenib in patients with cancer: a systematic review and meta-analysis. *Lancet Oncol.* (2008) 9:117–23. doi: 10.1016/S1470-2045(08)70003-2
192. Curigliano G, Mayer EL, Burstein HJ, Winer EP, Goldhirsch A. Cardiac toxicity from systemic cancer therapy: a comprehensive review. *Prog Cardiovasc Dis.* (2010) 53:94–104. doi: 10.1016/j.pcad.2010.05.006
193. Ewer MS, Suter TM, Lenihan DJ, Niculescu L, Breazna A, Demetri GD, et al. Cardiovascular events among 1090 cancer patients treated with sunitinib, interferon, or placebo: a comprehensive adjudicated database analysis demonstrating clinically meaningful reversibility of cardiac events. *Eur J Cancer.* (2014) 50:2162–70. doi: 10.1016/j.ejca.2014.05.013
194. Mourad J-J, Levy BI. Mechanisms of antiangiogenic-induced arterial hypertension. *Curr Hypertens Rep.* (2011) 13:289–93. doi: 10.1007/s11906-011-0206-y
195. Chintalgattu V, Rees ML, Culver JC, Goel A, Jiffar T, Zhang J, et al. Coronary microvascular pericytes are the cellular target of sunitinib malate-induced cardiotoxicity. *Sci Transl Med.* (2013) 5:187ra69. doi: 10.1126/scitranslmed.3005066
196. Kerkelä R, Grazette L, Yacobi R, Iliescu C, Patten R, Beahm C, et al. Cardiotoxicity of the cancer therapeutic agent imatinib mesylate. *Nat Med.* (2006) 12:908–16. doi: 10.1038/nm1446
197. Choksey A, Timm KN. Cancer therapy-induced cardiotoxicity-a metabolic perspective on pathogenesis, diagnosis and therapy. *Int J Mol Sci.* (2021) 23:441. doi: 10.3390/ijms23010441
198. McMullen CJ, Chalmers S, Wood R, Cunningham MR, Currie S. Sunitinib and imatinib display differential cardiotoxicity in adult rat cardiac fibroblasts that involves a role for calcium/calmodulin dependent protein kinase II. *Front Cardiovasc Med.* (2020) 7:630480. doi: 10.3389/fcvm.2020.630480
199. Latifi Y, Moccetti F, Wu M, Xie A, Packwood W, Qi Y, et al. Thrombotic microangiopathy as a cause of cardiovascular toxicity from the BCR-ABL1 tyrosine kinase inhibitor ponatinib. *Blood.* (2019) 133:1597–606. doi: 10.1182/blood-2018-10-881557
200. Singh AP, Glennon MS, Umbarkar P, Gupte M, Galindo CL, Zhang Q, et al. Ponatinib-induced cardiotoxicity: delineating the signalling mechanisms and potential rescue strategies. *Cardiovasc Res.* (2019) 115:966–77. doi: 10.1093/cvr/cvz006
201. Kalam K, Marwick TH. Role of cardioprotective therapy for prevention of cardiotoxicity with chemotherapy: a systematic review and meta-analysis. *Eur J Cancer.* (2013) 49:2900–9. doi: 10.1016/j.ejca.2013.04.030
202. Ganatra S, Nohria A, Shah S, Groarke JD, Sharma A, Venesy D, et al. Upfront dexrazoxane for the reduction of anthracycline-induced cardiotoxicity in adults with preexisting cardiomyopathy and cancer: a consecutive case series. *Cardio Oncol.* (2019) 5:1. doi: 10.1186/s40959-019-0036-7
203. Macedo AVS, Hajjar LA, Lyon AR, Nascimento BR, Putzu A, Rossi L, et al. Efficacy of dexrazoxane in preventing anthracycline cardiotoxicity in breast cancer. *JACC CardioOncol.* (2019) 1:68–79. doi: 10.1016/j.jaccao.2019.08.003
204. Simůnek T, Stérba M, Popelová O, Adamcová M, Hrdina R, Gersl V. Anthracycline-induced cardiotoxicity: overview of studies examining the roles of oxidative stress and free cellular iron. *Pharmacol Rep.* (2009) 61:154–71. doi: 10.1016/s1734-1140(09)70018-0
205. Lipshultz SE, Lipsitz SR, Kutok JL, Miller TL, Colan SD, Neuberg DS, et al. Impact of hemochromatosis gene mutations on cardiac status in doxorubicin-treated survivors of childhood high-risk leukemia. *Cancer.* (2013) 119:3555–62. doi: 10.1002/cncr.28256
206. Hasinoff BB, Schroeder PE, Patel D. The metabolites of the cardioprotective drug dexrazoxane do not protect myocytes from doxorubicin-induced cytotoxicity. *Mol Pharmacol.* (2003) 64:670–8. doi: 10.1124/mol.64.3.670
207. Cascales A, Sánchez-Vega B, Navarro N, Pastor-Quirante F, Corral J, Vicente V, et al. Clinical and genetic determinants of anthracycline-induced cardiac iron accumulation. *Int J Cardiol.* (2012) 154:282–6. doi: 10.1016/j.ijcard.2010.09.046
208. Lenèová-Popelová O, Jirkovskı E, Jansová H, Jirkovská-Vávrová A, Vostatková-Tichotová L, Mazurová Y, et al. Cardioprotective effects of inorganic nitrate/nitrite in chronic anthracycline cardiotoxicity: comparison with dexrazoxane. *J Mol Cell Cardiol.* (2016) 91:92–103. doi: 10.1016/j.yjmcc.2015.12.021
209. Martin E, Thougaard AV, Grauslund M, Jensen PB, Bjorkling F, Hasinoff BB, et al. Evaluation of the topoisomerase II-inactive bisdioxopiperazine ICRF-161 as a protectant against doxorubicin-induced cardiomyopathy. *Toxicology.* (2009) 255:72–9. doi: 10.1016/J.TOX.2008.10.011
210. Stìrba M, Popelová O, Vávrový A, Jirkovskı E, Kovaříková P, Geršl V, et al. Oxidative stress, redox signaling, and metal chelation in anthracycline cardiotoxicity and pharmacological cardioprotection. *Antioxid Redox Signal.* (2013) 18:899–929. doi: 10.1089/ars.2012.4795
211. Joseph P, Swedberg K, Leong DP, Yusuf S. The evolution of β-blockers in coronary artery disease and heart failure (part 1/5). *J Am Coll Cardiol.* (2019) 74:672–82. doi: 10.1016/J.JACC.2019.04.067
212. Freemantle N, Cleland J, Young P, Mason J, Harrison J. beta Blockade after myocardial infarction: systematic review and meta regression analysis. *BMJ.* (1999) 318:1730–7. doi: 10.1136/bmj.318.7200.1730
213. Kanduri J, More LA, Godishala A, Asnani A. Fluoropyrimidine-associated cardiotoxicity. *Cardiol Clin.* (2019) 37:399–405. doi: 10.1016/j.ccl.2019.07.004

214. Seicean S, Seicean A, Alan N, Plana JC, Budd GT, Marwick TH. Cardioprotective effect of β-adrenoceptor blockade in patients with breast cancer undergoing chemotherapy: follow-up study of heart failure. *Circ Heart Fail.* (2013) 6:420–6. doi: 10.1161/CIRCHEARTFAILURE.112.000055
215. Pituskin E, Mackey JR, Koshman S, Jassal D, Pitz M, Haykowsky MJ, et al. Multidisciplinary approach to novel therapies in cardio-oncology research (MANTICORE 101-breast): a randomized trial for the prevention of trastuzumab-associated cardiotoxicity. *J Clin Oncol.* (2017) 35:870–7. doi: 10.1200/JCO.2016.68.7830
216. Gulati G, Heck SL, Ree AH, Hoffmann P, Schulz-Menger J, Fagerland MW, et al. Prevention of cardiac dysfunction during adjuvant breast cancer therapy (PRADA): a 2 × 2 factorial, randomized, placebo-controlled, double-blind clinical trial of candesartan and metoprolol. *Eur Heart J.* (2016) 37:1671–80. doi: 10.1093/eurheartj/ehw022
217. Georgakopoulos P, Roussou P, Matsakas E, Karavidas A, Anagnostopoulos N, Marinakis T, et al. Cardioprotective effect of metoprolol and enalapril in doxorubicin-treated lymphoma patients: a prospective, parallel-group, randomized, controlled study with 36-month follow-up. *Am J Hematol.* (2010) 85:894–6. doi: 10.1002/ajh.21840
218. Spallarossa P, Garibaldi S, Altieri P, Fabbi P, Manca V, Nasti S, et al. Carvedilol prevents doxorubicin-induced free radical release and apoptosis in cardiomyocytes *in vitro*. *J Mol Cell Cardiol.* (2004) 37:837–46. doi: 10.1016/j.yjmcc.2004.05.024
219. Santos DL, Moreno AJM, Leino RL, Froberg MK, Wallace KB. Carvedilol protects against doxorubicin-induced mitochondrial cardiomyopathy. *Toxicol Appl Pharmacol.* (2002) 185:218–27. doi: 10.1006/taap.2002.9532
220. Matsui H, Morishima I, Numaguchi Y, Toki Y, Okumura K, Hayakawa T. Protective effects of carvedilol against doxorubicin-induced cardiomyopathy in rats. *Life Sci.* (1999) 65:1265–74. doi: 10.1016/s0024-3205(99)00362-8
221. Kalay N, Basar E, Ozdogru I, Er O, Cetinkaya Y, Dogan A, et al. Protective effects of carvedilol against anthracycline-induced cardiomyopathy. *J Am Coll Cardiol.* (2006) 48:2258–62. doi: 10.1016/j.jacc.2006.07.052
222. Tashakori Beheshti A, Mostafavi Toroghi H, Hosseini G, Zarifian A, Homaei Shandiz F, Fazlinezhad A. Carvedilol administration can prevent doxorubicin-induced cardiotoxicity: a double-blind randomized trial. *Cardiology.* (2016) 134:47–53. doi: 10.1159/000442722
223. Nabati M, Janbabai G, Baghyari S, Esmaili K, Yazdani J. Cardioprotective effects of carvedilol in inhibiting doxorubicin-induced cardiotoxicity. *J Cardiovasc Pharmacol.* (2017) 69:279–85. doi: 10.1097/FJC.0000000000000470
224. Avila MS, Ayub-Ferreira SM, de Barros Wanderley MR, das Dores Cruz F, Gonçalves Brandão SM, Rigaud VOC, et al. Carvedilol for prevention of chemotherapy-related cardiotoxicity: the CECCY trial. *J Am Coll Cardiol.* (2018) 71:2281–90. doi: 10.1016/j.jacc.2018.02.049
225. El-Shitany NA, Tolba OA, El-Shanshory MR, El-Hawary EE. Protective effect of carvedilol on adriamycin-induced left ventricular dysfunction in children with acute lymphoblastic leukemia. *J Card Fail.* (2012) 18:607–13. doi: 10.1016/j.cardfail.2012.06.416
226. Guglin M, Krischer J, Tamura R, Fink A, Bello-Matricaria L, McCaskill-Stevens W, et al. Randomized trial of lisinopril versus carvedilol to prevent trastuzumab cardiotoxicity in patients with breast cancer. *J Am Coll Cardiol.* (2019) 73:2859–68. doi: 10.1016/J.JACC.2019.03.495
227. Fongemie J, Felix-Getzik EA. Review of nebivolol pharmacology and clinical evidence. *Drugs.* (2015) 75:1349–71. doi: 10.1007/s40265-015-0435-5
228. de Nigris F, Rienzo M, Schiano C, Fiorito C, Casamassimi A, Napoli C. Prominent cardioprotective effects of third generation beta blocker nebivolol against anthracycline-induced cardiotoxicity using the model of isolated perfused rat heart. *Eur J Cancer.* (2008) 44:334–40. doi: 10.1016/j.ejca.2007.12.010
229. Mohamed EA, Kassem HH. Protective effect of nebivolol on doxorubicin-induced cardiotoxicity in rats. *Arch Med Sci.* (2018) 14:1450–8. doi: 10.5114/aoms.2018.79008
230. Kaya MG, Ozkan M, Gunebakmaz O, Akkaya H, Kaya EG, Akpek M, et al. Protective effects of nebivolol against anthracycline-induced cardiomyopathy: a randomized control study. *Int J Cardiol.* (2013) 167:2306–10. doi: 10.1016/j.ijcard.2012.06.023
231. Cochera F, Dinca D, Bordejevic DA, Citu IM, Mavrea AM, Andor M, et al. Nebivolol effect on doxorubicin-induced cardiotoxicity in breast cancer. *Cancer Manag Res.* (2018) 10:2071–81. doi: 10.2147/CMAR.S166481
232. Sobczuk P, Czerwińska M, Kleibert M, Cudnoch-Jêdrzejewska A. Anthracycline-induced cardiotoxicity and renin-angiotensin-aldosterone system-from molecular mechanisms to therapeutic applications. *Heart Fail Rev.* (2022) 27:295–319. doi: 10.1007/s10741-020-09977-1
233. Ayuna A, Abidin N. The role of neurohormonal blockers in the primary prevention of acute-, early-, and late-onset anthracycline-induced cardiotoxicity. *Egypt Hear J.* (2020) 72:59. doi: 10.1186/s43044-020-00090-0
234. Hanif K, Bid HK, Konwar R. Reinventing the ACE inhibitors: some old and new implications of ACE inhibition. *Hypertens Res.* (2010) 33:11–21. doi: 10.1038/hr.2009.184
235. Abd El-Aziz MA, Othman AI, Amer M, El-Missiry MA. Potential protective role of angiotensin-converting enzyme inhibitors captopril and enalapril against adriamycin-induced acute cardiac and hepatic toxicity in rats. *J Appl Toxicol.* (2001) 21:469–73. doi: 10.1002/jat.782
236. Boucek RJ, Steele A, Miracle A, Atkinson J. Effects of angiotensin-converting enzyme inhibitor on delayed-onset doxorubicin-induced cardiotoxicity. *Cardiovasc Toxicol.* (2003) 3:319–29. doi: 10.1385/ct:3:4:319
237. Hullin R, Métrich M, Sarre A, Basquin D, Maillard M, Regamey J, et al. Diverging effects of enalapril or eplerenone in primary prevention against doxorubicin-induced cardiotoxicity. *Cardiovasc Res.* (2018) 114:272–81. doi: 10.1093/cvr/cvx162
238. Okumura K, Jin D, Takai S, Miyazaki M. Beneficial effects of angiotensin-converting enzyme inhibition in adriamycin-induced cardiomyopathy in hamsters. *Jpn J Pharmacol.* (2002) 88:183–8. doi: 10.1254/jjp.88.183
239. Lipshultz SE, Lipsitz SR, Sallan SE, Simbre VC, Shaikh SL, Mone SM, et al. Long-term enalapril therapy for left ventricular dysfunction in doxorubicin-treated survivors of childhood cancer. *J Clin Oncol.* (2002) 20:4517–22. doi: 10.1200/JCO.2002.12.102
240. Jensen BV, Skovsgaard T, Nielsen SL. Functional monitoring of anthracycline cardiotoxicity: a prospective, blinded, long-term observational study of outcome in 120 patients. *Ann Oncol.* (2002) 13:699–709. doi: 10.1093/annonc/mdf132
241. Silber JH, Cnaan A, Clark BJ, Paridon SM, Chin AJ, Rychik J, et al. Enalapril to prevent cardiac function decline in long-term survivors of pediatric cancer exposed to anthracyclines. *J Clin Oncol.* (2004) 22:820–8. doi: 10.1200/JCO.2004.06.022
242. Soga M, Kamal FA, Watanabe K, Ma M, Palaniyandi S, Prakash P, et al. Effects of angiotensin II receptor blocker (candesartan) in daunorubicin-induced cardiomyopathic rats. *Int J Cardiol.* (2006) 110:378–85. doi: 10.1016/j.ijcard.2005.08.061
243. Cadeddu C, Piras A, Mantovani G, Deidda M, Dessì M, Madeddu C, et al. Protective effects of the angiotensin II receptor blocker telmisartan on epirubicin-induced inflammation, oxidative stress, and early ventricular impairment. *Am Heart J.* (2010) 160:487.e1–7. doi: 10.1016/j.ahj.2010.05.037
244. Dessì M, Madeddu C, Piras A, Cadeddu C, Antoni G, Mercuro G, et al. Long-term, up to 18 months, protective effects of the angiotensin II receptor blocker telmisartan on epirubin-induced inflammation and oxidative stress assessed by serial strain rate. *Springerplus.* (2013) 2:198. doi: 10.1186/2193-1801-2-198
245. Dessì M, Piras A, Madeddu C, Cadeddu C, Deidda M, Massa E, et al. Long-term protective effects of the angiotensin receptor blocker telmisartan on epirubicin-induced inflammation, oxidative stress and myocardial dysfunction. *Exp Ther Med.* (2011) 2:1003–9. doi: 10.3892/etm.2011.305
246. Boekhout AH, Gietema JA, Milojkovic Kerklaan B, van Werkhoven ED, Altena R, Honkoop A, et al. Angiotensin II-receptor inhibition with candesartan to prevent trastuzumab-related cardiotoxic effects in patients with early breast cancer: a randomized clinical trial. *JAMA Oncol.* (2016) 2:1030–7. doi: 10.1001/jamaoncol.2016.1726
247. Cardinale D, Colombo A, Lamantia G, Colombo N, Civelli M, De Giacomi G, et al. Anthracycline-induced cardiomyopathy: clinical relevance and response to pharmacologic therapy. *J Am Coll Cardiol.* (2010) 55:213–20. doi: 10.1016/j.jacc.2009.03.095
248. Leong DP, Cosman T, Alhussein MM, Kumar Tyagi N, Karampatos S, Barron CC, et al. Safety of continuing trastuzumab despite mild cardiotoxicity: a

phase I trial. *JACC CardioOncol.* (2019) 1:1–10. doi: 10.1016/j.jaccao.2019.06.004

249. Lynce F, Barac A, Geng X, Dang C, Yu AF, Smith KL, et al. Prospective evaluation of the cardiac safety of HER2-targeted therapies in patients with HER2-positive breast cancer and compromised heart function: the SAFE-HEaRt study. *Breast Cancer Res Treat.* (2019) 175:595–603. doi: 10.1007/s10549-019-05191-2
250. Ezekowitz JA, McAlister FA. Aldosterone blockade and left ventricular dysfunction: a systematic review of randomized clinical trials. *Eur Heart J.* (2009) 30:469–77. doi: 10.1093/eurheartj/ehn543
251. Akpek M, Ozdogru I, Sahin O, Inanc M, Dogan A, Yazici C, et al. Protective effects of spironolactone against anthracycline-induced cardiomyopathy. *Eur J Heart Fail.* (2015) 17:81–9. doi: 10.1002/ejhf.196
252. Berliner D, Bauersachs J. Current drug therapy in chronic heart failure: the new guidelines of the european society of cardiology (ESC). *Korean Circ J.* (2017) 47:543–54. doi: 10.4070/kcj.2017.0030
253. Zinman B, Wanner C, Lachin JM, Fitchett D, Bluhmki E, Hantel S, et al. Empagliflozin, cardiovascular outcomes, and mortality in type 2 diabetes. *N Engl J Med.* (2015) 373:2117–28. doi: 10.1056/NEJMoa1504720
254. Butler J, Packer M, Filippatos G, Ferreira JP, Zeller C, Schnee J, et al. Effect of empagliflozin in patients with heart failure across the spectrum of left ventricular ejection fraction. *Eur Heart J.* (2022) 43:416–26. doi: 10.1093/eurheartj/ehab798
255. Pan D, Xu L, Chen P, Jiang H, Shi D, Guo M. Empagliflozin in patients with heart failure: a systematic review and meta-analysis of randomized controlled trials. *Front Cardiovasc Med.* (2021) 8:683281. doi: 10.3389/fcvm.2021.683281
256. Barış VÖ, Dinçsoy AB, Gedikli E, Zırh S, Müftüoğlu S, Erdem A. Empagliflozin significantly prevents the doxorubicin-induced acute cardiotoxicity *via* non-antioxidant pathways. *Cardiovasc Toxicol.* (2021) 21:747–58. doi: 10.1007/s12012-021-09665-y
257. Quagliariello V, De Laurentiis M, Rea D, Barbieri A, Monti MG, Carbone A, et al. The SGLT-2 inhibitor empagliflozin improves myocardial strain, reduces cardiac fibrosis and pro-inflammatory cytokines in non-diabetic mice treated with doxorubicin. *Cardiovasc Diabetol.* (2021) 20:150. doi: 10.1186/s12933-021-01346-y
258. Sabatino J, De Rosa S, Tammè L, Iaconetti C, Sorrentino S, Polimeni A, et al. Empagliflozin prevents doxorubicin-induced myocardial dysfunction. *Cardiovasc Diabetol.* (2020) 19:66. doi: 10.1186/s12933-020-01040-5
259. Oh CM, Cho S, Jang JY, Kim H, Chun S, Choi M, et al. Cardioprotective potential of an SGLT2 inhibitor against doxorubicin-induced heart failure. *Korean Circ J.* (2019) 49:1183–95. doi: 10.4070/kcj.2019.0180
260. Ren C, Sun K, Zhang Y, Hu Y, Hu B, Zhao J, et al. Sodium-Glucose cotransporter-2 inhibitor empagliflozin ameliorates sunitinib-induced cardiac dysfunction *via* regulation of AMPK-mTOR signaling pathway-mediated autophagy. *Front Pharmacol.* (2021) 12:664181. doi: 10.3389/fphar.2021.664181
261. Corradi F, Paolini L, De Caterina R. Ranolazine in the prevention of anthracycline cardiotoxicity. *Pharmacol Res.* (2014) 79:88–102. doi: 10.1016/j.phrs.2013.11.001
262. Cappetta D, Esposito G, Coppini R, Piegari E, Russo R, Ciuffreda LP, et al. Effects of ranolazine in a model of doxorubicin-induced left ventricle diastolic dysfunction. *Br J Pharmacol.* (2017) 174:3696–712. doi: 10.1111/bph.13791
263. Wang YX, Korth M. Effects of doxorubicin on excitation-contraction coupling in guinea pig ventricular myocardium. *Circ Res.* (1995) 76:645–53. doi: 10.1161/01.res.76.4.645
264. Tocchetti CG, Carpi A, Coppola C, Quintavalle C, Rea D, Campesan M, et al. Ranolazine protects from doxorubicin-induced oxidative stress and cardiac dysfunction. *Eur J Heart Fail.* (2014) 16:358–66. doi: 10.1002/ejhf.50
265. Riccio G, Antonucci S, Coppola C, D'Avino C, Piscopo G, Fiore D, et al. Ranolazine attenuates trastuzumab-induced heart dysfunction by modulating ROS production. *Front Physiol.* (2018) 9:38. doi: 10.3389/fphys.2018.00038
266. Minotti G, Menna P, Calabrese V, Greco C, Armento G, Annibali O, et al. Pharmacology of ranolazine versus common cardiovascular drugs in patients with early diastolic dysfunction induced by anthracyclines or nonanthracycline chemotherapeutics: a phase 2b minitrial. *J Pharmacol Exp Ther.* (2019) 370:197–205. doi: 10.1124/jpet.119.258178
267. Fisher PW, Salloum F, Das A, Hyder H, Kukreja RC. Phosphodiesterase-5 inhibition with sildenafil attenuates cardiomyocyte apoptosis and left ventricular dysfunction in a chronic model of doxorubicin cardiotoxicity. *Circulation.* (2005) 111:1601–10. doi: 10.1161/01.CIR.0000160359.49478.C2
268. Koka S, Das A, Zhu S-G, Durrant D, Xi L, Kukreja RC. Long-acting phosphodiesterase-5 inhibitor tadalafil attenuates doxorubicin-induced cardiomyopathy without interfering with chemotherapeutic effect. *J Pharmacol Exp Ther.* (2010) 334:1023–30. doi: 10.1124/jpet.110.170191
269. Jin Z, Zhang J, Zhi H, Hong B, Zhang S, Guo H, et al. Beneficial effects of tadalafil on left ventricular dysfunction in doxorubicin-induced cardiomyopathy. *J Cardiol.* (2013) 62:110–6. doi: 10.1016/j.jjcc.2013.03.018
270. Das A, Xi L, Kukreja RC. Phosphodiesterase-5 inhibitor sildenafil preconditions adult cardiac myocytes against necrosis and apoptosis. Essential role of nitric oxide signaling. *J Biol Chem.* (2005) 280:12944–55. doi: 10.1074/JBC.M404706200
271. Bartolomaeus H, Balogh A, Yakoub M, Homann S, Markó L, Höges S, et al. Short-chain fatty acid propionate protects from hypertensive cardiovascular damage. *Circulation.* (2019) 139:1407–21. doi: 10.1161/CIRCULATIONAHA.118.036652
272. Chen X-F, Chen X, Tang X. Short-chain fatty acid, acylation and cardiovascular diseases. *Clin Sci (Lond).* (2020) 134:657–76. doi: 10.1042/CS20200128
273. Russo M, Guida F, Paparo L, Trinchese G, Aitoro R, Avagliano C, et al. The novel butyrate derivative phenylalanine-butyramide protects from doxorubicin-induced cardiotoxicity. *Eur J Heart Fail.* (2019) 21:519–28. doi: 10.1002/ejhf.1439
274. Thai PN, Miller CV, King MT, Schaefer S, Veech RL, Chiamvimonvat N, et al. Ketone ester D-β-hydroxybutyrate-(R)-1,3 butanediol prevents decline in cardiac function in type 2 diabetic mice. *J Am Heart Assoc.* (2021) 10:e020729. doi: 10.1161/JAHA.120.020729
275. Liao S, Tang Y, Yue X, Gao R, Yao W, Zhou Y, et al. β-hydroxybutyrate mitigated heart failure with preserved ejection fraction by increasing treg cells *via* Nox2/GSK-3β. *J Inflamm Res.* (2021) 14:4697–706. doi: 10.2147/JIR.S331320
276. Liu Y, Wei X, Wu M, Xu J, Xu B, Kang L. Cardioprotective roles of β-hydroxybutyrate against doxorubicin induced cardiotoxicity. *Front Pharmacol.* (2020) 11:603596. doi: 10.3389/fphar.2020.603596
277. Oesterle A, Laufs U, Liao JK. Pleiotropic effects of statins on the cardiovascular system. *Circ Res.* (2017) 120:229–43. doi: 10.1161/CIRCRESAHA.116.308537
278. Davignon J. Beneficial cardiovascular pleiotropic effects of statins. *Circulation.* (2004) 109:III39–43. doi: 10.1161/01.CIR.0000131517.20177.5a
279. Acar Z, Kale A, Turgut M, Demircan S, Durna K, Demir S, et al. Efficiency of atorvastatin in the protection of anthracycline-induced cardiomyopathy. *J Am Coll Cardiol.* (2011) 58:988–9. doi: 10.1016/J.JACC.2011.05.025
280. Seicean S, Seicean A, Plana JC, Budd GT, Marwick TH. Effect of statin therapy on the risk for incident heart failure in patients with breast cancer receiving anthracycline chemotherapy: an observational clinical cohort study. *J Am Coll Cardiol.* (2012) 60:2384–90. doi: 10.1016/j.jacc.2012.07.067
281. Chotenimitkhun R, D'Agostino R, Lawrence JA, Hamilton CA, Jordan JH, Vasu S, et al. Chronic statin administration may attenuate early anthracycline-associated declines in left ventricular ejection function. *Can J Cardiol.* (2015) 31:302–7. doi: 10.1016/j.cjca.2014.11.020
282. Abdel-Qadir H, Bobrowski D, Zhou L, Austin PC, Calvillo-Argüelles O, Amir E, et al. Statin exposure and risk of heart failure after anthracycline- or trastuzumab-based chemotherapy for early breast cancer: a propensity score—matched cohort study. *J Am Heart Assoc.* (2021) 10:e018393. doi: 10.1161/JAHA.119.018393
283. Calvillo-Argüelles O, Abdel-Qadir H, Michalowska M, Billia F, Suntheralingam S, Amir E, et al. Cardioprotective effect of statins in patients with HER2-positive breast cancer receiving trastuzumab therapy. *Can J Cardiol.* (2019) 35:153–9. doi: 10.1016/j.cjca.2018.11.028
284. Fukazawa R, Miller TA, Kuramochi Y, Frantz S, Kim YD, Marchionni MA, et al. Neuregulin-1 protects ventricular myocytes from anthracycline-induced apoptosis *via* erbB4-dependent activation of PI3-kinase/Akt. *J Mol Cell Cardiol.* (2003) 35:1473–9. doi: 10.1016/j.yjmcc.2003.09.012

285. Bian Y, Sun M, Silver M, Ho KKL, Marchionni MA, Caggiano AO, et al. Neuregulin-1 attenuated doxorubicin-induced decrease in cardiac troponins. *AJP Hear Circ Physiol.* (2009) 297:H1974–83. doi: 10.1152/ajpheart.01010.2008
286. Vasti C. Neuregulin-1/erbB activities with focus on the susceptibility of the heart to anthracyclines. *World J Cardiol.* (2014) 6:653. doi: 10.4330/wjc.v6.i7.653
287. Jay SM, Murthy AC, Hawkins JF, Wortzel JR, Steinhauser ML, Alvarez LM, et al. An engineered bivalent neuregulin protects against doxorubicin-induced cardiotoxicity with reduced proneoplastic potential. *Circulation.* (2013) 128:152–61. doi: 10.1161/CIRCULATIONAHA.113.002203
288. Demetri GD, Griffin JD. Granulocyte colony-stimulating factor and its receptor. *Blood.* (1991) 78:2791–808. doi: 10.1016/S0083-6729(01)63006-1
289. Li L, Takemura G, Li Y, Miyata S, Esaki M, Okada H, et al. Granulocyte colony-stimulating factor improves left ventricular function of doxorubicin-induced cardiomyopathy. *Lab Invest.* (2007) 87:440–55. doi: 10.1038/labinvest.3700530
290. Hamed S, Barshack I, Luboshits G, Wexler D, Deutsch V, Keren G, et al. Erythropoietin improves myocardial performance in doxorubicin-induced cardiomyopathy. *Eur Heart J.* (2006) 27:1876–83. doi: 10.1093/eurheartj/ehl044
291. Xu Y-J, Arneja AS, Tappia PS, Dhalla NS. The potential health benefits of taurine in cardiovascular disease. *Exp Clin Cardiol.* (2008) 13:57–65.
292. Huang W-P, Yin W-H, Chen J-S, Huang P-H, Chen J-W, Lin S-J. Fenofibrate attenuates doxorubicin-induced cardiac dysfunction in mice *via* activating the eNOS/EPC pathway. *Sci Rep.* (2021) 11:1159. doi: 10.1038/s41598-021-80984-4
293. Galán-Arriola C, Villena-Gutiérrez R, Higuero-Verdejo MI, Díaz-Rengifo IA, Pizarro G, López GJ, et al. Remote ischaemic preconditioning ameliorates anthracycline-induced cardiotoxicity and preserves mitochondrial integrity. *Cardiovasc Res.* (2021) 117:1132–43. doi: 10.1093/cvr/cvaa181
294. Bergmann O, Zdunek S, Felker A, Salehpour M, Alkass K, Bernard S, et al. Dynamics of cell generation and turnover in the human heart. *Cell.* (2015) 161:1566–75. doi: 10.1016/j.cell.2015.05.026
295. Bergmann O, Bhardwaj RD, Bernard S, Zdunek S, Barnabé-Heider F, Walsh S, et al. Evidence for cardiomyocyte renewal in humans. *Science.* (2009) 324:98–102. doi: 10.1126/science.1164680
296. Bongiovanni C, Sacchi F, Da Pra S, Pantano E, Miano C, Morelli MB, et al. Reawakening the intrinsic cardiac regenerative potential: molecular strategies to boost dedifferentiation and proliferation of endogenous cardiomyocytes. *Front Cardiovasc Med.* (2021) 8:750604. doi: 10.3389/fcvm.2021.750604
297. Eschenhagen T, Force T, Ewer MS, de Keulenaer GW, Suter TM, Anker SD, et al. Cardiovascular side effects of cancer therapies: a position statement from the heart failure association of the European society of cardiology. *Eur J Heart Fail.* (2011) 13:1–10. doi: 10.1093/eurjhf/hfq213

Conflict of Interest: The authors declare that the research was conducted in the absence of any commercial or financial relationships that could be construed as a potential conflict of interest.

Publisher's Note: All claims expressed in this article are solely those of the authors and do not necessarily represent those of their affiliated organizations, or those of the publisher, the editors and the reviewers. Any product that may be evaluated in this article, or claim that may be made by its manufacturer, is not guaranteed or endorsed by the publisher.

frontiers | Frontiers in Cardiovascular Medicine

ORIGINAL RESEARCH
published: 20 May 2022
doi: 10.3389/fcvm.2022.882167

Immune Checkpoint Inhibitor-Associated Cardiotoxicity in Solid Tumors: Real-World Incidence, Risk Factors, and Prognostic Analysis

*Xue Chen, Aimin Jiang, Rui Zhang, Xiao Fu, Na Liu, Chuchu Shi, Jingjing Wang, Xiaoqiang Zheng, Tao Tian, Xuan Liang, Zhiping Ruan and Yu Yao**

Department of Medical Oncology, The First Affiliated Hospital of Xi'an Jiaotong University, Xi'an, China

Background: Immune checkpoint inhibitors (ICIs) have achieved acknowledged progress in cancer therapy. However, ICI-associated cardiotoxicity as one of the most severe adverse events is potentially life-threatening, with limited real-world studies reporting its predictive factors and prognosis. This study aimed to investigate the real-world incidence, risk factors, and prognosis of ICI-related cardiotoxicity in patients with advanced solid tumors.

Methods: Electronic medical records from patients with advanced solid tumors receiving ICIs in the First Affiliated Hospital of Xi'an Jiaotong University were retrospectively reviewed. All patients were divided into the cardiotoxicity group and control group, with logistic regression analysis being implemented to identify potential risk factors of ICI-related cardiotoxicity. Furthermore, survival analysis was also performed to investigate the prognosis of patients with ICI-related cardiotoxicity.

Results: A total of 1,047 participants were enrolled in this retrospective study. The incidence of ICI-related cardiotoxicity in our hospital is 7.0%, while grade 3 and above cardiotoxicity was 2.4%. The logistic regression analysis revealed that diabetes mellitus [odds ratio (OR):1.96, 95% confidence Interval (CI): 1.05–3.65, $p = 0.034$] was an independent risk factor, whereas baseline lymphocyte/monocyte ratio (LMR) (OR: 0.59, 95% CI: 0.36–0.97, $p = 0.037$) was the protective factor of ICI-related cardiotoxicity. Survival analysis indicated that severe cardiotoxicity (≥grade 3) was significantly correlated with bleak overall survival (OS) than mild cardiotoxicity (≤grade 2) (8.3 months vs. not reached, $p = 0.001$). Patients with ICI-related overlap syndrome had poorer overall survival than patients with mere cardiotoxicity (9.4 vs. 24.7 months, $p = 0.033$). However, the occurrence of ICI-related cardiotoxicity was not significantly associated with the OS of overall population with solid tumors. Subgroup analysis showed that lung cancer and PD-L1 usage were significantly correlated with a higher incidence of severe cases.

Conclusion: Immune checkpoint inhibitor-related cardiotoxicity is more common in the real-world setting than the previously published studies. Diabetes mellitus and baseline

OPEN ACCESS

Edited by:
Feng Cao,
People's Liberation Army General Hospital, China

Reviewed by:
Alessandra Cuomo,
Federico II University Hospital, Italy
Irma Bisceglia,
San Camillo-Forlanini Hospital, Italy

****Correspondence:***
Yu Yao
yaoyu123@xjtufh.edu.cn

Specialty section:
This article was submitted to Cardio-Oncology, a section of the journal Frontiers in Cardiovascular Medicine

Received: *23 February 2022*
Accepted: *20 April 2022*
Published: *20 May 2022*

Citation:
Chen X, Jiang A, Zhang R, Fu X, Liu N, Shi C, Wang J, Zheng X, Tian T, Liang X, Ruan Z and Yao Y (2022) Immune Checkpoint Inhibitor-Associated Cardiotoxicity in Solid Tumors: Real-World Incidence, Risk Factors, and Prognostic Analysis. Front. Cardiovasc. Med. 9:882167. doi: 10.3389/fcvm.2022.882167

LMR are the potential predictive biomarkers of ICI-related cardiotoxicity. Although ICI-related cardiotoxicity is not correlated with the prognosis of these patients in our cohort, a systematic and comprehensive baseline examination and evaluation should be performed to avoid its occurrence.

Keywords: solid tumor, cardiotoxicity, rechallenge, risk factors, immune checkpoint inhibitor (ICI), prognosis

INTRODUCTION

Immune checkpoint inhibitors (ICIs) mainly act on the activation of T cells to fight against tumor cells. There are currently FDA-approved drugs that target cytotoxic T-lymphocyte-associated antigen-4 (CTLA-4), programmed cell death protein 1 (PD-1), and programmed cell death ligand 1 (PD-L1). Although ICI-related adverse effects are overall less severe than chemotherapy, there are potentially lethal adverse effects, such as cardiotoxicity, neuromuscular toxicity, and pulmonary toxicity.

The first case of fatal ICI-related myocarditis was reported by Läubli et al. in 2015 (1), in a 73-year-old patient with metastatic melanoma who developed ICI-associated myocarditis after receiving pembrolizumab, leading to acute heart failure. Two cases of fulminant myocarditis were reported in 2016. Both patients became symptomatic within 2 weeks of administration and aggravated rapidly, leading to death within a short period despite the admission of high-dose glucocorticoid and supportive care. These two cases of severe cardiotoxicity warned clinicians of the security of ICIs (2).

Cardiotoxicity associated with ICIs is broadly classified into myocarditis, pericarditis, and arrhythmia. Other clinical manifestations, such as hypertension, Takotsubo-like syndrome, myocardial ischemia, and myocardial infarction, are less reported (3, 4). In addition, some studies have roughly divided them into inflammatory (including myocarditis, pericarditis, etc.) and non-inflammatory (arrhythmia, myocardial infarction, etc.).

Early studies showed that the incidence of ICI-related cardiotoxicity is less than 1% (5). However, as Ganatra et al. (6) stated, the increasing application of ICIs in real-world and the diverse presentation of cardiotoxicity suggest a higher incidence of cardiotoxicity than previously reported. In addition, subclinical cases and increased awareness of toxicity may also be the contributing factors. Among these classifications, myocarditis maintained the highest incidence and fatality rate, as well as the worst prognosis. However, the presentations of cardiotoxicity in real-world were not separated. It is not rare for myocarditis to occur simultaneously with arrhythmia or pericarditis. Studies have found that approximately 19% of patients with pathologically defined cardiotoxicity developed arrhythmias (7). Two patients with fulminant myocarditis reported in 2016 also developed complete atrioventricular conduction block (2). The pathophysiological manifestation suggested the infiltrated T cells and macrophages in the conduction system. As reported, atrial fibrillation, ventricular arrhythmias, and conduction disturbances were detected in 17–30% of patients with ICI-related cardiotoxicity, of whom 3–13% had mere arrhythmias without myocarditis (8). Although the mechanism is unclear, the investigators concluded that there may be underlying undiagnosed myocarditis (8). There are limited studies on ICI-related pericardial disease. In addition, the incidence is unclear due to the lack of cardiovascular monitoring during ICI clinical trials but maybe more common than previously recognized. In an evaluation based on VigiBase, Salem et al. included 95 cases of pericardial disease associated with ICI, of which 60% were severe and 21% were associated with death (7). Unlike myocarditis, the incidence of pericarditis did not increase significantly with combination immunotherapy. In addition, the study found that more than half of the cases with pericardial diseases were reported in patients with lung cancer (7). Based on the preclinical and clinical studies, several possible influencing factors of ICI-related pericardial involvement were proposed. Given the disproportionately high incidence of pericardial disease in patients with lung cancer and synergy between radiotherapy and immunotherapy is considered a possible driver.

In the previous studies, autoimmune disease, prior heart disease, and combined ICI therapy can be the probable risk factors. Results are mostly derived from databases based on overall irAEs with few real-world studies based on cardiotoxicity. Therefore, we conducted a real-world retrospective study based on the whole immunotherapy population to explore the risk factors for ICI-related cardiotoxicity.

MATERIALS AND METHODS

Patients

Patients diagnosed with advanced solid tumors who were hospitalized from January 2020 to June 2021 at the departments of the medical oncology, surgical oncology, and radiation oncology at the First Affiliated Hospital of Xi'an Jiaotong University were included. We retrospectively screened patients into two groups according to whether cardiotoxicity happened during the administration of ICIs. Suspected cases were assessed mainly according to Bonaca diagnostic criteria (9). There were also cases that does not meet the criterion. In addition to that, we also consider ICI-related myocarditis according to the following two points:

1. Concurrent multi-organ damage with abnormal cardiac biomarkers responding to corticosteroids. Infection and autoimmune diseases were excluded.
2. Dynamical change in cardiac biomarker with ICI medication responding to corticosteroids. Infection and autoimmune diseases were excluded.

Immune checkpoint inhibitor-related pericarditis and arrhythmia were diagnosed according to Naranjo score: Suspected patients who suffered from cardiac damage during ICI therapy with a Naranjo scores $\geq$ 5 were included in the cardiotoxicity group.

Patients were categorized as "severe" cardiotoxicity if they displayed a grade 3–5 toxicity according to criteria adapted from the Common Terminology Criteria for Adverse Events V.5.0 (**Table 1**). Patients were categorized as "mild" cardiotoxicity if they displayed a grade 1–2 toxicity.

Statistical Analysis

Continuous variables are statistically described by means ± standard deviation (subject to normal distribution) or interquartile spacing (not subject to normal distribution); categorical variables are expressed in terms of number and percentage of cases. The SW test was used for the normality test, and one-way ANOVA was used for the variance homogeneity test. If the continuous variable obeys the normal distribution and the variance is homogeneous, the independent sample *t*-test is used, otherwise, the non-parametric rank sum test is used for statistical analysis. Categorical variables were statistically analyzed by the chi-square test or Fisher's exact probability. All patients were divided into occurrence group and non-occurrence group based on whether cardiotoxicity occurred during ICI treatment, with the univariate logistic regression analysis being exploited to investigate the possible risk factors of cardiotoxicity. Ultimately, the variables with $p < 0.05$ in univariate analysis were included in multivariate logistic regression analysis. All statistical analyses were performed in SPSS 23.0 and R 4.1.1 for Windows 64.0. Multiple imputations were used to supplement missing data.

Ethical Approval and Informed Consent

This study was conducted in strict accordance with the requirements of the Declaration of Helsinki. Our research also passed the ethics review of the First Affiliated Hospital of Xi'an Jiaotong University (no: XJTU1AF2020LSK-262).

RESULTS

Characteristics of the Whole Population

From January 2020 to July 2021, a total of 1,492 patients with advanced solid tumors were hospitalized and treated with ICIs in the departments of medical oncology, surgical oncology, and radiation oncology. A total of 391 patients who did not meet the requirements were excluded, and a total of 1,101 patients who met the research criteria were screened. There were 127 patients with cardiac damage, of which 54 patients did not meet the diagnostic criteria. In the end, 974 patients did not develop cardiotoxicity, and 73 patients developed ICI-related cardiotoxicity, including 25 patients with severe cardiotoxicity and 48 patients with mild cardiotoxicity (**Table 2**).

Among the 1,047 patients treated with ICI, there were 713 male patients (68.1%) and 334 female patients (31.9%). Most of the patients were younger than 65 years (673 cases, 64.3%), and the physical performance score was mostly 0–1 (866 cases, 82.7%). In terms of cancer types, respiratory tumors (360 cases, 34.4%) and digestive tumors (496 cases, 47.4%) accounted for the majority, followed by urethral tumors (83 cases, 7.9%) and malignant melanoma (43 cases, 3.9%). Other tumor types included skin tumors, mediastinal tumors, head and neck tumors, genital neoplasm, sarcomas, and other tumor types. There were 220 (44.4%) gastrointestinal patients involved in the digestive tumor group, whereas 78 patients (21.7%) with small-cell lung cancer were involved in the respiratory tumor groups. Heart disease (74 cases, 7.1%), diabetes (115 cases, 10.9%), and hypertension (241 cases, 23.0%) were the common comorbidities. There were 379 patients (36.2%) with a history of smoking and 89 patients (8.5%) with a family history of tumors. Most patients received ICI combined chemotherapy (975 cases, 93.1%). PD-1 was the most predominantly used ICIs in our cohort, accounting for 92.0% of cases. In the case of later-line immunotherapy, prior treatment included chemotherapy, radiotherapy, targeted therapy, and antiangiogenic therapy. During the course of immunotherapy, 128 patients developed ICI-associated pneumonia (12.2%), and 380 patients developed ICI-associated thyroid dysfunction (36.3%).

Risk Factors of Immune Checkpoint Inhibitor-Related Cardiotoxicity

Among the enrolled patients, 73 (7.0%) developed cardiotoxicity, including 48 mild cases (4.6%) and 25 severe cases (2.4%). Among the 115 patients with combined diabetes, 14 developed cardiotoxicity (12.2%). Whereas the occurrence rate of ICI-related cardiotoxicity among patients without diabetes was 6.3%, difference between these two groups was statistically significant ($p = 0.033$). Besides, patients who developed cardiotoxicity have lower LMR ($p = 0.01$). Respiratory tumors maintained the highest incidence of cardiotoxicity among all cancer types (8.6%), but there was no significant difference in the incidence of cardiotoxicity among tumor types. Combined cardiac diseases, ICI agents, history of previous antitumor therapy, and treatment modes have no correlation with the occurrence of cardiotoxicity. In terms of baseline laboratory levels, patients who suffered from cardiotoxicity have a lower lymphocyte ratio than patients without cardiotoxicity. But the difference was not statistically significant ($p = 0.066$). In addition, our research showed that the occurrence of ICI-related pneumonia ($p = 0.005$) and thyroid dysfunction ($p < 0.005$) during the course of ICI treatment were significantly associated with the occurrence of cardiotoxicity. Although most of the other two toxicities appear before cardiotoxicity, we cannot yet explain the relationship between ICI-related cardiotoxicity and ICI-related pneumonia or thyroid dysfunction. But this correlation suggests a link between adverse effects of different systems, and the presence of one toxicity may warn of another that may be more serious.

The univariate logistic regression analysis found that combined diabetes (OR = 2.05, 95% CI: 1.07–3.71, $p = 0.023$) may be a risk factor for cardiotoxicity, whereas lower baseline LMR (OR = 0.58, 95% CI: 0.35–0.93, $p = 0.027$) may be a protective factor (**Figure 1**). Ultimately, the multivariate regression analysis suggested that diabetes (OR = 1.96, 95% CI: 1.05–3.65, $p = 0.034$) was an independent risk factor for

TABLE 1 | Criteria for myocarditis severity scoring.

Grade	Criteria
1[a]	Elevated biomarkers without symptoms[b] (e.g., dyspnea, chest pain, etc.)
2	Elevated biomarkers without symptoms but not requiring patient hospitalization
3	Elevated biomarkers without symptoms requiring patient hospitalization (not requiring intensive care unit level of care); abnormal cardiovascular diagnostic studies (echocardiography showing reduction in LV function or wall motion abnormalities; abnormal cardiac MRI)
4	Deterioration of grade 3 clinical status or requirement for ICU level of care for cardiac symptoms with evidence of decreased cardiac output (cardiogenic shock) or arrhythmia
5	Death of the patient refractory to medical therapy

LV, left ventricular; MRI, magnetic resonance imaging; ICU, intensive care unit.
[a]CTCAE5.0 released in 2017 does not include grade 1 myocarditis. But this criterion cannot reflect the whole situation of the occurrence of myocarditis. This table is based on Bonaca and CTCAE4.0.
[b]Biomarkers for myocarditis are markers of myonecrosis, including cardiac troponin, CK-MB, or total CK.

the occurrence of ICI-related cardiotoxicity. In addition, lower baseline LMR (OR = 0.59, 95% CI: 0.36–0.97, $p = 0.037$) was a protective factor (**Figure 1**).

Severity of Myocarditis

The population with ICI-related cardiotoxicity included 48 mild cases and 25 severe cases (**Table 3**). Among them, 4 patients (5%) died in hospital. All in-hospital died patients were severe cardiotoxicity. When cardiotoxicity occurs, echocardiography was abnormal in 20 cases (26.3%), mainly with abnormal wall motion. A total of 24 patients (31.6%) had an abnormal electrocardiogram, including ST-T abnormality, conduction block, and other changes. In addition, 30 patients (41.1%) in the subgroup suffered from cardiotoxicity and concurrent ICI damage of other systems, among which abnormal liver function, myositis, skin rash, and abnormal thyroid function were more common.

Cardiotoxicity happened mainly in men (56, 76.7%). In terms of cancer types, the proportion of severe cases in respiratory tumors was significantly higher than in other tumors ($p = 0.045$), whereas the proportion in digestive tumors was significantly lower than other tumors ($p = 0.014$). The ICI agents were mainly PD-1 (65, 89.0%), of which 19 cases (29.2%) were severe, whereas 8 cases received PD-L1, and 6 cases (75.0%) were severe. The difference between the two groups was statistically significant ($p = 0.008$). We did not find that inflammatory parameters, such as NLR, PLR, and LMR, were associated with the severity of cardiotoxicity. Other indicators, including ECOG score, comorbidities, smoking history, family history, prior antitumor therapy, and treatment mode, were not significantly associated with the severity of cardiotoxicity. In addition, unlike the general population, the occurrence of ICI-related thyroid dysfunction ($p = 0.120$) and ICI-related pneumonia ($p = 0.327$) was not significantly associated with the severity of cardiotoxicity. There was no statistically significant difference in the occurrence time of mild and severe cardiotoxicities (median occurrence time: 105 vs. 134 days, $p = 0.345$) (**Figure 2**).

Survival Analysis

Survival analysis was performed in patients with or without cardiotoxicity. We investigated the difference with overall survival in these patients. The median follow-up time was 19.0 months. There was no significant difference with median overall survival time (mOS) between the two groups without cardiotoxicity and those with cardiotoxicity (29.1 vs. 24.7 months, $p = 0.184$) (**Figure 3A**). The mOS of severe cardiotoxicity was 8.3 months, while the mOS of mild cardiotoxicity was not reached ($p = 0.001$) (**Figure 3B**).

Survival analysis was performed on the subgroups of patients with respiratory tumors and digestive tumors due to different prognoses of different tumor types. There was no statistically significant difference between the two groups with or without cardiotoxicity in the respiratory tumors ($p = 0.360$) (**Figure 4A**). The mOS between the two groups without cardiotoxicity in the digestive system and those with cardiotoxicity was 21.6 and 15.3 months, respectively (**Figure 4B**). But the difference was also not statistically significant ($p = 0.509$). For all patients with cardiotoxicity, mOS was 17.0 months.

In addition, we also compared the survival difference between the groups with mere cardiotoxicity and those with concurrent cardiotoxicity and other toxicities. The mOS with mere cardiotoxicity was 24.7 months, and the mOS in the group with overlap syndrome was 9.4 months (**Figure 5A**). The difference was statistically significant ($p = 0.033$). In 2020, Dolladille et al. (10) analyzed the clinical characteristics of early and late cardiac adverse reactions through retrospective analysis of multicenter cases and data from the VigiBase using 90 days as a cutoff. They found differences in the characteristics of early and late cardiac cardiotoxicities. We furtherly plotted the survival curves of the two groups of patients with the occurrence time before 90 days and after 90 days. However, there was no significant difference between the two groups (**Figure 5B**).

Immune Checkpoint Inhibitor Rechallenge

Current guidelines suggest that restarting ICI is not recommended for grade 2 and above cardiotoxicity. We also strictly follow the recommendations in our clinical work. However, the complexity of real-world research results in patient diversity. In our study, some patients persisted in restarting ICI despite being fully informed of the risks. In the follow-up of patients who developed cardiotoxicity, there were 5 additional patients with grades 2 and 3 myocarditis who readmitted ICI after recovery (**Figure 6**). Only one of the five patients who

TABLE 2 | Characteristics of the whole population.

Characteristics	Groups	Number of patients (ratio)[a]		
		Without cardiotoxicity (*N* = 974)	With cardiotoxicity (*N* = 73)	*p*-value
Weight		62.2 ± 11.2	63.2 ± 9.4	0.447
Age		59.5 ± 11.2	59.8 ± 11.7	0.835
Gender	Male	657 (67.5%)	56 (76.7%)	0.132
	Female	317 (32.5%)	17 (23.3%)	
Cardiac disease	No	906 (93.0%)	67 (91.8%)	0.872
	Yes	68 (7.0%)	6 (8.2%)	
Hypertension	No	750 (77.0%)	56 (76.7%)	1.000
	Yes	224 (23.0%)	17 (23.3%)	
Diabetes	No	873 (89.6%)	59 (80.8%)	0.033
	Yes	101 (10.4%)	14 (19.2%)	
Cigarette	No	625 (64.2%)	43 (58.9%)	0.437
	Yes	349 (35.8%)	30 (41.1%)	
Family history	No	894 (91.8%)	64 (87.7%)	0.318
	Yes	80 (8.2%)	9 (12.3%)	
Respiratory tumors		329 (33.8%)	31 (42.5%)	0.159
Digestive tumors		467 (47.9%)	29 (39.7%)	0.183
Urinary tract tumors		74 (7.6%)	9 (12.3%)	0.173
Malignant melanoma		39 (4.0%)	2 (2.7%)	1.000
Other tumors[b]		65 (6.7%)	2 (2.7%)	0.315
Prior chemotherapy	No	482 (49.5%)	38 (52.1%)	0.763
	Yes	492 (50.5%)	35 (47.9%)	
Prior antiangiogenic therapy	No	837 (85.9%)	62 (84.9%)	0.950
	Yes	137 (14.1%)	11 (15.1%)	
Treatment line	First-line	486 (49.9%)	39 (53.4%)	0.646
	Post-line	488 (50.1%)	34 (46.6%)	
Lung metastasis	No	750 (77.0%)	60 (82.2%)	0.380
	Yes	224 (23.0%)	13 (17.8%)	
Liver metastasis	No	731 (75.1%)	48 (65.8%)	0.106
	Yes	243 (24.9%)	25 (34.2%)	
Brain metastasis	No	909 (93.3%)	72 (98.6%)	0.121
	Yes	65 (6.7%)	1 (1.4%)	
Bone metastasis	No	764 (78.4%)	60 (82.2%)	0.544
	Yes	210 (21.6%)	13 (17.8%)	
ECOG	0–1	803 (82.4%)	63 (86.3%)	0.496
	2–3	171 (17.6%)	10 (13.7%)	
Treatment	ICI monotherapy	66 (6.8%)	6 (8.2%)	0.818
	ICI combined with chemotherapy	908 (93.2%)	67 (91.8%)	
ICI agent	PD-1	898 (92.2%)	65 (89.0%)	0.463
	PD-L1	76 (7.8%)	8 (11.0%)	
LDH (U/L)	<250	505 (70.0%)	41 (70.7%)	1.000
	≥250	216(30.0%)	17 (29.3%)	
CK (U/L)	<310	701 (98.9%)	56 (98.2%)	1.000
	≥310	8 (1.1%)	1 (1.8%)	
CK-MB (U/L)	<24	599 (84.5%)	45 (78.9%)	0.362
	≥24	110(15.5%)	12 (21.1%)	
Hemoglobin (g/L; normal range 115–150)		126.7 ± 19.9	129.2 ± 18.8	0.296
Platelet count ($\times 10^9$/L; normal range 125–350)		234.3 ± 97.0	214.3 ± 98.5	0.091
White-cell count ($\times 10^9$/L; normal range 4.0–10.0)		6.9 ± 3.3	6.9 ± 2.6	0.892
Neutrophil count ($\times 10^9$/L; normal range 1.8–6.3)		4.9 ± 3.6	4.9 ± 2.5	0.937
Lymphocyte count ($\times 10^9$/L; normal range 1.1–3.2)		1.4 ± 0.6	1.4 ± 0.5	0.203
Monocytes (10^9/L; normal range 0.1–0.6)		0.4 ± 0.2	0.5 ± 0.4	0.166
Eosinophils (10^9/L; normal range 0.02–0.52)		0.2 ± 0.5	0.2 ± 0.3	0.482
Albumin (g/L; normal range 40–55)		39.2 ± 4.6	38.7 ± 4.6	0.379
Globulin (g/L; normal range 20–40)		29.5 ± 5.2	29.5 ± 5.0	0.958
TC (mmol/L; 3.10–5.69)		4.3 ± 1.0	4.5 ± 1.3	0.428
PLR		197.3 ± 156.9	183.3 ± 116.8	0.341
NLR		4.2 ± 4.6	4.4 ± 4.2	0.653
LMR		3.9 ± 3.4	3.3 ± 1.7	0.010
A/G		1.4 ± 0.3	1.3 ± 0.3	0.442
Neutrophil ratio (normal range 40–75%)		68.8% ± 39.6%	68.7% ± 10.0%	0.923
Lymphocyte ratio (normal range 20–50%)		23.0% ± 10.2%	21.1% ± 8.3%	0.066

ECOG, Eastern Cooperative Oncology Group; ICI, immune checkpoint inhibitor; LDH, lactate dehydrogenase; CK, creatine kinase; TC, total cholesterol; PLR, platelet to lymphocyte ratio; NLR, neutrophil to lymphocyte ratio; LMR, lymphocyte to monocyte ratio; A/G, albumin to globulin ratio.

[a] *Continuous variables are expressed as mean and standard deviation.*

[b] *Others include skin tumors, mediastinal tumors, head and neck tumors, genital neoplasm, sarcomas, and other tumor types.*

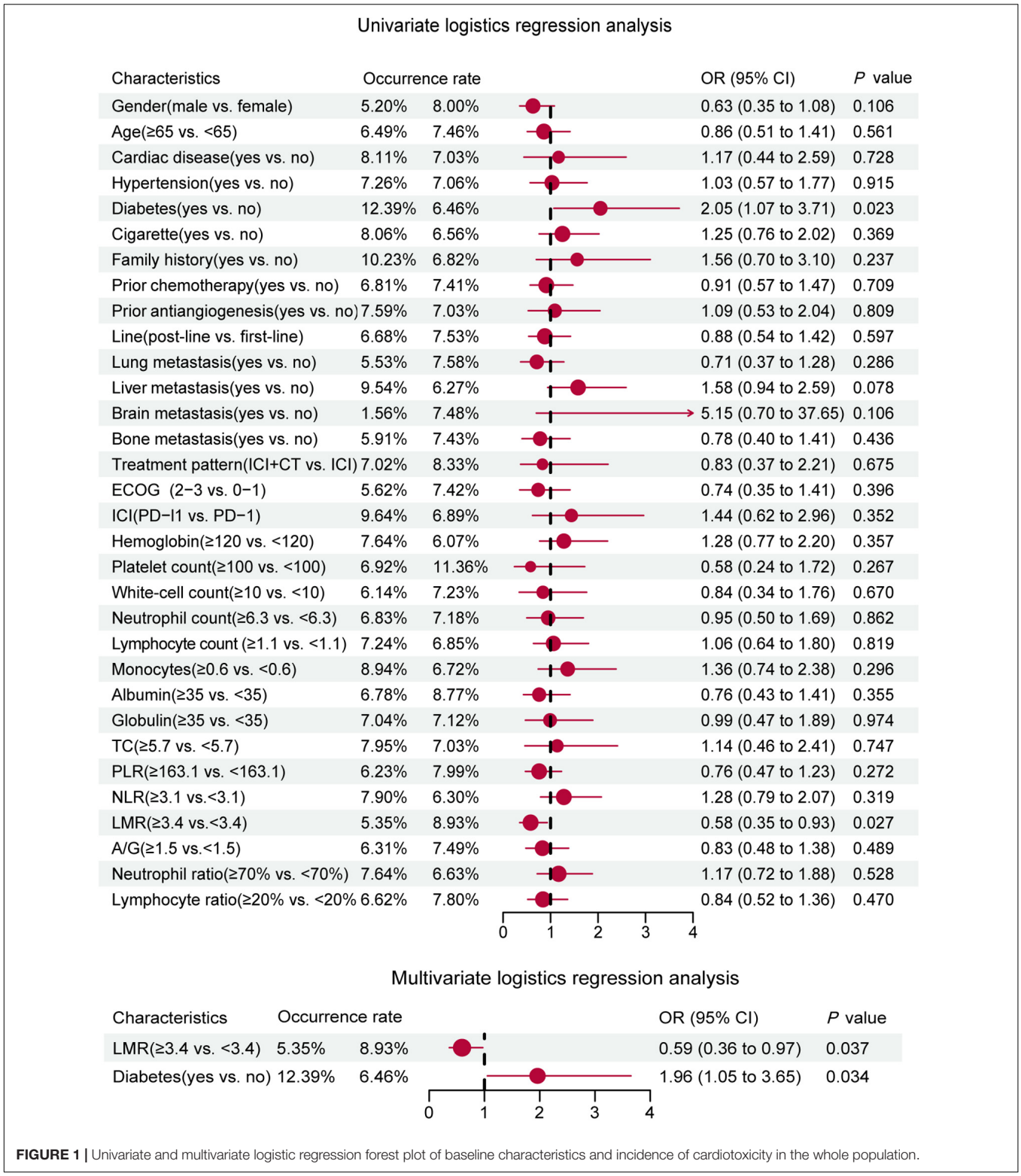

FIGURE 1 | Univariate and multivariate logistic regression forest plot of baseline characteristics and incidence of cardiotoxicity in the whole population.

had grade 3 myocarditis suffered grade 2 myocarditis after the rechallenge of ICI. No other grade 3 and above ICI toxicity were found in all patients. Following up for more than 1 year, only one case died of disease progression. The remaining patients were all alive. According to our investigation, the ICI rechallenge seems relatively secure. However, considering the small sample size in our cohort, more relevant studies are needed in the future to identify the safety of ICI rechallenge.

TABLE 3 | Characteristics of patients with cardiotoxicity.

Characteristics	Groups	≤Grade 2 (*N* = 48)	≥Grade3 (*N* = 25)	*p*-value
Age	<65 years old	33 (68.8%)	16 (64%)	0.883
	≥65 years old	15 (31.2%)	9 (36%)	
Gender	Male	38 (79.2%)	18 (72%)	0.692
	Female	10 (20.8%)	7 (28%)	
ECOG	0–1	43 (89.6%)	20 (80%)	0.440
	2–3	5 (10.4%)	5 (20%)	
Cardiac disease	No	44 (91.7%)	23 (92%)	1.000
	Yes	4 (8.3%)	2 (8%)	
Diabetes	No	38 (79.2%)	21 (84%)	0.854
	Yes	10 (20.8%)	4 (16%)	
Respiratory tumors		16 (33.3%)	15 (60%)	0.045
Digestive tumors		24 (50%)	5 (20%)	0.014
Urinary tract tumors		6 (12.5%)	3 (12%)	0.476
Malignant melanoma		1 (2.1%)	1 (4%)	-
Other tumors		1 (2.1%)	1 (4%)	-
Treatment[a]	ICI monotherapy	4 (8.3%)	2 (8%)	1.000
	ICI combined with chemotherapy	44 (91.7%)	23 (92%)	
ICI	PD-1	46 (95.8%)	19 (76%)	0.029
	PD-L1	2 (4.2%)	6 (24%)	
Neutrophil count ($\times 10^9$/L; normal range 1.8–6.3)	<6.3	38 (79.2%)	21 (84%)	0.854
	≥6.3	10 (20.8%)	4 (16%)	
Lymphocyte count ($\times 10^9$/L; normal range 1.1–3.2)	<1.1	14 (29.2%)	9 (36%)	0.741
	≥1.1	34 (70.8%)	16 (64%)	
Monocytes (10^9/L; normal range 0.1–0.6)	<0.6	35 (72.9%)	22 (88%)	0.238
	≥0.6	13 (27.1%)	3 (12%)	
PLR	<163.1	28 (58.3%)	13 (52%)	0.788
	≥163.1	20 (41.7%)	12 (48%)	
NLR	<3.1	20 (41.7%)	12 (48%)	0.788
	≥3.1	28 (58.3%)	13 (52%)	
LMR	<3.4	31 (64.6%)	14 (56%)	0.644
	≥3.4	17 (35.4%)	11 (44%)	
A/G	<1.5	36 (75%)	16 (64%)	0.476
	≥1.5	12 (25%)	9 (36%)	
Neutrophil ratio (normal range 40–75%)	<70%	22 (45.8%)	14 (56%)	0.563
	≥70%	26 (54.2%)	11 (44%)	
Lymphocyte ratio (normal range 20–50%)	<20%	22 (45.8%)	11 (44%)	1.000
	≥20%	26 (54.2%)	14 (56%)	

ECOG, Eastern Cooperative Oncology Group; ICI, immune checkpoint inhibitor; PLR, platelet to lymphocyte ratio; NLR, neutrophil to lymphocyte ratio; LMR, lymphocyte to monocyte ratio; A/G, albumin to globulin ratio.

[a]*Others include prostatic cancer, mediastinal tumor, head and neck squamous cell carcinoma, sarcoma.*

DISCUSSION

We found that the incidence of cardiotoxicity was 7.0%, which was higher than the previously reported. By collecting the cardiovascular risk factors of the enrolled patients, we found that diabetes was an independent risk factor for the occurrence of cardiotoxicity. This conclusion can be seen in the retrospective study of Mahmood et al. (11). Through a multicenter retrospective study of 35 patients, they found that myocarditis was more common in patients with diabetes mellitus, especially in patients receiving a combination of ICI therapy. Although they ultimately failed to prove it an independent risk factor, their research suggested a certain direction. In our analysis, an exact association of diabetes with the development of cardiotoxicity was found. However, we did not find an association between other cardiovascular risk factors, such as hypertension and the occurrence of cardiotoxicity.

The effect of diabetes on the development of ICI-related cardiotoxicity may be related to the long-term chronic inflammation in patients with diabetes. Till now, diabetes has been regarded as a chronic inflammatory disease. The high-glucose environment of diabetes significantly increases the cytokines, such as interleukin 4(IL-4), interleukin 5(IL-5), interleukin 6(IL-6), interleukin 13(IL-13), and tumor necrosis factorα (TNF-α). These cytokines maintained the balance of the autoimmune microenvironment. The chronic pathological state of immune imbalance caused by diabetes can promote many diseases (12–14). In addition, the oxidative stress produced by diabetes can also produce many inflammatory cytokines, such as TNF-α, IL-6, and transforming growth factor β (14).

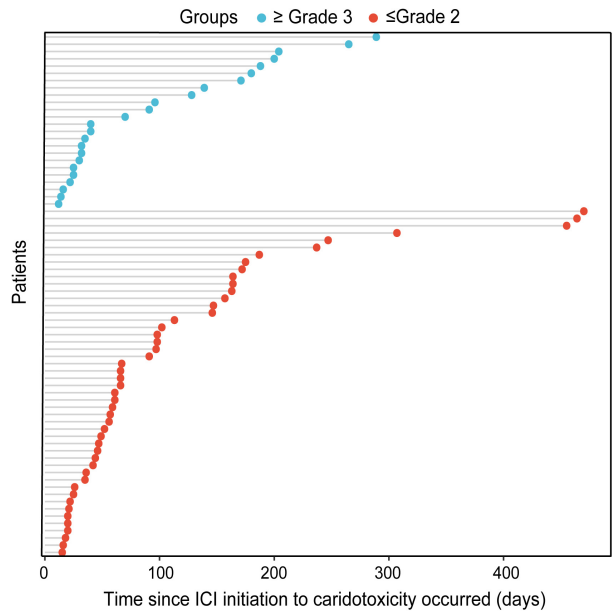

FIGURE 2 | Bubble chart of the time since ICI initiation to the occurrence of mild cardiotoxicity and severe cardiotoxicity.

The cytokine pathway has been confirmed to be closely related to irAEs in many studies (15). In addition, diabetes affects the number and activity of T cells, B cells, and NK cells in peripheral blood, and the result of immune imbalance may also play an important role (14). Moreover, whether diabetes, as an autoimmune disease, also plays an important role in irAEs like other types of autoimmune diseases remains to be further studied.

We also collected baseline inflammatory indicators, such as IL-6, C-reactive protein (CRP), and lactic dehydrogenase (LDH), of all patients and calculated NLR, PLR, and LMR. We found that lower baseline LMR was an independent risk factor for the development of cardiotoxicity. In previous studies, the correlation between peripheral lymphocyte levels and adverse reactions has already been investigated. In a study of risk factors for cardiotoxicity based on more than 4,000 immunotherapy patients (16), the authors identified the association between low baseline peripheral lymphocyte levels and cardiotoxicity through a machine learning method. In a retrospective study of NSCLC, an association of LMR with irAEs was also found (17). Activated T lymphocytes in patients with tumors after using PD-1/PD-L1 antibodies can not only attack tumor cells, but also cause irAEs. According to the autopsy result of patients with cardiotoxicity as previously reported, lymphocytic infiltration was widely seen in the diseased tissue (2). Therefore, lymphocytes may play a key role in the response of irAEs. However, no direct correlation between peripheral lymphocyte count (or percentage) and the occurrence of cardiotoxicity was found in our cohort. Moreover, these indicators are often dynamic during tumor treatment. Therefore, how does their changing act on adverse reactions? What role do lymphocytes play in it? They deserve further discussion.

In terms of gender, ICI was used in more men than women in our study, possibly due to the higher tumor prevalence in male patients. In this study, male patients received ICI proportionally more often than female patients, but no significant association between gender and the development of myocarditis was found. One study found higher occurrence rate of ICI associated cardiovascular with men (18). Several additional studies had the same finding (7, 11, 19). However, another research found a different result that women were at higher risk of ICI-related myocarditis. These studies suggested the relationship of gender and the occurrence of ICI-related myocarditis. In addition, we found a higher incidence of ICI-related cardiotoxicity in patients with respiratory neoplasms than in other types of neoplasms. Salem et al. (7) also found a higher rate of ICI-related pericardial disease among patients with lung cancer. Basic research has found upregulation of PD-L1 in models of myocardial injury induced by ischemiareperfusion and hypothermia, which may be a cytokine-mediated mechanism of cardiac protection. Besides, radiation therapy in patients with lung cancer may present with potential exposure to cardiac antigens. Immune activation thereby conferring them a higher incidence of cardiotoxicity. As for the correlation between comorbid autoimmune diseases and cardiotoxicity, there were numerous

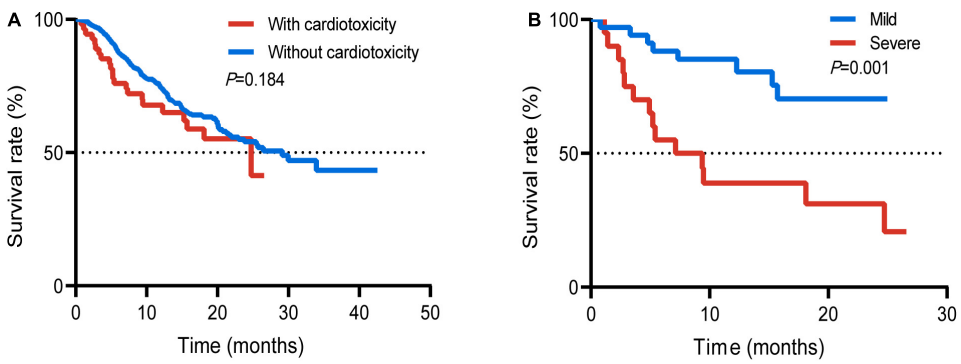

FIGURE 3 | Survival curve of the whole population with or without cardiotoxicity **(A)**; patients with mild or severe cardiotoxicity **(B)**.

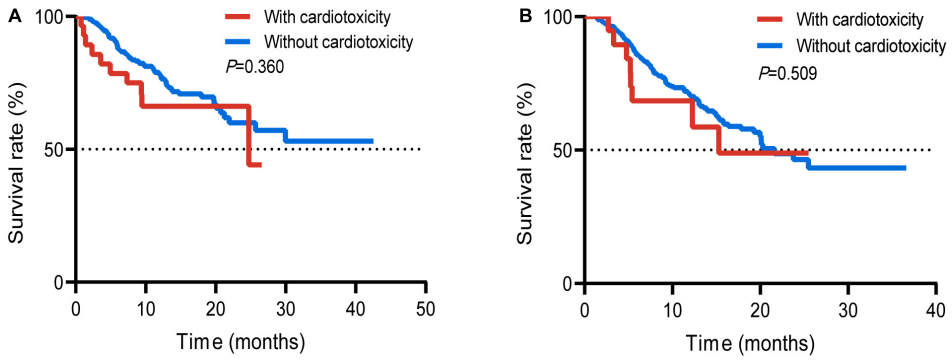

FIGURE 4 | Survival curve of the patients suffered respiratory tumor with or without cardiotoxicity **(A)**; patients suffered digestive tumor with or without cardiotoxicity **(B)**.

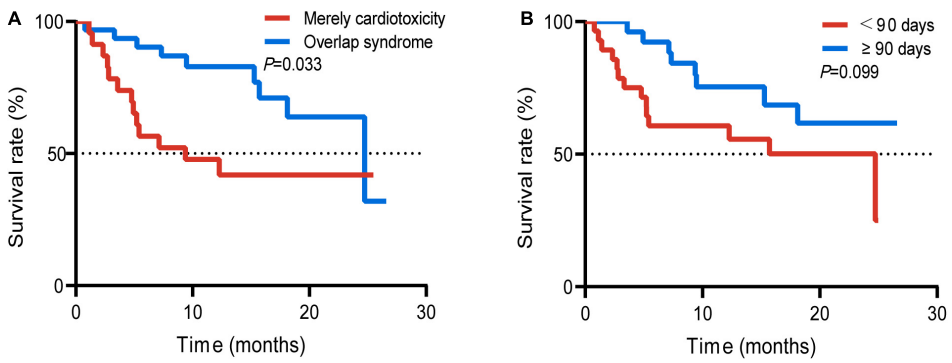

FIGURE 5 | Survival curve of the patients with mere cardiotoxicity and patients with concurrent cardiotoxicity and ICI targeted other functional disorder **(A)**; occurrence time (time since ICI initiation to the occurrence of ICI-related cardiotoxicity) of 90 days before and after 90 days **(B)**.

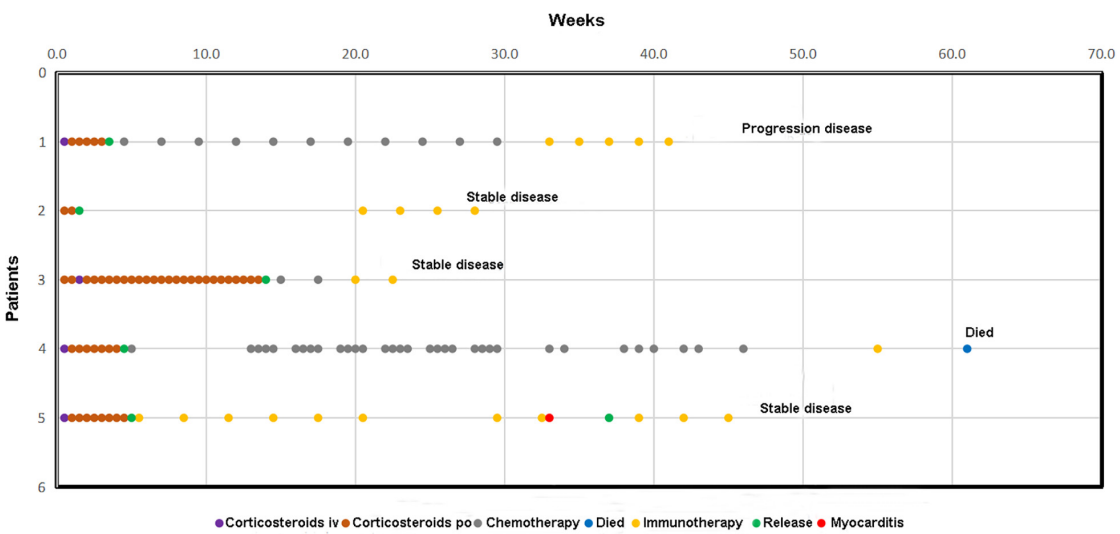

FIGURE 6 | Follow-up of patients who restart ICI therapy after suffering ICI-related cardiotoxicity.

reports of thymoma patients with ICI-related cardiotoxicity. Toi et al. (20) retrospectively recruited 137 patients with positive autoimmune antibody receiving ICI therapy. They found that positive autoimmune antibody was significantly associated with a higher occurrence of irAEs and better clinical benefit in NSCLC. In addition, another study also suggested

a relationship between autoimmune antibodies and irAEs (20). Therefore, we are more cautious about ICI initiation in patients with autoimmune diseases in real-world. Therefore, patients with active autoimmune disease were excluded from our study. Because the treatment of active autoimmune diseases is contrary to tumor treatment, they can affect the judgment to response of tumor treatment and drug-related adverse reactions.

In addition to ICI-related cardiotoxicity, we also collected ICI-related thyroid dysfunction and pneumonia. We found that both of them have a certain correlation with the occurrence of cardiotoxicity. Although the onset of ICI-related pneumonitis or abnormal thyroid function does not completely precede the onset of cardiotoxicity, we cannot establish a causal relationship between them. However, this finding suggests that there may be a link between the toxicities occurring at different times targeting different organs. The occurrence of toxicities targeting the lung or thyroid may then alert clinicians the occurrence of cardiotoxicity. Besides, myositis, hepatitis, and pneumonia may be complicated by the occurrence of cardiotoxicity. In the cardiotoxicity population, a total of 30 (41.1%) patients had concurrent toxicities targeting other organs. In a study based on the VigiBase database, serious combined ICI-related adverse reactions accounted for 42% of adverse reactions, most of which were ICI-related myocarditis and myositis (21). In a multicenter study, 32% of myositis was associated with concurrent myocarditis (22). In addition, the mortality rate is the highest in patients with combined myocarditis and myasthenia gravis. Therefore, in patients with symptoms of ICI-related myositis, they should be alert to the occurrence of myocarditis.

Previous studies have demonstrated a possible correlation between irAEs and tumor prognosis. A meta-analysis (23) explored the relationship between ICI-related adverse drug reactions and clinical benefits. It was suggested that in patients receiving ICIs, the development of irAEs was positively correlated with objective remission rate (ORR), progression-free survival (PFS), and OS, irrespective of disease site, type of ICI, and irAE. ORR was better in patients with grade 3 or higher toxicity, but OS was worse. However, in this study, we only did the analysis in overall survival, and no significant difference was found between patients with or without cardiotoxicity.

Till now, the National Comprehensive Cancer Network (NCCN) guidelines do not recommend rechallenge of ICI after grade 2 and above myocarditis. Subclinical myocarditis was recommended continue the use of ICI with close detection. In a single-center retrospective study in 2019 (24), the investigators included 93 patients with grade 2 or higher toxicity, including 43 grade 2 events, 36 grade 3 events, and 14 grade 4 events. Taking the occurrence of the second toxicity as the endpoint, the final results suggested that the time since ICI use to the occurrence of the initial irAE was related to the occurrence of the second irAE. Besides, the severity of the second irAE was not more severe than the first one. They concluded that the risk-reward ratio of anti-PD-1 or anti-PD-L1 rechallenge appears to be acceptable. However, patients with first ICI-related toxicity involving the heart were not included in this study. Conversely, there were also some studies restarting ICI after the occurrence of irAEs, resulting in recurrence of grade 5 toxicity in patients. Therefore, ICI rechallenge after irAEs is still controversial. Due to the small number of cases in our study, we cannot currently explain the safety of cardiotoxicity after restarting, because once cardiotoxicity occurs, it may be fatal drug toxicity, which is unacceptable for clinicians and patients' families. Moreover, the timing of ICI restarting among these patients also varied, and some patients even resumed ICI 1 month after ICI withdrawal. If there are large clinical studies to confirm the feasibility of restarting immunotherapy for ICI-related cardiotoxicity, the timing of restarting ICI will also be a major focus. Furthermore, there were many patients with grade 1 cardiotoxicity who continue to use immunotherapy under strict monitoring, and a small number of patients who suffered mild cardiotoxicity for not one time, but it does not affect the progress of tumor treatment.

CONCLUSION

We retrospectively analyzed the risk factors of ICI-related cardiotoxicity in the whole population receiving ICI therapy. We found a higher incidence of ICI-related cardiotoxicity, and a high proportion of severe cases than previous reported in real-world situation. Patients with diabetes mellitus and low baseline levels of LMR have an increased incidence of cardiotoxicity, which should be closely monitored during the use of ICIs. Besides, the incidence of severe cardiotoxicity was correlated with shorter overall survival.

SHORTAGE

Despite the advantages and potential insights on this study, there are some inevitable shortcomings in our study. First of all, some potential biases are still unavoidable due to the retrospective design of this study, such as investigator bias. Second, although the overall immunotherapy sample size we included is relatively large, the number of cardiotoxicity cases is relatively small, as well as the number of patients who rechallenge ICI. Finally, due to the serious lack of some data during the study period, we could not analyze the relationship between the baseline levels of some inflammatory markers (such as LDH, CRP, and cytokines) and the occurrence of cardiotoxicity. Hence, well-designed large-scale prospective studies are urgently needed in the future.

DATA AVAILABILITY STATEMENT

The raw data supporting the conclusions of this article will be made available by the authors, without undue reservation.

ETHICS STATEMENT

This study involving human participants was reviewed and approved by the Ethics Review of the First Affiliated Hospital of Xi'an Jiaotong University (no. XJTU1AF2020LSK-262) and was conducted in strict accordance with the requirements of the Declaration of Helsinki. Written informed consent was not required due to the retrospective nature of the study.

AUTHOR CONTRIBUTIONS

XC, TT, XL, ZR, and YY contributed to the design of the study. XC, AJ, RZ, XF, NL, JW, and XZ contributed to manuscript preparation. XC and AJ wrote the manuscript. RZ, YY, CS, and XL helped collect cases. All authors contributed to the article and approved the submitted version.

REFERENCES

1. Läubli H, Balmelli C, Bossard M, Pfister O, Glatz K, Zippelius A. Acute heart failure due to autoimmune myocarditis under pembrolizumab treatment for metastatic melanoma. *J Immunother Cancer.* (2015) 3:11. doi: 10.1186/s40425-015-0057-1
2. Johnson DB, Balko JM, Compton ML, Chalkias S, Gorham J, Xu Y, et al. Fulminant myocarditis with combination immune checkpoint blockade. *N Engl J Med.* (2016) 375:1749–55. doi: 10.1056/NEJMoa1609214
3. Geisler BP, Raad RA, Esaian D, Sharon E, Schwartz DR. Apical Ballooning and Cardiomyopathy in a melanoma patient treated with ipilimumab: a case of takotsubo-like syndrome. *J Immunother Cancer.* (2015) 3:4. doi: 10.1186/s40425-015-0048-2
4. Nykl R, Fischer O, Vykoupil K, Taborsky M. A unique reason for coronary spasm causing temporary st elevation myocardial infarction (inferior stemi) - systemic inflammatory response syndrome after use of pembrolizumab. *Arch Med Sci Atheroscler Dis.* (2017) 2:e100–2. doi: 10.5114/amsad.2017.72531
5. Upadhrasta S, Elias H, Patel K, Zheng L. Managing cardiotoxicity associated with immune checkpoint inhibitors. *Chronic Dis Transl Med.* (2019) 5:6–14. doi: 10.1016/j.cdtm.2019.02.004
6. Ganatra S, Neilan TG. Immune checkpoint inhibitor-associated myocarditis. *Oncologist.* (2018) 23:879–86. doi: 10.1634/theoncologist.2018-0130
7. Salem JE, Manouchehri A, Moey M, Lebrun-Vignes B, Bastarache L, Pariente A, et al. Cardiovascular toxicities associated with immune checkpoint inhibitors: an observational, retrospective, pharmacovigilance study. *Lancet Oncol.* (2018) 19:1579–89. doi: 10.1016/s1470-2045(18)30608-9
8. Escudier M, Cautela J, Malissen N, Ancedy Y, Orabona M, Pinto J, et al. Clinical features, management, and outcomes of immune checkpoint inhibitor-related cardiotoxicity. *Circulation.* (2017) 136:2085–7. doi: 10.1161/circulationaha.117.030571
9. Bonaca MP, Olenchock BA, Salem JE, Wiviott SD, Ederhy S, Cohen A, et al. Myocarditis in the setting of cancer therapeutics: proposed case definitions for emerging clinical syndromes in cardio-oncology. *Circulation.* (2019) 140:80–91. doi: 10.1161/circulationaha.118.034497
10. Dolladille C, Ederhy S, Allouche S, Dupas Q, Gervais R, Madelaine J, et al. Late cardiac adverse events in patients with cancer treated with immune checkpoint inhibitors. *J Immunother Cancer.* (2020) 8:e000261. doi: 10.1136/jitc-2019-000261
11. Mahmood SS, Fradley MG, Cohen JV, Nohria A, Reynolds KL, Heinzerling LM, et al. Myocarditis in patients treated with immune checkpoint inhibitors. *J Am Coll Cardiol.* (2018) 71:1755–64. doi: 10.1016/j.jacc.2018.02.037
12. Parikh RB, Min EJ, Wileyto EP, Riaz F, Gross CP, Cohen RB, et al. Uptake and survival outcomes following immune checkpoint inhibitor therapy among trial-ineligible patients with advanced solid cancers. *JAMA Oncol.* (2021) 7:1843–50. doi: 10.1001/jamaoncol.2021.4971
13. Tanaka S, Isoda F, Ishihara Y, Kimura M, Yamakawa T. T Lymphopaenia in relation to body mass index and TNF-alpha in human obesity: adequate weight reduction can be corrective. *Clin Endocrinol (Oxf).* (2001) 54:347–54. doi: 10.1046/j.1365-2265.2001.1139cn2155.x
14. Dong G, Li Y, Zhao Q, Pang B, Qi X, Wei J, et al. Effects of diabetes on the development of radiation pneumonitis. *Respir Res.* (2021) 22:160. doi: 10.1186/s12931-021-01754-4
15. Kang JH, Bluestone JA, Young A. Predicting and preventing immune checkpoint inhibitor toxicity: targeting cytokines. *Trends Immunol.* (2021) 42:293–311. doi: 10.1016/j.it.2021.02.006
16. Heilbroner SP, Few R, Mueller J, Chalwa J, Charest F, Suryadevara S, et al. Predicting cardiac adverse events in patients receiving immune checkpoint inhibitors: a machine learning approach. *J Immunother Cancer.* (2021) 9:e002545. doi: 10.1136/jitc-2021-002545
17. Egami S, Kawazoe H, Hashimoto H, Uozumi R, Arami T, Sakiyama N, et al. Peripheral blood biomarkers predict immune-related adverse events in non-small cell lung cancer patients treated with pembrolizumab: a multicenter retrospective study. *J Cancer.* (2021) 12:2105–12. doi: 10.7150/jca.53242
18. Wang DY, Salem JE, Cohen JV, Chandra S, Menzer C, Ye F, et al. Fatal toxic effects associated with immune checkpoint inhibitors: a systematic review and meta-analysis. *JAMA Oncol.* (2018) 4:1721–8. doi: 10.1001/jamaoncol.2018.3923
19. Reuben A, Petaccia de Macedo M, McQuade J, Joon A, Ren Z, Calderone T, et al. Comparative immunologic characterization of autoimmune giant cell myocarditis with ipilimumab. *Oncoimmunology.* (2017) 6:e1361097. doi: 10.1080/2162402x.2017.1361097
20. Toi Y, Sugawara S, Sugisaka J, Ono H, Kawashima Y, Aiba T, et al. Profiling preexisting antibodies in patients treated with Anti-Pd-1 therapy for advanced non-small cell lung cancer. *JAMA Oncol.* (2019) 5:376–83. doi: 10.1001/jamaoncol.2018.5860
21. Moslehi JJ, Salem JE, Sosman JA, Lebrun-Vignes B, Johnson DB. Increased reporting of fatal immune checkpoint inhibitor-associated myocarditis. *Lancet.* (2018) 391:933. doi: 10.1016/s0140-6736(18)30533-6
22. Moreira A, Loquai C, Pföhler C, Kähler KC, Knauss S, Heppt MV, et al. Myositis and neuromuscular side-effects induced by immune checkpoint inhibitors. *Eur J Cancer.* (2019) 106:12–23. doi: 10.1016/j.ejca.2018.09.033
23. Hussaini S, Chehade R, Boldt RG, Raphael J, Blanchette P, Maleki Vareki S, et al. Association between immune-related side effects and efficacy and benefit of immune checkpoint inhibitors – a systematic review and meta-analysis. *Cancer Treat Rev.* (2021) 92:102134. doi: 10.1016/j.ctrv.2020.102134
24. Simonaggio A, Michot JM, Voisin AL, Le Pavec J, Collins M, Lallart A, et al. Evaluation of readministration of immune checkpoint inhibitors after immune-related adverse events in patients with cancer. *JAMA Oncol.* (2019) 5:1310–7. doi: 10.1001/jamaoncol.2019.1022

Conflict of Interest: The authors declare that the research was conducted in the absence of any commercial or financial relationships that could be construed as a potential conflict of interest.

frontiers | Frontiers in Cardiovascular Medicine

ORIGINAL RESEARCH
published: 20 May 2022
doi: 10.3389/fcvm.2022.785246

Clinical Characteristics and Long-Term Outcomes of MINOCA Accompanied by Active Cancer: A Retrospective Insight Into a Cardio-Oncology Center Registry

Konrad Stepien[1,2,3]*, *Karol Nowak*[1,2], *Barbara Szlosarczyk*[1,2], *Jadwiga Nessler*[1,2] and *Jaroslaw Zalewski*[1,2]

[1] Department of Coronary Artery Disease and Heart Failure, Jagiellonian University Medical College, Kraków, Poland, [2] John Paul II Hospital, Kraków, Poland, [3] Club 30, Polish Cardiac Society, Kraków, Poland

Background: Clinical characteristics and long-term outcomes of patients with myocardial infarction with non-obstructive coronary arteries (MINOCA) and cancer are insufficiently elucidated.

Objectives: We sought to characterize these patients hospitalized in a tertiary cardio-oncology center and to find the potential determinants affecting their long-term mortality.

Methods: MINOCA was diagnosed in 72 of the 1,011 patients with consecutive myocardial infarction who underwent coronary angiography. Mortality rates and their determinants were analyzed within a median follow-up of 69.2 (37.8–79.9) months.

Results: Active cancer was identified in 21 (29.2%) of patients with MINOCA and in 113 (12.0%) patients with myocardial infarction and obstructive coronary artery disease (MI-CAD) ($p < 0.001$). MINOCA patients with cancer were characterized by a higher incidence of anemia (47.6 vs. 21.6%, $p = 0.03$) and more frequently Takotsubo syndrome (19.1 vs. 2.0%, $p = 0.01$) than in non-cancer MINOCA. The troponin T/hemoglobin ratio was higher in both cancer MINOCA and MI-CAD groups when compared with their respective non-cancer patients (both $p < 0.05$). The age and sex-standardized mortality rates were significantly higher in cancer MINOCA (26.7%/year) when compared with non-cancer MINOCA (2.3%/year, $p = 0.002$) and in cancer MI-CAD (25.0%/year) vs. non-cancer MI-CAD (3.7%/year, $p < 0.001$). Active cancer (HR 3.12, 95% CI 2.41–4.04) was independently associated with higher long-term mortality, while higher hemoglobin levels (HR 0.93, 95% CI 0.88–0.99, per g/dl) and a MINOCA diagnosis (HR 0.69, 95% CI 0.47–0.97) improved long-term survival.

Conclusion: Patients with MINOCA were comorbid with cancer more frequently than MI-CAD. In turn, an active malignancy was associated with an unfavorable long-term survival both in MI-CAD population and in patients with MINOCA.

Keywords: MINOCA, MI-CAD, cancer, anemia, cardio-oncology

OPEN ACCESS

Edited by:
Carlo Gabriele Tocchetti, University of Naples Federico II, Italy

Reviewed by:
Pietro Ameri, University of Genoa, Italy
Fernando Montenegro Sá, Hospital Pedro Hispano, Portugal

***Correspondence:**
Konrad Stepien
konste@interia.eu

Specialty section:
This article was submitted to Cardio-Oncology, a section of the journal Frontiers in Cardiovascular Medicine

Received: *28 September 2021*
Accepted: *19 April 2022*
Published: *20 May 2022*

Citation:
Stepien K, Nowak K, Szlosarczyk B, Nessler J and Zalewski J (2022) Clinical Characteristics and Long-Term Outcomes of MINOCA Accompanied by Active Cancer: A Retrospective Insight Into a Cardio-Oncology Center Registry. Front. Cardiovasc. Med. 9:785246. doi: 10.3389/fcvm.2022.785246

INTRODUCTION

Myocardial infarction with non-obstructive coronary arteries (MINOCA) is recognized if it meets the general criteria of myocardial infarction (MI) together with the absence of significant lesions in epicardial arteries in angiography (1). As shown in large MI registries, MINOCA concerns 1–13% of all patients with MI (2, 3). Recent reports indicate an unexpectedly unfavorable long-term prognosis in this group of patients. The SWEDEHEART registry included 9,092 patients with MINOCA, of whom 24% experienced a major cardiovascular event, and where 14% died within a mean follow-up period of 4.5 years (4).

The potential mechanisms responsible for MINOCA are heterogeneous (1, 5). According to the current knowledge, the underlying pathophysiological causes of MINOCA are grouped as coronary or non-coronary. Moreover, the latter are classified as myocardial disorders or as those that are typically extra-cardiac (6). Both historical (7) as well as current findings (8) indicate that hypercoagulable states, including the inherited thrombophilia, occurred in 15–25% of patients with MINOCA. This includes deficiency of protein C, protein S, or antithrombin. Additionally, the antiphospholipid syndrome was detected in 15.5% of patients. Concurrently, patients with cancer are a group that is at a particularly high prothrombotic risk, traditionally in the venous system (9). An analysis of the Surveillance, Epidemiology, and End Results involving nearly 280,000 patient pairs showed that the rate of arterial thromboembolic events was 4.7% in cancer patients compared with the 2.2% in controls (10). That predisposition for arterial thromboembolism, defined as MI, ischemic stroke, or peripheral arterial occlusion, has been confirmed recently in a large Danish population-based cohort study (1.5 vs. 0.8% in the 6-month observation, hazard ratio [HR]: 2.36, 95% confidence interval [CI]: 2.28–2.44] (11). Moreover, its occurrence among patients with cancer was associated with an increased risk of mortality (HR 3.28, 95% CI: 3.18–3.38) (11). As the arterial thromboembolic events immediately preceded cancer diagnosis and were correlated with the stage of cancer (10, 11), they can be considered paraneoplastic symptoms, which always require subsequent meticulous diagnostics toward a subclinical neoplastic process (12).

Recently, a review of the meta-regression analysis of nine studies including 26,636 patients with MINOCA has shown that 2.5% of them had a diagnosis of malignancy at presentation (13). Similar findings have been reported in the SWEDEHEART registry (14). Despite relatively low prevalence, both Nordenskjöld et al. (4) (HR: 2.40, 95% CI: 1.58–3.61, $p < 0.001$) and Pelliccia et al. (13) (coefficient: 0.001, 95% CI: −0.001 to 0.001, $p = 0.01$) have found cancer as an independent predictor of death in patients with MINOCA. Another meta-analysis including a higher number of patients with MINOCA, i.e., 36,932, did not confirm a similar relationship (15). Therefore, we sought to characterize subjects with MINOCA and cancer hospitalized in a tertiary cardio-oncology center in order to investigate the potential mechanisms affecting their long-term outcomes.

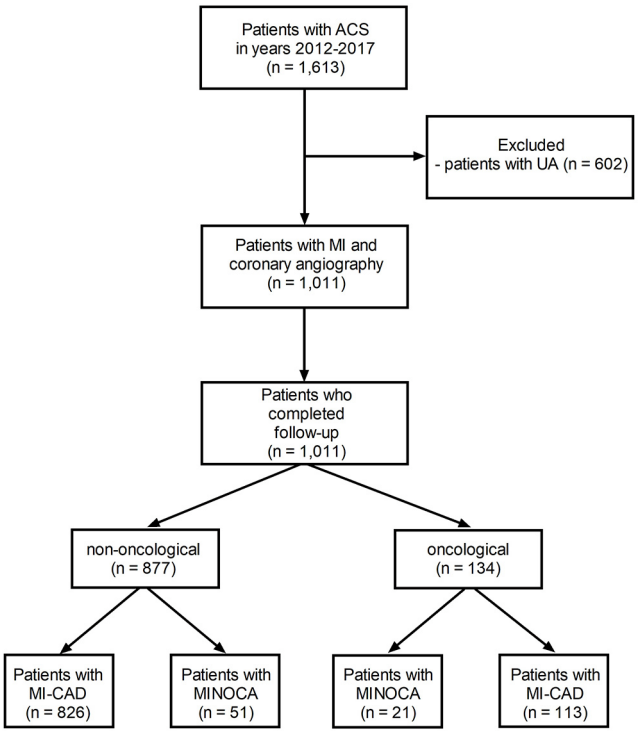

FIGURE 1 | The study flow-chart. MINOCA, myocardial infarction with non-obstructive coronary artery; MI-CAD, myocardial infarction and obstructive coronary artery disease.

MATERIALS AND METHODS

As has been stated retrospectively, in a tertiary cardio-oncology center including closely cooperating departments of cardiology (168 hospital beds), cardiac surgery (80 beds), pulmonology and oncology (74 beds), and thoracic surgery (48 beds), 1,011 consecutive patients underwent coronary angiography between 2012 and 2017 due to the diagnosis of MI based on clinical symptoms, electrocardiographic findings, and the evolution of myocardial necrotic biomarkers (16). MINOCA was recognized in 72 (7.1%) subjects (**Figure 1**) based on the universal criteria of MI (positive cardiac biomarkers rising and/or falling in serial measurements, with at least one value above the 99th percentile as the upper reference limit and at least one clinical sign of infarction). An additional inclusion criterion was a lack of obstructive lesions narrowing epicardial coronary segments by more than 50% in angiography (1, 17). Patients with ST-segment elevation of at least 1 mm in at least two contiguous leads were classified as ST-segment elevation MI (STEMI), whereas patients without ST-segment elevation on admission were diagnosed as non-ST-segment elevation MI (NSTEMI) (18). In addition, 134 (13.3%) patients were identified with active cancer, defined as cancer diagnosed within the past 6 months, receiving antimitotic treatment during the last 6 months, recurrent, metastatic, regionally advanced, or inoperable (19) (**Figure 1**). In the analyzed period of time, five MI patients with advanced cancer did not undergo coronary angiography and

TABLE 1 | Clinical and angiographic characteristics of the study patients.

	MINOCA		MI-CAD	
	Cancer *N* = 21	**Non-cancer *N* = 51**	**Cancer *N* = 113**	**Non-cancer *N* = 826**
Male gender	8 (38.1)	27 (52.9)	88 (77.9)	591 (71.6)
Age, years	75 (71–79)	70 (64–78)	73 (66–79)	68 (60–78)
Body mass index, kg/m^2	24.2 (22.1–27.4)	26.7 (23.6–31.5)	26.0 (23.4–29.1)	27.7 (25.0–30.9)
Diabetes mellitus	7 (33.3)	13 (25.5)	40 (35.4)	318 (38.6)
Hypertension	16 (76.2)	47 (92.2)	96 (85.0)	717 (87.1)
Dyslipidemia	12 (57.1)	38 (74.5)	73 (64.6)	695 (84.5)
Pre-ESRD or ESRD	1 (4.8)	2 (3.9)	2 (1.8)	20 (2.4)
Active smoking	0 (0.0)	6 (11.8)	18 (15.9)	203 (24.7)
Anemia	10 (47.6)	11 (21.6)	52 (46.0)	169 (20.5)
Thrombocytopenia	3 (14.3)	2 (3.9)	3 (2.7)	9 (1.1)
Prior myocardial infarction	3 (14.3)	9 (17.7)	39 (34.5)	239 (29.0)
Prior stroke	3 (14.3)	3 (5.9)	9 (8.0)	56 (6.8)
Killip class on admission				
I/II	19 (90.5)	47 (92.2)	98 (86.7)	757 (91.8)
III/IV	2 (9.5)	4 (7.8)	15 (13.3)	68 (8.2)
Clinical presentation				
NSTEMI	15 (71.4)	45 (88.2)	74 (65.5)	530 (64.2)
STEMI	6 (28.6)	6 (11.8)	39 (34.5)	296 (35.8)
Takotsubo syndrome	4 (19.1)	1 (2.0)	0 (0.0)	8 (1.0)
Perioperative myocardial infarction	1 (4.8)		3 (2.7)	
Type of cancer				
Genitourinary	8 (38.1)		36 (31.9)	
Breast	5 (23.8)		6 (5.3)	
Lung	3 (14.3)		27 (23.9)	
Gastrointestinal	2 (9.5)		18 (15.9)	
Other	3 (14.3)		26 (23.0)	
Metastatic disease				
Lymph nodes	0 (0.0)		16 (14.1)	
Distant	4 (19.1)		24 (21.2)	
Prior oncological treatment				
Surgery	6 (28.6)		24 (21.2)	
Surgery with curative intent	1 (4.8)		3 (2.7)	
Radiotherapy	3 (14.3)		13 (11.5)	
Chemotherapy	4 (19.1)		28 (24.8)	
Platinum compounds	2 (9.5)		9 (8.0)	
Taxanes	2 (9.5)		2 (1.8)	
Fluoropyrimidines	0 (0.0)		10 (8.8)	
Anthracyclines	0 (0.0)		3 (2.7)	
Other	0 (0.0)		4 (3.5)	
Hormonotherapy	2 (9.5)		17 (15.0)	
Newly diagnosed cancer during hospitalization	2 (9.5)		21 (18.6)	
Coronary angiography				
<30% stenosis	13 (61.9)	34 (66.7)		
30–50% stenosis	8 (38.1)	17 (33.3)		
≥50% stenosis in one or two coronary arteries			87 (77.0)	687 (83.2)
≥50% stenosis in three coronary arteries			26 (23.0)	139 (16.8)
≥50% stenosis in left main			19 (16.8)	98 (11.9)
Epicardial thrombus	0 (0.0)	1 (2.0)	14 (12.4)	116 (14.0)
Distal embolization	0 (0.0)	3 (5.9)	9 (8.0)	17 (2.1)

(Continued)

TABLE 1 | Continued

	MINOCA		MI-CAD	
	Cancer *N* = 21	Non-cancer *N* = 51	Cancer *N* = 113	Non-cancer *N* = 826
Treatment strategy				
Percutaneous coronary intervention			101 (89.4)	724 (87.7)
Coronary artery bypass graft surgery			3 (2.7)	24 (2.9)
Conservative			9 (8.0)	78 (9.4)
Pharmacotherapy				
Aspirin	19 (90.5)	44 (86.3)	108 (95.6)	810 (98.1)
P2Y12 inhibitor	10 (47.6)	27 (52.9)	105 (92.9)	785 (95.0)
Proton pump inhibitor	8 (38.1)	35 (68.6)	84 (74.3)	618 (75.3)
ACEI/ARB	17 (81.0)	44 (86.3)	103 (91.2)	728 (88.1)
β-blocker	16 (76.2)	36 (70.6)	101 (89.4)	743 (90.5)
Statin	14 (66.7)	39 (76.5)	99 (87.6)	774 (94.3)

Data are shown as number (percentage) or median (interquartile range), ACEI, angiotensin-converting enzyme inhibitor; ARB, angiotensin receptor blocker; ESRD, end-stage renal disease; MINOCA, myocardial infarction with non-obstructive coronary artery; MI-CAD, myocardial infarction and obstructive coronary artery disease; NSTEMI, non-ST-segment elevation myocardial infarction; STEMI, ST-segment elevation myocardial infarction.

were therefore excluded from further analysis. The study protocol complied with the Declaration of Helsinki and was approved by the Jagiellonian University Medical College Ethics Committee (Consent No. 1072.6120.59.2018). All included patients gave informed consent.

Patients Clinical and Laboratory Characteristics

Information on demographics, anthropometric parameters, cardiovascular risk factors, cardiovascular disease history, and comorbidities of all the study patients was gathered. Anemia was recognized if the hemoglobin level was <13 g/dl for men and <12 g/dl for women. The cut-off value for the thrombocytopenia was $100 \times 10^3/\mu l$ (20). Pre-end-stage renal disease and end-stage renal disease was diagnosed when creatinine clearance calculated using the Cockcroft-Gault formula was lower than 30 ml/min. Finally, creatine kinase serum activity (IU/L, upper limit of normal: 170 IU/L), isoenzyme MB of creatine kinase (IU/L, upper limit of normal: 24 IU/L), and concentration of high-sensitive cardiac troponin T (ng/ml, upper limit of normal: 0.014 ng/ml) were measured on admission and at least one time within the first 24 h.

Angiography

All coronary angiograms were analyzed off-line, using two contralateral projections for each artery at baseline and after angioplasty if applicable, by a cardiologist unaware of the clinical data. All coronary segments were carefully evaluated for the presence of visible thrombus, distal embolization, and degree of stenosis based on visual inspection (21, 22). In cases of borderline lesions between 40 and 70%, quantitative coronary angiography (QCA Quantcor, Siemens, Germany) was applied for precise assessment. According to the guidelines (1, 5), lesions narrowing the coronary artery by <50% were defined as insignificant. All patients with insignificant stenosis were divided into two groups with either i) normal coronary arteries or minimal intracoronary irregularities with stenosis of <30% or with ii) mild to moderate lesions of at least 30 and <50%.

Echocardiography

A two-dimensional transthoracic echocardiography was performed by a trained physician between the second and fourth day of hospitalization. It was performed at rest in a left decubitus position, using a Vivid S5 ultrasound (GE, Solingen, Germany) equipped with a multi-frequency harmonic transducer, 3Sc-RS (1.3-4 MHz). All measurements were carried out according to the recommendations of the American Society of Echocardiography and the European Association of Echocardiography (23). Standard parameters were collected to describe individual heart structures and enable their functional assessment. Screening for Takotsubo syndrome was also routinely conducted, the diagnosis of which was performed according to the InterTAK criteria (24), irrespective of the severity of coronary artery disease (25).

Clinical Follow-Up

The length of hospitalization was collected from hospital records, whereas long-term all-cause mortality was obtained from the National Health Registry. The additional data regarding the cause of death were obtained from the Polish Office of Statistics. The causes of death were categorized as cancer, cardiovascular, other (the most common causes included respiratory system disease or accident/trauma), or unknown. Major cardiovascular causes of death included coronary artery disease, cerebrovascular disease, heart failure, or atherosclerosis.

Statistical Analysis

Statistical analysis was performed with the SPSS Statistics software (Version 25.0.0.2, IBM, USA). Continuous variables were expressed as medians (interquartile range) and categorical variables as numbers (percentage). Continuous variables were

TABLE 2 | The selected laboratory and echocardiography characteristics.

	MINOCA		MI-CAD	
	Cancer *N* = 21	Non-cancer *N* = 51	Cancer *N* = 113	Non-cancer *N* = 826
Laboratory tests				
Hemoglobin, g/dl	12.9 (10.2–13.9)	14.1 (12.3–14.7)	12.8 (11.2–14.1)	14.0 (12.8–15.1)
Hematocrit, %	38.7 (31.7–41.9)	41.5 (36.6–42.8)	38.3 (34.6–41.3)	41.7 (38.4–44.6)
White blood cells, x10^3/μl	8.9 (6.1–11.7)	8.6 (6.5–11.5)	10.0 (7.3–13.3)	9.3 (7.5–12.0)
Platelet count, x10^3/μl	226 (166–284)	223 (163–263)	238 (182–292)	221 (184–271)
Creatinine, μmol/l	91 (76–124)	90 (73–113)	93 (77–112)	88 (76–103)
Glomerular filtration rate, ml/min	57.1 (36.7–71.2)	63.9 (53.0–88.1)	65.6 (52.7–86.0)	71.0 (57.2–86.3)
Glucose, mmol/l	7.5 (5.7–9.3)	6.3 (5.5–7.1)	7.5 (5.7–8.6)	6.9 (5.8–9.1)
Troponin, ng/ml	0.306 (0.102–0.680)	0.076 (0.027–0.265)	0.141 (0.046–1.070)	0.113 (0.033–0.429)
Troponin peak, ng/ml	0.489 (0.102–1.190)	0.145 (0.053–0.344)	0.952 (0.178–7.160)	0.897 (0.249–4.300)
Creatine kinase, IU/l	134 (51–163)	132 (90–266)	151 (82–376)	186 (109–381)
Creatine kinase peak, IU/l	137 (77–246)	150 (99–319)	313 (140–852)	553 (192–1,652)
Creatine kinase MB isoenzyme, IU/l	24 (13–35)	20 (14–29)	23 (15–61)	22 (15–45)
Creatine kinase MB isoenzyme peak, IU/l	27 (19–42)	21 (16–32)	44 (23–145)	61 (26–155)
Echocardiography characteristics				
Right ventricular systolic pressure, mmHg	45 (33–63)	32 (26–40)	36 (29–44)	28 (26–37)
TAPSE, mm	24 (20–28)	22 (20–25)	22 (16–24)	21.8 (19–25)
Left atrium, mm	36 (33–43)	42 (36–45)	41 (38–46)	42 (38–46)
E/A ratio	0.6 (0.5–0.8)	0.8 (0.6–1)	0.8 (0.7–1)	0.7 (0.6–1.1)
End-diastolic LV diameter, mm	45 (41–52)	50 (45–53)	51 (46–56)	51 (48–56)
End-systolic LV diameter, mm	25 (23–33)	32 (27–37)	34 (29–42)	32 (28–37)
LV ejection fraction, %	50 (40–59)	55 (45–60)	45 (36–55)	50 (40–55)
Aortic valve peak gradient, mmHg	8.5 (7–13.5)	7 (6–10)	7 (5–9)	7 (5–8)
Ascending aorta diameter, mm	34 (29–36)	36 (33–38)	35 (33–38)	36 (33–38)

Data are shown as median (interquartile range), HDL, high-density lipoprotein; LDL, low-density lipoprotein; LV, left ventricular; MINOCA, myocardial infarction with non-obstructive coronary artery; MI-CAD, myocardial infarction and obstructive coronary artery disease; TAPSE, tricuspid annular plane systolic excursion.

first checked for normal distribution using the Shapiro–Wilk test. Afterward, differences in the four groups were compared with an analysis of variance, followed by a *post-hoc* Bonferroni test if the data distribution was normal. Non-normally distributed data were analyzed *via* the Kruskal–Wallis test, and differences between the groups were identified using a test for multiple comparisons of mean ranks. Categorical variables were analyzed with the chi-square test or Fisher's exact test with a *post-hoc* z-test for comparison of column proportions with the Bonferroni method. The mortality rates were expressed as crude or age and sex-standardized for the European population based on Eurostat data available online (26). The Kaplan–Meier curves for overall mortality were constructed in order to estimate the survival rates, and a log-rank test with a Bonferroni-corrected threshold was performed to assess the differences in survival between the study groups. Finally, all independent variables with the potential to confound both the exposure and the outcome were included in the Cox proportional hazard regression model to determine independent predictors of long-term all-cause mortality. A two-tailed p-value of <0.05 was considered statistically significant.

RESULTS

Based on detailed angiographic and oncological characteristics, four groups of patients were created (**Figure 1**). Within 1,011 MI patients, active cancer and MINOCA were identified in 21 (2.1%) patients, whereas MINOCA without cancer was diagnosed in 51 (5.0%) subjects. Of the 939 remainders with type 1 MI with obstructive coronary artery disease (MI-CAD), 113 (11.2%) patients had active cancer and 826 (81.7%) had no evidence of active cancer. In 111 patients, the malignancy process was diagnosed before index MI, whereas new cancer was found during index hospitalization in two patients with MINOCA and in 21 with MI-CAD (**Table 1**).

Among the four groups, there were significant differences in the distribution of gender, anthropometric parameters, dyslipidemia, active smoking status, and initial clinical presentation ($p < 0.01$ for each) (**Table 1**). The angiographic analysis also revealed a different proportion of epicardial thrombus in the compared groups ($p = 0.02$). Hemoglobin levels were lower, whereas baseline high-sensitive troponin T was higher in both cancer groups compared with non-cancer

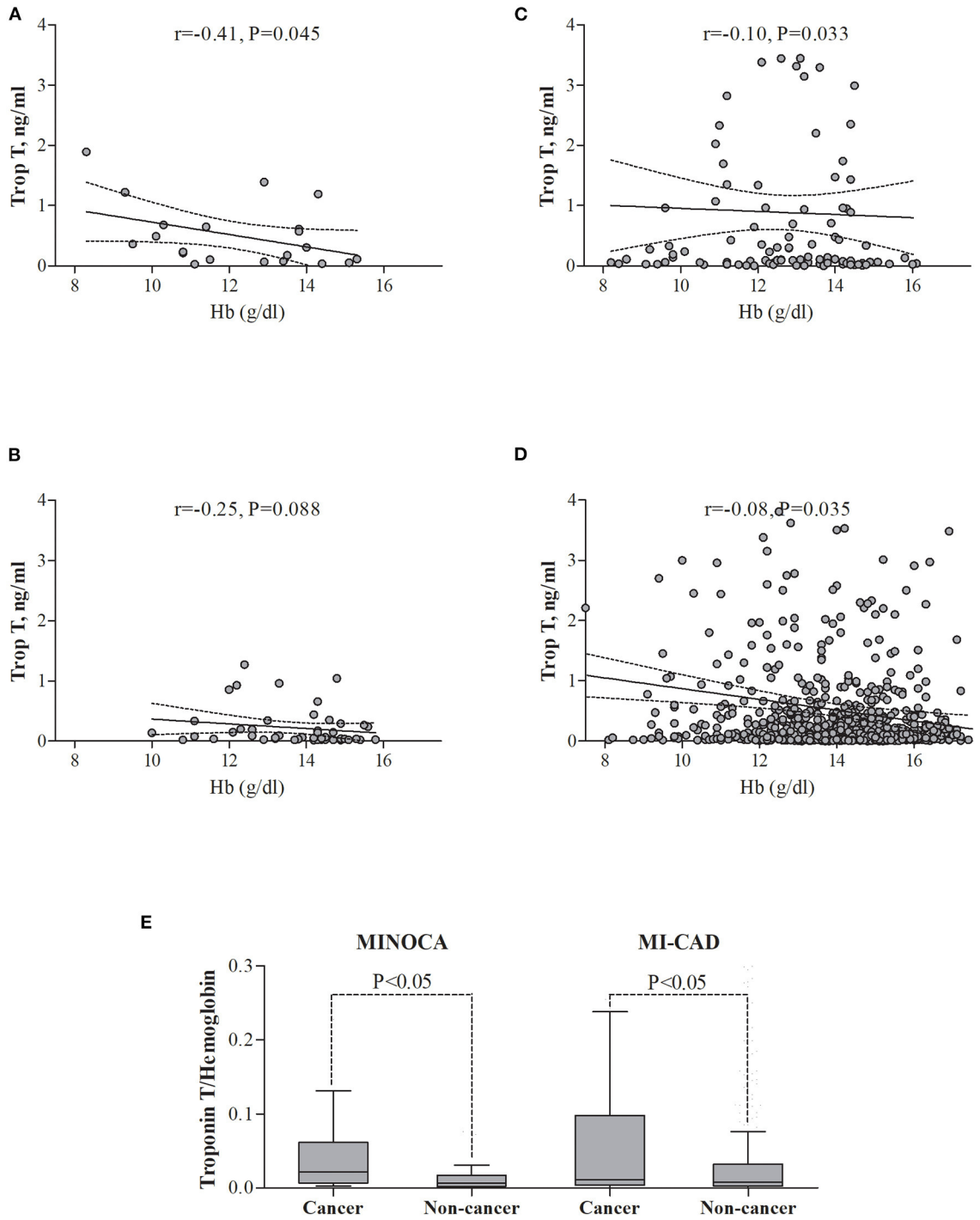

FIGURE 2 | The relationships between troponin T and hemoglobin level in the study groups. **(A)** Cancer MINOCA, **(B)** Non-cancer MINOCA, **(C)** Cancer MI-CAD, **(D)** Non-cancer MI-CAD, and **(E)** In both cancer groups, the ratio of troponin T to hemoglobin was higher than in the respective non-cancer groups. MINOCA, myocardial infarction with non-obstructive coronary artery; MI-CAD, myocardial infarction and obstructive coronary artery disease.

MINOCA subjects ($p < 0.05$ for all pairwise comparisons) with the blurring of differences during hospitalization in maximal peak values (**Table 2**). After adjustment for renal function, the highest inverse correlation between hemoglobin level and baseline troponin T concentration was found in the cancer MINOCA ($r = -0.41$, $p = 0.05$) group (**Figures 2A–D**). The

TABLE 3 | The long-term mortality and its causes.

	MINOCA		MI-CAD		*P*-value
	Cancer *N* = 21	Non-cancer *N* = 51	Cancer *N* = 113	Non-Cancer *N* = 826	
Patients who died during follow-up	14 (66.7)#,^	15 (29.4)	82 (72.6) #,^	256 (31.0)	<0.001*
Crude mortality rate, %/year	19.2#,^	5.9	31.7#,^	7.9	<0.001**
Age- and sex-standardized mortality rate, %/year	26.7#,^	2.3	25.0#,^	3.7	<0.001**
Causes of death, expressed as number (% of patients who died)					
Cancer	6 (42.8)#,^	3 (20.0)	46 (56.0)#,^	45 (17.6)	<0.001*
Unknown	0	1 (6.7)	3 (3.7)	8 (3.1)	
Other	2 (14.3)	3 (20.0)	9 (11.0)	54 (21.1)	
Cardiovascular:	6 (42.8)	8 (53.3)	24 (29.3)#,^	149 (58.2)	
Coronary artery disease	1 (7.1)	2 (13.3)	8 (9.8)	63 (24.6)	NA*
Cerebrovascular disease	1 (7.1)	2 (13.3)	4 (4.9)	22 (8.6)	
Heart failure	2 (14.3)	3 (20.0)	6 (7.3)	28 (10.9)	
Atherosclerosis	2 (14.3)	1 (6.7)	6 (7.3)	36 (14.1)	

Data are shown as number (percentage) unless otherwise indicated, MINOCA, myocardial infarction with non-obstructive coronary artery; MI-CAD, myocardial infarction and obstructive coronary artery disease; NA, not applicable; p-value for differences in four groups based on a chi-square test with a post-hoc z-test for comparison of column proportions with the Bonferroni method (*) or a log-rank test for multiple comparisons of survival curves with the Bonferroni-corrected threshold (**), #p < 0.05 non-cancer MINOCA, ^p < 0.05 non-cancer MI-CAD.

proposed ratio of troponin T to hemoglobin was higher in cancer patients with MINOCA and MI-CAD when compared with the respective non-cancer groups (**Figure 2E**). The time of hospitalization was insignificantly shorter in non-cancer MINOCA (4 (3–7) days) as compared with cancer MINOCA (6 (3–12) days), cancer MI-CAD (6 (3–9) days), and non-cancer MI-CAD (6 (4–8) days) and ($p = 0.07$).

Active Cancer Diagnosis Among MINOCA Patients

MINOCA was recognized significantly more often in cancer patients (21 of 134) compared with the non-cancer (51 of 877) cohort (15.7 vs. 5.8%, $p < 0.001$). A higher percentage of women was found in both cancer and non-cancer MINOCA groups than in the respective MI-CAD populations ($p < 0.05$ for both pairwise comparisons). A higher incidence of anemia was observed in cancer vs. non-cancer MINOCA group (47.6 vs. 21.6%, $p < 0.05$), without a significant difference in thrombocytopenia (14.3 and 3.9%). In both groups, the vast majority of MIs were classified as NSTEMI (71.4 and 88.2%, respectively). Similar treatment regimens were found in both MINOCA subgroups (**Table 1**). Aspirin was used in 90.5 and 86.3% of patients, respectively, whereas P2Y12 inhibitor was used in approximately half of the patients in both groups. Only proton pump inhibitors were used less frequently in cancer than in non-cancer MINOCA patients (38.1 vs. 68.6%, $p < 0.05$).

The echocardiographic screening showed more frequent Takotsubo syndrome in the oncological patients (19.1 vs. 2.0%, $p = 0.010$), with almost the same distribution of insignificant lesions in angiography in both groups (**Table 1**). Both epicardial thrombi and distal embolization were not found in cancer MINOCA and were reported only in the single non-cancer patients with MINOCA. Higher right ventricular systolic pressures ($p = 0.03$) and lower left atrium diameters ($p = 0.05$) (**Table 2**) were found in cancer vs. non-cancer patients with MINOCA with no differences in left ventricular ejection fraction (LVEF).

Active Cancer in Patients With MI With vs. Without Obstructive Coronary Artery Disease

Active cancer was found more often in patients with MINOCA (21 of 72) compared to patients (29.2 vs. 12.0%, $p < 0.001$) with MI-CAD (113 of 939) (**Table 1**). Men were almost two times as represented in the cancer MI-CAD group compared with the MINOCA subgroup (77.9 vs. 38.1%, $p < 0.05$). Almost half of the patients had anemia in both groups, and both cancer groups presented with thrombocytopenia less frequently than anemia (**Table 1**) in a similar proportion when compared with respective non-cancer populations. In-hospital use of P2Y12 inhibitors (47.6 vs. 92.9%, $p < 0.001$), proton pump inhibitors (38.1 vs. 74.3%, $p = 0.001$), and statins (66.7 vs. 87.6%, $p < 0.05$) was less frequent in cancer MINOCA than in cancer MI-CAD.

In half of the newly diagnosed neoplasms, the first symptom was bleeding associated with antiplatelet and/or antithrombotic treatment administered during index MI, including hematuria (26%), hemoptysis (13%), and bleeds from the gastrointestinal tract (13%). Genitourinary neoplasms were predominant in

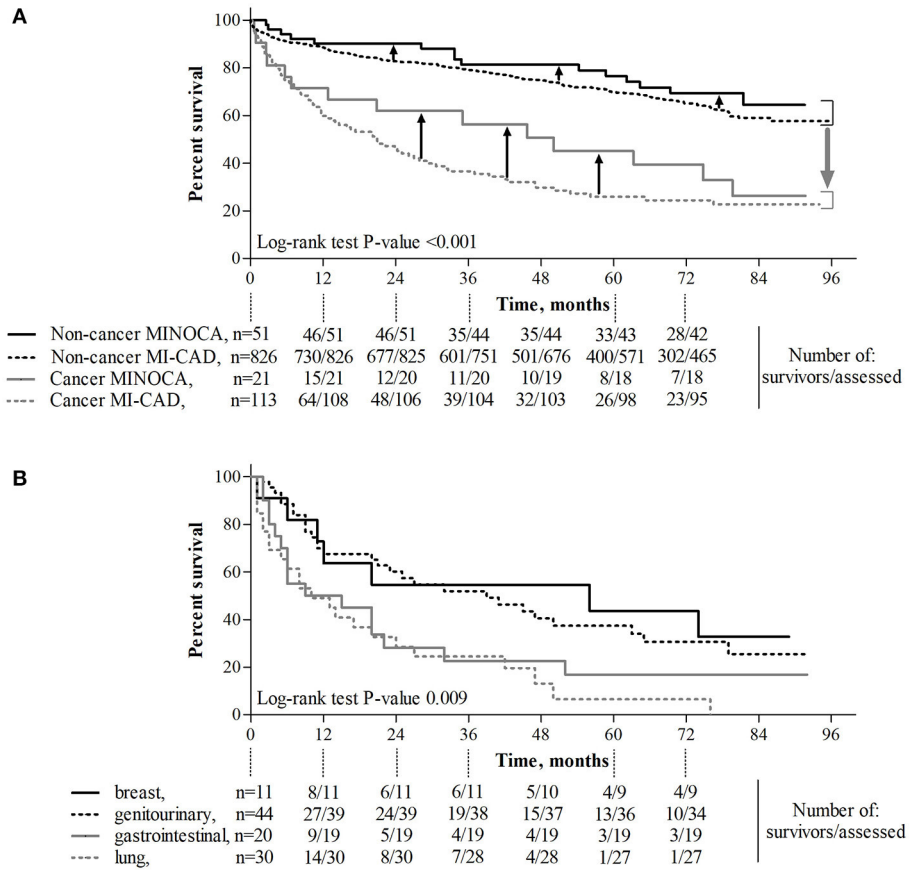

FIGURE 3 | The effect of cancer and its type and MINOCA on long-term survival. **(A)** Diagnosis of cancer was associated with significantly reduced long-term survival ($p < 0.001$, gray, wide arrow), whereas MINOCA diagnosis improved ($p = 0.048$, black, narrow arrows) long-term survival. **(B)** Long-term survival in patients with lung cancer was lower than that in those with genitourinary cancer ($p = 0.001$) or breast cancer ($p = 0.018$). MINOCA, myocardial infarction with non-obstructive coronary artery; MI-CAD, myocardial infarction and obstructive coronary artery disease.

both patients with MINOCA and MI-CAD (38.1 and 31.9%, respectively), whereas breast cancer was more frequent in the MINOCA group (23.8 vs. 5.3%, $p = 0.02$). There were significant differences neither in the locoregional and distant advancement of the neoplastic process nor in the anticancer treatment applied before the index MI (**Table 1**). The most commonly used chemotherapeutic agents in the MINOCA group were platinum compounds and taxanes. In turn, platinum compounds and fluoropyrimidines dominated in MI-CAD (**Table 1**).

Epicardial thrombus (12.4%) as well as distal embolization (8.0%) were observed numerically in a high percentage of cancer patients with MI-CAD but were not found in the cancer MINOCA group (**Table 1**). In the majority of cancer patients with MI-CAD, the significant atherosclerotic lesions were limited to one or two coronary arteries (77%). Most of these patients were treated with percutaneous coronary intervention (89.4%). In contrast, Takotsubo syndrome among patients with cancer was diagnosed only in the MINOCA group (19.1 vs. 0.0%, $p < 0.05$) (**Table 1**). There were no significant differences in right ventricular systolic pressure ($p = 0.18$) and LVEF ($p = 0.28$), but significantly larger end-diastolic ($p = 0.02$) and end-systolic ($p = 0.03$) left ventricular (LV) diameters were identified in the cancer MI-CAD group. Chemotherapy and radiotherapy administered before index MI did not affect LVEF ($p = 0.59$), end-diastolic ($p = 0.90$), or end-systolic ($p = 0.86$) LV diameters (**Table 2**).

Long-Term Mortality, Its Causes, and Predictors

The median follow-up time in patients with non-cancer MINOCA, non-cancer MI-CAD, cancer MINOCA, and cancer MI-CAD was 73.4 [33.7–81.7], 41.9 [28.1–73.5], 35.0 [6.2–77.2], and 17.3 [4.9–43.9] months, respectively ($p < 0.001$). Both crude or age- and sex-standardized mortality rates as well as causes of death differed among the four groups (**Table 3**). As expected, the higher prevalence of cancer deaths was more pronounced in both oncological groups. In turn, cardiovascular causes of death were predominant in both non-cancer MINOCA and MI-CAD groups. Long-term survival was significantly higher in non-cancer MINOCA when compared with cancer MINOCA (HR 4.07, 95% CI 1.72–9.64, $p = 0.002$) and in non-cancer MI-CAD when compared with cancer MI-CAD (HR 7.62, 95% CI 5.13–11.31, $p < 0.001$). Concurrently, there were no significant differences in long-term survival between both cancer groups of MINOCA and MI-CAD (HR 0.76, 95% CI 0.45–1.28, $p =$

TABLE 4 | The independent predictors of death in the whole group and in patients with MINOCA.

	Univariable model			Multivariable model		
	***P*-value**	**HR**	**95% CI for HR**	***P*-value**	**HR**	**95% CI for HR**
The whole group						
Age, per year	0.009	1.01	1.00–1.02	0.24	1.01	0.99–1.02
Male gender, yes/no	<0.001	0.65	0.53–0.80	0.53	0.93	0.74–1.17
Active cancer, yes/no	<0.001	3.33	2.64–4.21	<0.001	3.12	2.41–4.04
MINOCA, yes/no	0.18	0.90	0.65–1.15	0.048	0.69	0.47–0.97
Anemia, yes/no	<0.001	1.76	1.40–2.20	-		
Hemoglobin, per 1 g/dl	<0.001	0.88	0.84–0.93	0.018	0.93	0.88–0.99
LVEF, per 5%	0.74	1.00	0.99–1.01	-		
Killip 3/4 vs. 0/1 on admission	0.61	1.10	0.77–1.57	0.94	1.01	0.71–1.45
MINOCA patients						
Age, per 1 year	0.019	1.05	1.01–1.10	0.044	1.04	1.00–1.08
Female gender, yes/no	0.73	1.14	0.55–2.37	-		
Active cancer, yes/no	0.003	3.09	1.49–6.41	0.040	2.24	1.04–4.80
LVEF, per 5%	0.007	0.96	0.94–0.99	0.012	0.95	0.93–0.97

CI, confidence interval; HR, hazard ratio; LVEF, left ventricular ejection fraction; MINOCA, myocardial infarction with non-obstructive coronary artery.

0.31), as well as both non-cancer groups of MINOCA and MI-CAD (HR 0.80, 95% CI 0.50–1.28, $p = 0.35$) (**Figure 3A**). The median survival time irrespective of the type of MI was 56, 39, 12, and 10 months for breast, genitourinary, gastrointestinal, and lung cancer, respectively (**Figure 3B**). A significantly better survival rate was found in patients with genitourinary cancer vs. lung cancer (HR 0.34, 95% CI 0.18–0.65, $p = 0.001$) and in breast cancer vs. lung cancer (HR 0.39, 95% CI 0.18–0.85, $p = 0.02$).

In the MINOCA group, there were no significant differences in the long-term survival between patients with vs. without Takotsubo syndrome (**Supplementary Figure 1**). There was also a significantly higher long-term mortality rate in cancer vs. non-cancer patients matched for age, gender, body mass index, diabetes, hypertension, and hyperlipidemia (**Supplementary Table 1** and **Figure 2**). A Cox proportional hazard regression limited to patients matched for demographic parameters and cardiovascular risk factors showed that unfavorable prognosis was associated with active cancer, a lower hemoglobin level, and age of older patients. Simultaneously, hypertension, hyperlipidemia, and better LVEF independently improved long-term survival (**Supplementary Table 2**).

In the whole group, age, female gender, cancer, anemia, and lower hemoglobin level were identified as associated with a higher mortality rate in a univariate model (**Table 4**). Using a Cox proportional hazard regression, an active cancer was independently associated with a higher long-term mortality rate, while higher hemoglobin levels and MINOCA diagnosis improved long-term survival (**Table 4**). A Cox proportional hazard regression limited to only patients with MINOCA showed that age, cancer, and LVEF were independently associated with a long-term mortality rate (**Table 4**).

DISCUSSION

To our knowledge, this study is the first and most comprehensive analysis derived from a tertiary cardio-oncology center concerning the complex relationship between cancer and MINOCA, as well as its influence on long-term clinical outcomes. As shown, neoplasm has been identified more frequently in patients with MINOCA than in those with atherosclerosis and/or thrombus-based type 1 MI (defined as MI-CAD). However, a multivariable analysis showed that an active malignancy was associated with unfavorable long-term outcomes. We have also provided clinical features that characterized cancer patients with MINOCA, which might be useful in their differential diagnosis. It is important to note that the diagnosis of cancer in both MINOCA and MI-CAD groups was associated with an extremely high all-cause mortality in a 5-year observation. Moreover, a multivariable approach limited to only the MINOCA group showed that active cancer irrespective of age and lower left ventricular systolic function affected a higher mortality rate.

Patients with MI-CAD and cancer distinguished in our study were characterized by a highly unfavorable prognosis driven mostly by neoplastic disease. Although treatment of such patients should be strictly individualized, there are still limited data sufficiently addressing the optimal management of MI in patients with cancer (27). Further studies are warranted to establish an optimal antithrombotic regimen, especially in the acute phase, due to the proven high risk of stent thrombosis (9, 28). The results derived from the large Nationwide Inpatient Sample indicate that cancer in patients receiving percutaneous coronary intervention is common, but its prognostic impact depends on detailed oncological characteristics (29). Our results also indicate that, in both cancer and non-cancer MI-CAD patients, the rate of revascularization with the percutaneous coronary

intervention was almost 90% emphasizing current trends in interventional cardiology. While cancer patients with type 1 MI were historically less likely to receive primary percutaneous coronary intervention with first-generation drug-eluting stents mainly due to the need for a shorter course of dual antiplatelet therapy following bare-metal stents, the new drug-eluting stents requiring shorter antiplatelet therapy time have become more effective and as safe as bare-metal stents. According to the current registries, dual antiplatelet therapy was prescribed in only half of the patients with MINOCA, mainly in those with sinus rhythm, prior percutaneous coronary intervention, and active smokers (30).

In contrast, the prognosis in patients with MINOCA remains controversial, with the latest studies suggesting comparable (4, 31) or lower (15) long-term mortality rates in patients with MINOCA vs. MI-CAD. The abovementioned studies indicate that a history of cancer coexisting with 2–2.5% of patients with MINOCA (4, 13) is (13) or is not (15) an independent predictor of their long-term mortality. In our MINOCA and MI-CAD groups, a diagnosis of active cancer made before index MI was more common. This overrepresentation of neoplastic status was independently associated with unfavorable long-term survival. When compared with the available literature, such a high proportion of cancer patients is primarily a result of the structure of our center, as well as that of direct admissions from oncology and thoracic surgery departments to the cardiology ward. Interestingly, there is a visible trend toward more frequent admissions of cardio-oncology patients due to their prolonged survival time.

The etiology of MI in the oncological population is multifactorial. In previous studies, the role of cancer-induced immunological disorders, oxidative stress, prothrombotic state, and oncological treatment was underlined in MI development among cancer patients (32). Moreover, oncological patients are generally high-risk due to the significant prevalence of traditional cardiovascular risk factors, such as older age, hypertension, dyslipidemia, diabetes, obesity, or tobacco addiction (28). This was also corroborated in this current study. Most of the above-indicated factors contribute to the shifted oxidase-reductase balance and endothelial injury. This exacerbates coronary artery disease progression and promotes the rupture of atherosclerotic plaque associated with type I of MI, identified as MI-CAD (28, 32, 33) in our study. On the contrary, the influence of cancer and antitumor treatment is undeniable among MINOCA survivors. The rupture of non-obstructive plaque, distal embolization, hypercoagulable state with thrombus formation, transient artery spasm, microvascular dysfunction often caused by endothelial impairment, and supply-demand mismatch, among others, are all mechanisms responsible for MINOCA (5). It is worth noting that, each of these sequences of events might be triggered by both tumor and antineoplastic treatment (13). The classic chemotherapy drugs have been proven to damage the coronary arteries, mainly in their endothelium. Therefore, they can lead to acute thrombosis and coronary spasms (33). Drugs that particularly increase the risk of MI include fluoropyrimidines (5-fluorouracil, capecitabine, gemcitabine) and platinum compounds (33), which were also often used among the analyzed patients. Moreover, combining chemotherapeutics from different groups, especially those mentioned above, significantly increases the risk of MI (33). However, there is a lack of original reports demonstrating the relationship between chemotherapy and MINOCA. Our study provides detailed angiographic and echocardiographic characteristics of cancer patients with MINOCA, shedding light on their potential relationships. These findings might be helpful in further research dedicated for personalized treatment in this demanding group of patients.

A long-term prognosis is associated with myocardial infarct size. As we have shown, both cancer and non-cancer patients with MINOCA were characterized by a better preserved global LV function and lower peak high-sensitive troponin levels compared with the corresponding MI-CAD groups. This indirectly indicates a lower myocardial injury rate and most likely a smaller infarct size in patients with MINOCA. These findings are in line with previous data showing that, among the MINOCA population, patients with heart failure with preserved LV ejection fraction (34, 35) predominated. Post-infarction myocardial remodeling is also less frequently observed in this group. There are at least a few potential explanations for this relationship. First, the smaller myocardial infarct size is a consequence of a higher prevalence of NSTEMI in MINOCA (8). Second, cardiac magnetic resonance imaging provides evidence that, in patients with MINOCA, only small foci of necrosis are often observed, while myocardial edema is the dominant abnormality (36).

In this study, hemoglobin levels were lower in both cancer groups, compared with respective non-cancer MINOCA and MI-CAD groups. Moreover, as has been shown in our multivariable models, lower hemoglobin levels worsen long-term prognosis in the whole group, but not in the population limited to patients with MINOCA. According to criteria similar to ours, anemia at baseline was found in approximately 40% of patients in the European Cancer Anemia Survey (37). This proportion increased up to 60–70% during either anticancer treatment or cancer progression, affecting the higher overall mortality risk (38). In our cancer patients with MINOCA, lower hemoglobin levels were associated with higher baseline troponin concentrations, suggesting the possibility of anemia-induced myocardial injury (16). As has been shown previously, active cancer should be considered as a secondary cause of troponinosis that is not associated with acute coronary syndrome (39, 40). Moreover, troponin elevation was linked with a higher mortality rate, especially in patients with lung cancer (41). We have also found that the ratio of troponin T to hemoglobin was significantly higher in both cancer populations when compared to the respective non-cancer groups. Our findings are one more argument for the adoption of a higher troponin cut-off value for MI in patients with cancer (39, 40). The relatively high proportion of patients with cancer-induced anemia, also visible in our cohort, may require blood transfusion or other available methods of treatment (erythropoietin or iron supplementation). In a propensity-matched analysis, Salisbury et al. have demonstrated that blood transfusion was associated with a lower risk of in-hospital mortality (42). In turn, a meta

analysis done by Chatterjee et al. indicates that a liberal blood transfusion strategy is associated with higher all-cause mortality when compared to a more restricted strategy, which might be associated with volume overload, increased thrombogenicity, impaired oxygen delivery, and a risk of infection (43).

Limitations

Our study has several limitations. First, the analyzed cancer MINOCA group is relatively small. However, it represents a unique and comprehensively characterized cohort. Second, despite their obvious heterogeneity and applied various methods of anticancer treatment, due to the small sample size of patients with different types of cancer, a multivariable analysis had to be performed for all patients with cancer. Third, cardiac magnetic resonance and intracoronary imaging were not performed to confirm an alternative diagnosis including myocarditis (44, 45). Fourth, apart from death, we did not analyze other clinical outcomes, such as recurrent MI, ischemic stroke, or heart failure decompensation. Moreover, the fact of quitting smoking after the cancer diagnosis undoubtedly contributed to its underestimated self-reporting. Finally, we also did not perform specific coagulation tests that would determine the role of prothrombotic states involved in the etiology of MINOCA (8, 46, 47).

CONCLUSIONS

Our findings provide evidence that active cancer in the whole cohort of patients with MI, overrepresented among the MINOCA population, is associated with extremely high long-term mortality. A multivariable approach indicates that an active malignancy was independently associated with unfavorable long-term survival in the whole MI population as well as in patients with MINOCA.

DATA AVAILABILITY STATEMENT

The raw data supporting the conclusions of this article will be made available by the authors, without undue reservation.

ETHICS STATEMENT

The studies involving human participants were reviewed and approved by Jagiellonian University Medical College Ethics Committee (Consent No. 1072.6120.59.2018). The patients/participants provided their written informed consent to participate in this study.

AUTHOR CONTRIBUTIONS

KS conceived the concept of the study. KS, KN, and JZ contributed to the design of the research. KS, KN, and BS reviewed the literature and were involved in data acquisition. All authors analyzed and interpreted the data. JN and JZ supervised data processing. All authors edited and approved the final version of the manuscript.

SUPPLEMENTARY MATERIAL

The Supplementary Material for this article can be found online at: https://www.frontiersin.org/articles/10.3389/fcvm.2022.785246/full#supplementary-material

REFERENCES

1. Agewall S, Beltrame JF, Reynolds HR, Niessner A, Rosano G, Caforio AL, et al. ESC working group position paper on myocardial infarction with non-obstructive coronary arteries. *Eur Heart J.* (2017) 38:143–53. doi: 10.1093/eurheartj/ehw149
2. Gehrie ER, Reynolds HR, Chen AY, Neelon BH, Roe MT, Gibler WB, et al. Characterization and outcomes of women and men with non-ST-segment elevation myocardial infarction and non-obstructive coronary artery disease: results from the Can Rapid Risk Stratification of Unstable Angina Patients Suppress Adverse Outcomes with Early Implementation of the ACC/AHA Guidelines (CRUSADE) quality improvement initiative. *Am Heart J.* (2009) 158:688–94. doi: 10.1016/j.ahj.2009.08.004
3. Larsen AI, Galbraith PD, Ghali WA, Norris CM, Graham MM, Knudtson ML, et al. Characteristics and outcomes of patients with acute myocardial infarction and angiographically normal coronary arteries. *Am J Cardiol.* (2005) 95:261–3. doi: 10.1016/j.amjcard.2004.09.014
4. Nordenskjöld AM, Baron T, Eggers KM, Jernberg T, Lindahl B. Predictors of adverse outcome in patients with myocardial infarction with non-obstructive coronary artery (MINOCA) disease. *Int J Cardiol.* (2018) 261:18–23. doi: 10.1016/j.ijcard.2018.03.056
5. Tamis-Holland JE, Jneid H, Reynolds HR, Agewall S, Brilakis ES, Brown TM, et al. Contemporary diagnosis and management of patients with myocardial infarction in the absence of obstructive coronary artery disease: a scientific statement from the American heart association. *Circulation.* (2019) 139:e891–908. doi: 10.1161/CIR.0000000000000670
6. Pizzi C, Xhyheri B, Costa GM, Faustino M, Flacco ME, Gualano MR, et al. Non-obstructive vs. obstructive coronary artery disease in acute coronary syndrome: a meta-analysis. *J Am Heart Assoc.* (2016) 5:e004185. doi: 10.1161/JAHA.116.004185
7. Pasupathy S, Air T, Dreyer RP, Tavella R, Beltrame JF. Systematic review of patients presenting with suspected myocardial infarction and non-obstructive coronary arteries. *Circulation.* (2015) 131:861–70. doi: 10.1161/CIRCULATIONAHA
8. Stepien K, Nowak K, Wypasek E, Zalewski J, Undas A. High prevalence of inherited thrombophilia and antiphospholipid syndrome in myocardial infarction with non-obstructive coronary arteries: comparison with cryptogenic stroke. *Int J Cardiol.* (2019) 290:1–6. doi: 10.1016/j.ijcard.2019.05.037
9. Stepien K, Nowak K, Zalewski J, Pac A, Undas A. Extended treatment with non-vitamin K antagonist oral anticoagulants vs. low-molecular-weight heparins in cancer patients following venous thromboembolism. *A pilot study Vascul Pharmacol.* (2019) 120:106567. doi: 10.1016/j.vph.2019.106567
10. Navi BB, Reiner AS, Kamel H, Iadecola C, Okin PM, Elkind MSV, et al. Risk of arterial thromboembolism in patients with cancer. *J Am Coll Cardiol.* (2017) 70:926–38. doi: 10.1016/j.jacc.2017.06.047
11. Mulder FI, Horváth–Puhó E, van Es N, Büller HR, Bøtker HE, Sørensen HT. Arterial thromboembolism in cancer patients: a Danish population-based cohort study. *JACC: CardioOncol.* (2021) 3:205–18. doi: 10.1016/j.jaccao.2021.02.007
12. Navi BB, Reiner AS, Kamel H, Iadecola C, Okin PM, Tagawa ST, et al. Arterial thromboembolic events preceding the diagnosis of cancer in older persons. *Blood.* (2019) 133:781–9. doi: 10.1182/blood-2018-06-860874

13. Pelliccia F, Pasceri V, Tanzilli G, Speciale G, Camici PG, Gaudio C. Malignancy in patients with myocardial infarction and non-obstructive coronary arteries: a systematic review and meta-regression. *Eur J Intern Med.* (2020) 81:38–43. doi: 10.1016/j.ejim.2020.06.018
14. Nordenskjöld AM, Eggers KM, Jernberg T, Mohammad MA, Erlinge D, Lindahl B. Circadian onset and prognosis of myocardial infarction with non-obstructive coronary arteries (MINOCA). *PLoS ONE.* (2019) 14:e0216073. doi: 10.1371/journal.pone.0216073
15. Pelliccia F, Pasceri V, Niccoli G, Tanzilli G, Speciale G, Gaudio C, et al. Predictors of mortality in myocardial infarction and non-obstructed coronary arteries: a systematic review and meta-regression. *Am J Med.* (2020) 133:73–83. doi: 10.1016/j.amjmed.2019.05.048
16. Thygesen K, Alpert JS, Jaffe AS, Chaitman BR, Bax JJ, Morrow DA, et al. Fourth universal definition of myocardial infarction. *Circulation.* (2018) 138:e618–51. doi: 10.1161/CIR.0000000000000617
17. Stepień K, Nowak K, Nessler J, Zalewski J. Worse long-term prognosis in myocardial infarction occurring at weekends or public holidays with insight into myocardial infarction with non-obstructive coronary arteries. *Pol Arch Intern Med.* (2020) 130:942–52. doi: 10.20452/pamw.15615
18. Stepien K, Nowak K, Skorek P, Baravik V, Kozynacka A, Nessler J, et al. Baseline indicators of coronary artery disease burden in patients with non-ST-segment elevation acute coronary syndrome. *Minerva Cardioangiol.* (2019) 67:181–90. doi: 10.23736/S0026-4725.19.04838-2
19. Khorana AA, Noble S, Lee AYY, Soff G, Meyer G, O'Connell C, et al. Role of direct oral anticoagulants in the treatment of cancer-associated venous thromboembolism: guidance from the SSC of the ISTH. *J Thromb Haemost.* (2018) 16:1891–4. doi: 10.1111/jth.14219
20. Skorek P, Stepień K, Fila M, Hauer J, Kuzdzał J. Preoperative thrombocytosis in surgically treated patients with non-small cell lung cancer. *Pol Arch Intern Med.* (2018) 128:512–7. doi: 10.20452/pamw.4299
21. Zalewski J, Bogaert K, Desmet W, Sinnaeve P, Berger P, Grines C, et al. Intraluminal thrombus in facilitated vs. primary percutaneous coronary intervention: an angiographic sub-study of the ASSENT-4 PCI trial. *J Am Coll Cardiol.* (2011) 57:1867–73. doi: 10.1016/j.jacc.2010.10.061
22. Zalewski J, Zmudka K, Musiałek P, Zajdel W, Pieniazek P, Kadzielski A, et al. Detection of microvascular injury by evaluating epicardial blood flow in early reperfusion following primary angioplasty. *Int J Cardiol.* (2004) 96:389–96. doi: 10.1016/j.ijcard.2003.08.009
23. Lang R, Badano L, Mor-Avi V, Afilalo J, Armstrong A, Ernande L, et al. Recommendations for cardiac chamber quantification by echocardiography in adults: an update from the American society of echocardiography and the European association of cardiovascular imaging. *J Am Soc Echocardiogr.* (2015) 28:1–39. doi: 10.1016/j.echo.2014.10.003
24. Ghadri JR, Wittstein IS, Prasad A, Sharkey S, Dote K, Akashi YJ, et al. International expert consensus document on takotsubo syndrome (Part I): clinical characteristics, diagnostic criteria, and pathophysiology. *Eur Heart J.* (2018) 39:2032–46. doi: 10.1093/eurheartj/ehy076
25. Napp LC, Cammann VL, Jaguszewski M, Szawan KA, Wischnewsky M, Gili S, et al. Coexistence and outcome of coronary artery disease in Takotsubo syndrome. *Eur Heart J.* (2020) 41:3255–68. doi: 10.1093/eurheartj/ehaa210
26. Eurostat – European Statistics of European Commission. Available online at: https://ec.europa.eu/eurostat (accessed May, 05, 2021).
27. Potts JE, Iliescu CA, Lopez Mattei JC, Martinez SC, Holmvang L, Ludman P, et al. Percutaneous coronary intervention in cancer patients: a report of the prevalence and outcomes in the United States. *Eur Heart J.* (2019) 40:1790–800. doi: 10.1093/eurheartj/ehy769
28. Inohara T, Endo A, Melloni C. Unmet needs in managing myocardial infarction in patients with malignancy. *Front Cardiovasc Med.* (2019) 6:57. doi: 10.3389/fcvm.2019.00057
29. Rohrmann S, Witassek F, Erne P, Rickli H, Radovanovic D. Treatment of patients with myocardial infarction depends on history of cancer. *Eur Heart J Acute Cardiovasc Care.* (2018) 7:639–45. doi: 10.1177/2048872617729636
30. Montenegro Sá F, Carvalho R, Santos L, Ruivo C, Antunes A, Belo A, et al. Dual antiplatelet therapy in myocardial infarction with non-obstructive coronary artery disease - insights from a nationwide registry. *Rev Port Cardiol.* (2020) 39:679–84. doi: 10.1016/j.repc.2020.05.008
31. Choo EH, Chang K, Lee KY, Lee D, Kim JG, Ahn Y, et al. Prognosis and predictors of mortality in patients suffering myocardial infarction with non-obstructive coronary arteries. *J Am Heart Assoc.* (2019) 8:e011990. doi: 10.1161/JAHA.119.011990
32. Costa IBSDS, Andrade FTA, Carter D, Seleme VB, Costa MS, Campos CM, et al. Challenges and management of acute coronary syndrome in cancer patients. *Front Cardiovasc Med.* (2021) 8:590016. doi: 10.3389/fcvm.2021.590016
33. Zamorano JL, Lancellotti P, Rodriguez Munoz D, Aboyans V, Asteggiano R, Galderisi M, et al. 2016 ESC position paper on cancer treatments and cardiovascular toxicity developed under the auspices of the esc committee for practice guidelines: the task force for cancer treatments and cardiovascular toxicity of the european society of cardiology (ESC). *Eur Heart J.* (2016) 37:2768–801. doi: 10.1093/eurheartj/ehw211
34. Paolisso P, Foà A, Bergamaschi L, Donati F, Fabrizio M, Chiti C, et al. Hyperglycemia, inflammatory response and infarct size in obstructive acute myocardial infarction and MINOCA. *Cardiovasc Diabetol.* (2021) 20:33. doi: 10.1186/s12933-021-01222-9
35. Alkhawam H, Chaitman BR, Salloum MN, Abo-Salem E, Ghrair F, Saker E, et al. Myocardial infarct size and sex-related angiographic differences in myocardial infarction in non-obstructive coronary artery disease. *Coron Artery Dis.* (2021) 32:603–9. doi: 10.1097/MCA.0000000000001018
36. Baccouche H, Mahrholdt H, Meinhardt G, Merher R, Voehringer M, Hill S, et al. Diagnostic synergy of non-invasive cardiovascular magnetic resonance and invasive endomyocardial biopsy in troponin-positive patients without coronary artery disease. *Eur Heart J.* (2009) 30:2869–79. doi: 10.1093/eurheartj/ehp328
37. Ludwig H, Van Belle S, Barrett-Lee P, Birgegård G, Bokemeyer C, Gascón P, et al. The European Cancer Anaemia Survey (ECAS): a large, multinational, prospective survey defining the prevalence, incidence, and treatment of anaemia in cancer patients. *Eur J Cancer.* (2004) 40:2293–306. doi: 10.1016/j.ejca.2004.06.019
38. Macciò A, Madeddu C, Gramignano G, Mulas C, Tanca L, Cherchi MC, et al. The role of inflammation, iron, and nutritional status in cancer-related anemia: results of a large, prospective, observational study. *Haematologica.* (2015) 100:124–32. doi: 10.3324/haematol.2014.112813
39. Lippi G, Cervellin G. Cardiac troponin testing in acute coronary syndrome: personalised thresholds or generalized cut-offs. *J Lab Precis Med.* (2016) 1:1–6. doi: 10.21037/jlpm.2016.11.04
40. Danese E, Montagnana M, Giudici S, Aloe R, Franchi M, Guidi GC, et al. Highly-sensitive troponin I is increased in patients with gynecological cancers. *Clin Biochem.* (2013) 46:1135–8. doi: 10.1016/j.clinbiochem.2013.04.029
41. Lim E, Li Choy L, Flaks L, Mussa S, Van Tornout F, Van Leuven M, et al. Detected troponin elevation is associated with high early mortality after lung resection for cancer. *J Cardiothorac Surg.* (2006) 1:37. doi: 10.1186/1749-8090-1-37
42. Salisbury AC, Reid KJ, Marso SP, Amin AP, Alexander KP, Wang TY, et al. Blood transfusion during acute myocardial infarction: association with mortality and variability across hospitals. *J Am Coll Cardiol.* (2014) 64:811–9. doi: 10.1016/j.jacc.2014.05.040
43. Chatterjee S, Wetterslev J, Sharma A, Lichstein E, Mukherjee D. Association of blood transfusion with increased mortality in myocardial infarction: a meta-analysis and diversity-adjusted study sequential analysis. *JAMA Intern Med.* (2013) 173:132–9. doi: 10.1001/2013.jamainternmed.1001
44. Reynolds HR, Maehara A, Kwong RY, Sedlak T, Saw J, Smilowitz NR, et al. Coronary optical coherence tomography and cardiac magnetic resonance imaging to determine underlying causes of myocardial infarction with non-obstructive coronary arteries in women. *Circulation.* (2021) 143:624–40. doi: 10.1161/CIRCULATIONAHA.120.052008
45. Hausvater A, Smilowitz NR Li B, Redel-Traub G, Quien M, Qian Y, et al. Myocarditis in relation to angiographic findings in patients with provisional diagnoses of MINOCA. *JACC Cardiovasc Imag.* (2020) 13:1906–13. doi: 10.1016/j.jcmg.2020.02.037
46. Zalewski J, Lewicki L, Krawczyk K, Zabczyk M, Targonski R, Molek P, et al. Polyhedral erythrocytes in intracoronary thrombus and their association with reperfusion in myocardial infarction. *Clin Res Cardiol.* (2019) 108:950–62. doi: 10.1007/s00392-019-01425-x
47. Zalewski J, Bogaert J, Sadowski M, Woznicka O, Doulaptsis K, Ntoumpanaki M, et al. Plasma fibrin clot phenotype independently affects intracoronary

thrombus ultrastructure in patients with acute myocardial infarction. *Thromb Haemost.* (2015) 113:1258–69. doi: 10.1160/TH14-09-0801

Conflict of Interest: The authors declare that the research was conducted in the absence of any commercial or financial relationships that could be construed as a potential conflict of interest.

Publisher's Note: All claims expressed in this article are solely those of the authors and do not necessarily represent those of their affiliated organizations, or those of the publisher, the editors and the reviewers. Any product that may be evaluated in this article, or claim that may be made by its manufacturer, is not guaranteed or endorsed by the publisher.

frontiers | Frontiers in Cardiovascular Medicine

REVIEW
published: 20 May 2022
doi: 10.3389/fcvm.2022.847975

Interconnected Clinical and Social Risk Factors in Breast Cancer and Heart Failure

*Arjun Sinha[1], Avni Bavishi[2], Elizabeth A. Hibler[3], Eric H. Yang[4], Susmita Parashar[5], Tochukwu Okwuosa[6], Jeanne M. DeCara[7], Sherry-Ann Brown[8], Avirup Guha[9,10], Diego Sadler[11], Sadiya S. Khan[1], Sanjiv J. Shah[1], Clyde W. Yancy[1] and Nausheen Akhter[1]**

[1] Division of Cardiology, Department of Medicine, Northwestern University Feinberg School of Medicine, Chicago, IL, United States, [2] Department of Medicine, Northwestern University Feinberg School of Medicine, Chicago, IL, United States, [3] Department of Preventive Medicine, Division of Cancer Epidemiology and Prevention, Northwestern University Feinberg School of Medicine, Chicago, IL, United States, [4] UCLA Cardio-Oncology Program, Division of Cardiology, Department of Medicine, University of California, Los Angeles, Los Angeles, CA, United States, [5] Division of Cardiology, Department of Medicine, Emory University, Atlanta, GA, United States, [6] Division of Cardiology, Department of Medicine, Rush University Medical Center, Chicago, IL, United States, [7] Section of Cardiology, Department of Medicine, University of Chicago Medicine, Chicago, IL, United States, [8] Division of Cardiology, Department of Medicine, Medical College of Wisconsin, Milwaukee, WI, United States, [9] Cardio-Oncology Program, Division of Cardiology, Medical College of Georgia at Augusta University, Augusta, GA, United States, [10] Cardio-Oncology Program, Division of Cardiology, The Ohio State University Medical Center, Columbus, OH, United States, [11] Robert and Suzanne Tomsich Department of Cardiovascular Medicine, Heart, Vascular and Thoracic Institute, Cleveland Clinic Florida, Weston, FL, United States

OPEN ACCESS

Edited by:
Dong Han,
People's Liberation Army General Hospital, China

Reviewed by:
Zaza Iakobishvili,
Clalit Health Services, Israel
Dipti Gupta,
Memorial Sloan Kettering Cancer Center, United States

***Correspondence:**
Nausheen Akhter
n-akhter@northwestern.edu

Specialty section:
This article was submitted to Cardio-Oncology, a section of the journal Frontiers in Cardiovascular Medicine

Received: *03 January 2022*
Accepted: *13 April 2022*
Published: *20 May 2022*

Citation:
Sinha A, Bavishi A, Hibler EA, Yang EH, Parashar S, Okwuosa T, DeCara JM, Brown S-A, Guha A, Sadler D, Khan SS, Shah SJ, Yancy CW and Akhter N (2022) Interconnected Clinical and Social Risk Factors in Breast Cancer and Heart Failure. Front. Cardiovasc. Med. 9:847975. doi: 10.3389/fcvm.2022.847975

Breast cancer and heart failure share several known clinical cardiovascular risk factors, including age, obesity, glucose dysregulation, cholesterol dysregulation, hypertension, atrial fibrillation and inflammation. However, to fully comprehend the complex interplay between risk of breast cancer and heart failure, factors attributed to both biological and social determinants of health must be explored in risk-assessment. There are several social factors that impede implementation of prevention strategies and treatment for breast cancer and heart failure prevention, including socioeconomic status, neighborhood disadvantage, food insecurity, access to healthcare, and social isolation. A comprehensive approach to prevention of both breast cancer and heart failure must include assessment for both traditional clinical risk factors and social determinants of health in patients to address root causes of lifestyle and modifiable risk factors. In this review, we examine clinical and social determinants of health in breast cancer and heart failure that are necessary to consider in the design and implementation of effective prevention strategies that altogether reduce the risk of both chronic diseases

Keywords: breast cancer, heart failure, risk factors, social determinants of health, reverse cardio-oncology

INTRODUCTION

Cardiovascular disease (CVD) and cancer are the two leading causes of death in the United States in 2020 (1). Classically, the field of cardio-oncology has focused on the development of CVD directly from cardiotoxic effects of cancer biology and/or cancer therapies. But there is growing appreciation that the two diseases intersect at multiple levels, including shared clinical risk factors, shared social risk factors, and reverse cardio-oncology where CVD acts to promote cancer development (2). In this review, we focus specifically on the intersections between breast cancer

and heart failure (HF). Delving into anti-cancer therapies that cause cancer therapy-related cardiac dysfunction is beyond the scope of this review. Breast cancer remains the most common cancer in women, with one in eight women expected to develop breast cancer over the course of their lifetime (3). There have been notable improvements in survival rates for breast cancer due to earlier detection and advancements in treatment such that the 5-year relative survival rate from the mid-1970s to the present time has increased from 75 to 90% (4). Breast cancer survivors with a prior history of CVD who survive cancer for over 5 years are more likely to die of CVD, (5) and in breast cancer survivors age 66 years or older, CVD is often the primary cause of death (6). The lifetime risk of developing HF in women is even higher at one in five at age 40 and rises rapidly with increasing age (7, 8). The overall burden of HF continues to increase with the aging of the general population and with increases in HF risk factors such as obesity and diabetes. Thus, as women age they are at increased risk for both breast cancer and HF. Here we examine the shared pathophysiology and commonalities in clinical and social risk factors that lead to the high prevalence of both HF and breast cancer.

TABLE 1 | Impact of modifiable heart failure risk factors that increase risk for breast cancer and potential underlying mechanisms.

Modifiable heart failure risk factors	Risk of breast cancer	Mechanisms
Diabetes	20% Increased Risk (19)	Hyperinsulinemia. Adipocyte Dysfunction. Hypoxia. Immune Cell Recruitment. Expression of Aromatase. Hyperleptinemia
Obesity	25% Increased Risk (20)	
Hypertension	15% Increased Risk (36)	Angiotensin II
Hyperlipidemia	9% Increased Risk (41)	27-hydroxycholesterol
Atrial Fibrillation	35% Increased Risk (47)	Reactive Oxygen Species

Shared Clinical Risk Factors

Traditional clinical risk factors for HF in women are well established. Modifiable clinical HF risk factors that may also increase risk for breast cancer include diabetes, obesity, hypertension, hyperlipidemia, and atrial fibrillation (**Table 1**) (9). Inextricably linked with these risk factors are health behaviors such as tobacco use, alcohol use, physical inactivity, and an unhealthy diet. Prevention of risk factors (or primary prevention) and avoidance of poor health behaviors dramatically lower the risk of incident HF (10, 11). The causal pathways connecting these risk factors to increased risk of CVD and HF are well known (12–14). However, their association with increased risk of breast cancer is only starting to be appreciated (15). In this section, we summarize epidemiological and mechanistic evidence to better understand the relationship between some of the traditional cardiovascular risk factors and breast cancer.

Obesity and Glucose Dysregulation

Of the common modifiable risk factors, diabetes and obesity have the strongest association with HF in women (16, 17). Multiple studies have also shown an increased risk of breast cancer in women with diabetes. In a meta-analysis of 39 independent risk estimates from observational epidemiological studies, women with diabetes had a 27% higher risk of developing breast cancer (summary relative risk [SRR] 1.27, 95% confidence interval [CI], 1.16 – 1.39) (18). In prospective studies, the risk of developing breast cancer remained 23% higher in women with diabetes (SRR 1.23 [95% CI, 1.12–1.35]). Part of the risk was mediated through concomitant obesity, but the risk of developing breast cancer remained 16% higher after adjusting for body mass index (BMI). Of note, the risk of breast cancer was not elevated in premenopausal women with diabetes or women with Type 1 diabetes. A more recent review of meta-analyses estimated a 20% greater risk of developing breast cancer in women with diabetes (19). Similarly, the risk of breast cancer is 25% higher in post-menopausal women with obesity (20). The risk of breast cancer increases by 10% for every 5 kg/m^2 higher BMI above 25 kg/m^2 in postmenopausal women (21). This association is strongest in estrogen receptor positive breast cancer (22). Obesity contributes to a chronic low-grade inflammation that can promote both carcinogenesis and atherosclerosis. Changes in the adipose tissue microenvironment can switch from anti-inflammatory to pro-inflammatory in obesity (23).

Glucose dysregulation is central to both disease processes and is integral to understanding the pathophysiology underlying this association. Both obesity and diabetes lead to adipocyte dysfunction, insulin resistance, and hyperglycemia (24, 25). The excess growth of adipose tissue results in hypoxia and expression of hypoxia-inducible factor 1a (HIF1a) (26). This results in adipocyte dysfunction, which promotes breast cancer growth through multiple interconnected pathways. First, adipocyte hypoxia results in release of chemokines such as monocyte chemoattractant protein 1 (MCP1), which recruits immune cells and creates a pro-inflammatory environment (27). Second, there is increased expression of aromatase, the rate-limiting enzyme in estrogen synthesis, which leads to higher levels of circulating estrogen (28). Higher levels of estrogen promote estrogen-responsive malignancies including breast cancer. Third, there is dysregulation of adipocyte endocrine function. In individuals with obesity, the central nervous system develops resistance to leptin, a hormone that limits appetite in healthy individuals (29). The subsequent hyperleptinemia promotes breast cancer initiation, growth, and progression by promoting cellular growth, inhibiting apoptosis, activating cellular adhesion and inflammatory immune cells (30). In contrast, in obesity there is reduced production of protective hormones such as adiponectin and ghrelin, both of which reduce breast cancer risk by inhibiting aromatase and other pathways associated with increased cancer cell proliferation (31, 32).

In combination with inflammatory cytokines, hypoxia, elevated estrogen, and altered milieu of adipokines, hyperinsulinemia and hyperglycemia lead to dysregulation of multiple metabolic pathways in not only breast cancer cells but also local stromal and immune cells (33). These triggers stimulate signaling cascades by activating receptor tyrosine kinases leading to activation of the phosphoinositide 3-kinase (PI3K)-AKT pathway and inhibition of the AMP-activated protein kinase (AMPK); favoring a shift toward aerobic glycolysis, glucose uptake, and cell proliferation in cancer, stromal, and immune cells (34, 35). These pathways also lead to aromatase activation in stromal cells and release of inflammatory cytokines from immune cells resulting in a positive feedback cycle and tumor progression (33).

Hypertension

Hypertension is one of the most prevalent risk factors for both HF and breast cancer, especially as the population ages. Numerous observational studies have also evaluated the association of hypertension with risk of incident breast cancer. A large meta-analysis of 30 observational studies, including 11,643 cases of breast cancer, demonstrated a 15% higher risk of breast cancer in adults with hypertension (RR: 1.15; 95% CI 1.08 – 1.22) (36). In another meta-analysis of 13 prospective studies, the association between hypertension and breast cancer was again noted (RR: 1.07; 95% CI 0.84 – 1.35) (37). This was primarily driven by the association observed in postmenopausal women. Like diabetes, hypertension was not associated with increased risk of breast cancer among premenopausal women. Mechanisms behind hypertension and breast cancer risk are not well established. Since hypertension is often linked with diabetes and obesity, there are some shared pathways such as chronic inflammation as described above. One specific pathway that links both obesity and hypertension to breast cancer involves angiotensin II. While the renin-angiotensin system is well-known for its role in blood pressure and fluid regulation, it can be activated within dysregulated adipose tissue as well (38). Angiotensin II increases tumor angiogenesis in receptor-negative breast cancer and leads to activation of proinflammatory macrophages promoting tumor growth.

Cholesterol Dysregulation

Dysregulation in cholesterol metabolism is another traditional cardiovascular risk factor that is associated with breast cancer. Some studies have demonstrated an association between high-density lipoprotein cholesterol (HDL-C) and breast cancer risk (39). In a study of 4,670 women with increased mammographic density, higher levels of HDL-C were associated with a 23% increased risk of breast cancer (40). While observational data have not consistently shown an association between low-density lipoprotein cholesterol (LDL-C) and breast cancer risk, a large mendelian randomization of > 400,000 participants found a significant association between genetic risk factors for lifelong elevated LDL-C and increased risk of estrogen receptor positive breast cancer (41). There is also evidence that higher dietary intake of cholesterol is associated with an increased risk of breast cancer in a non-linear fashion (42). However, it is difficult to disentangle the effects of obesity and diabetes from hypercholesterolemia using observational data.

There is growing mechanistic evidence that links hypercholesterolemia with breast cancer. 27-hydroxycholesterol is an endogenous oxysterol that has activity as a selective estrogen receptor modulator (43). It is generated by the P450 enzyme sterol 27-hydroxylase CYP27A1 and is transported in conjunction with HDL-C and LDL-C. It has been shown to stimulate the growth of estrogen receptor positive breast cancer cells in human xenografts and animal models. Potential mechanisms include inhibition of tumor suppressor proteins, activation of growth factors, and immune dysregulation such as suppression of cytotoxic CD8+ T cells within tumors (44). More work is needed to better understand this pathway and how cholesterol lowering therapies such as statins may affect it. Current data do not show convincing evidence of statin therapy protecting against breast cancer development but there are multiple observational studies suggesting a benefit of lipophilic statins on breast cancer recurrence and mortality (45).

Atrial Fibrillation

There is an association between atrial fibrillation (AF) and cancer, with inflammation contributing to the development of both in part through the production of reactive oxygen species. Elevation in C-reactive protein levels and increased NLRP3 inflammasome activation have also been reported in AF (46). Whether atrial fibrillation itself increases the risk of developing cancer requires further investigation. In a cohort study of 34,691 women followed for a median of 19 years, new-onset AF was found to be a significant risk factor for incident breast cancer after age-adjusted models (hazard ratio [HR], 1.35; 95% CI, 1.01–1.81; $p < 0.04$). This risk was highest in the first 3 months after incident AF, but remained beyond 1 year (47). Atrial fibrillation may also be a marker for occult cancer. Patients with cancer have a higher prevalence of AF compared to those in the general population (48). Women with breast cancer diagnosis have a significantly higher incidence of AF, with increasing risk for those who present at a higher breast cancer stage. Incident AF in newly diagnosed breast cancer also increases 1-year CV mortality (49).

Inflammation

As described above, immune dysregulation and inflammation are common final pathways that link traditional HF risk factors to breast cancer development. Obesity can lead to a chronic low-grade inflammation which leads to accumulation of pro-inflammatory adipose tissue macrophages, increased levels of aromatase, estrogen biosynthesis, and increased risk for estrogen-dependent breast cancer after menopause (28). Some inflammatory pathways are shared in HF and cancer pathogenesis. Pro-inflammatory cytokines such as tumor necrosis factor (TNF), interleukin (IL)-1B, IL-6, and IL-18 have been shown to play a role in left ventricular dysfunction and adverse remodeling (50, 51). Increased expression of these cytokines, especially IL-1B, is due to activation of the NLRP3 inflammasome (52). The Canakinumab Anti-Inflammatory Thrombosis Outcome Study (CANTOS) evaluated the effect

TABLE 2 | Common social risk factors between heart failure and breast cancer.

Social risk factor	Heart failure	Breast cancer	Potential solutions
Low socioeconomic status	↑ Incidence of disease ↑ Mortality after 90 days of discharge ↓ Likely to be referred to subspecialist ↑ Hospitalizations, readmissions, and mortality	↑ Incidence of disease ↑ Aggressive premenopausal breast cancer ↑ Stage of breast cancer diagnosis ↑ Mortality	- Create a robust income safety net - Increase income benefits - Increase jobs/employment - Expand unemployment insurance
Neighborhood disadvantage	↑ Incidence of disease ↓ Ejection fractions ↑ Hospitalizations, readmissions, and mortality	↑ Stage of breast cancer diagnosis ↑ Breast cancer mortality	- Create a robust income safety net - Increase affordable public housing; prioritize for homeless - Rental assistance - Investment in low-income communities - Investment in schools, early childhood education, and mentorship programs - Build affordable transportation - Partner with social services addressing homelessness
Food insecurity	- Frailty and deconditioning - Poor access to low-sodium diet - Obesity, diabetes, hypertension more prevalent	- Dietary fat linked to reduced breast cancer - Obesity, diabetes, hypertension more prevalent	- Create a robust income safety net - Address food deserts - Expand food benefits - Expand universal free meals to children - Partner with local food banks and fridges
Poor access to healthcare	- Lack of continuity care - Lack of subspeciality care ↑ Medication costs	↓ Cancer screening ↑ Delays in diagnosis and treatment of breast cancer	- Create a robust income safety net - Affordable healthcare - Universal healthcare - Partner with community health centers - Prioritize access in health services
Social isolation	↓ Physical and mental health ↑ Hospitalizations, readmissions and mortality	↓ Physical and mental health ↓ Survival	- Access to mental health services - Increase social workers on healthcare teams - Patient support groups - Partner with local programs for the elderly

of canakinumab, a monoclonal antibody targeting interleukin-1B (IL-1B), on cardiovascular outcomes (53, 54). Canakinumab significantly reduced not only cardiovascular events and HF hospitalizations but incident lung cancer and decreased lung cancer-related death. While the trial did not have enough power to look at different cancer subtypes, breast cancer tumor cells have been shown to produce IL-1B, which promotes epithelial-to-mesenchymal transition, migration, and invasion of breast cancer cells (55). Animal models have shown reduction in breast cancer metastasis with IL-1B inhibition (55). Identification of these shared pathways may allow for targeted therapies for both breast cancer and HF.

Shared Social Risk Factors

Poverty and inequality form the backbone of underlying social risk factors that contribute to social determinants of health (SDOH). These are primary concerns for healthcare providers who must consider community-level factors that influence health outcomes. Thriving in a society involves addressing a complex association between personal, environmental, economic, and social factors that impact overall health. There are multiple SDOH assessment tools which have been developed to comprehensively evaluate these outcomes. SDOH screening tools must be better integrated into healthcare delivery schema in cardio-oncology. Several social risk factors derived from these tools are known to contribute to both cancer and HF, including socioeconomic status, neighborhood disadvantage, food insecurity, an inadequate healthcare system (lack of insurance, cost of medication), and social isolation (56, 57). These social issues have come to the forefront during the COVID-19 pandemic, where we have witnessed the selective effect of COVID-19 on disadvantaged communities. The pandemic has motivated a conversation to address these disparities in healthcare, which are deeply rooted in the structural inequities in our society. Potential mitigation strategies must be directed at multiple levels (**Table 2**). In this section, we summarize social risk factors that contribute to both breast cancer and HF.

Socioeconomic Status

There is a known association between socioeconomic characteristics and risk for both breast cancer and HF. Across racial and ethnic groups, increasing socioeconomic status is inversely correlated with breast cancer incidence in population studies (58). Low socioeconomic status is associated with increased risk of aggressive premenopausal breast cancer, later stage of diagnosis, and poorer survival (56). Breast cancer's 3-year survival is significantly affected by level of education, district of residence and social class in childhood (59). Mortality

is significantly higher in non-Hispanic Black breast cancer patients than non-Hispanic white patients, across all ages (60). Cardiovascular health is also worse in Black individuals who have a higher prevalence of HF risk factors such as obesity, diabetes, and hypertension than non-Hispanic white individuals (61, 62). Black individuals have higher rates of HF hospitalization and age-adjusted HF-related CVD death rates than their White counterparts (63). When compared to White survivors of breast cancer, Black survivors have an elevated risk of cardiotoxicity-associated morbidity and mortality (64).

Socioeconomic factors also predict outcomes from HF admissions. Those patients with adverse social factors in a Medicare dataset were 3-fold as likely to die within 90 days of discharge for a HF hospitalization as those without any social risk factors (65). In a study from Sweden evaluating HF outcomes, lower socioeconomic status was directly associated with patients being less likely to have a subspecialist referral (66). This may in part be due to the financial burden of care for cancer patients which is even higher when superimposed with atherosclerotic CVD (a major risk factor for HF), leading to difficulty paying bills, buying medications, and seeking care (67).

There is a linear relationship between number of socioeconomic risk factors and higher risk of HF hospitalization, cardiovascular events, and mortality (66). Prevention focusing on modifiable clinical risk factors is difficult for patients without socioeconomic support and resources. A patient with income instability must prioritize housing, food, utilities, and other needs over healthy activities such as a moderate-intensity exercise routine. Lower socioeconomic status is associated with a significant increase in body mass index, smoking prevalence, and diabetes (68). Other major risk factors for HF including coronary artery disease and hypertension also vary widely with levels of adverse social factors (69). Due to these underlying risk factors, those patients from lower socio-economic classes have a higher prevalence of incident HF 5 years earlier than those from more affluent backgrounds (68).

Neighborhood Disadvantage

Poor infrastructure and inadequate resources in low-income neighborhoods serve as barriers to healthcare. Housing insecurity, the role of public transportation, and travel costs may serve as physical impediments to access healthcare but have not been well studied. Geographic proximity and travel time to mammography facilities have not been shown to be associated with later stage breast cancer diagnosis (70). However, high census tract poverty (defined by the US census as $\geq$ 20% below poverty) and inner-city disadvantage have shown an association with risk of later stage breast cancer diagnosis (70, 71). In addition, concern for safety due to neighborhood violence or crime, lack of public spaces such as parks, and lack of exercise facilities can lead to a less active and more sedentary lifestyle. Obesity is highly correlated with neighborhood poverty (71), having both direct and indirect effects on breast cancer and HF. Stressors associated with poverty can cause a patient to turn to risky behaviors such as smoking, drinking, and drug use as coping mechanisms. High-income neighborhoods have demonstrated lower stress, anxiety, rates of obesity, and fewer other comorbidities (72).

Neighborhood deprivation index includes four main components: wealth and income, education, occupation, and housing quality (73). Akwo and colleagues demonstrated that neighborhood deprivation predicts risk of incident HF beyond individual socioeconomic status and traditional cardiovascular risk factors in low-income populations (74). Residents living in deprived neighborhoods have lower ejection fractions, more severe HF symptoms and higher odds of hospitalization for HF (75). Thirty-day HF readmission and mortality rates also increase with neighborhood deprivation (76). Neighborhood socioeconomic status is also an important factor in cancer-specific survival disparities in Black and non-Hispanic Whites (77).

Food Insecurity

Food insecurity is the lack of reliable access to nutritious food for healthy and active living, resulting in not having enough meals or cutting back on meals. It is a broad concept of adapting eating to social circumstances primarily driven by poverty, income instability, and neighborhood disadvantage. Food deserts are areas in primarily low-income neighborhoods where access to grocery stores that provide fresh fruits and vegetables is limited (78). This may also contribute to difficulty in adhering to a low-sodium diet for patients with HF when facing food insecurity. For patients with breast cancer and HF, food insecurity can have the potential to aggravate both conditions. Food insecurity and lack of healthy food is associated with HF risk factors and HF, but whether food insecurity and access to healthy food is associated with breast cancer requires further study.

One hypothesized mechanism for the association of SDOH and risk of HF is lack of access to healthy foods, more processed foods, and therefore higher dietary phosphate intake, which may increase circulating levels of inorganic phosphate and fibroblast growth factor 23 (FGF-23). FGF-23 has been correlated with increased myocardial fibrosis on cardiac MRI and a strong predictor of mortality and first HF hospitalization, especially in patients with HF with preserved ejection fraction (79). Further investigation is needed to understand the relationship between a high phosphate diet and breast cancer. Ultra-processed foods in diet have been associated with increased risks of overall and breast cancer (80). There may also be a possible link between lipids, higher HDL-C and apolipoprotein A1, and mammographic density which needs further study (40). A few studies have noted that dietary fat, n-3 PUFA, has an inverse link to breast cancer (81, 82).

Frailty and deterioration resulting from undernutrition has also been shown in patients with HF (83). Interventions such as the Supplemental Nutrition Assistance Program (SNAP), community partnerships through food pantries, school meals, and community fridges are needed to address food insecurity and health-related comorbidities.

Healthcare System

There are well-documented disparities in breast cancer survival and HF by socioeconomic status, access to health insurance, and

preventive care. Lack of adequate health insurance leads to high out of pocket medical costs, inability to pay for medications, lack of a primary care physician to perform screening studies, and provide subspeciality referral. The difficulty in navigating screening and treatment for HF or cancer is exacerbated by poverty, lack of insurance, and not having an established continuity clinic. Other socioeconomic factors such as lower education, health literacy, and higher stress levels were associated with lower HF clinic use (84). Patients without health insurance often seek care at safety-net or federally funded hospitals and indigent care clinics. When unable to afford healthcare or medications, patients may need to make trade-offs between basic needs and treatments.

Prevention is a large component in the management of both HF and breast cancer. It has been demonstrated that decreased cancer screening rates are associated with delayed diagnosis and treatment and poorer health outcomes (56). In a study by Kurani and colleagues, 78,302 patients eligible for breast cancer screening living in rural areas were 24% less likely to obtain breast cancer screening than those living in the city. Those living in the most deprived census blocks were 49% less likely to obtain breast cancer screening (85). Interventions such as providing transportation and childcare assistance, providing free screening services, or distributing educational resources through community partnerships have proven to be cost-effective measures at improving quality and length of life by increasing cancer screening (86). As previously outlined, socioeconomic factors effect access to heart failure care and subspeciality clinics (66). Racial disparities also exist in admission for heart failure, referral for diagnostic tests, and administration of advanced heart failure therapies (87, 88).

Social Isolation

Finally, the importance of social networks and connections for both breast cancer and HF patients has been well-established. High levels of social support have been shown to be protective for physical and mental health and quality of life (56, 89). In addition, several studies have demonstrated worse all-cause mortality and breast cancer mortality in patients without robust social support (90–92). These studies quantify social support based on both the number of people in the social network as well as the frequency of contact with friends/family following cancer diagnosis. In a study of 2,835 nurses from the Nurses' Health Study, participants that were socially isolated were twice as likely to die as those who were socially connected (90). Those with strong social support were also most likely to adhere to treatment regimens, access healthcare, and treatment options more effectively (93).

One prospective study of HF patients found that 6% of patients experienced severe social isolation; even after controlling for depression, these patients had >3.5 times increased risk of death 68% increased risk of hospitalization, and 57% increased risk of emergency department visits compared to those who did not report social isolation (94). In another study, loneliness was directly associated with more days hospitalized and more readmissions despite equivalent severity of HF (95).

Mitigation Strategies

To address the underlying factors that promote both HF and breast cancer, a multi-faceted approach is needed that focuses on SDOH and in turn clinical risk factors (**Table 2**). A singular theme across all domains of SDOH is a need for a robust income safety net for low-income individuals. Creation of policies that focus SDOH will have a transformational effect on comorbidities that affect HF and breast cancer. Health legislation such as the Patient Protection and Affordable Care Act expanded health insurance, largely through Medicaid, to low-income individuals with cancer and at rates similar to those without cancer (96). This led to increased diagnosis of early-stage breast cancer; however, there was no evidence of increase in timely initiation of cancer treatment due to earlier diagnosis (97). Similarly, although more low-income HF patients were now insured, largely through Medicaid expansion, this did not improve quality of care or in-hospital outcomes in low-income patients with HF (98). These findings underscore a need for an all-encompassing approach, beyond expansion of health insurance, that addresses affordable housing, transportation, food insecurity, access to healthcare, and building social support networks. An intervention such as the Supplemental Nutrition Assistance Program (SNAP) serves as an example for mitigating adverse health outcomes in individuals with food insecurity (99). Working alongside health and social policy makers, community partners, and patients to develop comprehensive intervention strategies that address structural inequities are needed to broaden our view of how to improve health outcomes for breast cancer and HF.

Reverse Cardio-Oncology

The newer concept whereby HF promotes cancer development is supported by both epidemiological and mechanistic data. In an initial case-control study, HF was associated with nearly 70% higher risk of incident cancer after adjusting for comorbidities (100). This association was present regardless of left ventricular ejection fraction. In a large population-based study of a Danish cohort, individuals with HF had a higher incidence of cancer across different age groups (101). Specifically, there was a 36% higher risk of breast cancer. In addition to incident cancer, two prospective cohort studies in early-stage breast cancer showed a 60% increased risk of recurrence in women who had an interim myocardial infarction (MI) (102). Baseline CVD risk factors, 10-year atherosclerotic CVD risk score, and natriuretic peptide concentrations are associated with increased risk of future cancer (103). Results from observational studies, however, can be biased due to increased surveillance in patients with HF and differences in treatment. Therefore, it is crucial to identify biological pathways that may explain this association.

Animal studies have provided important insights into the association between CVD and cancer. The initial hallmark study evaluated the effect of HF induced by a large anterior MI in mice prone to developing precancerous intestinal tumors (104). Mice with HF had significantly greater tumor growth. Tumor growth was associated with left ventricular dysfunction and myocardial scar. In their panel of candidate proteins, SerpinA3 consistently induced proliferative effects in the tumor via the Akt pathway. There have also been studies specifically evaluating the effect of

adverse cardiac remodeling in breast cancer models. In a mouse model of breast cancer, MI induced by coronary artery ligation led to 2-fold increase in tumor growth compared with controls (102). Analysis of the intra-tumoral immune cells showed an increase in monocytic myeloid-derived suppressor cells. These suppressor cells restricted infiltration of anti-tumor cytotoxic T cells, instead promoting pro-tumoral immunosuppressive T regulatory cells. These changes were in part mediated by epigenetic modification of monocytes in the bone marrow.

In a separate breast orthotopic cancer mouse model, pressure overload induced cardiac hypertrophy from transverse aortic constriction led to greater tumor growth and more metastases (105). Tumor growth correlated with the level of cardiac hypertrophy. The authors further identified increased messenger RNA expression of periostin in hypertrophied hearts and increased protein levels in serum. Depletion of periostin from the serum inhibited proliferation of cancer cells while addition of periostin promoted cancer cell proliferation in vitro. Periostin is an extracellular matrix protein that affects cancer cell proliferation, migration, and epithelial to mesenchymal transition. Interestingly, SerpinA3 was not elevated in this mouse model. This may represent differences in early and late stages of cardiac remodeling and HF or mode of cardiac injury. These studies further support the paradigm of reverse cardio-oncology but also reinforce the need for additional studies to better delineate the different pathways that connect CVD to cancer, specifically HF to breast cancer. Greater understanding of the mechanisms would not only allow for targeted therapy but more importantly emphasize the importance of HF and cancer prevention through aggressive risk factor modification by both patients and clinicians.

CONCLUSIONS

The interplay between risk factors associated with breast cancer and HF is very complex. Traditional cardiovascular risk factors, such as obesity, glucose dysregulation, hypertension, cholesterol dysregulation, atrial fibrillation and inflammation, are also closely linked with the development of breast cancer. HF itself has been shown to increase tumor growth and cancer development. Overarching social factors that lead

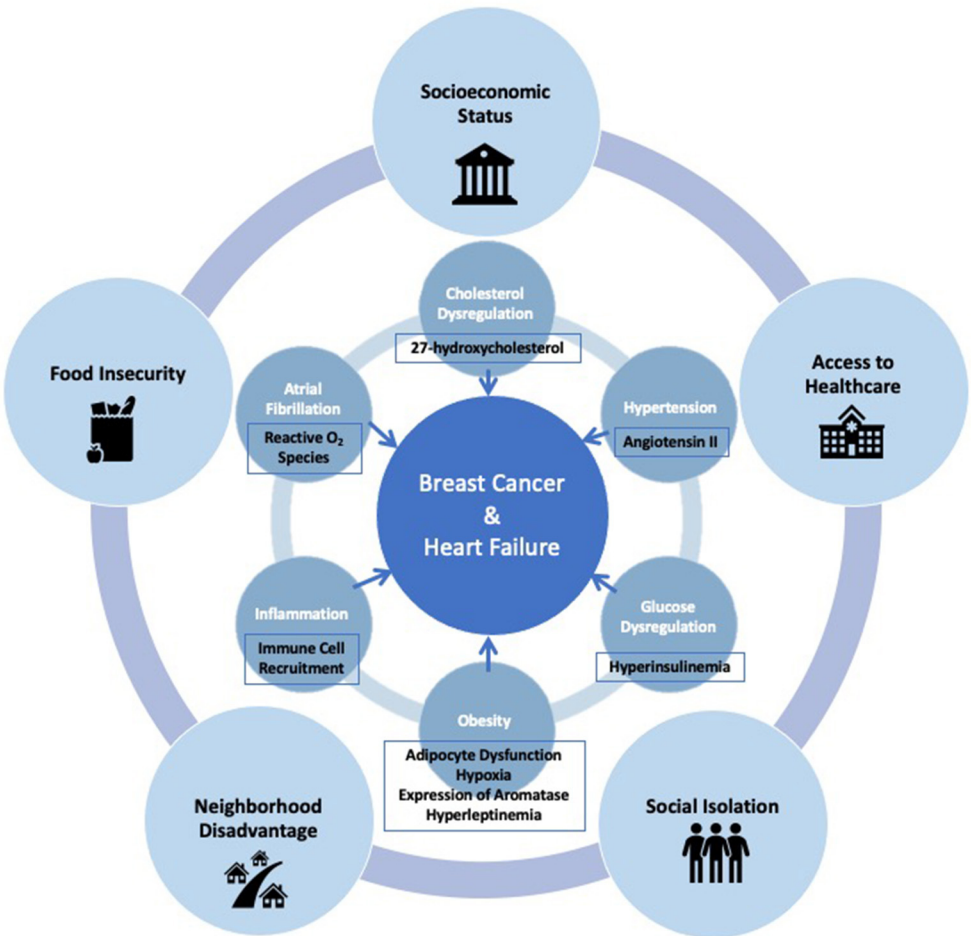

FIGURE 1 | Interconnected social and clinical risk factors, and mechanisms which link the development of breast cancer and heart failure.

to development of these cardiovascular risk factors, and in turn to breast cancer and HF, must simultaneously be addressed in order to comprehensively develop approaches for prevention of both chronic illnesses (**Figure 1**). Poverty and inequality are the root causes of several of these social risk factors, such as socioeconomic status, neighborhood disadvantage, food insecurity, an inadequate healthcare system, and social isolation. Implementation of prevention strategies must consider these social factors with equal importance when addressing common risk factors between breast cancer and HF.

AUTHOR CONTRIBUTIONS

NA, AS, and AB contributed to concept and design of the review and wrote sections of the the manuscript. NA and AB created the figure. All authors contributed to manuscript revision, read, and approved the submitted version.

REFERENCES

1. Ahmad FB, Minino A, Anderson RN, provisional mortality data - United States (2020). *MMWR Morb Mortal Wkly Rep*. (2021) 70:519–22. doi: 10.15585/mmwr.mm7014e1
2. Moslehi J, Zhang Q, Moore KJ. Crosstalk between the heart and cancer: beyond drug toxicity. *Circulation*. (2020) 142:684–7. doi: 10.1161/CIRCULATIONAHA.120.048655
3. Feuer EJ, Wun LM, Boring CC, Flanders WD, Timmel MJ, Tong T. The lifetime risk of developing breast cancer. *J Natl Cancer Inst*. (1993) 85:892–7. doi: 10.1093/jnci/85.11.892
4. American Cancer Society. *Cancer Facts and Figures*. Atlanta: American Cancer Society;. (2020).
5. Abdel-Qadir H, Austin PC, Lee DS, Amir E, Tu JV, Thavendiranathan P, et al. A population-Based study of cardiovascular mortality following early-Stage breast cancer. *JAMA Cardiol*. (2017) 2:88–93. doi: 10.1001/jamacardio.2016.3841
6. Patnaik JL, Byers T, DiGuiseppi C, Dabelea D, Denberg TD. Cardiovascular disease competes with breast cancer as the leading cause of death for older females diagnosed with breast cancer: a retrospective cohort study. *Breast Cancer Res*. (2011) 13:R64. doi: 10.1186/bcr2901
7. Huffman MD, Berry JD, Ning H, Dyer AR, Garside DB, Cai X, et al. Lifetime risk for heart failure among white and black americans: cardiovascular lifetime risk pooling project. *J Am Coll Cardiol*. (2013) 61:1510–7. doi: 10.1016/j.jacc.2013.01.022
8. Lloyd-Jones DM, Larson MG, Leip EP, Beiser A, D'Agostino RB, Kannel WB, et al. Lifetime risk for developing congestive heart failure: the framingham heart study. *Circulation*. (2002) 106:3068–72. doi: 10.1161/01.CIR.0000039105.49749.6F
9. Sinha A, Ning H, Carnethon MR, Allen NB, Wilkins JT, Lloyd-Jones DM, et al. Race- and sex-specific population attributable fractions of incident heart failure: a population-based cohort study from the lifetime risk pooling project. *Circ Heart Fail*. (2021) 14:e008113. doi: 10.1161/CIRCHEARTFAILURE.120.008113
10. Ogunmoroti O, Oni E, Michos ED, Spatz ES, Allen NB, Rana JS, et al. Life's simple 7 and incident heart failure: the multi-Ethnic study of atherosclerosis. *J Am Heart Assoc*. (2017) 6: e005180. doi: 10.1161/JAHA.116.005180
11. Folsom AR, Shah AM, Lutsey PL, Roetker NS, Alonso A, Avery CL, et al. American heart association's life's simple 7: avoiding heart failure and preserving cardiac structure and function. *Am J Med*. (2015) 128:970–6.e2. doi: 10.1016/j.amjmed.2015.03.027
12. Cleland JG, Progression from hypertension to heart failure. Mechanisms and management. *Cardiology*. (1999) 92:10-9; discussion 20–1. doi: 10.1159/000047289
13. Dunlay SM, Givertz MM, Aguilar D, Allen LA, Chan M, Desai AS, et al. Type 2 diabetes mellitus and heart failure: a Scientific statement from the american heart association and the heart failure society of america: this statement does not represent an update of the. (2017) ACC/AHA/HFSA heart failure guideline update. *Circulation*. (2019) 140:e294–324. doi: 10.1161/CIR.0000000000000691
14. Alpert MA, Lavie CJ, Agrawal H, Aggarwal KB, Kumar S. Obesity and heart failure: epidemiology, pathophysiology, clinical manifestations, and management. *Transl Res*. (2014) 164:345–56. doi: 10.1016/j.trsl.2014.04.010
15. Mehta LS, Watson KE, Barac A, Beckie TM, Bittner V, Cruz-Flores S, et al. Cardiovascular disease and breast cancer: where these entities intersect: a scientific statement from the american heart association. *Circulation*. (2018) 137:e30–66. doi: 10.1161/CIR.0000000000000556
16. Khan SS, Ning H, Wilkins JT, Allen N, Carnethon M, Berry JD, et al. Association of body mass index with lifetime risk of cardiovascular disease and compression of morbidity. *JAMA Cardiol*. (2018) 3:280–7. doi: 10.1001/jamacardio.2018.0022
17. Bibbins-Domingo K, Lin F, Vittinghoff E, Barrett-Connor E, Hulley SB, Grady D, et al. Predictors of heart failure among women with coronary disease. *Circulation*. (2004) 110:1424–30. doi: 10.1161/01.CIR.0000141726.01302.83
18. Boyle P, Boniol M, Koechlin A, Robertson C, Valentini F, Coppens K, et al. Diabetes and breast cancer risk: a meta-analysis. *Br J Cancer*. (2012) 107:1608–17. doi: 10.1038/bjc.2012.414
19. Tsilidis KK, Kasimis JC, Lopez DS, Ntzani EE, Ioannidis JP. Type 2 diabetes and cancer: umbrella review of meta-analyses of observational studies. *Bmj*. (2015) 350:g7607. doi: 10.1136/bmj.g7607
20. Dobbins M, Decorby K, Choi BC. The association between obesity and cancer risk: a Meta-Analysis of observational studies from 1985 to 2011. *ISRN Prev Med*. (2013) 2013:680536. doi: 10.5402/2013/680536
21. Renehan AG, Tyson M, Egger M, Heller RF, Zwahlen M. Body-mass index and incidence of cancer: a systematic review and meta-analysis of prospective observational studies. *Lancet*. (2008) 371:569–78. doi: 10.1016/S0140-6736(08)60269-X
22. Munsell MF, Sprague BL, Berry DA, Chisholm G, Trentham-Dietz A. Body mass index and breast cancer risk according to postmenopausal estrogen-progestin use and hormone receptor status. *Epidemiol Rev*. (2014) 36:114–36. doi: 10.1093/epirev/mxt010
23. Guha A, Wang X, Harris RA, Nelson AG, Stepp D, Klaassen Z, et al. Obesity and the bidirectional risk of cancer and cardiovascular diseases in African Americans: disparity vs. *ancestry Front Cardiovasc Med*. (2021) 8:761488. doi: 10.3389/fcvm.2021.761488
24. Xu CX, Zhu HH, Zhu Y. Diabetes cancer: associations. *mechanisms, and implications for medical practice World J Diabetes*. (2014) 5:372–80. doi: 10.4239/wjd.v5.i3.372
25. Kahn BB, Flier J. Obesity insulin resistance. *J Clin Invest*. (2000) 106:473–81. doi: 10.1172/JCI10842
26. Corvera S, Gealekman O. Adipose tissue angiogenesis: impact on obesity and type-2 diabetes. *Biochim Biophys Acta*. (1842) 2014: 463–72. doi: 10.1016/j.bbadis.2013.06.003
27. Engin A. The pathogenesis of obesity-associated adipose tissue inflammation. *Adv Exp Med Biol*. (2017) 960:221–45. doi: 10.1007/978-3-319-48382-5_9
28. Brown KA, Iyengar NM, Zhou XK, Gucalp A, Subbaramaiah K, Wang H, et al. Menopause is a determinant of breast aromatase expression and its associations with bMI, inflammation, systemic markers. *J Clin Endocrinol Metab*. (2017) 102:1692–701. doi: 10.1210/jc.2016-3606
29. Obradovic M, Sudar-Milovanovic E, Soskic S, Essack M, Arya S, Stewart AJ, et al. Obesity: role and clinical implication. *Front Endocrinol (Lausanne)*. (2021) 12:585887. doi: 10.3389/fendo.2021.585887

30. Sánchez-Jiménez F, Pérez-Pérez AL, de la cruz-Merino, sánchez-margalet V. *Obesity and breast cancer: role of leptin Front Oncol.* (2019) 9:596. doi: 10.3389/fonc.2019.00596
31. Macis D, Guerrieri-Gonzaga A, Gandini S. Circulating adiponectin and breast cancer risk: a systematic review and meta-analysis. *Int J Epidemiol.* (2014) 43:1226–36. doi: 10.1093/ije/dyu088
32. Au CC, Docanto MM, Zahid H, Raffaelli FM, Ferrero RL, Furness JB, et al. Des-acyl ghrelin inhibits the capacity of macrophages to stimulate the expression of aromatase in breast adipose stromal cells. *J Steroid Biochem Mol Biol.* (2017) 170:49–53. doi: 10.1016/j.jsbmb.2016.07.005
33. Brown KA. Metabolic pathways in obesity-related breast cancer. *Nat Rev Endocrinol.* (2021) 17:350–63. doi: 10.1038/s41574-021-00487-0
34. Hoxhaj G, Manning BD. The pI3K-AKT network at the interface of oncogenic signalling and cancer metabolism. *Nat Rev Cancer.* (2020) 20:74–88. doi: 10.1038/s41568-019-0216-7
35. Zadra G, Batista JL, Loda M. Dissecting the dual role of aMPK in cancer: from experimental to human studies. *Mol Cancer Res.* (2015) 13:1059–72. doi: 10.1158/1541-7786.MCR-15-0068
36. Han H, Guo W, Shi W, Yu Y, Zhang Y, Ye X, et al. Hypertension and breast cancer risk: a systematic review and meta-analysis. *Sci Rep.* (2017) 7:44877. doi: 10.1038/srep44877
37. Seretis A, Cividini S, Markozannes G, Tseretopoulou X, Lopez DS, Ntzani EE, et al. Association between blood pressure and risk of cancer development: a systematic review and meta-analysis of observational studies. *Sci Rep.* (2019) 9:8565. doi: 10.1038/s41598-019-45014-4
38. Rasha F, Ramalingam L, Gollahon L, Rahman RL, Rahman SM, Menikdiwela K, et al. Mechanisms linking the renin-angiotensin system, obesity, breast cancer. *Endocr Relat Cancer.* (2019) 26:R653–r672. doi: 10.1530/ERC-19-0314
39. Cedó L, Reddy ST, Mato E, Blanco-Vaca F, Escolà-Gil J, HDL. and LDL: potential new players in breast cancer development. *J Clin Med.* (2019) 8:853. doi: 10.3390/jcm8060853
40. Martin LJ, Melnichouk O, Huszti E, Connelly PW, Greenberg CV, Minkin S, et al. Serum lipids, lipoproteins, and risk of breast cancer: a nested case-control study using multiple time points. *J Natl Cancer Inst.* (2015) 107:32. doi: 10.1093/jnci/djv032
41. Nowak C, Ärnlöv J, A. mendelian randomization study of the effects of blood lipids on breast cancer risk. *Nat Commun.* (2018) 9:3957. doi: 10.1038/s41467-018-06467-9
42. Li C, Yang L, Zhang D, Jiang W. Systematic review and meta-analysis suggest that dietary cholesterol intake increases risk of breast cancer. *Nutr Res.* (2016) 36:627–35. doi: 10.1016/j.nutres.2016.04.009
43. Nelson ER, Wardell SE, Jasper JS, Park S, Suchindran S, Howe MK, et al. 27-hydroxycholesterol links hypercholesterolemia and breast cancer pathophysiology. *Science.* (2013) 342:1094–8. doi: 10.1126/science.1241908
44. Ma L, Wang L, Nelson AT, Han C, He S, Henn MA, et al. 27-Hydroxycholesterol acts on myeloid immune cells to induce T cell dysfunction, promoting breast cancer progression. *Cancer Lett.* (2020) 493:266–83. doi: 10.1016/j.canlet.2020.08.020
45. Zhong S, Zhang X, Chen L, Ma T, Tang J, Zhao J. Statin use and mortality in cancer patients: systematic review and meta-analysis of observational studies. *Cancer Treat Rev.* (2015) 41:554–67. doi: 10.1016/j.ctrv.2015.04.005
46. Leiva O, AbdelHameid D, Connors JM, Cannon CP, Bhatt DL. Common pathophysiology in cancer, atrial fibrillation, atherosclerosis, and thrombosis: jACC: cardioOncology state-of-the-Art review. *JACC CardioOncol.* (2021) 3:619–34. doi: 10.1016/j.jaccao.2021.08.011
47. Conen D, Wong JA, Sandhu RK, Cook NR, Lee IM, Buring JE, et al. Risk of malignant cancer among women with new-Onset atrial fibrillation. *JAMA Cardiol.* (2016) 1:389–96. doi: 10.1001/jamacardio.2016.0280
48. Kattelus H, Kesaniemi YA, Huikuri H, Ukkola O. Cancer increases the risk of atrial fibrillation during long-term follow-up. *(OPERA study) PLoS ONE.* (2018) 13:e0205454. doi: 10.1371/journal.pone.0205454
49. Guha A, Fradley MG, Dent SF, Weintraub NL, Lustberg MB, Alonso A, et al. Incidence, risk factors, and mortality of atrial fibrillation in breast cancer: a sEER-medicare analysis. *Eur Heart J.* (2022) 43:300–12. doi: 10.1093/eurheartj/ehab745
50. Adamo L, Rocha-Resende C, Prabhu SD, Mann DL. Reappraising the role of inflammation in heart failure. *Nat Rev Cardiol.* (2020) 17:269–85. doi: 10.1038/s41569-019-0315-x
51. Mann DL. Inflammatory mediators and the failing heart: past, present, and the foreseeable future. *Circ Res.* (2002) 91:988–98. doi: 10.1161/01.RES.0000043825.01705.1B
52. Mezzaroma E, Toldo S, Farkas D, Seropian IM, Van Tassell BW, Salloum FN, et al. The inflammasome promotes adverse cardiac remodeling following acute myocardial infarction in the mouse. *Proc Natl Acad Sci U S A.* (2011) 108:19725–30. doi: 10.1073/pnas.1108586108
53. Ridker PM, Everett BM, Thuren T, MacFadyen JG, Chang WH, Ballantyne C, et al. Antiinflammatory therapy with canakinumab for atherosclerotic disease. *N Engl J Med.* (2017) 377:1119–31. doi: 10.1056/NEJMoa1707914
54. Everett BM, Cornel JH, Lainscak M, Anker SD, Abbate A, Thuren T, et al. Anti-inflammatory therapy with canakinumab for the prevention of hospitalization for heart failure. *Circulation.* (2019) 139:1289–99. doi: 10.1161/CIRCULATIONAHA.118.038010
55. Tulotta C, Lefley DV, Freeman K, Gregory WM, Hanby AM, Heath PR, et al. Endogenous Production of IL1B by Breast Cancer Cells Drives Metastasis and Colonization of the Bone Microenvironment. *Clin Cancer Res.* (2019) 25:2769–82. doi: 10.1158/1078-0432.CCR-18-2202
56. Coughlin SS. Social determinants of breast cancer risk, stage, and survival. *Breast Cancer Res Treat.* (2019) 177:537–48. doi: 10.1007/s10549-019-05340-7
57. White-Williams C, Rossi LP, Bittner VA, Driscoll A, Durant RW, Granger BB, et al. addressing social determinants of health in the care of patients with heart failure: a scientific statement from the American heart association. *Circulation.* (2020) 141:e841–63. doi: 10.1161/CIR.0000000000000767
58. Yin D, Morris C, Allen M, Cress R, Bates J, Liu L. Does socioeconomic disparity in cancer incidence vary across racial/ethnic groups? *Cancer Causes Control.* (2010) 21:1721–30. doi: 10.1007/s10552-010-9601-y
59. Monfared ED, Mohseny M, Amanpour F, Mosavi Jarrahi A, Moradi Joo M, Heidarnia MA. Relationship of social determinants of health with the three-year survival rate of breast cancer. *Asian Pac J Cancer Prev.* (2017) 18:1121–6. doi: 10.22034/APJCP.2017.18.4.1121
60. Yedjou CG, Sims JN, Miele L, Noubissi F, Lowe L, Fonseca DD, et al. Health and racial disparity in breast cancer. *Adv Exp Med Biol.* (2019) 31–49. doi: 10.1007/978-3-030-20301-6_3
61. Carnethon MR, Pu J, Howard G, Albert MA, Anderson CAM, Bertoni AG, et al. Cardiovascular health in African Americans: a scientific statement from the american heart association. *Circulation.* (2017) 136:e393–423. 17. doi: 10.1161/CIR.0000000000000534
62. Fazal M, Malisa J, Rhee JW, Witteles RM, Rodriguez F. Racial and ethnic disparities in cardio-oncology: a call to action. *JACC CardioOncol.* (2021) 3:201–4. doi: 10.1016/j.jaccao.2021.05.001
63. Nayak A, Hicks AJ, Morris AA. Understanding the complexity of heart failure risk and treatment in black patients. *Circ Heart Fail.* (2020) 13:e007264. doi: 10.1161/CIRCHEARTFAILURE.120.007264
64. Ohman RE, Yang EH, Abel ML. Inequity in cardio-oncology: identifying disparities in cardiotoxicity and links to cardiac and cancer outcomes. *J Am Heart Assoc.* (2021) 10:e023852. doi: 10.1161/JAHA.121.023852
65. Sterling MR, Ringel JB, Pinheiro LC, Safford MM, Levitan EB, Phillips E, et al. Social determinants of health and 90-day mortality after hospitalization for heart failure in the rEGARDS study. *J Am Heart Assoc.* (2020) 9:e014836. doi: 10.1161/JAHA.119.014836
66. Schrage B, Lund LH, Benson L, Stolfo D, Ohlsson A, Westerling R, et al. Lower socioeconomic status predicts higher mortality and morbidity in patients with heart failure. *Heart.* (2021) 107:229–36. doi: 10.1136/heartjnl-2020-317216
67. Valero-Elizondo J, Chouairi F, Khera R, Grandhi GR, Saxena A, Warraich HJ, et al. Atherosclerotic cardiovascular disease, cancer, and financial toxicity among adults in the united states. *JACC CardioOncol.* (2021) 3:236–46. doi: 10.1016/j.jaccao.2021.02.006
68. Lawson CA, Zaccardi F, Squire I, Okhai H, Davies M, Huang W, et al. Risk factors for heart failure: 20-Year population-Based trends by sex, socioeconomic status, and ethnicity. *Circ Heart Fail.* (2020) 13:e006472. doi: 10.1161/CIRCHEARTFAILURE.119.006472

69. Kivimaki M, Shipley MJ, Ferrie JE, Singh-Manoux A, Batty GD, Chandola T, et al. Best-practice interventions to reduce socioeconomic inequalities of coronary heart disease mortality in UK: a prospective occupational cohort study. *Lancet.* (2008) 372:1648–54. doi: 10.1016/S0140-6736(08)61688-8
70. Henry KA, Boscoe FP, Johnson CJ, Goldberg DW, Sherman R, Cockburn M. Breast cancer stage at diagnosis: is travel time important? *J Community Health.* (2011) 36:933–42. doi: 10.1007/s10900-011-9392-4
71. DeGuzman PB, Cohn WF, Camacho F, Edwards BL, Sturz VN, Schroen AT. Impact of urban neighborhood disadvantage on late stage breast cancer diagnosis in virginia. *J Urban Health.* (2017) 94:199–210. doi: 10.1007/s11524-017-0142-5
72. Leventhal T, Brooks-Gunn J. Moving to opportunity: an experimental study of neighborhood effects on mental health. *Am J Public Health.* (2003) 93:1576–82. doi: 10.2105/AJPH.93.9.1576
73. Messer LC, Laraia BA, Kaufman JS, Eyster J, Holzman C, Culhane J, et al. The development of a standardized neighborhood deprivation index. *J Urban Health.* (2006) 83:1041–62. doi: 10.1007/s11524-006-9094-x
74. Akwo EA, Kabagambe EK, Harrell FE, Jr Blot WJ, Bachmann JM, Wang TJ, et al. Neighborhood deprivation predicts heart failure risk in a low-Income population of blacks and whites in the southeastern united states. *Circ Cardiovasc Qual Outcomes.* (2018) 11:e004052. doi: 10.1161/CIRCOUTCOMES.117.004052
75. Shirey TE, Hu Y, Ko YA, Nayak A, Udeshi E, Patel S, et al. Relation of neighborhood disadvantage to heart failure symptoms and hospitalizations. *Am J Cardiol.* (2021) 140:83–90. doi: 10.1016/j.amjcard.2020.10.057
76. Patel SA, Krasnow M, Long K, Shirey T, Dickert N, Morris AA. Excess 30-day heart failure readmissions and mortality in black patients increases with neighborhood deprivation. *Circ Heart Fail.* (2020) 13:e007947. doi: 10.1161/CIRCHEARTFAILURE.120.007947
77. Ellis L, Canchola AJ, Spiegel D, Ladabaum U, Haile R, Gomez S. Racial and ethnic disparities in cancer survival: the contribution of tumor, sociodemographic, institutional, neighborhood characteristics. *J Clin Oncol.* (2018) 36:25–33. doi: 10.1200/JCO.2017.74.2049
78. Kolak M, Bradley M, Block DR, Pool L, Garg G, Toman CK, et al. Urban foodscape trends: disparities in healthy food access in chicago, 2007–2014. *Health Place.* (2018) 52:231–9. doi: 10.1016/j.healthplace.2018.06.003
79. Roy C, Lejeune S, Slimani A, de meester C, As SAA, Rousseau MF, et al. Fibroblast growth factor 23: a biomarker of fibrosis and prognosis in heart failure with preserved ejection fraction. *ESC Heart Fail.* (2020) 7:2494–507. doi: 10.1002/ehf2.12816
80. Fiolet T, Srour B, Sellem L, Kesse-Guyot E, Alles B, Mejean C, et al. Consumption of ultra-processed foods and cancer risk: results from nutrinet-sante prospective cohort. *BMJ.* (2018) 360:k322. doi: 10.1136/bmj.k322
81. Wakai K, Tamakoshi K, Date C, Fukui M, Suzuki S, Lin Y, et al. Dietary intakes of fat and fatty acids and risk of breast cancer: a prospective study in japan. *Cancer Sci.* (2005) 96:590–9. doi: 10.1111/j.1349-7006.2005.00084.x
82. Zheng JS, Hu XJ, Zhao YM, Yang J, Li D. Intake of fish and marine n-3 polyunsaturated fatty acids and risk of breast cancer: meta-analysis of data from 21 independent prospective cohort studies. *BMJ.* (2013) 346:f3706. doi: 10.1136/bmj.f3706
83. Vitale C, Spoletini I, Rosano GM. Frailty in heart failure: implications for management. *Card Fail Rev.* (2018) 4:104–6. doi: 10.15420/cfr.2018.22.2
84. Gravely S, Ginsburg L, Stewart DE, Mak S, Grace SL I. Cardiac rehabilitation care continuity through automatic referral evaluation, referral and use of heart failure clinics: what factors are related to use? *Can J Cardiol.* (2012) 28:483–9. doi: 10.1016/j.cjca.2011.11.020
85. Kurani SS, McCoy RG, Lampman MA, Doubeni CA, Finney Rutten LJ, Inselman JW, et al. Association of neighborhood measures of social determinants of health with breast, cervical, and colorectal cancer screening rates in the USS midwest. *JAMA Netw Open.* (2020) 3:e200618. doi: 10.1001/jamanetworkopen.2020.0618
86. Mohan G, Chattopadhyay S. Cost-effectiveness of leveraging social determinants of health to improve breast, cervical, and colorectal cancer screening: a systematic review. *JAMA Oncol.* (2020) 6:1434–44. doi: 10.1001/jamaoncol.2020.1460
87. Eberly LA, Richterman A, Beckett AG, Wispelwey B, Marsh RH, Cleveland Manchanda EC, et al. Identification of racial inequities in access to specialized inpatient heart failure care at an academic medical center. *Circ Heart Fail.* (2019) 12:e006214. doi: 10.1161/CIRCHEARTFAILURE.120.007193
88. Greig D, Olivares G. Inequalities in the access to advanced therapy in heart failure. *Heart Fail Clin.* (2015) 11:523–8. doi: 10.1016/j.hfc.2015.07.014
89. Graells-Sans A, Serral G, Puigpinos-Riera R, Grupo Cohort D. Social inequalities in quality of life in a cohort of women diagnosed with breast cancer in Barcelona (DAMA cohort). *Cancer Epidemiol.* (2018) 54:38–47. doi: 10.1016/j.canep.2018.03.007
90. Kroenke CH, Kubzansky LD, Schernhammer ES, Holmes MD, Kawachi I. Social networks, social support, and survival after breast cancer diagnosis. *J Clin Oncol.* (2006) 24:1105–11. doi: 10.1200/JCO.2005.04.2846
91. Kroenke CH, Kwan ML, Neugut AI, Ergas IJ, Wright JD, Caan BJ, et al. Social networks, social support mechanisms, and quality of life after breast cancer diagnosis. *Breast Cancer Res Treat.* (2013) 139:515–27. doi: 10.1007/s10549-013-2477-2
92. Reynolds P, Boyd PT, Blacklow RS, Jackson JS, Greenberg RS, Austin DF, et al. The relationship between social ties and survival among black and white breast cancer patients. National Cancer Institute Black/White Cancer Survival Study Group. *Cancer Epidemiol Biomarkers Prev.* (1994) 3:253–9.
93. Gage-Bouchard EA. Social support, flexible resources, and health care navigation. *Soc Sci Med.* (2017) 190:111–8. doi: 10.1016/j.socscimed.2017.08.015
94. Manemann SM, Chamberlain AM, Roger VL, Griffin JM, Boyd CM, Cudjoe TKM, et al. Finney rutten, perceived social isolation and outcomes in patients with heart failure. *J Am Heart Assoc.* (2018) 7:e008069. doi: 10.1161/JAHA.117.008069
95. Lofvenmark C, Mattiasson AC, Billing E, Edner M. Perceived loneliness and social support in patients with chronic heart failure. *Eur J Cardiovasc Nurs.* (2009) 8:251–8. doi: 10.1016/j.ejcnurse.2009.05.001
96. Segel JE, Jung Coverage J. Financial burden and the patient protection and affordable care act for patients with cancer. *J Oncol Pract.* (2019) 15:e1035–49. doi: 10.1200/JOP.19.00138
97. Takvorian SU, Oganisian A, Mamtani R, Mitra N, Shulman LN, Bekelman JE, et al. Association of medicaid expansion under the affordable care act with insurance status, cancer stage, and timely treatment among patients with breast, colon, lung cancer. *JAMA Netw Open.* (2020) 3:e1921653. doi: 10.1001/jamanetworkopen.2019.21653
98. Wadhera RK, Joynt Maddox KE, Fonarow GC, Zhao X, Heidenreich PA, DeVore AD, et al. Association of the affordable care act's medicaid expansion with care quality and outcomes for low-Income patients hospitalized with heart failure. *Circ Cardiovasc Qual Outcomes.* (2018) 11:e004729. doi: 10.1161/CIRCOUTCOMES.118.004729
99. Pak TY, Kim G. Food stamps, food insecurity, and health outcomes among elderly americans. *Prev Med.* (2020) 130:105871. doi: 10.1016/j.ypmed.2019.105871
100. Hasin T, Gerber Y, McNallan SM, Weston SA, Kushwaha SS, Nelson TJ, et al. Patients with heart failure have an increased risk of incident cancer. *J Am Coll Cardiol.* (2013) 62:881–6. doi: 10.1016/j.jacc.2013.04.088
101. Banke A, Schou M, Videbaek L, Møller JE, Torp-Pedersen C, Gustafsson F, et al. Incidence of cancer in patients with chronic heart failure: a long-term follow-up study. *Eur J Heart Fail.* (2016) 18:260–6. doi: 10.1002/ejhf.472
102. Koelwyn GJ, Newman AAC, Afonso MS, van Solingen C, Corr EM, Brown EJ, et al. Myocardial infarction accelerates breast cancer via innate immune reprogramming. *Nat Med.* (2020) 26:1452–8. doi: 10.1038/s41591-020-0964-7
103. Lau ES, Paniagua SM, Liu E, Jovani M, Li SX, Takvorian K, et al. Cardiovascular risk factors are associated with future cancer. *JACC CardioOncol.* (2021) 3:48–58. doi: 10.1016/j.jaccao.2020.12.003
104. Meijers WC, Maglione M, Bakker SJL, Oberhuber R, Kieneker LM, de Jong S, et al. Heart failure stimulates tumor growth by circulating factors. *Circulation.* (2018) 138:678–91. doi: 10.1161/CIRCULATIONAHA.117.030816
105. Avraham S, Abu-Sharki S, Shofti R, Haas T, Korin B, Kalfon R, et al. Early cardiac remodeling promotes tumor growth and metastasis. *Circulation.* (2020) 142:670–83. doi: 10.1161/CIRCULATIONAHA.120.046471

Conflict of Interest: SS has received research grants from the National Institutes of Health (U54 HL160273, R01 HL107577, R01 HL127028, R01 HL140731, and R01 HL149423), Actelion, AstraZeneca, Corvia, Novartis, and Pfizer; and has received personal fees from Abbott, Actelion, AstraZeneca, Amgen, Aria CV,

Axon Therapies, Bayer, Boehringer-Ingelheim, Boston Scientific, Bristol-Myers Squibb, Cardiora, Coridea, CVRx, Cyclerion, Cytokinetics, Edwards Lifesciences, Eidos, Eisai, Imara, Impulse Dynamics, Intellia, Ionis, Ironwood, Lilly, Merck, MyoKardia, Novartis, Novo Nordisk, Pfizer, Prothena, Regeneron, Rivus, Sanofi, Shifamed, Tenax, Tenaya, and United Therapeutics.

The remaining authors declare that the research was conducted in the absence of any commercial or financial relationships that could be construed as a potential conflict of interest.

Publisher's Note: All claims expressed in this article are solely those of the authors and do not necessarily represent those of their affiliated organizations, or those of the publisher, the editors and the reviewers. Any product that may be evaluated in this article, or claim that may be made by its manufacturer, is not guaranteed or endorsed by the publisher.

frontiers | Frontiers in Cardiovascular Medicine

ORIGINAL RESEARCH
published: 31 May 2022
doi: 10.3389/fcvm.2022.916325

Predictors of Recurrence and Survival in Cancer Patients With Pericardial Effusion Requiring Pericardiocentesis

*Talha Ahmed[1,2], Elie Mouhayar[2], Juhee Song[3], Efstratios Koutroumpakis[2], Nicolas L. Palaskas[2], Syed Wamique Yusuf[2], Juan Lopez-Mattei[2], Saamir A. Hassan[2], Peter Kim[2], Mehmet Cilingiroglu[2], Konstantinos Marmagkiolis[2], Ara A. Vaporciyan[4], Stephen Swisher[4], Anita Deswal[2] and Cezar Iliescu[2]**

[1] Department of Cardiology, The University of Texas Health Science Center at Houston, Houston, TX, United States, [2] Department of Cardiology, The University of Texas MD Anderson Cancer Center, Houston, TX, United States, [3] Department of Biostatistics, The University of Texas Health Science Center at Houston, Houston, TX, United States, [4] Department of Thoracic and Cardiovascular Surgery, The University of Texas MD Anderson Cancer Center, Houston, TX, United States

OPEN ACCESS

Edited by:
Chun Liu,
Stanford University, United States

Reviewed by:
Weichieh Lee,
Chi Mei Medical Center, Taiwan
Andrew L. Morris,
University of Manitoba, Canada

***Correspondence:**
Cezar Iliescu
ciliescu@mdanderson.org

Specialty section:
This article was submitted to Cardio-Oncology, a section of the journal Frontiers in Cardiovascular Medicine

Received: *09 April 2022*
Accepted: *10 May 2022*
Published: *31 May 2022*

Citation:
Ahmed T, Mouhayar E, Song J, Koutroumpakis E, Palaskas NL, Yusuf SW, Lopez-Mattei J, Hassan SA, Kim P, Cilingiroglu M, Marmagkiolis K, Vaporciyan AA, Swisher S, Deswal A and Iliescu C (2022) Predictors of Recurrence and Survival in Cancer Patients With Pericardial Effusion Requiring Pericardiocentesis. Front. Cardiovasc. Med. 9:916325. doi: 10.3389/fcvm.2022.916325

Aim: This study investigated the factors predicting survival and the recurrence of pericardial effusion (PE) requiring pericardiocentesis (PCC) in patients with cancer.

Materials and Methods: We analyzed the data of patients who underwent PCC for large PEs from 2010 to 2020 at The University of Texas MD Anderson Cancer Center. The time to the first recurrent PE requiring PCC was the interval from the index PCC with pericardial drain placement to first recurrent PE requiring drainage (either repeated PCC or a pericardial window). Univariate and multivariate Fine-Gray models accounting for the competing risk of death were used to identify predictors of recurrent PE requiring drainage. Cox regression models were used to identify predictors of death.

Results: The study cohort included 418 patients with index PCC and pericardial drain placement, of whom 65 (16%) had recurrent PEs requiring drainage. The cumulative incidences of recurrent PE requiring drainage at 12 and 60 months were 15.0% and 15.6%, respectively. Younger age, anti-inflammatory medication use, and solid tumors were associated with an increased risk of recurrence of PE requiring drainage, and that echocardiographic evidence of tamponade at presentation and receipt of immunotherapy were associated with a decreased risk of recurrence. Factors predicting poor survival included older age, malignant effusion on cytology, non-use of anti-inflammatory agents, non-lymphoma cancers and primary lung cancer.

Conclusion: Among cancer patients with large PEs requiring drainage, young patients with solid tumors were more likely to experience recurrence, while elderly patients and those with lung cancer, malignant PE cytology, and non-use of anti-inflammatory agents showed worse survival.

Keywords: malignant pericardial effusion, recurrence, pericardiocentesis, survival, cancer patients

INTRODUCTION

Pericardial effusion (PE) is relatively common in cancer patients and is primarily caused by tumor invasion or disease treatment (1). Among cancer patients, malignant PE frequently occurs in those with advanced disease and is associated with worse outcomes (2, 3). The spectrum of malignant pericardial disease ranges from asymptomatic PE to hemodynamic instability in the setting of cardiac tamponade or constrictive physiology. Despite aggressive treatment, the prognosis of cancer patients with PE remains poor and is primarily dictated by the characteristics of the underlying disease (4). The treatment of PE attempts to correct hemodynamic instability and minimize interruptions in cancer therapy with the long-term goal to prevent effusion recurrence.

It is unknown which method of managing PE with imminent or recurrent tamponade is the most effective; however, pericardiocentesis (PCC) and surgical drainage (*via* a pericardiotomy or pericardial window) are widely used (5). The management of patients with PE and tamponade should be determined by the probability of recurrence of PE and expected survival time. Little information exists regarding the factors that may predict development of recurrent PE in these patients. The duration from the index PCC to first recurrence of PE requiring another drainage is also not well studied. Furthermore, the impact that recurrent PE has on the treatment and overall prognosis of cancer patients with PE is not known. Therefore, the aim of this study was to identify the factors predicting survival and recurrent PE requiring PCC in cancer patients.

MATERIALS AND METHODS

We conducted a retrospective analysis of a cohort of cancer patients who underwent index PCC from 2010 to 2020 at The University of Texas MD Anderson Cancer Center and were listed in "MD Anderson's Pericardiocentesis Cardiac Catheterization Lab Registry." The study was approved by MD Anderson's Institutional Review Board.

Patient Population

All patient data including imaging data was obtained using retrospective chart review. We collected patients' demographic and clinical data, including age, sex, type of malignancy, prior cancer therapy (chemotherapy, immunotherapy, stem cell transplantation, surgery, and radiation), laboratory values, and cancer stage at the time of the index procedure. We also documented the clinical symptoms, signs, and echocardiographic findings of patients presenting with PE. An echo-free space 2 cm or larger was indicative of a large PE while echocardiographic evidence of tamponade was defined by presence of chamber collapse, mitral and tricuspid valve inflow variation on Doppler images, and inferior vena cava size and respiratory variation (6). Computed tomography scans and echocardiograms were reviewed to detect primary or metastatic tumors involving the heart and described as "cardiac involvement by primary tumor or metastases. The effusion pathology and microbiology results obtained at the time of PCC were also reviewed to determine the percentage of patients with 'malignant effusion on cytology." Cancer groups were divided into solid and hematological malignancies and then further sub-classified into 7 major types, including lung; breast; colon and other gastrointestinal malignancies (such as esophageal, stomach, hepatic, and pancreatic malignancies); renal and genitourinary malignancies; other solid tumors; lymphomas; and leukemia and other hematological malignancies. Patients' cancers, were stratified as "advanced" (stage III or IV) or "non-advanced" (stage I or II). Determinants of recurrent PE requiring drainage were reviewed. A recurrent PE requiring drainage was defined as an effusion that caused clinical signs or symptoms as well as showed echocardiographic evidence of tamponade, and required drainage (either a pericardial window or repeated PCC). Patients who underwent a pericardial window for the index PE were excluded from the study.

Pericardiocentesis Procedure

Patients underwent primary percutaneous PCC, which, for therapeutic and/or diagnostic purposes, was guided by echocardiography, computed tomography, fluoroscopy, or combined echocardiography and fluoroscopy in the cardiac catheterization laboratory. Percutaneous PCC was performed using either the subcostal or the lateral/intercostal approach, whichever provided the shortest distance from the skin to the pericardial cavity and preferably lateral in the thrombocytopenic patients (7, 8). A pericardial drain was placed in each patient and was removed once the amount of drainage was less than 30 cc in a 24-h period or if the duration of the drain placement exceeded 7 days. Handheld bedside echocardiography was encouraged immediately prior to drain removal, but the decision to use it was left up to the treating physician. As a routine practice, formal echocardiography was performed prior to drain removal as well as at follow-up in the outpatient cardiology clinic at 4–6 weeks and at 3–6 months to assess for PE recurrence. Procedure failure was defined as failure to place the catheter in the pericardial space or the presence of less than 10 ml drainage during the initial procedure. Procedure complications were defined as cardiac death, cardiac perforation, pneumothorax, or bleeding requiring transfusion during or within a few days after the procedure, after ruling out other obvious causes of such events.

Data Analysis

Continuous variables were described as means ± standard deviations (SDs) or as medians with interquartile ranges (IQRs). Categorical variables were described as counts and percentages. The time to the first recurrent PE requiring drainage was defined as the time from the index PCC with pericardial drain placement to the first recurrent PE requiring drainage with either repeat PCC or a pericardial window. Patients without recurrent PE requiring drainage were censored at the time of death or last follow-up. The event of interest was recurrent PE requiring drainage with either repeat PCC or a pericardial window. Death without recurrent PE requiring drainage was considered as a competing risk event, an event that precludes the occurrence of the event of interest, recurrent PE (9). When a competing risk of

death exists, it may not be appropriate to simply censor patients who died before they had a chance to experience recurrent PE. Ignoring the competing risk could result in incorrect estimation of the risk of recurrent PE. Therefore, univariate and multivariate Fine-Gray models were used to assess the covariates' effects on the cumulative incidence of recurrent PE, accounting for death as a competing risk (10). Overall survival (OS) was defined as the time from the index PCC to death or last follow-up. Univariate and multivariate Cox regression models were used to identify risk factors associated with death. For model selection, the backward elimination method (for the Fine-Gray models) and stepwise selection method (for OS) were used. Subdistribution hazard ratios (sHRs) and 95% confidence intervals (CIs) were provided for Fine-Gray models and hazard ratios (HRs) and 95% CIs were provided for Cox regression models, as appropriate. *P*-values less than 0.05 were considered statistically significant. SAS version 9.4 (SAS Institute, Inc., Cary, North Carolina) was used for data analysis. Median follow up was determined using reverse Kaplan-Meier curve.

RESULTS

Patients' Baseline Characteristics

The cohort included 418 patients (mean age, 53 ± 16 years) with an index PCC. The patients' baseline characteristics are summarized in **Table 1**.

Most patients had advanced cancers (stage III or IV). All patients had large PEs, and most presented with echocardiographic evidence of tamponade (95%). Eight percent of patients had imaging evidence of cardiac metastasis. Two-thirds of the patients had malignant effusion on cytologic examination. Anti-inflammatory agents were prescribed in 11.8% of patients.

Follow-Up and Outcomes

The median follow-up time was 48 months (95% CI, 43–51 months), and the median OS duration was 3.9 months (**Figure 1**). Majority of patients (92%) reported improvement in symptoms after draining pericardial effusion. Among all the patients who had index PCC, the rates of procedure complications and procedure failure were very low (0.24% each); the single procedure complication was a cardiac perforation (**Table 2**). Recurrent PE requiring drainage occurred in 65 (15.6%) patients; in 63 (15%) of these patients, it occurred within 1 year of the index PCC (**Figure 2**). Three hundred thirty-eight (80.9%) patients died by the end of the follow-up period. Cumulative incidence plots showed a statistically significant increase in recurrence of pericardial effusion in young patients and with anti-inflammatory medication use (**Figure 3**).

Factors Determining Recurrence of Pericardial Effusion Requiring Drainage

The covariates that affect the incidence of recurrent PE requiring drainage are shown in **Table 3**. Univariate Fine-Gray models with death as a competing risk identified younger age, higher serum creatinine and hemoglobin levels, cardiac invasion by the tumor, and chemotherapy and surgery as the factors that have a significant increasing effect on the cumulative incidence of recurrent PE. The multivariate Fine-Gray model identified younger age, anti-inflammatory medication use, and solid malignancy as the factors with an increasing effect on the cumulative incidence of recurrent PE, while having echocardiographic evidence of tamponade at presentation and

TABLE 1 | Baseline characteristics of the patients (*N* = 418).

Characteristic	Count
Age (years), mean ± SD	53 ± 16
Sex, n (%)	
Female	193 (46.2)
Male	225 (53.8)
Laboratory values	
Hemoglobin (g/dL), mean ± SD	10.11 ± 1.89
Platelets (k/mL), median (IQR)	211.5 (106–321)
International normalized ratio, mean (SD)	1.24 ± 0.25
Creatinine (mg/dL), median (IQR)	0.84 (0.65–1.13)
Malignancy stage, n (%)	
Unknown	1
Non-advanced (stage I or II)	9 (2.2)
Advanced (stage III or IV),	408 (97.8)
Approach for PCC, n (%)	
Subcostal	256 (61.2)
Intercostal	162 (38.8)
Echocardiographic evidence of tamponade at presentation, n (%)	398 (95.2)
Malignant effusion on cytology, n (%)	269 (64.4)
Anti-inflammatory medication use (colchicine, steroids, or NSAIDs),	49 (11.7)
Cardiac involvement by primary tumor or tumor metastases, n (%)	35 (8.4)
Cancer subgroup, n (%)	
Unknown	3
Hematologic	144 (34.7)
Solid	271 (65.3)
Cancer type, n (%)	
Unknown	5
Lymphoma	61 (14.7)
Lung	127 (30.6)
Breast	42 (10.1)
Colon and other GI	26 (6.3)
Kidney and GU	43 (10.4)
Leukemia and other hematological	83 (20)
Other solid cancers	33 (8)
Cancer treatment, n (%)	
Radiation	165 (39.5)
Chemotherapy	367 (87.8)
Surgery	126 (30.1)
Immunotherapy	91 (21.8)
Stem cell Transplant	63 (15.1)

GI, gastrointestinal; GU, genitourinary; IQR, interquartile range; NSAID, non-steroidal anti-inflammatory drug; PCC, pericardiocentesis; SD, standard deviation.

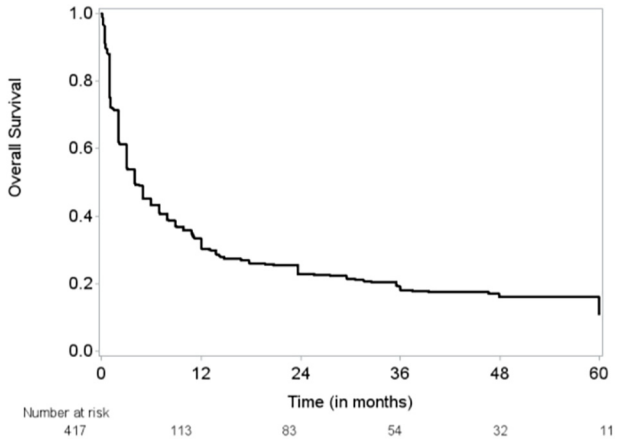

FIGURE 1 | Kaplan-Meier curve for overall survival (OS). Outcome for 1 patient was missing.

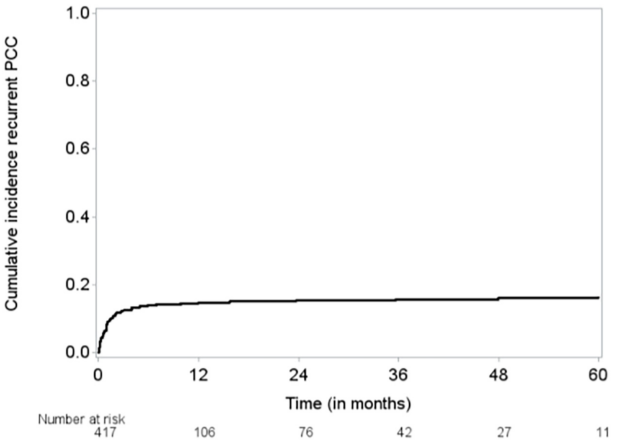

FIGURE 2 | Cumulative incidence of recurrent pericardial effusion requiring drainage by Aalen-Johansen estimator. Outcome for 1 patient was missing.

TABLE 2 | Outcomes of patients with index pericardiocentesis.

Outcome	n (%)
Symptomatic improvement	385 (92)
Recurrent PE requiring drainage	65 (15.6)
Survival at end of follow-up	80 (19.1)
Procedure complications	1 (0.24)
Procedure failure	1 (0.24)

PE: Pericardial Effusion.

receiving immunotherapy were associated with a decreasing effect on the cumulative incidence of recurrent PE.

Factors Determining Survival

The predictors of death are shown in **Table 4**. Univariate Cox regression models identified that older age, malignant effusion on cytological examination, and primary lung cancer were associated with an increased risk of death. Stem cell transplant and primary lymphoma were associated with a decreased risk of death. The multivariate Cox model identified that malignant effusion on cytological examination, not using anti-inflammatory agents, and non-lymphoma malignancies were associated with an increased risk of death.

DISCUSSION

In this study, we report on a cohort of 418 cancer patients presenting with PE treated with percutaneous PCC. Our study had several key findings. First, factors independently associated with an increasing effect on the cumulative incidence of recurrent PE requiring drainage included younger age, anti-inflammatory medication use, and solid tumors, whereas factors associated with a decreasing effect on the cumulative incidence of recurrent PE requiring drainage included having echocardiographic evidence of tamponade at presentation and receiving immunotherapy. Second, factors independently associated with poor OS included older age, malignant effusion on cytology, non-use of anti-inflammatory agents, non-lymphoma cancers and primary lung cancer. Third, PEs can be successfully drained with a very low rate of complications. Lastly, only 16% of patients presented with recurrent PEs requiring drainage, and almost all occurred within the first year after the index PCC.

In our study, the most frequent tumors associated with PEs requiring drainage were lung cancers (30.4%), followed by lymphomas (14.6%), leukemias (13.4%), and breast cancers (10.3%). While some studies have reported a similar percentage of cancer patients with pericardial effusion having hematological malignancies (1), others have reported a relatively less prevalence (4). Since most of these studies have been single center, this difference in observation can be explained by different patient population in each center. Most patients had advanced malignancies. In about two-thirds of our patients, cytological analysis of the pericardial fluid was positive for malignant cells; this was an independent predictor of a poor prognosis. This finding is in line with previous studies showing that recurrent, malignant PE occurs more commonly in patients with previously identified cardiac involvement than in those without it (11–14). In our study, 95% patients had echocardiographic evidence of tamponade while 5% patient underwent PCC for various reasons including clinical signs and symptoms related to large pericardial effusion, to establish the diagnosis of cancer, and for cancer staging.

In a retrospective analysis of cancer patients whose cumulative incidence of recurrent PE was 26.1% at 2-year interval from their index PCC, the use of anti-inflammatory agents was linked to a lower rate of death and PE recurrence (15). Similarly, we found that not using anti-inflammatory agents was associated with poor OS. However, in contrast to that study, we found that the risk of recurrence was higher with the use of these agents. This may represent a selection bias for the use of such therapies in patients who are generally thought to have

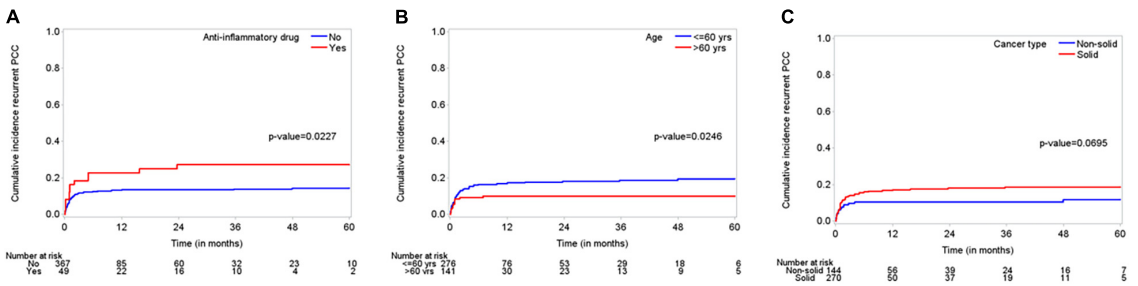

FIGURE 3 | "Cumulative incidence plots" displaying incidence of recurrent effusions for subgroups including **(A)**; anti-inflammatory medications (use versus non-use), **(B)**; age (young between 18 and 60 years versus elderly > 60 years), and **(C)**; cancer type (solid versus non-solid tumors).

a higher risk of recurrence or may reflect the use of anti-inflammatory agents to facilitate pericardial drain removal in patients requiring longer periods of pericardial drainage. This selection bias can also be due to use of such agents in patients with progressive primary cancer with increased tendency to develop recurrent effusions. Also, using anti-inflammatory agents in patients with hemorrhagic effusion can potentially lead to increased bleeding in pericardial space and increased recurrence risk (16, 17). In another study, rate of recurrence of pericardial effusion requiring pericardiocentesis was reduced from 23 to 11% with catheter drainage for 3-5 days as compared to not using an indwelling catheter (1). This alone was sufficient to reduce the risk of recurrence considerably and our data suggests that use of anti-inflammatory medications in the immediate peri-procedure phase (first week) might be hindering the beneficial effect of extended catheter drainage and mechanically induced adhesions.

Previous studies have shown conflicting evidence regarding the association between malignant cells in the pericardial fluid and poor outcomes in cancer patients (18–20). Our results indicate an association between malignant cells in the pericardial fluid and worse OS in cancer patients. Results from our analysis showed that patients with solid tumors had poor survival if they had malignant cells in the pericardial fluid; however, the outcomes did not differ for other cancer types when stratified by the results of cytological analysis.

In our study, almost all patients who developed recurrent PE developed it within 1 year after the index PCC. Specifically, the PE recurrence rate was only 15% in the first year after the index PCC and increased to only 16% after 5 years. This rate is lower than that reported previously (13). The low recurrence rate in our study can be explained by the close monitoring of the pericardial drain output, the standardized approach used for drain removal (based on 24-h drain output), and the encouraged use of echocardiography prior to drain removal. Among the patients who had recurrent PEs requiring drainage, the OS and recurrence rates did not differ between the patients who had had a pericardial window versus those who were treated percutaneously. This finding establishes the safety and utility of PCC in high-risk patients with cancer who present with PE recurrence (21, 22).

No randomized studies have compared the percutaneous drainage of PEs to the surgical drainage of PEs. Retrospective studies have shown that surgical drainage can reduce recurrence but increase the risk of peri-procedure complications (23). The American Heart Association and American College of Cardiology offer no guidelines on the management of pericardial disease. According to the 2015 European Society of Cardiology guidelines for pericardial disease, the treatment of cardiac tamponade related to a malignant PE effusion is a class I indication for PCC. Surgical pericardiotomy is indicated when PCC cannot be performed (class IIa; level of evidence B), but the surgical procedure may be associated with a higher rate of complications than PCC is and may not result in better outcomes (24). Guidelines for the treatment of PE recurrence do not exist. The choice between catheter-based and surgical drainage is usually made by a multidisciplinary team that includes the patient's oncologist, cardiologist, and thoracic surgical team, and it should be individualized to each patient and consider the patient's preference. In both percutaneous and PE treatment, the subcostal and intercostal (apical/lateral) approaches are similarly efficacious. Whether these approaches are successful depends primarily on the characteristics and location of the effusion, the stability of the patient, and various laboratory and clinical characteristics, including the presence of a chest wall tumor, the patient's history of chest wall radiation or abdominal surgery, or an apical loculation of the pericardial effusion (25–27). Our study found no difference in survival or PE recurrence between the 2 percutaneous approaches.

The safety of PCC was well demonstrated in our study in which the rates of procedure failure and complications were very low (0.24% each). One systematic review showed that the incidences of recurrent PE after isolated pericardiocentesis, PCC with extended catheter drainage, pericardial sclerosis, and percutaneous balloon pericardiotomy were 38.3%, 12.1%, 10.8%, and 10.3%, respectively (14). Despite being associated with a relatively high rate of recurrence, PCC continues to be a very attractive option for high-risk cancer patients. Some prefer to use surgical pericardial windows rather than PCC as the initial PE treatment in cancer patients owing to the high rate of cancer invasion into the pericardium and the high recurrence rate of PE; however, pericardial windows may be suboptimal for these patients because such patients tend to be frail and because the use of pericardial windows may delay their recovery from surgery and general anesthesia and thus affect their cancer treatment schedule. The high success rate of PCC and its low complication

TABLE 3 | Univariate and multivariate predictors of recurrent pericardial effusion requiring drainage.

	Univariate model		Multivariate model	
Covariate	**sHR (95% CI)**	***P*-value**	**sHR (95% CI)**	***P*-value**
Age (years)[1]	0.983 (0.968–0.998)	0.026	0.978 (0.960–0.997)	0.023
Sex				
Female	1.000			
Male	0.825 (0.508–1.339)	0.44		
Duration of drain placement[1], days	0.818 (0.626–1.067)	0.14		
Hemoglobin (g/dL)[1]	1.178 (1.051–1.322)	0.005		
Platelets (k/mL)[1]	0.999 (0.998–1.000)	0.17		
International normalized ratio[1]	0.883 (0.364–2.144)	0.78		
Creatinine (mg/dL)[1]	1.017 (1.014–1.020)	< 0.0001		
Malignancy stage				
Non-Advanced				
Advanced (stage III or IV)	3.168 (0.460–400.356)	0.42		
Approach for pericardiocentesis				
Subcostal	1.000			
Intercostal	0.777 (0.467–1.292)	0.33		
Echocardiographic evidence oftamponade at presentation[2]	0.134 (0.083–0.216)	< 0.0001	0.154 (0.095–0.250)	< 0.0001
Malignant effusion on cytology[2]	1.171 (0.698–1.965)	0.55		
Anti-inflammatory medication use[2](Colchicine, steroids or NSAIDs)	2.015 (1.109–3.662)	0.022	1.897 (1.046–3.441)	0.035
Cardiac involvement by primary tumor or tumor metastases[2]	2.090 (1.083–4.035)	0.028		
Cancer treatment				
Radiation therapy[2]	1.507 (0.930–2.443)	0.10		
Chemotherapy[2]	4.514 (1.076–18.937)	0.039		
Surgery[2]	1.955 (1.204–3.177)	0.007		
Immunotherapy[2]	0.346 (0.148–0.811)	0.015	0.312 (0.135–0.719)	0.006
Stem cell transplant[2]	0.544 (0.238–1.246)	0.15		
Cancer subgroup				
Hematologic	1.000		1.000	
Solid	1.668 (0.947–2.938)	0.08	2.357 (1.243–4.467)	0.009
Cancer type				
Lymphoma	1.000			
Lung	1.175 (0.544–2.539)	0.68		
Breast	1.268 (0.499–3.222)	0.62		
Colon and other GI	1.583 (0.570–4.397)	0.38		
Kidney and GU	0.963 (0.341–2.723)	0.94		
Leukemia; other hematologic	0.554 (0.205–1.499)	0.25		
Other solid cancers	1.505 (0.554–4.089)	0.42		

GI, gastrointestinal; GU, genitourinary; NSAID, non-steroidal anti-inflammatory drug; sHR, subdistribution hazard ratio (The sHR represents the ratio obtained from the Fine-Gray model with a competing risk of death).

[1]For this variable, the sHR is presented in 1-unit changes.

[2]For this variable, the sHR is presented considering "No" as a reference group.

and recurrence rates in our large cohort of cancer patients shows the value of the percutaneous procedure, with continued drainage over a few days, as a first line therapy for large PEs in these patients. That PCC is associated with no significant delay in cancer treatment (surgery, chemotherapy, immunotherapy, or radiation therapy) further supports its use in this population (28).

As suggested in our study, routine surveillance echocardiograms done at 3–6 weeks and at 4–6 months after index PCC can help determine which patients are more likely to develop recurrent effusions and may warrant closer monitoring and subsequent surveillance echocardiograms. In the current study, the median OS duration for cancer patients requiring PCC was 3.9 months (95% CI, 3–4.9 months). Although this duration is a little higher than that reported previously (15), the finding reiterates that PE requiring drainage is a poor prognostic marker in patients with cancer because it is indicative of advanced malignancy.

Study Limitations

Because this study was a retrospective chart review, it was subject to selection bias, as decisions regarding the procedure, entry site, imaging guidance, drainage duration, and use of anti-inflammatory agents were individualized to each patient and at the discretion of the treating physician. The use of standardized

TABLE 4 | Univariate and multivariate predictors of all-cause mortality.

	Univariate model		Multivariate model	
Covariate	**HR (95% CI)**	***P*-value**	**HR (95% CI)**	***P*-value**
Age (years)[1]	1.009 (1.002–1.016)	0.010	1.007 (1.000–1.014)	0.0489
Sex				
Female	1.000			
Male	1.071 (0.864–1.328)	0.53		
Duration of drain placement[1], days	0.987 (0.881–1.105)	0.82		
Hemoglobin (g/dL)[1]	0.961 (0.908–1.018)	0.18		
Platelets (k/mL)[1]	1.000 (0.999–1.000)	0.57		
International normalized ratio[1]	1.570 (0.987–2.500)	0.06		
Creatinine (mg/dL)[1]	1.002 (0.993–1.011)	0.65		
Malignancy stage				
Non-advanced	1.000			
Advanced (stage III or IV)	0.924 (0.458–1.864)	0.83		
Approach for pericardiocentesis				
Subcostal	1.000			
Intercostal	1.045 (0.840–1.300)	0.69		
Echocardiographic evidence of tamponade at presentation[2]	1.439 (0.869–2.383)	0.16		
Malignant effusion on cytology[2]	1.495 (1.188–1.881)	0.0006	1.286 (1.006–1.645)	0.04
Anti-inflammatory agents use[2](colchicine, steroids, or NSAIDs)	0.571 (0.398–0.819)	0.002	0.624 (0.426–0.916)	0.02
Cardiac involvement by primary[2]tumor or tumor metastases	1.308 (0.912–1.875)	0.14		
Cancer treatment				
Radiation therapy[2]	1.155 (0.929–1.435)	0.19		
Chemotherapy[2]	1.100 (0.781–1.549)	0.59		
Immunotherapy[2]	1.175 (0.934–1.480)	0.17		
Surgery[2]	0.833 (0.638–1.088)	0.18		
Stem cell transplant[2]	0.730 (0.534–0.996)	0.047		
Cancer subgroup				
Hematologic	1.000			
Solid	1.600 (1.266–2.022)	< 0.0001		
Cancer type				
Lymphoma	1.000		1.000	
Lung	2.533 (1.725–3.718)	< 0.0001	2.387 (1.622–3.513)	< 0.0001
Breast	2.338 (1.474–3.709)	0.0003	2.028 (1.273–3.233)	0.0029
Colon and other GI	2.139 (1.262–3.626)	0.005	2.048 (1.208–3.472)	0.0078
Kidney or GU	2.650 (1.647–4.265)	< 0.0001	2.692 (1.670–4.338)	< 0.0001
Leukemia and other hematologic malignancies	1.927 (1.280–2.902)	0.002	1.902 (1.263–2.866)	0.0021
Other solid cancers	1.784 (1.079–2.951)	0.024	1.745 (1.052–2.894)	0.0310

GI, gastrointestinal; GU, genitourinary; HR, hazard ratio; NSAID, non-steroidal anti-inflammatory drug.
[1]For this variable, the HR is presented in 1-unit changes.
[2]For this variable, the HR is presented considering "No" as a reference group.

protocols for PCC at our institution as well as protocols for surveillance imaging prior to and after drain removal may have helped counter the bias to some extent. Initial performance status data were not obtained, and symptomatic improvement and quality-of-life metrics were not quantified or collected owing to the urgent/emergent nature of the procedure, though immediate symptom relief was often recognized. Outcomes of patients with recurrent pericardial effusion managed with therapies such as pericardial window or instillation of intra-pericardial sclerosing agents were not included in our study. Since this study included patients from 'Cardiac Catheterization Lab' database, a direct comparison cannot be made with patients who had malignancy but did not meet inclusion criteria for the study and hence did not undergo PCC.

CONCLUSION

Pericardiocentesis is an attractive option in cancer patients with large pericardial effusion with acceptable recurrence rate. Aggressive cancers (younger patients with solid malignancy) have an increased risk of recurrent PE within the first year from the initial PCC, while elderly patients with lung cancer and malignant PE cytology have worse survival. Cancer patients

requiring treatment with immunotherapy appear less likely to require additional PCC. Future studies will continue to refine and align cancer and cardiovascular care to benefit patients facing this double jeopardy.

DATA AVAILABILITY STATEMENT

The raw data supporting the conclusions of this article will be made available by the authors, without undue reservation.

ETHICS STATEMENT

The studies involving human participants were reviewed and approved by MD Anderson Institutional Review Board. The ethics committee waived the requirement of written informed consent for participation.

AUTHOR CONTRIBUTIONS

TA, CI, AD, and EM contributed to the conception and design of the study. JS, EK, and NP organized the database. JS performed the statistical analysis. TA, JL-M, and PK wrote the first draft of the manuscript. SY, SH, MC, KM, AV, AD, CI, and SS wrote sections of the manuscript. All authors contributed to manuscript revision, read, and approved the submitted version.

FUNDING

NP was supported by the NIH/NCI 1P01CA261669-01, the Cancer Prevention & Research Institute of Texas (RP200670), the Sabin Family Foundation Fellowship, and the MD Anderson Department of Internal Medicine Research Development Award. AD was supported in part by the Ting Tsung and Wei Fong Chao Distinguished Chair. SH received funding and act as a consultant for TerSera Therapeutics, LLC.

ACKNOWLEDGMENTS

We thank Laura L. Russell, scientific editor, Research Medical Library, for editing this article.

REFERENCES

1. El Haddad D, Iliescu C, Yusuf SW, William WN Jr, Khair TH, Song J, et al. Outcomes of cancer patients undergoing percutaneous pericardiocentesis for pericardial effusion. *J Am Coll Cardiol.* (2015) 66:1119–28. doi: 10.1016/j.jacc.2015.06.1332
2. Maisch B, Ristic A, Pankuweit S. Evaluation and management of pericardial effusion in patients with neoplastic disease. *Prog Cardiovasc Dis.* (2010) 53:157–63. doi: 10.1016/j.pcad.2010.06.003
3. Virk SA, Chandrakumar D, Villanueva C, Wolfenden H, Liou K, Cao C. Systematic review of percutaneous interventions for malignant pericardial effusion. *Heart.* (2015) 101:1619–26. doi: 10.1136/heartjnl-2015-307907
4. Tsang TS, Seward JB, Barnes ME, Bailey KR, Sinak LJ, Urban LH, et al. Outcomes of primary and secondary treatment of pericardial effusion in patients with malignancy. *Mayo Clin Proc.* (2000) 75:248–53. doi: 10.4065/75.3.248
5. Kim SH, Kwak MH, Park S, Kim HJ, Lee HS, Kim MS, et al. Clinical characteristics of malignant pericardial effusion associated with recurrence and survival. *Cancer Res Treat.* (2010) 42:210–6. doi: 10.4143/crt.2010.42.4.210
6. Kearns MJ, Walley KR. Tamponade: hemodynamic and echocardiographic diagnosis. *Chest.* (2018) 153:1266–75. doi: 10.1016/j.chest.2017.11.003
7. Wilson NR, Lee MT, Gill CD, Serauto Canache A, Donisan T, Balanescu DV, et al. Prognostic factors and overall survival after pericardiocentesis in patients with cancer and thrombocytopenia. *Front Cardiovasc Med.* (2021) 8:638943. doi: 10.3389/fcvm.2021.638943
8. Iliescu C, Khair T, Marmagkiolis K, Iliescu G, Durand JB. Echocardiography and fluoroscopy-guided pericardiocentesis for cancer patients with cardiac tamponade and thrombocytopenia. *J Am Coll Cardiol.* (2016) 68:771–3. doi: 10.1016/j.jacc.2016.05.068
9. Austin PC, Fine JP. Practical recommendations for reporting fine-gray model analyses for competing risk data. *Stat Med.* (2017) 36:4391–400. doi: 10.1002/sim.7501
10. Bakoyannis G, Touloumi G. Practical methods for competing risks data: a review. *Stat Methods Med Res.* (2012) 21:257–72. doi: 10.1177/0962280210394479
11. Lekhakul A, Assawakawintip C, Fenstad ER, Pislaru SV, Thaden JJ, Sinak LJ, et al. Safety and outcome of percutaneous drainage of pericardial effusions in patients with cancer. *Am J Cardiol.* (2018) 122:1091–4. doi: 10.1016/j.amjcard
12. Jama GM, Scarci M, Bowden J, Marciniak SJ. Palliative treatment for symptomatic malignant pericardial effusion†. *Interact Cardiovasc Thorac Surg.* (2014) 19:1019–26. doi: 10.1093/icvts/ivu267
13. Santas E, Núñez J. Prognostic implications of pericardial effusion: the importance of underlying etiology. *Int J Cardiol.* (2016) 202:407. doi: 10.1016/j.ijcard.2015.09.051
14. Imazio M, Adler Y. Management of pericardial effusion. *Eur Heart J.* (2013) 34:1186–97. doi: 10.1093/eurheartj/ehs372
15. Kim SR, Kim EK, Cho J, Chang SA, Park SJ, Lee SC, et al. Effect of anti-inflammatory drugs on clinical outcomes in patients with malignant pericardial effusion. *J Am Coll Cardiol.* (2020) 76:1551–61. doi: 10.1016/j.jacc.2020.08.003
16. Imazio M, Belli R, Brucato A, Cemin R, Ferrua S, Beqaraj F, et al. Efficacy and safety of colchicine for treatment of multiple recurrences of pericarditis (CORP-2): a multicentre, double-blind, placebo-controlled, randomised trial. *Lancet.* (2014) 383:2232–7. doi: 10.1016/S0140-6736(13)62709-9
17. Strobbe A, Adriaenssens T, Bennett J, Dubois C, Desmet W, McCutcheon K, et al. Etiology and long-term outcome of patients undergoing pericardiocentesis. *J Am Heart Assoc.* (2017) 6:e007598. doi: 10.1161/JAHA.117.007598
18. Gornik HL, Gerhard-Herman M, Beckman JA. Abnormal cytology predicts poor prognosis in cancer patients with pericardial effusion. *J Clin Oncol.* (2005) 23:5211–6. doi: 10.1200/JCO.2005.00.745
19. Dragoescu EA, Liu L. Pericardial fluid cytology: an analysis of 128 specimens over a 6-year period. *Cancer Cytopathol.* (2013) 121:242–51. doi: 10.1002/cncy.21246
20. Saab J, Hoda RS, Narula N, Hoda SA, Geraghty BE, Nasar A, et al. Diagnostic yield of cytopathology in evaluating pericardial effusions: clinicopathologic analysis of 419 specimens. *Cancer Cytopathol.* (2017) 125:128–37. doi: 10.1002/cncy.21790
21. Imazio M, Colopi M, De Ferrari GM. Pericardial diseases in patients with cancer: contemporary prevalence, management and outcomes. *Heart.* (2020) 106:569–74. doi: 10.1136/heartjnl-2019-315852
22. Dequanter D, Lothaire P, Berghmans T, Sculier JP. Severe pericardial effusion in patients with concurrent malignancy: a retrospective analysis of prognostic factors influencing survival. *Ann Surg Oncol.* (2008) 15:3268–71. doi: 10.1245/s10434-008-0059-z
23. Patel N, Rafique AM, Eshaghian S, Mendoza F, Biner S, Cercek B, et al. Retrospective comparison of outcomes, diagnostic value, and complications of percutaneous prolonged drainage versus surgical pericardiotomy of

pericardial effusion associated with malignancy. *Am J Cardiol.* (2013) 112:1235–9. doi: 10.1016/j.amjcard.2013.05.066

24. Horr SE, Mentias A, Houghtaling PL, Toth AJ, Blackstone EH, Johnston DR, et al. Comparison of outcomes of pericardiocentesis versus surgical pericardial window in patients requiring drainage of pericardial effusions. *Am J Cardiol.* (2017) 120:883–90. doi: 10.1016/j.amjcard.2017.06.003
25. Adler Y, Charron P, Imazio M, Badano L, Barón-Esquivias G, Bogaert J, et al. 2015 ESC guidelines for the diagnosis and management of pericardial diseases: the task force for the diagnosis and management of pericardial diseases of the European society of cardiology (ESC) endorsed by: the European association for cardio-thoracic surgery (EACTS). *Eur Heart J.* (2015) 36:2921–64. doi: 10.1093/eurheartj/ehv318
26. Jacob R, Palaskas NL, Lopez-Mattei J, Hassan S, Kim P, Donisan T, et al. How to perform pericardiocentesis in cancer patients with thrombocytopenia: a single-center experience. *J Am Coll Cardiol CardioOncol.* (2021) 3:452–6. doi: 10.1016/j.jaccao.2021.05.005
27. Maggiolini S, De Carlini CC, Imazio M. Evolution of the pericardiocentesis technique. *J Cardiovasc Med (Hagerstown).* (2018) 19:267–73. doi: 10.2459/JCM.0000000000000649
28. Pennacchioni A, Nanni G, Sgura FA, Imberti JF, Monopoli DE, Rossi R, et al. Percutaneous pericardiocentesis for pericardial effusion: predictors of mortality and outcomes. *Intern Emerg Med.* (2021) 16:1771–7. doi: 10.1007/s11739-021-02642-x

Conflict of Interest: The authors declare that the research was conducted in the absence of any commercial or financial relationships that could be construed as a potential conflict of interest.

Publisher's Note: All claims expressed in this article are solely those of the authors and do not necessarily represent those of their affiliated organizations, or those of the publisher, the editors and the reviewers. Any product that may be evaluated in this article, or claim that may be made by its manufacturer, is not guaranteed or endorsed by the publisher.

frontiers | Frontiers in Cardiovascular Medicine

SYSTEMATIC REVIEW
published: 31 May 2022
doi: 10.3389/fcvm.2022.890082

Comparing Clinical Outcomes on Oncology Patients With Severe Aortic Stenosis Undergoing Transcatheter Aortic Valve Implantation: A Systematic Review and Meta-Analysis

Yumeng Song[1,2], *Yutong Wang*[1,2], *Zuoxiang Wang*[1,2], *Chang Xu*[1,2], *Jingshen Dou*[1,2] *and Tingbo Jiang*[1]*

[1] *Department of Cardiology, The First Affiliated Hospital of Soochow University, Suzhou, China,* [2] *Department of Medicine, Soochow University, Suzhou, China*

OPEN ACCESS

Edited by:
Reto Asmis,
Wake Forest School of Medicine, United States

Reviewed by:
Masahiko Asami,
Mitsui Memorial Hospital, Japan
Vladimir Uspenskiy,
Almazov National Medical Research Centre, Russia
Hemang Panchal,
Florida Atlantic University, United States

***Correspondence:**
Tingbo Jiang
jiangtingbo6797@163.com

Specialty section:
This article was submitted to Cardio-Oncology, a section of the journal Frontiers in Cardiovascular Medicine

Received: *07 March 2022*
Accepted: *19 April 2022*
Published: *31 May 2022*

Citation:
Song Y, Wang Y, Wang Z, Xu C, Dou J and Jiang T (2022) Comparing Clinical Outcomes on Oncology Patients With Severe Aortic Stenosis Undergoing Transcatheter Aortic Valve Implantation: A Systematic Review and Meta-Analysis. Front. Cardiovasc. Med. 9:890082. doi: 10.3389/fcvm.2022.890082

Objective: To compare the clinical outcomes of cancer and non-cancer patients with severe aortic stenosis (AS) after transcatheter aortic valve implantation (TAVI).

Methods: A computer-based search in PubMed, EMbase, The Cochrane Library, CBM, CNKI, and Wanfang databases from their date of inception to October 2021, together with reference screening, was performed to identify eligible clinical trials. Two reviewers independently screened the articles, extracted data, and evaluated their quality. Review Manger 5.3 and Stata 12.0 software were used for meta-analysis.

Results: The selected 11 cohort studies contained 182,645 patients, including 36,283 patients with cancer and 146,362 patients without cancer. The results of the meta-analysis showed that the 30-day mortality [OR = 0.68, 95%CI (0.63,0.74), I^2= 0, P < 0.00001] of patients with cancer in the AS group was lower than those in the non-cancer group; 1-year mortality [OR = 1.49, 95%CI(1.19,1.88), I^2= 58%, P = 0.0006] and late mortality [OR = 1.52, 95%CI(1.26,1.84), I^2= 55%, P < 0.0001] of patients with cancer in the AS group was higher than those in the non-cancer group. The results of the meta-analysis showed that the stroke [OR = 0.77, 95%CI (0.72, 0.82), I^2= 0, P < 0.00001] and the acute kidney injury [OR = 0.78, 95%CI (0.68, 0.90), I^2= 77%, P = 0.0005] of patients with cancer in the AS group was lower than those in the non-cancer group. The results of the meta-analysis showed no statistical difference in cardiovascular mortality, bleeding events, myocardial infarction, vascular complication, and device success rate.

Conclusion: It is more effective and safer in patients with cancer with severe AS who were undergoing TAVI. However, compared with patients with no cancer, this is still high in terms of long-term mortality, and further study of the role of TAVI in patients with cancer with AS is necessary.

Systematic Review Registration: Identifier [INPLASY CRD: 202220009].

Keywords: aortic stenosis, oncology, transcatheter aortic valve implantation, meta-analysis, mortality

INTRODUCTION

With the uptrend of aging in the world, the morbidity of valvular disease in the elderly is increasing, in which AS has gradually become the most common valvular heart disease in the elderly. The main manifestations of AS are angina pectoris, syncope, dyspnea, and even sudden death. The effect of conservative treatment is not good, though it can relieve the clinical symptoms, the aortic valve function cannot recover, affecting the quality of life of patients. The results of the American population survey showed that the incidence of severe valvular disease in the elderly is 2.5%, including 13.3% in people over 75 years old. European surveys showed that the incidence of AS in the population is 4%, and 2% in the elderly population (1). In addition, not only the incidence of AS is increasing year by year, but also the prognosis is very poor. Once the symptoms or cardiac function decrease, the mortality increases sharply. If only conservative treatment is performed, the 2-year fatality rate is 50% to 60%. Therefore, active intervention is needed.

Since transcatheter aortic valve implantation (TAVI) appeared in 2002, it has become a vital treatment of choice for patients with severe AS (2, 3). TAVI is sending the artificial valve to the aortic valve area to replace the aortic valve to perform its functions. TAVI indications listed in the 2017 European Valve Management guidelines: symptomatic patients with severe AS who are not suitable for surgery (I, B); or patients with higher surgical risk are defined as STS score or Euro SCORE II $\geq$4%, or other risk factors, such as weakness, porcelain aorta, and chest radiotherapy, especially suitable for elderly patients with femoral artery approach (I, B). The indications for TAVI listed in the 2017 American Valve Management guidelines are symptomatic in severe patients with AS with surgical taboos or high risk and expected survival of more than 12 months (I, A); surgical risk severe AS patients (II, a).

The TAVI has quickly developed all over the world because of its small trauma and rapid recovery. At present, more than 300,000 cases have been completed in more than 60 countries (4, 5). Among them, cancer patients with severe AS become a special group of valvular disease because of tumor recurrence, metastasis, and other characteristics. However, related research on the clinical efficacy and safety of TAVI in patients with cancer with severe AS is limited and the conclusion is still controversial. Therefore, the purpose of this study is to systematically evaluate the early and medium-term clinical efficacy of TAVI in patients with severe AS with cancer.

DATA AND METHODS

Data Sources

The Preferred Reporting Items for Systematic Reviews and Meta-Analyses Protocols (PRISMA-P) statement was followed. A comprehensive literature search was performed through the PubMed, Embase, The Cochrane Library, CBM, CNKI, and Wanfang databases from their establishment to October 2021 using the following terms: "transcatheter aortic valve implantation," "transcatheter aortic valve replacement," "TAVI," "TAVR," "neoplasm," "malignancy," "cancer," and "tumor" with no restrictions on language. Reference lists of reviewed articles were screened to identify further relevant studies. When outcomes reporting was incomplete, the study authors were contacted for further information.

Study Selection

Inclusion criteria were as follows: studies performed in patients with severe AS and cancer; study design comparing patients with cancer undergoing TAVI to patients without cancer undergoing TAVI; reporting the 30-day, 1-year, and late mortality. In the meta-analysis, we included patients with an active history of cancer.

Eligibility Criteria

All studies were included based on the following inclusion criteria: (1) the study enrolled patients with AS with cancer; (2) the study intervention was TAVI with no restrictions on the valve style (balloon- or self-expandable valve) or delivery route; (3) the study compared clinical outcomes of patients with cancer to patients without cancer undergoing TAVI; (4) the study design was randomized controlled trials (RCT) or cohort studies.

Studies will be excluded if one of the following conditions is met: (1) the type of study was case-control studies, case reports, conference abstracts, reviews, comments, or editorials were excluded; and (2) a significant amount of research data was missing or not available.

Study Selection and Data Extraction

The first author (YS) and the second author (YW) independently screened titles and abstracts of all identified records to exclude unrelated studies based on inclusion/exclusion criteria. After that, relevant studies and full articles were reviewed to further determine their suitability. Disagreements were resolved by discussions with a third reviewer (ZW) or by consensus.

Clinical Endpoints

The primary outcome is all-cause mortality in 30-days, 1-year, and late mortality. The second outcome included myocardial infarction (MI), stroke, bleeding events, major or minor vascular complications, new permanent pacemaker implantation, acute kidney injury (AKI), and device success.

Risk of Bias and Statistical Analysis

The Cochrane Collaboration's tool for assessing the risk of bias was utilized to assess the risk of bias in RCTs, including: (1) sequence generation; (2) allocation concealment; (3) blinding of participants and personnel; (4) blinding of outcome assessment; (5) incomplete outcome data; (6) selective outcome reporting; and (7) other bias. Moreover, the Newcastle-Ottawa Scale (NOS) (6) was used to assess the quality of cohort studies consisting of three factors: patient selection, comparability of the study groups, and the assessment of outcomes.

Categorical variables were reported as percentages, and continuous variables were presented as the mean $\pm$ SD. We reported clinical outcomes and their respective effect size in all

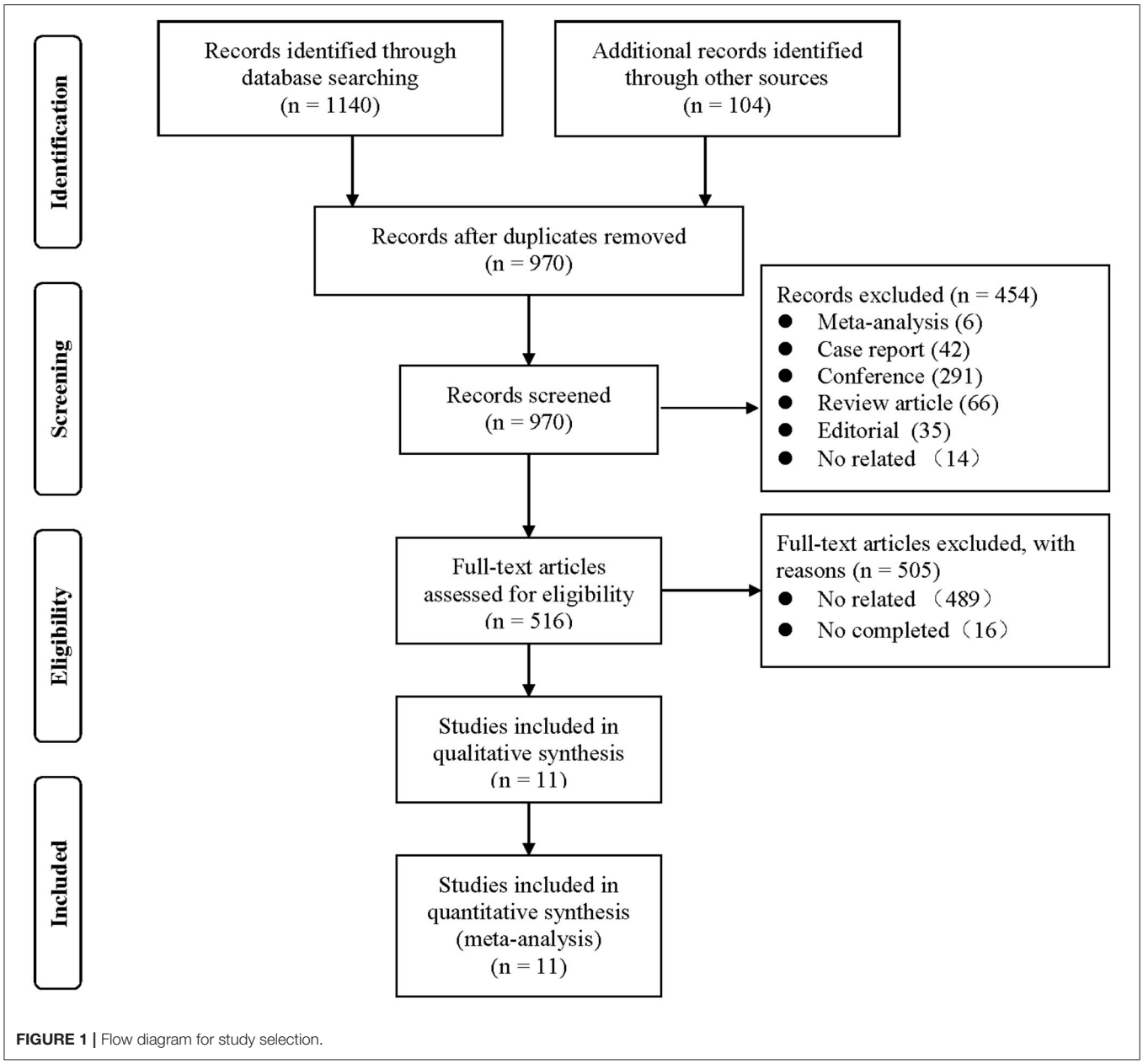

FIGURE 1 | Flow diagram for study selection.

included studies using odds ratios (ORs), with corresponding 95% confidence intervals (CIs).

Heterogeneity assessments were performed using χ2-based Q statistics and I^2 tests. If $P > 0.10$ and $I^2 \leq 50\%$, there was no statistical heterogeneity among results; if $P < 0.10$ and $I^2 > 50\%$, there was a considered significant heterogeneity. All the results were performed using the random effect model. Subgroup analyses were also performed to find more potential information based on a different type of event. The likelihood of publication bias was assessed directly through the funnel plots, evaluated using an Egger's test. All analyses were performed using Review Manger 5.3 and Stata 12.0 software.

RESULTS

Baseline Demographic and Quality Assessment

A total of 1,140 potentially eligible studies were identified in our initial search, and 11 clinical studies met the inclusion criteria (5, 7–16) (**Figure 1**). A total of 182,645 patients were enrolled, including 36,283 patients in the cancer group and 146,362 patients in the non-cancer group. The basic information of these studies is in **Table 1**. There were significant statistical differences in the mean Society of Thoracic Surgeons score (STS score) [$WMD = -0.76$, 95%CI $(-1.14, -0.37)$, $I^2 = 70\%$, $P =$

TABLE 1 | Characteristics of the studies included in this meta-analysis.

NO	Reference	Year	Type of research	Samples (E /C)	Characteristics(E/C)				Medical history(E/C)					Inspection report(E/C)			NOS
					Age(year)	Male(%)	BMI(Kg/m2)	Euro ScoreII(%)	Hypertension(%)	DM(%)	MI(%)	NYHA III,IV(%)	PAD(%)	STS score(%)	Valvular area(cm^2)	LVEF(%)	
1	Watanabe et al. (16)	2016	Cohort studies	47/702	83.0 ± 5.2/85.0 ± 4.4	45.0/33.0	23.6 ± 3.8/21.7 ± 3.6	3.1 ± 2.4/3.9 ± 2.8	75.0/75.6	30.0/25.0	11.0/8.0	40.0/48.0	23.0/15.0	5.4 ± 3.0/7.0 ± 3.6	0.65 ± 0.1/0.62 ± 0.2	65.9 ± 9.2/65.0 ± 7.8	8
2	Berkovitch et al. (7)	2018	Cohort studies	91/386	79.4 ± 8.6/81.8 ± 7.0	52.0/52.0	NR	4.5 ± 4.8/5.4 ± 5.9	82.0/85.0	34.0/40.0	NR	NR	NR	4.6 ± 3.0/5.7 ± 3.9	NR	NR	7
3	Mangner et al. (13)	2018	Cohort studies	350/1471	80.3 ± 5.7/81.0 ± 5.2	47.1/42.7	27.1 ± 4.9/27.4 ± 5.0	NR	92.6/93.6	40.6/43.6	12.3/12.0	78.3/77.1	10.3/11.7	6.4 ± 4.8/6.7 ± 4.8	0.6 ± 0.2/0.7 ± 0.2	58.4 ± 13.6/58.0 ± 14.8	8
4	Landes et al. (5)	2019	Cohort studies	222/2522	78.8 ± 7.5 /81.3 ± 7.1	62.1/45.0	26.6 ± 4.8/28.0 ± 5.0	4.2 ± 3.2/5.4 ± 4.4	76.0/92.0	28.0/36.0	13.0/9.0	76.0/83.0	16.0/14.0	4.9 ± 3.4/6.2 ± 4.4	0.72 ± 0.22/0.65 ± 0.20	56.0 ± 14.0/56.0 ± 8.0	8
5	Tabata et al. (15)	2019	Cohort studies	240/964	80.5 ± 5.9/81.0 ± 6.3	62.5/48.5	26.4 ± 5.1/27.0 ± 6.7	6.2 ± 5.7/6.8 ± 6.5	84.2/86.5	25.4/28.4	14.2/12.4	90.3/92.3	32.9/34.6	5.1 ± 4.1/5.6 ± 5.2	0.73 ± 0.16/0.72 ± 0.17	NR	8
6	Biancari et al. (8)	2020	Cohort studies	417/1713	80.6 ± 6.6/81.4 ± 6.6	48.9/44.0	NR	NR	NR	22.8/29.8	1.9/2.4	NR	NR	4.4 ± 3.2/4.6 ± 3.3	NR	NR	7
7	Grant et al. (9)	2020	Cohort studies	23670/ 99400	81.1 ± 7.9/80.1 ± 6.7	56.7/52.9	NR	NR	81.1/79.6	31.6/36.7	NR	NR	NR	NR	NR	NR	8
8	Guha et al. (10)	2020	Cohort studies	10670/ 36625	81.1 ± 0.2/80.8 ± 0.1	57.2/52.6	NR	NR	83.5/83.8	38.0/41.5	14.0/13.4	NR	NR	NR	NR	NR	7
9	Lind et al. (12)	2020	Cohort studies	249/839	81.1 ± 5.9/81.4 ± 5.4	50.6/45.5	NR	NR	94.0/94.7	33.7/34.6	7.2/6.6	85.1/89.0	17.7/20.2	5.1 ± 1.9/6.0 ± 2.4	NR	50.6 ± 11.3/51.3 ± 11.1	8
10	Tabata et al. (14)	2020	Cohort studies	298/1270	80.8 ± 5.8/81.1 ± 6.7	60.7/47.5	26.2 ± 5.0/27.0 ± 6.5	6.2 ± 5.7/6.8 ± 6.3	NR	25.0/28.7	12.3/11.9	NR	NR	5.4 ± 4.2/5.8 ± 5.2	0.73 ± 0.16/0.72 ± 0.17	NR	7
11	Karaduman et al. (11)	2021	Cohort studies	36/514	74.6 ± 6.5/77.8 ± 8.0	30.6/43.0	25.0 ± 3.9/27.9 ± 6.2	7.4 ± 4.9/9.1 ± 5.8	75.0/82.6	19.4/30.2	NR	58.3/72.4	NR	4.8 ± 3.2/6.1 ± 3.5	NR	NR	7

E, Experiment group; C,control group; E/C,%, proportion; BMI, Body Mass Index; Euro score, Logistic European score; DM, Diabetes Mellitus;PAD, Peripheral Artery Disease; MI,Myocardial Infarction; LVEF,Left Ventricular Ejection Fraction; NOS, Newcastle-Ottawa Quality Assessment Scale.

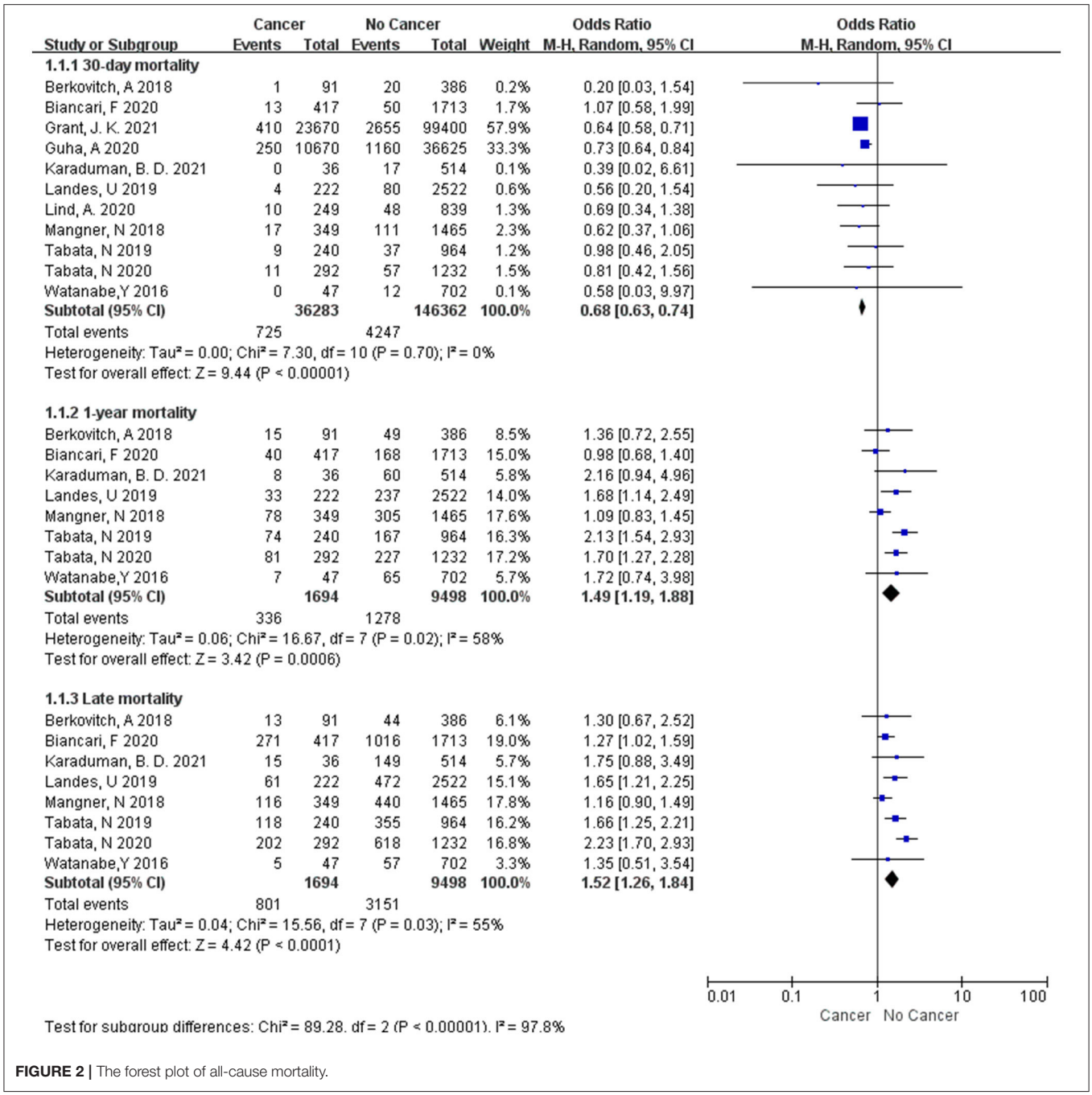

FIGURE 2 | The forest plot of all-cause mortality.

0.0001] and logistic European System for Cardiac Operative Risk Evaluation II (logistic Euro SCORE II) [$WMD = -0.95$, 95%CI $(-1.25, -0.65)$, $I^2 = 0$, $P < 0.00001$] between two groups.

Clinical Outcomes

All-Cause Mortality

For all-cause mortality, subgroup analysis of included studies illustrated that there were significant differences among them. At 30-day mortality, 11 studies were enrolled (5, 7–16) and the random effect model showed that the cancer group had a significantly lower all-cause mortality than the non-cancer group [$OR = 0.68$, 95%CI (0.63, 0.74), $I^2 = 0$, $P <$ in 0.00001]. However, cancer group had higher mortality than non-cancer group at 1-year (5, 7, 8, 11, 13–16) [OR=1.49, 95%CI (1.19,1.88), $I^2 =$ 58%, $P = 0.0006$] and late (5, 7, 8, 11, 13–16) [OR=1.52, 95%CI (1.26,1.84), $I^2 =$ 55%, $P < 0.0001$] (**Figure 2**).

Cardiovascular Mortality

There was no significant statistical difference in cardiovascular mortality [OR=1, 95%CI (0.83, 1.19), $I^2 =$ 2%, $P = 0.96$] between the two groups.

Stroke

There were 10 studies (5, 7, 9–16) included and the meta-analysis showed that the patients with cancer were associated with a significantly lower rate of stroke than the non-cancer group [$OR = 0.77$, 95%CI (0.72, 0.82), $I^2 = 0$, $P < 0.00001$] (**Figure 3A**).

Acute Kidney Injury

There were 7 studies (5, 7, 9, 10, 12, 13, 16) included and the meta-analysis showed that the patients with cancer were associated with a significantly lower rate of acute kidney injury (AKI) than the non-cancer group [$OR = 0.78$, 95%CI (0.68, 0.90), $I^2 = 77\%$, $P = 0.0005$] (**Figure 3B**).

New Permanent Pacemaker

There were 8 studies (5, 9–11, 13–16) included and the meta-analysis showed that the patients with cancer were associated with a significantly higher success rate of new permanent pacemakers than the non-cancer group [$OR = 1.11$, 95%CI (1.03, 1.19), $I^2 = 30\%$, $P = 0.005$] (**Figure 3C**).

Other Clinical Outcomes

There were no differences in any bleeding events [$OR = 1.13$, 95%CI (0.82, 1.56), $I^2 = 84\%$, $P = 0.45$], device success [$OR = 1.14$, 95%CI (0.63, 2.08), $I^2 = 56\%$, $P = 0.66$], myocardial infarction [$OR = 0.92$, 95% CI (0.30, 2.86), $I^2 = 57\%$, $P = 0.88$], major vascular complications [$OR = 1.16$, 95%CI (0.76, 1.78), $I^2 = 14\%$, $P = 0.48$], and minor vascular complications [$OR = 0.72$, 95%CI (0.35, 1,48), $I^2 = 76\%$, $P = 0.38$] between two groups.

Publication Bias

The funnel plot analysis and the Egger's test were used to examine the publication bias of included studies. Funnel plot analysis of all results did not show significant asymmetry. The Egger's test showed no significant publication bias in 30-day all-cause mortality ($P = 0.819$), 1-year all-cause mortality ($P = 0.668$), late and all-cause mortality ($P = 0.806$), stroke ($P = 0.509$), new permanent pacemaker implantation ($P = 0.991$), and AKI ($P = 0.589$) (**Figure 4**).

DISCUSSION

Patients with severe AS with tumors are a special group of valvular diseases (2, 3). The choice of intervention for AS is a matter of concern, because of their operation or drug intolerance, which will affect the choice of best anti-tumor therapy (5). The European Society of Cardiology (European Society of Cardiology, ESC) proposed that we can release the left heart failure caused by antineoplastic therapy by reducing the afterload of the left ventricle (17); while for AS, the afterload can be effectively reduced only through aortic valve intervention. The main clinical intervention methods for aortic valve include balloon valvuloplasty, aortic valve replacement (Surgical Aortic Valve Replacement, SAVR), and TAVI. It has been proved that balloon valvuloplasty cannot improve the survival rate of patients with AS, and has many complications (18, 19). Although SAVR can improve the survival rate of patients with cancer with severe AS (20), it will have higher perioperative mortality compared to non-cancer patients with AS because of its intolerance to open surgery (21). The revolutionary innovation of TAVI provides a great opportunity for the treatment of severe AS, which may also be the best treatment for patients with AS with cancer. TAVI has the advantages of minimal trauma and rapid recovery, which not only reduces the risk of bleeding and infection after SAVR but also avoids the interruption of perioperative antineoplastic therapy (21, 22).

The purpose of this study was to compare the difference in mortality between cancer and patients without cancer with severe AS in TAVI. The results of the meta-analysis showed that there was no significant difference in the cardiovascular mortality, any bleeding events, vascular complications, and myocardial infarction between the two groups, indicating that in patients undergoing TAVI, mortality was mainly affected by non-cardiac factors (23), such as cancer progression or metastasis. Meta-analysis showed that I^2 was >50% in 1-year and late all-cause mortality, but much <75%, while Egger test p-values were >0.05, which concluded that there was no significant heterogeneity. In the 30-day, the all-cause mortality in the cancer group was lower than the non-cancer group, while in the 1-year and late all-cause mortality, the mortality in the cancer group was higher than that. Maybe in short-term treatment, TAVI relieves patients' cardiac symptoms and plays a positive role in anti-tumor treatment (24), so the short-term survival rate is increased. In addition to this, the 2017 American Valve Management guidelines state that the indications for TAVI include a life expectancy of more than 12 months after treatment to correct AS (25). Patients with cancer who choose to undergo TAVI are generally younger and have a lower risk than patients without cancer, and they also have a higher survival rate in the short term. But compared with patients without cancer, even though the patients in the cancer group are younger and have lower STS scores, the long-term survival rate decreases due to the continuous influence of tumor factors (tumor progression, metastasis, recurrence, etc.).

This study also found that in the complications after TAVI, there were significant differences in the incidence of stroke, acute kidney injury, and new permanent pacemaker. The meta-analysis showed that in the cancer group, there was a lower rate of stroke and AKI than in the non-cancer group. Stroke is a common complication after TAVI and can be classified as perioperative (within 30 days after TAVI or during hospitalization), early period (between 30 days and 1 year after TAVI), and late period (more than 1 year) depending on the time of occurrence (26, 27). A stroke occurs in the perioperative period mainly due to debris dislodgement generated during TAVI, which includes aortic wall components, atherosclerotic tissue, and valves, and it may also be triggered by damage to the aortic wall caused by the procedure (28, 29); stroke occurs in the early and late periods mainly due to valve-related turbulence, vessel wall rupture, metal frame exposure, and other procedure-related factors (30). On the one hand, patients in the cancer group had lower STS and Euro II scores than those in the non-cancer group, we believe that patients in the oncology group had better vascular conditions than those in the non-oncology group and were less likely to have a stroke due to debris from vessel wall damage or poor valve placement. The ESC/EACTS,

A

Study or Subgroup	Cancer Events	Cancer Total	No Cancer Events	No Cancer Total	Weight	Odds Ratio M-H, Random, 95% CI
Berkovitch, A 2018	2	91	13	386	0.2%	0.64 [0.14, 2.91]
Grant, J. K. 2021	840	23670	4715	99400	74.9%	0.74 [0.69, 0.80]
Guha, A 2020	255	10670	1000	36625	21.6%	0.87 [0.76, 1.00]
Karaduman, B. D. 2021	1	36	28	514	0.1%	0.50 [0.07, 3.75]
Landes, U 2019	2	222	22	2522	0.2%	1.03 [0.24, 4.42]
Lind, A. 2020	10	249	28	839	0.8%	1.21 [0.58, 2.53]
Mangner, N 2018	16	341	67	1425	1.3%	1.00 [0.57, 1.74]
Tabata, N 2019	4	240	23	964	0.4%	0.69 [0.24, 2.02]
Tabata, N 2020	5	298	29	1270	0.5%	0.73 [0.28, 1.90]
Watanabe,Y 2016	0	47	18	702	0.1%	0.39 [0.02, 6.56]
Total (95% CI)		**35864**		**144647**	**100.0%**	**0.77 [0.72, 0.82]**
Total events	1135		5943			

Heterogeneity: Tau² = 0.00; Chi² = 7.20, df = 9 (P = 0.62); I² = 0%
Test for overall effect: Z = 7.86 (P < 0.00001)

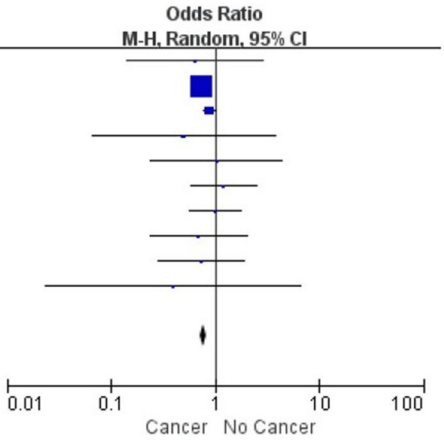

B

Study or Subgroup	Cancer Events	Cancer Total	No Cancer Events	No Cancer Total	Weight	Odds Ratio M-H, Random, 95% CI
Berkovitch, A 2018	15	91	83	386	4.6%	0.72 [0.39, 1.32]
Grant, J. K. 2021	2370	23670	13870	99400	35.1%	0.69 [0.66, 0.72]
Guha, A 2020	1525	10670	6340	36625	34.1%	0.80 [0.75, 0.85]
Landes, U 2019	8	222	139	2522	3.3%	0.64 [0.31, 1.32]
Lind, A. 2020	35	249	158	839	9.2%	0.70 [0.47, 1.05]
Mangner, N 2018	66	342	236	1433	13.4%	1.21 [0.90, 1.64]
Watanabe,Y 2016	0	47	17	702	0.2%	0.41 [0.02, 6.96]
Total (95% CI)		**35291**		**141907**	**100.0%**	**0.78 [0.68, 0.90]**
Total events	4019		20843			

Heterogeneity: Tau² = 0.01; Chi² = 26.05, df = 6 (P = 0.0002); I² = 77%
Test for overall effect: Z = 3.50 (P = 0.0005)

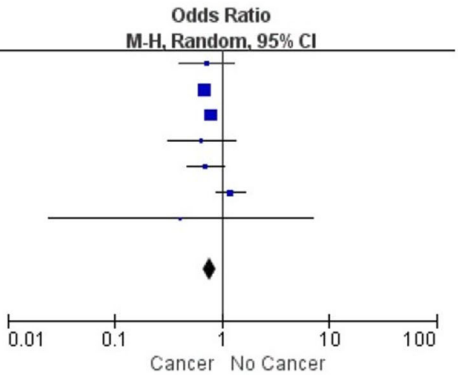

C

Study or Subgroup	Cancer Events	Cancer Total	No Cancer Events	No Cancer Total	Weight	Odds Ratio M-H, Random, 95% CI
Grant, J. K. 2021	1795	23670	6735	99400	43.5%	1.13 [1.07, 1.19]
Guha, A 2020	1210	10670	3990	36625	38.2%	1.05 [0.98, 1.12]
Karaduman, B. D. 2021	1	36	41	514	0.1%	0.33 [0.04, 2.47]
Landes, U 2019	43	222	337	2522	4.0%	1.56 [1.10, 2.21]
Mangner, N 2018	104	350	417	1470	7.2%	1.07 [0.83, 1.38]
Tabata, N 2019	38	240	123	964	3.2%	1.29 [0.87, 1.91]
Tabata, N 2020	41	298	150	1270	3.6%	1.19 [0.82, 1.73]
Watanabe,Y 2016	1	47	38	702	0.1%	0.38 [0.05, 2.83]
Total (95% CI)		**35533**		**143467**	**100.0%**	**1.11 [1.03, 1.19]**
Total events	3233		11831			

Heterogeneity: Tau² = 0.00; Chi² = 9.99, df = 7 (P = 0.19); I² = 30%
Test for overall effect: Z = 2.79 (P = 0.005)

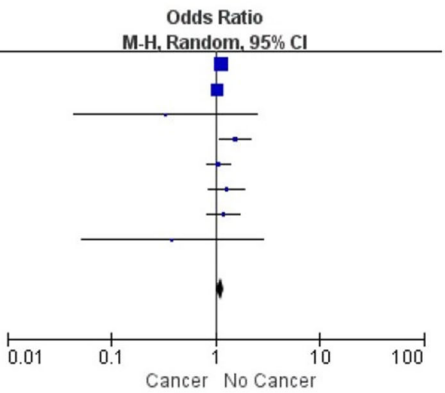

FIGURE 3 | The forest plots of **(A)** stroke, **(B)** AKI and **(C)** new permanent pacemaker.

AHA/ACC, and ESC/EAPCI committees have not reached a consensus on the choice of anticoagulation regimen after TAVI (31–33), but they all choose the appropriate anticoagulation therapy based on clinical experience and the patient's actual situation. Although patients in the cancer group are more likely to have hypercoagulable blood due to their tumors, routine

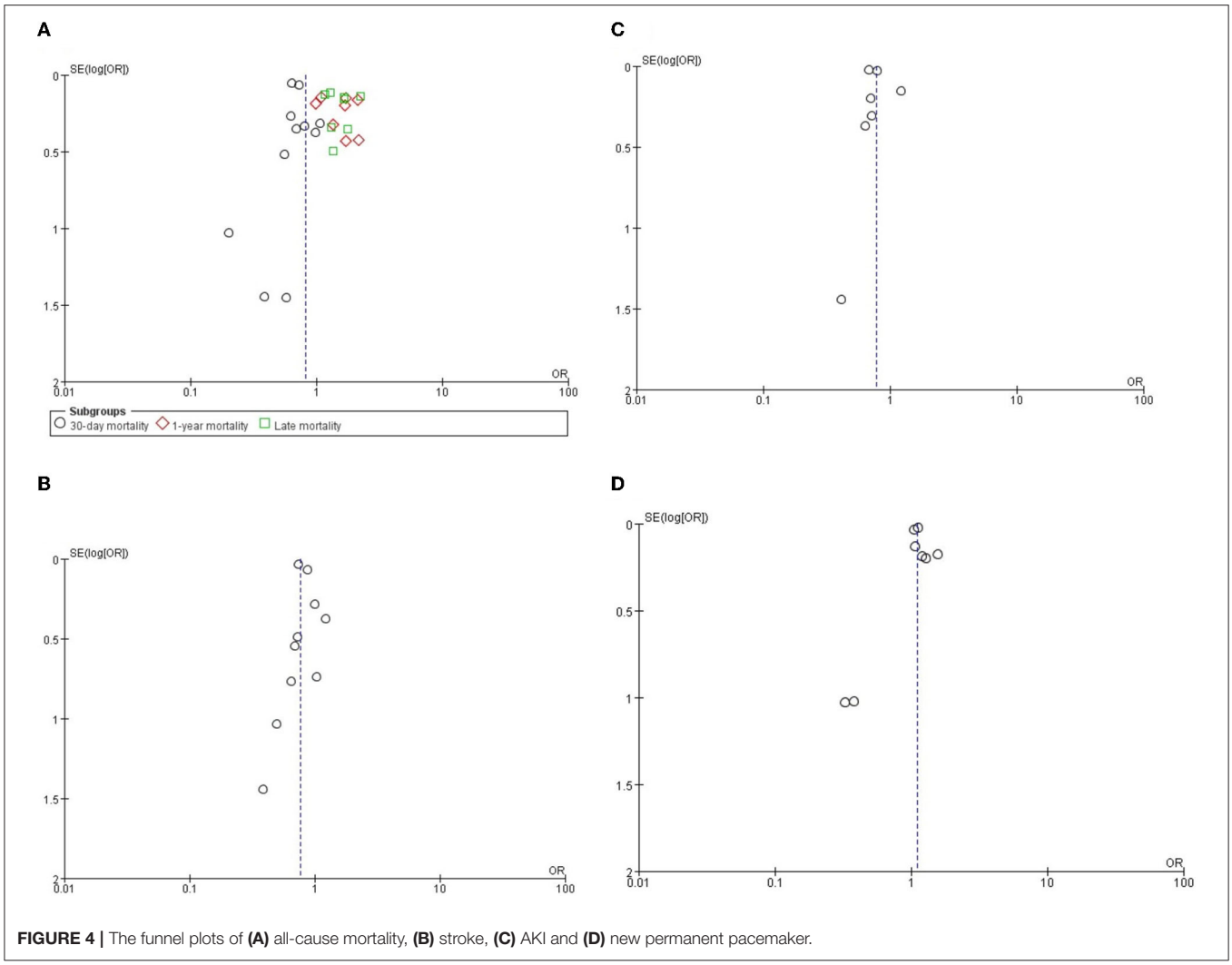

FIGURE 4 | The funnel plots of **(A)** all-cause mortality, **(B)** stroke, **(C)** AKI and **(D)** new permanent pacemaker.

anticoagulation after TAVI can reduce the risk. On the other hand, the meta-analysis showed that there is no statistically significant difference between the two groups in any bleeding events, which also demonstrates the effectiveness of either anticoagulation regimen in reducing blood hypercoagulability. While the large number of contrast media needed for an operation may cause acute renal function damage after the operation, we can see from the data that the age and STS scores of patients in the cancer group are lower than those in the non-cancer group. The lower score indicates that the patients in this group have fewer risk factors than the non-cancer group, which leads to a lower incidence of acute kidney injury after TAVI. The conduction block is also a common complication after TAVI, so 13% of patients after TAVI need permanent pacemakers to improve survival. In this study, there were statistical differences in the new permanent pacemaker implantation between the two groups. The cancer group had a higher implantation rate; however, data were collected in this meta-analysis without access to the preoperative ECG results of patients, including whether they had preoperative right bundle branch block (RBBB) or atrioventricular block (34), so we considered that the higher rate of permanent pacemaker implantation in the cancer group compared to the non-cancer group may be due to the possibility that they had a high degree of atrioventricular block or were unable to remove the temporary pacemaker after TAVI.

The strength of this meta-analysis is the inclusion of 11 articles including 182,645 patients, adequately comparing the differences between cancer and non-cancer groups in terms of various outcome indicators. This study also has the following limitations: (1) no published randomized controlled trials were included, meaning the study is only included in the cohort study for analysis, which may cause certain bias; (2) the study does not carry out a cost-benefit analysis, such as hospital stay, hospitalization costs, etc., so we cannot clarify the related economic burden of TAVI and cancer treatment; (3) due to the limitations of the follow-up time included in the study, the study only analyzed the outcome

indexes in the early and medium-term by Meta, and failed to explore the longer-term prognosis of TAVI in patients with severe AS with cancer; and (4) data were collected in this meta-analysis without access to the preoperative ECG results.

CONCLUSION

In conclusion, it is effective and safe to apply TAVI to the treatment of severe AS in patients with cancer, but compared with patients without cancer, the long-term mortality rate is still higher. More large samples and multicenter studies are needed in the future.

DATA AVAILABILITY STATEMENT

The original contributions presented in the study are included in the article/supplementary material, further inquiries can be directed to the corresponding author.

AUTHOR CONTRIBUTIONS

YS provided the idea and drafted the manuscript. YW provided statistical expertise. ZW, CX, and JD contributed to the development of the selection criteria, and the risk of bias assessment strategy. TJ read, provided feedback, and approved the final manuscript. All authors contributed to the article and approved the submitted version.

REFERENCES

1. Iung B, Vahanian A. Epidemiology of Acquired Valvular Heart Disease. *Can J Cardiol.* (2014) 30:962–70. doi: 10.1016/j.cjca.2014.03.022
2. Leon MB, Smith CR, Mack M, Miller DC, Moses JW, Svensson LG, et al. Transcatheter aortic-valve implantation for aortic stenosis in patients who cannot undergo surgery. *J Surv Anesthesiol.* (2011) 55:112–13. doi: 10.1097/01.SA.0000396024.48515.95
3. Smith CR, Leon MB, Mack MJ, Miller DC, Moses JW, Svensson LG, et al. Transcatheter versus surgical aortic-valve replacement in high-risk patients. *N Engl J Med.* (2011) 364:2187–98. doi: 10.1056/NEJMoa1103510
4. Bekeredjian R, Krumsdorf U, Chorianopoulos E, Kallenbach K, Karck M, Katus HA, et al. Usefulness of percutaneous aortic valve implantation to improve quality of life in patients >80 years of age. *Am J Cardiol.* (2010) 106:1777–81. doi: 10.1016/j.amjcard.2010.08.017
5. Landes U, Iakobishvili Z, Vronsky D, Zusman O, Barsheshet A, Jaffe R, et al. Transcatheter aortic valve replacement in oncology patients with severe aortic stenosis. *JACC Cardiovasc Interv.* (2019) 12:78–86. doi: 10.1016/j.jcin.2018.10.026
6. Stang A. Critical evaluation of the Newcastle-Ottawa scale for the assessment of the quality of nonrandomized studies in meta-analyses. *Eur J Epidemiol.* (2010) 25:603–5. doi: 10.1007/s10654-010-9491-z
7. Berkovitch A, Guetta V, Barbash IM, Fink N, Regev E, Maor E, et al. Favorable Short-term and long-term outcomes among patients with prior history of malignancy undergoing transcatheter aortic valve implantation. *J Invasive Cardiol.* (2018) 30:105–09.
8. Biancari F, Dahlbacka S, Juvonen T, Virtanen MPO, Maaranen P, Jaakkola J, et al. Favorable outcome of patients with cancer undergoing transcatheter aortic valve replacement. *Int J Cardiol.* (2020) 315:86–9. doi: 10.1016/j.ijcard.2020.03.038
9. Grant JK, Vincent L, Ebner B, Maning J, Singh H, Olorunfemi O, et al. In-Hospital outcomes in patients with a history of malignancy undergoing transcatheter aortic valve implantation. *Am J Cardiol.* (2021) 142:109–15. doi: 10.1016/j.amjcard.2020.11.029
10. Guha A, Dey AK, Arora S, Cavender MA, Vavalle JP, Sabik JF III, et al. Contemporary trends and outcomes of percutaneous and surgical aortic valve replacement in patients with cancer. *J Am Heart Assoc.* (2020) 9:e014248. doi: 10.1161/JAHA.119.014248
11. Karaduman BD, Ayhan H, Keleş T, Bozkurt E. Clinical outcomes after transcatheter aortic valve implantation in active patients with cancer and cancer survivors. *Turk Gogus Kalp Damar Cerrahisi Derg.* (2021) 29:45–51. doi: 10.5606/tgkdc.dergisi.2021.20622
12. Lind A, Totzeck M, Mahabadi AA, Jánosi RA, El Gabry M, Ruhparwar A, et al. Impact of cancer in patients undergoing transcatheter aortic valve replacement: a single-center study. *JACC CardioOncol.* (2020) 2:735–43. doi: 10.1016/j.jaccao.2020.11.008
13. Mangner N, Woitek FJ, Haussig S, Holzhey D, Stachel G, Schlotter F, et al. Impact of active cancer disease on the outcome of patients undergoing transcatheter aortic valve replacement. *J Interv Cardiol.* (2018) 31:188–96. doi: 10.1111/joic.12458
14. Tabata N, Al-Kassou B, Sugiura A, Kandt J, Shamekhi J, Stundl A, et al. Prognostic impact of cancer history in patients undergoing transcatheter aortic valve implantation. *Clin Res Cardiol.* (2020) 109:1243–50. doi: 10.1007/s00392-020-01615-y
15. Tabata N, Al-Kassou B, Sugiura A, Shamekhi J, Treede H, Ishii M, et al. Predictive value of the platelet-to-lymphocyte ratio in patients with cancer undergoing transcatheter aortic valve replacement. *JACC CardioOncol.* (2019) 1:159–69. doi: 10.1016/j.jaccao.2019.10.004
16. Watanabe Y, Kozuma K, Hioki H, Kawashima H, Nara Y, Kataoka A, et al. Comparison of results of transcatheter aortic valve implantation in patients with versus without active cancer. *Am J Cardiol.* (2016) 118:572–7. doi: 10.1016/j.amjcard.2016.05.052
17. Zamorano JL, Lancellotti P, Munoz DR, Aboyans V, Asteggiano R, Galderisi M, et al. 2016 ESC Position Paper on cancer treatments and cardiovascular toxicity developed under the auspices of the ESC Committee for Practice Guidelines. *Kardiol Pol.* (2016) 74:1193–233. doi: 10.5603/KP.2016.0156
18. Cubeddu R, Jneid H, Don C, Witzke C, Cruz-Gonzalez I, Gupta R, et al. Retrograde versus antegrade percutaneous aortic balloon valvuloplasty: immediate, short- and long-term outcome at 2 years. *Catheter Cardiovasc Interv.* (2009) 74:225–31. doi: 10.1002/ccd.22085
19. Lieberman EB, Bashore TM, Hermiller JB, Wilson JS, Pieper KS, Keeler GP, et al. Balloon aortic valvuloplasty in adults: failure of procedure to improve long-term survival. *J Am Coll Cardiol.* (1995) 26:1522–8. doi: 10.1016/0735-1097(95)00363-0
20. Yusuf SW, Sarfaraz A, Durand JB, Swafford J, Daher IN. Management and outcomes of severe aortic stenosis in patients with cancer. *Am Heart J.* (2011) 161:1125–32. doi: 10.1016/j.ahj.2011.03.013
21. Samuels LE, Kaufman MS, Morris RJ, Styler M, Brockman SK. Open heart surgery in patients with chronic lymphocytic leukemia. *Leuk Res.* (1999) 23:71–5. doi: 10.1016/S0145-2126(98)00126-X
22. Chan J, Rosenfeldt F, Chaudhuri K, Marasco S. Cardiac surgery in patients with a history of malignancy: increased complication rate but similar mortality. *Heart Lung Circ.* (2012) 21:255–9. doi: 10.1016/j.hlc.2012.02.004
23. Van Mieghem NM, van der Boon RM, Nuis RJ, Schultz C, van Geuns RJ, Serruys PW, et al. Cause of death after transcatheter aortic valve implantation. *Catheter Cardiovasc Interv.* (2014) 83:E277–82. doi: 10.1002/ccd.24597
24. Kogoj P, Devjak R, Bunc M. Balloon aortic valvuloplasty (BAV) as a bridge to aortic valve replacement in patients with cancer who require urgent non-cardiac surgery. *Radiol Oncol.* (2014) 48:62–6. doi: 10.2478/raon-2013-0078
25. Nishimura RA, Otto CM, Bonow RO, Carabello BA, Erwin JP 3rd, Fleisher LA, et al. 2017 AHA/ACC Focused Update of the 2014 AHA/ACC Guideline for the Management of Patients With Valvular Heart Disease: A Report of the American College of Cardiology/American Heart Association Task

Force on Clinical Practice Guidelines. *J Am Coll Cardiol*. (2017) 70:252–89. doi: 10.1016/j.jacc.2017.03.011
26. Généreux P, Piazza N, Alu MC, Nazif T, Hahn RT, Pibarot P, et al. Valve Academic Research Consortium 3: updated endpoint definitions for aortic valve clinical research. *Eur Heart J*. (2021) 42:1825–57. doi: 10.1093/eurheartj/ehaa799
27. Nombela-Franco L, Webb JG, de Jaegere PP, Toggweiler S, Nuis RJ, Dager AE, et al. Timing, predictive factors, and prognostic value of cerebrovascular events in a large cohort of patients undergoing transcatheter aortic valve implantation. *Circulation*. (2012) 126:3041–53. doi: 10.1161/CIRCULATIONAHA.112.110981
28. Schmidt T, Leon MB, Mehran R, Kuck KH, Alu MC, Braumann RE, et al. Debris heterogeneity across different valve types captured by a cerebral protection system during transcatheter aortic valve replacement. *JACC Cardiovasc Interv*. (2018) 11:1262–73. doi: 10.1016/j.jcin.2018.03.001
29. Van Mieghem NM, El Faquir N, Rahhab Z, Rodríguez-Olivares R, Wilschut J, Ouhlous M, et al. Incidence and predictors of debris embolizing to the brain during transcatheter aortic valve implantation. *JACC Cardiovasc Interv*. (2015) 8:718–24. doi: 10.1016/j.jcin.2015.01.020
30. Ranasinghe MP, Peter K, McFadyen JD. Thromboembolic and bleeding complications in transcatheter aortic valve implantation: insights on mechanisms, prophylaxis and therapy. *J Clin Med*. (2019) 8:280. doi: 10.3390/jcm8020280
31. Vahanian A, Beyersdorf F, Praz F, Milojevic M, Baldus S, Bauersachs J, et al. 2021 ESC/EACTS Guidelines for the management of valvular heart disease. *Eur J Cardiothorac Surg*. (2021) 60:727–800. doi: 10.1093/ejcts/ezab389
32. Otto CM, Nishimura RA, Bonow RO, Carabello BA, Erwin JP 3rd, Gentile F, et al. 2020 ACC/AHA Guideline for the Management of Patients With Valvular Heart Disease: Executive Summary: A Report of the American College of Cardiology/American Heart Association Joint Committee on Clinical Practice Guidelines. *J Am Coll Cardiol*. (2021) 77:450–500. doi: 10.1016/j.jacc.2020.11.035
33. Ten Berg J, Sibbing D, Rocca B, Van Belle E, Chevalier B, Collet JP, et al. Management of antithrombotic therapy in patients undergoing transcatheter aortic valve implantation: a consensus document of the ESC Working Group on Thrombosis and the European Association of Percutaneous Cardiovascular Interventions (EAPCI), in collaboration with the ESC Council on Valvular Heart Disease. *Eur Heart J*. (2021) 42:2265–69. doi: 10.1093/eurheartj/ehab196
34. Rodés-Cabau J, Ellenbogen KA, Krahn AD, Latib A, Mack M, Mittal S, et al. Management of conduction disturbances associated with transcatheter aortic valve replacement: JACC scientific expert panel. *J Am Coll Cardiol*. (2019) 74:1086–106. doi: 10.1016/j.jacc.2019.07.014

Conflict of Interest: The authors declare that the research was conducted in the absence of any commercial or financial relationships that could be construed as a potential conflict of interest.

Publisher's Note: All claims expressed in this article are solely those of the authors and do not necessarily represent those of their affiliated organizations, or those of the publisher, the editors and the reviewers. Any product that may be evaluated in this article, or claim that may be made by its manufacturer, is not guaranteed or endorsed by the publisher.

frontiers | Frontiers in Cardiovascular Medicine

ORIGINAL RESEARCH
published: 06 June 2022
doi: 10.3389/fcvm.2022.878211

A Prospective Study to Detect Immune Checkpoint Inhibitors Associated With Myocarditis Among Patients Treated for Lung Cancer

Clara Faubry[1†], *Maxime Faure*[2†], *Anne-Claire Toublanc*[1], *Rémi Veillon*[1], *Anne-Iris Lemaître*[2], *Charlotte Vergnenègre*[1], *Hubert Cochet*[3,4,5], *Sadia Khan*[6], *Chantal Raherison*[1,6], *Pierre Dos Santos*[2,3,4] *and Maeva Zysman*[1,7*]

[1] *Pulmonary Department, Centre Hospitalier Universitaire (CHU) Haut-Lévèque, Bordeaux, France,* [2] *Heart Failure Unit, Cardiology Department, Centre Hospitalier Universitaire (CHU) Haut-Lévèque, Bordeaux, France,* [3] *Department Cardiology, Lyric Institute, Fondation Bordeaux Université, Bordeaux, France,* [4] *Department Medicine, Universitaire Bordeaux, Institut National de la Santé et de la Recherche Médicale (INSERM), Bordeaux, France,* [5] *Department of Cardiovascular Imaging, Centre Hospitalier Universitaire (CHU) Bordeaux, Bordeaux, France,* [6] *Bordeaux University, Institut National de la Santé et de la Recherche Médicale (INSERM), Bordeaux Population Health Research Center, Bordeaux, France,* [7] *Centre de Recherche Cardio-Thoracique, Universitaire Bordeaux, Institut National de la Santé et de la Recherche Médicale (INSERM), Bordeaux, France*

OPEN ACCESS

Edited by:
Chun Liu,
Stanford University, United States

Reviewed by:
Chiara Lestuzzi,
Santa Maria degli Angeli Hospital Pordenone, Italy
Concetta Zito,
University of Messina, Italy

***Correspondence:**
Maeva Zysman
maeva.zysman@chu-bordeaux.fr

[†] *These authors have contributed equally to this work*

Specialty section:
This article was submitted to Cardio-Oncology, a section of the journal Frontiers in Cardiovascular Medicine

Received: *17 February 2022*
Accepted: *25 April 2022*
Published: *06 June 2022*

Citation:
Faubry C, Faure M, Toublanc A-C, Veillon R, Lemaître A-I, Vergnenègre C, Cochet H, Khan S, Raherison C, Dos Santos P and Zysman M (2022) A Prospective Study to Detect Immune Checkpoint Inhibitors Associated With Myocarditis Among Patients Treated for Lung Cancer. Front. Cardiovasc. Med. 9:878211. doi: 10.3389/fcvm.2022.878211

Background: Immune checkpoint inhibitors (ICIs) are widely used in lung cancer management. However, myocarditis, which is a rare, yet potentially severe adverse-related event associated with ICIs, could be under-reported.

Objectives: This study is aimed to prospectively evaluate the cumulative incidence rate of myocarditis, through systematic screening, among patients receiving ICIs for lung cancer.

Methods: All patients who received the first administration of ICIs for non-small cell (NSCLC) and small cell lung cancer (SCLC), between May and November 2020, in the pulmonary department of Bordeaux University Hospital, were included. Echocardiography (ECG), troponin-I, and natriuretic peptide dosages before ICIs' first administration and before each infusion were recorded. ECG and magnetic resonance imaging (MRI) were done additionally, in case of at least three times increase in troponin levels, ECG modifications, and the onset of cardiovascular symptoms. Second, if possible, coronarography than endomyocardial biopsy was assessed. The primary outcome was defined as ICIs related to myocarditis onset, while secondary outcomes included other cardiovascular events, disease-free, and overall survival.

Results: During the period of interest, 99 patients received their first infusion of ICIs for lung cancer (mean age 64 ± 9 years; 52 men, 67% with adenocarcinoma). Three cases of myocarditis without major adverse cardiac events (MACEs) occurred (two definite and one possible), and the mean duration between the first ICIs' administration and myocarditis onset was 144 ± 3 days. Median disease-free survival and overall survival were 169 [102; 233] days and 209 [147; 249] days, respectively.

Conclusion: In our study, systematic screening of myocarditis associated with ICIs leads to a more frequent incidence and a later onset than previously reported. None of them

were severe. Additional prospective evidence is needed before we could adopt routine cardiac screening in unselected patients starting ICIs; however, these data shed new light on the risk of myocarditis associated with ICIs administration.

Keywords: myocarditis, screening, immune checkpoint inhibitors, lung cancer, early diagnosis

INTRODUCTION

Immune checkpoint inhibitors (ICIs) have substantially improved clinical outcomes in multiple cancer types, such as lung cancer (1). In France, there are currently four approved ICIs in lung cancer, which are as follows: nivolumab, pembrolizumab, (both anti-programmed death-1, PD-1), atezolizumab, and durvalumab (both anti-programmed death ligand-1, PD-L1). The indications for their use in lung cancer treatment continue to expand and are often considered the first-line therapy (2). Unfortunately, these agents may induce a wide spectrum of immune-related adverse events (irAEs) by enhancing immune responses in non-target organs (3), including the cardiovascular system. While myocarditis is considered uncommon toxicity of ICIs with incidence varying from 0.01 to 1% (2). However, it is likely that myocarditis is under-reported, owing to an absence of systematic monitoring and coding mechanisms for cardiac events in immunotherapy trials. Moreover, myocarditis related to ICIs has been described to have a fulminant course, with a fatality rate of 30–50% (2). A meta-analysis of the incidence of immune-related adverse effects in patients treated for advanced non-small cell lung cancer (NSCLC) identified that myocarditis affects 0.5% of the whole population (3). Additionally, myocarditis has been reported to be differentially associated with available ICIs. For example, a combination of pembrolizumab and ipilimumab has shown a higher reporting of myocarditis as compared to one ICI alone or in combination with chemotherapy (4, 5). Although, myocarditis can also occur with immunotherapy administered alone (6). IrAEs may occur secondary to the inhibition of immune checkpoints leading to local and systemic auto-immune responses (CD4+ and CD8+ T cells recruitment along with macrophages infiltrate), which attack myocytes and cardiac conduction tissue that cause myocarditis (7).

Until now, the reported median time of the onset of myocarditis from the first ICIs' infusion ranges from 34 [21; 75] to 65 [2; 454] days (8). Since cardiac monitoring (e.g., ECG or troponin) is not routinely performed, in most immunotherapy trials or clinical practice, the true incidence of myocarditis remains still unknown. The diagnosis of myocarditis can be based on appropriate investigations as recommended by the European Society of Cardiology Guidelines (9). Interestingly, the clinical presentation of myocarditis ranges on a spectrum of mild-to-severe diseases from an asymptomatic increment in cardiac biomarkers to severe decompensation with end-organ damage, as suggested by clinical practice guidelines for the management of irAEs (10). Therefore, the need for increasing awareness to suspect, diagnose, and treat ICI-related myocarditis is pivotal in lung cancer patients who receive ICI treatment.

Hence, the aim of this study was to prospectively evaluate (1) the incidence of myocarditis associated with ICIs administration and (2) the frequency of other major cardiovascular events, such as ischemic heart disease or heart failure, in stages IIIB–IV lung cancer patients.

Abbreviations: C-MRI, cardiac magnetic resonance imaging; ECG, electrocardiogram; ICIs, immune checkpoint inhibitors; irAEs, immune-related adverse event; TTE, trans-thoracic echocardiography; MACEs, major adverse cardiovascular events.

MATERIALS AND METHODS

Study Design

All adult patients who initiated ICI treatment for stages IIIB–IV lung cancer between 1 May 2020 and 1 November 2020, in the pulmonary department of Bordeaux University Hospital, were included. All participants provided informed written consent. All patients who did not receive the first administration of ICI were excluded.

Sample Size

The cumulative incidence rate of myocarditis associated with ICIs' administration varies from 0.01 to 1% (2). The hypothesis is that the event is under-reported. Based on previous work, we had anticipated a cumulative incidence rate of 2%. For an α-error of 5% and a β-error of 10%, the number of patients required was 92. In order to take into account missing data or withdrawals of consent, a total of 98 patients needed to be included.

Ethical Approval and Consent to Participate

The study protocol was approved by the Ethics Committee of CHU Bordeaux (France) and registered with the following number CHUBX2020RE0275. This work complies with the protection of personal health data and the protection of privacy with the framework of application provided by article 65-2 of the amended Data Protection Act and the general data protection regulations. All subjects provided informed written consent. All authors provided consent to publication.

Data Collected

The following data were collected: demographic characteristics, smoking history, pre-existing cardiovascular diseases (coronary artery disease, arrhythmia, conduction abnormalities, and heart failure), lung cancer type [NSCLC and small lung cancer (SCLC)], grading [stages IIIB and IV, according to the 7th American Joint Comission on Cancer Tumor Node Metastasis (AJCC TNM) classification], ICI regimens, a combination of ICIs and chemotherapy, number of lines, pre-existing auto-immune diseases, and other immune side effects during treatment. We used The Strengthening the Reporting of Observational studies

in Epidemiology (STROBE) reporting guidelines in our study (**Supplementary Data 1**).

Myocarditis Suspicion

Baseline troponin and natriuretic peptide levels, ECG, and transthoracic echocardiography (TTE) were performed before the first ICI infusion to evaluate possible changes from baseline, e.g., changes in left ventricular ejection fraction (LVEF), diastolic function, new wall motion abnormalities, or pericardial effusion. Prior to ICI's administration, levels of biomarkers (troponin-I and natriuretic peptide) and ECG measurements were undertaken. Possible myocarditis was suspected, in case of any 1 of the following adverse events: new cardiovascular symptoms or at least 3 times increase in the levels of biomarkers beyond the level prior to ICI's administration, or any of the following ECG changes: new prolongation of the PR interval, atrioventricular block, ventricular arrhythmias, frequent premature ventricular complexes, ST depression, or diffuse T-wave inversions.

In the presence of an adverse event, additional scans were performed, which are as follows: TTE, cardiac magnetic resonance imaging (C-MRI), and coronarography. C-MRI was assessed with T2-weighted imaging, late gadolinium enhancement (LGE), extracellular volume fraction, and T1 and T2 mapping.

For the C-MRI diagnosis of myocarditis, the Lake Louise Criteria were used in our study, which states that if (2, 11) both myocardial edema and non-ischemic myocardial injury are identified on the C-MRI, it is highly suggestive of myocarditis.

Myocarditis Diagnosis

Any one of the following criteria is used to diagnose myocarditis in a clinical setting, the presence of two major criteria having the best diagnostic value:

a. Myocardial edema: Indicated by abnormal findings in T2 mapping or T2-weighted images.
b. Non-ischemic myocardial injury: Ascertained by abnormal findings on T1 mapping, LGE, or extracellular volume fraction.

Additional supportive criteria (below) can be suggestive of myocarditis, however, in the absence of the aforementioned two criteria, they cannot be considered definitively diagnostic of myocarditis.

a. Pericarditis: Indicated by either pericardial effusion or abnormal late gadolinium enhancement/T2 or T1 findings in the pericardium.
b. Left ventricular systolic dysfunction: Indicated by regional or global wall motion abnormalities.

Coronary angiography was performed to rule out significant coronary artery disease. Then, endomyocardial biopsies were performed when possible and guided according to C-MRI abnormalities. The myocardial tissue was evaluated using the histological Dallas criteria, which require two main components: inflammatory infiltrate and myocardial necrosis (12). If myocarditis was suspected, it was categorized as definite/probable/possible per consensus-based definition (13). Finally, treatments for myocarditis were decided according to international recommendations (2).

Statistical Analysis

Data are provided as mean or *n* (%), as appropriate. A value of $p \leq 0.05$ was considered statistically significant. All analyses were performed using Graph Pad Prism® statistical software.

RESULTS

Between 1 May 2020 and 1 November 2020, 99 patients (52% men, mean age: 64 ± 9 years) received the first administration of ICIs (**Figure 1**). In total, 38% of patients had pre-existing cardiovascular diseases and 15% suffered from pre-existing systolic or diastolic dysfunction. In addition, 6% of patients had positive troponin before starting treatment among whom, two patients had pre-existing stable ischemic heart disease and 1 presented tight aortic stenosis. The majority of the patients (66%) had adenocarcinoma (**Table 1**) and 67% were being treated with a combination of ICIs and chemotherapy, while 61% received first-line treatment. In total, 72% of patients received Pembrolizumab (**Table 2**).

Myocarditis was diagnosed in three patients during the 6-month follow-up (two definite and one possible, **Table 3**), indicating a cumulative incidence rate of 3%. All of them were asymptomatic. Troponin serum increment was seen for all three patients: 75.0 ng/l in the first case, 20.8 ng/l in the second case, and 202.0 ng/l in the third case. None of them had elevated troponin levels prior to ICIs. The mean duration between the first ICI administration and the onset of myocarditis was 144 ± 3 days (147 days for the first and the second cases; 141 days for the third case). Grade 1 skin toxicity (irAE) was seen between the first and second infusions for one patient with myocarditis (patient 2); however, no pre-existing auto-immune disease was previously reported (**Table 3**). No ECG abnormalities were seen, and TTE revealed preserved LVEF for all patients. We were able to distinguish myocarditis from myocardial ischemia or myocardial infarction with early systematic coronary angiography.

The first patient had an asymptomatic elevation of cardiac biomarkers. C-MRI showed myocardial edema in T2 mapping and LGE in a non-coronary distribution (**Figure 2**). Endomyocardial biopsies were performed according to C-MRI abnormalities and found non-specific edema. This patient was classified as having definite myocarditis because of increased cardiac biomarkers, positive C-MRI, and negative coronary angiography (13). The second patient was classified as possible myocarditis because of asymptomatic elevation of cardiac biomarkers, with negative C-MRI and angiography for coronary artery disease (13). In addition, the third case was classified as having definite myocarditis because of asymptomatic elevation of cardiac biomarkers, positive C-MRI but negative angiography for coronary artery disease (**Table 3**) (13).

All three patients received corticosteroids as recommended (10, 14, 15), intravenous methylprednisolone, at a dosage of 1 mg/kg/day for the first patient, and oral prednisone, at a dosage

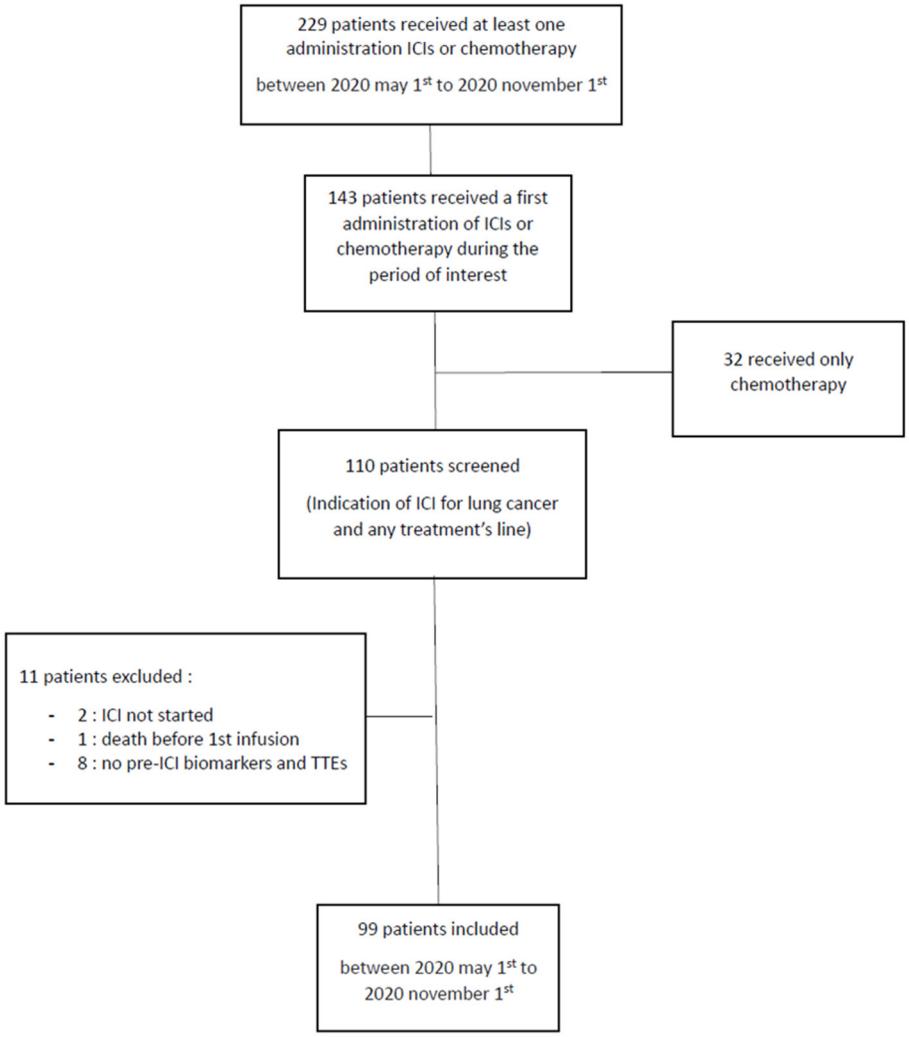

FIGURE 1 | Flow chart. ICI, immune checkpoint inhibitors; TTE, transthoracic echocardiogram.

of 1 mg/kg/day, with no additional immunosuppressant drugs for the remaining patients. The treatments administered were in line with the American Society of Clinical Oncology (ASCO) clinical practice guidelines for irAEs, and troponin monitoring was also done (10). All three patients had mild myocarditis and recovered without complications. No major adverse cardiac events (MACEs), e.g., cardiovascular death, cardiac arrest, cardiogenic shock, and hemodynamically significant complete heart block requiring a pacemaker, were noted.

Considering the non-severe presentation and the absence of alternative choice, ICIs rechallenge was performed in the first and second cases, after the normalization of troponin level. In the first case, nivolumab was administered 124 days after myocarditis and continued due to the absence of a recurrence. In the second case, pembrolizumab was re-administrated, 71 days after myocarditis and recurrence occurred 42 days (three infusions) after rechallenge. The recurrence was detected by ECG changes (*de novo* left ventricular block) and serum troponin increment, while C-MRI was normal. An endomyocardial biopsy was not performed because of a negative benefit-risk balance. Diagnosis of myocarditis was retained in view of ECG normalization under corticosteroid. No rechallenge was performed for the third patient.

After a 6-month follow-up, median disease-free survival and overall survival were 169 [102; 233] and 209 [147; 249] days, respectively. Mortality did not increase among patients with myocarditis at the end of follow-up ($p = 0.29$; not shown).

For one patient, due to the increased serum troponin levels, coronary angiography was performed and it confirmed an underlying coronary artery disease, which was treated with angioplasty. The patient had not previously reported pre-existing cardiovascular disease; however, several cardiovascular risk factors (current smoking, age >50 years) were noted. Finally, systematic TTE before ICIs' first administration allowed us to detect eight cases of unknown systolic or diastolic dysfunction, of which only one had LVEF between 40 and 50%, leading to

TABLE 1 | Patients' characteristics at inclusion.

	Patients' characteristics	Whole cohort *N* = 99 (%)
General		
	Mean age (years)	64
	Male gender	51 (52%)
Risk factor	Smoking	
	No	10 (10%)
	Cessation >3years	40 (40%)
	Current	49 (49%)
	Preexisting cardiovascular diseases	
	Coronary artery disease	14 (14%)
	Other artery disease	11 (11%)
	Arrhythmia/Conduction abnormality	13 (13%)
	Heart failure	
	LVEF <40%	1 (1%)
	LVEF 40–50%	6(6%)
	LVEF >50%	8(8%)
	Cardiovascular risk factors	
	Age (male >50 years; female >60 years)	80 (81%)
	Diabetes mellitus	19 (19%)
	Dyslipidaemia	32 (32%)
	Hypertension	18 (18%)
Primary cancer type	Adenocarcinoma	65 (66%)
	Squamous cell carcinoma	17 (17%)
	Small cell lung cancer	12 (12%)
	Others	5 (5%)
Pre-ICI biomarkers	Positive serum troponin before ICI	6 (6%)
	Troponin (ng/l)	13+/−21$^{\mu}$
	BNP (pg/ml)	44+/−41$^{\pi}$
	NT-pro-BNP (pg/ml)	341+/−448$^{\Omega}$
	CPK (UI/l)	64+/−55†
Pre-ICI ECG	*PR (ms)*	153+/−27‡
	QRS (ms)	94+/−21$^{\text{Þ}}$
Pre-ICI TTE	*LVEG (%)*	61%+/−6.5%$^{\overline{\text{T}}}$
	Strain (%)	−18%+/−3.1%$^{\prime\prime}$
	S'VD (cm/s)	13.6+/−2.66$^{\omega}$

Missing data : $\mu = 8$ *(8%),* $\pi = 25$ *(25%),* $^{\dagger} = 14$ *(14%),* $^{\ddagger} = 11$ *(11%),* $^{\text{Þ}} = 9$ *(9%),* $^{\overline{\text{T}}} = 2$ *(2%),* $^{\prime\prime} = 39$ *(39%),* $^{\omega} = 14$ *(14%)Patients concerned :* $\Omega = 15$ *(15%).*
ECG, electrocardiogram; ICI, Immune checkpoint inhibitors; TTE, Transthoracic echocardiogram; LVEG, Left ventricular ejection fraction.
Data were expressed as mean +/- standard deviation, as appropriate.

TABLE 2 | Patients' follow-up.

		Whole cohort *N* = 99(%)
ICI regimens	Pembrolizumab	71 (72%)
	Nivolumab	7 (7%)
	Atezolizumab	8 (8%)
	Durvalumab	11 (11%)
	Other	2 (2%)
Single agent or combined	Monotherapy	33 (33%)
	Combinaison	66 (67%)
Line of treatment	1st line	60 (61%)
	2nd line	33 (33%)
	≥3rd line	6 (6%)
Myocarditis		3 (3%)
Follow-up	Median follow-up (days)	209 [147 ; 249]
	Mortality rate	28 (28%)

ICI, Immune checkpoint inhibitors.

a specific treatment; while the remaining seven had diastolic heart failure. Additionally, concerning the five patients with positive troponin before starting treatment, two patients had known stable ischemic heart disease and one patient had severe unknown aortic stenosis without surgical indication. The two last patients had a spontaneous normalization of troponin levels.

DISCUSSION

In our prospective, hospital-based real-life cohort study, the screening of myocarditis was systematically assessed in 99 patients with lung cancer (stages IIIB–IV), receiving ICIs treatment. A 3% cumulative incidence rate of myocarditis was seen during a 6-month follow-up. All cases of myocarditis were mild and without MACEs. No increase in mortality was observed among patients with myocarditis. Finally, myocarditis occurred later than described in previous studies, i.e., the mean time of the onset between the first ICIs' administration and myocarditis was 144 ± 3 days.

No specific clinical characteristics were identified with myocarditis onset; the three cases were different, in terms of histological cancer type, ICIs regimens, combination regimen, and line number. None of the cases had an underlying auto-immune disease. The first case had a history of coronary artery disease without heart failure and the second had a history of valve disease, without associated heart failure.

In addition, the incidence of myocarditis (3%) was higher than previously reported, range of 0.06–1.14% (2), which could perhaps be explained by the rigorous systematic monitoring and subsequent early detection of myocarditis. Systematic monitoring to detect myocarditis is not routinely performed in patients receiving ICI; which might lead to its under-reporting. While the incidence of myocarditis was high (3%); however, the cases were mild and did not affect mortality. This finding was contrary to the previous reporting of a fatality rate of 30–50%, associated with myocarditis due to ICIs treatment (2). The lack of myocarditis-related mortality in our study could perhaps be due to the compliance of the patients with monotherapy, e.g., a large safety database suggests that myocarditis occurs more frequently and severely with the combination of ipilimumab and nivolumab when compared to monotherapy (5). Another hypothesis could be that systematic screening leads to earlier detection of myocarditis.

TABLE 3 | Description of myocarditis cases.

	1st patient	2nd patient	3rd patient
Primary cancer type	Squamous cell carcinoma	Adenocarcinoma	Small cell lung cancer
ICI regimens	Atezolizumab	Pembrolizumab	Atezolizumab
Single agent or combined	Monotherapy	Combinaison	Combinaison
Line of treatment	2nd line	1st line	1st line
Pre-existing auto-immune diseases	No	No	No
Other immune side effects during treatment	No	Dermatitis (grade I)	no
Time from first administration to myocarditis (days)	147	147	141
Biomarkers			
Serum troponin (ng/l) standard <15,6 (ng/l)	75	20,8	202
BNP (pg/ml)	13	21	45
CPK (UI/l)	38	57	33
ECG			
Sinus rythm	Yes	Yes	Yes
PR (ms)	160	178	160
QRS (ms)	100	96	80
TTE			
LVEF(%)	53	61	65
Strain(%)	−19.5	Not performed	Not performed
S'VD (cm/s)	11.5	Not performed	Not performed
Cardiac-MRI			
Edema by T2	Yes	No	Yes
Late Gadolinium enhancement	Yes	No	Yes
Coronary angiography	negative	Negative	Negative
Endomyocardial biopsy	Non specific edema	Not performed	Not performed
Final diagnosis	Definite myocarditis	Possible myocarditis	Definite myocarditis
ICI rechallenge			
Yes/no	yes	Yes	No
ICI regimen	Nivolumab	Pembrolizumab	-
Time to rechallenge (in days)	124	71	-
Recurrence yes/no	No	Yes	-

ECG, electrocardiogram; ICI, Immune checkpoint inhibitors; TTE, Transthoracic echocardiogram; LVEG, Left ventricular ejection fraction; Cardiac-MRI, Cardiac Magnetic Resonance Imaging.

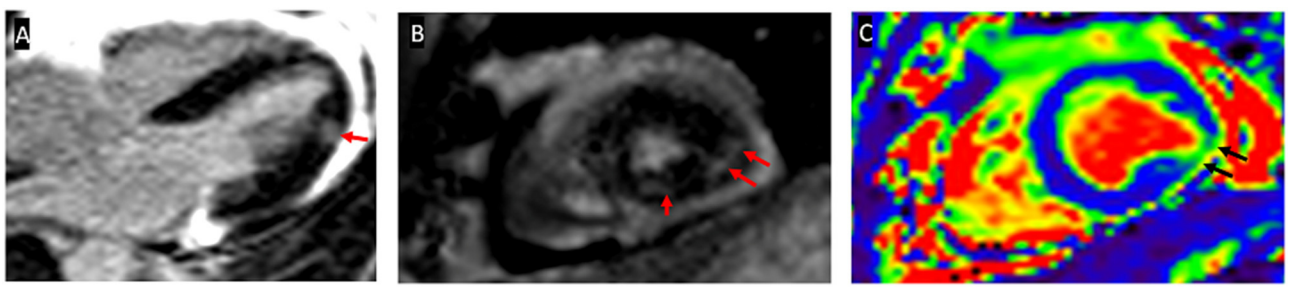

FIGURE 2 | Cardiac magnetic resonance imaging (C-MRI) imaging illustration of patient 1. **(A)** 4 cavity sections with a late enhancement of gadolinium and **(B)** transversal section showing infero-latero-medial mesomyocardic contrast (red arrows). **(C)** T2 mapping showing focal infero-latero-medial myocardial edema (black arrows).

This in turn allowed a prompt withdrawal of ICIs and initiation of corticosteroid treatment (intra-venous or oral) to avoid a fulminant course (16). Moreover, myocarditis had a later onset than previously observed in other studies (8, 16), which further underscores the need for prompt and rigorous systematic detection.

We also noticed a trend of better survival among patients who had myocarditis, suggesting a strong immune response. These

results correspond to the findings in the meta-analysis from Hussaini et al. (17) which state that immunotherapy has better efficacy in patients who developed irAEs in different cancers, such as lung cancer.

Besides, after troponin normalization under corticosteroid therapy and in the absence of therapeutic alternatives, rechallenge (8, 10) was considered in the first two cases, with a recurrence of mild myocarditis for the second case, but not for the first one.

Interestingly, all myocarditis presented a normal LVEF in TTEs. C-MRI was normal for one of the cases, and an endomyocardial biopsy was performed only once. Normal results are frequently seen in the early phase of the disease (7), with normal C-MRI being reported in almost 70% of patients (2). In conclusion, ICI-related myocarditis is a complex disease that bears resemblance to many other acute cardiac syndromes. Its diagnosis is difficult as it is based on a combination of different non-pathognomonic parameters, such as biomarkers (troponin, natriuretic, peptides), imaging (ECG, TTE, and C-MRI), and procedures (endomyocardial biopsy and coronary angiography). However, given the high incidence (3%) observed in this study, it is recommended to perform systemic screenings until more definitive data become available (18). C-MRI and endomyocardial biopsies are not available in all medical centers and due to their invasive nature might be unsuitable for asymptomatic patients. Our study indicates that while TTE does not help in the early diagnosis of myocarditis, it is relevant for screening other cardiovascular events. In fact, pre-therapeutic TTE detected 8 cases of heart failure and 3 cases of valve diseases. Of note, even if the first manifestations of myocarditis can be serious cardiac complications, e.g., ventricular arrhythmias and atrioventricular block, the LVEF is often preserved (5, 8, 16). For example, in a study by Mahmood et al. (18) 51% of patients with ICIs associated with myocarditis had a normal LVEF. In addition, in 38% of myocarditis patients, a normal LVEF was seen despite the development of MACEs.

Finally, smokers are at risk of lung cancer and atherosclerosis (19) making them a particularly vulnerable population for MACEs. In a large study, 66% of patients with cancer (n = 60,676) also presented with an acute coronary syndrome; and the most prevalent cancers were lymphoma (19%) and lung cancer (18.3%) (20). Contrastingly, in a more specific study by van-Herk-Sukel et al. (21) patients with lung cancer (N = 3,717) did not show a higher risk of developing myocardial infarction when compared with cancer-free controls. In our study, only 1 patient with cardiovascular risk factors had an elevation of troponin level linked to coronary artery disease and died a few months after diagnosis. However, cardiovascular co-morbidities (heart failure, myocardial infarction, and cardiac arrhythmias), which have been seen with low survival, in a study of 95,167 lung cancer patients, must be detected as earliest as possible (22).

Strengths and Clinical Perspectives

To our knowledge, this is the largest published prospective study of ICI-associated myocarditis among patients with lung cancer. While no specific clinical characteristics were identified with myocarditis onset, our study does outline the advantages of using an early and sustained systematic screening strategy for detecting myocarditis, when treating lung cancer patients with ICIs. The rigorous screening allowed for the early diagnosis and management of three cases of mild myocarditis and by extension could lead to a reduction in mortality.

Study Limitations

This study has several important limitations, such as the small number of patients; therefore, we could not compare overall survival and progression-free survival depending on myocarditis occurrence. Our study was also monocentric with a possible center effect, in particular, for C-MRI and endomyocardial biopsy access. While the probability of an over-diagnosis should be considered with any screening test; however, in our study there was only 1 troponin increment (leading to angioplasty).

CONCLUSION

This study outlines the usefulness of early monitoring for myocarditis in patients with lung cancer being treated with ICIs. Early monitoring is especially helpful in cases with non-specific symptoms and would help in decreasing the risk of fulminant progression of myocarditis. However, larger patient cohorts will be needed to estimate the true incidence of clinically meaningful immune-related cardiac events/myocarditis and importantly evaluate potential predictors to define higher-risk subgroups and refine screening and management strategies. Although improved detection and management of immune-related cardiovascular events are important, additional prospective evidence is needed before we can adopt routine cardiac screening in unselected patients starting ICI therapy.

DATA AVAILABILITY STATEMENT

The raw data supporting the conclusions of this article will be made available by the authors, without undue reservation.

ETHICS STATEMENT

The studies involving human participants were reviewed and approved by Ethics Committee of CHU Bordeaux (France) CHUBX2020RE0275. The patients/participants provided their written informed consent to participate in this study.

AUTHOR CONTRIBUTIONS

CF, MF, A-CT, RV, A-IL, CV, HC, SK, CR, PD, and MZ made substantial contributions to the conception and design, acquisition of data, analysis and interpretation of data, and involved in drafting the manuscript or revising it critically for important intellectual content and have given final approval of the version to be published. All authors contributed to the article and approved the submitted version.

ACKNOWLEDGMENTS

The authors thank coordination nurses of the thoracic oncology department, Irene Diouf, Sophie Estebam-Bisset, and Celine Lacave.

SUPPLEMENTARY MATERIAL

The Supplementary Material for this article can be found online at: https://www.frontiersin.org/articles/10.3389/fcvm.2022.878211/full#supplementary-material

REFERENCES

1. Salem JE, Manouchehri A, Moey M, Lebrun-Vignes B, Bastarache L, Pariente A, et al. Cardiovascular toxicities associated with immune checkpoint inhibitors: an observational, retrospective, pharmacovigilance study. *Lancet Oncol.* (2018) 19:1579–579:1579–89. doi: 10.1016/S1470-2045(18)30608-9
2. Zhang L, Awadalla M, Mahmood SS, Nohria A, Hassan MZO, Thuny F, et al. Cardiovascular magnetic resonance in immune checkpoint inhibitor-associated myocarditis. *EurHeart J 7 mai.* (2020) 41:1733–43. doi: 10.1093/eurheartj/ehaa051
3. Hu Y-B, Zhang Q, Li H-J, Michot JM, Liu H-B, Zhan P, et al. Evaluation of rare but severe immune related adverse effects in PD-1 and PD-L1 inhibitors in non-small cell lung cancer: a meta-analysis. *Transl Lung Cancer Res dLu.* (2017) 6:S8–20. doi: 10.21037/tlcr.2017.12.10
4. Fan Q, Hu Y, Yang C, Zhao B. Myocarditis following the use of different immune checkpoint inhibitor regimens: a real-world analysis of post-marketing surveillance data. *Int Immunopharmacol.* (2019) 76:105866. doi: 10.1016/j.intimp.2019.105866
5. Johnson DB, Balko JM, Compton ML, Chalkias S, Gorham J, Xu Y, et al. Fulminant myocarditis with combination immune checkpoint blockade. *N Engl J Med.* (2016) 375:1749–55. doi: 10.1056/NEJMoa1609214
6. Moslehi JJ, Salem J-E, Sosman JA, Lebrun-Vignes B, Johnson DB. Increased reporting of fatal immune checkpoint inhibitor-associated myocarditis. *The Lancet.* (2018) 391:933. doi: 10.1016/S0140-6736(18)30533-6
7. Thuny F, Alexandre J, Salem J-E, Mirabel M, Dolladille C, Cohen-Solal A, et al. Management of immune checkpoint inhibitor–induced myocarditis. *JACC CardioOncol.* (2021) 3:157–61. doi: 10.1016/j.jaccao.2020.12.001
8. Escudier M, Cautela J, Malissen N, Ancedy Y, Orabona M, Pinto J, et al. Clinical features, management, and outcomes of immune checkpoint inhibitor–related cardiotoxicity. *Circulation.* (2017) 136:2085–7. doi: 10.1161/CIRCULATIONAHA.117.030571
9. Caforio ALP, Marcolongo R, Jahns R, Fu M, Felix SB, Iliceto S. Immune-mediated and autoimmune myocarditis: clinical presentation, diagnosis and management. *Heart Fail Rev 1 nov.* (2013) 18:715–32. doi: 10.1007/s10741-012-9364-5
10. Brahmer JR, Lacchetti C, Schneider BJ, Atkins MB, Brassil KJ, Caterino JM, et al. Management of immune-related adverse events in patients treated with immune checkpoint inhibitor therapy: american society of clinical oncology clinical practice guideline. *J Clin Oncol Off J Am Soc Clin Oncol 10 juin.* (2018) 36:1714–68. doi: 10.1200/JCO.2017.77.6385
11. Ferreira VM, Schulz-Menger J, Holmvang G, Kramer CM, Carbone I, Sechtem U, et al. Cardiovascular magnetic resonance in non-ischemic myocardial inflammation. *J Am Coll Cardiol 18 d18.* (2018) 72:3158–76. doi: 10.1016/j.jacc.2018.09.072
12. Thomas Aretz H. Myocarditis: the Dallas criteria. *Hum Pathol 1 juin.* (1987) 18:619–24. doi: 10.1016/S0046-8177(87)80363-5
13. Bonaca MP, Olenchock BA, Salem JE, Wiviott SD, Ederhy S, Cohen A, et al. Myocarditis in the setting of cancer therapeutics. *Circulation.* (2019) 140:80–91. doi: 10.1161/CIRCULATIONAHA.118.034497
14. Zhang Lili, Zlotoff Daniel A, AwadallaMagid, Nohria Anju, Mahmood Syed S, Hassan Malek, et al. Major adverse cardiac events and the timing and dose of corticosteroids in immune checkpoint inhibitor-associated myocarditis. *Circulation.* (2019) 140(Suppl_1):A14733. doi: 10.1161/CIRCULATIONAHA.119.044703
15. Ball S, Ghosh RK, Wongsaengsak S, Bandyopadhyay D, Ghosh GC, Aronow WS, et al. Cardiovascular toxicities of immune checkpoint inhibitors. *J Am Coll Cardiol.* (2019) 74:1714–27. doi: 10.1016/j.jacc.2019.07.079
16. Mahmood SS, Fradley MG, Cohen JV, Nohria A, Reynolds KL, Heinzerling LM, et al. Myocarditis in patients treated with immune checkpoint inhibitors. *J Am Coll Cardiol.* (2018) 71:1755–64. doi: 10.1016/S0735-1097(18)31240-3
17. Hussaini S, Chehade R, Boldt RG, Raphael J, Blanchette P, MalekiVareki S, et al. Association between immune-related side effects and efficacy and benefit of immune checkpoint inhibitors - A systematic review and meta-analysis. *Cancer Treat Rev.* (2021) 92:102134. doi: 10.1016/j.ctrv.2020.102134
18. Palaskas N, Lopez-Mattei J, Durand JB, Iliescu C, Deswal A. Immune checkpoint inhibitor myocarditis: pathophysiological characteristics, diagnosis, and treatment. *J Am Heart Assoc.* (2020) 9:e013757. doi: 10.1161/JAHA.119.013757
19. Ravenel JG, Nance JW. Coronary artery calcification in lung cancer screening. *Transl Lung Cancer Res juin.* (2018) 7:361–7. doi: 10.21037/tlcr.2018.05.05
20. Mrotzek SM, Lena A, Hadzibegovic S, Ludwig R, Al-Rashid F, Mahabadi AA, et al. Assessment of coronary artery disease during hospitalization for cancer treatment. *Clin Res Cardiol.* (2021) 110:200–10. doi: 10.1007/s00392-020-01719-5
21. van Herk-Sukel MPP, Shantakumar S. Penning-van Beest FJA, Kamphuisen PW, Majoor CJ, Overbeek LIH, et al. Pulmonary embolism, myocardial infarction, and ischemic stroke in lung cancer patients: results from a longitudinal study. *Lung.* (2013) 191:501–9. doi: 10.1007/s00408-013-9485-1
22. Kravchenko J, Berry M, Arbeev K, Lyerly HK, Yashin A, Akushevich I. Cardiovascular comorbidities and survival of lung cancer patients: medicare data based analysis. *Lung Cancer.* (2015) 88:85–93. doi: 10.1016/j.lungcan.2015.01.006

Conflict of Interest: The authors declare that the research was conducted in the absence of any commercial or financial relationships that could be construed as a potential conflict of interest.

Publisher's Note: All claims expressed in this article are solely those of the authors and do not necessarily represent those of their affiliated organizations, or those of the publisher, the editors and the reviewers. Any product that may be evaluated in this article, or claim that may be made by its manufacturer, is not guaranteed or endorsed by the publisher.

frontiers | Frontiers in Cardiovascular Medicine

ORIGINAL RESEARCH
published: 16 June 2022
doi: 10.3389/fcvm.2022.851833

Cardiovascular Outcomes in the Patients With Colorectal Cancer: A Multi-Registry-Based Cohort Study of 197,699 Cases in the Real World

*Shilong Zhang[1], Yan Wang[1], Pengfei Zhang[1], Luoyan Ai[1] and Tianshu Liu[1,2]**

[1] Department of Medical Oncology, Zhongshan Hospital, Fudan University, Shanghai, China, [2] Centre for Evidence-Based Medicine, Fudan University, Shanghai, China

Purpose: We aimed to investigate the mortality patterns and quantitatively assess the risks of cardiovascular death (CVD) in patients with colorectal cancer (CRC). We also established a competing-risk model to predict the probability of CVD for patients with CRC.

Patients and Methods: Patients with CRC who diagnosed between 2007 and 2015 in the Surveillance, Epidemiology, and End Results (SEER) database were included in the present study. The cumulative incidence function (CIF) was used for CVD and other causes of death, and Gray's test was used to determine the subgroup difference in CIF. The Fine-Gray proportional subdistribution hazards model was used for identifying independent risk factors for CVD. A novel competing-risk model was established to evaluate the probability of CVD for patients with CRC. The performance of the nomogram was measured by concordance index (C-index), calibration curve, decision curve analysis (DCA), and risk stratification.

Results: After a median follow-up of 37.00 months, 79,455 deaths occurred, of whom 56,185 (70.71%) succumbed to CRC and 23,270 (29.29%) patients died due to non-CRC, among which CVD accounted for 9,702 (41.69%), being the major cause of non-cancer deaths. The 1-, 3-, and 5-year cumulative rates for CVD were 12.20, 24.25, and 30.51%, respectively. In multivariate analysis, age, race, marital status, tumor size, tumor stage, advanced stage, surgery, and chemotherapy were independent risk factors of CVD among patients with CRC. The nomogram was well calibrated and had good discriminative ability, with a c-index of 0.719 (95% CI, 0.738–0.742) in the training cohort and 0.719 (95% CI, 0.622–0.668) in the validation cohort. DCA demonstrated that nomogram produced more benefit within wide ranges of threshold probabilities for 1-, 3-, and 5-year CVD, respectively.

Conclusion: This study was the first to analyze the CIF and risk factors for CVD among CRC based on a competing-risk model. We have also built the first 1-, 3-, and 5-year competing nomogram for predicting CVD. This nomogram had excellent performance and could help clinicians to provide individualized management in clinical practice.

Keywords: SEER database, cardiovascular death, competing-risk model, nomogram, cause-specific death, colorectal cancer

OPEN ACCESS

Edited by:
Nazish Sayed,
Stanford University, United States

Reviewed by:
Qingan Jia,
Northwestern Polytechnical University, China
Zejuan Liu,
Capital Medical University, China
Xin Wang,
Shanghai Xuhui Central Hospital, China

***Correspondence:**
Tianshu Liu
liu.tianshu@zs-hospital.sh.cn

Specialty section:
This article was submitted to Cardio-Oncology, a section of the journal Frontiers in Cardiovascular Medicine

Received: *10 January 2022*
Accepted: *17 March 2022*
Published: *16 June 2022*

Citation:
Zhang S, Wang Y, Zhang P, Ai L and Liu T (2022) Cardiovascular Outcomes in the Patients With Colorectal Cancer: A Multi-Registry-Based Cohort Study of 197,699 Cases in the Real World. Front. Cardiovasc. Med. 9:851833. doi: 10.3389/fcvm.2022.851833

INTRODUCTION

Colorectal cancer (CRC), a common gastrointestinal cancer, is ranked as one of the three most common cancers worldwide, with 1,147,950 new cases and 53,200 deaths estimated in 2020 (1). The life expectancy of patients with CRC has considerably improved due to early diagnosis and treatment (2, 3). Therebefore, increasing mortality burden is not derived from cancer but from non-cancer causes. However, the political risk of non-cancer mortality is an objective existence, but it hasn't caused plenty of attention in academia.

In the past decade, cardiovascular death (CVD) has been regarded as one of the most common late complications of cancer therapy (4, 5). Indeed, the introduction of novel chemotherapeutic or immunotherapeutic drugs has brought considerable survival benefits for patients with advanced tumors (6). Unfortunately, these agents can cause a series of adverse events in clinical practice (7–10), mostly due to the induced overactivation of immunity or even direct killing of non-target organs, including the heart (11, 12). Therefore, it is an emerging issue that warrants increased awareness and investigation by cardiologists, oncologists, and immunologists.

Despite multiple studies showing how chemotherapeutic and immunotherapeutic drugs may contribute to the increased risk of CVD among cancer survivors, studies that focus on the cardiovascular outcomes in patients with CRC remain scarce. A prior descriptive analysis of Surveillance, Epidemiology, and End Results (SEER) data reported that patients with CRC were associated with an increased risk of CVD within 1 year of diagnosis. Although this analysis highlights the frequency of CVD among CRC survivors (13), it has mainly focused on CVD using the standard Cox proportional hazards regression approach. This conventional method might lead to unreliable results when competing events are present (14). Competing risks usually exist in the field of medicine, which may sway the occurrence of endpoint events. In addition, they would become particularly critical in terms of the elderly population or long prognosis (15). Thus, competing risks is certainly worth taking into consideration when investigating the CVD of patients with CRC, which would give a clearer picture of CVD risks that these patients would confront.

In the present study, we aimed to perform a population-based analysis of a cohort of patients with CRC between 2007 and 2015 in the SEER database to identify the risk factors for CVD among patients with CRC, including those within different subgroups. Since competitive events exist when analyzing CVD through Cox regression model (16), we used a competitive risk model when working for this type of data and objective of study. We comprehensively assessed the risks of CVD among more than 42,000 patients with CRC. Based on these results, we built and internally validated a competing-risk model to evaluate the probabilities of CVD for patients with CRC. Our findings can help clinicians adopt accurate risk stratification, weigh the advantages and disadvantages of therapies, and help with the cure of disease,

TABLE 1 | Demographic and clinicopathological characteristics of the included CRC patients.

Characteristics	Number (%)
Total	197,699
Year of diagnosis	
2007–2010	89,006 (45.0)
2011–2015	108,693 (55.0)
Age	
<65	98,682 (49.9)
≥65	99,017 (50.1)
Sex	
Female	95,030 (48.1)
Male	102,669 (51.9)
Race	
Black	23,557 (11.9)
White	156,015 (78.9)
Other	18,127 (9.2)
Marital status	
Married	111,210 (56.3)
Unmarried	86,489 (43.7)
Insurance	
Any Medicaid	24,892 (12.6)
Insured	165,937 (83.9)
Uninsured	6,870 (3.5)
Tumor site	
Left	101,144 (51.2)
Right	93,632 (47.4)
NOS	2,923 (1.5)
Tumor size	
≤5 cm	112,065 (56.7)
5–10 cm	52,078 (26.3)
>10 cm	33,556 (17.0)
Grade	
Grade I	21,461 (10.9)
Grade II	137,501 (69.6)
Grade III	33,300 (16.8)
Grade IV	5,437 (2.8)
SEER stage	
Localized	77,655 (39.3)
Regional	81,662 (41.3)
Distant	38,382 (19.4)
Surgery	
No	18,599 (9.4)
Yes	179,100 (90.6)
Radiotherapy	
No	168,962 (85.5)
Yes	28,737 (14.5)
Chemotherapy	
No	115,753 (58.6)
Yes	81,946 (41.4)
Causes	
Alive	118,244 (59.8)
Death form CRC	9,702 (4.9)
Death form CVD	56,185 (28.4)
Death form non-CVD	13,568 (6.9)

Other, American Indian/Alaska Native/Asian/Pacific Islander; NOS, not otherwise specified; SEER, Surveillance, Epidemiology, and End Results; CRC, colorectal cancer; CVD, cardiovascular death.

TABLE 2 | Cumulative incidence of cause-specific death and Gray's test in the whole set.

Characteristics	CVD (%)			*P*	Non-CVD (%)			*P*
	1-year	3-year	5-year		1-year	3-year	5-year	
Total	12.20	24.25	30.51		1.93	4.13	4.77	
Year of diagnosis				<0.001				0.01
2007–2010	1.84	3.47	4.99		2.10	4.30	6.60	
2011–2015	1.46	2.89	4.49		1.79	3.99	6.45	
Age				<0.001				<0.001
<65	0.44	0.94	1.39		0.87	1.95	2.99	
≥65	2.82	5.34	7.89		2.97	6.26	9.79	
Sex				0.210				0.010
Female	1.55	3.03	4.65		1.83	3.95	6.27	
Male	1.71	3.28	4.77		2.01	4.31	6.67	
Race				<0.001				<0.001
Black	1.72	3.23	4.46		1.99	4.27	6.35	
White	1.68	3.26	4.91		2.00	4.26	6.70	
Others	1.14	2.19	3.20		1.20	2.87	4.65	
Marital status				<0.001				<0.001
Married	1.23	2.40	3.63		1.46	3.26	5.31	
Unmarried	2.15	4.15	6.13		2.53	5.26	8.00	
Insurance status				<0.001				<0.001
Any Medicaid	1.89	3.65	5.16		2.63	5.33	7.66	
Insured	0.70	1.43	2.14		1.29	2.78	3.62	
Uninsured	1.63	3.16	4.75		1.85	4.01	6.42	
Tumor site				<0.001				<0.001
Left	1.34	2.65	3.89		1.55	3.40	5.32	
Right	1.94	3.69	5.59		2.30	4.90	7.71	
NOS	2.07	3.82	4.97		3.20	5.05	6.79	
Tumor size				<0.001				<0.001
≤5 cm	1.53	3.14	4.84		1.77	4.16	6.73	
5–10 cm	1.79	3.30	4.78		2.07	4.19	6.40	
>10 cm	1.72	3.02	4.18		2.22	3.97	5.76	
Grade				<0.001				<0.001
Grade I	1.22	2.86	4.58		1.64	3.90	6.46	
Grade II	1.64	3.20	4.83		1.86	4.17	6.59	
Grade III	1.86	3.18	4.34		2.25	4.08	6.06	
Grade IV	1.79	3.29	4.50		2.61	4.51	6.19	
SEER stage				<0.001				<0.001
Localized	1.71	3.72	5.93		1.99	4.81	8.08	
Regional	1.72	3.22	4.75		1.98	4.20	6.52	
Distant	1.29	1.91	2.17		1.69	2.63	3.15	
Surgery				<0.001				<0.001
No	2.48	3.55	4.13		3.05	4.55	5.40	
Yes	1.55	3.12	4.77		1.81	4.09	6.59	
Radiotherapy				<0.001				<0.001
No	1.78	3.42	5.08		2.09	4.42	6.90	
Yes	0.77	1.66	2.53		0.97	2.47	4.00	
Chemotherapy				<0.001				<0.001
No	2.36	4.47	6.62		2.74	5.60	8.74	
Yes	0.61	1.33	2.02		0.78	2.07	3.29	

Other, American Indian/Alaska Native/Asian/Pacific Islander; NOS, not otherwise specified; SEER, Surveillance, Epidemiology, and End Results.

improve the prognosis, and raise the quality of life for patients with CRC.

MATERIALS AND METHODS

Data Source and Study Cohort

The present study was a retrospective analysis of a cohort of patients with CRC that strictly followed the Strengthening the Reporting of Observational Studies in Epidemiology (STROBE) specifications (17). The data used in this study were taken from 18 SEER registries *via* the SEER*Stat software (2017 submission). The 18 SEER registries with additional treatment fields that were used in this study provided detailed data about demographic and clinicopathological characteristics, treatment protocols, and follow-up.

Study Population and Variables

This study included cases from the 18 SEER registries with CRC, which were proved by pathologic diagnosis. We selected the patients with CRC using the following topography codes: C18.0, C18.2, C18.3, C18.4, C18.5, C18.6, C18.7, C18.8, 18.9, C19.9, and C20.9. The dawn of tyrosine kinase inhibitors, 2007, was selected as a year of insurance that was accessible in the SEER database when investigating the role of socioeconomic factors in CVD (18). The eligible patients were selected using the following inclusion criteria: (1) diagnosed with CRC as the primary and only tumor; (2) diagnosed between 2007 and 2015; and (3) had active follow-up information and defined causes of mortalities. Then, the following information was obtained for each patient: year of diagnosis, age, sex, race, tumor stage, histological grade, tumor site, marital status, insurance status, surgery, radiotherapy, chemotherapy, survival months, and causes of death. Patients with missing data about any of above information were excluded.

Outcomes

Cardiovascular death was the primary endpoint and was measured as the time from the date of diagnosis of CRC to death due to CVD (19). As recorded in the SEER database, CVD has six causes of death, namely, disease of heart, hypertension without heart disease, cerebrovascular disease, atherosclerosis, aortic aneurysm and dissection, and other diseases of arteries, arterioles, and capillaries (20). The non-CVD was defined from other causes and was considered as competing events against CVD. Patients who survived until the last follow-up or who were lost to follow-up before the end of the observation period were regarded as censored observations.

Statistical Analysis

The difference of baseline characteristics between subgroups were compared with χ^2. Cumulative incidence function (CIF) was calculated to evaluate the probabilities of each event at 1-, 3-, and 5-year. Subgroup analyses were performed based on patient's characteristics, and respective curves for CIF were produced. The difference in CIF were determined through Gray's test (21). Fine and Gray's subdistribution

proportional hazards model was performed for identifying the independent risk factors for CVD among patients with CRC (22). Moreover, based on Fine-Gray's model, a novel competing-risk model was developed to predict the probabilities of CVD at 1-, 3-, 5-year for patients with CRC. We used the concordance index (C-index) to measure discriminative performance of the model, and the consistency was measured using a calibration curve (18). Decision curve analysis (DCA) was performed to visually investigate the clinical utilities and net benefits of this model (23, 24). The packages *cmprsk*, *survival*, *mstate*, *rms*, *pec,* and *riskRegression* in the R software (version 3.2.5) were used to establish and validate the nomogram. $p < 0.05$ in two-sided tests were statistically significant.

RESULTS

Patient Selections and Baseline Characteristics

Our study extracted 197,699 eligible patients diagnosed with CRC between 2007 and 2015 in the SEER program. The baseline characteristics of the whole study cohort are presented in **Table 1**. A larger proportion of patients were aged above 65 years (1,776, 65.7%), male (102,669, 51.9%), white (156,015, 78.9%), married (111,210, 56.3%), and insured (165,937, 83.9%). Most patients were diagnosed with grade II (69.6%), followed by grade III (16.8%), grade I (10.9%), and grade IV (2.8%) CRC. The distribution of SEER stage was as follows: 77,655 (39.3%) had localized stage, 81,662 (41.3%) had regional stage, and 38,382 (19.4%) had distant stage. A total of 179,100 (90.6%) patients were treated with surgery, 81,946 (41.4%) patients were treated with chemotherapy, and only 28,737 (14.5%) patients were treated with radiotherapy.

Cumulative Incidence Function Survival Analysis

The median follow-up of the whole cohort was 37 months (IQR: 17.00–119.00). In total, 79,455 patients died during the follow-up, of whom 56,185 (70.71%) succumbed to CRC and 23,270 (29.29%) died due to non-CRC, among which CVD accounted for 9,702 (41.69%), being the major cause of non-cancer deaths (**Table 1**). In consideration of competing risks (death from other causes), we further performed cumulative incidence analysis in the whole cohort (**Table 2**). Overall, the 1-, 3-, and 5-year CIF of death due to CRC were 1.63, 3.16, and 4.71%, respectively. The 1-, 3-, and 5-year CIF of CVD were 12.20, 24.25, and 30.51%, respectively, while the 1-, 3-, and 5-year CIF of non-CVD were 1.93, 4.13, and 4.77%, respectively (**Table 2**). Furthermore, the CIF of CVD were significantly decreased in recent years (**Figure 1** and **Table 2**).

In the subsequent subgroup analyses stratified by patient characteristics (**Table 2**), we found that a high CVD primarily occurred in patients aged ≥65 years (**Figure 2A**) whose race was White (**Figure 2C**); were unmarried (**Figure 2D**); had any Medicaid (**Figure 2E**); who had right tumors (**Figure 2F**), small tumor size (**Figure 2G**), and I-II grade of tumor (**Figure 2H**); had localized SEER stage (**Figure 2I**); and were not treated with surgery (**Figure 2J**), radiotherapy (**Figure 2K**), or chemotherapy (**Figure 2L**). In addition, no significant difference in CVD was found in sex subgroup analyses (**Figure 2B**).

Risk Factors for Cardiovascular Death Among Patients With Colorectal Cancer in the Training Cohort

As shown in **Table 3**, patients with CRC in the whole cohort were randomized into the training ($n = 138,391$) and validation cohort ($n = 59,308$) at a ratio of 7:3. The baseline characteristics between the two cohorts were well balanced. Furthermore, the

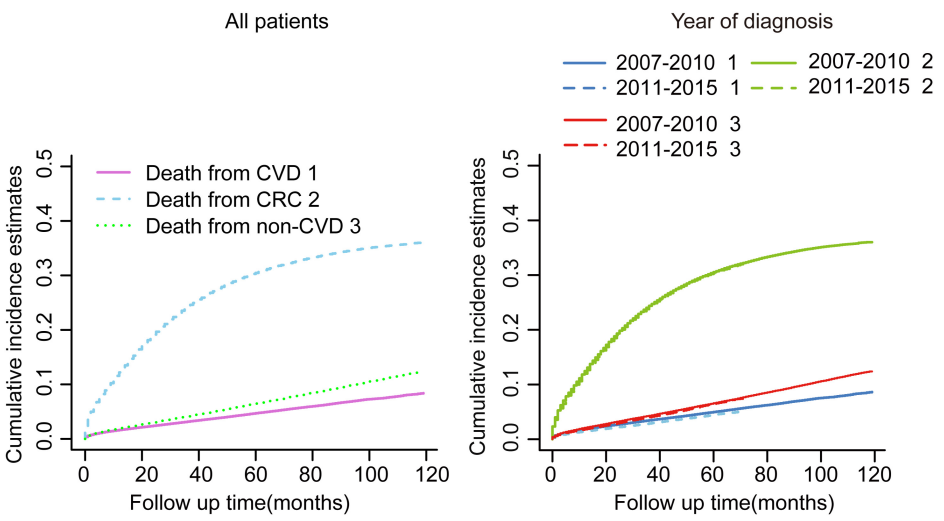

FIGURE 1 | Cumulative incidence estimates of cardiovascular death (CVD) among patients with colorectal cancer (CRC) in the whole cohort. Death from CVD was indicated as 1; death from CRC was indicated as 2; and death from non-CVD was indicated as 3.

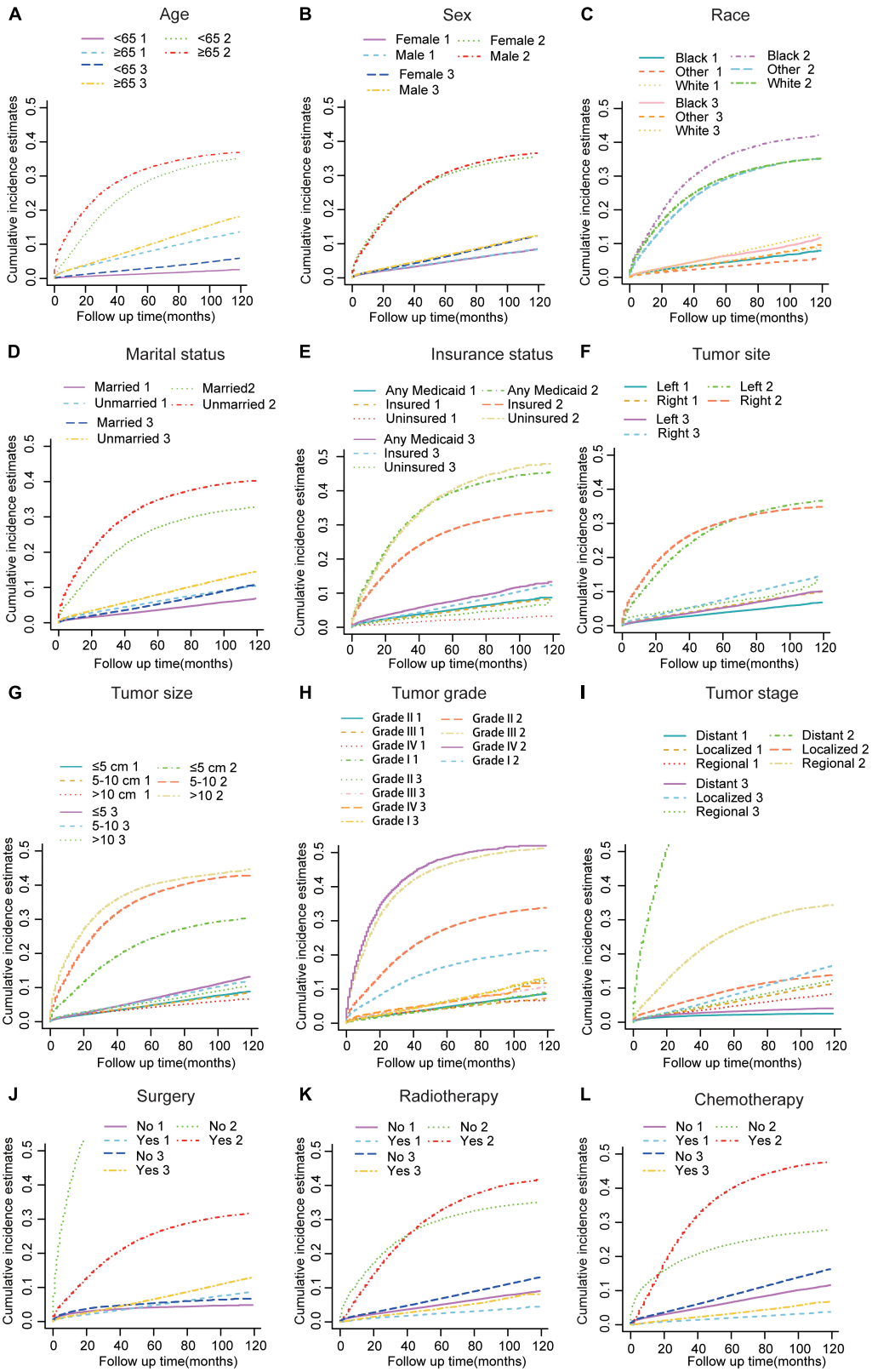

FIGURE 2 | Cumulative incidence estimates of CVD among patients with CRC according to **(A)** Age; **(B)** Sex; **(C)** Race; **(D)** Marital status; **(E)** Insurance status; **(F)** Tumor site; **(G)** Tumor size; **(H)** Grade; **(I)** SEER stage; **(J)** Surgery; **(K)** Radiotherapy; **(L)** and Chemotherapy. A solid line represents cause-specific death, while a dotted line represents other causes of death. Death from CVD was indicated as 1; death from CRC was indicated as 2; and death from non-CVD was indicated as 3.

TABLE 3 | Basic characteristics of patients in the training and validation cohorts.

Characteristics	Training cohort *N* (%)	Validation cohort *N* (%)	*P*
Total	**138,391 (100)**	**59,308 (100)**	
Age			0.217
<65	68,952 (49.8)	29,730 (40.1)	
≥65	69,439 (50.2)	29,578 (49.9)	
Sex			0.442
Female	66,443 (48.0)	28,587 (48.2)	
Male	71,948 (52.0)	30,721 (51.8)	
Race			0.488
Black	16,569 (12.0)	6,988 (11.8)	
White	109,146 (78.9)	46,869 (79.0)	
Other	12,676 (9.2)	5,451 (9.2)	
Year of diagnosis			0.499
2007–2010	62,374 (45.1)	26,632 (44.9)	
2011–2015	76,017 (54.9)	32,676 (55.1)	
Marital status			0.305
Married	78,031 (56.4)	33,179 (55.9)	
Unmarried	60,360 (43.6)	26,129 (44.1)	
Insurance			0.962
Any Medicaid	17,421 (12.6)	7,471 (12.6)	
Insured	116,171 (83.9)	49,766 (83.9)	
Uninsured	4,799 (3.5)	2,071 (3.5)	
Tumor site			0.248
Left	70,638 (51.0)	30,506 (51.4)	
Right	65,713 (47.5)	27,919 (47.1)	
NOS	2,040 (1.5)	883 (1.5)	
Tumor size			0.761
≤5 cm	78,372 (56.6)	33,693 (56.8)	
5–10 cm	36,503 (26.4)	15,575 (26.3)	
>10 cm	23,516 (17.0)	10,040 (16.9)	
Grade			0.238
Grade I	15,014 (10.8)	6,447 (10.9)	
Grade II	96,153 (69.5)	41,348 (69.7)	
Grade III	23,354 (16.9)	9,946 (16.8)	
Grade IV	3,870 (2.8)	1,567 (2.6)	
SEER stage			0.204
Localized	54,182 (39.2)	23,473 (39.6)	
Regional	57,291 (41.4)	24,371 (41.1)	
Distant	26,918 (19.5)	11,464 (19.3)	
Surgery			0.711
No	13,042 (9.4)	5,557 (9.4)	
Yes	125,349 (90.6)	53,751 (90.6)	
Radiotherapy			0.273
No	118,354 (85.5)	50,608 (85.3)	
Yes	20,037 (14.5)	8,700 (14.7)	
Chemotherapy			0.434
No	80,949 (58.5)	34,804 (58.7)	
Yes	57,442 (41.5)	24,504 (41.3)	
Death causes			0.267
Alive	82,788 (59.8)	35,456 (59.8)	
Death form CRC	39,417 (28.5)	16,768 (28.3)	
Death form CVD	6,712 (4.9)	2,990 (5.0)	
Death from non-CVD	9,474 (6.8)	4,094 (6.9)	

Other, American Indian/Alaska Native/Asian/Pacific Islander; NOS, not otherwise specified; SEER, Surveillance, Epidemiology, and End Results; CRC, colorectal cancer; CVD, cardiovascular death.

TABLE 4 | Univariate and multivariable competing risk analyses for cardiovascular death (CVD) among patients with colorectal cancer (CRC) in the training cohort.

	Univariate analysis		Multivariate analysis	
Variables	**sdHR (95% CI)**	***P***	**sdHR (95% CI)**	***P***
Age				
<65	Reference		Reference	
≥65	5.80 (5.42–6.21)	<0.001	4.65 (4.34–4.99)	<0.001
Sex				
Female	Reference			
Male	1.04 (0.99–1.10)	0.077		
Race				
Black	Reference		Reference	
White	1.07 (0.993–1.15)	0.07	0.94 (0.87–1.01)	0.095
Others	0.70 (0.62–0.78)	<0.001	0.67 (0.60–0.76)	<0.001
Marital status				
Married	Reference		Reference	
Unmarried	1.63 (1.55–1.71)	<0.001	1.33 (1.26–1.40)	<0.001
Insurance				
Insured	Reference		Reference	
Any Medicaid	2.81 (2.26–3.51)	<0.001	1.25 (1.00–1.56)	0.051
Uninsured	2.65 (2.14–3.27)	<0.001	1.01 (0.81–1.25)	0.940
Tumor site				
Left	Reference		Reference	
Right	1.10 (0.90–1.33)	0.35	0.96 (0.79–1.17)	0.710
NOS	0.75 (0.62–0.91)	0.003	0.94 (0.77–1.14)	0.520
Tumor size				
≤5 cm	Reference		Reference	
5–10 cm	1.01 (0.96–1.07)	0.710	1.07 (1.01–1.14)	0.017
>10 cm	0.85 (0.80–0.91)	<0.001	0.99 (0.92–1.07)	0.810
Grade				
Grade I	Reference			
Grade II	1.016 (0.94–1.10)	0.69		
Grade III	0.94 (0.86–1.04)	0.22		
Grade IV	0.86 (0.72–1.02)	0.08		
SEER stage				
Localized	Reference		Reference	
Regional	0.786 (0.75–0.83)	<0.001	0.99 (0.94–1.05)	0.930
Distant	0.334 (0.31–0.37)	<0.001	0.47 (0.43–0.52)	<0.001
Surgery				
No	Reference		Reference	
Yes	1.24 (1.13–1.36)	<0.001	0.81 (0.72–0.90)	<0.001
Radiotherapy				
No	Reference		Reference	
Yes	0.47 (0.43–0.52)	<0.001	1.01 (0.91–1.13)	0.780
Chemotherapy				
No	Reference		Reference	
Yes	0.30 (0.28–0.32)	<0.001	0.48 (0.45–0.52)	<0.001

sdHR, subdistribution hazard ratio; CI, confidence interval; Other, American Indian/Alaska Native/Asian/Pacific Islander; NOS, not otherwise specified; SEER, Surveillance, Epidemiology, and End Results; CRC, colorectal cancer; CVD, cardiovascular death.

CIF of CVD remained comparable between the two cohorts ($p = 0.57$). To identify the independent risk factors for CVD in the training cohort, we conducted the univariate and multivariate Fine-Gray hazard model analysis. The univariate analysis showed

that CVD was significantly associated with age, race, marital status, insurance status, tumor site, tumor size, SEER stage, surgery, radiotherapy, and chemotherapy (**Table 4**). However, sex and grade did not significantly influence cumulative incidences of CVD. To minimize the risks of producing false positive results, multivariate analyses based on Fine-Gray hazard model were conducted to control the significant covariates. Results showed that age, race, marital status, tumor size, SEER stage, surgery, and chemotherapy were independent risk factors for CVD (**Table 4**).

Construction of a Competing-Risk Model

The incidence of CVD in patients with CRC has tended to increase in the last decades. However, competing-risk model combining comprehensive factors for patients with CRC suffering CVD remains scarce. Thus, a nomogram predicting the probabilities of CVD at 1-, 3-, and 5-year was established (**Figure 3**) based on the Fine and Gray's model we built. With the help of this useful tool, an individual patient chance of CVD at different times could be easily obtained by adding the scores of each incorporated variable.

Validation and Risk Stratification of Competing-Risk Model

Then, this nomogram was validated using bootstrap and ten-fold cross-validation methods. The results showed that nomogram had a great discrimination ability in predicting overall survival (OS), with a C-index of 0.719 (95% CI, 0.738–0.742), and 0.719 (95% CI, 0.622–0.668) in the training and validation cohort, respectively. The calibration curves were shown in **Figure 4**, with the dots close to a 45° diagonal line, reflecting great consistency between the prediction by the nomogram and the actual observation of the probability of CVD at 1-, 3-, and 5-year. Furthermore, DCA was introduced to assess the clinical utility of the nomograms. As shown in **Figures 5A,B**, the clinical use of the nomogram showed high positive net benefits at a wider range

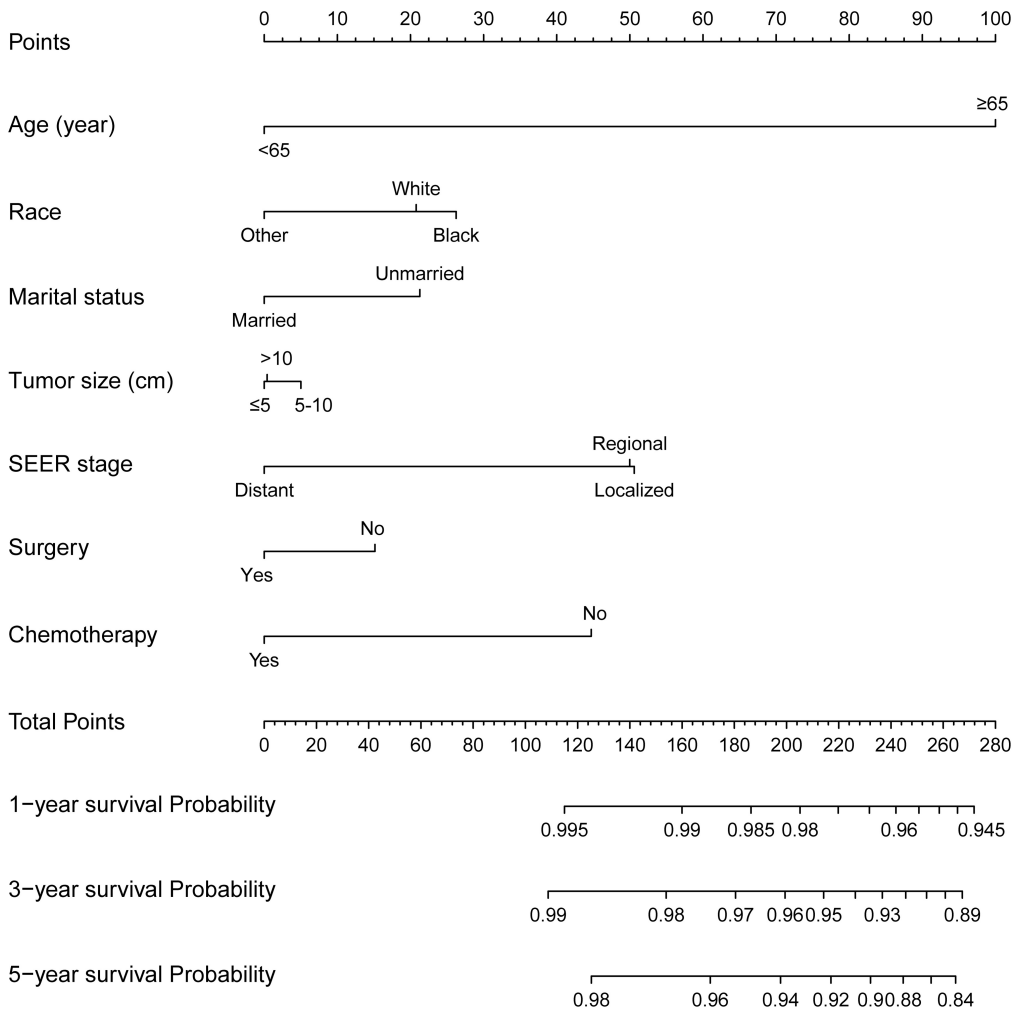

FIGURE 3 | Competing-risk model for predicting the 1-, 3-, and 5-year probabilities of CVD among patients with CRC. The "total points" of a certain patient was calculated by adding all the scores of the 7 parameters. Based on the total points, the possibilities of CVD at different timepoints and the prognostic group was obtained.

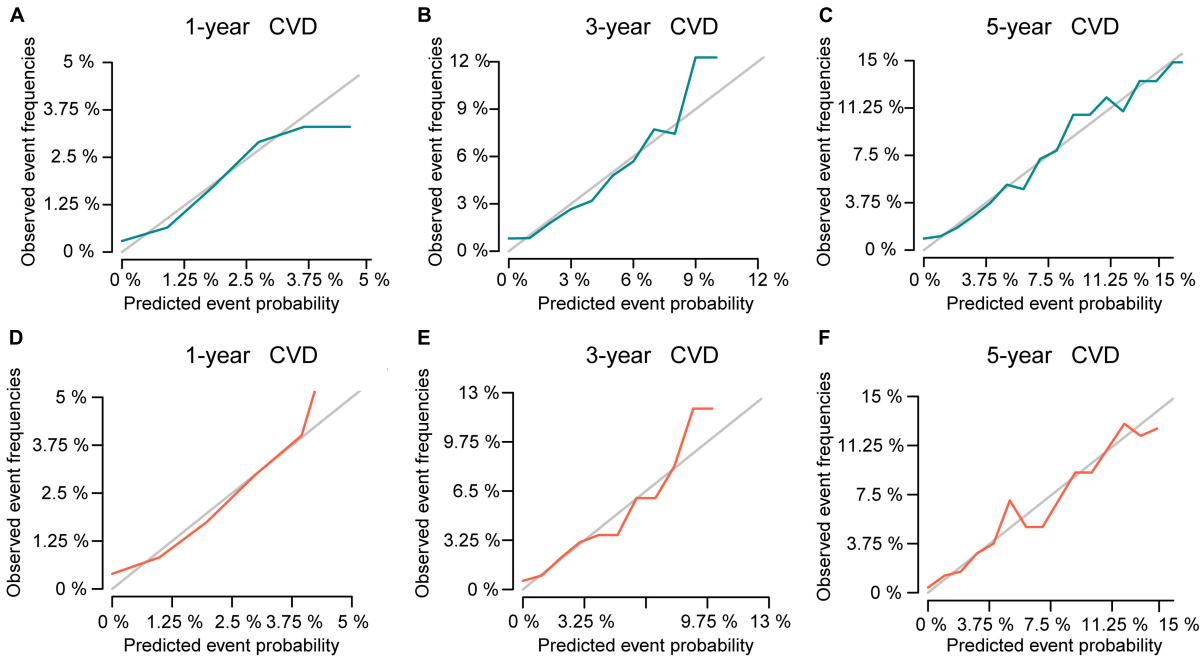

FIGURE 4 | The calibration curve for predicting the 1-, 3-, and 5-year probabilities of CVD in the training **(A–C)** and the validation cohort **(D–F)**, respectively.

of threshold likelihood, which depicted that the nomogram had a high clinical utility in predicting CVD.

According to the tertile values of the nomogram-based scores derived from the training cohort, the patients were categorized into high-risk, medium-risk, and low-risk groups in both cohorts. The high-risk group had the highest probabilities of CVD, followed by the medium-risk group and the low-risk group in both cohorts (**Figures 5C,D**). Hence, there is an important value of competing-risk model for clinical risk stratification and prognosis decision in patients with CRC.

DISCUSSION

In the past few decades, considerable advances in management of cancer have greatly prolonged the survival of patients suffering from CRC. On the other hand, we can also expect that non-cancer mortalities will become more prevalent, dominated by cardiovascular disease. Based on the SEER database, our current study provided important insights into the risk of CVD among patients with CRC diagnosed between 2007 and 2015. In total, 79,455 patients died throughout the follow-up, of whom 56,185 (70.71%) succumbed to CRC and 23,270 (29.29%) died due to non-CRC, among which CVD accounted for 9,702 (41.69%), being the major cause of non-cancer deaths. The 1-, 3-, and 5-year CIF of CVD were 12.20, 24.25, and 30.51%, respectively, while the 1-, 3-, and 5-year CIF of no-CVD were 1.93, 4.13, and 4.77%, respectively, indicating that CVD has become a main reason of death among CRC survivors during the follow-up period. Through competing risk analyses, we further identified that age, race, marital status, tumor size, SEER stage, surgery, and chemotherapy were independent risk factors for CVD. These results should not be ignored when evaluating the individual risks of CVD and work as an indication for more precise treatment and risk factors management, such as monitoring of blood sugar and hypertension and health education.

Currently, chemotherapy and widely used drugs for CRC, which involves several agents, such as oxaliplatin, fluorouracil, leucovorin, and so on (25, 26), are effective. Chemotherapy usually induces cardiotoxicity and increases CVD risk (27). In addition, drugs for CRC usually lead to higher CVD risk than the general population, particularly in the first few years of treatment (28). However, our analysis indicated that the risks of CVD were significantly lower among patients with CRC who were treated with chemotherapy than those were not. This result seemed to be contrary to the observed cardiotoxic effect of chemotherapy. However, consistent with the previous studies in other tumors (29, 30), this contradiction arises from the limited life expectancy of patients who received chemotherapy and succumbed to CVD events. Since the detailed information for chemotherapy regimen were missing in the SEER database, further investigation is required to clarify the effect of chemotherapy on the risk of CVD among patients with CRC. In addition, we also demonstrated that patients without cancer-direct surgery had an increased CVD compared to patients who received surgery, which was in line with previous findings (13, 31).

In recent years, the role of socioeconomic factors in influencing humans, including cultural and social values, insurance status, education level or employments status, and so on, are increasingly becoming the focus of medical attention (32, 33). In this study, we investigated the effects of insurance and marital status on the risks of CVD. Results showed that

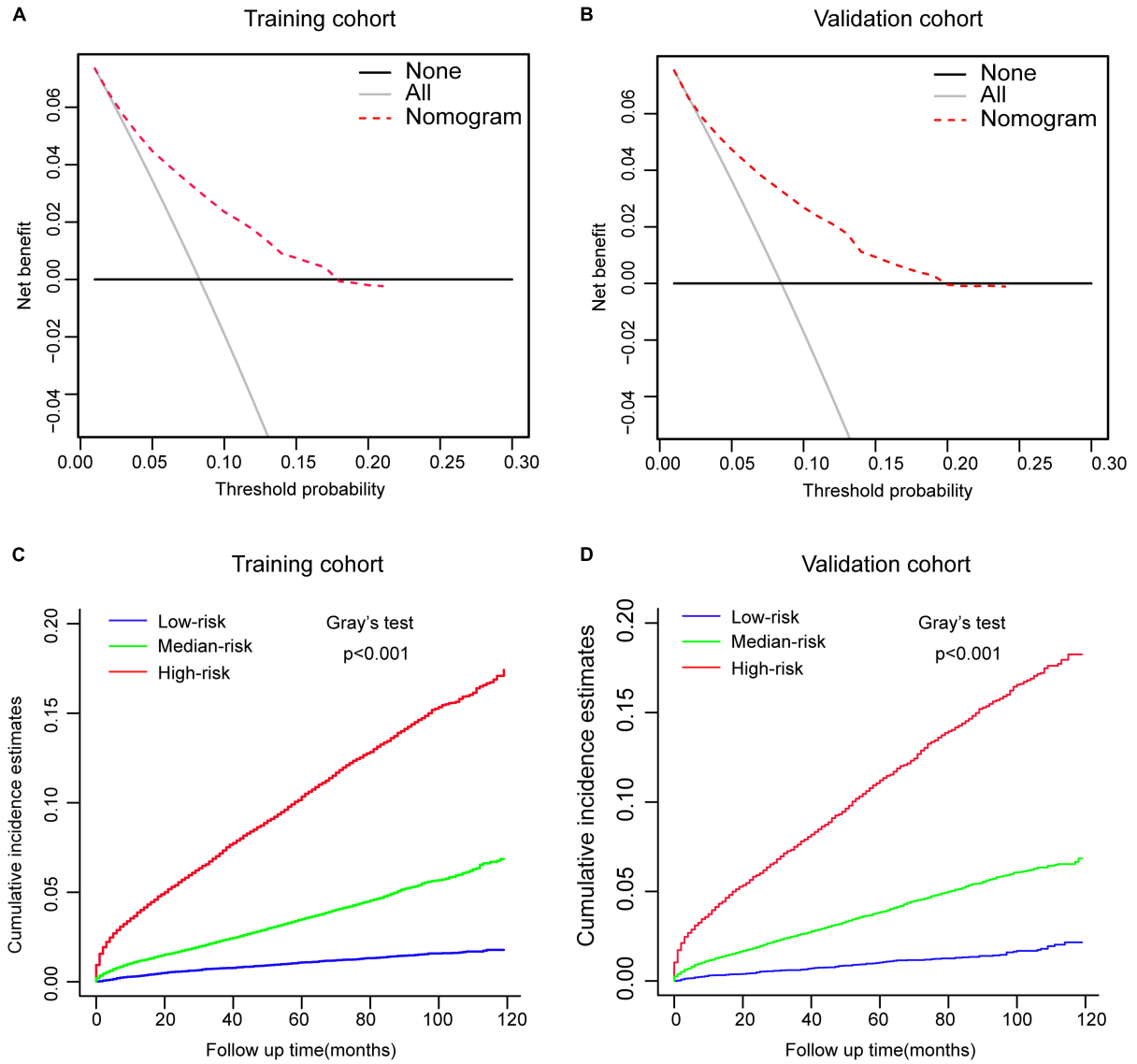

FIGURE 5 | Performance and risk stratification of the competing-risk model. **(A,B)** Decision curves of the nomogram predicting CVD in the training and validation cohort, respectively. **(C,D)** Cumulative incidence function (CIF) curves with the *p*-value of Gray's test for the training and validation cohort, respectively.

the insured patients had lower risk of CVD compared with those who were uninsured. For now, battling CRC has been regarded as a time-consuming, multidisciplinary, and expensive process. Uninsured patients usually suffer the brunt of shortage of medical services and supplies. Furthermore, we demonstrated that, among CRC survivors, marital status was a protection factor against CVD. Marital status is a potential marker of mental status, lifestyle, and social and family support, which have greatly affected the outcomes of patients with cardiovascular disease (34). Patients who are married display less distress and anxiety than their unmarried counterparts after a diagnosis of cancer (35–37), and this could contribute to increased family support, medication compliance, and survival advantages to a large extent. In addition, from the perspective of biological factors, a married status benefited to promote cardiovascular, endocrine, immune status, and nutrition behavior (34, 38). Collectively, we strongly recommend the integration of non-biological factors when assessing the individual risks of CVD among CRC survivors.

To facilitate patient counseling and clinical decision making, a prospective risk of potential cardiotoxicity for individual is imperative. From the clinical perspective, we constructed a competing-risk model with variables to investigate the probabilities of CVD at 1-, 3-, and 5-year. To the best of our knowledge, this is the first study that established and validated a competing-risk model based on the Fine-Gray proportional subdistribution hazard analysis to estimate the individual probabilities of CVD-specific mortality for patients

with CRC. All the variables included in this nomogram were easily available in clinical practice. With its aid, clinicians can more expediently devise clinical managements and, more importantly, remain vigilant for this complication when treating patients with CRC with immunotherapy. Our nomograms showed excellent accuracy and discriminative performance, as validated by C-index and calibration curves. Furthermore, we should be aware that high discrimination calibration does not necessarily imply an excellent clinical utility. Hence, DCA was employed to determine the clinical utility of this nomogram by calculating the net benefits at each risk threshold probability (23, 24). Results showed that using the nomogram to predict the probabilities of CVD provided more benefits. Collectively, these data demonstrated that this model had strong practicability and high reliability in the processes of clinical practice.

The major advantages of this study were that it had a large enough sample size and that it used competing risk analysis to investigate the risk of CVD among patients with CRC. Generally speaking, the SEER database, accounting for about a third of the United States population, provides large enough sample data to explore risk factors and further develop a nomogram based on competing risk analysis. More to the point, results from analyses that use population-level databases tend to be more generalizable and representative than those from single-center reports (24). Actually, sufficient incorporated samples are needed to guarantee the accuracy of nomograms, as demonstrated our recent publications (5, 18, 24). Notably, no competing-risk model has been established to evaluate the risk of CVD among patients with CRC so far. We established the first competing-risk model for these patients and made possible the individualized prediction of prognosis. Furthermore, our nomogram showed excellent discrimination power and clinical usefulness in clinical practice. In addition, the parameters included in the nomogram could be easily obtained in clinical practice.

Undoubtedly, this study was subject to several limitations. First, it had a retrospective design, making potential hidden biases. In addition, there is no way to know some the relevant information, such as gene mutations (HER-2 and RAS/RAF), making it impossible to adjust for these characteristics between the two groups. Second, the SEER database did not provide an explanation about comorbidity since it was a significant factor when physicians deciding treatment strategies. This lacking would, to certain degree, weaken the objectivity of our conclusions. In addition, it remains a main limitation that we established a model without comorbidity status. Third, data on chemotherapy regimen were not available in the SEER database, and some of which is closely associated with cardiotoxicity. Finally, although the competing-risk model had excellent performance in predicting the probabilities of CVD, it was validated by an internal patient cohort. Thus, additional external data is needed to verify the performance of the model further.

CONCLUSION

The present study was the first to use a competing-risk model to investigate the cumulative incidence and risk factors of CVD among patients with CRC. More importantly, we have successfully developed a nomogram for predicting the probabilities of CVD for patients with CRC. The internal and external validation demonstrated the excellent discrimination, calibration, and clinical usefulness of this model. With the help of this well-established nomogram, clinicians would make more individualized treatments, tighter control of modifiable risk factors, and follow-up schedules.

DATA AVAILABILITY STATEMENT

The datasets presented in this study can be found in online repositories. The names of the repository/repositories and accession number(s) can be found in the article/supplementary material.

ETHICS STATEMENT

Approval was waived by the Local Ethics Committee, as Surveillance, Epidemiology, and End Results (SEER) data is publicly available and de-identified.

AUTHOR CONTRIBUTIONS

TL and SZ were responsible for the conception and design of the study, assisted with the statistical analysis, and wrote and revised the manuscript. YW, PZ, and LA contributed to the data analysis and revision on the English language and grammar, and corrected the parts of the discussion. TL made the primary contribution in the later stage in the writing and modification of the manuscript, and review of the finalized article. All authors contributed to the article and approved the submitted version.

REFERENCES

1. Siegel RL, Miller KD, Jemal A. Cancer statistics, 2020. *CA Cancer J Clin.* (2020) 70:7–30. doi: 10.3322/caac.21590
2. Jiang Y, Yuan H, Li Z, Ji X, Shen Q, Tuo J, et al. Global pattern and trends of colorectal cancer survival: a systematic review of population-based registration data. *Cancer Biol Med.* (2021) 19:175–86. doi: 10.20892/j.issn.2095-3941.2020.0634
3. Sumransub N, Vantanasiri K, Prakash A, Lou E. Advances and new frontiers for immunotherapy in colorectal cancer: setting the stage for neoadjuvant success? *Mol Ther Oncolytics.* (2021) 22:1–12. doi: 10.1016/j.omto.2021.05.001
4. Cautela J, Lalevée N, Ammar C, Ederhy S, Peyrol M, Debourdeau P, et al. Management and research in cancer treatment-related cardiovascular toxicity: challenges and perspectives. *Int J Cardiol.* (2016) 224:366–75. doi: 10.1016/j.ijcard.2016.09.046
5. Qiu Z, Tang Y, Jiang Y, Su M, Wang X, Xu X, et al. Cardiovascular outcomes in the patients with primary central nervous system lymphoma: a multi-registry based cohort study of 4,038 cases. *Front Oncol.* (2021) 11:691038. doi: 10.3389/fonc.2021.691038

6. Makaremi S, Asadzadeh Z, Hemmat N, Baghbanzadeh A, Sgambato A, Ghorbaninezhad F, et al. Immune checkpoint inhibitors in colorectal cancer: challenges and future prospects. *Biomedicines.* (2021) 9:1075. doi: 10.3390/biomedicines9091075
7. Chen TW, Razak AR, Bedard PL, Siu LL, Hansen AR. A systematic review of immune-related adverse event reporting in clinical trials of immune checkpoint inhibitors. *Ann Oncol.* (2015) 26:1824–9. doi: 10.1093/annonc/mdv182
8. Boutros C, Tarhini A, Routier E, Lambotte O, Ladurie FL, Carbonnel F, et al. Safety profiles of anti-CTLA-4 and anti-PD-1 antibodies alone and in combination. *Nat Rev Clin Oncol.* (2016) 13:473–86. doi: 10.1038/nrclinonc.2016.58
9. Ricciuti B, Naqash AR, Naidoo J, Sehgal K, Miller A, Kehl K, et al. Association between immune-related adverse events and clinical outcomes to programmed cell death protein 1/Programmed death-ligand 1 blockade in SCLC. *JTO Clin Res Rep.* (2020) 1:100074. doi: 10.1016/j.jtocrr.2020.100074
10. Chhabra N, Kennedy J. A review of cancer immunotherapy toxicity: immune checkpoint inhibitors. *J Med Toxicol.* (2021) 17:411–24. doi: 10.1007/s13181-021-00833-8
11. Ji C, Roy MD, Golas J, Vitsky A, Ram S, Kumpf SW, et al. Myocarditis in cynomolgus monkeys following treatment with immune checkpoint inhibitors. *Clin Cancer Res.* (2019) 25:4735–48. doi: 10.1158/1078-0432.ccr-18-4083
12. Varricchi G, Marone G, Mercurio V, Galdiero MR, Bonaduce D, Tocchetti CG. Immune checkpoint inhibitors and cardiac toxicity: an emerging issue. *Curr Med Chem.* (2018) 25:1327–39. doi: 10.2174/0929867324666170407125017
13. Gaitanidis A, Spathakis M, Tsalikidis C, Alevizakos M, Tsaroucha A, Pitiakoudis M. Risk factors for cardiovascular mortality in patients with colorectal cancer: a population-based study. *Int J Clin Oncol.* (2019) 24:501–7. doi: 10.1007/s10147-018-01382-x
14. Noordzij M, Leffondré K, van Stralen KJ, Zoccali C, Dekker FW, Jager KJ. When do we need competing risks methods for survival analysis in nephrology? *Nephrol Dial Transplant.* (2013) 28:2670–7. doi: 10.1093/ndt/gft355
15. Berry SD, Ngo L, Samelson EJ, Kiel DP. Competing risk of death: an important consideration in studies of older adults. *J Am Geriatr Soc.* (2010) 58:783–7. doi: 10.1111/j.1532-5415.2010.02767.x
16. Abrahamowicz M, Du Berger R, Krewski D, Burnett R, Bartlett G, Tamblyn RM, et al. Bias due to aggregation of individual covariates in the Cox regression model. *Am J Epidemiol.* (2004) 160:696–706. doi: 10.1093/aje/kwh266
17. von Elm E, Altman DG, Egger M, Pocock SJ, Gøtzsche PC, Vandenbroucke JP. The Strengthening the Reporting of Observational Studies in Epidemiology (STROBE) Statement: guidelines for reporting observational studies. *Int J Surg.* (2014) 12:1495–9. doi: 10.1016/j.ijsu.2014.07.013
18. Zhang SL, Zhang ZY, Liu ZJ, Wang WR, Li ZM, Han B, et al. A real-world study of socioeconomic factors with survival in adults aged 18-64 years with renal cell carcinoma. *Future Oncol.* (2019) 15:2503–15. doi: 10.2217/fon-2018-0827
19. Weberpals J, Jansen L, Müller OJ, Brenner H. Long-term heart-specific mortality among 347 476 breast cancer patients treated with radiotherapy or chemotherapy: a registry-based cohort study. *Eur Heart J.* (2018) 39:3896–903. doi: 10.1093/eurheartj/ehy167
20. Fung C, Fossa SD, Milano MT, Sahasrabudhe DM, Peterson DR, Travis LB. Cardiovascular disease mortality after chemotherapy or surgery for testicular nonseminoma: a population-based study. *J Clin Oncol.* (2015) 33:3105–15. doi: 10.1200/jco.2014.60.3654
21. Satagopan JM, Ben-Porat L, Berwick M, Robson M, Kutler D, Auerbach AD. A note on competing risks in survival data analysis. *Br J Cancer.* (2004) 91:1229–35. doi: 10.1038/sj.bjc.6602102
22. He P, Eriksson F, Scheike TH, Zhang MJ. A proportional hazards regression model for the sub-distribution with covariates adjusted censoring weight for competing risks data. *Scand Stat Theory Appl.* (2016) 43:103–22. doi: 10.1111/sjos.12167
23. Vickers AJ, Cronin AM, Elkin EB, Gonen M. Extensions to decision curve analysis, a novel method for evaluating diagnostic tests, prediction models and molecular markers. *BMC Med Inform Decis Mak.* (2008) 8:53. doi: 10.1186/1472-6947-8-53
24. Zhang SL, Chen C, Rao QW, Guo Z, Wang X, Wang ZM, et al. Incidence, prognostic factors and survival outcome in patients with primary hepatic Lymphoma. *Front Oncol.* (2020) 10:750. doi: 10.3389/fonc.2020.00750
25. Ng M, Cunningham D, Norman AR. The frequency and pattern of cardiotoxicity observed with capecitabine used in conjunction with oxaliplatin in patients treated for advanced colorectal cancer (CRC). *Eur J Cancer.* (2005) 41:1542–6. doi: 10.1016/j.ejca.2005.03.027
26. Shiga T, Hiraide M. Cardiotoxicities of 5-fluorouracil and other fluoropyrimidines. *Curr Treat Options Oncol.* (2020) 21:27. doi: 10.1007/s11864-020-0719-1
27. Moslehi JJ. Cardiovascular toxic effects of targeted cancer therapies. *N Engl J Med.* (2016) 375:1457–67. doi: 10.1056/NEJMra1100265
28. Hsu PY, Mammadova A, Benkirane-Jessel N, Désaubry L, Nebigil CG. Updates on anticancer therapy-mediated vascular toxicity and new horizons in therapeutic strategies. *Front Cardiovasc Med.* (2021) 8:694711. doi: 10.3389/fcvm.2021.694711
29. Low SK, Giannis D, Bahaie NS, Trong BLH, Moris D, Huy NT. Competing mortality in patients with neuroendocrine tumors. *Am J Clin Oncol.* (2019) 42:668–74. doi: 10.1097/coc.0000000000000575
30. Guan T, Qiu Z, Su M, Yang J, Tang Y, Jiang Y, et al. Cardiovascular death risk in primary central nervous system lymphoma patients treated with chemotherapy: a registry-based cohort study. *Front Oncol.* (2021) 11:641955. doi: 10.3389/fonc.2021.641955
31. Du B, Wang F, Wu L, Wang Z, Zhang D, Huang Z, et al. Cause-specific mortality after diagnosis of thyroid cancer: a large population-based study. *Endocrine.* (2021) 72:179–89. doi: 10.1007/s12020-020-02445-8
32. Jakobsen L, Niemann T, Thorsgaard N, Thuesen L, Lassen JF, Jensen LO, et al. Dimensions of socioeconomic status and clinical outcome after primary percutaneous coronary intervention. *Circ Cardiovasc Interv.* (2012) 5:641–8. doi: 10.1161/circinterventions.112.968271
33. Shapiro M, Chen Q, Huang Q, Boosalis VA, Yoon CH, Saund MS, et al. Associations of socioeconomic variables with resection, stage, and survival in patients with early-stage pancreatic cancer. *JAMA Surg.* (2016) 151:338–45. doi: 10.1001/jamasurg.2015.4239
34. Aizer AA, Chen MH, McCarthy EP, Mendu ML, Koo S, Wilhite TJ, et al. Marital status and survival in patients with cancer. *J Clin Oncol.* (2013) 31:3869–76. doi: 10.1200/jco.2013.49.6489
35. Xie JC, Yang S, Liu XY, Zhao YX. Effect of marital status on survival in glioblastoma multiforme by demographics, education, economic factors, and insurance status. *Cancer Med.* (2018) 7:3722–42. doi: 10.1002/cam4.1688
36. Shi RL, Qu N, Lu ZW, Liao T, Gao Y, Ji QH. The impact of marital status at diagnosis on cancer survival in patients with differentiated thyroid cancer. *Cancer Med.* (2016) 5:2145–54. doi: 10.1002/cam4.778
37. Costa LJ, Brill IK, Brown EE. Impact of marital status, insurance status, income, and race/ethnicity on the survival of younger patients diagnosed with multiple myeloma in the United States. *Cancer.* (2016) 122:3183–90. doi: 10.1002/cncr.30183
38. Maselko J, Bates LM, Avendaño M, Glymour MM. The intersection of sex, marital status, and cardiovascular risk factors in shaping stroke incidence: results from the health and retirement study. *J Am Geriatr Soc.* (2009) 57:2293–9. doi: 10.1111/j.1532-5415.2009.02555.x

Conflict of Interest: The authors declare that the research was conducted in the absence of any commercial or financial relationships that could be construed as a potential conflict of interest.

frontiers | Frontiers in Cardiovascular Medicine

CASE REPORT
published: 23 June 2022
doi: 10.3389/fcvm.2022.889406

Case Report: Unusual Cause of Chest Pain: A Multi-Image Assessment of a Cardiac Mass

*Javier Serrano-Roman[1], Santiago Saenz-Ancira[1], Jose C. Armendariz-Ferrari[2], Valente Fernandez-Badillo[1], Enrique Solorzano-Pinot[1], Adrian Espejel-Guzman[1], Joaquin Berarducci[1], Alberto Aranda-Fraustro[3], Mauricio Garcia-Cardenas[1] and Nilda Espinola-Zavaleta[1,4]**

[1] Department of Nuclear Cardiology, National Institute of Cardiology Ignacio Chavez, Mexico City, Mexico, [2] Department of Clinical Cardiology and Echocardiography, Hospital Nacional Hipolito Unanue, Lima, Peru, [3] Department of Pathology, National Institute of Cardiology Ignacio Chavez, Mexico City, Mexico, [4] Department of Echocardiography, ABC Medical Center I.A.P, Mexico City, Mexico

OPEN ACCESS

Edited by:
Chun Liu,
Stanford University, United States

Reviewed by:
Gaetano Thiene,
University of Padua, Italy
Bruno Pinamonti,
University Health Organization
Giuliano Isontina (ASU GI), Italy

***Correspondence:**
Nilda Espinola-Zavaleta
niesza2001@hotmail.com

Specialty section:
This article was submitted to Cardio-Oncology, a section of the journal Frontiers in Cardiovascular Medicine

Received: 04 March 2022
Accepted: 31 May 2022
Published: 23 June 2022

Citation:
Serrano-Roman J, Saenz-Ancira S, Armendariz-Ferrari JC, Fernandez-Badillo V, Solorzano-Pinot E, Espejel-Guzman A, Berarducci J, Aranda-Fraustro A, Garcia-Cardenas M and Espinola-Zavaleta N (2022) Case Report: Unusual Cause of Chest Pain: A Multi-Image Assessment of a Cardiac Mass. Front. Cardiovasc. Med. 9:889406. doi: 10.3389/fcvm.2022.889406

Myxomas represent the most common benign primary cardiac tumor, they usually grow out of the interatrial septum into the left atrium with a pedunculated base. Intracardiac masses can be found incidentally on imaging studies, but symptomatology may arise secondary to the mass effect, embolization, and valvular function impairment. We present the case of a 75-year-old woman who arrived at the emergency department with atrial fibrillation and NSTEMI segment elevation myocardial infarction (NSTEMI) secondary to a highly vascularized neoplasm visible by coronary angiography and angiotomography. Scarce reports show high quality multi-imaging assessment of significantly vascularized myxomas with such atypical presentation. High-definition imaging studies played a fundamental role in the surgeon's management of a mass with a complex neovascularization.

Keywords: myxoma, tumor, neovascularization, echocardiography, computed tomography angiography

INTRODUCTION

Primary cardiac tumors are a rare entity with benign etiology in approximately 90%. Myxomas represent the most frequent type with almost 80% and tend to be located in the left atrium (1, 2). The clinical presentation depends on the location and size of the tumor, and whether it is associated with valvular insufficiency, obstruction, or embolic events. Such signs and symptoms may differ among them, such as dyspnea, pulmonary edema, auscultatory findings, and in cases of right-sided masses, foot edema, hepatomegaly, and even ascites.

Case series have shown a relatively high rate of neovascularization in left atrial myxomas (LAM), with an increased use of non-invasive imaging modalities such as Coronary Computed Tomography Angiography (CCTA) in the preoperative evaluation and characterization of highly vascularized neoplasms (3–5). We present a case in which a multi-imagen assessment was performed in order to understand the tumor's enormous blood supply, which influenced the surgical decisions and resulted in the complete recovery of the patient.

CASE DESCRIPTION

A 75-year-old female was admitted into the emergency department due to acute chest pain and dyspnea. There was no history of cardiovascular risk factors, prior heart disease, or trauma and the patient was otherwise in good health. On physical examination, jugular ingurgitation and bilateral rales in pulmonary fields were identified, heart sounds were arrhythmic and tachycardic (150 bpm) without murmurs. Other vital signs showed hypotension (80/60 mmHg) and tachypnea (26 rpm). Chest x-ray depicted cardiomegaly, left and right atrial enlargement and signs of pulmonary congestion. An initial electrocardiogram demonstrated atrial fibrillation (AF) and ST segment depression in the anterolateral wall (V1-V5), suggestive of a non-ST segment elevation myocardial infarction (NSTEMI) (**Table 1**). Baseline cardiac enzymes assessment surpassed the upper limit for CK 2919 U/L, CK-MB 57.5 U/L, and troponin I 0.058 ng/mL.

Risk stratification scales were calculated, obtaining 189 and 4 points in the GRACE and TIMI scores, respectively. Initial management included double antiplatelet therapy with aspirin and clopidogrel, and anticoagulation with enoxaparin. The atrial fibrillation reverted with the administration of Lanatoside C.

DIAGNOSTIC ASSESSMENT

The patient was initially managed as a NSTEMI, and an urgent coronary angiography (CA) was performed in order to discard coronary artery occlusion. The study showed abnormal and significant neovascularization within the left atrium and a 90% obstruction at the origin of the marginal branch, which suggested neovascularization of an atrial mass. (**Figures 1A,B** and **Supplementary Video 1**).

Transthoracic echocardiogram (TTE) showed a large echogenic oval mass in the left atrium attached to the interatrial septum by a short pedicle measuring 5 × 7 × 6 cm, as well as moderate to severe mitral regurgitation (MR) by color-Doppler. The biventricular systolic function was normal (LVEF-63% and TAPSE-21 mm). Two dimensional-Doppler-transesophageal echocardiography showed a giant vascularized heterogeneous mass. 3D-TTE accurately identified the mass protruding through the mitral valve into the left ventricle during end-diastole and the 2D-TTE color flow and continuous wave Doppler in four chamber view showed a diastolic mitral peak velocity of 2.08 m/s, maximum gradient of 17 mmHg and mean gradient of 10.33 mmHg (**Figures 2A–C** and **Supplementary Video 2**).

After the echocardiographic findings, the heart team agreed on performing a CCTA, which showed a non-infiltrative and very vascularized mass attached to the interatrial septum (**Figures 3A,B**). A 3D-CCTA reconstruction additionally showed the significant vascularity of the tumor, characterized the anatomy of the coronary arteries and the origin of the neovascularization (**Figure 3C**). Double arterial blood supply was observed, with anomalous vessels arising from the right coronary artery and the circumflex artery (**Figure 3D** and **Supplementary Video 3**).

The patient was scheduled for surgical resection, which consisted of median sternotomy, and bicaval bypass with cardioplegic cardiac arrest. Before the tumor resection, the surgical team ligated both feeding arteries. An oval mass presenting multiple hemorrhagic areas within was removed and the final measurement was 7 × 4 × 5 cm. Pathologic findings were consistent with a LAM (**Figures 4A–C**).

One month after surgery, a 2D-TTE demonstrated a diastolic mitral peak velocity of 0.67 m/s, maximum gradient of 1.79 mmHg, and mean gradient of 1.07 m/s and mild MR (**Figure 4D**). Atrial fibrillation and tumor recurrence were not detected in the following 18 months of follow-up.

TABLE 1 | Timeline.

Day 0
- A 75-year-old female was admitted into the emergency department due to acute chest pain and dyspnea.
- *Chest x-ray* evidenced cardiomegaly, atrial enlargement and pulmonary congestion.
- *Electrocardiogram*. Atrial fibrillation, non-ST segment elevation myocardial infarction.
- *Laboratory*. CK, CK-MB, and troponin I with increased values.
- *Urgent coronary angiography* showed abnormal neovascularity inside the left atrium and coronary artery disease.

Day 1
- *Transthoracic and transesophageal echocardiogram* evidenced an enormous and highly vascularized mass in the left atrium.

Day 2
- *Coronary computed tomography angiography* revealed the complex network of blood vessels inside the mass, which arised from the right coronary and circumflex arteries.

Day 4
- Artery ligation and tumor resection.

Day 6
- Histological confirmation of cardiac myxoma.

Month 1
- Follow-up Doppler echocardiography demonstrated adequate recovery, mild mitral regurgitation, and no tumor recurrence.
- Patient is asymptomatic.

DISCUSSION

The clinical presentation of left atrial tumors depends on location and size, and whether it is associated with valvular insufficiency, obstruction, or embolic events. The initial assessment of atypical presentations may be challenging. Regarding the case, the mechanisms responsible for the origin of the EKG findings and manifestations could be due to two different situations. Fast AF and hypotension may have resulted in an oxygen supply demand imbalance (type 2 NSTEMI), thus the absence of findings in the CA that could explain the ST segment abnormalities and the complete recovery after surgical removal. Similarly, LAM should always be considered as an embolic source in healthy patients with systemic thromboembolism, including coronary artery embolization, which is extremely rare (0.06%) (6). Spontaneous recanalization prior to CA could also explain the reported findings.

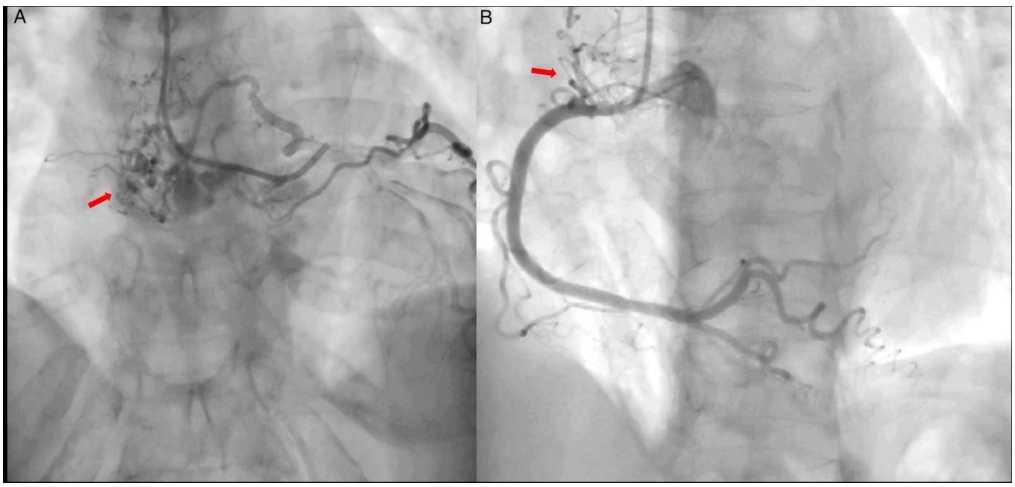

FIGURE 1 | Coronary angiography. **(A)** Left coronary artery showing abnormal vascular structures (arrow) suggestive of arteriovenous fistula and a highly vascularized mass. Marginal branch demonstrates proximal 90% obstruction (**Supplementary Video 1**). **(B)** Right coronary artery shows no obstruction, abnormal vascular structures are also present (arrow).

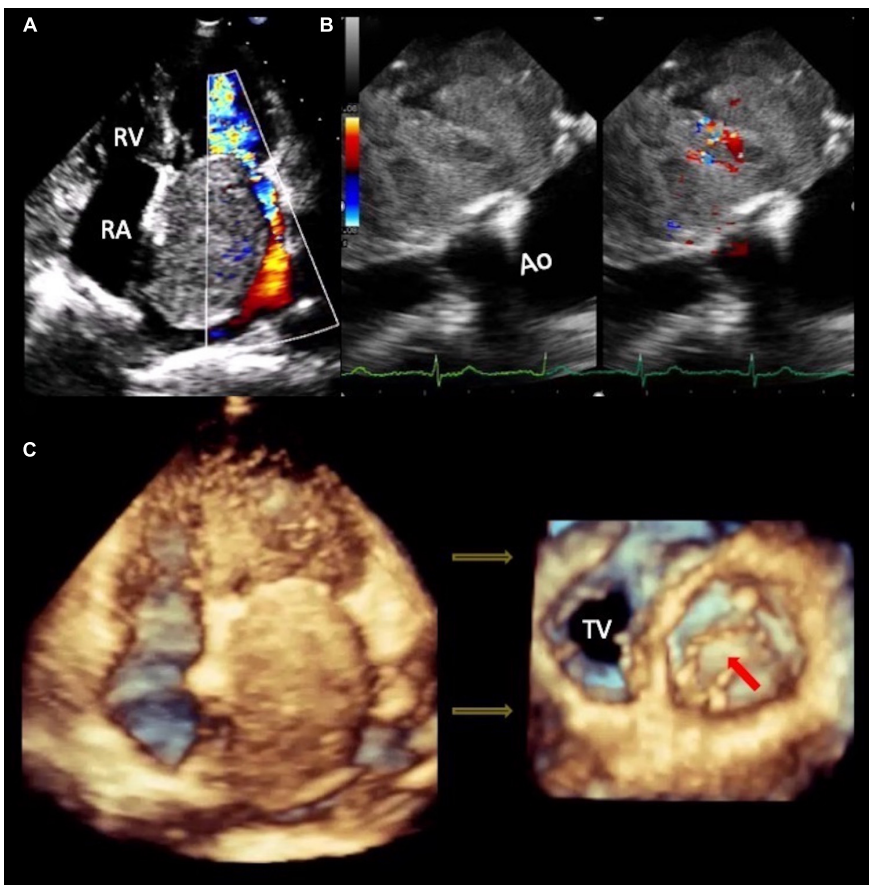

FIGURE 2 | Echocardiogram. **(A)** 2D-TTE four-chamber view shows a large echogenic oval mass that occupies practically the entire left atrium, with regular borders, heterogeneous echogenicity, adhered to the interatrial septum by a short pedicle and moderate to severe mitral regurgitation in the color Doppler. **(B)** 2D-Transesophageal echocardiogram and color-Doppler evidenced significant vascularization inside the mass. **(C)** 3D-TTE shows the mass protruding through the mitral valve into the left ventricle during end-diastole (**Supplementary Video 2**). Ao, aorta; RA, right atrium; RV, right ventricle; TTE, transthoracic echocardiogram; TV, tricuspid valve.

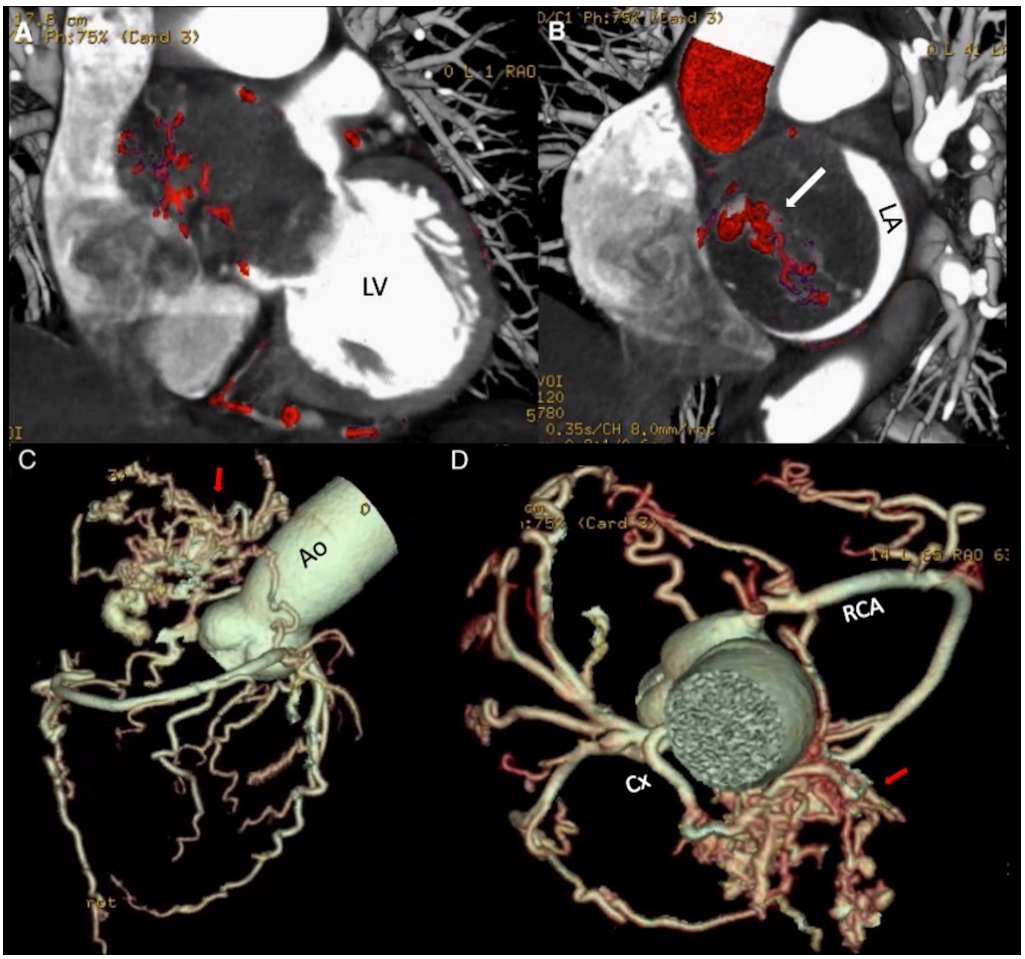

FIGURE 3 | (A,B) Coronary Computed Tomography Angiography. Hypodense mass located in the left atrium attached to the interatrial septum, with a dense network of blood vessels within. The intra- atrial mass protrudes through the mitral valve into the left ventricle during diastole, causing impairment of the atrial emptying and mitral valve closure. **(C,D)** Coronary Computed Tomography Angiography reconstruction. Complex blood vessel network (arrows) anastomosed to branches of the circumflex artery and the right coronary artery (**Supplementary Video 3**). Ao, aorta; Cx, circumflex artery; LA, left atrium; LV, left ventricle; RCA, right coronary artery.

In any case, the cardiac territory supplied by an obstructed artery is at increased risk of hypoxic cell injury, as seen during CA in the marginal branch, which showed a concomitant luminal reduction of 90%, which may have further contributed to the initial presentation in our patient.

Imaging evaluation of a cardiac mass includes echocardiography as the initial study to determine its location, size, and mobility. Other imaging modalities are required to visualize the characteristics of the coronary arteries and their relationship to the neovascularization that can be found in myxomas, however, these techniques may not be routinely available in some countries and were highly underused a few years ago, as described by Elbardissi et al. (7), when they evaluated 278 patients with cardiac masses, which were mainly diagnosed by echocardiography and only a few underwent CA (n = 33, 10%) or CCTA (n = 9, 3%). Case series have shown a relatively high rate of low neovascularization in myxomas, with an increased and standardized use of new imaging modalities such as cardiac magnetic resonance imaging (MRI) and CCTA for evaluating this type of tumors, either as a complementary tool of CA or by replacing it (3–5). CCTA overcomes the limitations of echocardiography and CA by displaying detailed images of the origin and morphology of tortuous and dilated blood vessels; and, at the same time, reliably ruling out coronary artery disease (CAD) in patients scheduled for surgical resection (4).

Kim et al. (5) described 2 patients who were initially diagnosed with LAM by echocardiography and subsequently underwent preoperative CCTA instead of coronary angiography to rule out concomitant CAD, which provided more information about the vasculature of the mass. On the other hand, this technique avoids the risk of embolization and other complications of CA and can provide information that modifies the chosen surgical method, such as ligation of the feeding arteries before surgical resection (4).

Differential diagnosis of LAM mainly includes cardiac malignant tumors such as angiosarcoma and thrombi. Large

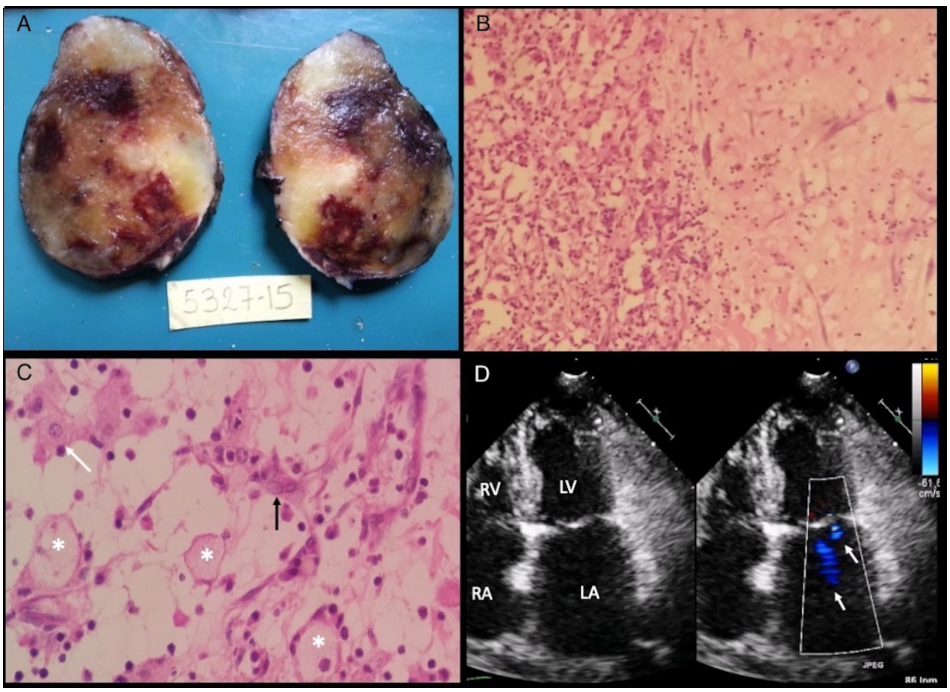

FIGURE 4 | Macroscopic and microscopic specimen findings. **(A)** Oval mass of 80 grams, 7 × 4 × 5 cm of diameter with a smooth surface showing white/yellow colors with zones of hemorrhagic aspect. Intact capsule that delimits the entire mass, compatible with its benign and non-invasive nature. **(B)** On the left side, a pattern of glanduloid/vascular cavities with abundant inflammatory lymphocytic infiltrate. On the right side, homogeneous stroma with clear spaces and isolated myxoma cells with fusi morphology. H/E10x **(C)** Myxoma's stroma shows decreased cellular density and multiple blood vessels (asterisks). Stellate appearance cells present eosinophilic cytoplasm and round nucleus (white arrow). Syncytial Cells with a string morphology (black arrow). H/E 40x. **(D)** Follow-up echocardiogram. 2D and color flow TTE in four-chamber view with 2 jets of mild mitral regurgitation (white arrows) and no cardiac mass in the left atrium. Abbreviations as before.

thrombi may represent a diagnostic challenge by using echocardiography alone, but characteristic findings include attachment to the posterior left atrial wall, a broad base and tend to be immobile, contrary to LAM. Additionally, malignant tumors tend to be highly vascularized masses which can be observed by using contrast echocardiography, which provides specific information for differentiating malignant from benign neoplasms. If low vascularization is present, slow contrast filling of the mass would be observed, as usually occurs in benign tumors, such as cardiac myxomas. In this particular case, due to the extreme vascularization, a contrast agent would show a rapid filling and late opacification, simulating a malignant process, which emphasizes the importance of pathologic findings for the final diagnosis of a cardiac tumor. Regarding thrombi, which are usually not vascularized, contrast echocardiography would show no filling of the contrast agent (8).

As mentioned, the pathological findings represent a fundamental tool for the final diagnosis of a cardiac mass, whereas a multi-imaging evaluation helps in the assessment of the morphology and characteristics of the tumor and its relationship with the surrounding cardiac and paracardiac structures, and therefore is particularly useful for the surgeon in order to precisely plan the surgical intervention.

In our case, CCTA showed that the tumor's enormous blood supply came from the right coronary and circumflex arteries, which helped the heart team understand the complexity of the myxoma vasculature and ligate both feeding arteries before the mass resection. Therefore, CCTA may confer a better alternative than CA in the evaluation of cardiac masses and in their differential diagnosis, especially in the context of a highly vascularized myxoma and when the patient is older than 40 years to rule out concomitant CAD.

On the other hand, cardiac MRI provides images suitable for the same purpose without exposing the patient to ionizing radiation, but it relies on patient cooperation, implanted magnetic devices, and is less useful than CCTA in evaluating coronary arteries during an acute event, which may be very important in the context of LAM, specifically in urgent atypical presentations as the one described in this case.

For the preoperative evaluation of myxomas, an imaging modality such as MRI, CCTA or CA must be performed in order to better characterize the mass and evaluate CAD. Preoperative CCTA represents an accurate method to assess myxoma morphology, vascularization, and avoids CA risks. Three-dimensional reconstructions may be even more useful in the decision making of the surgical team.

DATA AVAILABILITY STATEMENT

The datasets for this article are not publicly available due to concerns regarding participant/patient anonymity.

Requests to access the datasets should be directed to the corresponding author.

ETHICS STATEMENT

The studies involving human participants were reviewed and approved by the Research and Ethics Committee of National Institute of Cardiology Ignacio Chavez. The patients/participants provided their written informed consent to participate in this study. The patients/participants provided their written informed consent for the publication of the case report, and for the publication of any potentially identifiable images or data included in this article.

AUTHOR CONTRIBUTIONS

JS-R, SS-A, and NE-Z collected the data and headed the elaboration of the present manuscript. VF-B, ES-P, and AE-G reviewed the recent literature. JA-F performed the echocardiogram and analyzed the CCTA. JB and MG-C carefully revised the manuscript. AA-F interpreted the macroscopic and microscopic images. All authors contributed to the conception, analysis, and design of the complete case report, revising of the manuscript, enhancing its intellectual content, and approving the final version of the manuscript.

FUNDING

This work was supported by the National Institute of Cardiology Ignacio Chávez.

ACKNOWLEDGMENTS

We acknowledge the heart team of the National Institute of Cardiology Ignacio Chávez.

SUPPLEMENTARY MATERIAL

The Supplementary Material for this article can be found online at: https://www.frontiersin.org/articles/10.3389/fcvm.2022.889406/full#supplementary-material

REFERENCES

1. Reenen K. Cardiac myxomas. *N Engl J Med.* (1995) 333:1610–7. doi: 10.1056/NEJM199512143332407
2. Dubey L, Chaurasia A. Neovascularization in left atrial myxoma. *Int Cardiovasc Res J.* (2012) 6:133–4.
3. Jung H, Doh J, Chang W. Multi-modality imaging of a left atrial myxoma. *SAGE Open Med Case Rep.* (2017) 5:2050313X17736230. doi: 10.1177/2050313X17736230
4. Janas R, Jutley R, Fenton P, Sarkar P. Should we perform preoperative coronary angiography in all cases of atrial myxomas? *Catheter Cardiovasc Interv.* (2006) 67:379–83. doi: 10.1002/ccd.20643
5. Kim Y, Yong H, Kang E, Woo O. Left atrial myxoma with neovascularization: detected on cardiac computed tomography angiography. *Int J Cardiovasc Imaging.* (2009) 25(Suppl. 1):95–8. doi: 10.1007/s10554-008-9416-z
6. Latifi AN, Ibe U, Gnanaraj J. A case report of atrial myxoma presenting with systemic embolization and myocardial infarction. *Eur Heart J Case Rep.* (2019) 3:ytz104. doi: 10.1093/ehjcr/ytz104
7. Elbardissi AW, Dearani JA, Daly RC, Mullany CJ, Orszulak TA, Puga FJ, et al. Survival after resection of primary cardiac tumors: a 48year experience. *Circulation.* (2008) 118(14 Suppl.):S7–15. doi: 10.1161/CIRCULATIONAHA.107.783126
8. Uenishi EK, Caldas MA, Saroute AN, Tsutsui JM, Piotto GH, Falcão SN, et al. Contrast echocardiography for the evaluation of tumors and thrombi. *Arq Bras Cardiol.* (2008) 91:e48–52. doi: 10.1590/s0066-782x2008001700015

Conflict of Interest: The authors declare that the research was conducted in the absence of any commercial or financial relationships that could be construed as a potential conflict of interest.

Publisher's Note: All claims expressed in this article are solely those of the authors and do not necessarily represent those of their affiliated organizations, or those of the publisher, the editors and the reviewers. Any product that may be evaluated in this article, or claim that may be made by its manufacturer, is not guaranteed or endorsed by the publisher.

frontiers | Frontiers in Cardiovascular Medicine

TYPE Original Research
PUBLISHED 12 August 2022
DOI 10.3389/fcvm.2022.922811

OPEN ACCESS

EDITED BY
Reto Asmis,
Wake Forest School of Medicine,
United States

REVIEWED BY
Fabiana Lucà,
Grande Ospedale Metropolitano
Bianchi Melacrino Morelli, Italy
Chen Zhao,
Nanjing Medical University, China

*CORRESPONDENCE
Ben He
heben241@126.com

SPECIALTY SECTION
This article was submitted to
Cardio-Oncology,
a section of the journal
Frontiers in Cardiovascular Medicine

RECEIVED 18 April 2022
ACCEPTED 18 July 2022
PUBLISHED 12 August 2022

CITATION
Zhao Y, Qin F, Ji Q, Xia W and He B (2022) Primary site as a novel prognostic factor for cardiovascular mortality post-radiotherapy in limited-stage small cell lung cancer: A large population-based study.
Front. Cardiovasc. Med. 9:922811.
doi: 10.3389/fcvm.2022.922811

Primary site as a novel prognostic factor for cardiovascular mortality post-radiotherapy in limited-stage small cell lung cancer: A large population-based study

Yuwei Zhao[1], Fen Qin[2], Qingqi Ji[1], Wuyan Xia[3] and Ben He[1,4]*

[1]Department of Cardiology, Shanghai Chest Hospital, Shanghai Jiao Tong University, Shanghai, China, [2]Department of Cardiology, The First Affiliated Hospital of Zhengzhou University, Zhengzhou, China, [3]Department of Radiation Oncology, Shanghai Chest Hospital, Shanghai Jiao Tong University, Shanghai, China, [4]Clinical Research Center, Shanghai Jiao Tong University School of Medicine, Shanghai, China

Background: The effect of primary site on cardiovascular mortality (CVM) post-radiotherapy (RT) in patients with limited-stage small cell lung cancer (LS-SCLC) remains unclear.

Methods: We screened the Surveillance, Epidemiology, and End Results (SEER) database between 1988 and 2013. We used cumulative incidence function (CIF) curves to compare CVM incidences, and performed Cox proportional hazards and Fine-Gray competing risk analyses to identify independent risk factors of CVM. Propensity score matching (PSM) analysis was conducted.

Results: Among enrolled 4,824 patients (median age 57 years old, 49.2% were male), CVM accounts for 10.0% of all deaths after 5 years since cancer diagnosis. Hazard ratios (HRs) for CVM were 1.97 (95% CI: 1.23–3.16, $P = 0.005$) for main bronchus (MB) patients, 1.65 (95% CI: 1.04–2.63, $P = 0.034$) for lower lobe (LL) patients and 1.01 (95% CI: 0.40–2.59, $P = 0.977$) for middle lobe (ML) patients compared to upper lobe (UL) patients. CIF curves showed that the cumulative CVM incidence was greater in the re-categorized MB/LL group compared to UL/ML group both before PSM ($P = 0.005$) and after PSM ($P = 0.012$). Multivariate regression models indicated that MB/LL was independently associated with an increased CVM risk, before PSM (HR_{Cox}: 1.79, 95% CI: 1.23–2.61, $P = 0.002$; $HR_{Fine-Gray}$: 1.71, 95% CI: 1.18–2.48, $P = 0.005$) and after PSM (HR_{Cox}: 1.88, 95% CI: 1.20–2.95, $P = 0.006$; $HR_{Fine-Gray}$: 1.79, 95% CI: 1.15–2.79, $P = 0.010$).

Conclusions: MB/LL as the primary site is independently associated with an increased CVM risk post-RT in patients with LS-SCLC.

KEYWORDS

small cell lung cancer, radiotherapy, tumor primary site, cardiovascular mortality, SEER

Introduction

Radiotherapy (RT) is frequently used as an essential adjuvant to chemotherapy or surgery in thoracic malignancies. RT has been shown to improve cancer-specific survival; however, it has been implicated in pulmonary and cardiac complications because of reported acute and chronic radiation-induced injuries to healthy tissues in the radiation field (1–4). Some reports have focused on cardiovascular toxicities post-thoracic RT in long-term cancer survivors, including those with breast cancer and Hodgkin lymphoma (3, 5–7).

Lung cancer is a major malignancy that accounts for the highest morbidity and mortality rates worldwide (8). Adverse effects of RT on the cardiovascular system in patients with lung cancer have recently attracted wider attention and have gained increasing interest in the field of cardio-oncology. Previous studies have shown that RT could increase the incidence of cardiovascular complications in patients with non-small cell lung cancer (NSCLC) (9–14). However, investigations on RT-related cardiovascular sequelae in patients with limited-stage small cell lung cancer (LS-SCLC) remain scarce. This may be partially because, historically, LS-SCLC was considered to have an unfavorable median overall survival (OS) of approximately 1 year before the 1990s (15). Nevertheless, survival rates for patients with LS-SCLC have gradually improved due to wide-spread application of early chest CT screening in high-risk populations, advanced modern RT techniques, more accurate staging paradigms, and recent promising treatment strategies (16, 17). Thoracic RT combined with chemotherapy (CTX) is considered the first-line standard therapy for LS-SCLC (16, 17). However, more extensive studies are needed to evaluate RT-related cardiovascular toxicities in patients with LS-SCLC.

The primary site as a conventional clinical characteristic affecting a lung cancer treatment strategy has currently been recognized as an important prognostic factor for OS and tumor-specific prognosis (18–20). With a disparity in the distance between tumor location and heart/great vessels, potential RT-induced cardiovascular injury may be further distinctive risk (21); however, few relevant reports are available.

This study aimed to identify significant prognostic factors concerning CVM post-RT for patients with LS-SCLC, and to explore the effect of different primary site-based RTs on CVM in a large population of patients with LS-SCLC using data from the Surveillance, Epidemiology, and End Results (SEER) database.

Materials and methods

Patients and data sources

The SEER database [SEER 18 Regs Custom Data (with additional treatment fields), November 2018 Sub] was queried using SEER*Stat software (version 8.3.6). Inclusion criteria for patients were as follows: patients aged ≥18 and <65 years and diagnosed with LS-SCLC between 1988 and 2013; patients treated with external beam RT, and; patients with only one primary tumor, a positive histology, available clinical information, active follow-up, and complete dates. Older adult patients with more confounding factors such as coronary heart disease (CHD), hyperlipidemia, hypertension, and diabetes mellitus (DM) were not enrolled for the purpose of alleviating, at least partially, the effects of confounders on CVM in patients post-RT (1, 2, 14), and because younger patients are reported to be more vulnerable to radiation-induced cardiovascular injury (22). The specific time period of 1988–2013 was selected because American Joint Committee on Cancer (AJCC) staging for SCLC in the SEER database started in 1988, whereas 2013 was the final year for analysis in which adequate follow-up to assess post-treatment CVM was possible. Exclusion criteria included: unknown race, not the only primary cancer, receipt of surgical treatment, no/unknown external beam radiation, no/unknown chemotherapy, bilateral or unknown laterality, overlapping or unknown primary site or loss of follow-up information. Inclusion and exclusion criteria for the study population is outlined in Figure 1.

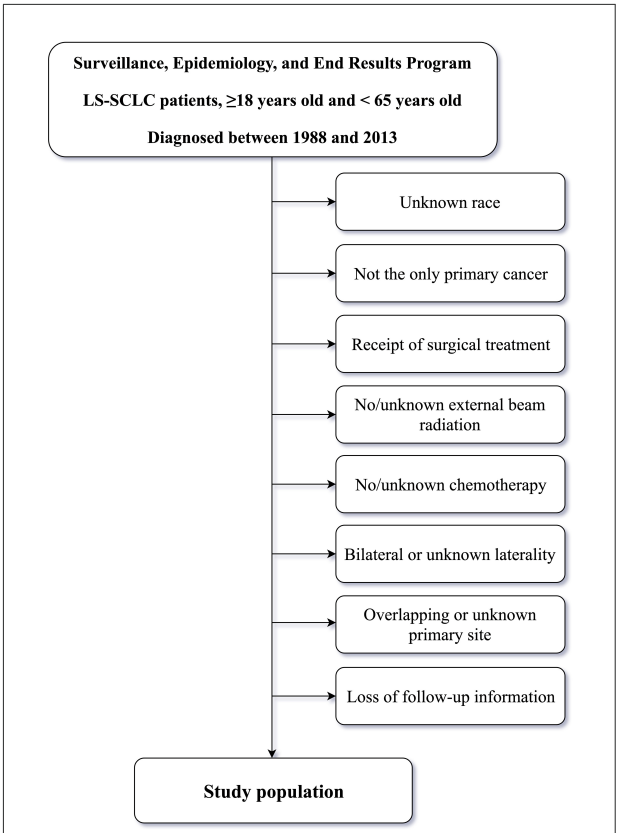

FIGURE 1
The flow chart of inclusion and exclusion criteria for the study population.

TABLE 1 The baseline clinical and prognostic characteristics of total study population.

Variables	Number	%
Total	4,824	100.0%
Primary site		
Upper lobe	2,890	59.9%
Middle lobe	247	5.1%
Main bronchus	748	15.5%
Lower lobe	939	19.5%
Age, years		
≤57	2,487	51.6%
>57	2,337	48.4%
Sex		
Male	2,373	49.2%
Female	2,451	50.8%
Race		
White	4,071	84.4%
Black	538	11.2%
Other	215	4.5%
Marriage		
Unmarried	1,957	40.6%
Married	2,717	56.3%
Unknown	150	3.1%
Year of diagnosis		
1988–2003	2,118	43.9%
2004–2013	2,706	56.1%
AJCC stage		
I-II	724	15.0%
III	4,100	85.0%
Laterality		
Left	1,965	40.7%
Right	2,859	59.3%
Prognosis		
CVM	113	2.3%
NCVM	4,212	87.3%
Alive	499	10.3%

AJCC, American Joint Committee on Cancer; CVM, cardiovascular mortality; NCVM, non-cardiovascular mortality. Percentages might not add up to 100% because of rounding.

This study was conducted in accordance with the Declaration of Helsinki (as revised in 2013) and complied with the requirements of the Institutional Review Board of Shanghai Chest Hospital, Shanghai Jiao Tong University. The authors have gotten the access to and approval from the SEER database (accession and approval number: 13236-November 2019). The need for informed consent has been waived due to the retrospective nature of the study and because SEER database is a public anonymized database.

Definition of LS-SCLC

LS-SCLC was defined as AJCC stage I-III malignancies with primary sites in the lung or bronchus [International Classification of Diseased for Oncology-3 (ICD-O-3)/WHO 2008: Lung and Bronchus]. Histological types were as follows: ICD-O-3 codes: 8002, 8041-8045. Primary sites were as follows: main bronchus (MB) (C34.0), upper lobe (UL) (C34.1), middle lobe (ML) (C34.2), and lower lobe (LL) (C34.3).

Research variables

Demographics and clinicopathologic data, such as age, sex, race, marriage, year of diagnosis, AJCC stage, laterality and primary site were collected. CVM was defined as death due to cardiovascular diseases using the following ICD-10 codes: I00-I52 and I70-I79, including conditions such as diseases of the heart, hypertension without heart disease, atherosclerosis, aortic aneurysm and dissection, and other diseases of the arteries, arterioles, and capillaries. Non-cardiovascular mortality (NCVM) was defined as death due to other causes, excluding CVM.

Statistical analysis

Statistical analysis was performed using either R (version 3.6.0, R Foundation for Statistical Computing, Vienna, Austria) or Stata (version 15.0, College Station, Texas, USA) software. All statistical tests were two-sided, and the significance level was set at 0.05. As the only continuous variable, age was expressed as median [with inter-quartile range (IQR)] for non-normally distributed data and compared using a Kruskal-Wallis test between the groups. Categorical variables were expressed as numbers (percentages) and then compared using a chi-square test.

We generated cumulative incidence function (CIF) curves using univariate Fine-Gray competing risk regression models to compare the cumulative incidences of CVM or NCVM between the groups. Univariate and multivariate Cox proportional hazards regression models were applied to identify factors associated with CVM or NCVM risk. Based on results obtained from multivariate Cox proportional hazards regression models, the UL and the ML as primary sites were re-categorized into a UL/ML group, and the MB and the LL were combined to form a MB/LL group. Accounting for mortality from other causes, univariate and multivariate Fine-Gray competing risk regression models (23) were used to validate factors associated with CVM risk and obtain more accurate results. The propensity score matching (PSM) method (24, 25) was used to balance the baseline bias between the UL/ML and MB/LL groups. A greedy

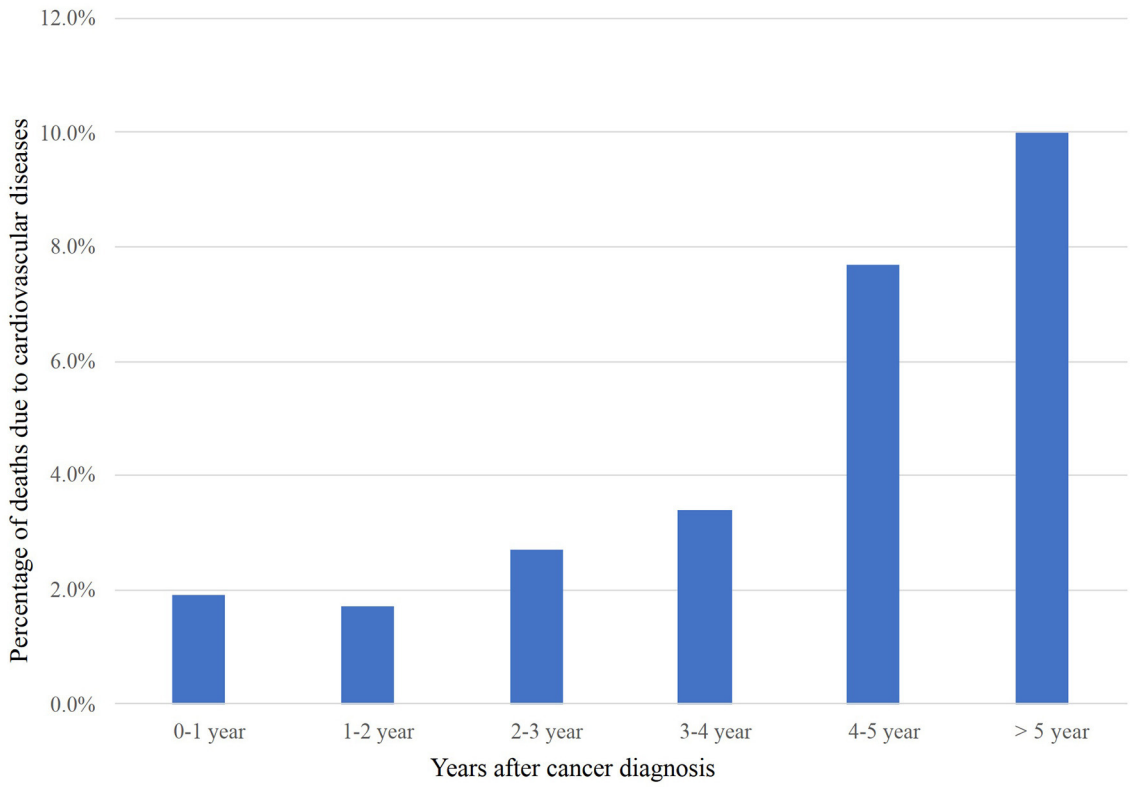

FIGURE 2
CVM post-radiotherapy as a proportion of all deaths within a given time period after LS-SCLC diagnosis. CVM, cardiovascular mortality; LS-SCLC, limited-stage small cell lung cancer.

matching algorithm was used for PSM and the caliper was set at 0.02.

Results

Patient demographics and clinical characteristics

A flowchart indicating inclusion and exclusion for the study population is outlined in Figure 1. We enrolled 4,824 patients with LS-SCLC {median age, 57 [interquartile range (IQR), 52–61] years; males, 49.2%}, of whom 2,487 (51.6%) were ≤57 years old, 2,373 (49.2%) were male, and 84.4% were of White ethnicity. There were 1,957 (40.6%) and 2,717 (56.3%) unmarried and married patients, respectively. In addition, 2,118 (43.9%) patients had been diagnosed with LS-SCLC in the 1988–2003 period, and 2,706 (56.1%) patients in the 2004–2013 period. In terms of AJCC stage, 15.0% and 85.0% of patients were classified in Stage I-II and Stage III, respectively. In terms of laterality, 1,965 (40.7%) patients had left-sided tumors and 2,859 (59.3%) had right-sided tumors. In terms of primary site tumor location, 2,890 (59.9%) patients had primary site tumors in the UL, 247 (5.1%) patients had primary site tumors in the ML, 748 (15.5%) patients had primary site tumors in the MB, and 939 (19.5%) patients had primary site tumors in the LL.

The overall incidence of CVM and NCVM at the follow-up endpoint (November 2018) was 2.3 and 87.3%, respectively. Baseline clinical and prognostic characteristics concerning the study population are shown in Table 1. The percentage of deaths due to cardiovascular diseases following diagnosis was tabulated (Figure 2). Within the first year of diagnosis, 1.9% of all deaths were CVM-related and this percentage increased from 1.7% in year two to 2.7% in year three, to 3.4% in year four, to 7.7% in year five, and to 10.0% after 5 years, showing an increasing trend for percentage of deaths due to CVM along with patients' survival time.

Analysis of CVM based on different variables

Primary sites were initially divided into UL, ML, MB, and LL groups. CIF curves showed no significant differences in cumulative incidences of CVM between groups according to age,

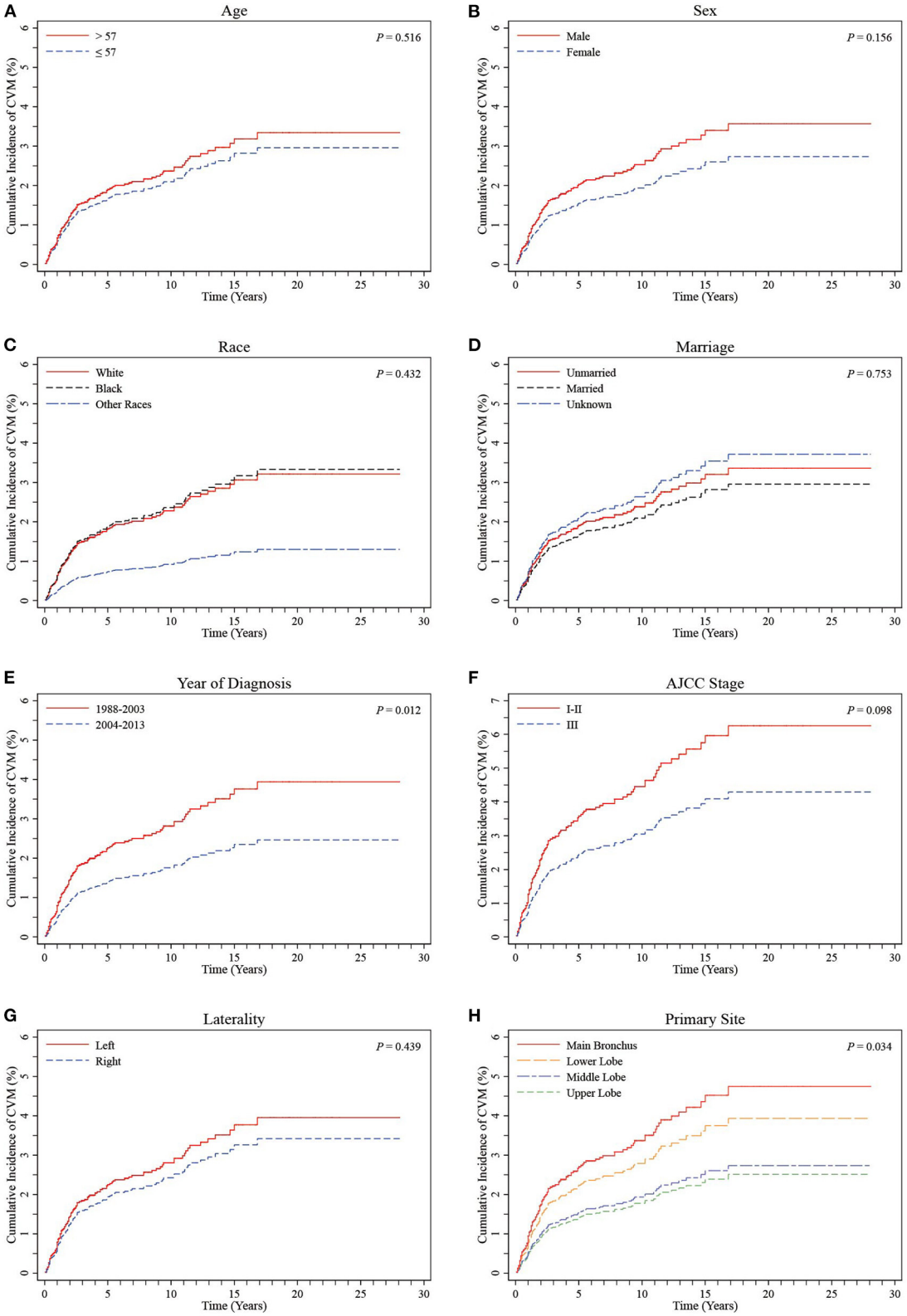

FIGURE 3
CIF curves of CVM by different variables in LS-SCLC patients. **(A)** Age; **(B)** Sex; **(C)** Race; **(D)** Marriage; **(E)** Year of diagnosis; **(F)** AJCC stage; **(G)** Laterality; **(H)** Primary site (stratified into UL, ML, MB and LL groups). CIF: cumulative incidence function; CVM: cardiovascular mortality; AJCC, American Joint Committee on Cancer; LS-SCLC, limited-stage small cell lung cancer.

TABLE 2 Cox proportional hazards regression models for predictors of CVM.

Variables	Group	Cox proportional hazards (Univariate)		Cox proportional hazards (Multivariate)	
		HR (95% CI)	*P*-value	HR (95% CI)	*P*-value
Primary site	Upper lobe	Reference		Reference	
	Middle lobe	0.97 (0.39–2.44)	0.957	1.01 (0.40–2.59)	0.977
	Main bronchus	1.91 (1.20–3.06)	0.007	1.97 (1.23–3.16)	0.005
	Lower lobe	1.65 (1.04–2.63)	0.033	1.65 (1.04–2.63)	0.034
Age, years	≤57	Reference		Reference	
	>57	1.41 (0.97–2.05)	0.071	1.45 (1.00–2.12)	0.052
Sex	Male	Reference		Reference	
	Female	0.64 (0.44–0.94)	0.021	0.59 (0.40–0.87)	0.007
Race	White	Reference		Reference	
	Black	1.15 (0.65–2.06)	0.631	1.07 (0.60–1.93)	0.813
	Other	0.41 (0.10–1.67)	0.213	0.37 (0.09–1.49)	0.161
Marriage	Unmarried	Reference		Reference	
	Married	0.75 (0.51–1.11)	0.150	0.70 (0.47–1.04)	0.075
	Unknown	1.01 (0.36–2.81)	0.982	1.03 (0.37–2.87)	0.953
Year of diagnosis	1988–2003	Reference		Reference	
	2004–2013	0.63 (0.42–0.92)	0.019	0.64 (0.43–0.95)	0.028
AJCC stage	I–II	Reference		Reference	
	III	0.94 (0.59–1.50)	0.808	1.03 (0.64–1.64)	0.913
Laterality	Left	Reference		Reference	
	Right	0.83 (0.57–1.20)	0.316	0.82 (0.56–1.21)	0.327

CVM, cardiovascular mortality; HR, hazard ratio; CI, confidence interval; AJCC, American Joint Committee on Cancer.

sex, ethnicity, marital status, AJCC stage, or laterality (all $P > 0.05$, Figures 3A–D,F,G). A comparison between time periods for diagnosis showed a significantly higher cumulative incidence of CVM in the 1988-2003 period relative to the 2004–2013 period ($P = 0.012$, Figure 3E). Additionally, there was a significant difference between the four groups in terms of the primary sites ($P = 0.034$, Figure 3H).

Multivariate Cox proportional hazards regression models showed independent predictors of CVM risk in patients with LS-SCLC, including sex [female vs. male: hazard ratio (HR) 0.59, 95% confidence interval (CI) 0.40–0.87; $P = 0.007$], time period for diagnosis (2004–2013 vs. 1988–2003, HR 0.64, 95% CI 0.43–0.95; $P = 0.028$), and primary site (ML *vs.* UL, HR 1.01, 95% CI 0.40–2.59, $P = 0.977$; MB vs. UL, HR 1.97, 95% CI 1.23–3.16, $P = 0.005$, and; LL vs. UL, HR 1.65, 95% CI 1.04–2.63, $P = 0.034$). A summary of the results of Cox proportional hazards regression models used to predict CVM risk are listed in Table 2.

Analysis of CVM based on primary site stratification across UL/ML and MB/LL groups before and after PSM

Based on the results obtained from multivariate Cox proportional hazards regression models, patients with UL and ML primary site tumors were grouped together into a UL/ML group, and patients with MB and LL primary site tumors were combined to form an MB/LL group. The proportion of patients with left-sided primary site tumors was significantly higher in the MB/LL group than in the UL/ML group before PSM (45.1 vs. 38.4%, $P < 0.001$). To prevent baseline bias, 1,687 patients in the UL/ML group were matched 1:1 with those from the MB/LL group using the PSM method, which showed a good match in terms of demographic and clinicopathologic characteristics (Table 3). We found a higher CVM incidence at the end of the follow-up (November 2018) in patients in the MB/LL group compared to those in the UL/ML group. We observed a before PSM CVM incidence of 3.2% and 1.9% ($P = 0.005$) in the MB/LL and UL/ML groups, respectively, and 3.2 and 1.8% ($P = 0.011$) after PSM, respectively (Table 3). CIF curves showed that the cumulative CVM incidence was significantly higher in the MB/LL group than in the UL/ML group before PSM ($P = 0.005$, Figure 4A) and after PSM ($P = 0.012$, Figure 4B).

Regression analyses showed that MB/LL primary site tumors were independently associated with an increased CVM risk compared with UL/ML primary site tumors in patients with LS-SCLC before and after PSM (Tables 4, 5). Specifically, multivariate Cox models showed an HR of 1.79 (95% CI 1.23–2.61, $P = 0.002$), whereas multivariate Fine-Gray models indicated an HR of 1.71 (95% CI 1.18–2.48, $P = 0.005$) before

TABLE 3 The baseline clinical and prognostic characteristics of LS-SCLC patients stratified into UL/ML and MB/LL groups by primary site before and after PSM.

Variables	Before PSM			After PSM		
	UL/ML ($n = 3,137$)	MB/LL ($n = 1,687$)	*P*-value	UL/ML ($n = 1,687$)	MB/LL ($n = 1,687$)	*P*-value
Age, years			0.915			0.470
≤57, no. (%)	1,615 (51.5%)	872 (51.7%)		850 (50.4%)	872 (51.7%)	
>57, no. (%)	1,522 (48.5%)	815 (48.3%)		837 (49.6%)	815 (48.3%)	
Sex			0.158			0.148
Male, no. (%)	1,567 (50.0%)	806 (47.8%)		849 (50.3%)	806 (47.8%)	
Female, no. (%)	1,570 (50.0%)	881 (52.2%)		838 (49.7%)	881 (52.2%)	
Race			0.696			0.704
White, no. (%)	2,652 (84.5%)	1,419 (84.1%)		1,430 (84.8%)	1,419 (84.1%)	
Black, no. (%)	351 (11.2%)	187 (11.1%)		186 (11.0%)	187 (11.1%)	
Other, no. (%)	134 (4.3%)	81 (4.8%)		71 (4.2%)	81 (4.8%)	
Marriage			0.892			0.994
Unmarried, no. (%)	1,275 (40.6%)	682 (40.4%)		683 (40.5%)	682 (40.4%)	
Married, no. (%)	1,762 (56.2%)	955 (56.6%)		953 (56.5%)	955 (56.6%)	
Unknown, no. (%)	100 (3.2%)	50 (3.0%)		51 (3.0%)	50 (3.0%)	
Year of diagnosis			0.401			0.603
1988–2003, no. (%)	1,363 (43.4%)	755 (44.8%)		739 (43.8%)	755 (44.8%)	
2004–2013, no. (%)	1,774 (56.6%)	932 (55.2%)		948 (56.2%)	932 (55.2%)	
AJCC stage			0.537			0.206
I–II, no. (%)	463 (14.8%)	261 (15.5%)		234 (13.9%)	261 (15.5%)	
III, no. (%)	2,674 (85.2%)	1,426 (84.5%)		1,453 (86.1%)	1,426 (84.5%)	
Laterality			<0.001			1.000
Left, no. (%)	1,205 (38.4%)	760 (45.1%)		760 (45.1%)	760 (45.1%)	
Right, no. (%)	1,932 (61.6%)	927 (54.9%)		927 (54.9%)	927 (54.9%)	
Prognosis						
CVM	59 (1.9%)	54 (3.2%)	0.005	30 (1.8%)	54 (3.2%)	0.011
NCVM	2,752 (87.7%)	1,460 (86.5%)	0.239	1,472 (87.3%)	1,460 (86.5%)	0.540
Alive	326 (10.4%)	173 (10.3%)	0.881	185 (11.0%)	173 (10.3%)	0.273

LS-SCLC, limited-stage small cell lung cancer; UL/ML, upper lobe/middle lobe; MB/LL, main bronchus/lower lobe; PSM, propensity score matching; AJCC, American Joint Committee on Cancer; CVM, cardiovascular mortality; NCVM, non-cardiovascular mortality. Percentages might not add up to 100% because of rounding.

PSM in patients with LS-SCLC in the MB/LL group compared with those in the UL/ML group (Table 4). After PSM, an HR of 1.88 (95% CI 1.20–2.95, $P = 0.006$) and an HR of 1.79 (95% CI 1.15–2.79, $P = 0.010$) were recorded for multivariate Cox proportional hazards regression and Fine-Gray models, respectively, for patients with LS-SCLC in the MB/LL group compared with those in the UL/ML group (Table 4).

CIF curves showed that cumulative CVM incidences were both significantly lower in the 1988–2003 period relative to the 2004–2013 period for diagnosis before PSM ($P = 0.012$, Figure 4C) and after PSM ($P = 0.004$, Figure 4D). Regression analyses, based on Cox proportional hazard regression and Fine-Gray competing risk models, showed that the 2004–2013 period was independently associated with lower CVM risk relative to the 1988–2003 before and after PSM (all $P > 0.05$, Tables 4, 5).

Analysis of NCVM based on different variables

There were no significant differences in cumulative NCVM incidences between the UL/ML and the LL/MB groups before PSM ($P = 0.442$, Figure 5A) and after PSM ($P = 0.324$, Figure 5B). The univariate and multivariate Fine-Gray competing risk regression analyses showed that primary site was not an independent predictor of NCVM post-RT in patients with LS-SCLC ($P > 0.05$, Supplementary Tables 1, 2).

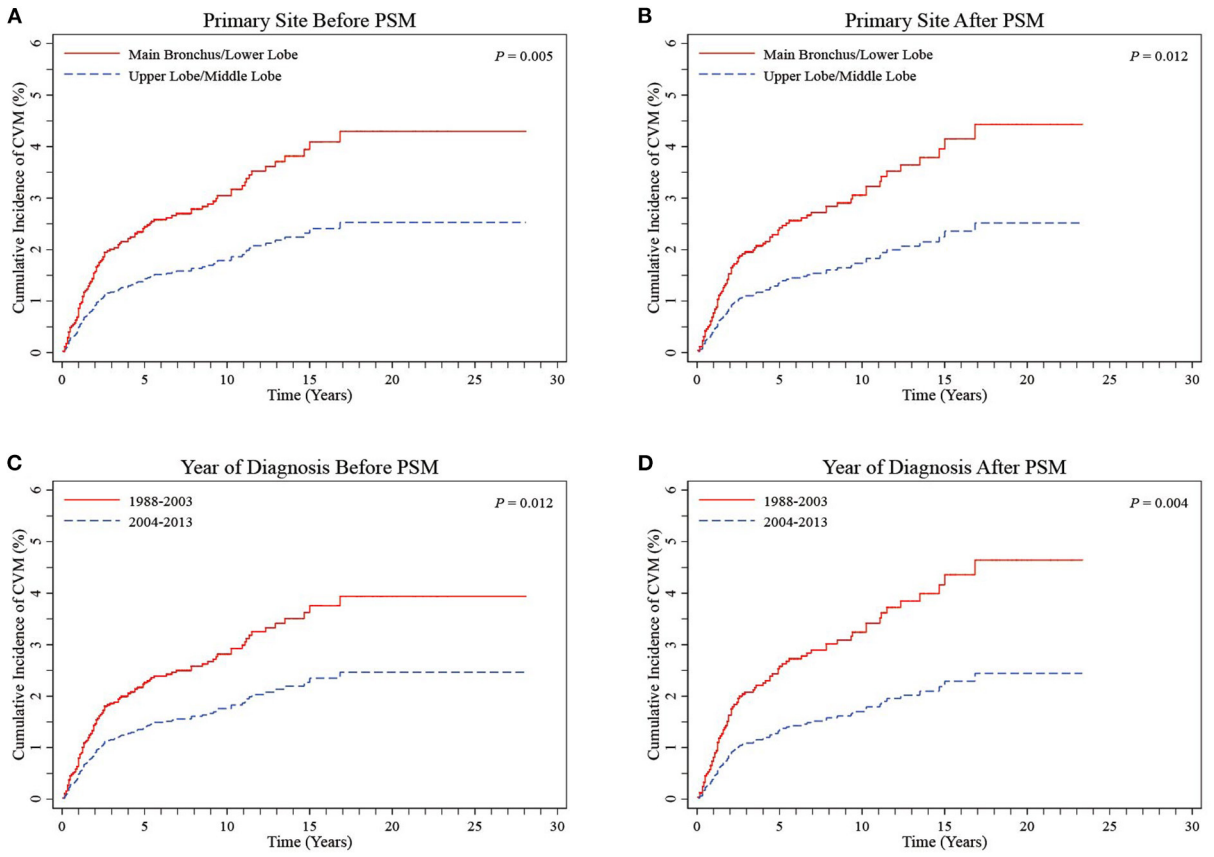

FIGURE 4
CIF curves of CVM stratified into UL/ML and MB/LL groups by primary site before **(A)** and after **(B)** PSM and stratified into 1988–2003 and 2004–2013 groups by year of diagnosis before **(C)** and after **(D)** PSM in LS-SCLC patients. CIF, cumulative incidence function; CVM, cardiovascular mortality; UL/ML, upper lobe/middle lobe; MB/LL, main bronchus/lower lobe; PSM, propensity score matching; LS-SCLC, limited-stage small cell lung cancer.

Discussion

Prior works

Studies have shown that RT can increase incidence of cardiovascular complications in lung cancer patients (9–14, 26, 27). For instance, Lally et al. (9) implicated postoperative RT with increased cardiac mortality in NSCLC patients. In the Radiation Therapy Oncology Group (RTOG) 0617 NSCLC trial, heart V5 (volume of heart receiving 5 Gy) and heart V30 were associated with increased risk of cardiac events (CE) as well as inferior survival rates (10). Dess et al. (11) presented a long-term grade 3 CE incidence, exceeding 10%, among a prospective locally advanced NSCLC (LA-NSCLC) cohort. In an analysis of prospective dose-escalation LA-NSCLC trial, Wang et al. (12) demonstrated that the radiation dose delivered to the heart was an independent predictor of CE. In addition, results of a SEER database analysis (13) among 52,624 LA-NSCLC patients receiving thoracic RT, showed that cardiac-specific mortality (CSM) in left-sided patients was significantly higher than that in right-sided patients. A recent study suggested that mean heart dose was a risk factor for major adverse cardiac events and all-cause mortality in a single-institution retrospective cohort study of LA-NSCLC patients (14).

In recent years, research focus has been directed toward long-term RT-related cardiovascular sequelae in patients with SCLC, due to parallels with NSCLC and the rise in life expectancy (16, 17). Ferris et al. (26) performed a data analysis using the SEER database and found that RT was associated with an approximate 10% absolute increase in CE at 5 years in patients with LS-SCLC and multivariate analysis has shown an independent association between RT and CE. A recent SEER database study showed an increased CSM in left vs. right-sided patients with LS-SCLC receiving thoracic RT (27). Currently, no prior study has investigated the effect of primary site on cardiovascular complications especially concerning CVM in patients with LS-SCLC post-RT. Our study has contributed an enhanced understanding to this research field.

TABLE 4 Univariate Cox proportional hazards and Fine-Gray competing risk regression models for predictors of CVM before and after PSM.

Variables	Group	Before PSM				After PSM			
		Cox proportional hazards (Univariate)		Fine-gray competing risk (Univariate)		Cox proportional hazards (Univariate)		Fine-gray competing risk (Univariate)	
		HR (95% CI)	*P*-value	HR (95% CI)	*P*-value	HR (95% CI)	*P*-value	HR (95% CI)	*P*-value
Primary site	UL/ML	Reference		Reference		Reference		Reference	
	MB/LL	1.78 (1.22–2.58)	0.003	1.71 (1.18–2.49)	0.005	1.86 (1.19–2.91)	0.007	1.78 (1.14–2.78)	0.012
Age, years	≤57	Reference		Reference		Reference		Reference	
	>57	1.41 (0.97–2.05)	0.071	1.13 (0.78–1.64)	0.516	1.58 (1.02–2.44)	0.039	1.25 (0.81–1.92)	0.310
Sex	Male	Reference		Reference		Reference		Reference	
	Female	0.64 (0.44–0.94)	0.021	0.76 (0.52–1.11)	0.156	0.60 (0.39–0.94)	0.024	0.73 (0.48–1.13)	0.161
Race	White	Reference		Reference		Reference		Reference	
	Black	1.15 (0.65–2.06)	0.631	1.04 (0.58–1.85)	0.904	1.53 (0.83–2.83)	0.173	1.35 (0.73–2.50)	0.336
	Other	0.41 (0.10–1.67)	0.213	0.40 (0.10–1.62)	0.199	0.56 (0.14–2.31)	0.426	0.56 (0.14–2.26)	0.412
Marriage	Unmarried	Reference		Reference		Reference		Reference	
	Married	0.75 (0.51–1.11)	0.150	0.88 (0.60–1.28)	0.503	0.73 (0.47–1.13)	0.156	0.87 (0.56–1.35)	0.527
	Unknown	1.01 (0.36–2.81)	0.982	1.11 (0.40–3.07)	0.844	1.08 (0.33–3.50)	0.900	1.16 (0.36–3.77)	0.800
Year of diagnosis	1988–2003	Reference		Reference		Reference		Reference	
	2004–2013	0.63 (0.42–0.92)	0.019	0.62 (0.43–0.90)	0.012	0.53 (0.34–0.84)	0.007	0.52 (0.34–0.81)	0.004
AJCC stage	I–II	Reference		Reference		Reference		Reference	
	III	0.94 (0.60–1.50)	0.808	0.68 (0.43–1.07)	0.098	0.83 (0.50–1.39)	0.481	0.58 (0.35–0.97)	0.038
Laterality	Left	Reference		Reference		Reference		Reference	
	Right	0.83 (0.57–1.20)	0.316	0.86 (0.59–1.25)	0.439	0.90 (0.58–1.38)	0.616	0.97 (0.63–1.49)	0.873

CVM, cardiovascular mortality; PSM, propensity score matching; HR, hazard ratio; CI, confidence interval; AJCC, American Joint Committee on Cancer; UL/ML, upper lobe/middle lobe; MB/LL, main bronchus/lower lobe.

Main findings

This study was the first to report the effects of primary site on CVM post-RT in patients with LS-SCLC. Our results showed that patients in the MB/LL group had a significantly higher cumulative CVM incidence than those in the UL/ML group. MB/LL as the primary site was associated with an increased risk of CVM, and the primary site was a novel prognostic factor for CVM post-RT. This study has many highlights and high reliability of the results. First, we used PSM to balance demographic and clinicopathologic characteristics. These characteristics, especially laterality, have been previously shown to affect occurrence of cardiovascular events in patients with cancer treated with thoracic RT (9, 13, 27). Previous SEER-based analyses involving patients with LA-NSCLC (13) or patients with LS-SCLC (27) receiving thoracic RT showed that CSM in patients with left-sided tumors was significantly higher than that in patients with right-sided tumors. In our study, the percentage of patients with left-sided tumors was significantly greater in the MB/LL patient group than in the UL/ML patient group; therefore, PSM was performed to eliminate possible laterality bias on CVM. Second, rather than using the Kaplan-Meier method, Fine-Gray competing risk regression models (23) that can correctly estimate the probability of an event in the presence of competing events were used in survival analysis to validate the results of Cox proportional hazards regression models. Third, we restricted our analysis to patients aged <65 years. Bias may be present and affect CVM results when comparing patients among all age groups in terms of an unbalanced burden of cardiovascular comorbidities. To address this challenge, we only enrolled patients aged <65 years to help determine any correlation between thoracic RT and CVM risk. We envisaged that this would minimize the effect of underlying cardiovascular risk factors or comorbidities on CVM occurrence. After taking these matters into account, we consider that this study provides a more accurate and reliable evaluation of the effect of thoracic RT on CVM in patients with SCLC.

Risk factors affecting CVM and potential mechanisms

Thoracic RT has been shown to result in injury to the heart and coronary artery, as well as to other vessels in the radiation field, including the aorta and pulmonary artery, resulting in aortic valve disease, porcelain aorta, and pulmonary artery aneurysm (28–31). The relative anatomical position between a tumor primary site and heart/great vessels might influence

TABLE 5 Multivariate Cox proportional hazards and Fine-Gray competing risk regression models for predictors of CVM before and after PSM.

Variables	Group	Before PSM				After PSM			
		Cox proportional hazards (Multivariate)		Fine-gray competing risk (Multivariate)		Cox proportional hazards (Multivariate)		Fine-gray competing risk (Multivariate)	
		HR (95% CI)	*P*-value	HR (95% CI)	*P*-value	HR (95% CI)	*P*-value	HR (95% CI)	*P*-value
Primary site	UL/ML	Reference		Reference		Reference		Reference	
	MB/LL	1.79 (1.23–2.61)	0.002	1.71 (1.18–2.48)	0.005	1.88 (1.20–2.95)	0.006	1.79 (1.15–2.79)	0.010
Age, years	≤57	Reference		Reference		Reference		Reference	
	>57	1.45 (0.99–2.10)	0.055	1.16 (0.80–1.68)	0.439	1.66 (1.07–2.58)	0.023	1.30 (0.85–2.00)	0.230
Sex	Male	Reference		Reference		Reference		Reference	
	Female	0.60 (0.41–0.87)	0.008	0.73 (0.50–1.07)	0.110	0.57 (0.37–0.89)	0.013	0.71 (0.46–1.10)	0.123
Race	White	Reference		Reference		Reference		Reference	
	Black	1.08 (0.60–1.94)	0.806	1.00 (0.56–1.79)	0.996	1.42 (0.76–2.66)	0.271	1.30 (0.71–2.40)	0.399
	Other	0.37 (0.09–1.49)	0.160	0.37 (0.09–1.49)	0.162	0.49 (0.12–2.00)	0.319	0.50 (0.12–2.06)	0.341
Marriage	Unmarried	Reference		Reference		Reference		Reference	
	Married	0.70 (0.47–1.04)	0.074	0.82 (0.56–1.20)	0.310	0.70 (0.44–1.09)	0.116	0.82 (0.53–1.26)	0.360
	Unknown	1.02 (0.37–2.83)	0.974	1.04 (0.38–2.86)	0.940	1.09 (0.33–3.53)	0.891	1.06 (0.33–3.37)	0.927
Year of diagnosis	1988–2003	Reference		Reference		Reference		Reference	
	2004–2013	0.64 (0.43–0.95)	0.025	0.64 (0.44–0.92)	0.016	0.55 (0.34–0.87)	0.010	0.54 (0.35–0.84)	0.006
AJCC stage	I–II	Reference		Reference		Reference		Reference	
	III	1.04 (0.65–1.66)	0.860	0.71 (0.46–1.12)	0.143	0.94 (0.56–1.58)	0.812	0.61 (0.37–1.01)	0.057
Laterality	Left	Reference		Reference		Reference		Reference	
	Right	0.83 (0.57–1.21)	0.322	0.89 (0.62–1.30)	0.555	0.86 (0.56–1.33)	0.507	0.96 (0.63–1.48)	0.865

CVM, cardiovascular mortality; PSM, propensity score matching; HR, hazard ratio; CI, confidence interval; AJCC, American Joint Committee on Cancer; UL/ML, upper lobe/middle lobe; MB/LL, main bronchus/lower lobe.

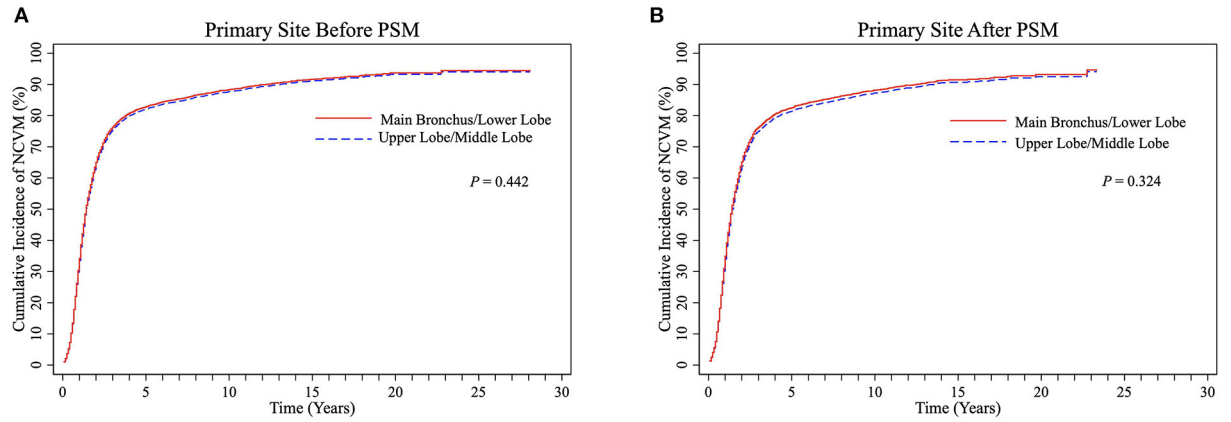

FIGURE 5
CIF curves of NCVM post-radiotherapy stratified into UL/ML and MB/LL groups by primary site before **(A)** and after **(B)** PSM in LS-SCLC patients. CIF, cumulative incidence function; CVM, cardiovascular mortality; UL/ML, upper lobe/middle lobe; MB/LL, main bronchus/lower lobe; PSM, propensity score matching; LS-SCLC, limited-stage small cell lung cancer.

the amount of radiation doses received by the heart or great vessels during RT. Anatomically, the LL is closely adjacent to the heart, and has been found to be associated with larger volume variability than the UL during radiation procedures (21). Furthermore, bilateral main bronchi are embedded in the hilum of the lung and are surrounded with several great vessels. Specifically, the right MB passes behind the ascending aorta, the superior vena cava, and the right pulmonary vessels, whereas the left MB passes behind the left pulmonary vessels, and extends across the arch formed by the arch of the aorta and the descending thoracic aorta. This close anatomical relationship makes it more likely for healthy tissues to receive additional

radiation exposure, especially heart and great vessel tissues located adjacent to the tumor in patients whose primary site is located in the MB and in the LL, consequently making them more vulnerable to radiation-induced injury. Recent clinical studies have reported that patients with NSCLC with primary sites in the left MB and left LL have lower OS rates (18–21). To date, the specific mechanism to explain this remains unclear, although it may be attributed, at least in part, to increased RT-induced severe adverse cardiovascular events in patients receiving RT with primary sites in the MB and LL (9–14). This explanation accords with our study findings. Two studies have shown that in patients with cancer receiving thoracic RT, left-sided laterality was associated with an increased incidence of cardiovascular complications, due to a shorter distance between the left-sided radiation field and the heart compared with patients with right-sided primary sites (13, 27). This finding provides support for the potential mechanisms involved concerning distinct incidences of CVM in different primary sites in our study.

Limitations

Although this study provides novel and clinically significant insights into CVM post-RT for patients with non-surgical LS-SCLC, there remain some limitations inherent to any retrospective analysis. First, the SEER database contains limited data concerning pre-existing cardiovascular comorbidities and risk factors. Next, similar to previous RT studies based on data from the SEER database (13, 26), we were unable to assess many important therapeutic parameters, such as total radiation dose, the dose per fraction, the volume of heart/great vessels irradiated, and chemotherapy agents. The validity of reporting RT using SEER data has been questioned. However, one recent study reported a high sensitivity and positive predictive value between RT records and the actual implementation of RT (32). Additionally, given the *post-hoc* nature of this study, limitations in terms of retrospective analyses apply. Nonetheless, MB/LL and UL/ML groups were matched to obviate the potential effect of unbalanced variables on CVM.

Conclusions

MB/LL as the primary site was found to be associated with an increased risk of CVM post-RT in patients with LS-SCLC. This study presented a propensity score-matched competing risk analysis in a large, population-based, real-world cohort, with which to analyze RT-linked sequelae and to stratify CVM risk during clinical decision-making. Our findings suggested that patients with MB/LL tumors undergoing RT may require better radioprotection not only for the heart, but also for the great vessels. More comprehensive cardiovascular management and closer follow-up are needed for patients with LS-SCLC undergoing RT.

Data availability statement

The raw data supporting the conclusions of this article will be made available by the authors, without undue reservation.

Ethics statement

Ethical review and approval was not required for the study on human participants in accordance with the local legislation and institutional requirements. Written informed consent for participation was not required for this study in accordance with the national legislation and the institutional requirements.

Author contributions

YZ contributed to writing the manuscript, SEER database access, and data acquisition and analysis. YZ, FQ, and BH contributed to the conception, design, and supervision of the study. QJ and WX contributed to data interpretation. All authors contributed to the article and approved the submitted version.

Funding

This work was supported by the National Natural Science Foundation of China (81830010), the Artificial intelligence project of Xuhui District, Shanghai (No. 2020-011), Clinical Research Plan of SHDC (SHDC2020CR1039B), Shanghai Jiao Tong University School of Medicine clinical research project (dly201512).

Acknowledgments

The authors would like to thank the Surveillance, Epidemiology, and End Results (SEER) Program tumor registries in the creation of the SEER database.

Conflict of interest

The authors declare that the research was conducted in the absence of any commercial or financial relationships that could be construed as a potential conflict of interest.

Publisher's note

All claims expressed in this article are solely those of the authors and do not necessarily represent those

of their affiliated organizations, or those of the publisher, the editors and the reviewers. Any product that may be evaluated in this article, or claim that may be made by its manufacturer, is not guaranteed or endorsed by the publisher.

Supplementary material

The Supplementary Material for this article can be found online at: https://www.frontiersin.org/articles/10.3389/fcvm.2022.922811/full#supplementary-material

References

1. Zamorano JL, Lancellotti P, Rodriguez MD, Aboyans V, Asteggiano R, Galderisi M, et al. 2016 ESC position paper on cancer treatments and cardiovascular toxicity developed under the auspices of the ESC committee for practice guidelines: the task force for cancer treatments and cardiovascular toxicity of the European society of cardiology (ESC). *Eur Heart J.* (2016) 37:2768–801. doi: 10.1093/eurheartj/ehw211

2. Desai MY, Windecker S, Lancellotti P, Bax JJ, Griffin BP, Cahlon O, et al. Prevention, diagnosis, and management of radiation-associated cardiac disease: JACC scientific expert panel. *J Am Coll Cardiol.* (2019) 74:905–27. doi: 10.1016/j.jacc.2019.07.006

3. Darby SC, Ewertz M, McGale P, Bennet AM, Blom-Goldman U, Bronnum D, et al. Risk of ischemic heart disease in women after radiotherapy for breast cancer. *N Engl J Med.* (2013) 368:987–98. doi: 10.1056/NEJMoa1209825

4. Venkatesulu BP, Mahadevan LS, Aliru ML, Yang X, Bodd MH, Singh PK, et al. Radiation-Induced endothelial vascular injury: a review of possible mechanisms. *JACC Basic Transl Sci.* (2018) 3:563–72. doi: 10.1016/j.jacbts.2018.01.014

5. Sardar P, Kundu A, Chatterjee S, Nohria A, Nairooz R, Bangalore S, et al. Long-term cardiovascular mortality after radiotherapy for breast cancer: a systematic review and meta-analysis. *Clin Cardiol.* (2017) 40:73–81. doi: 10.1002/clc.22631

6. van Nimwegen FA, Ntentas G, Darby SC, Schaapveld M, Hauptmann M, Lugtenburg PJ, et al. Risk of heart failure in survivors of hodgkin lymphoma: effects of cardiac exposure to radiation and anthracyclines. *Blood.* (2017) 129:2257–65. doi: 10.1182/blood-2016-09-740332

7. Maraldo MV, Brodin NP, Aznar MC, Vogelius IR, Munck ARP, Petersen PM, et al. Estimated risk of cardiovascular disease and secondary cancers with modern highly conformal radiotherapy for early-stage mediastinal hodgkin lymphoma. *Ann Oncol.* (2013) 24:2113–18. doi: 10.1093/annonc/mdt156

8. Siegel RL, Miller KD, Jemal A. Cancer statistics, 2020. *CA Cancer J Clin.* (2020) 70:7–30. doi: 10.3322/caac.21590

9. Lally BE, Detterbeck FC, Geiger AM, Thomas CJ, Machtay M, Miller AA, et al. The risk of death from heart disease in patients with nonsmall cell lung cancer who receive postoperative radiotherapy: analysis of the surveillance, epidemiology, and end results database. *Cancer-Am Cancer Soc.* (2007) 110:911–7. doi: 10.1002/cncr.22845

10. Bradley JD, Paulus R, Komaki R, Masters G, Blumenschein G, Schild S, et al. Standard-dose versus high-dose conformal radiotherapy with concurrent and consolidation carboplatin plus paclitaxel with or without cetuximab for patients with stage IIIA or IIIB non-small-cell lung cancer (RTOG 0617): a randomised, two-by-two factorial phase 3 study. *Lancet Oncol.* (2015) 16:187–99. doi: 10.1016/S1470-2045(14)71207-0

11. Dess RT, Sun Y, Matuszak MM, Sun G, Soni PD, Bazzi L, et al. Cardiac events after radiation therapy: combined analysis of prospective multicenter trials for locally advanced Non-Small-Cell lung cancer. *J Clin Oncol.* (2017) 35:1395–402. doi: 10.1200/JCO.2016.71.6142

12. Wang K, Eblan MJ, Deal AM, Lipner M, Zagar TM, Wang Y, et al. Cardiac toxicity after radiotherapy for stage III non-small-cell lung cancer: pooled analysis of dose-escalation trials delivering 70 to 90 Gy. *J Clin Oncol.* (2017) 35:1387–94. doi: 10.1200/JCO.2016.70.0229

13. Haque W, Verma V, Fakhreddine M, Butler EB, Teh BS, Simone CN. Trends in cardiac mortality in patients with locally advanced non-small cell lung cancer. *Int J Radiat Oncol Biol Phys.* (2018) 100:470–7. doi: 10.1016/j.ijrobp.2017.10.031

14. Atkins KM, Rawal B, Chaunzwa TL, Lamba N, Bitterman DS, Williams CL, et al. Cardiac radiation dose, cardiac disease, and mortality in patients with lung cancer. *J Am Coll Cardiol.* (2019) 73:2976–87. doi: 10.1016/j.jacc.2019.03.500

15. Pignon JP, Arriagada R, Ihde DC, Johnson DH, Perry MC, Souhami RL, et al. A meta-analysis of thoracic radiotherapy for small-cell lung cancer. *N Engl J Med.* (1992) 327:1618–24. doi: 10.1056/NEJM199212033272302

16. Faivre-Finn C, Snee M, Ashcroft L, Appel W, Barlesi F, Bhatnagar A, et al. Concurrent once-daily versus twice-daily chemoradiotherapy in patients with limited-stage small-cell lung cancer (CONVERT): An open-label, phase 3, randomised, superiority trial. *Lancet Oncol.* (2017) 18:1116–25. doi: 10.1016/S1470-2045(17)30318-2

17. Yang S, Zhang Z, Wang Q. Emerging therapies for small cell lung cancer. *J Hematol Oncol.* (2019) 12:47. doi: 10.1186/s13045-019-0736-3

18. Li C, Liu J, Lin J, Li Z, Shang X, Wang H. Poor survival of non-small-cell lung cancer patients with main bronchus tumor: a large population-based study. *Future Oncol.* (2019) 15:2819–27. doi: 10.2217/fon-2019-0098

19. Yang L, Wang S, Gerber DE, Zhou Y, Xu F, Liu J, et al. Main bronchus location is a predictor for metastasis and prognosis in lung adenocarcinoma: a large cohort analysis. *Lung Cancer.* (2018) 120:22–6. doi: 10.1016/j.lungcan.2018.03.011

20. Sun W, Yang X, Liu Y, Yuan Y, Lin D. Primary tumor location is a useful predictor for lymph node metastasis and prognosis in lung adenocarcinoma. *Clin Lung Cancer.* (2017) 18:e49–55. doi: 10.1016/j.cllc.2016.06.002

21. Jan N, Guy C, Reshko LB, Hugo GD, Weiss E. Lung and heart dose variability during radiation therapy of non-small cell lung cancer. *Int J Radiat Oncol Biol Phys.* (2017) 98:683–90. doi: 10.1016/j.ijrobp.2017.02.227

22. Hancock SL, Tucker MA, Hoppe RT. Factors affecting late mortality from heart disease after treatment of Hodgkin's disease. *JAMA.* (1993) 270:1949–55. doi: 10.1001/jama.270.16.1949

23. Wolbers M, Koller MT, Stel VS, Schaer B, Jager KJ, Leffondre K, et al. Competing risks analyses: objectives and approaches. *Eur Heart J.* (2014) 35:2936–41. doi: 10.1093/eurheartj/ehu131

24. Deb S, Austin PC, Tu JV, Ko DT, Mazer CD, Kiss A, et al. A review of propensity-score methods and their use in cardiovascular research. *Can J Cardiol.* (2016) 32:259–65. doi: 10.1016/j.cjca.2015.05.015

25. Austin PC. The use of propensity score methods with survival or time-to-event outcomes: Reporting measures of effect similar to those used in randomized experiments. *Stat Med.* (2014) 33:1242–58. doi: 10.1002/sim.5984

26. Ferris MJ, Jiang R, Behera M, Ramalingam SS, Curran WJ, Higgins KA. Radiation therapy is associated with an increased incidence of cardiac events in patients with small cell lung cancer. *Int J Radiat Oncol Biol Phys.* (2018) 102:383–90. doi: 10.1016/j.ijrobp.2018.05.066

27. Verma V, Fakhreddine MH, Haque W, Butler EB, Teh BS, Simone CN. Cardiac mortality in limited-stage small cell lung cancer. *Radiother Oncol.* (2018) 128:492–7. doi: 10.1016/j.radonc.2018.06.011

28. Daitoku K, Fukui K, Ichinoseki I, Munakata M, Takahashi S, Fukuda I. Radiotherapy-induced aortic valve disease associated with porcelain aorta. *Jpn J Thorac Cardiovasc Surg.* (2004) 52:349–52. doi: 10.1007/s11748-004-0069-0

29. Brosius FR, Waller BF, Roberts WC. Radiation heart disease. analysis of 16 young (aged 15 to 33 years) necropsy patients who received over 3,500 rads to the heart. *Am J Med.* (1981) 70:519–30. doi: 10.1016/0002-9343(81)90574-X

30. Coblentz C, Martin L, Tuttle R. Calcified ascending aorta after radiation therapy. *AJR Am J Roentgenol.* (1986) 147:477–8. doi: 10.2214/ajr.147.3.477

31. Ledoux B, Dupont M, Duplaquet F, Pirard L, Ocak S, Wanet M, et al. Illustration of a fatal radiation-induced lung aneurysm: is central lung stereotactic radiotherapy to be banned? *Cancer Radiother.* (2019) 23:926–9. doi: 10.1016/j.canrad.2019.05.016

32. Kraus RD, Hamilton AS, Carlos M, Ballas LK. Using hospital medical record data to assess the accuracy of the SEER Los Angeles cancer surveillance program for initial treatment of prostate cancer: a small pilot study. *Cancer Causes Control.* (2018) 29:815–21. doi: 10.1007/s10552-018-1057-5

frontiers | Frontiers in Cardiovascular Medicine

TYPE Original Research
PUBLISHED 08 September 2022
DOI 10.3389/fcvm.2022.930797

OPEN ACCESS

EDITED BY
Dong Han,
People's Liberation Army General Hospital, China

REVIEWED BY
Cristina M. Failla,
Institute of Immaculate Dermatology (IRCCS), Italy
Lars Michel,
Essen University Hospital, Germany

*CORRESPONDENCE
Vincenzo Quagliariello
quagliariello.enzo@gmail.com
Nicola Maurea
n.maurea@istitutotumori.na.it

SPECIALTY SECTION
This article was submitted to Cardio-Oncology, a section of the journal Frontiers in Cardiovascular Medicine

RECEIVED 28 April 2022
ACCEPTED 03 August 2022
PUBLISHED 08 September 2022

CITATION
Quagliariello V, Passariello M, Di Mauro A, Cipullo C, Paccone A, Barbieri A, Palma G, Luciano A, Buccolo S, Bisceglia I, Canale ML, Gallucci G, Inno A, De Lorenzo C and Maurea N (2022) Immune checkpoint inhibitor therapy increases systemic SDF-1, cardiac DAMPs Fibronectin-EDA, S100/Calgranulin, galectine-3, and NLRP3-MyD88-chemokine pathways. *Front. Cardiovasc. Med.* 9:930797. doi: 10.3389/fcvm.2022.930797

Immune checkpoint inhibitor therapy increases systemic SDF-1, cardiac DAMPs Fibronectin-EDA, S100/Calgranulin, galectine-3, and NLRP3-MyD88-chemokine pathways

Vincenzo Quagliariello[1]*, Margherita Passariello[2,3], Annabella Di Mauro[4], Ciro Cipullo[4], Andrea Paccone[1], Antonio Barbieri[5], Giuseppe Palma[5], Antonio Luciano[5], Simona Buccolo[1], Irma Bisceglia[6], Maria Laura Canale[7], Giuseppina Gallucci[8], Alessandro Inno[9], Claudia De Lorenzo[2,3] and Nicola Maurea[1]*

[1]Division of Cardiology, Istituto Nazionale Tumori- Istituto di Ricovero e Cura a Carattere Scientifico (IRCCS)- Fondazione G. Pascale, Naples, Italy, [2]Department of Molecular Medicine and Medical Biotechnology, University of Naples "Federico II", Naples, Italy, [3]Ceinge-Biotecnologie Avanzate s.c.a.r.l., Naples, Italy, [4]Pathology Unit, Istituto Nazionale Tumori- Istituto di Ricovero e Cura a Carattere Scientifico (IRCCS)- Fondazione G. Pascale, Naples, Italy, [5]Animal Facility, Istituto Nazionale Tumori- Istituto di Ricovero e Cura a Carattere Scientifico (IRCCS)- Fondazione G. Pascale, Naples, Italy, [6]Servizi Cardiologici Integrati, Dipartimento Cardio-Toraco-Vascolare, Azienda Ospedaliera San Camillo Forlanini, Rome, Italy, [7]U.O.C. Cardiologia, Ospedale Versilia, Lido di Camaiore (LU), Camaiore, Italy, [8]Cardiologia, Centro di Riferimento Oncologico della Basilicata (CROB) - Istituto di Ricovero e Cura a Carattere Scientifico (IRCCS), Rionero in Vulture, Italy, [9]Medical Oncology, Istituto di Ricovero e Cura a Carattere Scientifico (IRCCS) Ospedale Sacro Cuore Don Calabria, Negrar, Italy

Background: Immune checkpoint inhibitors (ICIs) have significantly changed the oncology clinic in recent years, improving survival expectations in cancer patients. ICI therapy have a broad spectrum of side effects from endocrinopathies to cardiovascular diseases. In this study, pro-inflammatory and pro-fibrotic effects of short-term ICIs therapy in preclinical models were analyzed.

Methods: Firstly, in a human *in vitro* model, human cardiomyocytes co-cultured with hPBMC were exposed to ICIs (with CTLA-4 or PD-1 blocking agents, at 200 nM) for 72 h. After treatment, production of DAMPs and 12 cytokines were analyzed in the supernatant through colorimetric and enzymatic assays. C57/Bl6 mice were treated with CTLA-4 or PD-1 blocking agents (15 mg/kg) for 10 days. Before (T0), after three days (T3) and after treatments (T10), ejection fraction, fractional shortening, radial and longitudinal strain were calculated by using bidimensional echocardiography (Vevo 2100, Fujfilm). Fibrosis, necrosis, hypertrophy and vascular NF-kB expression were analyzed through Immunohistochemistry. Myocardial expression of DAMPs (S100- Calgranulin, Fibronectin and Galectine-3), MyD88, NLRP3 and twelve cytokines have been analyzed. Systemic levels of SDF-1, IL-1β, and IL-6 were analyzed before, during and after ICIs therapy.

Results: Radial and longitudinal strain were decreased after 10 days of ICIs therapy. Histological analysis of NF-kB expression shows that short-term anti-CTLA-4 or anti-PD-1 treatment increased vascular and myocardial inflammation. No myocardial hypertrophy was seen with the exception of the pembrolizumab group. Myocardial fibrosis and expression of galectin-3, pro-collagen 1-α and MMP-9 were increased after treatment with all ICIs. Both anti-CTLA-4 or anti-PD-1 treatments increased the expression of DAMPs, NLRP3 inflammasome and MyD88 and induced both *in vitro* and *in vivo* the secretion of IL-1β, TNF-α and IL-6. Systemic levels of SDF-1, IL-1β and IL-6 were increased during and after treatment with ICIs.

Conclusions: Short therapy with PD-1 and CTLA-4 blocking agents increases vascular expression of NF-kB, systemic SDF-1, IL-1β, IL-6 levels and myocardial NLRP3, MyD88 and DAMPs expression in preclinical models. A pro-inflammatory cytokine storm was induced in myocardial tissues and in cultured cardiac cells after ICIs therapy. The overall picture of the study suggests new putative biomarkers of ICIs-mediated systemic and myocardial damages potentially useful in clinical cardioncology.

KEYWORDS

immunotherapy, biomarkers, preclinical study, mechanisms, inflammation, interleukin

Introduction

Immune checkpoint inhibitors (ICIs) includes monoclonal antibodies that activate the host immune system for efficient killing of cancer cells through unspecific activation mechanisms (1). ICIs are directed against programmed cell death protein (PD-1), its associated ligand (PD-L1) or CTLA-4 (Cytotoxic T-Lymphocyte Antigen 4) leading to activation of lymphocytes and NK cell activity against cancer cells (2, 3). Clinical benefits were seen in melanoma, non-small cell lung cancer and metastatic breast cancer patients; association therapies with radiotherapy or chemotherapy or with other ICIs are still proposed worldwide (2). ICIs-mediated side effects involves T-lymphocyte-driven inflammation and direct cytotoxicity in many tissues, such as skin, intestine, lungs, liver, endocrine organs and cardiovascular system (4, 5). ICIs mediated cardiotoxicities are rare but can affect anticancer regimens and quality of life in cancer patients (6). Cardiovascular complications in cancer patients treated with ICIs include fatal myocarditis, vasculitis, arrhythmia, fibrosis and heart failure (7, 8). In different types of cancer, different ICIs may show different cardiotoxicity spectra (9). The incidence of ICIs-related cardiovascular events ranged from 0.15 to 10%. For example, in melanomas, PD-1/PD-L1 inhibitor use was closely related to high blood pressure and myocarditis (8, 9). Lung cancer patients, commonly experienced acute coronary syndrome, arrhythmia and heart failure (9). The most common cardiotoxic events after nivolumab and pembrolizumab therapy in lung cancer patients are arrhythmia, cardiac-related chest pain, cardiomyopathy, and myopericardial diseases. Moreover, renal cell carcinomas patients treated with nivolumab associated to ipilimumab frequently experienced hypertension (9); patients with urothelial carcinoma treated with atezolizumab had frequently hypertension and arrhythmia. Therefore, a complex interaction between cancer-related and immune-related factors plays a key role in pathogenesis of cardiovascular toxicities.

Known mechanisms of ICIs-induced cardiotoxicity involves immune-infiltration of CD3 +, CD4 + and CD8 + T lymphocytes in myocardial tissues that can attack cardiomyocytes or endothelial cells leading to metabolic failure and reduced cell viability (10, 11). Notably, ICIs can induce a pro-inflammatory phenotype in cardiac and vascular tissues therefore the identification of new players of cardiotoxicity mediated by short-term ICIs therapy still need further attention. Recent consensus statements highlights on the importance of new predictive biomarkers of ICIs-mediated cardiotoxicity (12, 13). Indeed, echocardiographic biomarkers such as changes in global longitudinal strain (GLS) (12), or myocardial work (MW) (13) or increases in plasma levels of galectin-3 and cytokines (14) are of great interest in clinical cardioncology. Considering that Pembrolizumab and Ipilimumab recognize both human and mice PD-1 and CTLA-4 epitopes (15, 16), we have highlighted on the vascular and myocardial inflammation in female mice through immunohistochemistry and ELISA methods shedding light on potential pathways involved in ICIs cardiotoxicity, including NLRP3, MyD88 and DAMPs.

Materials and methods

Cell cultures

Human cardiac cells (HFC cell line; Innoprot, Derio, Spain) were cultured following the manufacturer's instructions (17, 18). Culture medium was supplemented with Fetal Bovine Serum at 10% v/V (FBS, Sigma Aldrich, St. Louis MO, USA), Penicillin at 50 U/ml, Streptomycin at50 µg/mL and L-Glutammine at 1% v/V.

In vitro cytotoxicity assays and cardiac cell lysis

Considering that PD-1 and CTLA-4 are expressed in human cardiomyocytes, as recently analyzed by our group through cell ELISA assays on human fetal cardiomyocytes with anti-PD-1 and anti-CTLA-4 mAbs (19), Ipilimumab and Pembrolizumab were added to HFC cells co-cultured with human lymphocytes. In brief, cells were plated in 96-well flat-bottom plates (at 10,000 cells/well) for 16 h. Human Peripheral Blood Mononuclear Cells (hPBMCs) were added at effector: target ratio 5:1 in the absence or presence of the mAbs (200 nM), and incubated for 24 h at 37°C, as previously described (20). Cells un-incubated or incubated with aspecific antibodies IgG were defined as control. After treatment with antibodies, lymphocytes were removed and adherent cells were washed and counted through trypan blue method. Lymphocytes can be easily removed by collecting the supernatant of co-cultures and by washing the tumor adherent cells as the lymphocytes are non-adherent. Cell survival was expressed as percent of viable cells tested with drugs compared to the untreated ones, used as a negative control. Cardiac cell lysis was determined as described in other recent work (21, 22) through the quantification of released LDH (LDH detection kit, Thermo-Fisher Scientific, Meridian Rd., Rockoford, IL USA), following the manufacturer's instructions.

ELISA assays on mouse purified proteins and PBMCs

The Enzyme-linked immunosorbent assay (ELISA) was performed on mouse PBMCs and purified recombinant target proteins to test the human-mouse cross-reactivity of the antibodies. Mouse lymphocytes (4×10^5 cells/well) activated with anti-CD3/CD28 beads for 3 days were plated on round-bottom 96-well plates. The purified recombinant human or mouse CTLA-4/Fc or the Fc portion (used as a negative control) were coated on flat bottom plates and blocked with a buffer solution (PBS/milk 5% v/v) for 1 h. The plates were incubated with increasing concentrations of antibodies in a buffer solution (PBS/milk 2.5% v/v) for 2 h. After washing, plates were incubated with HRP-conjugated anti-human IgG (Fab')2 goat monoclonal antibody in a buffer solution (PBS/BSA 3% v/v) for 1 h. The following steps were performed as previously described (23). The Absorbance values at 450 nm were measured by an Envision plate reader (Perkin Elmer, 2102, San Diego, CA, USA).

Animal studies

Twenty four C57Bl/6 mice (female, 6 weeks/age) were purchased from Harlan, San Pietro al Natisone (Italy). As standard protocol, firstly mice were housed and maintained on a 12 h light-12 h dark cycle in a room with a fixed temperature of 22°C with the appropriate foods water. The experimental protocols were approved by the Ministry of Health with authorization number 1467/17-PR of 13-02-2017, and institutional ethics committees: Organismo preposto al benessere degli animali (OPBA) in accordance with EU Directive 2010/63/EU for animal experiments and Italian D.L.vo 26/2014 law. Briefly, animals were randomly divided into three groups (6 mice per group) as followings:

- Control group: mice daily received normal saline injection (by i.p) every three days for 10 days
- Ipilimumab group: mice received a short therapy with a CTLA-4 blocking agent (Bristol-Myers Squibb, Princeton, New Jersey, US) (15 mg/kg/day by i.p) every three days for 10 days;
- Pembrolizumab group: mice received a short therapy with a PD-1 blocking agent (Merck & Co., Inc., Kenilworth, NJ, USA) (15 mg/kg/day by i.p) every 3 days for 10 days.

Notably, every drug was used in the clinically available formulation. The injected dose of 15 mg/kg mean body-weight was comparable to the uses of ICIs in clinical oncology (16, 17, 24–26); moreover, the dose used is within the range of doses administered intraperitoneally (1–30 mg/kg) in preclinical models for pharmacokinetic studies and anticancer studies with ICIs (15, 27, 28).

Echocardiographic evaluation of ventricular functions

To assess cardiac functions, the transthoracic echocardiography method was made in mice by using the Vevo 2100 (40-MHz transducer; Visual Sonics, Toronto, ON, Canada) which allows the determination of different cardiac function parameters in anesthetized mice (18, 29, 30). In brief, before (T0), after three days (T3) and at the end of treatments (T10) mice were prepared for cardiac function assessment by previous anesthesia through a solution composed by tiletamine zolazepam (both at 0,09 mg/g of weight) and atropine (at 0,04 mL/g of weight). The left

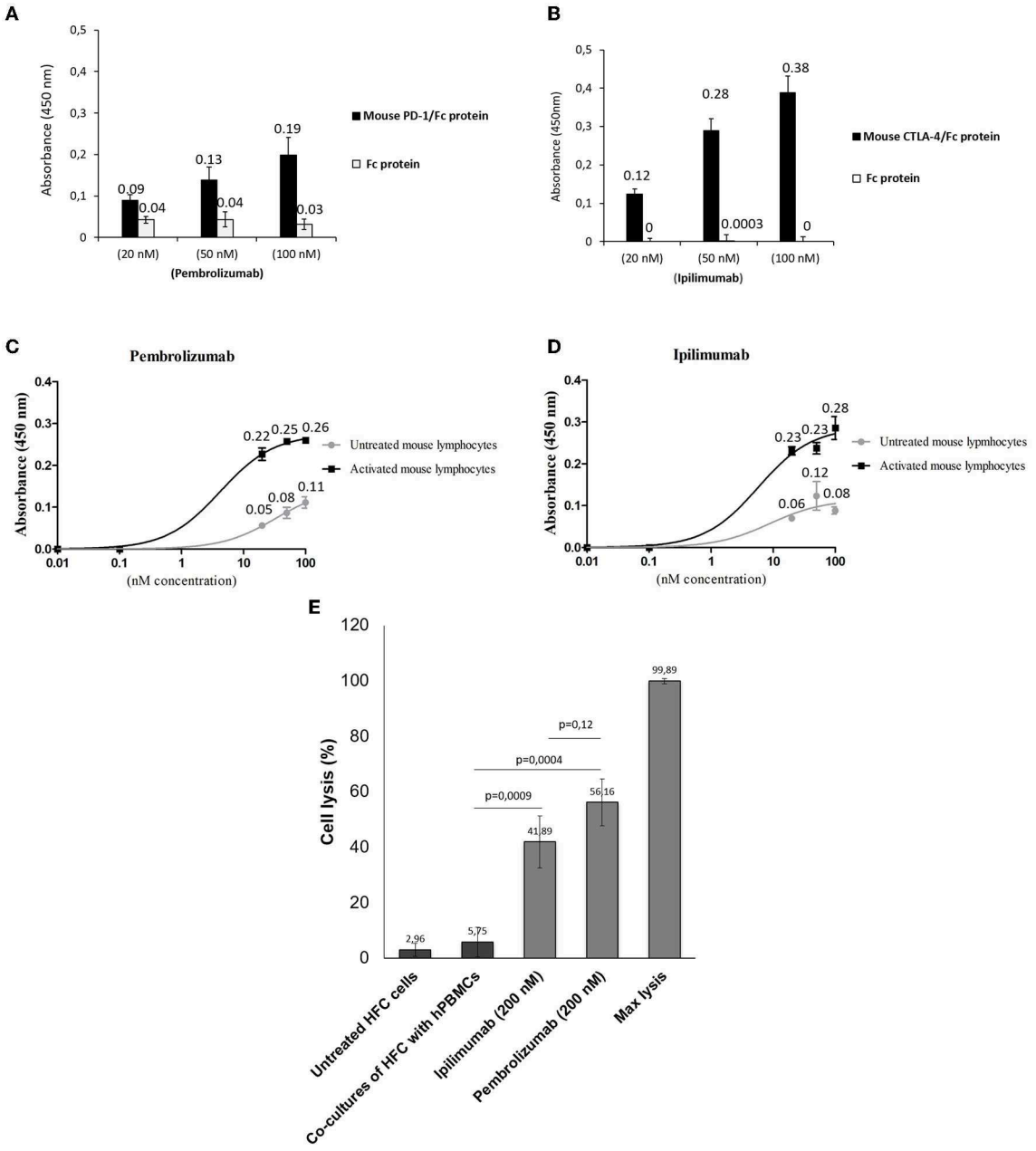

FIGURE 1
Binding assays of Pembrolizumab and Ipilimumab on mouse PBMCs and on human and mouse purified recombinant target proteins. ELISA assays were performed by using the indicated antibodies at increasing concentrations on mouse (black bars) CTLA-4/Fc or PD-1/Fc **(A,B)**. The binding of antibodies was also tested on the Fc portion (empty bars), used as a negative control. Cell ELISA assays were performed by testing Pembrolizumab **(C)** ($n = 3$) or Ipilimumab **(D)** ($n = 3$) on mouse PBMCs untreated or activated with anti-CD3/CD28 beads. **(E)** LDH assay on the supernatant of co-cultures of HFC and hPBMCs treated as indicated ($n = 3$). Cell lysis was measured as described in the materials and methods section. Error bars depict means ± SD.

ventricular echocardiography was performed in parasternal long-axis views (with a frame rate corresponding to 233 Hz). Firstly, in M-mode assessment, the left ventricular internal dimensions in diastole and a systole (LVID,d; LVID, s)were calculated from 3 to 5 beats. Fractional shortening and ejection fraction percentage (both in percentage) were determined as described in other recent work (15). Moreover, radial (RS, corresponding to the change in myocardial wall thickness) and longitudinal strain (LS, percent change in length of the ventricle) were calculated on long-axis views following the guide instructions of the Vevo 2100 software (15, 29).

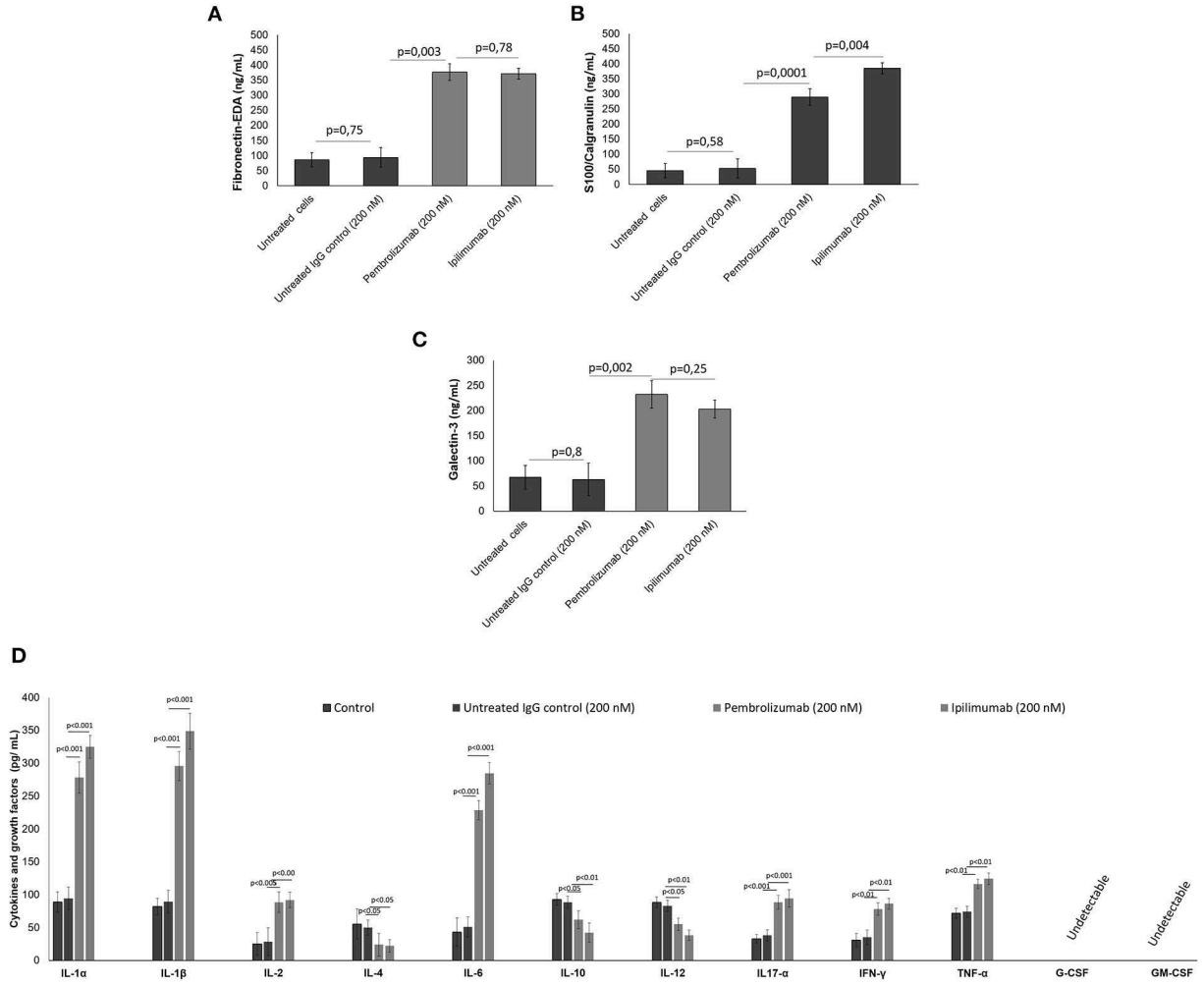

FIGURE 2
(A) DAMPs, including fibronectin, **(B)** S100 calgranulin, **(C)** galectin-3, and **(D)** cytokines and growth factors produced by cardiomyocytes in the supernatant of co-cultures of cardiomyocytes with hPBMC. The cytokines IL-1α, IL-1β, IL-2, IL-4, IL-6, IL-10, IL-12, IL17-α, IFN-γ, TNF-α, G-CSF, GM-CSF ($n = 3$) were quantified by ELISA assays. Error bars depict means ± SD.

Myocardial inflammation and DAMPs expression

After treatments, mice were anesthetized as described in section echocardiographic evaluation of ventricular functions and sacrificed via cervical dislocation. Hearts were excised, washed three times in physiological solution (to eliminate blood residues), weighed and divided into two parts through a proper longitudinal cut. One half was used for biochemical studies and the other part to histological analyzes. Firstly, hearts were lysed under ice in a lysis solution consisting of Triton × 100 1% V / v spiked with a protease inhibitor. To promote lysis, tissues were treated with ultrasounds for 5 min. After centrifugation at 4°C at 1,300 rpm for 10 min, the supernatant of the cardiac homogenates were used to quantitative analysis of six biomarkers of cardiac damages and inflammation, such as: myeloid differentiation primary response 88 (MYd-88) expression (through mouse MyD88 ELISA Kit (My Biosource, San Diego, CA, detection range of 78–5,000 pg/ml; sensitivity: 46.9 pg/ml); NOD-, LRR- and pyrin domain-containing protein 3 (NLRP-3) (through mouse NLRP3 ELISA Kit (OKEH05486, Aviva Systems Biology); Fibronectin-EDA, S100/Calgranulin and Galectine-3 [three DAMPs (quantified in cardiac tissues through selective quantitative assay); twelve cytokines and growth factors (IL-1α, IL-1β, IL-2, IL-4, IL-6, IL-10, IL-12, IL17-α, IFN-γ, TNF-α, G-CSF, GM-CSF) through a mouse cytokine Multiplex Assay kit (Qiagen, USA, pg/mg of heart tissue).

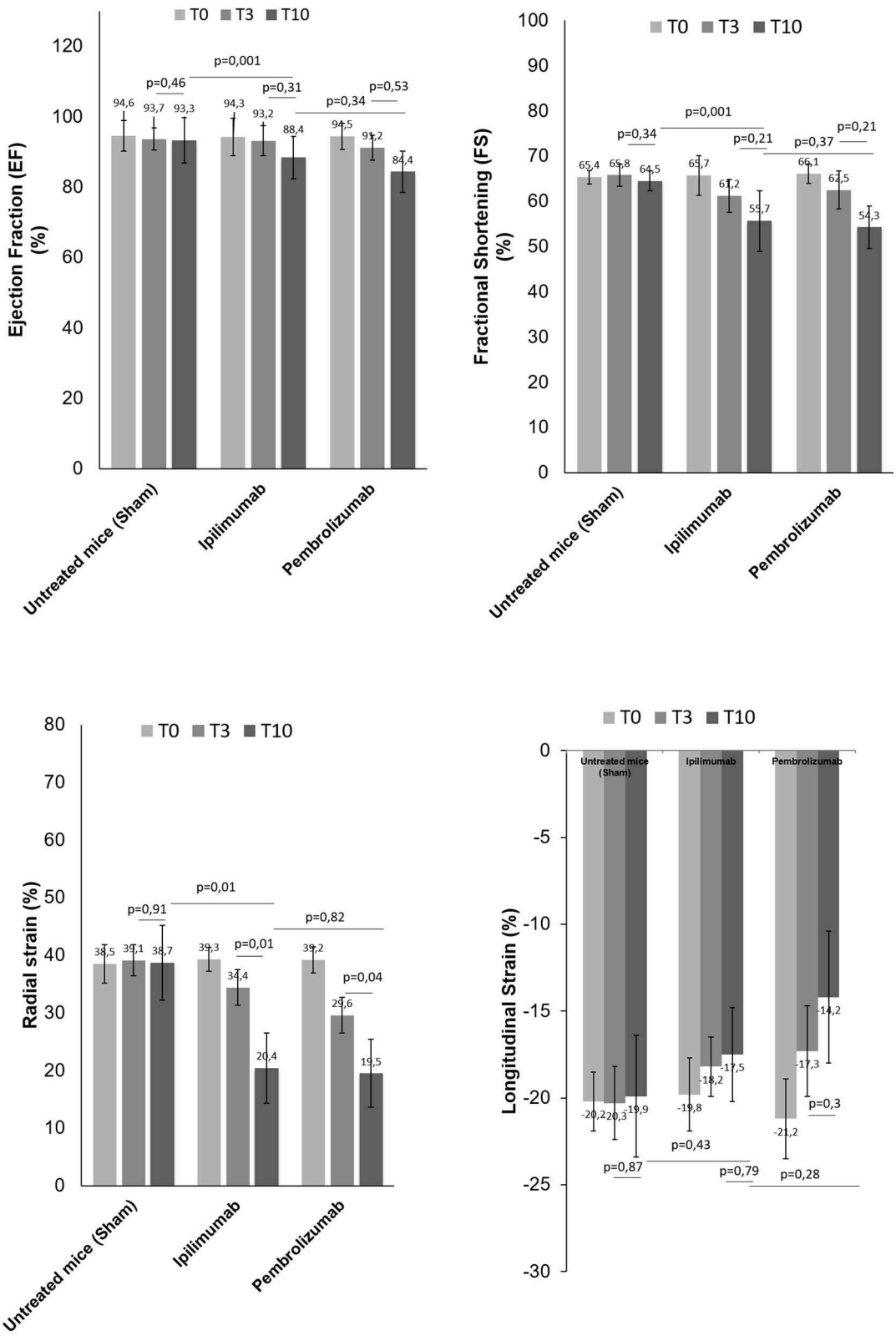

FIGURE 3
Cardiac function studies. Before (T0), after 3 days (T3) and at the end of treatments (T10) with saline or Ipilimumab or Pembrolizumab (15 mg/kg/die), cardiac functions studies were performed. Ejection fraction (%) ($n = 6$), fractional shortening (%) ($n = 6$), radial ($n = 6$) and longitudinal strain (%) ($n = 6$) were analyzed through VEVO 2100 echocardiography. Error bars depict means ± SD.

Systemic levels of SDF-1 (CXCL-12), IL-1β, IL-6

For systemic analysis, blood samples were collected in three points: before (T0), after three days (T3) and at the end of treatments (T10) in heparinised tubes and immediately centrifuged at 3,000 rpm for 10 min at 4°C in order to obtain plasma that was collected, frozen, and kept at −80°C until use. Circulating SDF-1 (CXCL-12), IL-1β, IL-6 were quantified in 0,1 mL of plasma through the use of mouse CXCL12/SDF-1 alpha Quantikine ELISA Kit (MCX120, R&D Systems, Minneapolis, MN, USA), mouse IL-1β ELISA kit (BMS6002, Thermo Fisher, Milan, Italy) and mouse IL-6 ELISA kit (KMC0061, Thermo Fisher, Milan, Italy).

Histology

Blinded histological examination of myocardial tissues were also performed. All selected samples were fixed in formalin and embedded in paraffin. Firstly, tissues were deparaffinized in a solution of xylene and rehydrated through graded alcohols. Antigen retrieval was performed with slides heated in 0.0.1 M edta buffer (pH 8.0.) for 10 min at 110 °C. Slides were rinsed with TBS and treated with a solution at 3 % v/V hydrogen peroxide. Another washing in BSA 5% v/V in PBS was performed as blocking step and an incubation for 12h with a primary antibody (diluted 1:100 in PBS) against mouse NF-kB (Abcam, Cambridge, UK) was performed. Sections were incubated with goat anti- anti-rabbit secondary IgG biotinylated secondary antibody for 0.5 h. Tissue reactivity was determined through the avidin–biotin–peroxydase method (Novocastra, Newcastle, UK) as described in other work (30). After, sections were counterstained with haematoxylin. To determine the structure of the heart, and to evaluate parameters such as hypertrophy, necrosis and fibrosis, the tissues of the heart were incubated with Mayer's hematoxylin for 30 s and washed properly with water (30). Antigen expression was evaluated by one experienced pathologist by using light microscopy. For NF-kB nuclear localization in vascular endothelium of the murine tissues under examination was considered. Immunostaining values were reported as percentage of positive cells in 10 non-overlapping fields by using magnification X400 (31).

Statistics

Data are presented as means ± standard errors (SE). All data were tested for normality by Shapiro–Wilk. Normally distributed data in two groups were tested with Student's *t*-test, and non-normally distributed data in two groups by Wilcoxon–Mann–Whitney. Normally distributed data in multiple groups were tested by one-way analysis of variance (ANOVA) with Sidak correction. Non-normally distributed data were tested by ANOVA with Holm–Sidak post-testing. Paired data were tested using the paired versions of t-Student.

Results

Pembrolizumab and Ipilimumab recognize and bind mouse PD-1 and CTLA-4 and induce cardiotoxic effect in human cardiomyocytes

We first verified the immunoreactivity of Pembrolizumab and Ipilimumab compared to murine epitopes of PD-1 and CTLA-4, respectively, through ELISA binding assays. As specified in Figure 1, and in line with other recent research (15, 22), Pembrolizumab and Ipilimumab are both able to bind to the mouse targets even though the affinity is lower than that observed for their human counterparts. Cardiotoxicity of Pembrolizumab and Ipilimumab in human *in vitro* models of co-cultures of hPBMC and human cardiomyocytes. To confirm in a human-like environment the results obtained in mouse models on the cardiotoxic effects of the immunomodulatory mAbs, we tested their effects in *in vitro* human models based on co-cultures of human cardiomyocytes (HFC) and lymphocytes. As shown in Figure 1, three mAbs induced a significant cardiac cell lysis (up to 50% for Pembrolizumab), thus indicating that they can indeed activate immune responses against cardiac cells.

ICI treatment promotes DAMPs and pro-inflammatory cytokine production in co-cultures of hPBMCs and human cardiomyocytes

It was verified if ICIs could affect the production of DAMPs, pro-inflammatory cytokines, chemokines, and growth factors in co-cultures of human cardiomyocytes with human peripheral blood mononuclear cells (hPBMCs) by analyzing the supernatant by ELISA assays. Firstly, in a similar fashion to the *in vivo* findings, all ICIs increased the production of Fibronectin-EDA (Figure 2A), S199/Calgranulin (Figure 2B) and Galectine-3 (Figure 2C) compared to untreated cells. However, the analysis of cytokines secretion indicated that only IL-1α, IL-1β, IL-6, and TNF-α were significantly increased after incubation with ICIs (Figure 2D).

Short-term ICI therapy reduces radial/longitudinal strain and ejection fraction

We determined the cardiotoxic effects of PD-1 and CTLA-4 blocking agents in C57Bl/6 mice through the study of FS, EF,

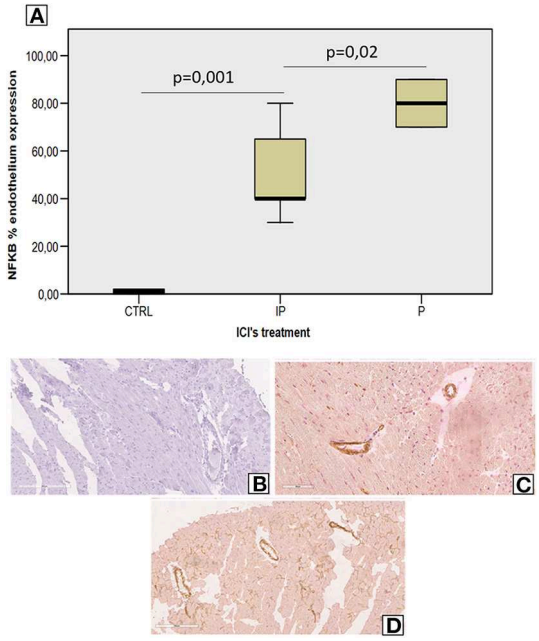

FIGURE 4
Endothelial NF-kB expression in myocardial tissues of mice treated with ICIs **(A)** Quantitative analysis of NF-kB endothelial expression (%) in mice untreated or treated with ICIs ($n = 6$). Vascular expression of NF-kB in mice untreated **(B)** or treated with Ipilimumab **(C)** or Pembrolizumab **(D)**.

RS, and LS by using two-dimensional echocardiography (Vevo Strain 2100, Fujifilm). Analysis of EF and FS indicated that short term of ICIs therapies significantly reduces the cardiac function (Figure 3). No differences were seen between groups. Instead, more significant reductions were observed for radial and longitudinal strain in ICIs groups vs. control. Again, no differences between the ICIs were seen (Figure 3).

Short-term ICI therapy increases vascular expression of nuclear factor kappa-light-chain-enhancer of activated B cells (NF-kB)

Analysis of vascular and myocardial NF-kB expression shows that short-term anti-CTLA-4 or anti-PD-1 treatment had differential effects (Figure 4). However, first, both ICIs increased significantly the vascular inflammation compared to untreated mice but the higher NF-kB expression was seen in Pembrolizumab compared to Ipilimumab group (Figure 4A). Histological characterization of the myocardial tissue phenotype confirms no detectable vascular NF-kB expression in untreated mice (Figure 4B) but a strong vascular expression was seen in ICIs groups (see arrows in Figures 2C,D).

Short-term Pembrolizumab therapy increases cardiac hypertrophy

Morphological characterization of the myocardial tissue phenotype in mice after short-term anti-CTLA-4 or anti-PD-1 treatment clearly indicates no cardiac hypertrophy with the exception of Pembrolizumab (Figure 5). Compared to control (sham), ematoxylin-eosin staining of longitudinal sections of mice treated with Ipilimumab did not show any significant hypertrophy; cardiomyocytes have a linear and homogeneous longitudinal aspect, the nucleus is not pycnotic and has a regular size and shape, and there are no cytoplasmic vacuoles. On the other hand, the cardiac longitudinal section of mice treated with Pembrolizumab shows a significant hypertrophy with evident increases in the cytoplasmic volume and an irregular course of the cardiomyocytes (Figure 5).

Short-term ICI therapy increases cardiac fibrosis and myocardial expression of MMP-9, Galectin-3, and pro-collagen-α1

Histological characterization of the myocardial tissue phenotype in mice after short-term anti-CTLA-4 or anti-PD-1 treatment showed that ICIs increased cardiac fibrosis compared to untreated mice (Figures 6A–C). In control group (Figure 6A) hematoxylin-eosin staining of longitudinal sections evidenced the absence of fibrosis, whereas treatment with Ipilimumab or Pembrolizumab (Figures 6B,C) increased drastically the fibrotic phenotype. Myocardial expression of galectin-3 (Figure 6D), mouse pro-collagen 1-α (Figure 6E) and MMP-9 (Figure 6F), biomarkers of fibrosis, corroborates these findings: galectin-3 is almost undetectable in control group while it is drastically increased after treatment with all ICIs (1.7 ± 1.2 vs. 24.5 ± 4.2 vs. 32.3 ± 4.3 ng/mg of tissue for control, Ipilimumab and Pembrolizumab, respectively; $p < 0.001$ for control vs. ICIs). Similar results were seen for procollagen 1α1 (3.4 ± 1.2 vs. 15.3 ± 3.1 vs. 16.8 ± 1.2 ng/mg of protein for control, Ipilimumab and Pembrolizumab, respectively; $p < 0.005$ for control vs. ICIs) and MMP-9 (407.8 ± 89.6 vs. 732.5 ± 102.2 vs. 895.5 ± 88.6 pg/mg of protein for control, Ipilimumab and Pembrolizumab, respectively; $p < 0.05$ for control vs. ICIs).

ICI therapy promotes DAMPs production, NLRP3, and MyD88 expression in myocardial tissues

We investigated on cardiac markers of inflammation and cell damages (DAMPs). Compared to untreated mice, ICIs increased significantly Fibronectin-EDA expression (Figure 6G) in heart lysates (2.3 ± 0.16 for Ipilimumab and $2.1 \pm$

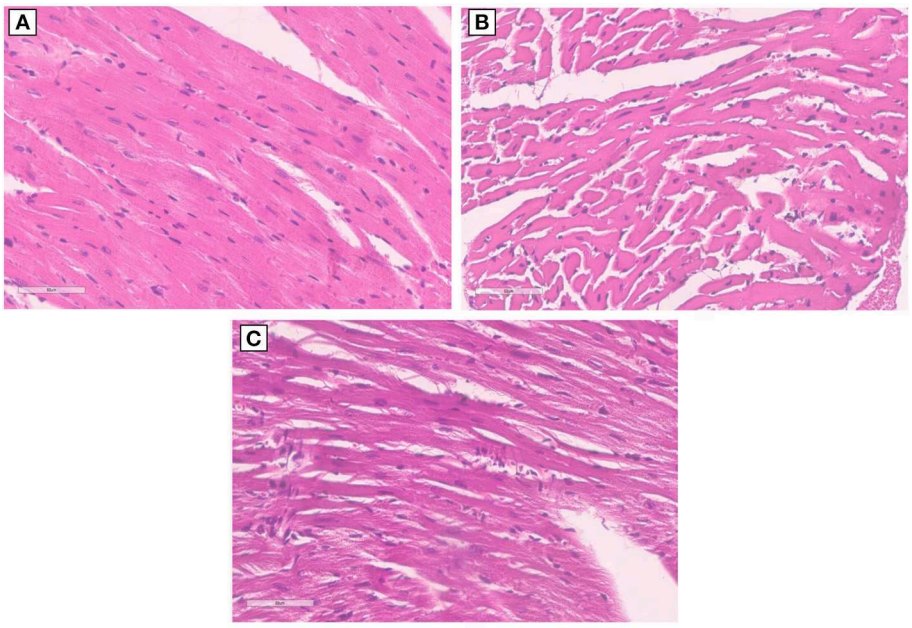

FIGURE 5
Hypertrophy analysis in myocardial tissues of mice treated with ICIs. **(A)** Hematoxylin-eosin staining of longitudinal sections with no hypertrophy in control untreated mice (x40); **(B)** hematoxylin-eosin staining of longitudinal sections with no hypertrophy in untreated mice and mice treated with Ipilimumab (×40); **(C)** hematoxylin-eosin staining of longitudinal sections highlights the development of marked hypertrophy in mice treated with Pembrolizumab (×40).

0.25 for Pembrolizumab; $p < 0.001$ for control vs. ICIs). Similarly another DAMP, called S100 Calgranulin (Figure 6H) was significantly enhanced by ICIs treatment (1.86 ± 0.21 for Ipilimumab and 1.96 ± 0.24 ng/mg of protein for Pembrolizumab; $p < 0.001$ for control vs. ICIs); no significant differences between ICIs were seen. Inflammasome and myddosome complex stimulates DAMPs, therefore, myocardial expression of NLRP type 3 and MyD type 88 were analyzed. A drastic increase in MyD-88 expression (Figure 6I) (33.2 pg/mg of protein ± 15.6 for untreated mice:198.6 ± 18.3 for Ipilimumab; 217.5 ± 17.4 for Pembrolizumab; $p < 0.005$ for ICIs vs. control). The same behavior was seen for NLRP3 expression after treatment with all ICIs (47.3 pg/mg of protein ± 13.5 for untreated mice: 132.1 ±15.1 for Ipilimumab; 126.6 ± 11.2 for Pembrolizumab; $p < 0.005$ for ICIs vs. control) (Figure 6J).

ICI therapy increases pro-inflammatory cytokine expression in myocardial tissues

Cytokines and chemokines are drivers of anticancer drug-induced cardiotoxicity, heart failure and myocarditis (32). Therefore, cytokines and chemokines in heart tissue of Ipilimumab or Pembrolizumab-treated female C57Bl6 mice were quantified (Figure 6K). Firstly, the family of IL-1 cytokines (IL-1α and IL-1β), increased in all ICIs treated group with respect to untreated mice ($p < 0.001$). IL-2 levels were also increased in ICIs group, highlighting immune-related reactions in myocardial tissue. Anti-inflammatory cytokines levels (IL-4 and IL-10) were reduced in ICIs group vs. untreated mice. Other pro-inflammatory cytokines (IL-6, IL17-α, IFN-γ, and TNF-α) were also increased in myocardial tissues of ICIs-treated mice vs. saline-treated groups. Levels of growth factors involved in heart failure and hypertrophy (G-CSF and GM-CSF) were also increased in ICIs groups (Figure 6K).

ICI therapy increases systemic levels of SDF-1 (CXCL12), inteleukin-1β, and interleukin-6

High plasma levels of Stromal Cell-Derived Factor 1 (SDF-1), IL-1β and IL-6 were associated to cardiac inflammation, heart failure and cardiovascular mortality (33). We analyzed if short term ICIs therapy could affect SDF-1, IL-1 β and IL-6 levels in plasma of C57/Bl6 mice (Figure 7). Before (T0), after three days (T3) and at the end of treatment (T10), systemic levels of all biomarkers were significantly increased with respect to control saline-treated mice ($p < 0.05$). For example, after 10 days of therapy, SDF-1 levels were 0.96 ng/ml ±0.24 for untreated mice; 2.75± 0.34 for Ipilimumab and 3.16 ± 0.29 for Pembrolizumab ($p < 0.005$ for ICIs vs. control). The same behavior was seen for

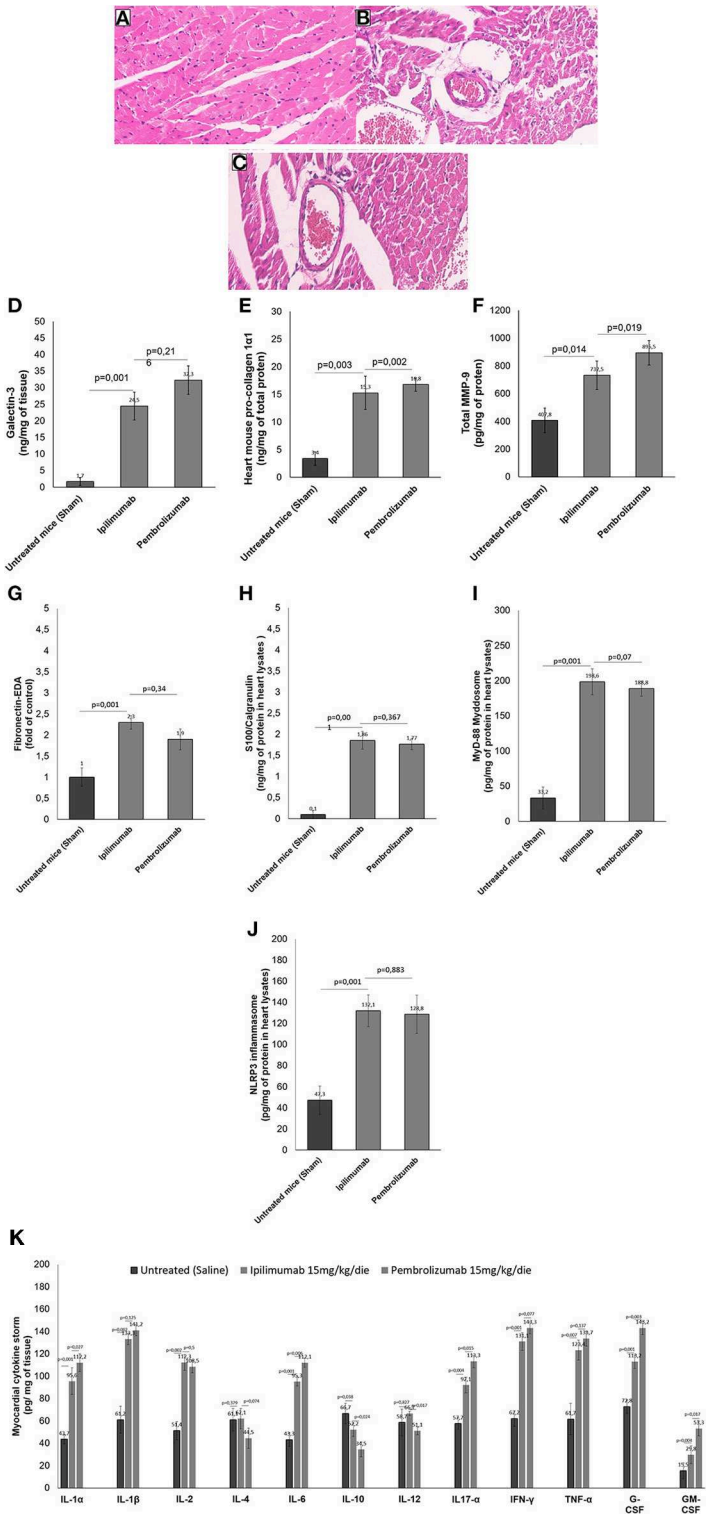

FIGURE 6
Histological analysis of the hearts of mice untreated or treated with ICIs. **(A)** Hematoxylin-eosin staining of longitudinal sections in control untreated mice (x40); **(B)** hematoxylin-eosin staining of longitudinal sections in mice treated with Ipilimumab (×40); **(C)** hematoxylin-eosin staining of longitudinal sections with fibrosis in mice treated with Pembrolizumab (×40). **(D)** Cardiac expression of galectin-3 (ng/mg of tissue), **(E)** mouse pro-collagen 1-α (ng/mg of total proten), **(F)** MMP-9 (pg/mg of protein), **(G)** Fibronectin EDA (fold of control), **(H)** S100 Calgranulin (ng/mg of protein in myocardial tissue lysate), **(I)** MyD-88 (pg/mg of protein in myocardial tissue lysate) and **(J)** NLRP-3 (pg/mg of protein in myocardial tissue lysate) after short-term treatment with ICIs. In **(K)**, Twelve cytokines (IL-1α, IL-1β, IL-2, IL-4, IL-6, IL-10, IL-12, IL17-α, IFN-γ, TNF-α, G-CSF, GM-CSF) were analyzed in heart lysates and reported as pg of cytokine normalized for mg of tissue. Error bars depict means ± SD ($n = 6$).

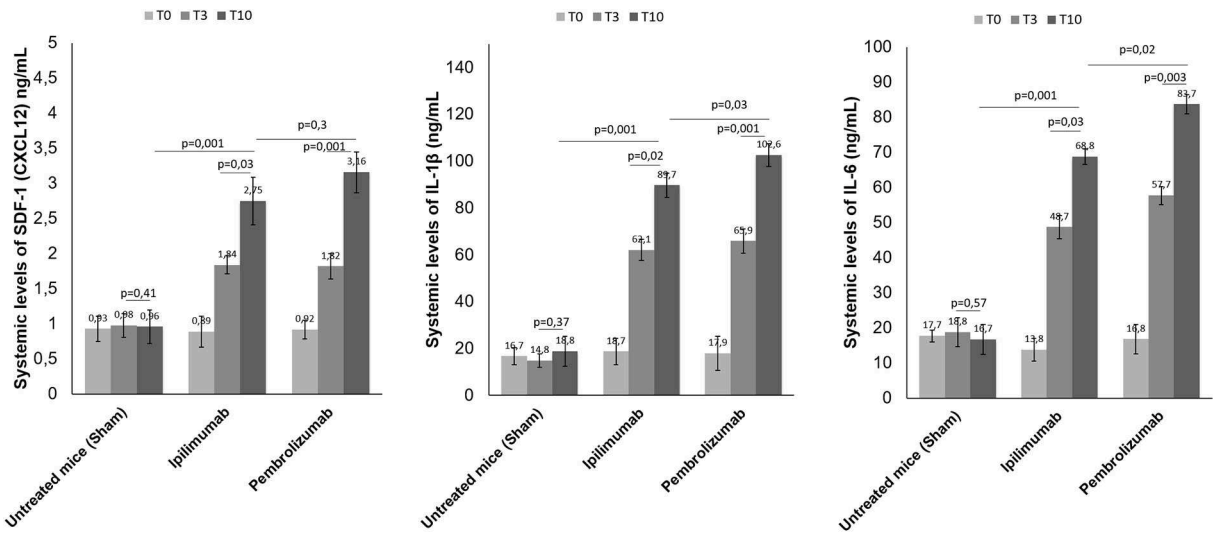

FIGURE 7
Effects of ICI treatment on plasma levels of SDF-1 (CXCL-12), Interleukin 1-β and Interleukin-6. Female C57/Bl6 mice were treated daily with anti-CTLA-4 or anti-PD-1 antibodies ($n = 6$) or left untreated ($n = 6$) for 10 days. Before (T0), after three days (T3) and at the end of treatments (T10), SDF-1 ($n = 6$), Interleukin 1-β ($n = 6$) and Interleukin-6 ($n = 6$) were quantified in plasma. Levels were reported in ng/ml of plasma.

IL-1 β and IL-6, indicating a systemic inflammation even after 3 days of treatment with ICIs (Figure 7).

Discussion

The current study aimed to evaluate the pro-inflammatory effects of short-term immune checkpoint inhibitors (ICIs) treatment in myocardial and vascular tissues in preclinical models (34, 35) (Figure 8). Notably, the use of ICIs in clinical oncology found significant clinical benefits in cancer patients, however, a wide spectrum of side effects are being seen (called irAEs): rash (maculopapular, lichenoid), diarrhea, colitis, mucositis, hypo or hyper thyroidism, hepatitis, inflammatory arthritis, myalgia (36). Endocrinopathies and inflammatory pathologies induced by PD-1 / PDL-1 or CTLA-4 blocking agents are frequently reported in both monotherapy and combinatorial therapies. Clinical studies report both short-term and long-term side effects in cancer patients and the mechanisms are not yet well-known (37). There are both immune-mediated and non-immune-mediated mechanisms involved in irAEs. A recent meta-analysis reports a high incidence of myocarditis (about 11 times higher than in other therapies) which reaches a mortality rate of about 50% in case of combination therapies (PD1 / PDL-1 associated to CTLA-4 blocking agents) (38, 39). Furthermore, ICIs have recently been shown to accelerate the process of atherosclerosis in both preclinical and clinical study models. Even just a short treatment with ICIs increases the inflammatory state in the vascular endothelium by accelerating the atherosclerotic process (39). Other recent studies show that short ICSi treatments can cause arrhythmias, Takotsubo syndrome and inflammatory vascular events (40, 41). Current data regarding ICIs- associated pericardial involvement are limited, but case-reports include pericarditis, pericardial effusion (42, 43). Notably, a deep knowledge of ICIs-induced myocardial injuries is needed. Immune cells uptake and infiltration in myocardial tissue were always seen in human histological studies (CD4, CD8 T cells and macrophages). Immune-related side effects involves several chemokines like CXCR 10, 9 and 3, high levels of granzyme B especially in myocardial tissue (44). Our data suggest that NLRP3 and MyD88 pathways could contribute to the increased vascular and myocardial inflammation of anti-CTLA-4/anti-PD-1 treatments. NLRP3 drives cytosolic damages, hypertrophy and inflammation through cytokines and overproduction of hs-CRP.

As described in Figure 6 and summarized in Figure 8, our data confirms that ICIs increases DAMPs in cardiomyocytes and myocardial tissue of mice models. It has been described that in patients with unstable angina or with AMI, endogenous DAMPs like Fibronectin-EDA, S100/Calgranulin, Galectine-3 are released from damaged cardiac cells and signal through TLR receptors. There is also emerging evidence for the involvement of Toll-like receptors type-9 in heart failure, which can be activated by endogenous DAMPs, including mitochondrial DNA, to modulate the progression of the disease (45, 46). The increases in DAMPs levels after short-term ICIs treatment in mice indicates myocardial injuries (46). Whether long-term ICI therapy affects myocardial stress and vascular inflammation is unknown. Nevertheless, our data suggest that even short-term

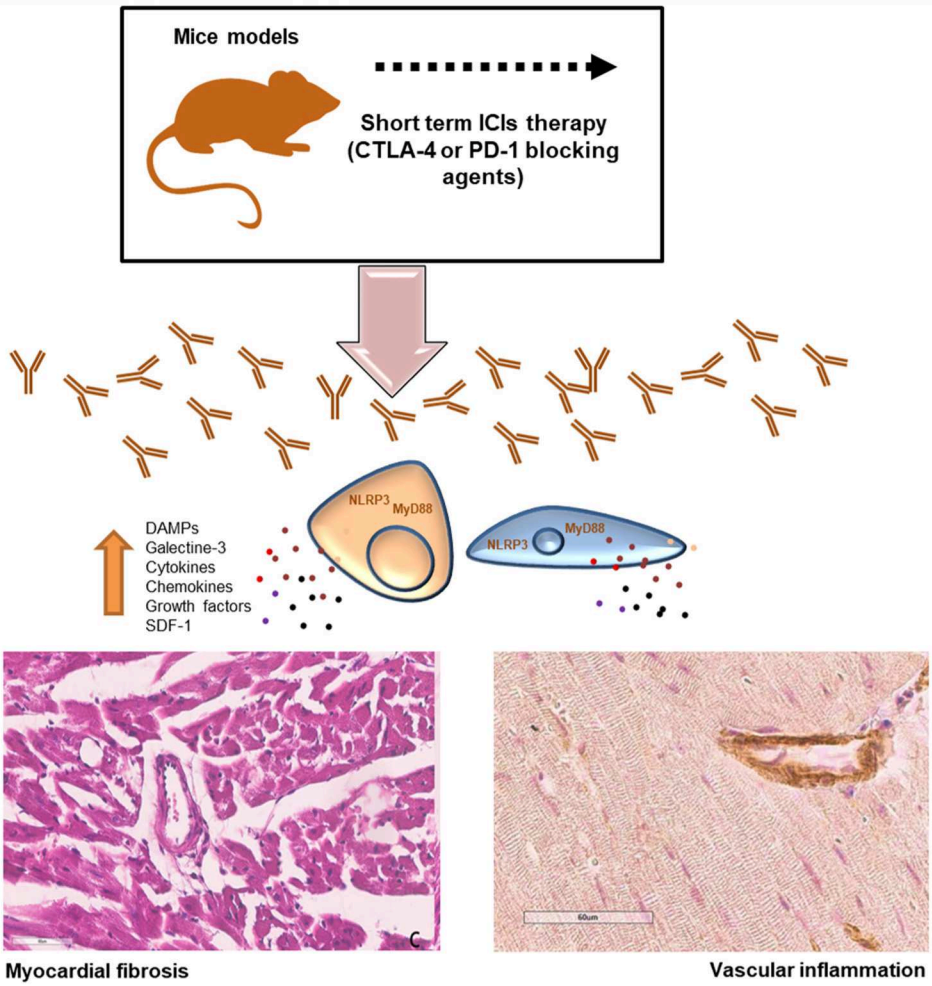

FIGURE 8
Short-term ICI Therapy increases DAMPs, NLRP3 and MyD-88 mediated fibrosis and vascular inflammation. Short-term treatment with immune checkpoint inhibitors (ICIs) induced significant increases in DAMPs, galectine-3, cytokines and chemokines through NLRP3 and MyD88 pathways inducing myocardial hypertrophy, fibrosis and strong vascular inflammation.

ICIs therapy induces vascular inflammation, fibrosis and levels of myocardial NLRP3 and MyD88 (Figure 8). Whether ICIs-induced inflammation persist after cessation of the therapy and how they affect myocardial work in the long-term is not currently known (47).

This work has several limitations: firstly, the use of a tumor-free mice model. As cardiovascular diseases and cancer share many pathophysiological pathways, including inflammation, the use of a tumor-bearing model would have increased the translational potential of our study. Moreover, there are clinical evidences that combination ICIs-therapy exerts the most frequent and pro-inflammatory cardiac and endocrine side effects compared to monotherapies (48) therefore, further cardiotoxic studies in preclinical models will be performed after the combination of anti-CTLA4 and anti-PD-1/PD-L1.

Another limitation is based on the short period of treatment with ICIs without a longer follow up. In real world clinical experience, cancer patients experienced ICIs-mediated side effects also many months after therapy cessation (47, 49). These effects could be also partially related to endocrine changes due to PD-1/CTLA-4 blocking pathways that exerts a detrimental cardiotoxic effects in these patients. Therefore, further preclinical studies on long-term cardiovascular side effects after ICIs therapy will be performed.

Another methodological limitation of this work is the absence of a more proper control group in animal studies based on the administration of IgG control antibody, however, as reported in cellular experiments (Figure 8), any changes in pro-inflammatory and cell dead markers were seen after incubation with control IgG. Moreover, it is plausible that the intraperitoneal administration of nonspecific IgG as a control

does not change neither cardiac functions nor cardiac and systemic inflammatory status in mouse models as confirmed by recent similar research papers (50, 51).

In conclusion, cardiotoxicity, although rare, is a clinically relevant problem in cancer patients undergoing ICIs. Long-term side effects of ICIs are reported, however, some biochemical changes may occur even a few days after treatment with ICIs, as specified in this work. The involvement of NLRP3 MyD-88 and some DAMPs in ICIs-associated cardiovascular disease was seen. Relevant histological effects such as cardiac endothelial inflammation and overexpression of pro-fibrotic and pro-inflammatory cytokines is a non-negligible fact that deserves further investigation. The increase in systemic levels of SDF-1, IL-1β and il-6 indicates systemic pro-inflammatory effects induced by ICIs that can directly and indirectly increase the risk of myocarditis, however more detailed studies on the mechanisms of systemic and direct cardiac toxicity will have to be carried out. Of note, considering that PD-1 and CTLA-4 blocking agents recognize the murine epitope with lower affinity than the human epitope, the effects observed in this work could also be underestimated (12) consequently, short and long term clinical studies during ICIs deserve urgent investigation. Moreover, the results of this study warrant further preclinical cardioprotective trials with anti-cytokine (52, 53), anti-NLRP3 (54–56) or anti-MyD88 (57, 58) therapies in primary or secondary prevention of ICIs-related cardiotoxicity.

This study suggests that short-term ICI therapy affects myocardial and vascular inflammation through DAMPs and cytokines through NLRP-3 and MyD-88 related pathways (Figure 8). It is plausible that ICIs exerts both systemic and cardiac toxicities through the activation of cytokines cascades that exacerbate the inflammatory damages in cardiomyocytes. These results are in line with another recent work (59) demonstrating pro-atherosclerotic effects of short-ICIs therapy in mice models. Clinical studies are required to elucidate the effects of ICIs on myocardial and vascular inflammation and confirms the role of NLRP3 and Myd88 in progression of ICIs-mediated cardiovascular diseases.

Data availability statement

The data presented in the study are deposited in the Zenodo repository, accession number https://zenodo.org/record/7040431#.YyMLcYrP1D9.

Ethics statement

The animal study was reviewed and approved by the experimental protocols, in accordance with EU Directive 2010/63/EU for animal experiments and Italian D.L.vo 26/2014 law, were approved by the Ministry of Health with authorization number 1467/17-PR of 13-02-2017, and institutional ethics committees: Organismo preposto al benessere degli animali (OPBA).

Author contributions

VQ, SB, MP, AD, CC, GG, AB, GP, and AL performed the experiments and analyzed the data. AP, IB, AI, and MC provided technical assistance. VQ, CD, and NM designed the study and drafted the manuscript. All authors read and approved the final manuscript.

Funding

This work was funded by a "Ricerca Corrente" grant from the Italian Ministry of Health titled "Cardiotossicità da chemioterapie, targeted therapies e immunoterapie, diagnosi precoce e cardioprotezione, Ricerca preclinica e clinica".

Conflict of interest

Authors MP and CD were employed by Ceinge - Biotecnologie Avanzate.

The remaining authors declare that the research was conducted in the absence of any commercial or financial relationships that could be construed as a potential conflict of interest.

Publisher's note

References

1. Meric-Bernstam F, Larkin J, Tabernero J, Bonini C. Enhancing anti-tumour efficacy with immunotherapy combinations. *Lancet.* (2021) 397:1010–22. doi: 10.1016/S0140-6736(20)32598-8

2. Rotte A, Jin JY, Lemaire V. Mechanistic overview of immune checkpoints to support the rational design of their combinations in cancer immunotherapy. *Ann Oncol.* (2018) 29:71–83. doi: 10.1093/annonc/mdx686

3. Davis AA, Patel VG. The role of PD-L1 expression as a predictive biomarker: an analysis of all US Food and Drug Administration (FDA) approvals of immune checkpoint inhibitors. *J Immunother Cancer.* (2019) 7:278. doi: 10.1186/s40425-019-0768-9

4. Boutros C, Tarhini A, Routier E, Lambotte O, Ladurie FL, Carbonnel F, et al. Safety profiles of anti-CTLA-4 and anti-PD-1 antibodies alone and in combination. *Nat Rev Clin Oncol.* (2016) 13:473–86. doi: 10.1038/nrclinonc.2016.58

5. Yin G, Guo W, Huang Z, Chen X. Efficacy of radiotherapy combined with immune checkpoint inhibitors in patients with melanoma: a systemic review and meta-analysis. *Melanoma Res.* (2022) 32:71–8. doi: 10.1097/CMR.0000000000000800

6. Johnson DB, Nebhan CA, Moslehi JJ, Balko JM. Immune-checkpoint inhibitors: long-term implications of toxicity. *Nat Rev Clin Oncol.* (2022) 19:254–67. doi: 10.1038/s41571-022-00600-w

7. Aras MA, Power JR, Moslehi JJ. Inflammatory biomarkers to detect immune checkpoint inhibitor-associated cardiotoxicity in lung cancer patients: ready for prime time? *JACC CardioOncol.* (2020) 2:503–5. doi: 10.1016/j.jaccao.2020.08.001

8. Geraud A, Gougis P, Vozy A, Anquetil C, Allenbach Y, Romano E, et al. Clinical pharmacology and interplay of immune checkpoint agents: a yin-yang balance. *Annu Rev Pharmacol Toxicol.* (2021) 61:85–112. doi: 10.1146/annurev-pharmtox-022820-093805

9. Dong M, Yu T, Zhang Z, Zhang J, Wang R, Tse G, et al. ICIs-Related cardiotoxicity in different types of cancer. *J Cardiovasc Dev Dis.* (2022) 9:203. doi: 10.3390/jcdd9070203

10. Wei SC, Meijers WC, Axelrod ML, Anang NAS, Screever EM, Wescott EC, et al. A genetic mouse model recapitulates immune checkpoint inhibitor-associated myocarditis and supports a mechanism-based therapeutic intervention. *Cancer Discov.* (2021) 11:614–25. doi: 10.1158/2159-8290.CD-20-0856

11. Michel L, Helfrich I, Hendgen-Cotta UB, Mincu RI, Korste S, Mrotzek SM, et al. Targeting early stages of cardiotoxicity from anti-PD1 immune checkpoint inhibitor therapy. *Eur Heart J.* (2022) 43:316–29. doi: 10.1093/eurheartj/ehab430

12. Awadalla M, Mahmood SS, Groarke JD, Hassan MZO, Nohria A, Rokicki A, et al. Global longitudinal strain and cardiac events in patients with immune checkpoint inhibitor-related myocarditis. *J Am Coll Cardiol.* (2020) 75:467–78. doi: 10.1016/j.jacc.2019.11.049

13. Vaz Ferreira V, Mano TB, Cardoso I, Coutinho Cruz M, Moura Branco L, Almeida-Morais L, et al. Myocardial work brings new insights into left ventricular remodelling in cardio-oncology patients. *Int J Environ Res Public Health.* (2022) 19:2826. doi: 10.3390/ijerph19052826

14. Besler C, Lang D, Urban D, Rommel KP, von Roeder M, Fengler K, et al. Plasma and cardiac galectin-3 in patients with heart failure reflects both inflammation and fibrosis: implications for its use as a biomarker. *Circ Heart Fail.* (2017) 10:e003804. doi: 10.1161/CIRCHEARTFAILURE.116.003804

15. Quagliariello V, Passariello M, Rea D, Barbieri A, Iovine M, Bonelli A, et al. Evidences of CTLA-4 and PD-1 blocking agents-induced cardiotoxicity in cellular and preclinical models. *J Pers Med.* (2020) 10:179. doi: 10.3390/jpm10040179

16. Department of Health and Ageing Australian Government. *Australian Public Assessment Report for IPILIMUMAB*. Bristol-Myers Squibb Australia Pty Ltd.: Mulgrave, Australia (2011).

17. Lu L, Xu X, Zhang B, Zhang R, Ji H, Wang X, et al. Combined PD-1 blockade and GITR triggering induce a potent antitumor immunity in murine cancer models and synergizes with chemotherapeutic drugs. *J Transl Med.* (2014) 12:36. doi: 10.1186/1479-5876-12-36

18. Peng Y, Popovic ZB, Sopko N, Drinko J, Zhang Z, Thomas D, et al. Speckle tracking echocardiography in the assessment of mouse models of cardiac dysfunction. *Am J Physiol Circ Physiol.* (2009) 297:H811–20. doi: 10.1152/ajpheart.00385.2009

19. Vetrei C, Passariello M, Froechlich G, Rapuano Lembo R, Zambrano N, De Lorenzo C. Immunomodulatory mAbs as tools to investigate on Cis-Interaction of PD-1/PD-L1 on tumor cells and to set up methods for early screening of safe and potent combinatorial treatments. *Cancers.* (2021) 13:2858. doi: 10.3390/cancers13122858

20. Rea D, Coppola C, Barbieri A, Monti MG, Misso G, Palma G, et al. Strain analysis in the assessment of a mouse model of cardiotoxicity due to chemotherapy: sample for preclinical research. *In Vivo.* (2016) 30:279–90.

21. De Lorenzo C, Paciello R, Riccio G, Rea D, Barbieri A, Coppola C, et al. Cardiotoxic effects of the novel approved anti-ErbB2 agents and reverse cardioprotective effects of ranolazine. *Onco Targets Ther.* (2018) 11:2241–50. doi: 10.2147/OTT.S157294

22. Quagliariello V, Passariello M, Coppola C, Rea D, Barbieri A, Scherillo M, et al. Cardiotoxicity and pro-inflammatory effects of the immune checkpoint inhibitor Pembrolizumab associated to Trastuzumab. *Int J Cardiol.* (2019) 292:171–9. doi: 10.1016/j.ijcard.2019.05.028

23. Passariello M, Yoshioka A, Takahashi K, Hashimoto SI, Rapuano Lembo R, Manna L, et al. Novel bi-specific immuno-modulatory tribodies potentiate T cell activation and increase anti-tumor efficacy. *Int J Mol Sci.* (2022) 23:3466. doi: 10.3390/ijms23073466

24. Selby MJ, Engelhardt JJ, Johnston RJ, Lu L-S, Han M, Thudium K, et al. Preclinical development of ipilimumab and nivolumab combination immunotherapy: mouse tumor models, *in vitro* functional studies, and cynomolgus macaque toxicology. *PLoS ONE.* (2016) 11:e0161779. doi: 10.1371/journal.pone.0161779

25. Chang CY, Park H, Malone DC, Wang CY, Wilson DL, Yeh YM, et al. Immune checkpoint inhibitors and immune-related adverse events in patients with advanced melanoma: a systematic review and network meta-analysis. *JAMA Netw Open.* (2020) 3:e201611. doi: 10.1001/jamanetworkopen.2020.1611

26. Ji C, Roy MD, Golas J, Vitsky A, Ram S, Kumpf SW, et al. Myocarditis in cynomolgus monkeys following treatment with immune checkpoint inhibitors. *Clin Cancer Res.* (2019) 25:4735–48. doi: 10.1158/1078-0432.CCR-18-4083

27. Sehgal K, Costa DB, Rangachari D. Extended-interval dosing strategy of immune checkpoint inhibitors in lung cancer: will it outlast the COVID-19 pandemic? *Front Oncol.* (2020) 10:1193. doi: 10.3389/fonc.2020.01193

28. Patnaik A, Kang SP, Rasco D, Papadopoulos KP, Elassaiss-Schaap J, Beeram M, et al. Phase I study of pembrolizumab (MK-3475; anti-PD-1 monoclonal antibody) in patients with advanced solid tumors. *Clin Cancer Res.* (2015) 21:4286–93. doi: 10.1158/1078-0432.CCR-14-2607

29. Riccio G, Antonucci S, Coppola C, D'Avino C, Piscopo G, Fiore D, et al. Ranolazine attenuates Trastuzumab-induced heart dysfunction by modulating ROS production. *Front Physiol.* (2018) 9:38. doi: 10.3389/fphys.2018.00038

30. Quagliariello V, De Laurentiis M, Rea D, Barbieri A, Monti MG, Carbone A, et al. The SGLT-2 inhibitor empagliflozin improves myocardial strain, reduces cardiac fibrosis and pro-inflammatory cytokines in non-diabetic mice treated with doxorubicin. *Cardiovasc Diabetol.* (2021) 20:150. doi: 10.1186/s12933-021-01346-y

31. Saito T, Hasegawa Y, Ishigaki Y, Yamada T, Gao J, Imai J, et al. Importance of endothelial NF-κB signalling in vascular remodelling and aortic aneurysm formation. *Cardiovasc Res.* (2013) 97:106–14. doi: 10.1093/cvr/cvs298

32. Subramanian S, Liu C, Aviv A, Ho JE, Courchesne P, Muntendam P, et al. Stromal cell-derived factor 1 as a biomarker of heart failure and mortality risk. *Arterioscler Thromb Vasc Biol.* (2014) 34:2100–5. doi: 10.1161/ATVBAHA.114.303579

33. Tschöpe C, Ammirati E, Bozkurt B, Caforio ALP, Cooper LT, Felix SB, et al. Myocarditis and inflammatory cardiomyopathy: current evidence and future directions. *Nat Rev Cardiol.* (2021) 18:169–93. doi: 10.1038/s41569-020-00435-x

34. Wang DY, Okoye GD, Neilan TG, Johnson DB, Moslehi JJ. Cardiovascular toxicities associated with cancer immunotherapies. *Curr Cardiol Rep.* (2017) 19:21. doi: 10.1007/s11886-017-0835-0

35. Leach DR, Krummel MF, Allison JP. Enhancement of antitumor immunity by CTLA-4 blockade. *Science.* (1996) 271:1734–6. doi: 10.1126/science.271.5256.1734

36. llouchery M, Beuvon C, Pérault-Pochat MC, Roblot P, Puyade M, Martin M. Safety of immune checkpoint inhibitor resumption after interruption for immune-related adverse events, a narrative review. *Cancers.* (2022) 14:955. doi: 10.3390/cancers14040955

37. Patel RP, Parikh R, Gunturu KS, Tariq RZ, Dani SS, Ganatra S, et al. Cardiotoxicity of immune checkpoint inhibitors. *Curr Oncol Rep.* (2021) 23:79. doi: 10.1007/s11912-021-01070-6

38. Tocchetti CG, Galdiero MR, Varricchi G. Cardiac toxicity in patients treated with immune checkpoint inhibitors: it is now time for cardio-immuno-oncology. *J Am Coll Cardiol.* (2018) 71:1765–7. doi: 10.1016/j.jacc.2018.02.038

39. Mahmood SS, Fradley MG, Cohen JV, Nohria A, Reynolds KL, Heinzerling LM, et al. Myocarditis in patients treated with immune checkpoint inhibitors. *J Am Coll Cardiol.* (2018) 71:1755–64. doi: 10.1016/j.jacc.2018.02.037

40. Carbone A, Bottino R, Russo V, D'Andrea A, Liccardo B, Maurea N, et al. Takotsubo cardiomyopathy as epiphenomenon of cardiotoxicity in patients with cancer: a meta-summary of case reports. *J Cardiovasc Pharmacol.* (2021) 78:e20–9. doi: 10.1097/FJC.0000000000001026

41. Serzan M, Rapisuwon S, Krishnan J, Chang IC, Barac A. Takotsubo cardiomyopathy associated with checkpoint inhibitor therapy: endomyocardial biopsy provides pathological insights to dual diseases. *JACC CardioOncol.* (2021) 3:330–4. doi: 10.1016/j.jaccao.2021.02.005

42. Braden J, Lee JH. Immune checkpoint inhibitor induced pericarditis and encephalitis in a patient treated with Ipilimumab and Nivolumab for metastatic

melanoma: a case report and review of the literature. *Front Oncol.* (2021) 11:749834. doi: 10.3389/fonc.2021.749834

43. Lal JC, Brown SA, Collier P, Cheng F. A retrospective analysis of cardiovascular adverse events associated with immune checkpoint inhibitors. *Cardiooncology.* (2021) 7:19. doi: 10.1186/s40959-021-00106-x

44. Johnson DB, Balko JM, Compton ML, Chalkias S, Gorham J, Xu Y, et al. Fulminant myocarditis with combination immune checkpoint blockade. *N Engl J Med.* (2016) 375:1749–55. doi: 10.1056/NEJMoa1609214

45. Yu L, Feng Z. The role of toll-like receptor signaling in the progression of heart failure. *Mediators Inflamm.* (2018) 2018:9874109. doi: 10.1155/2018/9874109

46. Christia P, Frangogiannis NG. Targeting inflammatory pathways in myocardial infarction. *Eur J Clin Invest.* (2013) 43:986–95. doi: 10.1111/eci.12118

47. Li C, Bhatti SA, Ying J. Immune checkpoint inhibitors-associated cardiotoxicity. *Cancers.* (2022) 14:1145. doi: 10.3390/cancers14051145

48. Agostinetto E, Eiger D, Lambertini M, Ceppi M, Bruzzone M, Pondé N, et al. Cardiotoxicity of immune checkpoint inhibitors: a systematic review and meta-analysis of randomised clinical trials. *Eur J Cancer.* (2021) 148:76–91. doi: 10.1016/j.ejca.2021.01.043

49. Zhang L, Reynolds KL, Lyon AR, Palaskas N, Neilan TG. The evolving immunotherapy landscape and the epidemiology, diagnosis, and management of cardiotoxicity: *JACC: CardioOncology* Primer. *JACC CardioOncol.* (2021) 3:35–47. doi: 10.1016/j.jaccao.2020.11.012

50. Giannoccaro MP, Menassa DA, Jacobson L, Coutinho E, Prota G, Lang B, et al. Behaviour and neuropathology in mice injected with human contactin-associated protein 2 antibodies. *Brain.* (2019) 142:2000–12. doi: 10.1093/brain/awz119

51. Kallikourdis M, Martini E, Carullo P, Sardi C, Roselli G, Greco CM, et al. T cell costimulation blockade blunts pressure overload-induced heart failure. *Nat Commun.* (2017) 8:14680. doi: 10.1038/ncomms14680

52. Ridker PM. Anticytokine agents: targeting interleukin signaling pathways for the treatment of atherothrombosis. *Circ Res.* (2019) 124:437–50. doi: 10.1161/CIRCRESAHA.118.313129

53. Quagliariello V, Paccone A, Iovine M, Cavalcanti E, Berretta M, Maurea C, et al. Interleukin-1 blocking agents as promising strategy for prevention of anticancer drug-induced cardiotoxicities: possible implications in cancer patients with COVID-19. *Eur Rev Med Pharmacol Sci.* (2021) 25:6797–812. doi: 10.26355/eurrev_202111_27124

54. Toldo S, Mauro AG, Cutter Z, Van Tassell BW, Mezzaroma E, Del Buono MG, et al. The NLRP3 inflammasome inhibitor, OLT1177 (Dapansutrile), reduces infarct size and preserves contractile function after ischemia reperfusion injury in the mouse. *J Cardiovasc Pharmacol.* (2019) 73:215–22. doi: 10.1097/FJC.0000000000000658

55. Murphy SP, Kakkar R, McCarthy CP, Januzzi JL Jr. Inflammation in heart failure: JACC state-of-the-art review. *J Am Coll Cardiol.* (2020) 75:1324–40. doi: 10.1016/j.jacc.2020.01.014

56. Quagliariello V, De Laurentiis M, Cocco S, Rea G, Bonelli A, Caronna A, et al. NLRP3 as putative marker of Ipilimumab-induced cardiotoxicity in the presence of hyperglycemia in estrogen-responsive and triple-negative breast cancer cells. *Int J Mol Sci.* (2020) 21:7802. doi: 10.3390/ijms21207802

57. Miao Y, Ding Z, Zou Z, Yang Y, Yang M, Zhang X, et al. Inhibition of MyD88 by a novel inhibitor reverses two-thirds of the infarct area in myocardial ischemia and reperfusion injury. *Am J Transl Res.* (2020) 12:5151–69.

58. Bayer AL, Alcaide P. MyD88: at the heart of inflammatory signaling and cardiovascular disease. *J Mol Cell Cardiol.* (2021) 161:75–85. doi: 10.1016/j.yjmcc.2021.08.001

59. Poels K, van Leent MMT, Boutros C, Tissot H, Roy S, Meerwaldt AE, et al. Immune checkpoint inhibitor therapy aggravates T cell-driven plaque inflammation in atherosclerosis. *JACC CardioOncol.* (2020) 2:599–610. doi: 10.1016/j.jaccao.2020.08.007

frontiers | Frontiers in Cardiovascular Medicine

TYPE Original Research
PUBLISHED 14 September 2022
DOI 10.3389/fcvm.2022.960240

OPEN ACCESS

EDITED BY
Dong Han,
People's Liberation Army General Hospital, China

REVIEWED BY
Antonio Avallone,
G. Pascale National Cancer Institute Foundation (IRCCS), Italy
Adriana Albini,
MultiMedica Holding SpA (IRCCS), Italy

*CORRESPONDENCE
Chiara Lestuzzi
chiara.lestuzzi@aas5.sanita.fvg.it

SPECIALTY SECTION
This article was submitted to Cardio-Oncology, a section of the journal Frontiers in Cardiovascular Medicine

RECEIVED 02 June 2022
ACCEPTED 16 August 2022
PUBLISHED 14 September 2022

CITATION
Cucciniello L, Bidoli E, Viel E, Canale ML, Gerratana L and Lestuzzi C (2022) The puzzling clinical presentation of fluoropyrimidines cardiotoxicity.
Front. Cardiovasc. Med. 9:960240.
doi: 10.3389/fcvm.2022.960240

The puzzling clinical presentation of fluoropyrimidines cardiotoxicity

Linda Cucciniello[1], Ettore Bidoli[2], Elda Viel[3], Maria Laura Canale[4], Lorenzo Gerratana[5] and Chiara Lestuzzi[3]*

[1]Department of Oncology, Centro di Riferimento Oncologico, Istituto di Ricovero e Cura a Carattere Scientifico (IRCCS), National Cancer Institute, Aviano, Italy, [2]Unit of Cancer Epidemiology, Centro di Riferimento Oncologico, Istituto di Ricovero e Cura a Carattere Scientifico (IRCCS), National Cancer Institute, Aviano, Italy, [3]Department of Cardiology, Azienda Sanitaria Friuli Occidentale, ASFO, Pordenone, Italy, [4]Ospedale Versilia, Azienda Usl Toscana nord ovest, Lido di Camaiore, Italy, [5]Department of Medical Oncology, Aviano Oncology Reference Center (IRCCS), Aviano, Italy

The cardiotoxicity of fluoropyrimidines (FP) [5-Fluorouracil and Capecitabine] is often reported as acute cardiac ischemia with rest typical angina, signs of ischemia at electrocardiogram (ECG), and ventricular kinetics abnormalities. However, silent ischemia, effort-related toxicity, and ventricular arrhythmias (VA) have been also described. The aim of this study is to report a consecutive series of 115 patients with FP cardiotoxicity observed in a single center both within clinical prospective studies and during the clinical routine. The clinical presentation widely varied as regards symptoms, ECG abnormalities, and clinical outcomes. We report also the strategies used to prevent cardiotoxicity in a subgroup of 35 patients who continued o rechallenged FP therapy after cardiotoxicity. In nearly half of the patients, the cardiotoxicity was triggered by physical effort. Typical angina was rare: the symptoms were absent in 51% of cases and were atypical in half of the other cases. ST-segment elevation and VA were the most frequent ECG abnormality; however, ST segment depression or negative T waves were the only abnormalities in 1/3 of the cases. Troponins essays were often within the normal limits, even in presence of extensive signs of ischemia. The most effective strategy to prevent cardiotoxicity at rechallenge was reducing FP dosage and avoiding physical effort. Anti-ischemic therapies were not always effective. Raltitrexed was a safe alternative to FP. Fluoropyrimidine cardiotoxicity shows a wide variety of clinical presentations in real life, from silent ischemia to atypical symptoms, acute coronary syndrome, left ventricular dysfunction (LVD), VA, or complete atrio-ventricular block. Physical effort is the trigger of cardiotoxicity in nearly half of the cases. The recognition of cardiotoxicity cannot rely on symptoms only but requires an active screening with ECG and stress test in selected cases.

KEYWORDS

cardiotoxicity, cardiotoxicity after chemotherapy, capecitabine, fluorouracil/adverse effects, fluoropyrimidine chemotherapeutics, fluoropyrimidine cardiotoxicity, 5-fluorouracil, capecitabine cardiotoxicity

Background

The fluoropyrimidines (FP) 5-fluorouracil (5-FU) and its prodrug capecitabine represent a mainstay of chemotherapy (CT) regimens for different types of malignancies, including head/neck, gastrointestinal, liver, and breast cancer. They can both induce cardiac toxicity (TOX), mostly in the form of myocardial ischemia (MI), ventricular arrhythmias (VA), left ventricular dysfunction (LVD), and sudden death (SD) (1–7). TOX of FP can be precipitated by effort and it can be asymptomatic, thus leading to an underdiagnosis in retrospective studies (8, 9). According to the literature, the most frequent clinical presentation of FP cardiotoxicity is angina with ST-segment elevation detected at Electrocardiogram (ECG) and mimicking vasospastic angina (**Table 1**). However, some prospective studies with Holter monitoring have reported transient asymptomatic ST segment elevation and ECG abnormalities different from ST-segment elevation have also been described (mostly ST segment depression and negative T waves) (10). A recent review analyzing data from 37 papers including the original data, reported wide variability in clinical presentation and risk factors, probably attributable to the different definitions provided for TOX and to the different modalities of data collection (11).

Aim of the study

To describe the clinical presentation of FP cardiotoxicity in patients treated with FP in a single Institution: CRO, National Cancer Institute of Aviano (PN, Italy) from 2001 to 2021, and to report the possibility of cardioprotection strategies in a group of patients who underwent a rechallenge therapy with FP after the first episode of cardiotoxicity.

Materials and methods

We searched the electronic database of the Cardiology Unit of the CRO from 2001 to 2021 and identified 141 patients who had been classified as having had FP cardiotoxicity. The clinical cardiologic and oncologic charts were reviewed by expert cardio-oncologists, in order to confirm the diagnosis and to collect data regarding the clinical history (before and after the diagnosis) whenever available. FP cardiotoxicity was defined as the presence of clinical, ECG, and/or echocardiographic signs of ischemia, Lown $\geq$2 VA, supraventricular arrhythmias, complete atrio-ventricular block, or LVD.

Symptoms were classified as follows: "typical chest pain" included typical angina (retrosternal constrictive or squeezing chest pain, radiated or not to the left arm or to jaws) and weight over the sternum; "atypical chest pain" included less defined chest pain or discomfort, burning sensation; "atypical symptoms" included jaw pain, throat constriction, malaise, dizziness, dyspnea.

The diagnosis of TOX had to be confirmed by the disappearance of clinical and instrumental abnormalities after withdrawing FP and by the exclusion of other causes of ischemia or arrhythmias.

After revision, 10 patients were excluded because the clinical diagnosis of cardiotoxicity was equivocal and another 26 patients (including two patients who died suddenly at home at the end of the 5-FU infusion) were excluded because it was not possible to collect detailed information about the ECG and the cardiovascular risk factors. The remaining 115 pts (74 males and 41 females, aged 19 to 79, mean 59 $\pm$11, median 61) are the object of our study (**Figure 1**). The cases had been observed both in daily practice and in two prospective studies where an effort stress test (EST) was obtained during FP treatment. We investigated also the clinical course of the patients in whom FP, after an episode of cardiotoxicity, was not discontinued or was later re-introduced in the therapy.

Results

Amongst the 115 patients evaluated in the present study, 79 had at least one CVRF, 15 had a clinical history of ischemic heart disease and 41 were on medical therapy with one or more cardiovascular drugs (in particular, 8 with calcium-channel blockers, 11 with beta-blockers, 22 with angiotensin-converting enzyme inhibitors, and 9 with nitrates). The FP administered was 5-FU in 64 patients and capecitabine in the remaining 51 patients (**Table 2**).

Cardiotoxicity (**Table 3**) was observed at rest in 63 patients and during physical effort in 52 patients. Furthermore, effort-related symptoms during daily life were reported by 10 patients who had cardiotoxicity confirmed by the EST. The ECG recorded at the time of cardiotoxicity diagnosis showed ischemic repolarization changes in 96 patients: ST-segment elevation (1 to 7 mm) in 53 patients, ST segment depression (1 to 7.5 mm) in 16, both ST-segment elevation and depression in 12 patients; negative T waves only in 15 patients. The number of ECG leads showing ST-T changes of ischemia ranged from 2 to 12 (median 5).

Arrhythmias were observed in 34 patients: in particular, 28 patients had ventricular ectopic beats and another 6 patients experienced other kinds of arrhythmias (supraventricular tachycardia, severe bradycardia, and atrio-ventricular block).

Typical angina was complained by 32 patients, atypical precordial pain, chest discomfort, or epigastric pain (suggestive of angina equivalents) were reported by 21 patients and other atypical symptoms (dyspnea, sore throat, jaw pain, palpitation, dizziness, and syncope) were instead experienced by 11 patients. Noteworthy, 51 patients were completely asymptomatic, and the diagnosis was made based on ECG and/or echocardiographic changes. The correlations between symptoms, ECG signs of ischemia, and arrhythmias are described in **Table 4**.

TABLE 1 Fluoropyrimidine Cardiotoxity reported in the literature.

Author	Title	Type	N cases	ECG ischemia	Angina	ARRH	AMI	Cardiac arrest/death
Saif et al. (31)	Fluoropyrimidine-associated cardiotoxicity: revisited.	Literature review *1	377	69%	45%	23%	22%	1.4%
Robben et al. (29)	The syndrome of 5-fluorouracil cardiotoxicity. An elusive cardiopathy	Review of case reports *1	135	75%	85%	15%	10%	13%
Dyhl-Polk et al. (20)	Cardiotoxicity in cancer patients treated with 5-fluorouracil or capecitabine: a systematic review of incidence, manifestations and predisposing factors	Review *1	94	6-33%		0-2%		0-2%
Zafar et al. (26)	The Incidence, Risk Factors, and Outcomes With 5-Fluorouracil– Associated Coronary Vasospasm	Retrospective analysis *1	87	73%	96%			
Khan et al. (24)	A retrospective study of cardiotoxicities induced by 5-fluouracil (5-FU) and 5-FU based chemotherapy regimens in Pakistani adult cancer patients at Shaukat Khanum Memorial Cancer Hospital & Research Center	Retrospective study *1	60	30%	37%%	81.6%	0%	3.3%
Dyhl-Polk et al. (27)	Incidence and risk markers of 5-fluorouracil and capecitabine cardiotoxicity in patients with colorectal cancer	Retrospective study *1	103	33%	43.6%		22.3%	9.7%
de Forni et al. (22)	Cardiotoxicity of high-dose continuous infusion fluorouracil: a prospective clinical study	Prospective study *1	28	64%	64%	3.5%		28.5%
Peng et al. (10)	Cardiotoxicity of 5-fluorouracil and capecitabine in Chinese patients: a prospective study	Prospective study *1	161	65.2%		68.3%	3.7%	
Kosmas et al. (3)	Cardiotoxicity of fluoropyrimidines in different schedules of administration: a prospective study	Prospective study *1	26	30%	42.3%	46.1%	30.7%	3.8%
Lestuzzi et al. (9)	Effort myocardial ischemia during chemotherapy with 5-fluorouracil: an underestimated risk	Prospective study *1	37 (21 at rest, 16 under effort)	95%	42%	50%	8.22%	
Dyhl-Polk et al. (29)	Myocardial Ischemia Induced by 5-Fluorouracil: A Prospective Electrocardiographic and Cardiac Biomarker Study	Prospective study *2	108 patients evaluated			1.85%	18.7%	0.92%
Lestuzzi et al. (14)	Cardiotoxicity from Capecitabine Chemotherapy: Prospective Study of Incidence at Rest and During Physical Exercise	Prospective study *1	32	100%	46.8%	53.1%		

*1 Percentages reported in relation to those experiencing a cardiotoxicity event. 2 Percentages reported in the relation to the whole group.

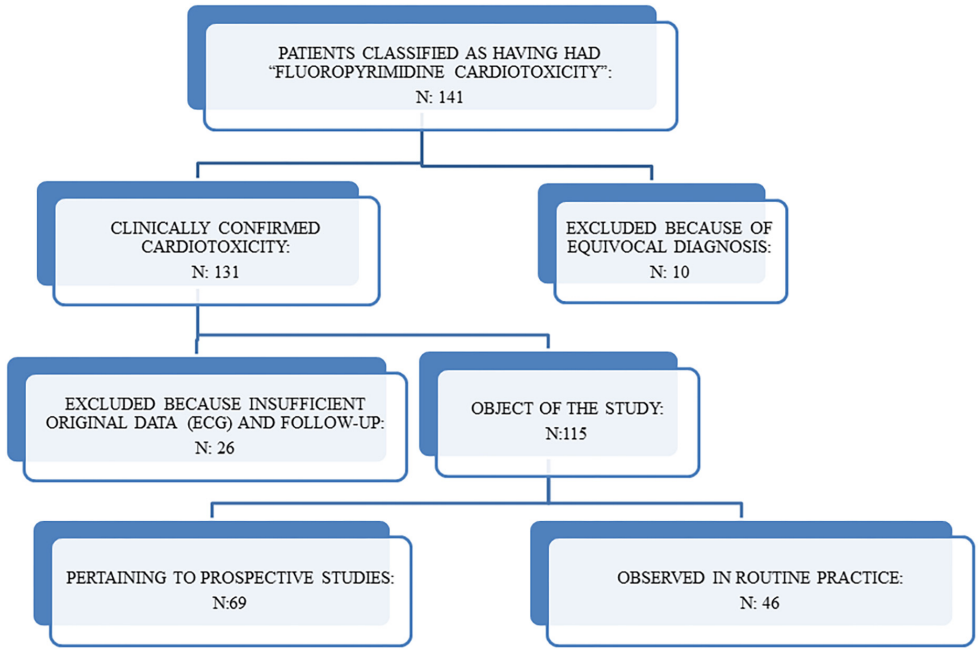

FIGURE 1
Selection of population reported in the study.

An echocardiogram was performed immediately at the time of detection of cardiotoxicity in 33 patients: it showed global or segmental kinetics abnormalities in 14 patients, while it was normal in the remaining 19 patients. Troponin was dosed in 28 patients and was above the normal limits of the laboratory in 8 cases.

After the diagnosis of FP cardiotoxicity, each patient was managed on an individual basis, according to the severity of toxicity, the stage of the neoplastic disease, and the availability of alternative treatments. The patients with acute coronary syndrome or severe arrhythmias were admitted to the Intensive Care Unit (ICU) and treated according to the best clinical practice. It is important to recall that uridine triacetate, which has been proven effective for severe FP toxicity, is currently not available for use in Italy (12, 13). The patients with minor signs or symptoms were either treated in the oncologic ward under cardiologic supervision or treated on an ambulatory basis. Cardiovascular therapy was prescribed according to the type of toxicity (MI, arrhythmias, LVD) and whether it occurred at rest or it was effort-related. If severe, even life-threatening toxicities (severe MI, arrhythmias, or LVD) occurred, or if the CT was considered avoidable (i.e., adjuvant treatment in patients with mild risk of relapse) or valid alternative regimens were available, FP-based CT was interrupted. In patients with minor toxicity or a strong indication to receive FP, the treatment was continued; in other patients, instead, it was interrupted but a rechallenge was attempted months or years later because of a relapse of the disease.

Overall, FP treatment was continued or re-introduced in 35 patients (Table 5). To prevent the recurrence of a cardiotoxicity event, several strategies (alone or in combination) were used: in 7 patients capecitabine was replaced by the 5-FU infusion

TABLE 2 Characteristics of the patients.

Sex	Males 74 Females 41
Age	19–79 years (median 61)
Tumor	Liver. 3
	Stomach, gut: 68
	Head, neck: 24
	Breast: 12
	Others: 8
Cardiovascular risk factors (CVRF)	Obesity: 8
	Diabetes: 8
	Hypertension: 41
	Active Smoking: 31
At least 1 CVRF	79
2 or more CVRF	41
Ischemic heart disease	15
On cardiovascular treatment	Beta-blockers: 11
	Calcium channel antagonists: 8
	Angiotensin Converting Enzime inhibitors: 22
	Nitrates: 9
Chemotherapy	5-Fluorouracil: 64
	Capecitabine: 51

10.3389/fcvm.2022.960240

TABLE 3 Symptoms, ECG and echocardiographic changes at rest and during stress.

ECG changes		N	Within group	Within all 115 patients
At rest (n = 62)	ST segment elevation	37	60%	32%
	ST segment depression	4	6%	3%
	Both ST elevation and depression	5	8%	4%
	Negative T waves	13	21%	11%
	Ventricular Ectopic Betas	5	6%	3%
Under/after effort (n = 49)	ST segment elevation	15	31%	13%
	ST segment depression	13	27%	11%
	Both ST elevation and depression	7	14%	6%
	Negative T waves	2	4%	2%
	Arrhythmias *	27	55%	23%
Symptoms				
No : 53 (46%)				
Yes: 62 (54%)		**N**	**Within group**	**Within all 115 patients**
Symptoms at rest (n = 30)	Typical chest pain	23	77%	20%
	Atypical chest pain	2	7%	2%
	Dyspnoea, dizziness, other atypical symptoms	5	17%	4%
Symptoms under effort (n = 32)	Typical chest pain	16	50%	14%
	Atypical chest pain	7	22%	6%
	Dyspnoea, dizziness, other atypical symptoms	9	28%	8%
Echocardiogram (n = 35)	Global dysfunction	9	26%	8%
	Segmental dysfunction	5	14%	4%
	No abnormalities	21	60%	

* Arrhythmias observed during/after effort were ventricular arrhythmias in 26 patients (3 had also ST segment abnormalities), and complete atrio-ventricular block in one. Typical chest pain includes typical angina and oppressive chest pain.

lasting ≤72 h; in 9 patients the FP dose was reduced by 25–50%; in 22 patients anti-ischemic and/or antiarrhythmic drugs (nitrates, calcium channel blockers, beta-blockers, ranolazine, and trimetazidine) were added to the therapy. A second rechallenge with a different approach (increase of FP dose after a successful attempt of rechallenge, or a different drug) was attempted in 7 patients. All the patients with effort-induced cardiotoxicity were screened with physical stress test during the rechallenge. The characteristics of the patients, the strategies applied and the results are reported in Table 5. Within the 35 patients who underwent the first rechallenge, 6 had again a severe cardiotoxicity event and the treatment was definitively interrupted in 5 of them (one of these patients was shifted to raltitrexed which, like FP, belongs to the CT class of anti-metabolites), instead, 4 patients had milder cardiotoxicity (evident only during stress test) and continued the therapy avoiding any physical effort and, finally, 25 patients were able to tolerate the rechallenge. Cardiotoxicity was completely prevented in 5 of the 7 patients who had an FP dose reduction only, in 10 of the 13 patients which received FP with dose reduction and anti-ischemic therapy, and in 4 of those patients who received a full dose FP and anti-ischemic therapy. Also, 4 patients with mild or no toxicity who received FP at a lower dose, experienced more severe toxicity when the drug dose was increased again. The 3 patients who shifted to raltitrexed did not have any cardiovascular adverse events and tolerated 3, 4, and 28 CT courses, respectively.

Discussion

In our experience, the clinical presentation of FP cardiotoxicity is extremely variable and often different from the classical description of "angina and ST-segment elevation at ECG," which is typical of vasospastic angina.

More than one-third of our patients were completely asymptomatic and cardiotoxicity was identified on the basis of ECG changes. This prevalence of asymptomatic cases is much higher than the one reported in other retrospective studies but lower than the prevalence observed in the two prospective studies conducted in our Institution where all the patients without rest cardiotoxicity performed a stress test (14). Actually, this study includes the cases detected in the two prospective studies conducted in our Institution, in which

TABLE 4 (A) Correlation between symptoms and ECG changes suggestive of ischemia. (B) Correlation between symptoms and ventricular arrhytmias.

(A)

Ischemic-like symptoms	ECG signs of ischemia			
	No	ST segment elevation	ST segment depression	Negative T waves
No	8	19	14	7
Dyspnoea		2		2
Atypical chest pain		17		3
Typical angina	6	23	1	1
Atypical symptoms		4	1	2

(B)

Symptoms	Ventricular arrhythmias		
	Rare	Frequent	Ventricular tachycardia
No	3	9	7
Dyspnoea			
Atypical chest pain	1	4	0
Typical angina	2	2	3
Atypical symptoms		9	4

cardiotoxicity was actively searched for with EST, and also those observed during daily clinical practice. It should be considered that, after our first observations of effort-induced cardiotoxicity and of asymptomatic ischemia in 2001 (15), we started active surveillance of cardiotoxicity even outside the prospective studies and this raised our chances of detecting the cardiotoxicity in regular clinical practice. For all patients, we perform a routine baseline ECG before the beginning of the treatment, we plan a second one after 2–4 days of CT with 5-FU or after 7–14 days of CT with capecitabine whenever possible (i.e., patients receiving in-hospital CT, patients undergoing daily radiotherapy, patients living near the hospital) and we advise the patients undergoing FP-based CT to avoid any physical effort and to promptly refer any new symptom (as chest pain, jaw pain, dyspnea, and palpitations) occurring during therapy. When a new ECG abnormality is observed and/or a new symptom is reported, the patient undergoes a cardiologic evaluation including an echocardiogram and/or stress test, if necessary, to define the diagnosis. This approach has been demonstrated to be effective in detecting several asymptomatic or oligosymptomatic toxicities, probably missed by most of the retrospective studies published so far, which included only those patients with clinical symptoms referred to the caring oncologists (16). At the same time, by advising to avoid physical efforts, the probability of eliciting effort-induced cardiotoxicity (which, according to our prospective studies with EST, accounts for half of the cases of cardiotoxicity) is reduced.

Concerning the ECG abnormalities, about half of the patients evaluated in the present study had ST-segment elevation (either alone or with specular ST segment depression), while other patients had negative T waves only or arrhythmias without typical ECG signs of ischemia. This contrasts with the hypothesis of vasospasm being the main cause of FP-related cardiotoxicity, which has been proposed for many years, and it is in support of multifactorial pathophysiology (17–21). Of note, ST-segment elevation was more frequent in the patients with rest cardiotoxicity, compared with those with stress-induced toxicity.

Other studies have reported retrospective or prospective series of FP-related cardiotoxicity, but it is not always easy to compare those data with ours, as the criteria for defining cardiotoxicity, and even the symptoms and the ECG changes, are equivocal.

In 1992, De Forni et al. prospectively studied 367 patients undergoing 96–120 h of 5-FU continuous infusion. Cardiotoxicity was observed in 28 patients (7.6%): 18 of them had angina, 12 presented cardiac collapse or pulmonary edema, and 8 patients died (5 suddenly and 3 of cardiogenic shock), ECG signs of ischemia were evident in 18 out of these 28 patients and global or segmental kinetics reduction was evident in 9 out of 16 patients who underwent an echocardiogram (22).

In a prospective study, Yilmaz et al. evaluated the role of Holter monitoring in 27 patients treated with 5FU: they did not observe any ST-T change (not even in the 2 patients who experienced chest pain); however, both a significant decrease in mean heart rate and an increase in the number of VA were reported (23).

TABLE 5 Patients with rechallenge chemotherapy after cardiotoxicity.

PT N	Sex, age	Drug with toxicity	Type of toxicity	Rechallenge: drug	Dose	Anti-ischemic drugs	Toxicity	N of cycles
1	F, 43	5FU	Angina	5FU	75%	Diltiazem, nitrates	No	8
2	F, 47	5FU	Silent ischemia	5FU	75%		No	2
3*	M, 59	Capecitabine	Effort silent ischemia	5FU	100%	Ranolazine	Severe	1
4	F, 65	5FU	Angina	5FU	100%	Nitrates, Ranolazine, ASA	Severe	1
5*	M, 49	Capecitabine	Effort silent ischemia	Capecitabine	50%		Mild	1
6	F, 68	Capecitabine	Effort silent ischemia	Capecitabine	75%	Betablockers	Mild	1
7*	F, 51	5FU	Angina	5FU	75%		No	1
8	M, 49	5FU	Angina	5FU	100%	Nitrates	No	2
9	M, 67	Capecitabine	Effort ischemia and arrhythmias	5FU	75%	Betablockers, amlodipine	Mild	1
10*	F, 69	5FU	Atypical	5FU	75%	Diltiazem	Mild	1
11	M, 61	5FU	Effort silent ischemia	5FU	75%		No	3
12	M, 69	Capecitabine	Silent ischemia	Capecitabine	75%	Betablockers	No	2
13	M, 61	Capecitabine	Effort Arrythmias	5FU	75%		No	1
14*	F, 73	5FU	Effort ischemia and arrhythmias	5FU	60%		No	6
15	F, 61	Capecitabine	Effort angina	5FU	100%	Diltiazem, nitrates	Severe	1
16*	M, 63	5FU	Angina	5FU	75%	Nifedipine, nitrates	No	6
17	F, 42	Capecitabine	Effort angina	Capecitabine	50%	Ranolazine	No	7
18	M, 63	5FU	Angina	5FU	75%	Nifedipine, nitrates	No	5
19	M, 73	5FU	Myocardial infarction	5FU	75%	Betablockers, nitrates	No	5
20	M, 53	5FU	Angina	5FU	75%		No	3
21	F, 24	5FU	Silent ischemia	5FU	66%	Ranolazine	No	3
22	M, 58	5FU	Silent ischemia	Capecitabine	100%	Diltiazem, nitrates	No	6
23	F, 65	Capecitabine	Angina	Capecitabine	75%	Verapamil, nitrates	No	2
24	F, 43	Capecitabine	Silent ischemia, LVD	Capecitabine	66%		Severe	1
25	M, 43	Capecitabine	Effort ischemia, atypical symptoms	Capecitabine	66%	Nitrates, ASA	No	1
26	M, 42	5FU	Angina	5FU		Diltiazem, nitrates	Severe	1
27	M, 57	Capecitabine	Effort arrhythmias	5FU	100%		No	3
28	M, 46	5FU	Effort silent ischemia	5FU	75%		No	3
29	M, 68	Capecitabine	Effort ischemia, atypical symptoms	Capecitabine		Betablockers, nitrates	Severe	1

(Continued)

TABLE 5 (Continued)

PT N	Sex, age	Drug with toxicity	Type of toxicity	Rechallenge: drug	Dose	Anti-ischemic drugs	Toxicity	N of cycles
30	M, 75	Capecitabine	Effort arrhythmias	5FU	100%		No	3
31	M, 67	5FU	ischemia, atypical symptoms	5FU	100%	Nitrates	No	3
32	F, 55	5FU	Takotsubo	Raltitrexed	100%		No	28
33	M, 55	Capecitabine	Effort arrhythmias	Capecitabine	100%	Betablockers	No	3
34	M, 47	5FU	Effort angina	5FU	100%	Nitrates	No	1
35*	F, 58	Capecitabine	Effort angina	Capecitabine	75%	Trimetazidine, nitrates	No	1
				Second rechallenge				
	DRUG 1st rechallenge		**Toxicity**	**Drug**	**Dose**			
3*	5FU		Severe	Raltitrexed	100%		No	4
5*	Capecitabine 50%		Mild	Capecitabine	75%		Severe	1
7*	5FU 75%		No	5FU	100%		Severe	1
10*	5FU 75%, Diltiazem		No	5FU	100%	Diltiazem	Severe	1
14*	5FU 75%		No	Capecitabine	75%		No	3
16*	5FU 75%, Nifedipine, nitrates		No	Raltitrexed	100%		No	3
35*	Capecitabine 75%, Trimetazidine, nitrates		No	Capecitabine	100%	Trimetazidine, nitrates	Mild	1

5FU, 5 Fluorouracil; ASA, Acetilsalycilc acid; LVD, left ventricular dysfunction; *, patients who had a second rechallenge with different approach.

Khan et al., in a 2012 retrospective study, reported 60 cases of "symptomatic cardiotoxicity" including 10 patients with not specified "ischemic ECG changes," 10 with "chest pain," 11 with ventricular tachycardia, 1 cardiac arrest, 36 with bradycardia, 18 with hypotension, 7 with hypertension, and 2 with atrio-ventricular block. The ECG repolarization abnormalities were described for 18 cases only: ST-segment elevation was detected in 5 patients, ST segment depression in 2 patients, and negative T waves in 11 patients (24).

Peng et al. (10) in 2018, published a multicentric prospective study evaluating data from 527 patients of which 161 experienced cardiotoxicity related to FP administration. In particular, 6 patients experienced a MI, 20 had heart failure (no cases of angina are reported) and 33 had "premature beats" (if ventricular or supraventricular is not specified). At ECG, a total of 105 "ischemic changes" were reported, including 70 "ST changes " and 47 "T wave changes".

Instead, in a retrospective study by Zafar et al., only 5-FU-induced coronary vasospasm was considered and only a very low rate of cardiotoxicity was reported: although the occurrence of 5-FU-related cardiotoxicity was likely underestimated, this actually confirms our observation that typical vasospastic angina probably accounts for no more than 50% of the cases of FP cardiotoxicity (25, 26).

In a 2016 retrospective study, Dyhl-Polk et al. reported data from 452 breast cancer patients treated with capecitabine. In this study, a total of 22 cases of cardiotoxicity were diagnosed on the basis of the appearance of cardiac symptoms: chest pain in 11 patients, MI in 2 patients, arrhythmias in 5 patients (one had a cardiac arrest), and dyspnea in 3 patients (27). Two recently published studies (one retrospective and one prospective) by the same group gave results comparable to the ones obtained in our study. In the retrospective study, conducted on patients with colorectal cancer (of which 995 were treated by 5-FU and 1241 with capecitabine), 103 cases of FP-related cardiotoxicity were reported (5.2% in the 5-FU group and 4.1% in the capecitabine group). The ECG (not obtained for all patients) showed ST-segment elevation in 17 cases, ST segment depression or negative T waves in 9 and 8 cases, respectively, and VA in 6 cases. Regarding the symptoms, 45 patients had unstable angina, 23 patients experienced acute MI (10 cases with ST-segment elevation and 13 cases without ST-segment elevation), 10 patients had atypical symptoms (chest pain, dizziness, and dyspnea), 2 patients experienced a syncope secondary to atrio-ventricular or sino-atrial block and a total of 10 patients experienced sudden death or cardiac arrest (28). In the prospective study, instead, the same group of authors reported MI detected by ECG Holter in 20 patients receiving FP

(18.7% of the whole group), and 16 of these patients (15% of the whole group evaluated, 80% of those with signs of ischemia) had silent ischemia (29). Six patients (5.6% of the whole study group) developed an acute coronary syndrome (in 3 cases the symptoms had been preceded by silent ischemia recorded at Holter) and 2 patients had symptomatic VT; 1 patient had a cardiac arrest after cessation of 5-FU and Holter recording revealed an ST-segment elevation. These two studies confirm some of our observations: first of all, in FP-related cardiotoxicity, ST segment depression or negative T waves are as frequent as ST-segment elevation. Secondly, that silent ischemia is rather frequent and can precede significant clinical events, such as acute coronary syndrome and/or cardiac arrest. Finally, the detection of FP-related cardiotoxicity is more than doubled in prospective studies in which planned ECG screening is performed.

It should be considered that, in our study, 24 out of 31 patients complaining of typical angina and 8 out of 9 patients with chest pain, presented ECG signs of ischemia, mostly represented by ST-segment elevation (assessed in 18 and 6 patients, respectively). This might explain why, in the studies identifying cardiotoxicity on the basis of clinical symptoms, ST-segment elevation is the most frequent ECG abnormality.

Another peculiar observation in our experience is that 55% of the patients with effort-induced cardiotoxicity had VA, which may cause syncope or sudden death. This is the main reason why we are presently giving to all the patients beginning a CT with capecitabine the advice to avoid any unusual physical effort when on therapy.

Another peculiar finding in our experience is that 60% of the echocardiograms performed shortly after detection of the cardiotoxicity were normal; it should be considered, however, that both symptoms and ECG abnormalities may vary over time, ad if the echocardiogram is not obtained during the acute episode it can be normal. Thus, a normal ECG and a normal echocardiogram in a patient who had reported angina symptoms during FP therapy but is presently asymptomatic cannot rule out the cardiotoxicity.

As regards the possibility that a dihydropyrimidine dehydrogenase (DPD) deficiency might have played a role in the cardiotoxicity of our patients, most of the cases had been observed before the routine use of the test in our Institution, and all those who were tested showed a wild-type gene. Thus, also a wild-type phenotype cannot exclude the possibility of cardiotoxicity. It should also be noted that the DPD polymorphism is a known risk factor for hematological and gastrointestinal, but not cardiac toxicity. (30, 31).

The rechallenge with the same drug after FP-induced cardiotoxicity poses a high risk of severe events and death; according to the suggestions provided by Saif et al., we limited the rechallenges to the patients with a strong indication of FP therapy and performed close monitoring with frequent ECG (or Holter monitoring), a close cardiologic follow-up and EST in selected cases (32, 33). The strategies employed to prevent cardiotoxicity when a rechallenge was considered necessary were variable and depended upon the available knowledge on FP toxicity, the anti-ischemic drugs available at different times, and also to the compliance of the patients. In the first years, we used mostly nitrates and nifedipine, according to the hypothesis of vasospasm; diltiazem was the preferred calcium channel blocker after a report on its utility in a small series of patients (34); beta-blockers were used in those patients with VA as the main manifestation of cardiotoxicity, in those with underlying coronary artery disease and in those with typical angina but with no signs of vasospasm. However, many patients were hypotensive and did not tolerate calcium channels blocker or beta blockers and others did not tolerate nitrates because of the onset of headaches. In some cases, the therapeutic approach was modified several times, using a treadmill stress test to assess the efficacy of the preventive measures, always trying to maintain the best anti-neoplastic effect, as previously described (33). Ranolazine, introduced in clinical practice in recent years, was well tolerated and it was effective in 2 patients, but not in a third. The number of patients undergoing a rechallenge is too little to allow an analysis of the efficacy of different cardiovascular treatments. However, our data suggest that the reduction of FP dose (associated with an anti-ischemic treatment if tolerated) and the shift from capecitabine to 5-FU or to a less cardiotoxic drug as raltitrexed, is probably the best approach, as already reported by other studies (35–40).

Raltitrexed is a quinazoline inhibitor of the enzyme thymidylate synthase and it is employed in the treatment of advanced malignant pleural mesothelioma [in association with cisplatin it has been demonstrated to improve the overall survival (41)] and in the treatment of advanced colorectal cancer. In patients with advanced colorectal cancer, raltitrexed has failed in demonstrating a superiority, in terms of survival outcome, when compared to 5-FU, at the cost of a higher incidence of hematological and gastrointestinal toxicity (42). However, in patients with cardiotoxicity induced by 5-FU or capecitabine, raltitrexed can represent a valid alternative, given the better cardiovascular tolerability profile (40, 42).

S1, an oral fluoropyrimidine composed of tegafur (a 5-FU prodrug), gimeracil (a dihydropyrimidine dehydrogenase, DPD, inhibitor), and potassium oxonate, is employed in Asia and in some European Countries for the treatment of different kinds of solid tumors, including advanced colorectal cancer. Lower toxicity of S-1 in the cardiovascular system could be explained by the fact that gimeracil inhibits DPD, which degrades 5-FU into its main metabolite alpha-fluoro-beta-alanine (43) (FbAL). Muneoka et al., in fact, described the case of a patient that experienced a MI after 5-FU administration and in which high levels of serum FbAL were detected. This same patient was later treated with S-1 and did not experience any additional cardiotoxicity (44).

Uracil/Tegafur (UTF), which is an oral agent composed of tegafur and uracil, is employed in Asia and also in South America in patients with advanced colorectal cancer that have experienced a cardiotoxicity event following the administration of 5-FU or capecitabine (45).

However, there is still not enough evidence regarding the potential cardiotoxicity of both S1 and UTF, thus requiring particular attention and close monitoring when employed (46).

Conclusion

Fluoropyrimidines (FP) cardiotoxicity is an elusive clinical condition and its recognition is challenging. At least half of the patients do not complain of angina or equivalents (and dizziness should be considered a warning symptom), and the ECG abnormalities may be absent at rest ECG.

Effort-induced clinical cardiotoxicity is characterized in about 50% of the cases by VA and by atypical symptoms (including dizziness). Thus, the patients undergoing FP therapy should be discouraged from affording any unusual physical effort.

ECG ischemic changes without angina, either detected at routine ECG, at Holter or evoked by a physical effort should be not disregarded as clinically irrelevant, as they may be a sign of even severe cardiotoxicity.

Active surveillance with ECG during CT and advising the patients to refer any new symptom may increase the detection of asymptomatic or oligosymptomatic cardiotoxicity. Also, a stress test, performed during active oncologic treatment, seems necessary to rule out the occurrence of cardiotoxicity events.

Data availability statement

The raw data supporting the conclusions of this article will be made available by the authors, without undue reservation.

Ethics statement

This study was reviewed and approved by the Internal Review Board of the Centro di Riferimento Oncologico (CRO), National Cancer Institute. Written informed consent was not required for this study in accordance with the local legislation and institutional requirements.

Author contributions

CL: study planning, data collection and review, writing the draft, and the final manuscript. LC and LG: analysis of the clinical data and writing the manuscript. EV: data collecting, clinical evaluation, and follow-up of the patients. EB: data analysis. MC: revision of ECG tracing and editing of the manuscript. All authors contributed to the article and approved the submitted version.

Funding

This study was financially supported by the Italian Ministry of Health-Ricerca Corrente to publishing this manuscript.

Conflict of interest

The authors declare that the research was conducted in the absence of any commercial or financial relationships that could be construed as a potential conflict of interest.

Publisher's note

References

1. Ng M, Cunningham D, Norman AR. The frequency and pattern of cardiotoxicity observed with capecitabine used in conjunction with oxaliplatin in patients treated for advanced colorectal cancer (CRC). *Eur J Cancer.* (2005) 41:1542–6. doi: 10.1016/j.ejca.2005.03.027

2. Stewart T, Pavlakis N, Ward M. Cardiotoxicity with 5-fluorouracil and capecitabine: more than just vasospastic angina. *Intern Med J.* (2010) 40:303–7. doi: 10.1111/j.1445-5994.2009.02144.x

3. Kosmas C, Kallistratos MS, Kopterides P, Syrios J, Skopelitis H, Mylonakis N, et al. Cardiotoxicity of fluoropyrimidines in different schedules of administration: a prospective study. *J Cancer Res Clin Oncol.* (2008) 134:75–82. doi: 10.1007/s00432-007-0250-9

4. McAndrew EN, Jassal DS, Goldenberg BA, Kim CA. Capecitabine-mediated heart failure in colorectal cancer: a case series. *Eur Heart J Case Rep.* (2021) 5:ytab079. doi: 10.1093/ehjcr/ytab079

5. Layoun ME, Wickramasinghe CD, Peralta MV, Yang EH. Fluoropyrimidine-induced cardiotoxicity: manifestations, mechanisms, and management. *Curr Oncol Rep.* (2016) 18:35. doi: 10.1007/s11912-016-0521-1

6. Kanduri J, More LA, Godishala A, Asnani A. Fluoropyrimidine-associated cardiotoxicity. *Cardiol Clin.* (2019) 37:399–405. doi: 10.1016/j.ccl.2019.07.004

7. More LA, Lane S, Asnani A. 5-FU cardiotoxicity: vasospasm, myocarditis, and sudden death. *Curr Cardiol Rep.* (2021) 23:17. doi: 10.1007/s11886-021-01441-2

8. Lestuzzi C, Viel E, Picano E, Meneguzzo N. Coronary vasospasm as a cause of effort-related myocardial ischemia during low-dose chronic continuous infusion of 5-fluorouracil. *Am J Med.* (2001) 111:316–8. doi: 10.1016/s0002-9343(01)00808-7

9. Lestuzzi C, Vaccher E, Talamini R, Lleshi A, Meneguzzo N, Viel E, et al. Effort myocardial ischemia during chemotherapy with 5-Fluorouracil: an underestimated risk. *Ann Oncol.* (2014) 25:1059–64. doi: 10.1093/annonc/mdu055

10. Peng J, Dong C, Wang C, Li W, Yu H, Zhang M, et al. Cardiotoxicity of 5-fluorouracil and capecitabine in Chinese patients: a prospective study. *Cancer Commun.* (2018) 38:22. doi: 10.1186/s40880-018-0292-1

11. Sara JD, Kaur J, Khodadadi R, Rehman M, Lobo R, Chakrabarti S, et al. 5-fluorouracil and cardiotoxicity: a review. *Ther Adv Med Oncol.* (2018) 10:1758835918780140. doi: 10.1177/1758835918780140

12. Ma WW, Saif MW, El-Rayes BF, Fakih MG, Cartwright TH, Posey JA, et al. Emergency use of uridine triacetate for the prevention and treatment of life-threatening 5-fluorouracil and capecitabine toxicity. *Cancer.* (2017) 123:345–56. doi: 10.1002/cncr.30321

13. Raber I, Frazer MB, Zerillo JA, Asnani A. Uridine triacetate for severe fluoropyrimidine cardiotoxicity in a patient with thymidylate synthase gene variants. *JACC CardioOncol.* (2020) 2:329–32. doi: 10.1016/j.jaccao.2020.04.005

14. Lestuzzi C, Stolfo D, De Paoli A, Banzato A, Buonadonna A, Bidoli E, et al. Cardiotoxicity from capecitabine chemotherapy: prospective study of incidence at rest and during physical exercise. *Oncologist.* (2022) 27:e158–67. doi: 10.1093/oncolo/oyab035

15. Hrovatin E, Viel E, Lestuzzi C, Tartuferi L, Zardo F, Brieda M, et al. Severe ventricular dysrhythmias and silent ischemia during infusion of the antimetabolite 5-fluorouracil and cis-platin. *J Cardiovasc Med.* (2006) 7:637–40. doi: 10.2459/01.JCM.0000237914.12915.dd

16. Jensen SA, Sørensen JB. Risk factors and prevention of cardiotoxicity induced by 5-fluorouracil or capecitabine. *Cancer Chemother Pharmacol.* (2006) 58:487–93. doi: 10.1007/s00280-005-0178-1

17. Mosseri M, Fingert HJ, Varticovski L, Chokshi S, Isner JM. In vitro evidence that myocardial ischemia resulting from 5-fluorouracil chemotherapy is due to protein kinase C-mediated vasoconstriction of vascular smooth muscle. *Cancer Res.* (1993) 53:3028–33.

18. Salepci T, Seker M, Uyarel H, Gumus M, Bilici A, Ustaalioglu BB, et al. 5-Fluorouracil induces arterial vasoconstrictions but does not increase angiotensin II levels. *Med Oncol.* (2010) 27:416–20. doi: 10.1007/s12032-009-9226-8

19. Sudhoff T, Enderle MD, Pahlke M, Petz C, Teschendorf C, Graeven U, et al. 5-Fluorouracil induces arterial vasocontractions. *Ann Oncol.* (2004) 15:661–4. doi: 10.1093/annonc/mdh150

20. Polk A, Vistisen K, Vaage-Nilsen M, Nielsen DL. A systematic review of the pathophysiology of 5-fluorouracil-induced cardiotoxicity. *BMC Pharmacol Toxicol.* (2014) 15:47. doi: 10.1186/2050-6511-15-47

21. Focaccetti C, Bruno A, Magnani E, Bartolini D, Principi E, Dallaglio K, et al. Effects of 5-fluorouracil on morphology, cell cycle, proliferation, apoptosis, autophagy and ROS production in endothelial cells and cardiomyocytes. *PLoS One.* (2015) 10:e0115686. doi: 10.1371/journal.pone.0115686

22. de Forni M, Malet-Martino MC, Jaillais P, Shubinski RE, Bachaud JM, Lemaire L, et al. Cardiotoxicity of high-dose continuous infusion fluorouracil: a prospective clinical study. *J Clin Oncol.* (1992) 10:1795–801. doi: 10.1200/JCO.1992.10.11.1795

23. Yilmaz U, Oztop I, Ciloglu A, Okan T, Tekin U, Yaren A, et al. 5-fluorouracil increases the number and complexity of premature complexes in the heart: a prospective study using ambulatory ECG monitoring. *Int J Clin Pract.* (2007) 61:795–801. doi: 10.1111/j.1742-1241.2007.01323.x

24. Khan MA, Masood N, Husain N, Ahmad B, Aziz T, Naeem A. A retrospective study of cardiotoxicities induced by 5-fluouracil (5-FU) and 5-FU based chemotherapy regimens in Pakistani adult cancer patients at Shaukat Khanum Memorial Cancer Hospital & Research Center. *J Pak Med Assoc.* (2012) 62:430–4.

25. Zafar A, Drobni ZD, Mosarla R, Alvi RM, Lei M, Lou UY, et al. The incidence, risk factors, and outcomes with 5-fluorouracil-associated coronary vasospasm. *JACC CardioOncol.* (2021) 3:101–9. doi: 10.1016/j.jaccao.2020.12.005

26. Dyhl-Polk A, Vaage-Nilsen M, Schou M, Vistisen KK, Lund CM, Kümler T, et al. Incidence and risk markers of 5-fluorouracil and capecitabine cardiotoxicity in patients with colorectal cancer. *Acta Oncol.* (2020) 59:475–83. doi: 10.1080/0284186X.2019.1711164

27. Polk A, Shahmarvand N, Vistisen K, Vaage-Nilsen M, Larsen FO, Schou M, et al. Incidence and risk factors for capecitabine-induced symptomatic cardiotoxicity: a retrospective study of 452 consecutive patients with metastatic breast cancer. *BMJ Open.* (2016) 6:e012798. doi: 10.1136/bmjopen-2016-012798

28. Dyhl-Polk A, Schou M, Vistisen KK, Sillesen AS, Serup-Hansen E, Faber J, et al. Myocardial ischemia induced by 5-fluorouracil: a prospective electrocardiographic and cardiac biomarker study. *Oncologist.* (2021) 26:e403–13. doi: 10.1002/onco.13536

29. Becker K, Erckenbrecht JF, Häussinger D, Frieling T. Cardiotoxicity of the antiproliferative compound fluorouracil. *Drugs.* (1999) 57:475–84. doi: 10.2165/00003495-199957040-00003

30. Kim W, Cho YA, Kim DC, Lee KE. Elevated risk of fluoropyrimidine-associated toxicity in European patients with *DPYD* genetic polymorphism: a systematic review and meta-analysis. *J Pers Med.* (2022) 12:225. doi: 10.3390/jpm12020225

31. Depetris I, Marino D, Bonzano A, Cagnazzo C, Filippi R, Aglietta M, et al. Fluoropyrimidine-induced cardiotoxicity. *Crit Rev Oncol Hematol.* (2018) 124:1–10. doi: 10.1016/j.critrevonc.2018.02.002

32. Wasif Saif M, Shah MM, Shah AR. Fluoropyrimidine-associated cardiotoxicity: revisited. *Expert Opin Drug Saf.* (2009) 8:191–202. doi: 10.1517/14740330902733961

33. Lestuzzi C, Crivellari D, Rigo F, Viel E, Meneguzzo N. Capecitabine cardiac toxicity presenting as effort angina: a case report. *J Cardiovasc Med.* (2010) 11:700–3. doi: 10.2459/JCM.0b013e328332e873

34. Ambrosy AP, Kunz PL, Fisher GA, Witteles RM. Capecitabine-induced chest pain relieved by diltiazem. *Am J Cardiol.* (2012) 110:1623–6. doi: 10.1016/j.amjcard.2012.07.026

35. Saif MW, Garcon MC, Rodriguez G, Rodriguez T. Bolus 5-fluorouracil as an alternative in patients with cardiotoxicity associated with infusion 5-fluorouracil and capecitabine: a case series. *In Vivo.* (2013) 27:531–4.

36. Deboever G, Hiltrop N, Cool M, Lambrecht G. Alternative treatment options in colorectal cancer patients with 5-fluorouracil- or capecitabine-induced cardiotoxicity. *Clin Colorectal Cancer.* (2013) 12:8–14. doi: 10.1016/j.clcc.2012.09.003

37. Kelly C, Bhuva N, Harrison M, Buckley A, Saunders M. Use of raltitrexed as an alternative to 5-fluorouracil and capecitabine in cancer patients with cardiac history. *Eur J Cancer.* (2013) 49:2303–10. doi: 10.1016/j.ejca.2013.03.004

38. Ransom D, Wilson K, Fournier M, Simes RJ, Gebski V, Yip D, et al. Final results of Australasian Gastrointestinal Trials Group ARCTIC study: an audit of raltitrexed for patients with cardiac toxicity induced by fluoropyrimidines. *Ann Oncol.* (2014) 25:117–21. doi: 10.1093/annonc/mdt479

39. Khan K, Rane JK, Cunningham D, Rao S, Watkins D, Starling N, et al. Efficacy and cardiotoxic safety profile of raltitrexed in fluoropyrimidines-pretreated or high-risk cardiac patients with GI malignancies: large single-center experience. *Clin Colorectal Cancer.* (2019) 18:64–71.e1. doi: 10.1016/j.clcc.2018.09.010

40. Sorrentino MF, Kim J, Foderaro AE, Truesdell AG. 5-fluorouracil induced cardiotoxicity: review of the literature. *Cardiol J.* (2012) 19:453–8. doi: 10.5603/cj.2012.0084

41. van Meerbeeck JP, Gaafar R, Manegold C, Van Klaveren RJ, Van Marck EA, Vincent M, et al. Randomized phase III study of cisplatin with or without raltitrexed in patients with malignant pleural mesothelioma: an intergroup study of the European organisation for research and treatment of cancer lung cancer group and the National cancer institute of Canada. *J Clin Oncol.* (2005) 23:6881–9. doi: 10.1200/JCO.20005.14.589

42. Maughan TS, James RD, Kerr DJ, Ledermann JA, McArdle C, Seymour MT, et al. Comparison of survival, palliation, and quality of life with three chemotherapy regimens in metastatic colorectal cancer: a multicentre randomised trial. *Lancet.* (2002) 359:1555–63. doi: 10.1016/s0140-6736(02)08514-8

43. Yamada Y, Hamaguchi T, Goto M, Muro K, Matsumura Y, Shimada Y, et al. Plasma concentrations of 5-fluorouracil and F-beta-alanine following oral administration of S-1, a dihydropyrimidine dehydrogenase inhibitory fluoropyrimidine, as compared with protracted venous infusion of 5-fluorouracil. *Br J Cancer.* (2003) 89:816–20. doi: 10.1038/sj.bjc.6601224

44. Muneoka K, Shirai Y, Yokoyama N, Wakai T, Hatakeyama K. 5-Fluorouracil cardiotoxicity induced by alpha-fluoro-beta-alanine. *Int J Clin Oncol.* (2005) 10:441–3. doi: 10.1007/s10147-005-0516-7

45. Shiga T, Hiraide M. Cardiotoxicities of 5-fluorouracil and other fluoropyrimidines. *Curr Treat Options Oncol.* (2020) 21:27. doi: 10.1007/s11864-020-0719-1

46. Osterlund P, Kinos S, Pfeiffer P, Salminen T, Kwakman JJM, Frödin JE, et al. Continuation of fluoropyrimidine treatment with S-1 after cardiotoxicity on capecitabine- or 5-fluorouracil-based therapy in patients with solid tumours: a multicentre retrospective observational cohort study. *ESMO Open.* (2022) 7:100427. doi: 10.1016/j.esmoop.2022.100427

frontiers | Frontiers in Cardiovascular Medicine

TYPE Mini Review
PUBLISHED 21 September 2022
DOI 10.3389/fcvm.2022.981838

OPEN ACCESS

EDITED BY
Dong Han,
People's Liberation Army General Hospital, China

REVIEWED BY
Josep M. Grinyó,
University of Barcelona, Spain
Lionel PE Rostaing,
Université Grenoble Alpes, France

*CORRESPONDENCE
Karim Sallam
sallam@stanford.edu

SPECIALTY SECTION
This article was submitted to Cardio-Oncology, a section of the journal Frontiers in Cardiovascular Medicine

RECEIVED 29 June 2022
ACCEPTED 30 August 2022
PUBLISHED 21 September 2022

CITATION
Elezaby A, Dexheimer R and Sallam K (2022) Cardiovascular effects of immunosuppression agents. *Front. Cardiovasc. Med.* 9:981838. doi: 10.3389/fcvm.2022.981838

Cardiovascular effects of immunosuppression agents

Aly Elezaby[1,2], Ryan Dexheimer[1] and Karim Sallam[1,2]*

[1]Stanford Cardiovascular Institute, Stanford University School of Medicine, Stanford, CA, United States, [2]Division of Cardiovascular Medicine, Department of Medicine, Stanford University, Stanford, CA, United States

Immunosuppressive medications are widely used to treat patients with neoplasms, autoimmune conditions and solid organ transplants. Key drug classes, namely calcineurin inhibitors, mammalian target of rapamycin (mTOR) inhibitors, and purine synthesis inhibitors, have direct effects on the structure and function of the heart and vascular system. In the heart, immunosuppressive agents modulate cardiac hypertrophy, mitochondrial function, and arrhythmia risk, while in vasculature, they influence vessel remodeling, circulating lipids, and blood pressure. The aim of this review is to present the preclinical and clinical literature examining the cardiovascular effects of immunosuppressive agents, with a specific focus on cyclosporine, tacrolimus, sirolimus, everolimus, mycophenolate, and azathioprine.

KEYWORDS

immunosuppression, cardiovascular, hypertrophy, hypertension, mitochondria, fibrosis, toxicity

Introduction

Medications that target and downregulate the immune system are utilized for the prevention and treatment of a variety of conditions, including neoplasms, autoimmune diseases, and acute rejection after solid organ transplantation (1). In a recent cohort, 2.8% of the adult population was treated with long-term immunosuppressive medications, consistent with prior self-reported estimates (2, 3). In addition to the well described increased risk of infection and malignancy in chronically immunosuppressed patients, many of these agents exhibit direct effects on the cardiovascular system including risk of left ventricular (LV) hypertrophy, myocardial fibrosis, arrhythmia, hypertension, dyslipidemia, and coronary atherosclerosis (4). Herein, we focus on the cardiovascular effects and mechanistic underpinnings of calcineurin inhibitors (CNI), mammalian target of rapamycin (mTOR) inhibitors, and purine synthesis inhibitors (Figure 1).

Hypertrophy and fibrosis

Cardiac hypertrophy is a feature of adverse cardiac remodeling that may be driven by genetic or acquired factors. Hypertrophy is frequently seen in association with diastolic dysfunction and represents an important marker for adverse remodeling (5, 6). Much of the focus on immunosuppression-induced cardiac remodeling has been on the effects on cardiac hypertrophy in native or transplanted hearts (7–9) (Table 1).

Calcineurin inhibitors

Calcineurin, a calcium and calmodulin-dependent phosphatase, plays a pivotal role in cardiac hypertrophy by translocating to the nucleus and dephosphorylating NFAT, allowing it to transcribe genes to activate hypertrophy in cardiomyocytes. Cyclosporine (CsA) binds to cyclophilin A, forming a complex with high affinity for calcineurin, which in turn inhibits its nuclear translocation. This is hypothesized to inhibit activation of NFAT-mediated hypertrophy (59). Tacrolimus binds to FK506-binding protein (FKBP12) to inhibit calcineurin activity driving reduced NFAT-mediated transcription of hypertrophic genes.

In early animal experiments, CsA successfully prevented or attenuated cardiac hypertrophy in mice overexpressing contractile elements (10, 29), genetic predispositions to hypertrophy (19), and treatment with exogenous chemical signals promoting hypertrophy (11, 15, 60). However, these data were challenged by the failure of CsA to prevent hypertrophy in several models of hypertension or pressure overload (16, 35, 61). Tacrolimus has also yielded mixed results. In murine models of genetic hypertrophic cardiomyopathy, tacrolimus exacerbated cardiac hypertrophy (37). In animal models of hypertrophy induced by phenylephrine stimulation, spontaneously hypertensive rats, or aortic banding, tacrolimus treatment had variable effects, with exacerbation or amelioration of the hypertrophic phenotype (16, 38, 61, 62).

Some hypothesized that the mixed results were driven by variability in hypertrophic signaling from genetic/sarcomeric-driven hypertrophic signaling vs. adaptive chemical or afterload-driven hypertrophy (37, 59). This hypothesis is somewhat weakened by mixed data for transverse aortic constriction rodent models.

Subsequent investigations suggested that CsA-induced effects on hypertrophic remodeling may be driven by increased fibrosis. Multiple studies have shown that CsA treatment led to increases in MMP2, MMP9, and Collagen I in dose dependent manner (20–22, 63). Rat hearts treated with CsA exhibited increased fibrosis/collagen content (64). Similar data of increased collagen deposition in response to tacrolimus treatment was observed in human induced pluripotent stem cell-derived cardiac organoids treated with tacrolimus (65). The *in vitro* findings suggest that increased fibrosis is not a result of calcineurin-induced hypertension.

Notwithstanding some of the conflicting data in animal models, the data from humans have been fairly consistent as to the effects of CsA and tacrolimus on human hearts. Endomyocardial biopsies from heart or liver transplant patients treated with CsA showed structural distortion, increased fibrosis, and increased collagen levels (25, 26). Furthermore, patients treated with CsA and tacrolimus had hypertrophy or increased LV mass on autopsy or imaging (8, 26, 27, 39, 40). A clinical trial investigating the effect of CsA in patients with hypertrophic cardiomyopathy was initiated, but it is unclear if the study was completed and findings, if any, were not published (66).

Despite some earlier reports of amelioration of cardiac hypertrophy by CNI, there is no clear evidence in humans to corroborate this finding. Supported by *in vitro* and human data, a consistent signal of increased hypertrophy and fibrosis associated with CNI treatment is observed (23, 28). Cellular data highlight that the increase in LV mass may be driven primarily by CNI-induced increase in fibrosis and collagen deposition rather than cardiomyocyte remodeling.

mTOR inhibitors

mTOR inhibitors, such as sirolimus and everolimus, inhibit mammalian target of rapamycin complex I, thereby inhibiting downstream pathways driving cell growth, proliferation, and survival. There are notable differences between sirolimus and everolimus (67). Everolimus is the 40-O-(2-hydroxyethyl) derivative of sirolimus, and differs in its subcellular distribution, pharmacokinetics and binding affinity. Compared to sirolimus, everolimus has higher bioavailability and shorter half-life. Both drugs form a complex with FKBP-12, which binds mTOR. However, everolimus binding to FKBP-12 is ∼3-fold weaker than that of sirolimus, leading to significant differences in inhibition of mTORC2 activation and downstream effects (68, 69). Clinically this has translated into differences in side effect profile and potency of each drug.

This class of drugs has garnered significant interest in solid organ transplantation owing to salutary effects on renal function, allograft vasculopathy and malignancy risk (70). Sirolimus has been shown to reduce cardiac hypertrophy and fibrosis in animal models of pressure overload, uremia, and adriamycin induced cardiomyopathy (42, 43, 71). In a rat model of myocardial infarction, everolimus improved post-infarct remodeling (72) although in the recently published CLEVER-ACS trial of patients with myocardial infarction, there everolimus treatment had no effect on myocardial remodeling (73). Cellular data suggest that attenuation of adverse cardiac remodeling by mTOR inhibitors may be related

10.3389/fcvm.2022.981838

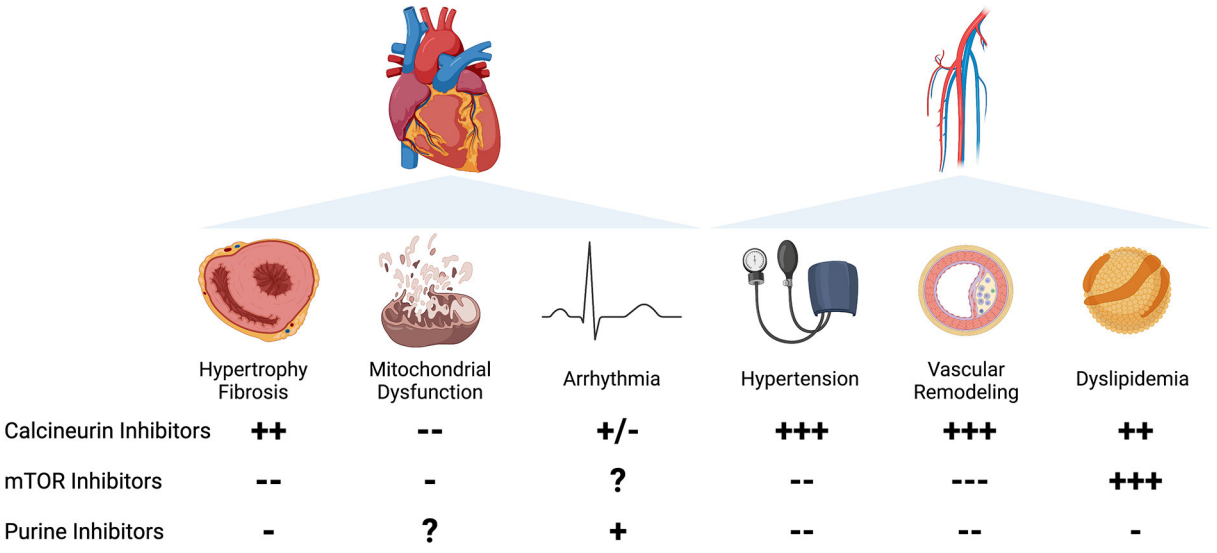

FIGURE 1
Left Panel: Cardiac effects of immunosuppression. Column A: Calcineurin inhibitors are associated with increased hypertrophy in clinical studies, with mixed preclinical evidence. mTOR inhibitors are associated with a decrease in cardiac hypertrophy in patients and animal studies. Purine synthesis inhibitors prevent cardiac remodeling in limited evidence in preclinical studies. Column B: Calcineurin inhibitors, particularly CsA, prevent mitochondrial dysfunction and mPTP opening. mTOR inhibitors may prevent mitochondrial dysfunction in preclinical studies. The effects of purine synthesis inhibitors on mitochondrial function in the heart are unknown. Column C: Calcineurin inhibitors are associated with arrhythmia in limited clinical case reports, with mixed effects in animal studies. The effects of mTOR inhibitors on arrhythmia are unknown. Purine synthesis inhibitors, particularly azathioprine, are weakly associated with increased atrial arrhythmias in clinical case reports. Right Panel: Vascular effects of immunosuppression. Column A: Hypertension. Calcineurin inhibitors are strongly associated with an increased incidence of hypertension in preclinical and clinical studies. mTOR inhibitors and purine synthesis inhibitors have a vasodilatory effect in animal models and limited clinical studies. Column B: Vascular remodeling. Calcineurin inhibitors are strongly associated with proliferative vasculopathy and vascular inflammation. mTOR inhibitors protect against vascular damage in clinical studies and preclinical models. Purine synthesis inhibitors are associated with improvement in vascular remodeling in preclinical studies and limited clinical reports. Column C: Dyslipidemia. Calcineurin inhibitors are associated with increased total serum cholesterol and LDL. mTOR inhibitors, particularly sirolimus, are strongly associated with an increase in serum cholesterol and triglycerides. Purine synthesis inhibitors are weakly associated with improvement in serum lipids.

in part to reduced cardiac fibroblast proliferation and collagen secretion (65).

The favorable signal for sirolimus has been validated in human studies, which largely compared outcomes to subjects treated with CNI. Sirolimus has been associated with improvement in diastolic dysfunction and filling pressures, possibly through attenuation of fibrosis (47–49). In patients with heart transplantation, everolimus treatment was associated with less myocardial fibrosis than mycophenolate treatment by biopsy and imaging (50, 51). The data in kidney transplant patients has been more mixed with some suggesting less LV hypertrophy with the use of everolimus (74), while a number of randomized trials showed no difference in LV mass index after conversion from CsA to everolimus post-kidney transplant (52–55). The incidence of adverse cardiovascular events from these studies was mixed with the majority showing no differences in outcomes (75–77). This discordant signal may be related to the fact that kidney transplant recipients often have concomitant hypertension and activation of the renin-angiotensin system that may have already contributed to significant adverse cardiac remodeling prior to kidney transplant—making it less likely to observe differences following kidney transplantation (75, 78). Additionally, most of the studies may have been underpowered to detect differences in cardiovascular outcomes.

Purine synthesis inhibitors

Purine synthesis inhibitors block cell proliferation by preventing the synthesis of DNA and RNA during S phase of the cell-cycle. Mycophenolate mofetil (MMF) treatment has been shown to prevent or attenuate ischemic injury and autoimmune myocarditis in animal models, with reduced secretion of inflammatory markers such as TLR4, NFκB, BAX expression, and TNFα (57, 58). There are no human studies suggesting a link between cardiac hypertrophy or fibrosis in association with MMF or azathioprine use.

Mitochondrial dysfunction

Mitochondria constitute a third of cardiomyocyte volume, and the heart, as a metabolically active organ, relies heavily on mitochondrial ATP production (79). Mitochondrial dysfunction

TABLE 1 Studies examining effects of immunosuppression on cardiac hypertrophy and fibrosis.

Agent	Species	Condition	Hypertrophy/Fibrosis	Studies
CsA	Rat, mouse	TAC	Attenuated LVH	(10–14)
	Mouse	TAC	No effect	(7, 15, 16)
	Rat	SHR	No effect	(16–18)
	Mouse	Gαq	Attenuated LVH	(19)
	Rat	Cardiac fibroblasts	No effect	(20)
	Rat	Cardiac fibroblasts	Induced fibrosis	(21–23)
	Rat	Langendorff	Decreased scar	(24)
	Human	Transplant	Increased LVH	(25–28)
	Human	LVH, HCM, CAD	Attenuated LVH	(29)
	Human	STEMI	Decreased scar	(30)
	Human	STEMI	No effect	(31–34)
Tacrolimus	Rat	SHR	Attenuated LVH	(35, 36)
	Mouse	Genetic HCM	Exacerbated LVH	(37)
	Rat	SHR, TAC	No effect	(16)
	Human	Transplant	Increased LVH	(26, 27, 38–40)
Sirolimus	Rat	Phenylephrine	Attenuated LVH	(41)
	Mouse, Rat	TAC	Attenuated LVH	(42, 43)
	Rat	Adriamycin	Attenuated fibrosis	(44)
	Mouse	Leprdb diabetic	Prevented fibrosis	(45)
	Rat	Zucker obese	Prevented fibrosis	(46)
		Zucker lean	Increased fibrosis	
	Human	Transplant	Regressed LVH	(47–49)
Everolimus	Human	Transplant	Attenuated LVH, fibrosis	(50, 51)
	Human	Transplant	No effect on LVH	(52–55)
	Rat	Metabolic syndrome	Attenuated LVH, fibrosis	(56)
MMF	Rat	Ischemia-reperfusion	Prevented apoptosis	(57)
	Rat	Myocarditis	Prevented LV dysfunction	(58)

TAC, Transverse Aortic Constriction; SHR, Spontaneously hypertensive rat; LVH, Left ventricular hypertrophy; HCM, hypertrophic cardiomyopathy; CAD, coronary artery disease; STEMI, ST elevation myocardial infarction.

is a feature of multiple types of cardiomyopathy, as it confers oxidative stress and changes in energetics to drive adverse cardiac remodeling. Immunosuppressive agents can exert direct effects on mitochondrial health to modulate cardiac remodeling and this has been subject of much investigation (Table 2).

Calcineurin inhibitors

Cyclophilin D is a protein in the inner mitochondrial matrix involved in opening of the mitochondrial permeability transition pore (mPTP) (94). mPTP opening results in mitochondrial calcium overload, release of cytochrome C, a process involved in apoptosis and implicated in myocardial ischemia-reperfusion (IR) injury (80). CsA interacts with cyclophilin D thereby preventing mPTP opening and protecting the mitochondria from calcium overload. Tacrolimus does not bind cyclophilin D and the effects of tacrolimus on mitochondrial function and mPTP opening are less defined. Multiple animal studies have sought to define the effect of both drugs on mitochondrial function.

CsA prevented mitochondrial-mediated injury and improved myocardial recovery in models of hypothermia, IR injury, and inborn errors of mitochondrial DNA polymerase (81–86, 95). In addition, CsA and/or tacrolimus have been associated with a favorable mitochondrial phenotype in the face of adriamycin treatment, hypoxia or endotoxemia (88–90).

Clinical data on the implications of these findings have been scant. In a single study of patients presenting with ST elevation myocardial infarction, CsA treatment decreased myocardial scar burden, which in combination with pre-clinical evidence provided promise for CsA as a "post-conditioning agent" during myocardial infarction (24, 30). However, follow-up studies failed to show any benefit to CsA treatment in regards to LV function, arrhythmia, or mortality (31–34). The discordance suggests that CsA protection from mitochondrial injury is largely a short term

TABLE 2 Studies examining effects of immunosuppression on cardiac mitochondrial function.

Agent	Species	Condition	Mito function	Studies
CsA	Rat	Isolated Mito	Protected from Ca^{2+} overload, prevented mPTP opening	(80)
	Rat	Hypothermia	Improved ATP levels	(81)
	Rat	IR injury	Prevented mito injury	(82, 83)
	Mouse	Mito DNA mutations	Prevented mito injury	(84)
	Pig, Rat	Cardioplegic arrest	Prevented mito injury	(85, 86)
	Pig	HFpEF	Attenuated mito dysfunction	(87)
	Mouse	Adriamycin	Prevented loss of mito membrane potential	(88)
	Feline	Endotoxemia	Normalized mito respiration	(89)
Tacrolimus	Mouse	Adriamycin	Did not prevent loss of mito membrane potential	(88)
	Feline	Endotoxemia	Normalized mito respiration	(89)
	Canine, Mouse	IR injury	Prevented loss of mito GSH and attenuated mito dysfunction	(90, 91)
Sirolimus	Mouse	Injection	Inhibited mito respiration	(92)
	Mouse	IR injury	Inhibited apoptosis, opened mito KATP channel	(93)

Mito, Mitochondrial; IR, ischemia-reperfusion; HFpEF, Heart failure with preserved ejection fraction.

TABLE 3 Studies examining effects of immunosuppression on arrhythmia.

Agent	Species	Condition	Arrhythmia	Studies
CsA	Rat	Injection	Sinus tachycardia, QT prolongation	(101)
	Rat	Oxidant stressor	Failed to suppress ventricular arrhythmia	(102)
	Rabbit	Atrial myocyte	Prevented cardiac alternans, decreased AF	(103)
	Canine	Pacing-induced AF	Prevented downregulation of LT Ca^{2+} channel α-1c expression	(104)
	Canine	Chronic AV block	Prevented polymorphic ventricular tachycardia	(105)
	Mouse	Iron overload	Prevented arrhythmia	(106)
	Human	STEMI	No effect	(31–34)
	Human	Transplant	Case reports of increased arrhythmia	(107, 108)
Tacrolimus	Guinea pig	Injection	Dose-dependent QT prolongation	(109, 110)
	Pig, rat	Isolated myocytes	Increased Ca^{2+} transients, prolonged action potential	(111–114)
	Rat	IR injury	Decreased ventricular arrhythmias	(115)
	Human	Transplant	Case reports of arrhythmias	(116–118)
Azathioprine	Human	Transplant	More atrial arrhythmias than MMF	(119)
	Human	Ulcerative colitis, psoriasis	Case reports of atrial fibrillation	(120–123)

STEMI, ST elevation myocardial infarction AF, Atrial fibrillation; IR, Ischemia-reperfusion; AV, atrioventricular.

or acute benefit. No human studies to date have evaluated the effect of CNI on mitochondrial structure and function in light of associated cardiac remodeling.

mTOR inhibitors

Sirolimus has been associated with a reduction in respiration and cellular energetics in cardiomyocytes (92). This effect has been attributed to the observation that mTOR may activate AMP-activated protein kinase to regulate cellular bioenergetics (96). In a mouse model of cardiac IR injury, sirolimus inhibited apoptosis and improved cardiac performance *via* interaction with the mitochondrial ATP-sensitive potassium channel (93) and appears to reduce ER stress and cytochrome C release (97). In brain, sirolimus enhances the distribution of CsA into mitochondria, accentuating its effects of decreasing mitochondrial metabolism, whereas everolimus appears to antagonize the effects of CsA in mitochondria to increase energy metabolism (67, 98). At therapeutically relevant concentrations, everolimus, but not sirolimus, distributes into brain mitochondria (99, 100). As cited above clinical studies have suggested a favorable effect for mTOR inhibitors on cardiac remodeling—but data examining mitochondrial function is lacking.

TABLE 4 Studies examining effects of immunosuppression on hypertension.

Agent	Species	Condition	Hypertension	Studies
CsA, Tacrolimus	Rat	Injection	Develop HTN prior to LVH	(101)
	Rat	Isolated arteries	Enhanced vasoconstriction, endothelin-1 receptor activation, decrease in eNOS	(127–129)
	Human	Transplant	Increase in HTN after transplant, more in CsA than tacrolimus	(130–132)
Sirolimus	Rat	Mineralocorticoid	Normalized systolic blood pressure	(133)
	Bovine	Endothelial cells	Restored eNOS-mediated vasodilation	(134)
	Human, mouse	PAH	Alleviated hypoxia-induced exacerbation of PAH	(135)
Everolimus	Human	Primary aldosteronism	Associated with improvement in blood pressure	(136)
	Human	Transplant	Lower incidence of HTN compared to CNI	(137)
	Human	PAH	Improvement in pulmonary vascular resistance	(138)
	Human	Renal cell carcinoma	Increased incidence of HTN when used in conjunction with Lenvatinib	(139)
MMF	Mouse	Systemic lupus erythematous	Lowered blood pressure	(140, 141)
	Rat	Lead-induced HTN	Attenuated HTN	(142)
	Rat	Mineralocorticoid HTN	Prevented hypertension	(143, 144)
	Human	Psoriasis, rheumatoid arthritis	Lowered blood pressure	(145)
Azathioprine	Rat	Pregnancy-associated HTN	Attenuated hypertension	(146)
	Human, Rat	PAH	Improved pulmonary vascular resistance	(147)
	Human	Transplant	Less likely to develop hypertension than CsA group	(148)

HTN, Hypertension; PAH, pulmonary arterial hypertension; eNOS, endothelial nitric oxide synthase.

Purine synthesis inhibitors

There are no reports of direct effects of MMF and Azathioprine on mitochondrial function in cardiomyocytes or heart tissue.

Arrhythmia

With described effects on myocardial structural remodeling and intracellular ion transporter function, immunosuppressive therapies may modulate the risk of arrhythmia. This poses significant short- and long-term risks, especially in patients with underlying structural heart disease and heart transplant recipients (Table 3).

Calcineurin inhibitors

Calcineurin affects intracellular calcium transients in cardiomyocytes *via* modulation of the ryanodine receptor and activation of the NFAT pathway, which drives transcriptional changes in proteins regulating intracellular calcium (124). Calcineurin inhibitors in turn can play a role in mediating changes in calcium transients impacting the electrical phenotype of the heart.

Delineating the precise effect of CNI on calcium regulation in human cardiomyocytes has proven elusive. In some models CsA appeared to reduce sarcoplasmic reticulum (SR) calcium release and cytosolic levels of Ca^{2+} (106). However, other models showed that both CsA and tacrolimus result in increased Ca^{2+} release events and an increase in QT prolongation. A possible mechanism of QT prolongation may be an increase in the duration of Ca^{2+} transients due to blockade of Na^{2+}/Ca^{2+} exchanger. It is possible that CsA and tacrolimus exert different electrical phenotypes owing to their differential role in mitochondrial Ca^{2+} regulation and mPTP opening. Nonetheless the results in animal models of both drugs have been equally mixed; in some animal models, the cellular phenotypes of CNI appeared to translate to a reduced propensity to arrhythmia (103, 105, 106), but not in other models (101, 102).

Clinically, in case reports, CsA and tacrolimus induced atrial fibrillation and tacrolimus induced QT prolongation and atrial arrhythmias (107, 116). However, neither signal was seen in clinical trials with either drug suggesting that the arrhythmic risk is low (125, 126).

mTOR inhibitors

There are no published reports of mTOR inhibitors modulating risk of arrhythmias. The recently published CLEVER-ACS trial showed no difference in atrial arrhythmias in patients treated with everolimus after myocardial infarction (73).

TABLE 5 Studies examining effects of immunosuppression on vascular remodeling.

Agent	Species	Condition	Vascular remodeling	Studies
CsA	Mouse	Endothelial and vascular smooth muscle cells	Increased endothelial cell activation, cytokines	(152)
	Rat	Isolated arteries	Increased endothelial dysfunction, oxidative stress, inflammation, smooth muscle proliferation	(128, 159–162)
	Human	Transplant	Associated with proliferative coronary vasculopathy	(163–165)
Tacrolimus	Human Rat	Norepinephrine Acetylcholine	Increased endothelial toxicity, impaired smooth muscle relaxation	(166)
	Human	Transplant	Less vasculopathy than CsA	(167–169)
Sirolimus	Rat	Mineralocorticoid, allografts, shear stress	Inhibited ROS, inflammation, intimal proliferation	(133, 170, 171)
	Pig Rat Human	Smooth muscle	Inhibited cell migration, proliferation	(172–174)
	Human	Transplant	Slowed coronary vasculopathy progression	(175, 176)
	Human	Transplant	Lowered PWV, arterial stiffness	(177, 178)
	Human	Coronary stenting	Prevented intimal proliferation	(179)
Everolimus	Rabbit	Carotid arteries	Improved vascular inflammation, thickening	(180)
	Mouse	LDL-receptor knockout	Prevented atherosclerosis	(181, 182)
	Human	PAH	Improved pulmonary vascular resistance	(138)
	Human	Transplant	Reduced CAV incidence/severity	(183, 184)
	Human	Transplant	No effect on pulse wave velocity	(75)
MMF	Rat	Lead-induced HTN	Decreased inflammation, intimal thickening	(142)
	Human	Transplant	Decrease in atherosclerosis, CAV	(119, 185, 186)
	Human	HUVEC + CNI	Prevented ROS production	(187)
AZA	Rat	Pregnancy-associated HTN	Attenuated endothelial cell dysfunction	(146)
	Rat	Subarachnoid hemorrhage	Attenuated vasospasm, reduced endothelin-1	(188)
	Mouse	Transgenic atherosclerosis	Inhibited atherosclerosis, decreased endothelial monocyte adhesion	(189)
	Human	HUVEC	Decreased cell proliferation	(190)

ROS, reactive oxygen species; PAH, pulmonary arterial hypertension; HUVEC, human umbilical vein endothelial cells; AZA, azathioprine; PWV, pulse wave velocity.

Purine synthesis inhibitors

Azathioprine use is associated with increased incidence of atrial arrhythmias. In a 3-year randomized controlled trial of azathioprine vs. MMF, heart transplant patients treated with azathioprine had a higher rate of atrial arrhythmias than those on MMF (119). The mechanism for this phenomenon is unknown. There are no published reports of MMF modulating arrhythmia risk.

Hypertension

Hypertension is a well described side effect of immunosuppressive medication use, particularly CNI, and is associated with increased risk of coronary artery disease, cerebrovascular events, renal dysfunction, and adverse cardiovascular remodeling (Table 4).

Calcineurin inhibitors

CNI are known to cause hypertension, with 50–80% of patients reported to have hypertension with chronic use. CsA is associated with a higher incidence compared to tacrolimus (130). CNI are implicated in afferent arteriole vasoconstriction and activation of the renin-angiotensin system, promoting sodium retention and volume expansion (127, 149). Furthermore, CsA and tacrolimus are associated with promoting direct vasoconstriction by one or more of the following

TABLE 6 Studies examining effects of immunosuppression on dyslipidemia.

Agent	Species	Condition	Dyslipidemia	Studies
CsA	Human	Transplant	Increased total cholesterol, LDL, decreased HDL	(202, 203)
	Human	Transplant	Increased cholesteryl ester transfer protein, lipoprotein lipase activity, decreased lipolysis	(204, 205)
	Human	Transplant	Pro-oxidant effect on LDL	(206, 207)
Tacrolimus	Mouse	High vs low dose	High dose developed hypercholesterolemia, low dose did not	(208)
	Human	Transplant	Less significant increase in LDL, total cholesterol than CsA	(130, 209–213)
	Human	Transplant	Less pro-oxidant effect on LDL than CsA	(206, 207)
	Human Mouse	HUVEC, diabetic mice	Decreases oxidized LDL uptake to endothelial cells, smooth muscle cells	(214–216)
	Mouse	Pcsk9 knockout	Increased PCSK9 expression, leading to decreased LDL receptor expression, increased LDL	(217)
	Human	Transplant	Increase in cholesterol, triglycerides	(70, 218)
	Human	Transplant	Increased apolipoprotein C-III, lipoprotein lipase	(204, 219)
Everolimus	Mouse	LDL-receptor knockout	Increased VLDL/LDL, inhibited atherosclerosis	(181, 182)
	Human	Transplant	No additive increase in total cholesterol and triglycerides	(220)
	Human	Transplant	Similar dyslipidemia to sirolimus	(221)
	Human	Transplant	Decreased oxidized LDL	(222)
	Human	Transplant	No change in lipids, increase in PCSK9	(223, 224)
MMF	Rabbit	High-cholesterol diet	No effect on LDL, HDL, or triglyceride levels	(225)
	Human	Transplant	Cholesteryl ester transfer protein activity unchanged with MMF	(131, 204, 226)
Azathioprine	Human	Transplant	Conversion from CsA decreased total cholesterol, LDL, triglycerides, improved LDL oxidation	(227)
	Human	Transplant	Did not alter serum lipids in comparison to MMF	(228)

mechanisms: increased tone of vascular smooth muscle (128, 150, 151), reduced nitric oxide production (129), and activation of endothelin-1 receptor (129). In cultured murine endothelial and vascular smooth muscle cells, both CsA and tacrolimus were associated with production of proinflammatory cytokines and endothelial activation, with increased superoxide production and NF-kB regulated synthesis of proinflammatory factors, which were prevented by pharmacological inhibition of TLR4. This raises the possibility that a proinflammatory milieu drives chronic endothelial dysfunction, contributing to CNI-induced hypertension (152).

There is some controversy as to whether the clinical hypertrophic phenotype is related to direct myocardial effects or is in fact due an increase in the incidence of hypertension associated with CsA use. Observations that rats treated with CsA develop hypertension prior to myocardial hypertrophy (4, 101, 153–155) supported the notion that perhaps the clinical hypertrophic phenotype is purely related to CNI-induced hypertension rather than direct myocardial effects. While hypertension may be a contributor to the hypertrophic phenotype observed, multiple animal and cellular models have supported a direct effect of CNI on myocardial remodeling.

mTOR inhibitors

mTOR inhibitors have been associated with a lower risk of hypertension compared to calcineurin inhibitors when used in solid organ transplant recipients (137, 156). The difference between effects of CNI and mTOR inhibitors is likely driven by multiple mechanisms with an overall vasodilatory effect of mTOR inhibitors (157, 158). Sirolimus and everolimus appear to increase nitric oxide production preventing endothelial hyperplasia and dysfunction (133, 134). This promising anti-hypertensive profile has led to the consideration of mTOR inhibitors as a primary therapy for specialized difficult-to-treat populations with hypertension including pulmonary arterial hypertension and primary hyperaldosteronism (138, 139).

Purine synthesis inhibitors

Purine synthesis inhibitors are not associated with hypertension and may in fact have an antihypertensive effect. In comparison to patients treated with CsA after heart transplantation, those treated with azathioprine were less likely to develop hypertension (148). Lower blood pressures have been reported in patients taking MMF for psoriasis and rheumatoid arthritis (145). Possible mechanisms for the favorable hypertensive profile include: lower pro-inflammatory signaling that drives endothelial dysfunction and hyperplasia, decreased circulating levels of endothelin-1, and reduced sodium reabsorption and neuro-hormonal activation leading to hypertension (142–144). Taken together, these data suggest that purine synthesis inhibitors carry a lower risk of systemic hypertension, and may in fact contribute to favorable mechanisms to reduce hypertension in pulmonary hypertension and renal dysfunction-associated hypertension.

Vascular remodeling

In addition to effects on hypertension, immunosuppressive agents may directly contribute to abnormal vascular remodeling to drive cardiovascular adverse events, independent of hypertension or dyslipidemia. Defining this risk and the contributing mechanisms for each drug is important in order to ensure appropriate follow up and identify potential actionable targets to modify the risk profile (Table 5).

Calcineurin inhibitors

CNI, particularly tacrolimus, have been associated with increased risk of allograft vasculopathy (167–169, 191). This notable complication of transplanted hearts represents a major driver of graft dysfunction and has significant implications for quality of life and longevity of heart transplant recipients (163–165). This has been replicated in animal models using both tacrolimus and CsA with adverse remodeling features of vascular stiffness, thickening, inflammation and fibrosis noted in treated animals (159, 160). The mechanisms for these include: decreased fibrinolytic activity in vessel walls, increased oxidative stress in endothelial cells, and possibly increased intracellular calcium in vascular smooth muscle cells (161, 162, 192).

mTOR inhibitors

Both sirolimus and everolimus have been associated with a more favorable vascular profile and their clinical efficacy in reducing the rate of progression of cardiac allograft vasculopathy has led to widespread use in heart transplant recipients (175, 176, 183). In addition to reducing signaling associated with endothelial dysfunction, mTOR inhibitors have been shown to reduce vascular smooth muscle proliferation, intimal hyperplasia, and infiltration by inflammatory cells (170–173, 193, 194). Everolimus, in particular, was shown to reduce pro-inflammatory signaling by decreasing IL-9, VEGF release, and TNFα induced adhesion of endothelial cells (184). These effects have led to wide adoption of everolimus- and sirolimus-eluting stents in the treatment of coronary artery disease (179, 195, 196).

In several trials of kidney transplant patients, a switch from CsA to mTOR inhibitor was associated with stabilization or improvement in parameters of arterial stiffness, including pulse wave velocity (PWV), carotid systolic blood pressure, pulse pressure, and augmentation index (177, 178). One notable exception was a secondary analysis of the ELEVATE trial, where no difference in PWV was found with switch from CsA to everolimus, which was attributed to significant variation in baseline PWV in the study population (75).

In addition to reducing allograft vasculopathy, the anti-vascular proliferation signal conferred by mTOR inhibitors has made the drug class of substantial interest in oncology to suppress tumor neovascularization. Nonetheless, while this anti-proliferation profile offers a substantial benefit, it carries some drawbacks; Namely, both mTOR inhibitor drugs are associated with an increased incidence of lymphedema, which is thought to be driven by inhibition of lymphatic endothelial cell proliferation (197, 198). The incidence of such side effects must be considered in oncologic therapy, where drug dosage is typically higher than that used in transplant immunosuppression (199).

Purine synthesis inhibitors

Purine synthesis inhibitors appear to confer a beneficial vascular remodeling profile. MMF has been associated with reduced atherosclerosis progression and CAV in patients and animal models (119, 142, 185). Animal models point to a signal of decreased vascular oxidative stress and inflammation as the driving mechanism of that benefit (187, 200, 201). Reduced endothelial and smooth muscle proliferation in association with MMF have also been proposed as a possible mechanism, although the evidence is more limited than for mTOR inhibitors (190).

Dyslipidemia

Immunosuppressive medications are associated with dyslipidemia. Each drug class is associated with individual variations in affected lipid particles and more importantly in the conferred risk of atherosclerosis (Table 6).

Calcineurin inhibitors

CsA use is associated with a dose-dependent increase in total cholesterol and low-density lipoprotein (LDL) cholesterol, a decrease in high-density lipoprotein (HDL) cholesterol, and an increase in serum triglycerides (202, 203). These changes are driven by a decrease in lipoprotein lipase and an increase in activity of cholesteryl ester transfer protein (204, 229). Additionally, CsA may reduce expression of the LDL receptor, thereby impairing LDL clearance (230–232). Tacrolimus is associated with a similar, but milder, dyslipidemia profile compared to CsA (130, 209–212). CsA appears to be associated with an increase in oxidized LDL, which confers a higher risk of atherosclerosis, while the data for tacrolimus effect on LDL oxidation are mixed (206–208).

mTOR inhibitors

Sirolimus is a stronger inducer of hyperlipidemia than CNI, associated clinically with an increase in serum LDL and triglyceride levels (70, 218, 233). The mechanism remains unclear, although it may be due to a combination of reduced catabolism, an increase in the free fatty acid pool, increased hepatic production of triglycerides, and secretion of very low density lipoprotein (VLDL) (204, 217). In addition, sirolimus is associated with an increase in serum PCSK9 levels, which acts as a post-transcriptional regulator of LDL receptor expression (234). Clinical data on the risk of dyslipidemia associated with everolimus has been mixed. In clinical studies, everolimus was not associated with an increased risk of dyslipidemia compared to CNI (220, 222, 223, 235–237). However, a meta-analysis comparing mTOR inhibitors to CNI adverse events has noted no difference between sirolimus and everolimus in the incidence of dyslipidemia (238). This suggests that everolimus may contribute to dyslipidemia, but at an intensity that is between CNI and sirolimus.

Interestingly, despite the increase in serum lipids, mTOR inhibitors are associated with an overall lower risk of atherosclerosis (195). Sirolimus reduces oxidized-LDL adhesion and uptake to endothelial cells, and can promote its autophagic degradation (214, 215). Additionally, sirolimus reduces intracellular lipid accumulation in vascular smooth muscle cells, and increases cholesterol efflux *via* increased expression of the ATP binding cassette protein ABCA1 (216). Similarly everolimus treatment in LDL receptor knockout mice, everolimus increased VLDL/LDL levels but reduced the rate of atherosclerosis. Thus, regardless of dyslipidemia profile, mTOR inhibitors appear to result in a net reduction in the rate of atherosclerosis, which may explain the overall clinical benefit observed.

Purine synthesis inhibitors

Both MMF and azathioprine appear to have a neutral effect on lipids with no significant changes observed in lipid profile in clinical studies (131, 226–228). *In vitro* studies suggest that MMF increases cholesterol efflux, but another study demonstrated inhibition of lipoprotein lipase activity—the opposing effects may explain the net neutral profile conferred by the drug.

Drug exposure and bioavailability

It is important to note that the bioavailability and exposure levels of the immunosuppression drugs have varied tremendously across clinic and scientific studies in the field. This may explain the differences observed between pre-clinical and clinical studies or even discrepancies between different clinical studies. Part of this variation is not simply investigator mediated, but is driven by variability in clinical practice by geographic area and changes in clinical practice over time. Early CsA trough concentrations in kidney transplant patients ranged 200–500 μg/ml, whereas in Europe, they were typically lower (100–200 μg/ml). Similarly, tacrolimus trough levels ranged 12–20 ηg/ml in the US, and lower in Europe (8–15 ηg/ml). There were also variations in sirolimus and everolimus levels when used in combination with CNI. MMF was previously prescribed at higher doses than is typically used now (2–3 g twice daily to 1 g twice daily) (12, 55, 107, 131).

Conclusions

Immunosuppressive agents exert significant effects on the heart and vasculature. Mechanistic studies point toward immunosuppression drug-specific influences on changes in cell proliferation, mitochondrial function, inflammatory cytokines, and altered calcium handling as potential mediators of these phenotypes. Calcineurin inhibitors promote cardiac hypertrophy, hypertension, dyslipidemia, and vascular remodeling, while mTOR inhibitors have an anti-proliferative effect with attenuation of cardiac hypertrophy and vascular remodeling despite promoting dyslipidemia. Purine synthesis inhibitor are less well studied, but may have a neutral to mildly positive effect on hypertension and vascular remodeling. These phenotypes are associated with significant morbidity in patients taking immunosuppressive medications, carrying increased risks of heart failure, cardiovascular disease, and kidney dysfunction. While preclinical studies have provided invaluable insight into mechanisms of cardiovascular remodeling, the discordance with clinical data, such as in the case of CNI and hypertrophy, highlights the importance of caution in generalizing the results of cell-based and animal models. Further translational research is needed to identify actionable

targets to treat associated cardiovascular side effects of immunosuppression drugs.

Data availability statement

The original contributions presented in the study are included in the article/supplementary material, further inquiries can be directed to the corresponding author.

Author contributions

AE, RD, and KS contributed to the writing and figures presented in the manuscript. All authors contributed to the article and approved the submitted version.

Funding

NIH T32 HL09427411A1 (AE), NIH K08 HL135343 (KS), and American Heart Association and Enduring Hearts Grant # 924127/Sallam and Hollander/2022 (KS).

Acknowledgments

Figures were created using Biorender.com.

Conflict of interest

The authors declare that the research was conducted in the absence of any commercial or financial relationships that could be construed as a potential conflict of interest.

Publisher's note

All claims expressed in this article are solely those of the authors and do not necessarily represent those of their affiliated organizations, or those of the publisher, the editors and the reviewers. Any product that may be evaluated in this article, or claim that may be made by its manufacturer, is not guaranteed or endorsed by the publisher.

References

1. Goldraich LA, Leitão SAT, Scolari FL, Marcondes-Braga FG, Bonatto MG, Munyal D, et al. A comprehensive and contemporary review on immunosuppression therapy for heart transplantation. *Curr Pharm Des.* (2020) 26:3351–84. doi: 10.2174/1381612826666200603130232

2. Wallace BI, Kenney B, Malani PN, Clauw DJ, Nallamothu BK, Waljee AK. Prevalence of immunosuppressive drug use among commercially insured US adults, 2018-2019. *JAMA Netw Open.* (2021) 4:e214920. doi: 10.1001/jamanetworkopen.2021.4920

3. Harpaz R, Dahl RM, Dooling KL. Prevalence of immunosuppression among US adults. *JAMA.* (2016) 316:2547–8. doi: 10.1001/jama.2016.16477

4. Miller LW. Cardiovascular toxicities of immunosuppressive agents. *Am J Transplant Off J Am Soc Transplant Am Soc Transpl Surg.* (2002) 2:807–18. doi: 10.1034/j.1600-6143.2002.20902.x

5. Levy D, Garrison RJ, Savage DD, Kannel WB, Castelli WP. Prognostic implications of echocardiographically determined left ventricular mass in the Framingham Heart Study. *N Engl J Med.* (1990) 322:1561–6. doi: 10.1056/NEJM199005313222203

6. Mottram PM, Marwick TH. Assessment of diastolic function: what the general cardiologist needs to know. *Heart Br Card Soc.* (2005) 91:681–95. doi: 10.1136/hrt.2003.029413

7. Luo Z, Shyu KG, Gualberto A, Walsh K. Calcineurin inhibitors and cardiac hypertrophy. *Nat Med.* (1998) 4:1092–3. doi: 10.1038/2578

8. Nakata Y, Yoshibayashi M, Yonemura T, Uemoto S, Inomata Y, Tanaka K, et al. Tacrolimus and myocardial hypertrophy. *Transplantation.* (2000) 69:1960–2. doi: 10.1097/00007890-200005150-00039

9. Paoletti E. mTOR inhibition and cardiovascular diseases: cardiac hypertrophy. *Transplantation.* (2018) 102:S41. doi: 10.1097/TP.0000000000001691

10. Sussman MA, Lim HW, Gude N, Taigen T, Olson EN, Robbins J, et al. Prevention of cardiac hypertrophy in mice by calcineurin inhibition. *Science.* (1998) 281:1690–3. doi: 10.1126/science.281.5383.1690

11. Meguro T, Hong C, Asai K, Takagi G, McKinsey TA, Olson EN, et al. Cyclosporine attenuates pressure-overload hypertrophy in mice while enhancing susceptibility to decompensation and heart failure. *Circ Res.* (1999) 84:735–40. doi: 10.1161/01.RES.84.6.735

12. Eto Y, Yonekura K, Sonoda M, Arai N, Sata M, Sugiura S, et al. Calcineurin is activated in rat hearts with physiological left ventricular hypertrophy induced by voluntary exercise training. *Circulation.* (2000) 101:2134–7. doi: 10.1161/01.CIR.101.18.2134

13. Lim HW, De Windt LJ, Steinberg L, Taigen T, Witt SA, Kimball TR, et al. Calcineurin expression, activation, and function in cardiac pressure-overload hypertrophy. *Circulation.* (2000) 101:2431–7. doi: 10.1161/01.CIR.101.20.2431

14. Hill JA, Karimi M, Kutschke W, Davisson RL, Zimmerman K, Wang Z, et al. Cardiac hypertrophy is not a required compensatory response to short-term pressure overload. *Circulation.* (2000) 101:2863–9. doi: 10.1161/01.CIR.101.24.2863

15. Ding B, Price RL, Borg TK, Weinberg EO, Halloran PF, Lorell BH. Pressure overload induces severe hypertrophy in mice treated with cyclosporine, an inhibitor of calcineurin. *Circ Res.* (1999) 84:729–34. doi: 10.1161/01.RES.84.6.729

16. Zhang W, Kowal RC, Rusnak F, Sikkink RA, Olson EN, Victor RG. Failure of calcineurin inhibitors to prevent pressure-overload left ventricular hypertrophy in rats. *Circ Res.* (1999) 84:722–8. doi: 10.1161/01.RES.84.6.722

17. Mervaala E, Müller DN, Park JK, Dechend R, Schmidt F, Fiebeler A, et al. Cyclosporin A protects against angiotensin II-induced end-organ damage in double transgenic rats harboring human renin and angiotensinogen genes. *Hypertens Dallas Tex.* (2000) 35:360–6. doi: 10.1161/01.HYP.35.1.360

18. Lassila M, Finckenberg P, Pere AK, Krogerus L, Ahonen J, Vapaatalo H, et al. Comparison of enalapril and valsartan in cyclosporine A-induced hypertension and nephrotoxicity in spontaneously hypertensive rats on high-sodium diet. *Br J Pharmacol.* (2000) 130:1339–47. doi: 10.1038/sj.bjp.0703422

19. Mende U, Kagen A, Cohen A, Aramburu J, Schoen FJ, Neer EJ. Transient cardiac expression of constitutively active Galphaq leads to hypertrophy and dilated cardiomyopathy by calcineurin-dependent and independent pathways. *Proc Natl Acad Sci U S A.* (1998) 95:13893–8. doi: 10.1073/pnas.95.23.13893

20. Eleftheriades EG, Ferguson AG, Samarel AM. Cyclosporine A has no direct effect on collagen metabolism by cardiac fibroblasts *in vitro*. *Circulation.* (1993) 87:1368–77. doi: 10.1161/01.CIR.87.4.1368

21. Chi J, Wang L, Zhang X, Fu Y, Liu Y, Chen W, et al. Cyclosporin A induces autophagy in cardiac fibroblasts through the NRP-2/WDFY-1 axis. *Biochimie.* (2018) 148:55–62. doi: 10.1016/j.biochi.2018.02.017

22. Rezzani R, Angoscini P, Rodella L, Bianchi R. Alterations induced by cyclosporine A in myocardial fibers and extracellular matrix in rat. *Histol Histopathol.* (2002) 17:761–6. doi: 10.14670/HH-17.761

23. Kolár F, Papousek F, MacNaughton C, Pelouch V, Milerová M, Korecky B. Myocardial fibrosis and right ventricular function of heterotopically transplanted hearts in rats treated with cyclosporin. *Mol Cell Biochem.* (1996) 163–164:253–60. doi: 10.1007/BF00408666

24. Minners J, van den Bos EJ, Yellon DM, Schwalb H, Opie LH, Sack MN. Dinitrophenol, cyclosporin A, and trimetazidine modulate preconditioning in the isolated rat heart: support for a mitochondrial role in cardioprotection. *Cardiovasc Res.* (2000) 47:68–73. doi: 10.1016/S0008-6363(00)00069-9

25. Stovin PG, English TA. Effects of cyclosporine on the transplanted human heart. *J Heart Transplant.* (1987) 6:180–5.

26. Roberts CA, Stern DL, Radio SJ. Asymmetric cardiac hypertrophy at autopsy in patients who received FK506 (tacrolimus) or cyclosporine A after liver transplant. *Transplantation.* (2002) 74:817–21. doi: 10.1097/00007890-200209270-00015

27. Espino G, Denney J, Furlong T, Fitzsimmons W, Nash RA. Assessment of myocardial hypertrophy by echocardiography in adult patients receiving tacrolimus or cyclosporine therapy for prevention of acute GVHD. *Bone Marrow Transplant.* (2001) 28:1097–103. doi: 10.1038/sj.bmt.1703304

28. Karch SB, Billingham ME. Cyclosporine induced myocardial fibrosis: a unique controlled case report. *J Heart Transplant.* (1985) 4:210–2.

29. Choudhary R, Sastry BKS, Subramanyam C. Positive correlations between serum calcineurin activity and left ventricular hypertrophy. *Int J Cardiol.* (2005) 105:327–31. doi: 10.1016/j.ijcard.2005.04.006

30. Piot C, Croisille P, Staat P, Thibault H, Rioufol G, Mewton N, et al. Effect of cyclosporine on reperfusion injury in acute myocardial infarction. *N Engl J Med.* (2008) 359:473–81. doi: 10.1056/NEJMoa071142

31. Ghaffari S, Kazemi B, Toluey M, Sepehrvand N. The effect of prethrombolytic cyclosporine-A injection on clinical outcome of acute anterior ST-elevation myocardial infarction. *Cardiovasc Ther.* (2013) 31:e34–39. doi: 10.1111/1755-5922.12010

32. Cung TT, Morel O, Cayla G, Rioufol G, Garcia-Dorado D, Angoulvant D, et al. Cyclosporine before PCI in patients with acute myocardial infarction. *N Engl J Med.* (2015) 373:1021–31. doi: 10.1056/NEJMoa1505489

33. Ottani F, Latini R, Staszewsky L, La VL, Locuratolo N, Sicuro M, et al. Cyclosporine A in reperfused myocardial infarction. *J Am Coll Cardiol.* (2016) 67:365–74. doi: 10.1016/j.jacc.2015.10.081

34. Chen -Scarabelli Carol, Scarabelli TM. Cyclosporine a prior to primary PCI in STEMI patients. *J Am Coll Cardiol.* (2016) 67:375–8. doi: 10.1016/j.jacc.2015.11.024

35. Sakata Y, Masuyama T, Yamamoto K, Nishikawa N, Yamamoto H, Kondo H, et al. Calcineurin inhibitor attenuates left ventricular hypertrophy, leading to prevention of heart failure in hypertensive rats. *Circulation.* (2000) 102:2269–75. doi: 10.1161/01.CIR.102.18.2269

36. Shimoyama M, Hayashi D, Zou Y, Takimoto E, Mizukami M, Monzen K, et al. [Calcineurin inhibitor attenuates the development and induces the regression of cardiac hypertrophy in rats with salt-sensitive hypertension]. *J Cardiol.* (2001) 37:114–8.

37. Fatkin D, McConnell BK, Mudd JO, Semsarian C, Moskowitz IG, Schoen FJ, et al. An abnormal Ca(2+) response in mutant sarcomere protein-mediated familial hypertrophic cardiomyopathy. *J Clin Invest.* (2000) 106:1351–9. doi: 10.1172/JCI11093

38. Kanazawa K, Iwai-Takano M, Kimura S, Ohira T. Blood concentration of tacrolimus and age predict tacrolimus-induced left ventricular dysfunction after bone marrow transplantation in adults. *J Med Ultrason.* (2001) 47:97–105. doi: 10.1007/s10396-019-00990-y

39. Atkison P, Joubert G, Barron A, Grant D, Paradis K, Seidman E, et al. Hypertrophic cardiomyopathy associated with tacrolimus in paediatric transplant patients. *Lancet Lond Engl.* (1995) 345:894–6. doi: 10.1016/S0140-6736(95)90011-X

40. Mano A, Nakatani T, Yahata Y, Kato T, Hashimoto S, Wada K, et al. Reversible myocardial hypertrophy induced by tacrolimus in a pediatric heart transplant recipient: case report. *Transplant Proc.* (2009) 41:3831–4. doi: 10.1016/j.transproceed.2009.05.040

41. Boluyt MO, Zheng JS, Younes A, Long X, O'Neill L, Silverman H, et al. Rapamycin Inhibits α1-Adrenergic Receptor–Stimulated Cardiac Myocyte Hypertrophy but Not Activation of Hypertrophy-Associated Genes. *Circ Res.* (1997) 81:176–86. doi: 10.1161/01.RES.81.2.176

42. Gao XM, Wong G, Wang B, Kiriazis H, Moore XL, Su YD, et al. Inhibition of mTOR reduces chronic pressure-overload cardiac hypertrophy and fibrosis. *J Hypertens.* (2006) 24:1663–70. doi: 10.1097/01.hjh.0000239304.01496.83

43. Gu J, Hu W, Song ZP, Chen YG, Zhang DD, Wang CQ. Rapamycin Inhibits Cardiac Hypertrophy by Promoting Autophagy *via* the MEK/ERK/Beclin-1 Pathway. *Front Physiol [Internet].* (2016). Available online at: https://www.frontiersin.org/article/10.3389/fphys.2016.00104 doi: 10.3389/fphys.2016.00104 (accessed April 28, 2022).

44. Yu SY, Liu L, Li P, Li J. Rapamycin inhibits the mTOR/p70S6K pathway and attenuates cardiac fibrosis in adriamycin-induced dilated cardiomyopathy. *Thorac Cardiovasc Surg.* (2013) 61:223–8. doi: 10.1055/s-0032-1311548

45. Reifsnyder PC, Ryzhov S, Flurkey K, Anunciado-Koza RP, Mills I, Harrison DE, et al. Cardioprotective effects of dietary rapamycin on adult female C57BLKS/J-Leprdb mice. *Ann N Y Acad Sci.* (2018) 1418:106–17. doi: 10.1111/nyas.13557

46. Luck C, DeMarco VG, Mahmood A, Gavini MP, Pulakat L. Differential Regulation of Cardiac Function and Intracardiac Cytokines by Rapamycin in Healthy and Diabetic Rats. *Oxid Med Cell Longev.* (2017) 2017:5724046. doi: 10.1155/2017/5724046

47. Raichlin E, Chandrasekaran K, Kremers WK, Frantz RP, Clavell AL, Pereira NL, et al. Sirolimus as primary immunosuppressant reduces left ventricular mass and improves diastolic function of the cardiac allograft. *Transplantation.* (2008) 86:1395–400. doi: 10.1097/TP.0b013e318189049a

48. Alnsasra H, Asleh R, Oh JK, Maleszewski JJ, Lerman A, Toya T, et al. Impact of sirolimus as a primary immunosuppressant on myocardial fibrosis and diastolic function following heart transplantation. *J Am Heart Assoc.* (2021) 10:e018186. doi: 10.1161/JAHA.120.018186

49. Kushwaha SS, Raichlin E, Sheinin Y, Kremers WK, Chandrasekaran K, Brunn GJ, et al. Sirolimus affects cardiomyocytes to reduce left ventricular mass in heart transplant recipients. *Eur Heart J.* (2008) 29:2742–50. doi: 10.1093/eurheartj/ehn407

50. Anthony C, Imran M, Pouliopoulos J, Emmanuel S, Iliff JW, Moffat KJ, et al. Everolimus for the prevention of calcineurin-inhibitor-induced left ventricular hypertrophy after heart transplantation (RADTAC Study). *JACC Heart Fail.* (2021) 9:301–13. doi: 10.1016/j.jchf.2021.01.007

51. Imamura T, Kinugawa K, Nitta D, Kinoshita O, Nawata K, Ono M. Everolimus attenuates myocardial hypertrophy and improves diastolic function in heart transplant recipients. *Int Heart J.* (2016) 57:204–10. doi: 10.1536/ihj.15-320

52. Krishnan A, Teixeira-Pinto A, Chan D, Chakera A, Dogra G, Boudville N, et al. Impact of early conversion from cyclosporin to everolimus on left ventricular mass index: a randomized controlled trial. *Clin Transplant.* (2017) 31:10. doi: 10.1111/ctr.13043

53. Murbraech K, Holdaas H, Massey R, Undset LH, Aakhus S. Cardiac response to early conversion from calcineurin inhibitor to everolimus in renal transplant recipients: an echocardiographic substudy of the randomized controlled CENTRAL trial. *Transplantation.* (2014) 97:184–8. doi: 10.1097/TP.0b013e3182a92728

54. Murbraech K, Massey R, Undset LH, Midtvedt K, Holdaas H, Aakhus S. Cardiac response to early conversion from calcineurin inhibitor to everolimus in renal transplant recipients–a three-yr serial echocardiographic substudy of the randomized controlled CENTRAL trial. *Clin Transplant.* (2015) 29:678–84. doi: 10.1111/ctr.12565

55. de Fijter JW, Holdaas H, Øyen O, Sanders JS, Sundar S, Bemelman FJ, et al. Early conversion from Calcineurin inhibitor- to Everolimus-based therapy following kidney transplantation: results of the randomized ELEVATE trial. *Am J Transplant Off J Am Soc Transplant Am Soc Transpl Surg.* (2017) 17:1853–67. doi: 10.1111/ajt.14186

56. Uchinaka A, Yoneda M, Yamada Y, Murohara T, Nagata K. Effects of mTOR inhibition on cardiac and adipose tissue pathology and glucose metabolism in rats with metabolic syndrome. *Pharmacol Res Perspect.* (2017) 5:4. doi: 10.1002/prp2.331

57. Li T, Yu J, Chen R, Wu J, Fei J, Bo Q, et al. Mycophenolate mofetil attenuates myocardial ischemia-reperfusion injury *via* regulation of the TLR4/NF-κB signaling pathway. *Pharm.* (2014) 69:850–5. doi: 10.1691/ph.2014.4598

58. Kamiyoshi Y, Takahashi M, Yokoseki O, Yazaki Y, Hirose SI, Morimoto H, et al. Mycophenolate mofetil prevents the development of experimental autoimmune myocarditis. *J Mol Cell Cardiol.* (2005) 39:467–77. doi: 10.1016/j.yjmcc.2005.04.004

59. Molkentin JD. Calcineurin and beyond: cardiac hypertrophic signaling. *Circ Res.* (2000) 87:731–8. doi: 10.1161/01.RES.87.9.731

60. Zhu W, Zou Y, Shiojima I, Kudoh S, Aikawa R, Hayashi D, et al. Ca2+/calmodulin-dependent kinase II and calcineurin play critical roles in

endothelin-1-induced cardiomyocyte hypertrophy. *J Biol Chem.* (2000) 275:15239–45. doi: 10.1074/jbc.275.20.15239

61. Zhang W. Old and new tools to dissect calcineurin's role in pressure-overload cardiac hypertrophy. *Cardiovasc Res.* (2002) 53:294–303. doi: 10.1016/S0008-6363(01)00451-5

62. Taigen T, De Windt LJ, Lim HW, Molkentin JD. Targeted inhibition of calcineurin prevents agonist-induced cardiomyocyte hypertrophy. *Proc Natl Acad Sci U S A.* (2000) 97:1196–201. doi: 10.1073/pnas.97.3.1196

63. Pan B, Li J, Parajuli N, Tian Z, Wu P, Lewno MT, et al. The calcineurin-TFEB-p62 pathway mediates the activation of cardiac macroautophagy by proteasomal malfunction. *Circ Res.* (2020) 127:502–18. doi: 10.1161/CIRCRESAHA.119.316007

64. Nayler WG, Gu XH, Casley DJ, Panagiotopoulos S, Liu J, Mottram PL. Cyclosporine increases endothelin-1 binding site density in cardiac cell membranes. *Biochem Biophys Res Commun.* (1989) 163:1270–4. doi: 10.1016/0006-291X(89)91115-7

65. Sallam K, Thomas D, Gaddam S, Lopez N, Beck A, Beach L, et al. Modeling effects of immunosuppressive drugs on human hearts using induced pluripotent stem cell-derived cardiac organoids and single-cell RNA sequencing. *Circulation.* (2022) 145:1367–9. doi: 10.1161/CIRCULATIONAHA.121.054317

66. National Heart, Lung, and Blood Institute (NHLBI). *Double Blind Placebo Controlled Study of Cyclosporin A in Patients With Left Ventricular Hypertrophy Caused by Sarcomeric Gene Mutations [Internet]. clinicaltrials*. (2008). Available online at: https://clinicaltrials.gov/ct2/show/NCT00001965 (accessed May 16, 2022).

67. Klawitter J, Nashan B, Christians U. Everolimus and sirolimus in transplantation-related but different. *Expert Opin Drug Saf.* (2015) 14:1055–70. doi: 10.1517/14740338.2015.1040388

68. Mabasa VH, Ensom MHH. The role of therapeutic monitoring of everolimus in solid organ transplantation. *Ther Drug Monit.* (2005) 27:666–76. doi: 10.1097/01.ftd.0000175911.70172.2e

69. Stenton SB, Partovi N, Ensom MHH. Sirolimus: the evidence for clinical pharmacokinetic monitoring. *Clin Pharmacokinet.* (2005) 44:769–86. doi: 10.2165/00003088-200544080-00001

70. Kahan BD, Podbielski J, Napoli KL, Katz SM, Meier-Kriesche HU, Van Buren CT. Immunosuppressive effects and safety of a sirolimus/cyclosporine combination regimen for renal transplantation. *Transplantation.* (1998) 66:1040–6. doi: 10.1097/00007890-199810270-00013

71. Haller ST, Yan Y, Drummond CA, Xie J, Tian J, Kennedy DJ, et al. Rapamycin Attenuates Cardiac Fibrosis in Experimental Uremic Cardiomyopathy by Reducing Marinobufagenin Levels and Inhibiting Downstream Pro-Fibrotic Signaling. *J Am Heart Assoc.* (2016) 5:e004106. doi: 10.1161/JAHA.116.004106

72. Buss SJ, Muenz S, Riffel JH, Malekar P, Hagenmueller M, Weiss CS, et al. Beneficial effects of mammalian target of rapamycin inhibition on left ventricular remodeling after myocardial infarction. *J Am Coll Cardiol.* (2009) 54:2435–46. doi: 10.1016/j.jacc.2009.08.031

73. Klingenberg R, Stähli BE, Heg D, Denegri A, Manka R, Kapos I, et al. Controlled-Level EVERolimus in Acute Coronary Syndrome (CLEVER-ACS)—A phase II, randomized, double-blind, multi-center, placebo-controlled trial. *Am Heart J.* (2022) 247:33–41. doi: 10.1016/j.ahj.2022.01.010

74. Pascual J. Everolimus in clinical practice—renal transplantation. *Nephrol Dial Transplant*. (2006) 21:iii18–23. doi: 10.1093/ndt/gfl300

75. Holdaas H, de Fijter JW, Cruzado JM, Massari P, Nashan B, Kanellis J, et al. Cardiovascular parameters to 2 years after kidney transplantation following early switch to Everolimus without Calcineurin inhibitor therapy: an analysis of the randomized ELEVATE study. *Transplantation.* (2017) 101:2612–20. doi: 10.1097/TP.0000000000001739

76. Pipeleers L, Abramowicz D, Broeders N, Lemoine A, Peeters P, Van Laecke S, et al. 5-Year outcomes of the prospective and randomized CISTCERT study comparing steroid withdrawal to replacement of cyclosporine with everolimus in de novo kidney transplant patients. *Transpl Int.* (2021) 34:313–26. doi: 10.1111/tri.13798

77. van Dijk M, van Roon AM, Said MY, Bemelman FJ, Homan van der Heide JJ, de Fijter HW, et al. Long-term cardiovascular outcome of renal transplant recipients after early conversion to everolimus compared to calcineurin inhibition: results from the randomized controlled MECANO trial. *Transpl Int Off J Eur Soc Organ Transplant.* (2018) 31:1380–90. doi: 10.1111/tri.13322

78. Jennings DL, Taber DJ. Use of renin-angiotensin-aldosterone system inhibitors within the first eight to twelve weeks after renal transplantation. *Ann Pharmacother.* (2008) 42:116–20. doi: 10.1345/aph.1K471

79. Gustafsson AB, Gottlieb RA. Heart mitochondria: gates of life and death. *Cardiovasc Res.* (2008) 77:334–43. doi: 10.1093/cvr/cvm005

80. Yarana C, Sripetchwandee J, Sanit J, Chattipakorn S, Chattipakorn N. Calcium-induced cardiac mitochondrial dysfunction is predominantly mediated by cyclosporine A-dependent mitochondrial permeability transition pore. *Arch Med Res.* (2012) 43:333–8. doi: 10.1016/j.arcmed.2012.06.010

81. Rajesh KG, Sasaguri S, Ryoko S, Maeda H. Mitochondrial permeability transition-pore inhibition enhances functional recovery after long-time hypothermic heart preservation. *Transplantation.* (2003) 76:1314–20. doi: 10.1097/01.TP.0000085660.93090.79

82. Xie JR Yu LN. Cardioprotective effects of cyclosporine A in an *in vivo* model of myocardial ischemia and reperfusion. *Acta Anaesthesiol Scand.* (2007) 51:909–13. doi: 10.1111/j.1399-6576.2007.01342.x

83. Griffiths EJ, Halestrap AP. Protection by Cyclosporin A of ischemia/reperfusion-induced damage in isolated rat hearts. *J Mol Cell Cardiol.* (1993) 25:1461–9. doi: 10.1006/jmcc.1993.1162

84. Mott JL, Zhang D, Freeman JC, Mikolajczak P, Chang SW, Zassenhaus HP. Cardiac disease due to random mitochondrial DNA mutations is prevented by cyclosporin A. *Biochem Biophys Res Commun.* (2004) 319:1210–5. doi: 10.1016/j.bbrc.2004.05.104

85. Nathan M, Friehs I, Choi YH, Cowan DB, Cao-Danh H, McGowan FX, et al. Cyclosporin a but not FK-506 protects against dopamine-induced apoptosis in the stunned heart. *Ann Thorac Surg.* (2005) 79:1620–6. doi: 10.1016/j.athoracsur.2004.10.030

86. Gao L, Hicks M, Villanueva JE, Doyle A, Chew HC, Qui MR, et al. Cyclosporine A as a cardioprotective agent during donor heart retrieval, storage, or transportation: benefits and limitations. *Transplantation.* (2019) 103:1140–51. doi: 10.1097/TP.0000000000002629

87. Hiemstra JA, Gutiérrez-Aguilar M, Marshall KD, McCommis KS, Zgoda PJ, Cruz-Rivera N, et al. A new twist on an old idea part 2: cyclosporine preserves normal mitochondrial but not cardiomyocyte function in mini-swine with compensated heart failure. *Physiol Rep.* (2014) 2:e12050. doi: 10.14814/phy2.12050

88. Marechal X, Montaigne D, Marciniak C, Marchetti P, Hassoun SM, Beauvillain JC, et al. Doxorubicin-induced cardiac dysfunction is attenuated by ciclosporin treatment in mice through improvements in mitochondrial bioenergetics. *Clin Sci.* (2011) 121:405–13. doi: 10.1042/CS20110069

89. Joshi MS, Julian MW, Huff JE, Bauer JA, Xia Y, Crouser ED. Calcineurin regulates myocardial function during acute endotoxemia. *Am J Respir Crit Care Med.* (2006) 173:999–1007. doi: 10.1164/rccm.200411-1507OC

90. Nishinaka Y, Sugiyama S, Yokota M, Saito H, Ozawa T. Protective effect of FK506 on ischemia/reperfusion-induced myocardial damage in canine heart. *J Cardiovasc Pharmacol.* (1993) 21:448–54. doi: 10.1097/00005344-199303000-00015

91. Sharp WW, Fang YH, Han M, Zhang HJ, Hong Z, Banathy A, et al. Dynamin-related protein 1 (Drp1)-mediated diastolic dysfunction in myocardial ischemia-reperfusion injury: therapeutic benefits of Drp1 inhibition to reduce mitochondrial fission. *FASEB J Off Publ Fed Am Soc Exp Biol.* (2014) 28:316–26. doi: 10.1096/fj.12-226225

92. Albawardi A, Almarzooqi S, Saraswathiamma D, Abdul-Kader HM, Souid AK, Alfazari AS. The mTOR inhibitor sirolimus suppresses renal, hepatic, and cardiac tissue cellular respiration. *Int J Physiol Pathophysiol Pharmacol.* (2015) 7:54–60.

93. Khan S, Salloum F, Das A, Xi LW, Vetrovec G, Cukreja R. Rapamycin confers preconditioning-like protection against ischemia–reperfusion injury in isolated mouse heart and cardiomyocytes. *J Mol Cell Cardiol.* (2006) 41:256–64. doi: 10.1016/j.yjmcc.2006.04.014

94. Johnson N, Khan A, Virji S, Ward JM, Crompton M. Import and processing of heart mitochondrial cyclophilin D. *Eur J Biochem.* (1999) 263:353–9. doi: 10.1046/j.1432-1327.1999.00490.x

95. Hausenloy DJ, Boston-Griffiths EA, Yellon DM. Cyclosporin A and cardioprotection: from investigative tool to therapeutic agent. *Br J Pharmacol.* (2012) 165:1235–45. doi: 10.1111/j.1476-5381.2011.01700.x

96. Tennant DA, Durán RV, Gottlieb E. Targeting metabolic transformation for cancer therapy. *Nat Rev Cancer.* (2010) 10:267–77. doi: 10.1038/nrc2817

97. Zhu J, Hua X, Li D, Zhang J, Xia Q. Rapamycin attenuates mouse liver ischemia and reperfusion injury by inhibiting endoplasmic reticulum stress. *Transplant Proc.* (2015) 47:1646–52. doi: 10.1016/j.transproceed.2015.05.013

98. Klawitter J, Gottschalk S, Hainz C, Leibfritz D, Christians U, Serkova NJ. Immunosuppressant neurotoxicity in rat brain models: oxidative stress and cellular metabolism. *Chem Res Toxicol.* (2010) 23:608–19. doi: 10.1021/tx900351q

99. Serkova N, Christians U. Transplantation: toxicokinetics and mechanisms of toxicity of cyclosporine and macrolides. *Curr Opin Investig Drugs Lond Engl.* (2003) 4:1287–96.

100. Serkova N, Jacobsen W, Niemann CU, Litt L, Benet LZ, Leibfritz D, et al. Sirolimus, but not the structurally related RAD (everolimus), enhances the negative effects of cyclosporine on mitochondrial metabolism in the rat brain. *Br J Pharmacol.* (2001) 133:875–85. doi: 10.1038/sj.bjp.0704142

101. Tavares P, Reis F, Ribeiro CAF, Teixeira F. Cardiovascular effects of cyclosporin treatment in an experimental model. *Rev Port Cardiol Orgao Of Soc Port Cardiol Port J Cardiol Off J Port Soc Cardiol.* (2002) 21:141–55.

102. Biary N, Xie C, Kauffman J, Akar FG. Biophysical properties and functional consequences of reactive oxygen species (ROS)-induced ROS release in intact myocardium. *J Physiol.* (2011) 589:5167–79. doi: 10.1113/jphysiol.2011.214239

103. Oropeza-Almazán Y, Blatter LA. Mitochondrial calcium uniporter complex activation protects against calcium alternans in atrial myocytes. *Am J Physiol Heart Circ Physiol.* (2020) 319:H873–81. doi: 10.1152/ajpheart.00375.2020

104. Huang Y, Lu CY, Yan W, Gao L, Chen Q, Zhang YJ. [Influence of cyclosporine A on atrial L-type calcium channel alpha1c subunit in a canine model of atrial fibrillation]. *Zhonghua Xin Xue Guan Bing Za Zhi.* (2009) 37:112–4.

105. Schreiner KD, Kelemen K, Zehelein J, Becker R, Senges JC, Bauer A, et al. Biventricular hypertrophy in dogs with chronic AV block: effects of cyclosporin A on morphology and electrophysiology. *Am J Physiol Heart Circ Physiol.* (2004) 287:H2891–2898. doi: 10.1152/ajpheart.01051.2003

106. Gordan R, Fefelova N, Gwathmey JK, Xie LH. Iron overload, oxidative stress and calcium mishandling in cardiomyocytes: role of the mitochondrial permeability transition pore. *Antioxidants.* (2020) 9:758. doi: 10.3390/antiox9080758

107. Ko WJ, Lin FL, Wang SS, Chu SH. Hypomagnesia and arrhythmia corrected by replacing cyclosporine with FK506 in a heart transplant recipient. *J Heart Lung Transplant Off Publ Int Soc Heart Transplant.* (1997) 16:980–2.

108. Mayer AD, Dmitrewski J, Squifflet JP, Besse T, Grabensee B, Klein B, et al. Multicenter randomized trial comparing tacrolimus (FK506) and cyclosporine in the prevention of renal allograft rejection: a report of the European Tacrolimus Multicenter Renal Study Group. *Transplantation.* (1997) 64:436–43. doi: 10.1097/00007890-199708150-00012

109. Minematsu T, Ohtani H, Sato H, Iga T. Sustained QT prolongation induced by tacrolimus in guinea pigs. *Life Sci.* (1999) 65:PL197–202. doi: 10.1016/S0024-3205(99)00396-3

110. Minematsu T, Ohtani H, Yamada Y, Sawada Y, Sato H, Iga T. Quantitative relationship between myocardial concentration of tacrolimus and QT prolongation in guinea pigs: pharmacokinetic/pharmacodynamic model incorporating a site of adverse effect. *J Pharmacokinet Pharmacodyn.* (2001) 28:533–54.

111. McCall E, Li L, Satoh H, Shannon TR, Blatter LA, Bers DM. Effects of FK-506 on contraction and Ca2+ transients in rat cardiac myocytes. *Circ Res.* (1996) 79:1110–21. doi: 10.1161/01.RES.79.6.1110

112. DuBell WH, Wright PA, Lederer WJ, Rogers TB. Effect of the immunosupressant FK506 on excitation—contraction coupling and outward K+ currents in rat ventricular myocytes. *J Physiol.* (1997) 501:509–16. doi: 10.1111/j.1469-7793.1997.509bm.x

113. Bell WH, Gaa ST. Lederer WJ, Rogers TB. Independent inhibition of calcineurin and K+ currents by the immunosuppressant FK-506 in rat ventricle. *Am J Physiol.* (1998) 275:H2041–2052. doi: 10.1152/ajpheart.1998.275.6.H2041

114. Katanosaka Y, Iwata Y, Kobayashi Y, Shibasaki F, Wakabayashi S, Shigekawa M. Calcineurin inhibits Na+/Ca2+ exchange in phenylephrine-treated hypertrophic cardiomyocytes. *J Biol Chem.* (2005) 280:5764–72. doi: 10.1074/jbc.M410240200

115. Li X, Bilali A, Qiao R, Paerhati T, Yang Y. Association of the PPARγ/PI3K/Akt pathway with the cardioprotective effects of tacrolimus in myocardial ischemic/reperfusion injury. *Mol Med Rep.* (2018) 17:6759–67.

116. Hodak SP, Moubarak JB, Rodriguez I, Gelfand MC, Alijani MR, Tracy CM, et al. prolongation and near fatal cardiac arrhythmia after intravenous tacrolimus administration: a case report. *Transplantation.* (1998) 66:535–7. doi: 10.1097/00007890-199808270-00021

117. Kim BR, Shin HS, Jung YS, Rim H, A. case of tacrolimus-induced supraventricular arrhythmia after kidney transplantation. *Sáo Paulo Med J Rev Paul Med.* (2013) 131:205–7. doi: 10.1590/1516-3180.2013.1313472

118. Nishimura M, Kim K, Uchiyama A, Fujino Y, Nishimura S, Taenaka N, et al. Tacrolimus-induced life-threatening arrhythmia in a pediatric liver-transplant patient. *Intensive Care Med.* (2002) 28:1683–4. doi: 10.1007/s00134-002-1479-z

119. Eisen HJ, Kobashigawa J, Keogh A, Bourge R, Renlund D, Mentzer R, et al. Three-year results of a randomized, double-blind, controlled trial of mycophenolate mofetil vs. azathioprine in cardiac transplant recipients. *J Heart Lung Transplant Off Publ Int Soc Heart Transplant.* (2005) 24:517–25. doi: 10.1016/j.healun.2005.02.002

120. Cassinotti A, Massari A, Ferrara E, Greco S, Bosani M, Ardizzone S, et al. New onset of atrial fibrillation after introduction of azathioprine in ulcerative colitis: case report and review of the literature. *Eur J Clin Pharmacol.* (2007) 63:875–8. doi: 10.1007/s00228-007-0328-y

121. Riccioni G, Bucciarelli V, Di Ilio E, Scotti L, Aceto A, D'Orazio N, et al. Recurrent atrial fibrillation in a patient with ulcerative colitis treated with azathioprine: case report and review of the literature. *Int J Immunopathol Pharmacol.* (2011) 24:247–9. doi: 10.1177/039463201102400131

122. Dodd HJ, Tatnall FM, Sarkany I. Fast atrial fibrillation induced by treatment of psoriasis with azathioprine. *Br Med J Clin Res Ed.* (1985) 291:706. doi: 10.1136/bmj.291.6497.706

123. Murphy G, Fulton RA, Keegan DJ. Fast atrial fibrillation induced by azathioprine. *Br Med J Clin Res Ed.* (1985) 291:1049–1049. doi: 10.1136/bmj.291.6501.1049-a

124. Saygili E, Rana OR, Günzel C, Rackauskas G, Saygili E, Noor-Ebad F, et al. Rate and irregularity of electrical activation during atrial fibrillation affect myocardial NGF expression *via* different signalling routes. *Cell Signal.* (2012) 24:99–105. doi: 10.1016/j.cellsig.2011.08.007

125. Sommerer C, Suwelack B, Dragun D, Schenker P, Hauser IA, Witzke O, et al. An open-label, randomized trial indicates that everolimus with tacrolimus or cyclosporine is comparable to standard immunosuppression in de novo kidney transplant patients. *Kidney Int.* (2019) 96:231–44. doi: 10.1016/j.kint.2019.01.041

126. U.S. Multicenter FK506 Liver Study Group. A comparison of tacrolimus (FK 506) and cyclosporine for immunosuppression in liver transplantation. *N Engl J Med.* (1994) 331:1110–5. doi: 10.1056/NEJM199410273311702

127. Hošková L, Málek I, Kautzner J, Honsová E, van Dokkum RPE, Husková Z, et al. Tacrolimus-induced hypertension and nephrotoxicity in Fawn-Hooded rats are attenuated by dual inhibition of renin–angiotensin system. *Hypertens Res.* (2014) 37:724–32. doi: 10.1038/hr.2014.79

128. Grześk E, Malinowski B, Wiciński M, Szadujkis-Szadurska K, Sinjab TA, Manysiak S, et al. Cyclosporine-A, but not tacrolimus significantly increases reactivity of vascular smooth muscle cells. *Pharmacol Rep PR.* (2016) 68:201–5. doi: 10.1016/j.pharep.2015.08.012

129. Tekes E, Soydan G, Tuncer M. The role of endothelin in FK506-induced vascular reactivity changes in rat perfused kidney. *Eur J Pharmacol.* (2005) 517:92–6. doi: 10.1016/j.ejphar.2005.05.029

130. Taylor DO, Barr ML, Radovancevic B, Renlund DG, Mentzer RM, Smart FW, et al. A randomized, multicenter comparison of tacrolimus and cyclosporine immunosuppressive regimens in cardiac transplantation: decreased hyperlipidemia and hypertension with tacrolimus. *J Heart Lung Transplant Off Publ Int Soc Heart Transplant.* (1999) 18:336–45. doi: 10.1016/S1053-2498(98)00060-6

131. Stegall MD, Wachs ME, Everson G, Steinberg T, Bilir B, Shrestha R, et al. Prednisone withdrawal 14 days after liver transplantation with mycophenolate: a prospective trial of cyclosporine and tacrolimus. *Transplantation.* (1997) 64:1755–60. doi: 10.1097/00007890-199712270-00023

132. Canzanello VJ, Schwartz L, Taler SJ, Textor SC, Wiesner RH, Porayko MK, et al. Evolution of cardiovascular risk after liver transplantation: a comparison of cyclosporine A and tacrolimus (FK506). *Liver Transplant Surg Off Publ Am Assoc Study Liver Dis Int Liver Transplant Soc.* (1997) 3:1–9. doi: 10.1002/lt.500030101

133. Temiz-Resitoglu M, Guden DS, Senol SP, Vezir O, Sucu N, Kibar D, et al. Pharmacological inhibition of mammalian target of rapamycin attenuates deoxycorticosterone acetate salt–induced hypertension and related pathophysiology: regulation of oxidative stress, inflammation, and cardiovascular hypertrophy in male rats. *J Cardiovasc Pharmacol.* (2022) 79:355–67. doi: 10.1097/FJC.0000000000001187

134. Kim JA, Jang HJ, Martinez-Lemus LA, Sowers JR. Activation of mTOR/p70S6 kinase by ANG II inhibits insulin-stimulated endothelial nitric oxide synthase and vasodilation. *Am J Physiol Endocrinol Metab.* (2012) 302:E201–208. doi: 10.1152/ajpendo.00497.2011

135. He Y, Zuo C, Jia D, Bai P, Kong D, Chen D, et al. Loss of DP1 aggravates vascular remodeling in pulmonary arterial hypertension *via* mTORC1 signaling. *Am J Respir Crit Care Med.* (2020) 201:1263–76. doi: 10.1164/rccm.201911-2137OC

136. Trinh B, Burkard T. The mTOR-inhibitor everolimus reduces hypervolemia in patients with primary aldosteronism. *Minerva Endocrinol.* (2021) 20:1. doi: 10.23736/S2724-6507.21.03382-0

137. Andreassen AK, Broch K, Eiskjær H, Karason K, Gude E, Mølbak D, et al. Blood Pressure in De Novo Heart Transplant Recipients Treated With Everolimus Compared With a Cyclosporine-based Regimen: Results From the Randomized SCHEDULE Trial. *Transplantation.* (2019) 103:781–8. doi: 10.1097/TP.0000000000002445

138. Seyfarth HJ, Hammerschmidt S, Halank M, Neuhaus P, Wirtz HR. Everolimus in patients with severe pulmonary hypertension: a safety and efficacy pilot trial. *Pulm Circ.* (2013) 3:632–8. doi: 10.1086/674311

139. Bendtsen MAF, Grimm D, Bauer J, Wehland M, Wise P, Magnusson NE, et al. Hypertension Caused by Lenvatinib and everolimus in the treatment of metastatic renal cell carcinoma. *Int J Mol Sci.* (2017) 18:1736. doi: 10.3390/ijms18081736

140. Lewis MJ, D'Cruz D. Adhesion molecules, mycophenolate mofetil and systemic lupus erythematosus. *Lupus.* (2005) 14 Suppl 1:s17–26. doi: 10.1177/096120330501400105

141. Taylor EB, Ryan MJ. Immunosuppression with mycophenolate mofetil attenuates hypertension in an experimental model of autoimmune disease. *J Am Heart Assoc.* (2017) 6:e005394. doi: 10.1161/JAHA.116.005394

142. Bravo Y, Quiroz Y, Ferrebuz A, Vaziri ND, Rodríguez-Iturbe B. Mycophenolate mofetil administration reduces renal inflammation, oxidative stress, and arterial pressure in rats with lead-induced hypertension. *Am J Physiol Renal Physiol.* (2007) 293:F616–623. doi: 10.1152/ajprenal.00507.2006

143. Moes AD, Severs D, Verdonk K, van der Lubbe N, Zietse R, Danser AHJ, et al. Mycophenolate mofetil attenuates DOCA-salt hypertension: effects on vascular tone. *Front Physiol.* (2018) 9:578. doi: 10.3389/fphys.2018.00578

144. Quiroz Y, Pons H, Gordon KL, Rincón J, Chávez M, Parra G, et al. Mycophenolate mofetil prevents salt-sensitive hypertension resulting from nitric oxide synthesis inhibition. *Am J Physiol Renal Physiol.* (2001) 281:F38–47. doi: 10.1152/ajprenal.2001.281.1.F38

145. Herrera J, Ferrebuz A, MacGregor EG, Rodriguez-Iturbe B. Mycophenolate mofetil treatment improves hypertension in patients with psoriasis and rheumatoid arthritis. *J Am Soc Nephrol JASN.* (2006) 17:S218–225. doi: 10.1681/ASN.2006080918

146. Tinsley JH, Chiasson VL, South S, Mahajan A, Mitchell BM. Immunosuppression improves blood pressure and endothelial function in a rat model of pregnancy-induced hypertension. *Am J Hypertens.* (2009) 22:1107–14. doi: 10.1038/ajh.2009.125

147. Botros L, Szulcek R, Jansen SMA, Kurakula K, Goumans MJTH, van Kuilenburg ABP, et al. The effects of mercaptopurine on pulmonary vascular resistance and BMPR2 expression in pulmonary arterial hypertension. *Am J Respir Crit Care Med.* (2020) 202:296–9. doi: 10.1164/rccm.202003-0473LE

148. Thompson ME, Shapiro AP, Johnsen AM, Itzkoff JM, Hardesty RL, Griffith BP, et al. The contrasting effects of cyclosporin-A and azathioprine on arterial blood pressure and renal function following cardiac transplantation. *Int J Cardiol.* (1986) 11:219–29. doi: 10.1016/0167-5273(86)90181-6

149. Ventura HO, Mehra MR, Stapleton DD, Smart FW. Cyclosporine-induced hypertension in cardiac transplantation. *Med Clin North Am.* (1997) 81:1347–57. doi: 10.1016/S0025-7125(05)70587-3

150. Textor SC, Taler SJ, Canzanello VJ, Schwartz L, Augustine JE. Posttransplantation hypertension related to calcineurin inhibitors. *Liver Transplant Off Publ Am Assoc Study Liver Dis Int Liver Transplant Soc.* (2000) 6:521–30. doi: 10.1053/jlts.2000.9737

151. Tang Q, Zheng YM, Song T, Reyes-García J, Wang C, Wang YX. Inhibition of big-conductance Ca2+-activated K+ channels in cerebral artery (vascular) smooth muscle cells is a major novel mechanism for tacrolimus-induced hypertension. *Pflugers Arch.* (2021) 473:53–66. doi: 10.1007/s00424-020-02470-6

152. Rodrigues-Diez R, González-Guerrero C, Ocaña-Salceda C, Rodrigues-Diez RR, Egido J, Ortiz A, et al. Calcineurin inhibitors cyclosporine A and tacrolimus induce vascular inflammation and endothelial activation through TLR4 signaling. *Sci Rep.* (2016) 6:27915. doi: 10.1038/srep27915

153. Porter GA, Bennett WM, Sheps SG. Cyclosporine-associated hypertension. *National High Blood Pressure Education Program Arch Intern Med.* (1990) 150:280–3. doi: 10.1001/archinte.150.2.280

154. Blum A, Aravot D. Heart transplantation–an update. *Clin Cardiol.* (1996) 19:930–8. doi: 10.1002/clc.4960191206

155. Miller LW, Schlant RC, Kobashigawa J, Kubo S, Renlund DG. 24th Bethesda conference: Cardiac transplantation. *Task Force 5: Complications J Am Coll Cardiol.* (1993) 22:41–54. doi: 10.1016/0735-1097(93)90814-H

156. Oberbauer R, Kreis H, Johnson RWG, Mota A, Claesson K, Ruiz JC, et al. Long-term improvement in renal function with sirolimus after early cyclosporine withdrawal in renal transplant recipients: 2-year results of the Rapamune Maintenance Regimen Study. *Transplantation.* (2003) 76:364–70. doi: 10.1097/01.TP.0000074360.62032.39

157. Sessa A, Esposito A, Giliberti A, Iavicoli G, Costa C, Bergallo M, et al. Immunosuppressive Agents and Metabolic Factors of Cardiovascular Risk in Renal Transplant Recipients. *Transplant Proc.* (2009) 41:1178–82. doi: 10.1016/j.transproceed.2009.02.045

158. Boots JMM, Christiaans MHL, van Hooff JP. Effect of immunosuppressive agents on long-term survival of renal transplant recipients. *Drugs.* (2004) 64:2047–73. doi: 10.2165/00003495-200464180-00004

159. Mennander A, Tiisala S, Paavonen T, Halttunen J, Häyry P. Chronic rejection of rat aortic allograft. II Administration of cyclosporin induces accelerated allograft arteriosclerosis. *Transpl Int Off J Eur Soc Organ Transplant.* (1991) 4:173–9. doi: 10.1007/BF00335340

160. Mennander A, Paavonen T, Häyry P. Cyclosporine-induced endothelialitis and accelerated arteriosclerosis in chronic allograft rejection. *Transplant Proc.* (1992) 24:341.

161. Diederich D, Skopec J, Diederich A, Dai FX. Cyclosporine produces endothelial dysfunction by increased production of superoxide. *Hypertens Dallas Tex.* (1994) 23:957–61. doi: 10.1161/01.HYP.23.6.957

162. Redondo-Horcajo M, Romero N, Martínez-Acedo P, Martínez-Ruiz A, Quijano C, Lourenço CF, et al. Cyclosporine A-induced nitration of tyrosine 34 MnSOD in endothelial cells: role of mitochondrial superoxide. *Cardiovasc Res.* (2010) 87:356–65. doi: 10.1093/cvr/cvq028

163. Gao SZ, Schroeder JS, Alderman EL, Hunt SA, Valantine HA, Wiederhold V, et al. Prevalence of accelerated coronary artery disease in heart transplant survivors. comparison of cyclosporine and azathioprine regimens. *Circulation.* (1989) 80:III100–105.

164. Mehra MR, Ventura HO, Chambers RB, Ramireddy K, Smart FW, Stapleton DD. The prognostic impact of immunosuppression and cellular rejection on cardiac allograft vasculopathy: time for a reappraisal. *J Heart Lung Transplant Off Publ Int Soc Heart Transplant.* (1997) 16:743–51.

165. Gamba A, Mamprin F, Fiocchi R, Senni M, Troise G, Ferrazzi P, et al. The risk of coronary artery disease after heart transplantation is increased in patients receiving low-dose cyclosporine, regardless of blood cyclosporine levels. *Clin Cardiol.* (1997) 20:767–72. doi: 10.1002/clc.4960200911

166. De Lima JJ, Xue H, Coburn L, Andoh TF, McCarron DA, Bennett WM, et al. Effects of FK506 in rat and human resistance arteries. *Kidney Int.* (1999) 55:1518–27. doi: 10.1046/j.1523-1755.1999.00366.x

167. Klauss V, König A, Spes C, Meiser B, Rieber J, Siebert U, et al. Cyclosporine vs. tacrolimus (FK 506) for prevention of cardiac allograft vasculopathy. *Am J Cardiol.* (2000) 85:266–9. doi: 10.1016/S0002-9149(99)00631-1

168. Reichart B, Meiser B, Viganò M, Rinaldi M, Martinelli L, Yacoub M, et al. European multicenter tacrolimus (FK506) Heart Pilot Study: one-year results–European tacrolimus multicenter heart study group. *J Heart Lung Transplant Off Publ Int Soc Heart Transplant.* (1998) 17:775–81.

169. Koglin J, Muscholl M, Petrakopoulou P, Groetzner J, Weis M, Meiser B, et al. Tacrolimus excels cyclosporine a in prevention of cardiac allograft vasculopathy—a prospective IVUS, angiography and doppler study. *J Heart Lung Transplant.* (2002) 21:68. doi: 10.1016/S1053-2498(01)00471-5

170. Cheng C, Tempel D, Oostlander A, Helderman F, Gijsen F, Wentzel J, et al. Rapamycin modulates the eNOS vs. shear stress relationship. *Cardiovasc Res.* (2008) 78:123–9. doi: 10.1093/cvr/cvm103

171. Pham SM, Shears LL, Kawaharada N, Li S, Venkataramanan R, Sehgal S. High local production of nitric oxide as a possible mechanism by which rapamycin prevents transplant arteriosclerosis. *Transplant Proc.* (1998) 30:953–4. doi: 10.1016/S0041-1345(98)00107-9

172. Poon M, Marx SO, Gallo R, Badimon JJ, Taubman MB, Marks AR. Rapamycin inhibits vascular smooth muscle cell migration. *J Clin Invest.* (1996) 98:2277–83. doi: 10.1172/JCI119038

173. Marx SO, Jayaraman T, Go LO, Marks AR. Rapamycin-FKBP inhibits cell cycle regulators of proliferation in vascular smooth muscle cells. *Circ Res.* (1995) 76:412–7. doi: 10.1161/01.RES.76.3.412

174. Bruemmer D, Yin F, Liu J, Kiyono T, Fleck E, Van Herle AJ, et al. Rapamycin inhibits E2F-dependent expression of minichromosome maintenance proteins in vascular smooth muscle cells. *Biochem Biophys Res Commun.* (2003) 303:251–8. doi: 10.1016/S0006-291X(03)00343-7

175. Mancini D, Pinney S, Burkhoff D, LaManca J, Itescu S, Burke E, et al. Use of rapamycin slows progression of cardiac transplantation vasculopathy. *Circulation.* (2003) 108:48–53. doi: 10.1161/01.CIR.0000070421.38604.2B

176. Potena L, Fearon WF, Sydow K, Holweg C, Luikart H, Chin C, et al. Asymmetric dimethylarginine and cardiac allograft vasculopathy progression: modulation by sirolimus. *Transplantation.* (2008) 85:827–33. doi: 10.1097/TP.0b013e318166a3a4

177. Joannidès R, Monteil C, de Ligny BH, Westeel PF, Iacob M, Thervet E, et al. Immunosuppressant regimen based on sirolimus decreases aortic stiffness in renal transplant recipients in comparison to cyclosporine. *Am J Transplant Off J Am Soc Transplant Am Soc Transpl Surg.* (2011) 11:2414–22. doi: 10.1111/j.1600-6143.2011.03697.x

178. Seckinger J, Sommerer C, Hinkel UP, Hoffmann O, Zeier M, Schwenger V. Switch of immunosuppression from cyclosporine A to everolimus: impact on pulse wave velocity in stable de-novo renal allograft recipients. *J Hypertens.* (2008) 26:2213–9. doi: 10.1097/HJH.0b013e32830ef940

179. Sousa JE, Costa MA, Abizaid A, Abizaid AS, Feres F, Pinto IM, et al. Lack of neointimal proliferation after implantation of sirolimus-coated stents in human coronary arteries: a quantitative coronary angiography and three-dimensional intravascular ultrasound study. *Circulation.* (2001) 103:192–5. doi: 10.1161/01.CIR.103.2.192

180. Baetta R, Granata A, Canavesi M, Ferri N, Arnaboldi L, Bellosta S, et al. Everolimus inhibits monocyte/macrophage migration *in vitro* and their accumulation in carotid lesions of cholesterol-fed rabbits. *J Pharmacol Exp Ther.* (2009) 328:419–25. doi: 10.1124/jpet.108.144147

181. Beutner F, Brendel D, Teupser D, Sass K, Baber R, Mueller M, et al. Effect of everolimus on pre-existing atherosclerosis in LDL-receptor deficient mice. *Atherosclerosis.* (2012) 222:337–43. doi: 10.1016/j.atherosclerosis.2012.03.003

182. Mueller MA, Beutner F, Teupser D, Ceglarek U, Thiery J. Prevention of atherosclerosis by the mTOR inhibitor everolimus in LDLR–/– mice despite severe hypercholesterolemia. *Atherosclerosis.* (2008) 198:39–48. doi: 10.1016/j.atherosclerosis.2007.09.019

183. Eisen HJ, Tuzcu EM, Dorent R, Kobashigawa J, Mancini D. Valantine-von Kaeppler HA, et al. Everolimus for the prevention of allograft rejection and vasculopathy in cardiac-transplant recipients. *N Engl J Med.* (2003) 349:847–58. doi: 10.1056/NEJMoa022171

184. Norum HM, Michelsen AE, Lekva T, Arora S, Otterdal K, Olsen MB, et al. Circulating delta-like Notch ligand 1 is correlated with cardiac allograft vasculopathy and suppressed in heart transplant recipients on everolimus-based immunosuppression. *Am J Transplant Off J Am Soc Transplant Am Soc Transpl Surg.* (2019) 19:1050–60. doi: 10.1111/ajt.15141

185. Placebo-controlled study of mycophenolate mofetil combined with cyclosporin and corticosteroids for prevention of acute rejection. European Mycophenolate Mofetil cooperative study group. *Lancet Lond Engl.* (1995) 345:1321–5. doi: 10.1016/S0140-6736(95)92534-1

186. Kobashigawa J, Miller L, Renlund D, Mentzer R, Alderman E, Bourge R, et al. A randomized active-controlled trial of mycophenolate mofetil in heart transplant recipients. *Mycophenolate Mofetil Investigators Transplantation.* (1998) 66:507–15. doi: 10.1097/00007890-199808270-00016

187. Krötz F, Keller M, Derflinger S, Schmid H, Gloe T, Bassermann F, et al. Mycophenolate acid inhibits endothelial NAD(P)H oxidase activity and superoxide formation by a rac1-dependent mechanism. *Hypertension.* (2007) 49:201–8. doi: 10.1161/01.HYP.0000251162.14782.d4

188. Chang CZ, Wu SC, Kwan AL, Lin CL, Hwang SL. 6-Mercaptopurine reverses experimental vasospasm and alleviates the production of endothelins in NO-independent mechanism-a laboratory study. *Acta Neurochir (Wien).* (2011) 153:939–49. doi: 10.1007/s00701-010-0865-5

189. Pols TWH, Bonta PI, Pires NMM, Otermin I, Vos M, de Vries MR, et al. 6-mercaptopurine inhibits atherosclerosis in apolipoprotein e*3-leiden transgenic mice through atheroprotective actions on monocytes and macrophages. *Arterioscler Thromb Vasc Biol.* (2010) 30:1591–7. doi: 10.1161/ATVBAHA.110.205674

190. Weigel G, Griesmacher A, DeAbreu RA, Wolner E, Mueller MM. Azathioprine and 6-mercaptopurine alter the nucleotide balance in endothelial cells. *Thromb Res.* (1999) 94:87–94. doi: 10.1016/S0049-3848(98)00199-6

191. Valantine H. Cardiac allograft vasculopathy after heart transplantation: risk factors and management. *J Heart Lung Transplant Off Publ Int Soc Heart Transplant.* (2004) 23:S187–193. doi: 10.1016/j.healun.2004.03.009

192. Atkison PR, Joubert GI, Guiraudon C, Armstrong R, Wall W, Asfar S, et al. Arteritis and increased intracellular calcium as a possible mechanism for tacrolimus-related cardiac toxicity in a pediatric transplant recipient. *Transplantation.* (1997) 64:773–5. doi: 10.1097/00007890-199709150-00020

193. Autieri MV. Allograft-induced proliferation of vascular smooth muscle cells: potential targets for treating transplant vasculopathy. *Curr Vasc Pharmacol.* 1:1–9. doi: 10.2174/1570161033386772

194. Vitiello D, Neagoe PE, Sirois MG, White M. Effect of everolimus on the immunomodulation of the human neutrophil inflammatory response and activation. *Cell Mol Immunol.* (2015) 12:40–52. doi: 10.1038/cmi.2014.24

195. Martinet W, De Loof H, De Meyer GRY. mTOR inhibition: a promising strategy for stabilization of atherosclerotic plaques. *Atherosclerosis.* (2014) 233:601–7. doi: 10.1016/j.atherosclerosis.2014.01.040

196. Wessely R. New drug-eluting stent concepts. *Nat Rev Cardiol.* (2010) 7:194–203. doi: 10.1038/nrcardio.2010.14

197. Kobayashi S, Kishimoto T, Kamata S, Otsuka M, Miyazaki M, Ishikura H. Rapamycin, a specific inhibitor of the mammalian target of rapamycin, suppresses lymphangiogenesis and lymphatic metastasis. *Cancer Sci.* (2007) 98:726–33. doi: 10.1111/j.1349-7006.2007.00439.x

198. Huber S, Bruns CJ, Schmid G, Hermann PC, Conrad C, Niess H, et al. Inhibition of the mammalian target of rapamycin impedes lymphangiogenesis. *Kidney Int.* (2007) 71:771–7. doi: 10.1038/sj.ki.5002112

199. Verheijen RB, Atrafi F, Schellens JHM, Beijnen JH, Huitema ADR, Mathijssen RHJ, et al. Pharmacokinetic optimization of everolimus dosing in oncology: a randomized crossover trial. *Clin Pharmacokinet.* (2018) 57:637–44. doi: 10.1007/s40262-017-0582-9

200. Allison AC, Eugui EM. Preferential suppression of lymphocyte proliferation by mycophenolic acid and predicted long-term effects of mycophenolate mofetil in transplantation. *Transplant Proc.* (1994) 26:3205–10.

201. Voloshyna I, Teboul I, Kasselman LJ, Salama M, Carsons SE, DeLeon J, et al. Macrophage lipid accumulation in the presence of immunosuppressive drugs mycophenolate mofetil and cyclosporin A. *Inflamm Res Off J Eur Histamine Res Soc Al.* (2019) 68:787–99. doi: 10.1007/s00011-019-01262-8

202. Kasiske BL, Tortorice KL, Heim-Duthoy KL, Awni WM, Rao KV. The adverse impact of cyclosporine on serum lipids in renal transplant recipients. *Am J Kidney Dis Off J Natl Kidney Found.* (1991) 17:700–7. doi: 10.1016/S0272-6386(12)80355-6

203. Ballantyne CM, Podet EJ, Patsch WP, Harati Y, Appel V, Gotto AM, et al. Effects of cyclosporine therapy on plasma lipoprotein levels. *JAMA.* (1989) 262:53–6. doi: 10.1001/jama.262.1.53

204. Tory R, Sachs-Barrable K, Hill JS, Wasan KM. Cyclosporine A and Rapamycin induce *in vitro* cholesteryl ester transfer protein activity, and suppress lipoprotein lipase activity in human plasma. *Int J Pharm.* (2008) 358:219–23. doi: 10.1016/j.ijpharm.2008.03.026

205. Derfler K, Hayde M, Heinz G, Hirschl MM, Steger G, Hauser AC, et al. Decreased postheparin lipolytic activity in renal transplant recipients with cyclosporin A. *Kidney Int.* (1991) 40:720–7. doi: 10.1038/ki.1991.266

206. Apanay DC, Neylan JF, Ragab MS, Sgoutas DS. Cyclosporine increases the oxidizability of low-density lipoproteins in renal transplant recipients. *Transplantation.* (1994) 58:663–9. doi: 10.1097/00007890-199409000-00005

207. Cofan F, Cofan M, Campos B, Guerra R, Campistol JM, Oppenheimer F. Effect of calcineurin inhibitors on low-density lipoprotein oxidation. *Transplant Proc.* (2005) 37:3791–3. doi: 10.1016/j.transproceed.2005.10.068

208. Bai L, Gabriels K, Wijnands E, Rousch M, Daemen MJAP, Tervaert JWC, et al. Low- but not high-dose FK506 treatment confers atheroprotection due to alternative macrophage activation and unaffected cholesterol levels. *Thromb Haemost.* (2010) 104:143–50. doi: 10.1160/TH09-07-0502

209. Jiang Y, Xie XB, Peng LK, Peng FH, Lan GB, Wang Y, et al. Dyslipidemia in human kidney transplant recipients receiving cyclosporine and tacrolimus is associated with different expression of CD36 on peripheral blood monocytes. *Transplant Proc.* (2011) 43:1612–5. doi: 10.1016/j.transproceed.2011.03.015

210. Deleuze S, Garrigue V, Delmas S, Chong G, Swarcz I, Cristol JP, et al. New onset dyslipidemia after renal transplantation: is there a difference between tacrolimus and cyclosporine? *Transplant Proc.* (2006) 38:2311–3. doi: 10.1016/j.transproceed.2006.06.125

211. Steinmüller TM, Gräf KJ, Schleicher J, Leder K, Bechstein WO, Mueller AR, et al. The effect of FK506 vs. cyclosporine on glucose and lipid metabolism–a randomized trial. *Transplantation.* (1994) 58:669–74. doi: 10.1097/00007890-199409000-00006

212. Abouljoud MS, Levy MF, Klintmalm GB. Hyperlipidemia after liver transplantation: long-term results of the FK506/cyclosporine A US multicenter trial. *US Multicenter Study Group Transplant Proc.* (1995) 27:1121–3.

213. Claesson K, Mayer AD, Squifflet JP, Grabensee B, Eigler FW, Behrend M, et al. Lipoprotein patterns in renal transplant patients: a comparison between FK 506 and cyclosporine a patients. *Transplant Proc.* (1998) 30:1292–4. doi: 10.1016/S0041-1345(98)00246-2

214. Zhou YD, Cao XQ, Liu ZH, Cao YJ, Liu CF, Zhang YL, et al. Rapamycin inhibits oxidized low density lipoprotein uptake in human umbilical vein endothelial cells *via* mTOR/NF-κB/LOX-1 pathway. *PLoS One.* (2016) 11:e0146777. doi: 10.1371/journal.pone.0146777

215. Choi SK, Kwon Y, Byeon S, Lee YH. Stimulation of autophagy improves vascular function in the mesenteric arteries of type 2 diabetic mice. *Exp Physiol.* (2020) 105:192–200. doi: 10.1113/EP087737

216. Ma KL, Ruan XZ, Powis SH, Moorhead JF, Varghese Z. Anti-atherosclerotic effects of sirolimus on human vascular smooth muscle cells. *Am J Physiol Heart Circ Physiol.* (2007) 292:H2721–2728. doi: 10.1152/ajpheart.01174.2006

217. Ai D, Chen C, Han S, Ganda A, Murphy AJ, Haeusler R, et al. Regulation of hepatic LDL receptors by mTORC1 and PCSK9 in mice. *J Clin Invest.* (2012) 122:1262–70. doi: 10.1172/JCI61919

218. Brattström C, Wilczek H, Tydén G, Böttiger Y, Säwe J, Groth CG. Hyperlipidemia in renal transplant recipients treated with sirolimus (rapamycin). *Transplantation.* (1998) 65:1272–4. doi: 10.1097/00007890-199805150-00023

219. Tur MD, Garrigue V, Vela C, Dupuy AM, Descomps B, Cristol JP, et al. Apolipoprotein CIII is upregulated by anticalcineurins and rapamycin: implications in transplantation-induced dyslipidemia. *Transplant Proc.* (2000) 32:2783–4. doi: 10.1016/S0041-1345(00)01884-4

220. Levy G, Schmidli H, Punch J, Tuttle-Newhall E, Mayer D, Neuhaus P, et al. Safety, tolerability, and efficacy of everolimus in de novo liver transplant recipients: 12- and 36-month results. *Liver Transplant Off Publ Am Assoc Study Liver Dis Int Liver Transplant Soc.* (2006) 12:1640–8. doi: 10.1002/lt.20707

221. Kasiske BL, de Mattos A, Flechner SM, Gallon L, Meier-Kriesche HU, Weir MR, et al. Mammalian Target of Rapamycin Inhibitor Dyslipidemia in Kidney Transplant Recipients. *Am J Transplant.* (2008) 8:1384–92. doi: 10.1111/j.1600-6143.2008.02272.x

222. Rosing K, Fobker M, Kannenberg F, Gunia S. Dell'Aquila AM, Kwiecien R, et al. Everolimus therapy is associated with reduced lipoprotein-associated phospholipase A2 (Lp-Pla2) activity and oxidative stress in heart transplant recipients. *Atherosclerosis.* (2013) 230:164–70. doi: 10.1016/j.atherosclerosis.2013.07.007

223. Engelen MA, Amler S, Welp H, Vahlhaus C, Gunia S, Sindermann JR, et al. Prospective study of everolimus with calcineurin inhibitor-free immunosuppression in maintenance heart transplant patients: results at 2 years. *Transplantation.* (2011) 91:1159–65. doi: 10.1097/TP.0b013e31821774bd

224. Sato S, Akamine Y, Kagaya H, Saito M, Inoue T, Numakura K, et al. Changes in PCSK9 and LDL cholesterol concentrations by everolimus treatment and their effects on polymorphisms in PCSK9 and mTORC1. *Pharmacol Rep PR.* (2020) 72:622–30. doi: 10.1007/s43440-020-00090-6

225. Schreiber TC, Greenstein SM, Kim DY, Calderon TM, Sun S, Schechner RS, et al. Effect of Mycophenolate Mofetil on Atherosclerosis in a Rabbit Model: Initial Histologic and Immunohistochemical Analyses 11Supported by Roche, Inc (Nutley, NJ). *Transplant Proc.* (1998) 30:961–2. doi: 10.1016/S0041-1345(98)00111-0

226. Perrea DN, Moulakakis KG, Poulakou MV, Vlachos IS, Nikiteas N, Kostakis A. Correlation between lipid abnormalities and immunosuppressive therapy in renal transplant recipients with stable renal function. *Int Urol Nephrol.* (2008) 40:521–7. doi: 10.1007/s11255-007-9266-y

227. van den Dorpel MA, Ghanem H, Rischen-Vos J, Man in't Veld AJ, Jansen H, Weimar W. Conversion from cyclosporine A to azathioprine treatment improves LDL oxidation in kidney transplant recipients. *Kidney Int.* (1997) 51:1608–12. doi: 10.1038/ki.1997.221

228. Akman B, Uyar M, Afsar B, Sezer S, Ozdemir FN, Haberal M. Lipid profile during azathioprine or mycophenolate mofetil combinations with cyclosporine and steroids. *Transplant Proc.* (2007) 39:135–7. doi: 10.1016/j.transproceed.2006.10.210

229. de Groen PC. Cyclosporine, low-density lipoprotein, and cholesterol. *Mayo Clin Proc.* (1988) 63:1012–21. doi: 10.1016/S0025-6196(12)64916-7

230. Rayyes O, Wallmark A, Florén C. Cyclosporine inhibits catabolism of low-density lipoproteins in HepG2 cells by about 25%. *Hepatology.* (1996) 24:613–9. doi: 10.1002/hep.510240325

231. López-Miranda J, Vilella E, Pérez-Jiménez F, Espino A. Jiménez-Perepérez JoséA, Masana L, et al. Low-density lipoprotein metabolism in rats treated with cyclosporine. *Metabolism.* (1993) 42:678–83. doi: 10.1016/0026-0495(93)90232-D

232. Kockx M, Kritharides L. Chapter 25—Cyclosporin A-Induced Dyslipidemia and LDL Receptors. In: Patel VB, editor. *The Molecular Nutrition of Fats [Internet]. Academic Pr.* (2019). p. 323–33. Available online at: https://www.sciencedirect.com/science/article/pii/B9780128112977000251 (accessed June 18, 2022).

233. MacDonald AS. RAPAMUNE Global Study Group. A worldwide, phase III, randomized, controlled, safety and efficacy study of a sirolimus/cyclosporine regimen for prevention of acute rejection in recipients of primary mismatched renal allografts. *Transplantation.* (2001) 71:271–80. doi: 10.1097/00007890-200101270-00019

234. Simha V, Qin S, Shah P, Smith BH, Kremers WK, Kushwaha S, et al. Sirolimus therapy is associated with elevation in circulating PCSK9 levels in cardiac transplant patients. *J Cardiovasc Transl Res.* (2017) 10:9–15. doi: 10.1007/s12265-016-9719-8

235. Vitko S, Tedesco H, Eris J, Pascual J, Whelchel J, Magee JC, et al. Everolimus with optimized cyclosporine dosing in renal transplant recipients: 6-month safety and efficacy results of two randomized studies. *Am J Transplant Off J Am Soc Transplant Am Soc Transpl Surg.* (2004) 4:626–35. doi: 10.1111/j.1600-6143.2004.00389.x

236. Holdaas H, Potena L, Saliba F. mTOR inhibitors and dyslipidemia in transplant recipients: A cause for concern? *Transplant Rev.* (2015) 29:93–102. doi: 10.1016/j.trre.2014.08.003

237. Pascual J. Concentration-controlled everolimus (Certican): combination with reduced dose calcineurin inhibitors. *Transplantation.* (2005) 79:S76–79. doi: 10.1097/01.TP.0000162434.62591.F3

238. Murakami N, Riella LV, Funakoshi T. Risk of metabolic complications in kidney transplantation after conversion to mTOR inhibitor: a systematic review and meta-analysis. *Am J Transplant.* (2014) 14:2317–27. doi: 10.1111/ajt.12852

frontiers | Frontiers in Cardiovascular Medicine

TYPE Original Research
PUBLISHED 23 September 2022
DOI 10.3389/fcvm.2022.922095

OPEN ACCESS

EDITED BY
Dong Han,
People's Liberation Army General Hospital, China

REVIEWED BY
Zaza Iakobishvili,
Tel Aviv University, Israel
Alessandra Cuomo,
Federico II University Hospital, Italy

*CORRESPONDENCE
Junke Long
drburkes@csu.edu.cn

SPECIALTY SECTION
This article was submitted to Cardio-Oncology, a section of the journal Frontiers in Cardiovascular Medicine

RECEIVED 17 April 2022
ACCEPTED 22 August 2022
PUBLISHED 23 September 2022

CITATION
Peng X, Zheng Y, Zhu Z, Liu N, Zhou S and Long J (2022) Which cardiac parameters best predict the cardiovascular outcomes among patients with anti-PD-1 immunotherapy-induced myocardial injury?
Front. Cardiovasc. Med. 9:922095.
doi: 10.3389/fcvm.2022.922095

Which cardiac parameters best predict the cardiovascular outcomes among patients with anti-PD-1 immunotherapy-induced myocardial injury?

Xiongjun Peng[1], Yawen Zheng[2], Zhaowei Zhu[3], Na Liu[3], Shenghua Zhou[3] and Junke Long[3]*

[1]The Second Xiangya Hospital, Central South University, Changsha, China, [2]National Clinical Research Center for Geriatric Disorders, Department of Geriatrics, Xiangya Hospital, Central South University, Changsha, China, [3]Department of Cardiovascular Medicine, The Second Xiangya Hospital, Central South University, Changsha, China

Aim: To explore the association of cardiac parameters with different clinical outcomes in patients with anti-PD-1 immunotherapy-induced myocardial injury.

Methods and results: We screened 3,848 patients who received anti-PD-1 immunotherapy from June 2018 to Oct 2021 at the Second Xiangya Hospital of Central South University. Among those patients, 134 patients were diagnosed with anti-PD-1 immunotherapy-induced myocardial injury. Twenty-four patients with cardiovascular symptoms were divided into the major adverse cardiac events (MACE) group, and 110 patients without cardiovascular symptoms were divided into the non-MACE group. We compared creatine kinase isozyme (CK-MB), high-sensitivity troponin T (hsTNT), N-terminal pro–B-type natriuretic peptide (NT-ProBNP), electrocardiography (ECG), and echocardiographic parameters between the two groups of patients. CK-MB, hsTNT, NT-proBNP [2,600.0 (1,317.00–7,950.00) vs. 472.9 (280.40–788.80), $p \leq 0.001$], left ventricular end-diastolic diameter (LVEDd), left ventricular ejection fraction (LVEF) and QRS interval were significantly different. The receiver operating characteristic (ROC) curve was used to compare the accuracy of various indicators to predict the occurrence of MACE events. NT-ProBNP (area under the curve [*AUC*] 97.1) was the best predictor, followed by CK-MB (*AUC* = 94.1), LVEF (*AUC* = 83.4), LVEDd (*AUC* = 81.5), and other indicators. In the MACE group, 11/24 patients had experienced cardiogenic death by the end of follow-up. There were significant differences in the CK-MB, hsTNT, NT-proBNP, LVEDd, LVEF, and QRS intervals between the deceased patients and the survivors. The ROC curve shows that hsTNT is the most accurate marker for predicting cardiogenic death in the MACE group (*AUC* = 91.6).

Conclusion: In patients with myocardial injury after PD-1 inhibitor treatment, NT-proBNP is the parameter of choice to predict the likelihood of developing cardiovascular symptoms, whereas, in symptomatic patients, hsTNT is the

optimal parameter associated with the outcome of death compared with other cardiac parameters.

KEYWORDS

cardiac parameters, anti-PD-1 immunotherapy, myocardial injury, prognostic predictor, cardiogenic death

Introduction

Cancer and cardiovascular diseases are the two most important categories of diseases affecting human health (1). Immunotherapy has advanced rapidly in the treatment of tumors in recent decades (2). In particular, immune checkpoint inhibitors (ICIs) represented by anti-programmed cell death-1 (PD-1) antibody therapy are one of the most commonly used immunotherapy methods worldwide (3). According to the guidelines published by multiple oncology organizations around the world (4, 5), PD-1 inhibitors have become a standard treatment for a variety of solid advanced malignancies, and immunotherapy-induced myocardial injury has increasingly been recognized with the widespread use of these agents (6). Some patients have only isolated elevation of serum markers of myocardial injury without any complaints, such as creatine kinase isozyme (CK-MB), high-sensitivity troponin T (hsTnT), and N-terminal pro–B-type natriuretic peptide (NT-proBNP). However, some patients treated with anti-PD-1 inhibitors also have severe cardiovascular manifestations, such as heart failure (HF), malignant arrhythmias, and death, even though a lower incidence of 0.3–2% has been reported in the literature (7, 8). The mechanism leading to this completely different clinical outcome is not yet been fully understood and may be related to the excessive activation of inflammation. In addition, whether patients with asymptomatic myocardial injury need treatment is unclear. Regardless, it is foreseeable that the use of ICIs will continue to increase as the cost decreases, and therefore, how to accurately identify the severity of PD-1 inhibitor-induced myocardial injury at an early stage is of great importance but remains unclear.

Our objective was to identify the association of cardiac parameters with different clinical outcomes in patients with anti-PD-1 immunotherapy-induced myocardial injury and find a better cardiac parameter to predict these outcomes of different severities.

Patients and methods

Patients

This is a retrospective cohort study, we screened 3,848 patients who received anti-PD-1 immunotherapy from June 2018 to Oct 2021 at the Second Xiangya Hospital of Central South University. Among those patients, 134 patients were diagnosed with anti-PD-1 immunotherapy-induced myocardial injury. These patients were from the Department of Oncology, Department of Respiratory Medicine, Department of Cardiology, Department of Thoracic Surgery, Department of Critical Medicine, and Department of Emergency. Medical records are from the inpatient, outpatient, and emergency medical systems. Data including demographic characteristics, comorbidities, main complaint at diagnosis, laboratory testing results, electrocardiography (ECG), echocardiographic findings, and treatment were obtained. The study protocol conformed to the ethical guidelines of the Declaration of Helsinki (9) as reflected by prior approval from the human research committee of the Second Xiangya Hospital of Central South University. Written informed consent was obtained from patients while the patient was in a clinically stable, non-congested condition or from their family members who could give informed consent on behalf of patients after they were informed about the objectives and procedures of the study. Their rights to refuse participation any time they wanted were assured. For this purpose, a one-page consent letter was attached as a cover page of each questionnaire stating the general objective of the study and issues of confidentiality that were discussed by the data collectors before proceeding with the data collection.

Diagnostic procedures

A total of 3,848 patients who received PD-1 antibody therapy were evaluated. The inclusion criteria were as follows: (1) High-sensitivity troponin T was negative in patients before PD-1 antibody treatment, but the concentration increased in patients after treatment. The exclusion criteria were: (1) Acute or suspected renal function injury leading to false elevation of high-sensitivity troponin T levels; and (2) Use of other drugs that may cause myocardial injuries, such as anthracycline chemotherapeutic drugs, cyclophosphamide, and trastuzumab. Finally, 134 patients were included in the study (see flowchart in Figure 1 for details).

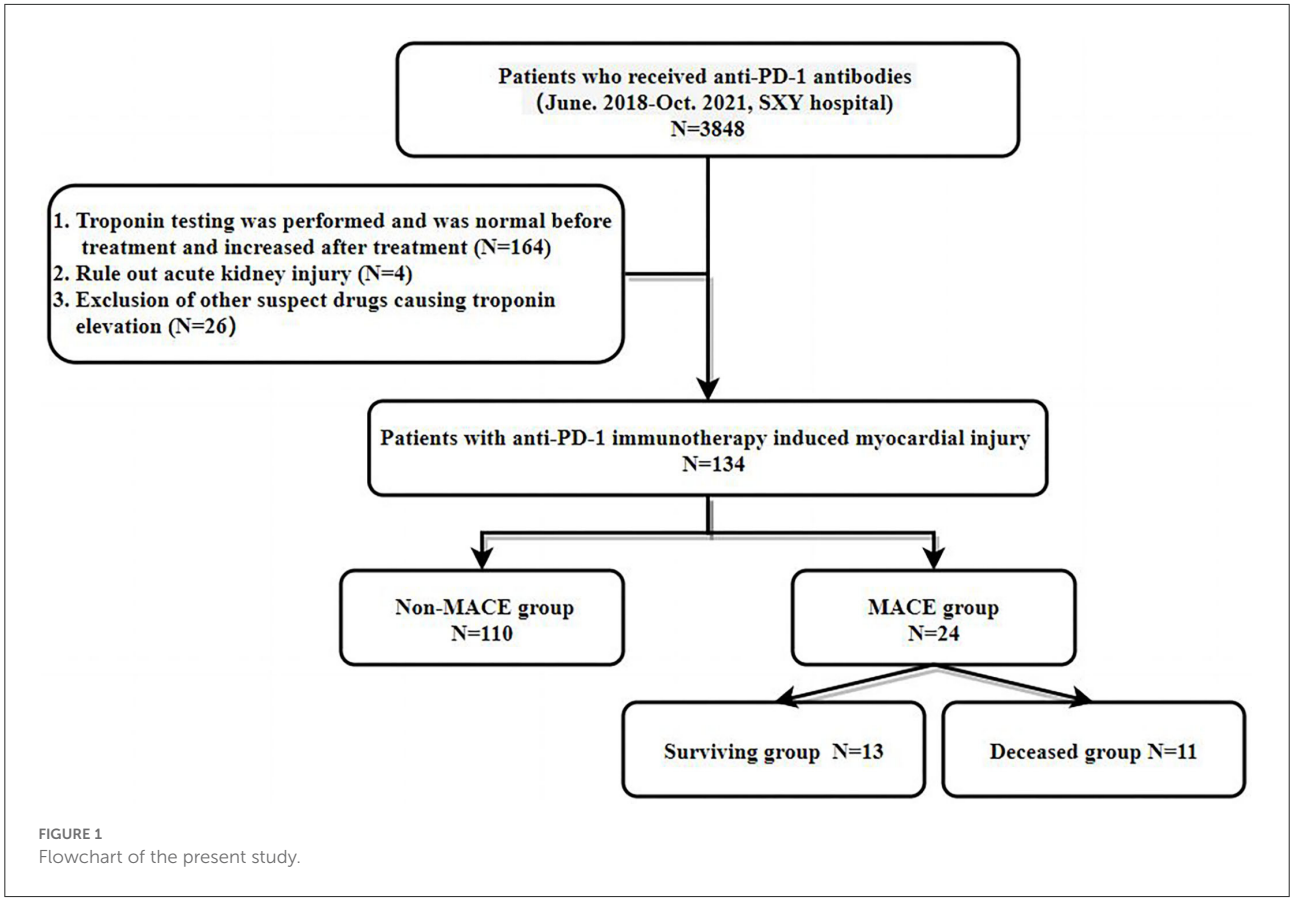

FIGURE 1
Flowchart of the present study.

Data collection

Demographic and clinical characteristics were collected when the diagnosis of PD-1 inhibitor-induced myocardial injury was confirmed. Blood test parameters, ECG, and cardiac ultrasound parameters were the first reports obtained after diagnosis. Patient-reported comorbidities were listed according to what the patient told our doctor on admission and what we diagnosed after discharge. The tracking of hsTNT and NT-proBNP is generally divided into two situations. The first is that it is detected in our hospital when symptoms appear. The second is the routine detection of asymptomatic patients on admission for anti-tumor treatment. High-sensitivity troponin T (hsTnT) was measured by electrochemiluminescence (Roche, Germany). The upper limit of the reference value (99th quantile) in the manual is 14 pg/ml.

Definitions and outcome

The outcome of interest, major adverse cardiac events (MACE), was a composite of cardiovascular death, cardiac arrest, HF, and arrhythmias that cause hemodynamic abnormalities such as tachyarrhythmias/bradyarrhythmias and acute myocardial infarction (AMI). For cases where cardiac arrest, HF, arrhythmias, and AMI led to death, the outcome was counted as cardiac death. Standard definitions were used for cardiovascular death, cardiac arrest, HF, and AMI (10, 11). Survival time (days) was measured as the duration between the first day of hospitalization when the patient received PD-1 antibody therapy to the date of MACE or death from any cause. Data were obtained from medical records or from telephone interviews with patients or relatives by 2 trained physicians. We chose to set the follow-up time to 90 days because previous clinical studies showed that the vast majority of cardiotoxicity occurred within 90 days following the use of PD-1 inhibitors (12). Patients were followed until 16 October 2021. Patients were censored if they were still alive at the end of the research period or were lost to follow-up, on which occasion their last clinic visit or correspondence time was used.

Statistical analysis

Normally distributed parameters are expressed as the mean ± standard deviation (*SD*), whereas non-normally distributed parameters are expressed as the median with interquartile range (*IQR*). Categorical values are presented as numbers

(percentages). Categorical data were reported as frequencies and percentages and were compared using the chi-squared or Fisher's exact test. Comparison of continuous variables between two independent groups was performed using an unpaired Student's *t*-test (if normally distributed) or the Mann–Whitney *U* test (non-normally distributed variables), and in cases where more than two groups were compared, one-way analysis of variance (ANOVA) or the Kruskal–Wallis test was used. Univariate analyses were performed to examine the correlates between cardiac parameters and different outcomes using the logistic regression models. The receiver operating characteristic (ROC) curve was used to reflect the accuracy of different cardiac parameters in predicting different outcomes by the area under the curve (AUC). Survival was evaluated with Kaplan–Meier curves. All tests were two-tailed and a p-value of < 0.05 was considered to indicate statistically significant. Statistical analysis was performed using SPSS 26.0 (IBM Software Inc), EmpowerStats 3.0 software, and R (version 3.3.2).

Results

Patient characteristics

In the MACE group, 16 patients had a new onset HF, 3 patients had non-ST segment elevation myocardial infarction (NSTEMI), 3 patients had new-onset symptomatic arrhythmia, and 1 patient had a sudden cardiac arrest. In the non-MACE group ($n = 110$), no patients presented with clinical symptoms of the cardiovascular system. Although high-sensitivity troponin T or NT-proBNP levels were significantly higher than before PD-1 antibody administration. The MACE group was older than the non-MACE group (66.5 ± 8.1 vs. 60.4 ± 9.9 $p = 0.01$). In addition, the MACE group had more concurrent side effects, such as PD-1-mediated pneumonia [7/24 (29.2%) vs. 1/110 (0.9%)], hepatitis [3/24 (12.5%) vs. 3/110 (2.7%)], myositis [4/24 (16.7%) vs. 3/110 (2.7%)], and thyroid dysfunction [5/24 (20.8%) vs. 16/110 (14.5%)]. Regarding sex, 75% (18/24) of patients in the MACE group were male, and 78.2% (86/110) in the non-MACE group were male. There was no significant difference in the gender distribution between the two groups (Table 1).

Cancer characteristics of interest

The time from the first day of PD-1 inhibitor treatment to the date when PD-1 inhibitor-induced myocardial injury diagnosis was confirmed was 37.04 ± 20.26 days for the MACE group and 32.85 ± 17.97 days for the non-MACE group. Regarding the tumor proportion scores (TPS) of PD-1 expression by tumor tissue immunohistochemistry, there was no difference between the two groups (47.35 ± 27.51 vs. 44.12 ± 27.23, $p = 0.654$). Regarding the anti-tumor regimen, 7 (29.2%) patients in the MACE group and 40 (36.4%) patients in the non-MACE group received PD-1 inhibitor monotherapy. The remaining cases were treated with chemotherapy combined with immunotherapy. More than half of the patients' primary tumors were non-small-cell lung cancer (NSCLC), followed by esophageal cancer, liver cancer, and other tumors (details in Table 1).

Cardiac parameters among subjects

In the MACE group, CK-MB (108.97 ± 57.09 vs. 31.86 ± 43.66, $p \leq 0.001$), hsTNT [195.5 (108.75–302.50) vs. 78.00 (47.85–124.00), $p \leq 0.001$], and NT-proBNP [2,600.0 (1,317.00–7,950.00) vs. 472.9 (280.40–788.80), $p \leq 0.001$] levels were significantly higher than those in the non-MACE group. Regarding the parameters of echocardiography, in the MACE group, patients had a higher left ventricular end-diastolic diameter (LVEDd) (51.5 ± 6.1 vs. 43.5 ± 6.2, $p \leq 0.001$) and lower left ventricular ejection fraction (LVEF) (46.7 ± 9.1 vs. 57.2 ± 7.5, $p \leq 0.001$) than those in the non-MACE group. There were no significant differences in other cardiac parameters between the two groups (Table 2). The ECG parameters between the two groups were also somewhat different. The incidence of bradyarrhythmia and tachyarrhythmia in the MACE group was higher than that in the non-MACE. The QRS interval of the MACE group was significantly wider than that of the non-MACE group (127.2 ± 33.5 vs. 93.7 ± 16.1, $p = 0.001$), but the corrected QT interval of the two groups was no different (details in Table 2).

Outcome of all cases

The median follow-up of all cases was 90 days (12–102 days). In the MACE group, 13/24 of patients survived after careful treatment. The number of all-cause deaths in the MACE group was 12 (50%) as of the end of follow-up, and one of them was non-cardiogenic death (lung infection). For the non-MACE group, 16/110 (14.5%) of patients had non-cardiogenic deaths, and the rest were still alive at the end of follow-up. The K–M survival curves of the two groups are shown in Figure 2.

Cardiac parameters among survivors and deceased patients in the MACE group

In the MACE group, 13/24 of patients survived after treatment, and 11/24 died after treatment. Compared with those of the survivors, the CK-MB (146.4 ± 56.2 vs. 77.3 ± 35.3, $p \leq 0.001$), hsTNT [300.0 (218.5–729.0) vs. 112.0 (84.0–122.0), $p \leq 0.001$], and NT-proBNP [8,400.0 (3,850.0–14,000.0) vs. 1,890.0 (1,200.0–2,400.0), $p \leq 0.001$] levels of the deceased

TABLE 1 Characteristics of 134 patients with programmed cell death (PD-1)-related myocardial injury.

	No MACE ($n = 110$)	MACE ($n = 24$)	*P*-value
Age, years	60.4 (9.9)	66.5 (8.1)	0.010
Male, *n* (%)	86(78.2)	18 (75)	0.735
SBP, mmHg	115.48 (21.13)	119.25 (17.52)	0.233
DBP, mmHg	70.45 (11.57)	70.46 (13.47)	0.738
NYHA, *n* (%)			< 0.001
Class I–II	110(100)	9(37.5)	
Class III–IV	–	15(62.5)	
SpO_2, %	96.45 (2.43)	96.25 (2.72)	0.962
TPS, %	47.35 (27.51)	44.12 (27.23)	0.654
Days from first dose	32.85 (17.97)	37.04 (20.26)	0.257
Primary cancer type, *n* (%)			0.822
Lung cancer	66 (60)	16 (66.7)	
Esophageal cancer	14 (12.7)	2 (8.3)	
Liver cancer	10 (9.1)	3 (12.5)	
Other tumors	20 (18.2)	3 (12.5)	
Comorbidities, *n* (%)			0.356
COPD	15 (13.6)	5 (20.8)	
Hypertension	38 (34.5)	8 (33.3)	
Hyperlipidemia	28 (25.5)	6 (25)	
CKD	22 (20)	5 (20.8)	
T2DM	16 (14.6)	2 (8.4)	
Stroke	15 (13.6)	2 (8.3)	
CHD	16 (14.5)	6 (25)	
Anti-tumor regimen, *n* (%)			0.188
PD-1 monotherapy	40(36.4)	7 (29.2)	
Combined chemotherapy	70 (63.6)	17 (70.8)	
Concurrent side effects, *n* (%)			0.001
Pneumonitis	1 (0.9)	7 (29.2)	
Hepatitis	3 (2.7)	3 (12.5)	
Thyroid dysfunction	16 (14.5)	5 (20.8)	
Myositis	3 (2.7)	4 (16.7)	
Baseline cardiac parameters			
Cardiac troponin T, pg/mL	8.0 (6.3–10.2)	7.6 (5.3–9.8)	0.285
PR interval, ms	154.9 ± 17.3	161.2 ± 36.4	0.214
Corrected QT interval, ms	452.6 ± 36.2	448.5 ± 52.2	0.654
QRS duration, ms	95.2 ± 19.4	87.0 ± 17.1	0.058
Baseline cardiovascular medications			
Aspirin	15 (13.6%)	5 (20.8%)	0.370
ACEI or ARB	10 (9.1%)	4 (16.7%)	0.272
βblockers	11 (10.0%)	4 (16.7%)	0.348

Data are (N) Mean (SD) or (N) n (%), Median (Q3–Q1), where N is the total number of patients with available data. SBP, Systolic Blood Pressure; DBP, Diastolic Blood Pressure; SpO_2, Saturation of Peripheral Oxygen; TPS, Tumor Proportion Score; NYHA, New York Heart Association Functional Classification; CHD, Coronary Heart Disease; COPD, Chronic Obstructive Pulmonary Disease; CKD, Chronic Kidney Disease; T2DM, Type 2 Diabetes Mellitus; PD-1,Programmed Cell Death.

patients were significantly higher. Regarding the parameters of echocardiography, deceased patients had higher LVEDd (54.7 ± 4.7 vs. 48.7 ± 5.8, $p \leq 0.009$) and lower LVEF (39.7 ± 6.4 vs. 52.6 ± 6.5, $p \leq 0.001$) than those survivors. The QRS interval of the deceased patient group was significantly longer than that of the survivor groups (144.0 ± 37.5 vs. 113.1 ± 20.5, $p = 0.020$). There were no significant differences in other cardiac parameters between the two groups (Table 3).

TABLE 2 Laboratory, echocardiographic, and electrocardiographic characteristics and treatment of 134 patients with PD-1-related myocardial injury.

	No MACE ($n = 110$)	MACE ($n = 24$)	*P*-value
Laboratory results			
CK-MB, u/L	31.86 (43.66)	108.97 (57.09)	**<0.001**
Cardiac troponin T, pg/mL	78.00 (47.85–124.00)	195.5 (108.75–302.50)	**<0.001**
NT-proBNP, pg/mL	472.9 (280.40–788.80)	2600.0(1317.00–7950.00)	**<0.001**
Echocardiographic findings			
LVEDd, mm	43.5 (6.2)	51.5 (6.1)	**<0.001**
RVEDd, mm	33.7 (4.3)	33.0(4.3)	0.380
LAESd, mm	36.5 (5.9)	37.4 (5.0)	0.201
RAESd, mm	34.1 (5.3)	33.5 (5.1)	0.614
LVEF, (%)	57.2 (7.5)	46.7 (9.1)	**<0.001**
ECG findings			
Atrial fibrillation, *n* (%)	11 (10)	1 (4.2)	0.693
Advanced AV block, *n* (%)	2 (1.8)	8 (33.3)	**0.001**
Bundle branch block	24 (21.8)	7 (29.2)	0.256
FVP or VT, *n* (%)	19 (17.3)	11 (45.8)	**0.006**
PR interval, ms	170.6 (32.2)	168.3 (26.2)	0.929
Corrected QT interval, ms	457.3 (34.1)	470.5 (35.4)	0.173
QRS duration, ms	93.7 (16.1)	127.2 (33.5)	**<0.001**
Therapeutic cardiovascular medications			
Aspirin	16 (14.5)	8 (33.3)	**0.040**
ACEI or ARB	12 (10.9)	10 (41.7)	0.010
βblockers	16 (14.5)	5 (20.8)	0.743
Furosemide	2 (1.8)	17 (70.8)	**<0.001**
Inotropic agents	0 (0)	6 (25)	**<0.001**
Glucocorticoid	1 (0.9)	13 (54.2)	**<0.001**

Data are (N) Mean (SD) or (N) n (%), Median (Q3–Q1), where N is the total number of patients with available data. CK-MB, Creatine Kinase isoenzyme MB; NT-proBNP, N-terminal pro–B-type Natriuretic Peptide; LAESd, Left Atrium End Systolic diameter; LVEDd, Left Ventricular End Diastolic diameter; RAESd, Right Atrium End Systolic diameter; RVEDd, Right Ventricular End Diastolic diameter; LVEF, Left Ventricular Ejection Fraction; FVP, Frequent Ventricular Premature; VT, Ventricular Tachycardia.

The association between cardiac parameters and different outcomes

Univariate logistic regression was used to analyze the association between cardiac parameters and different outcomes. Age ($OR = 1.08$, 95% $CI = 1.02–1.14$, $p = 0.007$), CK-MB ($OR = 1.03$, 95% $CI = 1.01–1.04$, $p < 0.001$), hsTNT ($OR = 1.01$, 95% $CI = 1–1.01$, $p = 0.001$), NT-proBNP ($OR = 1.0$, 95% $CI = 1.0–1$, $p < 0.001$), LVEDd ($OR = 1.21$, 95% $CI = 1.12–1.32$, $p < 0.001$), LVEF ($OR = 0.87$, 95% $CI = 0.82–0.93$, $p < 0.001$), and QRS interval ($OR = 1.04$, 95% $CI = 1.02–1.06$, $p < 0.001$) were predictive of the development of cardiovascular symptoms (MACE events) in patients with PD-1 inhibitor-induced myocardial injury. The ROC curve was used to compare the accuracy of various indicators to predict the occurrence of MACE events. NT-ProBNP ($AUC = 97.1$) was the best predictor, followed by CK-MB ($AUC = 94.1$), LVEF ($AUC = 83.4$), LVEDd ($AUC = 81.5$), and other indicators, as shown in Figure 3A. In the MACE group, CK-MB ($OR = 1.04$, 95% $CI = 1.01–1.07$, $p < 0.021$), NT-proBNP ($OR = 1.0$, 95% $CI = 1–1$, $p < 0.042$), hsTNT ($OR = 1.02$, 95% $CI = 1–1.04$, $p < 0.034$), and QRS duration ($OR = 1.04$, 95% $CI = 1–1.07$, $p < 0.032$) were predictors of death. The ROC curve revealed that hsTNT was the most accurate predictive marker ($AUC = 91.6$; more details in Table 4 and Figure 3B).

Discussion

This is a retrospective case analysis from a large referral hospital. We are deeply concerned about the increase in high-sensitivity troponin T levels after PD-1 inhibitor treatment, and previous studies have reported that the incidence is very low. In the safety study of more than 2,000 patients with immunotherapy released by Bristol–Myers Squibb, the rate of myocarditis in patients treated with ipilimumab or nivolumab

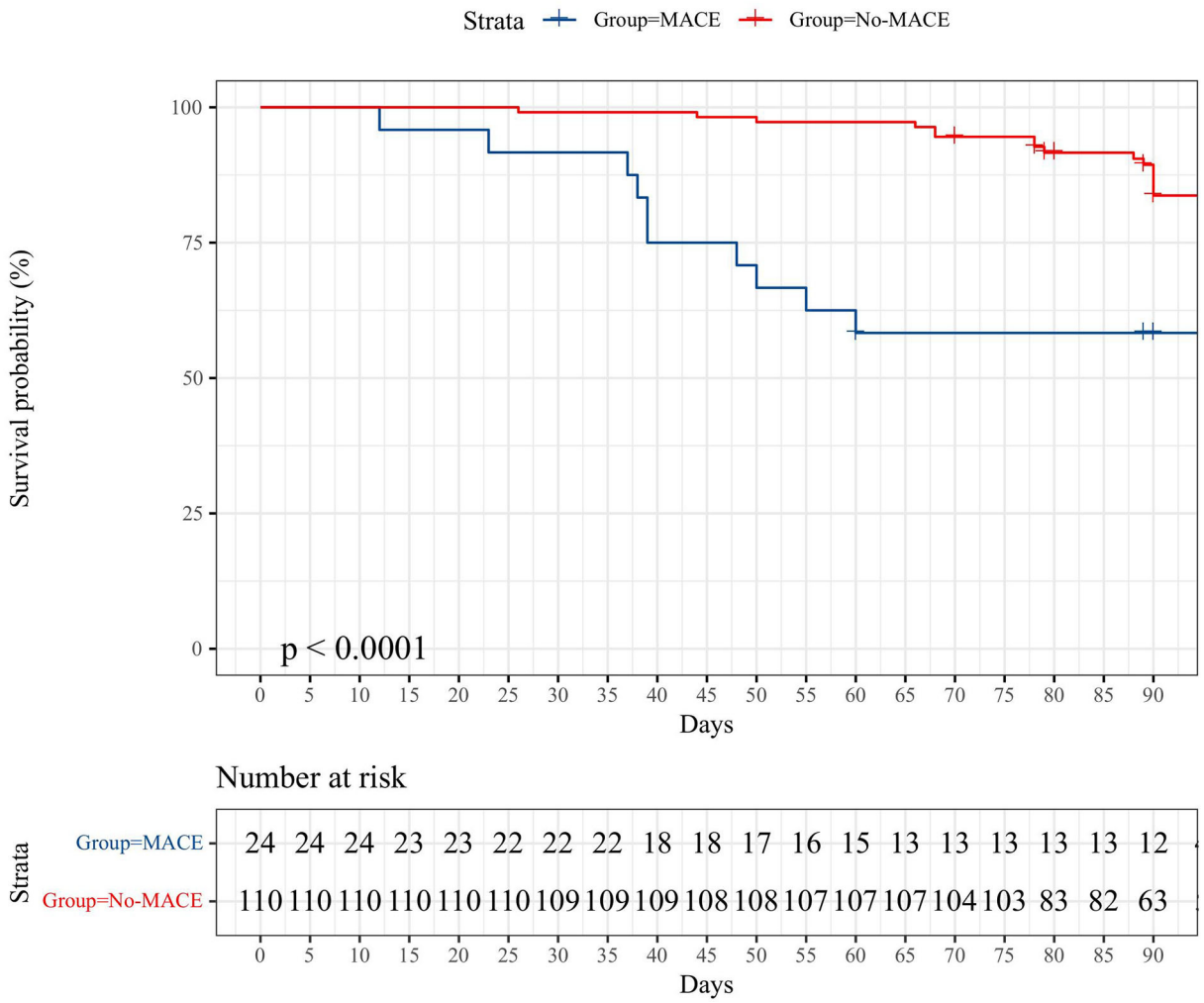

FIGURE 2
The K–M survival curve compares the 90-day all-cause deaths between the two groups.

was 0.09%. Among patients receiving combination therapy, the incidence of myocarditis is approximately 0.3%, and its severity is greater than that of patients receiving monotherapy (8). A retrospective case study of PD-1 inhibitor treatment reported that the prevalence of myocarditis was 1.14% with a median time of onset of 34 days after starting PD-1 inhibitor treatment (*IQR*: 21–75 days) (13). Since many patients do not routinely have ECG and markers of myocardial injury monitored, some studies suggest or believe that the proportion of myocarditis caused by PD-1 inhibitors may be higher than 1% (7). However, in clinical practice, we often encounter patients who show only elevated levels of cardiac troponin, a marker of myocardial injury but have no symptoms after treatment with PD-1 inhibitors. These patients have not been well evaluated. Our study showed that 3.48% (134/3848) of patients had increased high-sensitivity troponin T levels after PD-1 inhibitor monotherapy. This ratio is very high and still underestimated because some patients without cardiovascular symptoms have not been monitored for troponin levels. Our study indicated that 24 patients (0.62%) had cardiovascular symptoms, and 11 of them suffered cardiogenic death. If these symptomatic patients are defined as having myocarditis, this is equivalent to the incidence rate of previous studies.

Our study supports the need for routine monitoring of cardiac parameters in patients using PD-1 inhibitors. Oncologists in many countries currently recommend routine detection of myocardial injury markers, such as CK-MB, CK, troponin, and BNT-proBNP, during each cycle of PD-1 inhibitors (14, 15). However, the importance of the elevated levels of each marker is unclear, and cardiovascular physicians often go to the oncology department for consultation. Our study indicates that the higher the increase in these cardiac

TABLE 3 Cardiac parameters among survivors and deceased patients.

	Survived ($N = 13$)	Deceased ($N = 11$)	*P*-value
Age, years	63.8 (7.7)	69.6 (7.6)	0.124
Male, *n* (%)	11 (84.6%)	7 (63.6%)	0.357
Cardiovascular manifestations			
Dyspnea	8 (61.5%)	9 (81.8%)	0.386
Edema	2 (15.4%)	2 (18.2%)	0.855
Palpitation	3 (23.1%)	0 (0.0%)	0.233
Chest pain	4 (30.8%)	1 (9.1%)	0.327
Days from first dose to onset	36.7 (20.4)	37.5 (21.0)	0.772
Cardiac parameters			
SBP, mmHg	124.5 (17.3)	113.1 (16.5)	0.111
DBP, mmHg	74.6 (10.2)	65.5 (15.6)	0.147
CK-MB, u/L	77.3 (35.3)	146.4 (56.2)	**0.003**
Cardiac troponin T, pg/mL	112.0 (84.0–122.0)	300.0 (218.5–729.0)	**0.001**
NT-proBNP, pg/mL	1,890.0 (1,200.0–2,400.0)	8,400.0 (3,850.0–14,000.0)	**0.002**
Echocardiographic findings			
LVEDd, mm	48.7 (5.8)	54.7 (4.7)	**0.009**
RVEDd, mm	32.1 (3.7)	34.2 (5.0)	0.222
LAESd, mm	35.9 (6.1)	39.1 (2.5)	0.130
RAESd, mm	32.9 (5.9)	34.1 (4.2)	0.662
LVEF, (%)	52.6 (6.5)	39.7 (6.4)	**<0.001**
ECG findings			
Atrial fibrillation, *n* (%)	0 (0.0%)	1 (9.1%)	0.458
Advanced AV block, *n* (%)	3 (23.1%)	5 (45.5%)	0.390
Bundle branch block	2 (15.4%)	5 (45.5%)	0.182
FVP or VT, *n* (%)	4 (30.8%)	7 (63.6%)	0.107
PR interval, ms	173.9 (28.2)	161.7 (23.0)	0.234
Corrected QT interval, ms	471.2 (40.9)	469.7 (29.7)	0.977
QRS duration, ms	113.1 (20.5)	144.0 (37.5)	**0.020**

Data are (N) Mean (SD) or (N) n (%), Median (Q3–Q1), where N is the total number of patients with available data. For other abbreviations, see Table 2.

markers levels, the greater the probability of occurrence of cardiac symptoms. In addition, our study indicates that the QRS interval on ECG is also a clinical indicator for predicting whether patients will have symptoms, which suggests that ECG is also very important in monitoring patients for adverse drug reactions. This is similar to a previous study by Zlotoff et al., which showed that the QRS duration is increased in ICI myocarditis and is associated with increased MACE risk, especially in patients whose QRS interval is greater than 110 ms (16). We think this is mainly related to the occurrence of more ventricular arrhythmias in the MACE group. With an increasing number of ventricular arrhythmias, the probability of cardiovascular symptoms will obviously increase. Of course, cardiac ultrasound is a very accurate tool to judge whether a patient has cardiac dysfunction, especially the LVEF is a very important indicator. However, using the ROC curve for comparison, NT-proBNP is the best cardiac parameter predicting clinical symptoms in patients with PD-1 inhibitor-mediated myocardial injury. This may be related to the fact that most patients in the MACE group present with symptoms of HF.

Our study indicated that the most common occurrence of cardiovascular system symptoms after PD-1 inhibitor treatment is HF symptoms, manifested as dyspnea and edema. Then, five patients presented with chest pain, four patients experienced palpitations, and one patient died suddenly after elevated troponin levels were observed. Notably, 62.5% (16/24) of patients in the MACE group entered the intensive care unit for treatment. However, 45.8% (11/24) of the patients eventually experienced cardiogenic death. Such a high mortality rate is similar to that reported in Western countries (17–19). Additionally, the proportion of corticosteroid treatment was

TABLE 4 Logistic regression analysis of the association between cardiac parameters and different outcomes.

Variables	MACE among 124 patients OR (95% CI)	*p*-value
Age	1.08 (1.02∼1.14)	**0.007**
Male	1.19 (0.43∼3.34)	0.735
CK-MB	1.03 (1.01∼1.04)	**<0.001**
Cardiac troponin T	1.01 (1∼1.01)	**0.001**
NT-proBNP	1.0 (1.00∼1)	**<0.001**
LVEDd, mm	1.21 (1.12∼1.32)	**<0.001**
RVEDd, mm	0.97 (0.87∼1.07)	0.515
LAESd, mm	1.03 (0.95∼1.11)	0.505
RAESd, mm	0.98 (0.89∼1.06)	0.569
LVEF	0.87 (0.82∼0.93)	**<0.001**
PR interval	1 (0.98∼1.01)	0.75
Corrected QT interval	1.01 (1∼1.02)	0.093
QRS duration	1.04 (1.02∼1.06)	**<0.001**
Cardiac death among 24 patients		
Age	1.11(0.99∼1.25)	0.086
Male	3.14 (0.45∼21.96)	0.248
CK-MB	1.04 (1.01∼1.07)	**0.021**
Cardiac troponin T	1.02 (1∼1.04)	**0.034**
NT-proBNP	1 (1∼1)	**0.042**
LVEDd, mm	0.87(0.7∼1.07)	0.184
RVEDd, mm	1.13 (0.92∼1.39)	0.24
LAESd, mm	1.17 (0.95∼1.43)	0.135
RAESd, mm	1.05 (0.89∼1.23)	0.57
LVEF	0.88 (0.75∼1.04)	0.136
PR interval	0.98 (0.95∼1.01)	0.258
Corrected QT interval	1 (0.98∼1.02)	0.916
QRS duration	1.04 (1∼1.07)	**0.032**

relatively low compared to that in Western countries; 23 patients in the MACE group received treatment, and 13 patients received glucocorticoids. A recent study (20) showed that the dose of corticosteroids is negatively correlated with the mortality of patients with PD-1 inhibitor-mediated myocarditis. However, these results increase the possibility that myocardial injury can be mitigated by early and intensive corticosteroid therapy. Nevertheless, the decision of whether to administer high-dose corticosteroids during clinical practice still requires consideration of various other aspects, especially infection. Certainly, we cannot rule out that this mortality rate is related to the conservative use of corticosteroid therapy. Despite the high mortality rate, we still need to risk stratify patients. We also used a logistic model to evaluate the relationship between various cardiac parameters and cardiogenic death. CK-MB, hsTNT, NT-proBNP, and QRS duration were statistically significant in predicting cardiogenic death in the MACE group. Using ROC curves for mutual comparison, hsTNT was the best marker for predicting cardiogenic death in the MACE group patients.

In 2018, the American Society for Clinical Oncology (ASCO) issued the clinical practice guidelines (21, 22) for cardiotoxicity related to ICIs. Based on this guideline, cardiotoxicity is divided into four levels according to severity (23). Patients who exhibit only increased levels of markers of myocardial injury without any symptoms are divided into 1 level and do not need corticosteroid treatment, however, monitoring of cardiac parameters needs to be continued. The results of this study may help clinicians identify, early in the course of the disease, which patients with level 1 will continue to develop symptoms and which patients with symptoms will continue to progress to death. In view of the very high mortality rate of PD-1 inhibitor-related myocarditis, these results may help us to stay aware of specific patients and provide more appropriate treatments in the early stages of disease deterioration.

This study also has some limitations. First of all, this is a single-center retrospective study. Although we want to clarify the specific probability of myocardial injury after PD-1 inhibitor treatment, a large proportion of the data is incomplete,

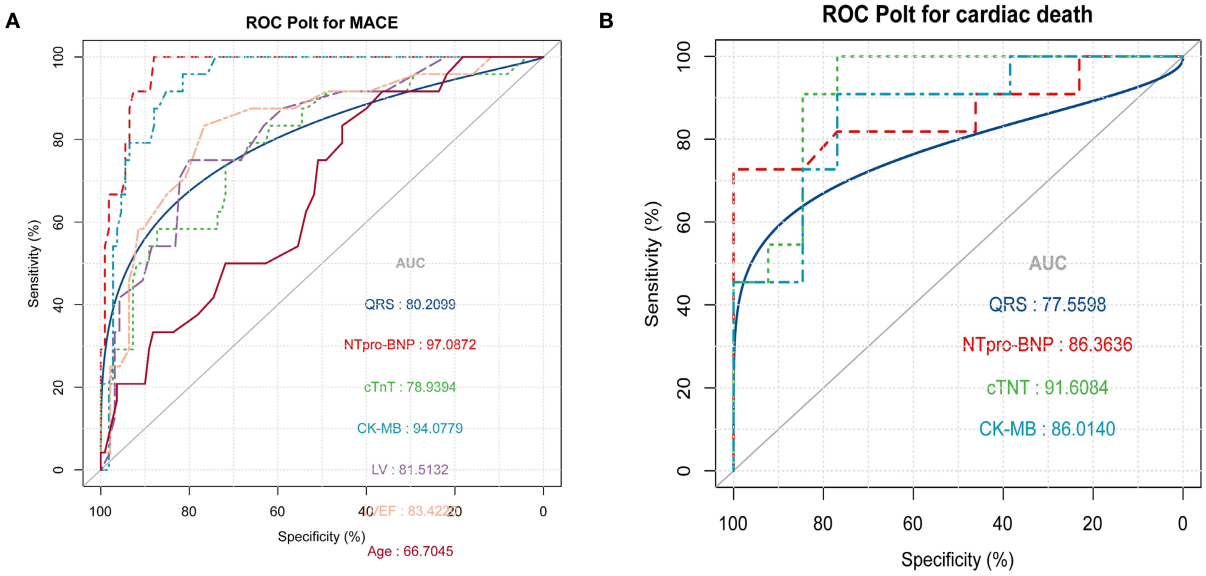

FIGURE 3
(A) Receiver operating characteristic (ROC) was used to compare the accuracy of various indicators to predict the occurrence of major adverse cardiac events (MACE) **(B)** ROC curve shows that high-sensitivity troponin T (hsTNT) is the most accurate marker for predicting cardiogenic death in the MACE group.

and there are many deviations. Laboratory indicators and ECG indicators are complete, but there are missing data on cardiac ultrasound. Thus, we used the mean instead. This led to a shift in the research results. Second, we cannot completely rule out myocardial damage caused by other drugs, such as chemotherapy drugs, such as paclitaxel and platinum, although these drugs are rarely reported to cause myocardial damage, at the same time, we cannot completely rule out myocardial infarction, stress cardiomyopathy, and other causes of myocardial injury in these patients because of the lack of very complete clinical examination results. Third, the small sample size and information bias may affect the results of our study. Further research should be conducted with larger sample size and minimize the information bias for more reliable results.

Conclusion

In patients with myocardial injury after PD-1 inhibitor treatment, NT-proBNP is the superior parameter of choice to predict the likelihood of developing cardiovascular symptoms, whereas, in symptomatic patients, hsTnT is superior to other cardiac parameters and is associated with the development of death.

Data availability statement

The raw data supporting the conclusions of this article will be made available by the authors, without undue reservation.

Ethics statement

The studies involving human participants were reviewed and approved by Human Research Committee of the Second Xiangya Hospital of Central South University. The patients/participants provided their written informed consent to participate in this study.

Author contributions

JL designed this study and performed quality control of data authenticity. XP drafted the manuscript and collected and analyzed the data. ZZ, NL, SZ, YZ, and JL revised the paper. All authors approved the final version.

Funding

This research was supported by the National Natural Science Foundation of China (82100314).

Conflict of interest

The authors declare that the research was conducted in the absence of any commercial or financial relationships that could be construed as a potential conflict of interest.

Publisher's note

References

1. Vos T, Lim SS, Abbafati C, Abbas KM, Abbasi M, Abbasifard M, et al. Global burden of 369 diseases and injuries in 204 countries and territories, 1990-2019: a systematic analysis for the global burden of disease study 2019. *Lancet.* (2020) 396:1204–22. doi: 10.1016/S0140-6736(20)30925-9

2. Zaha VG, Meijers WC, Moslehi J. Cardio-immuno-oncology. *Circulation.* (2020) 141:87–9. doi: 10.1161/CIRCULATIONAHA.119.042276

3. Dall'Olio FG, Marabelle A, Caramella C, Garcia C, Aldea M, Chaput N, et al. Tumour burden and efficacy of immune-checkpoint inhibitors. *Nat Rev Clin Oncol.* (2021) 19:75–90. doi: 10.1038/s41571-021-00564-3

4. Schneider BJ, Ismaila N, Aerts J, Chiles C, Daly ME, Detterbeck FC, et al. Lung cancer surveillance after definitive curative-intent therapy: ASCO Guideline. *J Clin Oncol.* (2020) 38:753–66. doi: 10.1200/JCO.19.02748

5. Siddiqui AZ, Almhanna K. Beyond Chemotherapy, PD-1, and HER-2: novel targets for gastric and esophageal cancer. *Cancers.* (2021) 13:4322. doi: 10.3390/cancers13174322

6. Kondapalli L, Neilan TG. Immune checkpoint inhibitors and cardiovascular events among patients with cancer: a window into the critical role of the immune system in cardiovascular biology. *Eur Heart J.* (2021) 42:4978–80. doi: 10.1093/eurheartj/ehab708

7. Zimmer L, Goldinger SM, Hofmann L, Loquai C, Ugurel S, Thomas I, et al. Neurological, respiratory, musculoskeletal, cardiac and ocular side-effects of anti-PD-1 therapy. *Eur J Cancer.* (2016) 60:210–25. doi: 10.1016/j.ejca.2016.02.024

8. Johnson DB, Balko JM, Compton ML, Chalkias S, Gorham J, Xu Y, et al. Fulminant myocarditis with combination immune checkpoint blockade. *New England J Med.* (2016) 375:1749–55. doi: 10.1056/NEJMoa1609214

9. World Medical Association declaration of Helsinki. Recommendations guiding physicians in biomedical research involving human subjects. *JAMA.* (1997) 277:925–6. doi: 10.1001/jama.277.11.925

10. Hicks KA, Tcheng JE, Bozkurt B, Chaitman BR, Cutlip DE, Farb A, et al. ACC/AHA key data elements and definitions for cardiovascular endpoint events in clinical trials: a report of the American college of cardiology/American heart association task force on clinical data standards (writing committee to develop cardiovascular endpoints data standards). *Circulation.* (2015) 132:302–61. doi: 10.1161/CIR.0000000000000156

11. McDonagh TA, Metra M, Adamo M, Gardner RS, Baumbach A, Böhm M, et al. 2021 ESC guidelines for the diagnosis and treatment of acute and chronic heart failure. *Eur Heart J.* (2021) 42:3599–726. doi: 10.1093/eurheartj/ehab368

12. Stein-Merlob AF, Rothberg MV, Ribas A, Yang EH. Cardiotoxicities of novel cancer immunotherapies. *Heart.* (2021) 107:1694–1703. doi: 10.1136/heartjnl-2020-318083

13. Mahmood SS, Fradley MG, Cohen JV, Nohria A, Reynolds KL, Heinzerling LM et al. myocarditis in patients treated with immune checkpoint inhibitors. *J Am Coll Cardiol.* (2018) 71:1755–64. doi: 10.1016/j.jacc.2018.02.037

14. Neilan TG, Rothenberg ML, Amiri-Kordestani L, Sullivan RJ, Steingart RM, Gregory W, et al. myocarditis associated with immune checkpoint inhibitors: an expert consensus on data gaps and a call to action. *Oncologist.* (2018) 23:874–8. doi: 10.1634/theoncologist.2018-0157

15. Puzanov I, Diab A, Abdallah K, Bingham CO, Brogdon C, Dadu R, et al. Managing toxicities associated with immune checkpoint inhibitors: consensus recommendations from the society for immunotherapy of Cancer (SITC) toxicity management working group. *J Immunother Cancer.* (2017) 5:95. doi: 10.1186/s40425-017-0300-z

16. Zlotoff DA, Hassan M, Zafar A, Alvi RM, Awadalla M, Mahmood SS, et al. Electrocardiographic features of immune checkpoint inhibitor associated myocarditis. *J Immunother Cancer.* (2021) 9:e002007. doi: 10.1136/jitc-2020-002007

17. Rubio-Infante N, Ramírez-Flores YA, Castillo EC, Lozano O, García-Rivas G, Torre-Amione G. Cardiotoxicity associated with immune checkpoint inhibitor therapy: a meta-analysis. *Eur J Heart Fail.* (2021) 23–1793–47. doi: 10.1002/ejhf.2289

18. Puzanov I, Subramanian P, Yatsynovich YV, Jacobs DM, Chilbert MR, Sharma UC, et al. Clinical characteristics, time course, treatment and outcomes of patients with immune checkpoint inhibitor-associated myocarditis. *J Immunother Cancer.* (2021) 9:e002553. doi: 10.1136/jitc-2021-002553

19. Pathak R, Katel A, Massarelli E, Villaflor V, Sun V, Salgia R. Immune checkpoint inhibitor-induced myocarditis with myositis/myasthenia gravis overlap syndrome: a systematic review of cases. *Oncologist.* (2021) 26:1052–61. doi: 10.1002/onco.13931

20. Zhang L, Zlotoff DA, Awadalla M, Mahmood SS, Nohria A, Hassan M, et al. Major adverse cardiovascular events and the timing and dose of corticosteroids in immune checkpoint inhibitor-associated myocarditis. *Circulation.* (2020) 141:2031–4. doi: 10.1161/CIRCULATIONAHA.119.044703

21. Schneider BJ, Naidoo J, Santomasso BD, Lacchetti C, Adkins S, Anadkat M, et al. Management of immune-related adverse events in patients treated with immune checkpoint inhibitor therapy: ASCO guideline update. *J Clin Oncol.* (2021) 39:4073–4126. doi: 10.1200/JCO.21.01440

22. Brahmer JR, Lacchetti C, Schneider BJ, Atkins MB, Brassil KJ, Caterino JM, et al. Management of immune-related adverse events in patients treated with immune checkpoint inhibitor therapy: American society of clinical oncology clinical practice guideline. *J Clin Oncol.* (2018) 36:1714–68. doi: 10.1200/JCO.2017.77.6385

23. Lyon AR, Dent S, Stanway S, Earl H, Brezden-Masley C, Cohen-Solal A, et al. Baseline cardiovascular risk assessment in cancer patients scheduled to receive cardiotoxic cancer therapies: a position statement and new risk assessment tools from the cardio-oncology study group of the heart failure association of the european society of cardiology in collaboration with the international cardio-oncology society. *Eur J Heart Fail.* (2020) 22:1945–60. doi: 10.1002/ejhf.1920

frontiers | Frontiers in Cardiovascular Medicine

TYPE Review
PUBLISHED 23 September 2022
DOI 10.3389/fcvm.2022.932347

OPEN ACCESS

EDITED BY
Feng Cao,
People's Liberation Army General Hospital, China

REVIEWED BY
Maria Teresa Palano,
MultiMedica (IRCCS), Italy
Daniel Chen,
University College London, United Kingdom

*CORRESPONDENCE
Vlad G. Zaha
vlad.zaha@utsouthwestern.edu

SPECIALTY SECTION
This article was submitted to Cardio-Oncology, a section of the journal Frontiers in Cardiovascular Medicine

RECEIVED 29 April 2022
ACCEPTED 16 August 2022
PUBLISHED 23 September 2022

CITATION
Rao A, Stewart A, Eljalby M, Ramakrishnan P, Anderson LD Jr, Awan FT, Chandra A, Vallabhaneni S, Zhang K and Zaha VG (2022) Cardiovascular disease and chimeric antigen receptor cellular therapy. *Front. Cardiovasc. Med.* 9:932347. doi: 10.3389/fcvm.2022.932347

Cardiovascular disease and chimeric antigen receptor cellular therapy

Anjali Rao[1,2,3], Andrew Stewart[3,4], Mahmoud Eljalby[3,4], Praveen Ramakrishnan[5], Larry D. Anderson Jr.[5,6], Farrukh T. Awan[5], Alvin Chandra[1,2,3], Srilakshmi Vallabhaneni[1,2,3], Kathleen Zhang[1,2,3] and Vlad G. Zaha[1,2,3]*

[1]Division of Cardiology, Department of Internal Medicine, UT Southwestern Medical Center, Dallas, TX, United States, [2]Cardio-Oncology Program, Harold C. Simmons Comprehensive Cancer Center, UT Southwestern Medical Center, Dallas, TX, United States, [3]Parkland Health and Hospital System, Dallas, TX, United States, [4]Department of Internal Medicine, UT Southwestern Medical Center, Dallas, TX, United States, [5]Division of Hematology and Oncology, Department of Internal Medicine, UT Southwestern Medical Center, Dallas, TX, United States, [6]Myeloma, Waldenstrom's, and Amyloidosis Program, Harold C. Simmons Comprehensive Cancer Center, UT Southwestern Medical Center, Dallas, TX, United States

Chimeric antigen receptor T-cell (CAR T) therapy is a revolutionary personalized therapy that has significantly impacted the treatment of patients with hematologic malignancies refractory to other therapies. Cytokine release syndrome (CRS) is a major side effect of CAR T therapy that can occur in 70–90% of patients, with roughly 40% of patients at grade 2 or higher. CRS can cause an intense inflammatory state leading to cardiovascular complications, including troponin elevation, arrhythmias, hemodynamic instability, and depressed left ventricular systolic function. There are currently no standardized guidelines for the management of cardiovascular complications due to CAR T therapy, but systematic practice patterns are emerging. In this review, we contextualize the history and indications of CAR T cell therapy, side effects related to this treatment, strategies to optimize the cardiovascular health prior to CAR T and the management of cardiovascular complications related to CRS. We analyze the existing data and discuss potential future approaches.

KEYWORDS

chimeric antigen receptor (CAR T), cardio-oncology, immunotherapy, cytokine release syndrome (CRS), cellular therapy, cardiovascular disease

Introduction

The power of the immune system in treating neoplastic diseases has long been recognized in the medical community. However, starting from adoptive cell transfer, the precursor of CAR T, various cardiovascular toxic side effects have also been identified. Herein we review the available data, and propose a strategy for prevention, surveillance and management of cardiovascular toxicity in patients receiving immune cellular therapies.

Adoptive cell transfer

Adoptively acquired immunity is the process through which active immune tissues are transferred from a donor to a recipient (1–3). Initial studies performed in the 1950's demonstrated in mouse that immune tissue (i.e., spleen or lymph nodes) but not antigens or peripheral cells from a primary transplant tolerant host induced sustained resistance to rejection in a secondary host (1). In a landmark paper published in 1957, E. Donnall Thomas and colleagues demonstrated a sustained response after bone marrow infusion in several patients with bone marrow deficiency following radiation and chemotherapy (3). This led to the first allogeneic bone marrow transplantations in the early 1960s, using bone marrow from twin siblings. With the subsequent development of autologous stem cell transplantation, adoptive cellular therapies have become a mainstay in the treatment of hematologic malignancies (4).

Modern development of cellular therapies

Following the historic success of bone marrow transplantation, the next phase of adoptive cell transfer came in the 1980s with the emergence of tumor-infiltrating lymphocytes (TIL) (5–8). In this therapy, B- and T-cells isolated from the tumor biopsy are expanded in a laboratory and subsequently infused back into the original host after a dose of chemotherapy (5, 6). TIL were combined with interleukin-2, a key cytokine in the proliferation and differentiation of effector T cells, to enhance their antitumor effects (5, 6).

With the advent of gene-transfer techniques, the potential of peripheral blood T cells was further harnessed through genetic modifications that increase their specificity and augment their function (9, 10). These "first-generation" genetically modified T cells were engineered to express a chimeric antigen receptor (CAR)—composed of an extracellular single-chain variable fragment (scFv) that serves as the targeting moiety, a transmembrane spacer, and intracellular signaling/activation domain(s)—to target surface-exposed tumor-associated antigens (10–12). Over time, CARs evolved to more complex "second-" and "third-generation" CARs that have augmented T cell persistence and proliferation (13–16).

Chimeric antigen receptor T-cell therapy mechanism and indications

The development of CAR T cell therapy triggered a paradigm shift in cancer immunotherapy, demonstrating remarkable success particularly in CD-19 expressing malignancies, as the first genetically engineered personalized therapy option. This therapeutic option has become a viable and commercially available treatment option for several hematologic malignancies (Table 1). Promising results emerged from the initial CAR T trials of tisagenlecleucel (tisa-cel) and axicabtagene ciloleucel (axi-cel) in 2017 (17). Tisa-cel was the first anti-CD-19 CAR T product approved by the Food and Drug Administration (FDA), for patients up to 25 years of age with relapsed or refractory B-cell precursor acute lymphoblastic leukemia (ALL) in 2017 (17). Axi-cel, an anti-CD-19 targeting CAR T-cell, approval followed soon after in 2017 for patients with relapsed or refractory diffuse large B-cell lymphoma (18). Axi-cel was subsequently also approved for the management of patients with relapsed or refractory follicular lymphoma after 2 prior lines of therapy (19). Since then, the FDA has approved 6 total CAR T therapies for the treatment of hematologic malignancies, including lisocabtagene maraleucel (liso-cel) for relapsed or refractory diffuse large B-cell lymphoma, brexucabtagene autoleucel (brexu-cel) for relapsed or refractory mantle cell lymphoma and relapsed or refractory ALL, and idecabtagene vicleucel (ide-cel) and ciltacabtagene autoleucel (cita-cel) for relapsed and refractory multiple myeloma (18, 20–23) (Table 1). Responses for all these agents average around 60 to 80% with complete remissions achieved in approximately 40 to 60% of the patients (17–19, 21, 22). These results are especially striking given the failure of conventional chemotherapy, including high-dose chemotherapy and stem cell transplantation in this population.

Chimeric antigen receptor T-cell therapy induction and administration

The administration of CAR T requires the identification of optimal patients who would generally be considered healthy and fit to undergo this procedure. While there is no established consensus on the optimal patient profile that would be considered suitable, various guidelines suggest

Abbreviations: ALL, acute lymphocytic leukemia; CAD, coronary artery disease; CAR T-cell, chimeric antigen receptor T-cell; CAR NK-cell, chimeric antigen receptor natural killer cell; CEA, carcinoembryonic antigen; CHF, congestive heart failure; CMR, cardiac magnetic resonance; CRS, cytokine release syndrome; CV, cardiovascular; CVD, cardiovascular disease; ECG, electrocardiogram; FAP, fibroblast activation protein; FDA, Food and Drug Administration; GD2, disialoganglioside 2; HER2, human epidermal growth factor receptor 2; HLH, hemophagocytic lymphohystiocytosis; ICANS, immune cell-associated neurotoxicity syndrome; IFN-γ, interferon-gamma; IL, interleukin; L1CAM, L1 cell adhesion molecule; MCP-1, monocyte chemoattractant protein-1; MI, myocardial infarction; MIP-1β, macrophage inflammatory protein-1 beta; REMS, risk evaluation and mitigation strategy; TIL, tumor-infiltrating lymphocytes; TNFα, tumor necrosis factor alpha; TTE, transthoracic echocardiogram.

TABLE 1 Summary of current FDA-approved CAR T generic names, trade names, and indications.

CAR product (generic name)	CAR product (trade name)	Indication(s)
Tisagenlecleucel	Kymriah	Acute lymphoblastic leukemia, B-cell lymphoma (17)
Axicabtagene ciloleucel	Yescarta	B-cell lymphoma, follicular lymphoma (18, 19)
Lisocabtagene maraleucel	Breyanzi	B-cell lymphoma (20)
Brexucabtagene autoleucel	Tecartus	Mantle cell lymphoma (21)
Idecabtagene vicleucel	Abecma	Multiple myeloma (22)
Ciltacabtagene autoleucel (cita-cel)	Carvykti	Multiple myeloma (23)

CAR, chimeric antigen receptor.

utilizing established fitness and morbidity scores to determine eligibility (24–26). After harvesting the peripheral blood product through a routine apheresis procedure, the cells typically require processing and manufacturing which can take up to 4–6 weeks. During this interval, patients frequently require "bridging therapy" to ensure that they do not have rapid and symptomatic disease progression. Following successful manufacturing and receipt of the product, patients undergo lymphodepleting chemotherapy typically with fludarabine and cyclophosphamide over 3 days for up to a week prior to reinfusion of the cells. Patients are subsequently monitored closely for the development of cytokine release syndrome (CRS) and neurotoxicity which can manifest for approximately the first month after reinfusion of cells (24, 25). Because of the risks noted with CRS, patients must enter a risk evaluation and mitigation strategy (REMS) program and stay within 2 h of the CAR T center for the first month and must not drive for 2 months following CAR T.

Immune cell-related adverse events

Robust systemic release of a high level of cytokines following overwhelming T cell activation as well as specific interactions between the CAR and its target antigen expressed by non-malignant cells are two mechanisms thought to mediate CAR T toxicities (27). One of the most common CAR T cell-related adverse events is CRS. CRS is a multisystem inflammatory response mediated by a surge of cytokines triggered by an infusion of CAR T cells. Among other toxic phenomena, CRS, in particular, affects 37–93% of patients with lymphoma (28), and 77–93% of patients with leukemia (28–31). Clinical manifestations can range from fevers and constitutional symptoms to hypoxia, hypotension, end-organ damage, and even sepsis-like syndrome or death in severe cases (29). CRS is thought to result from widespread simultaneous activation of T-cells and release of cytokines and chemokines (30, 32). CRS has been associated with elevation of interleukin (IL)-6, IL-8, IL-10, IL-15, GM-CSF, interferon (IFN)-g, MCP-1, MIP-1b, ferritin, CRP, and in severe cases soluble IL-2 receptor (28, 33). Management includes supportive care and antipyretics in mild cases, administration of IL-6-receptor antagonists like tocilizumab in moderate CRS or those not responding to supportive care, and corticosteroids like dexamethasone in more severe cases of CRS (34, 35). CRS can occasionally mimic macrophage activation syndrome (MAS) or hemophagocytic lymphohistiocytosis (HLH) in severe cases, which is often treated with anakinra, an IL-1 receptor antagonist, if the above measures are not effective (36–39). Serum inflammatory markers (acute phase reactants) including c-reactive protein (CRP) and ferritin may be followed clinically to help aid in prediction of impending CRS or to monitor response to therapy, though cytokine levels are not often readily available in real time (39).

CRS may contribute to the development of immune cell-associated neurotoxicity syndrome (ICANS), which can manifest along a spectrum from mild delirium with confusion to cerebral edema, seizures, and even death (34, 40). Cardiovascular manifestations of CRS Although the underlying mechanism of ICANS is incompletely understood compared to CRS, studies have also shown a correlation with elevated levels of inflammatory cytokines like IL-6, IFN-γ and TNFα (33, 41, 42). These signals are postulated to cause endothelial damage and activation with disruption of the blood brain barrier and capillary leak. It requires careful monitoring, frequent assessments, and promptly initiated therapy. ICANS has also been associated with sinus bradycardia that is often self-limited without need for intervention but should be monitored closely (43). Other constitutional, hematologic, renal, gastrointestinal, and dermatologic toxicities have also been observed (28, 41, 44–46).

Cardiovascular complications of cellular imunotherapies

While there has been a consistent trend of improvement in the survival following both autologous and allogeneic hematopoietic cell transplantation bone marrow transplant therapies decade over decade (47, 48), cardiovascular toxicities (49) continue to be frequent complications, along with infections and graft vs. host disease. This has resulted in evolving practice guidelines targeting preventive evaluations pretransplant, monitoring peri-transplant, and surveillance in long term survivors (50, 51). With regard to CAR T therapy, the current information about cardiovascular side

effects related to CAR T therapies is limited to a few retrospective studies (Table 2), but concepts established for other adoptive cell transfers likely apply. In particular, with the growing prevalence of cardiovascular disease combined with the increase in available CAR T cell therapies for the treatment of hematologic malignancies, attempting to understand the mechanisms of these complications is essential as this may help guide interventions.

The impact of CAR T cell therapy on the cardiovascular system manifests as hemodynamic compromise, myocardial injury/dysfunction, and/or cardiac arrhythmias (60, 61). There is also the potential for pericardial complications, such as in a case report (62) describing a patient with high-grade lymphoma who developed a pericardial effusion and tamponade with cardiogenic shock after CAR T therapy. Higher-grade CRS appears to be linked to adverse cardiovascular events of all types. This is likely driven by the release of inflammatory cytokines into the bloodstream with CAR T therapy, particularly the secretion of interleukin-6 (IL-6). This cytokine is a mediator of systemic inflammation, leading to hemodynamic compromise and even circulatory collapse in CRS. Of the studies published so far in patients treated with CAR T cell therapy, cardiovascular monitoring was performed in 3 pediatric studies and 5 adult studies (52–59). All studies in adult populations were retrospective, single-center observational cohort studies. Across all studies, cardiovascular complications have been inconsistently monitored. In children, transient and reversible hypotension in the setting of high-grade CRS was more commonly noted. In studies that monitored for cardiovascular complications in adults, the most frequently observed were cardiac arrhythmias and heart failure, albeit with relatively low event rates overall. Interestingly, preexisting cardiovascular disease (including heart failure) has not been shown to be reliably associated with the development of cardiovascular complications after CAR T cell therapy in one cohort study (57). In contrast, in another cohort study (55), troponin elevation was notably associated with cardiovascular adverse events in patients undergoing CAR T cell therapy. The patients with troponin elevation in this study were older and had more traditional cardiovascular risk factors. In both these cohort studies cardiovascular complications occurred with increased frequency at higher grades of CRS (2 or greater). As such, additional studies in larger cohorts are needed to establish risk factors, biomarker elevation patterns, imaging findings, event rates, and outcomes after CAR T cell therapy.

CRS monitoring and grading

Most patients undergoing CAR T can be managed on the regular cell therapy hospital floor with only a minority requiring ICU care, but close monitoring and specialty care is. due to rapid onset of CRS, it is recommended that this therapy is given at a specialized center with CAR T experience and credentialling.

Grading of CRS is now done per the American Society of Transplantation and Cellular Therapy (ASTCT) consensus guidelines (Table 3) (34).

CRS management

Rates of CRS and median time to onset vary depending on the particular CAR T product and disease burden. For example, in the KarMMa study of ide-cel for relapsed/refractory multiple myeloma (22), CRS was seen in 84% of patients, but most cases were only grade 1 or 2, with only 5% of patients developing grade 3–5. Median time to onset of CRS in the KarMMa study was 1 day (range 1–12 days) with a median duration of 5 days (range 1–63).

Management of CRS required tocilizumab in 52% patients, but only 15% required glucocorticoids (22, 63). On the other hand, in the Zuma-1 study of axi-cel for relapsed/refractory large B-cell lymphomas, CRS was a nearly universal side effect, with 93% of patients experiencing any grade CRS and 11% with grade 3 or higher, and hypotension was seen in 63%, tachycardia in 40%, and hypoxia in 34% (64). The median time to onset of CRS was 2 days (range 1–12) with a median duration of 8 days (65). All patients had resolution of their CRS, except for one patient who died from complications of HLH, and another patient who died of cardiac arrest with ongoing CRS. Tocilizumab was given in 43% and corticosteroids were required in 27% of Zuma-1 patients; however, more recently the FDA has issued a new label change for axi-cel allowing the prophylactic use of 3 days of corticosteroids based on a study showing much less severe CRS and ICANS without impairment of lymphoma response rates (66). The decision regarding inpatient vs. outpatient care and aggressive early therapy vs. minimal therapy for CRS is not only made based on the track record of the particular CAR T product but also based on risk factors such as age, frailty, and tumor burden, as higher tumor burden consistently correlates with increased incidence and severity of CRS (67).

Surveillance for cardiovascular toxicity

At our institution, cardiovascular (CV) surveillance for CAR-T therapy begins with CV risk stratification prior to infusion. Patients with CV comorbidities (especially heart failure, coronary artery disease, arrhythmias) or new/worsening CV symptoms (i.e., chest pain, dyspnea on exertion, lower extremity edema) represent a high CV risk group. Older age and prior cardiotoxic cancer therapy (i.e., anthracyclines, chest radiation) may also raise the risk of CV toxicity after treatment (68). In these high CV

TABLE 2 Summary of pediatric and adult studies investigated cardiovascular complications and CAR T-cell therapy.

References	No. of subjects	Oncologic diagnosis	CAR T* therapy	Preexisting cardiovascular disease–n (%)	Patients with CRS+ [%, (grade)]	Adverse cardiovascular events – n (%)
Fitzgerald et al. (52)[a]	39	Acute lymphoblastic leukemia	CD19-directed T-cells	Not captured	92% (any grade); 46% (3,4)	Vasoplegic shock—13 (36) Cardiomyopathy—1 (2)[c]
Burstein et al. (53)[a]	98	Leukemia/lymphoma	CD19-directed T-cells	Cardiomyopathy—10 (10) Structural disease—6 (6)	24% (≥2)	Shock—24 (24) Cardiac dysfunction—10 (10)[d]
Shalabi et al. (54)[a]	52	Leukemia/lymphoma	CD19-directed T-cells	Not captured	12% (any grade)	Cardiomyopathy—6 (11)[e] Sinus tachycardia—36 (69)
Alvi et al. (55)[b]	137	Lymphoma, multiple myeloma	axi-cel, tisa-cel	Coronary artery disease—10 (7) Heart failure—5 (4) Atrial fibrillation—18 (13)	59% (any grade); 39% (≥2)	Cardiovascular mortality—6 (4)[f] Heart failure—6 (4)[e] Arrhythmia—5 (4)[g]
Ganatra et al. (56)[b]	187	Leukemia/lymphoma	axi-cel, tisa-cel	Coronary artery disease—20 (11)	83% (any grade); 46% (≥2)	Cardiomyopathy—12 (6)[e] Arrhythmia—13 (7)
Lefebvre et al. (57)[b]	145	Leukemia/lymphoma	axi-cel, tisa-cel	Coronary artery disease—14 (10) Heart failure—12 (8) Atrial fibrillation—4 (3)	72% (any grade)	Heart failure—21 (15)[h] Atrial fibrillation—11 (7)
Brammer et al. (58)[b]	90	Lymphoma	Axi-cel, tisa-cel, brexu-cel	Coronary artery disease—7 (8) Heart failure—8 (9) Atrial fibrillation—10 (11)	49% (≥2)	Arrhythmia—11 (12)[i] Myocarditis—2 (2) Heart failure—1 (1)[h]
Steiner et al. (59)[b]	165	Lymphoma	axi-cel, tisa-cel	Coronary artery disease—15 (9) Heart failure—14 (8)	14% (≥3)	Arrhythmia—15 (9)[j] Heart failure—3 (2)[h] Myocardial infarction—3 (2)[k]

*CAR T, chimeric antigen receptor T-cell + CRS, cytokine release syndrome.

Study specific parameters: [a] Pediatric population; [b] Adult population; [c] Cardiomyopathy, defined as decreased left ventricular systolic function requiring milrinone; [d] Cardiac dysfunction, defined as either an echocardiographic decrease of ≥10% in ejection fraction or ≥5% in shortening fraction from normal baseline ejection fraction > 55% or shortening fraction > 28%; [e] Cardiac dysfunction, defined as either a >10% absolute decrease in LVEF compared with baseline or new-onset LV systolic dysfunction (LVEF <50%); [f] Cardiovascular mortality, defined as a combination of death due to heart failure, cardiogenic shock, cardiac arrest, or an arrhythmia; [g] Arrhythmia, defined as new-onset supraventricular tachycardia, atrial fibrillation, or atrial flutter requiring intervention; [h] Heart failure, defined as clinical signs of heart failure on physical examination, laboratory or imaging or radiographic findings of heart failure (B-type natriuretic peptide or N-terminal pro–B-type natriuretic peptide, Kerley B-lines or pulmonary edema, pleural effusion, decreased left ventricular ejection fraction, and initiation of new treatment for heart failure (pharmacological therapies such as diuretic agents and/or mechanical support); [i]Arrhythmia, defined as atrial fibrillation, ventricular tachycardia; [j] Arrhythmia, defined as non-sustained ventricular tachycardia, atrial fibrillation; [k] Myocardial infarction, defined as angina or anginal equivalent symptoms with cardiac enzyme elevation, with or without EKG/echocardiographic changes.

PubMed search performed using the following terms: Chimeric antigen receptor; cardiovascular; cytokine release syndrome.

10.3389/fcvm.2022.932347

TABLE 3 American Society of Blood and Marrow Transplantation (ASBMT) consensus grading of cytokine release syndrome (CRS) severity (34).

Cytokine release syndrome parameter	Grade 1	Grade 2	Grade 3	Grade 4
Fever	Temperature ≥38°C	Temperature ≥38°C	Temperature ≥38°C	Temperature ≥38°C
With				
Hypotension	None	Not requiring vasopressors	Requiring one vasopressor with or without vasopressin	Requiring multiple vasopressors (excluding vasopressin)
And/or*				
Hypoxia	None	Requiring low-flow nasal cannula or blow-by	Requiring high-flow nasal cannula, facemask, nonrebreather mask, or Venturi mask	Requiring positive pressure (e.g., CPAP, BiPAP, intubation, and mechanical ventilation)

CPAP, Continuous Positive Airway Pressure; BiPAP, Bilevel Positive Airway Pressure.
*CRS grade is determined by the more severe event: hypotension or hypoxia not attributable to any other cause.
Fever is defined as temperature≥38°C not attributable to any other cause. In patients who have CRS then receive antipyretic or anti-cytokine therapy such as tocilizumab or steroids, fever is no longer required to grade subsequent CRS severity.
Low-flow nasal cannula is defined as oxygen delivered at ≤6 L/min. Lowflow also includes blow-by oxygen delivery, sometimes used in pediatrics. High-flow nasal cannula is defined as oxygen delivered at>6 L/min.

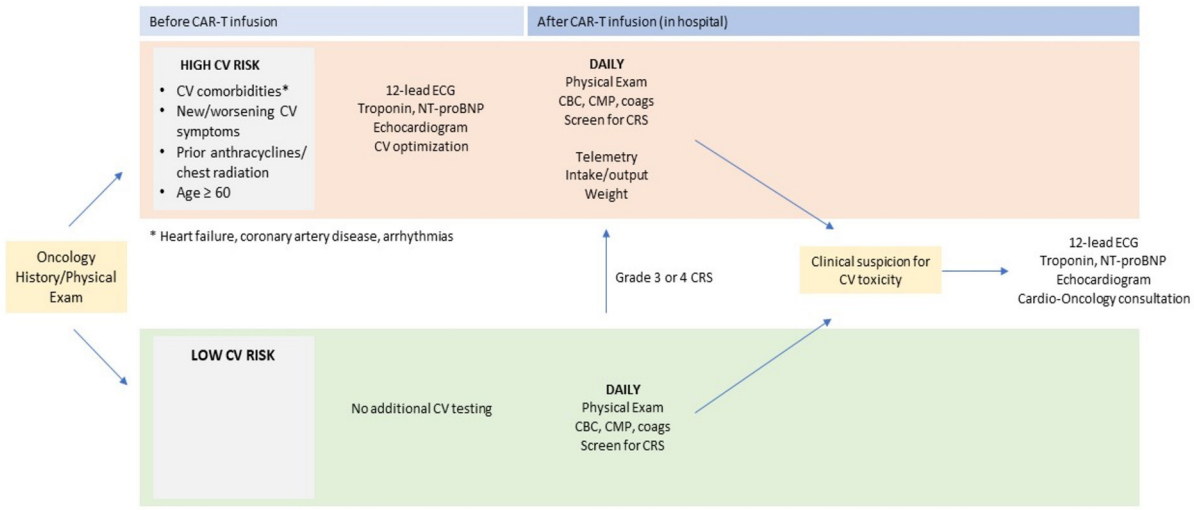

FIGURE 1
Proposed pre- and post-CAR T cardiac screening. CAR, chimeric antigen receptor; ECG, electrocardiography; NT-proBNP, N-terminal pro–B-type natriuretic peptide. *arrhythmias, coronary artery disease, heart failure.

risk patients, standard baseline testing should include a 12-lead electrocardiogram, cardiac biomarkers (troponin, NT-proBNP), and transthoracic echocardiography. In some cases, cardiac MRI may clarify features of cardiac structure and/or function that would guide optimization of CV therapy. Cardioprotective therapies such as beta-blockers and renin-angiotensin-aldosterone system blockers, diuretics, and/or antiarrhythmics should be utilized as clinically indicated. In addition, any patient with the above cardiovascular comorbidities, and whose baseline electrocardiogram or transthoracic echocardiogram is abnormal, should be considered for cardio-oncology referral pre-CAR T therapy.

Inpatient monitoring after CAR-T infusion is strongly recommended for patients with increased baseline CV risk. Figure 1 shows our institutional algorithm for surveillance and monitoring in this population. Standard monitoring protocols after CAR-T infusion include daily blood counts and metabolic profiling, physical examination, and screening for CRS (69). Patients at high baseline CV risk should additionally be monitored on telemetry with close monitoring of oral and intravenous fluid input, urine output, and daily

body weight measurement. Given the observed association between CRS and CV events after CAR-T (55, 57), all patients with grade 3 or 4 CRS should also be placed on these CV monitoring protocols.

The utility of routine cardiac biomarker testing for detection of CV toxicity after CAR-T is uncertain. Where there is clinical suspicion for a CV event after CAR-T infusion based on symptoms or monitoring, initial evaluation should include cardiac biomarkers (troponin, NT-proBNP), 12-lead electrocardiogram (ECG), and transthoracic echocardiography (TTE). Cardio-oncology consultation should be obtained, if available, to direct further diagnostic evaluation and management.

Data are limited regarding the optimal surveillance and testing protocol for patients undergoing CAR T cell therapy. Current standards of practice have been previously published by Hayden et al. (26), Ghosh et al. (60), and Totzeck et al. (70), with similar approaches to our institution and each other with regard to screening and surveillance while on CAR T therapy. Ghosh et al. propose that all patients undergo baseline cardiac magnetic resonance imaging (CMR) with follow-up CMR in patients with abnormal biomarkers, ECG, and/or TTE. We generally agree with these publications on the initial evaluation of patients after a cardiovascular event with CAR-T infusion, including cardiac blood biomarkers (troponin, NT-proBNP), ECG, and TTE, with judicious use of CMR in appropriate cases. By contrast, there is some variability in the post-CAR T surveillance and monitoring approaches proposed by the other consensus approaches. For example, Ghosh et al. recommend for all patients to follow-up with cardio-oncology 3 months after CAR T cell therapy, whereas the other two consensus recommendations propose a 7-day follow-up visit. We propose a patient-specific approach depending on the type of cardiovascular event that patient experienced. The utility of monitoring for late effects (i.e., at 3 months post CAR-T and beyond) and the potential for long-term CV consequences of CAR-T itself stand out as areas for future study.

Future directions

Current targets of CAR T are malignant immune cells, but new targets continue to develop. There has been an expanding focus on targeting solid tumors, and overall, nearly 600 clinical trials are underway (71–73). Multiple new endeavors are focusing on solid tumor surface antigens such as carcinoembryonic antigen (CEA), ganglioside GD2 subtype, mesothelin, interleukin-13 receptor α (IL-13Rα), human epidermal growth factor receptor 2 (HER2), fibroblast activation protein (FAP), and L1 cell adhesion molecule (L1CAM) (16, 74–79).

Multiple trials are currently ongoing evaluating various CAR T products in different disease entities including allogeneic products utilizing various T-cell and NK-cell engineering and manufacturing procedures. Moreover, the well-documented side effects of CAR T–most notably, CRS–have spurred the recent discussion surrounding CAR NK-cell therapy, a potential avenue to mitigatehe systemic immune effects (73). CAR T has been shown to effectively target and remove activated cardiac fibroblasts in mice, suggesting potential applications to address myocardial scar and fibrosis (80, 81). At the same time, early signals have raised concerns about the unique dangers of systemic immune effects in patients with preceding cardiovascular diseases or cardiovascular risks, with limited information about cardiotoxicity available from the initial CAR T trials. Clinical practice guidelines are emerging to address immune cell-related adverse events (82). Next steps also include validated risk prediction tools for cardiovascular complications after CAR-T, elucidate mechanisms of these immune-mediated complications, development of preventative therapies by integrating timelines of cardiac blood biomarkers and immunophenotyping in this population.

Conclusions

The rapid development of immunocellular personalized therapeutic modalities is creating unprecedented opportunities for treatment of cancers. To optimize the cardiovascular outcomes in patients treated with CAR T several lessons learned from other anticancer therapies and from early CAR T studies may be beneficial. While early studies have established the specific indications for these therapies, cardiovascular risk profiles will need to be defined further during their real-life application. The awareness of interactions between the cardiovascular risks, underlying cardiovascular problems and the cytokine release syndrome is prompting the definition of systematic assessments before and during CAR T therapy. Yet unknown potential latent effects, such as vascular inflammation seen after other immunotherapeutic interventions (i.e., immune checkpoint inhibitor therapies) will need to be taken in consideration for long-term cardiovascular surveillance. Inclusion of cardiovascular endpoints in trials, as well as broad collaborative, prospective clinical registries have the potential to provide new information about these risks. And not the least, the further investigation of such observations in targeted research studies has the potential to refine this technology and expand its safe applicability.

Author contributions

AR and VZ organized the outline and the components of the manuscript, as well. AR, AS, and ME performed an extensive literature search of cardiovascular disease and chimeric antigen receptor T cell therapy. PR, LA, and FA

wrote individual sections on CAR T therapy and provided feedback on the manuscript. AC, SV, and KZ created the figure and wrote the section on surveillance and monitoring. All authors contributed to the writing efforts and the editing of this manuscript.

Funding

VZ received support from the Cancer Prevention Research Institute of Texas (RP180404).

Conflict of interest

Author FA has provided consultancy to: Genentech, Astrazeneca, Abbvie, Janssen, Pharmacyclics, Gilead sciences, Kite pharma, Celgene, Karyopharm, MEI Pharma, Verastem, Incyte, Beigene, Johnson and Johnson, Dava Oncology, BMS, Merck, Cardinal Health, ADCT therapeutics, and Epizyme.

The remaining authors declare that the research was conducted in the absence of any commercial or financial relationships that could be construed as a potential conflict of interest.

Publisher's note

References

1. Billingham RE, Brent L, Medawar PB. Quantitative studies on tissue transplantation immunity. II. The origin, strength and duration of actively and adoptively acquired immunity. *Proc R Soc Lond B Biol Sci.* (1954) 143:58–80. doi: 10.1098/rspb.1954.0054

2. Lorenz E, Uphoff D, Reid TR, Shelton E. Modification of irradiation injury in mice and guinea pigs by bone marrow injections. *J Natl Cancer Inst.* (1951) 12:197–201.

3. Thomas ED, Lochte HL Jr, Lu WC, Ferrebee JW. Intravenous infusion of bone marrow in patients receiving radiation and chemotherapy. *N Engl J Med.* (1957) 257:491–6. doi: 10.1056/NEJM195709122571102

4. Thomas ED. A history of haemopoietic cell transplantation. *Br J Haematol.* (1999) 105:330–9. doi: 10.1111/j.1365-2141.1999.01337.x

5. Rosenberg SA, Lotze MT, Muul LM, Leitman S, Chang AE, Ettinghausen SE, et al. Observations on the systemic administration of autologous lymphokine-activated killer cells and recombinant interleukin-2 to patients with metastatic cancer. *N Engl J Med.* (1985) 313:1485–92. doi: 10.1056/NEJM198512053132327

6. Rosenberg SA, Spiess P, Lafreniere R. A new approach to the adoptive immunotherapy of cancer with tumor-infiltrating lymphocytes. *Science.* (1986) 233:1318–21. doi: 10.1126/science.3489291

7. Rosenberg SA, Packard BS, Aebersold PM, Solomon D, Topalian SL, Toy ST, et al. Use of tumor-infiltrating lymphocytes and interleukin-2 in the immunotherapy of patients with metastatic melanoma. A preliminary report. *N Engl J Med.* (1988) 319:1676–80. doi: 10.1056/NEJM198812223192527

8. Zhang Y, Zhang Z. The history and advances in cancer immunotherapy: understanding the characteristics of tumor-infiltrating immune cells and their therapeutic implications. *Cell Mol Immunol.* (2020) 17:807–21. doi: 10.1038/s41423-020-0488-6

9. Kershaw MH, Westwood JA, Parker LL, Wang G, Eshhar Z, Mavroukakis SA, et al. A phase I study on adoptive immunotherapy using gene-modified T cells for ovarian cancer. *Clin Cancer Res.* (2006) 12(20 Pt 1):6106–15. doi: 10.1158/1078-0432.CCR-06-1183

10. Brentjens RJ, Riviere I, Park JH, Davila ML, Wang X, Stefanski J, et al. Safety and persistence of adoptively transferred autologous CD19-targeted T cells in patients with relapsed or chemotherapy refractory B-cell leukemias. *Blood.* (2011) 118:4817–28. doi: 10.1182/blood-2011-04-348540

11. Porter DL, Levine BL, Kalos M, Bagg A, June CH. Chimeric antigen receptor-modified T cells in chronic lymphoid leukemia. *N Engl J Med.* (2011) 365:725–33. doi: 10.1056/NEJMoa1103849

12. Kochenderfer JN, Dudley ME, Feldman SA, Wilson WH, Spaner DE, Maric I, et al. B-cell depletion and remissions of malignancy along with cytokine-associated toxicity in a clinical trial of anti-CD19 chimeric-antigen-receptor-transduced T cells. *Blood.* (2012) 119:2709–20. doi: 10.1182/blood-2011-10-384388

13. Ritchie DS, Neeson PJ, Khot A, Peinert S, Tai T, Tainton K, et al. Persistence and efficacy of second generation CAR T cell against the LeY antigen in acute myeloid leukemia. *Mol Ther.* (2013) 21:2122–9. doi: 10.1038/mt.2013.154

14. Lee DW, Kochenderfer JN, Stetler-Stevenson M, Cui YK, Delbrook C, Feldman SA, et al. T cells expressing CD19 chimeric antigen receptors for acute lymphoblastic leukaemia in children and young adults: a phase 1 dose-escalation trial. *Lancet.* (2015) 385:517–28. doi: 10.1016/S0140-6736(14)61403-3

15. Caruana I, Savoldo B, Hoyos V, Weber G, Liu H, Kim ES, et al. Heparanase promotes tumor infiltration and antitumor activity of CAR-redirected T lymphocytes. *Nat Med.* (2015) 21:524–9. doi: 10.1038/nm.3833

16. Wang LC, Lo A, Scholler J, Sun J, Majumdar RS, Kapoor V, et al. Targeting fibroblast activation protein in tumor stroma with chimeric antigen receptor T cells can inhibit tumor growth and augment host immunity without severe toxicity. *Cancer Immunol Res.* (2014) 2:154–66. doi: 10.1158/2326-6066.CIR-13-0027

17. Maude SL, Laetsch TW, Buechner J, Rives S, Boyer M, Bittencourt H, et al. Tisagenlecleucel in children and young adults with b-cell lymphoblastic leukemia. *N Engl J Med.* (2018) 378:439–48. doi: 10.1056/NEJMoa1709866

18. Neelapu SS, Locke FL, Bartlett NL, Lekakis LJ, Miklos DB, Jacobson CA, et al. Axicabtagene ciloleucel CAR T-cell therapy in refractory large B-Cell lymphoma. *N Engl J Med.* (2017) 377:2531–44. doi: 10.1056/NEJMoa1707447

19. Jacobson CA, Chavez JC, Sehgal AR, William BM, Munoz J, Salles G, et al. Axicabtagene ciloleucel in relapsed or refractory indolent non-Hodgkin lymphoma (ZUMA-5): a single-arm, multicentre, phase 2 trial. *Lancet Oncol.* (2022) 23:91–103. doi: 10.1016/S1470-2045(21)00591-X

20. Abramson JS, Palomba ML, Gordon LI, Lunning MA, Wang M, Arnason J, et al. Lisocabtagene maraleucel for patients with relapsed or refractory large B-cell lymphomas (TRANSCEND NHL 001): a multicentre seamless design study. *Lancet.* (2020) 396:839–52. doi: 10.1016/S0140-6736(20)31366-0

21. Wang M, Munoz J, Goy A, Locke FL, Jacobson CA, Hill BT, et al. KTE-X19 CAR T-cell therapy in relapsed or refractory mantle-cell lymphoma. *N Engl J Med.* (2020) 382:1331–42. doi: 10.1056/NEJMoa1914347

22. Munshi NC, Anderson LD Jr, Shah N, Madduri D, Berdeja J, et al. Idecabtagene vicleucel in relapsed and refractory multiple myeloma. *N Engl J Med.* (2021) 384:705–16. doi: 10.1056/NEJMoa2024850

23. Berdeja JG, Madduri D, Usmani SZ, Jakubowiak A, Agha M, Cohen AD, et al. Ciltacabtagene autoleucel, a B-cell maturation antigen-directed chimeric antigen receptor T-cell therapy in patients with relapsed or refractory multiple myeloma (CARTITUDE-1): a phase 1b/2 open-label study. *Lancet.* (2021) 398:314–24. doi: 10.1016/S0140-6736(21)00933-8

24. Yakoub-Agha I, Chabannon C, Bader P, Basak GW, Bonig H, Ciceri F, et al. Management of adults and children undergoing chimeric antigen receptor T-cell therapy: best practice recommendations of the european society for blood and marrow transplantation (EBMT) and the joint accreditation committee of ISCT and EBMT (JACIE). *Haematologica.* (2020) 105:297–316. doi: 10.3324/haematol.2019.229781

25. Hayden PJ, Sirait T, Koster L, Snowden JA, Yakoub-Agha I. An international survey on the management of patients receiving CAR T-cell therapy for haematological malignancies on behalf of the chronic malignancies working party of EBMT. *Curr Res Transl Med.* (2019) 67:79–88. doi: 10.1016/j.retram.2019.05.002

26. Hayden PJ, Roddie C, Bader P, Basak GW, Bonig H, Bonini C, et al. Management of adults and children receiving CAR T-cell therapy: 2021 best practice recommendations of the european society for blood and marrow transplantation (EBMT) and the joint accreditation committee of ISCT and EBMT (JACIE) and the European Haematology Association (EHA). *Ann Oncol.* (2022) 33:259–75. doi: 10.1016/j.annonc.2021.12.003

27. Rafiq S, Hackett CS, Brentjens RJ. Engineering strategies to overcome the current roadblocks in CAR T cell therapy. *Nat Rev Clin Oncol.* (2020) 17:147–67. doi: 10.1038/s41571-019-0297-y

28. Maude SL, Barrett D, Teachey DT, Grupp SA. Managing cytokine release syndrome associated with novel T cell-engaging therapies. *Cancer J.* (2014) 20:119–22. doi: 10.1097/PPO.0000000000000035

29. Frey N, Porter D. Cytokine release syndrome with chimeric antigen receptor T cell therapy. *Biol Blood Marrow Transplant.* (2019) 25:e123–e7. doi: 10.1016/j.bbmt.2018.12.756

30. Bonifant CL, Jackson HJ, Brentjens RJ, Curran KJ. Toxicity and management in CAR T-cell therapy. *Mol Ther Oncolytics.* (2016) 3:16011. doi: 10.1038/mto.2016.11

31. Lee DW, Gardner R, Porter DL, Louis CU, Ahmed N, Jensen M, et al. Current concepts in the diagnosis and management of cytokine release syndrome. *Blood.* (2014) 124:188–95. doi: 10.1182/blood-2014-05-552729

32. Dai H, Wang Y, Lu X, Han W. Chimeric antigen receptors modified T-cells for cancer therapy. *J Natl Cancer Inst.* (2016) 108:djv439. doi: 10.1093/jnci/djv439

33. Hay KA, Hanafi LA, Li D, Gust J, Liles WC, Wurfel MM, et al. Kinetics and biomarkers of severe cytokine release syndrome after CD19 chimeric antigen receptor-modified T-cell therapy. *Blood.* (2017) 130:2295–306. doi: 10.1182/blood-2017-06-793141

34. Lee DW, Santomasso BD, Locke FL, Ghobadi A, Turtle CJ, Brudno JN, et al. ASTCT consensus grading for cytokine release syndrome and neurologic toxicity associated with immune effector cells. *Biol Blood Marrow Transplant.* (2019) 25:625–38. doi: 10.1016/j.bbmt.2018.12.758

35. Thompson JA, Schneider BJ, Brahmer J, Andrews S, Armand P, Bhatia S, et al. Management of Immunotherapy-Related Toxicities, Version 1.2019. *J Natl Compr Canc Netw.* (2019) 17:255–89. doi: 10.6004/jnccn.2019.0013

36. Giavridis T, van der Stegen SJC, Eyquem J, Hamieh M, Piersigilli A, Sadelain M. CAR T cell-induced cytokine release syndrome is mediated by macrophages and abated by IL-1 blockade. *Nat Med.* (2018) 24:731–8. doi: 10.1038/s41591-018-0041-7

37. Norelli M, Camisa B, Barbiera G, Falcone L, Purevdorj A, Genua M, et al. Monocyte-derived IL-1 and IL-6 are differentially required for cytokine-release syndrome and neurotoxicity due to CAR T cells. *Nat Med.* (2018) 24:739–48. doi: 10.1038/s41591-018-0036-4

38. Reagan PM, Neelapu SS. How I manage: pathophysiology and management of toxicity of chimeric antigen receptor T-cell therapies. *J Clin Oncol.* (2021) 39:456–66. doi: 10.1200/JCO.20.01616

39. Greenbaum U, Strati P, Saliba RM, Torres J, Rondon G, Nieto Y, et al. CRP and ferritin in addition to the EASIX score predict CAR-T-related toxicity. *Blood Adv.* (2021) 5:2799–806. doi: 10.1182/bloodadvances.2021004575

40. Sheth VS, Gauthier J. Taming the beast: CRS and ICANS after CAR T-cell therapy for ALL. *Bone Marrow Transplant.* (2021) 56:552–66. doi: 10.1038/s41409-020-01134-4

41. Brudno JN, Kochenderfer JN. Recent advances in CAR T-cell toxicity: mechanisms, manifestations and management. *Blood Rev.* (2019) 34:45–55. doi: 10.1016/j.blre.2018.11.002

42. Hunter BD, Jacobson CA. CAR T-cell associated neurotoxicity: mechanisms, clinicopathologic correlates, and future directions. *J Natl Cancer Inst.* (2019) 111:646–54. doi: 10.1093/jnci/djz017

43. Catala E, Iacoboni G, Vidal-Jordana A, Oristrell G, Carpio C, Vilaseca A, et al. Neurotoxicity-associated sinus bradycardia after chimeric antigen receptor T-cell therapy. *Hematol Oncol.* (2022) 40:482–7. doi: 10.1002/hon.2976

44. Fischer JW, Bhattarai N. CAR-T cell therapy: mechanism, management, and mitigation of inflammatory toxicities. *Front Immunol.* (2021) 12:693016. doi: 10.3389/fimmu.2021.693016

45. Penack O, Koenecke C. Complications after CD19+ CAR T-Cell therapy. *Cancers (Basel).* (2020) 12:12113445. doi: 10.3390/cancers12113445

46. Rubin DB, Vaitkevicius H. Neurological complications of cancer immunotherapy (CAR T cells). *J Neurol Sci.* (2021) 424:117405. doi: 10.1016/j.jns.2021.117405

47. Bhatia S, Dai C, Landier W, Hageman L, Wu J, Schlichting E, et al. Trends in late mortality and life expectancy after allogeneic blood or marrow transplantation over 4 decades: a blood or marrow transplant survivor study report. *JAMA Oncol.* (2021) 7:1626–34. doi: 10.1001/jamaoncol.2021.3676

48. Bhatia S, Dai C, Landier W, Hageman L, Wu J, Schlichting E, et al. Trends in late mortality and life expectancy after autologous blood or marrow transplantation over three decades: a BMTSS report. *J Clin Oncol.* (2022) 2022:JCO2102372. doi: 10.1200/JCO.21.02372

49. Herrmann J, Lenihan D, Armenian S, Barac A, Blaes A, Cardinale D, et al. Defining cardiovascular toxicities of cancer therapies: an International Cardio-Oncology Society (IC-OS) consensus statement. *Eur Heart J.* (2022) 43:280–99. doi: 10.1093/eurheartj/ehab674

50. Saad A, de Lima M, Anand S, Bhatt VR, Bookout R, Chen G, et al. Hematopoietic cell transplantation, version 2.2020, NCCN clinical practice guidelines in oncology. *J Natl Compr Canc Netw.* (2020) 18:599–634. doi: 10.6004/jnccn.2020.0021

51. Tevaarwerk A, Denlinger CS, Sanft T, Ansbaugh SM, Armenian S, Baker KS, et al. Survivorship, version 1.2021. *J Natl Compr Canc Netw.* (2021) 19:676–85. doi: 10.6004/jnccn.2021.0028

52. Fitzgerald JC, Weiss SL, Maude SL, Barrett DM, Lacey SF, Melenhorst JJ, et al. Cytokine release syndrome after chimeric antigen receptor T Cell therapy for acute lymphoblastic leukemia. *Crit Care Med.* (2017) 45:e124–e31. doi: 10.1097/CCM.0000000000002053

53. Burstein DS, Maude S, Grupp S, Griffis H, Rossano J, Lin K. Cardiac profile of chimeric antigen receptor T cell therapy in children: a single-institution experience. *Biol Blood Marrow Transplant.* (2018) 24:1590–5. doi: 10.1016/j.bbmt.2018.05.014

54. Shalabi H, Sachdev V, Kulshreshtha A, Cohen JW, Yates B, Rosing DR, et al. Impact of cytokine release syndrome on cardiac function following CD19 CAR-T cell therapy in children and young adults with hematological malignancies. *J Immunother Cancer.* (2020) 8:1159. doi: 10.1136/jitc-2020-001159

55. Alvi RM, Frigault MJ, Fradley MG, Jain MD, Mahmood SS, Awadalla M, et al. Cardiovascular events among adults treated with chimeric antigen receptor T-cells (CAR-T). *J Am Coll Cardiol.* (2019) 74:3099–108. doi: 10.1016/j.jacc.2019.10.038

56. Ganatra S, Redd R, Hayek SS, Parikh R, Azam T, Yanik GA, et al. Chimeric antigen receptor T-cell therapy-associated cardiomyopathy in patients with refractory or relapsed non-hodgkin lymphoma. *Circulation.* (2020) 142:1687–90. doi: 10.1161/CIRCULATIONAHA.120.048100

57. Lefebvre B, Kang Y, Smith AM, Frey NV, Carver JR, Scherrer-Crosbie M. Cardiovascular effects of CAR T cell therapy: a retrospective study. *JACC CardioOncol.* (2020) 2:193–203. doi: 10.1016/j.jaccao.2020.04.012

58. Brammer JE, Braunstein Z, Katapadi A, Porter K, Biersmith M, Guha A, et al. Early toxicity and clinical outcomes after chimeric antigen receptor T-cell (CAR-T) therapy for lymphoma. *J Immunother Cancer.* (2021) 9:2303. doi: 10.1136/jitc-2020-002303

59. Steiner RE, Banchs J, Koutroumpakis E, Becnel M, Gutierrez C, Strati P, et al. Cardiovascular events in patients treated with chimeric antigen receptor t-cell therapy for aggressive B-cell lymphoma. *Haematologica.* (2021) 107:1555–66. doi: 10.3324/haematol.2021.280009

60. Ghosh AK, Chen DH, Guha A, Mackenzie S, Walker JM, Roddie C. CAR T cell therapy-related cardiovascular outcomes and management: systemic disease or direct cardiotoxicity? *JACC CardioOncol.* (2020) 2:97–109. doi: 10.1016/j.jaccao.2020.02.011

61. Jamal FA, Khaled SK. The cardiovascular complications of chimeric antigen receptor T cell therapy. *Curr Hematol Malig Rep.* (2020) 15:130–2. doi: 10.1007/s11899-020-00567-4

62. Moriyama S, Fukata M, Yokoyama T, Ueno S, Nunomura T, Mori Y, et al. Case report: cardiac tamponade in association with cytokine release syndrome following CAR-T cell therapy. *Front Cardiovasc Med.* (2022) 9:848091. doi: 10.3389/fcvm.2022.848091

63. Anderson LD Jr. Idecabtagene vicleucel (ide-cel) CAR T-cell therapy for relapsed and refractory multiple myeloma. *Future Oncol.* (2022) 18:277–89. doi: 10.2217/fon-2021-1090

64. Locke FL, Ghobadi A, Jacobson CA, Miklos DB, Lekakis LJ, Oluwole OO, et al. Long-term safety and activity of axicabtagene ciloleucel in refractory large B-cell lymphoma (ZUMA-1): a single-arm, multicentre, phase 1-2 trial. *Lancet Oncol.* (2019) 20:31–42. doi: 10.1016/S1470-2045(18)30864-7

65. Riedell PA, Bishop MR. Safety and efficacy of axicabtagene ciloleucel in refractory large B-cell lymphomas. *Ther Adv Hematol.* (2020) 11:2040620720902899. doi: 10.1177/2040620720902899

66. Oluwole OO, Bouabdallah K, Munoz J, De Guibert S, Vose JM, Bartlett NL, et al. Prophylactic corticosteroid use in patients receiving axicabtagene ciloleucel for large B-cell lymphoma. *Br J Haematol.* (2021) 194:690–700. doi: 10.1111/bjh.17527

67. Yan Z, Zhang H, Cao J, Zhang C, Liu H, Huang H, et al. Characteristics and risk factors of cytokine release syndrome in chimeric antigen receptor T cell treatment. *Front Immunol.* (2021) 12:611366. doi: 10.3389/fimmu.2021.611366

68. Armenian SH, Lacchetti C, Barac A, Carver J, Constine LS, Denduluri N, et al. Prevention and monitoring of cardiac dysfunction in survivors of adult cancers: American Society of Clinical Oncology clinical practice guideline. *J Clin Oncol.* (2017) 35:893–911. doi: 10.1200/JCO.2016.70.5400

69. Yanez L, Sanchez-Escamilla M, Perales MA. CAR T cell toxicity: current management and future directions. *Hemasphere.* (2019) 3:e186. doi: 10.1097/HS9.0000000000000186

70. Totzeck M, Michel L, Lin Y, Herrmann J, Rassaf T. Cardiotoxicity from chimeric antigen receptor-T cell therapy for advanced malignancies. *Eur Heart J.* (2022) 43:1928–40. doi: 10.1093/eurheartj/ehac106

71. Albinger N, Hartmann J, Ullrich E. Current status and perspective of CAR-T and CAR-NK cell therapy trials in Germany. *Gene Ther.* (2021) 28:513–27. doi: 10.1038/s41434-021-00246-w

72. Marofi F, Al-Awad AS, Sulaiman Rahman H, Markov A, Abdelbasset WK, Ivanovna Enina Y, et al. CAR-NK cell: a new paradigm in tumor immunotherapy. *Front Oncol.* (2021) 11:673276. doi: 10.3389/fonc.2021.673276

73. Liu E, Marin D, Banerjee P, Macapinlac HA, Thompson P, Basar R, et al. Use of CAR-transduced natural killer cells in CD19-positive lymphoid tumors. *N Engl J Med.* (2020) 382:545–53. doi: 10.1056/NEJMoa1910607

74. Cha SE, Kujawski M, P JY, Brown C, Shively JE. Tumor regression and immunity in combination therapy with anti-CEA chimeric antigen receptor T cells and anti-CEA-IL2 immunocytokine. *Oncoimmunology.* (2021) 10:1899469. doi: 10.1080/2162402X.2021.1899469

75. Yu AL, Gilman AL, Ozkaynak MF, London WB, Kreissman SG, Chen HX, et al. Anti-GD2 antibody with GM-CSF, interleukin-2, and isotretinoin for neuroblastoma. *N Engl J Med.* (2010) 363:1324–34. doi: 10.1056/NEJMoa0911123

76. Brown CE, Badie B, Barish ME, Weng L, Ostberg JR, Chang WC, et al. Bioactivity and safety of IL13Ralpha2-redirected chimeric antigen receptor $CD8^+$ T cells in patients with recurrent glioblastoma. *Clin Cancer Res.* (2015) 21:4062–72. doi: 10.1158/1078-0432.CCR-15-0428

77. Le Q, Castro S, Tang T, Loeb AM, Hylkema T, McKay CN, et al. Therapeutic targeting of mesothelin with chimeric antigen receptor T cells in acute myeloid leukemia. *Clin Cancer Res.* (2021) 27:5718–30. doi: 10.1158/1078-0432.CCR-21-1546

78. Ahmed N, Brawley VS, Hegde M, Robertson C, Ghazi A, Gerken C, et al. Human epidermal growth factor receptor 2 (HER2) -specific chimeric antigen receptor-modified T cells for the immunotherapy of HER2-positive sarcoma. *J Clin Oncol.* (2015) 33:1688–96. doi: 10.1200/JCO.2014.58.0225

79. Hong H, Brown CE, Ostberg JR, Priceman SJ, Chang WC, Weng L, et al. L1 cell adhesion molecule-specific chimeric antigen receptor-redirected human T cells exhibit specific and efficient antitumor activity against human ovarian cancer in mice. *PLoS ONE.* (2016) 11:e0146885. doi: 10.1371/journal.pone.0146885

80. Aghajanian H, Kimura T, Rurik JG, Hancock AS, Leibowitz MS, Li L, et al. Targeting cardiac fibrosis with engineered T cells. *Nature.* (2019) 573:430–3. doi: 10.1038/s41586-019-1546-z

81. Rurik JG, Tombacz I, Yadegari A, Mendez Fernandez PO, Shewale SV, Li L, et al. CAR T cells produced *in vivo* to treat cardiac injury. *Science.* (2022) 375:91–6. doi: 10.1126/science.abm0594

82. Maus MV, Alexander S, Bishop MR, Brudno JN, Callahan C, Davila ML, et al. Society for immunotherapy of cancer (SITC) clinical practice guideline on immune effector cell-related adverse events. *J Immunother Cancer.* (2020) 8:1511. doi: 10.1136/jitc-2020-001511

frontiers | Frontiers in Cardiovascular Medicine

TYPE Original Research
PUBLISHED 19 October 2022
DOI 10.3389/fcvm.2022.901431

OPEN ACCESS

EDITED BY
Dong Han,
People's Liberation Army General Hospital, China

REVIEWED BY
Dinu Valentin Balanescu,
Beaumont Hospital, United States
Tatsuhiko Otsuka,
Itabashi Chuo Medical Center, Japan

*CORRESPONDENCE
Cezar A. Iliescu
ciliescu@mdanderson.org

†These authors have contributed equally to this work

SPECIALTY SECTION
This article was submitted to Cardio-Oncology, a section of the journal Frontiers in Cardiovascular Medicine

RECEIVED 21 March 2022
ACCEPTED 13 September 2022
PUBLISHED 19 October 2022

CITATION
Ahmed T, Pacha HM, Addoumieh A, Koutroumpakis E, Song J, Charitakis K, Boudoulas KD, Cilingiroglu M, Marmagkiolis K, Grines C and Iliescu CA (2022) Percutaneous coronary intervention in patients with cancer using bare metal stents compared to drug-eluting stents. *Front. Cardiovasc. Med.* 9:901431. doi: 10.3389/fcvm.2022.901431

Percutaneous coronary intervention in patients with cancer using bare metal stents compared to drug-eluting stents

Talha Ahmed[1,2†], Homam Moussa Pacha[1,2†], Antoine Addoumieh[1,2], Efstratios Koutroumpakis[2], Juhee Song[3], Konstantinos Charitakis[1], Konstantinos Dean Boudoulas[4], Mehmet Cilingiroglu[2], Konstantinos Marmagkiolis[2,5], Cindy Grines[6] and Cezar A. Iliescu[2*]

[1]Division of Cardiovascular Medicine, University of Texas Health Science Center at Houston, Houston, TX, United States, [2]Division of Cardiovascular Medicine, MD Anderson Cancer Center, University of Texas, Houston, TX, United States, [3]Department of Biostatistics, MD Anderson Cancer Center, University of Texas, Houston, TX, United States, [4]Division of Cardiovascular Medicine, The Ohio State University, Columbus, OH, United States, [5]University of South Florida, Tampa, FL, United States, [6]Division of Cardiovascular Medicine, Northside Hospital Cardiovascular Institute, Atlanta, GA, United States

Background: Management of coronary artery disease (CAD) is unique and challenging in cancer patients. However, little is known about the outcomes of using BMS or DES in these patients. This study aimed to compare the outcomes of percutaneous coronary intervention (PCI) in cancer patients who were treated with bare metal stents (BMS) vs. drug-eluting stents (DES).

Methods: We identified cancer patients who underwent PCI using BMS or DES between 2013 and 2020. Outcomes of interest were overall survival (OS) and the number of revascularizations. The Kaplan–Meier method was used to estimate the survival probability. Multivariate Cox regression models were utilized to compare OS between BMS and DES.

Results: We included 346 cancer patients who underwent PCI with a median follow-up of 34.1 months (95% CI, 28.4–38.7). Among these, 42 patients were treated with BMS (12.1%) and 304 with DES (87.9%). Age and gender were similar between the BMS and DES groups ($p = 0.09$ and 0.93, respectively). DES use was more frequent in the white race, while black patients had more BMS ($p = 0.03$). The use of DES was more common in patients with NSTEMI ($p = 0.03$). The median survival was 46 months (95% CI, 34–66). There was no significant difference in the number of revascularizations between the BMS and DES groups ($p = 0.43$). There was no significant difference in OS between the BMS and DES groups in multivariate analysis ($p = 0.26$). In addition, independent predictors for worse survival included age > 65 years, BMI ≤ 25 g/m^2, hemoglobin level ≤ 12 g/dL, and initial presentation with NSTEMI.

Conclusions: In our study, several revascularizations and survival were similar between cancer patients with CAD treated with BMS and DES. This finding

suggests that DES use is not associated with an increased risk for stent thrombosis, and as cancer survival improves, there may be a more significant role for DES.

KEYWORDS

percutaneous coronary intervention, bare metal stents, drug-eluting stents, cardio-oncology, revascularization

Introduction

Cardiovascular disease and cancer frequently coexist in an increasingly aging population and share the same risk factors (1). They are also the leading causes of death in developed countries, accounting for two-thirds of disease-related mortality (1). Despite the increased prevalence of thrombocytopenia and bleeding tendencies, cancer is often associated with a hypercoagulable state with increased platelet activation and aggregation. In addition, many chemotherapeutic agents are associated with angina, myocardial infarction (MI), and acceleration of pre-existing coronary artery disease (CAD), while radiotherapy is associated with CAD through direct endothelial injury (2–4). All the aforementioned factors make the management of cancer patients' CAD unique as well as challenging.

A history of cancer is independently associated with an increased risk of major adverse cardiovascular events (MACE) (5–7). The current generation of drug-eluting stents (DES) has been proven to reduce the risk of restenosis and stent thrombosis compared to bare-metal stents (BMS). However, data suggesting the preference of DES over BMS in the cancer population are lacking. The perceived need for a shorter course of dual antiplatelet treatment (DAPT) used to make the use of BMS an attractive alternative, particularly in patients with increased bleeding risk and an expectant need for cancer-directed surgery and/or procedures (8, 9).

There are limited data on the outcomes of cancer patients requiring PCI when directly comparing BMS with DES. Additionally, most randomized controlled trials making such comparisons exclude patients with active malignancy and treatment. With a growing number of patients with cancer, it is essential to study the outcomes of different types of stents and the duration of antiplatelet agents (10). The current study examines clinical and procedural characteristics and clinical outcomes in cancer patients with CAD treated with BMS vs. DES.

Materials and methods

Patient population

This was a single-center, retrospective, observational study approved by the MD Anderson Cancer Center Institutional Review Board. The requirement to obtain informed consent was waived, and the data were deidentified. All cancer patients who underwent PCI between January 2013 and December 2020 were included. Patients were further divided into two groups based on the type of intervention performed using either BMS or DES. Patients treated with balloon angioplasty alone were excluded. The decision to treat a patient with either of these strategies was based on the clinical characteristics of the individual patient. It was left to the discretion of the treating physicians.

Patient characteristics were collected using electronic medical records, including age, sex, race, body mass index, indication for primary PCI, comorbidities (history of diabetes mellitus, hypertension, hyperlipidemia, end-stage renal disease, peripheral vascular disease, stroke, or transient ischemic attack, previous coronary artery bypass graft, and PCI, etc.), as well as laboratory variables (hemoglobin, platelet count, creatinine, lipid panel, troponin, and B type natriuretic peptide/BNP, etc.), type of malignancy (solid vs. hematological), and intracoronary imaging used (intravascular ultrasound/IVUS and optical coherence tomography/OCT), as MD Anderson Catheterization laboratory is not an ST-elevation myocardial infarction (STEMI) receiving center, so these patients were not included. All other indications of revascularizations include "cardiomyopathy," "positive stress test," "unstable angina," "non STEMI," and "angina with prior history of CAD." Propensity score matching was conducted to select patients treated with BMS and comparable patients treated with DES. Furthermore, information related to primary outcomes was collected. The term "number of revascularizations" was defined by the total number of revascularizations needed for either the target vessel stented with either BMS or DES during the index procedure or for other arteries.

TABLE 1 Descriptive statistics by the intervention (BMS vs. DES).

Variable	BMS ($n = 42$)	DES ($n = 304$)	P-value[a]
Age (years)[b]	70.04 ± 9.79	67.16 ± 10.27	0.0870[c]
Number of revascularizations[d]	0 (0–0)	0 (0–0)	0.4263
Platelet count (10^3/uL)[d]	178 (158–246)	188 (138–253)	0.7883
Absolute Neutrophil Count (10^3/uL)[d]	3.9 (2.7–5.9)	4.44 (3–6)	0.5012
INR[d]	1.1 (1.02–1.27)	1.1 (1.01–1.2)	0.4705
Creatinine (mg/dL)[d]	1.08 (0.8–1.3)	1.03 (0.84–1.24)	0.7664
Hemoglobin (g/dL)[b]	11.89 ± 2.32	11.65 ± 2.13	0.4985[c]
Triglyceride (mg/dL)[d]	131 (80–224)	127 (88–170)	0.9536
Cholesterol (mg/dL)[d]	163 (145–224)	143 (114–171)	0.0243
HDL (mg/dL)[c]	45.00 ± 15.03	40.98 ± 13.93	0.2678[c]
LDL (mg/dL)[d]	91.5 (65.5–146)	73 (48–99)	0.0462
VLD (mg/dL)[d]	31 (16–45)	23.5 (17–34)	0.6332
BNP (pg/mL)[d]	347.5 (100–785.5)	422 (165–644)	0.6398
Troponin (ng/mL)[d]	0.66 (0.03–5.1)	0.4 (0.03–2.4)	0.5883
BMI (kg/m^2)[b]	28.82 ± 6.06	28.91 ± 6.09	0.9329[c]
Gender			
Male	33 (78.6%)	237 (78%)	0.9286[e]
Female	9 (21.4%)	67 (22%)	
Race			
White	20 (47.6%)	206 (68.4%)	0.0282[e]
Black	5 (11.9%)	23 (7.6%)	
Other	17 (40.5%)	72 (23.9%)	
Number of revascularization			
0	39 (92.9%)	271 (89.1%)	0.8719[f]
1	3 (7.1%)	20 (6.6%)	
2	0 (0.0%)	10 (3.3%)	
3	0 (0.0%)	3 (1%)	
Intracoronary imaging			
None	16 (38.1%)	118 (38.8%)	0.5256[e]
IVUS	24 (57.1%)	156 (51.3%)	
OCT	2 (4.8%)	30 (9.9%)	
Cancer type			
Solid	34 (81%)	198 (71.2%)	0.1881[e]
Hematological	8 (19%)	80 (28.8%)	
Smoker ≥1 years	24 (58.5%)	182 (69.3%)	0.5087[e]
Hypertension	38 (92.7%)	264 (91.7%)	1.0000[f]
Dyslipidemia	31 (77.5%)	232 (82%)	0.4954[e]
Family History Premature CAD	13 (34.2%)	34 (11.8%)	0.0002[e]
Prior MI	8 (21.1%)	103 (37.7%)	0.0444[e]
Prior Heart Failure	8 (20.5%)	65 (25.4%)	0.5108[e]
Peripheral Artery Disease	3 (7.9%)	42 (16.6%)	0.1663[e]
Chronic Lung Disease	3 (7.9%)	44 (17.4%)	0.1380[e]
Diabetes	11 (28.9%)	128 (48.7%)	0.0226[e]
Prior PCI	2 (11.1%)	66 (35.1%)	0.0386[e]
Prior CABG	0 (0.0%)	24 (13.4%)	0.1361[f]
Indication for Revascularization			
Cardiomyopathy	6 (14.3%)	43 (14.1%)	0.9804[e]
Abnormal Stress test	16 (38.1%)	73 (24%)	0.0503[e]
Stable CAD	16 (38.1%)	130 (42.8%)	0.5659[e]
Unstable Angina	7 (16.7%)	71 (23.4%)	0.3309[e]
NSTEMI	5 (11.9%)	82 (27%)	0.0323[e]

BMI, Body mass index; IVUS, Intravascular ultrasound; OCT, optical coherence tomography; MI, myocardial Infarction; CAD, coronary artery disease; PCI, Percutaneous coronary intervention; CABG, coronary artery bypass grafting; NSTEMI, non-ST elevation MI.

[a]Wilcoxon rank-sum test was used unless specified, [b]Mean ± SD are presented, [c] Two sample t-test was used, [d]Median (IQR) are presented, [e]Chi-square test was used, and [f]Fisher's exact test was used. P value < 0.05 suggesting statistical significance.

Outcomes

The primary endpoints included all-cause mortality and the number of revascularizations at the end of the follow-up period, while the secondary outcome was cardiovascular death.

Statistical analysis

Continuous variables were described as means ± standard deviations (SDs) or medians with interquartile ranges (IQRs). As appropriate, categorical variables were described as counts and percentages. Patient characteristics were compared between BMS and DES by a two-sample t-test or Wilcoxon rank-sum test for continuous variables and a Chi-square test or Fisher's exact test for categorical variables. Overall, survival time was defined as the interval between index PCI intervention and death. It was determined at the last follow-up if the patient was alive during the follow-up. The Kaplan–Meier method was used to estimate the survival probability. Univariate and multivariate Cox regression models were used to compare BMS and DES overall survival. The multivariate logistic regression model initially included covariates with a significant or marginally significant p-value based on univariate logistic regression analysis. The stepwise selection method was then utilized to include significant variables in the multivariate model. The propensity score, the predicted probability of receiving BMS, was calculated using a multivariate logistic regression model including significant factors. 1:1 propensity score matching and a 1:2 propensity score matching were conducted to select patients treated with BMS and comparable patients treated with DES using a one-to-many match macro using a greedy algorithm. A univariate Cox regression model was utilized to compare overall survival between BMS and DES in propensity score-matched cohorts. A $p < 0.05$ indicates

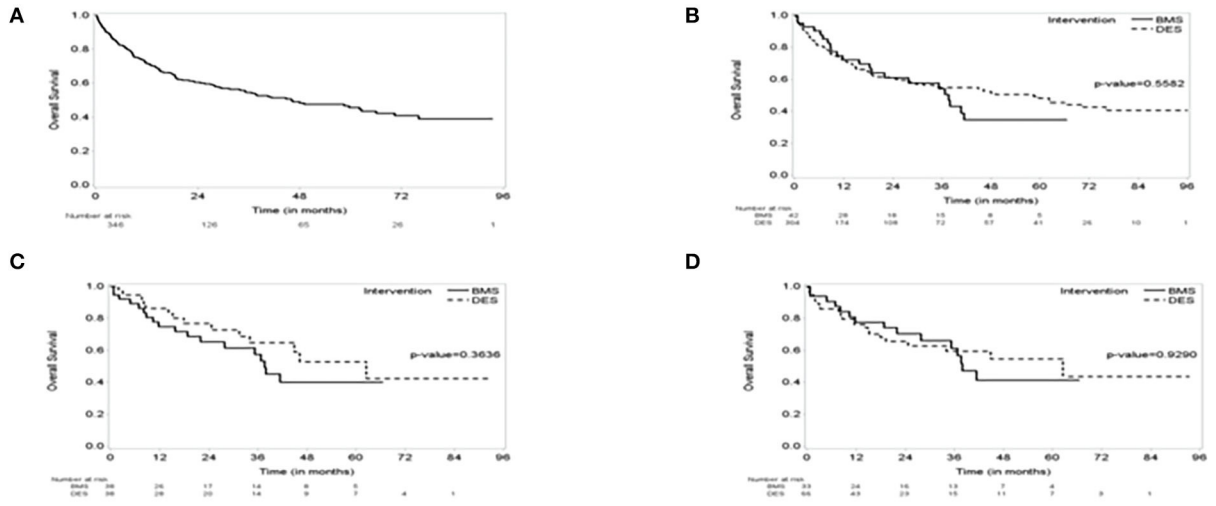

FIGURE 1
The Kaplan–Meier (KM) survival curve. **(A)** The KM curve of the entire group showing Median survival: 46 months (95% CI, 34–66); median follow-up of 34 months (95% CI, 28–39). **(B)** KM Survival curve by intervention showing no difference in survival over the follow-up period between bare metal stent (BMS) vs. drug-eluting stent (DES). **(C)** a 1:1 propensity score-matched cohorts of BMS vs. DES showing no difference in survival. **(D)** a 1:2 propensity score-matched cohorts of BMS vs. DES showing no difference in survival.

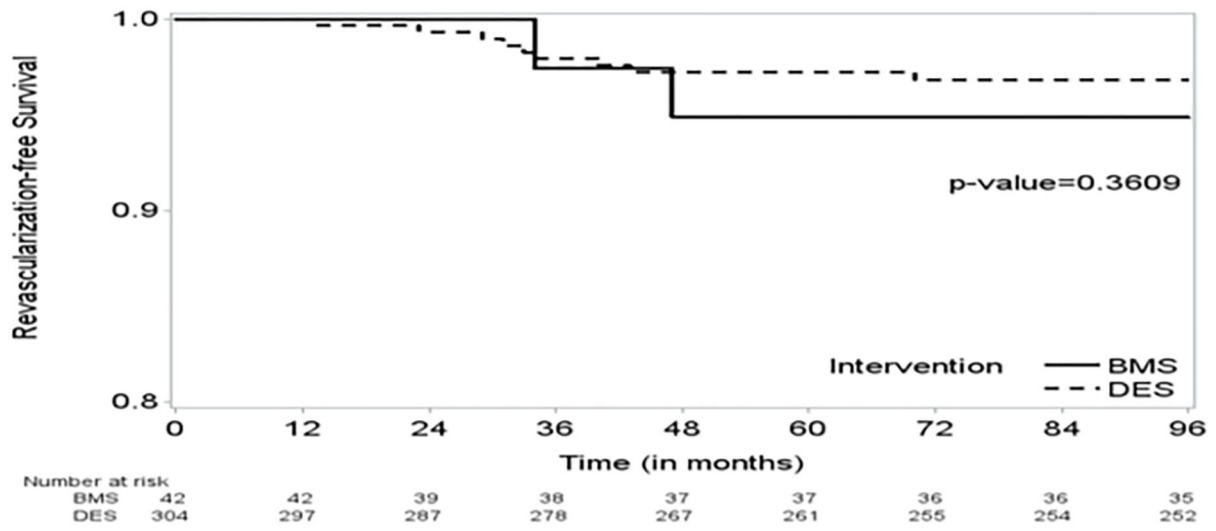

FIGURE 2
The Kaplan–Meier (KM) curve on time to revascularization shows no significant difference in time to revascularization between the BMS and DES groups.

statistical significance. For data analysis, SAS version 9.4 (SAS Institute, Inc., Cary, North Carolina) was used.

Results

Baseline characteristics

The study included 346 CAD cancer patients treated with BMS (n = 42) or DES (n = 304), while patients treated with POBA (n = 9) were excluded (Table 1). The median follow-up time, estimated by the reverse of the Kaplan–Meier method, was 34.1 months (95% CI, 28.4–38.7). The median survival time was 46.2 months (95% CI, 34.0–66.0) (Figures 1, 2). Patient characteristics of the intervention (BMS vs. DES) are summarized in Table 1. Some variables showed significant differences between the BMS and DES groups: BMS was more prevalent in blacks, while DES was more commonly seen in whites. Lipid panels, including

TABLE 2 Univariate Cox model (on overall survival time); with 346 who performed BMS or DES (147 deaths).

Variable	HR (95% CI)	*P*-value
Age (years)[a]	1.031 (1.013–1.049)	0.0006
Platelet count (10^3/uL)[a]	0.999 (0.997–1.001)	0.3660
Absolute Neutrophil Count (10^3/uL)[a]	1.029 (0.992–1.068)	0.1273
INR	0.984 (0.940–1.031)	0.5088
Creatinine (mg/dL)[a]	1.002 (0.981–1.022)	0.8784
Hemoglobin (g/dL) [a]	0.800 (0.737–0.869)	<0.0001
Triglyceride (mg/dL)[a]	0.999 (0.996–1.002)	0.4313
Cholesterol (mg/dL)[a]	0.998 (0.994–1.003)	0.4079
HDL (mg/dL)[a]	0.990 (0.974–1.006)	0.2084
LDL (mg/dL)[a]	0.999 (0.994–1.004)	0.7545
VLD (mg/dL)[a]	1.000 (0.982–1.018)	0.9775
BNP (pg/mL)[a]	1.000 (1.000–1.000)	0.9188
Troponin (ng/mL)[a]	0.984 (0.953–1.017)	0.3335
BMI (kg/m^2)[a]	0.943 (0.915–0.972)	0.0002
Gender		
Male	1.000	
Female	1.071 (0.720–1.592)	0.7344
Race		
White	1.000	
Black	1.442 (0.836–2.488)	0.1880
Other	0.824 (0.553–1.229)	0.3424
Intervention group		
BMS	1.000	
DES	0.873 (0.554–1.375)	0.5585
Intracoronary imaging		
IVUS	1.000	
None	1.130 (0.802–1.592)	0.4838
OCT	1.036 (0.575–1.865)	0.9072
Cancer type		
Solid	1.000	
Hematological	0.824 (0.572–1.187)	0.2990
Smoker≥1 year[b]	1.181 (0.838–1.665)	0.3408
Hypertension[b]	0.594 (0.358–0.987)	0.0443
Dyslipidemia[b]	1.095 (0.710–1.689)	0.6816
Family History Premature CAD[b]	1.439 (0.932–2.223)	0.1008
Prior MI[b]	0.760 (0.523–1.103)	0.1486
Prior Heart Failure[b]	1.350 (0.918–1.986)	0.1270
Peripheral Artery Disease[b]	1.215 (0.767–1.923)	0.4063
Chronic Lung Disease[b]	1.493 (0.974–2.289)	0.0661
Diabetes[b]	0.942 (0.661–1.341)	0.7383
Prior PCI[b]	1.063 (0.666–1.697)	0.7969
Prior CABG[b]	0.975 (0.484–1.962)	0.9430
Indication for Revascularization		
Cardiomyopathy[b]	1.092 (0.699–1.705)	0.6989
Abnormal Stress test[b]	0.707 (0.482–1.038)	0.0766
Stable CAD[b]	1.072 (0.775–1.484)	0.6739
Unstable Angina[b]	0.718 (0.473–1.091)	0.1203
NSTEMI[b]	1.961 (1.386–2.774)	0.0001

The number of revascularization is not included in this analysis as this variable is not a baseline characteristic. (i.e., patients with revascularization are likely to have longer survival as the survival time is calculated from initial vascularization and patients need to be survived to be revascularized).

BMI, Body mass index; IVUS, Intravascular ultrasound; OCT, Optical coherence tomography; MI, Myocardial Infarction; CAD, Coronary artery disease; PCI, Percutaneous coronary intervention; CABG, Coronary artery bypass grafting; NSTEMI, Non ST-elevation MI.

[a]HR in 1 unit change is presented along with 95% CI.

[b]HR considering no group as a reference, is presented along with 95% CI. P value < 0.05 suggesting statistical significance.

TABLE 3 Multivariate Cox model (on overall survival time).

Variable	Level	HR (95% CI)	*P*-value
Age group	≤65 years	1.000	
	>65 years	1.592 (1.087–2.334)	0.0170
Hemoglobin group	≤12 g/dL	1.000	
	>12 g/dL	0.481 (0.328–0.706)	0.0002
Intervention group	BMS	1.000	
	DES	0.763 (0.479–1.216)	0.2561
BMI group	≤25 g/m2	1.000	
	25–30 g/m2	0.811 (0.541–1.216)	0.3102
	>30 g/m2	0.585 (0.378–0.906)	0.0163
Indication: NSTEMI	No	1.000	
	Yes	1.629 (1.110–2.391)	0.0127

Including 323 patients with either BMS or DES considering age, hemoglobin (12 g/dL as a cutoff value), intervention, BMI, and an indication of NSTEMI.

cholesterol and mean LDL, were higher in the BMS group. The BMS group had a higher prevalence of family history of premature CAD, while those treated with DES had a significantly increased number of prior MI and PCI. DES use was more common in patients with non-ST segment elevation MI (NSTEMI).

Univariate Cox analysis results

Univariate analysis results are presented in Table 2. Age, higher INR, lower hemoglobin, lower body mass index (BMI), absence of hypertension, and primary PCI indication of NSTEMI were significantly associated with an increased risk of death.

Multivariate Cox analysis results

A multivariate Cox model initially considered the age at intervention, INR group, hemoglobin group, family

TABLE 4 Propensity score matching.

		Univariate Cox model		Multivariate Cox model	
Variable	**Level**	**HR (95% CI)**	***P*-value**	**HR (95% CI)**	***P*-value**
(a) 1:1 matching for BMS to DES (38 BMS vs. 38 DES were chosen)					
Intervention group	BMS	1.000		1.000	
	DES	0.724 (0.360–1.457)	0.3657	0.739 (0.367–1.489)	0.3974
Hemoglobin group	≤12 g/dL			1.000	
	>12 g/dL			0.516 (0.257–1.036)	0.0629
		Univariate Cox model		**Multivariate Cox model**	
Variable	**Level**	**HR (95% CI)**	***P*-value**	**HR (95% CI)**	***P*-value**
(b) 1:2 matching for BMS to DES (33 BMS vs. 66 DES were chosen)					
Intervention group	BMS	1.000		1.000	
	DES	0.971 (0.508–1.856)	0.9287	0.941 (0.489–1.809)	0.8545
Hemoglobin group	≤12 g/dL			1.000	
	>12 g/dL			0.517 (0.271–0.988)	0.0460

TABLE 5 Analysis of the number of revascularizations between BMS vs. DES group, including 1:1 and 1:2 propensity-matched analysis.

Covariate	**Levels**	**BMS ($n = 42$)**	**DES ($n = 304$)**	***P*-value**
(a) Including all patients with BMS or DES				
Number of revascularization	Median (Q1-Q3)	0 (0–0)	0 (0–0)	0.4263
	Mean ± SD	0.07 ± 0.26	0.16 ± 0.51	0.0745
Number of revascularization	0	39 (92.9%)	271 (89.1%)	0.8719
	1	3 (7.1%)	20 (6.6%)	
	2	0 (0%)	10 (3.3%)	
	3	0 (0%)	3 (1%)	
Covariate	**Levels**	**BMS ($n = 38$)**	**DES ($n = 38$)**	***P*-value**
(b) 1:1 Propensity score matched cohorts				
Number of revascularization	Median (Q1-Q3)	0 (0–0)	0 (0–0)	0.6560
	Mean (SD)	0.08 ± 0.27	0.16 ± 0.49	0.3927
Number of revascularization	0	35 (92.1%)	34 (89.5%)	0.6745
	1	3 (7.9%)	2 (5.3%)	
	2	0 (0%)	2 (5.3%)	
Covariate	**Levels**	**BMS ($n = 33$)**	**DES ($n = 66$)**	***P*-value**
(c) 1:2 propensity score matched cohorts				
Number of revascularization	Median (Q1-Q3)	0 (0–0)	0 (0–0)	0.6144
	Mean (SD)	0.09 ± 0.29	0.17 ± 0.48	0.3353
Number of revascularization	0	30 (90.9%)	58 (87.9%)	0.7447
	1	3 (9.1%)	5 (7.6%)	
	2	0 (0%)	3 (4.5%)	

TABLE 6 Cardiovascular specific survival: Univariate Fine-Gray models, considering cardiovascular specific death as an event of interest and death as a competing risk event.

Variable	HR (95% CI)	*P*-value
Age (years)	1.034 (0.970–1.104)	0.3064
Platelet count (10^3/uL)	1.000 (0.997–1.003)	0.9275
Absolute Neutrophil Count (10^3/uL)	1.056 (1.019–1.095)	0.0030
INR	1.002 (0.976–1.028)	0.8864
Creatinine (mg/dL)	0.995 (0.977–1.012)	0.5368
Hemoglobin (g/dL)	0.874 (0.716–1.066)	0.1848
Triglyceride (mg/dL)	1.003 (0.998–1.007)	0.2097
Cholesterol (mg/dL)	0.989 (0.978–0.999)	0.0354
HDL (mg/dL)	0.982 (0.942–1.024)	0.3983
LDL (mg/dL)	0.978 (0.963–0.994)	0.0071
VLD (mg/dL)	1.025 (0.998–1.054)	0.0682
BNP (pg/mL)	1.000 (0.999–1.000)	0.5436
Troponin (ng/mL)	0.866 (0.730–1.028)	0.0995
BMI (kg/m^2)	0.955 (0.907–1.005)	0.0765
Gender		
Female	1.000	
Male	1.443 (0.498–4.181)	0.4996
Race		
White	1.000	
Black	1.572 (0.462–5.344)	0.4687
Other	0.600 (0.201–1.787)	0.3588
Intervention group		
BMS	1.000	
DES	3.394 (0.464–24.830)	0.2288
Intracoronary imaging		
IVUS	1.000	
None	1.455 (0.633–3.341)	0.3770
OCT	1.040 (0.240–4.506)	0.9582
Cancer type		
Solid	1.000	
Hematological	0.839 (0.347–2.026)	0.6960
Indication for Revascularization		
Cardiomyopathy	1.618 (0.610–4.290)	0.3336
Abnormal Stress test	0.243 (0.059–1.008)	0.0512
Stable CAD	0.947 (0.422–2.125)	0.8957
Unstable Angina	1.144 (0.457–2.861)	0.7743
NSTEMI	2.232 (0.995–5.005)	0.0515

history of premature CAD, chronic lung disease, BMI group, and an indication of primary PCI (abnormal stress test or NSTEMI). Age, hemoglobin, BMI, and indication of NSTEMI remained significant in multivariate analysis. Therefore, multivariate models, including age group, hemoglobin group (using 12 g/dl as a cutoff value), BMI group, and an indication of NSTEMI, are presented in Table 3. After adjusting for age, hemoglobin, BMI, and indication of NSTEMI, BMS and DES did not show a significant difference in overall survival.

TABLE 7 Number of patients with BMS vs. DES per year (2013–2020).

Frequency	BMS *n* (%)	DES *n* (%)
2013	0 (0)	38 (100)
2014	4 (9.5)	38 (90.5)
2015	18 (39)	28 (61)
2016	12 (21.4)	44 (78.6)
2017	5 (11.6)	38 (88.4)
2018	2 (4.1)	47 (95.9)
2019	0 (0)	49 (100)
2020	1 (4.3)	22 (95.7)

Propensity score matching

Some patients were treated with BMS, while others with DES, and these interventions were not randomly allocated. To make a fair comparison between BMS and DES in outcomes, we calculated the propensity score using a logistic regression model to predict being treated with BMS. The logistic regression model initially considered significant or marginally significant variables in univariate logistic regression models (age at intervention, family history of premature CAD, race, prior MI, and diabetes). The stepwise selection method selected family history of premature CAD, race, and diabetes in the final multivariate logistic regression model. Using this model, we calculated the propensity score as the predicted probability of receiving BMS for given covariates. Using these propensity scores, we selected a 1:1 propensity score-matched cohorts (38 BMS vs. 38 DES) and a 1:2 propensity score-matched cohorts (33 BMS vs. 66 DES). In these cohorts, BMS and DES did not show significant differences in overall survival (Tables 4a,b).

The "number of revascularizations" was compared between the two groups: BMS vs. DES (Table 5a). Propensity score matching was also performed for the "number of revascularizations" (Tables 5b,c).

Secondary outcomes and other statistical analysis

Univariate Fine-Gray models, considering cardiovascular-specific death as an event of interest and death as a competing risk event, revealed no significant difference in cardiovascular outcomes between BMS vs. DES (Table 6). Detailed cancer characteristics for patients in the BMS and DES groups are provided in Table 7. The number of patients

10.3389/fcvm.2022.901431

TABLE 8 Cancer characteristics by intervention.

Covariate	Levels	BMS	DES	*P*-value
Cancer type	Solid	34 (81%)	198 (71.2%)	0.1881
	Hematologic	8 (19%)	80 (28.8%)	
Primary Cancer Type	1 Leukemia	7 (16.7%)	32 (11.6%)	0.0075
	2 Myeloma	1 (2.4%)	21 (7.6%)	
	3 Lymphoma	0 (0%)	26 (9.4%)	
	4 Lung	1 (2.4%)	41 (14.8%)	
	5 Colon/rectal	4 (9.5%)	15 (5.4%)	
	6 Breast	2 (4.8%)	11 (4%)	
	7 Pancreatic	3 (7.1%)	6 (2.2%)	
	8 Uterine	0 (0%)	2 (0.7%)	
	9 Ovarian/Endometrial	0 (0%)	3 (1.1%)	
	11 Prostate	1 (2.4%)	19 (6.9%)	
	12 Skin	2 (4.8%)	5 (1.8%)	
	13 Melanoma	4 (9.5%)	8 (2.9%)	
	14 Stomach/Esophageal	1 (2.4%)	12 (4.3%)	
	15 Renal/bladder	3 (7.1%)	31 (11.2%)	
	16 Other	3 (7.1%)	9 (3.2%)	
	17 Thyroid	1 (2.4%)	8 (2.9%)	
	18 ENT	4 (9.5%)	15 (5.4%)	
	19 Neurological	1 (2.4%)	2 (0.7%)	
	20 Liver	4 (9.5%)	8 (2.9%)	
	21 Endocrine	0 (0%)	3 (1.1%)	
Primary cancer group	1 Leukemia	7 (16.7%)	32 (11.6%)	0.0049
	2 Myeloma	1 (2.4%)	21 (7.6%)	
	3 Lymphoma	0 (0%)	26 (9.4%)	
	4 Lung	1 (2.4%)	41 (14.8%)	
	5 GI	12 (28.6%)	40 (14.4%)	
	6 Breast	2 (4.8%)	10 (3.6%)	
	7 Gynecological	0 (0%)	5 (1.8%)	
	8 Prostate/Testicular	1 (2.4%)	22 (7.9%)	
	9 Skin	6 (14.3%)	13 (4.7%)	
	10 Renal/bladder	3 (7.1%)	28 (10.1%)	
	11 Other	4 (9.5%)	12 (4.3%)	
	12 Endocrine	1 (2.4%)	9 (3.2%)	
	13 ENT	4 (9.5%)	18 (6.5%)	
Prior Chemotherapy	0	8 (33.3%)	61 (31.1%)	0.8256
	1	16 (66.7%)	135 (68.9%)	
Prior radiation	0	15 (62.5%)	118 (59.9%)	0.8058
	1	9 (37.5%)	79 (40.1%)	
Active Chemotherapy	0	14 (58.3%)	116 (58.3%)	0.9969
	1	10 (41.7%)	83 (41.7%)	

who underwent BMS and DES each year during the study duration (2013–2020) is provided in Table 8. A descriptive patient flowchart for inclusion in the study is provided in Figure 3.

Discussion

Our study showed that 1) the number of revascularizations (including target and other vessels) in cancer patients with CAD treated with BMS vs. DES was similar during the follow-up period, and 2) the all-cause mortality between BMS and DES did not differ significantly. These are important findings since cancer and cardiovascular disease are the most prevalent diseases worldwide. Data on outcomes after percutaneous intervention in these patients are scant, and the evidence-based treatment regimen for CAD in this group of patients is not well established (11–13).

Several comorbid conditions affect patients with cancer, which influence their treatment in the setting of PCI. While cancer and its treatment can predispose patients to bleeding tendencies and thrombocytopenia, neoplasia by itself is a pro-coagulant state (14). This poses a unique challenge and highlights the need to evaluate thrombosis and bleeding risks carefully. In the setting of PCI, this information has a tremendous impact on the options for stenting and antiplatelet therapy (14). Several clinical studies have proven the superiority of DES over BMS in reducing the risk of restenosis and stent thrombosis compared with bare-metal stents (BMS) in non-cancer high-risk patients (9). In-stent restenosis, although of concern, may not be significant due to shorter-term survivorship from cancer. As cancer survival rates keep improving, the role of DES in improved restenosis becomes more important. A study using OCT to evaluate stent healing after DES placement showed adequate stent healing in cancer patients despite a shorter course of DAPT (<6 months) in 61% of them. Findings were matched with stent healing value for DES in non-cancer patients (15).

Another concern for DES use in cancer patients is stent thrombosis, given the need for a shorter course of antiplatelet therapy in selected cases (16). In our study, the number of revascularizations was similar between the DES and BMS groups. Hence, DES is likely not associated with increased thrombotic risk in the cancer patient population. The idea of abbreviated DAPT after BMS appeals to the high-risk group of cancer patients (17). With recent advancements, the current-generation DES now possesses a reduced stent strut thickness and a unique drug fast-release profile that results in less powerful inhibition of intimal hyperplasia and rapid reendothelialization of stent struts. Given these qualities, a shorter duration of DAPT seems more feasible (18).

Recently published trials showed that 1 month of DAPT after PCI followed by aspirin monotherapy was non-inferior to 6 or 12 months of full antiplatelet therapy (18, 19). Interestingly, there was no difference in the occurrence of major bleeding and stent thrombosis between both groups. Similar studies are needed in a cancer population. Currently, the latest American College of Cardiology/American Heart Association

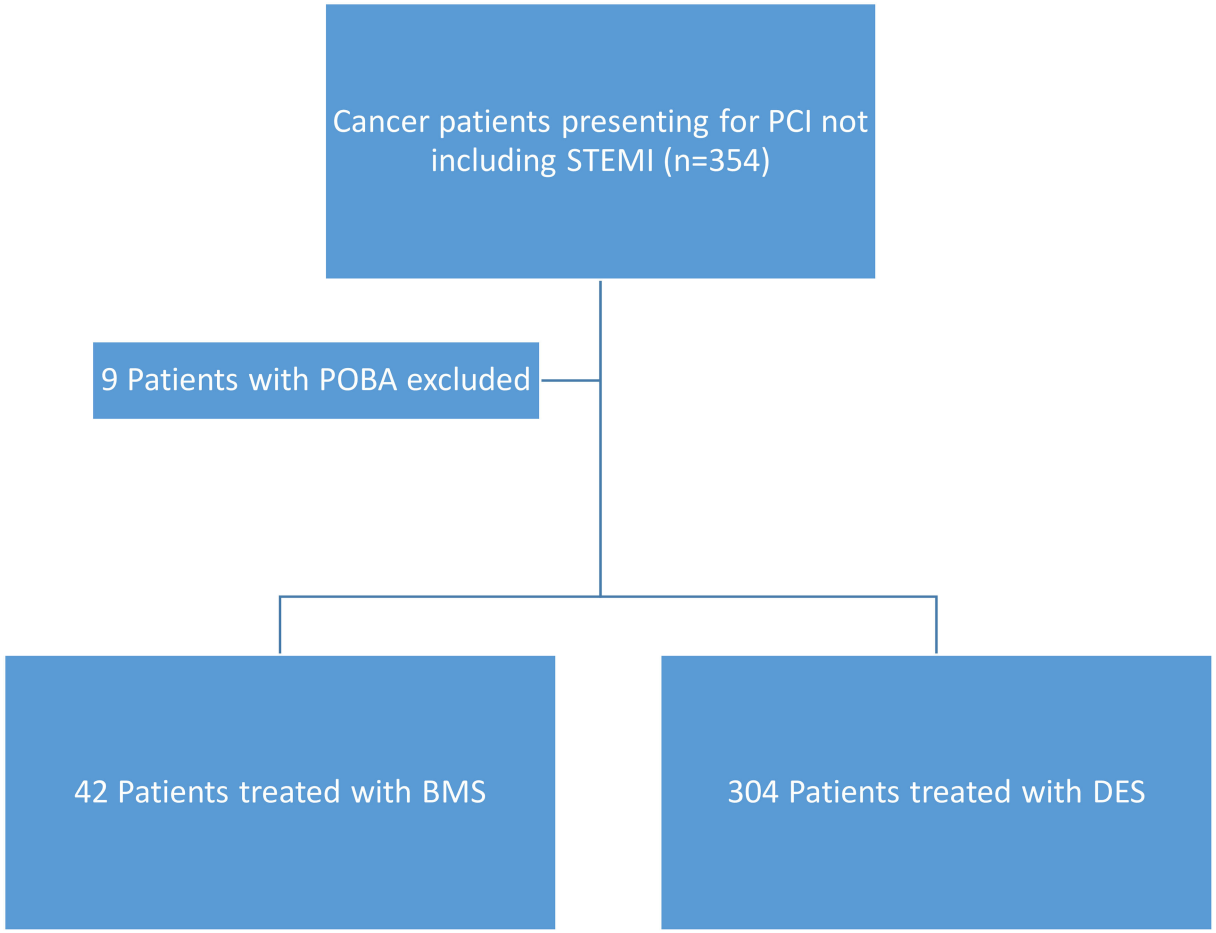

FIGURE 3
Patient flow chart showing inclusion criteria for the patients. STEMI, ST-elevation myocardial infarction; POBA, plain old balloon angioplasty; BMS, bare metal stents; DES, drug-eluting stents.

(ACC/AHA) guidelines and European Society of Cardiology (ESC) guidelines still emphasize a class I recommendation for at least 6 months of DAPT in non-ACS for DES and 1 month for BMS, and 12 months of DAPT in ACS settings for both DES and BMS (20, 21). According to the ACC/AHA guidelines, discontinuation of aspirin may be considered 1–3 months after DES implantation with continued P2Y12 monotherapy in both stable ischemic heart disease (SIHD) and ACS patients (class 2a recommendation) (20). We believe future guidelines will continue to implement shorter courses of DAPT as more data supporting this becomes available, especially with advanced technology in stent development. This will favor DES use in such a high-risk cancer population.

Another important consideration is the increased requirement for anticoagulation in cancer patients due to their higher propensity for thrombosis and atrial fibrillation. The management of triple therapy in these patients poses its own challenges due to the high risk of bleeding and a decision regarding the timing of re-initiation of chemotherapy (22, 23). A recent large study on a national database suggested superior outcomes in patients with cancer with a DES placed compared with those with a bare-metal stent (BMS) placed (8). However, this was driven by higher in-hospital mortality and increased bleeding events in the BMS group, signifying a selection bias to use BMS for sicker patients requiring early discontinuation of DAPT for various reasons, including initiation of cancer therapy due to advanced disease (24, 25). Although the choice of a stent in our study was at the treating physician's discretion after shared decision-making with the patient, a key difference in baseline characteristics between the two groups was an increased number of patients with NSTEMI in the DES group.

A significant interplay exists between cancer and CAD. Given a high bleeding risk in patients with cancer, shorter-duration DAPT and BMS were historically preferred in the setting of percutaneous coronary intervention. However, factors such as chronic inflammation and

chemotherapy/radiation-induced cardiotoxicity increase the risk of stent thrombosis and in-stent restenosis. Another important observation from this study is that in cancer patients, despite the increased inflammatory and prothrombotic state, the use of DES was not associated with a need for more revascularizations as compared to BMS. In a recent Italian registry, the use of BMS was extremely low, at 0.3 %, with the main reasons for BMS use being advanced age, ST-elevation myocardial infarction (STEMI), and physicians' perception of a high risk of bleeding (25).

Moreover, recent evidence from multiple studies suggests that shorter-duration DAPT is feasible with newer-generation DES and that percutaneous coronary intervention outcomes with the current generation of DES are better than with BMS (26, 27). Although the utilization of these stents in cancer patients is yet to be tested, in light of the current evidence, there is no reason for using BMS in any situation except for some cost-effectiveness. Moreover, the revolution of BMS vs. DES in our study indicates a stronger preference for using DES in the later years, with improvement in the design and generations of these stents.

Recent data suggest that routine use of intracoronary imaging leads to superior outcomes, which is paramount when shorter durations of DAPT are required (28–30). In our study, > 50% of the patients in either arm had IVUS as a part of their intervention, while almost 5% in BMS and 10% in DES underwent OCT. This highlights the role of optimizing PCI in this patient population, particularly given the increased likelihood that a shorter duration of DAPT may be required. This approach can avoid stent under-sizing and malapposition and residual untreated complications such as edge dissections, all of which may lead to worse outcomes, especially with a shorter duration of DAPT (13). When possible, bifurcation and overlapping stents should be avoided to reduce the risk of stent thrombosis (13).

Study limitations

Our study included a large cohort of patients with cancer patients undergoing PCI with DES vs. BMS reported to date. However, it was a single-center retrospective observational study with known limitations, including relatively small sample size. Also, mortality data may be underestimated because we rely on our electronic medical records. Furthermore, the successful continuation of DAPT therapy in both arms could not be accurately confirmed due to the study's retrospective nature. Moreover, our study did not use the newest generations of stents, including zatarolimus-coated stents, polymer-free stents, nano-coated stents, etc., requiring shorter-term DAPT therapy. Some data regarding index procedure details, including the number of stents used and the type of target vessel for revascularization, which can potentially affect the future need for revascularization, were not obtained and hence can affect the outcomes of the study. This calls for more detailed data collection for cancer patients in large-scale PCI registries to further validate the findings of our study.

Conclusion

In conclusion, cancer patients with CAD treated with BMS had similar overall survival and need for revascularizations compared to patients treated with DES. Our study revealed no increased risk of stent thrombosis or restenosis as well as all-cause mortality in cancer patients when comparing BMS vs. DES. As cancer therapy continues to evolve, the survival of these patients is expected to increase. Hence, greater use of DES may benefit these patients over a longer follow-up period. As such, the choice of stents in these patients should factor in the stage of cancer, expectant survival, and overall prognosis.

Data availability statement

The raw data supporting the conclusions of this article will be made available by the authors, without undue reservation.

Ethics statement

The studies involving human participants were reviewed and approved by the MD Anderson Cancer Center Institutional Review Board. Written informed consent for participation was not required for this study in accordance with the national legislation and the institutional requirements.

Author contributions

TA contributed to conception or design of the work, acquisition, analysis, or interpretation of data for the work, and drafting the work or revising it critically for important intellectual content. HP and AA contributed to the acquisition, analysis, or interpretation of data for the work, and drafting the work. EK contributed to revising it critically for important intellectual content. JS did analysis of the data and provided approval for publication of the content. KC, KM, KB, MC, and CG contributed to revising it critically for important intellectual content and final approval. CI contributed to revising it critically, provided final approval of publication, agreed to be accountable for all aspects of the work in ensuring that questions related to the accuracy or integrity of any part of the work are appropriately investigated, and

resolved. All authors contributed to the article and approved the submitted version.

Funding

The statistical analysis work was supported in part by cancer center support Grant No. 24 (NCI Grant No. PA30 CA016672).

Conflict of interest

The authors declare that the research was conducted in the absence of any commercial or financial relationships that could be construed as a potential conflict of interest.

Publisher's note

All claims expressed in this article are solely those of the authors and do not necessarily represent those of their affiliated organizations, or those of the publisher, the editors and the reviewers. Any product that may be evaluated in this article, or claim that may be made by its manufacturer, is not guaranteed or endorsed by the publisher.

References

1. Strongman H, Gadd S, Matthews A, Mansfield KE, Stanway S, Lyon AR, et al. Medium and long-term risks of specific cardiovascular diseases in survivors of 20 adult cancers: a population-based cohort study using multiple linked UK electronic health records databases. *Lancet.* (2019) 394:1041–54. doi: 10.1016/S0140-6736(19)31674-5

2. Xu XR, Yousef GM, Ni H. Cancer and platelet crosstalk: opportunities and challenges for aspirin and other antiplatelet agents. *Blood.* (2018) 131:1777–89. doi: 10.1182/blood-2017-05-743187

3. Roule V, Verdier L, Blanchart K, Ardouin P, Lemaitre A, Bignon M, et al. Systematic review and meta-analysis of the prognostic impact of cancer among patients with acute coronary syndrome and/or percutaneous coronary intervention. *BMC Cardiovasc Disord.* (2020) 20:38. doi: 10.1186/s12872-020-01352-0

4. Yeh ET, Bickford CL. Cardiovascular complications of cancer therapy: incidence, pathogenesis, diagnosis, and management. *J Am Coll Cardiol.* (2009) 53:2231–47. doi: 10.1016/j.jacc.2009.02.050

5. Kurisu S, Iwasaki T, Ishibashi K, Mitsuba N, Dohi Y, Kihara Y. Comparison of treatment and outcome of acute myocardial infarction between cancer patients and non-cancer patients. *Int J Cardiol.* (2013) 167:2335–7. doi: 10.1016/j.ijcard.2012.11.009

6. Landes U, Kornowski R, Bental T, Assali A, Vaknin-Assa H, Lev E, et al. Long-term outcomes after percutaneous coronary interventions in cancer survivors. *Coron Artery Dis.* (2017) 28:5–10. doi: 10.1097/MCA.0000000000000429

7. Wang F, Gulati R, Lennon RJ, Lewis BR, Park J, Sandhu GS, et al. Cancer history portends worse acute and long-term noncardiac (but not cardiac) mortality after primary percutaneous coronary intervention for acute ST-segment elevation myocardial infarction. *Mayo Clin Proc.* (2016) 91:1680–92. doi: 10.1016/j.mayocp.2016.06.029

8. Potts JE, Iliescu CA, Lopez Mattei JC, Martinez SC, Holmvang L, Ludman P, et al. Percutaneous coronary intervention in cancer patients: a report of the prevalence and outcomes in the United States. *Eur Heart J.* (2019) 40:1790–800. doi: 10.1093/eurheartj/ehy769

9. Neupane S, Khawaja O, Edla S, Singh H, Othman H, Bossone E, et al. Meta-analysis of drug eluting stents compared with bare metal stents in high bleeding risk patients undergoing percutaneous coronary interventions. *Catheter Cardiovasc Interv.* (2019) 94:98–104. doi: 10.1002/ccd.28045

10. Balanescu DV, Aziz MK, Donisan T, Palaskas N, Lopez-Mattei J, Hassan S, et al. Cancer treatment resumption in patients with new-generation drug-eluting stents. *Coron Artery Dis.* (2021) 32:295–301. doi: 10.1097/MCA.0000000000000986

11. Hess CN, Roe MT, Clare RM, Chiswell K, Kelly J, Tcheng JE, et al. Relationship between cancer and cardiovascular outcomes following percutaneous coronary intervention. *J Am Heart Assoc.* (2015) 4:e001779. doi: 10.1161/JAHA.115.001779

12. Ueki Y, Vögeli B, Karagiannis A, Zanchin T, Zanchin C, Rhyner D, et al. Ischemia and bleeding in cancer patients undergoing percutaneous coronary intervention. *JACC Cardio Oncol.* (2019) 1:145–155. doi: 10.1016/j.jaccao.2019.11.001

13. Iliescu CA, Grines CL, Herrmann J, Yang EH, Cilingiroglu M, Charitakis K, et al. SCAI Expert consensus statement: Evaluation, management, and special considerations of cardio-oncology patients in the cardiac catheterization laboratory (endorsed by the cardiological society of india, and sociedad Latino Americana de Cardiologia intervencionista). *Catheter Cardiovasc Interv.* (2016) 87:E202–23. doi: 10.1002/ccd.26379

14. Ramcharan KS, Lip GY, Stonelake PS, Blann AD. Effect of standard chemotherapy and antiangiogenic therapy on plasma markers and endothelial cells in colorectal cancer. *Br J Cancer.* (2014) 111:1742–9. doi: 10.1038/bjc.2014.491

15. Aziz MK, Herrmann J, Marmagkiolis K, Balanescu DV, Donisan T, Pushparaji B, et al. Coronary stent healing in cancer patients-an optical coherence tomography perspective. *Front Cardiovasc Med.* (2021) 8:665303. doi: 10.3389/fcvm.2021.665303

16. Nardi Agmon I, Perl L, Bental T, Itzhaki Ben Zadok O, Vaknin-Assa H, et al. Temporal trends in short and long-term outcomes after percutaneous coronary interventions among cancer patients. *Heart Vessels.* (2021) 36:1283–9. doi: 10.1007/s00380-021-01817-y

17. Quintana RA, Monlezun DJ, Davogustto G, Saenz HR, Lozano-Ruiz F, Sueta D, et al. Outcomes following percutaneous coronary intervention in patients with cancer. *Int J Cardiol.* (2020) 300:106–12. doi: 10.1016/j.ijcard.2019.09.016

18. Hong SJ, Kim JS, Hong SJ, Lim DS, Lee SY, Yun KH, et al. One-month DAPT investigators. 1-month dual-antiplatelet therapy followed by aspirin monotherapy after polymer-free drug-coated stent implantation: one-month DAPT trial. *JACC Cardiovasc Interv.* (2021) 14:1801–11. doi: 10.1016/j.jcin.2021.06.003

19. Valgimigli M, Cao D, Angiolillo DJ, Bangalore S, Bhatt DL, Ge J, et al. Duration of dual antiplatelet therapy for patients at high bleeding risk undergoing PCI. *J Am Coll Cardiol.* (2021) 78:2060–2072. doi: 10.1016/j.jacc.2021.08.074

20. Lawton JS, Tamis-Holland JE, Bangalore S, Bates ER, Beckie TM, Bischoff JM, et al. 2021 ACC/AHA/SCAI guideline for coronary artery revascularization: a report of the American College of Cardiology/American Heart Association joint committee on clinical practice guidelines. *J Am Coll Cardiol.* (2022) 79:e21–e129. doi: 10.1161/CIR.0000000000001039

21. Valgimigli M, Bueno H, Byrne RA, Collet JP, Costa F, Jeppsson A, et al. 2017 ESC focused update on dual antiplatelet therapy in coronary artery disease developed in collaboration with EACTS. *Eur J Cardiothorac Surg.* (2018) 53:34–78. doi: 10.1093/eurheartj/ehx419

22. Urban P, Meredith IT, Abizaid A, Pocock SJ, Carrié D, Naber C, et al. Polymer-free drug-coated coronary stents in patients at high bleeding risk. *N Engl J Med.* (2015) 373:2038–47. doi: 10.1056/NEJMoa1503943

23. Kandzari DE, Kirtane AJ, Windecker S, Latib A, Kedhi E, Mehran R, et al. One-month dual antiplatelet therapy following percutaneous coronary intervention with zotarolimus-eluting stents in high-bleeding-risk patients. *Circ Cardiovasc Interv.* (2020) 13:e009565. doi: 10.1161/CIRCINTERVENTIONS.120.009565

24. Jain D, Russell RR, Schwartz RG, Panjrath GS, Aronow W. Cardiac complications of cancer therapy: pathophysiology, identification, prevention, treatment, and future directions. *Curr Cardiol Rep.* (2017) 19:36. doi: 10.1007/s11886-017-0846-x

25. Giannini F, Pagnesi M, Campo G, Donahue M, Ferri LA, Briguori C, et al. Italian multicenter registry of bare metal stent use in modern percutaneous coronary intervention era (AMARCORD): a multicenter observational study. *Catheter Cardiovasc Interv.* (2021) 97:411–20. doi: 10.1002/ccd.28798

26. Giacoppo D, Matsuda Y, Fovino LN, D'Amico G, Gargiulo G, Byrne RA, et al. Short dual antiplatelet therapy followed by P2Y12 inhibitor monotherapy vs. prolonged dual antiplatelet therapy after percutaneous coronary intervention with second-generation drug-eluting stents: a systematic review and meta-analysis of randomized clinical trials. *Eur Heart J.* (2021) 42:308–19. doi: 10.1093/eurheartj/ehaa739

27. Wang W, Liu J, Fang J, Liu Y, An T, Zou M, et al. The optimal discontinuation of dual antiplatelet therapy in patients undergoing percutaneous coronary intervention with drug-eluting stents: a meta-analysis of randomized trials. *Int J Cardiol.* (2017) 235:73–86. doi: 10.1016/j.ijcard.2017.02.091

28. Kirtane AJ, Stoler R, Feldman R, Neumann FJ, Boutis L, Tahirkheli N, et al. Primary results of the EVOLVE short DAPT study: evaluation of 3-month dual antiplatelet therapy in high bleeding risk patients treated with a bioabsorbable polymer-coated everolimus-eluting stent. *Circ Cardiovasc Interv.* (2021) 14:e010144. doi: 10.1161/CIRCINTERVENTIONS.120.010144

29. Shin DH, Hong SJ, Mintz GS, Kim JS, Kim BK, Ko YG, et al. Effects of Intravascular ultrasound-guided versus angiography-guided new-generation drug-eluting stent implantation: meta-analysis with individual patient-level data from 2,345 randomized patients. *JACC Cardiovasc Interv.* (2016) 9:2232–9. doi: 10.1016/j.jcin.2016.07.021

30. Zhang J, Gao X, Kan J, Ge Z, Han L, Lu S, et al. Intravascular ultrasound versus angiography-guided drug-eluting stent implantation: the ULTIMATE trial. *J Am Coll Cardiol.* (2018) 72:3126–37. doi: 10.1016/j.jacc.2018.09.013

frontiers | Frontiers in Cardiovascular Medicine

TYPE Review
PUBLISHED 08 November 2022
DOI 10.3389/fcvm.2022.966182

OPEN ACCESS

EDITED BY
Feng Cao,
People's Liberation Army General Hospital, China

REVIEWED BY
Daniela Di Lisi,
Azienda Ospedaliera Universitaria Policlinico Paolo Giaccone, Italy
Anna Sicuranza,
University of Siena, Italy

*CORRESPONDENCE
Luwen Shi
shilu@bjmu.edu.cn
Xiaoyan Nie
niexy@pku.edu.cn

†These authors have contributed equally to this work

SPECIALTY SECTION
This article was submitted to Cardio-Oncology, a section of the journal Frontiers in Cardiovascular Medicine

RECEIVED 10 June 2022
ACCEPTED 18 October 2022
PUBLISHED 08 November 2022

CITATION
Li S, He J, Zhang X, Cai Y, Liu J, Nie X and Shi L (2022) Cardiovascular adverse events in chronic myeloid leukemia patients treated with nilotinib or imatinib: A systematic review, meta-analysis and integrative bioinformatics analysis.
Front. Cardiovasc. Med. 9:966182.
doi: 10.3389/fcvm.2022.966182

Cardiovascular adverse events in chronic myeloid leukemia patients treated with nilotinib or imatinib: A systematic review, meta-analysis and integrative bioinformatics analysis

Sicong Li[1†], Jinshan He[2†], Xinyi Zhang[1], Yuchun Cai[1], Jian Liu[2], Xiaoyan Nie[1*] and Luwen Shi[1*]

[1]School of Pharmaceutical Sciences, Peking University, Beijing, China, [2]Department of Cardiovascular, Peking University People's Hospital, Beijing, China

Objective: The aim of this article is to assess the risk and potential mechanisms of cardiovascular adverse events in patients treated with nilotinib or imatinib by conducting a systematic review, meta-analysis and integrative bioinformatics analysis.

Materials and methods: Three databases were systematically searched for studies published from inception to May 29, 2022. Differential expression analysis and weighted gene coexpression network analysis (WGCNA) were performed to search for modules of genes most associated with cardiotoxicity. Protein-protein interaction (PPI) network analysis was then performed to identify hub genes for the cardiotoxicity of nilotinib. Molecular docking was used to analyze the effects of rosuvastatin and aspirin on these targets.

Results: Patients treated with nilotinib as first-line treatment were associated with a higher risk of CAE (OR = 3.43 [95% CI 2.77–4.25]), CAD (OR = 5.30 [95% CI 3.85–7.29]), ACS (OR 2.7 [95% CI 1.60–4.54]), CVA (OR 5.76 [95% CI 2.84–11.28]), PAOD (OR 5.57 [95% CI 3.26–9.50]) and arrhythmia (OR 2.34 [1.17,4.67]) than those treated with imatinib, while no significant difference was found in the risk of HF (OR 1.40 [95% CI 0.42–4.69]) between the two groups. Patients who were treated with more than 600 mg daily dosage of nilotinib or followed up for more than 5 years had a higher risk of ACS and CVA. IL6, CXCL8, CCL2, SOD2, NFKBIA, and BIRC3 were identified as the top 6 hub genes in the magenta module (human cardiomyocyte samples) and were mainly enriched in the NOD-like receptor signaling pathway, IL-17 signaling pathway, TNF signaling pathway, lipid and atherosclerosis signaling pathway. TYROBP and CSF1R were identified as hub genes in the turquoise module (liver samples from Mus musculus). GSEA results showed that type II diabetes mellitus, B-cell receptor, apoptosis, insulin, natural killer cell mediated cytotoxicity,

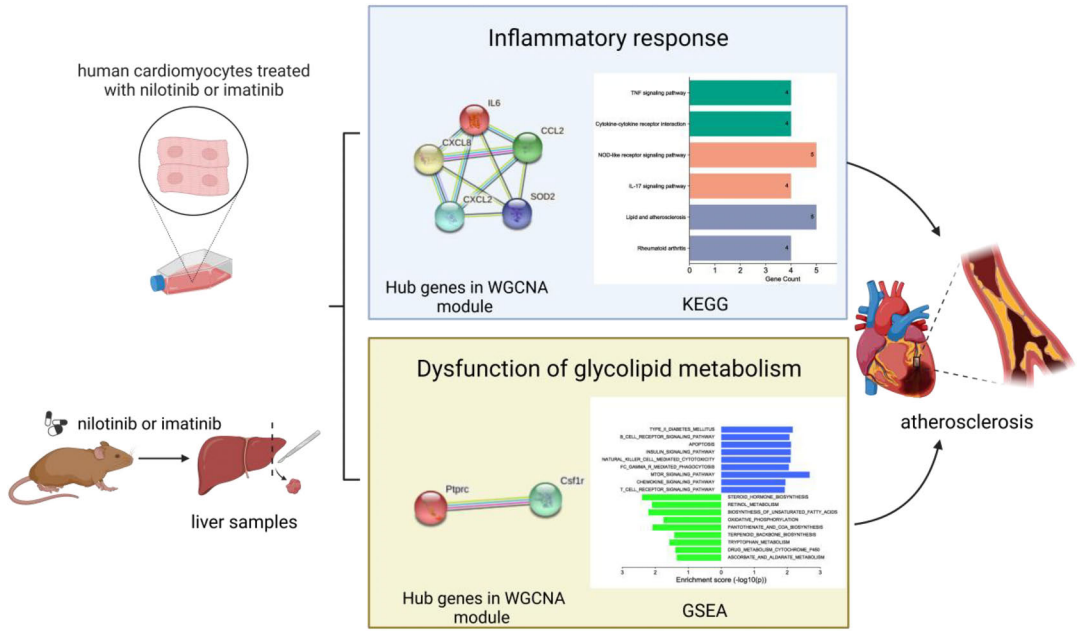

GRAPHICAL ABSTRACT
Study design for the bioinformatics analysis.

mTOR, chemokine, and T-cell receptor signaling pathways were related to the higher risk of atherosclerosis caused by nilotinib. Rosuvastatin can effectively bind to most of the hub targets and proteins enriched in the inflammatory pathways above.

Conclusion: CML patients who start with nilotinib have a higher risk of CAE than those with imatinib. Atherosclerosis caused by the inflammatory response and glycolipid metabolism disorder is the key mechanism of nilotinib cardiotoxicity. Rosuvastatin may be an effective treatment for the cardiotoxicity of nilotinib.

KEYWORDS

chronic myeloid leukemia, nilotinib, imatinib, cardiovascular adverse events, atherosclerosis

Introduction

Chronic myeloid leukemia (CML) is a malignant hematopoietic system disease that severely endangers the life of patients. CML patients possess the Philadelphia chromosome, which contains the Bcr-Abl that encodes the oncoprotein BCR-ABL. As the first TKI approved by the FDA, imatinib can improve the outcomes of CML patients and prolong their overall survival to a point that is similar to their age-matched healthy individuals (1). However, inevitable drug resistance to imatinib and the majority of relapses upon withdrawal have occurred frequently due to several mutations in the BCR-ABL kinase. Effective against most BCR-ABL1 mutations (T315I excluded), nilotinib has been approved as a first-line treatment and second-line treatment for CML patients with intolerance or resistance to imatinib (2), with a 10- to 50-fold higher BCR/ABL kinase inhibition activity than imatinib (3). The clinical efficacy of nilotinib (300 mg BID, 400 mg BID) in newly diagnosed chronic phase CML was demonstrated in the randomized phase III ENESTnd trial (4). As reported in the phase II study GIMEMA CML 0307, the 10-year overall survival and progression-free survival in patients treated with nilotinib

were 94.5% (5). The rates of major (MMR) and deep (MR4) molecular responses were 96% and 83%, respectively (5).

Apart from hematological, musculoskeletal, gastrointestinal and subcutaneous toxicity, nilotinib can also lead to adverse effects different from those of imatinib, such as cardiovascular adverse events (1, 6). A total of 23.3% of patients have at least one arterial obstructive event, which suggests that cardiovascular toxicity remains a concern. Nilotinib (NILO) can cause accelerated atherosclerosis and arterial thrombotic events (myocardial ischemia, stroke, and peripheral artery obstructive disease), hyperglycemia and hyperlipidemia (7, 8). The risk increases with the nilotinib administration duration (9). TKIs have become the current standard of care for CML, so their cardiotoxicity should be given enough attention in this population. The mechanisms underlying the cardiovascular adverse events induced by nilotinib or imatinib remain unclear.

Nowadays, statins have been recommended for optimal atherosclerotic cardiovascular disease (ASCVD) risk reduction by American College of Cardiology/American Heart Association (ACC/AHA) Guideline (10) and European Society of Cardiology/European Atherosclerosis Society (ESC/EAS) Guideline (11). As inhibitors of 3-hydroxy 3-methylglutaryl coenzyme A reductase, statins can reduce circulating low-density lipoprotein (LDL) and cholesterol levels by 25 to 50%. Moreover, statins bring about cardiovascular benefits via anti-inflammation and atherosclerotic plaque stabilization (12). As was reported in the Network Meta-Analyses conducted by Xiaodan Zhang et al. (13), rosuvastatin ranked first in lowering low-density lipoprotein cholesterol (LDL-C), apolipoprotein B (ApoB) and increasing apolipoprotein A1 (ApoA1) efficacy. Rosuvastatin, at moderate and high intensity doses, was the most effective in reducing levels of non-high density lipoprotein cholesterol in patients with diabetes (14). Therefore, we assess the therapeutic potential of rosuvastatin and aspirin, an important drug in prevention of ASCVD, so as to provide reference for researches on cardiotoxicity of nilotinib.

Abbreviations: ACS, Acute coronary syndrome; BIRC3, Baculoviral IAP Repeat Containing 3; BP, biological process; CAE, Cardiovascular Adverse events; CCL2, C-C Motif Chemokine Ligand 2; CCL20, C-C Motif Chemokine Ligand 20; CC, cellular component; CVA, cerebrovascular accident; CNKI, China National Knowledge Internet; CML, chronic myeloid leukemia; ceRNA, competing endogenous RNA; CAD, coronary artery disease; CXCL2, C-X-C Motif Chemokine Ligand 2; CXCL8, C-X-C Motif Chemokine Ligand 8; DM, diabetes mellitus; DEGs, differentially expressed genes; ES, enrichment score; FDR, false discovery rate; FC, fold change; GEO, Gene Expression Omnibus database; GO, Gene Ontology; GSEA, Gene Set Enrichment Analysis; HF, heart failure; hs-CRP, high-sensitivity C-reactive protein; HTN, hypertension; IGM, impaired glucose metabolism; IL10, interleukin 10; IL6, Interleukin 6; IHD, ischemic heart disease; KEGG, Kyoto Encyclopedia of Gene and Genomes; ME, module eigengene; MM, module membership; MF, molecular function; NFKBIA, NFKB Inhibitor Alpha; NILO, Nilotinib; NES, normalized enrichment score; PAOD, peripheral artery occlusive disease; PRISMA, Preferred Reporting Items for Systematic Reviews and Meta-Analyses; PDB, Protein Data Bank; PPI, protein-protein interaction; PH, pulmonary hypertension; RCT, randomized controlled trial; SOD2, Superoxide Dismutase 2; TIA, transient ischemic attack; TNFα, Tumor Necrosis Factor-α; TKIs, tyrosine kinase inhibitors; VSMCs, vascular smooth muscle cells; WGCNA, weighted gene coexpression network analysis.

Method

Meta-analysis

Literature data sources and search strategy

This systematic review and meta-analysis were registered on the PROSPERO platform (CRD42022334398) and performed in accordance with the Preferred Reporting Items for Systematic Reviews and Meta-Analyses (PRISMA) guidelines (15). The Embase, PubMed, and Cochrane Library databases were searched for articles. Moreover, we searched https://www.isrctn.com, https://www.clinicaltrials.gov, and http://www.chictr.org.cn/index.aspx for registered trials. The retrieval time was from inception to May 29, 2022. The detailed search strategy is described in **Supplementary Tables 1–3**.

Inclusion and exclusion criteria

Inclusion criteria

(1) Chronic myeloid leukemia patients who started with nilotinib or imatinib as first-line treatment. (2) Sufficient data and full text available for meta-analysis. (3) Study types were randomized controlled trials (RCTs) or observational studies. (4) Articles published in English.

Exclusion criteria

(1) Patients treated with a TKI except for imatinib or nilotinib. (2) Rotation of imatinib and nilotinib during follow-up. (3) Study types were case reports, single-cell sequencing studies, animal experiments, conference presentations, study protocols, meta-analyses or network meta-analyses.

Definition of the outcome

Cardiovascular adverse events (CAE), which were defined as the combination of any of the following events (1) coronary artery disease (CAD), which included but not was limited to stable angina, or acute coronary syndrome(ACS) (including unstable angina, ST or non-ST segment elevation myocardial infarction) (2) cerebrovascular accident (CVA), including stroke or transient ischemic attack (TIA) (3) peripheral artery occlusive disease(PAOD) (4) heart failure(HF) (5) pulmonary hypertension (PH) (6) arrhythmia.

Study selection and data extraction

Two review authors (Sicong Li and Jinshan He) independently reviewed the titles and abstracts of studies with potential eligibility. After that, we downloaded the full texts of studies eligible for inclusion. Two authors (Xinyi Zhang and Yuchun Cai) independently extracted the following data: (1) basic information, including first author, publication year,

sample size, follow-up time and study design; (2) characteristics of patients, including sex, age and country; (3) details about the TKI treatment: dosage and duration of nilotinib or imatinib treatment; and (4) information on quality assessment. Any disagreement concerning data extraction was settled through consensus among authors.

Strategy for meta-analysis

This meta-analysis was performed by using R (version 4.0.3). The chi-square test and I2 value were used to measure statistical heterogeneity. $I^2 < 50\%$ and $P > 0.05$ indicated no significant heterogeneity, and a fixed-effects model was used to pool the value of OR/HR and 95% confidence interval; otherwise, a random-effects model was used. Subgroup analysis was conducted to analyze sources of heterogeneity. Sensitivity analysis was conducted by excluding one study each time. Begg's and Egger's tests were used to assess publication bias. Statistical significance was set as $\alpha = 0.05$ in this study.

Quality assessment

XZ and YC assessed the quality of eligible studies independently by using the Newcastle–Ottawa Quality Assessment Scale (NOS) (16). The NOS assessed the quality of studies from the aspects of selection, comparability, and exposure, with a total score ranging from 0 to 9 points. More than 6 points was defined as a high-quality study. The results are presented in **Supplementary Table 5**.

Bioinformatics analysis

Data acquisition and quality control

By using "Tyrosine kinase inhibitor," "cardiotoxicity" and "atherosclerosis" as keywords, the Gene Expression Omnibus (GEO) repository[1] was searched for datasets about the cardiotoxicity of nilotinib or imatinib. GSE146095 and GSE146096 with expression profiling of cardiomyocytes from Homo sapiens and GSE103908 with expression profiling of liver tissues from Mus musculus were obtained for further analysis (17). No vascular endothelial cell samples treated with TKI were found on the GEO website. We first used the inSilicoMerging package of R software to merge the two datasets (GSE146095 and GSE146096) (18). Then, we used the method illustrated by Johnson we et al. (19) to remove the batch effect and finally obtained the transcriptomic profile matrix of human heart-derived primary cardiomyocyte-like cell lines from 16 nilotinib samples and 20 imatinib samples.

The liver plays a central role in cholesterol metabolism and lipoprotein distribution. Moreover, the liver is the main organ for the degradation of insulin, which inhibits gluconeogenesis and promotes glycogen decomposition and the synthesis and metabolism of long-chain fatty acids and triglycerides.

In the study of GSE103908, histopathological analysis of atherosclerosis and transcriptome analysis of the liver were performed on female APOE*3Leiden CETP transgenic mice. Sixteen of them were treated with imatinib (150 mg/kg BID), and eight of them were treated with nilotinib (10 or 30 mg/kg QD). Baseline was defined as the time point after 3 weeks on a Western-type diet containing saturated fat from 15% (w/w) cacao butter and 0.15% cholesterol. Nilotinib decreased collagen content by 32% ($p = 0.003 < 0.05$) and the lesion stability index by 43% ($p = 0.003 < 0.05$). Increased expression of macrophage-derived chemokine monocyte chemoattractant protein-1 (MCP-1) was observed in the nilotinib group. Imatinib reduced average cholesterol and triglyceride levels by 69% ($p < 0.001$) and 36% ($p = 0.019$), respectively, which was related to inhibiting VLDL production and intestinal absorption of cholesterol (20).

Analysis of differentially expressed genes

First, the probe names were converted into gene symbol names. Second, DEGs were identified by using the "limma" package (adjusted $p < 0.05$ and $|\log2FoldChange| > 1$). All of the DEGs were shown in a volcano plot, and the top 10 DEGs are shown in a heatmap.

Weighted gene co-expression analysis

The WGCNA package in R software was used to find clusters of highly correlated genes (with hierarchical clustering) and to summarize these clusters as module eigengenes (MEs) by liaising with cardiotoxicity and assigning module membership (MM) to genes. After obtaining the expression profile of differentially expressed genes, we removed the genes with a standard deviation of 0 in each sample, removed the outlier genes and samples by using the goodSamplesGenes method in the WGCNA package, and further constructed the scale-free coexpression network. Specifically, first, Pearson's correlation matrices and the average linkage method were both performed for all pairwise genes. Then, a weighted adjacency matrix was constructed using the power function $A\_mn = |C\_mn|^{\beta}$ (C_mn = Pearson's correlation between Gene_m and Gene_n; A_mn = adjacency between Gene m and Gene n). β was a soft-thresholding parameter that could emphasize strong correlations between genes and penalize weak correlations. After choosing the power of 20, the adjacency was transformed into a topological overlap matrix (TOM), which could measure the network connectivity of a gene defined as the sum of its adjacency with all other genes for network Gene ratio, and the corresponding dissimilarity (1-TOM) was calculated. To classify genes with similar expression profiles into gene modules, average linkage hierarchical clustering was conducted according to the TOM-based dissimilarity measure with a minimum size (gene group) of 30 for the gene dendrogram. Sensitivity was set as 2. To further analyze the module, we calculated the

1 https://www.ncbi.nlm.nih.gov/gds/

dissimilarity of module genes, chose a cut line for the module dendrogram and merged some modules. In addition, we also combined modules with a distance less than 0.25 and finally obtained four coexpression modules. Genes in the module most related to the cardiotoxicity of nilotinib were obtained for further analysis.

Gene ontology and kyoto encyclopedia of gene and genomes enrichment analysis

We used the DAVID website[2] to perform GO function and KEGG pathway enrichment analyses for genes in the most relevant module (21). Each term was calculated with a P value by using Fisher's exact test. $P < 0.05$ was considered statistically significant. All of the results were visualized by using the bioinformatic website.[3]

Construction and analysis of the protein-protein interaction network

The PPI network was constructed by using the STRING database[4] with a confidence score > 0.4 (4). The downloaded results were imported into Cytoscape 3.8.2 (22) software for further analysis. The top 10 hub genes in the PPI network were screened out by using the cytoHubba plugin. UpsetR was used to take the intersection of the top 10 hub genes according to 5 criteria.

Construction of the competing endogenous RNA network

miRNA–mRNA and miRNA–lncRNA interactions were obtained by searching lncACTdb (23).[5] In this database, we searched for ceRNA interactions supported by low- and high-throughput experiments. Finally, the ceRNA network was visualized in a Sankey plot by the R package "ggalluvial."

Gene set enrichment analysis

We obtained GSEA software (version 3.0) from the GSEA website[6] (24). We downloaded the c2.cp.kegg.v7.4.symbols.gmt subset from the Molecular Signatures Database[7] (19) to evaluate the relevant pathways and molecular mechanisms based on gene expression profiles and phenotypic grouping. The default weighted enrichment method was used for the enrichment analysis. The random combination was set for 1000 times (25). $|NES| > 1$, FDR < 0.25, NOM $p < 0.05$ were considered significant enrichment.

2 https://david.ncifcrf.gov/
3 http://www.bioinformatics.com.cn/
4 https://www.string-db.org
5 http://www.biobigdata.ta.net/LncACTdb/
6 http://software.broadinstitute.org/gsea/index.jsp
7 http://www.gsea-msigdb.org/gsea/downloads.jsp

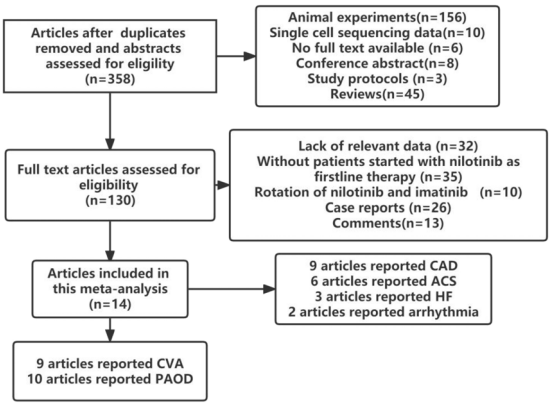

FIGURE 1
Flow chart of the study selection.

Molecular docking

Molecular docking was performed to predict the binding of rosuvastatin and aspirin to the hub proteins and the targets enriched in the atherosclerosis signaling pathway. The three-dimensional structures of rosuvastatin and aspirin were obtained from the PubChem database,[8] and the three-dimensional structures of hub proteins were obtained from the RCSB Protein Data Bank (PDB) database.[9] Molecular docking simulations between rosuvastatin, aspirin and the target proteins were performed by using the AutoDock Tool (version 1.5.6) and AutoDock Vina 1.1.2 (Molecular Graphics Laboratory, Scripps Institute, 2011). A minimum binding energy less than 5 indicated a good binding ability. The results were finally visualized by using the PyMOL molecular graphics system (v.2.4.0, Schrödinger, LLC) (26).

Results

Results of meta-analysis

Literature search

In total, 14 studies involving 9699 patients with CML were found to meet the inclusion criteria. Wang et al. (27) and Kantarjian et al. (28) reported open labeled randomized controlled studies, Anna Sicuranza et al. reported prospective cohort studies (29), while others reported retrospective cohort studies (30–40). The flow chart of the study selection process is presented in **Figure 1**.

8 https://pubchem.ncbi.nlm.nih.gov/
9 http://www.rcsb.org/

TABLE 1 Basic characteristics of the included studies.

Author	Country	Sample size	Age (year-old)	Sex male(%)	CAE outcomes reported	Duration of nilotinib	Duration of imatinib	Nilotinib dose	Imatinib dose	Follow-up time
Subramanian et al. (24)	Japan	369	53.0 (range 18–89)	224 (60.70%)	CAD, CVA,PAOD	464 person-years	1336 person-years	150 mg QD,300 mg QD, 400 mg QD, 300 mg BID,	400 mg QD	71.8 (range 1–196) months
Zhao et al. (25)	Sweden	1601	imatinib 60 (range 46–70), nilotinib 60 (range 45–69)	715 (64%)	ACS,CAD,PAOD	2.8 (range0.8–5.6) years	3.2 (range1.1–7.8) years	NA	NA	6 (range 3–10) years
Trott and Olson (26)	Slovakia	82	55.82 ± 13	48 (58.54%)	CAD, CVA,PAOD	51.6 (range3.0–123.6) months	126.25 (range3.33–198.00) months	300 mg BID,400 mg BID	400 mg QD	median 61.3 months
Kantarjian et al. (27)	Sweden	896	58.2 ± 17.0	485 (54.1%)	ACS, CVA, POAD	167 person-years	2350 person-years	NA	NA	4.2 (range1.9–7.1) years
Wang et al. (28)	China	1,111	Nilotinib 48.3 ± 14.4; Imatinib 49.0 ± 16.4	NA	CAD,CVA,POAD	91.2 ± 277.6 days	35.8 ± 130.9 days	NA	NA	5 years
Sicuranza et al. (29)	USA	531	49 ± 15	321 (60%)	CAD, PAOD, HF, CVA,PH, Arrhythmia	77 (range 3–134) months	imatinib 400 mg cohort 144 (range, 2–195)months, imatinib 800 mg cohort 136 (2-186)months	400 mg BID	400 mg QD,400 mg BID	94 (range 2-196) months
Fujioka et al. (30)	Japan	506	56(range 18-92)	329(65%)	PAOD, ACS, HF, arrhythmia, CVA	65.3 (range2.0–89.2) months	77.9 (range 1.7–97.8) months	300 mg QD, 300 mg BID	300 mg QD	5 years
Dahlén et al. (31)	Ireland	1857	nilotinib median 47;imatinib median 49	1089(58.64%)	CAE	36 (range,0–47) months	45 (range 0–67) months	300 mg BID, 400 mg BID	400 mg QD, 400 mg BID	6 (IQR, 3-10) years
Petrikova et al. (32)	China	1207	46.38 ± 14.96	728 (60.31)	CAD, CVA, PAOD	median 2.40 years	median 3.74 years	NA	NA	NA
Szklarczyk et al. (4)	USA	846	NA	NA	CAD,CVA,PAOD	median 82.8 months in the 300-mg BID group, 87.5 months in the 400-mg BID group	median 64.0 months	300-mg BID, 400-mg BID	400 mg QD	10 years

(Continued)

10.3389/fcvm.2022.966182

TABLE 1 (Continued)

Author	Country	Sample size	Age (year-old)	Sex male(%)	CAE outcomes reported	Duration of nilotinib	Duration of imatinib	Nilotinib dose	Imatinib dose	Follow-up time
Wang et al. (23)	Italy	186	60 (range 24–90)	(107/79)	ACS,CVA,PAOD	24 (range 12–64.5)months	21 (range 12–62.7) months	NA	NA	23.3 (range 12–64.6)months
Dahlén et al. (33)	Germany	159	53 (range 21–85)	(84/75)	PAOD	36 (range 6–72) months	97.5 (range 8–146)months	300 mg BID, 400 mg BID, 1200 mg QD, 600 mg BID	400 mg QD, 400 mg BID	74 (4–269) months
Ragueneau et al. (22)	China	267	nilotinib 41 (range 18–76), imatinib 39 (range 19–74)	172 (64.42%)	CVA	2 years	2 years	300 mg BID	400 mg QD	2 years
Chen et al. (34)	Italy	81	Median [IQR]:nilotinib 60 [53–66]; imatinib 62 [51–69]	43(53.09%)	ACS, HF, CVA	3.59 [IQR 2.23–4.76] years	4.55 [IQR 1.39–7.89] years	NA	NA	5.93 (IQR 3.64–9.25) years

Study characteristics

The included studies were published between 2013 and 2022 and were conducted in Italy, China, Sweden, Slovakia, the USA, Germany, Japan, and Ireland. The average follow-up time ranged from 4.2 years to 10 years. Six studies did not report the dosage of nilotinib and imatinib. The relevant characteristics of the included studies are detailed in **Table 1**. Pulmonary hypertension was not included in this analysis because only one study reported it.

Results for cardiovascular adverse events

In logistic regression and survival analysis, patients treated with nilotinib as first-line treatment suffered from a higher risk of CAE (OR 3.43 [95% CI 2.77–4.25], HR = 3.75 [95% CI 1.90, 7.40]) than those treated with imatinib (see **Figure 2**). No individual study was found to significantly influence the pooled HR and 95% CI in the sensitivity analysis. No significant publication bias was found by Begg's and Egger's tests. Torsten Dahlén (33) contributed the most to the overall heterogeneity and the overall results. In the subgroup analysis, different definitions of CAE might be the main source of heterogeneity. In terms of survival analysis, we did not construct funnel plots or perform Begg's test and Egger's test to assess publication bias due to the less than recommended arbitrary minimum number of studies.

Results for other outcomes

Patients treated with nilotinib as first-line treatment had a higher risk of CAD (OR 5.30 [95% CI 3.85–7.29]), ACS (OR 2.7 [95% CI 1.60–4.54]), CVA (OR 5.76 [95% CI 2.84–11.28]), POAD (OR 5.57 [95% CI 3.26–9.50]) and arrhythmia (OR 2.34 [1.17,4.67]) than those treated with imatinib, while no significant difference was found in the risk of HF (OR 1.40 [95% CI 0.42–4.69]) between the two groups (**Figure 3**). The results of the publication bias assessment, sensitivity analysis and baujat plots for heterogeneity analysis are presented in **Supplementary Figures 7–10**.

Regarding the outcomes of HF and arrhythmia, we did not construct funnel plots or perform Begg's test and Egger's test to assess publication bias due to the less than recommended arbitrary minimum number of studies.

In subgroup analysis, sample size may be the source of heterogeneity in the comparison of ACS, CVA and CAD. Nilotinib treatment in studies with sample sizes greater than 1000 tended to show a higher risk of ACS, CVA and CAD than imatinib treatment. The median follow-up time, dosage and duration of nilotinib may be the source of heterogeneity in the comparison of ACS, which indicated that patients treated with more than 600 mg daily dosage or longer than 5 years of nilotinib treatment or who were followed up for more than 5 years suffered from a higher risk of ACS. In the comparison of CVA, patients treated with nilotinib tended to have a higher risk of CVA than those treated with imatinib. In studies where

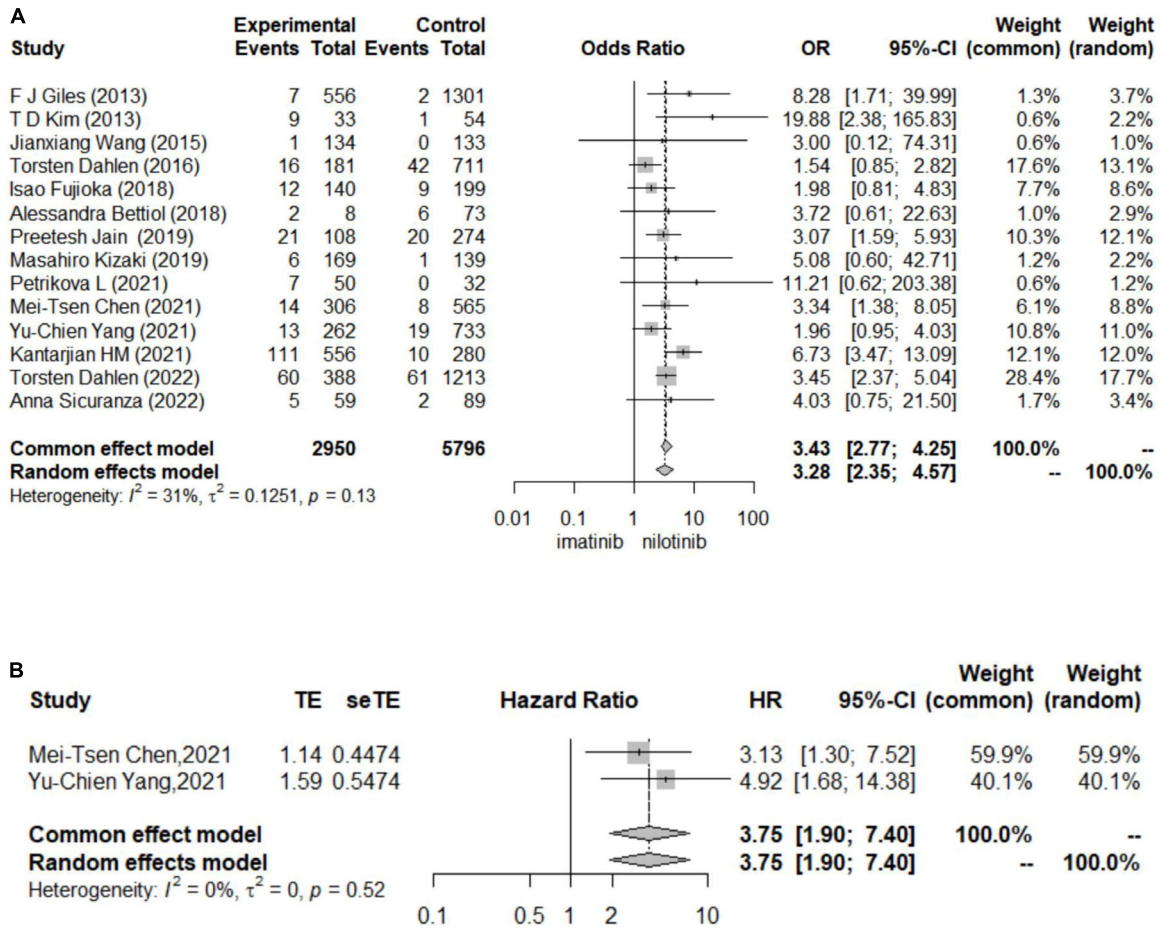

FIGURE 2
Forest plots for cardiovascular adverse events **(A)**. The results for logistic regression **(B)**. The results for survival analysis.

patients took more than 600 mg daily dosage of nilotinib or more than 400 mg daily dosage of imatinib, the duration of imatinib or total follow-up time was more than 5 years (**Supplementary Figures 1–6**).

Results of bioinformatics analysis

Results of differentially expressed genes

In terms of human cardiomyocytes treated with nilotinib, 55 upregulated and 759 downregulated DEGs were identified through fold change (FC) and P value filtering ($|\log2FC| > 1$ and $P < 0.05$) (see **Figure 4**). Interleukin 6 (IL6), C-X-C motif chemokine ligand 8 (CXCL8), C-C motif chemokine ligand 2 (CCL2), superoxide dismutase 2 (SOD2), NFKB inhibitor alpha (NFKBIA), baculoviral IAP repeat containing 3 (BIRC3), C-C motif chemokine ligand 20 (CCL20), and C-X-C motif chemokine ligand 2 (CXCL2) were upregulated in the nilotinib group, while insulin receptor substrate 1 (IRS1) was downregulated.

In liver samples of Mus musculus treated with nilotinib, CCL2, CXCL2, BIRC3, Transmembrane Immune Signaling Adaptor (TYROBP), and Colony Stimulating Factor 1 Receptor (CSF1R) were upregulated, while Low Density Lipoprotein Receptor (LDLR), very Low Density Lipoprotein Receptor (VLDLR), and Insulin Receptor Substrate 1 (IRS1) were downregulated compared with those treated with imatinib. TYROBP and CSF1R are important functional regulators of macrophages, which are the main inflammatory cells in vulnerable plaques and are closely related to the occurrence, development and rupture of vulnerable plaques. Decreased expression of LDLR and VLDLR in the liver can lead to hypercholesterolemia, while decreased expression of IRS1 can lead to insulin resistance (IR).

Weighted gene coexpression network analysis

In terms of human cardiomyocyte samples, WGCNA was performed on the 814 DEGs (see **Figure 5**). The soft threshold for network construction was selected as 20. Meanwhile, the fitting degree of the scale-free topological model was 0.85. This

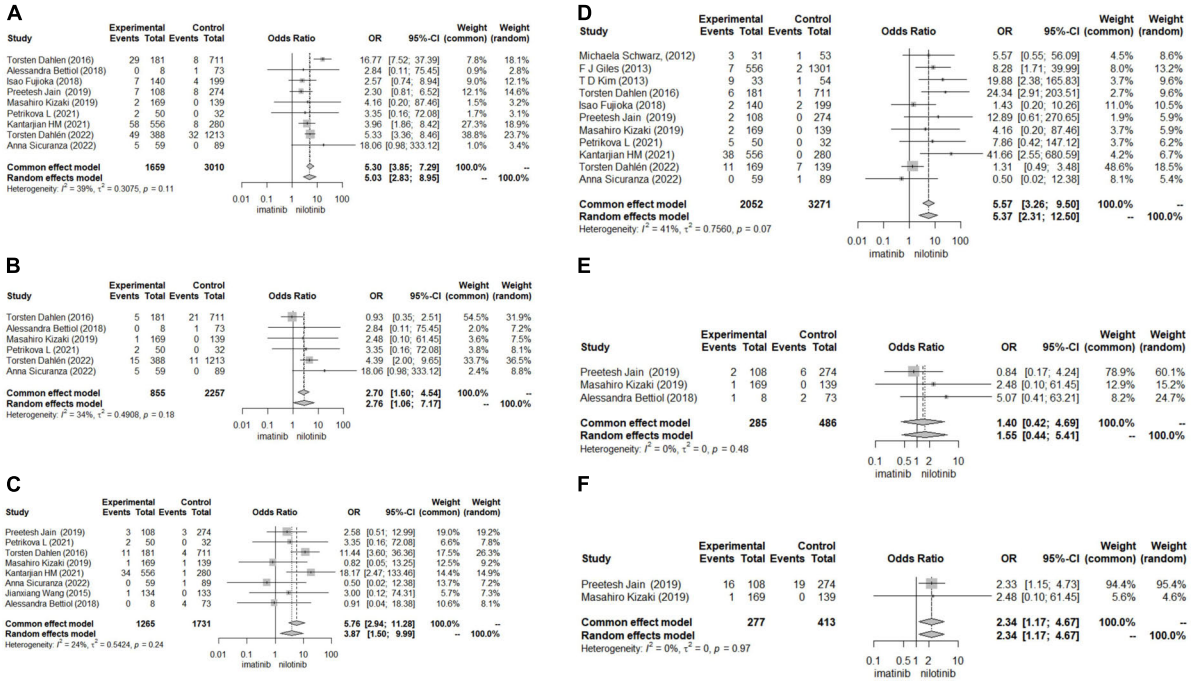

FIGURE 3
Forest plots for other outcomes. **(A)** Coronary artery disease (CAD). **(B)** Acute coronary syndrome (ACS). **(C)** Cerebrovascular accident (CVA). **(D)** Peripheral artery occlusive disease (POAD). **(E)** Heart failure (HF). **(F)** Arrhythmia.

network conformed to the power-law distribution and was closer to the real biological network state (41). Four modules were identified based on average linkage hierarchical clustering and soft-thresholding power. Among them, the magenta module showed the highest correlation with the cardiotoxicity of nilotinib (correlation index: 0.56, $P = 3.4e^{-4} < 0.05$). Thirty-five genes in the magenta module were selected for further analysis.

In terms of liver samples from Mus musculus, the soft threshold for network construction was selected as 6. Finally, 36 modules were identified based on average linkage hierarchical clustering and soft-thresholding power. Among them, the turquoise module showed the highest correlation with atherosclerosis related to nilotinib (correlation index: 0.77, $P = 9.7e^{-6} < 0.05$). A total of 182 genes in the turquoise module were selected for further analysis.

Gene ontology and kyoto encyclopedia of gene and genomes enrichment analysis

In terms of human cardiomyocyte samples, 35 genes in the magenta module were analyzed by using the DAVID database. Thirty-two biological processes (BPs), 5 cellular components (CCs), and 8 molecular functions (MFs) were found. The top 5 results in terms of count with a significant difference ($P < 0.05$) and KEGG results with a count larger than 2 are presented in the bar graph according to the P value (**Figures 6A,B**). The smaller the P value is, the greater the color of the bar tends to be red. The greater the number of enriched genes, the longer the area of the bar was. The 35 genes were mainly associated with the NOD-like receptor signaling pathway, IL-17 signaling pathway, TNF signaling pathway, lipid and atherosclerosis, cytokine-cytokine receptor interaction and AGE-RAGE signaling pathway in diabetic complications.

In terms of liver samples from Mus musculus, genes in the turquoise module were enriched in 232 biological processes (BPs), 77-cellular components (CCs), and 8 molecular functions (MFs). In terms of KEGG analysis, genes in the turquoise module were mainly enriched in the regulation of actin cytoskeleton, chemokine signaling pathway, leukocyte transendothelial migration, PI3K-Akt, focal adhesion, Fc gamma R-mediated phagocytosis, platelet activation, natural killer cell mediated cytotoxicity, Rap1, and lipid and atherosclerosis signaling pathways (see **Figures 6C,D**). The results above indicated that the inflammatory response and abnormal glycolipid metabolism are the essential mechanisms in atherosclerosis related to nilotinib.

Protein-protein interaction network analysis

The PPI network was constructed by Cytoscape based on the STRING database. In terms of human samples, the PPI network consists of 26 nodes and 54 edges (**Figure 7A**). The top 10 hub genes according to 5 kinds of criteria were identified by using the cytoHubba plugin (**Supplementary Figure 11**

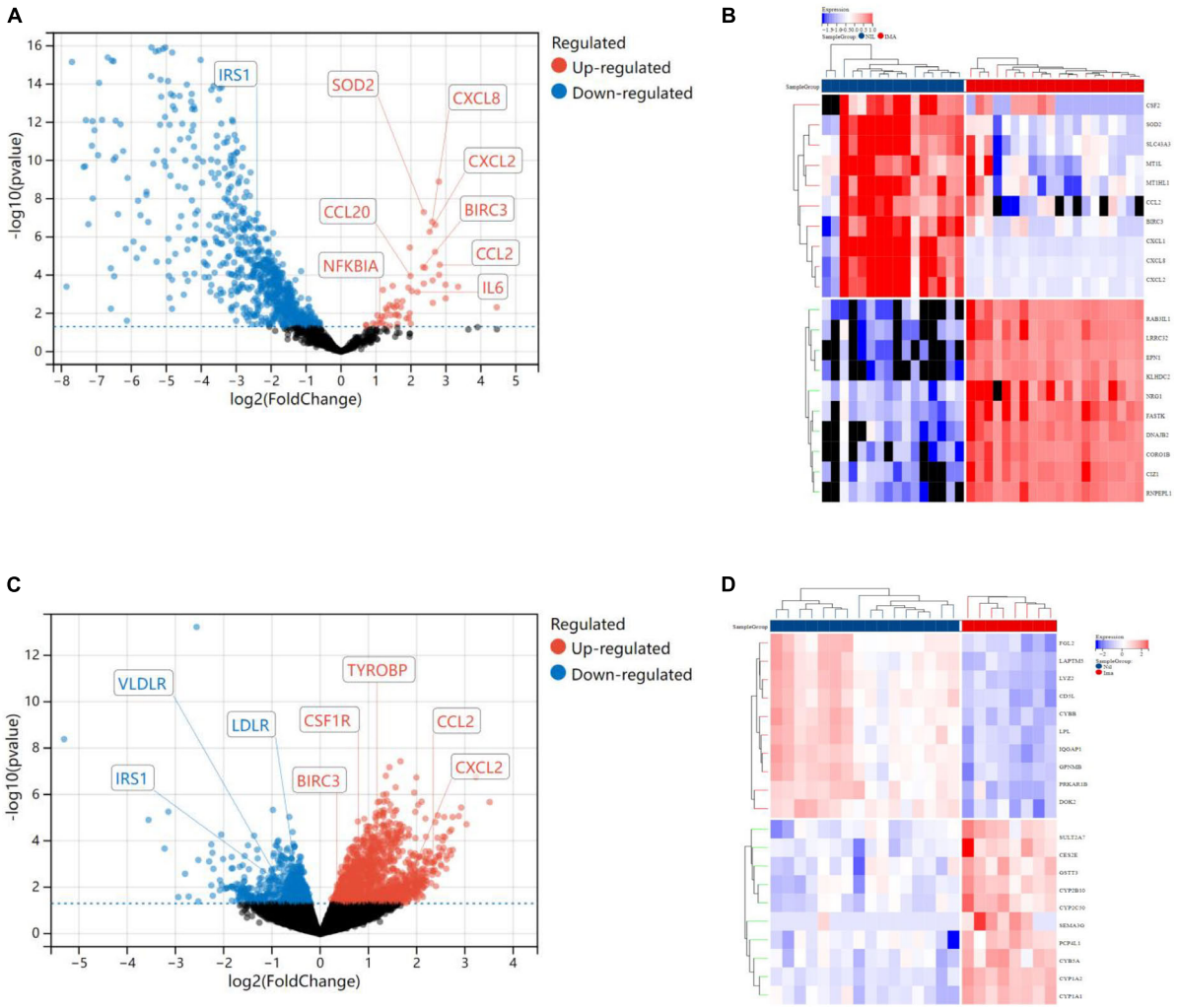

FIGURE 4
Visualized plots for differentially expressed genes (DEGs). **(A)** Volcano plots (human cardiomyocytes samples). **(B)** Heatmap (human cardiomyocytes samples). **(C)** Heatmap (liver samples from Mus musculus). **(D)** Volcanoplots (liver samples from Mus musculus).

and Supplementary Table 6). We took their intersection by using UpsetR (Supplementary Figure 11), and 6 hub genes were finally identified (Table 2). GO term enrichment analysis showed that the top 6 genes were enriched in the inflammatory response and signal transduction in biological processes. Cell component analysis found that they were significantly enriched in the extracellular space and extracellular region. For the molecular function analysis, they were principally involved in chemokine activity and cytokine activity. KEGG analysis suggested that they were mainly involved in the NOD-like receptor signaling pathway, IL-17, lipid and atherosclerosis pathway.

In terms of samples from Mus musculus, the PPI network consists of 171 nodes and 1403 edges (Figure 7B). after taking the intersection of the top 10 hub genes according to 5 kinds of criteria, TYROBP and CSF1R were found to be hub genes, which were enriched in the osteoclast differentiation signaling pathway (Supplementary Figure 12 and Supplementary Table 7). Osteoclasts are involved in calcification formation in atherosclerotic plaques.

Construction of the competing endogenous RNA regulatory network for the hub genes

As shown in Figure 8, a ceRNA coexpression network consisting of 11 lncRNAs, 14 miRNAs, and 6 mRNAs was visualized by a Sankey plot after merging these predicted results. We did not find experimentally validated ceRNAs related to TYROBP in the lncACTdb database.

Results of gene set enrichment analysis

Gene set enrichment analysis (GSEA) was performed to analyze the signaling pathway enrichment in the two groups.

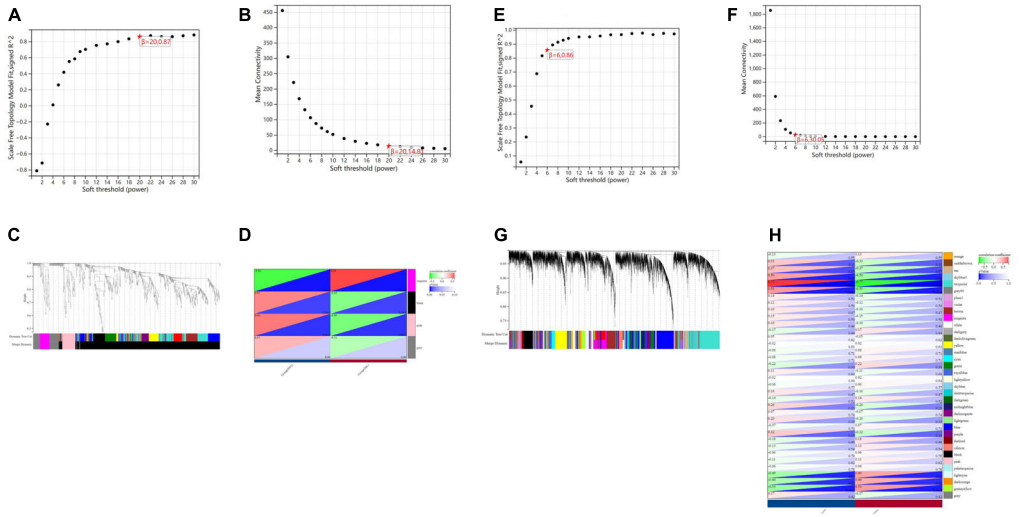

FIGURE 5
Visualization of weighted gene coexpression network analysis (WGCNA) results. **(A)** The scale-free fit index for soft-thresholding powers (human cardiomyocytes samples). **(B)** Mean connectivity (human cardiomyocytes samples). **(C)** Dendrogram of the DEGs clustered (human cardiomyocytes samples). **(D)** Heatmap showing the correlation between TKI and cardiotoxicity (human cardiomyocytes samples). **(E)** The scale-free fit index for soft-thresholding powers (liver samples from Mus musculus). **(F)** Mean connectivitys (liver samples from Mus musculus). **(G)** Dendrogram of the DEGs clustered (liver samples from Mus musculus). **(H)** Heatmap showing the correlation between TKI and atherosclerosis (liver samples from Mus musculus).

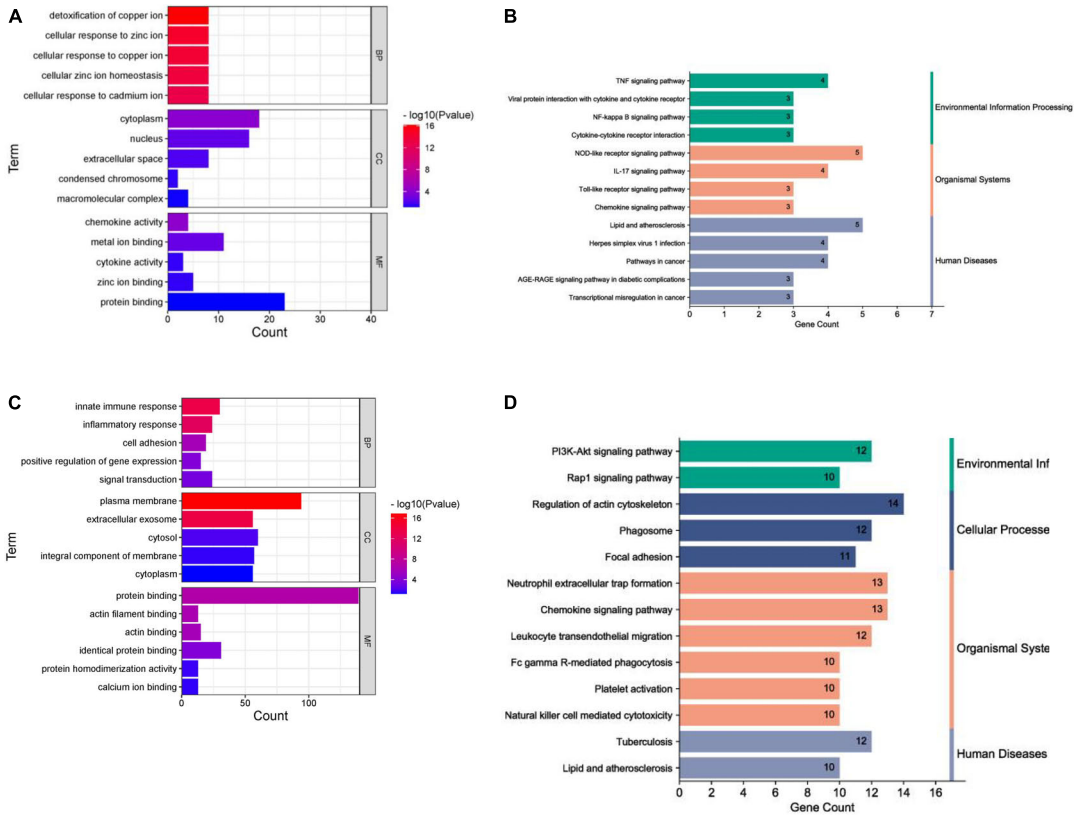

FIGURE 6
Enrichment analysis results. **(A)** GO analysis (human cardiomyocytes samples). **(B)** KEGG analysis (human cardiomyocytes samples). **(C)** GO analysis (liver samples from Mus musculus). **(D)** KEGG analysis (liver samples from Mus musculus).

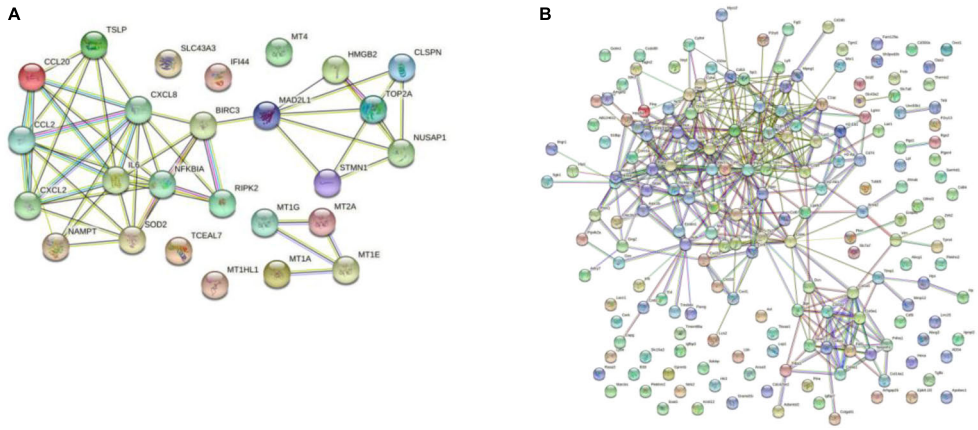

FIGURE 7
Results of the Cytoscape analysis. **(A)** PPI network (human cardiomyocytes samples). **(B)** PPI network (liver samples from Mus musculus).

TABLE 2 Results of the cytoHubba analysis.

node_name	MCC	Degree	EPC	EcCentricity	Betweenness
IL6	432	10	11.80	0.27	31.47
CXCL8	432	10	11.77	0.27	31.47
CCL2	384	8	11.55	0.20	3.63
NFKBIA	288	8	11.65	0.27	14.57
SOD2	168	7	11.43	0.27	12.67
BIRC3	49	6	11.37	0.40	120.50
TYROBP	25563	27	31.03	0.19	1026.7662
CSF1R	24447	19	28.642	0.19	372.18325

FIGURE 8
Sankey plot for ceRNAs.

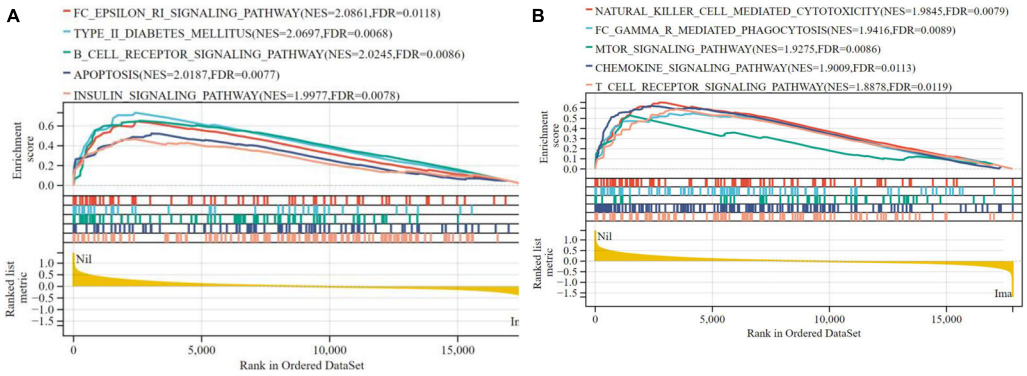

FIGURE 9
Visualized plot for the GSEA for liver samples from Mus musculus (top 10 according to NES). **(A)** Top 1–5 GSEA results and **(B)** Top 6–10 GSEA results.

TABLE 3 The results of GSEA.

Term	ES	NES	pvalue	FDR
FC_EPSILON_RI_SIGNALING_PATHWAY	0.6471	2.0861	0.002	0.0118
TYPE_II_DIABETES_MELLITUS	0.7333	2.0697	0.0068	0.012
B_CELL_RECEPTOR_SIGNALING_PATHWAY	0.6517	2.0245	0.0086	0.018
APOPTOSIS	0.5231	2.0187	0.0077	0.021
INSULIN_SIGNALING_PATHWAY	0.4691	1.9977	0.0078	0.025
NATURAL_KILLER_CELL_MEDIATED_CYTOTOXICITY	0.6578	1.9845	0.0079	0.03
FC_GAMMA_R_MEDIATED_PHAGOCYTOSIS	0.5508	1.9416	0.0089	0.041
MTOR_SIGNALING_PATHWAY	0.5287	1.9275	0.0021	0.0086
CHEMOKINE_SIGNALING_PATHWAY	0.6229	1.9009	0.0113	0.063
T_CELL_RECEPTOR_SIGNALING_PATHWAY	0.5899	1.8878	0.0119	0.072

The enrichment score (ES) and normalized enrichment score (NES) were used to indicate the analysis results across gene sets. The false discovery rate (FDR) was used to judge whether a set was significantly enriched. In human cardiomyocyte samples, no pathway was found to be significantly associated with risk scores in the nilotinib group according to the criteria ($|NES| > 1$, $FDR < 0.25$, NOM $p < 0.05$).

In terms of liver samples from Mus musculus, 10 pathways were found to be significantly associated with risk scores in the nilotinib group, including FC epsilon RI, type II diabetes mellitus, B-cell receptor, apoptosis, insulin, natural killer cell mediated cytotoxicity, FC gamma R mediated phagocytosis, mTOR, chemokine, and T-cell receptor signaling pathways (Figure 9 and Table 3). The results indicated that nilotinib caused atherosclerosis by triggering inflammatory response and abnormal glycolipid metabolism.

Molecular docking simulation

Rosuvastatin effectively bound to the proteins encoded by CCL20, CXCL2, NFKB1A, SOD2, BIRC3, TYROBP, and CSF1R, which were mainly enriched in the TNF and cytokine-cytokine receptor interaction signaling pathways. Aspirin could only bind to the proteins encoded by CCL20, CXCL2, and NFKB1A, which were also enriched in the TNF signaling pathway. The molecular docking scores are presented in Table 4, while the molecular docking is visualized in Figures 10, 11. The results indicated that rosuvastatin might be effective in the treatment of atherosclerosis caused by nilotinib.

TABLE 4 Molecular docking results in terms of the minimum binding energy (kcal/mol).

Targets	Rosuvastatin	Aspirin
CCL2	−6.7	−5.3
IL6	−4.8	−4.6
CXCL8	−4.2	−2.7
CXCL2	−5.6	−5.4
NFKB1A	−6.5	−5.8
SOD2	−5.2	−0.9
BIRC3	−5.6	−4.6
TYROBP	−5.7	−4.3
CSF1R	−6.1	−4.7

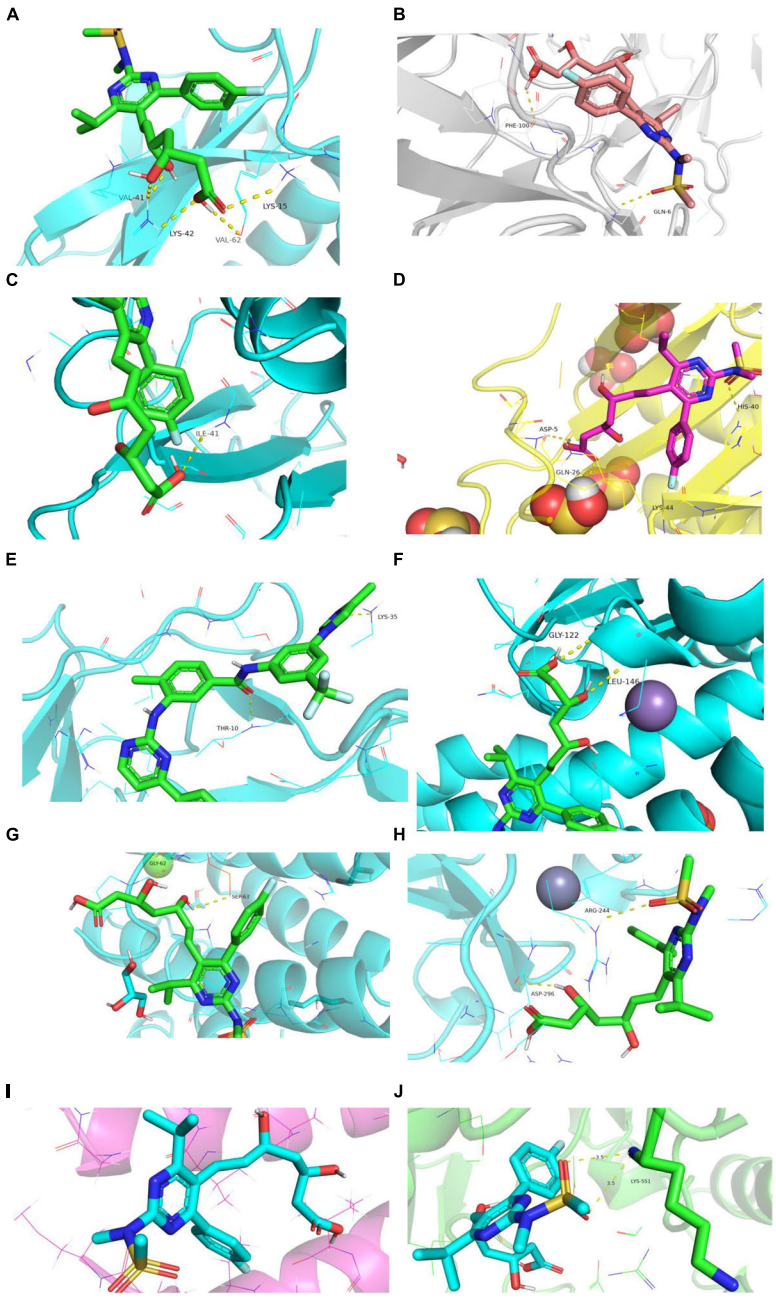

FIGURE 10
Diagram of structural interactions between rosuvastatin and hub targets. **(A)** CXCL8 **(B)** IL6 **(C)** CXCL2 **(D)** CCL20 **(E)** CCL2 **(F)** SOD2 **(G)** NFKBIA **(H)** BIRC3 **(I)** TYROBP **(J)** CSF1R.

Discussion

In this meta-analysis, we conclude that patients who start with nilotinib as first-line treatment have a higher risk of CAE, CAD, ACS, CVA, POAD and arrhythmia than those with imatinib. The evidence suggests that nilotinib is not recommended for patients with advanced age, previous cardiovascular disease or high-risk factors for CAEs. It is essential to screen for vascular risk factors, such as hypertension, hypercholesterolemia, diabetes mellitus (DM), or dyslipidemia, prior to starting nilotinib and to maintain follow-up during treatment. CML patients can be stratified according to the new Systematic Coronary Risk Evaluation (SCORE) scoring system. Patients with high and very high SCORE risk suffered from higher risk of arterial occlusive events (HR = 3.5; 95% CI = 1.4–8.7 and HR = 4.4; 95% CI = 2–9.8, respectively) (42).

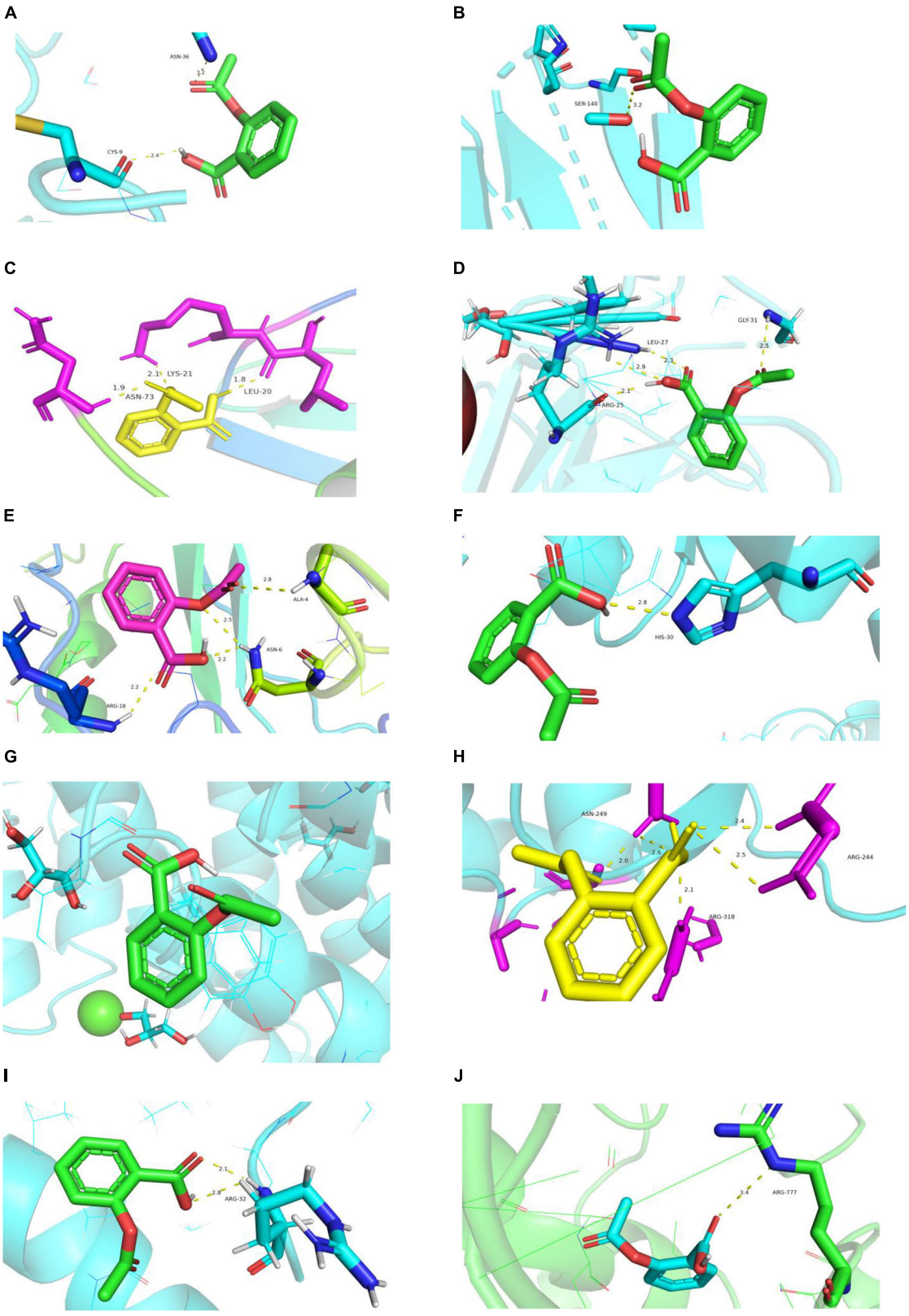

FIGURE 11
Diagram of structural interactions between aspirin and hub targets. **(A)** CXCL8 **(B)** IL6 **(C)** CXCL2 **(D)** CCL20 **(E)** CCL2 **(F)** SOD2 **(G)** NFKBIA **(H)** BIRC3 **(I)** TYROBP **(J)** CSF1R.

Atherosclerosis has been considered the leading cause of CAD, ACS, CVA and POAD. Sudden rupture of vulnerable atherosclerotic plaques that are characterized by large necrotic cores, thin fibrous caps, calcification, and intraplaque hemorrhage can lead to acute cardiovascular adverse events (43). In this article, atherosclerosis caused by the inflammatory response and glycolipid metabolism disorder were considered the key mechanisms for the cardiotoxicity of nilotinib.

Nilotinib can upregulate the expression of cytokines and chemokines, such as CCL2, IL6, CXCL8, CXCL2, CXCL20, TYROBP and CSF1R, leading to a complex cascade that results in the formation and disruption of atherosclerotic plaques. Moreover, nilotinib downregulated the expression of LDLR, VLDLR and IRS1. LDLR is mainly involved in the catabolism of low-density lipoprotein (LDL), while VLDL is mainly involved in endogenous triglyceride transportation. Nilotinib can inhibit the ability of adipose tissue to store lipids, which results in the ectopic accumulation of fat and the development of insulin resistance (44, 45). Type 2 diabetes was also frequently observed in patients treated with nilotinib (8). As insulin receptors, downregulation of IRS1 can lead to insulin resistance, which can accelerate the decomposition of adipose tissue and increase the flow of free fatty acids (FFAs) into the liver (46), leading to the accumulation of diacylglycerol (DAG), activating protein kinase C (PKC), inhibiting the expression of IRS-1, and aggravating IR in the liver (47, 48). In the IR state, a high concentration of FFA can promote the activation of M1-type macrophages in the liver and promote the secretion of chemokines, such as CCL2 (MCP-1), TNF-α, CXCL8, CXCL2, and IL-6, which contribute to the development of atherosclerosis by regulating the activation of leukocytes, the development of foam cells and thrombosis, the proliferation of smooth muscle cells, cell egress from lesions, angiogenesis (49, 50), damage to endothelial cells and vessels (51) and the recruitment of an increasing number of monocytes and macrophages (52, 53). As a transmembrane receptor in neutrophils and monocytes/macrophages (54), TYROBP is involved in macrophage activation, lipid deposition and plaque inflammation. In the bioinformatics analysis reported by Liu et al. (55), Liu et al. (56), Zhang et al. (57), Hao and Wang (58), TYROBP was found to be one of the key Genes Involved in Advanced Atherosclerosis. CSF1R plays an important role in the survival, proliferation and differentiation of macrophages and monocytes.

However, imatinib has a positive impact on glycolipid metabolism. Imatinib can enhance the insulin-mediated vasoreactivity of resistance arteries (59), increase insulin secretion, protect against human beta-cell death (60), and reduce non-alcoholic fatty liver disease by targeting inflammatory and lipogenic pathways. Noa Markovits reported a retrospective cohort study in which long-term use of imatinib significantly reduced HbA1c (0.53%, IQR[0.09,1.19]) and FPG (10.2 mg/dL, IQR[−3.5,32.2]) in patients with diabetes, independent of demographics and glucose-lowering drug utilization, which suggested durable metabolic benefits of imatinib (61).

As the mainstream lipid-lowering drugs, statins can block cholesterol biosynthesis in liver cells enhance the intake and clearance of LDL cholesterol (LDL-C) in blood. Moreover, statins confer cardiovascular benefits through anti-inflammatory effects (62). Rosuvastatin treatment can reduce hs-CRP and IL-6 levels in patients with coronary artery ectasia (63) and inhibit the TLR4/MyD88/NF-$_{K}$B signaling pathway (64). In this article, rosuvastatin was found to bind to most of the hub genes and genes enriched in the lipid and atherosclerosis signaling pathways, which indicates that rosuvastatin may be effective in the treatment of CAE caused by nilotinib.

Our study had several limitations. First, the dosage was an important factor when discussing adverse drug reactions. Six studies did not report the dosage of nilotinib or imatinib, which might lead to some degree of heterogeneity. Second, some studies did not introduce the risk factors or previous history of cardiovascular events of patients included, which might lead to some degree of bias. Third, vascular endothelial cells or cardiomyocytes from CML patients treated with nilotinib or imatinib may provide more information about atherosclerosis related to nilotinib, but no dataset in this respect was found in the GEO database. Fourth, bioinformatics analysis and molecular docking can only suggest the potential mechanism and potential therapeutic drugs, which lacks experimental validation. We will conduct relevant experiments in the future.

Conclusion

This meta-analysis suggests that patients who start with nilotinib as first-line treatment have a higher risk of cardiovascular adverse events than those with imatinib. Atherosclerosis caused by the inflammatory response and glycolipid metabolism disorders are the key mechanisms of nilotinib cardiotoxicity. Rosuvastatin may be beneficial in the treatment of CAE caused by nilitinib.

Author contributions

XN, LS, and JL conceived of the study and design. XN conceived the early ideas for the application of the analysis models and worked on the critical revision of the manuscript. SL and JH collected data, led the analysis and interpretation of findings, and drafted the initial and subsequent versions of the manuscript. XZ and YC helped with data extraction and interpretation. All authors contributed to the analysis and interpretation of the data, revised the manuscript

for important intellectual content, and contributed to the manuscript as presented here.

Funding

This work was supported by the National Natural Science Foundation of China to XN (Grant No. 81803497).

Acknowledgments

We would like to thank all the scholars who have made outstanding contributions to the treatment of CML.

Conflict of interest

The authors declare that the research was conducted in the absence of any commercial or financial relationships that could be construed as a potential conflict of interest.

Publisher's note

All claims expressed in this article are solely those of the authors and do not necessarily represent those of their affiliated organizations, or those of the publisher, the editors and the reviewers. Any product that may be evaluated in this article, or claim that may be made by its manufacturer, is not guaranteed or endorsed by the publisher.

Supplementary material

The Supplementary Material for this article can be found online at: https://www.frontiersin.org/articles/10.3389/fcvm.2022.966182/full#supplementary-material

References

1. Ma Y, Liu X, Bi Y, Wang T, Chen C, Wang Y, et al. Alteration of N6-Methyladenosine mRNA methylation in a human stem cell-derived cardiomyocyte model of tyrosine kinase inhibitor-induced cardiotoxicity. *Front Cardiovasc Med.* (2022) 23:849175. doi: 10.3389/fcvm.2022.849175

2. O'Hare T, Eide CA, Deininger MW. Bcr-Abl kinase domain mutations, drug resistance, and the road to a cure for chronic myeloid leukemia. *Blood.* (2007) 110:2242–9. doi: 10.1182/blood-2007-03-066936

3. Weisberg E, Manley PW, Breitenstein W, Brüggen J, Cowan-Jacob SW, Ray A, et al. Characterization of AMN107, a selective inhibitor of native and mutant Bcr-Abl. *Cancer Cell.* (2005) 7:129–41. doi: 10.1016/j.ccr.2005.01.007

4. Szklarczyk D, Morris JH, Cook H, Kuhn M, Wyder S, Simonovic M, et al. The STRING database in 2017: quality-controlled protein-protein association networks, made broadly accessible. *Nucleic Acids Res.* (2017) 45:D362–8. doi: 10.1093/nar/gkw937

5. Nakamae H, Yamamoto M, Sakaida E, Kanda Y, Ohmine K, Ono T, et al. Nilotinib vs. imatinib in Japanese patients with newly diagnosed chronic myeloid leukemia in chronic phase: 10-year follow-up of the Japanese subgroup of the randomized ENESTnd trial. *Int J Hematol.* (2022) 115:33–42. doi: 10.1007/s12185-021-03216-5

6. Santoro M, Mancuso S, Accurso V, Di Lisi D, Novo G, Siragusa S. Cardiovascular issues in tyrosine kinase inhibitors treatments for chronic myeloid leukemia: a review. *Front Physiol.* (2021) 12:675811. doi: 10.3389/fphys.2021.675811

7. Wang Z, Wang X, Wang Z, Feng Y, Jia Y, Jiang L, et al. Comparison of hepatotoxicity associated with new BCR-ABL tyrosine kinase inhibitors vs imatinib among patients with chronic myeloid leukemia: a systematic review and meta-analysis. *JAMA Netw Open.* (2021) 4:e2120165. doi: 10.1001/jamanetworkopen.2021.20165

8. Racil Z, Koritakova E, Sacha T, Klamova H, Belohlavkova P, Faber E, et al. Insulin resistance is an underlying mechanism of impaired glucose metabolism during nilotinib therapy. *Am J Hematol.* (2018) 93:E342–5. doi: 10.1002/ajh.25232

9. Novo G, Di Lisi D, Bronte E, Macaione F, Accurso V, Badalamenti G, et al. Cardiovascular toxicity in cancer patients treated with tyrosine kinase inhibitors: a real-world single-center experience. *Oncology.* (2020) 98:445–51. doi: 10.1159/000505486

10. Arnett DK, Blumenthal RS, Albert MA, Buroker AB, Goldberger ZD, Hahn EJ, et al. 2019 ACC/AHA guideline on the primary prevention of cardiovascular disease: a report of the American College of Cardiology/American Heart Association Task Force on Clinical Practice Guidelines. *Circulation.* (2019) 140:e596–646. doi: 10.1161/CIR.0000000000000678

11. Pavlović J, Greenland P, Franco OH, Kavousi M, Ikram MK, Deckers JW, et al. Recommendations and associated levels of evidence for statin use in primary prevention of cardiovascular disease: a comparison at population level of the American Heart Association/American College of Cardiology/Multisociety, US Preventive Services Task Force, Department of Veterans Affairs/Department of Defense, Canadian Cardiovascular Society, and European Society of Cardiology/European Atherosclerosis Society Clinical Practice Guidelines. *Circ Cardiovasc Qual Outcomes.* (2021) 14:e007183. doi: 10.1161/CIRCOUTCOMES.120.007183

12. Hussain MA, Saposnik G, Raju S, Salata K, Mamdani M, Tu JV, et al. Association between statin use and cardiovascular events after carotid artery revascularization. *J Am Heart Assoc.* (2018) 7:e009745. doi: 10.1161/JAHA.118.009745

13. Zhang X, Xing L, Jia X, Pang X, Xiang Q, Zhao X, et al. Comparative lipid-lowering/increasing efficacy of 7 statins in patients with dyslipidemia, cardiovascular diseases, or diabetes mellitus: systematic review and network meta-analyses of 50 randomized controlled trials. *Cardiovasc Ther.* (2020) 2020:3987065. doi: 10.1155/2020/3987065

14. Hodkinson A, Tsimpida D, Kontopantelis E, Rutter MK, Mamas MA, Panagioti M. Comparative effectiveness of statins on non-high density lipoprotein cholesterol in people with diabetes and at risk of cardiovascular disease: systematic review and network meta-analysis. *BMJ.* (2022) 376:e067731. doi: 10.1136/bmj-2021-067731

15. Page MJ, McKenzie JE, Bossuyt PM, Boutron I, Hoffmann TC, Mulrow CD, et al. The PRISMA 2020 statement: an updated guideline for reporting systematic reviews. *Syst Rev.* (2021) 10:89. doi: 10.1186/s13643-021-01626-4

16. Stang A. Critical evaluation of the Newcastle-Ottawa scale for the assessment of the quality of nonrandomized studies in meta-analyses. *Eur J Epidemiol.* (2010) 25:603–5. doi: 10.1007/s10654-010-9491-z

17. van Hasselt JGC, Rahman R, Hansen J, Stern A, Shim JV, Xiong Y, et al. Transcriptomic profiling of human cardiac cells predicts protein kinase inhibitor-associated cardiotoxicity. *Nat Commun.* (2020) 11:4809. doi: 10.1038/s41467-020-18396-7

18. Taminau J, Meganck S, Lazar C, Steenhoff D, Coletta A, Molter C, et al. Unlocking the potential of publicly available microarray data using inSilicoDb and inSilicoMerging R/Bioconductor packages. *BMC Bioinformatics.* (2012) 13:335. doi: 10.1186/1471-2105-13-

19. Johnson WE, Li C, Rabinovic A. Adjusting batch effects in microarray expression data using empirical Bayes methods. *Biostatistics.* (2007) 8:118–27. doi: 10.1093/biostatistics/kxj037

20. Pouwer MG, Pieterman EJ, Verschuren L, Caspers MPM, Kluft C, Garcia RA, et al. The BCR-ABL1 inhibitors imatinib and ponatinib decrease plasma cholesterol and atherosclerosis, and nilotinib and ponatinib activate coagulation in a translational mouse model. *Front Cardiovasc Med.* (2018) 5:55. doi: 10.3389/fcvm.2018.00055

21. Sherman BT, Hao M, Qiu J, Jiao X, Baseler MW, Lane HC, et al. DAVID: a web server for functional enrichment analysis and functional annotation of gene lists. *Nucleic Acids Res.* (2022) 50:W216–21. doi: 10.1093/nar/gkac194

22. Ragueneau E, Shrivastava A, Morris JH, Del-Toro N, Hermjakob H, Porras P. IntAct App: a Cytoscape application for molecular interaction network visualization and analysis. *Bioinformatics.* (2021) 37:3684–5. doi: 10.1093/bioinformatics/btab319

23. Wang P, Guo Q, Qi Y, Hao Y, Gao Y, Zhi H, et al. LncACTdb 3.0: an updated database of experimentally supported ceRNA interactions and personalized networks contributing to precision medicine. *Nucleic Acids Res.* (2022) 50:D183–9. doi: 10.1093/nar/gkab1092

24. Subramanian A, Tamayo P, Mootha VK, Mukherjee S, Ebert BL, Gillette MA, et al. Gene set enrichment analysis: a knowledge-based approach for interpreting genome-wide expression profiles. *Proc Natl Acad Sci U.S.A.* (2005) 102:15545–50. doi: 10.1073/pnas.0506580102

25. Zhao X, Zhang L, Wang J, Zhang M, Song Z, Ni B, et al. Correction to: Identification of key biomarkers and immune infiltration in systemic lupus erythematosus by integrated bioinformatics analysis. *J Transl Med.* (2021) 19:64. doi: 10.1186/s12967-021-02728-2

26. Trott O, Olson AJ. AutoDock Vina: improving the speed and accuracy of docking with a new scoring function, efficient optimization, and multithreading. *J Comput Chem.* (2010) 31:455–61. doi: 10.1002/jcc.21334

27. Kantarjian HM, Hughes TP, Larson RA, Kim DW, Issaragrisil S, Le Coutre P. Long-term outcomes with frontline nilotinib versus imatinib in newly diagnosed chronic myeloid leukemia in chronic phase: ENESTnd 10-year analysis. *Leukemia.* (2021) 35:440–53. doi: 10.1038/s41375-020-01111-2

28. Wang J, Shen ZX, Saglio G, Jin J, Huang H, Hu Y, et al. Phase 3 study of nilotinib vs imatinib in Chinese patients with newly diagnosed chronic myeloid leukemia in chronic phase: ENESTchina. *Blood.* (2015) 125:2771–8. doi: 10.1182/blood-2014-09-601674

29. Sicuranza A, Ferrigno I, Abruzzese E, Iurlo A, Galimberti S, Gozzini A, et al. Pro-Inflammatory and pro-oxidative changes during nilotinib treatment in CML patients: results of a prospective multicenter front-line TKIs study (KIARO Study). *Front Oncol.* (2022) 12:835563. doi: 10.3389/fonc.2022.835563

30. Fujioka I, Takaku T, Iriyama N, Tokuhira M, Kimura Y, Sato E, et al. Features of vascular adverse events in Japanese patients with chronic myeloid leukemia treated with tyrosine kinase inhibitors: a retrospective study of the CML cooperative study group database. *Ann Hematol.* (2018) 97:2081–8. doi: 10.1007/s00277-018-3412-8

31. Dahlén T, Edgren G, Ljungman P, Flygt H, Richter J, Olsson-Strömberg U, et al. Adverse outcomes in chronic myeloid leukemia patients treated with tyrosine kinase inhibitors: Follow-up of patients diagnosed 2002-2017 in a complete coverage and nationwide agnostic register study. *Am J Hematol.* (2022) 97:421–30. doi: 10.1002/ajh.26463

32. Petrikova L, Slezakova K, Sninska Z, Harvanova L, Martisova M, Hatalova A, et al. Cardiovascular events and atherogenic lipid profile in chronic myeloid leukemia patients treated with nilotinib versus imatinib. *Bratisl Lek Listy.* (2021) 122:531–7. doi: 10.4149/BLL_2021_085

33. Dahlén T, Edgren G, Lambe M, Höglund M, Björkholm M, Sandin F, et al. Cardiovascular events associated with use of tyrosine kinase inhibitors in chronic myeloid leukemia: a population-based cohort study. *Ann Intern Med.* (2016) 165:161–6. doi: 10.7326/M15-2306

34. Chen MT, Huang ST, Lin CW, Ko BS, Chen WJ, Huang HH, et al. Tyrosine kinase inhibitors and vascular adverse events in patients with chronic myeloid leukemia: a population-based, propensity score-matched cohort study. *Oncologist.* (2021) 26:974–82. doi: 10.1002/onco.13944

35. Jain P, Kantarjian H, Boddu PC, Nogueras-González GM, Verstovsek S, Garcia-Manero G, et al. Analysis of cardiovascular and arteriothrombotic adverse events in chronic-phase CML patients after frontline TKIs. *Blood Adv.* (2019) 3:851–61. doi: 10.1182/bloodadvances.2018025874

36. Kizaki M, Takahashi N, Iriyama N, Okamoto S, Ono T, Usui N, et al. Efficacy and safety of tyrosine kinase inhibitors for newly diagnosed chronic-phase chronic myeloid leukemia over a 5-year period: results from the Japanese registry obtained by the New TARGET system. *Int J Hematol.* (2019) 109:426–39. doi: 10.1007/s12185-019-02613-1

37. Giles FJ, Mauro MJ, Hong F, Ortmann CE, McNeill C, Woodman RC, et al. Rates of peripheral arterial occlusive disease in patients with chronic myeloid leukemia in the chronic phase treated with imatinib, nilotinib, or nontyrosine kinase therapy: a retrospective cohort analysis. *Leukemia.* (2013) 27:1310–5. doi: 10.1038/leu.2013.69

38. Yang YC, Huang RY, Tsai HJ, Li PC, Yang YH, Hsieh KP. Cardiovascular events in patients with chronic myeloid leukemia treated with tyrosine kinase inhibitors in Taiwan: a nationwide population-based study. *Eur J Prev Cardiol.* (2021) 28:zwab043. doi: 10.1093/eurjpc/zwab043

39. Kim TD, Rea D, Schwarz M, Grille P, Nicolini FE, Rosti G, et al. Peripheral artery occlusive disease in chronic phase chronic myeloid leukemia patients treated with nilotinib or imatinib. *Leukemia.* (2013) 27:1316–21. doi: 10.1038/leu.2013.70

40. Bettiol A, Marconi E, Lombardi N, Crescioli G, Gherlinzoni F, Walley T, et al. Pattern of use and long-term safety of tyrosine kinase inhibitors: a decade of real-world management of chronic myeloid leukemia. *Clin Drug Investig.* (2018) 38:837–44. doi: 10.1007/s40261-018-0676-7

41. Yang Q, Wang R, Wei B, Peng C, Wang L, Hu G, et al. Candidate biomarkers and molecular mechanism investigation for glioblastoma multiforme utilizing WGCNA. *Biomed Res Int.* (2018) 2018:4246703. doi: 10.1155/2018/4246703

42. Caocci G, Mulas O, Capodanno I, Bonifacio M, Annunziata M, Galimberti S. Low-density lipoprotein (LDL) levels and risk of arterial occlusive events in chronic myeloid leukemia patients treated with nilotinib. *Ann Hematol.* (2021) 100:2005–14. doi: 10.1007/s00277-020-04392-w

43. Ilyas I, Little PJ, Liu Z, Xu Y, Kamato D, Berk BC, et al. Mouse models of atherosclerosis in translational research. *Trends Pharmacol Sci.* (2022) 43:920–39. doi: 10.1016/j.tips.2022.06.009

44. Sadiq S, Owen E, Foster T, Knight K, Wang L, Pirmohamed M, et al. Nilotinib-induced metabolic dysfunction: insights from a translational study using in vitro adipocyte models and patient cohorts. *Leukemia.* (2019) 33:1810–4. doi: 10.1038/s41375-018-0337-0

45. Fitter S, Vandyke K, Schultz CG, White D, Hughes TP, Zannettino AC. Plasma adiponectin levels are markedly elevated in imatinib-treated chronic myeloid leukemia (CML) patients: a mechanism for improved insulin sensitivity in type 2 diabetic CML patients? *J Clin Endocrinol Metab.* (2010) 95:3763–7. doi: 10.1210/jc.2010-0086

46. Li YC, Qiao JY, Wang BY, Bai M, Shen JD, Cheng YX. Paeoniflorin ameliorates fructose-induced insulin resistance and hepatic steatosis by activating LKB1/AMPK and AKT Pathways. *Nutrients.* (2018) 10:1024. doi: 10.3390/nu10081024

47. Bazotte RB, Silva LG, Schiavon FP. Insulin resistance in the liver: deficiency or excess of insulin? *Cell Cycle.* (2014) 13:2494–500. doi: 10.4161/15384101.2014.947750

48. Ma S, Fan L, Cao F. Combating cellular senescence by sirtuins: implications for atherosclerosis. *Biochim Biophys Acta Mol Basis Dis.* (2019) 1865:1822–30. doi: 10.1016/j.bbadis.2018.06.011

49. Hedayati-Moghadam M, Hosseinian S, Paseban M, Shabgah AG, Gholizadeh J, Jamialahmadi T, et al. The role of chemokines in cardiovascular diseases and the therapeutic effect of curcumin on CXCL8 and CCL2 as pathological chemokines in atherosclerosis. *Adv Exp Med Biol.* (2021) 1328:155–70. doi: 10.1007/978-3-030-73234-9_11

50. Wang Y, Zhang Y, Wang Z, Zhang J, Qiao RR, Xu M, et al. Optical/MRI dual-modality imaging of M1 macrophage polarization in atherosclerotic plaque with MARCO-targeted upconversion luminescence probe. *Biomaterials.* (2019) 219:119378. doi: 10.1016/j.biomaterials.2019.119378

51. Shapouri-Moghaddam A, Mohammadian S, Vazini H, Taghadosi M, Esmaeili SA, Mardani F, et al. Macrophage plasticity, polarization, and function in health and disease. *J Cell Physiol.* (2018) 233:6425–40. doi: 10.1002/jcp.26429

52. McLaren JE, Michael DR, Ashlin TG, Ramji DP. Cytokines, macrophage lipid metabolism and foam cells: implications for cardiovascular disease therapy. *Prog Lipid Res.* (2011) 50:331–47. doi: 10.1016/j.plipres.2011.04.002

53. Momtazi-Borojeni AA, Abdollahi E, Nikfar B, Chaichian S, Ekhlasi-Hundrieser M. Curcumin as a potential modulator of M1 and M2 macrophages: new insights in atherosclerosis therapy. *Heart Fail Rev.* (2019) 24:399–409. doi: 10.1007/s10741-018-09764-z

54. Kobayashi M, Konishi H, Takai T, Kiyama HA. DAP12-dependent signal promotes pro-inflammatory polarization in microglia following nerve injury and exacerbates degeneration of injured neurons. *Glia.* (2015) 63:1073–82. doi: 10.1002/glia.22802

55. Liu C, Zhang H, Chen Y, Wang S, Chen Z, Liu Z, et al. Identifying RBM47, HCK, CD53, TYROBP, and HAVCR2 as hub genes in advanced atherosclerotic plaques by network-based analysis and validation. *Front Genet.* (2021) 11:602908. doi: 10.3389/fgene.2020.602908

56. Liu Y, Huan W, Wu J, Zou S, Qu L. IGFBP6 is downregulated in unstable carotid atherosclerotic plaques according to an integrated bioinformatics analysis and experimental verification. *J Atheroscler Thromb.* (2020) 27:1068–85. doi: 10.5551/jat.52993

57. Zhang L, Gu J, Wang S, He F, Gong K. Identification of key differential genes in intimal hyperplasia induced by left carotid artery ligation. *PeerJ.* (2022) 10:e13436. doi: 10.7717/peerj.13436

58. Huo TM, Wang ZW. Comprehensive analysis to identify key genes involved in advanced atherosclerosis. *Dis Markers.* (2021) 2021:4026604. doi: 10.1155/2021/4026604

59. Box CVJ, Sandhu AK, Turaihi AH, Xiaoké P, Dallinga-Thie G, Aman J, et al. Effects of imatinib on vascular insulin sensitivity and free fatty acid transport in early weight gain. *PLoS One.* (2021) 16:e0250442. doi: 10.1371/journal.pone.0250442

60. AlAsfoor S, Rohm TV, Bosch AJT, Dervos T, Calabrese D, Matter MS, et al. Imatinib reduces nonalcoholic fatty liver disease in obese mice by targeting inflammatory and lipogenic pathways in macrophages and liver. *Sci Rep.* (2018) 8:15331. doi: 10.1038/s41598-018-32853-w

61. Markovits N, Kurnik D, Friedrich C, Gueta I, Halkin H, David S, et al. Effects of imatinib on glycemic and lipid profiles: a retrospective cohort study. *Leuk Lymphoma.* (2022) 63:2224–32. doi: 10.1080/10428194.2022.2068003

62. Kao TW, Huang CC. Inflammatory burden and immunomodulative therapeutics of cardiovascular diseases. *Int J Mol Sci.* (2022) 23:804. doi: 10.3390/ijms23020804

63. Fan CH, Hao Y, Liu YH, Li XL, Huang ZH, Luo Y, et al. Anti-inflammatory effects of rosuvastatin treatment on coronary artery ectasia patients of different age groups. *BMC Cardiovasc Disord.* (2020) 20:330. doi: 10.1186/s12872-020-01604-z

64. Koushki K, Shahbaz SK, Mashayekhi K, Sadeghi M, Zayeri ZD, Taba MY, et al. Anti-inflammatory action of statins in cardiovascular disease: the role of inflammasome and toll-like receptor pathways. *Clin Rev Allergy Immunol.* (2021) 60:175–99. doi: 10.1007/s12016-020-08791-9

frontiers | Frontiers in Cardiovascular Medicine

TYPE Original Research
PUBLISHED 05 January 2023
DOI 10.3389/fcvm.2022.974402

OPEN ACCESS

EDITED BY
Feng Cao,
People's Liberation Army General Hospital, China

REVIEWED BY
Zhenyu Huo,
Guangzhou Medical University, China
Danilo Menichelli,
Sapienza University of Rome, Italy
Alice Giontella,
University of Verona, Italy

*CORRESPONDENCE
Wei Wang
✉ wangwei9500@hotmail.com;
✉ wwei9500@smu.edu.cn

†These authors share co-first authorship

SPECIALTY SECTION
This article was submitted to Cardio-Oncology, a section of the journal Frontiers in Cardiovascular Medicine

RECEIVED 21 June 2022
ACCEPTED 07 December 2022
PUBLISHED 05 January 2023

CITATION
Li W, Huang M, Wang R and Wang W (2023) Impact of genetically predicted atrial fibrillation on cancer risks: A large cardio-oncology Mendelian randomization study using UK biobank. *Front. Cardiovasc. Med.* 9:974402. doi: 10.3389/fcvm.2022.974402

Impact of genetically predicted atrial fibrillation on cancer risks: A large cardio-oncology Mendelian randomization study using UK biobank

Wenjie Li[1†], Mingkai Huang[2†], Rong Wang[1] and Wei Wang[1*]

[1]Department of Radiation Oncology, Nanfang Hospital, Southern Medical University, Guangzhou, China, [2]Department of Cardiology, Union Hospital, Tongji Medical College, Huazhong University of Science and Technology, Wuhan, China

Background: Increasing incidences of both atrial fibrillation (AF) and cancer have been observed in recent years. However, the casual association of both serious conditions has been scarcely evaluated and is considered to be a blank slate in cardio-oncology. Thus, we introduced Mendelian randomization (MR) methods to estimate the effects of AF on cancer risks.

Methods: We performed univariable and multivariable two-sample MR analyses to evaluate the effects of AF on the risk of 19 site-specific types of cancer. This MR study was conducted based on 111 independent AF-associated genetic instruments from genome-wide association studies and summarized-level data from corresponding cancer consortia. Multiple sensitivity analyses, including the leave-one-out analysis, MR-Egger regression, and MR-PRESSO tests, were further performed to examine the potential directional pleiotropic effects. Functional annotation was performed for common differentially expressed genes of AF and prostate cancer (PCA).

Results: A total of 6,777,155 European-descent people, including 533,725 cases and 6,243,430 controls, were included in the present MR analysis. Univariable MR analyses demonstrated a causal effect of AF on the incidence of PCA [odds ratio (OR): 0.96; 95% confidence interval (CI) 0.92–0.99, $p = 0.01$], and the causal effect remained significant (OR: 0.65; 95% CI 0.47–0.90, $p = 0.01$) after adjusting for potential confounders through the multivariable MR approach. However, no casual associations between AF and the other 18 site-specific cancer risks were observed (all p-values were > 0.05). The consistency of outcomes across complementary sensitivity MR methods further supported the causality. The functional analysis emphasized the essential role of antioxidant and xenobiotic catabolic processes in AF and PCA.

Conclusion: Contrary to the findings of several previous observational studies, our comprehensive MR analyses did not corroborate a causal role for AF in increasing the risk of various types of cancer. They did, however, demonstrate that AF may decrease the risk of PCA. Studies from larger sample sizes and

individuals with different ethnic backgrounds are required to further support our conclusions.

KEYWORDS

cancer, Mendelian randomization, single-nucleotide polymorphism, atrial fibrillation, prevention

1. Introduction

Atrial fibrillation (AF) is the most common cardiac arrhythmia (1) that imposes a substantial risk of death from many cardiovascular diseases and huge societal healthcare burdens. It is presumed that 6–12 million people will develop AF in the USA by 2050 and 17.9 million citizens in Europe by 2060 (2). Interestingly, a recent prospective cohort study has reported that cancer is the leading causes of death in high-income countries, accounting for two times as many deaths as cardiovascular diseases (3). Moreover, abundant evidence based on large populations shows that patients with cancer are related to an increased incidence of AF (4). However, the effect of AF on cancer risks is an uncharted field in cardio-oncology (5). Given the unacceptably high prevalence and treatment costs of both serious conditions, cardio-oncology should not be only concerned with the cardiac side effects of antineoplastic drugs in this case (6). Thus, a specific study is urgently required to find the potential associations between AF and cancer risks, which may provide new insights into the possible mechanisms and therapeutic targets.

Several observational studies have described the ambiguous effects of AF on types of cancer (7–12) due to shared risk factors and predisposing biological processes (13, 14). Prior evidence shows that patients with new-onset AF would have a noticeably increased risk of a malignant diagnosis (7), which was consistent with those of population-based cohort studies that showed that AF was related to a higher malignant incidence (8, 9, 11). However, several intrinsic methodological limitations in prior study designs may impact the observed results, thus resulting in contradictory conclusions. It is difficult, for example, for observational studies to rule out several important lifestyle differences or residual confounders (e.g., smoking, alcohol consumption, diabetes, or hypertension) in both AF and types of cancer (14). Moreover, observational results suggest that an observed association might be attributable to instances associated with a cancer diagnosis and detection bias instead of a causal relationship (9). Consequently, there is an urgent need for a reliable study design that will assess the exact causal association between AF and cancer risks.

Mendelian randomization (MR) analysis has recently become a promising and novel epidemiological approach to assess the causal relationship between exposures and outcomes, using genetic variants as instrumental variables (IVs). Adopting genetic variants as the IVs in the MR analysis can make it less susceptible to reverse causality and hypothetical confounders. A two-sample MR analysis can be performed with robust statistical power using summary-level data from large genome-wide association studies (GWAS) (15). Hence, to solve the aforementioned issue regarding AF and types of cancer, we aimed to evaluate the causal relationship between AF and the risks of 19 site-specific types of cancer with univariable and multivariable two-sample MR methods. Given the tight association between AF and heart failure (HF) (16), we also evaluated the causality between HF and cancer risks.

2. Method

2.1. Mendelian randomization assumptions

To enable a valuable interpretation, all analyses in our MR study were based on the following three core hypotheses or study designs (17): (i) the IVs were convincingly correlated with exposures, (ii) the IVs influenced tumors only through their effects on exposures, and (iii) the IVs were independent of any confounders from the AF/HF cancer association (Figure 1A).

2.2. Selection of genetic instruments for exposures

The flowchart of this study is shown in Figure 1B. Exposures considered in this analysis included AF and HF. Variant AF/HF relationships were derived and manually extracted from the available summary-level GWAS. Nielsen et al. (18) carried out a GWAS with 60,620 AF cases and 970,216 controls to distinguish genetic variations. This study was mainly derived from six

Abbreviations: AF, atrial fibrillation; ANP, atrial natriuretic peptide; CIs, confidence intervals; DEG, differentially expressed gene; GWAS, genome-wide association study; GO, Gene Ontology; HF, heart failure; IVW, inverse-variance weighted; KEGG, Kyoto Encyclopedia of Genes and Genomes; LD, linkage disequilibrium; MR, Mendelian randomization; OR, odds ratio; PCA, prostate cancer; MR-PRESSO, MR Pleiotropy Residual Sum and Outlier; SNP, single-nucleotide polymorphism.

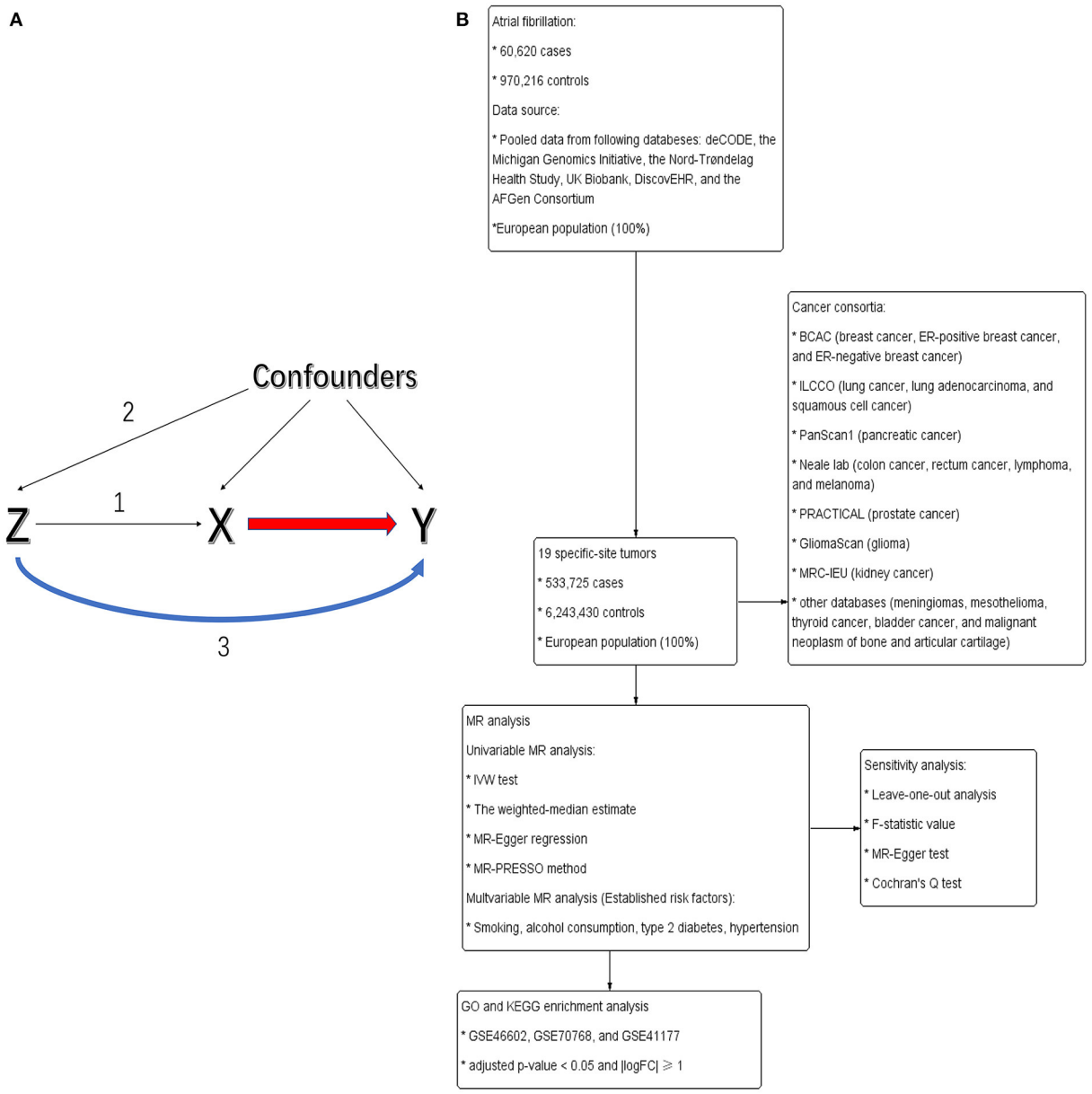

FIGURE 1
(A) Directed acyclic graph portraying the design of Mendelian randomization and potential pleiotropy. Genetic variants (Z) served as genetic instruments to evaluate whether exposures (X) were causally related to outcomes (Y). Numbers 1–3 represent assumptions 1–3. **(B)** The flowchart of this study.

databases [deCODE, the Michigan Genomics Initiative (MGI), the Nord-Trøndelag Health Study (HUNT), UK Biobank, DiscovEHR, and the AFGen Consortium]. All enrolled patients were of European descent and generally elder people (the median age at first AF diagnosis: MGI: 65; deCODE: 74; HUNT: 76). The genetic variation of HF was derived from a GWAS meta-analysis of HF comprising 47,309 European-descent cases and 930,014 controls from the Heart Failure Molecular Epidemiology for Therapeutic Targets Consortium (19).

Given that the violation of three MR assumptions may lead to unreliable conclusions, the following steps would help choose the best IVs. First, we extracted accessible summary-level data from Nielsen et al. (18) and Sonia et al. (19) and set up a significance threshold of $p < 5 \times 10^{-8}$. Detailed information about AF/HF-related single-nucleotide polymorphisms (SNPs) is shown in Supplementary Table 1. To measure genetic correlation, we further conducted a linkage disequilibrium (LD) clumping test at an $R^2 < 0.001$ and

10,000 kb window to preserve the SNPs that were most robustly associated with the AF/HF for downstream analysis. To exclude bias from weak instruments, the F-statistic value was assessed on the bias of the formula $F = \frac{R2(N-k-1)}{k(1-R2)}$, where R^2 is the proportion of variance explained by the IVs, k and N are the number of SNPs and enrolled patients, respectively. F-statistic values > 10 were robust enough to avoid weak instrument bias. Eventually, several SNPs were excluded to eradicate the genetic bias created by palindromes with intermediate allele frequencies (20), and we created a total of 111 and 12 SNPs as the original AF- and HF-IVs, respectively.

2.3. Study participants of various types of cancer

To obtain genetic data for 19 site-specific tumors, we analyzed the following European cancer consortia: Breast Cancer Association Consortium (BCAC) (21) (breast cancer: 122,977 patients and 105,974 controls; ER-positive breast cancer: 69,501 patients and 105,974 controls; and ER-negative breast cancer: 21,468 patients and 105,974 controls), Prostate Cancer Association Group to Investigate Cancer Associated Alterations in the Genome (PRACTICAL) (22) [prostate cancer (PCA): 79,148 patients and 61,106 controls], International Lung Cancer Consortium (ILCCO) (23) (lung cancer: 11,348 patients and 15,861 controls, lung adenocarcinoma: 3,442 patients and 14,895 controls; and squamous cell cancer: 3,275 patients and 15,038 controls), PanScan1 (24) (pancreatic cancer: 1,896 patients, 1,939 controls), GliomaScan (25) (glioma: 6,811 patients, 1,856 controls), the Medical Research Council-Integrative Epidemiology Unit (MRC-IEU) consortium (kidney cancer: 1,114 patients, 461,896 controls; pancreatic cancer: 1,114 patients, 461,896 controls; rectum cancer: 1,470 patients, 461,540 controls), Neale lab (colon cancer: 2,437 patients, 358,757 controls; lymphoma: 1,752 patients, 359,442 controls; melanoma: 3,598 patients, 459,335 controls), and other databases (malignant neoplasm of bone and articular cartilage: 119 patients, 174,006 controls; thyroid cancer: 989 patients, 174,006 controls; bladder cancer: 1,279 patients, 372,016 controls; mesothelioma: 133 patients, 174,006 controls; meningiomas: 455 patients, 86,713 controls) (Table 1).

2.4. Statistical analysis of MR estimates

All MR analyses were performed in R 4.0.5 using the package TwoSampleMR (version 0.5.0).

2.4.1. Two-sample MR method

We performed the inverse-variance weighted (IVW) test, which can provide a coherent estimation of the causality between genetically determined exposures and outcomes. It is made up of a meta-analysis of a single SNP's Wald ratio between the exposures and outcomes using a random-effects inverse-variance method, which can weigh every single Wald ratio according to its standard error to judge potential measurable heterogeneity (20). The causal effects were calculated and presented in the form of odds ratios (ORs) with 95% confidence intervals (CIs) for 14 site-specific types of cancer. Two-sided p-values < 0.05 were considered to be statistically significant. Of note, the results of IVW tests might be biased given the horizontal pleiotropy in invalid instrumental variables. Hence, the MR-Egger regression and the weighted-median estimate were conducted to predominantly assess the MR outcomes (20, 26). The MR-Egger regression can amend the IVW test by allowing a nonzero intercept that can provide an exploration of pleiotropy and an evaluation of the causality adjusted for pleiotropy (20). The weighted-median analysis is used to pool the median effects of all SNPs and can return an unbiased estimate once 50% of the SNPs are valid instruments (20). Finally, the MR Pleiotropy Residual Sum and Outlier (MR-PRESSO) test was conducted using the "MRPRESSO" R package to distinguish outlying SNPs that may result in horizontal pleiotropy and causal effects.

2.4.2. Multivariable MR analysis

To support the univariate MR results and the third assumption, multivariable MR analyses adjusted for confounders, including smoking (trait ID: ukb-a-225), alcohol consumption (trait ID: ukb-d-20117_2), type 2 diabetes (trait ID: ebi-a-GCST006867), and hypertension (trait ID: ukb-b-14057) were introduced. Multivariable MR showed that the SNPs used in univariate MR analyses were also related to these confounders. Then, multivariable MR estimated the effects of each exposure on a single outcome. That is, this can simultaneously assess the effects of all risk factors that share a set of overlapping SNPs and make sure that the direct effects of each exposure on outcomes will not be mediated by other factors (27). As we included MR analyses of 19 site-specific types of cancer, a Bonferroni-adjusted p-value less than the threshold (i.e., 0.05/19 = 0.0026) was deemed as a significant causality to adjust for multiple-comparison tests. A potential relationship was considered significant if a p-value is between 0.05 and 0.0026.

2.5. Pleiotropy and sensitivity analysis

We conducted the leave-one-out analyses to assess whether the results of the IVW tests would be biased by single-sensitive SNPs (26). The aforementioned Egger intercept analysis was then performed to estimate the horizontal pleiotropy. The MR-heterogeneity analysis was ultimately performed to single

TABLE 1 Details of studies in the present Mendelian randomization analyses.

Phenotype	Consortium	Sample size	Number of patients	Number of controls	Number of variants	GWAS Trait ID	Ethnicity	F-statistic
Exposure								
Atrial fibrillation	NA	103,0836	60,620	970,216	33,519,037	ebi-a-GCST006414	European	NA
Heart failure	NA	977,323	47,309	930,014	77,73,021	ebi-a-GCST009541	European	NA
Outcome								
Overall cancer	UK Biobank	4,42239	70,223	3,72,016	12,321,875	ieu-b-4966	European	277.9
Breast cancer	BCAC	228,951	122,977	105,974	10,680,257	ieu-a-1126	European	281
ER+ breast cancer	BCAC	175,475	69,501	105,974	10,680,257	ieu-a-1127	European	281
ER– breast cancer	BCAC	127,442	21,468	105,974	10,680,257	ieu-a-1135	European	281
Lung cancer	ILCCO	85,716	29,266	56,450	89,45,893	ieu-a-966	European	281.4
Lung adenocarcinoma	ILCCO	66,756	11,273	55,483	88,81,354	ieu-a-965	European	281.4
Squamous cell lung cancer	ILCCO	63,053	7,426	55,627	88,93,750	ieu-a-967	European	281.4
Prostate cancer	PRACTICAL	140,254	79,148	61,106	19,733,911	ebi-a-GCST006085	European	273.8
Glioma	GliomaScan	6,811	1,856	4,955	309,636	ieu-a-1013	European	326
Kidney cancer	MRC-IEU	463,010	1,114	461,896	98,51,867	ukb-b-1316	European	275.6
Pancreatic cancer	MRC-IEU	46,3010	233	462,777	521,863	ieu-a-822	European	369.1
Rectum cancer	MRC-IEU	463010	1470	461540	9851867	ukb-b-1251	European	261.2
Lymphoma	Neale Lab	361,194	1,752	359,442	361,194	ukb-d-C_LYMPHOMA	European	273.8
Melanoma	Neale Lab	337,159	2,677	334,482	10,855,955	ukb-d-C3_MELANOMA_SKIN	European	273.8
Colon cancer	Neale Lab	36,1194	2,437	358,757	10,788,369	ukb-d-C3_COLON	European	349.6
Mesothelioma	NA	17,4139	133	174,006	16,380,303	finn-b-C3_MESOTHELIOMA_EXALLC	European	293.8
Meningiomas	NA	87,168	455	86,713	16,152,119	finn-a-CD2_BENIGN_MENINGES_EXALLC	European	NA
Thyroid cancer	NA	17,4995	989	174,006	16,380,316	finn-b-C3_THYROID_GLAND_EXALLC	European	293
Bladder cancer	NA	373,295	1,279	372,016	99,049,26	ieu-b-4874	European	290
Malignant neoplasm of bone and articular cartilage	NA	174,125	119	174,006	16,380,303	finn-b-C3_BONE_CARTILAGE_EXALLC	European	293.8

MR, Mendelian Randomization; GWAS, Genome Wide Association Study; BCAC, Breast Cancer Association Consortium; ILCCO, International Lung Cancer Consortium; PRACTICAL, Prostate Cancer Association Group to Investigate Cancer Associated Alterations in the Genome; MRC-IEU, Medical Research Council-Integrative Epidemiology Unit; NA, not available.

10.3389/fcvm.2022.974402

out SNPs that were responsible for heterogeneity in casual estimation by means of Cochran's *Q*-test (28).

2.6. Identification and enrichment analyses of DEGs

Two PCA-related microarray datasets [GSE46602 (29) and GSE70768 (30)] and one AF-related dataset [GSE41177 (31)] were downloaded from the GEO (http://www.ncbi.nlm.nih.gov/geo) database to select differentially expressed genes (DEGs). Herein, genes with an adjusted *p*-value of < 0.05 and $|\log FC| \geq 1$ were considered DEGs. Gene Ontology (GO) and Kyoto Encyclopedia of Genes and Genomes (KEGG) pathway were performed to explore the potential biological functions of DEGs.

3. Results

In general, this MR study included a total of 6,334,916 European-descent people, with 463,502 cases and 5,871,414 controls (Table 1). Considering the variation in sample sizes of different cancers, *F*-statistics values in this study ranged from 273.8 to 369.1. The instruments ($F > 100$) used in our MR analyses were very strong to avoid bias (Table 1). All the MR evaluations for multi-polymorphism scores are shown in Tables 2, 3. Our results indicated that the genetically predicted AF was associated with a decreased risk of cancers of PCA and found no detrimental effects of AF/HF on the other 18 site-specific cancer risks (Tables 2, 3). The estimated effect sizes of the SNPs on both exposure (AF) and outcomes (PCA, breast cancer, lung cancer, and kidney cancer) are displayed in scatterplots (Figure 2).

3.1. Association of genetic liability to exposures with cancer risks

3.1.1. Univariable MR results

The results of the IVW test revealed a suggestive association of genetic liability to AF and PCA (OR = 0.96; 95% CI 0.92–0.99, $p = 0.01$) (Table 2). However, no relationships of genetic liability to AF with lower odds of breast cancer (OR = 1.003; 95% CI 0.97–1.035, $p = 0.87$), ER-negative breast cancer (OR = 1.009; 95% CI 0.96–1.06, $p = 0.7$), ER-positive breast cancer (OR = 0.99; 95% CI 0.96–1.03, $p = 0.76$), lung cancer (OR = 1.00; 95% CI 0.94–1.06, $p = 0.97$), lung adenocarcinoma (AF: OR = 1.01; 95% CI 0.93–1.10, $p = 0.76$), and squamous cell lung cancer (OR = 1.004; 95% CI 0.92–1.10, $p = 0.93$) were observed. Regarding other 12 site-specific types of cancer, limited evidence validated a causal association of genetic liability to AF with the risk of kidney cancer (OR = 1.0001; 95% CI 0.9996–1.0006, $p = 0.71$), melanoma (OR = 1.0003; 95% CI 0.9999–1.0011, $p = 0.93$), lymphoma (OR = 1.00016; 95% CI 0.995–1.00049, $p = 0.95$), glioma (OR = 1.15; 95% CI 0.97–1.36, $p = 0.12$), colon cancer (OR = 0.9998; 95% CI 0.9992–1.0004, $p = 0.44$), rectum cancer (OR = 1.0002; 95% CI 0.9997–1.00068, $p = 0.27$), meningiomas (OR = 0.95; 95% CI 0.76–1.18, $p = 0.65$), thyroid cancer (OR = 0.95; 95% CI 0.84–1.09, $p = 0.48$), and bladder cancer (OR = 0.9999; 95% CI 0.9996–1.00038, $p = 0.9$); malignant neoplasm of bone and articular cartilage (OR = 0.78; 95% CI 0.54–1.13, $p = 0.2$); and mesothelioma (OR = 1.24; 95% CI 0.85–1.81, $p = 0.27$) (Table 2). Some outliers were observed with the MR-PRESSO analysis, and the results remained in line with the original ones after removing these outliers (Supplementary Table 2). Additionally, we also found no associations between HF and 19 site-specific cancer risks (Table 3).

3.1.2. Multivariable MR analysis

As illustrated in Figure 3 and Supplementary Table 3, after adjusting for potential pleiotropic or mediating effects, multivariable MR still expounded strong independent associations between genetic predisposition to AF and PCA (OR = 0.94; 95% CI 0.90–0.98, $p = 0.0048$) and yielded similar results that AF was not associated with the increased risk of other site-specific cancer types.

3.2. Assessment of MR assumptions

The first assumption was met because our included SNPs were selected at the genome-wide significance threshold of $p < 5 \times 10^{-8}$ and *F*-statistics values ranged from 273.8 to 369.1 ($F > 100$). Leave-one-out analysis suggested that individual SNPs had no impact on the overall effect of AF on cancer risks. Moreover, the MR-Egger regression analysis suggested that the impact of pleiotropy was negligible because intercepts were not statistically significant (all *p*-values$>$0.05) (Supplementary Table 4). Sensitive analyses demonstrated that the second MR assumption was not violated. Although the Cochrane *Q*-tests showed certain horizontal pleiotropy, little influence affected the overall results because no pleiotropy biased the results of the MR-Egger and MR-PRESSO tests (32). With regard to the third MR assumption, multivariable MR and MR-PRESSO analyses eliminated pleiotropic effects, which abided by the third MR assumption.

3.3. Analysis of the functional characteristics of common DEGs

In total, 51 common DEGs between AF-related and PCA-related datasets were identified (Figure 4A). Results of the KEGG pathway demonstrated that several significant

TABLE 2 Mendelian randomization estimates of the casual relationships between atrial fibrillation and cancer risks.

Exposure	nSNPs	IVW method		Weighted median method		MR–Egger	
		OR (95% CI)	P-value	OR (95% CI)	P-value	OR (95% CI)	P-value
Overall cancer	107	1.0025 (0.9999–1.0052)	0.06	1.0017 (0.9974–1.0060)	0.4	1.0051 (0.9999–1.01)	0.06
Breast cancer	99	1.0026 (0.97–1.035)	0.87	1.00 (0.97–1.028)	0.87	1.026 (0.96–1.090)	0.41
ER+ breast cancer	99	0.99 (0.96–1.030)	0.76	0.98 (0.94–1.025)	0.42	1.014 (0.95–1.084)	0.69
ER– breast cancer	99	1.0089 (0.96–1.060)	0.73	0.99 (0.92–1.06)	0.7	1.07 (0.97–1.18)	0.16
Lung cancer	104	1.00 (0.94–1.060)	0.97	1.049 (0.96–1.14)	0.3	1.019 (0.91–1.14)	0.75
Lung adenocarcinoma	104	1.01 (0.93–1.10)	0.76	1.06 (0.92–1.20)	0.42	1.05 (0.90–1.24)	0.52
Squamous cell lung cancer	104	1.004 (0.92–1.10)	0.93	1.02 (0.88–1.18)	0.78	0.98 (0.83–1.17)	0.85
Prostate cancer	108	0.96 (0.92–0.99)	**0.01**	0.96 (0.92–1.0080)	0.11	0.94 (0.88–1.0040)	0.07
Glioma	50	1.15 (0.97–1.36)	0.12	1.22 (0.93–1.59)	0.14	1.24 (0.92–1.66)	0.16
Kidney cancer	44	1.000096 (0.9996–1.00060)	0.71	1.0003 (0.9996–1.001)	0.42	0.9997 (0.9984–1.0010)	0.67
Pancreatic cancer	52	0.87 (0.72–1.06)	0.16	0.83 (0.62–1.10)	0.19	0.78 (0.57–1.09)	0.15
Lymphoma	108	1.00016 (0.995–1.00049)	0.95	0.9995 (0.9987–1.00036)	0.27	0.9997 (0.9988–1.00063)	0.52
Melanoma	108	1.00036 (1.00–1.0010)	0.27	1.0010 (1.00–1.0020)	**0.045**	1.0011 (1.00–1.0020)	0.07
Colon cancer	108	0.9998 (0.9992–1.0004)	0.44	0.9990 (0.9980–1.00)	**0.041**	0.9995 (0.9983–1.0006)	0.39
Malignant neoplasm of bone and articular cartilage	106	0.78 (0.54–1.13)	0.2	0.71 (0.37–1.37)	0.31	0.75 (0.37–1.53)	0.43
Mesothelioma	106	1.24 (0.85–1.81)	0.27	1.25 (0.64–2.43)	0.51	1.02 (0.49–2.12)	0.96
Rectum cancer	61	1.002 (0.9997–1.00068)	0.5	1.009 (0.9994–1.00094)	0.61	1.000065 (0.9986–1.0015)	0.93
Meningiomas	83	0.95 (0.76–1.18)	0.65	0.90 (0.61–1.31)	0.57	0.87 (0.58–1.31)	0.50
Thyroid cancer	106	0.95 (0.84–1.09)	0.48	1.02 (0.8–1.3)	0.88	0.90 (0.70–1.15)	0.4
Bladder cancer	107	0.9999 (0.9996–1.00038)	0.9	0.9999 (0.9991–1.00065)	0.76	0.9993 (0.9986–1.00014)	0.11

The bold values are statistically significant ($p < 0.05$).

10.3389/fcvm.2022.974402

Frontiers in Cardiovascular Medicine

TABLE 3 Mendelian randomization estimates of the associations between heart failure and cancer risks.

Exposure	nSNPs	IVW method		Weighted median method		MR–Egger	
		OR (95% CI)	P-value	OR (95% CI)	P-value	OR (95% CI)	P-value
Overall cancer	9	0.99 (0.98–1.01)	0.56	1.0053 (0.99–1.02)	0.45	1.03 (0.99–1.07)	0.19
Breast cancer	9	0.93 (0.65–1.31)	0.66	1.065 (0.93–1.23)	0.38	1.35 (0.47–3.86)	0.59
ER+ breast cancer	9	0.95 (0.67–1.32)	0.75	1.00 (0.85–1.17)	0.96	1.31 (0.47–3.38)	0.62
ER– breast cancer	9	0.90 (0.61–1.34)	0.61	0.94 (0.69–1.28)	0.71	1.07 (0.31–3.66)	0.91
Lung cancer	9	1.0081 (0.75–1.35)	0.96	1.03 (0.75–1.41)	0.85	0.64 (0.28–1.44)	0.32
Lung adenocarcinoma	9	1.042 (0.64–1.70)	0.87	1.12 (0.67–1.86)	0.67	0.62 (0.15–0.59)	0.53
Squamous cell lung cancer	9	1.10 (0.77–1.56)	0.60	1.32 (0.83–2.11)	0.24	0.53 (0.20–1.44)	0.25
Prostate cancer	9	1.11 (0.92–1.35)	0.25	1.09 (0.94–1.28)	0.25	1.58 (0.94–2.66)	0.13
Glioma	6	0.78 (0.30–2.01)	0.61	1.33 (0.52–3.39)	0.55	3.88 (0.14–111.11)	0.47
Kidney cancer	2	0.9979 (0.9922–1.0036)	0.48	NA	NA	NA	NA
Pancreatic cancer	6	2.11 (0.41–10.87)	0.37	0.99 (0.37–2.64)	0.99	0.14 (0.00051–40.12)	0.54
Lymphoma	NA	NA	NA	NA	NA	NA	NA
Melanoma	9	1.00054 (0.9978–1.0034)	0.71	0.9996 (0.9959–1.0033)	0.82	1.0065 (0.9989–1.014)	0.14
Colon cancer	9	0.9984 (0.9959–1.00092)	0.21	0.9986 (0.9955–1.0018)	0.4	1.00054 (0.9933–1.0078)	0.89
Malignant neoplasm of bone and articular cartilage	9	0.33 (0.06–1.83)	0.21	0.25 (0.026–2.45)	0.23	0.08 (0.00047–12.14)	0.35
Mesothelioma	9	0.61 (0.12–3.09)	0.55	0.73 (0.09–5.67)	0.76	2.19 (0.017–279.04)	0.76
Rectum cancer	2	0.9975 (0.9940–1.0011)	0.18	NA	NA	NA	NA
Meningiomas	8	0.93 (0.33–2.58)	0.88	0.65 (0.19–2.21)	0.49	0.71 (0.028–18.015)	0.84
Thyroid cancer	9	1.18 (0.64–2.16)	0.59	1.28 (0.57–2.88)	0.55	1.02 (0.17–6.18)	0.99
Bladder cancer	9	1.00022 (0.9980–1.0025)	0.84	1.00023 (0.9978–1.0026)	0.85	0.9984 (0.9917–1.0052)	0.66

10.3389/fcvm.2022.974402

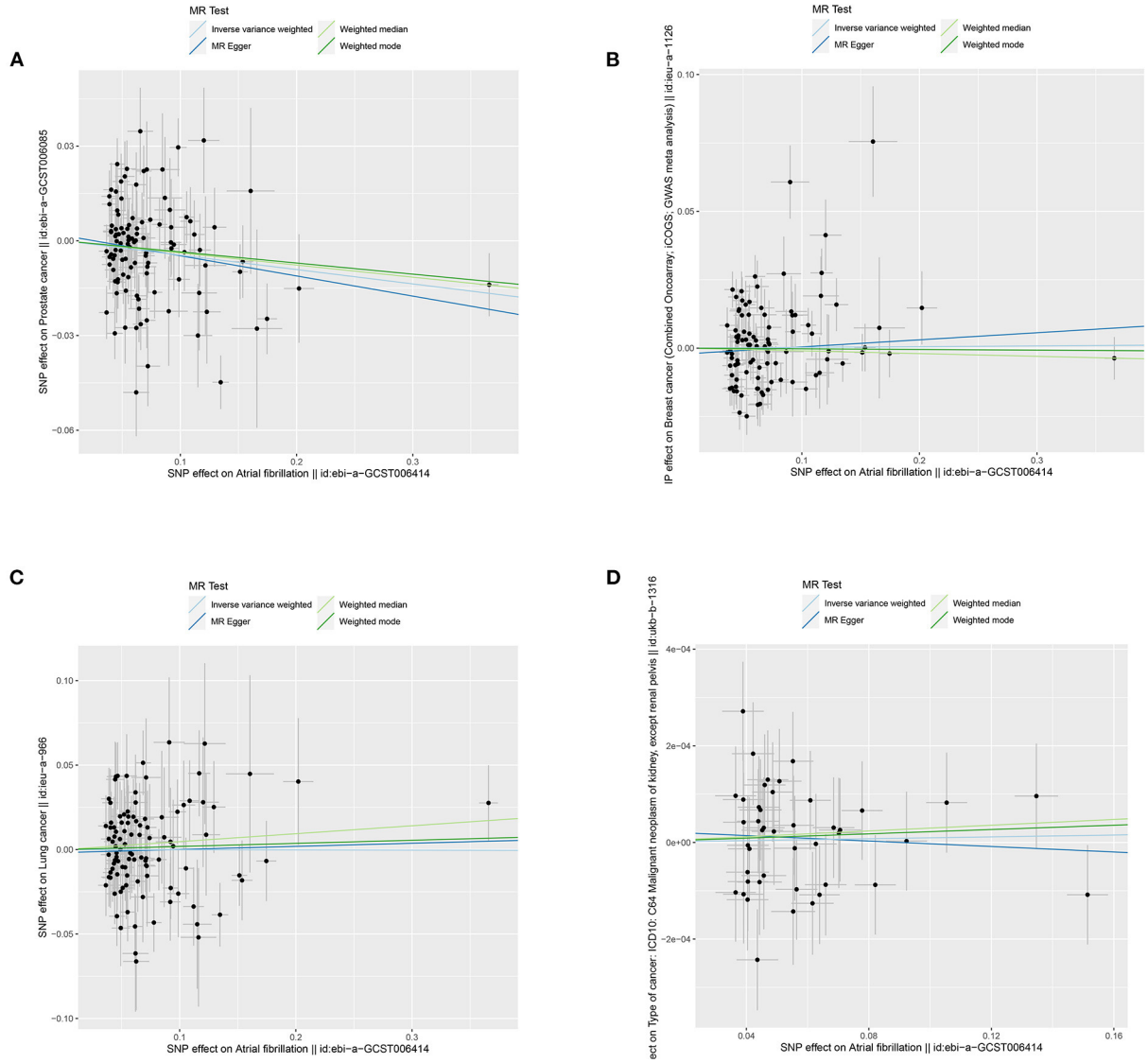

FIGURE 2
Scatterplots for MR analyses of the causal effect of atrial fibrillation on cancer risks: **(A)** prostate cancer; **(B)** breast cancer; **(C)** lung cancer; and **(D)** kidney cancer. The x-axis represents the previously published β-estimate for the association of each SNP with atrial fibrillation. The y-axis outlines the β-estimate for the relationship of each SNP with cancer risks by means of the multivariate logistic regression model. Lines represent causal estimates from the different methods. The slope of each line indicates the estimated MR effect per method. Circles correspond to marginal genetic associations with atrial fibrillation and risk of outcome for each variant. Error bars indicate 95% confidence intervals. SD, standard error; MR, Mendelian randomization.

enrichment pathways were noted, such as glutathione metabolism and metabolism of xenobiotics by cytochrome P450 (all p-values were <0.05) (Figure 4B). Regarding GO analysis, these DEGs were mainly enriched in cellular detoxification, xenobiotic metabolic process, glutathione derivative metabolic process, cellular response to xenobiotic stimulus, glutathione binding, and antioxidant activity (all p-values were <0.05) (Figures 4C, D). These outcomes firmly revealed that the antioxidant activity, xenobiotic catabolic process, and cytochrome P450 metabolism were involved in the development of AF and PCA.

4. Discussion

4.1. Principal findings

In this study, we performed MR analyses to evaluate whether genetic evidence supported a causal association between AF and

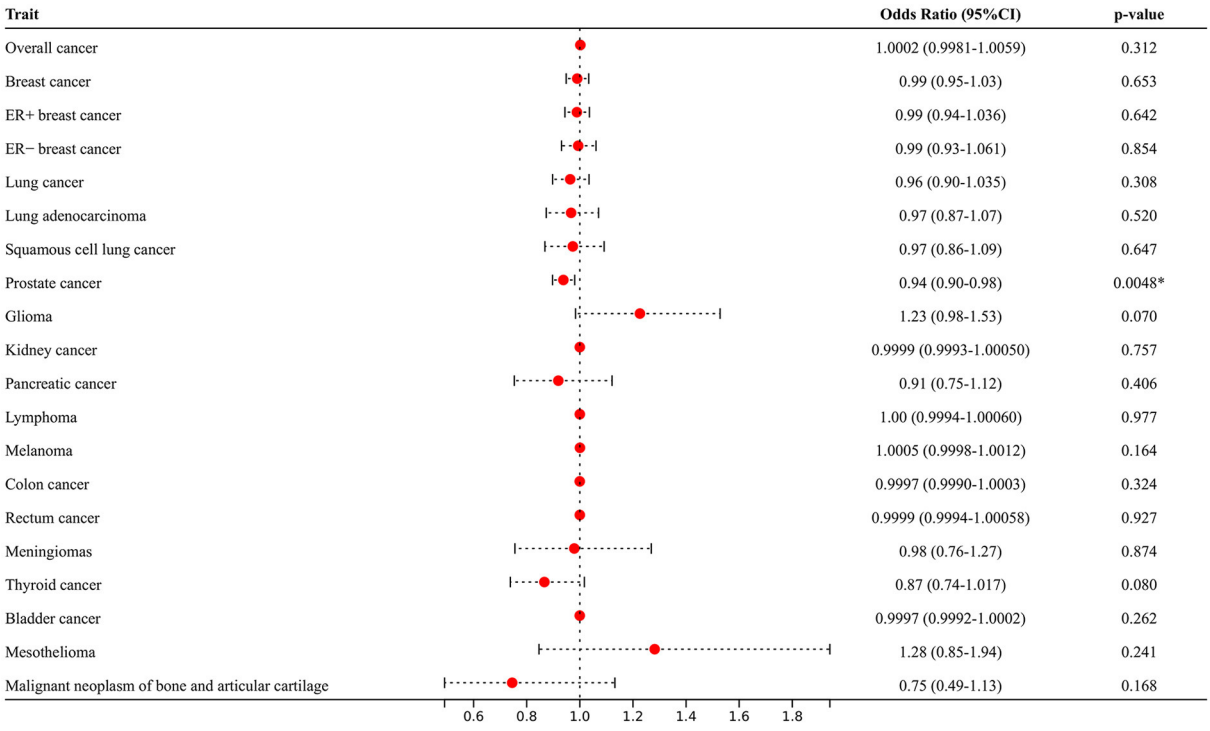

FIGURE 3
Multivariable Mendelian randomization analyses adjusted for smoking, alcohol consumption, diabetes, and hypertension. *Means statistically significance.

the risk of 19 site-specific types of cancer. To the best of our knowledge, this is the first cardio-oncology MR study involving 6,334,916 people to explicate that AF may casually reduce the risk of PCA. Moreover, little evidence demonstrated that AF and closely related HF were casually related to the increased risks of lung cancer, breast cancer, PCA, kidney cancer, glioma, pancreatic cancer, colon cancer, rectum cancer, meningiomas, thyroid cancer, bladder cancer, lymphoma, or melanoma, with less susceptibility to potential confounders and inverse causation. Based on our findings, cancer screening beyond standard routine healthcare may not be currently merited with a new diagnosis of AF. Nonetheless, a tight collaboration between cardiologists and oncologists is still essential to improve the management of patients, which may provide crucial mechanistic and therapeutic insights with regard to both serious conditions.

4.2. Previous research

The present MR findings do not support previous observational studies, suggesting that the manifestation of AF was a marker of occult cancer. Several sporadic epidemiological trials have described the underlying effect of AF on site-specific malignancies, but their findings were very controversial. An observational cohort study by Conen et al. (12) included 34,691 women and revealed that women with new-onset AF may have an elevated cancer risk beyond 1 year of AF diagnosis. This questionnaire-derived study also indicated that new-onset AF was statistically significant for the risk of colon cancer, whereas significant multivariable-adjusted relationships for breast cancer were not observed (12). These findings were consistent with a Danish population-based cohort study enrolling 26,222 men and 28,879 women free of AF (8). In this cohort trial, AF was not related to breast cancer or PCA (8), but the risk of colorectal cancer and lung cancer was paradoxically remarkably high within the initial 90 days following the diagnosis of AF (8). A retrospective cohort of 5,130 patients, however, demonstrated that the standard incidence ratio of lung and colon cancer was significantly high in patients with AF, although there was no significant increase in the risks of liver or breast cancer (11). Interestingly, evidence from a prospective cohort study even reached a contrasting conclusion that AF was related to decreased odds of the new diagnosis of breast cancer and colorectal cancer, indicating that an association noted in a previous study may be caused by potential detection bias instead of a causal relationship (9).

Atrial fibrillation and HF are often presented together with each other (16), and a similar scenario also holds for the relationship between HF and cancer risks. Retrospective research has suggested that the prevalence of malignancy in

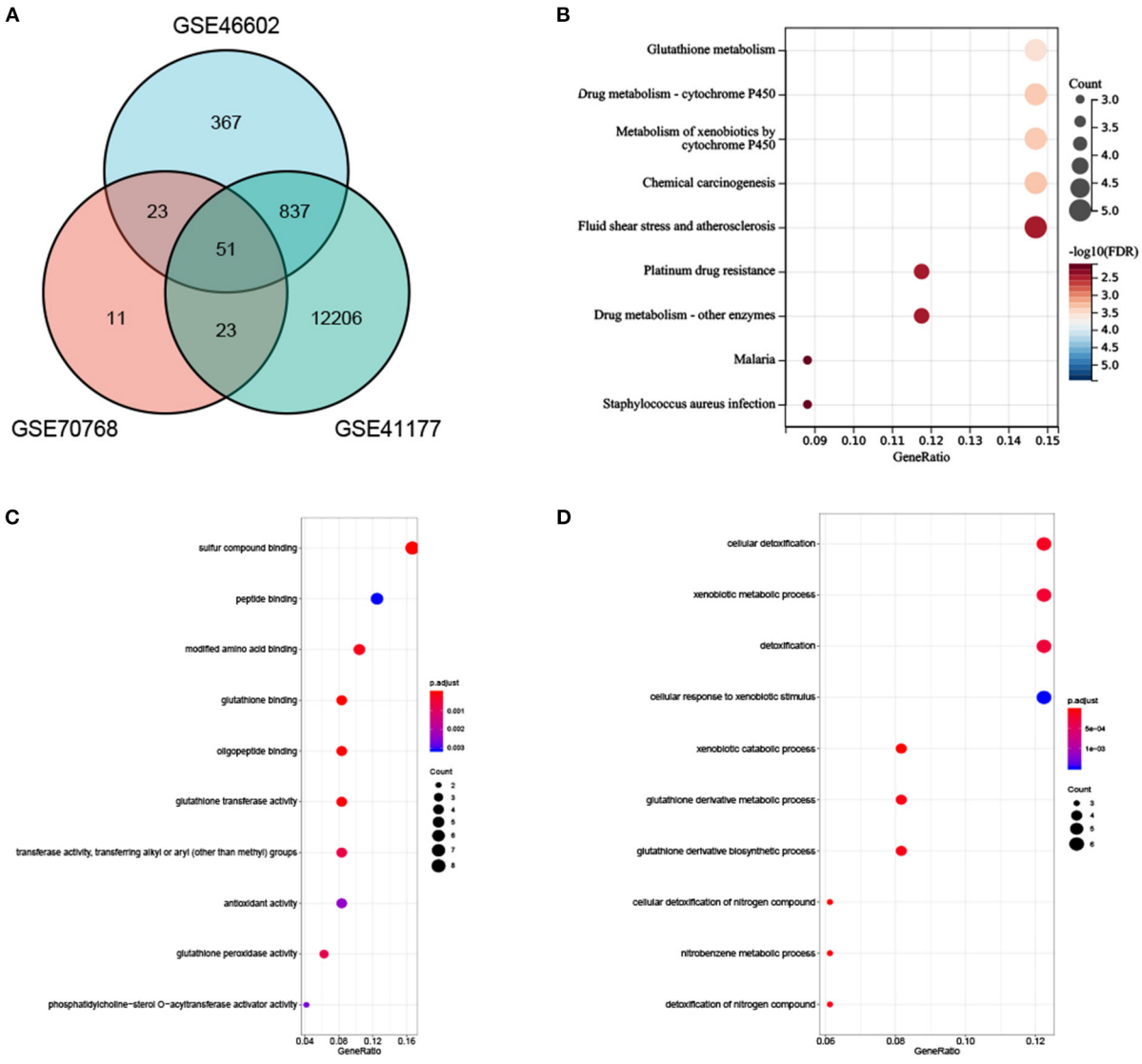

FIGURE 4
(A) Venn diagram showed an overlap of 51 DEGs. **(B)** The enrichment analysis results of KEGG Pathway. **(C, D)** The enrichment analysis results of GO terms.

established HF ranges from 18.9 to 33.7 per 1,000 person-years (33–35). Conversely, a study with larger cohorts and longer follow-up durations explicated that HF was neither associated with an increased risk of cancer nor cancer-specific deaths (36). Overall, according to previous studies, an association between AF and malignant tumors has been reported but is largely controversial.

4.3. The interpretation of the observed results

The potential limitations in previous epidemiological studies may bias the observed outcomes. The conflicting outcomes regarding cancer risks and AF in prior studies may be mediated by lots of possibilities, and some of the potential relationships are complex.

First, it was not surprising to see elevated cancer risks in patients with AF because related treatments render clinically overt cancer that could be otherwise asymptomatic. Several cardiovascular drugs, including spironolactone (37) and aspirin (38), have been shown to lower the carcinogenesis of certain types of cancer. In addition to the effect of related treatments, inherent drawbacks in observational study design, such as shorter follow-up duration, possible selection/surveillance bias (8, 12), and a lack of comprehensive data on shared risk factors (14, 39), could explain the perplexing results. The median time from AF/HF to malignancy diagnosis in some

prior investigations was <3 years (33, 35), which might be too short of a period to expound a causal association. With regard to selection or surveillance bias, some questionnaire-based studies may be unable to accurately determine whether patients underwent the examination before or after AF diagnosis (12). Besides, patients with screen-detected AF are more possible to have cancer screenings at an early stage, which is usually missed in the general population. For instance, if silent malignancies stay undetected, AF-related antithrombotic (40) or anticoagulant agents (8, 12) could increase the positivity rate of intestinal hemorrhage or hematuria, thus followed by several cancer detections (41). Third, AF and cancer are complex conditions and share many common risk factors, including alcohol consumption, smoking, hypertension, and diabetes (42). The risk of malignancy in patients with AF will naturally increase with the presence of the number of these risk factors. Hence, minimizing the effects of confounders and limitations of study designs is necessary for the evaluation of causality.

4.4. Possible mechanisms

In the present MR analysis, we found that AF may lower the risk of PCA using univariable and multivariable MR methods. The observed findings may be first attributed to an atrial natriuretic peptide (ANP), which may provide meaningful information about the underlying mechanism. AF is an independent determinant of ANP that exerts an important role in restraining tumor growth (43, 44). The inhibition of malignant cell proliferation by ANP is mediated by both intracellular acidity and Wnt/β-catenin signaling (45). ANP might also hinder the adhesion of malignant cells to microvascular endothelial cells by suppressing the E-selectin expression, which is regulated by inflammation (46). Second, AF-related hypercoagulability would alter cancer cell adhesion and tumor progression by decreasing matrix metalloproteinases (MMPs) in tissue and increasing circulating levels of inhibitors of matrix metalloproteinases (TIMPs) (5). TIMPs could control MMP that could lead to the degradation of the extracellular matrix and, consequently, organize the path for malignant cells to progress and spread to distant secondary areas (47). Third, certain immune-related genes identified in AF have recently been linked to the prognosis and immune infiltration in several tumor types (48). Herein, present KEGG and GO enrichment analyses of 51 common DEGs also revealed that these genes were significantly enriched in antioxidant activity, xenobiotic catabolic processes, and cytochrome P450 metabolism pathways. It has been expounded that the cause of PCA occurrence might be the outcome of an imbalance of antioxidants (49). Antioxidant defenses might be notably attenuated in patients with PCA (50). Moreover, environmental xenobiotics are largely involved in PCA development and are metabolized by cytochrome P450 in the human organism (51).

4.5. Strengths and limitations

The present MR study has several notable strengths. First, this is the first MR study conducted to evaluate the causal association between AF and cancer risks. MR analysis is deemed a reliable epidemiological method to evaluate the causality between exposures and outcomes. Residual confounding from unmeasured variations of baseline information may not ascertain cause–effect associations in previous studies (7, 8, 11, 12). The MR analysis, however, may better diminish the interference of confounders and inverse causation. Moreover, we were more likely to portray a relatively independent causal inference from AF to cancer risks with the multivariable MR approach adjusted for confounders. Second, the included AF-associated SNPs as IVs were gained from all documented GWASs, which may better explicate the variation of AF. Third, the present genetic summary data of certain types of cancer were obtained from large-scale consortia (namely, ILCCO, BCAC, and PRACTICAL), including millions of cases, which were far more than some previous studies (7, 11, 12). Compared with the low-occurrence rates of certain tumors in the previous studies (7, 11, 12), the present results from a relatively large sample size and strongly related IVs could present sufficient statistical power and a precise assessment of causal effects.

Some drawbacks should be taken into account to better elucidate the present findings. The participants in our study were of European descent. Thus, the results of our analysis were less likely to be biased by population stratification, but whether our assertion could be generalizable to other populations for different genetic backgrounds needs to be verified. Besides, the sample size of several site-specific cancer types in our analysis was small. For example, the consortium of malignant plasma cell neoplasms consisted of only 180 patients compared with its vast number of 87,061 controls. The statistical power may not estimate their causality accurately. Finally, the association between AF and PCA was not maintained in the results of MR weighted-median and MR-Egger analyses. However, the direction of MR estimates was consistent among IVW, weighted median, and MR–Egger methods in this study. Moreover, MR-PRESSO and multivariable MR tests were conducted to distinguish possible horizontal pleiotropy and supported the original IVW results.

5. Conclusion

This large cardio-oncology study revealed that AF may reduce the risk of PCA. Despite the lack of a causal relationship between AF and increased cancer risks, we should not ignore the two diseases' shared risk factors and pathophysiological mechanisms. Numerous studies still investigate the complicated interrelations between AF and cancer stay and, with an aging population, it

represents a valuable field for future investigation. A multidisciplinary approach is still needed to better understand the underlying mechanisms regarding the links between AF and cancer risks.

Data availability statement

The datasets presented in this study can be found in online repositories. The names of the repository/repositories and accession number(s) can be found in the article/Supplementary material.

Ethics statement

Ethical review and approval was not required for the study on human participants. Written informed consent was not required to participate in this study.

Author contributions

WL, MH, and WW conceived and designed the study, collected, analyzed, and interpreted the data. The first version of the manuscript was written by WL, RW, and WW. All authors contributed to the article and approved the submitted version.

Funding

This study was supported by the National Natural Science Foundation of China Grants (81172243 and 81572966 to WW) and the Natural Science Foundation of Guangdong Province (2017A030313883 to WW).

Acknowledgments

The authors would like to appreciate the efforts of the consortia in providing high-quality GWAS resources for scholars. Data and material can be available from the corresponding GWAS consortium.

Conflict of interest

The authors declare that the research was conducted in the absence of any commercial or financial relationships that could be construed as a potential conflict of interest.

Publisher's note

Supplementary material

The Supplementary Material for this article can be found online at: https://www.frontiersin.org/articles/10.3389/fcvm.2022.974402/full#supplementary-material

References

1. Rahman F, Kwan G, Benjamin E. Global epidemiology of atrial fibrillation. *Nat Rev. Cardiol.* (2014) 11:639–54. doi: 10.1038/nrcardio.2014.118

2. Lippi G, Sanchis-Gomar F, Cervellin G. Global epidemiology of atrial fibrillation: an increasing epidemic and public health challenge. *Int J Stroke Off.* (2021) 16:217–21. doi: 10.1177/1747493019897870

3. Walli-Attaei M, Joseph P, Rosengren A, Chow C, Rangarajan S, Lear S, et al. Variations between women and men in risk factors, treatments, cardiovascular disease incidence, and death in 27 high-income, middle-income, and low-income countries (Pure): a prospective cohort study. *Lancet.* (2020) 396:97–109. doi: 10.1016/S0140-6736(20)30543-2

4. Erichsen R, Christiansen C, Mehnert F, Weiss N, Baron J, Sørensen H. Colorectal cancer and risk of atrial fibrillation and flutter: a population-based case-control study. *Intern Emerg Med.* (2012) 7:431–8. doi: 10.1007/s11739-011-0701-9

5. Chu G, Versteeg H, Verschoor A, Trines S, Hemels M, Ay C, et al. Atrial fibrillation and cancer - an unexplored field in cardiovascular oncology. *Blood Rev.* (2019) 35:59–67. doi: 10.1016/j.blre.2019.03.005

6. Roderburg C, Loosen S, Jahn J, Gänsbacher J, Luedde T, Kostev K, et al. Heart failure is associated with an increased incidence of cancer diagnoses. *ESC Heart Failure.* (2021) 8:3628–33. doi: 10.1002/ehf2.13421

7. Ostenfeld E, Erichsen R, Pedersen L, Farkas D, Weiss N, Sørensen H. Atrial Fibrillation as a marker of occult cancer. *PLoS ONE.* (2014) 9:e102861. doi: 10.1371/journal.pone.0102861

8. Vinter N, Christesen A, Fenger-Grøn M, Tjønneland A, Frost L. Atrial fibrillation and risk of cancer: a Danish population-based cohort study. *J Am Heart Assoc.* (2018) 7:e009543. doi: 10.1161/JAHA.118.009543

9. Saliba W, Rennert H, Gronich N, Gruber S, Rennert G. Association of atrial fibrillation and cancer: analysis from two large population-based case-control studies. *PLoS ONE.* (2018) 13:e0190324. doi: 10.1371/journal.pone.0190324

10. Karnik A, Benjamin E, Trinquart L. Breast cancer and atrial fibrillation-a malignant combination? *Heart Rhythm.* (2019) 16:349–50. doi: 10.1016/j.hrthm.2018.11.016

11. Hung C, Chang C, Lin J, Ho Y, Chen M. The association between new onset atrial fibrillation and incident cancer-a nationwide cohort study. *PLoS ONE.* (2018) 13:e0199901. doi: 10.1371/journal.pone.0199901

12. Conen D, Wong J, Sandhu R, Cook N, Lee I, Buring J, et al. Risk of malignant cancer among women with new-onset atrial fibrillation. *JAMA Cardiol.* (2016) 1:389–96. doi: 10.1001/jamacardio.2016.0280

13. Conen D, Ridker P, Everett B, Tedrow U, Rose L, Cook N, et al. A multimarker approach to assess the influence of inflammation on the incidence of atrial fibrillation in women. *Eur Heart J.* (2010) 31:1730–6. doi: 10.1093/eurheartj/ehq146

14. Koene R, Prizment A, Blaes A, Konety S. Shared risk factors in cardiovascular disease and cancer. *Circulation.* (2016) 133:1104–14. doi: 10.1161/CIRCULATIONAHA.115.020406

15. Burgess S, Scott R, Timpson N, Davey Smith G, Thompson S. Using published data in mendelian randomization: a blueprint for efficient identification of causal risk factors. *Eur J Epidemiol.* (2015) 30:543–52. doi: 10.1007/s10654-015-0011-z

16. Carlisle M, Fudim M, DeVore A, Piccini J. Heart failure and atrial fibrillation, like fire and fury. *JACC Heart Failure.* (2019) 7:447–56. doi: 10.1016/j.jchf.2019.03.005

17. VanderWeele T, Tchetgen Tchetgen E, Cornelis M, Kraft P. Methodological challenges in Mendelian randomization. *Epidemiology.* (2014) 25:427–35. doi: 10.1097/EDE.0000000000000081

18. Nielsen J, Thorolfsdottir R, Fritsche L, Zhou W, Skov M, Graham S, et al. Biobank-driven genomic discovery yields new insight into atrial fibrillation biology. *Nat Genet.* (2018) 50:1234–9. doi: 10.1038/s41588-018-0171-3

19. Shah S, Henry A, Roselli C, Lin H, Sveinbjörnsson G, Fatemifar G, et al. Genome-wide association and mendelian randomisation analysis provide insights into the pathogenesis of heart failure. *Nat Commun.* (2020) 11:163. doi: 10.1038/s41467-019-13690-5

20. Hemani G, Zheng J, Elsworth B, Wade K, Haberland V, Baird D, et al. The Mr-base platform supports systematic causal inference across the human phenome. *Elife.* (2018) 7:34408. doi: 10.7554/eLife.34408

21. Michailidou K, Lindström S, Dennis J, Beesley J, Hui S, Kar S, et al. Association analysis identifies 65 new breast cancer risk loci. *Nature.* (2017) 551:92–4. doi: 10.1038/nature24284

22. Schumacher F, Al Olama A, Berndt S, Benlloch S, Ahmed M, Saunders E, et al. Association analyses of more than 140,000 men identify 63 new prostate cancer susceptibility loci. *Nat Genet.* (2018) 50:928–36. doi: 10.1038/s41588-018-0142-8

23. Wang Y, McKay J, Rafnar T, Wang Z, Timofeeva M, Broderick P, et al. Rare variants of large effect in brca2 and chek2 affect risk of lung cancer. *Nat Genet.* (2014) 46:736–41.

24. Amundadottir L, Kraft P, Stolzenberg-Solomon R, Fuchs C, Petersen G, Arslan A, et al. Genome-wide association study identifies variants in the abo locus associated with susceptibility to pancreatic cancer. *Nat Genet.* (2009) 41:986–90. doi: 10.1038/ng.429

25. Rajaraman P, Melin B, Wang Z, McKean-Cowdin R, Michaud D, Wang S, et al. Genome-wide association study of glioma and meta-analysis. *Hum Genet.* (2012) 131:1877–88. doi: 10.1007/s00439-012-1212-0

26. Verbanck M, Chen C, Neale B, Do R. Detection of widespread horizontal pleiotropy in causal relationships inferred from Mendelian randomization between complex traits and diseases. *Nat Genet.* (2018) 50:693–8. doi: 10.1038/s41588-018-0099-7

27. Burgess S, Thompson S. Multivariable mendelian randomization: the use of pleiotropic genetic variants to estimate causal effects. *Am J Epidemiol.* (2015) 181:251–60. doi: 10.1093/aje/kwu283

28. Bowden J, Del Greco M F, Minelli C, Davey Smith G, Sheehan N, Thompson J, et al. Framework for the investigation of pleiotropy in two-sample summary data Mendelian randomization. *Stat Med.* (2017) 36:1783–802. doi: 10.1002/sim.7221

29. Mortensen M, Høyer S, Lynnerup A, Ørntoft T, Sørensen K, Borre M, et al. Expression profiling of prostate cancer tissue delineates genes associated with recurrence after prostatectomy. *Sci Rep.* (2015) 5:16018. doi: 10.1038/srep16018

30. Ross-Adams H, Lamb A, Dunning M, Halim S, Lindberg J, Massie C, et al. Integration of copy number and transcriptomics provides risk stratification in prostate cancer: a discovery and validation cohort study. *EBioMedicine.* (2015) 2:1133–44. doi: 10.1016/j.ebiom.2015.07.017

31. Yeh Y, Kuo C, Lee Y, Lin Y, Nattel S, Tsai F, et al. Region-specific gene expression profiles in the left atria of patients with valvular atrial fibrillation. *Heart Rhythm.* (2013) 10:383–91. doi: 10.1016/j.hrthm.2012.11.013

32. Burgess S, Thompson S. Interpreting findings from mendelian randomization using the Mr-egger method. *Eur J Epidemiol.* (2017) 32:377–89. doi: 10.1007/s10654-017-0255-x

33. Hasin T, Gerber Y, Weston S, Jiang R, Killian J, Manemann S, et al. Heart failure after myocardial infarction is associated with increased risk of cancer. *J Am Coll Cardiol.* (2016) 68:265–71. doi: 10.1016/j.jacc.2016.04.053

34. Hasin T, Gerber Y, McNallan S, Weston S, Kushwaha S, Nelson T, et al. Patients with heart failure have an increased risk of incident cancer. *J Am Coll Cardiol.* (2013) 62:881–6. doi: 10.1016/j.jacc.2013.04.088

35. Banke A, Schou M, Videbaek L, Møller J, Torp-Pedersen C, Gustafsson F, et al. Incidence of cancer in patients with chronic heart failure: a long-term follow-up study. *Eur J Heart Fail.* (2016) 18:260–6. doi: 10.1002/ejhf.472

36. Selvaraj S, Bhatt D, Claggett B, Djoussé L, Shah S, Chen J, et al. Lack of association between heart failure and incident cancer. *J Am Coll Cardiol.* (2018) 71:1501–10. doi: 10.1016/j.jacc.2018.01.069

37. Mackenzie I, Morant S, Wei L, Thompson A, MacDonald T. Spironolactone use and risk of incident cancers: a retrospective, matched cohort study. *Br J Clin Pharmacol.* (2017) 83:653–63. doi: 10.1111/bcp.13152

38. Fu B, Wang K, Mucci L, Clinton S, Giovannucci E. Aspirin use and prostate tumor angiogenesis. *Cancer Causes Control.* (2021) 33:149–51. doi: 10.1007/s10552-021-01501-6

39. Meijers W, De Boer R. Common risk factors for heart failure and cancer. *Cardiovasc Res.* (2019) 115:844–53. doi: 10.1093/cvr/cvz035

40. Ameri P, Canepa M, Anker M, Belenkov Y, Bergler-Klein J, Cohen-Solal A, et al. Cancer diagnosis in patients with heart failure: epidemiology, clinical implications and gaps in knowledge. *Eur J Heart Fail.* (2018) 20:879–87. doi: 10.1002/ejhf.1165

41. Papanastasiou A, Morsi-Yeroyannis A, Karagiannidis E, Kartas A, Doundoulakis I, Karvounis H, et al. Association of anticoagulant-related bleeding events with cancer detection in atrial fibrillation: a systematic review and meta-analysis. *Hellenic J Cardiol.* (2020) 5:359–65. doi: 10.1016/j.hjc.2020.11.007

42. Menichelli D, Vicario T, Ameri P, Toma M, Violi F, Pignatelli P, et al. Cancer and atrial fibrillation: epidemiology, mechanisms, and anticoagulation treatment. *Prog Cardiovasc Dis.* (2021) 66:28–36. doi: 10.1016/j.pcad.2021.04.004

43. Rossi A, Enriquez-Sarano M, Burnett J, Lerman A, Abel M, Seward J. Natriuretic peptide levels in atrial fibrillation: a prospective hormonal and Doppler-echocardiographic study. *J Am Coll Cardiol.* (2000) 35:1256–62. doi: 10.1016/S0735-1097(00)00515-5

44. Vesely D. Cardiac and renal hormones: anticancer effects *in vitro* and *in vivo*. *J Invest Med.* (2009) 57:22–8. doi: 10.2310/JIM.0b013e3181948b25

45. Serafino A, Moroni N, Psaila R, Zonfrillo M, Andreola F, Wannenes F, et al. Anti-proliferative effect of atrial natriuretic peptide on colorectal cancer cells: evidence for an Akt-mediated cross-talk between Nhe-1 activity and Wnt/B-catenin signaling. *Biochim Biophys Acta.* (2012) 1822:1004–18. doi: 10.1016/j.bbadis.2012.02.016

46. Nojiri T, Hosoda H, Tokudome T, Miura K, Ishikane S, Otani K, et al. Atrial natriuretic peptide prevents cancer metastasis through vascular endothelial cells. *Proc Natl Acad Sci U S A.* (2015) 112:4086–91. doi: 10.1073/pnas.1417273112

47. Bourboulia D, Stetler-Stevenson W. Matrix metalloproteinases (Mmps) and tissue inhibitors of metalloproteinases (Timps): positive and negative regulators in tumor cell adhesion. *Semin Cancer Biol.* (2010) 20:161–8. doi: 10.1016/j.semcancer.2010.05.002

48. Yan T, Zhu S, Shi Y, Xie C, Zhu M, Zhang Y, et al. Anxa4pan-cancer analysis of atrial-fibrillation-related innate immunity gene. *Front Cardiovas Med.* (2021) 8:713983. doi: 10.3389/fcvm.2021.713983

49. Ahmed Amar S, Eryilmaz R, Demir H, Aykan S, Demir C. Determination of oxidative stress levels and some antioxidant enzyme activities in prostate cancer. *J Int Soc Stud Aging Male.* (2019) 22:198–206. doi: 10.1080/13685538.2018.1488955

50. Sajjaboontawee N, Supasitthumrong T, Tunvirachaisakul C, Nantachai K, Snabboon T, Reiche E, et al. Lower thiol, glutathione, and glutathione peroxidase levels in prostate cancer: a meta-analysis study. *J Int Soc Stud Aging Male.* (2020) 23:1533–44. doi: 10.1080/13685538.2020.1858048

51. Maksymchuk O, Kashuba V. Dietary lipids and environmental xenobiotics as risk factors for prostate cancer: the role of cytochrome P450. *Pharmacol Rep.* (2019) 71:826–32. doi: 10.1016/j.pharep.2019.04.011

frontiers | Frontiers in Cardiovascular Medicine

TYPE Original Research
PUBLISHED 07 February 2023
DOI 10.3389/fcvm.2023.888366

OPEN ACCESS

EDITED BY
Dong Han,
The People's Liberation Army General Hospital, China

REVIEWED BY
Oliver Königsbrügge,
Medical University of Vienna, Austria
Elisabetta Abruzzese,
University of Rome Tor Vergata, Italy
Massimiliano Bonifacio,
University of Verona, Italy
Mario Annunziata,
Antonio Cardarelli Hospital, Italy

*CORRESPONDENCE
Rafael Amorim Belo Nunes
ra.nunes16@gmail.com

SPECIALTY SECTION
This article was submitted to Frontiers in Cardiovascular Medicine | Cardio-Oncology, a section of the journal Frontiers in Cardiovascular Medicine

RECEIVED 02 March 2022
ACCEPTED 09 January 2023
PUBLISHED 07 February 2023

CITATION
Nunes RAB, Neves PDMM, da Costa LMA, Bachour P, Cantarelli MJC, Oliveira GBF and Avezum Á Jr (2023) Five-year cardiovascular outcomes in patients with chronic myeloid leukemia treated with imatinib, dasatinib, or nilotinib: A cohort study using data from a large multinational collaborative network. *Front. Cardiovasc. Med.* 10:888366. doi: 10.3389/fcvm.2023.888366

Five-year cardiovascular outcomes in patients with chronic myeloid leukemia treated with imatinib, dasatinib, or nilotinib: A cohort study using data from a large multinational collaborative network

Rafael Amorim Belo Nunes[1]*, Precil Diego Miranda de Menezes Neves[2], Leandro Menezes Alves da Costa[1], Philip Bachour[3], Marcelo José de Carvalho Cantarelli[1], Gustavo Bernardes de Figueiredo Oliveira[2] and Álvaro Avezum Jr.[2]

[1]Department of Cardiology, Hospital Alemão Oswaldo Cruz, São Paulo, Brazil, [2]International Research Center, Hospital Alemão Oswaldo Cruz, São Paulo, Brazil, [3]Department of Hematology and Bone Marrow Transplant, Hospital Alemão Oswaldo Cruz, São Paulo, Brazil

Background: Breakpoint cluster region-Abelson gene (BCR-ABL) tyrosine kinase inhibitors (TKIs) have revolutionized the treatment of patients with chronic myeloid leukemia (CML). However, concern has arisen about the cardiac safety profile of these drugs.

Objectives: This study aims to compare long-term risks of adverse cardiovascular and cerebrovascular events (ACE), heart failure or left ventricular ejection fraction (LVEF) $< 50\%$, and venous thromboembolic events (VTE) in patients with CML treated with BCR-ABL TKIs, using data from a large multinational network.

Methods: Patients aged $\geq$ 18 years with CML treated with imatinib, dasatinib, or nilotinib without prior cardiovascular or cerebrovascular disease were included. We used propensity score matching to balance the cohorts. The 5-year cumulative incidences and hazard ratios were calculated.

Results: We identified 3,722 patients with CML under treatment with imatinib (n = 1,906), dasatinib (n = 1,269), and nilotinib (n = 547). Patients with imatinib compared to dasatinib showed a higher hazard ratio (HR) for ACE (HR 2,13, 95% CI 1.15–3.94, p = 0.016). Patients with imatinib presented a lower HR than nilotinib for ACE (HR 0.50, 95% CI 0.30–0.83, p = 0.0074). In relation to heart failure or LVEF $< 50\%$, patients with imatinib had a higher HR than dasatinib (HR 9.41, 95% CI 1.22–72.17, p = 0.03), but no significant difference was observed between imatinib and nilotinib (HR 0.48, 95% CI 0.215–1.01, p = 0.064).

Conclusion: In this retrospective study with a large number of patients with CML, those treated with nilotinib had a higher 5-year ratio of ACE, while patients with dasatinib showed a lower ratio than patients with imatinib. The ratio of heart failure was higher in patients with imatinib than in patients with dasatinib, but not when compared to nilotinib.

KEYWORDS

cardiovascular safety, chronic myeloid leukemia, tyrosine kinase inhibitor (TKI), breakpoint cluster region-abelson (BCR-ABL), cardio-onco-hematology

Introduction

Chronic myeloid leukemia (CML) is a myeloproliferative disorder caused by a balanced chromosomal translocation involving a fusion of the Abelson gene (ABL1) from chromosome 9q34 with the breakpoint cluster region (BCR) gene on chromosome 22q11, known as the Philadelphia chromosome, which encodes the BCR-ABL protein with protein tyrosine kinase activity (1). The advent of BCR-ABL tyrosine kinase inhibitors (TKI) was a big breakthrough in the treatment of patients with CML, improving their outcomes and quality of life. In 2001, imatinib was the first BCR-ABL TKI approved for the treatment of patients with CML (2). Posteriorly, other BCR-ABL TKIs such as dasatinib and nilotinib were also approved for this purpose.

Despite their well-known benefits for CML treatment, concerns have been raised about short- and long-term cardiac and pulmonary safety profiles of BCR-ABL TKIs. Cardiac toxicities associated with TKIs are heterogeneous and may include QT prolongation, arrhythmias, decreased left ventricular ejection fraction (LVEF), congestive heart failure, acute coronary syndrome, arterial thrombosis, pulmonary, and systemic hypertension (3–10). TKI-induced cardiotoxicity mechanisms are miscellaneous and may be drug-specific, even to same-class drugs. Proposed mechanisms may include disruption of mitochondrial function within the cardiomyocyte, off-target inhibition of other kinases, disturbing cardiomyocyte cellular oxidative phosphorylation, and caspase-mediated mitochondrial apoptosis (11).

Despite data from clinical trials and cohort studies, there is still a need for more robust information about the long-term cardiac safety profile of BCR-ABL TKIs, especially real-world data. Trials evaluating BCR-ABL TKIs in patients with CML have enrolled participants with a history of cardiovascular disease but, when cardiac endpoints were reported, these patients were not analyzed as a separate group (12). Also, the definition of cardiovascular outcomes in TKI studies was heterogeneous and generally, they were not the same as those of cardiologic trials as well as they were not specifically designed to determine cardiac safety.

Based on the previous literature data, we hypothesized that cardiovascular outcomes may differ according to the treatment with specific BCR-ABL TKIs. In this study, we aimed to evaluate the 5-year incidence and compare the ratios of significant cardiovascular outcomes in patients with CML without a past history of heart or cerebrovascular diseases treated with Bcr-ABL TKIs imatinib, dasatinib, or nilotinib, using data from a large multinational network based on electronic medical records.

Materials and methods

Data source

We used global-based data from the network TriNetX (TriNetX, Inc., Cambridge, MA, United States), a multinational collaborative clinical research platform, that collects real-time medical records, including demographics, diagnoses, procedures, medications, laboratory values, and vital statuses. This network included 70 healthcare organizations at the time of analysis, including data from around 69.8 million patients. The TriNetX platform uses aggregated counts and statistical summaries of de-identified information so that no protected health information or personal data are made available to users of the platform. Data were extracted and analyzed from the Global Collaborative Network on the TriNetX platform between 27 August and 30 August 2021.

Study population

We queried the databank to select patients of both sexes and with age $\geq$ 18 years with CML, BCR-ABL positive, based on International Classification of Diseases, Tenth Revision (ICD-10) diagnosis codes (ICD-10 code C92.1) during the past 10 years before the analysis. The patients needed to be under treatment with a BCR-ABL TKI (imatinib, dasatinib, or nilotinib), and they must not be prescribed another TKI anytime. The index date was determined by the earliest date of identification of the use of a BCR-ABL TKI. Patients with past ischemic heart disease, other forms of heart disease (including patients with LVEF $<$ 50% identified in the TriNetX databank), cerebrovascular disease, and pulmonary hypertension (ICD-10 codes I20-I25, I27, I30-I52, and I60-I69) before the index date were excluded from the analysis.

Study design

In this population-based retrospective cohort study, we aimed to analyze the 5-year incidence of cardiovascular outcomes [adverse cardiovascular and cerebrovascular events (ACE), heart failure or LVEF $<$ 50%, and venous thromboembolic events (VTE)] and their comparative hazard ratios (HR) in patients with CML BCR-ABL positive under treatment with imatinib, dasatinib, or nilotinib. The time window for the outcome was the treatment starting with a BCR-ABL TKI up to 5 years after. To avoid interactions in

cardiovascular outcomes from patients with CML that were changed from one TKI to another, patients with switch therapy were excluded from the analysis.

Outcomes

The three analyzed cardiovascular outcomes are as follows:

Adverse cardiovascular and cerebrovascular events (ACE): the composite of ischemic heart disease (ICD-10 codes I20–I25) or cerebrovascular disease (ICD-10 codes I60–69) or myocardial revascularization (coronary angioplasty code or coronary artery bypass graft surgery, ICD-10 codes Z95.1, Z95.5, and Z98.61).

Heart failure or left ventricular ejection fraction (LVEF) < 50%: ICD-10 code I50 or TriNetX code 2003. LVEF < 50% was chosen as a surrogate for ventricular dysfunction.

Venous thromboembolism (VTE): ICD-10 I82 or I26.

Statistical analysis

The baseline characteristics for each group were compared with the chi-square test for categorical variables and the Student *t*-test for continuous variables. Propensity score matching was used to balance cohorts with baseline characteristics. In relation to outcome comparisons, we used the imatinib group as the reference, comparing it with the two other groups (dasatinib and nilotinib). Kaplan–Meier analysis was performed to estimate the probability of outcomes after the index date from 1 day up to 5 years. Comparisons between cohorts were made using a log-rank test. We calculate the HRs and their associated 95% confidence intervals (CI), together with the test for proportionality based on the scaled Schoenfeld residual, using R's Survival package v3.2-3.

Statistical analyses were done within TriNetX (13). Statistical significance was set at a two-sided p-value of < 0.05.

Propensity score matching and covariates

The propensity score matching was calculated using logistic regression implemented by the function logistic regression of the scikit-learn package in Python version 3.7. "Greedy nearest neighbor matching" was used with a caliper of 0.1 pooled standard deviations (13). 1:1 matching was adjusted for covariates that could be confounders for the predefined cardiovascular outcomes as follows: demographic variables such as age, sex, and race (defined as white, black or African American, Asian, or unknown); health conditions related to cardiovascular risk and recorded identified from ICD-10-CM codes in electronic medical records: overweight or obesity, hypertension, chronic kidney disease, dyslipidemia, diabetes mellitus, and nicotine dependence; and use of cardiovascular and antimetabolite medications: hydroxyurea, diuretics, ACE inhibitors or angiotensin II receptor blockers, beta-blockers, lipid-lowering drugs, and antiarrhythmics, before starting BCR-ABL TKIs.

Ethics

TriNetX-derived studies with de-identified information were approved by the Institutional Review Board of Hospital Alemão Oswaldo Cruz.

Results

Characteristics of the study population

Using the electronic medical records from the platform TriNetX, we identified 24,921 patients with CML BCR/ABL positive (ICD-10 C92.1). From this cohort, we selected, using inclusion and exclusion criteria, 3,722 patients with CML and without past heart disease treated with imatinib (n = 1,906), dasatinib (n = 1,269), and nilotinib (n = 547). The exposure time for each analyzed TKI was as follows: imatinib (median 1,198 days, range 1–1,826 days), dasatinib (median 647 days, range 1–1,826 days), and nilotinib (median 790 days, range 1–1,826 days).

Compared to imatinib, patients with dasatinib were younger during the start of treatment with a TKI (age 55 vs. 47.7 years old, $p < 0.0001$), had a lower rate of hypertension (21 vs. 16%, $p < 0.0001$), and had diabetes mellitus (10 vs. 7%, $p = 0.002$). The patients with dasatinib had a higher rate of previous treatment with hydroxyurea ($p < 0.0001$) and antiarrhythmics ($p < 0.0001$) than patients in the imatinib group.

Compared to the imatinib group, patients from the nilotinib group were younger (55 vs. 53 years old, $p = 0.008$), had a higher proportion of female patients (46 vs. 52%, $p = 0.007$), and had a higher proportion of black or African American patients (11 vs. 15%, $p = 0.02$). Patients with nilotinib had a lower rate of use of antiarrhythmics than patients with imatinib. The baseline characteristics before propensity score matching of the three study groups are detailed in **Table 1**.

Outcome incidences during 5-year follow-up before the propensity score matching

The number and cumulative incidence of patients with ACE in the Imatinib group were 99 (5.23%), in the dasatinib group were 15 (1.19%), and in the nilotinib group were 44 (8.1%). For the composite outcome heart failure or LVEF < 50%, the number and cumulative incidence in the imatinib group were 35 (1.83%), in the dasatinib group were 10 (0.78%), and in the nilotinib group were 17 (3.1%). The composite outcome VTE or pulmonary embolism occurred in 45 (2.4%) patients in the imatinib group, 25 (2%) patients in the dasatinib group, and 10 (1.8%) patients in the nilotinib group.

5-year outcomes in imatinib, dasatinib, and nilotinib groups after propensity score matching

After the propensity score matching, the imatinib group (n = 1,153) compared to the dasatinib group (n = 1,153) showed a

10.3389/fcvm.2023.888366

TABLE 1 Baseline characteristics of the cohort for the imatinib, dasatinib, and nilotinib groups.

	Imatinib	Dasatinib	*P*-value*	Nilotinib	*P*-value**
Cohort size, *n*	1906	1269		547	
Demographics					
Mean age (SD), years	55 (16)	47.7 (15)	<0.0001	53 (15)	0.0086
Sex					
Male, *n* (%)	1029 (54)	700 (55)	NS	261 (48)	0.0092
Female, *n* (%)	877 (46)	569 (45)	NS	285 (52)	0.0073
Race					
White, *n* (%)	1323 (69)	820 (65)	0.0281	362 (66)	NS
Black or African American, *n* (%)	215 (11)	185 (15)	0.0026	81 (15)	0.0230
Asian, *n* (%)	35 (2)	30 (2)	NS	10 (2)	NS
Unknown, *n* (%)	323 (17)	223 (18)	NS	97 (18)	NS
Comorbidities					
Overweight or obesity, *n* (%)	133 (7)	75 (6)	NS	30 (5)	NS
Nicotine dependence, *n* (%)	113 (6)	79 (6)	NS	29 (5)	NS
Disorders of lipid metabolism, *n* (%)	228 (12)	117 (9)	NS	61 (11)	NS
Diabetes mellitus, *n* (%)	187 (10)	85 (7)	0.0002	57 (10)	NS
Hypertension, *n* (%)	401 (21)	202 (16)	<0.0001	96 (18)	NS
Chronic kidney disease, *n* (%)	79 (4)	28 (2)	<0.0001	13 (2)	NS
Medications					
Hydroxyurea, *n* (%)	252 (13)	328 (26)	<0.0001	66 (12)	NS
Antilipemic agentes, *n* (%)	311 (16)	164 (13)	0.002	92 (17)	NS
Beta blockers, *n* (%)	269 (14)	124 (10)	<0.0001	87 (16)	NS
ACE inhibitors, *n* (%)	200 (10)	174 (14)	0.0002	57 (10)	NS
Angiotensin II inhibitors, *n* (%)	127 (7)	62 (5)	0.003	34 (6)	NS
Antiarrhythmics	362 (19)	317 (25)	0.0002	56 (10)	0.0001
Diuretics, *n* (%)	323 (17)	165 (13)	<0.0001	70 (13)	0.018

SD, standard deviation; ACE, angiotensin-converting enzyme; NS, non-significant. *imatinib vs. dasatinib; **imatinib vs. nilotinib.

higher HR for ACE (HR 2.13, 95% CI 1.15–3.94, $p = 0.016$). When compared with the nilotinib group ($n = 533$), the matched imatinib group ($n = 533$) presented a lower HR for ACE (HR 0.50, 95% CI 0.30–0.83, $p = 0.0074$). In relation to heart failure or LVEF < 50%, patients with imatinib had a higher ratio than patients with dasatinib (HR 9.41, 95% CI 1.22–72.17, $p = 0.03$), but no significant difference was observed between imatinib and nilotinib groups (HR 0.48, 95% CI 0.215–1.01, $p = 0.064$). There were no significant differences between the three groups in relation to VTE or pulmonary embolism. Five-year Kaplan–Meier curves for ACE, heart failure, and venous thromboembolism between dasatinib vs. imatinib and nilotinib vs. imatinib are depicted in **Figure 1**.

Discussion

We used a large electronic medical record network to create propensity score-matched cohorts of patients with CML without a past history of heart or cerebrovascular diseases according to the treatment with three commonly used BCR-ABL TKIs for comparing ratios of cardiovascular outcomes (ACE, heart failure or LVEF < 50%, and VTE or pulmonary embolism) during a 5-year period. As patients of the imatinib group were older than patients of the other groups and had more cardiovascular risk factors than patients of the dasatinib group, we opted for matching the cohorts as a reasonable approach to compare the groups with similar baseline characteristics for reducing bias. Using this approach, we found that when compared with patients from the imatinib group, patients with dasatinib had a significantly lower ratio of ACE, while patients from the nilotinib group had a significantly higher rate of ACE.

Cardiovascular events, including ischemic heart disease, cerebrovascular disease, and peripheral artery disease, are major concerns in patients with CML, particularly in those under treatment with second- and third-generation Bcr-ABL TKIs nilotinib and ponatinib, respectively (14). In this population, cardiovascular disease may be responsible for up to 16.5 and 5% of potential years of life lost in men and women, respectively (15). In the 3-year follow-up of the ENESTnd trial, which included a total of 846 patients with newly diagnosed Ph + CML-CP, the incidence of ischemic heart disease was higher with nilotinib than with imatinib: nine patients (3.2%) in the nilotinib 300 mg twice-daily arm, 11 patients (4.0%) in the nilotinib 400 mg twice-daily arm, and three patients (1.1%) in imatinib arm (9). These results were more evident with a 5-year update of the ENESTnd trial, in which 28 of 279 (10%) patients

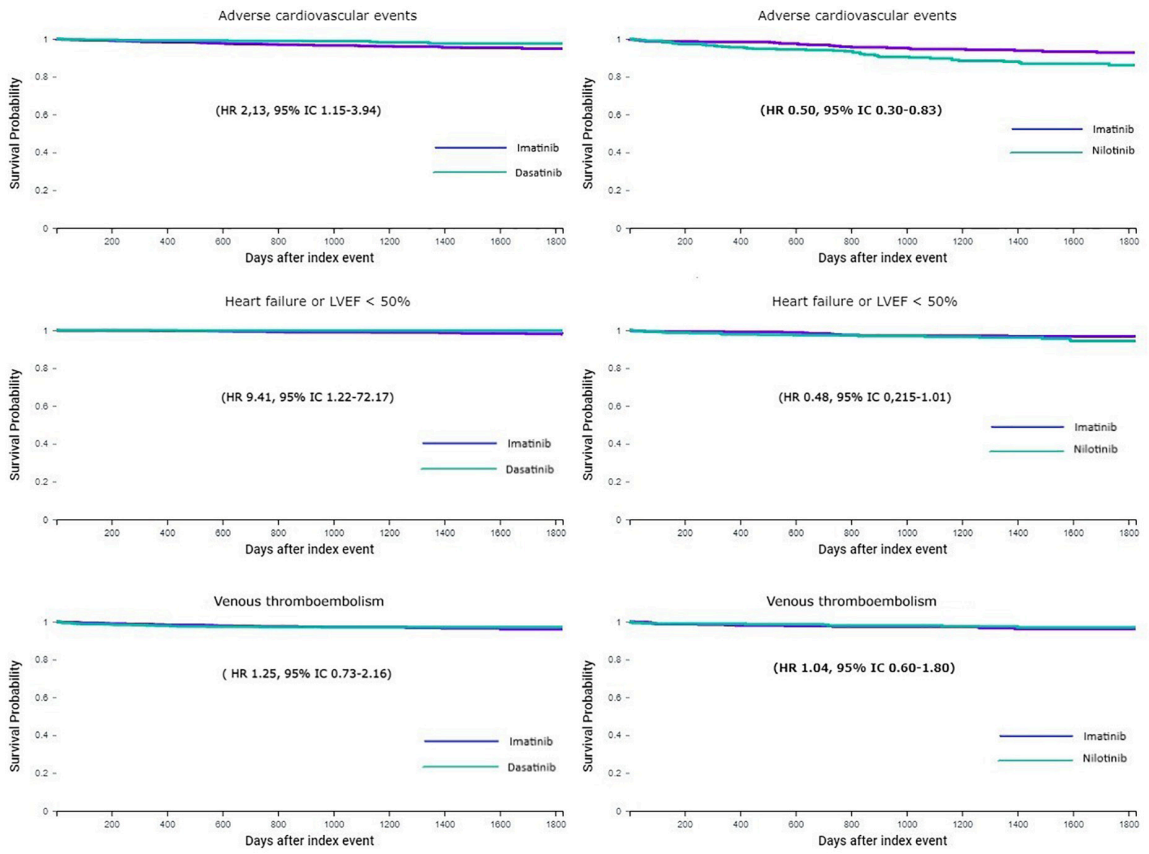

FIGURE 1
5-year Kaplan–Meier curves for adverse cardiovascular or cerebrovascular events, heart failure or LVEF < 50%, and VTE or pulmonary embolism in patients treated with imatinib vs. dasatinib (**left** column) and imatinib vs. nilotinib (**right** column). LVEF, left ventricular ejection fraction; HR, hazard ratio; CI, confidence interval; VTE, venous thromboembolism.

treated with nilotinib at 300 mg twice per day, 44 of 277 patients (15.9%) treated with nilotinib at 400 mg twice per day, and 7 (2.5%) of 280 patients treated with imatinib 400 once per day had ischemic events (16). Interestingly, a retrospective study using data from 1,390 patients with CML from IRIS, TOPS, and ENESTnd trials showed a lower risk of peripheral arterial disease in patients treated with imatinib vs. nilotinib or patients with CML treated without TKIs, suggesting a possible protective role of imatinib in atherosclerotic vascular diseases (10). The supposed mechanisms related to nilotinib cardiovascular toxicities are complex and may involve different pathways. Nilotinib may lead to overexpression of cell adhesion proteins on human endothelium, including ICAM1, VCAM1, and E-selectin, which may enroll inflammatory cells and platelets and increase the risk of cardiovascular events (14). Nilotinib also represses endothelial cell proliferation and migration and may inhibit other kinases related to angiogenesis (17). In our study, in line with previous data, we have also observed a higher risk of cardiovascular disease, including cerebrovascular and ischemic heart disease or myocardial revascularization, in patients with nilotinib when compared with imatinib, even excluding patients with a past history of heart and cerebrovascular disease and adjusting the analysis for baseline cardiovascular risk factors.

The risk of cardiovascular ischemic events induced by dasatinib is not well-established. Despite the higher incidence of cardiovascular events in patients treated with dasatinib in relation to imatinib (4 vs. 2%) at the 5-year follow-up of the DASISION trial (8), a *post hoc* analysis that included patients from the DASISION trial showed that the cardiovascular events occurred mainly in patients with a history of cardiovascular disease (18). In a retrospective study that analyzed data from 105 patients with CML in Polish tertiary health centers, patients treated with dasatinib had lower rates of vascular events (4%) than patients with nilotinib (11%) (19). We showed in our analysis a lower HR of cardiovascular and cerebrovascular events in patients with dasatinib compared to imatinib, differing from other analyses by being a real-world cohort and excluding patients with overt cardiovascular and cerebrovascular diseases before the start of a TKI. It is also essential to keep in mind the TKIs used for CML treatment differ in their potency and activity against BCR-ABL1 and other kinases, which also exert relevant functions on the cardiovascular system. This can in part explains the observed discrepancy in the cardiovascular risk between the different TKIs.

A warning signal for the risk of heart failure in patients with CML treated with BCR-ABL TKIs was suggested in 2006 by Kerkelä and colleagues when reporting a case series of 10 patients treated with imatinib that had developed heart failure with reduced LVEF. Myocardial biopsies in two patients and three imatinib-treated mice showed mitochondrial abnormalities and accumulation of membrane whorls in both vacuoles and sarcoplasmic reticulum, suggesting toxic myopathy possibly associated with ABL inhibition (20). However, a further follow-up study of patients treated with imatinib did not demonstrate a higher risk of heart failure or cardiomyopathy (21). In our cohort, the unmatched incidences of the composite outcome

heart failure or LVEF < 50% were higher in the imatinib group (1.83%) and the nilotinib group (3.1%) than in the dasatinib group (0.78%). After matching for baseline risk factors, patients treated with imatinib showed a greater ratio for heart failure or a reduced LVEF than patients with dasatinib but not in relation to patients with nilotinib, suggesting that in a long term, dasatinib may exert less toxicity on ventricular function than imatinib or nilotinib. However, we should take into account that heart failure incidence was low in the three treatment groups.

In our study, patients with CML who were switched from one TKI to another were excluded from the analysis. One might question that patients on dasatinib who stopped medication for pleural effusion, which is a common adverse event with this medication, might have a higher incidence of heart failure and lead to a selection bias. However, the physiopathology of pleural effusion in patients treated with dasatinib is not related to heart failure, given that dasatinib-induced pleural effusions are generally lymphocyte-predominant exudates (22). In addition, data indicate dasatinib-induced pleural effusion could be related to strong inhibition of the platelet-derived growth factor receptor β, leading to a decreased interstitial fluid pressure and higher vascular permeability (23).

Venous thromboembolic events have not been described as a significant adverse effect of BCR-ABL TKIs. An exception was a phase 2 study that included patients with CML for ponatinib treatment, which showed moderate rates of VTE, mostly deep vein thrombosis and pulmonary embolism, that occurred in 5% of patients (24). In our study, the overall incidence of VTE or pulmonary embolism was low in the three TKI groups, and we have not observed a difference in risk between them.

The strengths of this study are the sample size, considering the low incidence of CML in many healthcare organizations, the capacity of adjusting the outcomes for baseline cardiovascular characteristics, and the real-world essence of the data. We must recognize several limitations of this study. First, it involved analyses of a retrospective observational cohort, which led to baseline differences among the treatment arms, such as older individuals with more cardiovascular risks in the imatinib group. This fact led us to use propensity score matching, which may have some problems like trying to mimic a randomized experiment, without the same precision and control against confounding. Also, propensity score matching may create a "propensity score paradox," in which unit pruning causes increased imbalance after a point (25).

Due to its observational retrospective nature, the study may be inherently subject to bias. Therefore, we should carefully avoid making cause–effect relationships and, instead, consider the results as a hypothesis generator. Second, despite the matching, we cannot exclude the influence of residual confounding, which was not captured, such as TKIs and cardiovascular medications dosage, administration timing since the beginning of the follow-up, and lifestyle habits such as physical activity and diet. Particularly TKI dosage may be an important factor for cardiotoxicity as showed in the ENESTnd trial, in which a higher dosage of nilotinib was associated with a higher incidence of arterial events in relation to a lower dosage or with imatinib (15). We were also unable to analyze the treatment discontinuation rates for the three BCR-ABL TKI groups, which could influence the timing of exposition to the TKI and their cardiovascular effect. Third, the outcomes and baseline characteristics were based on 10 ICD codes, which are not accurate when compared with adjudicated outcomes in randomized clinical trials.

In conclusion, we found in a large sample of patients with CML treated with BCR-ABL TKIs that when compared with imatinib treatment, patients treated with nilotinib had a higher ratio of ACE, while patients treated with dasatinib showed a lower ratio of cardiovascular and cerebrovascular events. The ratio of heart failure was greater in patients with imatinib when compared to dasatinib but not compared to nilotinib. These results raise the hypothesis that, when comparing three commonly used BCR-ABL TKIs, nilotinib presents a higher probability of cardiovascular toxicity and dasatinib presents a better cardiovascular safety profile. These findings may be particularly relevant in patients with CML and underlying cardiovascular risk factors, in which a BCR-ABL TKI is being considered for treatment.

Data availability statement

The original contributions presented in this study are included in the article/supplementary material, further inquiries can be directed to the corresponding author.

Ethics statement

The studies involving human participants were reviewed and approved by Comissão de Ética em Pesquisa do Hospital Alemão Oswaldo Cruz. Written informed consent for participation was not required for this study in accordance with the national legislation and the institutional requirements.

Author contributions

All authors listed have made a substantial, direct, and intellectual contribution to the work, and approved it for publication.

Acknowledgments

We thank Hospital Alemão Oswaldo Cruz for the access to the collaborative research network TriNetX.

Conflict of interest

The authors declare that the research was conducted in the absence of any commercial or financial relationships that could be construed as a potential conflict of interest.

Publisher's note

References

1. Jabbour E, Kantarjian H. Chronic myeloid leukemia: 2020 update on diagnosis, therapy and monitoring. *Am J Hematol.* (2020) 95:691–709.

2. Wood A, Savage D, Antman K. Imatinib mesylate–a new oral targeted therapy. *N Engl J Med.* (2002) 346:683–93. doi: 10.1056/NEJMra013339

3. Bojan A, Torok-Vistai T, Parvu A. Assessment and management of cardiotoxicity in hematologic malignancies. *Dis Markers.* (2021) 2021:6616265. doi: 10.1155/2021/6616265

4. Atallah E, Durand J, Kantarjian H, Cortes J. Congestive heart failure is a rare event in patients receiving imatinib therapy. *Blood.* (2007) 110:1233–7.

5. Chen Z, Ai D. Cardiotoxicity associated with targeted cancer therapies. *Mol Clin Oncol.* (2016) 4:675–81.

6. Hatfield A, Owen S, Pilot P. In reply to 'Cardiotoxicity of the cancer therapeutic agent imatinib mesylate'. *Nat Med.* (2007) 13:13.

7. Montani D, Bergot E, Günther S, Savale L, Bergeron A, Bourdin A, et al. Pulmonary arterial hypertension in patients treated by dasatinib. *Circulation.* (2012) 125:2128–37.

8. Cortes JE, Saglio G, Kantarjian HM, Baccarani M, Mayer J, Boqu C, et al. Final 5-year study results of DASISION: the dasatinib versus imatinib study in treatment-naïve chronic myeloid leukemia patients trial. *J Clin Oncol.* (2016) 34:2333–40. doi: 10.1200/JCO.2015.64.8899

9. Larson RA, Hochhaus A, Hughes TP, Clark RE, Etienne G, Kim D, et al. Nilotinib vs imatinib in patients with newly diagnosed Philadelphia chromosome-positive chronic myeloid leukemia in chronic phase: ENESTnd 3-year follow-up. *Leukemia.* (2012) 26:2197–203.

10. Giles FJ, Mauro MJ, Hong F, Ortmann C, McNeill C, Woodman RC, et al. Rates of peripheral arterial occlusive disease in patients with chronic myeloid leukemia in the chronic phase treated with imatinib, nilotinib, or non-tyrosine kinase therapy: a retrospective cohort analysis. *Leukemia.* (2013) 27:1310–5. doi: 10.1038/leu.2013.69

11. Chaar M, Kamta J, Ait-Oudhia S. Mechanisms, monitoring, and management of tyrosine kinase inhibitors-associated cardiovascular toxicities. *Onco Targets Ther.* (2018) 11:6227–37. doi: 10.2147/OTT.S170138

12. Aghel N, Delgado D, Lipton J. Cardiovascular toxicities of BCR-ABL tyrosine kinase inhibitors in chronic myeloid leukemia: preventive strategies and cardiovascular surveillance. *Vasc Health Risk Manag.* (2017) 13:293–303. doi: 10.2147/VHRM.S108874

13. Taquet M, Luciano S, Geddes J, Harrison P. Bidirectional associations between COVID-19 and psychiatric disorder: retrospective cohort studies of 62?354 COVID-19 cases in the USA. *Lancet Psychiatry.* (2021) 8:130–40. doi: 10.1016/S2215-0366(20)30462-4

14. Manouchehri A, Kanu E, Mauro M, Aday A, Lindner J, Moslehi J. Tyrosine kinase inhibitors in leukemia and cardiovascular events: from mechanism to patient care. *Arterioscler Thromb Vasc Biol.* (2020) 40:301–8.

15. Caocci G, Mulas O, Annunziata M, Luciano L, Abruzzese E, Bonifacio M, et al. Long-term mortality rate for cardiovascular disease in 656 chronic myeloid leukaemia patients treated with second- and third-generation tyrosine kinase inhibitors. *Int J Cardiol.* (2020) 301:163–6. doi: 10.1016/j.ijcard.2019.10.036

16. Hochhaus A, Saglio G, Hughes TP, Larson RA, Kim D, Issaragrisil S, et al. Long-term benefits and risks of frontline nilotinib vs imatinib for chronic myeloid leukemia in chronic phase: 5-year update of the randomized ENESTnd trial. *Leukemia.* (2016) 30:1044–54. doi: 10.1038/leu.2016.5

17. Saglio G, le Coutre P, Cortes J, Mayer J, Rowlings P, Mahon F, et al. Evaluation of cardiovascular ischemic event rates in dasatinib-treated patients using standardized incidence ratios. *Ann Hematol.* (2017) 96:1303–13. doi: 10.1007/s00277-017-3012-z

18. Hadzijusufovic E, Albrecht-Schgoer K, Huber K, Hoermann G, Grebien F, Eisenwort G, et al. Nilotinib-induced vasculopathy: identification of vascular endothelial cells as a primary target site. *Leukemia.* (2017) 31:2388–97. doi: 10.1038/leu.2017.245

19. Gora-Tybor J, Medras E, Calbecka M, Kolkowska-Leśniak A, Ponikowska-Szyba E, Robak T, et al. Real-life comparison of severe vascular events and other non-hematological complications in patients with chronic myeloid leukemia undergoing second-line nilotinib or dasatinib treatment. *Leuk Lymphoma.* (2015) 56:2309–14.

20. Kerkel R, Grazette L, Yacobi R, Iliescu C, Patten R, Beahm C, et al. Cardiotoxicity of the cancer therapeutic agent imatinib mesylate. *Nat Med.* (2006) 12:908–16.

21. Druker B, Guilhot F, O'Brien S, Gathmann I, Kantarjian H, Gattermann N, et al. Five-year follow-up of patients receiving imatinib for chronic myeloid leukemia. *N Engl J Med.* (2006) 355:2408–17.

22. Brixey A, Light R. Pleural effusions due to dasatinib. *Curr Opin Pulm Med.* (2010) 16:351–6.

23. Cortes J, Jimenez C, Mauro M, Geyer A, Pinilla-Ibarz J, Smith B. Pleural effusion in dasatinib-treated patients with chronic myeloid leukemia in chronic phase: identification and management. *Clin Lymphoma Myeloma Leuk.* (2017) 17:78–82. doi: 10.1016/j.clml.2016.09.012

24. Jain P, Kantarjian H, Jabbour E, Gonzalez G, Borthakur G, Pemmaraju N, et al. Ponatinib as first-line treatment for patients with chronic myeloid leukaemia in chronic phase: a phase 2 study. *Lancet Haematol.* (2015) 2:e376–83.

25. Li F, Morgan KL, Zaslavsky AM. Balancing covariates via propensity score weighting. *J Am Stat Assoc.* (2018) 113:390–400.

Frontiers in
Cardiovascular Medicine

Innovations and improvements in cardiovascular treatment and practice

Focuses on research that challenges the status quo of cardiovascular care, or facilitates the translation of advances into new therapies and diagnostic tools.

Discover the latest Research Topics

See more →

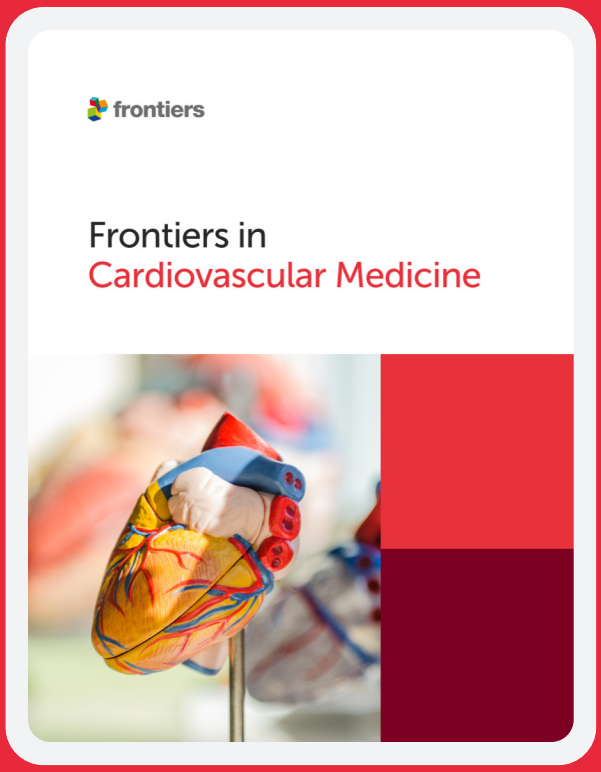

Frontiers

Avenue du Tribunal-Fédéral 34
1005 Lausanne, Switzerland
frontiersin.org

Contact us

+41 (0)21 510 17 00
frontiersin.org/about/contact